

Atmospheric deposition of organic contaminants into the North Sea and the western Baltic Sea

Ph. D. Thesis

for the achievement of an academic degree as

Dr. rer. nat.

at the Department of Chemistry
of the University of Hamburg

Presented by

Carolin Mai
born in Kirn

Hamburg 2012

This thesis was written between 03.12.2008 and 31.05.2012 at the Federal Maritime and Hydrographic Agency of Germany (BSH) in Hamburg under support and supervision of Dr. N. Theobald, Prof. Dr. H. Hühnerfuss and Prof. Dr. G. Lammel.

1st Consultant: Prof. Dr. H. Hühnerfuss

2nd Consultant: Dr. M. Steiger

Date of Disputation: 29.06.2012

Acknowledgement

First, I would like to thank my Ph.D supervisor Prof. Dr. Hühnerfuss for the honour to be one of the last Ph. D. students in his well established and successful working group. Additionally, I thank Prof. Dr. Lammel for the scholarship at the International Max Planck Research School for Maritime Affairs (IMPRS) making this Ph. D. thesis possible, for his advice and support throughout my studies. In this sense, I also thank the directorate of the IMPRS for the permission of financial support throughout my Ph. D study.

Special thanks go to Dr. Theobald for the allocation of a very interesting Ph. D. topic, for the freedom of making it my own and for welcoming me into his working group. Furthermore, I would like to express my gratitude to the members of the division marine chemistry (M3) at the Federal Maritime and Hydrographic Agency (BSH) for their support, advice and appreciation throughout my time there. Especially Udo Ziebarth and Wolfgang Gerwinski are thanked for their support. My office mate Uta Kraus is thanked for making good times better and bad times less hard. The members of the mechanic workshop (M24) and the division of the marine monitoring network (M23) are thanked for providing their knowledge and support, which contributed to the success of the air sampling campaigns.

I deeply acknowledge Uwe Wiegand and Dr. Jan Rueß for their teamwork in data acquisition at Sylt and the Baltic Sea. Moreover, I would like to thank Dr. Annetrin Dreyer and Dr. Christian Temme for showing me the right direction at the early beginning of my project. Further thanks go to the Research Centre for Toxic Compounds in the Environment (RECETOX) at the Masaryk University in Brno (Czech Republic) for the supply of the passive air sampling equipment and to the department of environmental chemistry of the Helmholtz-Zentrum Geesthacht (HZG) borrowing me the equipment for my first sampling campaign at sea. In addition, I thank the members of the Federal Environmental Agency (UBA), the Federal Maritime and Hydrographic Agency (BSH) and the Institute for Baltic Sea research (IOW) for the complementing data to my investigations.

Finally, I would like to show my gratitude to Prof. Dr. Knepper, the supervisor of my diploma thesis, for his advice and support helping me to start this Ph.D. project.

Last but certainly not least, I thank my family for their faith and never-ending support encouraging me to finish this work.

Table of contents

1. Introduction	1
1.1 Context	1
1.2 State of the art	2
1.3 Objectives	7
2. Theory	9
2.1 Occurrence and fate of organic pollutants in the atmosphere	9
2.2 Atmospheric transport of organic pollutants	11
2.2.1 The role of aerosol particles in atmospheric transport and deposition.....	13
2.2.2 The role of clouds in atmospheric transport, deposition and transformation processes....	16
2.3 Air-sea and sea-air exchange mechanisms of organic pollutants	16
2.3.1 Influence of biogeochemical processes in the water column	17
2.3.2 Influence of bubbling processes in surface waters	18
2.4 Atmospheric Deposition	20
2.4.1 Direction of the net flux of diffusive gas exchange	20
2.4.2 Quantification of the dry gaseous deposition	21
2.4.3 Quantification of the dry particulate deposition	22
2.4.4 Quantification of the wet deposition	24
3. Methodology	25
3.1 Air-sampling methods	25
3.1.1 High-volume active air samplers	25
3.1.2 PUF disk passive air samplers	30
3.2 Air sampling campaigns	33
3.2.1 Active air sampling campaigns	33
3.2.2 Passive air sampling campaigns	38
3.3 Target compounds	42
3.4 Analysis - Extraction, Evaporation, Clean-up and Quantification	53
3.5 Air mass backward trajectories	56
3.6 Surface Water Samples	58
4. Method Validation	59
4.1 Validation of air sampling	59
4.1.1 Side-by-side air sampling experiments	59
4.1.2 Desorption experiments	60
4.1.3 Stability tests of exposed air sampling materials	64

4.2 Validation of air sample preparation methods	68
4.2.1 Blanks	69
4.2.2 Spike controls	74
4.2.3 Reproducibility of air sample preparation	78
4.2.4 Extraction efficiency	80
4.3 Validation of Quantification	80
4.3.1 Limits of quantification	80
4.3.2 Limits of detection	82
5. Results and Discussion	85
5.1 Assessment of the current status of the cycling processes of organic contaminants between the marine atmosphere and the sea surface water of the German EEZ, the North Sea and the Baltic Sea	86
5.1.1 Polycyclic Aromatic Hydrocarbons	86
5.1.2 Chlorinated Benzenes	102
5.1.3 Hexachlorocyclohexanes	111
5.1.4 Cyclodiene pesticides	120
5.1.5 DDT isomers and metabolites	126
5.1.6 Polychlorinated Biphenyls	136
5.1.7 Triazine Herbicides	146
5.1.8 Organophosphate Insecticides	159
5.1.9 Phenylurea Herbicides	164
5.1.10 Phenoxyalkanoic acid and Thiadiazine Herbicides	179
5.1.11 Dinitroaniline, Chloroacetanilide and Carbamate Pesticides	189
5.1.12 Perfluorinated compounds	207
5.1.13 Organophosphorus and Brominated Flame Retardants	217
5.1.14 Pharmaceuticals	220
5.2 Vertical distributions of organic contaminants in the North Sea atmosphere	227
5.2.1 Influence of the vertical wind velocity profile on the sampling rates	228
5.2.2 Vertical profiles of PAH abundances in the marine atmosphere	230
5.2.3 Vertical profiles of organochlorine pesticides and PCBs in the marine atmosphere	231
5.2.4 Vertical profiles of polar pesticides in the marine atmosphere	232
5.2.5 Vertical profiles of perfluorinated compounds in the marine atmosphere	234
5.3 Estimations of the dry particle and wet deposition fluxes to the surface seawaters	235
5.3.1 Wet deposition	236
5.3.2 Dry particle deposition	238

6. Summary	241
7. Zusammenfassung	244
8. Perspectives	247
9. Experimental	248
9.1 List of materials	248
9.2 List of instruments	254
9.3 Standard Solutions	255
9.3.1 Performance reference compound (PRC) standard solutions	255
9.3.2 Internal standard (IS) solutions	255
9.3.3 Spike standard solutions of target compounds	256
9.4 Processing methods	257
9.4.1 Pre-cleaning of sampling material	257
9.4.2 Sample collection	257
9.4.3 Sample preparation	258
9.4.4 Quality control samples	262
9.5 Mass spectrometry - Acquisition methods	264
9.5.1 GC-MS	264
9.5.2 GC-MS/MS	265
9.5.3 HPLC-MS/MS	266
9.6 Mass spectrometry - Quantification methods	267
9.6.1 GC-MS	267
9.6.2 GC-MS/MS	268
9.6.3 HPLC-MS/MS	268
9.7 Calculation of atmospheric concentrations	269
10. References	270
11. Annexes	283
Annex 1 (A1): Atmospheric concentrations of target analytes	283
Annex 2 (A2): Field blanks and control samples	304
Annex 3 (A3): Recoveries of performance reference compounds (PRCs)	339
Annex 4 (A4): Air mass backward trajectories – Original Hysplit 4.9 plottings	344
Annex 5 (A5): Surface water concentrations of target analytes	383
Annex 6 (A6): Concentrations of target analytes in suspended particulate matter	409
Annex 7 (A7): Henry’s law constants of target analytes	410
Annex 8 (A8): Concentrations of organic compounds in rain water samples	411

List of figures

Figure 2.1: Schematic illustration of environmental mechanisms affecting the occurrence and fate of organic pollutants in the atmosphere	10
Figure 2.2: Illustration of thermodynamically expected atmospheric transport processes referring to the global fractionation hypothesis and grasshopper-effect	11
Figure 2.3: Distribution characteristics of organic pollutants defined by the partition coefficients (A); Transport behaviour categorization of several organic pollutants (B)	13
Figure 2.4: Overview of the mass size distribution, atmospheric lifetimes, sources and sinks of aerosol particles	14
Figure 2.5: Schematic presentation of the air-water-phytoplankton coupling model	17
Figure 2.6: (A) Schematic presentation of sea-air-interactions via bubble bursting, (B) White capping and sea spray	19
Figure 2.7: Surface size distribution of various aerosol types	23
Figure 3.1: Schematic diagrams of high-volume active air samplers including a photograph of the inlet, respectively; (A) AAS of the HZG; (B) AAS of the University of Hamburg	26
Figure 3.2: Schematic diagram of the Digital DHM-60 high-volume active air sampler and a photograph from the top deck of the research ship Pelagia	27
Figure 3.3: (A) Gauze-insertions; (B) The fine-meshed gauze prevent the loss of XAD-2 from the adsorber cartridge (PUF/XAD-2/PUF sandwich)	27
Figure 3.4: Size segregation characteristic of the single-stage impactor in the Digital DHM-60 high-volume active air sampler at 15°C ambient temperature, 1013 mbar air pressure and 50% relative humidity	28
Figure 3.5: Housings of the adsorber cartridge of the Digital DHM-60 systems; (A) Housing with a screw cap; (B) Housing with a hinged lid; (C) Adsorber cartridge fitting for insertion in the housings	29
Figure 3.6: Schematic diagram of a conventional PUF disk passive air sampler and a photograph illustrating the installation at the top deck of the research vessels	30
Figure 3.7: Modified PUF disk passive air sampler	32
Figure 3.8: Ship positions corresponding to air samples collected during the Baltic Sea research cruise in April 2009	34
Figure 3.9: Ship positions corresponding to air samples collected during the research cruise in the German EEZ in May/June 2009.....	35
Figure 3.10: GFF contaminated by ship fumes (A); GFF air sample without ship fumes (B)	36
Figure 3.11: Ship positions corresponding to air samples collected during the research cruise in the North Sea in August/September 2009.....	36
Figure 3.12: Ship positions corresponding to air samples collected during the research cruise in the German EEZ in May 2010	37
Figure 3.13: Geographical positions of the sampling sites in Sülldorf/Hamburg, Tinnum/Sylt and the FINO stations in the German EEZ	39
Figure 3.14: PAS deployment at FINO 1 in the German EEZ	41
Figure 3.15: Illustration of the parallel-evaporator with regard to adjustable parameters including the temperature profile established at a heating plate temperature of 50°C and at a water recirculation cooler temperature of 30°C	53

Figure 3.16: Optimization of parallel-evaporation parameters; The quantification is standardized to the internal standard PCB 185, which resists evaporation; Target compounds are sorted by increasing retention time	54
Figure 3.17: Schematic illustration of extraction, evaporation and clean-up of air samples	55
Figure 3.18: Air mass backward trajectories (black arrows) of the air samples (red and green lines) collected over the German EEZ in May/June 2009 (A) and in May 2010 (B), respectively	56
Figure 3.19: Air mass backward trajectories (black arrows) of the air samples (red lines) collected over the North Sea in August/September 2009	57
Figure 3.20: Air mass backward trajectories (black arrows) of the air samples collected during the Baltic Sea research cruise in April 2009.....	57
Figure 3.21: Sea currents of the North Sea (A) and the Baltic Sea (B).....	58
Figure 4.1: Desorption test for prometryn-D ₆ ; (A) PUF plug adsorber cartridge; (B) PUF/XAD-2/PUF adsorber cartridge	61
Figure 4.2: Desorption test for simazine-D ₁₀ ; (A) PUF plug adsorber cartridge; (B) PUF/XAD-2/PUF adsorber cartridge	61
Figure 4.3: Desorption test for γ -HCH- ¹³ C ₆ D ₆ ; (A) PUF plug adsorber cartridge; (B) PUF/XAD-2/PUF adsorber cartridge	62
Figure 4.4: Desorption test for polychlorinated biphenyl 30; (A) PUF plug adsorber cartridge; (B) PUF/XAD-2/PUF adsorber cartridge	62
Figure 4.5: Desorption test for polychlorinated biphenyl 104; (A) PUF plug adsorber cartridge; (B) PUF/XAD-2/PUF adsorber cartridge	62
Figure 4.6: Desorption test for polychlorinated biphenyl 145; (A) PUF plug adsorber cartridge; (B) PUF/XAD-2/PUF adsorber cartridge	63
Figure 4.7: Desorption test for polychlorinated biphenyl 204; (A) PUF plug adsorber cartridge; (B) PUF/XAD-2/PUF adsorber cartridge	63
Figure 4.8: Desorption test for phenanthrene-D ₁₀ ; (A) PUF plug adsorber cartridge; (B) PUF/XAD-2/PUF adsorber cartridge	63
Figure 4.9: Desorption test for fluoranthene-D ₁₀ ; (A) PUF plug adsorber cartridge; (B) PUF/XAD-2/PUF adsorber cartridge	64
Figure 4.10: Desorption test for benzo[<i>a</i>]anthracene-D ₁₂ ; (A) PUF plug adsorber cartridge; (B) PUF/XAD-2/PUF adsorber cartridge	64
Figure 4.11: Stability test of prometryn-D ₆ ; (A) PUF/XAD-2/PUF adsorber cartridge, (B) PUF disk	65
Figure 4.12: Stability test of simazine-D ₁₀ ; (A) PUF/XAD-2/PUF adsorber cartridge, (B) PUF disk	65
Figure 4.13: Stability test of γ -HCH- ¹³ C ₆ D ₆ ; (A) PUF/XAD-2/PUF adsorber cartridge, (B) PUF disk	66
Figure 4.14: Stability test of polychlorinated biphenyl 30; (A) PUF/XAD-2/PUF adsorber cartridge, (B) PUF disk	66
Figure 4.15: Stability test of polychlorinated biphenyl 104; (A) PUF/XAD-2/PUF adsorber cartridge, (B) PUF disk	66
Figure 4.16: Stability test of polychlorinated biphenyl 145; (A) PUF/XAD-2/PUF adsorber cartridge, (B) PUF disk	67

Figure 4.17: Stability test of polychlorinated biphenyl 204; (A) PUF/XAD-2/PUF adsorber cartridge, (B) PUF disk	67
Figure 4.18: Stability test of phenanthrene-D ₁₀ ; (A) PUF/XAD-2/PUF adsorber cartridge, (B) PUF disk	67
Figure 4.19: Stability test of fluoranthene-D ₁₀ ; (A) PUF/XAD-2/PUF adsorber cartridge, (B) PUF disk	68
Figure 4.20: Stability test of benzo[<i>a</i>]anthracene-D ₁₂ ; (A) PUF/XAD-2/PUF adsorber cartridge, (B) PUF disk	68
Figure 4.21: Glass jars of the parallel-evaporator system glazed with tenacious PUF residues	74
Figure 4.22: White and aged polyurethane foam (A) with respective methanol extracts (B)	79
Figure 4.23: PRC recovery results of (A) 20 GFF air samples and (B) of 12 PUF disk air samples	79
Figure 4.24: PRC recovery results of (A) 10 PUF plug adsorber cartridge air samples and (B) 9 PUF/XAD-2/PUF adsorber cartridge air samples	80
Figure 5.1: Atmospheric concentrations of organic pollutants in the atmosphere of the North Sea (plot of active air sampling data of the research cruises in the German EEZ 2009/2010 and the wider North Sea 2009)	85
Figure 5.2: (A) Atmospheric bulk concentrations of PAHs above the German EEZ in May/Jun. 2009; (B) Interpretation by location and sources (backward trajectories)	88
Figure 5.3: Atmospheric bulk concentrations of PAHs above the German EEZ in May 2010	89
Figure 5.4: Atmospheric bulk concentrations of PAHs above the North Sea in Aug./Sep. 2009 ...	90
Figure 5.5: Concentrations of PAHs in the gaseous mass fraction of the atmosphere above the Baltic Sea in Apr. 2009	90
Figure 5.6: Seasonal variation of atmospheric PAH levels plotted in correlation with the ambient temperature for the PUF disk passive air sampler sampling sites Sülldorf/Hamburg (A) and Tinum/Sylt (B)	91
Figure 5.7: Comparison of atmospheric bulk concentrations of PAHs determined by active air sampling campaigns in winter (arithmetic mean of 20 air samples) and spring/summer (arithmetic mean of two air samples)	92
Figure 5.8: Gas-particle partitioning of PAHs in correlation with ambient air temperatures	93
Figure 5.9: Gas-particle partitioning of individual PAH components sorted by their vapour pressures ^[69] , at different ambient air temperatures	94
Figure 5.10: Occurrence and distribution of PAHs (aqueous and particulate phase) in the surface water (5m) of the German EEZ in May/Jun. 2009; (A) Spatial distribution; (B) PAH abundances in relation to suspended particulate matter (SPM) concentration and salinity for each water sampling site	95
Figure 5.11: Occurrence and distribution of PAHs (aqueous and particulate phase) in the surface water (5m) of the German EEZ in May 2010; (A) Spatial distribution; (B) PAH abundances in relation to suspended particulate matter (SPM) concentration and salinity for each water sampling site	96
Figure 5.12: Occurrence and distribution of PAHs (aqueous and particulate phase) in the surface water (5m) of the North Sea in Aug./Sep. 2009; (A) Spatial distribution; (B) PAH abundances in relation to suspended particulate matter (SPM) concentration and salinity for each water sampling site	97

Figure 5.13: Spatial distribution of PAHs (aqueous and particulate phase) in the surface water (6m) of the Baltic Sea in Feb. 2005	98
Figure 5.14: PAH abundances of suspended particulate matter (SPM) collected in the estuary of the river Elbe (Apr./Jun. 2009) in relation to logKOW (obtained from ^[64])	99
Figure 5.15: Net flux of diffusive gas exchange of fluorene and phenanthrene; Fugacity ratio < 0.5: Atmosphere --> Sea; Fugacity ratio > 2: Sea --> Atmosphere; (A) German EEZ May/Jun. 2009; (B) German EEZ May 2010; (C) North Sea Aug./Sep. 2009; (D) Baltic Sea Apr. 2009	101
Figure 5.16: Gas phase concentrations of chlorinated benzenes in the atmosphere above the German EEZ in May/Jun. 2009	104
Figure 5.17: Gas phase concentrations of chlorinated benzenes in the atmosphere above the German EEZ in May 2010	104
Figure 5.18: Gas phase concentrations of chlorinated benzenes in the atmosphere above the North Sea in Aug./Sep. 2009	105
Figure 5.19: Gas phase concentrations of chlorinated benzenes in the atmosphere above the Baltic Sea in Apr. 2009	105
Figure 5.20: Occurrence and spatial distribution of chlorinated benzenes in the surface water (5m) of the German EEZ in May/Jun. 2009	107
Figure 5.21: Occurrence and spatial distribution of chlorinated benzenes in the surface water (5m) of the German EEZ in May 2010	107
Figure 5.22: Occurrence and distribution of chlorinated benzenes in the surface water (5m) of the North Sea in Aug./Sep. 2009	108
Figure 5.23: Spatial distribution of hexachlorobenzene (HCB) in the surface water (6m) of the Baltic Sea in Feb. 2005	108
Figure 5.24: Net flux of diffusive gas exchange of chlorinated benzenes; Fugacity ratio < 0.5: Atmosphere --> Sea; Fugacity ratio > 2: Sea --> Atmosphere; (A) German EEZ May/Jun. 2009; (B) German EEZ May 2010; (C) North Sea Aug./Sep. 2009; (D) Baltic Sea Apr. 2009	109
Figure 5.25: (A) Gas phase concentrations of hexachlorocyclohexanes in the atmosphere above the German EEZ in May/Jun. 2009; (B) Air mass history (24 h backward trajectories)	112
Figure 5.26: (A) Gas phase concentrations of hexachlorocyclohexanes in the atmosphere above the German EEZ in May 2010; (B) Air mass history (24 h backward trajectories)	112
Figure 5.27: (A) Gas phase concentrations of hexachlorocyclohexanes in the atmosphere above the North Sea in Aug./Sep. 2009; (B) Air mass history (24 h backward trajectories)	113
Figure 5.28: (A) Gas phase concentrations of hexachlorocyclohexanes in the atmosphere above the Baltic Sea in Apr. 2009; (B) Air mass history (24 h backward trajectories)	113
Figure 5.29: Seasonal variations in atmospheric hexachlorocyclohexane levels plotted in correlation with the ambient temperature for the PUF disk passive air sampler sampling sites Sülldorf/Hamburg (A) and Tinnum/Sylt (B)	114
Figure 5.30: Occurrence and distribution of hexachlorocyclohexanes in the surface water (5m) of the German EEZ in Apr./May 2009	115
Figure 5.31: Occurrence and distribution of hexachlorocyclohexanes in the surface water (5m) of the German EEZ in May 2010	116
Figure 5.32: Occurrence and distribution of hexachlorocyclohexanes in the surface water (5m) of the North Sea in Aug./Sep. 2009	117

Figure 5.33: Occurrence and distribution of hexachlorocyclohexanes in the surface water (5m) of the German EEZ in the Baltic Sea in July 2009	118
Figure 5.34: Net flux of diffusive gas exchange of α -HCH and γ -HCH; Fugacity ratio < 0.5: Atmosphere --> Sea; Fugacity ratio > 2: Sea --> Atmosphere; (A) German EEZ May/Jun. 2009; (B) German EEZ May 2010; (C) North Sea Aug./Sep. 2009; (D) Baltic Sea Apr. 2009	119
Figure 5.35: Atmospheric concentrations (gaseous phase) of dieldrin above the German EEZ in May/Jun. 2009	121
Figure 5.36: Atmospheric concentrations (gaseous phase) of dieldrin above the German EEZ in May 2010	122
Figure 5.37: Atmospheric concentrations (gaseous phase) of dieldrin above the North Sea in Aug./Sep. 2009	122
Figure 5.38: Occurrence and distribution of cyclodiene pesticides in the surface water (5 m) of the German EEZ in May/Jun. 2009	124
Figure 5.39: Occurrence and distribution of cyclodiene pesticides in the surface water (5 m) of the German EEZ in May 2010	124
Figure 5.40: Occurrence and distribution of cyclodiene pesticides in the surface water (5 m) of the North Sea in Aug./Sep. 2009	125
Figure 5.41: Net flux of diffusive gas exchange of dieldrin; Fugacity ratio < 0.5: Atmosphere --> Sea; Fugacity ratio > 2: Sea --> Atmosphere; (A) German EEZ May/Jun. 2009; (B) German EEZ May 2010; (C) North Sea Aug./Sep. 2009	125
Figure 5.42: Atmospheric bulk concentrations of DDT isomers and metabolites above the German EEZ in May/Jun. 2009	127
Figure 5.43: Atmospheric bulk concentrations of DDT isomers and metabolites above the German EEZ in May 2010	128
Figure 5.44: Atmospheric bulk concentrations of DDT isomers and metabolites above the North Sea in Aug./Sep. 2009	129
Figure 5.45: Concentrations of DDT isomers and metabolites in the gaseous mass fraction of the atmosphere above the Baltic Sea in Apr. 2009	130
Figure 5.46: Seasonal variability in atmospheric levels of the DDT isomers and metabolites of the PUF disk passive air sampler sampling sites in Sülldorf/Hamburg (A) and Tinnum/Sylt (B)	131
Figure 5.47: Occurrence and spatial distribution of DDTTP and metabolites in the surface water (5m) of the German EEZ in May/Jun. 2009	133
Figure 5.48: Occurrence and spatial distribution of the DDTTP and metabolites in the surface water (5m) of the German EEZ in May 2010	134
Figure 5.49: Occurrence and distribution of DDTTP and metabolites in the surface water (5m) of the North Sea in Aug./Sep. 2009	134
Figure 5.50: Occurrence and spatial distribution of DDTTP and metabolites in the surface water (6m) of the Baltic Sea in Feb. 2005	135
Figure 5.51: Atmospheric bulk concentrations of PCBs above the German EEZ in May/Jun. 2009	137
Figure 5.52: Atmospheric bulk concentrations of PCBs above the German EEZ in May 2010 ...	138

Figure 5.53: Atmospheric bulk concentrations of PCBs above the North Sea in Aug./Sep. 2009	138
Figure 5.54: Concentrations of PCBs in the gaseous mass fraction of the atmosphere above the Baltic Sea in Apr. 2009	139
Figure 5.55: Seasonal variation in atmospheric abundances of PCBs at the PUF disk passive air sampler sampling sites Sülldorf/Hamburg (A) and Tinum/Sylt (B)	140
Figure 5.56: Occurrence and distribution of PCBs in the surface water (5m) of the German EEZ in May/Jun. 2009	143
Figure 5.57: Occurrence and distribution of PCBs in the surface water (5m) of the German EEZ in May 2010	143
Figure 5.58: Occurrence and distribution of PCBs in the surface water (5m) of the North Sea in Aug./Sep. 2009	144
Figure 5.59: Occurrence and distribution of PCBs in the surface water (6 m) of the Baltic Sea in Feb. 2005	145
Figure 5.60: Atmospheric bulk concentrations of triazine herbicides above the German EEZ in May/Jun. 2009	148
Figure 5.61: Concentrations of triazine herbicides in the gaseous mass fraction of the atmosphere above the Baltic Sea in Apr. 2009	148
Figure 5.62: Seasonal variations in atmospheric levels of the triazine herbicides terbuthylazine and terbutryn observed at the sampling sites Sülldorf/Hamburg and Tinum/Sylt	150
Figure 5.63: Occurrence and distribution of triazine herbicides in the aqueous phase of the surface water (5m) of the German EEZ in May/Jun. 2009	153
Figure 5.64: Occurrence and distribution of triazine herbicides in the aqueous phase of the surface water (5m) of the German EEZ in May 2010	154
Figure 5.65: Occurrence and distribution of triazine herbicides in the aqueous phase of the surface water (5m) of the North Sea in Aug./Sep. 2009	155
Figure 5.66: Seasonal variations in the surface water concentrations (5 m) of the triazine herbicides in the estuary of the river Elbe (A) and of terbuthylazine at selected sampling sites throughout the German EEZ (B)	156
Figure 5.67: Occurrence and distribution of triazine herbicides in the aqueous phase of the surface water (6m) of the Baltic Sea in Jun./Jul. 2008	157
Figure 5.68: Net flux of diffusive gas exchange of terbuthylazine and atrazine; Fugacity ratio < 0.5: Atmosphere --> Sea; Fugacity ratio > 2: Sea --> Atmosphere; (A) German EEZ May/Jun. 2009; (B) Baltic Sea Apr. 2009	158
Figure 5.69: Seasonal variations in the atmospheric abundances of the organophosphate insecticides observed at the sampling sites Sülldorf/Hamburg and Tinum/Sylt	161
Figure 5.70: Occurrence and distribution of organophosphate insecticides in the aqueous phase of the surface water (5m) of the German EEZ in May/Jun. 2009	162
Figure 5.71: Occurrence and distribution of organophosphate insecticides in the aqueous phase of the surface water (5m) of the German EEZ in May 2010	163
Figure 5.72: Occurrence and distribution of organophosphate insecticides in the aqueous phase of the surface water (5m) of the North Sea in Aug./Sep. 2009	163

Figure 5.73: Net flux of diffusive gas exchange of diazinone between the surface water and the atmosphere of the North Sea in Aug./Sep. 2009; Fugacity ratio < 0.5: Atmosphere --> Sea; Fugacity ratio > 2: Sea --> Atmosphere	164
Figure 5.74: Atmospheric bulk concentrations of phenylurea herbicides above the German EEZ in May/Jun. 2009	166
Figure 5.75: Atmospheric bulk concentrations of phenylurea herbicides above the German EEZ in May 2010	167
Figure 5.76: Atmospheric bulk concentrations of phenylurea herbicides above the North Sea in Aug./Sep. 2009	167
Figure 5.77: Concentrations of phenylurea herbicides in the gaseous mass fraction of the atmosphere above the Baltic Sea in Apr. 2009	168
Figure 5.78: Seasonal variations in the atmospheric abundances of phenylurea herbicides observed at the sampling sites Sülldorf/Hamburg (A) and Tinnum/Sylt (B)	170
Figure 5.79: Occurrence and distribution of phenylurea herbicides in the aqueous phase of the surface water (5 m) of the German EEZ in May/Jun. 2009	173
Figure 5.80: Occurrence and distribution of phenylurea herbicides in the aqueous phase of the surface water (5 m) of the German EEZ in May 2010	174
Figure 5.81: Occurrence and distribution of phenylurea herbicides in the aqueous phase of the surface water (5 m) of the North Sea in Aug./Sep. 2009	175
Figure 5.82: Occurrence and distribution of phenylurea herbicides in the aqueous phase of the surface water (6 m) of the Baltic Sea in Jun./Jul. 2008	176
Figure 5.83: Seasonal variations in the surface water concentrations (5 m) of the phenylurea herbicides displayed for selected sampling sites in the German EEZ in 2009	177
Figure 5.84: Atmospheric concentrations of phenoxyalkanoic acids (gaseous mass fraction) and bentazone (bulk concentrations) above the German EEZ in May/Jun. 2009	180
Figure 5.85: Atmospheric concentrations of phenoxyalkanoic acids (gaseous mass fraction) and bentazone (bulk concentrations) above the German EEZ in May 2010	181
Figure 5.86: Atmospheric concentrations of phenoxyalkanoic acids (gaseous mass fraction) and bentazone (bulk concentrations) above the North Sea in Aug./Sep. 2009	181
Figure 5.87: Seasonal variations in the atmospheric abundances of bentazone observed at the sampling sites Sülldorf/Hamburg (A) and Tinnum/Sylt (B)	182
Figure 5.88: Occurrence and spatial distribution of phenoxyalkanoic acids and bentazone in the aqueous phase of the surface water (5 m) of the German EEZ in May/Jun. 2009	184
Figure 5.89: Occurrence and spatial distribution of phenoxyalkanoic acids and bentazone in the aqueous phase of the surface water (5 m) of the German EEZ in May 2010	185
Figure 5.90: Occurrence and spatial distribution of phenoxyalkanoic acids and bentazone in the aqueous phase of the surface water (5 m) of the North Sea in Aug./Sep. 2009	185
Figure 5.91: Occurrence and spatial distribution of phenoxyalkanoic acids and bentazone in the aqueous phase of the surface water (6 m) of the Baltic Sea in Jun./Jul. 2008	186
Figure 5.92: Seasonal variations in the surface water concentrations (5 m) of the phenoxyalkanoic acids and bentazone displayed for selected sampling sites in the German EEZ in 2009	187
Figure 5.93: Atmospheric bulk concentrations of dinitroaniline, chloroacetanilide and carbamate pesticides above the German EEZ in May/Jun. 2009	190

Figure 5.94: Atmospheric bulk concentrations of dinitroaniline, chloroacetanilide and carbamate pesticides above the German EEZ in May 2010	190
Figure 5.95: Atmospheric bulk concentrations of dinitroaniline, chloroacetanilide and carbamate pesticides above the North Sea in Aug./Sep. 2009	191
Figure 5.96: Concentrations of dinitroaniline, chloroacetanilide and carbamate pesticides in the gaseous mass fraction of the atmosphere above the Baltic Sea in Apr. 2009	191
Figure 5.97: Seasonal variations in the atmospheric abundances of dinitroaniline, chloroacetanilide and carbamate pesticides at the sampling sites Sülldorf/Hamburg and Tinnum/Sylt	194
Figure 5.98: Gas-particle partitioning of pendimethalin in correlation with the ambient air temperatures	195
Figure 5.99: Occurrence and distribution of dinitroaniline, chloroacetanilide and carbamate pesticides in the aqueous phase of the surface water (5 m) of the German EEZ in May/Jun. 2009	197
Figure 5.100: Occurrence and distribution of dinitroaniline, chloroacetanilide and carbamate pesticides in the aqueous phase of the surface water (5 m) of the German EEZ in May 2010	198
Figure 5.101: Occurrence and distribution of dinitroaniline, chloroacetanilide and carbamate pesticides in the aqueous phase of the surface water (5 m) of the North Sea in Aug./Sep. 2009	201
Figure 5.102: Occurrence and distribution of dinitroaniline, chloroacetanilide and carbamate pesticides in the aqueous phase of the surface water (6 m) of the Baltic Sea in Jun./Jul. 2008	202
Figure 5.103: Seasonal variations in the surface water concentrations (5 m) of the dinitroaniline, chloroacetanilide and carbamate pesticides displayed for selected sampling sites in the German EEZ in 2009	203
Figure 5.104: Net flux of diffusive gas exchange of the dinitroaniline and chloroacetanilide herbicides; Fugacity ratio < 0.5: Atmosphere --> Sea; Fugacity ratio > 2: Sea --> Atmosphere; (A) German EEZ May/Jun. 2009; (B) German EEZ May 2010; (C) North Sea Aug./Sep. 2009; (D) Baltic Sea Apr. 2009	205
Figure 5.105: Atmospheric bulk concentrations of the PFCs above the German EEZ in May/Jun. 2009	208
Figure 5.106: Atmospheric bulk concentrations of the PFCs above the German EEZ in May 2010	209
Figure 5.107: Atmospheric bulk concentrations of PFCs above the North Sea in Aug./Sep. 2009	210
Figure 5.108: Arithmetic mean bulk concentrations of PFOS and PFOA in pg/m ³ at sea and land based sampling sites	210
Figure 5.109: Occurrence and distribution of PFCs in the aqueous phase of the surface water (5 m) of the German EEZ in May/Jun. 2009	212
Figure 5.110: Occurrence and distribution of PFCs in the aqueous phase of the surface water (5 m) of the German EEZ in May 2010	213
Figure 5.111: Occurrence and distribution of PFCs in the aqueous phase of the surface water (5 m) of the North Sea in Aug./Sep. 2009	214
Figure 5.112: Occurrence and distribution of PFCs in the aqueous phase of the surface water (6 m) of the Baltic Sea in Jun./Jul. 2008	215

Figure 5.113: Composition of the targeted PFCs in the surface water (5-6 m) of the North Sea, the German EEZ and the Baltic Sea	216
Figure 5.114: Occurrence and spatial distribution of pharmaceuticals in the aqueous phase of the surface water of the German EEZ in May/Jun. 2009	223
Figure 5.115: Occurrence and spatial distribution of pharmaceuticals in the aqueous phase of the surface water of the German EEZ in May 2010	224
Figure 5.116: Occurrence and spatial distribution of pharmaceuticals in the aqueous phase of the surface water of the North Sea in Aug./Sep. 2009	225
Figure 5.117: Occurrence and spatial distribution of pharmaceuticals in the aqueous phase of the surface water of the Baltic Sea in Jun./Jul. 2008	226
Figure 5.118: Vertical wind profile monitored at the FINO 3 platform in the period of the 10 August to the 1 September 2010	228
Figure 5.119: Vertical gradients of the atmospheric abundances of PAHs in the marine atmosphere of the German EEZ in the period of August to October 2010	230
Figure 5.120: Vertical gradients of the atmospheric abundances of organochlorine pesticides and PCBs in the marine atmosphere of the German EEZ in the period of August to October 2010	232
Figure 5.121: Vertical gradients of the atmospheric abundances of polar pesticides in the marine atmosphere of the German EEZ in the period of August to October 2010	233
Figure 5.122: Vertical gradients of the atmospheric abundances of perfluorinated compounds in the marine atmosphere of the German EEZ in the period of August to October 2010	234
Figure 9.1. Insertion of the sampling material in respective sampler holders; (A) Adsorber cartridge; (B) Glass fibre filter; (C) PUF disk with stainless steel ring	258
A4 Figure 1: Air mass backward trajectories of the air sample AL 1	344
A4 Figure 2: Air mass backward trajectories of the air sample AL 2	345
A4 Figure 3: Air mass backward trajectories of the air sample AL 3	346
A4 Figure 4: Air mass backward trajectories of the air sample AL 4	347
A4 Figure 5: Air mass backward trajectories of the air sample AL 5	348
A4 Figure 6: Air mass backward trajectories of the air sample AL 6	349
A4 Figure 7: Air mass backward trajectories of the air sample AL 7	350
A4 Figure 8: Air mass backward trajectories of the air sample AL 8	351
A4 Figure 9: Air mass backward trajectories of the air sample AL 9	352
A4 Figure 10: Air mass backward trajectories of the air sample AL 10	353
A4 Figure 11: Air mass backward trajectories of the air sample 09AT 2	354
A4 Figure 12: Air mass backward trajectories of the air sample 09AT 3	355
A4 Figure 13: Air mass backward trajectories of the air sample 09AT 4	356
A4 Figure 14: Air mass backward trajectories of the air sample 09AT 5	357
A4 Figure 15: Air mass backward trajectories of the air sample 09AT 7	358
A4 Figure 16: Air mass backward trajectories of the air sample 09AT 8	359
A4 Figure 17: Air mass backward trajectories of the air sample 09AT 9	360

A4 Figure 18: Air mass backward trajectories of the air sample 09AT 11	361
A4 Figure 19: Air mass backward trajectories of the air sample 09AT 12	362
A4 Figure 20: Air mass backward trajectories of the air sample PE 1	363
A4 Figure 21: Air mass backward trajectories of the air sample PE 3	364
A4 Figure 22: Air mass backward trajectories of the air sample PE 4	365
A4 Figure 23: Air mass backward trajectories of the air sample PE 6.....	366
A4 Figure 24: Air mass backward trajectories of the air sample PE 7	367
A4 Figure 25: Air mass backward trajectories of the air sample PE 8	368
A4 Figure 26: Air mass backward trajectories of the air sample PE 9	369
A4 Figure 27: Air mass backward trajectories of the air sample PE 10	370
A4 Figure 28: Air mass backward trajectories of the air sample PE 11	371
A4 Figure 29: Air mass backward trajectories of the air sample PE 15	372
A4 Figure 30: Air mass backward trajectories of the air sample PE 16	373
A4 Figure 31: Air mass backward trajectories of the air sample PE 17	374
A4 Figure 32: Air mass backward trajectories of the air sample PE 18	375
A4 Figure 33: Air mass backward trajectories of the air sample 10AT 1	376
A4 Figure 34: Air mass backward trajectories of the air sample 10AT 2	377
A4 Figure 35: Air mass backward trajectories of the air sample 10AT 3	378
A4 Figure 36: Air mass backward trajectories of the air sample 10AT 4	379
A4 Figure 37: Air mass backward trajectories of the air sample 10AT 5	380
A4 Figure 38: Air mass backward trajectories of the air sample 10AT 6	381
A4 Figure 39: Air mass backward trajectories of the air sample 10AT 7	382
A5 Figure 1: Observational network of BSH water sampling sites in the German EEZ	383
A5 Figure 2: Observational network of BSH water sampling sites in the North Sea	384
A5 Figure 3: Observational network of water sampling sites in the Baltic Sea for the research cruise in Feb. 2005	384
A5 Figure 4: Observational network of water sampling sites in the Baltic Sea for the research cruise in Jun./Jul. 2008	385
A5 Figure 5: Observational network of water sampling sites in the Baltic Sea for the research cruise in Jul. 2009	385

List of tables

Table 2.1: Predicted deposition velocities (cm/s) of (NH ₄) ₂ SO ₄ aerosol particles with a mass median diameter of 0.56 μm at different wind speeds v_D (m/s) and relative humidity (r.h.) above natural waters	23
Table 3.1: Active air samples collected during the research cruise in the Baltic Sea in April 2009	33
Table 3.2: Active air samples collected during the research cruise in the German EEZ in May/June 2009	35
Table 3.3: Active air samples collected during the research cruise in the North Sea in August/September 2009	36
Table 3.4: Active air samples collected during the research cruise in the German EEZ in May 2010;	37
Table 3.5: Active air samples collected in Sülldorf/Hamburg in November/December 2010	38
Table 3.6: Passive air samples collected during sea cruises	39
Table 3.7: Passive air samples collected in Sülldorf/Hamburg	40
Table 3.8: Passive air samples collected in Tinnum/Sylt	40
Table 3.9: Passive air samples collected at the FINO research stations	41
Table 3.10: Target compounds	42
Table 4.1: Reproducibility (precision) of air sampling data based on all analytes exceeding LOQ in all samples collected simultaneously.....	60
Table 4.2: Air sample preparation sequences	68
Table 4.3: Field blanks	70
Table 4.4: Laboratory blanks	73
Table 4.5: Recovery of target compounds in spike controls.....	75
Table 4.6: Limits of quantification in ng/mL extract applied to the air sample preparation sequences 1-5	81
Table 4.7: Limits of detection in ng/mL extract applied to the air sample preparation sequences 1-5	83
Table 5.1: Hexachlorobenzene (HCB) and pentachlorobenzene (QCB) concentrations in the marine atmosphere	106
Table 5.2: Comparison of atmospheric concentrations of DDTTP and DDEPP determined at sea and land based sampling sites.....	130
Table 5.3: Comparison of the atmospheric bulk concentrations of PCBs (in pg/m ³) determined at sea and land based sampling sites.....	140
Table 5.4: Occurrence and concentrations (pg/m ³) of triazine herbicides in the atmosphere above the German EEZ, the wider North Sea, the Baltic Sea and Sülldorf/Hamburg	147
Table 5.5: Concentration ranges of the triazine herbicides in the surface water of the German EEZ, the wider North Sea and the Baltic Sea	152

Table 5.6: Occurrence and bulk concentrations (pg/m ³) of organophosphate insecticides in the atmosphere above the German EEZ, North Sea, Baltic Sea and Sülldorf/Hamburg	160
Table 5.7: Atmospheric concentrations of diuron and fenuron in Sülldorf/Hamburg in December 2010 determined during the side-by-side air sampling experiments	169
Table 5.8: Occurrence and bulk concentrations (pg/m ³) of organophosphorus and brominated flame retardants in the atmosphere above the German EEZ, the wider North Sea, the Baltic Sea and Sülldorf/Hamburg	218
Table 5.9: Occurrence and bulk concentrations of carbamazepine, primidone and oxazepam and concentrations of clofibric acid, diclofenac and naproxen in the particle associated mass fraction of the atmosphere of the German EEZ, the wider North Sea, the Baltic Sea and of Sülldorf/Hamburg	221
Table 5.10: Recovery (%) of PRCs in the PUF disk passive air samples exposed at the FINO research platforms	229
Table 5.11: Scavenging ratios	236
Table 5.12: Annual wet deposition fluxes of organic pollutants to the coastal sampling sites Tinnum and Zingst (calculated from the data of the UBA, annex 8) as well as estimated wet deposition fluxes to the surface seawater of the German EEZ, the wider North Sea and the Baltic Sea.....	237
Table 5.13: Sea surface water concentrations calculated from the annual wet deposition fluxes and real water concentrations observed in 5-6 m of depth	238
Table 5.14: Estimations of the dry particulate deposition fluxes to the sea surface water of the German EEZ and the North Sea	239
Table 5.15: Estimations of the annual dry particle deposition fluxes of PFCs and organophosphorus flame retardants to the sea surface water of the German EEZ and the North Sea	240
Table 5.16: Dry particulate deposition fluxes (F_{DD}), deposition velocities (v_D) and concentrations in the particulate mass fraction in the atmosphere (c_p) reported in the literature	240
Table 9.1: List of solvents	248
Table 9.2: List of chemicals	248
Table 9.3: Further materials	253
Table 9.4: PRC-LC (methanol solution)	255
Table 9.5: PRC-GC (hexane solution)	255
Table 9.6: IS-LC (methanol solution)	255
Table 9.7: IS-GC (hexane solution)	256
Table 9.8: Spike-LC (methanol solution)	256
Table 9.9: Spike-GC (hexane solution)	256
Table 9.10: Büchi evaporation parameters and time-pressure gradient for the evaporation of 350 mL acetone/hexane/methanol (75/20/5, v/v/v) solvent mixture at rack 4	259
Table 9.11: Büchi evaporation parameters and time-pressure gradient for the evaporation of 100 mL acetone/hexane/methanol (75/20/5, v/v/v) solvent mixture at rack 12	260
Table 9.12: Büchi evaporation parameters and time-pressure gradient for the evaporation of 40 mL hexane at rack 4	260

Table 9.13: Büchi evaporation parameters and time-pressure gradient for the evaporation of 40 mL methanol at rack 4	260
Table 9.14: Büchi evaporation parameters and time-pressure gradient for the evaporation of 40 mL hexane at rack 12	260
Table 9.15: Büchi evaporation parameters and time-pressure gradient for the evaporation of 40 mL methanol at rack 12	261
Table 9.16: Amounts of target analytes, performance reference compounds and internal standard added to laboratory blanks and spike control samples.....	262
Table 9.17: Composition of the single-point calibration standard LC-Cal (methanol solution) ...	263
Table 9.18: Composition of the single-point calibration standard GC-Cal (hexane solution)	263
Table 9.19: GC gradient program (GC-MS method)	264
Table 9.20: MS parameters (MS method type: segmented SIM)	264
Table 9.21: GC gradient program (GC-MS/MS method)	265
Table 9.22: MS parameters (MS method type: segmented MRM).....	265
Table 9.23: HPLC gradient program	266
Table 9.24: Common scheduled MRM parameters in positive (p) and negative (n) ESI mode	266
Table 9.25: Scheduled MRM mass transition parameters in positive (p) and negative (n) ESI mode	266
Table 9.26: GC-MS analytes and their corresponding internal standards	267
Table 9.27: GC-MS/MS analytes and their corresponding internal standards	268
Table 9.28: HPLC-MS/MS analytes and their corresponding internal standards	268
A1 Table 1: Atmospheric concentrations of target compounds in pg/m ³ determined by high-volume active air sampling.....	283
A1 Table 2: Atmospheric concentrations of target compounds in ng/PUF disk determined by passive air sampling.....	297
A2 Table 1: Field blanks of Glass Fibre Filters (GFFs)	304
A2 Table 2: Field blanks of PUF plug adsorber cartridges	307
A2 Table 3: Field blanks of PUF/XAD-2/PUF adsorber cartridges	308
A2 Table 4: Field blanks of PUF disk passive air samplers	311
A2 Table 5: Laboratory blanks – Extraction blanks	318
A2 Table 6: Laboratory blanks – Bottle blanks	320
A2 Table 7: Laboratory blanks – Evaporation blanks	321
A2 Table 8: Laboratory blanks – Clean-up blanks	324
A2 Table 9: Recovery of target compounds in spike control samples	326
A2 Table 10: Soxhlet extraction efficiency – Peak areas of labeled analytes (IS and PRCs) in the extract of the first sample preparation and in the extract of the second sample preparation ..	334
A2 Table 11: Efficiency of the GFF extraction – Peak areas of labeled analytes (IS and PRCs) in the extract of the first sample preparation and in the extract of the second sample preparation	336

A3 Table 1: Reproducibility of the sample preparation for GFFs; Recoveries (%) of Performance Reference Compounds spiked prior extraction to the environmental samples	339
A3 Table 2: Reproducibility of the sample preparation for PUF plug adsorber cartridges; Recoveries (%) of Performance Reference Compounds spiked prior extraction to the environmental samples	339
A3 Table 3: Reproducibility of the sample preparation for PUF/XAD-2/PUF adsorber cartridges; Recoveries (%) of Performance Reference Compounds spiked prior extraction to the environmental samples	340
A3 Table 4: Reproducibility of the sample preparation for PUF disks; Recoveries (%) of Performance Reference Compounds spiked prior extraction to the environmental samples.....	340
A3 Table 5: Desorption from PUF plug adsorber cartridges; Recoveries (%) of Performance Reference Compounds spiked prior to air sampling.....	340
A3 Table 6: Desorption from PUF/XAD-2/PUF adsorber cartridges; Recoveries (%) of Performance Reference Compounds spiked prior to air sampling	341
A3 Table 7: Stability of frozen PUF/XAD-2/PUF adsorber cartridges; Recoveries (%) of Performance Reference Compounds in field blanks spiked prior to storage	342
A3 Table 8: Stability of frozen PUF disks; Recoveries (%) of Performance Reference Compounds in field blanks spiked prior to storage	342
A3 Table 9: PRC recoveries (%) in the PUF disk passive air samples spiked prior to exposure at Tinnun/Sylt (28 days), Sülldorf/Hamburg (28 days) and at the FINO platforms	343
A5 Table 1: Surface water concentrations (5 m, A5 figure 1) in ng/L determined during the research cruise in the German EEZ in May/Jun. 2009; with respective LOQs, PSU= Practical Salinity units; SPM = Suspended particulate matter in mg/L	386
A5 Table 2: Surface water concentrations (5 m, A5 figure 1) in ng/L determined during the research cruise in the German EEZ in May 2010; with respective LOQs, PSU = Practical Salinity units; SPM = Suspended particulate matter in mg/L	390
A5 Table 3: Surface water concentrations (5 m, A5 figure 2) in ng/L determined during the research cruise in the North Sea in Aug./Sep. 2009; with respective LOQs, PSU = Practical Salinity units; SPM = Suspended particulate matter in mg/L	394
A5 Table 4: Surface water concentrations (5 m, A5 figure 3) in ng/L of the Baltic Sea in Feb. 2005; data >LOQs, PSU = Practical Salinity units; SPM = Suspended particulate matter in mg/L	400
A5 Table 5: Surface water concentrations (6 m, A5 figure 4) in ng/L of the Baltic Sea in Jun./Jul. 2008; with respective LOQs, PSU = Practical Salinity units; SPM = Suspended particulate matter in mg/L	400
A5 Table 6: Surface water concentrations (5 m, A5 figure 5) in ng/L of the Baltic Sea in Jul. 2009, data >LOQs, PSU = Practical Salinity units; SPM = Suspended particulate matter in mg/L	403
A5 Table 7: Surface water concentrations (5 m, A5 figure 5) in ng/L of the German EEZ in September 2009; PSU = Practical Salinity units; SPM = Suspended particulate matter in mg/L	403
A5 Table 8: Surface water concentrations (5 m, A5 figure 5) in ng/L of the German EEZ in November 2009; PSU = Practical Salinity units; SPM = Suspended particulate matter in mg/L	406

A6 Table 1: Concentrations (ng/g) of target analytes in suspended particulate matter collected at four water sampling sites (refer to A4 figure 1) by centrifugation of surface water; TOC = Concentration (mg/g) of total organic carbon in the suspended particulate matter	409
A7 Table 1: Henry's law constants applied for the calculation of the net flux of diffusive gas exchange of target analytes between the surface water and the atmosphere	410
A8 Table 1: Concentrations (ng/L) of organic compounds in monthly rain water samples collected in Zingst in 2009 and 2010, respectively	411
A8 Table 2: Concentrations (ng/L) of organic compounds in monthly rain water samples collected in Tinum/Sylt in 2009 and 2010, respectively	412

List of abbreviations

AAS	Active air sampling
ABL	Atmospheric boundary layer
ACE	Acenaphthene
ACE-D ₁₀	Acenaphthene-D ₁₀
ACY	Acenaphthylene
AL	Research ship Alkor
ALD	Aldrin
AMETRYN	Ametryn
ANT	Anthracene
ANT-D ₁₀	Anthracene-D ₁₀
ARGE-BLMP	Arbeitsgemeinschaft Bund-Länder-Messprogramm
ARL	Air resources laboratory
ASE	Accelerated Soxhlet extraction
AT	Research ship Atair
ATRAZ	Atrazine
ATRAZ-D ₅	Atrazine-D ₅
AZINPH-E	Azinphos-ethyl
AZINPH-M	Azinphos-methyl
AZINPH-M-D ₆	Azinphos-methyl-D ₆
B.S.	Baltic Sea
BAA	Benzo[<i>a</i>]anthracene
BAA-D ₁₂	Benzo[<i>a</i>]anthracene-D ₁₂
BAP	Benzo[<i>a</i>]pyrene
BBF	Benzo[<i>b</i>]fluoranthene
BENTAZ	Bentazone
BEP-D ₁₂	Benzo[<i>e</i>]pyrene-D ₁₂
BGHIP	Benzo[<i>g,h,i</i>]perylene
BGHIP-D ₁₂	Benzo[<i>g,h,i</i>]perylene-D ₁₂
BLMP	Bund-Länder-Messprogramm
BSH	Federal Maritime and Hydrographic Agency of Germany
<i>C</i>	Cunningham slip correction factor
<i>c_a</i>	Concentration of a given compound in air (pg/m ³)
CARBAMAZ	Carbamazepine
CARBEND	Carbendazim
CB104	Polychlorinated Biphenyl 104

CB145	Polychlorinated Biphenyl 145
CB204	Polychlorinated Biphenyl 204
CB30	Polychlorinated Biphenyl 30
CB138	Polychlorinated Biphenyl 138
CB153	Polychlorinated Biphenyl 153
CB153- ¹³ C ₁₂	Polychlorinated Biphenyl 153 – ¹³ C ₁₂
CB185	Polychlorinated Biphenyl 185
CB28	Polychlorinated Biphenyl 28
CB52	Polychlorinated Biphenyl 52
CB52- ¹³ C ₁₂	Polychlorinated Biphenyl 52 – ¹³ C ₁₂
CBzs	Chlorinated benzenes
CCN	Cloud condensation nuclei
CFC	Chlorofluorocarbon
CHLORFENV	Chlorfenvinphos
CHLORTUR	Chlorotoluron
CHR	Chrysene
CHRTR	Sum parameter of chrysene and triphenylene
CLOFIBRS	Clofibric acid
<i>c_{Prec}</i>	Concentration of an organic compound in precipitation (ng/L)
<i>c_r</i>	Concentration of a given compound in rain water (ng/L)
CUP	Currently used pesticide
<i>D</i>	Diffusion coefficient
d(ae) ₅₀	Aerodynamic diameter of particulate matter segregated with 50% efficiency (µm)
DBAHA	Dibenzo[<i>a,h</i>]anthracene
DDDPP	<i>p,p'</i> -Dichlorodiphenyldichloroethane
DDEPP	<i>p,p'</i> -Dichlorodiphenyldichloroethylene
DDT	1,1,1-trichloro-2,2-di(4-chlorophenyl)ethane
DDTOP	<i>o,p'</i> -Dichlorodiphenyltrichloroethane
DDTPP	<i>p,p'</i> -Dichlorodiphenyltrichloroethane
DDTPP-D ₈	<i>p,p'</i> -Dichlorodiphenyltrichloroethane-D ₈
DEATRAZ	Desethylatrazine
DEATRAZ-D ₆	Desethylatrazine-D ₆
DHI	German Hydrographic Institute
DIAZINON	Diazinone
DICHLPR	Dichlorprop
DICLOF	Diclofenac

DIELD	Dieldrin
DIMETH	Dimethoate
DIURON	Diuron
DIURON-D ₆	Diuron-D ₆
d_j	Nozzle diameter (mm)
D_s	Sampling duration (h)
DWD	Deutscher Wetterdienst
EEZ	Exclusive economic zone
EMEP	European Monitoring and Evaluation Programme
END	Endrin
EVA	Ethyl-vinyl-acetate
f	Fugacity
f_A	Fugacity of a given compound in air
F_{AW}	Flux of diffusive air-water exchange (ng/(m ² d))
F_{DD}	Flux of dry particulate deposition (ng/(m ² d))
FENUR	Fenuron
FL	Fluorene
FLU	Fluoranthene
FLU-D ₁₀	Fluoranthene-D ₁₀
FR	Fugacity ratio
f_w	Fugacity of a given compound in water
F_{Wet}	Flux of wet deposition (ng/(m ² d))
G. EEZ	German exclusive economic zone of the North Sea / German Bight
GAPS	Global atmospheric passive sampling study
GC	Gas chromatography
GDAS	Global data assimilation system
GFF	Glass fibre filter
QFF	Quartz fibre filter
H	Henry's law constant (Pa m ³ / mol)
H'	Dimensionless Henry's law constant
HBCDA	α -Hexabromocyclododecane
HBCDA-D ₁₈	α -Hexabromocyclododecane-D ₁₈
HBCDB	β -Hexabromocyclododecane
HBCDG	γ -Hexabromocyclododecane
HBCDBG	Sum parameter of HBCDB and HBCDG
HCB	Hexachlorobenzene
HCB- ¹³ C ₆	Hexachlorobenzene- ¹³ C ₆

HCFC	Hydrochlorofluorocarbon
HCH	Hexachlorocyclohexane
HCHA	α -Hexachlorocyclohexane
HCHB	β -Hexachlorocyclohexane
HCHD	δ -Hexachlorocyclohexane
HCHE	ε -Hexachlorocyclohexane
HCHG	γ -Hexachlorocyclohexane / Lindane
HCHG- $^{13}\text{C}_6\text{D}_6$	Lindane- $^{13}\text{C}_6\text{D}_6$
HELCOM	Baltic Marine Environment Protection Commission / Helsinki Commission
HEXAZIN	Hexazinone
HVS	High-volume sampler
HZG	Helmholtz-Zentrum Geesthacht
I123P	Indeno[1,2,3- <i>cd</i>]pyrene
IfM	Institute of marine science
IOW	Institute for Baltic Sea Research
IRGAROL	Irgarol
ISOD	Isodrin
ISOPRUR	Isoproturon
k_A	Pollutant mass transfer rate in the air (m/d)
K_{A, H_2O}	Mass transfer coefficient of H_2O in the air
k_{AW}	Air-water mass transfer rate (m/d)
K_{AW}	Air-water partition coefficient
K_{OA}	Octanol-air partition coefficient
K_{OW}	Octanol-water partition coefficient
k_W	Pollutant mass transfer rate in the water (m/d)
K_{W, CO_2}	Mass transfer coefficient of CO_2 in the water
LC	Liquid chromatography
LDPE	Low density polyethylene
LINUR	Linuron
LLE	Liquid-liquid-extraction
LOD	Limit of detection
LOQ_{Blank}	Limit of quantification calculated from field blanks
$\text{LOQ}_{S/N}$	Limit of quantification calculated from the signal to noise ratio
LVS	Low volume sampler
MAE	Microwave assisted extraction
MALATH	Malathion
MALATH-D ₁₀	Malathion-D ₁₀

MCPA	(4-Chloro-2-methylphenoxy)ethanoic acid
MCPA-D ₃	(4-Chloro-2-methylphenoxy)ethanoic acid-D ₃
MECOPR	Mecoprop
MECOPR-D ₃	Mecoprop-D ₃
METAZCHL	Metazachlor
METHABZT	Methabenzthiazuron
METOLA	Metolachlor
MMD	Mass median diameter
MS	Mass spectrometry / Mass spectrometer
NAPROX	Naproxen
NCEP	National centers for environmental prediction
N_i	Number of nozzles
NOAA	National oceanic and atmospheric administration
N_t	Total number of maritime aerosol particles
OC	Organic carbon
OCP	Organochlorine pesticide
OM	Organic matter
OSPAR	Convention for the protection of the marine environment of the North-East Atlantic
OXAZEP	Oxazepam
P di	PUF disk
P pl	PUF plug adsorber cartridge
p	Air pressure (hPa)
P	Total precipitation flux (L/(m ² d))
PAH	Polycyclic aromatic hydrocarbon
PAS	Passive air sampler / Passive air sampling
PBDE	Polybrominated diphenyl ethers
PBT	Persistent bioaccumulative and toxic chemicals
PCB	Polychlorinated biphenyl
PCDD	Polychlorinated dibenzodioxin
PCDF	Polychlorinated dibenzofuran
PE	Research ship Pelagia
PENDIMETH	Pendimethalin
PER-D ₁₂	Perylene-D ₁₂
PFBS	Perfluorobutanesulfonic acid
PFC	Perfluorinated compounds
PFCA	Perfluoroalkyl carboxylate

PFDEA	Perfluorodecanoic acid
PFHPA	Perfluoroheptanoic acid
PFHXA	Perfluorohexanoic acid
PFHXS	Perfluorohexanesulfonic acid
PFHXS- ¹⁸ O ₂	Perfluorohexanesulfonic acid - ¹⁸ O ₂
PFNOA	Perfluorononanoic acid
PFOA	Perfluorooctanoic acid
PFOA- ¹³ C ₂	Perfluorooctanoic acid - ¹³ C ₂
PFOS	Perfluorooctanesulfonic acid
PFOS- ¹³ C ₄	Perfluorooctanesulfonic acid - ¹³ C ₄
PFOSA	Perfluorooctanesulfonamide
PFSA	Perfluoroalkyl sulfonate
PHEN	Phenanthrene
PHEN-D ₁₀	Phenanthrene-D ₁₀
PIRIMIC	Pirimicarb
PLE	Automated pressurized liquid extraction
PM	Particulate matter
POG	Polymer coated glass
POP	Persistent organic pollutant
PRC	Performance reference compound
PRIMID	Primidone
PROMETR	Prometryn
PROMETR-D ₆	Prometryn-D ₆
PROPAZ	Propazin
PSU	Practical salinity units
PTFE	Polytetrafluoroethylene
PTS	Persistent toxic substances
PUF	Polyurethane foam
PVDF	Polyvinylidene fluoride
PXP	PUF/XAD-2/PUF adsorber cartridge / sandwich cartridge
PYR	Pyrene
QCB	Pentachlorobenzene
<i>R</i>	Ideal gas constant (8.314 Pa m ³ /(mol K))
<i>r.h.</i>	Relative humidity (%)
<i>Sc</i>	Schmidt number, dimensionless
SCCPs	Short-chain chloroparaffins
SIMAZ	Simazine

SIMAZ-D ₁₀	Simazine-D ₁₀
SIP	Sorbent-impregnated polyurethane foam
SPM	Suspended particulate matter
SPMD	Semi-permeable membrane device
Stk_{50}	Dimensionless Stokes number
SVOC	Semi-volatile organic compound
T	Air temperature (°C)
t	Precipitation sampling time (d)
T_A	Absolute air temperature (K)
TBEP	Tris(2-butoxy-ethyl)phosphate
TBP	Tributyl phosphate
TERBAZ	Terbutylazine
TERBAZ-D ₅	Terbutylazine-D ₅
TERBUTR	Terbutryn
TPP	Triphenyl phosphate
TR	Triphenylene
TRIFLU	Trifluralin
TRIFLU-D ₁₄	Trifluralin-D ₁₄
TWA	Time-weighted averaged concentration
u	wind velocity (m/s)
U_{10}	Wind speed at 10 m height
UBA	Federal Environmental Agency
UFP	Ultrafine particles
UNEP	United nations environment programme
V	Volume collected by the wet deposition sampler (L)
V_F	Air volume flow (m ³ /s)
V_p	Volume of a single maritime aerosol particle (m ³)
V_t	Total volume of maritime aerosol particles (m ³)
W_t	Total scavenging ratio
XAD-2	A hydrophobic cross-linked polystyrene copolymer resin
Z	Fugacity capacity
Z_A	Fugacity capacity of air
Z_W	Fugacity capacity of water
a	Sampling area of the wet deposition collector (m ²)
η	Dynamic viscosity (kg/(m s))
ρ_p	Standard density of idealised spherical particles (kg/m ³)
24D	(2,4-Dichlorophenoxy)ethanoic acid

1. Introduction

1.1 Context

The monitoring and assessment of the environmental condition of the North Sea and the Baltic Sea was initiated in Germany in the 1970s. 1980 a common monitoring program, named “Bund-Länder-Messprogramm” (BLMP), for the North Sea was arranged between the German federation and the coastal federal states of Germany.

During the DDR era the Baltic Sea was monitored by the German Hydrographic Institute (DHI, Hamburg), by the institute of marine science at the University of Kiel, by the Leibniz Institute for Baltic Sea Research in Warnemünde (IfM) and by the “Wasserwirtschaftsdirektion Küste” in Stralsund. Since the German reunification in 1990 the monitoring of the Baltic Sea has been divided between the Federal Maritime and Hydrographic Agency of Germany (BSH) and the responsible agencies of the coastal federal states Mecklenburg-Vorpommern, Schleswig-Holstein and the Institute for Baltic Sea Research (IOW) in Warnemünde.

In April 1997 a consortium, named “Arbeitsgemeinschaft Bund-Länder-Messprogramm” (ARGE-BLMP), was founded including the responsible resorts of the German federation and the coastal federal states Hamburg, Mecklenburg-Vorpommern, Schleswig-Holstein and Lower Saxony for a joint monitoring of the North Sea and the Baltic Sea. The intention of this arrangement is to improve the coordination of several monitoring and assessment programmes. In addition, actual studies are accommodated to national and international agreements and regulations, like the international agreement for the protection of the marine environment of the Baltic Sea (HELCOM-Helsinki-Commission) and the North-East-Atlantic (OSPAR).^[1-3]

Today several annual monitoring cruises in the North Sea and the Baltic Sea aim to investigate a variety of important physical, biological and chemical parameters, the occurrence and distribution of organic contaminants in sea surface water, among others. As a result of the extended observational network the riverine input of organic contaminants to the sea is well investigated.^[1] By contrast, the atmospheric deposition, a further important and effective input pathway for several organic contaminants, is less examined so far. Organic compounds may undergo long-range transport in the atmosphere enabling the deposition from distant sources within and beyond Europe. For this reason knowledge about atmospheric concentrations and pathways of organic contaminants is essential for the establishment of effective national and international environmental regulations and politics.^[4] Therefore, systematic field studies, investigating the atmospheric concentrations, spatial distribution and deposition of organic contaminants at sea are of great importance for the extension of the current state of knowledge and for the evaluation of model simulations.^[5-8]

1.2 State of the art

In 1995 the Governing Council of the United Nations Environment Programme (UNEP) negotiated the Stockholm Convention in order to reduce the release of persistent organic pollutants (POPs) to the environment. POPs are hardly degradable in the environment and accumulate along the food chain causing possible health hazards to humans and wildlife. Today POPs are globally distributed. Enhanced concentrations have been detected even in remote regions like the Arctic, where they have never been used. ^[9] During the first period, twelve organic compounds (“dirty dozen”) have been subject to the convention, namely aldrin, chlordane, 1,1,1-trichloro-2,2-di(4-chlorophenyl)ethane (DDT), dieldrin, endrin, heptachlor, hexachlorobenzene (HCB), polychlorinated biphenyls (PCBs), polychlorinated dibenzodioxins (PCDDs) and polychlorinated dibenzofurans (PCDFs). In May 2009 nine additional POPs were incorporated in the convention, i.e., α -hexachlorocyclohexane, β -hexachlorocyclohexane, lindane, chlordecone, hexabromobiphenyl, hexabromodiphenyl ether and heptabromodiphenyl ether, pentachlorobenzene, perfluorooctane sulfonic acid and perfluorooctane sulfonyl fluoride, tetrabromodiphenyl ether and pentabromodiphenyl ether. Endosulfan was classified as 22nd POP in April 2011. Moreover, a further category named persistent bioaccumulative and toxic (PBT) chemicals is defined by UNEP, including the POPs as an integral part. The PBT group additionally contains among others trace metals and organo-metal compounds as well as further organic compounds, e.g., perfluorooctanoic acid and polycyclic musks, which may be prospective POP candidates. In order to verify the effectiveness of the Stockholm Convention, comprehensive monitoring data of all environmental compartments are required. Especially, the atmosphere is expected to be an efficient indicator of decreasing POP releases, because atmospheric concentrations change rapidly according to variations in primary sources. ^[10-13] Europe, USA, Canada and the Russian Federation additionally ratified the POP protocol of the Convention on Long-Range Transboundary Air Pollution originally negotiated in Geneva 1979. It was entered into force in 2003 and comprises a more extensive spectrum of organic compounds than the “dirty dozen” of the Stockholm convention, e.g., additionally including hexachlorocyclohexanes (HCHs) and polycyclic aromatic hydrocarbons (PAHs). In this context the European Monitoring and Evaluation Programme (EMEP) runs an air monitoring network throughout Europe. Currently the network encloses more than 100 sampling sites, whereof 20 sampling sites distributed in 14 countries are measuring POPs in the atmosphere. Sampling sites on sea are not established. ^[4, 6, 14]

A variety of air sampling methods has been developed for monitoring atmospheric concentrations of organic contaminants in ambient air. Principally they can be grouped in active air sampling (AAS) techniques and passive air sampling (PAS) techniques.

High-volume Samplers (HVSs) and Low Volume Samplers (LVSs) are the most frequently used active air sampling systems. They are based on an active pumping of ambient air through a filter followed by a solid adsorbent providing a differentiation between gaseous mass fraction and particle associated mass fraction of organic compounds in the atmosphere. Glass fibre filters (GFFs) and quartz fibre filters (QFFs) are applied as separator of particle associated and gaseous mass fraction. Organic contaminants present in the gaseous mass fraction may be collected hereafter by different adsorber materials, such as XAD-2, a hydrophobic cross-linked polystyrene copolymer resin and polyurethane foam (PUF), the same material as used for furniture upholstery and mattresses. XAD-2 is additionally deployed in combination with PUF cylinders in order to increase the sampling efficiency and in combination with a further polymer resin named Tenax TA. [15] Extensively investigated organic compounds are the organochlorine pesticides (OCPs) and the polycyclic aromatic hydrocarbons. Active air sampling methods reveal several advantages for the investigation of both contaminant classes. In the case of the organochlorine pesticides active air sampling provides a reliable quantification of the trace pollutants in ambient air due to the possibility of increased sample volumes and an accurate air volume measurement. PAHs undergo gas-particle partitioning in the atmosphere. Due to the separation between gaseous and particle bound mass fraction, this phenomenon is verifiable using active air sampling techniques. [16-18] A standard sample volume for the measurement of organic compounds in the atmosphere is not defined, because it depends on the purpose of sampling, the atmospheric concentrations of target analytes and the detection limits of analytical methods. Diffusion denuder systems proved to be an alternative sampling tool to phase-segregated active high-volume sampling. These systems were applied to the quantification of semi-volatile organic compounds (SVOCs) in numerous studies. [19-21]

Passive air sampling is based on the diffusion of target compounds to an accumulating medium. The advantages of passive air samplers are the inexpensive sampler design and the operation without the need of electrical power, enabling the deployment at numerous sampling sites even in remote regions. Hence, passive air sampling is a useful and attractive tool to complement active air sampling data of at least gaseous compounds and to investigate the global distribution of organic compounds as already carried out in the Global Atmospheric Passive Sampling (GAPS) study. [22, 23] Passive air samplers record time-weighted averaged concentrations (TWA), because of required sampling durations ranging from weeks to months. Therefore, daily fluctuations in air concentrations need to be documented by active air sampling methods. [24] A variety of passive air sampler designs currently exists. The most commonly used adsorbent for passive air sampling is the PUF disk. [15] Further adsorber materials are XAD-2, sorbent-impregnated polyurethane foam (SIP) disks coated with XAD powder, semi-permeable membrane devices (SPMDs) consisting of

low density polyethylene (LDPE) bags filled with triolein and polymer coated glass (POG) covered with ethyl-vinyl acetate (EVA).^[25-28] The accumulating medium is placed in a protection chamber to minimize the effects of environmental impacts like wind speed, rain, sunlight and particle deposition on the diffusion processes. Newest developments may even differentiate between gaseous and particle associated mass fraction, being once only a characteristic feature of active air samplers.^[29]

In order to obtain volumetric air concentrations the sampling rates of passive air sampler systems need to be calibrated for the target compounds. The calibration procedures are based on the characterisation of atmospheric uptake by passive air samplers according to Fick's first law of diffusion and the Whitman two-film approach: When a passive air sampler is deployed in ambient air, the amount of target analytes will increase until equilibrium is established.^[30] Two general methods for passive air sampler calibration are discussed in the literature. One possibility is the calibration with the aid of an active air sampler system (HVS or LVS), by deploying active air samplers and passive air sampling devices simultaneously. The equivalent air volume is calculated by dividing the mass of a compound accumulated on the passive air sampler adsorbent by the concentration in ambient air measured with the active air sampler system. A repetition of this procedure for a duration of several months provides the determination of sampling rates of the targeted compounds by plotting the equivalent air volume versus time. The sampling rate is derived from the slope of the linear portion of the regression curve. It is specific for the wind velocity regime of the calibration period.^[26, 31] A further calibration possibility uses depuration compounds, which are spiked on the PAS adsorber prior to exposure. Depuration compounds may be isotopically labeled or unlabeled organic compounds that exhibit negligible concentrations in air. The uptake of SVOCs from ambient air by the passive air sampling devices is defined to be air-side controlled and follows a first order rate expression. Hence, the rate of uptake of the target compounds from air is the same as the rate of loss of the depuration compounds from the PAS adsorber material.^[32, 33]

Numerous calibration studies are discussed in the literature displaying increased aberrations in their results. However, a common fact is the variability of sampling rates among congeners and compounds possibly ranging from 0.6 m³/d to 24 m³/d.^[23, 34-36] A number of environmental impacts are discussed causing these fluctuations, namely gas particle partitioning, changes in ambient air concentrations, wind speed and the concentration and mass size distribution of particles. It has been established that PUF disk PAS collect even the particle associated mass fraction of target compounds in the atmosphere. Therefore, sampling rates need to be calibrated on the base of the bulk air concentrations of the target compounds. Particle sampling is highly variable and can be

partly calibrated using depuration compounds. It depends primarily on the concentration and size distribution of particles in ambient air. Smaller particles ($< 2 \mu\text{m}$) are assumed to diffuse to the PAS similar to the gaseous compounds and may be calibrated with depuration compounds. By contrast, particles of increased sizes are collected by PAS probably due to sedimentation, impaction and interception processes, which are highly influenced by wind speed, sampler housing and the density of the adsorber material itself.^[31, 37] Gas particle partitioning, especially observed for the PAHs, may prevent the free exchange of the particle associated mass fraction with ambient air thus complicating the prediction of the particle uptake.^[38] Increased wind speeds reduce the thickness of the air-side boundary layer resulting in an increase in the sampling rates.^[39] A combination of changes in wind speed and wind direction may cause the collection of different air masses of passive and active air sampling devices during a simultaneous exposure for calibration studies. An adaption of the sampling rates of the active air sampler to the sampling rates of the passive air sampler renders air masses collected by the active air sampler more representative. For this reason the application of low volume active air sampler systems instead of high-volume active air sampler systems is recommended for an external calibration of passive air sampling devices in an actual literature review and calibration study.^[31] To sum up, the volumetric air concentrations obtained from passive air samplers are semi-quantitative and are not as reliable as active air sampling data. Nevertheless, passive air sampling is a useful methodology especially for long-term field studies in remote regions and is indispensable for a completion of active air sampling results.

Analytical procedures applied to the analyses of the collected air samples in general encompass the steps extraction, clean-up, analysis and quantification. Classical Soxhlet-extraction is the most frequently used method for a quantitative elution of the target compounds from the adsorber materials and filters. It has been adopted in some standardized analytical procedures.^[15, 23, 40, 41] Soxhlet-extraction is a time and solvent consuming technique. In addition long heating periods may cause a transformation of thermally labile analytes during extraction. For this reason some alternative extraction techniques are described in literature, e.g., the automated pressurized liquid extraction (PLE), also known as accelerated solvent extraction (ASE), ultrasonic extraction and microwave assisted extraction (MAE).^[42-46] Typical extraction solvents are dichloromethane, hexane, acetone, petroleum ether, ethyl acetate and cyclohexane. They are used as single solvents or in combination to achieve an optimized polarity for the elution of the target compounds. Extraction solvents of highest polarity like methanol are not found in literature, probably because polar pollutants in the atmosphere are usually not targeted as less abundant and less harmful for humans and wildlife.^[2-4, 15] After extraction and evaporation a clean-up step is executed, in order to minimize matrix effects during analyses and to maintain instrument performance. The most common clean-up materials are normal phases consisting of Florisil (magnesium silicate), silica gel

and aluminium oxide as single sorbents or in combination. Extracts of increased polarity like ethyl acetate extracts undergo a clean-up with a reversed phase C₁₈ silica gel material. ^[15, 40, 41] Finally, the environmental samples are analysed on mass spectrometer (MS) systems, a universal detection method of highest sensitivity. Mass spectrometers may be used in combination with gas-chromatography (GC) and liquid chromatography (LC) separation methods. Organic compounds analysed on a GC-MS instrument need to be volatile and thermally stable, whereas compounds of increased polarity have best performances in LC-MS analyses. Newest developments in the last decades further improved the selectivity and sensitivity of mass spectrometers by the combination of up to three mass analysers in a single system. ^[47] Today GC-MS/MS and LC-MS/MS analyses are the methods of choice for a reliable determination of trace levels of organic compounds in environmental samples.

In recent years, a large variety of organic contaminants in the atmosphere in remote, rural and urban zones nearly globally has been reported from monitoring. In the case of passive air sampler studies, especially PAHs, OCPs, PCBs and polybrominated diphenyl ethers (PBDEs) have been intensively investigated. ^[23, 31, 34, 36, 48] In active air sampler studies a wider spectrum of organic compounds is targeted, ranging from PAHs and OCPs to currently used pesticides (CUPs) in agriculture and industrial products/byproducts. ^[4, 15, 49, 50] In particular, the levels and distributions of SVOCs in the atmosphere are subject to worldwide monitoring programmes. Their occurrences in the atmosphere are explained in the context of hypotheses on processes determining the global circulation of POPs in the environment, i.e., global fractionation, grasshopper effect and mountain cold trapping (chapter 2.2). In addition, PAH concentrations in air and their distribution between particles and gaseous mass fraction have been examined in the last decades and spark political interest in questions of particulate matter reduction. PAHs are ubiquitously distributed in the atmosphere, because they originate from any kind of combustion processes, causing air concentrations in the ng/m³ range. PAHs, consisting of four or more condensed aromatic rings, occur in higher abundances in the particle associated mass fraction of the atmosphere. During inhalation PAH contaminated particulate matter may be deposited in the pulmonary alveoli, hence posing a human health hazard. For this reason benzo-*a*-pyrene, a five ring aromatic system is used as a criteria pollutant to assess toxicity and mutagenicity. In general, toxicity and mutagenicity are mostly related to PAH transformation products like nitro-PAHs. ^[51-53] Moreover, perfluorinated compounds have been subject of extensive research in recent years. Analogue to the OCP and other POPs they come into public focus due to their global occurrence in wildlife and humans. Although their main transport pathway was anticipated to be the oceanic circulation system, studies investigating atmospheric concentrations are executed hypothesizing the atmosphere as a second principal transport pathway of perfluorinated compounds. Potential precursor compounds like

fluorotelomer alcohols, perfluorinated sulfonamido ethanols and perfluorinated sulfonamides have been examined in those studies due to their volatility. ^[49, 54-56] CUPs are mostly subject to monitoring campaigns in agricultural regions in order to investigate their emission to the atmosphere by spray drift and subsequent volatilisation as well as post-application emissions (volatilisation from crops and leaves, wind erosion) throughout the year. ^[57-59]

1.3 Objectives

This study aims to monitor the occurrence and spatial distribution of organic compounds in the North Sea atmosphere. A variety of polar to non-polar organic contaminants, routinely investigated by the BSH in the North Sea surface water and sediments, are incorporated in this study. The target chemicals comprise the pollutant classes of polycyclic aromatic hydrocarbons, selected polychlorinated biphenyls, organochlorine pesticides, currently used/polar pesticides like triazines, organophosphates, phenylureas, phenoxyalkanoic acids, carbamates, dinitroanilines and chloroacetanilides. Moreover, a selection of perfluorinated compounds, organophosphorus and brominated flame retardants and pharmaceuticals are investigated. In the literature no further study may be found encompassing such a diversified spectrum of organic contaminants measured in the marine atmosphere.

First of all, a technique for the collection of marine air during sea cruises has to be established. For this purpose, high-volume sampling is assumed to be the method of choice due to the need of spatial resolution limiting the sampling durations and because of the analytical limitations related to low volumes of sampled air. ^[49, 55, 60-67] With respect to the utmost probability of extreme weather and working conditions, the high-volume sampler needs to be robust, less error-prone, waterproof and subject to easy handling. Active air sampling campaigns were to be performed on the top deck of research vessels during cruises in the exclusive economic zone (EEZ) of Germany, in the wider North Sea and for comparison in the Baltic Sea. In order to complement active air sampling data PAS studies were to be executed at two different sampling sites. PUF disk passive air samplers were to be installed in Sülldorf/Hamburg, an urban (residential) land based sampling site, and in Tinnum/Sylt, a rural and coastal sampling site. PUF disks had to be changed every 4 weeks in order to monitor seasonal fluctuations of atmospheric pollutant concentrations. In addition, a further installation of PUF disk passive air samplers was planned on the FINO research platforms in the EEZ of Germany. The heights of the mast positioned on these stations range from 80m to 90m, allowing an examination of vertical fluctuations in atmospheric concentrations of organic contaminants.

Secondly, a reliable sample preparation technique for filters, adsorber cartridges and PUF disks had to be developed. Due to limitations concerning the availability of high-volume samplers and sampling materials, the sample preparation technique needs to provide the determination of polar and non-polar organic pollutants from a single environmental sample. Hence, the approved methods described in the literature had to be advanced and improved due to the broad diversity of target compounds investigated in this study. A comprehensive validation of the sampling techniques and sample preparation methods had to be performed. In contrast, GC-MS, GC-MS/MS and LC-MS/MS quantification methods had to be adopted from the routine monitoring procedures of the BSH.

Thirdly, the gas-particle partitioning of organic compounds in air, the comparison of sea and land based measurements, air mass history as well as the passive sampling characteristics had to be established to describe the occurrence and spatial distribution of organic contaminants in the marine atmosphere.

Finally, additional data sets describing the occurrence and distribution of the target compounds in the surface water of the EEZ of Germany, North Sea and Baltic Sea (provided by the BSH and IOW) and in precipitation (provided by the Federal Environmental Agency (UBA)), had to be used for further interpretations of the measurements in air. The direction of gas exchange between atmosphere and sea and the atmospheric deposition trends of organic compounds had to be assessed. Deposition velocities derived from literature as well as precipitation data of coastal sampling sites (provided by the UBA) were used to quantify atmospheric deposition fluxes.

2. Theory

2.1 Occurrence and fate of organic pollutants in the atmosphere

Organic contaminants enter the atmosphere via primary and secondary emissions. In addition to sporadic natural inputs due to wildfires and volcanic activities, the primary emissions of organic pollutants are dominated by anthropogenic sources such as fuel burning, waste deposition in landfills, waste water treatment plants, industry and agriculture. A prominent example concerning the direct input of pesticides into the atmosphere is the spray loss during application. It may range from a few percent to 20-30 % and in special cases even up to 50 % depending on the weather conditions and pesticide formulations. ^[68] In addition, the heating period during winter time essentially contributes to a seasonal increase in atmospheric PAH abundances by several orders of magnitude. Decelerations in photodegradation as well as the less efficient mixing due to a lower mean boundary layer height in winter may further support the seasonal enrichment of PAHs. ^[69] Moreover, several environmentally relevant organic compounds, e.g., polychlorinated biphenyls, perfluorinated compounds and phthalates are integral parts of a variety of industrial products. Hence, the primary sources are numerous and difficult in their traceability.

Additional input pathways of organic contaminants to atmosphere, summarized under the term “secondary emissions” or “post-application emissions”, are based on complex exchange processes between the environmental compartments (figure 2.1). Important mechanisms affecting the secondary input of organic contaminants into the troposphere are the volatilisation from soil, plants and water surfaces, the wind erosion of contaminated soil particles and the sea spray generated above the oceans. The extent and effectiveness of exchange predominantly depends on the physico-chemical properties of the organic pollutants, the meteorological conditions as well as the properties of soil and water bodies. Today the oceans and soils act as natural sinks for a variety of organic pollutants. Due to secondary exchange processes they may be re-emitted from these reservoirs resulting in a continuous contamination of the troposphere.

Once an organic contaminant enters the atmosphere it is dispersed within the atmospheric boundary layer and transported by the wind. SVOCs are capable of undergoing gas-particle partitioning. The distribution among both phases affects the residence times of organic compounds in the atmosphere, which in turn determines the long-range transport potential. ^[70] Besides the physico-chemical properties and the atmospheric concentrations of the organic pollutants, the type and concentration of particulate matter, humidity and temperature are the most influencing factors on gas-particle partitioning. ^[71-73]

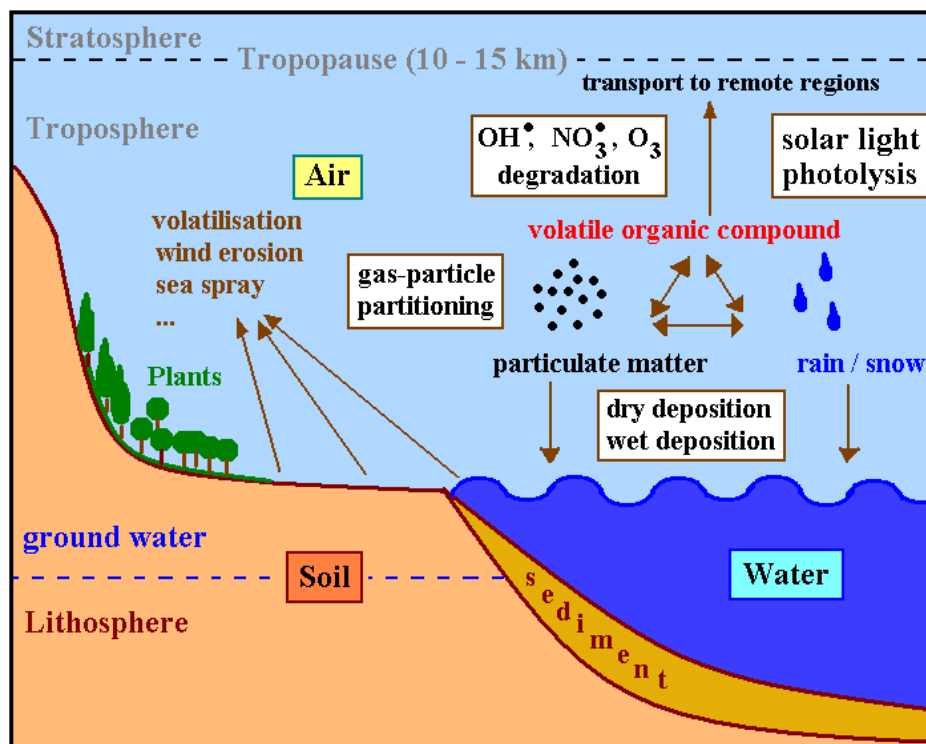


Figure 2.1: Schematic illustration of environmental mechanisms affecting the occurrence and fate of organic pollutants in the atmosphere

Organic contaminants are removed from the atmosphere via diffusive gas exchange with other environmental compartments like water, soil and plants (dry gaseous deposition). Additional removal mechanisms are the dry particulate deposition, wet deposition and chemical transformation. Dry particulate deposition describes a sedimentation and interception process of particulate matter and hence of particle associated organic contaminants from the atmosphere. The effectivity of dry deposition depends on particle size. Typical tropospheric particles, exhibiting sizes in the range of 0.01 μm to 5 μm , have dry deposition lifetimes exceeding one day. Wet deposition describes the “wash out” of pollutants from the atmosphere by hydrometeors, e.g., rain, snow and ice. It combines in-cloud and below-cloud scavenged material. In-cloud scavenging encompasses uptake processes into hydrometeors within clouds, whereas below-cloud scavenging encompasses uptake of gaseous and particulate material by falling hydrometeors (precipitation) during their way to the ground. Wet deposition of particle associated organic contaminants is highly efficient and may result in a complete removal from the atmosphere. In contrast, organic pollutants present in the gas phase are less efficiently scavenged. Hence, organic contaminants preferentially adsorbed to particulate matter exhibit a more efficient deposition from atmosphere predicting limited residence times and long-range transport. Transformation and degradation of organic contaminants in the atmosphere may occur by photolysis in the UV and visible part of the spectrum and chemical reactions with ozone, hydroxyl and nitrate radicals. Highest radical

concentrations and thus accelerated degradation rates are achieved in summer at high altitudes during day time. ^[74-76]

2.2 Atmospheric transport of organic pollutants

Several hypotheses in environmental chemistry have been established and verified by multi-media approaches and field studies elucidating the atmosphere as a major pathway for the long-range transport of organic contaminants, especially for semi-volatile pollutants (revealing saturated vapour pressures in the range of 10^{-6} Pa to 10^{-2} Pa at 20 °C): Persistent semi-volatile organic compounds may undergo a multitude of cycles consisting of (secondary) emission, atmospheric transport and deposition (mechanisms described in chapter 2.1). As a result they are ubiquitously distributed throughout the environmental compartments worldwide. The long-range transport of organic compounds in the atmosphere due to subsequent cycles of emission and deposition is named grasshopper effect or multi-hopping. Several persistent organic compounds accumulate in the environment of the polar regions, because the low ambient temperatures favour their condensation and prevent a further re-emission from water, soil and ice reservoirs. In addition, the gradual decrease in temperature with increasing latitude causes a global fractionation of pollutants according to their volatility (figure 2.2). Analogue to the latitudinal fractionation pollutants may even accumulate with increasing elevation, which is termed mountain cold trapping. ^[9, 77-81]

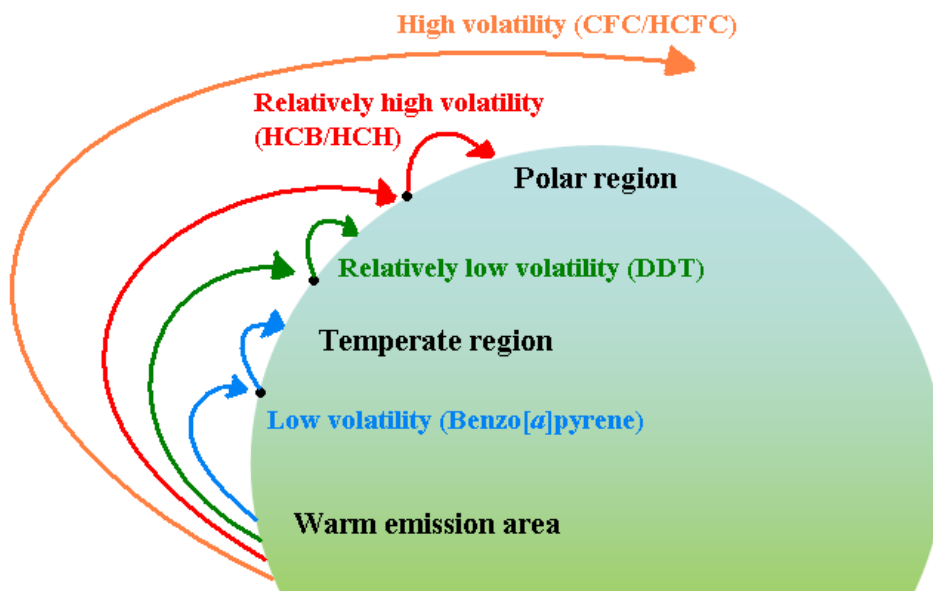


Figure 2.2: Illustration of thermodynamically expected atmospheric transport processes referring to the global fractionation hypothesis and grasshopper-effect; (•) re-emission source; adopted and modified from the AMAP assessment report 2002. ^[9]

More long-range transport mechanisms than exclusively atmospheric distribution are relevant for the global cycling of pollutants. This was shown by studies of environmentally relevant organic

pollutants, varying largely in volatility and water solubility. The transport of contaminated sediment particles and dissolved pollutants by ocean currents and rivers as well as the transport in tissues of migratory animals and thus the transport by the food chain are additional factors influencing global distribution and fate of pollutants.

In the UNEP global report 2003 on the “Regionally Based Assessment of Persistent Toxic Substances (PTS)” organic pollutants are classified according to their long-range transport behaviour into four categories. Although the terminology of the categories relies on the grasshopper effect hypothesis, the multitude of transport mechanisms is considered in the classification grouping organic pollutants as no-hopping, multi-hopping and single-hopping contaminants as well as pollutants without the need of hopping for a global distribution. “No hoppers” like chlorofluorocarbons (CFCs) and hydrochlorofluorocarbons (HCFCs) are organic pollutants of highest volatility remaining in the atmosphere without any significant atmospheric deposition. The term “multi-hopper” refers to chemicals, which are distributed according to the above mentioned grasshopper-effect. Some prominent examples for multi-hopping organic contaminants are PCBs, lighter PCDDs and PCDFs, toxaphene, dieldrin, chlordane and endosulfan. Pollutants of lowest volatility and water solubility predominantly adsorb to suspended particles in the atmosphere and water and are carried with them until sedimentation. Once removed from the atmosphere and water currents, a further transport of those pollutants may only occur due to a resuspension of the contaminated particles, e.g., during storm events and floods. The limited remobilisation possibilities of organic chemicals sorbed to particles result in their classification as “single hoppers”. Heavier PCDDs and PCDFs, benzo[*a*]pyrene, heavy PBDEs, mirex and decachlorobipenyl are considered as typical “single hopping” pollutants. The fourth category includes organic contaminants of high water solubility, e.g., HCHs, atrazine, phthalates and perfluorooctanesulfonic acid (PFOS). Compounds predominantly occurring in the water phase undergo long-range transport primary by rivers and ocean currents. Therefore, “hopping” between the atmosphere and the earth’s surface is not necessary for their spatial distribution.^[82]

As already illustrated organic pollutants are multicompartiment compounds typically penetrating the total environment. The extent of atmospheric transport and the fate of organic pollutants in the environment may be predicted from partition coefficients describing the distribution properties between the environmental compartments (figure 2.3). Low air-water partition coefficients (K_{AW}) also referred to as Henry’s law constants (*H*) indicate an accumulation in the hydrosphere. The octanol-water partition coefficient (K_{OW}) is used as a predictor for an enrichment of pollutants in biota (i.e., aquatic and terrestrial plants and animals), sediments and the organic fraction of deposited particulate matter (e.g., on snow and ice). The distribution of an organic compound

between the atmosphere and soil, vegetation and atmospheric particulate matter is described by the octanol-air partition coefficient (K_{OA}).^[81, 82]

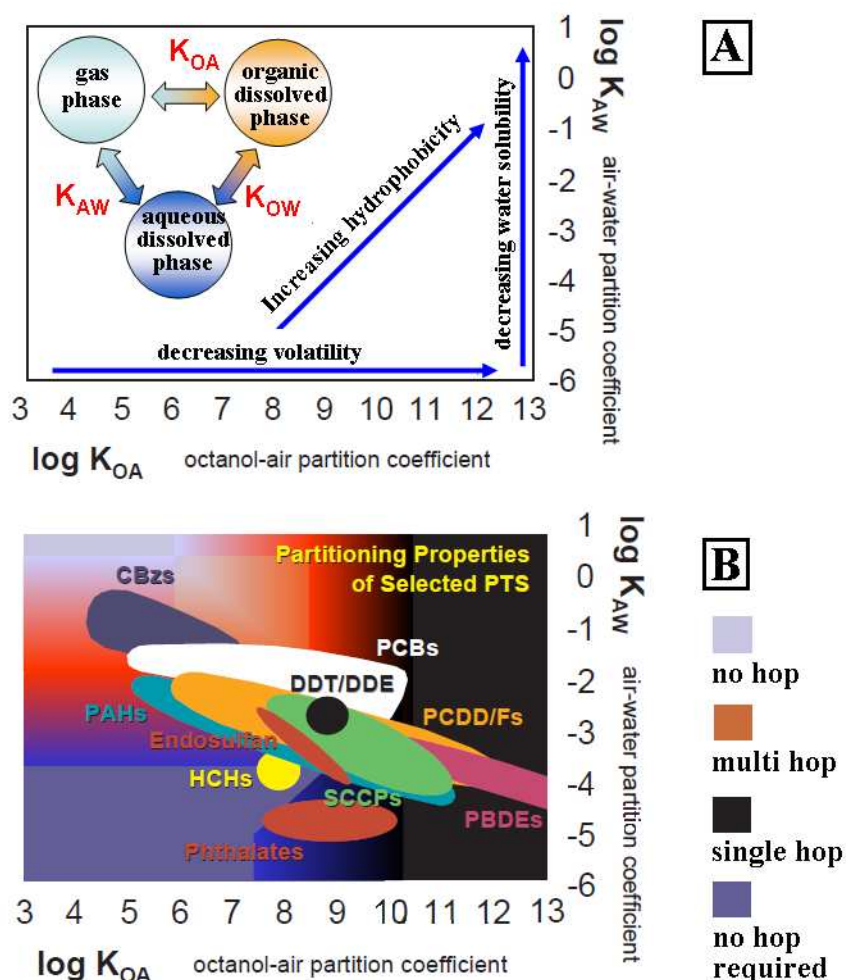


Figure 2.3: Distribution characteristics of organic pollutants defined by the partition coefficients (A); Transport behaviour categorization of several organic pollutants (B); adopted and modified from the UNEP Global Report 2003.^[82]

2.2.1 The role of aerosol particles in atmospheric transport and deposition

Aerosol particles also named particulate matter (PM) may act as atmospheric transport vehicles of pollutants. Persistent pollutants, e.g., heavy metals and organic contaminants like PAHs and PCBs may be incorporated in their structure and transported with them during their formation and growth. Aerosol particles are efficiently washed out by rain. Nevertheless, they are capable of accumulating in the atmosphere under dry conditions providing a means of transport over long distances, especially if mixed to higher altitudes. The distribution and deposition of organic contaminants is highly affected by aerosol particles and their atmospheric dynamics. For this reason a short overview on their composition, formation and growth is given here (figure 2.4).^[83]

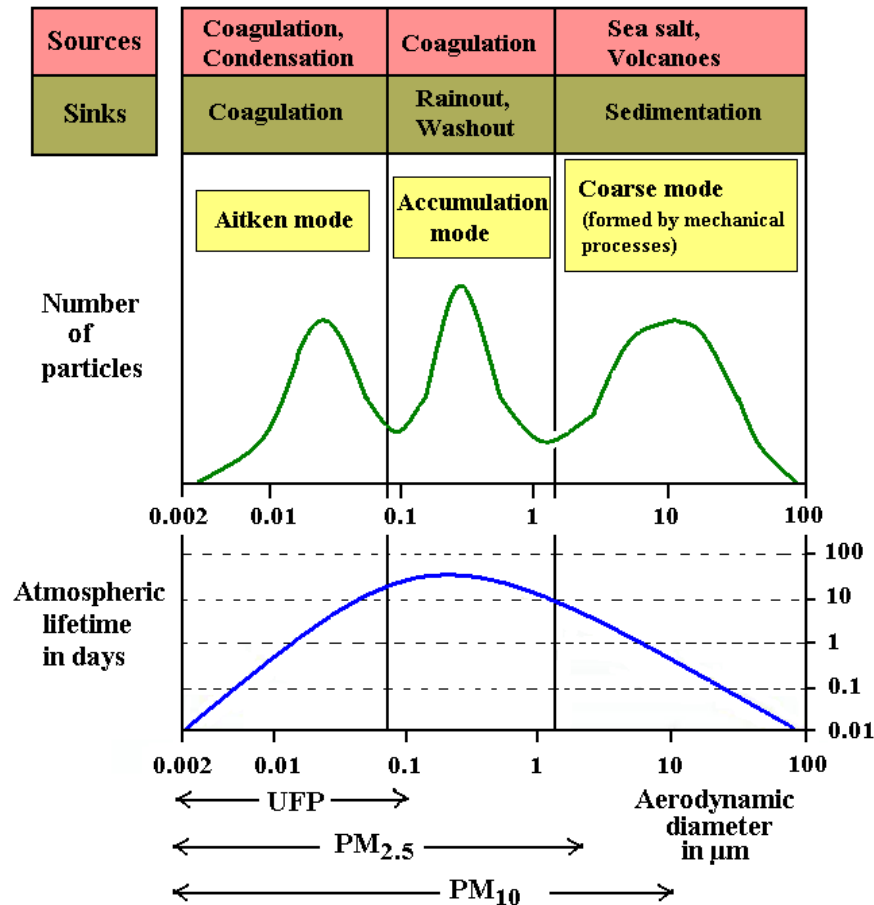


Figure 2.4: Overview of the mass size distribution, atmospheric lifetimes, sources and sinks of aerosol particles, adopted and modified from ^[84, 85]

An aerosol is a mixture of a gas with dispersed particles of diameters in the range from 1 nm to 100 μm . Airborne particles have irregular shapes. For this reason, their size determination often refers to the diameter of idealised spherical particles having a density of 1 g/cm^3 (aerodynamic diameters). Hence, particles of different dimensions and shapes may exhibit the same aerodynamic diameter. Aerosol particles are classified by their particle sizes/aerodynamic diameters into ultrafine particles (UFP, <100 nm), fine particles (< 2.5 μm) and coarse particles ($> 2.5\mu\text{m}$ and < 10 μm). For health hazard reasons (analogy to characteristics of the human respiratory tract) aerosol particle sampling by impaction collectors with size-selective inlets often addresses $\text{PM}_{2.5}$ (< 2.5 μm) and PM_{10} (< 10 μm). It is based on a 50 % efficiency cut-off at 10 μm and 2.5 μm aerodynamic sizes, respectively.

Primary aerosol particles are directly introduced into the atmosphere, e.g., from sea salt emissions above the oceans and desert dust. Secondary aerosol particles may be formed in the atmosphere from precursor gases like sulfur dioxide, nitrogen oxides and ammonia originating e.g. from volcanoes, fossil fuel or biomass burning and livestock. Aerosol particles predominantly consist of

water. Nevertheless, they need to be distinguished from cloud droplets, which act as cloud condensation nuclei (CCN) and exhibit sizes of 10 μm to 3 mm. The morphology and chemical composition of aerosol particles is rather complex. Besides water, the main components of aerosol particles originating from polluted regions are sulphate, nitrate, ammonium, sea salt, dust (soil), elemental carbon (soot, “black carbon”) and an organic fraction (“organic matter” (OM), “organic carbon” (OC))^[84]

The hydrophilic/hydrophobic properties of aerosol particles change during particle growth due to various processes affecting chemical composition and morphology. Nucleation, condensation and coagulation are the three major mechanisms of aerosol physics. The formation of new aerosol particles from precursor gases in the atmosphere is referred to as nucleation. Condensation describes the growth of particles by attachment of gaseous molecules (mostly water vapour). Collisions of aerosol particles may cause the formation of larger particles, which is termed coagulation. Larger particles efficiently grow by collection of smaller particles. Atmospheric aerosols are grouped by their size distribution into four different modes: Nucleation mode (3-20 nm, recently formed particles by nucleation), Aitken mode (20 - 100 nm, ultrafine particles), accumulation mode (100 nm - 2.5 μm , fine particles) and coarse mode (> 2.5 μm and < 10 μm). Very small and very large particles have short lifetimes due to diffusion (to surfaces) and sedimentation, respectively. Therefore, the largest part of the aerosol particles is found in the accumulation mode. Their increased particle mass causes a slower movement and decreases the possibility of collisions with other aerosol particles. For this reason, aerosol particles in the accumulation mode reveal the longest lifetimes in atmosphere of about one week (figure 2.4). Accumulation mode particles are predominantly removed from the atmosphere by wet deposition. However, numerous rain drops are evaporated before they reach the Earth's surface, causing the formation of new aerosol particles from the remaining solutes and undissolved material. In contrast, particles in the coarse mode are frequently formed by wind erosion and bubble bursting processes in surface waters. They are prone to sedimentation and wet deposition.^[83]

As already mentioned the most prominent organic pollutants undergoing gas-particle partitioning in the atmosphere are the PAHs. Their distribution characteristics are linked to their molecular weight and volatility. PAHs of higher molecular weight (> 228 g/mol) are predominantly connected to accumulation mode aerosol particles. Their atmospheric lifetimes of several days in the absence of precipitation provide a chance for long-range transport above the atmospheric boundary layer over thousands of kilometres. Coarse mode aerosol particles reveal significant amounts of low molecular weight PAHs (178-202 g/mol) adsorbed to the particle surface. For this

reason, PAHs of lower molecular weight are more prone to dry particle deposition than the heavier PAHs (>228 g/mol) primarily connected to accumulation mode particles. ^[83, 86]

2.2.2 The role of clouds in atmospheric transport, deposition and transformation processes

Clouds in various ways affect the distribution and transformation processes of organic contaminants in the atmosphere. In particular, they influence their atmospheric transport by cloud venting processes and provide a medium for aqueous chemistry in cloud droplets and precipitation particles. In addition, clouds are an efficient sink for organic contaminants in the atmosphere when precipitating. Moreover, they influence photochemical transformation mechanisms.

The vertical transport of gaseous matter and aerosol particles from the lower troposphere to the middle and upper troposphere (cloud layer) being generated by clouds is termed cloud venting. Deep convection is a key driver in cloud venting processes due to the accompanied updraft and downdraft providing the fast exchange of gaseous and particulate material and hence organic contaminants in both directions. Under the influence of deep convective clouds or supercell thunderstorms updraft wind velocities between 10 to 30 m/s and up to 40 m/s, respectively might be established for several hours. These strong updrafts facilitate the vertical transport of organic contaminants across the troposphere within one to a few hours providing further chances for their long-range transport. In comparison, the vertical wind velocities in the cloud-free atmosphere and in non-convective clouds are low, leading to vertical mixing within days.

Clouds provide a medium for the physical and chemical transformation of organic pollutants. Especially, those present in non-precipitating clouds are prone to altering processes. In addition cloud chemistry may affect the concentration of other reactants, e.g., oxidants, which in turn influence the atmospheric residence times of organic pollutants.

Characteristic properties of clouds are the absorption and scattering of solar light effecting a strong influence on atmospheric photochemistry and thus on the atmospheric transformation of pollutants. The photolysis rates below cloud layers are significantly reduced, whereas they increase in the upper layers and above the clouds. ^[76]

2.3 Air-sea and sea-air exchange mechanisms of organic pollutants

The sea plays a key role in controlling the transport, fate and sinks of organic contaminants. Dry deposition, wet deposition and gas exchange are the three main mechanisms controlling the atmospheric input of organic contaminants to the sea surface layer. The diffusive gas exchange between the atmospheric boundary layer (ABL) and the sea surface is reported to be the dominating depositional process above the oceans, whereas dry particle and wet deposition fluxes may be extended, e.g., during rainy seasons, in regions of high marine aerosol production, in

regions close to urban areas with increased particulate matter concentrations and for chemicals with a strong affinity to particulate matter. In addition, the exchange of organic contaminants between sea and atmosphere is highly affected by bubbling processes in surface waters. ^[87-91]

2.3.1 Influence of biogeochemical processes in the water column

Biogeochemical processes in the oceans water column, especially phytoplankton growth and particle settling to the deep oceans, is considered to be a key driver of atmospheric depositional fluxes as it limits the atmospheric residence times of organic pollutants in the surface mixed layer. Hence, areas of primary production may affect atmospheric distribution over the oceans and the large-scale chemodynamics of organic pollutants. In several studies a coupling of the diffusive air-water exchange mechanism with the oceanic biological pump has been pointed out (figure 2.5).

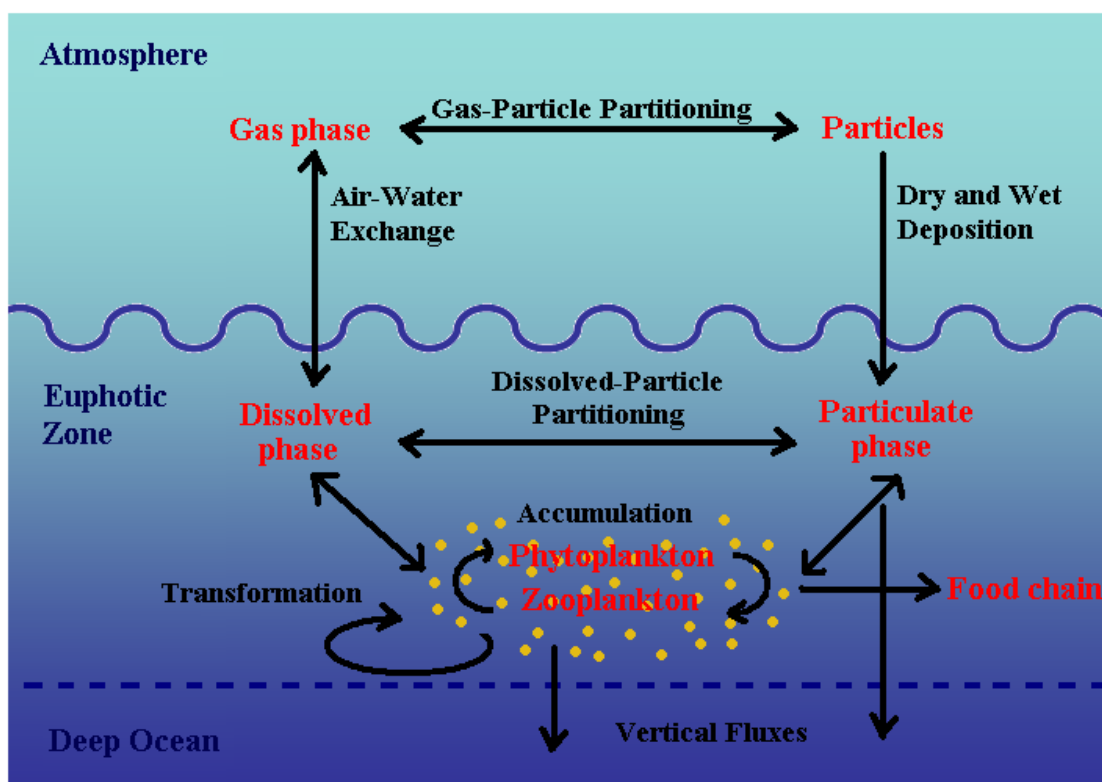


Figure 2.5: Schematic presentation of the air-water-phytoplankton coupling model, adopted and modified from ^[93]

The biological pump is a phytoplankton based food web transporting carbon from the surface euphotic zone to the deep ocean by a sequence of biologically mediated processes. Organic contaminants may be incorporated into the biological pump due to bioaccumulation in phytoplankton resulting in contaminated particle settling to the deep oceans. In addition, the microbial activity in the phytoplankton food web may favour the biodegradation of organic contaminants. In areas of high primary productivity the phytoplankton growth and associated

settling fluxes cause dissolved organic contaminants to decrease, forcing air and water concentrations out of equilibrium. As a consequence, the diffuse air-sea gas exchange of organic contaminants is enhanced to compensate for the disequilibrium.^[90, 92]

In a recent study the air-water-phytoplankton coupling in the Mediterranean Sea has been investigated for several persistent organic pollutants, such as PCBs, HCHs and HCB: Less hydrophobic compounds like PCB 28, PCB 52 and HCB (log K_{ow} : 5.62, 6.09 and 5.73, respectively) provide a fast gas exchange mechanism from the atmosphere to the sea, which is capable of balancing the depletion of pollutants by the phytoplankton. In such a case, the concentration of organic contaminants in the phytoplankton is independent of the amount of biomass. In contrast, the air-water exchange of more hydrophobic PCBs like PCB 138 and PCB 180 (log K_{ow} : 7.44 and 8.27, respectively) is a much slower process resulting in a decrease of dissolved and particulate (phytoplankton, zooplankton, detritus) associated concentrations with increasing biomass production. This observation is termed “biomass dilution effect”. Hexachlorocyclohexanes (log K_{ow} of γ -HCH: 3.72) are less hydrophobic than the PCBs and are not prone to a biomass dilution effect. Nevertheless, it has been found that the phytoplankton concentrations of HCHs significantly decrease with increasing biomass. HCHs are known to be less persistent than PCBs and undergo microbial transformation in marine environments. For this reason, the observed biomass dilution effect of HCHs may be based on enhanced biodegradation rates of HCHs in areas of phytoplankton growth, a process not covered by the air-water-phytoplankton coupling model.^[93]

2.3.2 Influence of bubbling processes in surface waters

The gas exchange between sea and atmosphere is strongly influenced by bubbling processes in the water column. Three different types of bubbles are differentiated by their sources, namely benthic bubbles, cavitation bubbles and atmospheric bubbles. Benthic bubbles are released from the seafloor by volcanic activities and predominantly consist of methane and carbondioxide. Bubbles produced by anthropogenic sources such as ship propellers are referred to as cavitation bubbles. Both types account negligibly to sea-air interactions. Atmospheric bubbles are generated by two mechanisms: A minor part of atmospheric bubbles is produced by fumigation in air saturated surface water. The major source of bubbles in the surface water of the sea is the entrainment of air within the water flow occurring during wave breaking, rainfall or any other kind of atmospheric precipitation. At wind speeds of approximately > 4 m/s quite large volumes of air are entrapped by wave breaking resulting in the formation of white caps (figure 2.6). The bursting of white cap bubbles generates sea spray which is transferred into the atmosphere as sea-salt aerosol particles

(primary aerosol). Due to the steady agitation of water surfaces atmospheric bubbles are dominating the gas exchange between sea and air. ^[91, 94, 95]

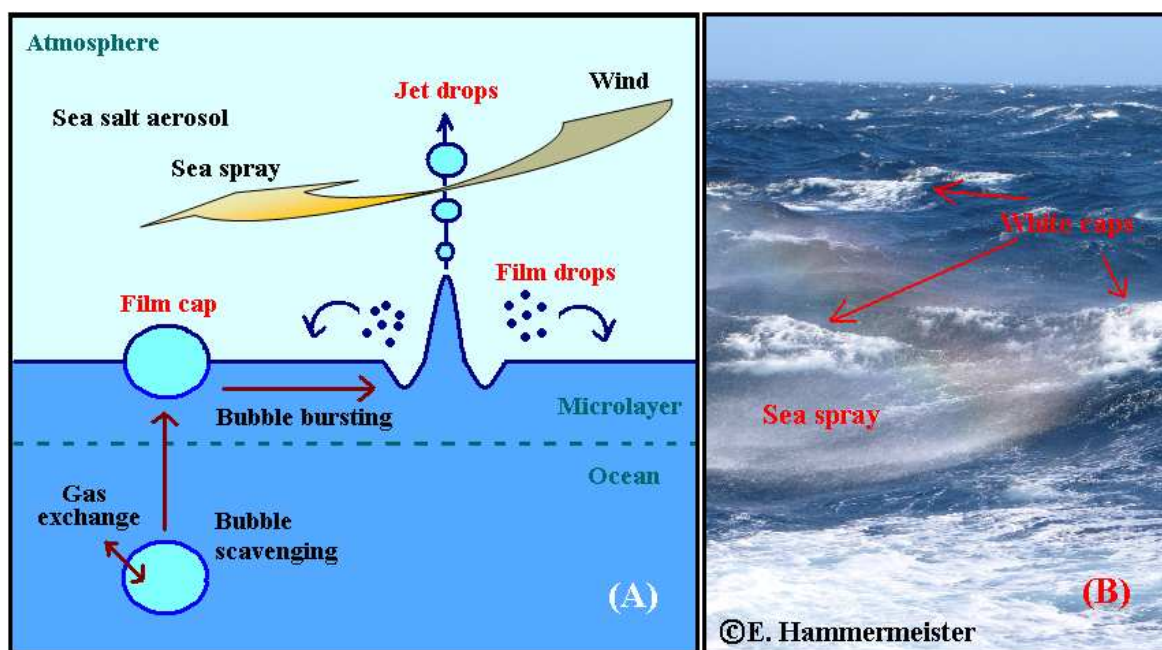


Figure 2.6: (A) Schematic presentation of sea-air-interactions via bubble bursting, modified from ^[91] (B) White capping and sea spray

Bubbles are capable of accumulating dissolved and particulate substances on their surfaces (bubble scavenging). They are transferred to the atmosphere by the following mechanism (figure 2.6): The upper surface of a bubble moves through the water-air interface and forms a “film cap”. The bursting of the film cap produces several smaller “film drops” of diameters ranging from $< 1 \mu\text{m}$ to $10 \mu\text{m}$, which are quickly dropped back to the water surface. Simultaneously, the remaining cavity collapses inwards and generates a “Worthington jet”, which in turn decomposes into “jet drops”. These are vertically ejected into the air and may be captured by the wind resulting in the formation of sea salt aerosols. Organic material, metal ions, viruses, bacteria and even organic contaminants are emitted into the atmosphere by the bubbling processes in the water surfaces. ^[96]

In a recent dissertation the impact of bubbling processes on the sea-air exchange of α -HCH, *cis*-chlordane, PCB 153 and ibuprofen has been investigated in a model wave channel. By successive variation of environmental conditions, the influence of salt water, wind speed, the rising paths of bubbles, bubbles sizes and surface films on the exchange rates has been addressed. It has been pointed out, that salt water significantly supports the exchange rates of PCB 153 and *cis*-chlordane, whereas the transport of α -HCH and ibuprofen is unaffected. In addition, ibuprofen exchange only occurs at high wind speeds. Moreover, the transport potential of *cis*-chlordane and PCB 153

increases with a larger travel distance of a bubble through the water column and with increasing bubbling sizes. ^[91]

2.4 Atmospheric Deposition

As already described in the chapters above, diffusive gas exchange (dry gaseous deposition) in most cases is the dominating deposition process of organic pollutants from air to sea. However, this transfer (flux) proceeds in both directions making the seas even to a possible source of atmospheric pollution.

2.4.1 Direction of the net flux of diffusive gas exchange

The direction of the net flux of the diffusive gas exchange of a given compound may be predicted from the fugacity in the respective phases. Fugacity, which describes the tendency of a compound to leave a phase, depends on the compound concentration, the physical-chemical properties of the compound as well as on the environmental characteristics of the phase itself. In addition the fugacity concept is an equilibrium model assuming that the compounds reside in two adjacent homogenous phases (particles ignored). Hence, it needs to be noted, that the reliability of the fugacity model results may be limited, e.g., by the dynamics (mass transfer kinetics) and partial irreversibility of gas-particle partitioning in both the atmosphere and the seawater.

Fugacity f expressed in units of pressure (Pa) is equalized to the concentration c (mol/m³) through a fugacity capacity Z (ng/(m³Pa)):

$$c = f \cdot Z \quad (\text{equation 1})$$

The fugacity capacities for water (Z_w) and air (Z_A) are given by

$$Z_w = \frac{1}{H} \quad (\text{equation 2})$$

and

$$Z_A = \frac{1}{R \cdot T_A} \quad (\text{equation 3}),$$

respectively, where H is the Henry's Law constant (Pa m³/mol) corrected for a given water temperature, R is the ideal gas constant (8.314 Pa m³/(mol K)) and T_A is the absolute air temperature (K). By insertion of equation 2 in equation 1 and equation 3 in equation 1 following expressions for the fugacities of a given compound in water (f_w) and air (f_A) are obtained:

$$f_W = c_W \cdot H \quad (\text{equation 4})$$

and

$$f_A = c_A \cdot R \cdot T_A \quad (\text{equation 5})$$

On the basis of the fugacity ratio f_W/f_A the flux direction is estimated. Fugacity ratios <1 indicate a dry gaseous deposition from atmosphere to sea, whereas fugacity ratios >1 suggest the opposite. A fugacity ratio of 1 refers to equilibrium conditions. Because of the above mentioned limitations of the fugacity approach, additional uncertainties in Henry constants and other experimental parameters, the obtained ratios need to be interpreted within an appropriate uncertainty range. Thus, values >2 and <0.5 are considered to be significant for net volatilization and atmospheric deposition, respectively. ^[97, 98] Henry coefficients for flux-calculations are tabulated in the annex 7.

2.4.2 Quantification of the dry gaseous deposition

The diffusive air-water exchange (F_{AW} in $\text{ng}/(\text{m}^2 \text{d})$) is given by

$$F_{AW} = k_{AW} \cdot \left(\frac{c_A}{H'} - c_W \right) \quad (\text{equation 6}),$$

where k_{AW} is the air-water mass transfer rate (m/d), c_A is the gas phase concentration in the atmosphere (ng/m^3), c_W is the dissolved POP concentration in sea water (ng/m^3) and H' is the temperature corrected and dimensionless Henry's law constant. The reciprocal of k_{AW} (equation 7) is additionally defined as the sum of the resistances to pollutant mass transfer in the air (k_A) and water (k_W) phases in units of m/d, respectively.

$$\frac{1}{k_{AW}} = \frac{1}{k_A \cdot H'} + \frac{1}{k_W} \quad (\text{equation 7})$$

k_W of a given pollutant is estimated from the mass transfer coefficient of CO_2 (k_{W,CO_2}), whereas k_A may be calculated from the mass transfer coefficient of H_2O . Both variables are a function of the wind speed at 10 m height (U_{10} in m/s).

$$k_{W,\text{CO}_2} = 0.24 \cdot U_{10}^2 + 0.061 \cdot U_{10} \quad (\text{equation 8})$$

$$k_W = k_{W,\text{CO}_2} \cdot \left(\frac{Sc_{OC}}{Sc_{\text{CO}_2}} \right)^{-0.5} \quad (\text{equation 9})$$

$$k_{A,H_2O} = 0.2 \cdot U_{10} + 0.3 \quad (\text{equation 10})$$

$$k_A = k_{A,H_2O} \cdot \left(\frac{D_{OC,a}}{D_{H_2O,a}} \right)^{0.61} \quad (\text{equation 11})$$

Sc is the Schmidt number, which is dimensionless and characterizes the fluid flow via convective and diffusive mass transport, e.g., of an organic contaminant (Sc_{OC}). Schmidt numbers are highly affected by the weather conditions, i.e., wind speed, cloud cover and temperature. For this reason, a reliable estimation of the Schmidt numbers requires stable atmospheric conditions during the sampling duration. D is the diffusion coefficient in air describing the diffusion mobility of a given compound. In this case $D_{OC,a}$ and $D_{H_2O,a}$ are the diffusion coefficients of the organic contaminant and water in the air, respectively. ^[90, 98, 99]

2.4.3 Quantification of the dry particulate deposition

The flux of the dry particulate deposition (F_{DD} in $\text{ng}/(\text{m}^2 \text{d})$) is defined by

$$F_{DD} = v_D \cdot c_p \quad (\text{equation 12})$$

where v_D is the overall dry deposition velocity (m/d) and c_p is the atmospheric concentration of the organic contaminant in the particulate phase. Aerosol size distributions, wind speed and the atmospheric stability are the major factors controlling v_D . ^[88] Experimentally determined data of dry particle deposition fluxes are scarce and have to be estimated. The mass median diameter (MMD) of a given aerosol size distribution may be used to assess the overall dry deposition velocities of organic contaminants. A typical maritime aerosol size distribution is given by Jaenicke. ^[100] According to the general acceptance of a homogenous density and spherical form of aerosol particles, the mass median diameter may be calculated from the total volume (V_t) and total number (N_t) of maritime aerosol particles of the complete size range (radii $r > 0.001 \mu\text{m}$) as described in equations 13 - 15. A mass median aerodynamic diameter of about $0.56 \mu\text{m}$ is derived.

$$V_t = 1.6 \cdot 10^{-11} \quad [l], \quad N_t = 1.78 \cdot 10^2 \quad [1/\text{cm}^3]$$

$$V_p = \frac{V_t}{N_t}, \quad V_p = 8.99 \cdot 10^{-14} \quad [\text{cm}^3] \quad (\text{equation 13})$$

$$r_p = \sqrt[3]{\frac{V_p \cdot 3}{4 \cdot \pi}}, \quad r_p = 0.28 \quad [\mu\text{m}] \quad (\text{equation 14})$$

$$MMD = 2 \cdot r_p, \quad MMD = 0.56 \quad [\mu\text{m}] \quad (\text{equation 15})$$

Figure 2.7 additionally illustrates the surface size distribution of various aerosol types. Marine aerosol is defined as the sum of background aerosol and seasalt. Hence, the background aerosol graph plotted in figure 2.7 is assumed to be most similar to the surface size distribution of marine aerosol.

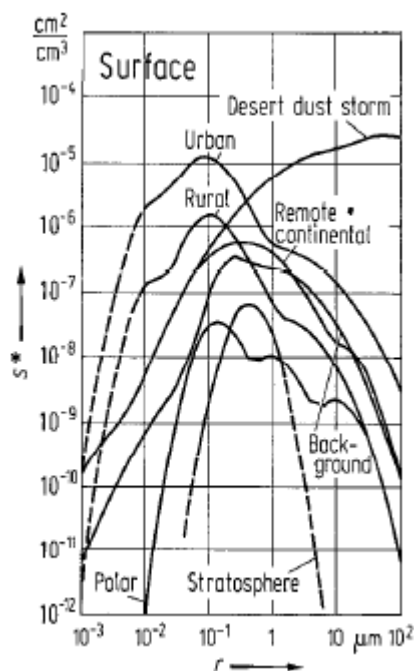


Figure 2.7: Surface size distribution of various aerosol types, adopted from ^[100]

The simplification achieved by the determination of a MMD provides the estimation of dry deposition velocities via an empirical relation published by Slinn & Slinn, by plotting the dry deposition velocity against the dry aerosol particle radius for different wind speeds and relative humidity. The derived dry deposition velocities are summarized in table 2.1. ^[101]

Table 2.1: Predicted deposition velocities (cm/s) of $(\text{NH}_4)_2\text{SO}_4$ aerosol particles with a mass median diameter of $0.56 \mu\text{m}$ at different wind speeds v_D (m/s) and relative humidity (r.h.) above natural waters

	v_D (m/s)	r.h. 100 %	r.h. 99 %	r.h. 0 %
wind speeds:	1 m/s	0.1	0.02	0.002
	5 m/s	0.3	0.02	0.004
	15 m/s	0.5	0.02	0.01

A relative humidity of 0 % refers to hydrophobic particles. Their deposition velocities may be excluded for this study, because the sea salt content of marine aerosol particles makes them highly hydrophilic. The deposition velocities for 100 % relative humidity may be applied to aerosol particles collected during fog and sea smoke.

2.4.4 Quantification of the wet deposition

Wet deposition F_{Wet} (ng/(m² d)) is defined as

$$F_{Wet} = c_{Prec} \cdot P \quad (\text{equation 16})$$

where c_{Prec} is the concentration in precipitation (ng/L) and P is the total precipitation flux (L/(m² d)).^[102] An additional definition enabling the determination of the wet deposition rate without knowledge of the total precipitation flux is given in equation 17.

$$F_{Wet} = \frac{c_{Prec} \cdot V}{a \cdot t} \quad (\text{equation 17})$$

V is the volume (L) collected by the wet deposition sampler, a refers to the sampling cross section (m²) of the wet deposition collector and t is the precipitation sampling time (d).^[103] Moreover, a rough estimate of wet deposition rates can be based on scavenging ratios published in the literature (equation 18).

$$F_{Wet} = 10^3 \cdot W_t \cdot c_a \cdot P \quad (\text{equation 18})$$

$$W_t = 10^3 \cdot \frac{c_r}{c_a} \quad (\text{equation 19})$$

W_t is the total scavenging ratio defining the volume of air washed out by the volume of rainwater for a given compound. It could be calculated (equation 19) from the concentrations (total of gaseous/soluble and particulate phase) of a given compound in air (c_a in ng/m³) and in the rainwater (c_r in ng/L).^[104]

3. Methodology

The results of this study are based on atmospheric concentrations of organic target analytes in the marine atmosphere, which were predominantly determined during ship based air-sampling campaigns in the North Sea, the German Exclusive Economic Zone (EEZ) and the Baltic Sea. This chapter gives a brief summary of the methods, of the target analytes and of the air-sampling campaigns carried out. A detailed list of material and instruments as well as sample processing methods may be found in chapter 9.

3.1 Air-sampling methods

Air sampling was performed by high-volume active air samplers and PUF-disk passive air samplers. High-volume active air samplers were applied to the volumetric quantification of atmospheric trace concentrations of organic pollutants (8–10 hours), whereas seasonal and vertical fluctuations in atmospheric concentrations were monitored by time integrating (4–6 weeks) passive air sampling studies.

3.1.1 High-volume active air samplers

When starting this study, high-volume samplers were not available, but had to be procured. Commercially available active air-sampler systems are designed for land based measurements. For this reason, their utilisability and performance on the top deck of research vessels during seafarings under extreme weather and working conditions had to be tested and evaluated before ordering. A high-volume sampler model, which had been applied already for ship based measurements, was borrowed from the Helmholtz-Zentrum Geesthacht-Centre for Materials and Coastal Research (HZG) in order to obtain first experience in active air sampling. A second high-volume sampler was tested by the University of Hamburg during a sea cruise in the Baltic Sea ^[91] and a fraction of the obtained air samples were provided for this study.

The high-volume samplers are comparable in their construction. They consist of a turbine sucking the ambient air through a filter followed by a solid adsorbent and a flow meter determining the volume of collected air. The particle associated mass fraction of organic pollutants is separated on glass fibre filters (GFFs), whereas the gaseous mass fraction is trapped in an adsorber cartridge consisting either of PUF plugs or PUF/XAD-2/PUF sandwiches. They differ in the assembly of the inlet as illustrated in figure 3.1.

Both high-volume samplers were successfully operated during sea cruises. Nevertheless, there was a need for optimization with regard to the following observations: The inlet of the high-volume sampler provided by the university was prone to water intrusion (sea spray, rain) limiting the

offshore usage. By contrast, the inlet of the HZG active air sampler was in the majority of cases water tight, but the numerous gaskets make the system vulnerable for leakage, e.g., during strong winds. Moreover, the exchange of filters and adsorber cartridges was more complex, inadequately for operation on the top deck. In addition, a loss of XAD-2 was observed, which was ascribed to a deformation of the PUF/XAD-2/PUF sandwich caused by a partial vacuum occurring during sampling. Furthermore, both inlets were not adequate for a size-selective collection of particulate matter in accordance with the PM_{10} or $PM_{2.5}$ classification. Besides, the total volume of collected air measured during a sampling event was biased by lost heat, because the flowmeter was installed behind the turbine. The flowrate of ambient air passing the glass fibre filter and adsorber cartridge was controlled by an adjustable turbine frequency. During a sampling period, the flow resistance of GFF and adsorber cartridge increased due to a clogging of the filter by collected particulate matter and a compression of adsorber material in the cartridge, which in turn decreased the flow rate. Thus, the adjustment of a constant flow rate was almost unfeasible and required a continuous control and regulation of flow rate and turbine frequency.

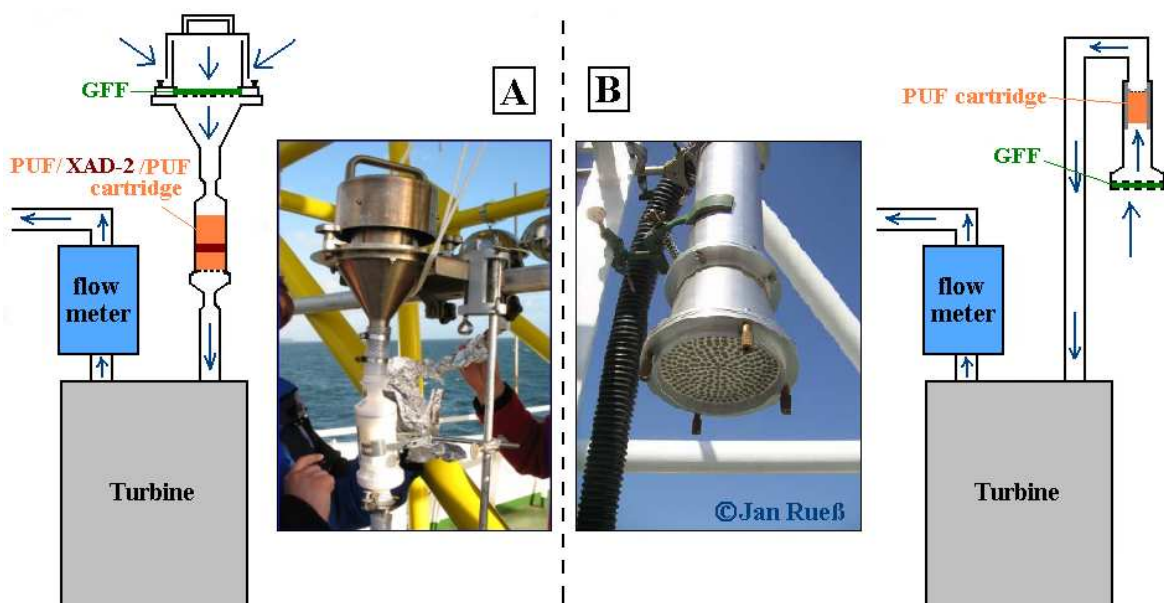


Figure 3.1: Schematic diagrams of high-volume active air samplers including a photograph of the inlet, respectively; (A) AAS of the HZG; (B) AAS of the University of Hamburg

Considering the above listed difficulties, a Digital DHM-60 high-volume active air sampler was purchased. It is equipped with a PM_{10} impactor, a size-selective inlet based on a 50% efficiency cut-off at $10 \mu m$ aerodynamic particle size. The impactor additionally protects the system from water intrusion. Furthermore, the collected air volumes are pressure and temperature corrected due to pressure/temperature-sensors at the inlet and at the flow meter. The Digital-sampler is supplied

with a rotary flow meter, providing the adjustment of a constant flow rate via a light barrier. Moreover, the date of sampling, start and stop of the sampling event, pressure and temperature monitored by the sensors, collected air volumes as well as occurring sampler errors are electronically stored on a PCMCIA memory card (figure 3.2).

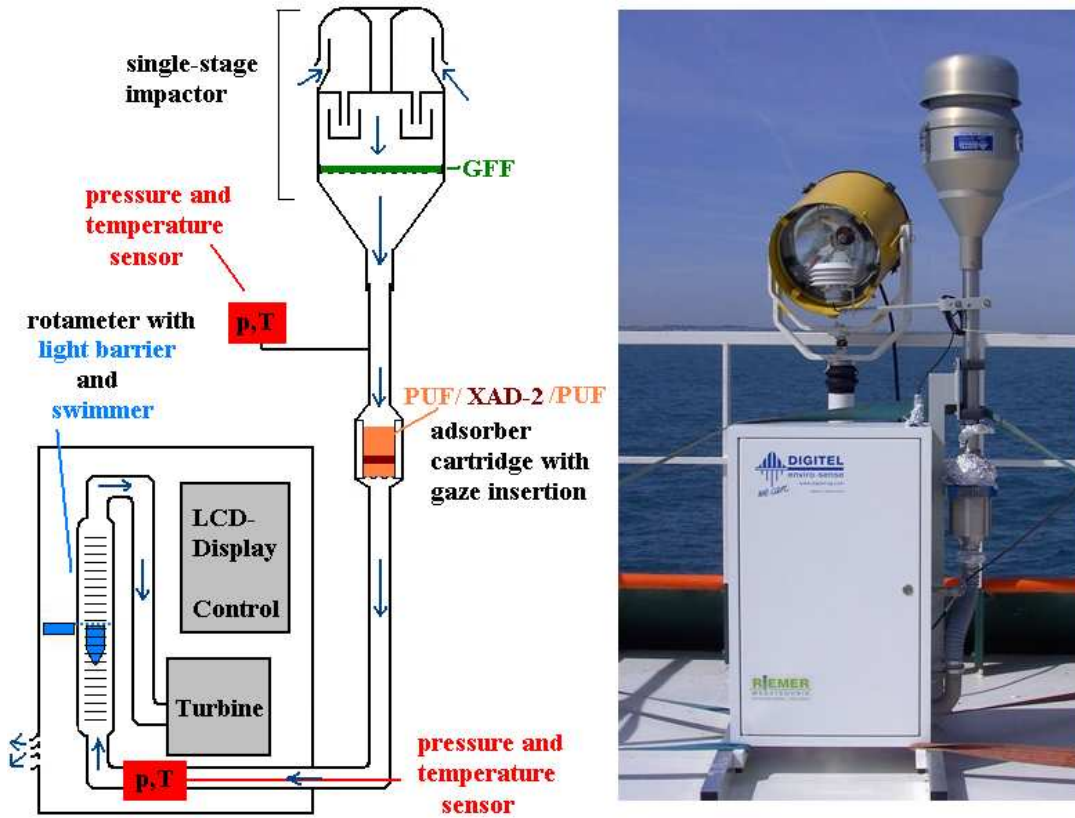


Figure 3.2: Schematic diagram of the Digitel DHM-60 high-volume active air sampler and a photography for the top deck of the research ship Pelagia

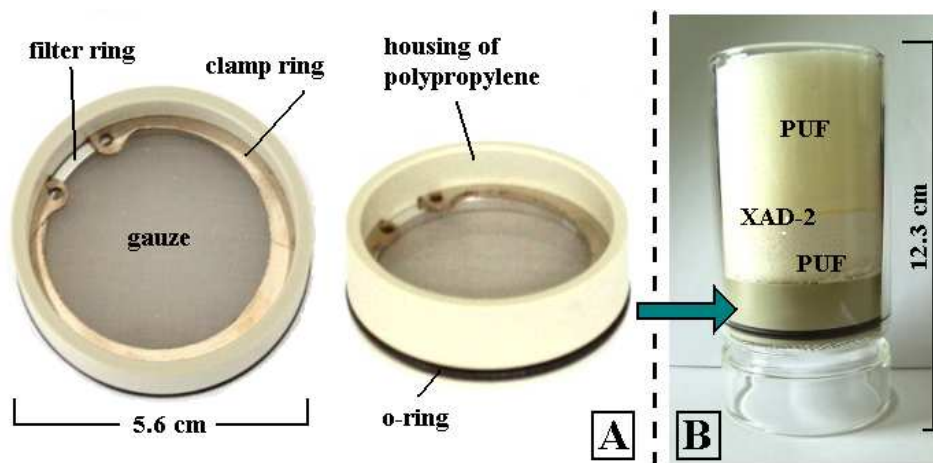


Figure 3.3: (A) Gauze-insertions; (B) The fine-meshed gauze prevent the loss of XAD-2 from the adsorber cartridge (PUF/XAD-2/PUF sandwich)

In cooperation with the mechanic workshop of the BSH gauze-insertions were developed. They were inserted into the adsorber cartridge preventing the loss and contamination of the high-volume sampler by XAD-2 (figure 3.3).

The application of gauze insertions increases the flow resistance of the PUF/XAD-2/PUF adsorber cartridge requiring a reduction of the flow rate to 425 L/min (25.5 m³/h). For this reason, the impactor cut-off needs to be recalculated, because the Digital sampler was calibrated for PM₁₀ sampling at a constant flow rate of 500 L/min. The aerodynamic diameter of particulate matter, which is segregated with 50% efficiency by a single-stage impactor ($d(ae)_{50}$) may be calculated by the Theory of Marple:

$$d(ae)_{50} = \sqrt{\frac{9 \cdot \pi \cdot Stk_{50} \cdot \eta \cdot d_j^3 \cdot N_i}{4 \cdot C \cdot \rho_p \cdot V_F}} \quad (\text{equation 19})$$

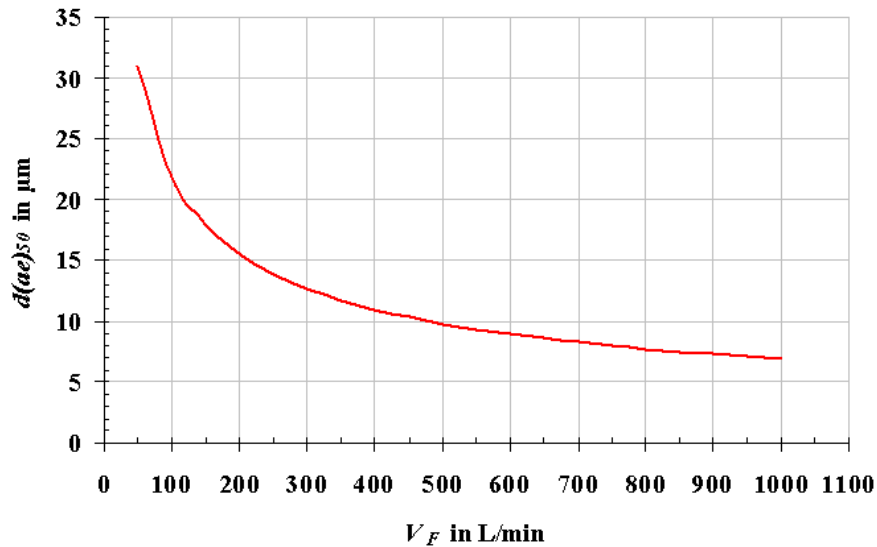


Figure 3.4: Size segregation characteristic of the single-stage impactor in the Digital DHM-60 high-volume active air sampler at 15°C ambient temperature, 1013 mbar air pressure and 50% relative humidity

Stk_{50} is the dimensionless Stokes number describing the ratio of the stopping distance of a particle to the radius of the impactor nozzle. Exact Stokes numbers are determined by calibration. Here a mean Stokes number of 0.24 for a round nozzle impactor is assumed. η is the dynamic viscosity depending on the temperature and gas composition. A dynamic viscosity of $1.79 \cdot 10^{-5}$ kg/(m s) at 15 °C is supposed. d_j and N_i are the nozzle diameter ($13.8 \cdot 10^{-3}$ m) and number of nozzles (10), respectively. The Cunningham slip correction factor C describes the influence of gas molecules on the movement of particles, which is negligible for particles of 10µm aerodynamic size ($C = 1$). The aerodynamic diameter of aerosol particles is an equivalent diameter referring to idealised spherical

particles of a standard density (ρ_P) of 1000 kg/m³. V_F is the air volume flow in m³/s. A flow rate of 0.006 m³/s (400 L/min) corresponds to a 50% efficiency cut-off at 11 μ m (aerodynamic particle diameter).^[105, 106] The size segregation characteristic of the single-stage impactor being applied in the Digital high-volume active air samplers DHM-60 is plotted in figure 3.4.

The Digital sampler was successfully operated during cruises in the open North Sea and the German EEZ. Hence, an identical second Digital DHM-60 sampler was ordered for purposes of method validation and side-by-side sampling. In comparison to the first sampler, the PCMCIA data output is replaced by a USB flash drive interface. In addition, the housing of the adsorber cartridge is equipped with a hinged lid instead of a screw cap to eliminate the possibility of cartridge contamination by silicone grease (figure 3.5 B).



Figure 3.5: Housings of the adsorber cartridge of the Digital DHM-60 systems; (A) Housing with a screw cap; (B) Housing with a hinged lid; (C) Adsorber cartridge fitting for insertion in the housings

It should be mentioned that high-volume active air sampling is prone to artefacts causing a possible misrepresentation of the gas-particle partitioning of organic contaminants in air. On the one hand, artefacts are due to adsorption of gaseous pollutants to the particulate matter accumulated on the filter or even to the filter material itself. This phenomenon is named blow-on effect. On the other hand, artefacts may occur due to volatilization of organic contaminants from the particulate matter collected on the glass fibre filter, which is termed blow-off effect and results in an underestimation of the particle associated mass fraction. The extent of volatilization losses may depend on the pressure gradient existing through the filter, the ambient temperature during sampling as well as the physico-chemical properties of organic compounds. Average volatilization losses of PCBs under ambient temperatures of 7-22°C range from 70% to 98%, whereas the extent of volatilization loss of *n*-alkanes is between 20% and 80% depending on the chain length (C_{21} to

C₃₅). The blow-off of PAHs (PAHs consisting of 3 to 4 aromatic rings) is determined in the range of 50% to 90%, whereof four-ring PAHs with lowest vapour pressures reveal lowest volatilization losses. The average volatilization losses listed above were determined by a charcoal diffusion denuder system, which is placed upstream of the particle collecting filter. It removes the gaseous associated mass fraction of organic contaminants from the air flow effecting a shift in gas-particle equilibrium, which in turn causes increased volatilization losses as compared without denuder. For this reason, the extent of the blow-off effect is not directly assignable to the high-volume active air samplers as applied in this study. ^[107, 108]

The sampling durations and air volumes collected by high-volume active air samplers differed depending on the weather conditions and the course of the ship. During ship based measurements the high-volume active air sampler was placed on the top deck to minimize the collection of high amounts of sea spray. The sole exception was the Baltic Sea cruise, where the sampler was positioned on the foredeck. An overview of the high-volume active air sampling campaigns and sampling parameters is given in chapter 3.2.

3.1.2 PUF disk passive air samplers

This study applies PUF disks of 14 cm diameter, 1.4 cm thickness and 0.0213 g/cm³ density. They are placed in a stainless steel protection chamber during exposure. The conventional construction of a PUF disk passive air sampler is illustrated in figure 3.6.

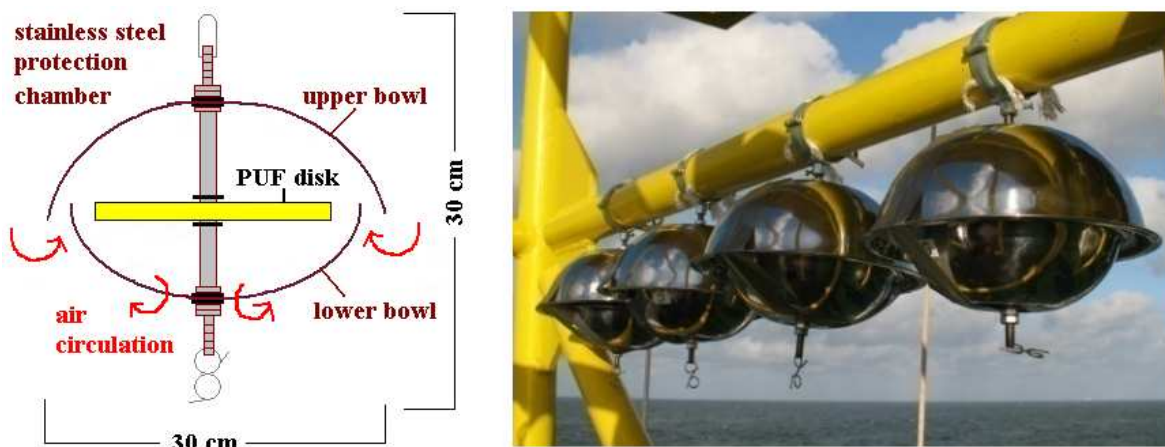


Figure 3.6: Schematic diagram of a conventional PUF disk passive air sampler (adopted and modified from ^[15]) and a photography illustrating the installation at the top deck of the research vessels

The protection chamber, which reminds of a “flying saucer”, is composed of a lower and an upper bowl being connected with a thread rod allowing the adjustment of the PUF disk inside the

chamber. An important feature of the PUF disk housing is to keep the sampling rates of gaseous organic pollutants in ambient air constant, e.g., due to a shielding of the PUF disk from wind speed. Furthermore, the chamber protects the PUF disk from any kind of precipitation, reduces particle deposition and prevents from the photodegradation of adsorbed pollutants by sunlight. ^[15]

A calibration of the PUF disk sampling rates in order to obtain time weighted average air concentrations of organic contaminants was not performed in this study due to several reasons. On the one hand the long-term studies with passive air samplers aim to monitor seasonal and vertical trends in fluctuations of organic pollutants in the atmosphere, whereas the quantification of volumetric marine air concentrations was the subject of ship based active air sampling campaigns. For this reason, the quantification of the total amount of organic pollutants accumulated on the PUF disk was sufficient for the investigations of trends. On the other hand, the passive air sampler (PAS) calibration studies published in the literature exhibit high aberrations and variability in calculated sampling rates of PUF disk passive air samplers, which may be more affected by ambient weather conditions, e.g., wind speed, than by compound and congener specific physico-chemical properties. ^[23, 33] Furthermore, wind tunnel experiments support the observation of biased air samples towards windy days. It is reported that the “flying saucer” design keeps the uptake rates constant up to a wind velocity of approximately 4 m/s. Higher wind speeds increase the sampling rates sharply, for example, a wind velocity of 7 m/s may increase the uptake rates up to 40 m³/d. ^[109] Average wind speeds during sea cruises ranged from 5 m/s to 17 m/s during a sampling period. Hence, sampling rates determined from land based calibration studies were not adequate for the calculation of time integrated average concentrations of organic pollutants in marine atmosphere. Typical sampling rates of organic pollutants from ambient air determined under weather conditions allowing the sampler housing an efficient dampening of the wind effect are reported to range from 1 m³/d to 5 m³/d. In consequence, the determination of time weighted average concentrations of target analytes in marine atmosphere requires an optimization of the PUF disk housing with regard to the wind dampening effect at high wind speeds and thereafter a recalibration of sampling rates. Considering the limitations in the given study time and the available equipment, this option was discarded.

In order to carry out trend investigations based on the total amount of organic pollutant adsorbed to the PAS (ng/PAS) the following principles had to be applied: The monitoring of the seasonal fluctuations in atmospheric concentrations was performed at land based sampling sites. Hence, the wind dampening effect of the “flying saucer” housing was supposed to keep the sampling rates constant. The PUF disks were simultaneously exchanged in fixed time intervals of 28 days enabling the comparability of collected passive air samples. By contrast, the vertical profiles in

atmospheric pollutant concentrations were monitored at the FINO research stations in the German EEZ of the North Sea in 60 m, 80 m and 100 m height above sea level. Here, the wind dampening effect of the PUF disk protection chamber was insufficient. Nevertheless, comparability of the air samples collected in the different heights is ensured by the simultaneous exposure of the samplers. In addition, the PUF disks were spiked with performance reference compounds (PRCs) prior to exposure. PRCs are isotopically labeled or unlabeled organic compounds exhibiting negligible concentrations in ambient air. After exposure and analysis the recoveries of the PRCs were calculated. According to the usage of deuration compounds (see chapter 1.2), the comparable PRC recoveries in air samples collected in identical time intervals over the monitoring periods were used as indicators for comparable sampling rates and thus comparable air samples. Air temperatures and wind speed were monitored over the deployment period at each sampling site.

First experiences in passive air sampling in the marine atmosphere were made during sea cruises. PUF disk passive air samplers were installed on the top deck close to the high-volume active air sampler. At high wind velocities (> 7 m/s) a deformation of the protection chamber was observed requiring an additional fixation of the bowls with adhesive tape. In consequence, the “flying saucer” protection chambers installed at the FINO stations needed to be modified in order to obtain a more stabilized construction resisting strong winds and storms over extended sampling periods. In principal the modification of the sampler housing was based on the connection of the bowls by a hinge-joint providing a more effective fixation of the bowls and a simplified exchange of PUF disks at sampling sites difficult to reach. A photography illustrating the modified sampler housing is shown in figure 3.7. An overview of the passive air sampling campaigns and sampling parameters is given in chapter 3.2.



Figure 3.7: Modified PUF disk passive air sampler

3.2 Air sampling campaigns

This study comprises the results of four high-volume active air sampling campaigns, which were performed during research cruises in the German EEZ, the wider North Sea and the Baltic Sea. A land based active air sampling campaign was carried out in Sülldorf/Hamburg for purposes of method validation and for comparison of sea and land based collected air samples. In addition, long-term monitoring studies of seasonal fluctuations in atmospheric pollutant concentrations via passive air sampling were performed. PUF disk air samples were collected every month from October 2009 to December 2010 at an urban sampling site (Sülldorf/Hamburg) and a coastal sampling site (Tinnum/Sylt). Moreover, vertical profiles of pollutant concentrations in marine atmosphere were investigated at the FINO stations in the German EEZ. Atmospheric concentrations of target analytes are listed in the annex 1 for all sampling campaigns.

3.2.1 Active air sampling campaigns

This chapter is a brief overview of collected high-volume active air samples, including the geographical position of sampling sites, sampling parameters and meteorological conditions.

The sampling durations depended on the prevailing wind direction. Backward winds required an interruption of sampling in order to avoid the collection of ship emissions. Therefore, sampling duration and time of the sampling period may differentiate in the tables below. Meteorological parameters were obtained from ship based measurements. The mean values of air temperature, air pressure, relative humidity and wind velocity monitored over a sampling period are listed in the following tables.

Baltic Sea - April 2009

Air samples of the Baltic Sea atmosphere were obtained from a cooperative work with the University of Hamburg. The active air sampler (schematic illustration see figure 3.1(B)) was placed at the foredeck of the research ship Alkor (AL). GFFs and PUF plugs were used as trapping materials, whereof the GFF samples were not available for this sampling. Three PUF plugs (AL11, AL12 and AL13) were stored as field blanks (refer to chapter 4 and annex 2). Sampling parameters and sampling sites are given in table 3.1 and figure 3.8.

Table 3.1: Active air samples collected during the research cruise in the Baltic Sea in April 2009; D_s = sampling duration, V_s = sample volume, R_s = sampling rate, T = air temperature, p = air pressure, $r.h.$ = relative humidity, u = wind velocity

Sample name	Start of sampling		End of sampling		D_s in h	V_s in m ³	R_s in m ³ /h	T in °C	p in hPa	$r.h.$ in %	u in m/s
	Date	Time	Date	Time							
AL 1	26.04.09	20:24	27.04.09	07:24	11	437	40	11	1004	86	9
AL 2	27.04.09	08:47	28.04.09	07:26	23	875	39	11	1005	93	6
AL 3	28.04.09	07:51	28.04.09	20:55	13	525	40	10	1005	94	9

Table 3.1 continued:

Sample name	Start of sampling		End of sampling		D_s in h	V_s in m^3	R_s in m^3/h	T in $^{\circ}C$	p in hPa	$r.h.$ in %	u in m/s
	Date	Time	Date	Time							
AL 4	28.04.09	21:55	29.04.09	12:35	15	581	40	12	1008	80	5
AL 5	29.04.09	12:48	30.04.09	10:19	22	809	38	10	1015	92	9
AL 6	30.04.09	10:52	01.05.09	12:34	26	555	22	7	1024	97	11
AL 7	01.05.09	12:54	02.05.09	12:33	23	918	39	7	1027	92	4
AL 8	02.05.09	13:12	03.05.09	08:15	19	763	40	8	1024	88	6
AL 9	03.05.09	08:35	03.05.09	22:03	13	562	42	8	1019	93	7
AL 10	03.05.09	22:21	04.05.09	16:32	18	733	40	7	1013	98	7

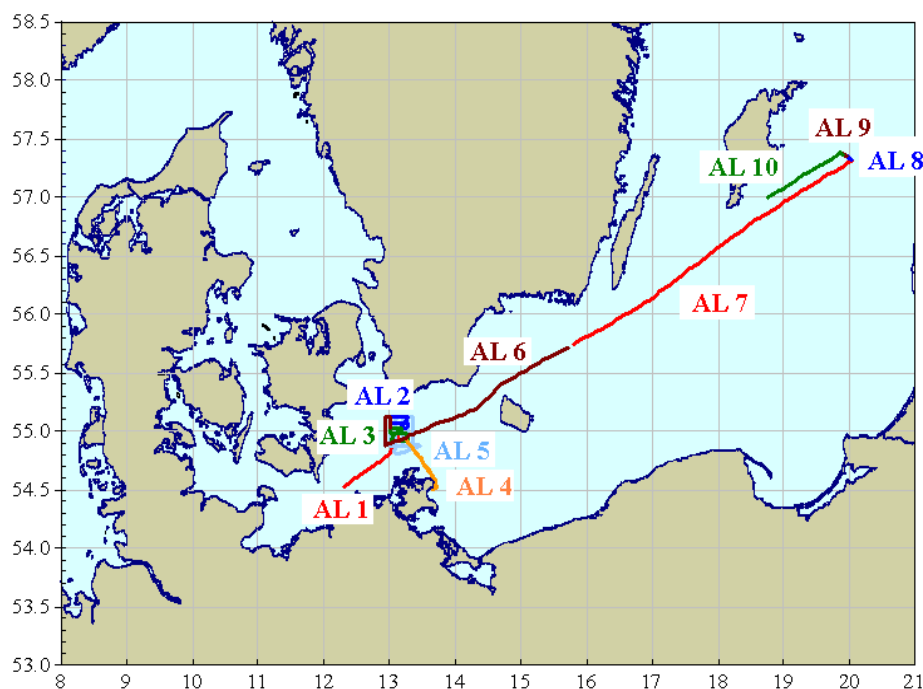


Figure 3.8: Ship positions corresponding to air samples collected during the Baltic Sea research cruise in April 2009

German EEZ – May/June 2009

The first air samples of the North Sea atmosphere were collected with a HZG high-volume active air sampler (schematic illustration see figure 3.1 (A)). It was installed on the top deck of the research vessel Atair (AT). GFFs and PUF/XAD-2/PUF sandwich cartridges were used as sampling materials. Four GFFs and adsorber cartridges (09AT 1, 09AT 6, 09AT 10, 09AT 13) were stored as field blanks, respectively (refer to chapter 4 and annex 2). Sampling parameters and sampling sites are given in table 3.2 and figure 3.9.

Table 3.2: Active air samples collected during the research cruise in the German EEZ in May/June 2009; D_s = sampling duration, V_s = sample volume, R_s = sampling rate, T = air temperature, p = air pressure, $r.h.$ = relative humidity, u = wind velocity

Sample name	Start of sampling		End of sampling		D_s in h	V_s in m ³	R_s in m ³ /h	T in °C	p in hPa	$r.h.$ in %	u in m/s
	Date	Time	Date	Time							
09AT 2	27.05.09	11:35	27.05.09	18:20	7	144	21	13	1019	77	14
09AT 3	28.05.09	07:41	28.05.09	19:47	12	182	15	11	1026	79	12
09AT 4	28.05.09	19:57	29.05.09	07:20	12	267	23	11	1032	89	9
09AT 5	29.05.09	07:30	29.05.09	18:45	11	241	21	12	1034	95	7
09AT 7	30.05.09	07:38	30.05.09	20:20	13	241	19	13	1032	93	7
09AT 8	30.05.09	20:28	31.05.09	17:45	21	508	24	13	1030	92	7
09AT 9	31.05.09	21:30	01.06.09	14:50	17	414	24	13	1029	94	7
09AT 11	01.06.09	17:00	02.06.09	07:20	14	332	23	12	1024	89	11
09AT 12	02.06.09	21:10	03.06.09	06:50	10	159	16	11	1019	77	14

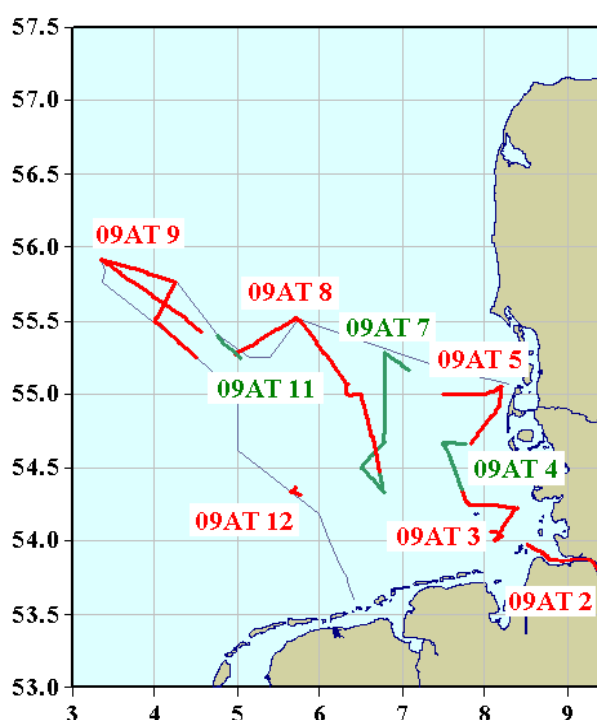


Figure 3.9: Ship positions corresponding to air samples collected during the research cruise in the German EEZ in May/June 2009

North Sea – August/September 2009

Air samples of the entire North Sea atmosphere were collected in August/September 2009 on the top deck of the research vessel Pelagia (PE). High-volume active air sampling was performed with the Digital DHM-60 system (schematic illustration see figure 3.2). GFFs and PUF/XAD-2/PUF sandwich cartridges equipped with gaze insertions to prevent the loss of XAD-2 were applied as trapping materials. Three GFFs and adsorber cartridges (PE 2, PE 12, PE 13) were stored as field blanks, respectively (refer to chapter 4 and annex 2). Two collected air samples (PE 5, PE 14)

contaminated by ship fumes were excluded from this study. The criterion for rejection was visible blackening (extreme example in figure 3.10) and/or wind direction (from close to the ship's stack). Sampling parameters and sampling sites are given in table 3.3 and figure 3.11.

Table 3.3: Active air samples collected during the research cruise in the North Sea in August/September 2009; D_s = sampling duration, V_s = sample volume, R_s = sampling rate, T = air temperature, p = air pressure, $r.h.$ = relative humidity, u = wind velocity

Sample name	Start of sampling		End of sampling		D_s in h	V_s in m ³	R_s in m ³ /h	T in °C	p in hPa	$r.h.$ in %	u in m/s
	Date	Time	Date	Time							
PE 1	21.08.09	06:02	21.08.09	17:11	9	222	25	17	1018	69	10
PE 3	22.08.09	10:47	22.08.09	22:47	12	297	25	17	1024	64	5
PE 4	23.08.09	13:27	24.08.09	10:13	21	518	25	17	1007	75	5
PE 6	26.08.09	14:01	26.08.09	21:24	7	174	25	20	1011	71	9
PE 7	27.08.09	07:36	27.08.09	18:00	10	251	25	17	1011	85	5
PE 8	28.08.09	07:24	28.08.09	15:11	7	219	30	14	1002	74	15
PE 9	30.08.09	05:43	30.08.09	18:01	12	316	26	15	1012	71	12
PE 10	31.08.09	06:48	31.08.09	17:47	11	284	26	17	1004	92	13
PE 11	02.09.09	06:39	02.09.09	18:39	12	311	26	15	1006	77	10
PE 15	04.09.09	05:21	04.09.09	17:21	12	314	26	14	991	85	14
PE 16	05.09.09	07:08	05.09.09	17:21	9	230	26	13	1008	82	7
PE 17	06.09.09	06:11	06.09.09	10:17	4	106	26	14	1011	14	8
PE 18	07.09.09	04:34	07.09.09	10:05	5	142	26	14	1000	14	17

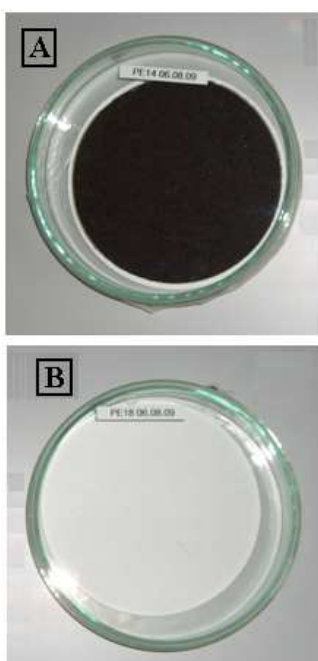


Figure 3.10: GFF contaminated by ship fumes (A); GFF air sample without ship fumes (B)

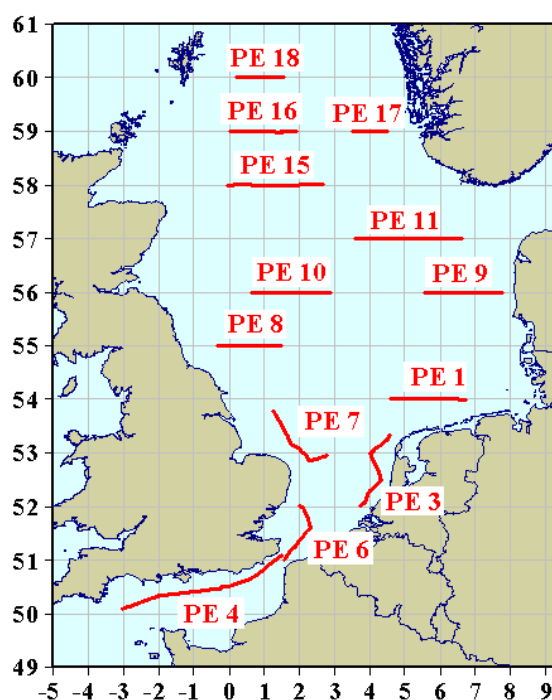


Figure 3.11: Ship positions corresponding to air samples collected during the research cruise in the North Sea in August/September 2009

German EEZ – May 2010

A second air sampling campaign in the German EEZ was carried out at the research vessel Atair in May 2010. The Digital DHM-60 sampler equipped with GFFS, PUF/XAD-2/PUF sandwich cartridges and gaze insertions was positioned on the top deck. Three GFFs and adsorber cartridges (10AT 8, 10AT 9, 10AT 10) were stored as field blanks, respectively (refer to chapter 4 and annex 2). Sampling parameters and sampling sites are given in table 3.4 and figure 3.12.

Table 3.4: Active air samples collected during the research cruise in the German EEZ in May 2010; D_s = sampling duration, V_s = sample volume, R_s = sampling rate, T = air temperature, p = air pressure, $r.h.$ = relative humidity, u = wind velocity

Sample name	Start of sampling		End of sampling		D_s in h	V_s in m ³	R_s in m ³ /h	T in °C	p in hPa	$r.h.$ in %	u in m/s
	Date	Time	Date	Time							
10AT 1	18.05.10	10:52	18.05.10	17:07	6	159	26	10	1025	81	N/A
10AT 2	19.05.10	08:18	19.05.10	17:52	8	206	26	10	1025	89	N/A
10AT 3	20.05.10	07:24	20.05.10	17:27	10	250	25	11	1029	85	N/A
10AT 4	21.05.10	07:25	22.05.10	03:48	12	306	26	10	1028	89	N/A
10AT 5	22.05.10	07:41	22.05.10	19:33	7	193	26	10	1026	94	N/A
10AT 6	22.05.10	20:31	23.05.10	07:12	10	261	26	11	1024	95	N/A
10AT 7	23.05.10	07:50	23.05.10	18:21	10	254	26	12	1020	96	N/A

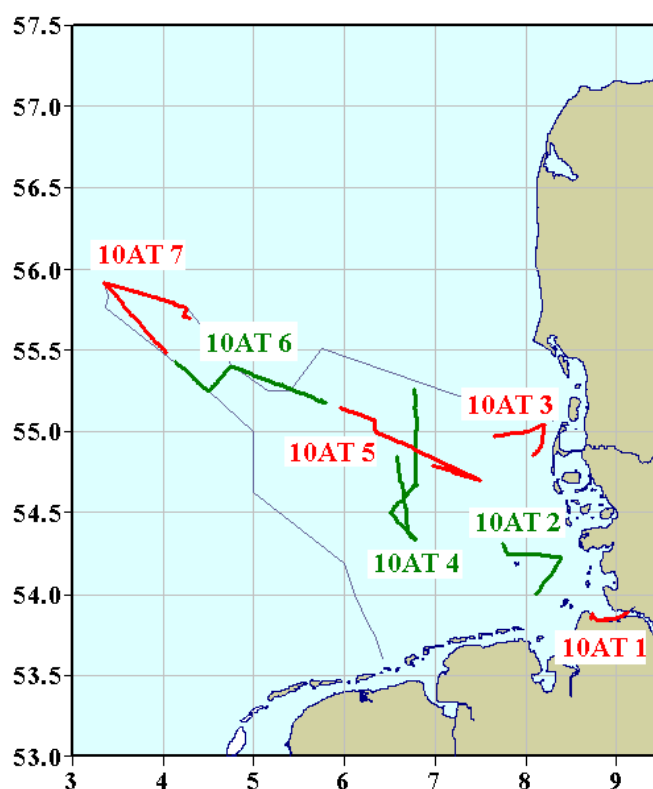


Figure 3.12: Ship positions corresponding to air samples collected during the research cruise in the German EEZ in May 2010

Sülldorf/Hamburg – November/December 2010

For purposes of method validation (refer to chapter 4), two Digital DHM-60 samplers (S1 and S2) were simultaneously deployed in Sülldorf/Hamburg on the ground of the BSH laboratory. The samplers were equipped with GFFs, PUF plugs and PUF/XAD-2/PUF sandwich adsorber cartridges including gaze insertions. Three field blanks of GFFs, PUF plugs and PUF/XAD-2/PUF sandwich cartridges were obtained, respectively. Sampling parameters and the geographical position of the sampling site are given in table 3.5 and figure 3.13.

Table 3.5: Active air samples collected in Sülldorf/Hamburg in November/December 2010; R = number of side-by-side sampler run; S = HVS number; D_s = sampling duration, V_s = sample volume, R_s = sampling rate

Sample name	Start of sampling		End of sampling		D_s in h	V_s in m ³	R_s in m ³ /h	Type of adsorber cartridge
	Date	Time	Date	Time				
R1S1	15.11.10	08:58	16.11.10	14:36	29	779	27	PUF plug
R1S2	15.11.10	09:04	16.11.10	18:24	33	879	27	PUF plug
R2S1	17.11.10	09:29	18.11.10	04:00	18	485	27	PUF plug
R2S2	17.11.10	09:29	18.11.10	04:00	18	475	27	PUF plug
R3S1	18.11.10	09:53	18.11.10	19:09	9	244	27	PUF plug
R3S2	18.11.10	09:52	18.11.10	19:08	9	230	27	sandwich
R4S1	22.11.10	08:22	22.11.10	19:29	11	294	27	PUF plug
R4S2	22.11.10	08:20	22.11.10	19:27	11	275	27	sandwich
R5S1	23.11.10	09:36	23.11.10	22:36	13	342	27	PUF plug
R5S2	23.11.10	09:37	23.11.10	22:35	13	325	27	sandwich
R6S1	29.11.10	08:42	29.11.10	23:31	14	386	27	PUF plug
R6S2	29.11.10	08:41	29.11.10	23:30	14	378	27	PUF plug
R7S1	30.11.10	09:06	30.11.10	20:14	11	287	27	PUF plug
R7S2	30.11.10	09:06	30.11.10	20:12	11	282	27	PUF plug
R8S1	01.12.10	09:43	01.12.10	18:59	9	231	27	sandwich
R8S2	01.12.10	09:42	01.12.10	18:58	9	224	27	sandwich
R9S1	02.12.10	09:15	02.12.10	20:22	10	280	27	sandwich
R9S2	02.12.10	09:14	02.12.10	20:21	10	271	27	sandwich
R10S1	06.12.10	07:35	06.12.10	20:33	12	329	27	sandwich
R10S2	06.12.10	07:33	06.12.10	20:31	12	322	27	sandwich

3.2.2 Passive air sampling campaigns

The seasonal and vertical transects of organic contaminants in the marine atmosphere were examined via PUF disk passive air samplers. This chapter summarizes the passive air samples collected in Sülldorf/Hamburg, Tinnum/Sylt and at the FINO research stations of the German EEZ. Monthly averaged meteorological parameters were obtained from the Deutscher Wetterdienst (DWD) for the sampling sites Fuhlsbüttel (Hamburg), List (Sylt) and Heligoland.

Moreover, passive air samplers were exposed during sea cruises in the German EEZ and the wider North Sea in order to obtain first experiences in passive air sampling in the marine

atmosphere. One field blank was obtained for each collected air sample (chapter 4 and annex 2). Sampling parameters are listed in table 3.6.

Table 3.6: Passive air samples collected during sea cruises; 09AT = Atair cruise in the German EEZ in May/June 2009; 10AT = Atair cruise in the German EEZ in May 2010; PE = Pelagia cruise in the North Sea in August/September 2009; D_s = sampling duration, T = air temperature, p = air pressure, $r.h.$ = relative humidity, u = wind velocity

Sample name	Sampling site	Start of sampling	End of sampling	D_s in d	T in °C [2m]	p in hPa	$r.h.$ in %	u in m/s
09AT A	German EEZ	27.05.09	04.06.09	9	12	1026	85	9
09AT C	German EEZ	27.05.09	04.06.09	9	12	1026	85	9
09AT E	German EEZ	27.05.09	04.06.09	9	12	1026	85	9
09AT G	German EEZ	27.05.09	04.06.09	9	12	1026	85	9
10AT A	German EEZ	18.05.10	26.05.10	9	11	1025	90	N/A
10AT C	German EEZ	18.05.10	26.05.10	9	11	1025	90	N/A
PE A	North Sea	21.08.09	08.09.09	19	16	1008	67	10
PE C	North Sea	21.08.09	08.09.09	19	16	1008	67	10

Seasonal fluctuations of organic contaminants in atmosphere

Passive air samples were collected in Sülldorf/Hamburg, an urban (residential) sampling site, and in Tinum/Sylt, a coastal (rural) sampling site. Tinum is located approximately in 2–3 km distance from Westerland and the the coast, respectively. Sülldorf is an outer urban district in the west of Hamburg. PUF disks were simultaneously exchanged in fixed time intervals of 28 days in the period from October 2009 to December 2010. The long-term study with constant sampling durations enables the monitoring of seasonal profiles of pollutant concentrations in the urban and coastal atmospheres. In general, one PUF disk per month and sampling site was stored as field blank (chapter 4 and annex 2). Sampling sites and parameters are given in figure 3.13, table 3.7 and table 3.8.

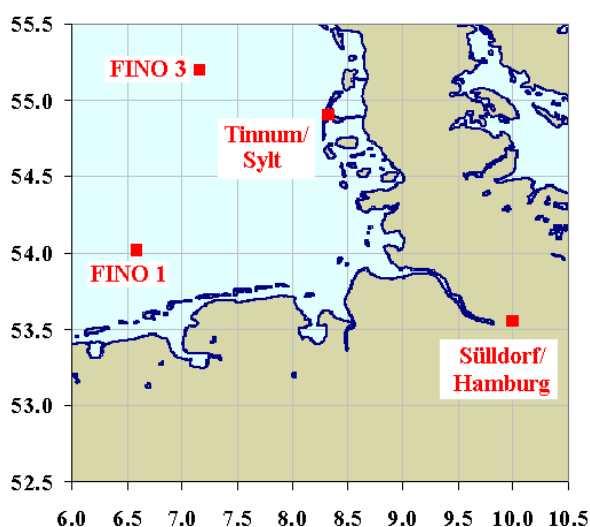


Figure 3.13: Geographical positions of the sampling sites in Sülldorf/Hamburg, Tinum/Sylt and the FINO stations in the German EEZ

Table 3.7: Passive air samples collected in Sülldorf/Hamburg; D_s = sampling duration, T = air temperature, p = air pressure, $r.h.$ = relative humidity, u = wind velocity

Sample name	Month	Start of sampling	End of sampling	D_s in d	T in °C [2m]	p in hPa	$r.h.$ in %	u in m/s
Sülld. G	Oct. 2009	12.10.2009	09.11.2009	28	7	1012	84	4
Sülld. I	Nov. 2009	09.11.2009	07.12.2009	28	8	1005	84	5
Sülld. K	Dec. 2009	07.12.2009	04.01.2010	28	0	1007	87	4
Sülld. M	Jan. 2010	04.01.2010	01.02.2010	28	-3	1015	85	4
Sülld. O	Feb. 2010	01.02.2010	01.03.2010	28	0	1003	86	4
Sülld. Q	Feb. 2010	01.02.2010	01.03.2010	28	0	1003	86	4
Sülld. S	Mar. 2010	01.03.2010	29.03.2010	28	4	1015	81	4
Sülld. U	Apr. 2010	29.03.2010	26.04.2010	28	8	1016	70	4
Sülld. W	May 2010	26.04.2010	25.05.2010	29	10	1013	78	4
Sülld. Y	Jun. 2010	25.05.2010	21.06.2010	27	14	1011	75	3
Sülld. Z	Jul. 2010	21.06.2010	19.07.2010	28	21	1016	63	3
Sülld. AB	Aug. 2010	19.07.2010	16.08.2010	28	19	1012	74	3
Sülld. AC	Aug. 2010	19.07.2010	16.08.2010	28	19	1012	74	3
Sülld. AE	Sep. 2010	16.08.2010	13.09.2010	28	15	1012	81	4
Sülld. AG	Oct. 2010	13.09.2010	11.10.2010	28	12	1012	85	4
Sülld. AI	Nov. 2010	11.10.2010	08.11.2010	28	8	1010	88	4
Sülld. AK	Dec. 2010	08.11.2010	06.12.2010	28	2	1003	89	4

Table 3.8: Passive air samples collected in Tinnum/Sylt; D_s = sampling duration, T = air temperature, p = air pressure, $r.h.$ = relative humidity, u = wind velocity

Sample name	Month	Start of sampling	End of sampling	D_s in d	T in °C [2m]	p in hPa	$r.h.$ in %	u in m/s
Sylt A	Oct. 2009	12.10.2009	09.11.2009	28	8	1010	86	7
Sylt C	Nov. 2009	09.11.2009	07.12.2009	28	8	1001	90	9
Sylt E	Dec. 2009	07.12.2009	04.01.2010	28	1	1005	91	7
Sylt G	Jan. 2010	04.01.2010	01.02.2010	28	-2	1013	91	7
Sylt H	Feb. 2010	01.02.2010	01.03.2010	28	-1	1001	92	7
Sylt I	Mar. 2010	01.03.2010	29.03.2010	28	3	1012	90	7
Sylt K	Apr. 2010	29.03.2010	26.04.2010	28	7	1011	80	7
Sylt M	May 2010	26.04.2010	25.05.2010	29	9	1012	80	8
Sylt O	Jun. 2010	25.05.2010	21.06.2010	27	13	1010	78	7
Sylt Q	Jul. 2010	21.06.2010	19.07.2010	28	18	1015	76	6
Sylt R	Aug. 2010	19.07.2010	17.08.2010	29	18	1010	79	6
Sylt S	Sep. 2010	17.08.2010	13.09.2010	27	16	1010	80	8
Sylt U	Oct. 2010	13.09.2010	11.10.2010	28	13	1009	84	8
Sylt W	Nov. 2010	11.10.2010	08.11.2010	28	9	1006	85	8
Sylt Y	Dec. 2010	08.11.2010	06.12.2010	28	2	1002	90	7

Vertical distribution of organic contaminants in the marine atmosphere

Three air sampling campaigns were performed at the research platforms FINO 1 and FINO 3 in the EEZ of Germany. The masts positioned on these stations enabled the simultaneous deployment of passive air samplers in 40 m, 60 m and 80 m height above the FINO platform (installed 20 m above the sea level) for periods ranging from 5 to 7 weeks. The campaigns aim to investigate vertical

variations of pollutant concentrations in the marine atmosphere. Geographical positions and photography of the sampling sites are illustrated in figures 3.13 and 3.14, respectively. FINO 1 is located at the Borkum Riffgrund in approximately 40 km distance to the coast, whereas FINO 3 is positioned approximately 70 km west of the island Sylt. Three PUF disks per campaign were stored as field blanks. Sampling parameters are given in table 3.9. The meteorological parameters for Heligoland were obtained from the DWD.



Figure 3.14: PAS deployment at FINO 1 in the German EEZ

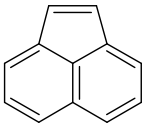
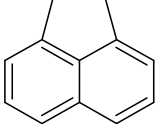
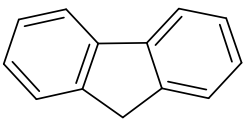
Table 3.9: Passive air samples collected at the FINO research stations; D_s = sampling duration, T = air temperature, p = air pressure, $r.h.$ = relative humidity, u = wind velocity

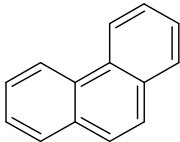
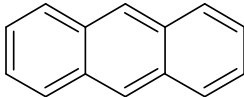
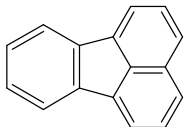
Sample name	Sampling height in m	Start of sampling	End of sampling	D_s in d	T in °C [2m]	p in hPa	$r.h.$ in %	u in m/s
FINO1 A	40	03.08.2010	22.09.2010	50	16	1012	77	8
FINO1 B	60	03.08.2010	22.09.2010	50	16	1012	77	8
FINO1 C	80	03.08.2010	22.09.2010	50	16	1012	77	8
FINO3 A	40	10.08.2010	29.09.2010	50	16	1011	78	8
FINO3 C	60	10.08.2010	29.09.2010	50	16	1011	78	8
FINO3 E	80	10.08.2010	29.09.2010	50	16	1011	78	8
FINO1 G	40	22.09.2010	26.10.2010	34	12	1012	78	9
FINO1 H	60	22.09.2010	26.10.2010	34	12	1012	78	9
FINO1 I	80	22.09.2010	26.10.2010	34	12	1012	78	9

3.3 Target compounds

A total of 87 organic pollutants, known to be present in the surface water of the North Sea and the river Elbe are targeted in this study. According to their structural characteristics and their field of application, they may be grouped into polycyclic aromatic hydrocarbons, organochlorine pesticides, polychlorinated biphenyls, polar pesticides, perfluorinated compounds, organophosphorus/brominated flame retardants and pharmaceuticals. An overview is given in table 3.10.

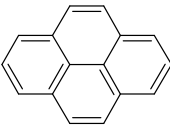
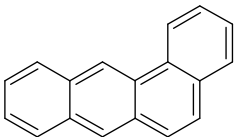
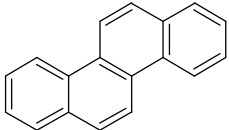
Table 3.10: Target compounds

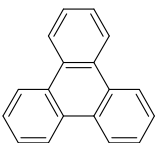
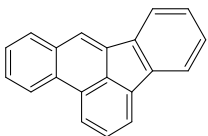
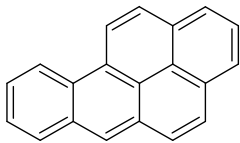
Pollutant group	Polycyclic Aromatic Hydrocarbons (PAHs)		
Pollutant sub group	2 benzene rings		
Common name	Acenaphthylene	Acenaphthene	Fluorene
IUPAC name	Acenaphthylene	Acenaphthene	Fluorene
Abbreviation	ACY	ACE	Fl
Chemical Structure			
Sum formula	C ₁₂ H ₈	C ₁₂ H ₈	C ₁₃ H ₁₀
Molar mass	152.19 g/mol	152.19 g/mol	166.22 g/mol

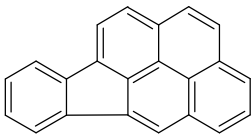
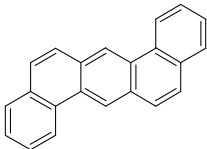
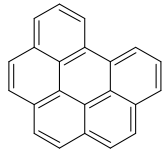
Pollutant sub group	3 benzene rings		
Common name	Phenanthrene	Anthracene	Fluoranthene
IUPAC name	Phenanthrene	Anthracene	Fluoranthene
Abbreviation	PHEN	ANT	FLU
Chemical Structure			
Sum formula	C ₁₄ H ₁₀	C ₁₄ H ₁₀	C ₁₆ H ₁₀
Molar mass	178.23 g/mol	178.23 g/mol	202.25 g/mol

Pollutant sub group	4 benzene rings		
Common name	Pyrene	Benzo[<i>a</i>]anthracene	Chrysene
IUPAC name	Pyrene	Benzo[<i>a</i>]anthracene	Chrysene

Table 3.10 continued:

Abbreviation	PYR	BAA	CHR
Chemical Structure			
Sum formula	C ₁₆ H ₁₀	C ₁₈ H ₁₂	C ₁₈ H ₁₂
Molar mass	202.25 g/mol	228.29 g/mol	228.29 g/mol

Pollutant sub group	4 benzene rings		5 benzene rings
Common name	Triphenylene	Benzo[<i>b</i>]fluoranthene	Benzo[<i>a</i>]pyrene
IUPAC name	Triphenylene	Benzo[<i>b</i>]fluoranthene	Benzo[<i>a</i>]pyrene
Abbreviation	TR	BBF	BAP
Chemical Structure			
Sum formula	C ₁₈ H ₁₂	C ₂₀ H ₁₂	C ₂₀ H ₁₂
Molar mass	228.29 g/mol	252.31 g/mol	252.31 g/mol

Pollutant sub group	5 benzene rings		6 benzene rings
Common name	Indeno[1,2,3- <i>cd</i>]pyrene	Dibenzo[<i>a,h</i>]anthracene	Benzo[<i>g,h,i</i>]perylene
IUPAC name	Indeno[1,2,3- <i>cd</i>]pyrene	Dibenzo[<i>a,h</i>]anthracene	Benzo[<i>g,h,i</i>]perylene
Abbreviation	I123P	DBAHA	BGHIP
Chemical Structure			
Sum formula	C ₂₂ H ₁₂	C ₂₂ H ₁₄	C ₂₂ H ₁₂
Molar Mass	276.33 g/mol	278.35 g/mol	276.33 g/mol

Pollutant group	Organochlorine Pesticides (OCPs)		
Pollutant sub group	Chlorinated Benzenes		Hexachlorocyclohexanes
Common name	Pentachlorobenzene	Hexachlorobenzene	α-Hexachlorocyclohexane
IUPAC name	1,2,3,4,5-Pentachlorobenzene	1,2,3,4,5,6-Hexachlorobenzene	1 <i>R</i> ,2 <i>R</i> ,3 <i>S</i> ,4 <i>R</i> ,5 <i>S</i> ,6 <i>S</i> -Hexachlorocyclohexane

Table 3.10 continued:

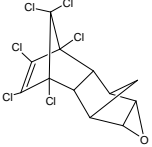
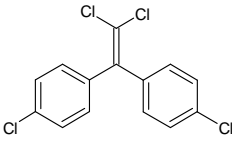
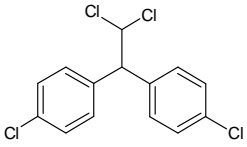
Abbreviation	QCB	HCB	HCHA
Chemical Structure			
Sum formula	C ₆ HCl ₅	C ₆ Cl ₆	C ₆ H ₆ Cl ₆
Molar mass	250.32 g/mol	284.76 g/mol	290.81 g/mol

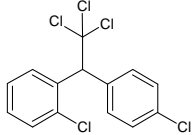
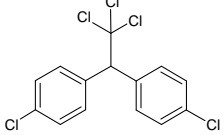
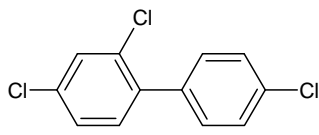
Pollutant sub group	Hexachlorocyclohexanes		
Common name	β-Hexachlorocyclohexane	γ-Hexachlorocyclohexane / Lindane	δ-Hexachlorocyclohexane
IUPAC name	1 <i>R</i> ,2 <i>S</i> ,3 <i>R</i> ,4 <i>S</i> ,5 <i>R</i> ,6 <i>S</i> -Hexachlorocyclohexane	1 <i>R</i> ,2 <i>R</i> ,3 <i>S</i> ,4 <i>R</i> ,5 <i>R</i> ,6 <i>S</i> -Hexachlorocyclohexane	1 <i>R</i> ,2 <i>R</i> ,3 <i>R</i> ,4 <i>S</i> ,5 <i>R</i> ,6 <i>S</i> -Hexachlorocyclohexane
Abbreviation	HCHB	HCHG	HCHD
Chemical Structure			
Sum formula	C ₆ H ₆ Cl ₆	C ₆ H ₆ Cl ₆	C ₆ H ₆ Cl ₆
Molar mass	290.81 g/mol	290.81 g/mol	290.81 g/mol

Pollutant sub group	Cyclodienes		
Common name	Aldrin	Isodrin	Dieldrin
IUPAC name	(1 <i>R</i> ,4 <i>S</i> ,4 <i>aS</i> ,5 <i>S</i> ,8 <i>R</i> ,8 <i>aR</i>)-1,2,3,4,10,10-hexachloro-1,4,4 <i>a</i> ,5,8,8 <i>a</i> -hexahydro-1,4:5,8-dimethanonaphthalene	(1 <i>R</i> ,4 <i>S</i> ,5 <i>R</i> ,8 <i>S</i>)-1,2,3,4,10,10-hexachloro-1,4,4 <i>a</i> ,5,8,8 <i>a</i> -hexahydro-1,4:5,8-dimethanonaphthalene	(1 <i>R</i> ,4 <i>S</i> ,4 <i>aS</i> ,5 <i>R</i> ,6 <i>R</i> ,7 <i>S</i> ,8 <i>S</i> ,8 <i>aR</i>)-1,2,3,4,10,10-hexachloro-1,4,4 <i>a</i> ,5,6,7,8,8 <i>a</i> -octahydro-6,7-epoxy-1,4:5,8-dimethanonaphthalene
Abbreviation	ALD	ISOD	DIELD
Chemical Structure			
Sum formula	C ₁₂ H ₈ Cl ₆	C ₁₂ H ₈ Cl ₆	C ₁₂ H ₈ Cl ₆ O
Molar mass	364.89 g/mol	364.89 g/mol	380.89 g/mol

Pollutant sub group	Cyclodienes	DDT	
Common name	Endrin	<i>p,p'</i> -Dichlorodiphenyl-dichloroethylene	<i>p,p'</i> -Dichlorodiphenyl-dichloroethane

Table 3.10 continued:

IUPAC name	(1 <i>R</i> ,4 <i>S</i> ,4 <i>aS</i> ,5 <i>S</i> ,6 <i>S</i> ,7 <i>R</i> ,8 <i>R</i> ,8 <i>aR</i>)-1,2,3,4,10,10-hexachloro-1,4,4 <i>a</i> ,5,6,7,8,8 <i>a</i> -octahydro-6,7-epoxy-1,4:5,8-dimethanonaphthalene	1,1-bis-(4-chlorophenyl)-2,2-dichloroethene	1-chloro-4-[2,2-dichloro-1-(4-chlorophenyl)ethyl] benzene
Abbreviation	END	DDEPP	DDDPP
Chemical Structure			
Sum formula	C ₁₂ H ₈ Cl ₆ O	C ₁₄ H ₈ Cl ₄	C ₁₄ H ₁₀ Cl ₄
Molar mass	380.89 g/mol	318.01 g/mol	320.03 g/mol

Pollutant sub group	DDT		Polychlorinated Biphenyls (PCBs)
Common name	<i>o,p'</i> -Dichlorodiphenyl-trichloroethane	<i>p,p'</i> -Dichlorodiphenyl-trichloroethane	Polychlorinated Biphenyl 28
IUPAC name	1,1,1-trichloro-2-(2-chlorophenyl)-2-(4-chlorophenyl)ethane	1,1,1-trichloro-2,2-di(4-chlorophenyl) ethane	2,4,4'-Trichlorobiphenyl
Abbreviation	DDTOP	DDTPP	CB28
Chemical Structure			
Sum formula	C ₁₄ H ₉ Cl ₅	C ₁₄ H ₉ Cl ₅	C ₁₂ H ₇ Cl ₃
Molar mass	354.47 g/mol	354.47 g/mol	257.53 g/mol

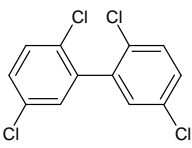
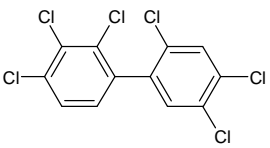
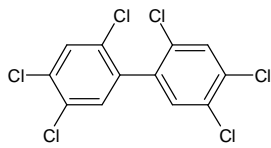
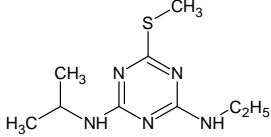
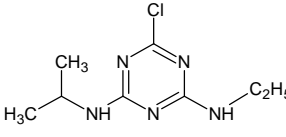
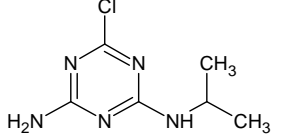
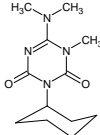
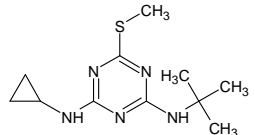
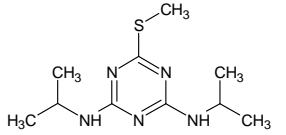
Pollutant sub group	Polychlorinated Biphenyls (PCBs)		
Common name	Polychlorinated Biphenyl 52	Polychlorinated Biphenyl 138	Polychlorinated Biphenyl 153
IUPAC name	2,2',5,5'-Tetrachlorobiphenyl	2,2',3,4,4',5'-Hexachlorobiphenyl	2,2',4,4',5,5'-Hexachlorobiphenyl
Abbreviation	CB52	CB138	CB153
Chemical Structure			
Sum formula	C ₁₂ H ₆ Cl ₄	C ₁₂ H ₄ Cl ₆	C ₁₂ H ₄ Cl ₆
Molar mass	291.98 g/mol	360.86 g/mol	360.86 g/mol

Table 3.10 continued:

Pollutant group	Polar Pesticides		
Pollutant sub group	Triazines		
Common name	Ametryn	Atrazine	Desethylatrazine
IUPAC name	<i>N</i> 2-ethyl- <i>N</i> 4-(1-methylethyl)-6-methylthio-1,3,5-triazine-2,4-diamine	6-chloro- <i>N</i> 2-ethyl- <i>N</i> 4-(1-methylethyl)-1,3,5-triazine-2,4-diamine	6-chloro- <i>N</i> 2-(1-methylethyl)-1,3,5-triazine-2,4-diamine
Abbreviation	AMETRYN	ATRAZ	DEATRAZ
Chemical Structure			
Sum formula	C ₉ H ₁₇ N ₅ S	C ₈ H ₁₄ ClN ₅	C ₆ H ₁₀ ClN ₅
Molar mass	227.32 g/mol	215.68 g/mol	187.63 g/mol

Pollutant sub group	Triazines		
Common name	Hexazinone	Irgarol	Prometryn
IUPAC name	3-cyclohexyl-1-methyl-6-(dimethylamino)-1,3,5-triazine-2,4-dione	<i>N</i> 4-cyclopropyl- <i>N</i> 2-(1,1-dimethylethyl)-6-methylthio-1,3,5-triazine-2,4-diamine	<i>N</i> 2, <i>N</i> 4-bis(1-methylethyl)-6-methylthio-1,3,5-triazine-2,4-diamine
Abbreviation	HEXAZIN	IRGAROL	PROMETR
Chemical Structure			
Sum formula	C ₁₂ H ₂₀ N ₄ O ₂	C ₁₁ H ₁₉ N ₅ S	C ₁₀ H ₁₉ N ₅ S
Molar mass	252.31 g/mol	253.36 g/mol	241.35 g/mol

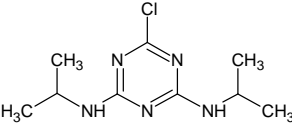
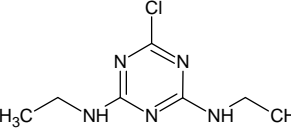
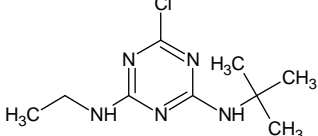
Pollutant sub group	Triazines		
Common name	Propazin	Simazine	Terbutylazine
IUPAC name	6-chloro- <i>N</i> 2, <i>N</i> 4-bis(1-methylethyl)-1,3,5-triazine-2,4-diamine	6-chloro- <i>N</i> 2, <i>N</i> 4-diethyl-1,3,5-triazine-2,4-diamine	6-chloro- <i>N</i> 4-ethyl- <i>N</i> 2-(1,1-dimethylethyl)-1,3,5-triazine-2,4-diamine
Abbreviation	PROPAZ	SIMAZ	TERBAZ
Chemical Structure			
Sum formula	C ₉ H ₁₆ ClN ₅	C ₇ H ₁₂ ClN ₅	C ₉ H ₁₆ ClN ₅
Molar mass	229.71 g/mol	201.65 g/mol	229.71 g/mol

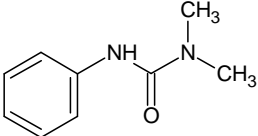
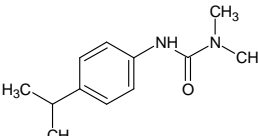
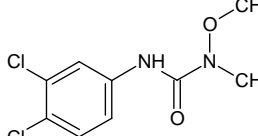
Table 3.10 continued:

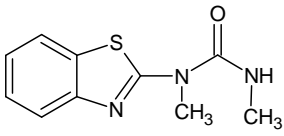
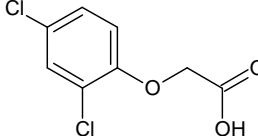
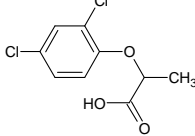
Pollutant sub group	Triazines	Organophosphates	
Common name	Terbutryn	Chlorfenvinphos	Malathion
IUPAC name	<i>N</i> 4-ethyl- <i>N</i> 2-(1,1-dimethylethyl)-6-methylthio-1,3,5-triazine-2,4-diamine	2-chloro-1-(2,4-dichlorophenyl)vinyl diethyl phosphate	diethyl-2-[(dimethoxyphosphorothioyl)sulfanyl]butanedioate
Abbreviation	TERBUTR	CHLORFENV	MALATH
Chemical Structure			
Sum formula	C ₁₀ H ₁₉ N ₅ S	C ₁₂ H ₁₄ Cl ₃ O ₄ P	C ₁₀ H ₁₉ O ₆ PS ₂
Molar mass	241.35 g/mol	359.54 g/mol	330.35 g/mol

Pollutant sub group	Organophosphates		
Common name	Azinphos-ethyl	Azinphos-methyl	Diazinone
IUPAC name	3-(diethoxyphosphinothioylsulfanylmethyl)-1,2,3-benzotriazin-4-one	3-(dimethoxyphosphinothioylsulfanylmethyl)-1,2,3-benzotriazin-4-one	<i>O,O</i> -diethyl- <i>O</i> -[2-(1-methylethyl)-6-methylpyrimidin-4-yl]phosphorothioate
Abbreviation	AZINPH-E	AZINPH-M	DIAZINON
Chemical Structure			
Sum formula	C ₁₂ H ₁₆ N ₃ O ₃ PS ₂	C ₁₀ H ₁₂ N ₃ O ₃ PS ₂	C ₁₂ H ₂₁ N ₂ O ₃ PS
Molar mass	345.37 g/mol	317.31 g/mol	304.34 g/mol

Pollutant sub group	Organophosphates	Phenylureas	
Common name	Dimethoate	Chlortoluron	Diuron
IUPAC name	<i>O,O</i> -Dimethyl- <i>S</i> -[2-(methylamino)-2-oxoethyl]dithiophosphate	3-(3-chloro-4-methylphenyl)-1,1-dimethylurea	3-(3,4-dichlorophenyl)-1,1-dimethylurea
Abbreviation	DIMETH	CHLORTUR	DIURON
Chemical Structure			
Sum formula	C ₅ H ₁₂ N ₃ O ₃ PS ₂	C ₁₀ H ₁₃ ClN ₂ O	C ₉ H ₁₀ Cl ₂ N ₂ O
Molar mass	229.25 g/mol	212.67 g/mol	233.09 g/mol

Table 3.10 continued:

Pollutant sub group	Phenylureas		
Common name	Fenuron	Isoproturon	Linuron
IUPAC name	1,1-dimethyl-3-phenylurea	3-(4-(1-methyl-ethyl)phenyl)-1,1-dimethylurea	3-(3,4-dichlorophenyl)-1-methoxy-1-methylurea
Abbreviation	FENUR	ISOPRUR	LINUR
Chemical Structure			
Sum formula	C ₉ H ₁₂ N ₂ O	C ₁₂ H ₁₈ N ₂ O	C ₉ H ₁₀ Cl ₂ N ₂ O ₂
Molar mass	164.20 g/mol	206.28 g/mol	249.09 g/mol

Pollutant sub group	Phenylureas	Phenoxyacetic acids	
Common name	Methabenzthiazuron	2,4-D	Dichlorprop
IUPAC name	1-(1,3-benzothiazol-2-yl)-1,3-dimethylurea	(2,4-dichlorophenoxy) acetic acid	2-(2,4-dichlorophenoxy) propanoic acid
Abbreviation	METHABZT	24-D	DICHLPR
Chemical Structure			
Sum formula	C ₁₀ H ₁₁ N ₃ OS	C ₈ H ₆ Cl ₂ O ₃	C ₉ H ₈ Cl ₂ O ₃
Molar mass	221.27 g/mol	221.03 g/mol	235.06 g/mol

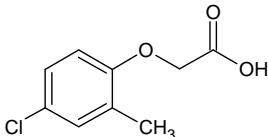
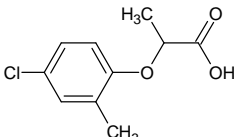
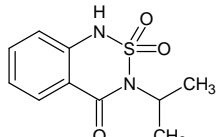
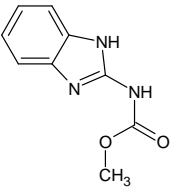
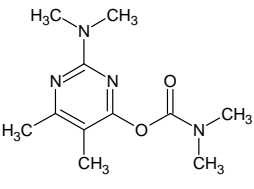
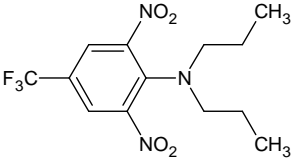
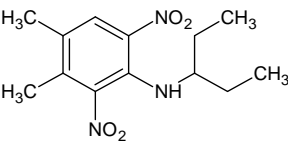
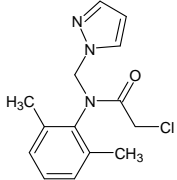
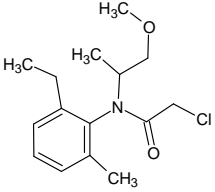
Pollutant sub group	Phenoxyacetic acids		Thiadiazine
Common name	MCPA	Mecoprop	Bentazon
IUPAC name	(4-chloro-2-methylphenoxy) acetic acid	2-(4-chloro-2-methylphenoxy) propanoic acid	3-(1-methylethyl)-1 <i>H</i> -2,1,3-benzothiadiazin-4(3 <i>H</i>)-one-2,2-dioxide
Abbreviation	MCPA	MECOPR	BENTAZ
Chemical Structure			
Sum formula	C ₉ H ₉ ClO ₃	C ₁₀ H ₁₁ ClO ₃	C ₁₀ H ₁₂ N ₂ O ₃ S
Molar mass	200.62 g/mol	214.64 g/mol	240.27 g/mol

Table 3.10 continued:

Pollutant sub group	Carbamates		2,6-Dinitroanilines
Common name	Carbendazim	Pirimicarb	Trifluralin
IUPAC name	Methyl-benzimidazol-2-yl-carbamate	(2-Dimethylamino-5,6-dimethylpyrimidin-4-yl)- <i>N,N</i> -dimethyl-carbamate	2,6-Dinitro- <i>N,N</i> -dipropyl-4-(trifluoromethyl)-aniline
Abbreviation	CARBEND	PIRIMIC	TRIFLU
Chemical Structure			
Sum formula	C ₉ H ₉ N ₃ O ₂	C ₁₁ H ₁₈ N ₄ O ₂	C ₁₃ H ₁₆ F ₃ N ₃ O ₄
Molar mass	191.19 g/mol	238.29 g/mol	335.28 g/mol

Pollutant sub group	2,6-Dinitroanilines	Chloroacetanilides	
Common name	Pendimethalin	Metazachlor	Metolachlor
IUPAC name	3,4-Dimethyl-2,6-dinitro- <i>N</i> -pentan-3-yl-aniline	2-Chloro- <i>N</i> -(pyrazol-1-yl-methyl)-acet-2',6'-xylylidide	2-Chloro- <i>N</i> -(2-ethyl-6-methyl-phenyl)- <i>N</i> -(1-methoxypropan-2-yl)acetamide
Abbreviation	PENDIMETH	METAZCHL	METOLA
Chemical Structure			
Sum formula	C ₁₃ H ₁₉ N ₃ O ₄	C ₁₄ H ₁₆ ClN ₃ O	C ₁₅ H ₂₂ ClNO ₂
Molar mass	281.31 g/mol	277.75 g/mol	283.79 g/mol

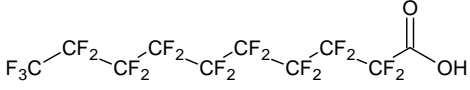
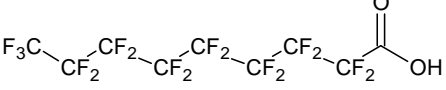
Pollutant group	Perfluorinated Compounds (PFCs)	
Pollutant sub group	Perfluoroalkyl Carboxylates (PFCAs)	
Common name	Perfluorodecanoic acid	Perfluorononanoic acid
IUPAC name	2,2,3,3,4,4,5,5,6,6,7,7,8,8,9,9,10,10-Nonadecafluorodecanoic acid	2,2,3,3,4,4,5,5,6,6,7,7,8,8,9,9,9-Heptadecafluorononanoic acid
Abbreviation	PFDEA	PFNOA
Chemical Structure		
Sum formula	C ₁₀ HF ₁₉ O ₂	C ₉ HF ₁₇ O ₂
Molar mass	514.08 g/mol	464.08 g/mol

Table 3.10 continued:

Pollutant sub group	Perfluoroalkyl Carboxylates (PFCAs)	
Common name	Perfluorooctanoic acid	Perfluoroheptanoic acid
IUPAC name	2,2,3,3,3,4,4,5,5,6,6,7,7,8,8,8-Pentadecafluorooctanoic acid	2,2,3,3,3,4,4,5,5,6,6,7,7,7-Tridecafluoroheptanoic acid
Abbreviation	PFOA	PFHPA
Chemical Structure		
Sum formula	C ₈ HF ₁₅ O ₂	C ₇ HF ₁₃ O ₂
Molar mass	414.07 g/mol	364.06 g/mol

Pollutant sub group	Perfluoroalkyl Carboxylates (PFCAs)	Perfluoroalkyl sulfonates (PFSAs)
Common name	Perfluorohexanoic acid	Perfluorooctanesulfonic acid
IUPAC name	2,2,3,3,3,4,4,5,5,6,6,6-Undecafluorohexanoic acid	1,1,2,2,3,3,3,4,4,5,5,6,6,7,7,8,8,8-Hepta-decafluoro-1-octane sulfonic acid
Abbreviation	PFHXA	PFOS
Chemical Structure		
Sum formula	C ₆ HF ₁₁ O ₂	C ₈ HF ₁₇ O ₃ S
Molar mass	314.05 g/mol	500.12 g/mol

Pollutant sub group	Perfluoroalkyl sulfonates (PFSAs)	
Common name	Perfluorohexanesulfonic acid	Perfluorobutanesulfonic acid
IUPAC name	1,1,2,2,3,3,3,4,4,5,5,6,6,6-Tridecafluorohexane-1-sulfonic acid	1,1,2,2,3,3,3,4,4,4-Nonafluorobutane-1-sulfonic acid
Abbreviation	PFHXS	PFBS
Chemical Structure		
Sum formula	C ₆ HF ₁₃ O ₃ S	C ₄ HF ₉ O ₃ S
Molar mass	400.11 g/mol	300.09 g/mol

Pollutant sub group	Perfluorinated sulfonamide
Common name	Perfluorooctanesulfonamide
IUPAC name	1,1,2,2,3,3,3,4,4,5,5,6,6,7,7,8,8,8-Hepta-decafluorooctane-1-sulfonamide

Table 3.10 continued:

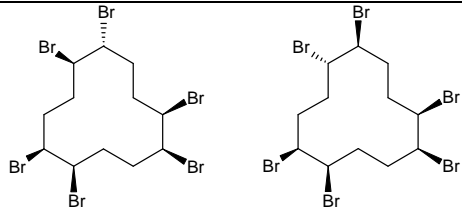
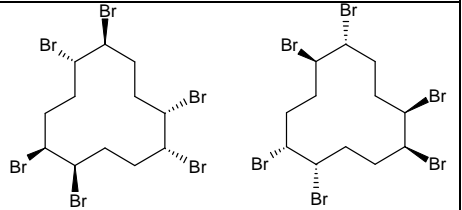
Abbreviation	PFOSA
Chemical Structure	
Sum formula	C ₈ H ₂ F ₁₇ NO ₂ S
Molar mass	499.14 g/mol

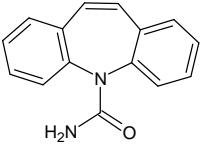
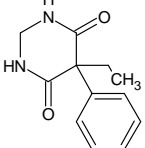
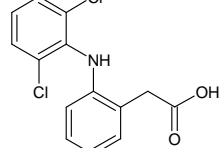
Pollutant group	Flame Retardants	
Pollutant sub group	Organophosphorus Flame Retardants	
Common name	Tris(2-butoxyethyl) phosphate	Tributyl phosphate
IUPAC name	Tris(2-butoxyethyl) phosphate	Tributyl phosphate
Abbreviation	TBEP	TBP
Chemical Structure		
Sum formula	C ₁₈ H ₃₉ O ₇ P	C ₁₂ H ₂₇ O ₄ P
Molar mass	398.47 g/mol	266.31 g/mol

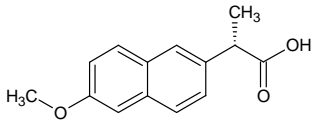
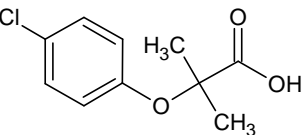
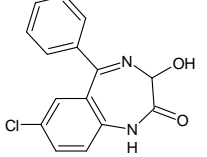
Pollutant sub group	Organophosphorus Flame Retardants	Brominated Flame Retardants
Common name	Triphenyl phosphate	α-Hexabromocyclododecane
IUPAC name	Triphenyl phosphate	1 <i>R</i> ,2 <i>R</i> ,5 <i>S</i> ,6 <i>R</i> ,9 <i>R</i> ,10 <i>S</i> -Hexabromocyclododecane
Abbreviation	TPP	HBCDA
Chemical Structure		
Sum formula	C ₁₈ H ₁₅ O ₄ P	C ₁₂ H ₁₈ Br ₆
Molar mass	326.28 g/mol	641.69 g/mol

Pollutant sub group	Brominated Flame Retardants	
Common name	β-Hexabromocyclododecane	γ-Hexabromocyclododecane
IUPAC name	1 <i>R</i> ,2 <i>R</i> ,5 <i>R</i> ,6 <i>S</i> ,9 <i>R</i> ,10 <i>S</i> - Hexabromocyclododecane	1 <i>R</i> ,2 <i>R</i> ,5 <i>R</i> ,6 <i>S</i> ,9 <i>S</i> ,10 <i>R</i> - Hexabromocyclododecane

Table 3.10 continued:

Abbreviation	HBCDB	HBCDG
Chemical Structure		
Sum formula	$C_{12}H_{18}Br_6$	$C_{12}H_{18}Br_6$
Molar mass	641.69 g/mol	641.69 g/mol

Pollutant group	Pharmaceuticals		
Common name	Carbamazepine	Primidone	Diclofenac
IUPAC name	5 <i>H</i> -dibenzo[<i>b,f</i>]azepine-5-carboxamide	5-ethyl-5-phenyl-1,3-diazinane-4,6-dione	2-[2-(2,6-dichlorophenylamino)phenyl]acetic acid
Abbreviation	CARBAMAZ	PRIMID	DICLOF
Chemical Structure			
Sum formula	$C_{15}H_{12}N_2O$	$C_{12}H_{14}N_2O_2$	$C_{14}H_{11}Cl_2NO_2$
Molar mass	236.27 g/mol	218.25 g/mol	296.14 g/mol

Common name	Naproxen	Clofibric acid	Oxazepam
IUPAC name	(<i>S</i>)-2-(6-methoxynaphthalen-2-yl)propanoic acid	2-(4-chlorophenoxy)-2-methylpropanoic acid	8-chloro-3-hydroxy-5-phenyl-1 <i>H</i> -1,4-benzodiazepin-2-one
Abbreviation	NAPROX	CLOFIBRS	OXAZEP
Chemical Structure			
Sum formula	$C_{14}H_{14}O_3$	$C_{10}H_{11}ClO_3$	$C_{15}H_{11}ClN_2O_2$
Molar mass	230.26 g/mol	214.64 g/mol	286.70 g/mol

3.4 Analysis - Extraction, Evaporation, Clean-up and Quantification

Approved air sample preparation methods predominantly describe the determination of PAHs, OCPs, PCBs and perfluorinated compounds, as already mentioned in chapter 1.2. The implementation of these methods in the current study was limited, due to the broad diversity of target compounds. Restrictions in the availability of sampling material and sampler equipment additionally required the quantification of polar and non-polar organic contaminants from a single environmental sample. Hence, the sample preparation methods described in the literature had to be modified and optimized to the requirements of this study as summarized below:

The air samples were successively extracted by two azeotropic solvent mixtures, namely acetone/hexane (60/40; v/v) and acetone/methanol (90/10; v/v), in order to enable the quantitative elution of non-polar to polar target analytes. PUF disks and adsorber cartridges are Soxhlet extracted, whereas GFFs are eluted by diffusion. Thereafter, the successive azeotropic extracts are unified to a single homogeneous solution. The target compounds are quantified using GC-MS/MS and LC-MS/MS systems requiring different solvents (hexane for GC-MS/MS, methanol for LC-MS/MS) and clean-up procedures. Therefore, the acetone/hexane/methanol-extract is divided into two aliquot parts. Subsequently, the aliquots are evaporated in a parallel-evaporator (figure 3.15).

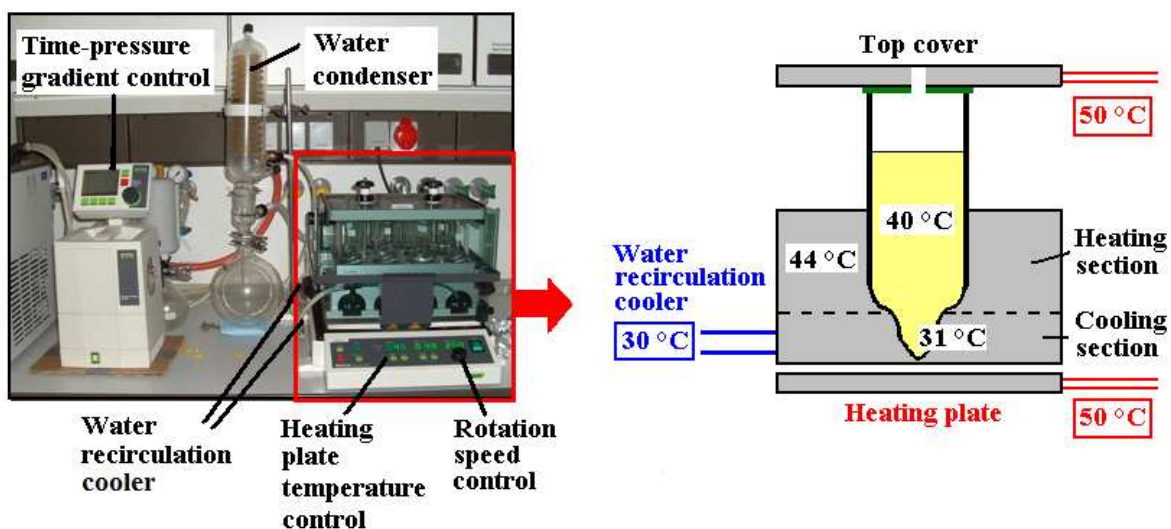


Figure 3.15: Illustration of the parallel-evaporator with regard to adjustable parameters including the temperature profile established at a heating plate temperature of 50 °C and at a water recirculation cooler temperature of 30 °C

Evaporation is a critical step in sample preparation, especially for the acetone/hexane/methanol solvent mixture applied in this study. It strongly influences the recoveries of target analytes. Thus, the evaporation needs to be uniform for all environmental samples. The parallel-evaporator allows the programming of individual time-pressure gradients with regard to the solvent mixture providing

the consistent evaporation of 4 to 12 air samples simultaneously. Parameters of evaporation are successively optimized with regard to recoveries of the target analytes. In order to give an overview, influences of the time-pressure gradient, adjusted temperatures, solvent mixture and evaporation duration are exemplarily compared for selected organic contaminants in figure 3.16.

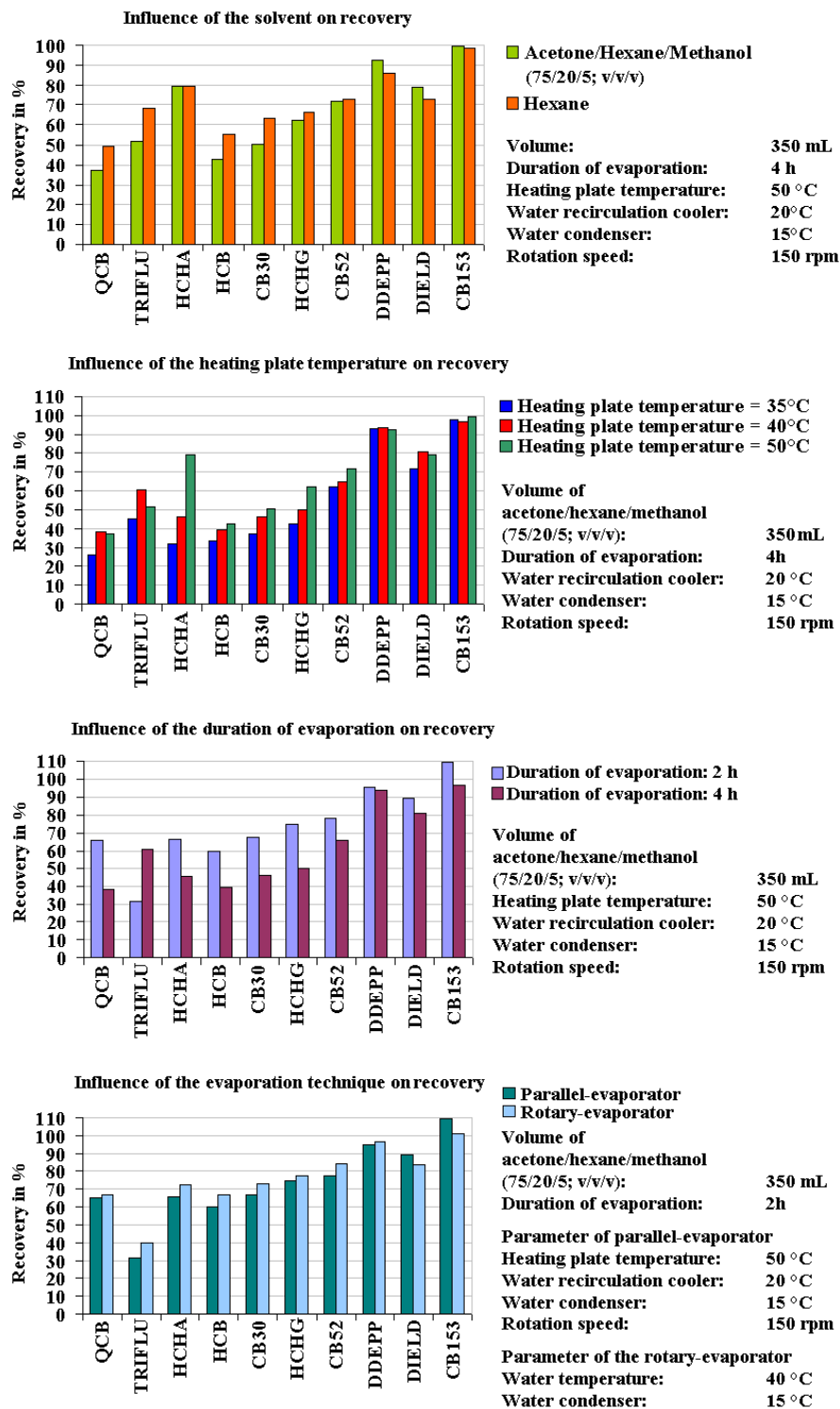


Figure 3.16: Optimization of parallel-evaporation parameters; The quantification is standardized to the internal standard PCB 185, which resists evaporation; Target compounds are sorted by increasing retention time

Acetone is the remaining solvent after evaporation allowing a simple solvent exchange to hexane and methanol by replenishing the samples with an excess of hexane or methanol. Optimized temperatures and time-pressure gradients for parallel evaporation are listed in chapter 9.

Finally the aliquots were centrifuged. The precipitated pellet was discarded, whereas the supernatant underwent a final clean-up in order to minimize matrix effects and to maintain instrument performances. Silica gel was used as clean-up material for the hexane-aliquot analysed by GC-MS/MS. Additional precipitation in the methanol aliquot was removed using syringe filters prior to analysis by LC-MS/MS. An overview of the sample preparation methods for glass fibre filters, adsorber cartridges and PUF disks is given in figure 3.17. Detailed work instructions and mass spectrometer methods may be found in chapter 9. The results in method validation are summarized in chapter 4.

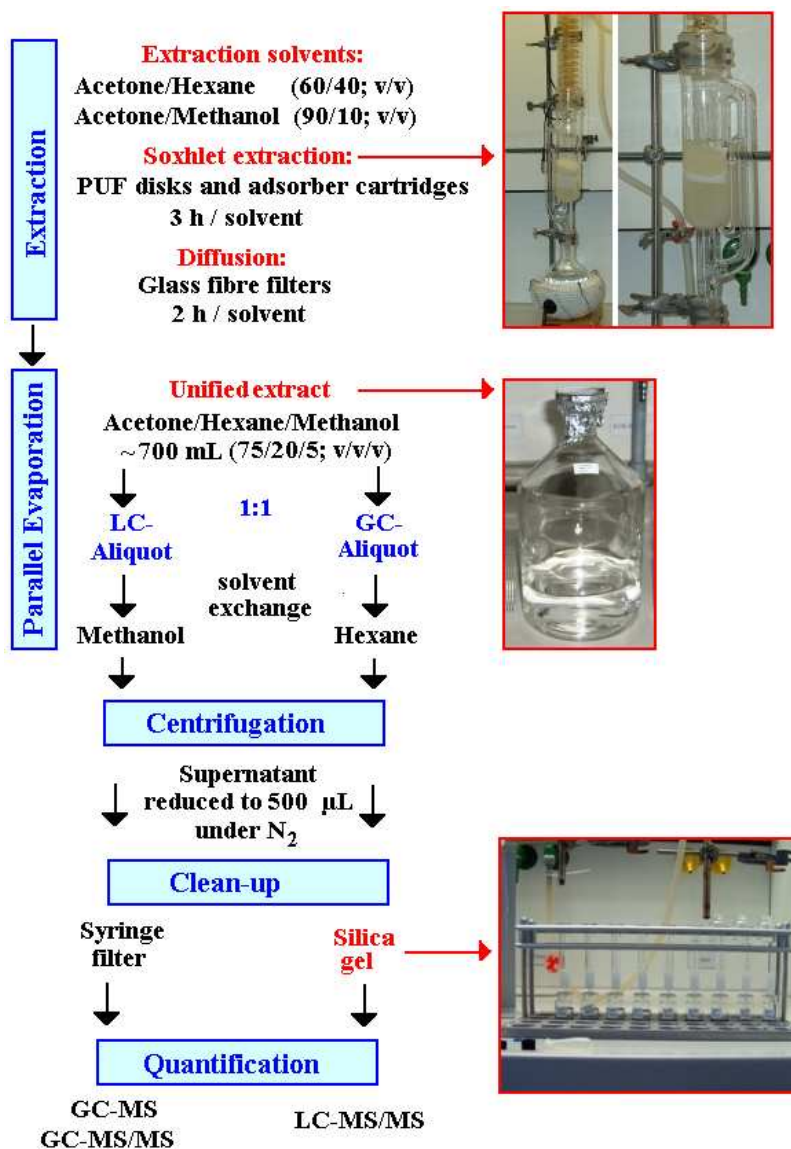


Figure 3.17: Schematic illustration of extraction, evaporation and clean-up of air samples

3.5 Air mass backward trajectories

The origin of collected air is significant for the interpretation of its pollution level. Air mass backward trajectories are calculated by usage of the model Hysplit 4.9 (Hybrid Single-Particle Lagrangian Integrated Trajectory) provided by the US National Oceanic and Atmospheric Administration (NOAA)-Air Resources Laboratory (ARL). Meteorological data is obtained from the US National Centre for Environmental Prediction (NCEP)-Global Data Assimilation System (GDAS) with 1 degree latitude/longitude resolution. ^[110] Seven days and 24 hours backward trajectories were calculated for arrival heights of 16 m, 200 m, 500 m and 1000 m in order to verify the results of these computations.

Air mass backward trajectories were determined for all air samples collected at the four active air sampling campaigns in the German EEZ, North Sea and Baltic Sea. In order to give an overview the results of 24 h backward trajectories are assembled and plotted in the figures 3.18 – 3.20 below. More exact outputs of the Hysplit model (original plots) are given in annex 4.

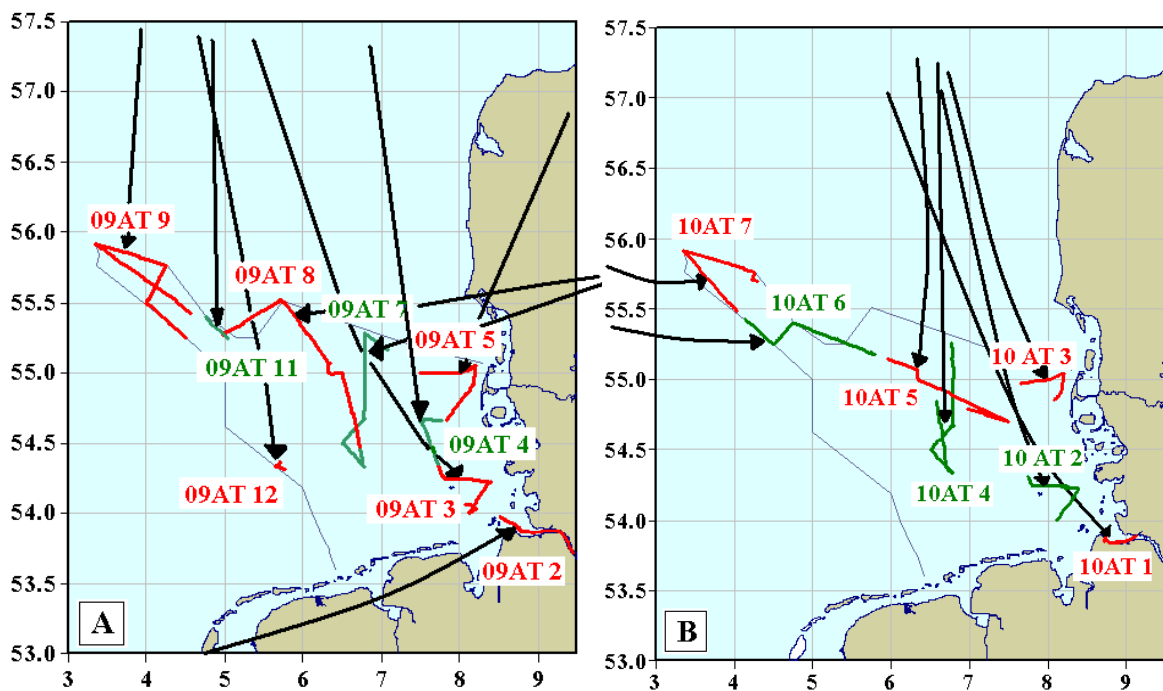


Figure 3.18: Air mass backward trajectories (black arrows) of the air samples (red and green lines) collected over the German EEZ in May/June 2009 (A) and in May 2010 (B), respectively

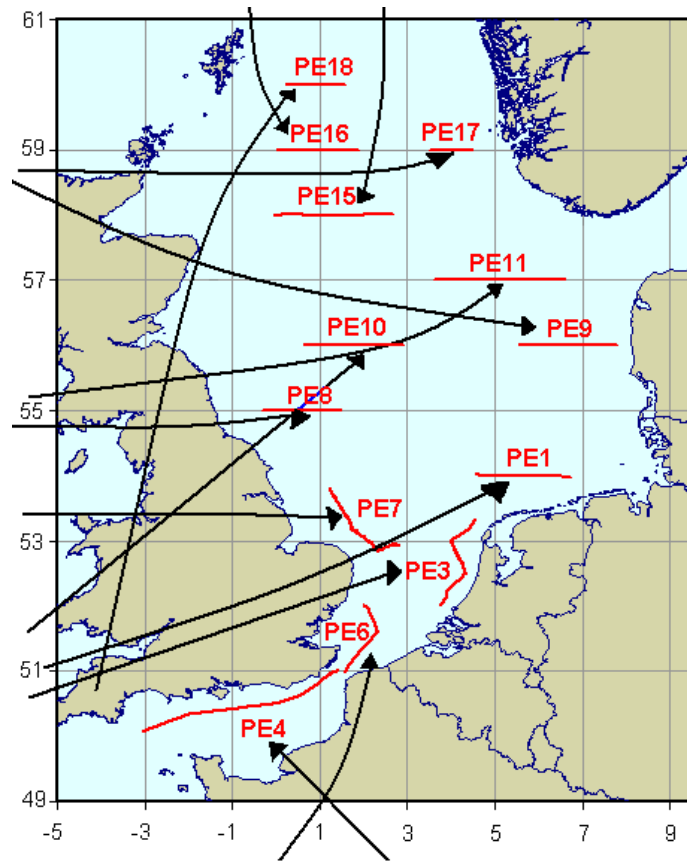


Figure 3.19: Air mass backward trajectories (black arrows) of the air samples (red lines) collected over the North Sea in August/September 2009

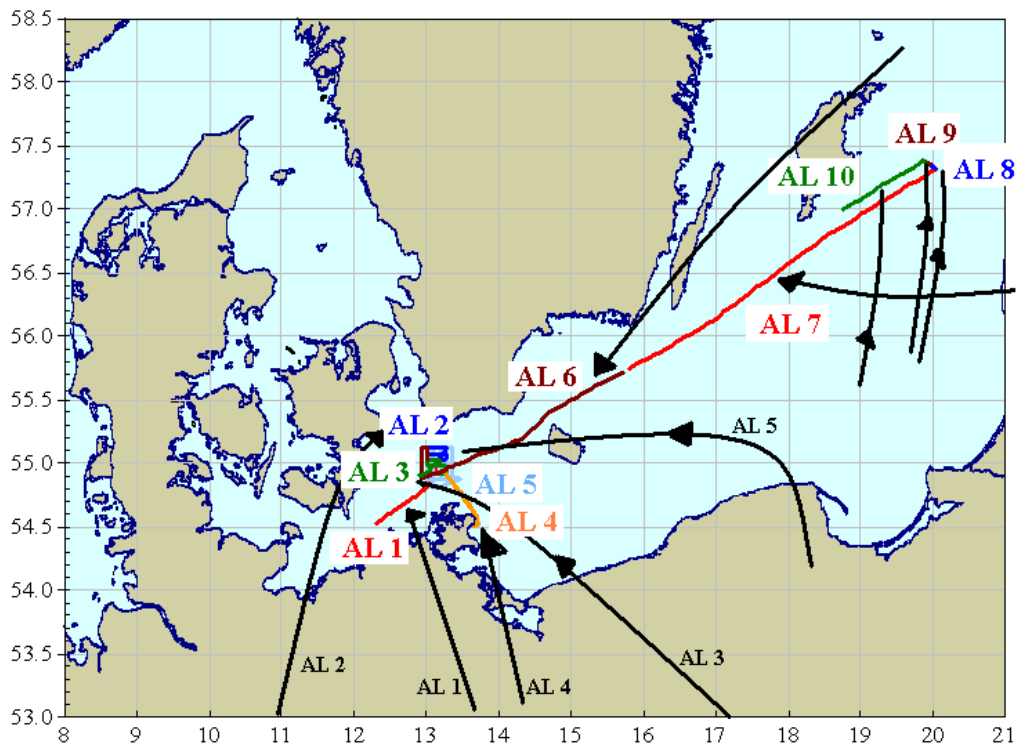


Figure 3.20: Air mass backward trajectories (black arrows) of the air samples collected during the Baltic Sea research cruise in April 2009

3.6 Surface Water Samples

Surface water samples were obtained in parallel to air samples during the routine monitoring cruises of the BSH in the German EEZ and the North Sea. They were analysed for target compounds by the BSH and provided for this study. Concentrations of target compounds in the surface water of the Baltic Sea were not available for the Alkor journey in April 2009. Instead, data for PAHs, OCPs and PCBs were obtained from the MUDAB database (Meeresumwelt-Datenbank) for February 2005. ^[111] More current data was available for the HCHs from July 2009. Surface water concentrations of polar pesticides, PFCs, PBFRs and pharmaceuticals were provided from a special BSH monitoring cruise in the Baltic Sea in June/July 2008.

Preparation and analysis of surface water samples were performed by the BSH. The following aspects of sample preparation should be considered for data interpretation: Polar pesticides, PFCs, PBFRs and pharmaceuticals are extracted from filtered sea water by solid phase extraction (SPE), whereas the water concentrations of PAHs, OCPs, PCBs and trifluralin are determined by liquid-liquid-extraction (LLE) from unfiltered sea water. Hence the surface water concentrations of target compounds exhibiting high adsorption to suspended particulate matter and determined by LLE, e.g., four- to six-ring PAHs and higher chlorinated PCBs, may be biased due to partitioning to the seawater particulate phase.

The spatial distribution of target analytes in the surface waters of the North Sea and the Baltic Sea are influenced by fluxes and locations of riverine input sources (estuaries) and the sea currents. Thus, the mean surface currents of the North Sea and Baltic Sea (illustrated in figure 3.21) are shown as background information for the discussion in chapter 5. Details of water sampling sites in the German EEZ, the wider North Sea and the Baltic Sea and the corresponding target compound concentrations in the surface water are listed in the annex 5.

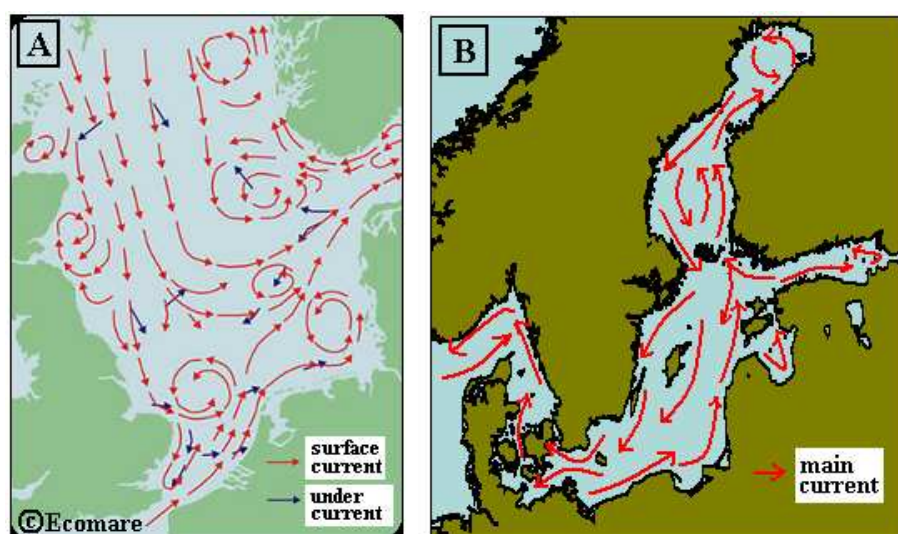


Figure 3.21: Sea currents of the North Sea (A) and the Baltic Sea (B)

4. Method Validation

As already mentioned in previous chapters, the broad diversity of target compounds as well as limitations in air sampling equipment required an advancement of approved air sample preparation methods described in the literature. Hence, a major part of this study was dedicated to purposes of method validation. A comprehensive validation of the air sampling techniques and air sample preparation methods was performed, as summarized below.

4.1 Validation of air sampling

Air sampling techniques were tested for reproducibility in order to assess the reliability and comparability of collected air samples. Furthermore, the retention capacities of PUF plug adsorber cartridges and PUF/XAD-2/PUF adsorber cartridges were verified. In addition, investigations on the stability of collected air samples during storage in the freezer were performed.

4.1.1 Side-by-side air sampling experiments

The reproducibility of air sampling data was estimated by simultaneous side-by-side exposures of two PUF disk passive air samplers and two active air samplers (Digital DHM-60). GFF, PUF/XAD-2/PUF adsorber cartridge, PUF plug and PUF disk air samples were taken in parallel and analysed for target compounds. The deviation of each pair of values was calculated in %. Each side-by-side air sampling experiment with active air samplers was carried out in triplicate as listed in table 3.5 (three side-by-side sampling experiments with PUP plug adsorber cartridges: R2, R6 and R7, three side-by-side sampling experiments with PUF/XAD-2/PUF adsorber cartridges: R8, R9 and R10 and three parallel exposures of PUF plug and PUF/XAD-2/PUF adsorber cartridges: R3, R4 and R5). In addition, six side-by-side passive air sample exposures were performed, whereof four exposures originated from ship based measurements (refer to table 3.6) and two from the sampling site Sülldorf/Hamburg (refer to table 3.7). Air concentration data is listed in the annex 1.

Most target compounds occurred in the atmosphere in trace concentrations of a few pg/m^3 often close to or below the LOQ. In addition, numerous currently used pesticides were only quantifiable during their main agricultural application season. For these reasons, side-by-side sampling data was often incomplete and in consequence insufficient for an adequate reproducibility calculation of each single target compound. Therefore, the calculations are limited to those exceeding LOQ for all samples collected simultaneously. Reproducibility results were grouped in accordance with the quantification of target analytes (GC-MS, GC-MS/MS, LC-MS/MS) and sampling material (GFF, PUF/XAD-2/PUF adsorber cartridge, PUF plug and PUF disk). The calculated mean deviations

with their standard deviations revealed the mean error (precision) of the overall data acquisition procedure including air sampling, air sample preparation and mass spectrometry (table 4.1).

Table 4.1: Reproducibility (precision) of air sampling data based on all analytes exceeding LOQ in all samples collected simultaneously

Mean Deviation in %	GC-MS	GC-MS/MS	LC-MS/MS
GFF	12 ± 4	9 ± 4	18 ± 15
PUF plug	13 ± 8	14 ± 7	24 ± 16
PUF/XAD-2/PUF (sandwich)	19 ± 15	12 ± 6	27 ± 14
PUF disk	11 ± 9	9 ± 8	26 ± 22
PUF plug - PUF/XAD-2/PUF (sandwich)	12 ± 6	17 ± 9	17 ± 12

PUF plug and PUF/XAD-2/PUF adsorber cartridges were exposed side-by-side in order to assure the comparability of air samples collected with the distinct trapping materials. In fact, this experiment aimed to assess the comparability of atmospheric target analyte concentrations originating from the Baltic Sea active air sampling campaign with those of the North Sea campaigns. The obtained mean deviations (table 4.1; PUF plug – PUF/XAD-2/PUF) were assimilable with mean deviations of identical trapping materials. Thus comparability of collected air samples among each other was ensured.

4.1.2 Desorption experiments

Active air sampling adsorbents need to be in contact with a large quantity of air, because atmospheric target analyte concentrations usually range from <0.1 pg/m³ to 1 ng/m³. Moreover, sampling durations during ship cruises were limited to at most 1 day, in order to obtain an adequate spatial resolution of sampling sites. Hence, an important source of error limiting the reproducibility of active air sampling, might be a break-through of trapped pollutants from the adsorber cartridge caused by large sample volumes in short time intervals. The maximum volume of air collected without break-through is referred to as retention capacity. It is supposed that break-through observations predominantly originate from desorption of trapped pollutants rather than from insufficient retention capacities of adsorber cartridges. Thus desorption experiments were an important implement controlling active air sampling performances.

Desorption of trapped pollutants was investigated by spiking performance reference compounds to the adsorber cartridge prior to sampling. The occurrence of desorption would cause a decrease of PRC recoveries by increasing volumes of collected air. The recoveries are plotted against the volume of sampled air and a linear regression was calculated for each PRC compound (figure 4.1 – 4.10). Confidence limits (95 %) and prediction limits (95 %) account for the variation of recovery

data and are applied to evaluate the trends of the linear regression curves: The upper and lower confidence limits display the area, which contains the true regression curve with a probability of 95 %. The upper and lower prediction limits mark the area in which 95 % of the data points of PRC recovery would be expected. The sample volume of 0 m³ corresponded to the PRC recoveries in field blanks. Applied PRCs as well as spiked concentrations are listed in chapter 9.

Considering the confidence and prediction limits, a significant desorption was exclusively observed for Prometryn-D₆, a sixfold deuterium labeled triazine pesticide (figure 4.1). Sampling of 900 m³ ambient air resulted in ~ 30 % loss of Prometryn-D₆ in the PUF plug cartridge, whereas ~ 35 % loss was displayed for the PUF/XAD-2/PUF adsorber cartridge at 500 m³ air volume. As summarized in chapter 3, mean sample volumes usually varied between 100 m³ and 300 m³. In this range, sampling errors caused by desorption were predicted to be less than 15%.

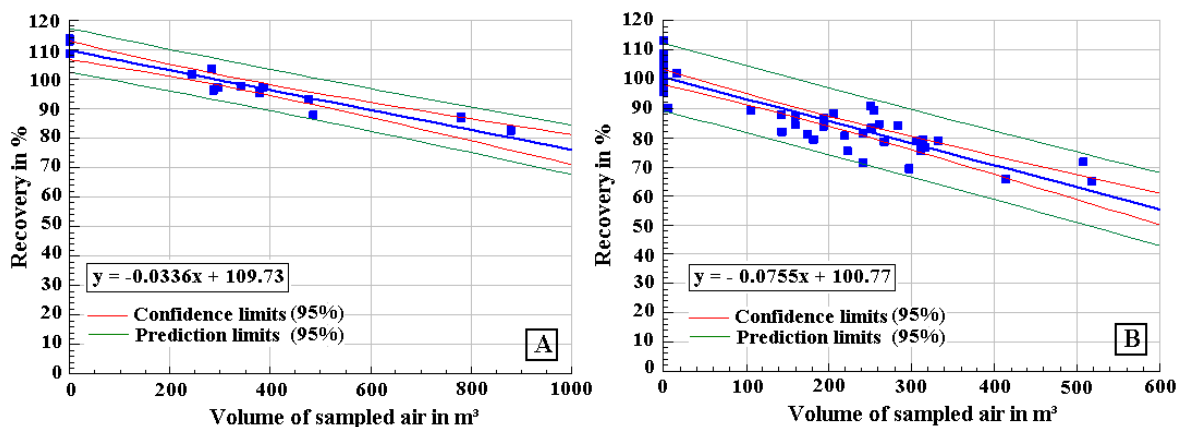


Figure 4.1: Desorption test for prometryn-D₆; (A) PUF plug adsorber cartridge; (B) PUF/XAD-2/PUF adsorber cartridge

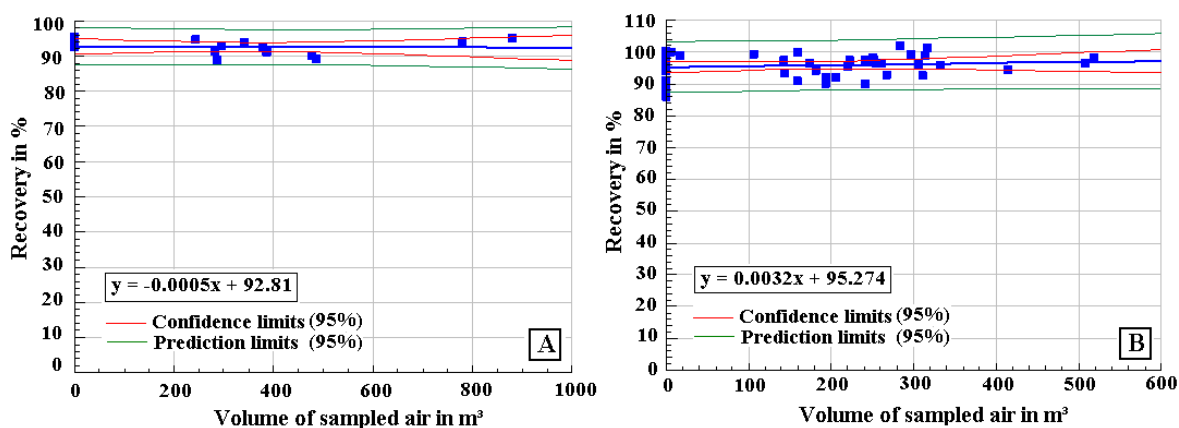


Figure 4.2: Desorption test for simazine-D₁₀; (A) PUF plug adsorber cartridge; (B) PUF/XAD-2/PUF adsorber cartridge

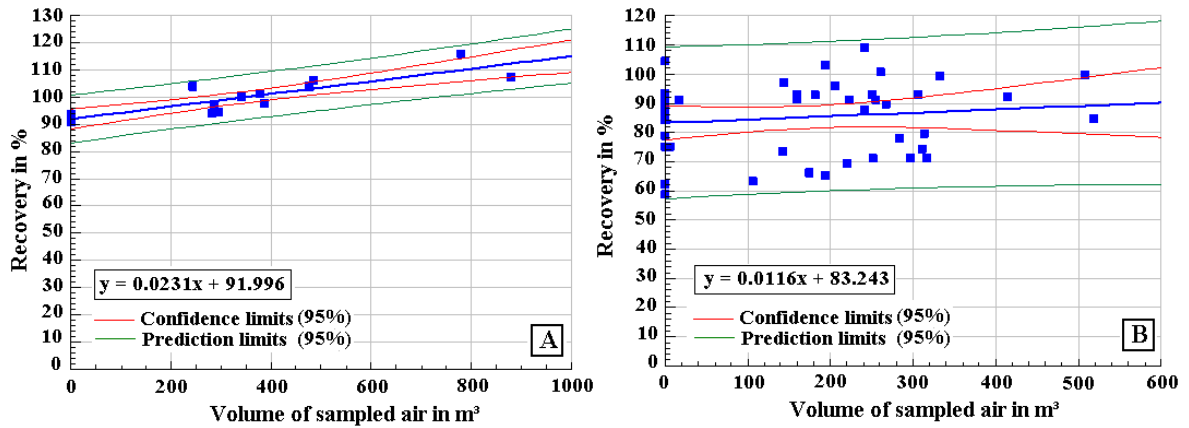


Figure 4.3: Desorption test for γ -HCH- $^{13}\text{C}_6\text{D}_6$; (A) PUF plug adsorber cartridge; (B) PUF/XAD-2/PUF adsorber cartridge

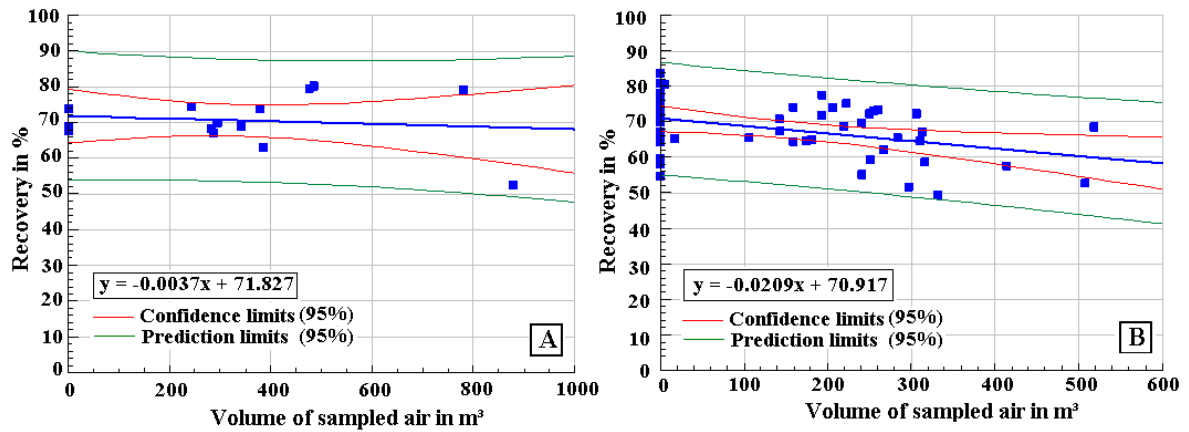


Figure 4.4: Desorption test for polychlorinated biphenyl 30; (A) PUF plug adsorber cartridge; (B) PUF/XAD-2/PUF adsorber cartridge

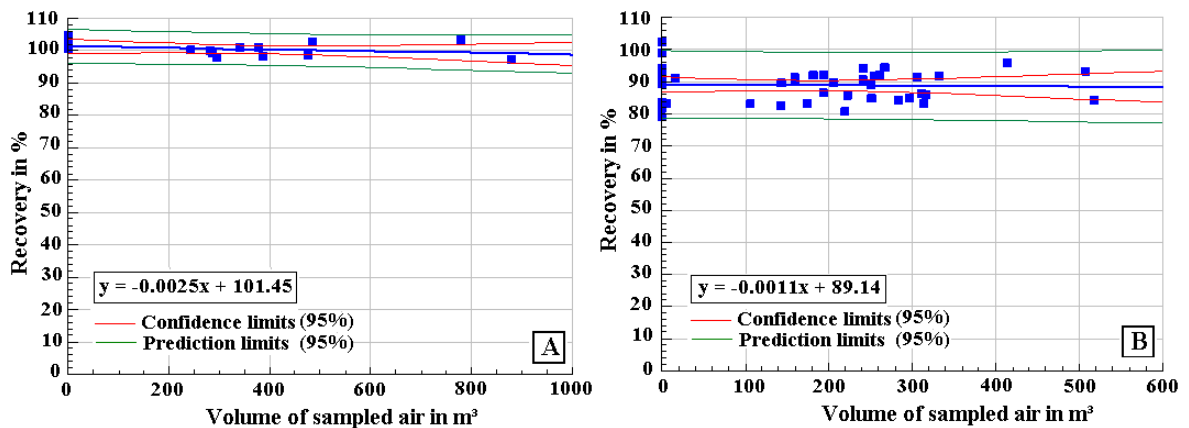


Figure 4.5: Desorption test for polychlorinated biphenyl 104; (A) PUF plug adsorber cartridge; (B) PUF/XAD-2/PUF adsorber cartridge

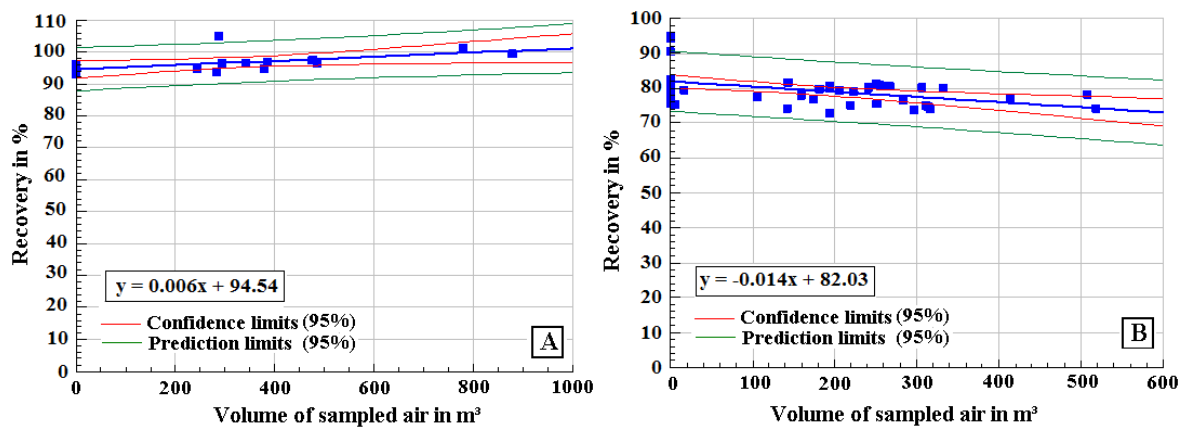


Figure 4.6: Desorption test for polychlorinated biphenyl 145; (A) PUF plug adsorber cartridge; (B) PUF/XAD-2/PUF adsorber cartridge

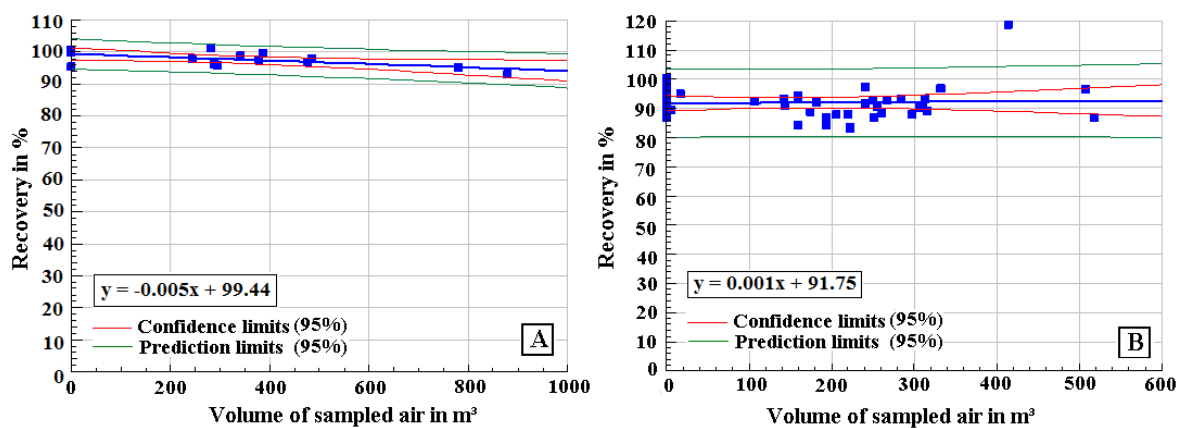


Figure 4.7: Desorption test for polychlorinated biphenyl 204; (A) PUF plug adsorber cartridge; (B) PUF/XAD-2/PUF adsorber cartridge

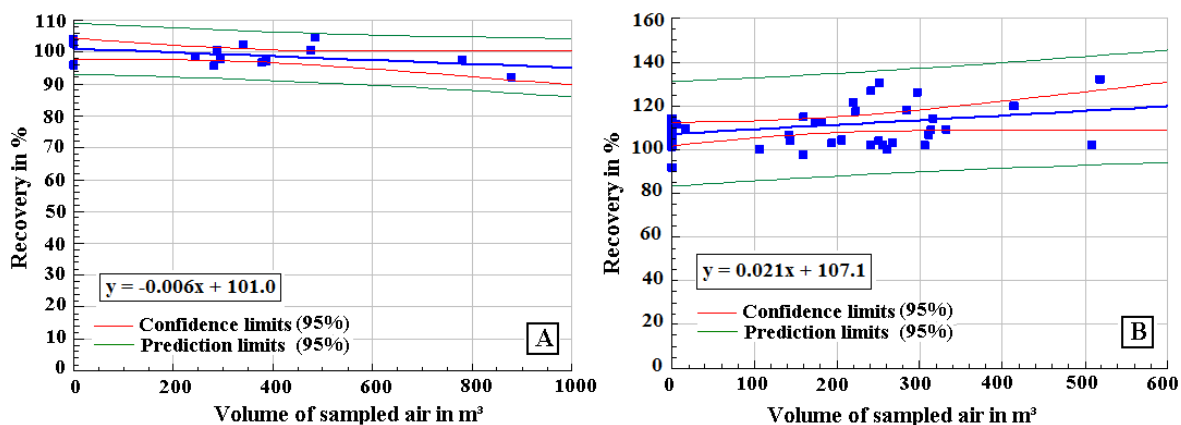


Figure 4.8: Desorption test for phenanthrene-D₁₀; (A) PUF plug adsorber cartridge; (B) PUF/XAD-2/PUF adsorber cartridge

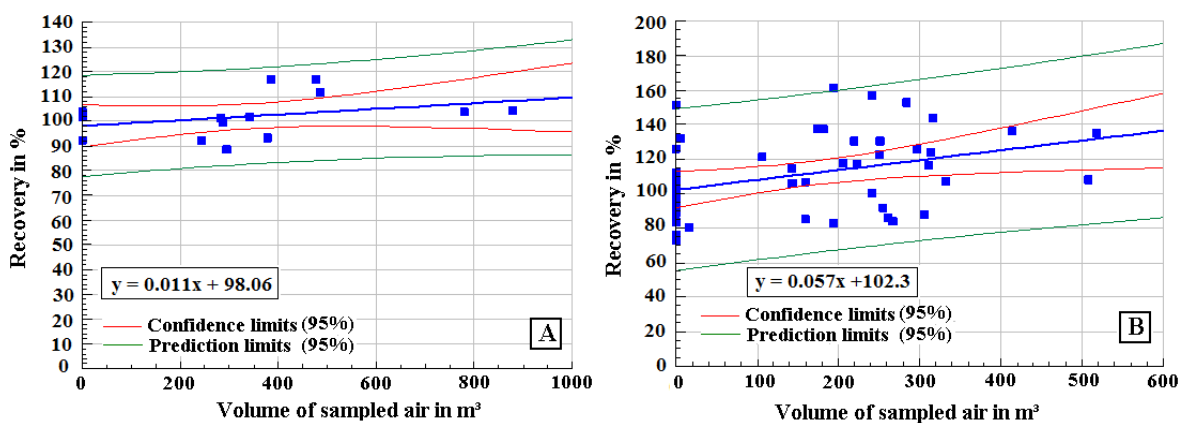


Figure 4.9: Desorption test for fluoranthene-D₁₀; (A) PUF plug adsorber cartridge; (B) PUF/XAD-2/PUF adsorber cartridge

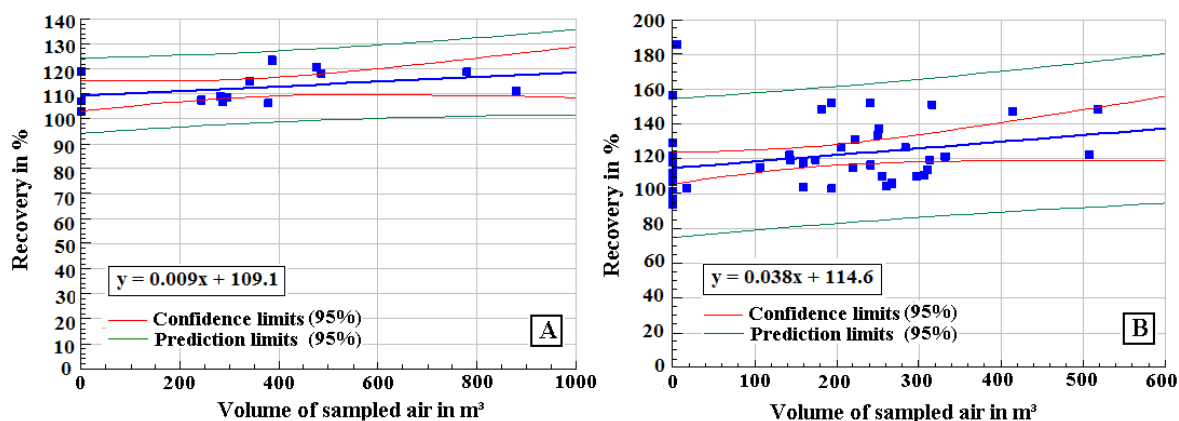


Figure 4.10: Desorption test for benzo[a]anthracene-D₁₂; (A) PUF plug adsorber cartridge; (B) PUF/XAD-2/PUF adsorber cartridge

PUF/XAD-2/PUF adsorber cartridges were expected to show an increased retention capacity on target analytes than solely PUF plug adsorber cartridges. Hence PUF/XAD-2/PUF was the adsorbent of choice for this study. However, side-by-side sampling and desorption experiments disproved expected advantages of PUF/XAD-2/PUF adsorber cartridges compared to PUF plugs. Considering additional difficulties in XAD-2 handling, e.g., the electrostatic properties, the loss of XAD-2 during sampling and the increased air-flow resistance, PUF plugs are proposed as trapping material for further campaigns beyond this study.

4.1.3 Stability tests of exposed air sampling materials

Exposed PUF disks, adsorber cartridges and GFFs were stored in a freezer (-20 °C) for several weeks until extraction. The stability of frozen PUF disks and PUF/XAD-2/PUF adsorber cartridge air samples was controlled by the recoveries of performance reference compounds spiked to field

blanks. Storage durations of 0 weeks corresponded to sampling material immediately spiked prior to extraction. Applied PRCs as well as spiked concentrations are listed in chapter 9.

The stability of PUF disk and PUF/XAD-2/PUF adsorber cartridge air samples was ensured over storage time, as displayed in figures 4.11 - 4.20. Stability results of PUF plug air samples were not available, because the PRC standards were not established at the time of the Baltic Sea active air sampling campaign. However, PUF disks and PUF plugs are the same sampling material in different dimensions. Therefore, stability data of PUF disks might be completely conferrable to PUF plugs. In addition, particulate matter air sample stabilities could not be tested, because spiked PRCs immediately evaporate from GFF surfaces. Though, the hermetically sealed storage at -20 °C was expected to reduce gas exchange of the particle associated mass fraction of target compounds adequately.

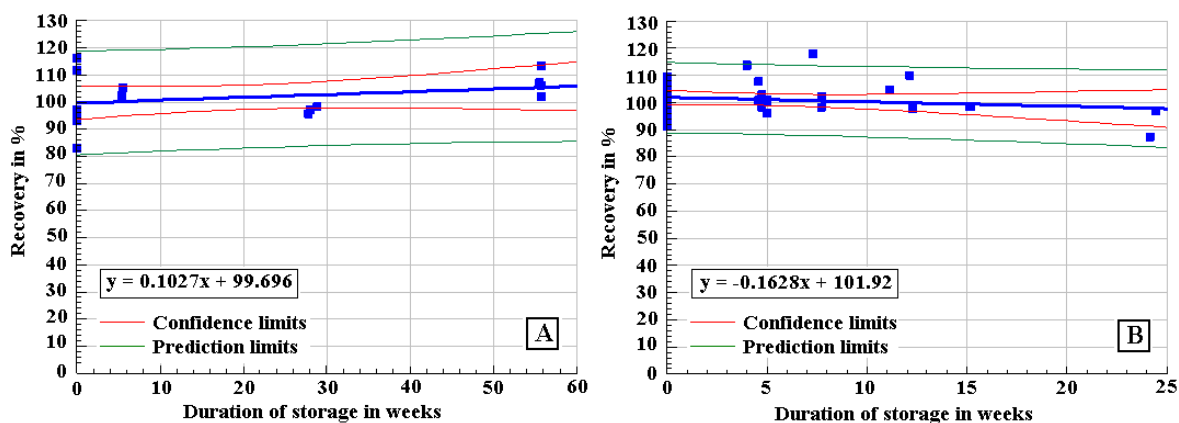


Figure 4.11: Stability test of prometryn-D₆; (A) PUF/XAD-2/PUF adsorber cartridge, (B) PUF disk

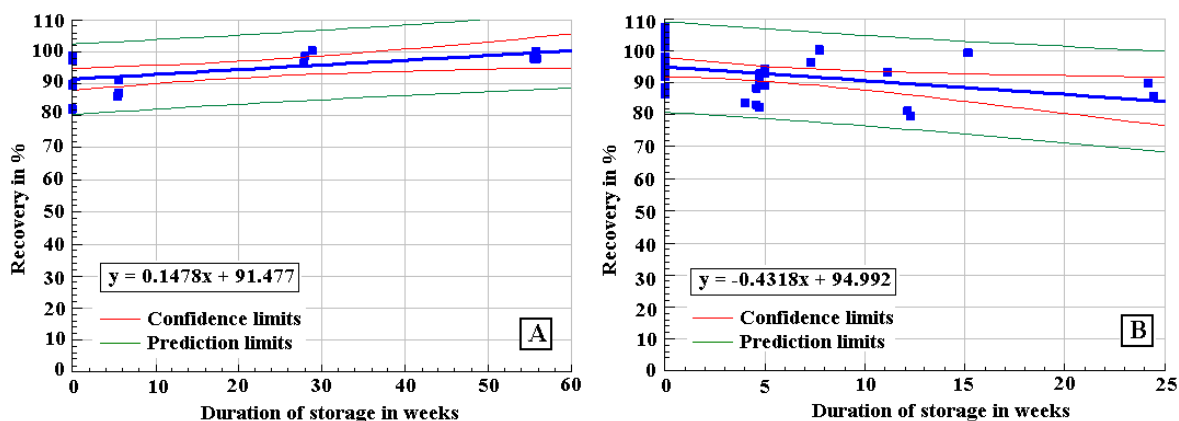


Figure 4.12: Stability test of simazine-D₁₀; (A) PUF/XAD-2/PUF adsorber cartridge, (B) PUF disk

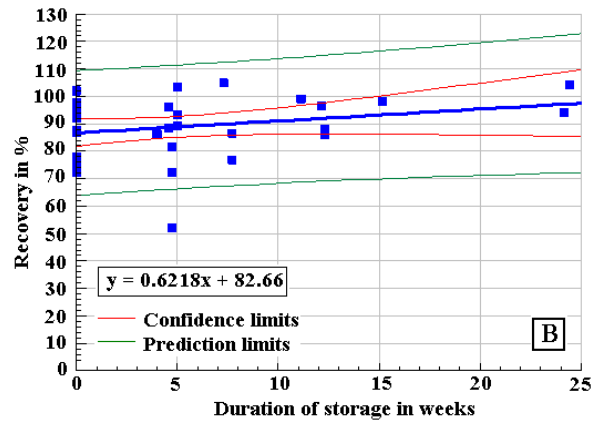
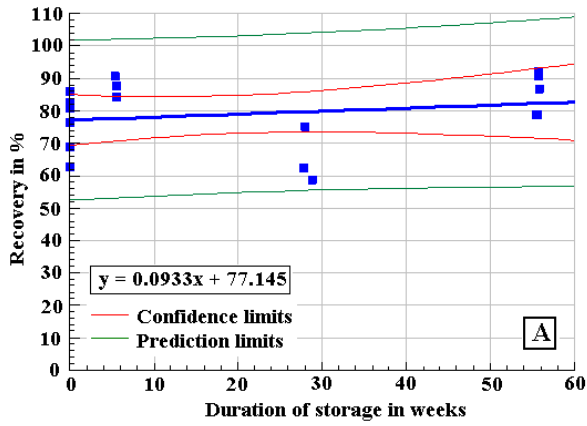


Figure 4.13: Stability test of $\gamma\text{-HCH-}^{13}\text{C}_6\text{D}_6$; (A) PUF/XAD-2/PUF adsorber cartridge, (B) PUF disk

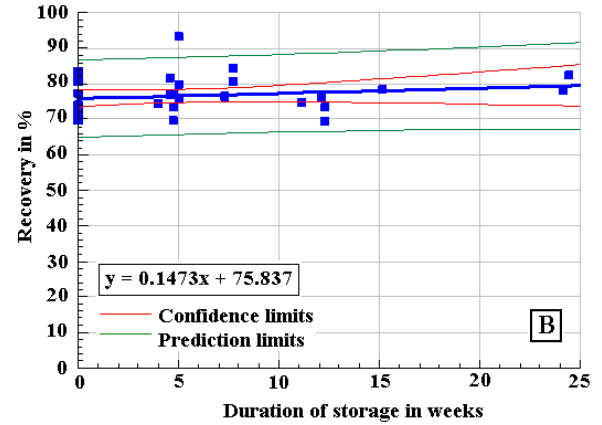
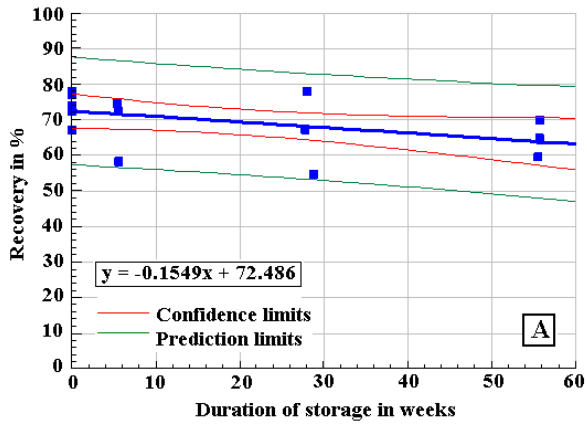


Figure 4.14: Stability test of polychlorinated biphenyl 30; (A) PUF/XAD-2/PUF adsorber cartridge, (B) PUF disk

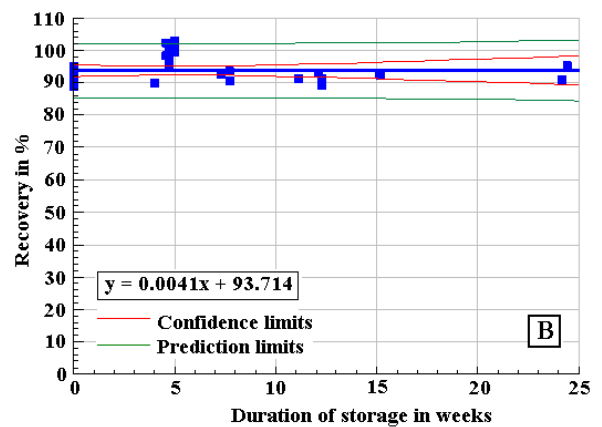
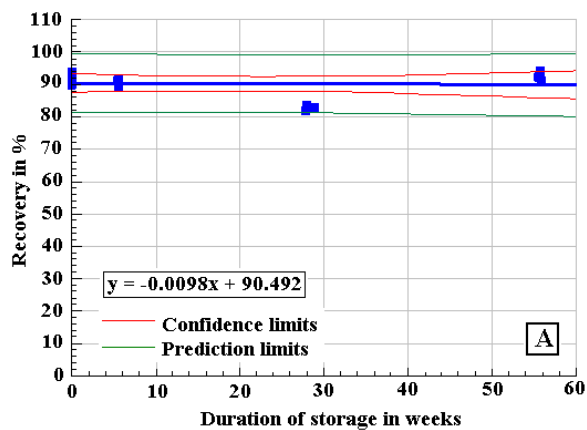


Figure 4.15: Stability test of polychlorinated biphenyl 104; (A) PUF/XAD-2/PUF adsorber cartridge, (B) PUF disk

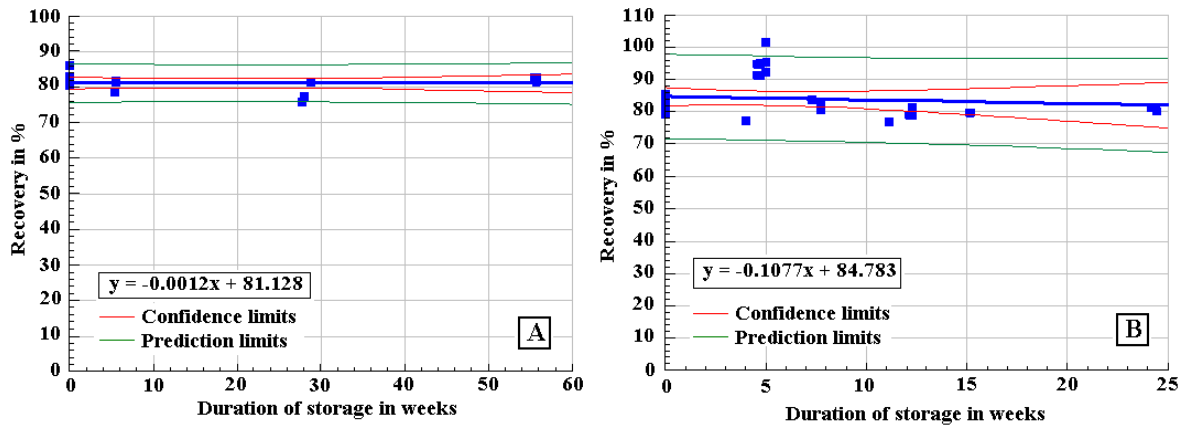


Figure 4.16: Stability test of polychlorinated biphenyl 145; (A) PUF/XAD-2/PUF adsorber cartridge, (B) PUF disk

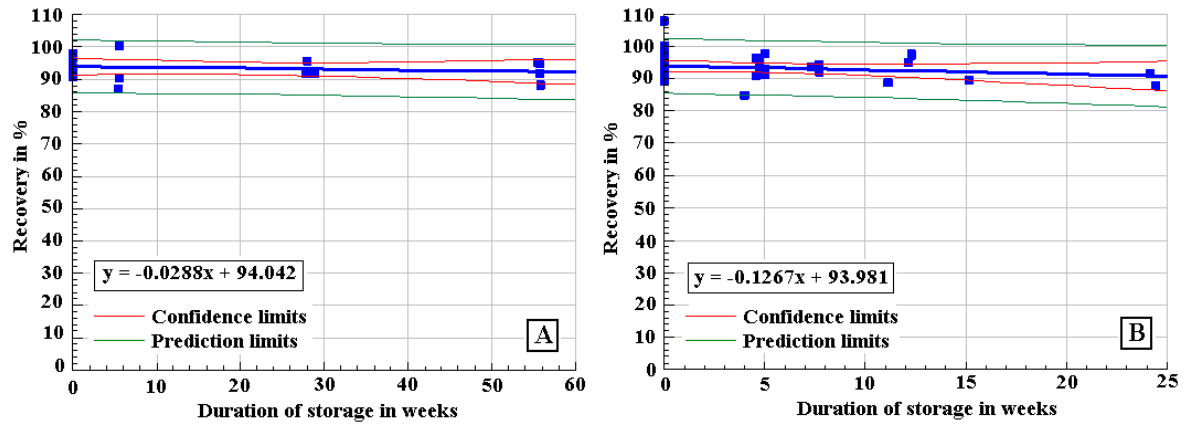


Figure 4.17: Stability test of polychlorinated biphenyl 204; (A) PUF/XAD-2/PUF adsorber cartridge, (B) PUF disk

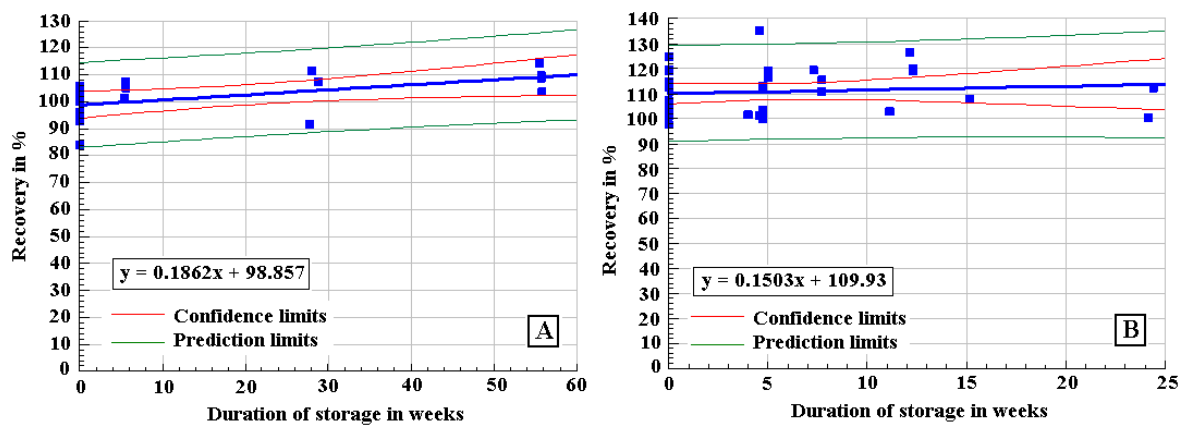


Figure 4.18: Stability test of phenanthrene-D₁₀; (A) PUF/XAD-2/PUF adsorber cartridge, (B) PUF disk

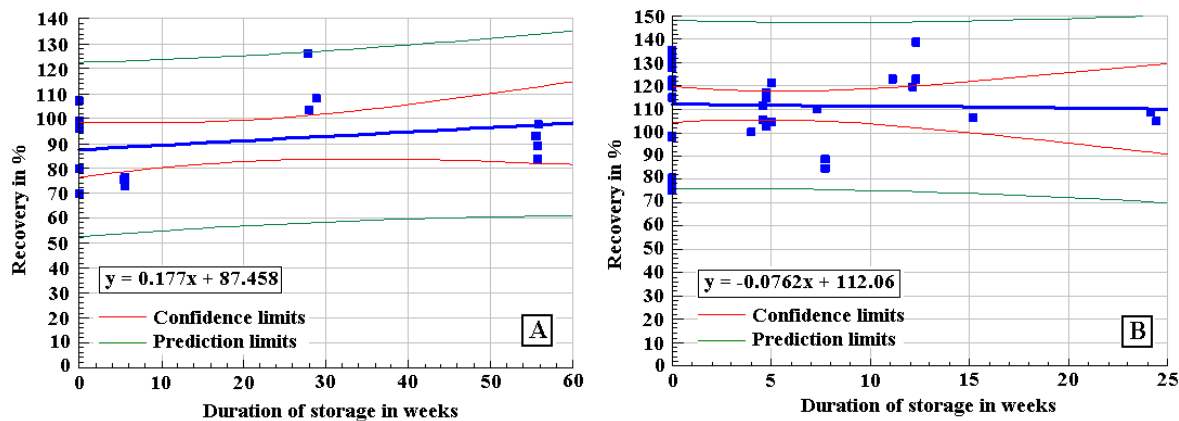


Figure 4.19: Stability test of fluoranthene-D₁₀; (A) PUF/XAD-2/PUF adsorber cartridge, (B) PUF disk

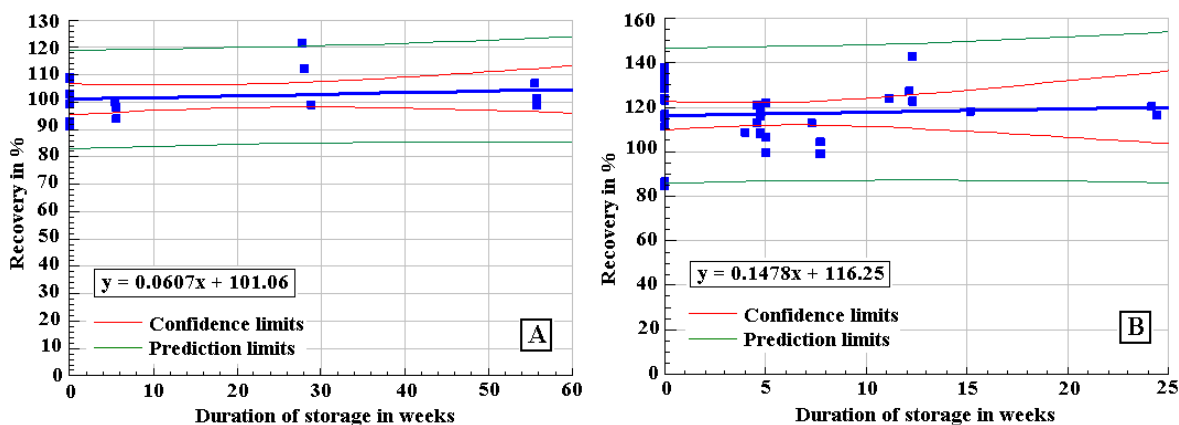


Figure 4.20: Stability test of Benzo[a]anthracene-D₁₂; (A) PUF/XAD-2/PUF adsorber cartridge, (B) PUF disk

4.2 Validation of air sample preparation methods

Air samples and corresponding field blanks were extracted in five preparation sequences. Quality assurance of sample preparation was performed by laboratory blanks and spike experiments for each sequence. An overview is given in table 4.2.

Table 4.2: Air sample preparation sequences; 1 = Baltic Sea in Apr. 2009 (table 3.1); 2 = North Sea in Aug./Sep. 2009 (tables 3.3 and 3.6); 3 = German EEZ in May/Jun. 2009 and May 2010 (tables 3.2, 3.4 and 3.6); 4 = PUF disk passive air samples (tables 3.7 - 3.9); 5 = Sülldorf/Hamburg Nov./Dec.2010 (table 3.5)

Preparation Sequence:	1	2	3	4	5
Number of air samples:					
PUF disk	-	2	6	41	-
GFF	-	13	16	-	20
PUF plug adsorber cartridge	10	-	-	-	11
PUF/XAD-2/PUF adsorber cartridge	-	13	16	-	9

Table 4.2 continued:

Preparation Sequence:	1	2	3	4	5
Number of field blanks:					
PUF disk	-	2	6	37	-
GFF	-	3	7	-	3
PUF plug adsorber cartridge	3	-	-	-	3
PUF/XAD-2/PUF adsorber cartridge	-	3	7	-	3
Number of laboratory blanks:					
Soxhlet blank	1	1	1	1	1
Petri dish blank	-	1	1	-	1
2.0 L bottle blank	1	1	1	1	1
0.5 L bottle blank	-	1	1	-	1
Evaporation-350 mL blank	3	3	1	1	1
Evaporation-100 mL blank	-	3	1	-	1
Syringe filtration blank	-	-	1	1	1
Silica gel blank	3	3	1	1	1
Number of spike samples:					
PUF disk	-	2	3	3	3
GFF	-	-	3	-	6
PUF plug adsorber cartridge	3	-	-	-	3
PUF/XAD-2/PUF adsorber cartridge	-	3	3	-	3
Evaporation-350 mL spike	3	3	1	1	1
Evaporation-100 mL spike	-	3	1	-	1
Syringe filtration spike	-	3	1	1	1
Silica gel spike	3	3	1	1	1

4.2.1 Blanks

Twelve types of blanks were subject to the quality assurance of air concentration data generated in this study. They may be grouped in field blanks and laboratory blanks. Arithmetic means, medians and standard deviations of each type of blank and target analyte were summarized in the tables below. Results for single blank samples are tabulated in the annex 2.

Field blanks

Field blanks of PUF disks, PUF plug adsorber cartridges, PUF/XAD-2/PUF adsorber cartridges and GFFs were prepared. Field blanks were used as control samples displaying possible contamination sources of air samples during transportation, their insertion in respective sampler holders, sample preparation and quantification. Hence, field blanks provided the data for the blank correction of air concentration data. Finally, field blank results were used to calculate the limits of quantification and limits of detection of air sample analysis (refer to chapter 4.3).

Pre-cleaning, transportation and sample preparation procedures as well as mass spectrometry quantification methods were identical for air samples and field blanks. As described in chapter 9.4.2 field blanks were defrosted and spiked with PRC standard solutions in parallel with the air

sampling material. During pre-installation of the air sampling material in respective sampler holders in laboratory, they were exposed to ambient air. Thereafter, they were stored in the freezer until extraction together with the collected air samples. In order to give an overview, arithmetic means, medians and standard deviations of organic target compounds in field blanks were calculated enclosing the whole data set produced in the five preparation sequences. Results are listed in units of ng/mL extract in table 4.3.

Table 4.3: Field blanks; n = number of field blanks, \bar{x}_{arithm} = arithmetic mean (ng/mL), \bar{x}_{med} = median (ng/mL), σ = standard deviation (ng/mL); n.q. = not quantified

Type of field blank	GFF				PUF disk				PUF plug adsorber cartridge				PUF/XAD-2/PUF adsorber cartridge			
	n	\bar{x}_{arithm}	\bar{x}_{med}	σ	n	\bar{x}_{arithm}	\bar{x}_{med}	σ	n	\bar{x}_{arithm}	\bar{x}_{med}	σ	n	\bar{x}_{arithm}	\bar{x}_{med}	σ
24-D	13	0.000	0.000	0.000	n.q.	n.q.	n.q.	n.q.	n.q.	n.q.	n.q.	n.q.	n.q.	n.q.	n.q.	n.q.
ACE	13	1.158	1.910	1.124	45	2.063	2.709	1.992	6	2.640	3.770	2.057	13	2.725	3.485	1.711
ACY	13	0.000	0.000	0.000	45	8.112	6.764	6.313	6	4.228	2.171	6.336	13	6.909	4.010	13.07
ALD	13	0.000	0.000	0.000	45	0.000	0.000	0.000	6	0.000	0.000	0.000	13	0.000	0.000	0.000
AMETRYN	13	0.002	0.000	0.002	45	0.006	0.000	0.013	6	0.000	0.000	0.000	13	0.000	0.000	0.000
ANT	13	0.000	0.000	0.000	45	0.000	0.000	0.000	6	0.000	0.000	0.000	13	0.260	0.000	0.901
ATRAZ	13	0.000	0.000	0.000	45	0.000	0.000	0.000	6	0.000	0.000	0.000	13	0.000	0.000	0.000
AZINPH-E	13	0.000	0.000	0.000	45	0.000	0.000	0.000	6	0.000	0.000	0.000	13	0.000	0.000	0.000
AZINPH-M	13	0.000	0.000	0.000	45	0.000	0.000	0.000	6	0.000	0.000	0.000	13	0.000	0.000	0.000
BAA	13	0.000	0.000	0.000	45	0.000	0.000	0.000	6	0.000	0.000	0.000	13	0.389	0.000	0.705
BAP	13	0.000	0.000	0.000	45	0.000	0.000	0.000	6	0.000	0.000	0.000	13	0.836	0.000	1.612
BBF	13	0.000	0.000	0.000	45	0.000	0.000	0.000	6	0.000	0.000	0.000	13	0.876	0.000	1.316
BENTAZ	13	0.000	0.000	0.000	45	0.004	0.000	0.009	6	0.000	0.000	0.000	13	0.001	0.000	0.002
BGHIP	13	0.000	0.000	0.000	45	0.000	0.000	0.000	6	0.000	0.000	0.000	13	2.667	0.000	3.964
CARBAMAZ	13	0.000	0.000	0.000	45	0.003	0.000	0.015	6	0.000	0.000	0.000	13	0.000	0.000	0.000
CARBEND	13	0.000	0.000	0.000	45	0.000	0.000	0.000	6	0.000	0.000	0.000	13	0.000	0.000	0.000
CB138	13	0.000	0.000	0.000	45	0.095	0.000	0.245	6	0.146	0.091	0.180	13	0.257	0.252	0.212
CB153	13	0.038	0.000	0.094	45	0.168	0.240	0.159	6	0.311	0.353	0.172	13	0.276	0.228	0.172
CB28	13	0.051	0.000	0.141	45	0.283	0.292	0.137	6	0.083	0.000	0.202	13	0.246	0.134	0.214
CB52	13	0.000	0.000	0.000	45	0.041	0.000	0.104	6	0.000	0.000	0.000	13	0.231	0.162	0.276
CHLORFENV	13	0.000	0.000	0.000	45	0.000	0.000	0.000	6	0.000	0.000	0.000	13	0.214	0.000	0.352
CHLORTUR	13	0.000	0.000	0.000	45	0.003	0.000	0.014	6	0.007	0.002	0.010	13	0.000	0.000	0.000
CHRTR	13	0.000	0.000	0.000	45	0.579	0.000	1.492	6	0.000	0.000	0.000	13	1.636	0.000	2.450
CLOFIBRS	13	0.000	0.000	0.000	n.q.	n.q.	n.q.	n.q.	n.q.	n.q.	n.q.	n.q.	n.q.	n.q.	n.q.	n.q.
DBAHA	13	0.000	0.000	0.000	45	0.000	0.000	0.000	6	0.000	0.000	0.000	13	0.478	0.000	1.655
DDPP	13	0.000	0.000	0.000	45	0.000	0.000	0.000	6	0.012	0.000	0.028	13	0.000	0.000	0.000
DDEPP	13	0.000	0.000	0.000	45	0.071	0.000	0.116	6	0.000	0.000	0.000	13	0.000	0.000	0.000
DDTOP	13	0.000	0.000	0.000	45	0.000	0.000	0.000	6	0.000	0.000	0.000	13	0.000	0.000	0.000
DDTPP	13	0.000	0.000	0.000	45	0.003	0.000	0.021	6	0.000	0.000	0.000	13	0.000	0.000	0.000
DEATRAZ	13	0.000	0.000	0.000	45	0.000	0.000	0.000	6	0.000	0.000	0.000	13	0.000	0.000	0.000
DIAZINON	13	0.000	0.000	0.000	45	0.002	0.000	0.011	6	0.000	0.000	0.000	13	0.000	0.000	0.000
DICHLPR	13	0.000	0.000	0.000	n.q.	n.q.	n.q.	n.q.	n.q.	n.q.	n.q.	n.q.	n.q.	n.q.	n.q.	n.q.
DICLOF	13	0.000	0.000	0.000	n.q.	n.q.	n.q.	n.q.	n.q.	n.q.	n.q.	n.q.	n.q.	n.q.	n.q.	n.q.
DIELD	13	0.000	0.000	0.000	45	0.000	0.000	0.000	6	0.000	0.000	0.000	13	0.000	0.000	0.000
DIMETH	13	0.000	0.000	0.000	45	0.003	0.000	0.009	6	0.000	0.000	0.000	13	0.001	0.000	0.002
DIURON	13	0.000	0.000	0.000	45	0.002	0.000	0.009	6	0.072	0.035	0.096	13	0.053	0.000	0.087

Table 4.3 continued:

field Type of blank	GFF			PUF disk			PUF plug adsorber cartridge			PUF/XAD-2/PUF adsorber cartridge						
Target compound	n	\bar{x}_{arithm}	\bar{x}_{med}	σ	n	\bar{x}_{arithm}	\bar{x}_{med}	σ	n	\bar{x}_{arithm}	\bar{x}_{med}	σ	n	\bar{x}_{arithm}	\bar{x}_{med}	σ
END	13	0.000	0.000	0.000	45	0.000	0.000	0.000	6	0.000	0.000	0.000	13	0.000	0.000	0.000
FENUR	13	0.000	0.000	0.001	45	0.035	0.019	0.045	6	0.025	0.011	0.041	13	1.561	0.355	2.848
FL	13	1.938	0.000	2.554	45	5.414	6.851	3.829	6	4.382	4.976	3.836	13	5.244	6.561	3.398
FLU	13	1.557	0.000	1.776	45	6.069	5.049	2.782	6	2.060	2.445	1.811	13	13.06	7.627	17.70
HBCD-A	13	0.000	0.000	0.001	45	0.004	0.000	0.010	6	0.087	0.066	0.100	13	0.020	0.000	0.032
HBCD-BG	13	0.001	0.001	0.002	45	0.007	0.000	0.026	6	0.200	0.144	0.241	13	0.001	0.000	0.005
HCB	13	0.123	0.148	0.072	45	0.242	0.245	0.145	6	0.108	0.102	0.118	13	0.269	0.193	0.234
HCHA	13	0.000	0.000	0.000	45	0.005	0.000	0.025	6	0.021	0.000	0.051	13	0.027	0.000	0.052
HCHB	13	0.000	0.000	0.000	45	0.000	0.000	0.000	6	0.000	0.000	0.000	13	0.000	0.000	0.000
HCHD	13	0.000	0.000	0.000	45	0.018	0.000	0.099	6	0.000	0.000	0.000	13	0.000	0.000	0.000
HCHG	13	0.000	0.000	0.000	45	0.061	0.000	0.123	6	0.099	0.078	0.110	13	0.166	0.210	0.096
HEXAZIN	13	0.000	0.000	0.000	45	0.008	0.000	0.036	6	0.000	0.000	0.000	13	0.000	0.000	0.000
I123P	13	0.000	0.000	0.000	45	0.000	0.000	0.000	6	0.000	0.000	0.000	13	1.233	0.000	2.083
IRGAROL	13	0.000	0.000	0.000	45	0.000	0.000	0.000	6	0.000	0.000	0.000	13	0.000	0.000	0.000
ISOD	13	0.000	0.000	0.000	45	0.000	0.000	0.000	6	0.037	0.000	0.090	13	0.017	0.000	0.060
ISOPRUR	13	0.000	0.000	0.000	45	0.006	0.000	0.014	6	0.001	0.000	0.002	13	0.001	0.000	0.002
LINUR	13	0.000	0.000	0.000	45	0.000	0.000	0.000	6	0.000	0.000	0.000	13	0.000	0.000	0.000
MALATH	13	0.000	0.000	0.000	45	0.000	0.000	0.000	6	0.000	0.000	0.000	13	0.000	0.000	0.000
MCPA	13	0.000	0.000	0.000	n.q.	n.q.	n.q.	n.q.	n.q.	n.q.	n.q.	n.q.	n.q.	n.q.	n.q.	n.q.
MECOPR	13	0.000	0.000	0.000	n.q.	n.q.	n.q.	n.q.	n.q.	n.q.	n.q.	n.q.	n.q.	n.q.	n.q.	n.q.
METAZCHL	13	0.000	0.000	0.000	45	0.026	0.000	0.084	6	0.000	0.000	0.000	13	0.002	0.000	0.006
METHABZT	13	0.000	0.000	0.000	45	0.000	0.000	0.002	6	0.000	0.000	0.000	13	0.000	0.000	0.000
METOLA	13	0.020	0.020	0.020	45	0.072	0.049	0.102	6	0.014	0.000	0.022	13	0.314	0.205	0.327
NAPROX	13	0.000	0.000	0.000	n.q.	n.q.	n.q.	n.q.	n.q.	n.q.	n.q.	n.q.	n.q.	n.q.	n.q.	n.q.
OXAZEP	13	0.000	0.000	0.000	45	0.000	0.000	0.000	6	0.000	0.000	0.000	13	0.000	0.000	0.000
PENDIMETH	13	0.047	0.056	0.034	45	0.225	0.167	0.190	6	0.203	0.173	0.108	13	0.183	0.178	0.083
PFBS	13	0.003	0.003	0.002	45	0.018	0.013	0.013	6	0.006	0.006	0.006	13	0.020	0.016	0.009
PFDEA	13	0.000	0.000	0.000	45	0.004	0.000	0.010	6	0.017	0.017	0.016	13	0.006	0.000	0.012
PFHPA	13	0.014	0.013	0.008	45	0.123	0.090	0.117	6	0.021	0.030	0.017	13	0.054	0.057	0.036
PFHXA	13	0.011	0.009	0.008	45	0.145	0.123	0.100	6	0.053	0.046	0.021	13	0.090	0.090	0.029
PFHXS	13	0.001	0.001	0.001	45	0.008	0.006	0.007	6	0.010	0.010	0.009	13	0.014	0.015	0.008
PFNOA	13	0.024	0.028	0.017	45	0.075	0.072	0.079	6	0.012	0.011	0.014	13	0.102	0.109	0.077
PFOA	13	0.048	0.048	0.018	45	0.659	0.487	0.899	6	0.124	0.152	0.064	13	0.409	0.328	0.190
PFOS-1	13	0.023	0.015	0.022	45	0.165	0.129	0.128	6	0.087	0.081	0.024	13	0.204	0.199	0.108
PFOSA-1	13	0.033	0.020	0.029	45	0.125	0.099	0.092	6	0.066	0.075	0.029	13	0.591	0.531	0.500
PHEN	13	1.684	2.853	1.628	45	12.20	9.824	7.215	6	7.997	8.651	3.091	13	13.47	11.86	7.267
PIRIMIC	13	0.000	0.000	0.000	45	0.001	0.000	0.006	6	0.000	0.000	0.000	13	0.000	0.000	0.000
PRIMID	13	0.000	0.000	0.000	45	0.000	0.000	0.000	6	0.000	0.000	0.000	13	0.000	0.000	0.000
PROMETR	13	0.074	0.078	0.017	45	0.105	0.078	0.079	6	0.070	0.071	0.012	13	0.073	0.075	0.007
PROPAZ	13	0.000	0.000	0.000	45	0.000	0.000	0.000	6	0.000	0.000	0.000	13	0.000	0.000	0.000
PYR	13	2.181	3.572	2.144	45	10.44	7.722	6.281	6	3.899	2.880	4.613	13	26.34	9.764	26.59
QCB	13	0.000	0.000	0.000	45	0.168	0.215	0.084	6	0.286	0.245	0.186	13	0.270	0.214	0.132
SIMAZ	13	0.000	0.000	0.000	45	0.000	0.000	0.000	6	0.000	0.000	0.000	13	0.000	0.000	0.000
TBEP	13	2.931	0.933	3.147	45	0.783	0.357	1.262	6	0.622	0.721	0.453	13	2.784	2.427	1.932
TBP	13	2.219	2.180	0.380	45	20.62	14.40	13.48	6	7.746	7.480	2.296	13	12.18	14.30	9.467
TERBAZ	13	0.091	0.080	0.047	45	0.064	0.037	0.068	6	0.033	0.032	0.009	13	0.148	0.090	0.135
TERBUTR	13	0.000	0.000	0.000	45	0.047	0.000	0.147	6	0.000	0.000	0.000	13	0.000	0.000	0.000
TPP	13	0.798	0.583	0.450	45	3.688	2.800	2.345	6	1.846	1.725	0.851	13	33.03	11.80	42.77
TRIFLU	13	0.000	0.000	0.000	45	0.013	0.000	0.063	6	0.111	0.104	0.123	13	0.024	0.000	0.087

Laboratory blanks

Eight different types of laboratory blanks were examined in order to localize possible sources of air sample contamination during sample preparation (table 4.2). Blanks were obtained for three different stages of the sample preparation method, namely extraction including the unification in narrow neck bottles, evaporation and clean-up. Extraction blanks revealed the overall contamination level of the sample preparation method. Evaporation blanks displayed contamination sources originating from parallel evaporation and following sample preparation stages. Clean-up blanks controlled the last sample preparation step.

Extraction blanks were obtained by extraction of empty petri dishes (“petri dish blank”) and Soxhlet apparatus (“Soxhlet blank”) according to the extraction methods described in chapter 9. The air sample extracts were collected in narrow neck bottles of sizes of 2.0 L and 0.5 L. Blanks of both bottle sizes (“2.0 L bottle blank”, “0.5 L bottle blank”) were generated by rinsing them with an acetone/hexane/methanol (75/20/5; v/v/v) solvent mixture. The 2.0 L narrow neck bottle was rinsed with 700 mL solvent mixture, whereas the 0.5 L bottle was flushed out with 200 mL.

The air sample extracts were divided in two equal parts. Thereafter, the aliquots were evaporated and solvent exchanged either to methanol or hexane in a parallel-evaporation system. As described in chapter 9, two different volumes of air sample extracts (350 mL and 100 mL) needed to be evaporated. Hence, two evaporation blanks (“evaporation-350 mL blank”, “evaporation-100 mL blank”) were obtained.

The last sample preparation step for the methanol aliquot was a syringe filtration. Blanks of syringe filtration (“syringe filtration blank”) were obtained by filtration of 250 μ L methanol instead of the air sample extract. Silica gel was used as clean-up material for the hexane aliquot. Silica gel blanks (“silica gel blank”) were produced by transferring 500 μ L of hexane instead of the air sample extract into the clean-up column.

Arithmetic means, medians and standard deviations of organic target compounds in laboratory blanks were calculated enclosing the whole data set of the five preparation sequences. For reasons of clarity and readability exclusively the laboratory blanks of PAHs and organophosphorus flame retardants are listed in table 4.4, because only these compounds exhibit significant blank results. Single laboratory blank data for each target analyte is tabulated in annex 2.

Table 4.4: Laboratory blanks; n = number of field blanks, \bar{x}_{arithm} = arithmetic mean (ng/mL), \bar{x}_{med} = median (ng/mL), σ = standard deviation (ng/mL); n.q. = not quantified

Type of lab blank	Soxhlet blank				Petri dish blank				2.0 L bottle blank			0.5 L bottle blank				
	Target compound	n	\bar{x}_{arithm}	\bar{x}_{med}	σ	n	\bar{x}_{arithm}	\bar{x}_{med}	σ	n	\bar{x}_{arithm}	\bar{x}_{med}	σ	n	\bar{x}_{arithm}	\bar{x}_{med}
ACE	5	0.264	0.000	0.591	3	0.013	0.000	0.023	5	0.318	0.000	0.712	3	0.000	0.000	0.000
ACY	5	1.161	0.000	2.597	3	0.000	0.000	0.000	5	0.210	0.000	0.470	3	0.000	0.000	0.000
ANT	5	0.000	0.000	0.000	3	0.000	0.000	0.000	5	0.000	0.000	0.000	3	0.000	0.000	0.000
BAA	5	0.000	0.000	0.000	3	0.000	0.000	0.000	5	0.000	0.000	0.000	3	0.000	0.000	0.000
BAP	5	0.000	0.000	0.000	3	0.000	0.000	0.000	5	0.000	0.000	0.000	3	0.000	0.000	0.000
BBF	5	0.000	0.000	0.000	3	0.000	0.000	0.000	5	0.000	0.000	0.000	3	0.000	0.000	0.000
BGHIP	5	0.000	0.000	0.000	3	0.000	0.000	0.000	5	0.000	0.000	0.000	3	0.000	0.000	0.000
CHRTR	5	0.016	0.000	0.037	3	0.000	0.000	0.000	5	0.000	0.000	0.000	3	0.000	0.000	0.000
DBAHA	5	0.000	0.000	0.000	3	0.000	0.000	0.000	5	0.000	0.000	0.000	3	0.000	0.000	0.000
FL	5	0.316	0.000	0.651	3	0.017	0.000	0.030	5	0.249	0.000	0.558	3	0.010	0.000	0.018
FLU	5	0.421	0.000	0.827	3	0.002	0.000	0.003	5	0.008	0.000	0.019	3	0.001	0.000	0.002
P123I	5	0.000	0.000	0.000	3	0.000	0.000	0.000	5	0.000	0.000	0.000	3	0.000	0.000	0.000
PHEN	5	2.078	0.670	2.564	3	0.124	0.000	0.215	5	0.250	0.000	0.517	3	0.066	0.000	0.115
PYR	5	0.212	0.000	0.435	3	0.000	0.000	0.000	5	0.006	0.000	0.012	3	0.000	0.000	0.000
TBEP	5	1.489	0.341	2.577	3	1.543	0.407	2.089	5	1.679	0.373	2.962	3	1.465	0.333	1.999
TBP	5	15.23	12.10	14.11	3	1.973	2.060	0.261	5	7.557	6.430	3.707	3	1.720	1.630	0.276
TPP	5	1.228	1.060	0.840	3	0.528	0.373	0.620	5	0.878	0.776	0.580	3	0.439	0.372	0.476

Type of lab blank	Evaporation-350 mL blank				Evaporation-100 mL blank				Syringe filtration blank				Silica gel blank			
	Target compound	n	\bar{x}_{arithm}	\bar{x}_{med}	σ	n	\bar{x}_{arithm}	\bar{x}_{med}	σ	n	\bar{x}_{arithm}	\bar{x}_{med}	σ	n	\bar{x}_{arithm}	\bar{x}_{med}
ACE	9	0.021	0.000	0.043	5	0.064	0.000	0.143	n.q.	n.q.	n.q.	n.q.	9	0.004	0.000	0.013
ACY	9	1.994	0.271	3.591	5	0.996	0.000	2.024	n.q.	n.q.	n.q.	n.q.	9	0.000	0.000	0.000
ANT	9	0.000	0.000	0.000	5	0.000	0.000	0.000	n.q.	n.q.	n.q.	n.q.	9	0.000	0.000	0.000
BAA	9	0.000	0.000	0.000	5	0.000	0.000	0.000	n.q.	n.q.	n.q.	n.q.	9	0.000	0.000	0.000
BAP	9	0.000	0.000	0.000	5	0.000	0.000	0.000	n.q.	n.q.	n.q.	n.q.	9	0.000	0.000	0.000
BBF	9	0.000	0.000	0.000	5	0.000	0.000	0.000	n.q.	n.q.	n.q.	n.q.	9	0.000	0.000	0.000
BGHIP	9	0.000	0.000	0.000	5	0.000	0.000	0.000	n.q.	n.q.	n.q.	n.q.	9	0.000	0.000	0.000
CHRTR	9	0.002	0.000	0.007	5	0.000	0.000	0.000	n.q.	n.q.	n.q.	n.q.	9	0.000	0.000	0.000
DBAHA	9	0.000	0.000	0.000	5	0.000	0.000	0.000	n.q.	n.q.	n.q.	n.q.	9	0.000	0.000	0.000
FL	9	0.008	0.000	0.023	5	0.059	0.000	0.132	n.q.	n.q.	n.q.	n.q.	9	0.000	0.000	0.001
FLU	9	0.003	0.000	0.010	5	0.003	0.000	0.007	n.q.	n.q.	n.q.	n.q.	9	0.000	0.000	0.000
I123P	9	0.000	0.000	0.000	5	0.000	0.000	0.000	n.q.	n.q.	n.q.	n.q.	9	0.000	0.000	0.000
PHEN	9	0.050	0.000	0.137	5	0.067	0.000	0.151	n.q.	n.q.	n.q.	n.q.	9	0.023	0.000	0.069
PYR	9	0.022	0.000	0.066	5	0.003	0.000	0.007	n.q.	n.q.	n.q.	n.q.	9	0.001	0.000	0.002
TBEP	9	0.645	0.295	1.202	5	0.560	0.200	0.907	3	0.437	0.113	0.586	n.q.	n.q.	n.q.	n.q.
TBP	9	5.321	4.010	3.375	5	1.330	1.160	0.905	3	0.206	0.042	0.321	n.q.	n.q.	n.q.	n.q.
TPP	9	0.798	0.741	0.441	5	0.268	0.256	0.271	3	0.109	0.000	0.188	n.q.	n.q.	n.q.	n.q.

Increased blanks (field blanks / laboratory blanks) were predominantly observed for the PAHs and the organophosphorus flame retardants. In particular the organophosphorus flame retardants (tris(2-butoxyethyl)phosphate, tributyl phosphate and triphenyl phosphate) exhibited highest laboratory blanks, which indicated to an overall contamination of the laboratory equipment: A gradual increase in organophosphorus flame retardant contamination with proceeding sample preparation was observed. Thus, contamination was supposed to origin from diffusive sources,

which could not be definitely located throughout this study. It was assumed that the contamination partly originated from a 2 % Mucosol® solution, which was necessary for the purification of laboratory glass jars from tenacious PUF residues (figure 4.21).

The PAHs, in particular those of high volatility (acenaphthene, acenaphthylene, fluorene, phenanthrene, fluoranthene and pyrene) exhibited increased field blanks. By contrast, PAH contamination was comparable low in laboratory blanks. Hence, the most important factor on PAH contamination was presumed in the last step of the pre-cleaning procedure consisting of an enhanced dessication period in a vacuum desiccator (chapter 9).



Figure 4.21: Glass jars of the parallel-evaporator system glazed with tenacious PUF residues

4.2.2 Spike controls

The quality assurance of air concentration data included eight different spike controls. The recoveries of target analytes from GFFs, PUF disks, PUF plug adsorber cartridges and PUF/XAD-2/PUF adsorber cartridges were determined by spiking pre-cleaned sampling material with specified amounts of target analytes, performance reference compounds and internal standards (refer to chapter 9). Most organic compounds (labeled and unlabeled) immediately evaporated from GFF surfaces without atmospheric particle coating. Thus, target analytes, performance reference compounds and internal standards were added to the first extraction solvent (acetone/hexane) in the petri dishes.

In addition, recovery controls of certain air sample preparation steps, namely evaporation (“evaporation-350 mL spike”, “evaporation-100 mL spike”) and clean-up (“silica gel spike”, “syringe filtration spike”), were performed. Evaporation spike controls were carried out with

350 mL and 100 mL of an acetone/hexane/methanol (75/20/5, v/v/v) solvent mixture contaminated with defined amounts of target analytes, performance reference compounds and internal standards (refer to chapter 9). Clean-up spikes were performed with specified solvent volumes of methanol (250 µL) and hexane (500 µL) spiked with distinct amounts of respective target analytes, performance reference compounds and internal standards (refer to chapter 9).

Arithmetic means, medians and standard deviations of target compound recoveries in spike samples were calculated for the whole data set enclosing five preparation sequences. Recoveries (in %) are listed in table 4.5. Results for single spike samples are tabulated in the annex 2.

Table 4.5: Recovery of target compounds in spike controls; n = number of spike samples, \bar{x}_{arithm} = arithmetic mean (%), \bar{x}_{med} = median (%), σ = standard deviation (%); n.q. = not quantified

Type of spike sample	GFF				PUF disk				PUF plug adsorber cartridge				PUF/XAD-2/PUF adsorber cartridge			
	n	\bar{x}_{arithm}	\bar{x}_{med}	σ	n	\bar{x}_{arithm}	\bar{x}_{med}	σ	n	\bar{x}_{arithm}	\bar{x}_{med}	σ	n	\bar{x}_{arithm}	\bar{x}_{med}	σ
24-D	9	100	103	7	n.q.	n.q.	n.q.	n.q.	n.q.	n.q.	n.q.	n.q.	n.q.	n.q.	n.q.	n.q.
ACE	9	105	103	12	11	101	100	14	6	97	100	8	9	118	103	26
ACY	9	97	97	12	11	63	66	13	6	117	118	62	9	78	70	29
ALD	9	79	74	13	11	91	89	7	6	81	79	8	9	89	87	6
AMETRYN	9	131	132	15	11	106	110	11	6	109	108	9	9	110	114	10
ANT	9	105	104	13	11	99	99	13	6	92	93	11	9	99	102	11
ATRAZ	9	101	101	1	11	98	96	4	6	102	103	2	9	100	101	3
AZINPH-E	9	116	116	9	11	168	163	53	6	131	118	40	9	140	127	34
AZINPH-M	9	103	104	3	11	103	102	10	6	105	105	3	9	104	105	5
BAA	9	97	91	14	11	107	104	10	6	116	108	32	9	112	111	18
BAP	9	105	101	16	11	89	88	10	6	87	92	15	9	94	94	13
BBF	9	111	106	15	11	108	109	4	6	104	103	6	9	109	105	13
BENTAZ	9	106	106	2	11	84	78	15	6	92	94	12	9	70	69	8
BGHIP	9	106	104	13	11	98	98	6	6	101	102	4	9	97	98	9
CARBAMAZ	9	105	107	5	11	90	93	11	6	99	101	6	9	101	102	6
CARBEND	9	84	87	26	11	70	76	19	6	86	100	26	9	70	64	17
CB138	9	102	101	15	11	102	99	5	6	104	104	3	9	102	103	5
CB153	9	104	102	13	11	102	101	5	6	104	102	4	9	102	100	4
CB28	9	98	96	12	11	98	99	4	6	95	96	6	9	100	101	5
CB52	9	102	100	13	11	101	100	6	6	101	102	6	9	104	104	5
CHLORFENV	9	107	107	6	11	106	93	22	6	97	97	1	9	123	114	39
CHLORTUR	9	100	99	2	11	71	80	15	6	94	96	11	9	93	95	8
CHRTR	9	97	92	14	11	114	114	14	6	120	111	38	9	125	129	15
CLOFIBRS	9	101	102	3	n.q.	n.q.	n.q.	n.q.	n.q.	n.q.	n.q.	n.q.	n.q.	n.q.	n.q.	n.q.
DBAHA	9	108	103	16	11	107	106	5	6	106	107	12	9	105	107	6
DDPP	9	100	102	19	11	96	98	7	6	104	103	9	9	103	106	9
DDEPP	9	118	118	24	11	108	105	10	6	108	103	12	9	107	109	8
DDTOP	9	165	147	54	11	100	99	20	6	106	106	6	9	98	102	13
DDTPP	9	115	109	18	11	98	96	7	6	104	103	5	9	98	96	7
DEATRAZ	9	102	103	3	11	105	107	7	6	102	101	3	9	98	99	3
DIAZINON	9	81	82	8	11	108	113	14	6	101	102	5	9	100	94	16
DICHLPR	9	101	101	2	n.q.	n.q.	n.q.	n.q.	n.q.	n.q.	n.q.	n.q.	n.q.	n.q.	n.q.	n.q.
DICLOF	9	103	107	12	n.q.	n.q.	n.q.	n.q.	n.q.	n.q.	n.q.	n.q.	n.q.	n.q.	n.q.	n.q.

Table 4.5 continued:

Type of spike sample	GFF				PUF disk				PUF plug adsorber cartridge				PUF/XAD-2/PUF adsorber cartridge			
Target compound	n	\bar{x}_{arithm}	\bar{x}_{med}	σ	n	\bar{x}_{arithm}	\bar{x}_{med}	σ	n	\bar{x}_{arithm}	\bar{x}_{med}	σ	n	\bar{x}_{arithm}	\bar{x}_{med}	σ
DIELD	9	67	72	17	11	86	89	12	6	76	76	4	9	87	86	9
DIMETH	9	96	96	5	11	107	98	28	6	94	96	7	9	116	104	38
DIURON	9	103	104	4	11	116	115	9	6	108	108	6	9	106	105	7
END	9	82	80	28	11	125	120	29	6	103	100	66	9	134	140	38
FENUR	9	120	116	11	11	92	95	20	6	102	101	6	9	145	104	101
FL	9	110	106	14	11	134	126	21	6	119	124	17	9	124	126	55
FLU	9	67	64	14	11	102	98	16	6	128	120	30	9	128	117	35
HBCD-A	9	91	91	4	11	71	76	15	6	86	94	15	9	80	86	22
HBCD-BG	9	53	53	9	11	53	49	22	6	75	96	37	9	61	68	33
HCB	9	102	100	14	11	99	99	5	6	96	95	7	9	98	99	2
HCHA	9	12	12	9	11	71	74	23	6	109	112	33	9	71	80	21
HCHB	9	312	260	144	11	116	106	34	6	123	110	36	9	116	111	26
HCHD	9	0	0	0	11	50	55	30	6	40	44	35	9	49	58	36
HCHG	9	16	11	13	11	73	77	22	6	72	76	11	9	74	78	21
HEXAZIN	9	117	119	9	11	93	92	12	6	102	103	4	9	96	94	8
I123P	9	109	106	14	11	102	103	6	6	99	98	7	9	98	99	15
IRGAROL	9	140	138	16	11	90	91	10	6	106	104	8	9	103	101	11
ISOD	9	96	92	14	11	95	95	6	6	89	87	8	9	93	95	9
ISOPRUR	9	99	99	3	11	94	91	10	6	100	98	8	9	101	98	7
LINUR	9	93	93	3	11	106	107	8	6	103	102	5	9	106	100	9
MALATH	9	92	98	37	11	97	97	3	6	97	100	6	9	99	96	7
MCPA	9	104	107	5	n.q.	n.q.	n.q.	n.q.	n.q.	n.q.	n.q.	n.q.	n.q.	n.q.	n.q.	n.q.
MECOPR	9	101	101	3	n.q.	n.q.	n.q.	n.q.	n.q.	n.q.	n.q.	n.q.	n.q.	n.q.	n.q.	n.q.
METAZCHL	9	137	136	19	11	85	82	7	6	106	105	6	9	104	101	9
METHABZT	9	141	141	17	11	83	81	6	6	102	101	8	9	105	108	11
METOLA	9	119	119	11	11	121	124	13	6	113	112	13	9	114	115	10
NAPROX	9	95	97	9	n.q.	n.q.	n.q.	n.q.	n.q.	n.q.	n.q.	n.q.	n.q.	n.q.	n.q.	n.q.
OXAZEP	9	98	99	8	11	82	85	18	6	91	99	23	9	90	94	28
PENDIMETH	9	105	111	15	11	48	64	40	6	52	52	54	9	63	74	42
PFBS	9	214	245	89	11	217	120	178	6	310	228	285	9	249	107	224
PFDEA	9	102	102	2	11	109	112	12	6	109	105	11	9	109	109	6
PFHPA	9	105	104	2	11	82	78	15	6	98	98	3	9	90	90	8
PFHXA	9	104	104	2	11	84	86	11	6	91	92	6	9	86	87	7
PFHXS	9	102	103	2	11	100	100	4	6	103	103	2	9	103	102	5
PFNOA	9	102	102	2	11	102	108	16	6	106	102	9	9	104	100	7
PFOA	9	103	104	3	11	108	109	18	6	106	103	8	9	105	104	5
PFOS-1	9	103	104	2	11	103	104	5	6	104	104	5	9	105	105	4
PFOSA-1	9	101	102	2	11	87	89	17	6	97	99	7	9	113	107	24
PHEN	9	107	105	12	11	128	124	11	6	188	187	68	9	196	162	84
PIRIMIC	9	106	108	8	11	105	115	16	6	108	108	9	9	106	111	9
PRIMID	9	136	136	31	11	130	135	22	6	112	110	12	9	106	112	18
PROMETR	9	131	131	15	11	109	113	12	6	114	112	15	9	110	116	15
PROPAZ	9	105	107	4	11	99	99	6	6	105	105	6	9	106	104	5
PYR	9	70	66	15	11	111	114	18	6	161	150	36	9	166	146	53
QCB	9	110	102	18	11	84	91	14	6	81	82	13	9	80	76	12
SIMAZ	9	105	105	3	11	83	81	7	6	99	100	3	9	91	91	5
TBEP	9	130	131	5	11	107	99	32	6	103	99	12	9	131	112	72
TBP	9	153	141	38	11	447	385	257	6	254	243	169	9	202	244	90
TERBAZ	9	106	105	3	11	105	102	7	6	106	105	8	9	105	104	5
TERBUTR	9	130	130	14	11	107	110	12	6	111	109	11	9	108	111	12
TPP	9	190	104	261	11	118	111	58	6	130	100	48	9	1623	152	3076
TRIFLU	9	94	90	12	11	62	83	41	6	186	82	207	9	91	88	13

Table 4.5 continued:

Type of spike sample	Evaporation-350 mL				Evaporation-100 mL				Syringe filtration				Silica gel			
	n	\bar{x}_{arithm}	\bar{x}_{med}	σ	n	\bar{x}_{arithm}	\bar{x}_{med}	σ	n	\bar{x}_{arithm}	\bar{x}_{med}	σ	n	\bar{x}_{arithm}	\bar{x}_{med}	σ
24-D	n.q.	n.q.	n.q.	n.q.	5	93	93	3	3	90	89	3	n.q.	n.q.	n.q.	n.q.
ACE	9	104	99	16	5	108	107	9	n.q.	n.q.	n.q.	n.q.	9	99	99	8
ACY	9	107	108	20	5	100	95	11	n.q.	n.q.	n.q.	n.q.	9	101	98	8
ALD	9	77	76	6	5	84	84	4	n.q.	n.q.	n.q.	n.q.	9	100	102	6
AMETRYN	9	108	107	9	5	106	105	5	6	99	97	5	n.q.	n.q.	n.q.	n.q.
ANT	9	89	89	9	5	105	102	8	n.q.	n.q.	n.q.	n.q.	9	98	98	10
ATRAZ	9	97	96	4	5	94	93	3	6	96	95	3	n.q.	n.q.	n.q.	n.q.
AZINPH-E	9	106	102	10	5	99	97	3	6	98	97	4	n.q.	n.q.	n.q.	n.q.
AZINPH-M	9	99	96	5	5	97	97	2	6	97	98	3	n.q.	n.q.	n.q.	n.q.
BAA	9	96	95	10	5	87	87	4	n.q.	n.q.	n.q.	n.q.	9	100	99	8
BAP	9	98	97	5	5	105	100	10	n.q.	n.q.	n.q.	n.q.	9	95	97	6
BBF	9	102	102	6	5	105	102	8	n.q.	n.q.	n.q.	n.q.	9	93	91	7
BENTAZ	9	701	94	949	5	95	95	2	6	79	79	6	n.q.	n.q.	n.q.	n.q.
BGHIP	9	96	97	5	5	100	100	2	n.q.	n.q.	n.q.	n.q.	9	98	95	8
CARBAMAZ	9	128	123	20	5	96	94	5	6	99	99	4	n.q.	n.q.	n.q.	n.q.
CARBEND	9	93	97	31	5	105	105	2	6	80	89	22	n.q.	n.q.	n.q.	n.q.
CB138	9	99	98	3	5	98	99	5	n.q.	n.q.	n.q.	n.q.	9	100	99	11
CB153	9	103	102	4	5	99	99	3	n.q.	n.q.	n.q.	n.q.	9	101	102	6
CB28	9	95	94	8	5	92	89	5	n.q.	n.q.	n.q.	n.q.	9	97	100	12
CB52	9	97	97	6	5	98	101	7	n.q.	n.q.	n.q.	n.q.	9	99	99	7
CHLORFENV	9	128	101	47	5	100	99	4	6	102	101	3	n.q.	n.q.	n.q.	n.q.
CHLORTUR	9	126	117	14	5	96	95	4	6	99	98	3	n.q.	n.q.	n.q.	n.q.
CHRTR	9	96	97	13	5	94	94	9	n.q.	n.q.	n.q.	n.q.	9	102	105	12
CLOFIBRS	n.q.	n.q.	n.q.	n.q.	5	96	96	2	3	96	96	1	n.q.	n.q.	n.q.	n.q.
DBAHA	9	99	98	6	5	110	114	8	n.q.	n.q.	n.q.	n.q.	9	96	98	7
DDPP	9	116	113	19	5	105	105	10	n.q.	n.q.	n.q.	n.q.	9	101	99	19
DDEPP	9	94	97	7	5	88	92	6	n.q.	n.q.	n.q.	n.q.	9	103	101	9
DDTOP	9	92	85	24	5	86	84	8	n.q.	n.q.	n.q.	n.q.	9	117	100	28
DDTPP	9	99	96	9	5	97	96	5	n.q.	n.q.	n.q.	n.q.	9	97	98	5
DEATRAZ	9	97	96	1	5	97	96	3	6	98	98	1	n.q.	n.q.	n.q.	n.q.
DIAZINON	9	83	84	7	5	83	83	1	6	81	92	29	n.q.	n.q.	n.q.	n.q.
DICHLPR	n.q.	n.q.	n.q.	n.q.	5	96	96	3	3	96	96	2	n.q.	n.q.	n.q.	n.q.
DICLOF	n.q.	n.q.	n.q.	n.q.	5	96	94	6	3	93	94	7	n.q.	n.q.	n.q.	n.q.
DIELD	9	91	90	23	5	89	90	8	n.q.	n.q.	n.q.	n.q.	9	103	99	12
DIMETH	9	121	97	41	5	98	96	7	6	97	98	5	n.q.	n.q.	n.q.	n.q.
DIURON	9	100	97	7	5	97	94	6	6	97	97	3	n.q.	n.q.	n.q.	n.q.
END	9	149	100	89	5	159	155	35	n.q.	n.q.	n.q.	n.q.	9	78	87	30
FENUR	9	106	102	8	5	104	102	6	6	99	99	3	n.q.	n.q.	n.q.	n.q.
FL	9	149	108	72	5	140	154	33	n.q.	n.q.	n.q.	n.q.	9	103	98	12
FLU	9	70	72	14	5	64	65	4	n.q.	n.q.	n.q.	n.q.	9	98	100	5
HBCD-A	9	89	88	6	5	3616	89	7885	6	101	102	5	n.q.	n.q.	n.q.	n.q.
HBCD-BG	9	76	78	10	5	3452	86	7527	6	99	100	3	n.q.	n.q.	n.q.	n.q.
HCB	9	99	100	3	5	98	98	1	n.q.	n.q.	n.q.	n.q.	9	97	98	4
HCHA	9	79	69	45	5	83	87	11	n.q.	n.q.	n.q.	n.q.	9	97	96	4
HCHB	9	107	100	14	5	105	103	8	n.q.	n.q.	n.q.	n.q.	9	96	99	7
HCHD	9	70	101	52	5	86	106	48	n.q.	n.q.	n.q.	n.q.	9	94	100	10
HCHG	9	74	84	27	5	86	89	10	n.q.	n.q.	n.q.	n.q.	9	96	95	5
HEXAZIN	9	105	104	14	5	102	99	7	6	102	102	2	n.q.	n.q.	n.q.	n.q.
I123P	9	95	98	7	5	107	108	6	n.q.	n.q.	n.q.	n.q.	9	92	91	8
IRGAROL	9	113	115	16	5	112	110	5	6	99	98	3	n.q.	n.q.	n.q.	n.q.
ISOD	9	87	88	7	5	91	91	2	n.q.	n.q.	n.q.	n.q.	9	97	95	6
ISOPRUR	9	126	123	13	5	94	93	5	6	100	98	6	n.q.	n.q.	n.q.	n.q.

Table 4.5 continued:

Type of spike sample	Evaporation-350 mL				Evaporation-100 mL				Syringe filtration				Silica gel			
	n	\bar{x}_{arithm}	\bar{x}_{med}	σ	n	\bar{x}_{arithm}	\bar{x}_{med}	σ	n	\bar{x}_{arithm}	\bar{x}_{med}	σ	n	\bar{x}_{arithm}	\bar{x}_{med}	σ
LINUR	9	117	123	15	5	91	91	3	6	102	99	9	n.q.	n.q.	n.q.	n.q.
MALATH	9	95	96	3	5	98	96	7	6	95	95	2	n.q.	n.q.	n.q.	n.q.
MCPA	n.q.	n.q.	n.q.	n.q.	5	94	93	4	3	98	97	2	n.q.	n.q.	n.q.	n.q.
MECOPR	n.q.	n.q.	n.q.	n.q.	5	96	95	2	3	98	98	1	n.q.	n.q.	n.q.	n.q.
METAZCHL	9	112	105	12	5	110	107	6	6	102	101	4	n.q.	n.q.	n.q.	n.q.
METHABZT	9	112	112	13	5	109	107	6	6	97	95	4	n.q.	n.q.	n.q.	n.q.
METOLA	9	102	101	7	5	99	100	2	6	99	97	6	n.q.	n.q.	n.q.	n.q.
NAPROX	n.q.	n.q.	n.q.	n.q.	5	97	96	6	3	89	87	3	n.q.	n.q.	n.q.	n.q.
OXAZEP	9	120	118	11	5	93	92	2	6	99	98	9	n.q.	n.q.	n.q.	n.q.
PENDIMETH	9	71	74	18	5	84	86	9	6	98	97	6	n.q.	n.q.	n.q.	n.q.
PFBS	9	105	98	13	5	103	97	13	6	91	92	4	n.q.	n.q.	n.q.	n.q.
PFDEA	9	94	94	3	5	97	98	2	6	100	100	2	n.q.	n.q.	n.q.	n.q.
PFHPA	9	93	95	7	5	99	99	0	6	96	96	3	n.q.	n.q.	n.q.	n.q.
PFHXA	9	93	95	7	5	99	99	1	6	89	87	6	n.q.	n.q.	n.q.	n.q.
PFHXS	9	99	99	2	5	99	99	2	6	97	98	2	n.q.	n.q.	n.q.	n.q.
PFNOA	9	93	95	6	5	96	97	2	6	97	97	3	n.q.	n.q.	n.q.	n.q.
PFOA	9	100	101	2	5	98	98	2	6	98	99	2	n.q.	n.q.	n.q.	n.q.
PFOS-1	9	99	99	2	5	99	99	2	6	99	100	3	n.q.	n.q.	n.q.	n.q.
PFOSA-1	9	96	96	3	5	98	99	3	6	102	101	4	n.q.	n.q.	n.q.	n.q.
PHEN	9	96	97	10	5	95	99	7	n.q.	n.q.	n.q.	n.q.	9	98	99	6
PIRIMIC	9	93	94	7	5	95	94	4	6	98	96	6	n.q.	n.q.	n.q.	n.q.
PRIMID	9	113	101	26	5	110	108	5	6	102	99	9	n.q.	n.q.	n.q.	n.q.
PROMETR	9	106	101	11	5	108	107	4	6	101	99	6	n.q.	n.q.	n.q.	n.q.
PROPAPZ	9	98	96	4	5	96	94	5	6	97	95	5	n.q.	n.q.	n.q.	n.q.
PYR	9	71	68	14	5	71	71	6	n.q.	n.q.	n.q.	n.q.	9	100	96	11
QCB	9	98	98	7	5	97	97	3	n.q.	n.q.	n.q.	n.q.	9	101	102	4
SIMAZ	9	97	97	3	5	97	95	4	6	98	97	3	n.q.	n.q.	n.q.	n.q.
TBEP	9	125	123	16	5	111	112	3	6	101	103	9	n.q.	n.q.	n.q.	n.q.
TBP	9	160	117	74	5	106	99	13	6	96	94	12	n.q.	n.q.	n.q.	n.q.
TERBAZ	9	98	98	3	5	96	94	4	6	98	96	4	n.q.	n.q.	n.q.	n.q.
TERBUTR	9	107	107	9	5	105	103	5	6	99	97	5	n.q.	n.q.	n.q.	n.q.
TPP	9	164	116	171	5	93	98	11	6	155	102	115	n.q.	n.q.	n.q.	n.q.
TRIFLU	9	88	83	12	5	99	99	1	n.q.	n.q.	n.q.	n.q.	9	97	99	5

4.2.3 Reproducibility of air sample preparation

The above tabulated spike control samples were a useful tool in the verification of air sampling data. However, they insufficiently accounted for matrix influences on air sample preparation and mass spectrometer analyses. Besides the matrix originating from atmosphere, the condition of polyurethane foam determined the matrix content in the sample. White polyurethane foam used for adsorber cartridges and for passive air sampling aged (turned yellow) during long sampling periods. Aged polyurethane foam caused extended precipitation during sample preparation and observably pigmented the final air sample extract. An example of the increased matrix content in extracts originating from aged polyurethane foam is illustrated in figure 4.22.

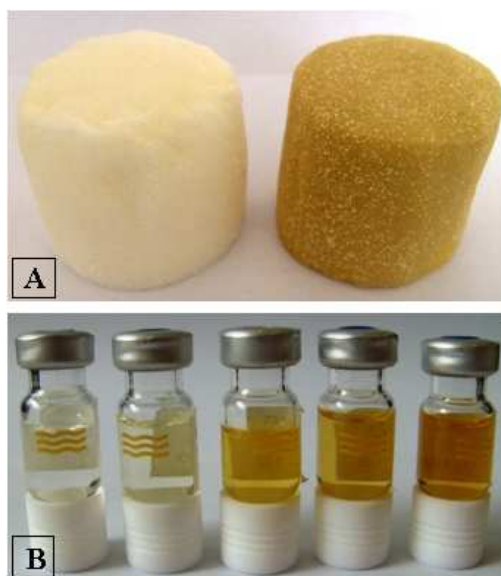


Figure 4.22: White and aged polyurethane foam (A) with respective methanol extracts (B)

For this reason, reproducibility of air sample preparation was tested by a further experiment: Air samples, consisting of target analytes, atmospheric matrix as well as more or less aged sampling material, were spiked with performance reference compounds after exposure and prior to extraction. The reproducibility of PRC recovery results (plotted in figures 4.23 - 4.26) were used as indicator of the sample preparation precision.

Standard deviations were less than 10 %, except in four cases. The recovery results of prometryn-D₆ in the GFF sample preparation, γ -HCH-¹³C₆D₆ and fluoranthene-D₁₀ in the PUF disk sample preparation and polychlorinated biphenyl 30 in the PUF/XAD-2/PUF adsorber cartridge sample preparation displayed standard deviations less than 20 %. Arithmetic mean recoveries ranged from 60 % to 127 %.

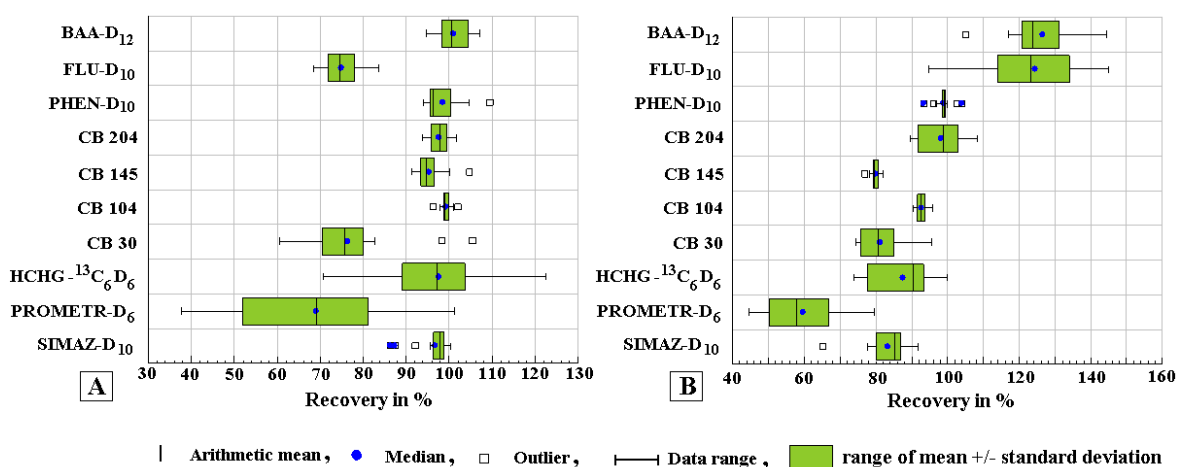


Figure 4.23: PRC recovery results of (A) 20 GFF air samples and (B) of 12 PUF disk air samples

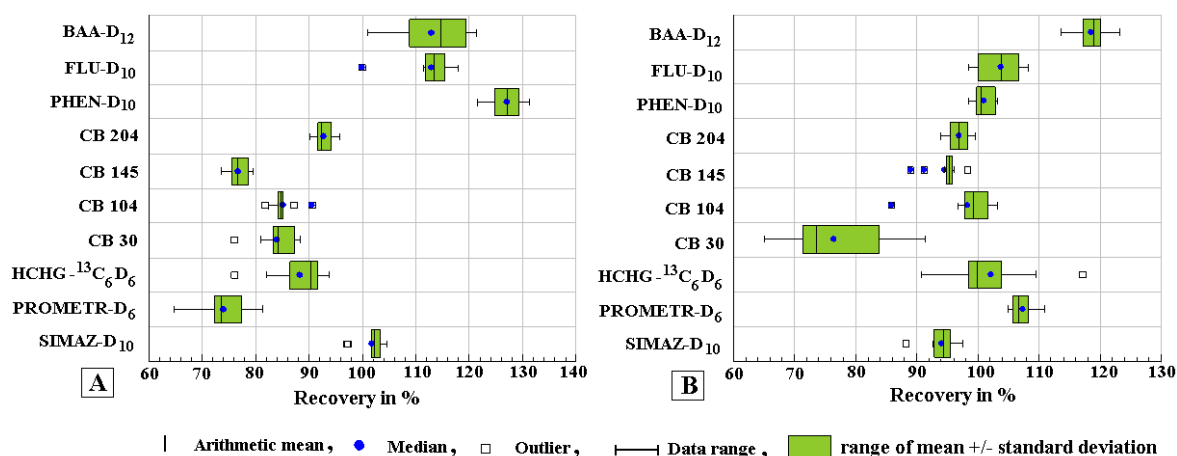


Figure 4.24: PRC recovery results of (A) 10 PUF plug adsorber cartridge air samples and (B) 9 PUF/XAD-2/PUF adsorber cartridge air samples

4.2.4 Extraction efficiency

The quantitative extraction of target analytes was necessary for a reliable air sample preparation and an optimized quantification. Extraction efficiencies of the Soxhlet and GFF extraction were controlled by a repetition of the sample preparation procedure. The fraction of labeled analytes (performance reference compounds and internal standards) in the first extract was > 98 %. Peak area data is tabulated in the annex 2.

4.3 Validation of Quantification

The limits of quantification (LOQ) and the limits of detection (LOD) were specified for each preparation sequence (refer to table 4.2) as a function of both the respective field blanks and the system performance of the mass spectrometers. LOQ and LOD were defined in concentrations of ng/mL air sample extract.

4.3.1 Limits of quantification

The limits of quantification were calculated from field blank results (LOQ_{blank}) by equation 20, where \bar{x}_{arithm} referred to the arithmetic mean and σ was the standard deviation. In addition LOQs ($LOQ_{S/N}$) were determined by the signal (S) to noise (N) ratio according to equation 21. The higher LOQ was applied. LOQs are listed in table 4.6.

$$LOQ_{blank} = \bar{x}_{arithm} + 3 \cdot \sigma \quad (\text{equation 20})$$

$$LOQ_{S/N} = S = 3 \cdot N \quad (\text{equation 21})$$

Table 4.6: Limits of quantification in ng/mL extract applied to the air sample preparation sequences 1-5; 1 = Baltic Sea in Apr. 2009, 2 = North Sea in Aug/Sep. 2009, 3 = German EEZ in May/Jun. 2009 and May 2010, 4 = PUF disk passive air samples, 5 = Sülldorf/Hamburg Nov./Dec. 2010, P pl = PUF plug adsorber cartridge, PXP = PUF/XAD-2/PUF adsorber cartridge, P di = PUF disk, n.q. = not quantified, *LOQ_{blank}*, *LOQ_{S/N}*

Preparation Sequence	1	2			3						4			5		
Sampling site	B.S.	North Sea			G. EEZ 2009			G. EEZ 2010			HH	Sylt	FINO	HH		
Matrix	P pl	GFF	PXP	P di	GFF	PXP	P di	GFF	PXP	P di	P di	P di	P di	GFF	P pl	PXP
24-D	n.q.	0.17	n.q.	n.q.	0.17	n.q.	n.q.	0.17	n.q.	n.q.	n.q.	n.q.	n.q.	0.17	n.q.	n.q.
ACE	2.69	3.00	6.67	6.67	0.88	1.43	2.91	0.83	1.79	2.63	1.88	2.97	2.93	1.33	1.68	1.67
ACY	0.33	3.33	31.28	3.33	1.00	1.00	1.57	1.00	1.76	4.54	10.72	10.82	5.47	1.33	9.65	4.74
ALD	0.05	0.17	0.05	0.05	0.13	0.13	0.13	0.13	0.13	0.13	0.13	0.13	0.13	0.33	0.33	0.33
AMETRYN	0.01	0.01	0.01	0.01	0.01	0.01	0.01	0.01	0.01	0.02	0.01	0.01	0.02	0.01	0.01	0.01
ANT	0.33	3.33	3.33	3.33	1.00	1.00	1.00	1.00	1.00	1.00	1.00	1.00	1.00	1.33	1.67	2.73
ATRAZ	0.03	0.03	0.03	0.03	0.03	0.03	0.03	0.03	0.03	0.03	0.03	0.03	0.03	0.03	0.03	0.03
AZINPH-E	0.03	0.03	0.03	0.03	0.03	0.03	0.03	0.03	0.03	0.03	0.03	0.03	0.03	0.03	0.03	0.03
AZINPH-M	0.17	0.17	0.17	0.17	0.17	0.17	0.17	0.17	0.17	0.17	0.17	0.17	0.17	0.17	0.17	0.17
BAA	0.83	1.67	3.33	3.33	0.50	0.67	0.50	0.50	0.67	0.50	1.33	1.33	1.33	1.67	1.67	1.67
BAP	1.00	2.33	3.33	3.33	0.67	0.67	0.67	0.67	2.43	0.67	1.00	1.00	1.00	1.67	1.67	1.67
BBF	0.83	3.33	3.33	3.33	1.00	1.34	1.00	1.00	1.00	1.00	1.33	1.33	1.33	1.67	1.67	1.67
BENTAZ	0.01	0.01	0.01	0.01	0.01	0.01	0.01	0.01	0.01	0.02	0.01	0.01	0.02	0.01	0.01	0.01
BGHIP	0.83	1.67	4.40	1.67	0.50	0.67	0.50	0.50	7.14	0.50	1.00	1.00	1.00	1.33	1.33	3.37
CARBAMAZ	0.01	0.01	0.01	0.01	0.01	0.01	0.01	0.01	0.01	0.01	0.03	0.01	0.01	0.01	0.01	0.01
CARBEND	0.01	0.01	0.01	0.01	0.01	0.01	0.01	0.01	0.01	0.01	0.01	0.01	0.01	0.01	0.01	0.01
CB138	0.23	0.10	0.12	0.03	0.10	0.22	0.66	0.10	0.13	0.17	0.20	0.13	0.13	0.20	0.20	0.46
CB153	0.23	0.16	0.06	0.05	0.10	0.10	0.13	0.18	0.10	0.10	0.23	0.22	0.12	0.15	0.33	0.36
CB28	0.07	0.07	0.08	0.07	0.10	0.07	0.28	0.07	0.07	0.10	0.13	0.13	0.13	0.34	0.34	0.33
CB52	0.05	0.05	0.12	0.06	0.07	0.07	0.12	0.07	0.08	0.07	0.13	0.13	0.13	0.13	0.13	0.71
CHLORFENV	0.03	0.03	0.07	0.03	0.03	0.03	0.03	0.03	0.54	0.03	0.03	0.03	0.03	0.03	0.03	0.19
CHLORTUR	0.03	0.03	0.03	0.03	0.03	0.03	0.03	0.03	0.03	0.03	0.03	0.03	0.03	0.03	0.03	0.03
CHRTR	0.33	3.33	10.00	10.00	1.00	1.00	1.47	1.00	1.67	1.48	1.00	1.00	1.00	2.33	2.33	5.28
CLOFIBRS	n.q.	0.03	n.q.	n.q.	0.03	n.q.	n.q.	0.03	n.q.	n.q.	n.q.	n.q.	n.q.	0.03	n.q.	n.q.
DBAHA	0.83	3.33	3.95	3.33	0.83	1.00	1.00	0.83	1.00	1.00	1.00	1.00	1.00	1.67	1.33	1.33
DDDPP	0.05	0.10	0.10	0.10	0.07	0.07	0.07	0.07	0.07	0.07	0.08	0.08	0.08	0.13	0.10	0.10
DDEPP	0.10	0.10	0.10	0.10	0.10	0.10	0.10	0.10	0.10	0.10	0.16	0.12	0.10	0.17	0.17	0.17
DDTOP	0.10	0.10	0.10	0.10	0.07	0.07	0.07	0.07	0.07	0.07	0.10	0.10	0.10	0.13	0.10	0.10
DDTPP	0.03	0.03	0.03	0.03	0.07	0.07	0.07	0.07	0.07	0.12	0.07	0.07	0.07	0.10	0.10	0.10
DEATRAZ	0.03	0.03	0.03	0.03	0.03	0.03	0.03	0.03	0.03	0.03	0.03	0.03	0.03	0.03	0.03	0.03
DIAZINON	0.03	0.03	0.03	0.03	0.03	0.03	0.03	0.03	0.03	0.03	0.03	0.03	0.03	0.03	0.03	0.03
DICHLPR	n.q.	0.03	n.q.	n.q.	0.03	n.q.	n.q.	0.03	n.q.	n.q.	n.q.	n.q.	n.q.	0.03	n.q.	n.q.
DICLOF	n.q.	0.17	n.q.	n.q.	0.17	n.q.	n.q.	0.17	n.q.	n.q.	n.q.	n.q.	n.q.	0.17	n.q.	n.q.
DIELD	0.50	0.10	0.07	0.07	0.13	0.13	0.13	0.13	0.13	0.13	0.13	0.13	0.13	0.27	0.27	0.27
DIMETH	0.03	0.03	0.03	0.03	0.03	0.03	0.03	0.03	0.03	0.03	0.03	0.03	0.03	0.03	0.03	0.03
DIURON	0.03	0.03	0.03	0.03	0.03	0.03	0.03	0.03	0.05	0.03	0.03	0.03	0.03	0.03	0.13	0.19
END	0.03	0.17	0.17	0.17	0.17	0.17	0.17	0.17	0.17	0.17	0.17	0.17	0.17	0.33	0.33	0.33
FENUR	0.07	0.02	0.24	0.02	0.02	0.02	0.07	0.02	5.80	0.04	0.05	0.05	0.09	0.02	0.02	0.84
FL	6.79	6.67	6.67	6.67	3.88	3.87	9.00	2.33	3.36	4.19	5.11	2.75	4.40	1.67	2.69	1.73
FLU	1.50	3.33	3.14	2.67	2.21	1.50	5.73	1.28	10.02	2.11	3.81	4.28	3.42	3.33	3.33	51.35
HBCD-A	0.17	0.17	0.17	0.17	0.17	0.17	0.17	0.17	0.17	0.17	0.17	0.17	0.17	0.17	0.17	0.17
HBCD-BG	0.30	0.17	0.17	0.17	0.17	0.17	0.17	0.17	0.17	0.17	0.17	0.17	0.17	0.17	0.17	0.17
HCB	0.08	0.07	0.09	0.07	0.07	0.08	0.21	0.07	0.07	0.07	0.10	0.10	0.17	0.17	0.17	0.62
HCHA	0.09	0.10	0.04	0.04	0.10	0.10	0.10	0.10	0.10	0.10	0.10	0.10	0.10	0.17	0.17	0.17
HCHB	0.10	0.10	0.10	0.10	0.13	0.13	0.13	0.13	0.13	0.13	0.17	0.17	0.17	0.20	0.20	0.20

Table 4.6 continued:

Preparation Sequence	1	2			3						4			5		
Sampling site	B.S.	North Sea			G. EEZ 2009			G. EEZ 2010			HH	Sylt	FINO	HH		
Matrix	P pl	GFF	PXP	P di	GFF	PXP	P di	GFF	PXP	P di	P di	P di	P di	GFF	P pl	PXP
HCHD	0.10	0.10	0.10	0.10	0.10	0.13	0.13	0.10	0.13	0.13	0.13	0.13	0.13	0.20	0.23	0.23
HCHG	0.10	0.10	0.09	0.13	0.13	0.13	0.25	0.13	0.13	0.13	0.13	0.13	0.13	0.20	0.20	0.20
HEXAZIN	0.01	0.01	0.01	0.01	0.01	0.01	0.13	0.01	0.01	0.01	0.01	0.01	0.01	0.01	0.01	0.01
I123P	0.67	2.67	4.45	2.67	0.67	0.67	0.67	0.67	1.63	0.67	1.00	1.00	1.00	1.67	1.67	1.67
IRGAROL	0.01	0.01	0.01	0.01	0.01	0.01	0.01	0.01	0.01	0.01	0.01	0.01	0.01	0.01	0.01	0.01
ISOD	0.15	0.15	0.15	0.15	0.17	0.17	0.17	0.17	0.17	0.17	0.17	0.17	0.17	0.33	0.33	0.33
ISOPRUR	0.02	0.02	0.02	0.02	0.02	0.02	0.02	0.02	0.02	0.02	0.02	0.02	0.02	0.02	0.02	0.02
LINUR	0.17	0.17	0.17	0.17	0.17	0.17	0.17	0.17	0.17	0.17	0.17	0.17	0.17	0.17	0.17	0.17
MALATH	0.03	0.03	0.03	0.03	0.03	0.03	0.03	0.03	0.03	0.03	0.03	0.03	0.03	0.03	0.03	0.03
MCPA	n.q.	0.03	n.q.	n.q.	0.03	n.q.	n.q.	0.03	n.q.	n.q.	n.q.	n.q.	n.q.	0.03	n.q.	n.q.
MECOPR	n.q.	0.03	n.q.	n.q.	0.03	n.q.	n.q.	0.03	n.q.	n.q.	n.q.	n.q.	n.q.	0.03	n.q.	n.q.
METAZCHL	0.02	0.02	0.02	0.02	0.02	0.02	0.02	0.02	0.02	0.02	0.15	0.02	0.02	0.02	0.02	0.02
METHABZT	0.02	0.02	0.02	0.02	0.02	0.02	0.02	0.02	0.02	0.02	0.02	0.02	0.02	0.02	0.02	0.02
METOLA	0.01	0.01	0.02	0.01	0.03	0.43	0.17	0.02	0.29	0.08	0.14	0.02	0.05	0.01	0.03	0.01
NAPROX	n.q.	0.17	n.q.	n.q.	0.17	n.q.	n.q.	0.17	n.q.	n.q.	n.q.	n.q.	n.q.	0.17	n.q.	n.q.
OXAZEP	0.17	0.17	0.17	0.17	0.17	0.17	0.17	0.17	0.17	0.17	0.17	0.17	0.17	0.17	0.17	0.17
PENDIMETH	0.17	0.03	0.09	0.06	0.03	0.16	0.18	0.04	0.07	0.08	0.28	0.09	0.15	0.03	0.20	0.10
PFBS	0.01	0.01	0.01	0.01	0.01	0.01	0.01	0.01	0.01	0.03	0.01	0.01	0.03	0.01	0.01	0.02
PFDEA	0.03	0.03	0.03	0.03	0.03	0.03	0.03	0.03	0.03	0.03	0.03	0.03	0.03	0.03	0.03	0.03
PFHPA	0.02	0.01	0.01	0.01	0.01	0.04	0.07	0.01	0.04	0.04	0.24	0.08	0.06	0.01	0.02	0.06
PFHXA	0.04	0.01	0.06	0.02	0.01	0.06	0.13	0.01	0.06	0.06	0.19	0.09	0.08	0.01	0.01	0.05
PFHXS	0.01	0.01	0.01	0.01	0.01	0.01	0.01	0.01	0.02	0.02	0.01	0.01	0.02	0.01	0.01	0.02
PFNOA	0.02	0.02	0.02	0.02	0.02	0.10	0.10	0.02	0.12	0.13	0.07	0.11	0.07	0.02	0.02	0.07
PFOA	0.11	0.03	0.22	0.04	0.04	0.45	0.48	0.02	0.14	0.39	1.82	0.42	0.28	0.02	0.07	0.24
PFOS-1	0.06	0.02	0.15	0.04	0.05	0.18	0.08	0.01	0.18	0.15	0.26	0.09	0.07	0.01	0.05	0.05
PFOSA-1	0.05	0.03	0.88	0.01	0.06	0.50	0.08	0.02	0.17	0.12	0.18	0.09	0.04	0.01	0.04	0.04
PHEN	6.07	3.33	6.57	3.55	1.13	3.96	23.14	1.22	9.58	6.54	10.57	11.93	7.71	1.67	4.63	19.97
PIRIMIC	0.02	0.02	0.02	0.02	0.02	0.02	0.02	0.02	0.02	0.02	0.02	0.02	0.02	0.02	0.02	0.02
PRIMID	0.17	0.17	0.17	0.17	0.17	0.17	0.17	0.17	0.17	0.17	0.17	0.17	0.17	0.17	0.17	0.17
PROMETR	0.03	0.02	0.03	0.02	0.03	0.03	0.02	0.03	0.03	0.04	0.17	0.03	0.05	0.04	0.03	0.03
PROPAZ	0.03	0.03	0.03	0.03	0.03	0.03	0.03	0.03	0.03	0.03	0.03	0.03	0.03	0.03	0.03	0.03
PYR	0.67	2.67	11.82	6.11	1.19	2.00	11.60	1.59	47.41	3.29	9.26	12.54	9.80	3.33	5.36	20.45
QCB	0.09	0.10	0.06	0.06	0.10	0.10	0.10	0.10	0.10	0.10	0.10	0.10	0.10	0.20	0.39	0.20
SIMAZ	0.03	0.03	0.03	0.03	0.03	0.03	0.03	0.03	0.03	0.03	0.03	0.03	0.03	0.03	0.03	0.03
TBEP	0.85	0.36	0.43	0.11	4.72	2.34	1.64	5.38	3.92	4.93	0.36	0.09	0.24	0.50	0.29	1.34
TBP	6.03	1.35	3.09	7.46	0.86	11.24	30.47	0.84	0.86	16.35	16.59	6.42	14.16	1.23	3.50	5.81
TERBAZ	0.02	0.10	0.03	0.05	0.05	0.20	0.11	0.03	0.10	0.08	0.08	0.02	0.05	0.06	0.01	0.01
TERBUTR	0.01	0.01	0.01	0.01	0.01	0.01	0.19	0.01	0.01	0.01	0.01	0.01	0.01	0.01	0.01	0.01
TPP	0.85	0.73	19.43	0.55	0.33	2.82	1.25	0.23	31.07	1.48	4.18	1.33	2.12	0.94	1.48	95.20
TRIFLU	0.10	0.10	0.21	0.11	0.10	0.10	0.10	0.10	0.10	0.10	0.10	0.10	0.10	0.20	0.17	0.17

4.3.2 Limits of detection

The limits of detection were calculated from the LOQs tabulated above, as defined by equation 22. Applied LODs are listed in table 4.7.

$$LOD = \frac{LOQ}{3} \quad (\text{equation 22})$$

Table 4.7: Limits of detection in ng/mL extract applied to the air sample preparation sequences 1-5; 1 = Baltic Sea in Apr. 2009, 2 = North Sea in Aug/Sep. 2009, 3 = German EEZ in May/June. 2009 and May 2010, 4 = PUF disk passive air samples, 5 = Sülldorf/Hamburg Nov./Dec. 2010, P pl = PUF plug adsorber cartridge, PXP = PUF/XAD-2/PUF adsorber cartridge, P di = PUF disk, n.q. = not quantified

Preparation Sequence	1	2			3						4			5		
Sampling site	B.S.	North Sea			G. EEZ 2009			G. EEZ 2010			HH	Sylt	FINO	HH		
Matrix	P pl	GFF	PXP	P di	GFF	PXP	P di	GFF	PXP	P di	P di	P di	P di	GFF	P pl	PXP
24-D	n.q.	0.17	n.q.	n.q.	0.17	n.q.	n.q.	0.17	n.q.	n.q.	n.q.	n.q.	n.q.	0.17	n.q.	n.q.
ACE	2.69	3.00	6.67	6.67	0.88	1.43	2.91	0.83	1.79	2.63	1.88	2.97	2.93	1.33	1.68	1.67
ACY	0.33	3.33	31.28	3.33	1.00	1.00	1.57	1.00	1.76	4.54	10.72	10.82	5.47	1.33	9.65	4.74
ALD	0.05	0.17	0.05	0.05	0.13	0.13	0.13	0.13	0.13	0.13	0.13	0.13	0.13	0.33	0.33	0.33
AMETRYN	0.01	0.01	0.01	0.01	0.01	0.01	0.01	0.01	0.01	0.02	0.01	0.01	0.02	0.01	0.01	0.01
ANT	0.33	3.33	3.33	3.33	1.00	1.00	1.00	1.00	1.00	1.00	1.00	1.00	1.00	1.33	1.67	2.73
ATRAZ	0.03	0.03	0.03	0.03	0.03	0.03	0.03	0.03	0.03	0.03	0.03	0.03	0.03	0.03	0.03	0.03
AZINPH-E	0.03	0.03	0.03	0.03	0.03	0.03	0.03	0.03	0.03	0.03	0.03	0.03	0.03	0.03	0.03	0.03
AZINPH-M	0.17	0.17	0.17	0.17	0.17	0.17	0.17	0.17	0.17	0.17	0.17	0.17	0.17	0.17	0.17	0.17
BAA	0.83	1.67	3.33	3.33	0.50	0.67	0.50	0.50	0.67	0.50	1.33	1.33	1.33	1.67	1.67	1.67
BAP	1.00	2.33	3.33	3.33	0.67	0.67	0.67	0.67	2.43	0.67	1.00	1.00	1.00	1.67	1.67	1.67
BBF	0.83	3.33	3.33	3.33	1.00	1.34	1.00	1.00	1.00	1.00	1.33	1.33	1.33	1.67	1.67	1.67
BENTAZ	0.01	0.01	0.01	0.01	0.01	0.01	0.01	0.01	0.01	0.02	0.01	0.01	0.02	0.01	0.01	0.01
BGHIP	0.83	1.67	4.40	1.67	0.50	0.67	0.50	0.50	7.14	0.50	1.00	1.00	1.00	1.33	1.33	3.37
CARBAMAZ	0.01	0.01	0.01	0.01	0.01	0.01	0.01	0.01	0.01	0.01	0.03	0.01	0.01	0.01	0.01	0.01
CARBEND	0.01	0.01	0.01	0.01	0.01	0.01	0.01	0.01	0.01	0.01	0.01	0.01	0.01	0.01	0.01	0.01
CB138	0.23	0.10	0.12	0.03	0.10	0.22	0.66	0.10	0.13	0.17	0.20	0.13	0.13	0.20	0.20	0.46
CB153	0.23	0.16	0.06	0.05	0.10	0.10	0.13	0.18	0.10	0.10	0.23	0.22	0.12	0.15	0.33	0.36
CB28	0.07	0.07	0.08	0.07	0.10	0.07	0.28	0.07	0.07	0.10	0.13	0.13	0.13	0.34	0.34	0.33
CB52	0.05	0.05	0.12	0.06	0.07	0.07	0.12	0.07	0.08	0.07	0.13	0.13	0.13	0.13	0.13	0.71
CHLORFENV	0.03	0.03	0.07	0.03	0.03	0.03	0.03	0.03	0.54	0.03	0.03	0.03	0.03	0.03	0.03	0.19
CHLORTUR	0.03	0.03	0.03	0.03	0.03	0.03	0.03	0.03	0.03	0.03	0.03	0.03	0.03	0.03	0.03	0.03
CHRTR	0.33	3.33	10.00	10.00	1.00	1.00	1.47	1.00	1.67	1.48	1.00	1.00	1.00	2.33	2.33	5.28
CLOFIBRS	n.q.	0.03	n.q.	n.q.	0.03	n.q.	n.q.	0.03	n.q.	n.q.	n.q.	n.q.	n.q.	0.03	n.q.	n.q.
DBAHA	0.83	3.33	3.95	3.33	0.83	1.00	1.00	0.83	1.00	1.00	1.00	1.00	1.00	1.67	1.33	1.33
DDDDPP	0.05	0.10	0.10	0.10	0.07	0.07	0.07	0.07	0.07	0.07	0.08	0.08	0.08	0.13	0.10	0.10
DDEPP	0.10	0.10	0.10	0.10	0.10	0.10	0.10	0.10	0.10	0.10	0.16	0.12	0.10	0.17	0.17	0.17
DDTOP	0.10	0.10	0.10	0.10	0.07	0.07	0.07	0.07	0.07	0.07	0.10	0.10	0.10	0.13	0.10	0.10
DDTTP	0.03	0.03	0.03	0.03	0.07	0.07	0.07	0.07	0.07	0.12	0.07	0.07	0.07	0.10	0.10	0.10
DEATRAZ	0.03	0.03	0.03	0.03	0.03	0.03	0.03	0.03	0.03	0.03	0.03	0.03	0.03	0.03	0.03	0.03
DIAZINON	0.03	0.03	0.03	0.03	0.03	0.03	0.03	0.03	0.03	0.03	0.03	0.03	0.03	0.03	0.03	0.03
DICHLPR	n.q.	0.03	n.q.	n.q.	0.03	n.q.	n.q.	0.03	n.q.	n.q.	n.q.	n.q.	n.q.	0.03	n.q.	n.q.
DICLOF	n.q.	0.17	n.q.	n.q.	0.17	n.q.	n.q.	0.17	n.q.	n.q.	n.q.	n.q.	n.q.	0.17	n.q.	n.q.
DIELD	0.50	0.10	0.07	0.07	0.13	0.13	0.13	0.13	0.13	0.13	0.13	0.13	0.13	0.27	0.27	0.27
DIMETH	0.03	0.03	0.03	0.03	0.03	0.03	0.03	0.03	0.03	0.03	0.03	0.03	0.03	0.03	0.03	0.03
DIURON	0.03	0.03	0.03	0.03	0.03	0.03	0.03	0.03	0.05	0.03	0.03	0.03	0.03	0.03	0.13	0.19
END	0.03	0.17	0.17	0.17	0.17	0.17	0.17	0.17	0.17	0.17	0.17	0.17	0.17	0.33	0.33	0.33
FENUR	0.07	0.02	0.24	0.02	0.02	0.02	0.07	0.02	5.80	0.04	0.05	0.05	0.09	0.02	0.02	0.84
FL	6.79	6.67	6.67	6.67	3.88	3.87	9.00	2.33	3.36	4.19	5.11	2.75	4.40	1.67	2.69	1.73
FLU	1.50	3.33	3.14	2.67	2.21	1.50	5.73	1.28	10.02	2.11	3.81	4.28	3.42	3.33	3.33	51.35
HBCD-A	0.17	0.17	0.17	0.17	0.17	0.17	0.17	0.17	0.17	0.17	0.17	0.17	0.17	0.17	0.17	0.17
HBCD-BG	0.30	0.17	0.17	0.17	0.17	0.17	0.17	0.17	0.17	0.17	0.17	0.17	0.17	0.17	0.17	0.17
HCB	0.08	0.07	0.09	0.07	0.07	0.08	0.21	0.07	0.07	0.07	0.10	0.10	0.17	0.17	0.17	0.62
HCHA	0.09	0.10	0.04	0.04	0.10	0.10	0.10	0.10	0.10	0.10	0.10	0.10	0.10	0.17	0.17	0.17
HCHB	0.10	0.10	0.10	0.10	0.13	0.13	0.13	0.13	0.13	0.13	0.17	0.17	0.17	0.20	0.20	0.20

Table 4.7 continued:

Preparation Sequence	1	2			3						4			5		
Sampling site	B.S.	North Sea			G. EEZ 2009			G. EEZ 2010			HH	Sylt	FINO	HH		
Matrix	P pl	GFF	PXP	P di	GFF	PXP	P di	GFF	PXP	P di	P di	P di	P di	GFF	P pl	PXP
HCHD	0.10	0.10	0.10	0.10	0.10	0.13	0.13	0.10	0.13	0.13	0.13	0.13	0.13	0.20	0.23	0.23
HCHG	0.10	0.10	0.09	0.13	0.13	0.13	0.25	0.13	0.13	0.13	0.13	0.13	0.13	0.20	0.20	0.20
HEXAZIN	0.01	0.01	0.01	0.01	0.01	0.01	0.13	0.01	0.01	0.01	0.01	0.01	0.01	0.01	0.01	0.01
I123P	0.67	2.67	4.45	2.67	0.67	0.67	0.67	0.67	1.63	0.67	1.00	1.00	1.00	1.67	1.67	1.67
IRGAROL	0.01	0.01	0.01	0.01	0.01	0.01	0.01	0.01	0.01	0.01	0.01	0.01	0.01	0.01	0.01	0.01
ISOD	0.15	0.15	0.15	0.15	0.17	0.17	0.17	0.17	0.17	0.17	0.17	0.17	0.17	0.33	0.33	0.33
ISOPRUR	0.02	0.02	0.02	0.02	0.02	0.02	0.02	0.02	0.02	0.02	0.02	0.02	0.02	0.02	0.02	0.02
LINUR	0.17	0.17	0.17	0.17	0.17	0.17	0.17	0.17	0.17	0.17	0.17	0.17	0.17	0.17	0.17	0.17
MALATH	0.03	0.03	0.03	0.03	0.03	0.03	0.03	0.03	0.03	0.03	0.03	0.03	0.03	0.03	0.03	0.03
MCPA	n.q.	0.03	n.q.	n.q.	0.03	n.q.	n.q.	0.03	n.q.	n.q.	n.q.	n.q.	n.q.	0.03	n.q.	n.q.
MECOPR	n.q.	0.03	n.q.	n.q.	0.03	n.q.	n.q.	0.03	n.q.	n.q.	n.q.	n.q.	n.q.	0.03	n.q.	n.q.
METAZCHL	0.02	0.02	0.02	0.02	0.02	0.02	0.02	0.02	0.02	0.02	0.15	0.02	0.02	0.02	0.02	0.02
METHABZT	0.02	0.02	0.02	0.02	0.02	0.02	0.02	0.02	0.02	0.02	0.02	0.02	0.02	0.02	0.02	0.02
METOLA	0.01	0.01	0.02	0.01	0.03	0.43	0.17	0.02	0.29	0.08	0.14	0.02	0.05	0.01	0.03	0.01
NAPROX	n.q.	0.17	n.q.	n.q.	0.17	n.q.	n.q.	0.17	n.q.	n.q.	n.q.	n.q.	n.q.	0.17	n.q.	n.q.
OXAZEP	0.17	0.17	0.17	0.17	0.17	0.17	0.17	0.17	0.17	0.17	0.17	0.17	0.17	0.17	0.17	0.17
PENDIMETH	0.17	0.03	0.09	0.06	0.03	0.16	0.18	0.04	0.07	0.08	0.28	0.09	0.15	0.03	0.20	0.10
PFBS	0.01	0.01	0.01	0.01	0.01	0.01	0.01	0.01	0.01	0.03	0.01	0.01	0.03	0.01	0.01	0.02
PFDEA	0.03	0.03	0.03	0.03	0.03	0.03	0.03	0.03	0.03	0.03	0.03	0.03	0.03	0.03	0.03	0.03
PFHPA	0.02	0.01	0.01	0.01	0.01	0.04	0.07	0.01	0.04	0.04	0.24	0.08	0.06	0.01	0.02	0.06
PFHXA	0.04	0.01	0.06	0.02	0.01	0.06	0.13	0.01	0.06	0.06	0.19	0.09	0.08	0.01	0.01	0.05
PFHXS	0.01	0.01	0.01	0.01	0.01	0.01	0.01	0.01	0.02	0.02	0.01	0.01	0.02	0.01	0.01	0.02
PFNOA	0.02	0.02	0.02	0.02	0.02	0.10	0.10	0.02	0.12	0.13	0.07	0.11	0.07	0.02	0.02	0.07
PFOA	0.11	0.03	0.22	0.04	0.04	0.45	0.48	0.02	0.14	0.39	1.82	0.42	0.28	0.02	0.07	0.24
PFOS-1	0.06	0.02	0.15	0.04	0.05	0.18	0.08	0.01	0.18	0.15	0.26	0.09	0.07	0.01	0.05	0.05
PFOSA-1	0.05	0.03	0.88	0.01	0.06	0.50	0.08	0.02	0.17	0.12	0.18	0.09	0.04	0.01	0.04	0.04
PHEN	6.07	3.33	6.57	3.55	1.13	3.96	23.14	1.22	9.58	6.54	10.57	11.93	7.71	1.67	4.63	19.97
PIRIMIC	0.02	0.02	0.02	0.02	0.02	0.02	0.02	0.02	0.02	0.02	0.02	0.02	0.02	0.02	0.02	0.02
PRIMID	0.17	0.17	0.17	0.17	0.17	0.17	0.17	0.17	0.17	0.17	0.17	0.17	0.17	0.17	0.17	0.17
PROMETR	0.03	0.02	0.03	0.02	0.03	0.03	0.02	0.03	0.03	0.04	0.17	0.03	0.05	0.04	0.03	0.03
PROPAZ	0.03	0.03	0.03	0.03	0.03	0.03	0.03	0.03	0.03	0.03	0.03	0.03	0.03	0.03	0.03	0.03
PYR	0.67	2.67	11.82	6.11	1.19	2.00	11.60	1.59	47.41	3.29	9.26	12.54	9.80	3.33	5.36	20.45
QCB	0.09	0.10	0.06	0.06	0.10	0.10	0.10	0.10	0.10	0.10	0.10	0.10	0.10	0.20	0.39	0.20
SIMAZ	0.03	0.03	0.03	0.03	0.03	0.03	0.03	0.03	0.03	0.03	0.03	0.03	0.03	0.03	0.03	0.03
TBEP	0.85	0.36	0.43	0.11	4.72	2.34	1.64	5.38	3.92	4.93	0.36	0.09	0.24	0.50	0.29	1.34
TBP	6.03	1.35	3.09	7.46	0.86	11.24	30.47	0.84	0.86	16.35	16.59	6.42	14.16	1.23	3.50	5.81
TERBAZ	0.02	0.10	0.03	0.05	0.05	0.20	0.11	0.03	0.10	0.08	0.08	0.02	0.05	0.06	0.01	0.01
TERBUTR	0.01	0.01	0.01	0.01	0.01	0.01	0.19	0.01	0.01	0.01	0.01	0.01	0.01	0.01	0.01	0.01
TPP	0.85	0.73	19.43	0.55	0.33	2.82	1.25	0.23	31.07	1.48	4.18	1.33	2.12	0.94	1.48	95.20
TRIFLU	0.10	0.10	0.21	0.11	0.10	0.10	0.10	0.10	0.10	0.10	0.10	0.10	0.10	0.20	0.17	0.17

5. Results and Discussion

In order to give a first brief overview of atmospheric concentrations of the pollutants targeted in this study, concentration ranges of the individual pollutant classes in the North Sea air are plotted in figure 5.1.

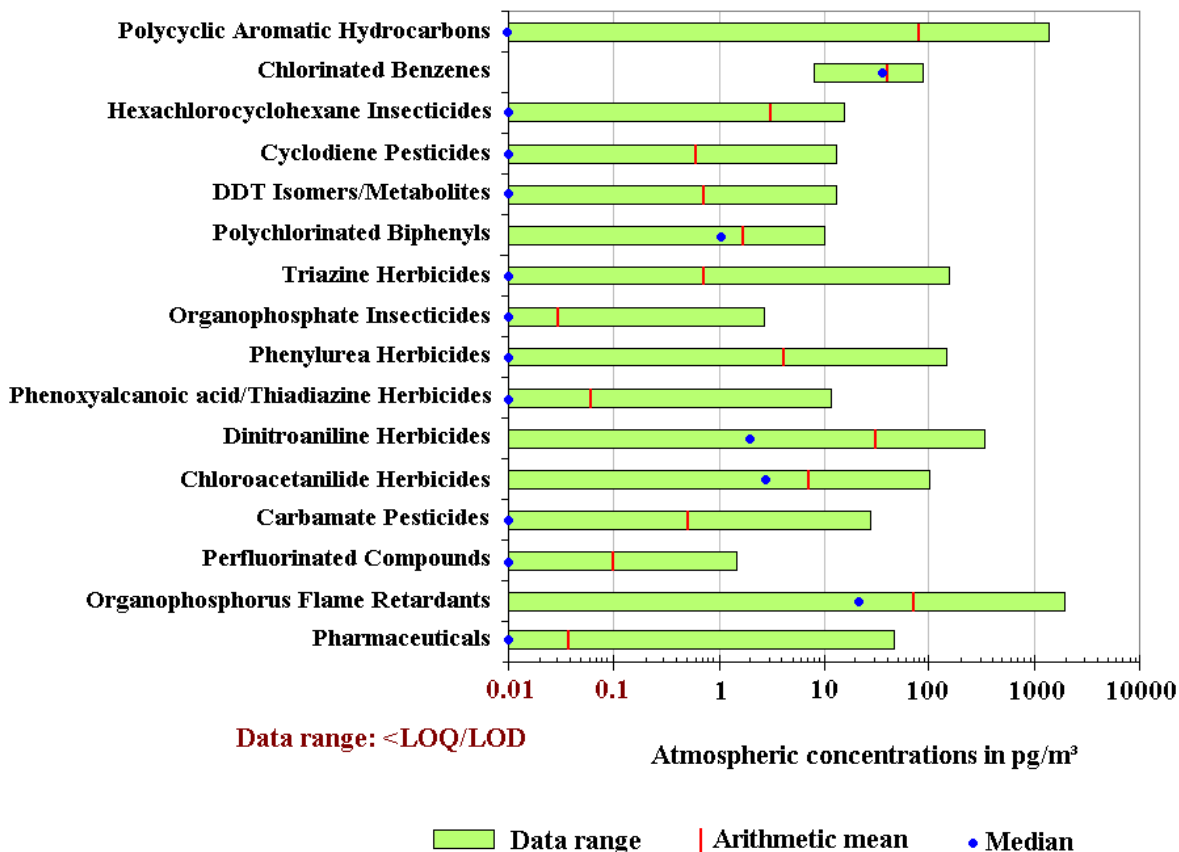


Figure 5.1: Atmospheric concentrations of organic pollutants in the atmosphere of the North Sea (plot of active air sampling data of the research cruises in the German EEZ 2009/2010 and the wider North Sea 2009)

The atmospheric concentrations of targeted pollutants were observed to be highly variable concerning the data ranges between (maxima of atmospheric concentrations) and even in (deviation of median and arithmetic mean) the individual pollutant classes. Exclusively the chlorinated benzenes could be determined in each air sample and exhibited the lowest variability in their atmospheric concentrations. The PAHs and the organophosphorus flame retardants reached the highest concentrations in the marine atmosphere of up to ~ 2000 pg/m³. Lowest atmospheric concentrations (maxima < 10 pg/m³) were observed for the perfluorinated compounds and the organophosphate insecticides. The deviation of arithmetic mean and median within a pollutant class was caused either by seasonal variations in atmospheric pollutant concentrations and/or by atmospheric concentrations <LOQ/<LOD of individual target compounds of the pollutant class. A

detailed view on the variability in concentrations and spatial distributions of target analytes in the atmosphere is given in the following chapters:

The first chapter is an assessment of the current status of the cycling processes of organic contaminants in the marine environment of the German EEZ, the North Sea and the Baltic Sea based on their spatial distribution in the marine atmosphere and the surface seawater. Vertical distributions of organic target analytes in the marine atmosphere observed at FINO stations are summarized in the second part of this chapter. The third part is an estimation on the dry particle and wet deposition fluxes of selected target analytes from the atmosphere to the surface seawaters, which is based on the atmospheric concentrations determined in this study, precipitate contamination data provided by the UBA as well as dry deposition velocities published in the literature.

5.1 Assessment of the current status of the cycling processes of organic contaminants between the marine atmosphere and the surface seawater of the German EEZ, the North Sea and the Baltic Sea

The occurrence and spatial distribution of target analytes in the marine atmosphere was interpreted by air mass backward trajectories, by comparison of sea and land based measurements, by investigations of gas-particle partitioning as well as seasonal fluctuations monitored by PUF disk passive air samplers. Additional data sets specifying the occurrence and distribution of organic contaminants in respective surface waters enabled the calculation of the direction of diffusive gas exchange between atmosphere and sea, which was reported to be the dominant exchange process at open seas (refer to chapter 2.3). Moreover, different characteristics in surface water distributions of individual pollutants could point to riverine input as well as atmospheric deposition. The results provided the assessment of the current status of the cycling processes of the targeted organic contaminants in the marine environment of the German EEZ, the wider North Sea and the Baltic Sea, which was summarized for pollutant groups as well as pollutant sub groups (table 3.10) in the following subchapters.

5.1.1 Polycyclic Aromatic Hydrocarbons

PAHs originate as byproducts from almost any kind of combustion processes. Thus they are ubiquitously present in the atmosphere. Due to their carcinogenic and mutagenic properties, they are important contributors to the toxicity potential of ambient aerosols. In particular toxicity is related to PAHs consisting of more than 4 rings like Benzo[*a*]pyrene and their reaction products, e.g., nitro PAHs. The most important primary sources of PAHs are domestic heating, thermal

power stations, road traffic and industrial emissions. ^[69, 112, 113] Ship emissions are expectedly relevant, too in the study area.

Occurrence and distribution of PAHs in the marine atmosphere

All targeted PAH components (table 3.10) were quantified in the marine atmosphere. Fluorene (FL) and phenanthrene (PHEN) were the main PAH components. Concentrations of up to 1000 pg/m³ were exclusively quantified in the gaseous mass fraction. In addition acenaphthene (ACE), fluoranthene (FLU) and pyrene (PYR) were detected in the majority of marine air samples in bulk concentrations (sum of gaseous and particle bound mass fraction) less than 300 pg/m³. Other PAH compounds, especially those of vapour pressures less than $2.8 \cdot 10^{-5}$ Pa (4-6 ring PAHs) were scarcely detected and accounted negligibly to the total PAH content in the marine atmosphere. They occurred solely in air masses originating from the continent (24 h and 7 d air mass backward trajectories) or in air samples collected close to continent. Moreover, a significant decrease in bulk PAH concentrations with increasing distance to the continent and thus increasing distance to major primary sources was observed. Atmospheric concentrations above the Baltic Sea and the North Sea were at the same order of magnitude. These results were in agreement with previous studies investigating PAH concentrations at a North-South transect in the marine atmosphere above the Atlantic Ocean. ^[60] The occurrence and distribution of PAHs in the marine atmosphere of North Sea, German EEZ and Baltic Sea is illustrated in figures 5.2 - 5.5.

Interpretation of atmospheric concentrations by air mass backward trajectories

Atmospheric PAH concentrations could be partly interpreted by the air mass backward trajectories, which were summarized in chapter 3.5 (original Hysplit graphics in the annex 4). In most cases air samples of identical trajectories displayed comparable atmospheric PAH concentrations, e.g., PE 16 and PE 15, PE 7 and PE 10, 09AT 7 and 09 AT 8, 10AT 6 and 10AT 7. On the other side, aberrations in atmospheric concentrations could be interpreted by further influencing factors like the location of the sampling site and thus proximity to continental sources as well as variable primary sources at high seas, e.g., passing ships.

An example of interpretation of atmospheric concentrations by air mass history is given in figure 5.2 (research cruise in the German EEZ in May/Jun. 2009): According to the air mass backward trajectories calculated for 24 h, air samples could be grouped in air masses originating either from continent (09AT 2, 09AT 7, 09AT 8) or sea (09AT 3, 09AT 4, 09AT 5, 09AT 9, 09AT 11, 09AT 12). In the air masses originating from continent the whole spectrum of targeted PAHs could be detected and quantified. Two of them revealed identical 24 h backward trajectories (09AT 7, 09AT 8) and were consistent in their PAH concentrations (1100 pg/m³) and composition.

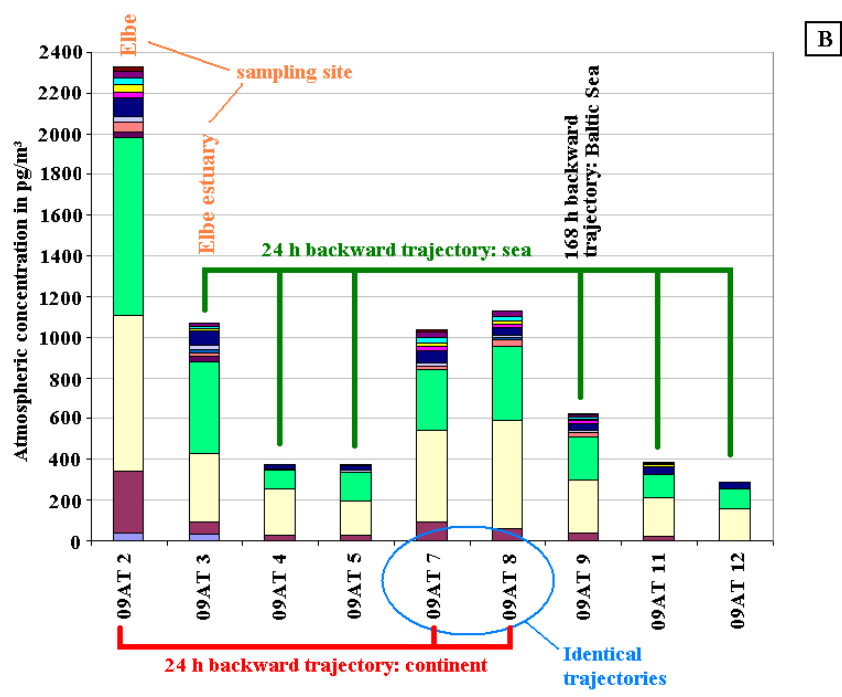
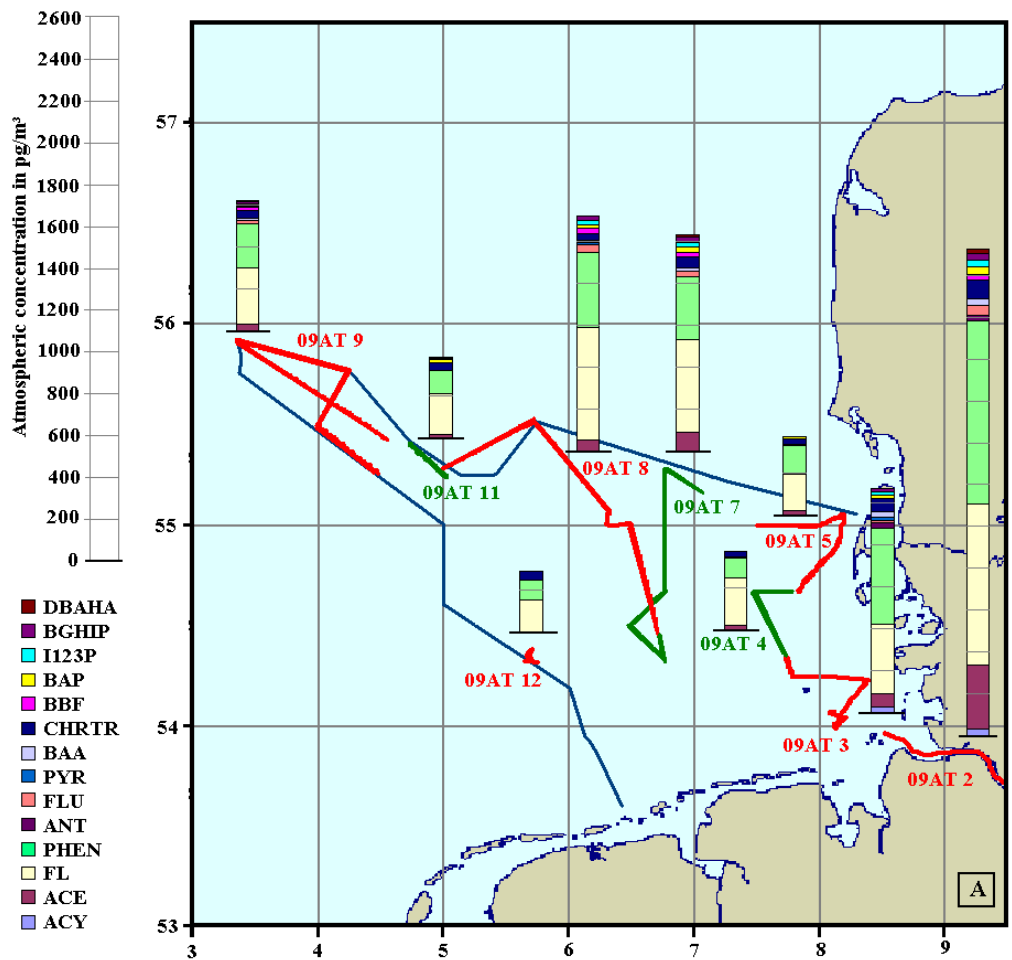


Figure 5.2: (A) Atmospheric bulk concentrations of PAHs above the German EEZ in May/June 2009; (B) Interpretation by location and sources (backward trajectories)

The third air sample with a 24h backward trajectory from continent was collected above the river Elbe (09AT 2), which was referred to as land based sampling site. The PAH concentrations were approximately two times higher (2300 pg/m³) than in the air samples 09AT7 and 09AT8. However, all three air samples with air masses from continent revealed similar PAH patterns. In comparison the six air samples with 24 h air mass backward trajectories originating from sea, displayed a reduced PAH spectrum and decreased concentrations. Four of them (09AT 4, 09AT 5, 09AT 11, 09AT 12) were similar in their composition and concentration. They predominantly consisted of fluorene, phenanthrene, pyrene and acenaphthene with a total concentration of approximately 350 pg/m³. The other two additionally displayed individual 4-6 ring PAHs and total PAH concentrations in the range 600 – 1100 pg/m³. In the case of the air sample 09AT3, the variation in concentrations and composition were attributed to the sampling site located in the Elbe estuary and thus proximity to a major shipping line and primary sources on the continent. In contrast, the increased PAH spectrum and concentrations in air sample 09AT 9 was comprehensible by the 168h air mass backward trajectory, which pointed to an air mass origin in the Baltic Sea region.

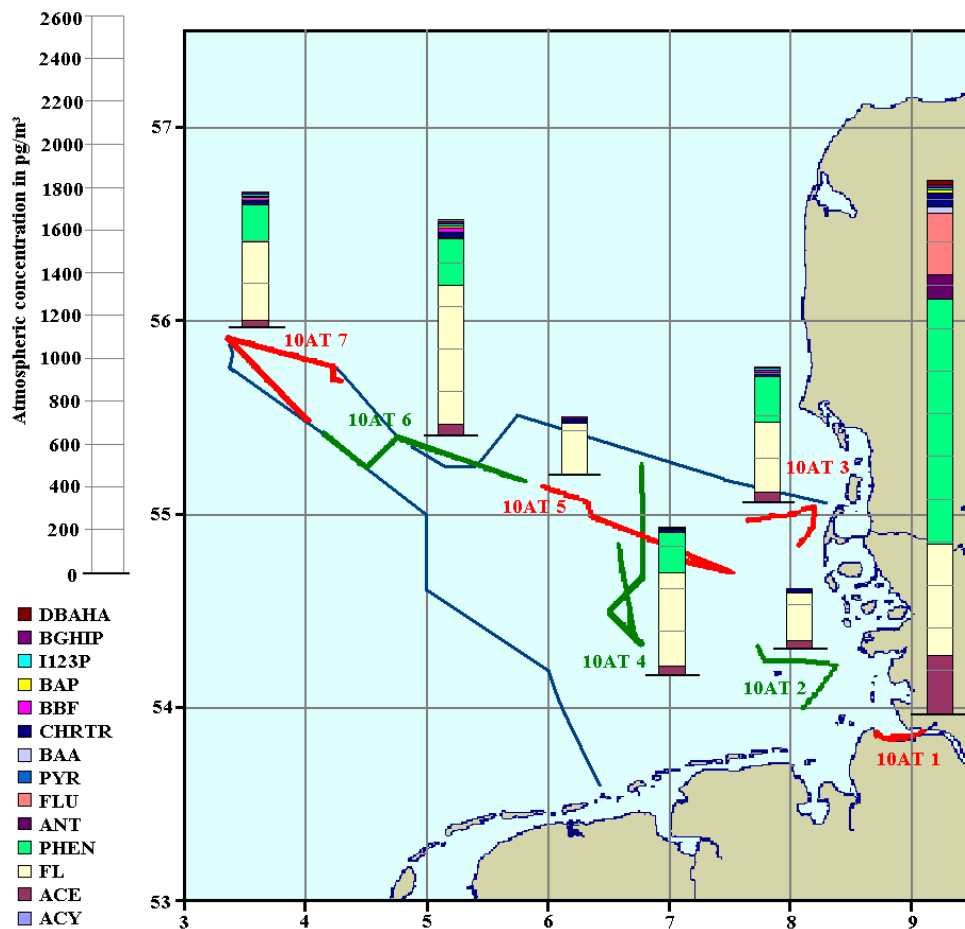


Figure 5.3: Atmospheric bulk concentrations of PAHs above the German EEZ in May 2010

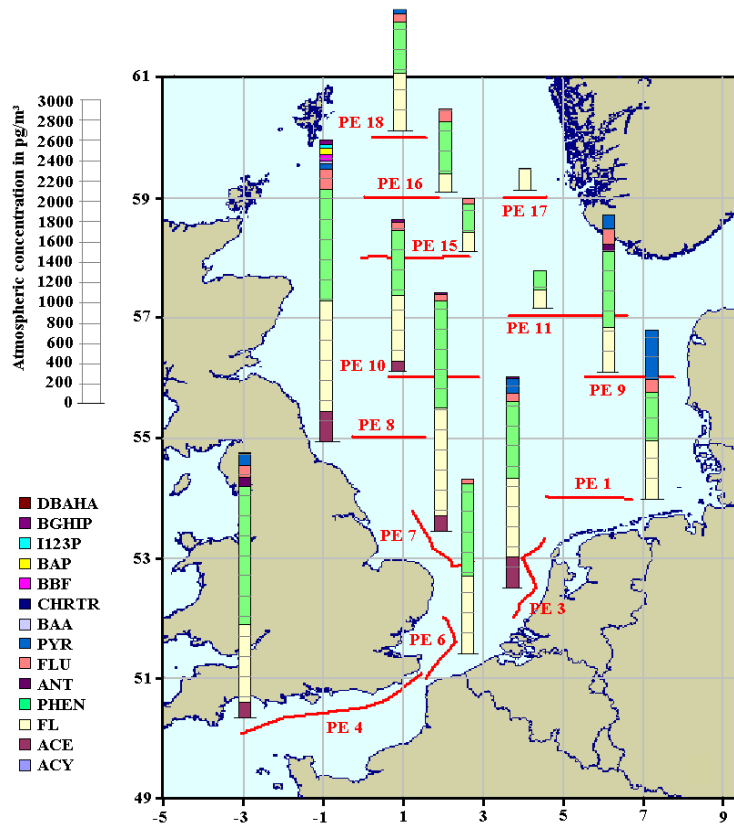


Figure 5.4: Atmospheric bulk concentrations of PAHs above the North Sea in Aug./Sep. 2009

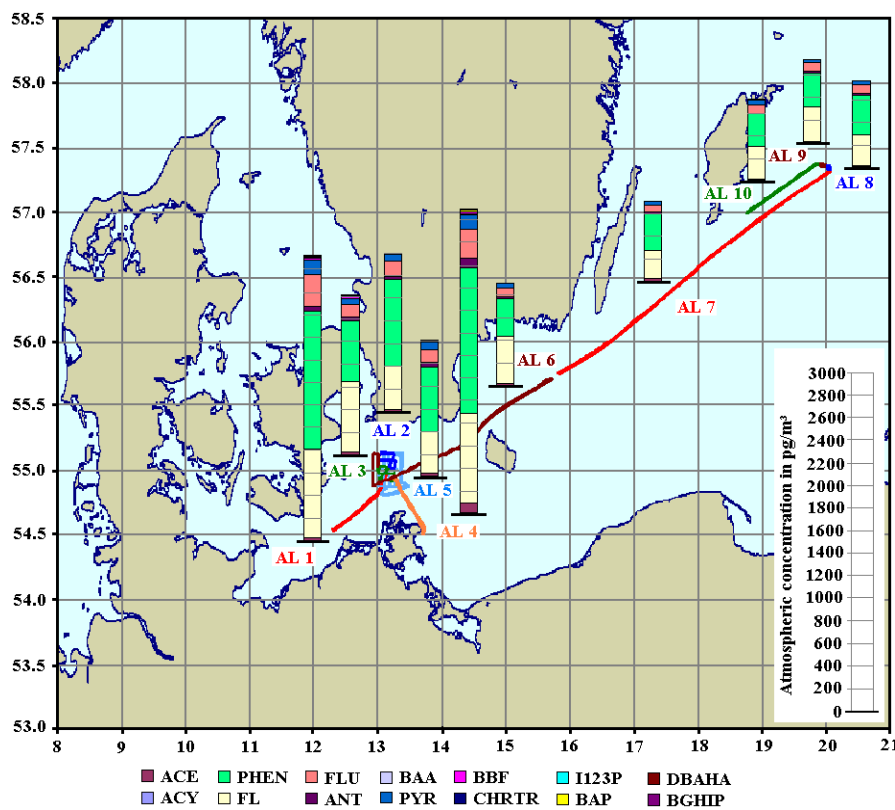


Figure 5.5: Concentrations of PAHs in the gaseous mass fraction of the atmosphere above the Baltic Sea in Apr. 2009

Comparison of PAH concentrations determined at sea and land based sampling sites

A comparison of marine and continental atmospheric PAH concentrations was difficult, because respective active air sampling campaigns were performed in different seasons. However, the samples collected during the cruises in the spring along the river Elbe could be considered as land based sampling sites. On average, atmospheric PAH concentrations determined above the river Elbe were 3 - 4 times higher than in the German EEZ.

Seasonal variations in atmospheric PAH concentrations

The PUF disk passive air sampler seasonal profiles (figure 5.6) displayed a significant increase in PAH abundances at ambient temperatures (monthly mean temperatures) less than 2 °C. Significant

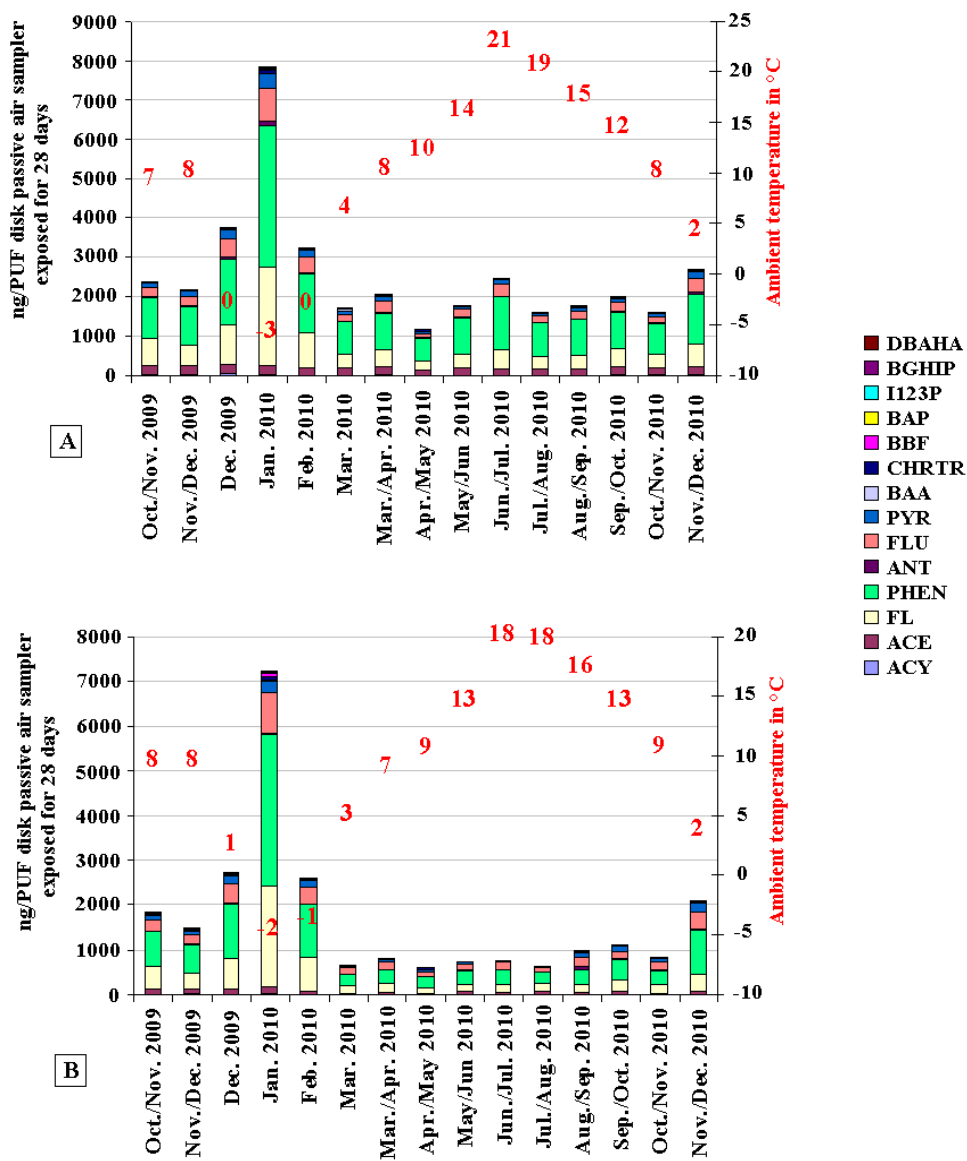


Figure 5.6: Seasonal variation of atmospheric PAH levels plotted in correlation with the ambient temperature for the PUF disk passive air sampler sampling sites Sülldorf/Hamburg (A) and Tinnum/Sylt (B)

differences in the atmospheric PAH patterns depending on the season were not monitored by passive air samplers, because PUF disk passive air samplers accounted negligibly for the particle associated mass fraction of PAHs. Thus, active air sampling data obtained from comparable sampling sites in spring and winter were additionally summarized in figure 5.7. On average the total PAH concentrations were 9 - 10 times higher in winter than in spring. Furthermore, the mass fraction of the main components fluorene and phenanthrene was two times higher in spring than in winter air samples. On average the atmospheric concentrations of 4-6 ring PAHs were found to be 10 times higher in winter than in spring air samples. PAHs originate from combustion processes. As already reported and confirmed by this study (figure 5.6 and 5.7), atmospheric concentrations of PAHs were significantly higher in winter, due to the heating period. A less efficient mixing of the boundary layer and less photodegradation in winter additionally contributed to an amplification of summer time atmospheric PAH concentrations. [69, 114, 115]

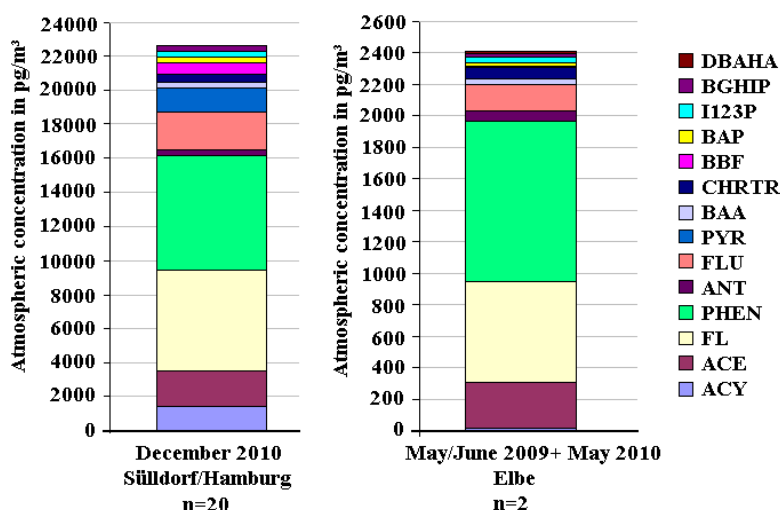


Figure 5.7: Comparison of atmospheric bulk concentrations of PAHs determined by active air sampling campaigns in winter (arithmetic mean of 20 air samples) and spring/summer (arithmetic mean of two air samples)

Gas-particle partitioning

Besides the seasonal variations in atmospheric concentrations due to variable primary sources, the differences in PAH patterns of summer and winter air samples was additionally influenced by the gas-particle partitioning behaviour of PAHs. The gas-particle partitioning was investigated in five active air sampling campaigns performed in different seasons. Two of them were executed at ambient air temperatures of -3 °C and 6 °C in Sülldorf/Hamburg. Three data sets originated from sea cruises in the German EEZ and North Sea at air temperatures ranging from 11°C to 16°C. The particle associated and gaseous mass fractions of PAHs were plotted in % against the ambient air temperatures, where 100% referred to the sum of all air samples per campaign (figure 5.8 and 5.9).

A correlation in gas-particle partitioning of PAHs with ambient air temperature was observed in this study as illustrated in figure 5.8. In winter the particle associated mass fraction reached up to 17 % of the total atmospheric PAH concentration. In contrast, only 2 % of total PAH adsorbed to atmospheric particles in summer. On average approximately 90 % of total PAH was present in the gaseous mass fraction of the atmosphere. This ratio in gas-particle partitioning was in line with previous studies reporting the occurrence of a comparable spectrum of PAHs in the atmosphere at land based sampling sites. ^[69, 116]

The increase of the particle associated mass fraction of PAHs in winter could be ascribed to complex interactions of the seasonal variations in primary sources and meteorological conditions as well as the physico-chemical properties of the PAHs: As mentioned above atmospheric PAH abundances are elevated in winter season due to the heating period, a less efficient mixing of the boundary layer and a deceleration of photo-chemical reactions. ^[69, 114] Moreover, the adsorption to soot is an important factor for the gas-particle partitioning process. The heating period additionally leads to higher levels of soot in the atmosphere, which in turn results in higher abundances of particle associated PAHs. Furthermore, low ambient temperatures favour the adsorption of PAHs on particulate matter. ^[69, 117, 118]

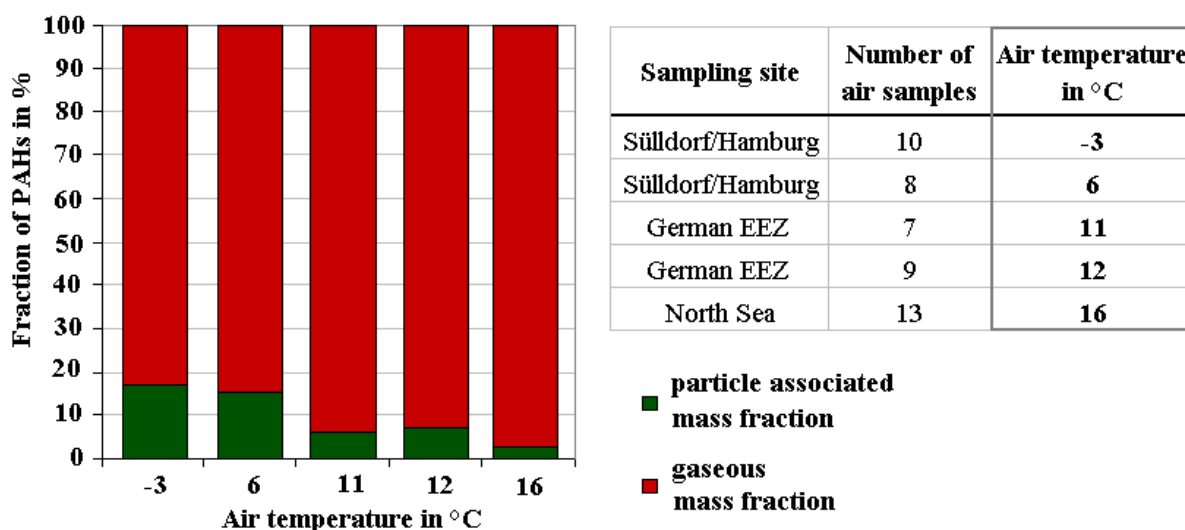


Figure 5.8: Gas-particle partitioning of PAHs in correlation with ambient air temperatures

In addition, the gas-particle partitioning was influenced by the physico-chemical properties of the PAH compounds, as displayed in figure 5.9. The distribution of individual PAHs between the gaseous and particle mass fraction was in agreement with their saturation vapour pressures (p_{sat}) and thus with their boiling point, molecular weight and chemical structure. PAHs of vapour pressures less than $2.8 \cdot 10^{-5}$ Pa (25 °C) predominantly occurred in the particle associated mass fraction. Significant changes in their gas-particle behaviour with ambient temperature were not

observed. In contrast, PAHs of vapour pressures more than $2.8 \cdot 10^{-5}$ Pa (25°C) were mainly found in the gaseous mass fraction. Significant effects of ambient temperature on the gas-particle partitioning were observed for several PAHs in the gaseous mass fraction, namely anthracene, phenanthrene, fluoranthene and pyrene. In particular, the gas-particle partitioning of fluoranthene ($p_{\text{sat}} = 1.2 \cdot 10^{-3}$ Pa, 25°C) and pyrene ($p_{\text{sat}} = 6.0 \cdot 10^{-4}$ Pa, 25°C) revealed the highest influence of ambient temperature. These observations were in agreement with a previous study.^[16]

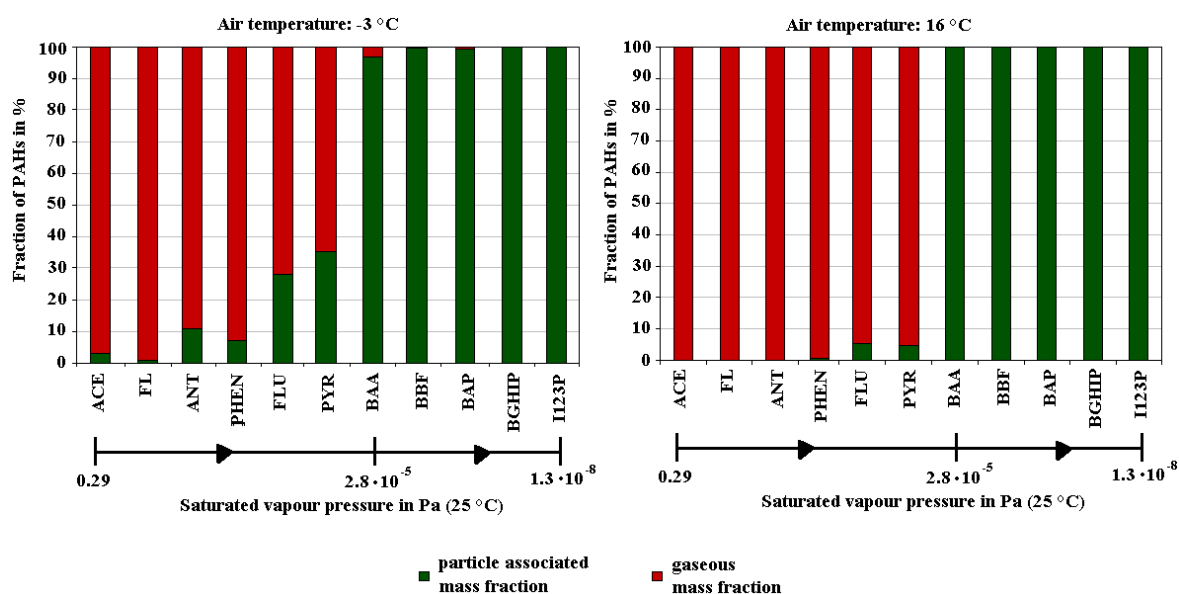


Figure 5.9: Gas-particle partitioning of individual PAH components sorted by their vapour pressures^[69] at different ambient air temperatures

The effects of ambient temperature on the gas-particle partitioning of individual PAHs could be interpreted by a preferential adsorption to the different modes of aerosol particles: As described in chapter 2.2.1 PAHs of lower molecular weight (< 202 g/mol) were observed to adsorb in significant abundances to the surfaces of coarse mode particles. Therefore, a free-exchange with the ambient atmosphere and thus a temperature driven equilibrium between particle and gaseous phase might be predicted for those compounds. In contrast, PAHs of higher molecular weight (>228 g/mol) were found to be predominantly connected to accumulation mode particles. These particles evolve by coagulation with smaller particles, which might effect an incorporation of adsorbed PAHs into the aerosol structure. Hence, a free-exchange with the ambient atmosphere could not be provided limiting the influence of ambient temperature on the gas-particle partitioning mechanism.^[38, 83, 86]

Occurrence and distribution of PAHs in the surface seawater

The spatial distribution of PAHs in the surface water of the German EEZ, the wider North Sea and the Baltic Sea is illustrated in figures 5.10 - 5.13. The data sets of the cruises in the German EEZ

and the Baltic Sea comprised only selected PAH components. Nevertheless, they were found to be sufficient for a further interpretation of atmospheric PAH concentrations in relation to the respective surface seawater abundances.

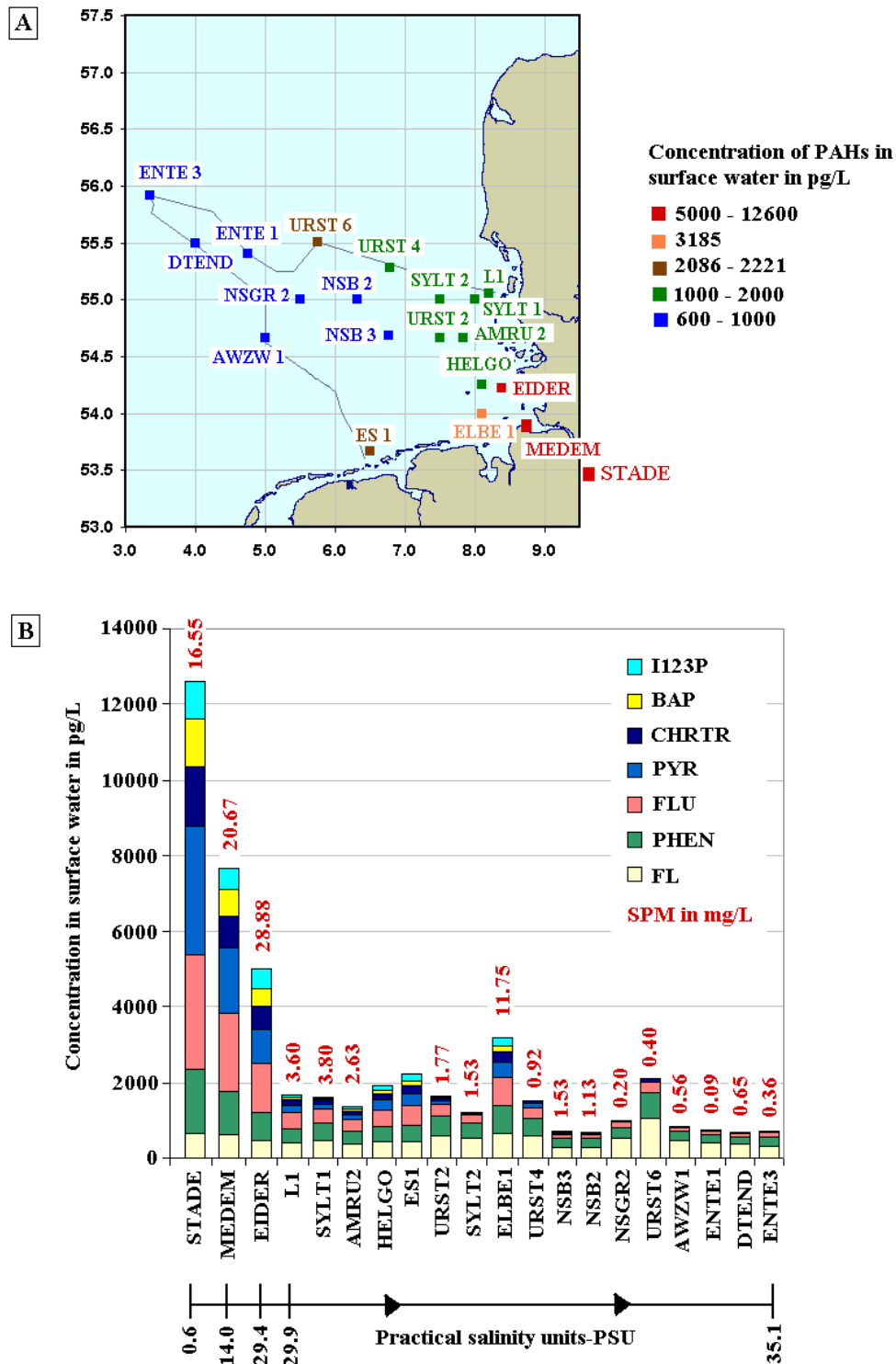


Figure 5.10: Occurrence and distribution of PAHs (aqueous and particulate phase) in the surface water (5m) of the German EEZ in May/June 2009; (A) Spatial distribution; (B) PAH abundances in relation to suspended particulate matter (SPM) concentration and salinity for each water sampling site

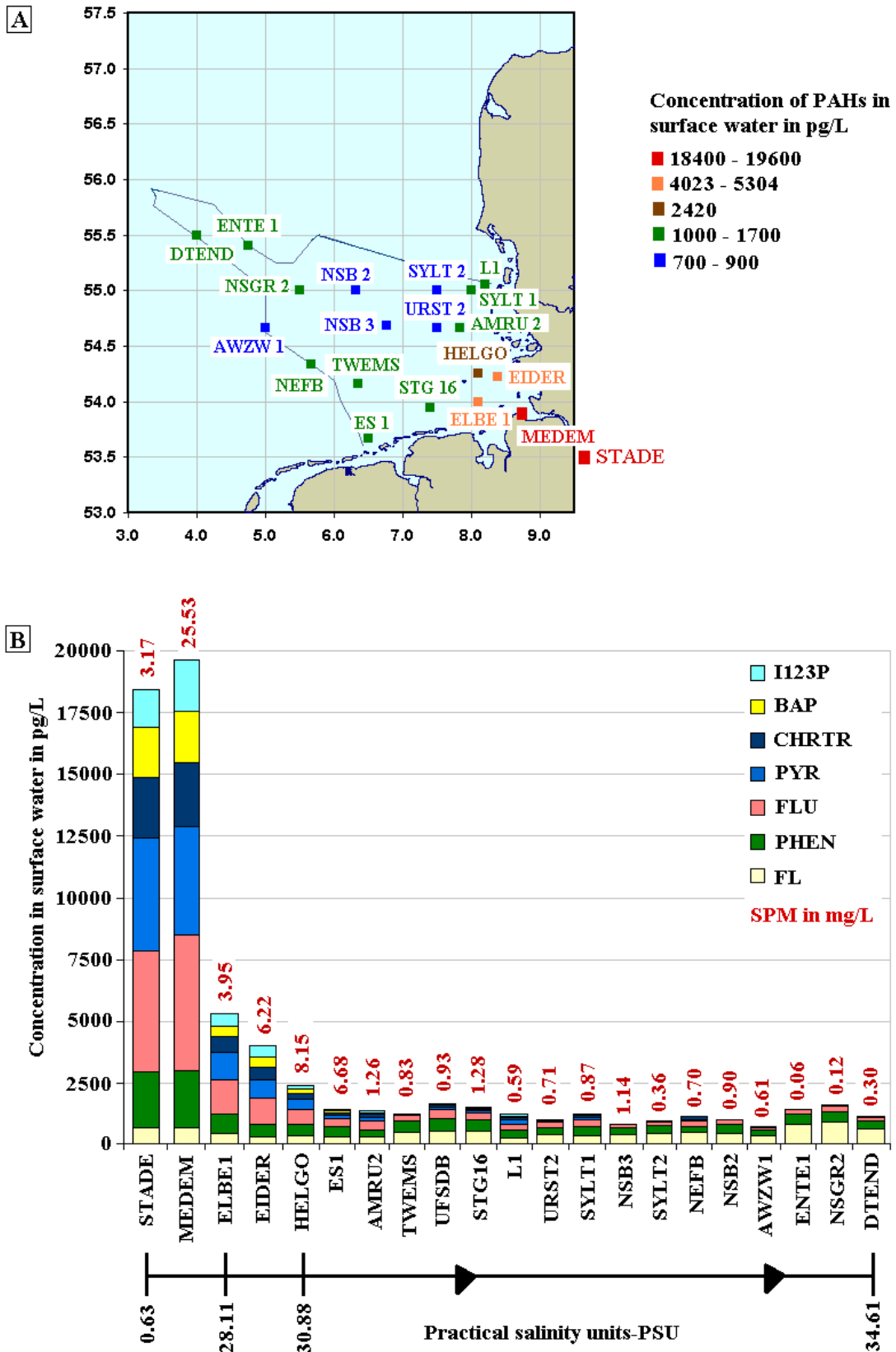


Figure 5.11: Occurrence and distribution of PAHs (aqueous and particulate phase) in the surface water (5m) of the German EEZ in May 2010; (A) Spatial distribution; (B) PAH abundances in relation to suspended particulate matter (SPM) concentration and salinity for each water sampling site

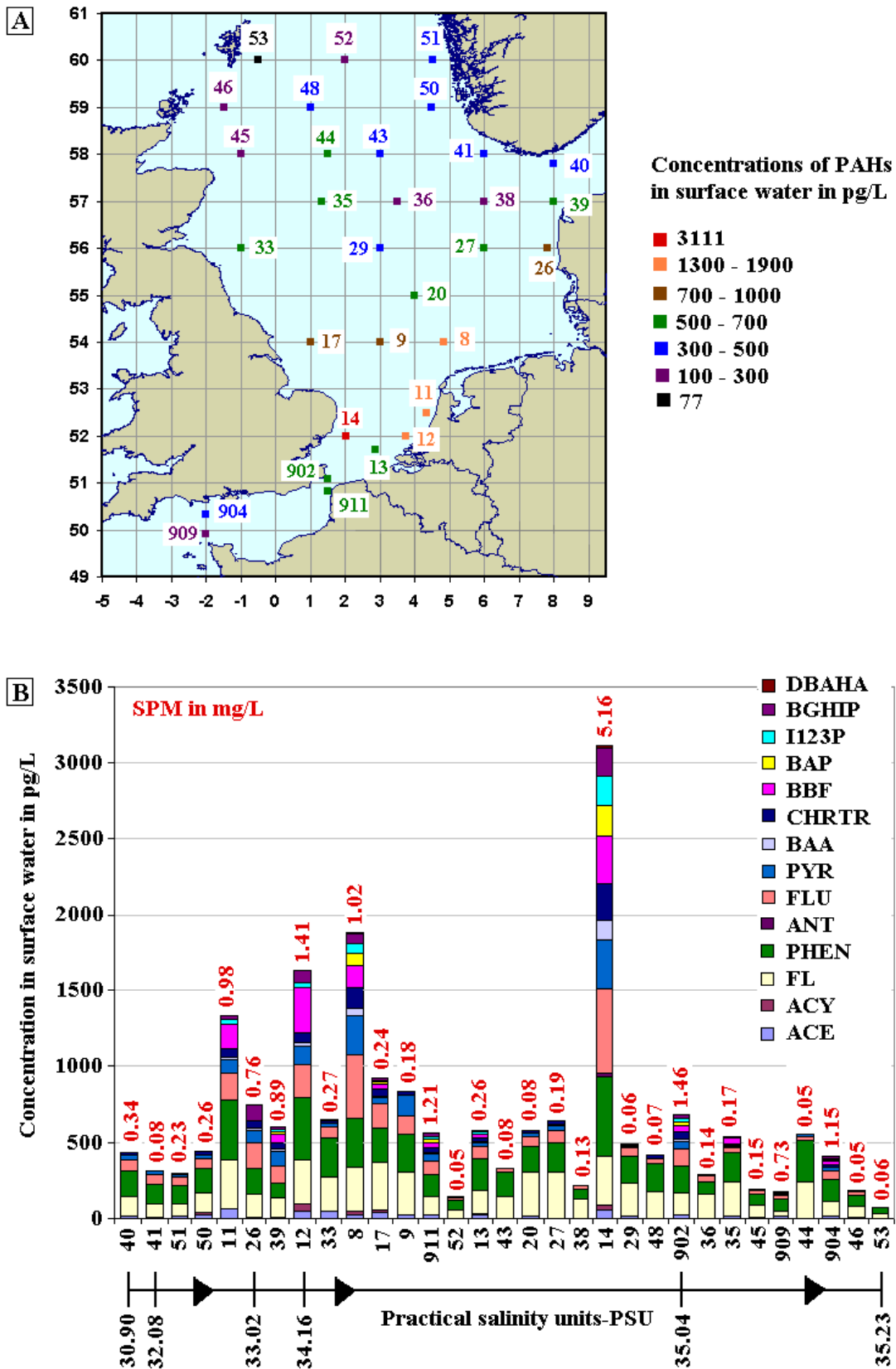


Figure 5.12: Occurrence and distribution of PAHs (aqueous and particulate phase) in the surface water (5m) of the North Sea in Aug./Sep. 2009; (A) Spatial distribution; (B) PAH abundances in relation to suspended particulate matter (SPM) concentration and salinity for each water sampling site

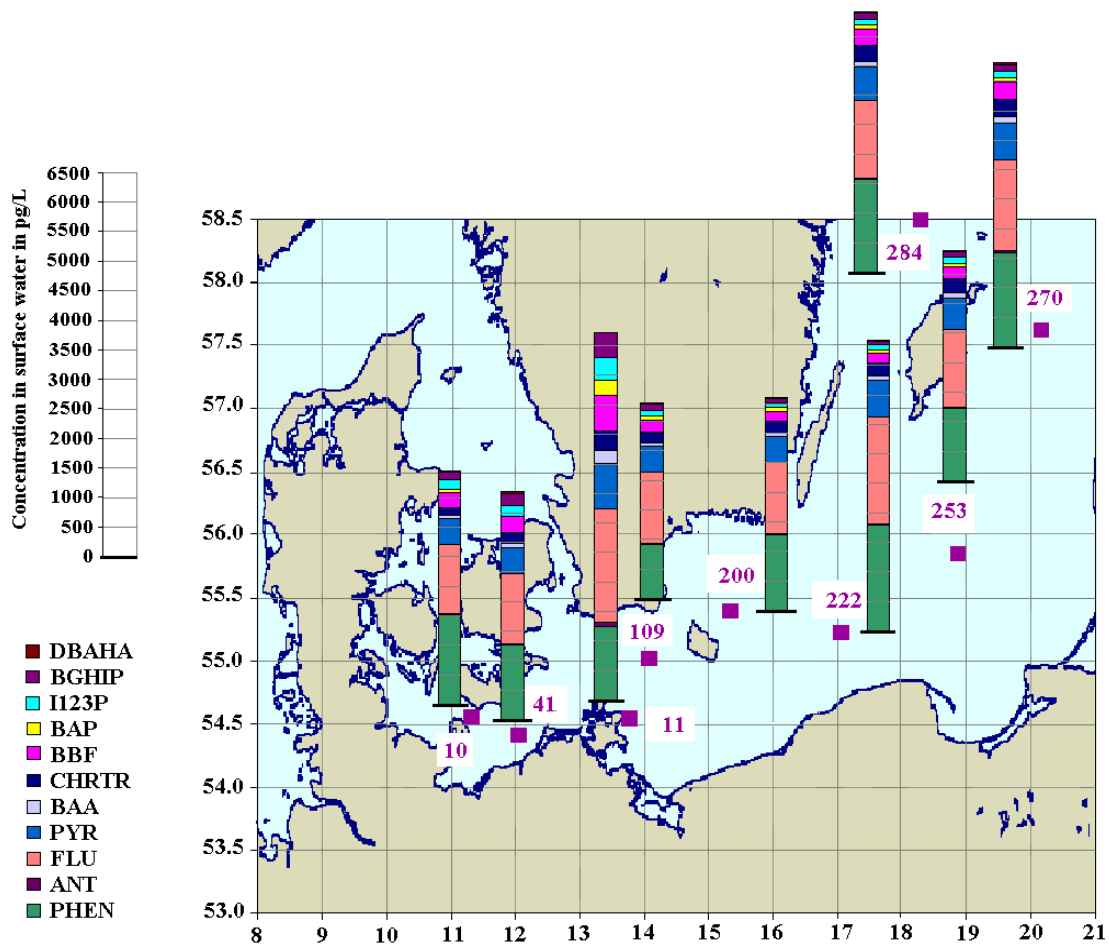


Figure 5.13: Spatial distribution of PAHs (aqueous and particulate phase) in the surface water (6m) of the Baltic Sea in Feb. 2005

The spatial distributions of PAHs in the surface seawater displayed a significant decrease in concentration with increasing distance to estuaries and river plumes. Highest gradients of total PAH concentrations were monitored from the Elbe (STADE, MEDEM) to the western sampling sites (ENTE 1, ENTE 3) of the German EEZ. Gradients of approximately 12-18 pg/L were documented for the years 2009 and 2010, respectively (figures 5.10 and 5.11). The spatial distributions of PAHs in surface seawater were consistent with the sea currents of the German EEZ (refer to figure 3.21). Typical river plumes of the Elbe, Ems and Weser were observed. The Elbe plume revealed the highest concentration levels, which pointed to a major riverine input source of PAHs into the German EEZ. A comparable slight decrease in surface seawater concentrations (e.g. from sampling sites 14 to 52) of approximately 3 ng/L was observed for the wider North Sea (figure 5.12). Highest concentrations were quantified in the southern part of the North Sea inside the river plumes of Thames and Rhine. A decrease of PAH abundances towards the water exchange regions with the Atlantic Ocean in the northern part of the North Sea and the English Channel was documented. The spatial distribution of PAHs in the surface water of the North Sea was in agreement with river estuaries, the outflow of the Baltic Sea and sea currents (refer to figure 3.21)

indicating a dominant riverine input of PAHs. In contrast, the surface water of the Baltic Sea (figure 5.13) showed a homogenous PAH distribution in the area of the longitudes 11° E to 21° E. Total PAH concentrations of approximately 4 ng/L \pm 1 ng/L were monitored, which was comparable with concentrations detected in water samples of the estuaries of Elbe and Thames. On average the total PAH concentrations in the Baltic Sea (Feb. 2005) were three times higher than in the German EEZ (May/Jun. 2009/2010). This could be due to the seasonal variation in surface water concentrations of PAHs: Along with the seasonal fluctuations in atmospheric concentrations, the surface water concentrations were several times higher in winter. It was reported that the surface water concentration of phenanthrene was three times higher in winter (January) than in summer (July). No significant trends in PAH surface seawater concentrations were monitored. ^[119]

The occurrence and distribution of PAHs in the surface seawater and the atmosphere displayed comparable characteristics: The main PAH components in the surface seawater beyond coastal sampling sites were fluorene and phenanthrene, the same as in the atmosphere. They were detected even at the remote sampling sites in the northern North Sea. Maximum concentrations of fluorene and phenanthrene were quantified in the river Elbe with 700 pg/L and 2000 pg/L, respectively. Moreover, the partitioning of PAHs between aqueous and particulate (SPM) phases was comparable to the atmospheric gas-particle partitioning. Those PAHs, which were predominantly found in the particulate matter phase in surface water were identical with the particle associated PAHs in the atmosphere. PAHs of increased logK_{OW} occurred in highest mass fractions in suspended particulate matter ^[119], as illustrated in figure 5.14. In consequence, 4-6 ring PAHs were predominantly observed in water samples with significant SPM amounts (coastal sampling sites, river estuaries), as illustrated in figures 5.10 - 5.12.

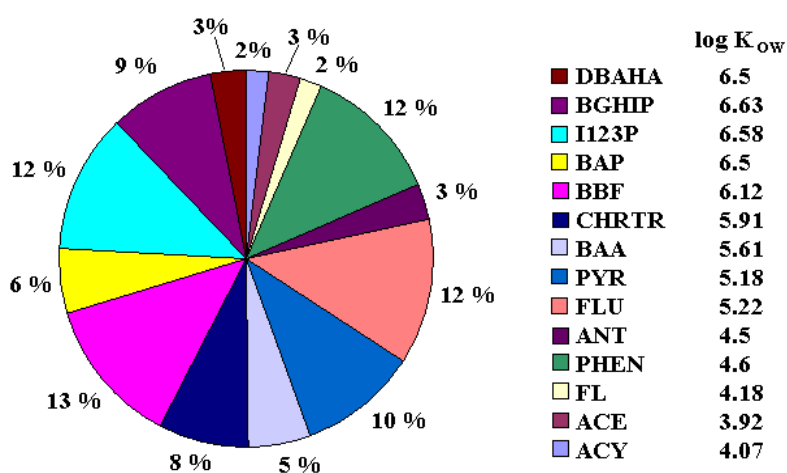


Figure 5.14: PAH abundances of suspended particulate matter (SPM) collected in the estuary of the river Elbe (Apr./Jun. 2009) in relation to logK_{OW} (obtained from ^[69])

The river estuaries were found to be major input sources of PAHs to the surface seawater. However, it had to be differentiated between the individual PAH components. It was noticed that the concentration gradients of individual PAH components either decreased or did not exist with decreasing $\log K_{OW}$ and thus a decreasing tendency of particle adsorption. Fluorene ($\log K_{OW} = 4.18$ [69]) displayed an almost constant surface water concentration of approximately $0.47 \text{ ng/L} \pm 0.15 \text{ ng/L}$ throughout the German EEZ, which was unaffected by the suspended particulate matter and riverine fresh water content (decreasing practical salinity units (PSU)). In addition, a slight increase in surface water concentrations towards the western sampling sites of the German EEZ (ENTE1, NSGR2, DTEND) was observed indicating atmospheric deposition of fluorene in this sea region (refer to figure 5.11). A significant contribution of atmospheric deposition to the surface sea water contamination beyond coastal waters could be additionally assumed for phenanthrene ($\log K_{OW} = 4.6$ [69]). Phenanthrene, which was found to be a main PAH component in the marine atmosphere, displayed a small concentration gradient within the German EEZ pointing to a significant pre-contamination of “clean” background water presumably by atmospheric deposition. In contrast, the other PAH components revealed much stronger concentration gradients, especially those which adsorbed in significant fractions to SPM. The contaminated SPM settled down to the sea bottom and was consequently less transported with surface sea currents. Atmospheric deposition of 4-6 ring PAHs to the surface sea water was assumed to be a minor input pathway, because they occurred scarcely in the atmosphere and were not detected in the surface seawater at remote sampling sites.

Net flux of diffusive gas exchange of PAHs between the marine atmosphere and the sea surface water

In order to assess the occurrence of atmospheric dry gaseous deposition, the direction of the net flux of diffusive gas exchange was calculated as defined in chapter 2.4.1 for gaseous compounds. Fugacity ratios were exclusively calculated for phenanthrene and fluorene, the major PAH components in the aqueous phase of the surface seawater and the gaseous mass fraction of the atmosphere (figure 5.15). Surface water concentrations of the Baltic Sea were exclusively available for February 2005, whereas atmospheric concentrations originated from a research cruise in April 2009. No significant trend in surface water concentrations of PAHs were observed, which provided the comparison of data from different years. However, a seasonal variation of surface water concentrations from February to April could not be excluded. The phenanthrene concentration was reported to be three times higher in water samples from July than in water samples from January. [119] Therefore, the flux calculation of the Baltic Sea was probably biased by increased water concentrations, which in turn increased the fugacity ratios.

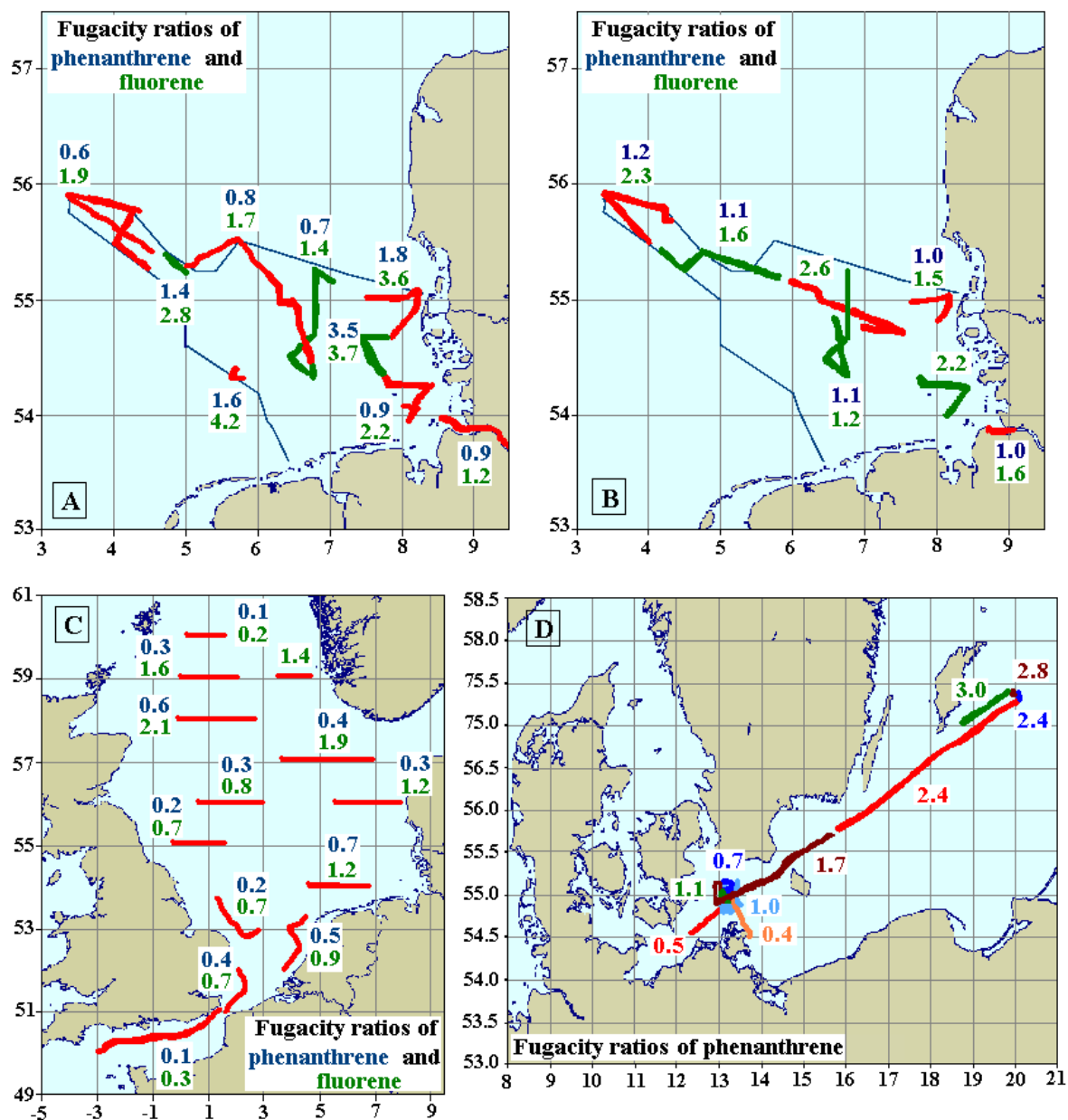


Figure 5.15: Net flux of diffusive gas exchange of fluorene and phenanthrene; Fugacity ratio < 0.5: Atmosphere → Sea; Fugacity ratio > 2; Sea → Atmosphere; (A) German EEZ May/Jun. 2009; (B) German EEZ May 2010; (C) North Sea Aug./Sep. 2009; (D) Baltic Sea Apr. 2009

The results indicated a net volatilisation of fluorene from the surface seawater of the German EEZ, whereas a tendency to equilibrium in gas exchange was determined for phenanthrene. In addition, an atmospheric deposition of phenanthrene and equilibrium conditions in gas exchange of fluorene was calculated for the wider North Sea. The diffusive gas exchange direction for the Baltic Sea could only be assessed for phenanthrene, because fluorene concentrations of surface water were not available. At the sampling sites west of 14°E an atmospheric deposition of phenanthrene with a trend to equilibrium was observed. This could be due to the proximity of the sampling sites to continent and thus primary sources. At the eastern sampling sites of the Baltic Sea (east of 14°E)

the flux direction changed and pointed to a net volatilisation of phenanthrene from surface water. The net flux of diffusive gas exchange was affected by air and water temperatures (chapter 2.4) as well as seasonal variations in environmental concentrations of phenanthrene and fluorene. Thus, the calculated direction of the net flux of diffusive gas exchange was only valid for the seasons of the respective research campaigns.

Conclusions

In conclusion, the atmospheric deposition of the free gaseous PAH components fluorene and phenanthrene to the surface water of the North Sea was documented and gaining importance outside of river plumes, estuaries and the Baltic Sea outflow. Atmospheric deposition of particle associated PAHs was found to be less significant, as their atmospheric concentrations were mostly below the LOQ. Riverine input was a major PAH source to the surface seawaters, predominantly for particle bound PAH components. A net volatilisation of fluorene from surface seawater was observed within river plumes and estuaries. These observations were made in the months May/Jun. 2009, May 2010, Aug./Sep 2009. They could change with season due to seasonal fluctuations in PAH concentrations in surface water and atmosphere as well as variations in water and air temperature.

In the Baltic Sea an atmospheric deposition of phenanthrene with a trend to equilibrium was documented at sampling sites west of 14°E. This was attributed to the proximity of the sampling sites to continent and thus primary sources. At the eastern sampling sites of the Baltic Sea (east of 14°E) the flux direction changed and pointed to a net volatilisation of phenanthrene from surface water. The direction of the net flux of diffusive gas exchange of fluorene in the Baltic Sea could not be determined, because respective surface water concentrations were not available.

On average the atmospheric bulk concentrations (sum of gaseous and particle associated mass fraction) of PAHs were approximately ten times higher in December (Sülldorf/Hamburg) than in May (Elbe). A seasonality of atmospheric deposition of PAHs along with the increase in atmospheric concentrations in winter was not reported in this study, but was still observed in previous investigations. ^[119]

5.1.2 Chlorinated Benzenes

Besides a variety of applications, agriculture was an important input source of chlorinated benzenes to the environment. Hexachlorobenzene (HCB) was used as fungicide especially for the seed treatment of wheat and was an integral part of several pesticide formulations. Its application was

prohibited in Germany in 1981. Pentachlorobenzene (QCB) was prepared as an intermediate for the production of the pesticide pentachloronitrobenzene, which usage was prohibited in Germany in 1992. In addition, they were used in a chlorobenzene mixture accompanied with PCBs in electrical equipment. Today, both chlorinated benzenes are banned under the Stockholm Convention. Nevertheless, there are still potential emission sources of chlorinated benzenes today. Waste incineration, revolatilisation from contaminated soil as well as chlorination processes in industry are current emission sources of chlorinated benzenes to the atmosphere. ^[120-123]

Occurrence and distribution of chlorinated benzenes in the marine atmosphere

Hexachlorobenzene and pentachlorobenzene were quantified throughout all sampling sites in the gaseous mass fraction of the atmosphere. They were only sporadically detected in the particle associated mass fraction. This was anticipated regarding their semi-volatility and in agreement with other observations. ^[66, 124] Seasonal fluctuations in atmospheric concentrations of HCB and QCB were not documented during this study.

Hexachlorobenzene as well as pentachlorobenzene displayed negligible variations in atmospheric concentrations. They were almost homogeneously distributed, without significant alignment to sampling sites and air mass backward trajectories (figures 5.16-5.19). However, a slight decrease in atmospheric hexachlorobenzene concentrations with increasing distance to continent and sea origin (according to 24 h backward trajectories) was indicated for the Baltic Sea campaign (AL 7, AL 8, AL 9, AL 10).

Mean atmospheric concentrations and standard deviations (table 5.1) of chlorinated benzenes quantified during the research cruises in the German EEZ and the North Sea were comparable. In contrast, hexachlorobenzene and pentachlorobenzene concentrations were approximately two to six times lower in the Baltic Sea atmosphere, respectively. This difference was presumably significantly influenced by a systematic error in air sample analysis identified during a side-by-side sampling experiment with PUF plug and PUF/XAD-2/PUF adsorber cartridges (chapter 4.1.1, annex 1): It was observed that QCB concentrations quantified on PUF/XAD-2/PUF adsorber cartridges (applied during cruises in the German EEZ and North Sea) were two times higher than those obtained from PUF plug adsorber cartridges (applied during the Baltic Sea research cruise). HCB was quantified in approximately 1.5 times higher concentrations on PUF/XAD-2/PUF adsorber cartridges than on PUF plugs. Due to the reproducibility of the results (data is tabulated in the annex 1) a systematic error might be predicted. However, the source of error was still unknown. The most probable assumption could be a break through of chlorinated benzenes during active air sampling with PUF plug adsorber cartridges, as still reported in a previous study. ^[17] Typical HCB concentrations in the marine atmosphere documented during research cruises in the North Atlantic

and Arctic Ocean ranged from 40 pg/m^3 to 50 pg/m^3 .^[66] This was in agreement with the atmospheric concentrations of North Sea and German EEZ determined during this study. Considering the homogeneity in chlorinated benzene distributions and the results of the side-by-side sampling experiments, no significant differences in atmospheric concentrations above the Baltic Sea and above the North Sea were assumed.

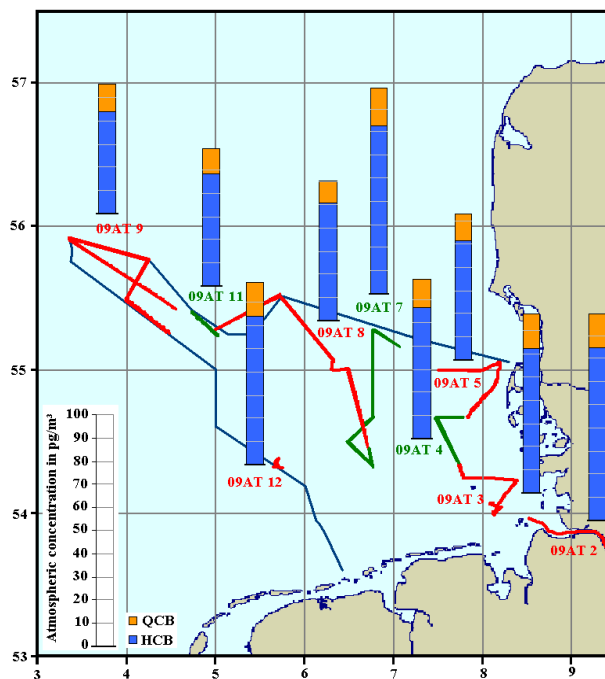


Figure 5.16: Gas phase concentrations of chlorinated benzenes in the atmosphere above the German EEZ in May/June, 2009

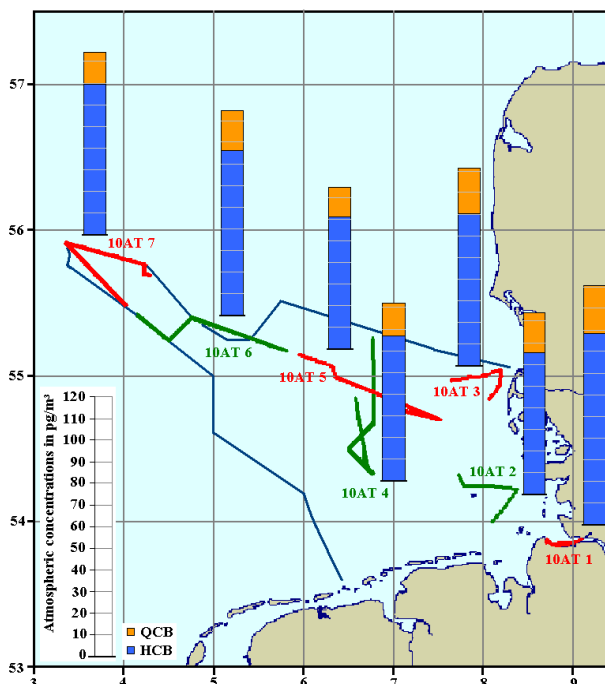


Figure 5.17: Gas phase concentrations of chlorinated benzenes in the atmosphere above the German EEZ in May 2010

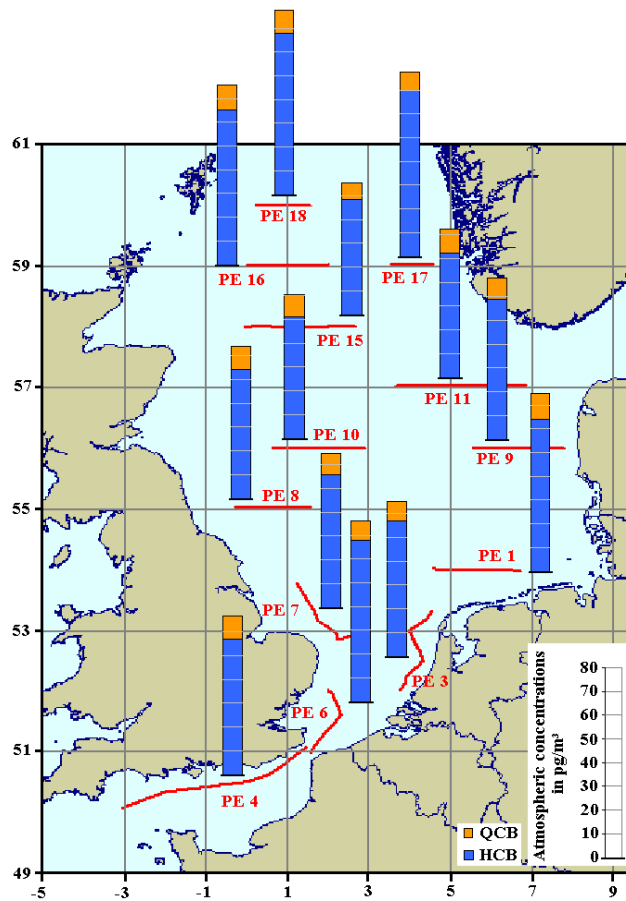


Figure 5.18: Gas phase concentrations of chlorinated benzenes in the atmosphere above the North Sea in Aug./Sep. 2009

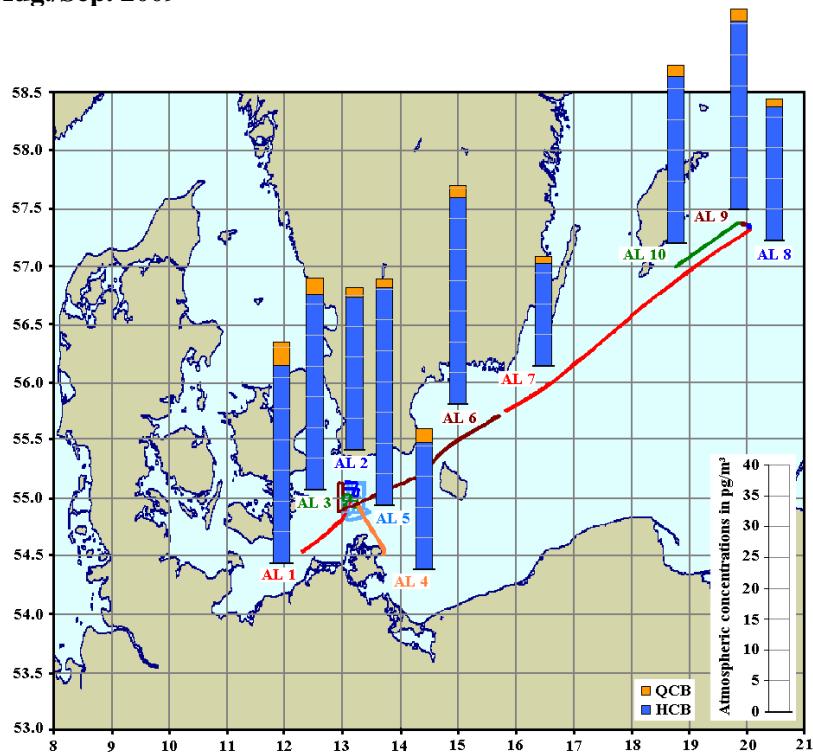


Figure 5.19: Gas phase concentrations of chlorinated benzenes in the atmosphere above the Baltic Sea in Apr. 2009

Table 5.1: Hexachlorobenzene (HCB) and pentachlorobenzene (QCB) concentrations in the marine atmosphere; P pl = PUF plug adsorber cartridge; PXP = PUF/XAD-2/PUF adsorber cartridge; \bar{x}_{arithm} = arithmetic mean of concentration in pg/m^3 ; σ_a = standard deviation of atmospheric concentrations in pg/m^3 ; σ_r = standard deviation of atmospheric concentration in % of the arithmetic mean

Sampling campaign	Adsorber cartridge	HCB			QCB		
		\bar{x}_{arithm}	$\pm \sigma_a$	$\pm \sigma_r$	\bar{x}_{arithm}	$\pm \sigma_a$	$\pm \sigma_r$
Baltic Sea 09	P pl	27.3	6.3	23	2.0	0.7	35
North Sea 09	PXP	59.3	7.0	12	9.1	1.1	12
G. EEZ 09	PXP	58.3	10.8	19	13.0	2.2	17
G. EEZ 10	PXP	71.2	9.0	13	17.6	3.3	19

Occurrence and distribution of chlorinated benzenes in the surface seawater

HCB and QCB could be quantified throughout all sampling sites in the German EEZ. Decreasing surface water concentrations with increasing distance to the river plume of the Elbe were documented for both chlorinated benzenes. Surface water concentrations of 7-8 pg/L and 11-18 pg/L of chlorinated benzenes were documented at sampling sites within the Elbe plume for the years 2009 and 2010, respectively. At the western sampling sites of the German EEZ the surface water concentrations decrease to approximately 0.4-4 pg/L and 5 pg/L for the years 2009 and 2010, respectively (figures 5.20 and 5.21).

HCB was homogeneously distributed with a mean concentration of 3 pg/L in the surface water of the wider North Sea. In contrast, QCB was exclusively quantified at three sampling sites within or adjacent to the river plume of the Rhine (12, 11, 8) in concentrations of approximately 2-4 pg/L (figure 5.22). The small concentration gradients of HCB within the German EEZ and its homogeneous distribution in the North Sea surface water could be interpreted by a predominant atmospheric deposition of HCB and lesser significance of riverine input. Although QCB was quantified in constant concentrations throughout the entire North Sea atmosphere, it was not present at concentrations above LOQ in the surface water of the North Sea (except in the river plume of the Rhine). The QCB concentration gradient within the German EEZ and its occurrence within the river plume of the Rhine pointed to a riverine input of QCB to the surface seawaters.

At first sight a comparison of HCB surface water concentrations of the North Sea and the Baltic Sea could be difficult, because the data sets originated from different years and seasons (refer to figure 5.22 and 5.23). However, constant surface water concentrations of HCB were reported over many years. Moreover, the seasonal variations in HCB concentrations in the period from February to April were supposed to be negligible, because they were reported to differ by only a factor of two in the period of January to July. ^[119] Therefore, a comparison of both data sets appeared to be possible. HCB was homogeneously distributed throughout the investigated Baltic Sea region. The mean HCB surface water concentration was approximately 7 pg/L and was comparable with

concentrations quantified in the river plume of the Elbe. The constant concentrations indicated an atmospheric input of HCB to the surface water of the Baltic Sea for the sea region displayed in figure 5.23. QCB surface water concentrations of the Baltic Sea were not available.

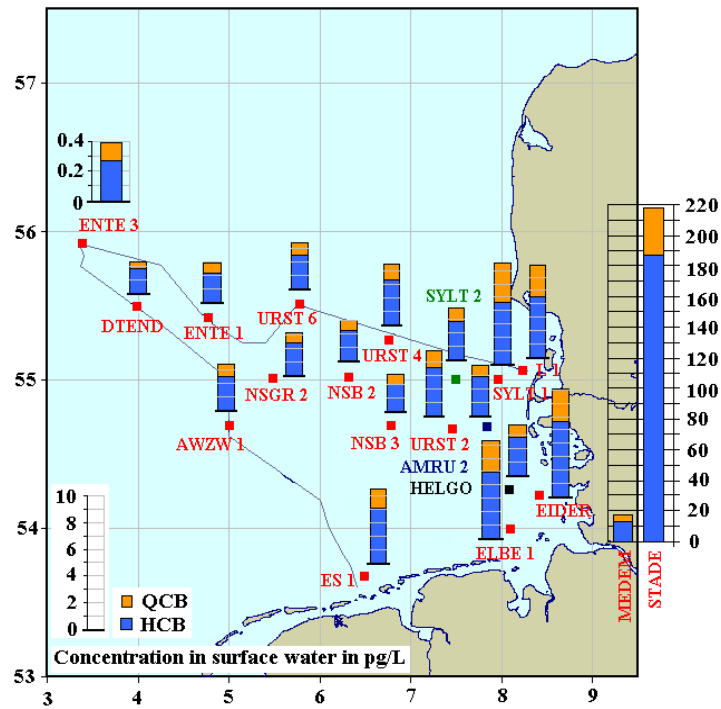


Figure 5.20: Occurrence and spatial distribution of chlorinated benzenes in the surface water (5m) of the German EEZ in May/June, 2009

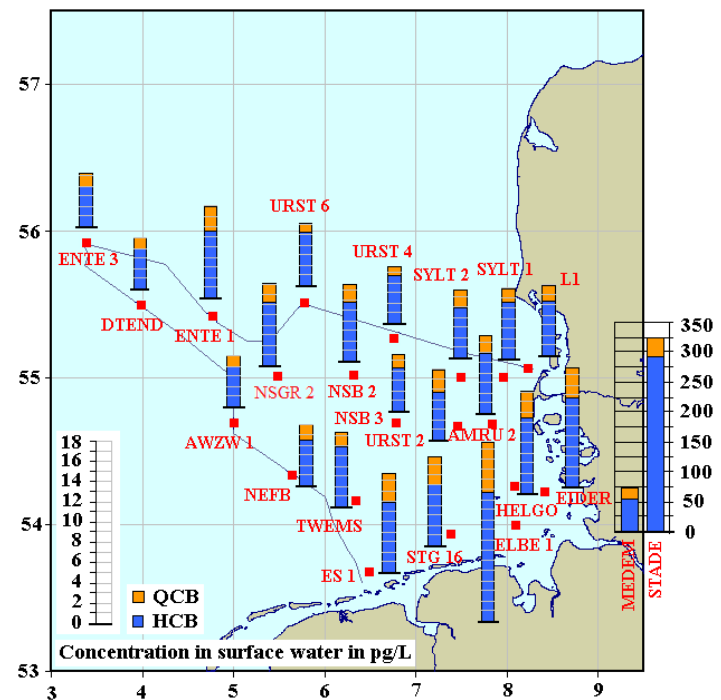


Figure 5.21: Occurrence and spatial distribution of chlorinated benzenes in the surface water (5m) of the German EEZ in May 2010

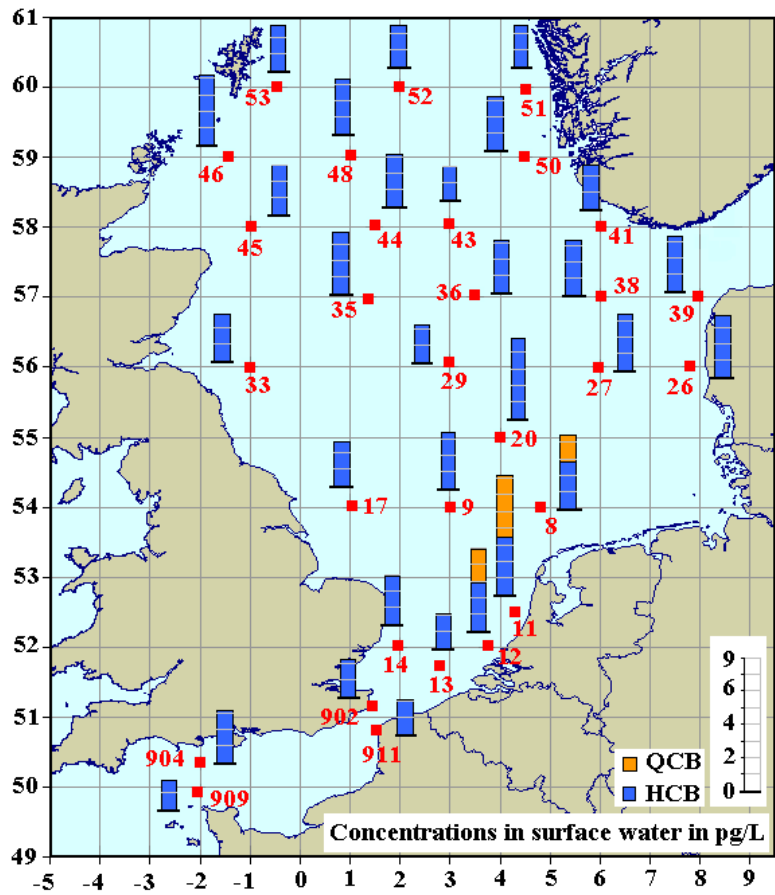


Figure 5.22: Occurrence and distribution of chlorinated benzenes in the surface water (5m) of the North Sea in Aug./Sep. 2009

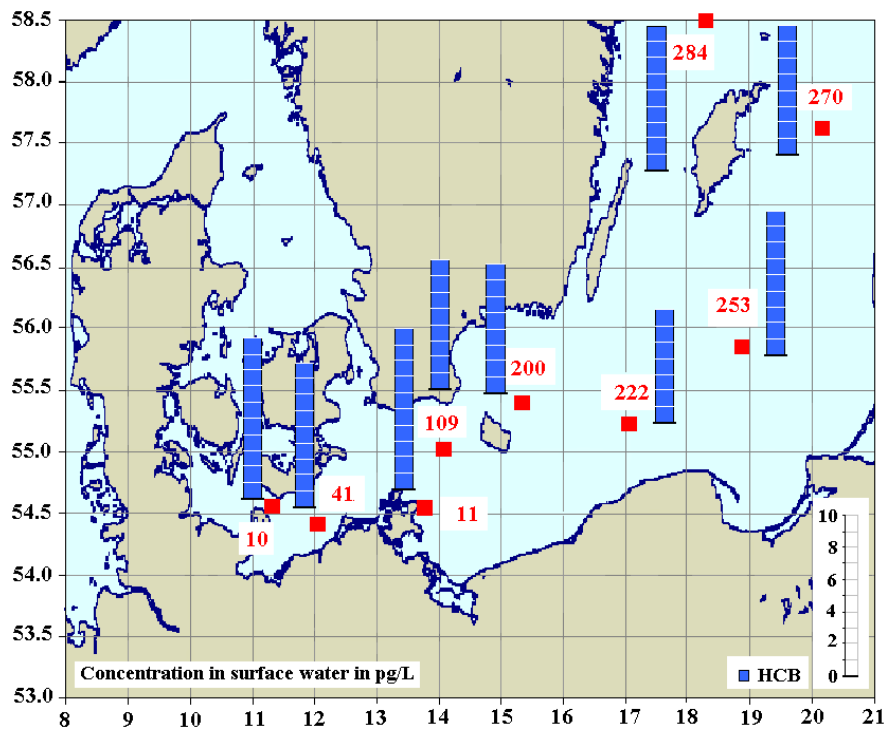


Figure 5.23: Spatial distribution of hexachlorobenzene (HCB) in the surface water (6m) of the Baltic Sea in Feb. 2005

Due to the negligible water solubility of chlorinated benzenes and $\log K_{OW}$ of 5-6, absorption to suspended particulate matter in the water phase would be expected. ^[125] However, a correlation between the surface water concentrations of chlorinated benzenes and the SPM content was not observed. Moreover, the constant concentrations of HCB within the surface water contraindicated significant particle adsorption of HCB. Further studies confirmed the predominant occurrence of chlorinated benzenes in the aqueous phase, where on average approximately 90 % of total HCB had been found dissolved in the water phase. ^[119] In addition the low SPM content in the surface water beyond coastal sampling sites suggested that the particle associated mass fraction of chlorinated benzenes contributed negligibly to the reported surface seawater concentrations.

Net flux of diffusive gas exchange of chlorinated benzenes between the marine atmosphere and the surface water

As discussed above chlorinated benzenes were predominantly present in the particle unbound mass fraction of the atmosphere and the surface seawater. Hence, the direction of the net flux of diffusive gas exchange could be calculated (figure 5.24) as described in chapter 2.4.1.

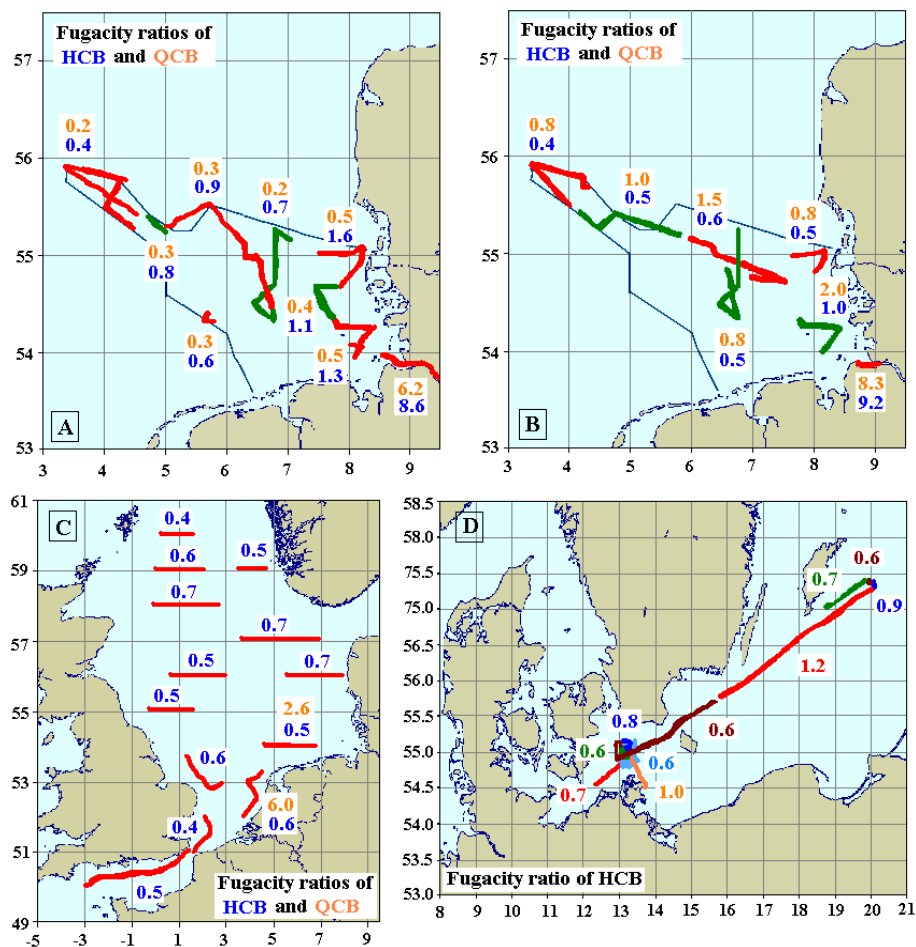


Figure 5.24: Net flux of diffusive gas exchange of chlorinated benzenes; Fugacity ratio < 0.5: Atmosphere → Sea; Fugacity ratio > 2: Sea → Atmosphere; (A) German EEZ May/Jun. 2009; (B) German EEZ May 2010; (C) North Sea Aug./Sep. 2009; (D) Baltic Sea Apr. 2009

The atmospheric concentrations of chlorinated benzenes above the Baltic Sea were corrected by a factor of 2 for the calculation, because of the systematic error in air sample analysis described above. The surface water concentrations of HCB in the Baltic Sea from the year 2005 were predicted to be representative for the calculation of the gas exchange direction, because no significant trend in water concentrations was reported within the years. ^[119]

The gas exchange of HCB within the river plume of the Elbe was close to phase equilibrium, whereas net deposition was suggested for the western areas of the German EEZ. In addition, the results confirmed the atmospheric input of chlorinated benzenes to the surface waters of the North Sea, whereas the gas exchange in the investigated region of the Baltic Sea was found close to phase equilibrium. The results for QCB were ambiguous. For the research cruise in 2009 atmospheric deposition of QCB was calculated throughout the entire German EEZ, whereas in the year 2010 the gas exchange was found close to phase equilibrium. For the sampling site on the river Elbe net volatilisation of both components was calculated. However, this result was probably biased by particle bound chlorinated benzenes in the river water with high SPM content and should not undergo further interpretation.

Conclusions

Atmospheric deposition was found to be the major input source of HCB to the surface waters of the German EEZ, the wider North Sea and the Baltic Sea. Evidence was given by the homogenous distribution of HCB throughout the marine atmosphere and surface waters of the North Sea and the Baltic Sea as well as by the calculation of the direction of the net flux of diffusive gas exchange. A minor riverine input of HCB by the Elbe was documented by a small concentration gradient in the surface water of the German EEZ. The gas exchange of HCB between atmosphere and sea was close to phase equilibrium within the river plume of the Elbe and in the studied areas of the Baltic Sea. To sum up, the results of this study confirmed the consideration that HCB is the POP closest to equilibrium in its large-scale (at least regional) distribution. ^[66]

No such conclusion was possible for QCB. Although QCB was found in homogeneous concentrations throughout the marine atmosphere, surface water concentrations were only quantified in the German EEZ and the river plume of the Rhine. A predominant atmospheric deposition by diffusive gas exchange was calculated for the German EEZ in the year 2009. A minor riverine input by the Elbe was indicated by a small concentration gradient within the German EEZ. An atmospheric deposition of QCB to the North Sea could not be documented, because of levels below LOQ in most surface water samples. However, an atmospheric deposition could not be excluded, because of the abundances of QCB in the North Sea air.

5.1.3 Hexachlorocyclohexanes

Hexachlorocyclohexanes were intensively used as insecticides from the late 1940s to the 1990s. They were formulated and applied as technical HCH containing the stable isomers α , β , γ , δ , and ϵ -HCH in percentages of 55–80 %; 5–14 %; 8–15 %; 2–16 %, and 3–5 %, respectively. The active ingredient was found to be γ -hexachlorocyclohexane, which was isolated and used under the trademark lindane since the 1950s. Today hexachlorocyclohexanes are banned under the Stockholm Convention on persistent organic pollutants. However, lindane is still used as pharmaceutical for the treatment of, e.g., scabies, acarions and lice. ^[126]

Occurrence and distribution of hexachlorocyclohexanes in the marine atmosphere

Hexachlorocyclohexanes occurred in the gaseous mass fraction of the atmosphere. A gas-particle partitioning was not observed. β -HCH and δ -HCH were scarcely observed in the marine atmosphere in concentrations mostly below the LOQs, whereas α -HCH and γ -HCH were detected throughout all sampling sites.

α -HCH was homogeneously distributed in the marine atmosphere. Mean concentrations of 3-5 pg/m^3 were quantified above the German EEZ, North Sea and Baltic Sea, which were unaffected by the origin of collected air masses (figure 5.25 - 5.28). These observations indicated a close to equilibrium distribution of α -HCH in the marine environment of the North Sea and the Baltic Sea, which had been already documented for other parts of the world. In particular, a close to equilibrium state was reported for the Arctic Ocean in the early 1990s, which changed to a net-volatilisation of α -HCH in ice-free regions of high and mid latitudes. ^[127, 128] This was in agreement with the constant α -HCH concentrations quantified in air masses from the North Atlantic (figure 5.27), which were collected at the remote sampling sites in the North Sea (PE 15, PE 16, PE 17). Aberrations to the homogeneous distribution were observed above the river Elbe, where 2-3 times higher α -HCH concentrations were determined (figure 5.25 and 5.26). In addition, the sampling sites in the Baltic Sea west of 14°E in proximity to land, displayed slightly increased α -HCH concentrations of 6-8.5 pg/m^3 (figure 5.28). These aberrations were attributed to the proximity of the sampling sites to continent and thus proximity to volatilisation processes from contaminated soil.

In contrast, the spatial distribution of γ -HCH in the marine atmosphere was highly variable. Atmospheric concentrations in the range of 1 pg/m^3 to 16 pg/m^3 were determined (figures 5.25 – 5.28). It was observed that the γ -HCH abundances strongly depended on the origin of collected air masses. Highest concentrations were quantified in air masses originating (24 h air mass backward trajectories) from England and France (figure 5.27). However, a definite source region of γ -HCH was not determined, which was anticipated considering the multi-hopping phenomenon of long

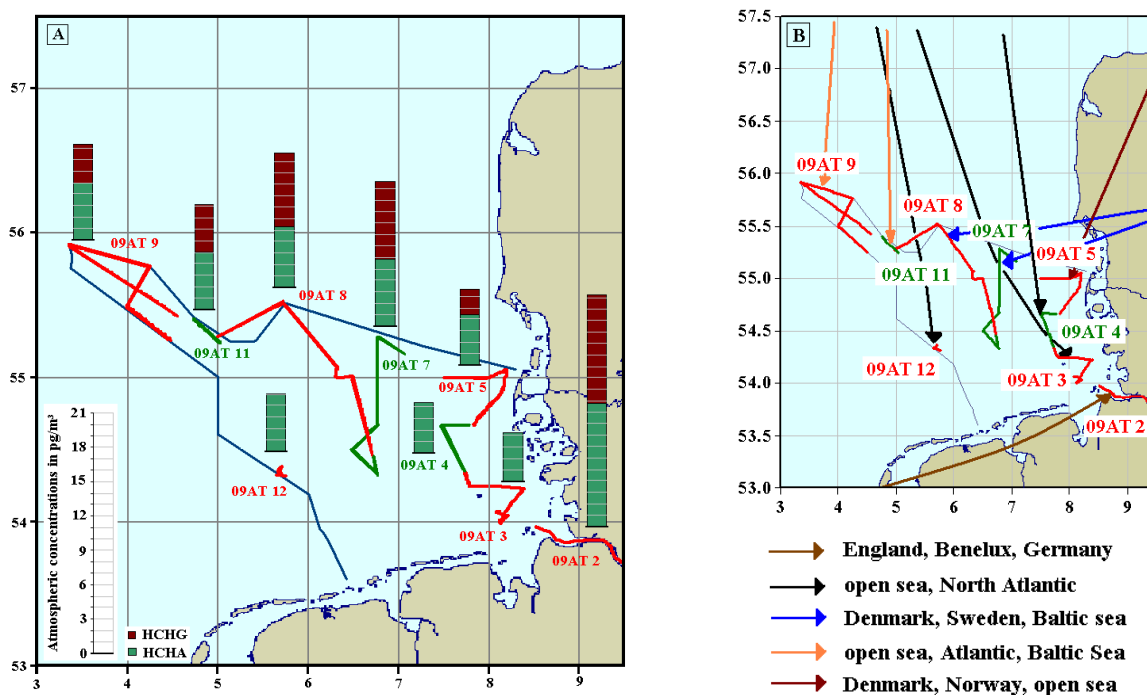


Figure 5.25: (A) Gas phase concentrations of hexachlorocyclohexanes in the atmosphere above the German EEZ in May/June, 2009; (B) Air mass history (24 h backward trajectories)

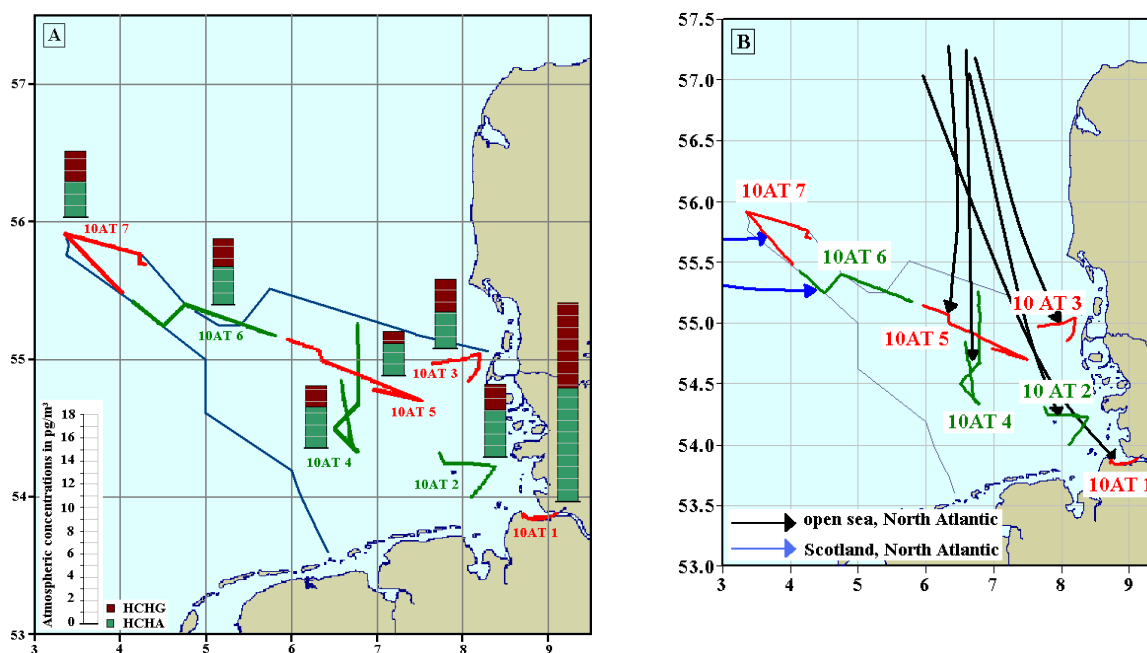


Figure 5.26: (A) Gas phase concentrations of hexachlorocyclohexanes in the atmosphere above the German EEZ in May 2010; (B) Air mass history (24 h backward trajectories)

living semi-volatile compounds (chapter 2.2). The γ -HCH concentration increased the longer the air masses had passed the continent, which was attributed to an uptake of re-emitted γ -HCH from contaminated soil. Besides, the air masses passing long distances over sea revealed lower γ -HCH abundances. Less than 4 pg/m^3 were determined in air samples without significant γ -HCH input

from the continent. These observations could be interpreted by an atmospheric deposition of re-emitted γ -HCH from continental contaminated soil to the surface waters of the North Sea and the Baltic Sea.

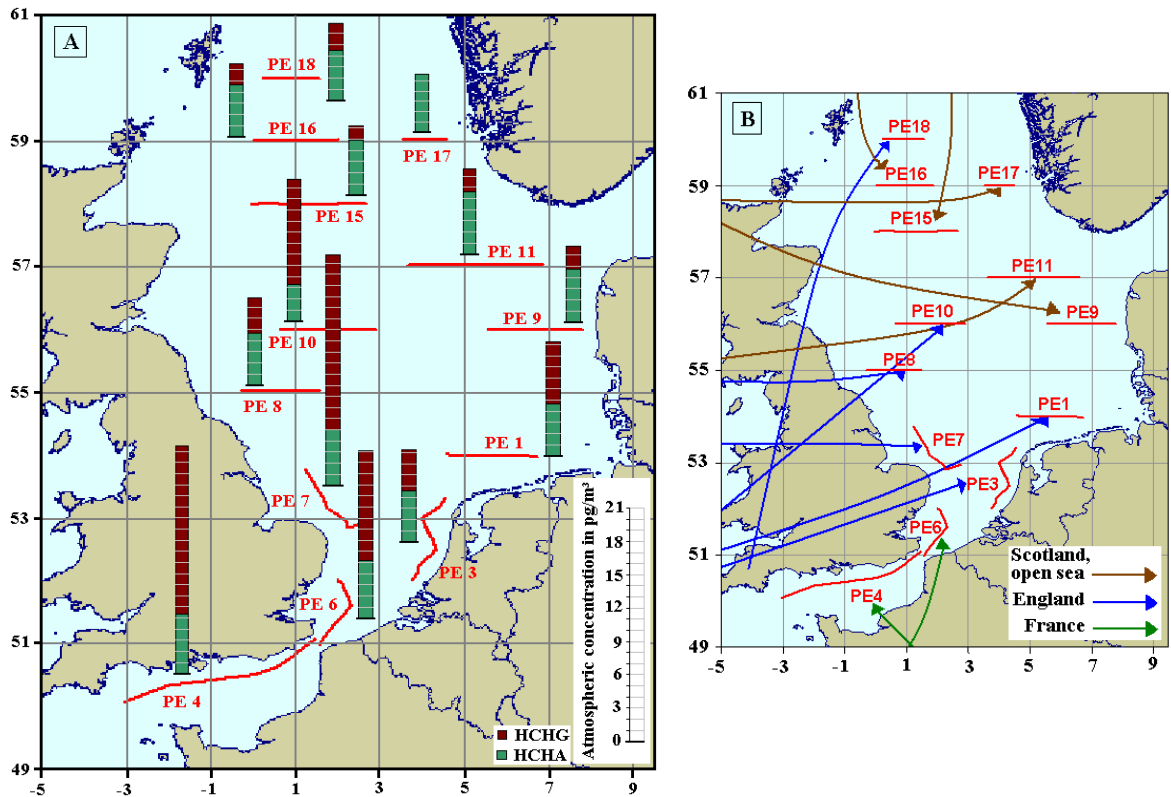


Figure 5.27: (A) Gas phase concentrations of hexachlorocyclohexanes in the atmosphere above the North Sea in Aug./Sep. 2009; (B) Air mass history (24 h backward trajectories)

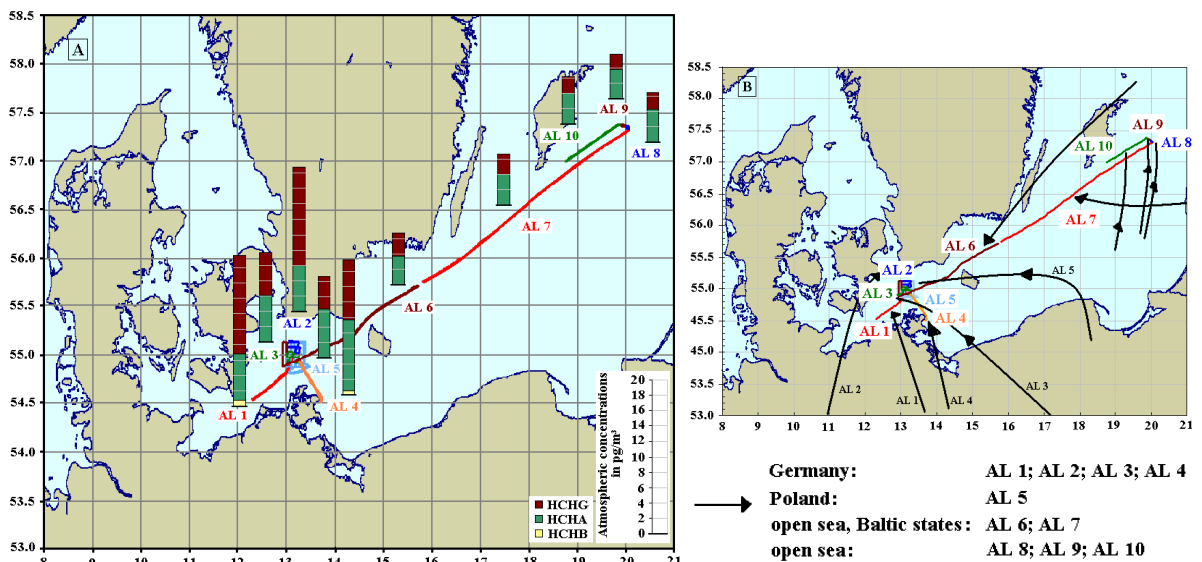


Figure 5.28: (A) Gas phase concentrations of hexachlorocyclohexanes in the atmosphere above the Baltic Sea in Apr. 2009; (B) Air mass history (24 h backward trajectories)

Seasonal variations in atmospheric concentrations

The PUF disk passive air samplers (figure 5.29) documented a seasonal variation of the γ -HCH abundances in air, which could be correlated with ambient temperature. Highest γ -HCH concentrations were found in June and July, the months with the maximum ambient temperature, whereas lowest concentrations were determined in January ($r^2 = 0.91$ for Hamburg and 0.86 for Sylt; figure 5.29). These results were attributed to the higher efficiency of the revolatilisation processes from contaminated soil at increased temperatures in the summer months. The maximum amplitude in atmospheric γ -HCH levels of approximately 12 ng/PUF disk PAS was observed at the urban sampling site in Sülldorf/Hamburg. An amplitude of 5 ng/PUF disk PAS was determined at Tinnum/Sylt an coastal sampling site. These observations provided further evidence that continental contaminated soil was a major source of γ -HCH to the atmosphere, as described above.

A significant seasonal variation of the atmospheric α -HCH abundances was not observed. Maximum amplitudes of 1-2 ng/PUF disk PAS were determined at the sampling sites Hamburg and Sylt, respectively.

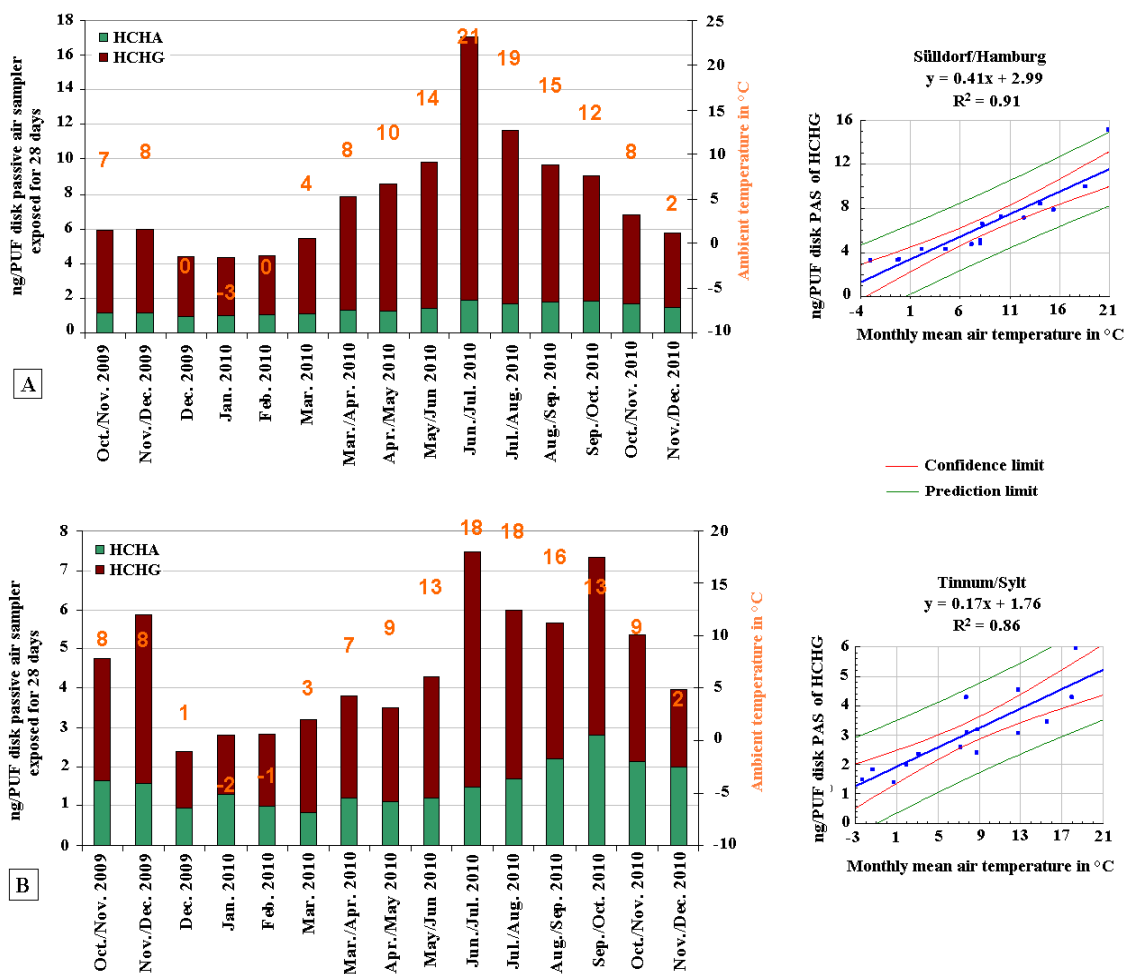


Figure 5.29: Seasonal variations in atmospheric hexachlorocyclohexane levels plotted in correlation with the ambient temperature for the PUF disk passive air sampler sampling sites Sülldorf/Hamburg (A) and Tinnum/Sylt (B)

Occurrence and distribution of hexachlorocyclohexanes in the surface seawater

α -, β - and γ -HCH were quantified throughout all sampling sites in the surface waters of the German EEZ, the wider North Sea and the German EEZ of the Baltic Sea (figures 5.30-5.33), whereas δ -HCH was only determined in the region of the Baltic Sea outflow and within the river plumes of Elbe, Ems, Weser, Rhine and Thames (δ -HCH surface water concentrations of the Baltic Sea were not available). Regarding the total of HCH isomers in surface water, a decreasing concentration with increasing distance to river plumes and the Baltic Sea outflow was observed. Maximum spatial concentration gradients of approximately 100 pg/L (sampling sites 909 and 11) and 3000 pg/L (sampling sites STADE and ENTE3) were observed for the surface water of the North Sea and the German EEZ, respectively. Thus, rivers and the outflow of the Baltic Sea were found to be important input sources of HCHs to the surface water of the North Sea. Besides, the slightly decreasing concentrations in the surface water of the open North Sea additionally indicated a dilution effect with significantly pre-contaminated surface water presumably due to net atmospheric deposition. In contrast, the German EEZ of the Baltic Sea displayed more constant HCH surface water concentrations in the range of 460-610 pg/L. A spatial gradient was not observed. The composition of the HCH fraction in surface water revealed significant discrepancies requiring a more detailed investigation of the occurrence of individual HCH isomers, as described below.

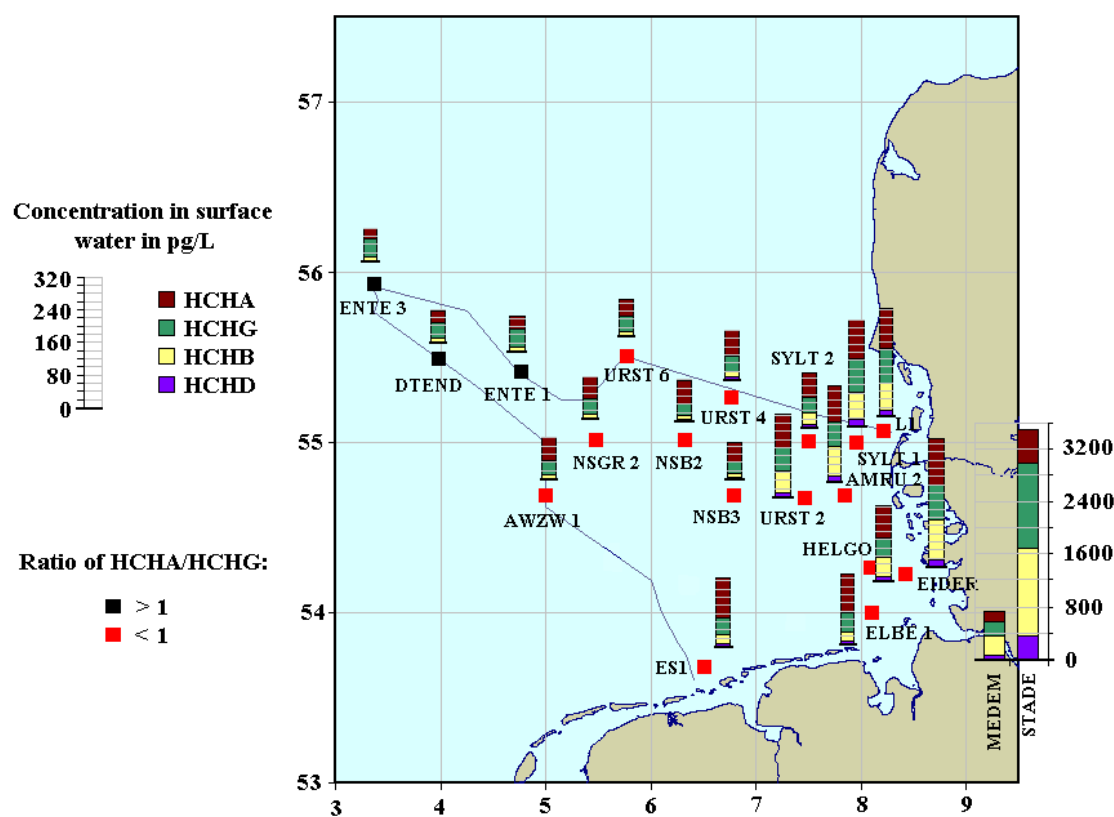


Figure 5.30: Occurrence and distribution of hexachlorocyclohexanes in the surface water (5m) of the German EEZ in Apr./May 2009

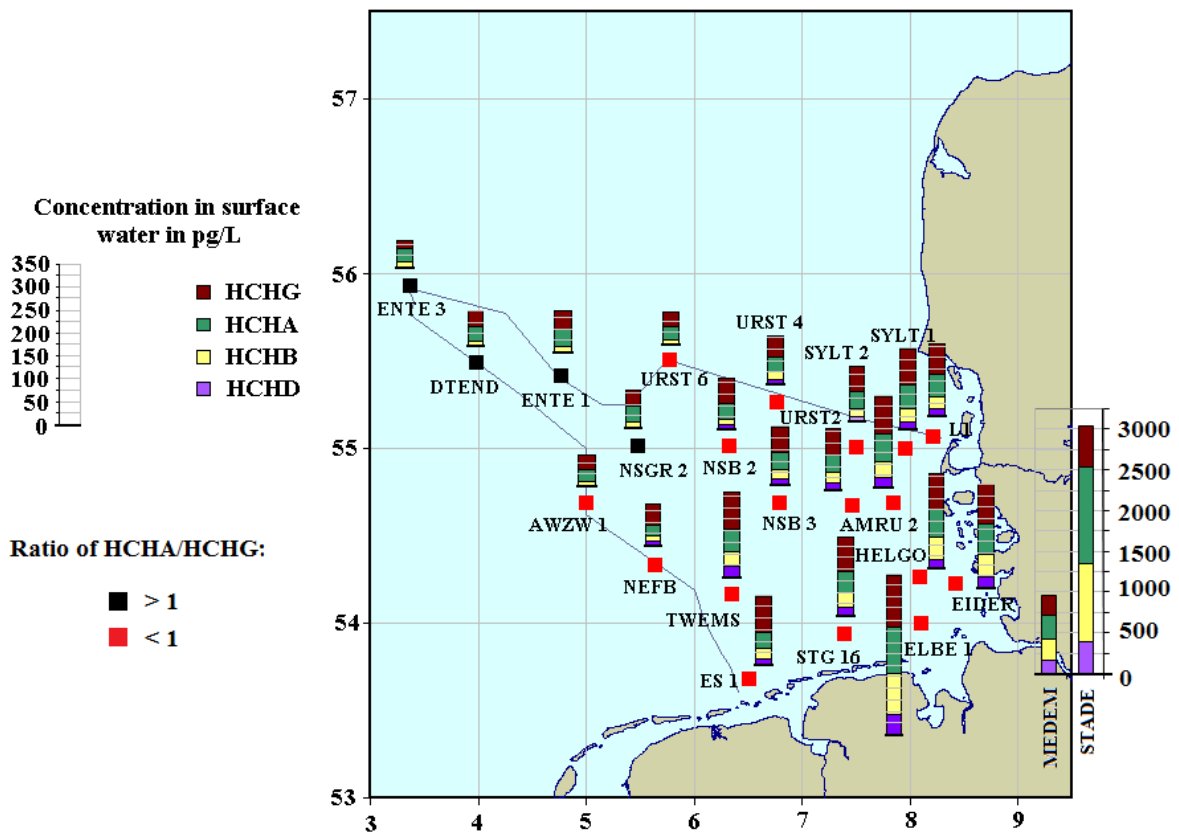


Figure 5.31: Occurrence and distribution of hexachlorocyclohexanes in the surface water (5m) of the German EEZ in May 2010

In the water samples of the river Elbe β - and δ - HCH were quantified in approximately the same concentrations like α -HCH and γ -HCH, respectively (figure 5.30 and 5.31). In contrast, the β -HCH isomer accounted for only a quarter of the total HCH concentration at the western sampling sites (ENTE1), whereas δ - HCH was not detected. Considering the predominant occurrence of α -HCH and γ -HCH in the marine atmosphere, these fluctuations in the HCH patterns of surface water samples from the German EEZ provided evidence of the significance of their atmospheric deposition.

α -HCH and γ -HCH were the main components in the surface seawater of the North Sea (figure 5.32). This was in agreement with their dominant occurrence in the marine atmosphere. Their surface water concentrations in the North Sea ranged from 7 – 48 pg/L and 12 - 65 pg/L, respectively. Highest concentrations of γ -HCH were quantified in the southern part of the North Sea and these decreased with increasing distance to the river estuaries and the Baltic Sea outflow. In contrast, the surface water concentrations of α -HCH were highest at northern sampling sites and these decreased towards the southern part of the North Sea. This opposite distribution could be described by the ratios of α -HCH/ γ -HCH (HCHA/HCHG) calculated for each water sample. A ratio of approximately 0.4 was determined at the sampling sites inside the river plumes of Thames

and Rhine implying a 2.5 times higher γ -HCH abundance in this region. A gradual increase of the α -HCH/ γ -HCH ratio towards the northern surface water was determined achieving its maximum in the range 2-3. Thus, 2-3 times higher α -HCH than γ -HCH concentrations were quantified at the remote sampling sites in the northern North Sea. These observations were supplemented by the α -HCH/ γ -HCH ratios calculated for the German EEZ (figure 5.30 and 5.31). The ratio increased towards the western sampling sites (ENTE 3, DTEND, ENTE 1) to a maximum of approximately 1.8. The ratios inside the estuary of the Elbe were the same as determined in the river plumes of Thames and Rhine.

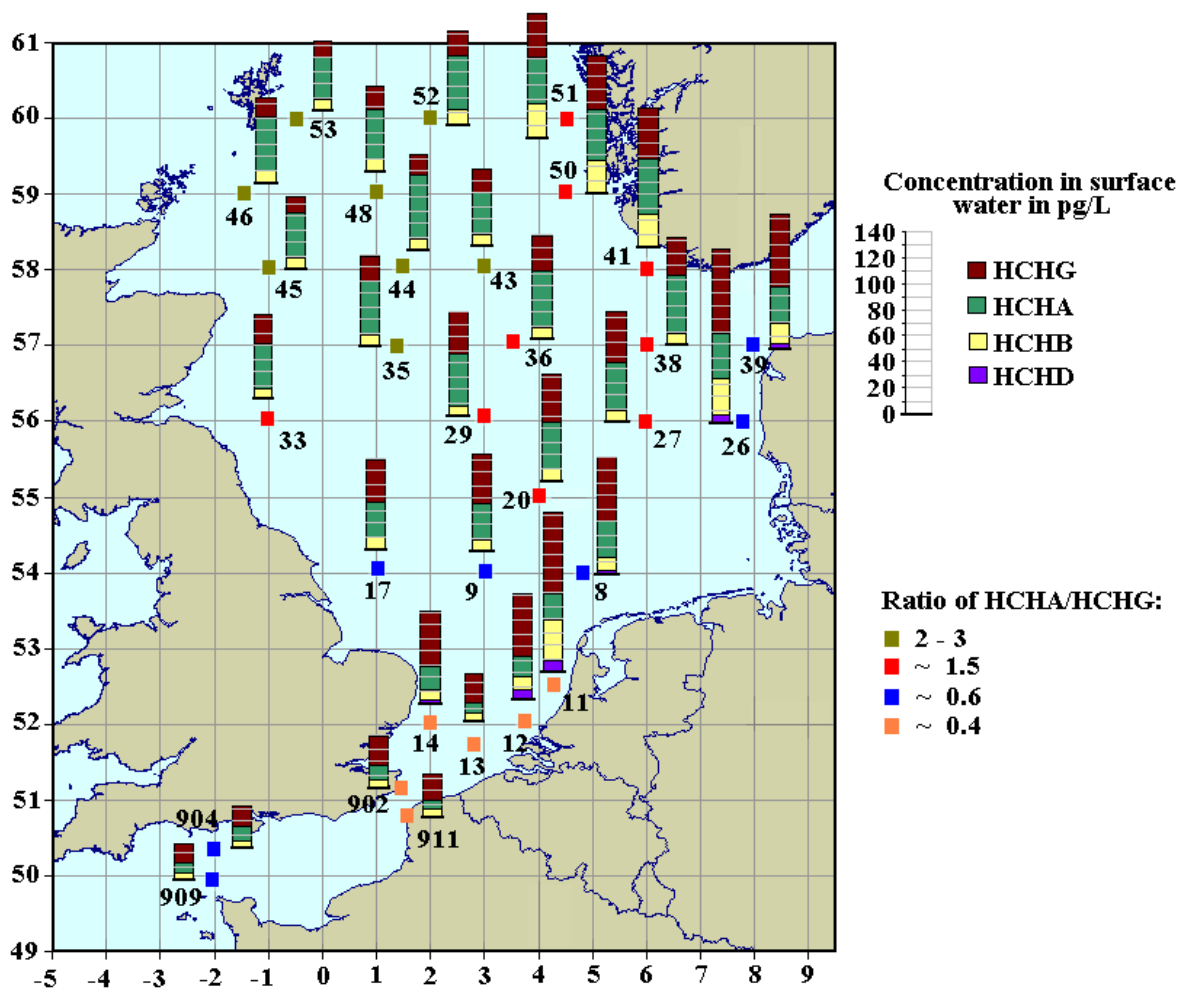


Figure 5.32: Occurrence and distribution of hexachlorocyclohexanes in the surface water (5m) of the North Sea in Aug./Sep. 2009

α -HCH/ γ -HCH ratios for the Baltic Sea (figure 5.33) were determined in the range from 0.8 to 1.1, which were comparable with those calculated for the German EEZ of the North Sea. The spatial trends in the α -HCH/ γ -HCH ratios were influenced by several factors: As mentioned above, γ -HCH is currently used for medical treatments and has been applied as lindane from 1980 to the 1990s, whereas α -HCH predominantly originates from the usage of technical HCH in earlier years.

Thus, γ -HCH could be still found in higher concentrations inside the river plumes and estuaries than α -HCH. A further important factor could be the different stability of individual HCH isomers. The most stable isomer is α -HCH occurring in 55-80 % in technical HCH. ^[126] It was reported that γ -HCH was transformed more readily by photooxidation and marine microorganisms than α -HCH. In addition a transformation of γ -HCH to α -HCH was observed. ^[129] Thus, the concentration of α -HCH exceeded the concentration of γ -HCH with increasing distance to riverine input. Moreover, atmospheric deposition might even contributed to the hexachlorocyclohexane abundances in the sea surface water, because both hexachlorocyclohexanes could be quantified in the marine atmosphere throughout all sampling campaigns.

To sum up, riverine input was an important source of HCHs to the surface seawater as displayed by the increased concentration gradients observed in the German EEZ. In addition, the abundances of α -HCH and γ -HCH in the marine atmosphere pointed to the possibility of a significant atmospheric deposition into the surface seawater of both compounds.

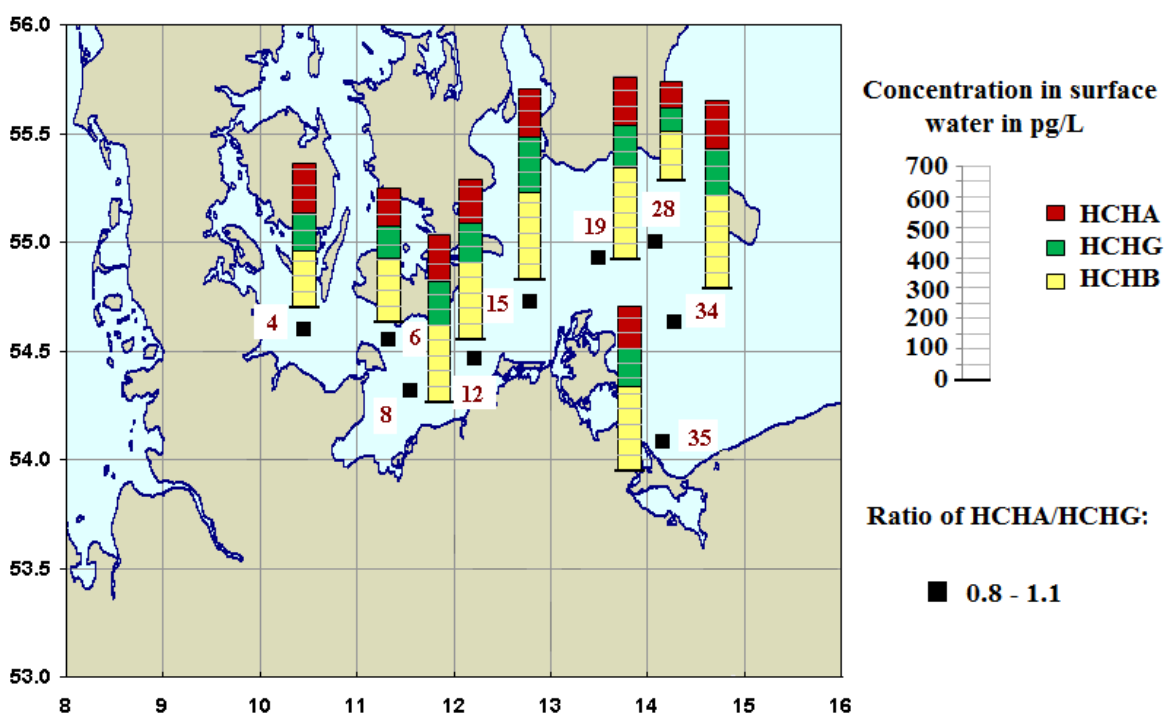


Figure 5.33: Occurrence and distribution of hexachlorocyclohexanes in the surface water (5m) of the German EEZ in the Baltic Sea in July 2009

Net flux of diffusive gas exchange of hexachlorocyclohexanes between the marine atmosphere and the surface water

HCHs were absent in the particle phases of both surface seawater (refer to annex 6) and air. Thus, a calculation of the direction of the net flux of diffusive gas exchange of α -HCH and γ -HCH was possible (figure 5.34), as defined in chapter 2.4.1.

γ -HCH displayed an overall dry gaseous atmospheric deposition to the surface waters of the German EEZ, the wider North Sea and the Baltic Sea. A trend to equilibrium of diffusive gas exchange was observed within the river plume of the Elbe. Equilibrium of the gaseous exchange of α -HCH was observed in the central and northern parts of the North Sea and inside the river plume of the Elbe, whereas net atmospheric deposition was indicated for the southern part. These results confirmed the significance of atmospheric deposition, as discussed above.

It was reported that α -HCH and γ -HCH evaporate from the surface seawater of the Elbe estuary in summer. [5, 130] Net volatilisation in spring was not indicated in this study. However, it would be predicted for observed (spring time) concentrations under summer temperatures.

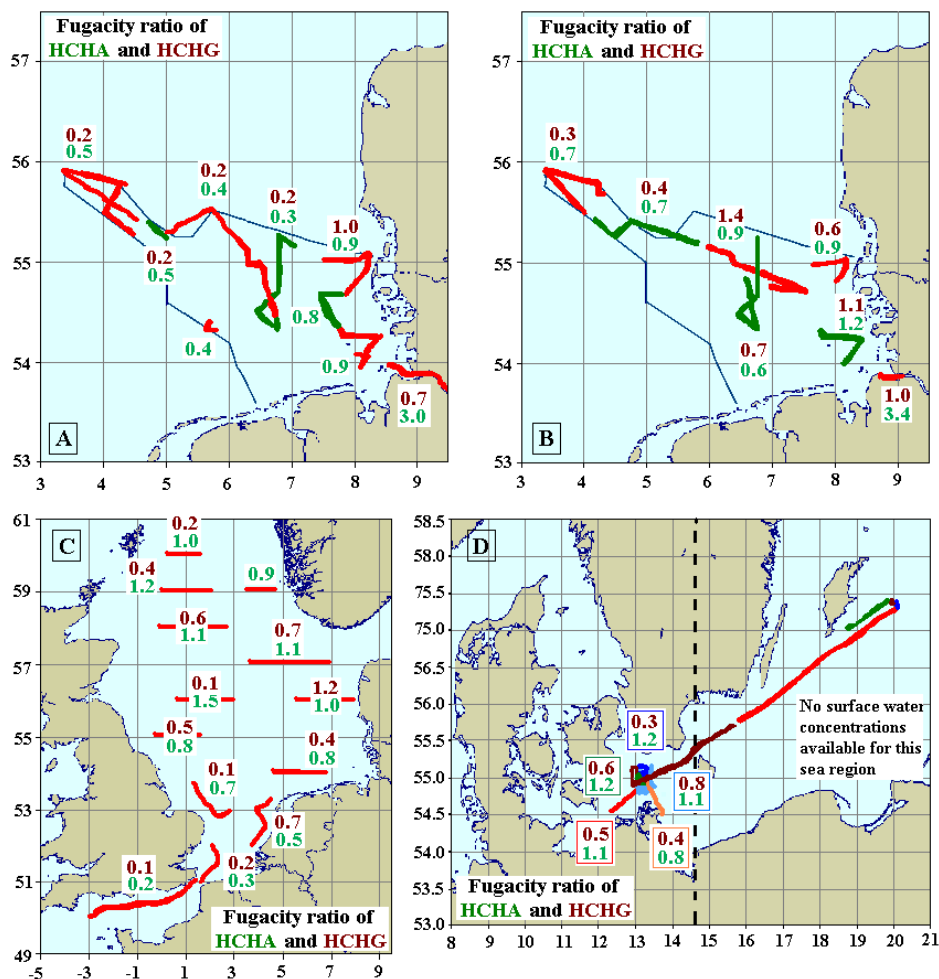


Figure 5.34: Net flux of diffusive gas exchange of α -HCH and γ -HCH; Fugacity ratio < 0.5: Atmosphere \rightarrow Sea; Fugacity ratio > 2: Sea \rightarrow Atmosphere; (A) German EEZ May/Jun. 2009; (B) German EEZ May 2010; (C) North Sea Aug./Sep. 2009; (D) Baltic Sea Apr. 2009

Conclusions

A close to equilibrium distribution of α -HCH was observed in the marine environment of the North Sea. α -HCH was homogeneously distributed in the marine atmosphere. Constant atmospheric concentrations were even detected in air masses originating from the North Atlantic, which could be interpreted by the outgassing of α -HCH from the North Atlantic and ice-free regions of the Arctic Ocean. Gradually increasing surface water concentrations of α -HCH towards the northern North Sea were in agreement with the significance of atmospheric deposition, the history of usage and the higher stability of the α -isomer against biodegradation in seawater. A riverine input of α -HCH was only observed for the Elbe. The net flux of diffusive gas exchange was found close to equilibrium in a large area, i.e. from the central to the northern North Sea and the Elbe estuary, whereas net atmospheric deposition was indicated in the southern North Sea.

An overall net dry deposition of γ -HCH to the surface waters of the German EEZ, the wider North Sea and Baltic Sea was documented. The atmospheric concentrations of γ -HCH were highly variable and strongly depended on the origin of air mass. It was observed that the γ -HCH concentration increased the longer the air mass had passed over the continent. Thus, re-emission from continental contaminated soil was indicated to be a major source of γ -HCH to the marine atmosphere. In addition, the PUF disk passive air samplers documented a seasonal increase in atmospheric γ -HCH abundances, which indicated a higher revolatilisation flux of γ -HCH from land during summer months. Besides atmospheric deposition, the Baltic Sea outflow as well as riverine input in the southern part of the North Sea were major sources of γ -HCH to the surface seawaters.

An atmospheric deposition of β - and δ -HCH was not observed, because their atmospheric concentrations are very low (usually below LOQ).

5.1.4 Cyclodiene pesticides

Aldrin, dieldrin, endrin and isodrin are named after the Diels-Alder reaction by which they are synthesized. Up to the 1990s they were applied as insecticides in agriculture and against vectors of animal disease, such as the tsetse fly. Today the application of dieldrin, aldrin and endrin is banned under the Stockholm Convention. Dieldrin is the main metabolite of aldrin and is observed in the highest concentrations of the targeted cyclodiene pesticides in the environment. ^[131]

Occurrence and distribution of cyclodiene pesticides in the marine atmosphere

The cyclodiene pesticides were scarcely detected in the marine atmosphere. Exclusively the occurrence and spatial distribution of dieldrin in the atmosphere of the North Sea and German EEZ could be reported in this study, whereas aldrin, endrin and isodrin were not detected in any air sample. In the atmosphere of the Baltic Sea neither the occurrence of aldrin, endrin and isodrin nor

the presence of dieldrin could be observed. This was attributed to the approximately 4 times higher LOQ of dieldrin applied to the air sample preparation sequence of the Baltic Sea air samples depending on the system performance at this time (refer to chapter 4.3.1).

Dieldrin was exclusively quantified in the gaseous mass fraction of the atmosphere. Typical atmospheric concentrations of dieldrin in the German EEZ and North Sea varied between 1.5 pg/m³ and 3.5 pg/m³ (figures 5.35 – 5.37). The spatial distribution of dieldrin in the marine atmosphere was almost homogenous and seemed to be unaffected by the air mass backward trajectories. This observation pointed to a close to equilibrium distribution of dieldrin in the marine environment. However, two air samples, namely PE 7 and PE 10, collected during the research cruise in the North Sea in Aug./Sep. 2009 (figure 5.37) revealed significantly elevated dieldrin concentrations of 11.4 pg/m³ and 13.0 pg/m³. The air mass backward trajectory analysis (refer to chapter 3.5 and annex 4) indicated a common source region in central England. In addition, the air mass history pointed to a revolatilisation of dieldrin from the North Atlantic Ocean due to the occurrence of dieldrin in air samples of the northern part of the North Sea unaffected by air advected from the continent (PE 15, PE 16, PE 17, figure 5.37). Dieldrin concentrations below the LOQs were assigned to decreased sample volumes (refer to chapter 3.2).

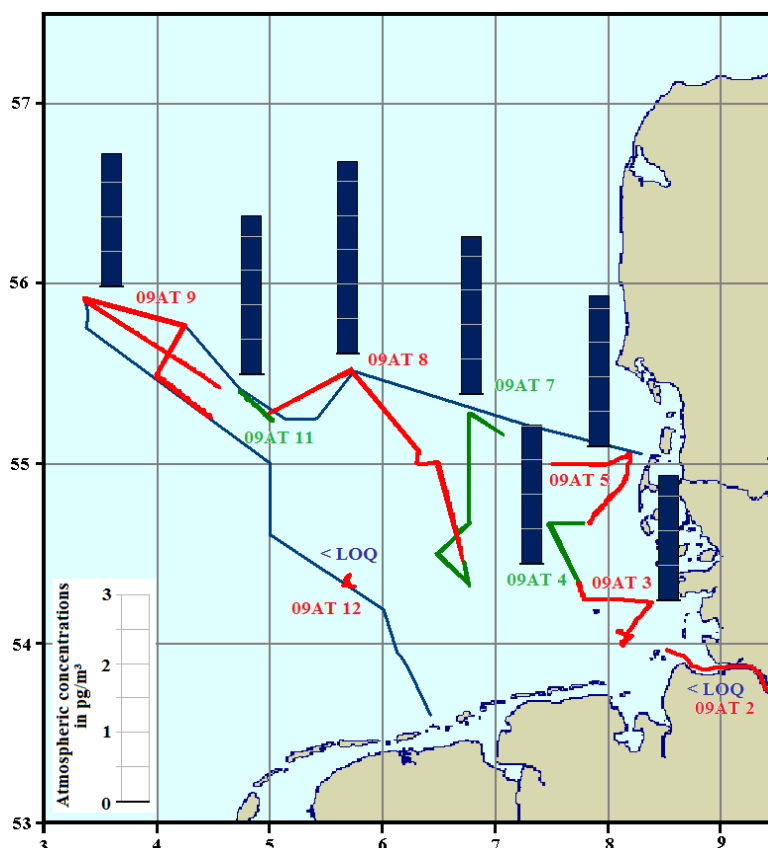


Figure 5.35: Atmospheric concentrations (gaseous phase) of dieldrin above the German EEZ in May/June 2009

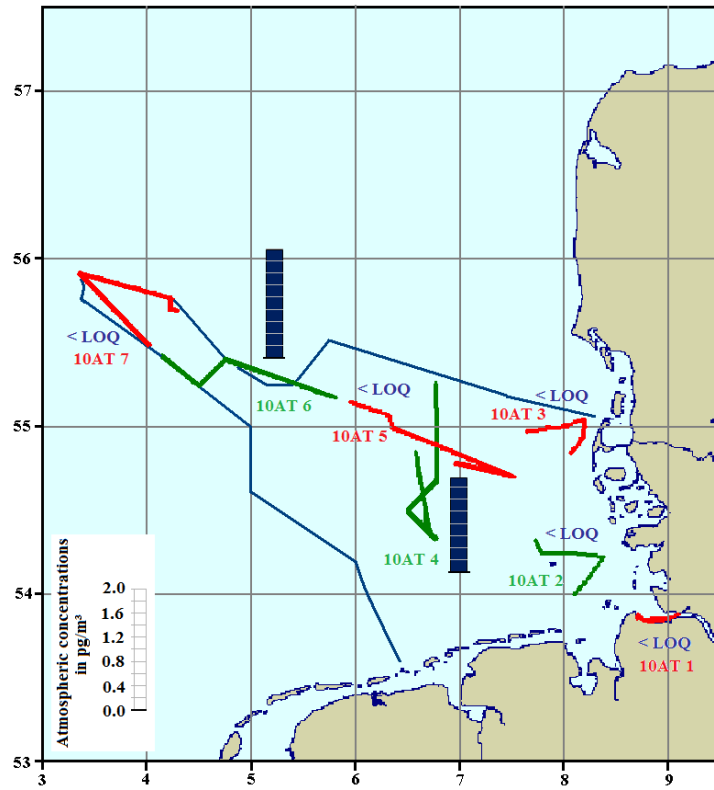


Figure 5.36: Atmospheric concentrations (gaseous phase) of dieldrin above the German EEZ in May 2010

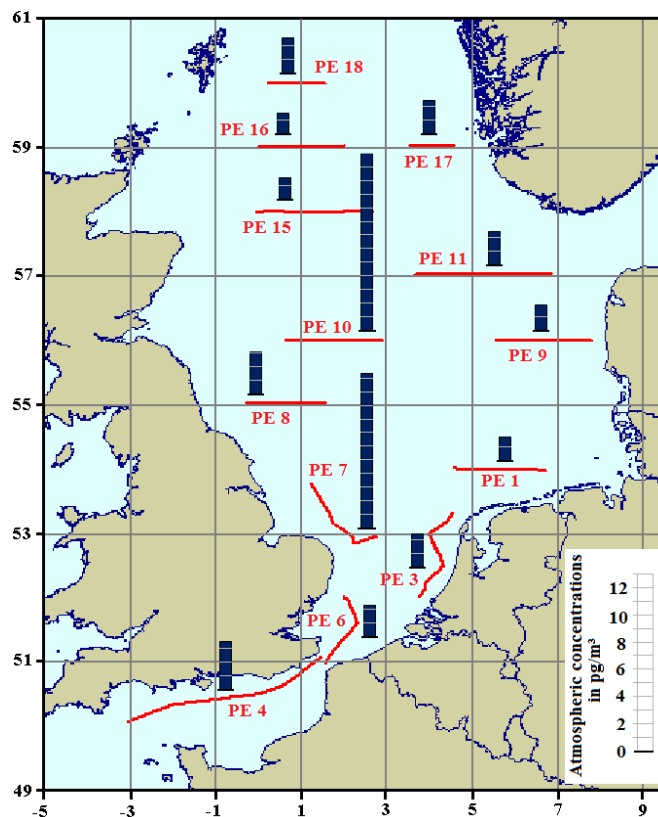


Figure 5.37: Atmospheric concentrations (gaseous phase) of dieldrin above the North Sea in Aug./Sep. 2009

Seasonal variations in atmospheric dieldrin concentrations were not observed. Therefore a comparison of dieldrin concentrations in continental and marine atmosphere, which originated from different seasons, was possible. Atmospheric concentrations of dieldrin in the atmosphere of Sülldorf/Hamburg in November/December 2010 ranged from 2.56 pg/m³ to 4.75 pg/m³ and were comparable to those in the marine atmosphere of the North Sea and the German EEZ. Due to the observed homogeneity of atmospheric dieldrin concentrations similar concentrations were suggested for the Baltic Sea atmosphere.

Occurrence and distribution of cyclodiene pesticides in the surface seawater

Dieldrin was detected in the surface water throughout all sampling sites, whereas endrin and isodrin were only observed in 3 and 1 water sample, respectively. The occurrence of aldrin could not be reported in any surface water sample. Dieldrin surface water concentrations of the Baltic Sea were not available.

The surface water concentrations of dieldrin in the German EEZ and the wider North Sea (figures 5.38-5.40) varied between 3.1 pg/L and 19.6 pg/L. Highest concentrations were quantified inside of the river estuaries and river plumes, which pointed to a riverine input. However, small concentration gradients towards the open sea indicated a significant pre-contamination of the surface waters presumably due to an atmospheric deposition. Further evidence on atmospheric deposition was given by the comparable high dieldrin concentrations of 9 -11 pg/L in the central North Sea, in particular at the sampling sites 17, 9 and 20 (figure 5.40). These elevated concentrations could be excluded to originate from riverine input considering the sea current profile in the surface water of the North Sea (refer to chapter 3.6). This conclusion was additionally supported by the increased atmospheric concentrations of dieldrin (PE 7 and PE 10, figure 5.37) detected in this sea area.

The south-central part of the North Sea revealing highest dieldrin concentrations is named Dogger Bank, a shallow region, which is known for its high primary productivity throughout the year.^[132] It might be imaginable that the increased phytoplankton growth enhanced the atmospheric deposition in this sea region according to the air-water-phytoplankton coupling mechanism described in chapter 2.3.1. The hydrophicity of dieldrin ($\log K_{OW} = 4.5$ to 5.5 ,^[125]) was found to be comparable to those organic compounds, which exhibited a fast gas exchange from atmosphere to sea, balancing the depletion of pollutants by the phytoplankton.^[92, 93] Considering that the observed surface water concentrations in the Dogger Bank originated from unfiltered water samples (and thus including phytoplankton), elevated dieldrin concentrations could be explained.

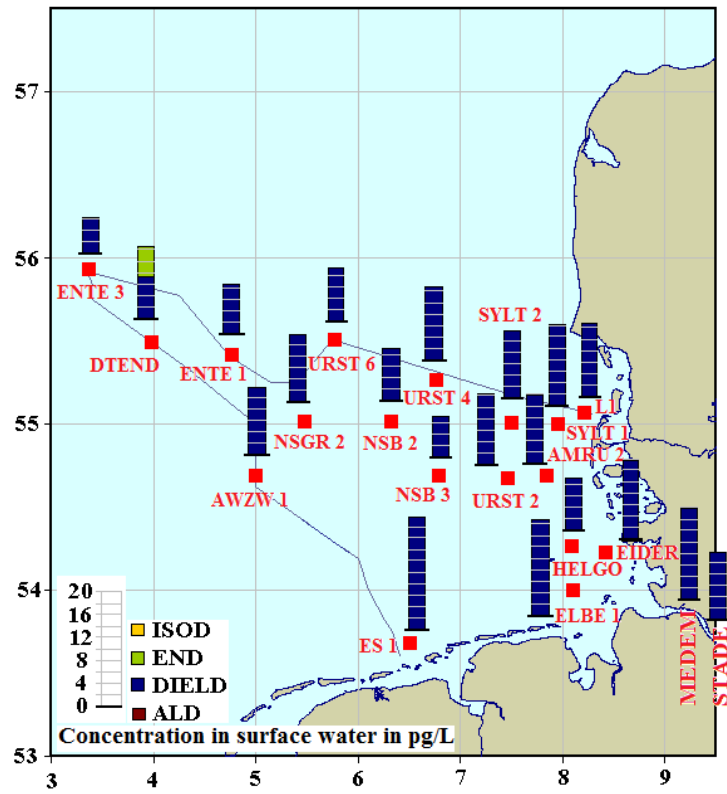


Figure 5.38: Occurrence and distribution of cyclodiene pesticides in the surface water (5 m) of the German EEZ in May/June, 2009

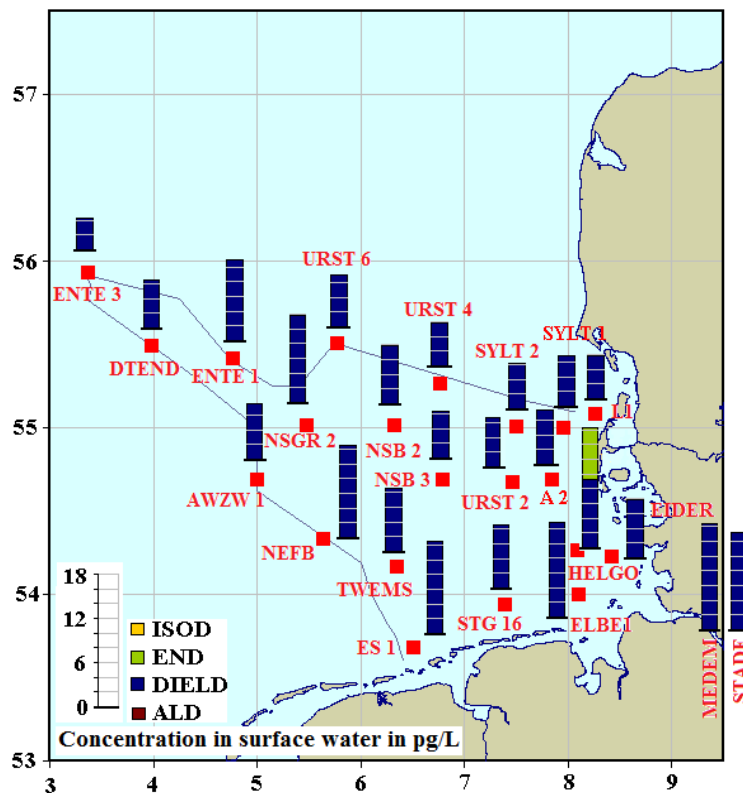


Figure 5.39: Occurrence and distribution of cyclodiene pesticides in the surface water (5 m) of the German EEZ in May 2010; A2 = water sampling site AMRU 2

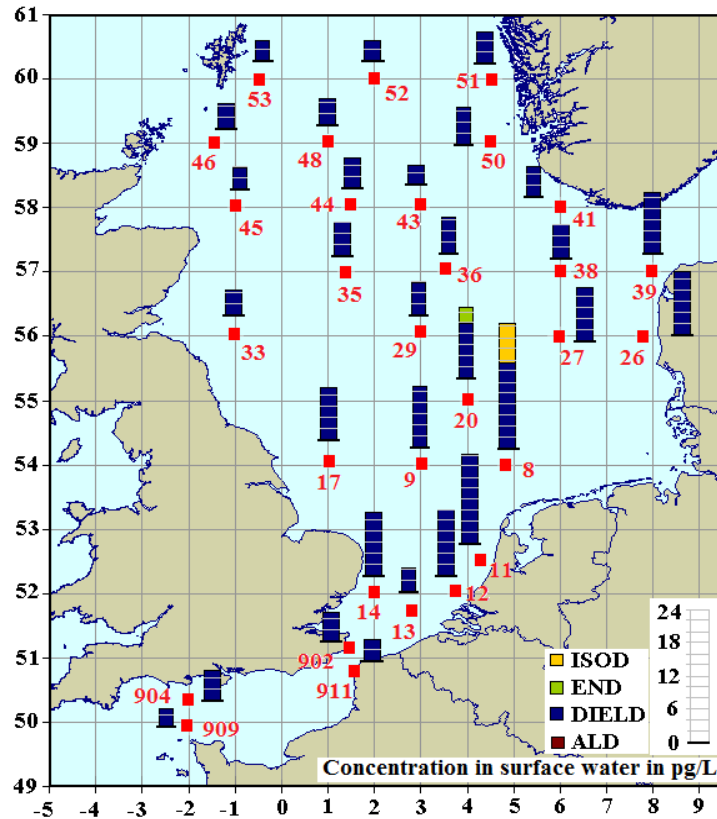


Figure 5.40: Occurrence and distribution of cyclodiene pesticides in the surface water (5 m) of the North Sea in Aug./Sep. 2009

Net flux of diffusive gas exchange of cyclodiene pesticides between the marine atmosphere and the surface water

Dieldrin was predominantly present in the gaseous mass fraction of the atmosphere and in the aqueous fraction of the surface water. Thus, a calculation of the direction of the net flux of diffusive gas exchange was possible (figure 5.41), as described in chapter 2.4.1.

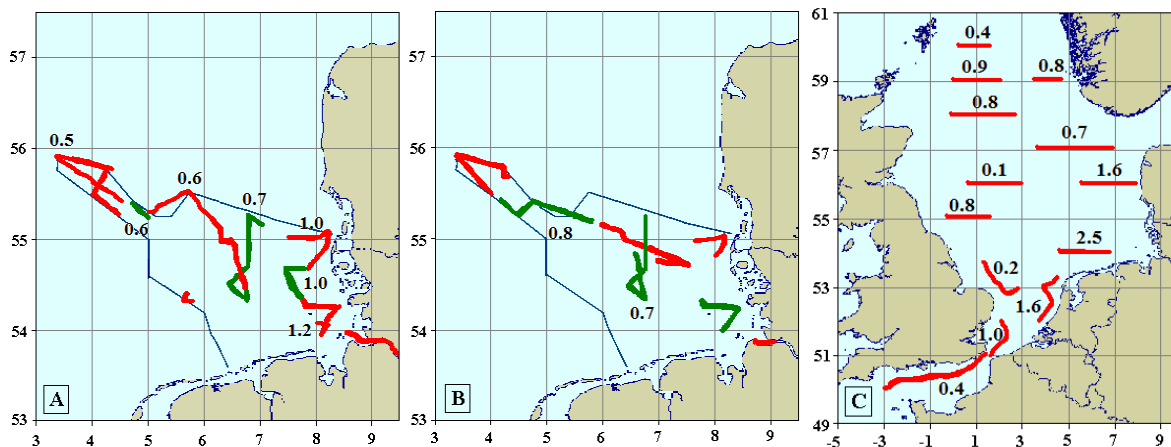


Figure 5.41: Net flux of diffusive gas exchange of dieldrin; Fugacity ratio < 0.5: Atmosphere → Sea; Fugacity ratio > 2: Sea → Atmosphere; (A) German EEZ May/June 2009; (B) German EEZ May 2010; (C) North Sea Aug./Sep. 2009

A trend to equilibrium, which was consistent with the almost homogenous atmospheric concentrations, was calculated for the German EEZ and the North Sea. Lowest fugacity ratios and thus a significant net atmospheric deposition were calculated for the exchange regions with the Atlantic Ocean (English Channel, northern part of the North Sea) and for elevated atmospheric concentrations of dieldrin (PE7, PE10, figure 5.37).

Conclusions

Dieldrin was almost homogeneously distributed in the marine atmosphere of the North Sea and the German EEZ. Small concentration gradients in the surface waters from the river estuaries to the open sea as well as the calculation of the direction of the net flux of diffusive gas exchange indicated a predominant atmospheric input of dieldrin to the surface seawaters. Increased surface water concentrations of dieldrin, which could be excluded to originate from riverine input due to the prevailing sea currents, were observed in the south-central part of North Sea (Dogger Bank region). Elevated atmospheric dieldrin concentrations were observed in air masses originating from central England above or in proximity to this sea region, which could be possible sources of dieldrin to the Dogger Bank. In addition, the high primary productivity and thus phytoplankton growth of the shallow Dogger Bank throughout the year was supposed to enhance the dry gaseous deposition by the coupling mechanisms of phytoplankton growth and air-water exchange as described in chapter 2.3.1.

Atmospheric concentrations of dieldrin above the Baltic Sea as well as the respective surface water concentrations were not available. The occurrence and spatial distribution of aldrin, isodrin and endrin could not be investigated in this study, because their environmental concentrations were almost exclusively below the LODs.

5.1.5 DDT isomers and metabolites

DDT is an insecticide, which was intensively applied from the 1940s to the 1990s in the agriculture. Today DDT is regulated under the Stockholm convention but a number of tropical countries have reserved exemptions for combat of insect vectors of human diseases, e.g., malaria and typhus. DDT is slowly degradable in the environment and persists in soils and seawater. It accumulates along terrestrial and marine food chains. ^[133, 134] *p,p'*-DDT (DDTPP), the isomer *o,p'*-DDT (DDTOP), which are the major components of technical DDT as well as the metabolites *p,p'*-DDD (DDDPP) and *p,p'*-DDE (DDEPP) are targeted in this study (table 3.10).

Occurrence and distribution of DDT isomers and metabolites in the marine atmosphere

The DDT isomers and metabolites could be observed in the marine atmosphere of the North Sea and Baltic Sea, but the concentrations of DDDPP were exclusively below the LOQ (figures 5.42 – 5.45). The metabolite DDEPP was found to be the main component of the DDT group in the atmosphere. Concentrations ranging from 0.7 pg/m³ to 13 pg/m³ were determined in marine air samples. DDTTP was the most frequently observed DDT isomer with atmospheric concentrations in the range from 0.4 pg/m³ to 3.6 pg/m³. Whenever observed, the DDTOP isomer was quantified in almost the same concentration as DDTTP.

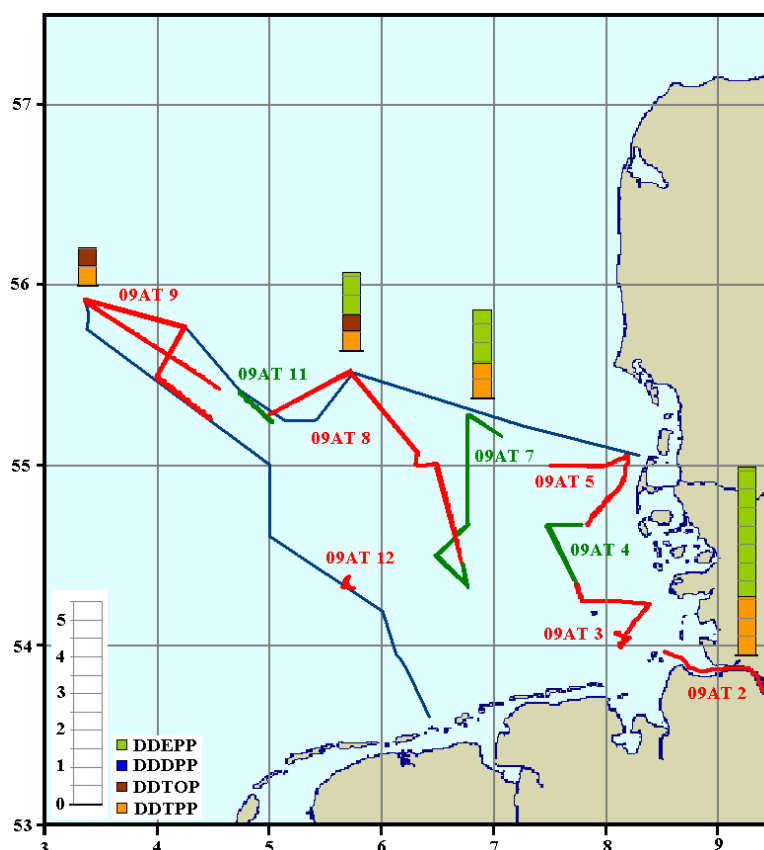


Figure 5.42: Atmospheric bulk concentrations of DDT isomers and metabolites above the German EEZ in May/June 2009

Although detected, the DDT isomers and metabolites could be only sporadically quantified in the atmosphere of the German EEZ (spring campaigns of 2009 and 2010). Their atmospheric concentrations were mostly below LOQ (figures 5.42-5.43). In contrast, DDTTP was quantified in every air sample collected during the North Sea campaign (summer 2009), whereas DDEPP was detected in twelve of the thirteen air samples (figure 5.44). A slight decrease in their atmospheric concentrations with increasing distance to continent was observed within the North Sea atmosphere. This indicated minor influences of secondary emission sources of the DDT group from continent. DDEPP and DDTTP were even detected in air masses collected at the remote sampling

sites in the northern North Sea (PE 15, PE 16, PE 17, figure 5.44), which originated from the North Atlantic Ocean and passed the sea within seven days. Two air samples from the North Sea atmosphere (PE 7 and PE 10, figure 5.44) pointed to an increased input from continental sources. Besides elevated DDEPP abundances, both air samples revealed DDTOP concentrations comparable to those of DDTPP. The air mass backward trajectory analysis indicated a common source region of the collected air masses in central England, which was consistent with the identical DDT group pattern and concentrations of both air samples.

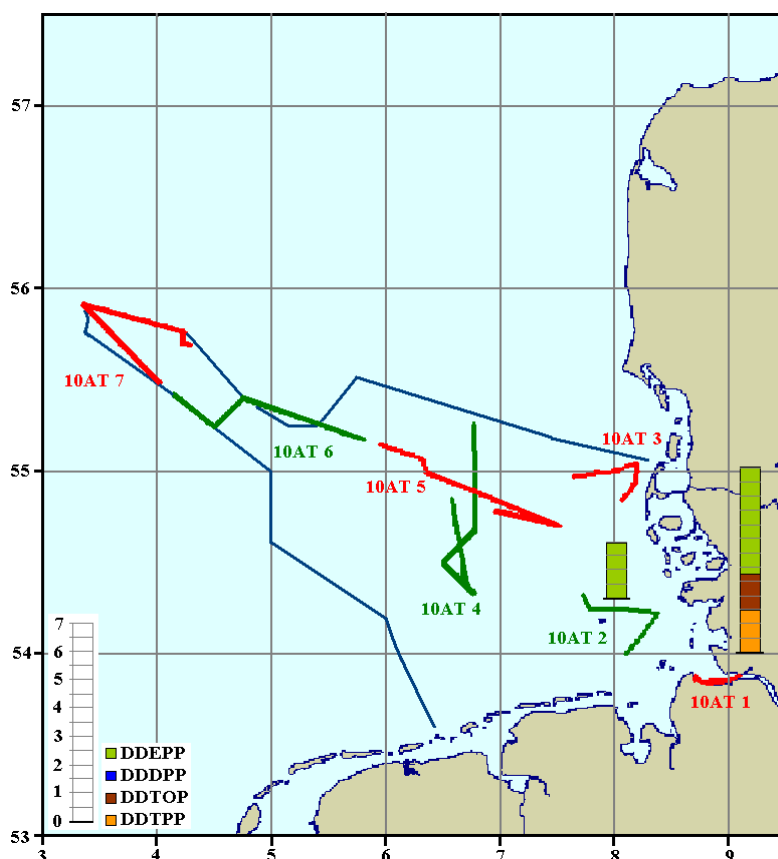


Figure 5.43: Atmospheric bulk concentrations of DDT isomers and metabolites above the German EEZ in May 2010

The atmospheric concentrations of the DDT isomers and metabolites above the Baltic Sea (figure 5.45) were at the same order of magnitude as observed above the North Sea. In contrast to the sampling campaigns in the North Sea and the German EEZ, the atmospheric concentrations of both DDT isomers and DDEPP could be quantified throughout all sampling sites. Besides, e.g., unknown seasonal events and intercontinental transport, this could be additionally influenced by enhanced air volumes collected during this campaign. Air samples collected above the Baltic Sea revealed approximately 2 to 3 times higher sample volumes than those collected above the North Sea and German EEZ (refer to chapter 3.2). As illustrated in figure 5.45, the atmospheric concentrations of DDTTP, DDTOP and DDEPP significantly decreased towards the eastern sea

region with increasing distance to continent. At the sampling sites west of 14°E the atmospheric concentrations were more variable than those observed at the sampling sites east of 14°E. In agreement with the observations in the North Sea atmosphere DDEPP displayed the highest fluctuations in atmospheric concentrations with an amplitude of 7.8 pg/m³. At the sampling sites in the eastern sea region (AL 7, AL 8, AL 9, AL 10) DDTTP, DDTOP as well as DDEPP revealed comparable atmospheric concentration levels of approximately 0.5 pg/m³, respectively.

The spatial distribution of the DDT group in the atmosphere of the Baltic Sea was in agreement with the location of the sampling sites and the air mass history (refer to chapter 3.5 and annex 4). The sampling sites west of 14°E were located close to continent and revealed 24 h air mass backward trajectory, which originated from continent. Thus the higher atmospheric concentrations and increased atmospheric fluctuations could be attributed to continental sources. In contrast, the air samples west of 14°E were collected with a greater distance from continent and revealed 24 h air mass backward trajectories, which had passed the sea. Hence, the influence of continental sources was limited resulting in almost constant atmospheric concentrations.

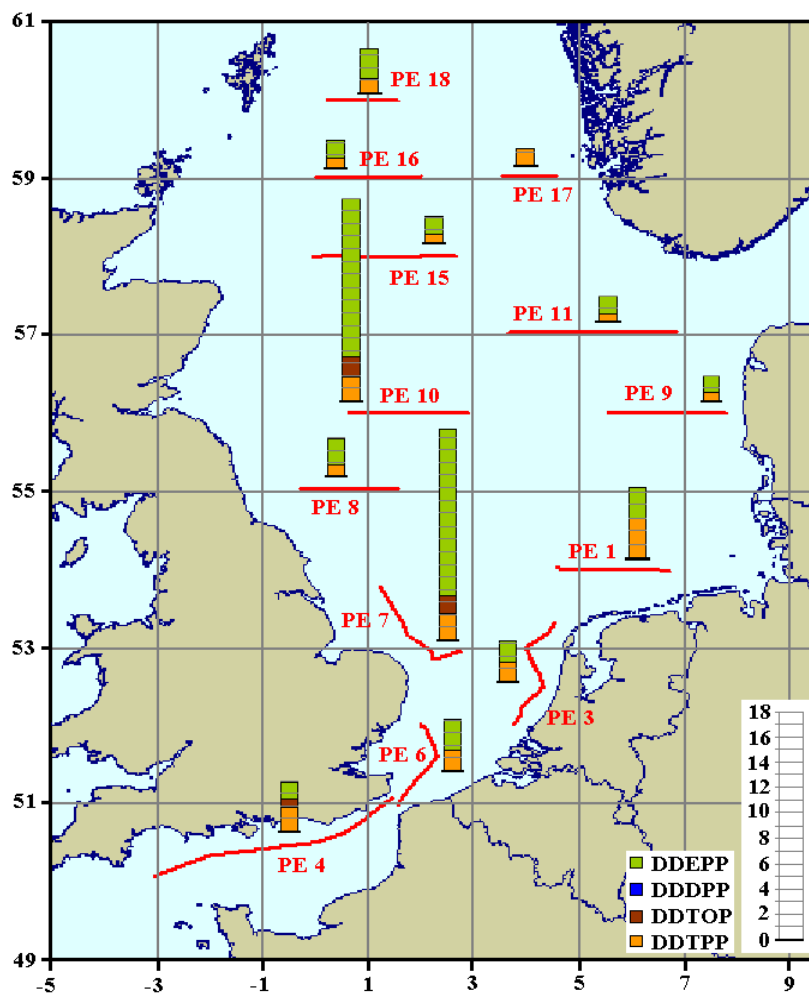


Figure 5.44: Atmospheric bulk concentrations of DDT isomers and metabolites above the North Sea in Aug./Sep. 2009

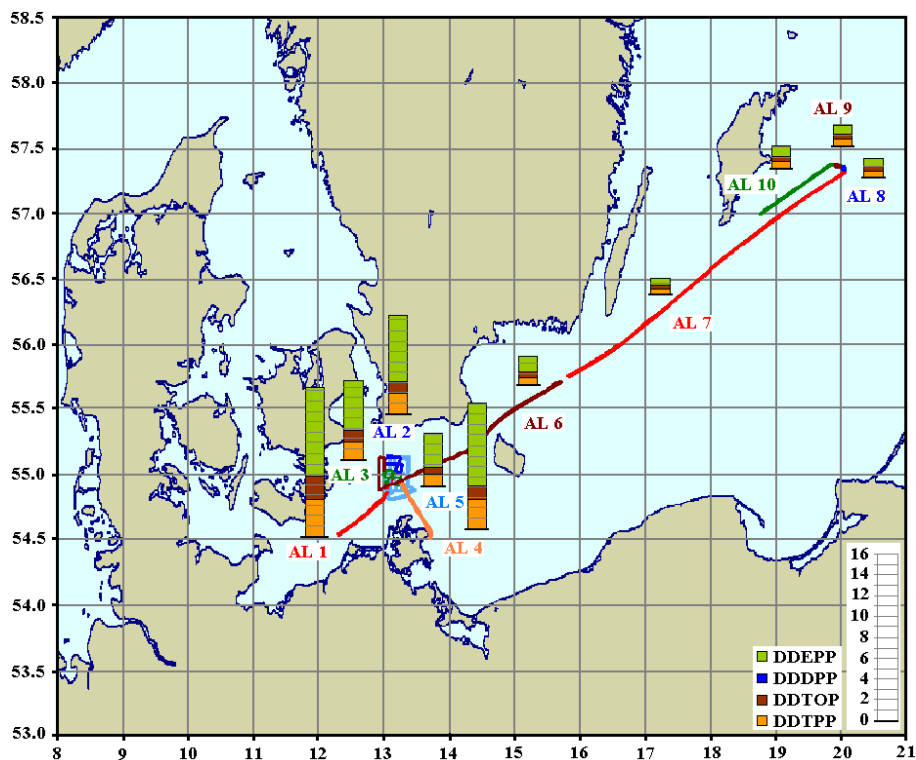


Figure 5.45: Concentrations of DDT isomers and metabolites in the gaseous mass fraction of the atmosphere above the Baltic Sea in Apr. 2009

Comparison of atmospheric concentrations determined at sea and land based sampling sites

A significant seasonality in the atmospheric concentrations of the DDT isomers and metabolites was not observed (figure 5.46). Thus a comparison of the marine and continental air samples collected in different seasons might be possible (table 5.2). The atmospheric concentrations of DDTTP were two times higher above the continent than above the North Sea and the Baltic Sea. DDEPP abundances above the continent were higher by a factor of 3. Hence, the concentrations of DDTTP and DDEPP in continental and marine atmosphere were almost at the same order of magnitude. This was in agreement with the minor influence of air mass history on the spatial distribution of the DDT isomers and metabolites observed in the marine atmosphere.

Table 5.2: Comparison of atmospheric concentrations of DDTTP and DDEPP determined at sea and land based sampling sites, n = number of air samples; \bar{x}_{arithm} = arithmetic mean of the air concentrations in pg/m^3 , σ = standard deviation of the atmospheric concentrations in pg/m^3

Sampling site	DDTTP			DDEPP		
	n	\bar{x}_{arithm}	$\pm \sigma$	n	\bar{x}_{arithm}	$\pm \sigma$
Sülldorf/Hamburg (Dec. 2010)	8	2.9	1.6	8	9.5	8.0
North Sea (Aug./Sep. 2009)	13	1.3	0.6	12	3.6	4.3
Baltic Sea (Apr. 2009)	10	1.4	3.6	10	3.6	3.1

Seasonal variations in atmospheric concentrations

The atmospheric concentrations of DDEPP displayed a small seasonal increase from September to October, whereas the variability of the concentrations of the DDT isomers was low (figure 5.46). A correlation with the ambient air temperature was not observed. Therefore, a higher efficiency of the revolatilisation processes from contaminated surfaces at increased ambient temperatures could be excluded as explanation. This was additionally supported by the more distinct seasonality at the coastal sampling site Tinum/Sylt than at the urban sampling site Sülldorf/Hamburg, the latter being expected to be more adjacent to possible re-emission sources. The weak DDEPP seasonality could be influenced by the sensitivity of the DDEPP sampling rate of the PUF disk passive air sampler to wind velocity (refer to chapter 3.2). However, the variability of DDEPP concentrations cannot be explained by current knowledge and further interpretation would be hypothetical.

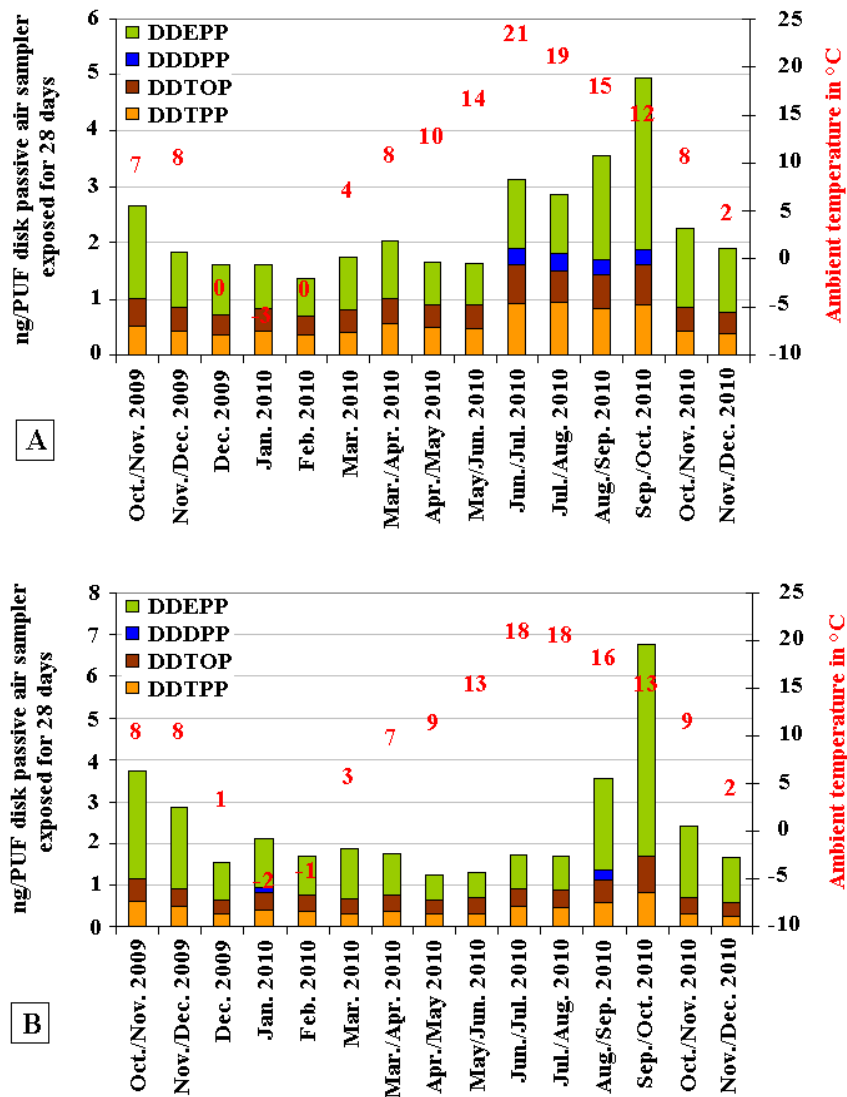


Figure 5.46: Seasonal variability in atmospheric levels of the DDT isomers and metabolites of the PUF disk passive air sampler sampling sites in Sülldorf/Hamburg (A) and Tinum/Sylt (B)

Gas-particle partitioning

DDT isomers and metabolites were predominantly observed in the gaseous mass fraction of the atmosphere. The gas-particle partitioning of DDTTP and DDEPP could be investigated in air samples collected in Sülldorf/Hamburg in December 2010. Less than 40 % of DDTTP and less than 30 % of DDEPP were present in the particulate mass fraction of the continental atmosphere in winter season. The gas-particle partitioning of DDTOP could not be quantified, because the atmospheric concentrations in the particle mass fraction were exclusively below the LOQ. DDDPP could not be quantified in the ambient air by active air sampling.

Occurrence and distribution of DDT isomers and metabolites in the surface seawater

The concentrations and spatial distributions of DDTTP and metabolites were highly variable within the surface water of the German EEZ, considering the concentrations observed at individual sampling sites of a single research cruise as well as the fluctuations within the research cruises of two successive years (figures 5.47-5.48). On average the sum concentrations of DDTTP, DDDPP and DDEPP inside the river plumes of ELBE, EMS and Weser were two times higher in May 2010 than during May/June 2009. In addition the spatial distributions observed within two years displayed significant aberrations. A concentration gradient of approximately 27 pg/L (EIDER to ENTE 3) was observed for 2009, whereat DDTTP, DDEPP and DDDPP were quantified even in the western part of the German EEZ (ENTE 3, DTEND, ENTE 1). In the year 2010 only DDEPP was determined at these western sampling sites and a concentration gradient of approximately 50 pg/m³ (ELBE 1 to ENTE 3) was reached. These strong variations were attributed to the strong adsorption of DDT isomers ($\log K_{OW} = 5 - 6$) and metabolites ($\log K_{OW} = 5 - 6$) to the suspended particulate matter in the water column.^[119, 125] Therefore, the particle load of rivers, resuspension processes of contaminated sediments, e.g., during storm events and phytoplankton growth were supposed to be important factors influencing the spatial distribution of DDTTP and metabolites. Although the trend of increasing surface water concentrations with increasing SPM content could be observed, a linear correlation was not determined. This was ascribed to the inhomogeneity of the SPM composition and thus a variable affinity of DDTTP and the metabolites. The spatial distribution of DDTTP, DDEPP and DDDPP indicated a major riverine input to the surface water of the German EEZ.

The metabolites DDEPP and DDDPP could be quantified in the surface water of the North Sea, whereas DDTTP was exclusively observed at the sampling site 909 adjacent to the exchange region with the Atlantic Ocean (figure 5.49). The spatial distribution gave evidence of a predominant riverine input of DDEPP and DDDPP to the surface water of the North Sea. Highest sum concentrations of 1.5 to 4.5 pg/L were determined inside the river plumes of Thames (14), Rhine

(12, 11, 8) and Elbe (26) as well as in the region of water exchange with the Baltic Sea (39). Towards the northern sampling sites the concentrations decreased below the LOQs.

The surface water concentrations of DDTTP, DDEPP and DDDPP of the Baltic Sea (figure 5.50) were at the same order of magnitude than in the Elbe estuary in spring 2009. The sum of the concentrations varied between 13 pg/L and 28 pg/L. A small concentration gradient towards the eastern sampling sites was observed.

DDTOP surface water concentrations of the German EEZ, North Sea and Baltic Sea were not available.

Although DDDPP reached the highest concentrations in surface water of the German EEZ, North Sea and Baltic Sea, it was not quantified in the marine atmosphere. The dominant occurrence of DDDPP in surface water as well as the dominant occurrence of DDEPP in the marine atmosphere may be interpreted by their transformation processes from DDT. It was reported that DDD was formed by the reductive dechlorination of DDTTP. This process was enhanced under anaerobic conditions and was the major microbial transformation mechanism under reducing conditions, as it might occur, e.g., in soil and sediments. Besides, dehydrochlorination processes in bacteria and animals, DDEPP additionally originated from photochemical reactions in the presence of sunlight, which might be enhanced in the atmosphere.^[135]

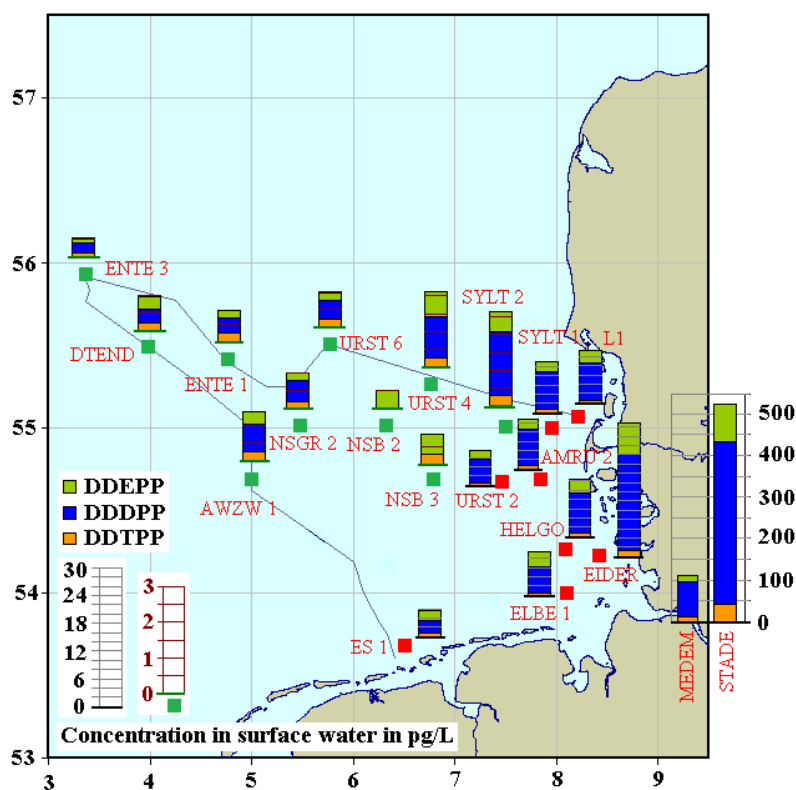


Figure 5.47: Occurrence and spatial distribution of DDTTP and metabolites in the surface water (5 m) of the German EEZ in May/June, 2009; Note the variable concentration scales displayed in the legend

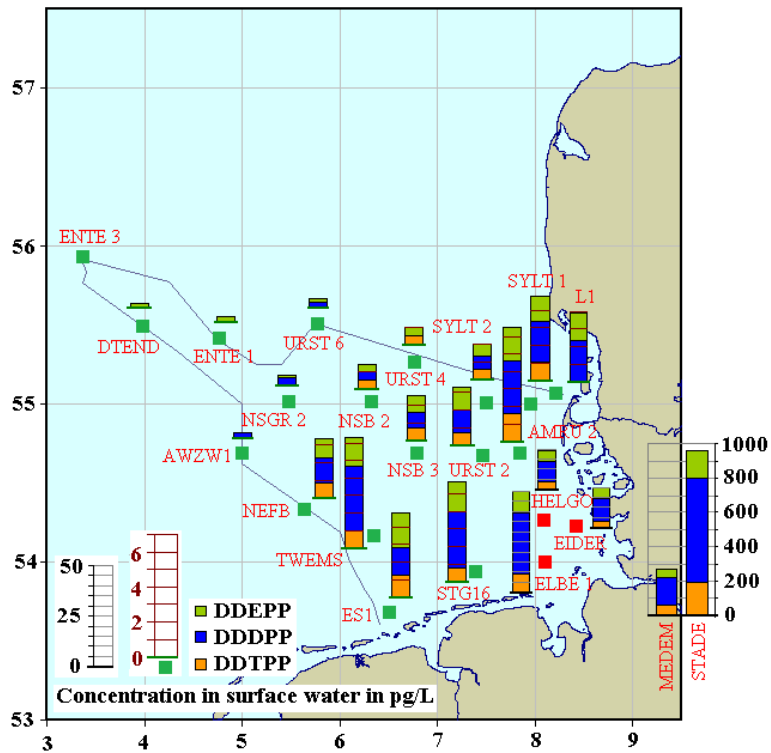


Figure 5.48: Occurrence and spatial distribution of the DDTTP and metabolites in the surface water (5 m) of the German EEZ in May 2010; Note the variable concentration scales displayed in the legend

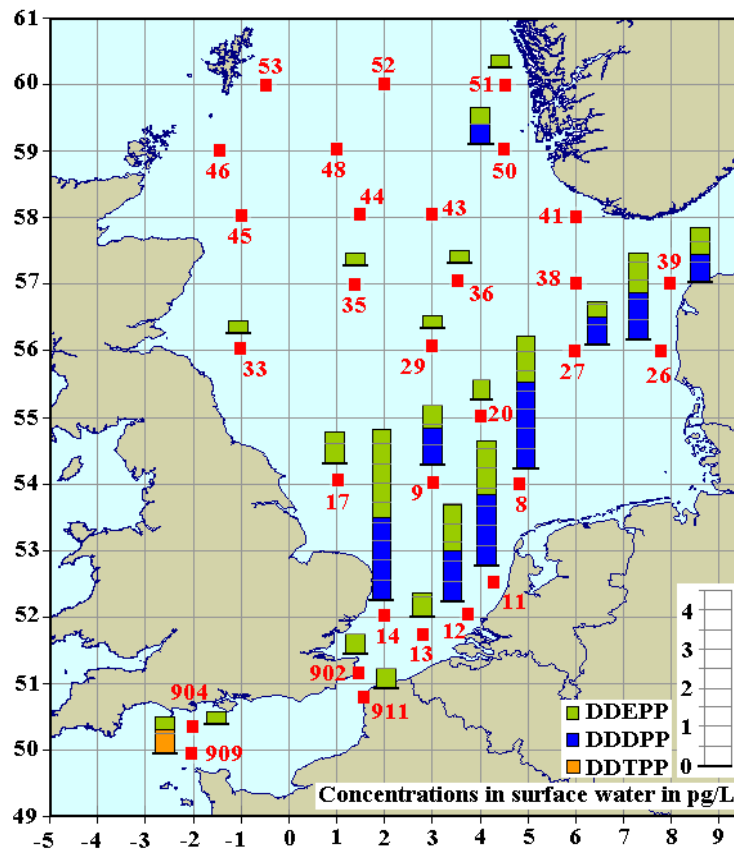


Figure 5.49: Occurrence and distribution of DDTTP and metabolites in the surface water (5m) of the North Sea in Aug./Sep. 2009

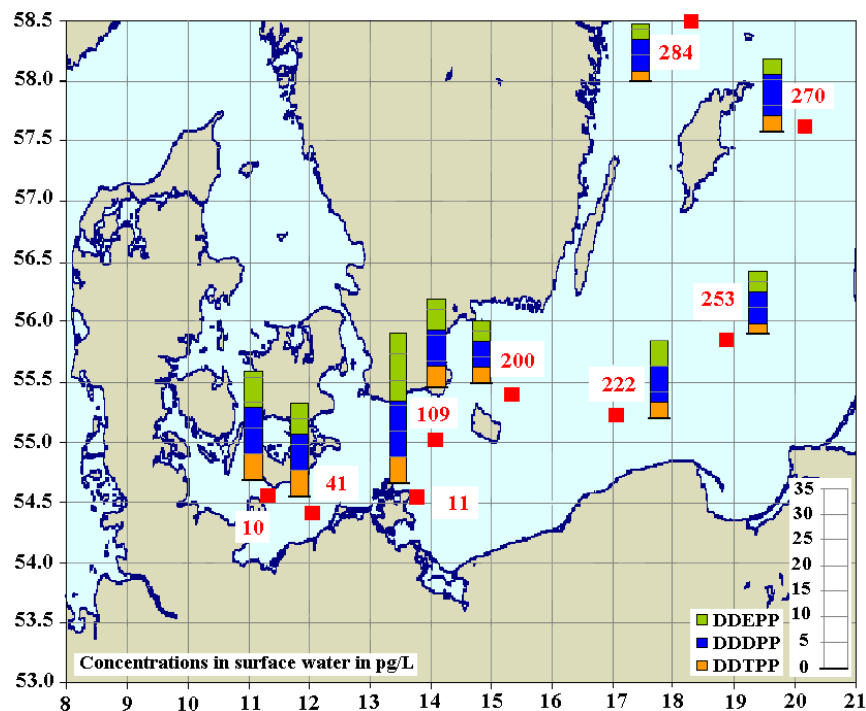


Figure 5.50: Occurrence and spatial distribution of DDTTP and metabolites in the surface water (6 m) of the Baltic Sea in Feb. 2005

Regarding the spatial distributions of DDTTP and metabolites in the surface water of the German EEZ (figure 5.48) and the North Sea (figure 5.49), an atmospheric deposition of DDEPP to the North Sea surface water could be assumed: In the Elbe estuary (EIDER, HELGO) the concentration of DDDPP was approximately two times higher than the concentration of DDEPP. A gradual approximation of the concentration levels of both metabolites with decreasing water concentrations towards the western sampling sites was observed. At the western sampling sites of the German EEZ (ENTE 3, DTEND, ENTE 1) exclusively DDEPP was quantified in the surface water, whereas the DDDPP concentrations were below LOQ. The same was observed for the North Sea surface water. Although DDDPP revealed the highest surface water concentrations inside the river plumes and estuaries, exclusively DDEPP was quantified towards the northern sampling sites. These changes in metabolite pattern could not be fully interpreted by a dilution effect with pristine water or sedimentation of suspended particulate matter to the sea bottom. Considering the dominant occurrence of DDEPP in the marine atmosphere, it might be rather interpreted by an atmospheric deposition of DDEPP.

Net flux of diffusive gas exchange of DDT isomers and metabolites between marine atmosphere and surface water

The direction of the net flux of diffusive gas exchange could not be calculated, because the surface water concentrations discussed above were significantly biased by the particle associated mass

fraction of the DDT isomers and metabolites. Concentrations of the DDT isomers and metabolites in the aqueous phase of the surface water were not available.

The air-sea gaseous exchange of DDEPP, DDTTP and DDTOP was investigated in 1989/1990 for parts of the North Atlantic Ocean between 20° to 40° northern latitude. A net depositional flux was calculated of less than 10 ng/(m² d). The atmospheric concentrations of the DDT isomers were approximately three times higher than observed in this study, which could be attributed to the differences in the geographical locations of the sampling sites as well as the long-term trend (environmental response reflecting global usage restrictions). In contrast, the atmospheric concentration levels of DDEPP as well as the surface water concentrations were still at the same order of magnitude as determined in this study.^[136] In consequence a net depositional flux into the surface waters of the North Sea beyond river plumes and estuaries, especially for the metabolite DDEPP due to its dominant occurrence in the marine atmosphere, could be suggested.

Conclusion

DDTTP and metabolites strongly adsorb to the suspended particulate matter in the water column. Thus, their occurrence and spatial distribution in surface water was highly variable and depended on the composition and concentration of the SPM. Due to their strong particle adsorption a reliable calculation of the direction of the net flux of diffusive gas exchange was not possible. A net depositional flux of DDEPP to the surface water of the North Sea was indicated by the dominant occurrence of DDEPP in the marine atmosphere and the changes in metabolite patterns observed in the surface water towards the open sea.

5.1.6 Polychlorinated Biphenyls

Polychlorinated biphenyls (PCBs) have been widely used in industry, e.g., as dielectric and heat transfer fluids, plasticizers, wax extenders and flame retardands.^[137] 209 possible PCB congeners exist exhibiting one to ten chlorine substituents on the biphenyl ring system. In 1980 K. Ballschmiter and M. Zell introduced the systematic PCB number, which simplifies identification and prevents confusions. It is based on the numbering of the PCB congeners from 1 to 209 after the sorting by their structural names.^[138] Today the PCBs are banned under the Stockholm Convention, because of their ubiquitous occurrence in the environment, persistence and toxicity potential.^[10] Four PCB congeners, which are routinely monitored in the surface water of the North Sea are targeted in this study, namely the trichlorobiphenyl PCB28, the tetrachlorobiphenyl PCB52 as well as the hexachlorobiphenyls PCB138 and PCB153. In order to avoid confusion with the target compound pentachlorobenzene, they are referred to as CB28, CB52, CB138 and CB153 in this study (table 3.10).

Occurrence and distribution of PCBs in the marine atmosphere

All targeted PCB congeners were quantifiable in the marine atmosphere of the German EEZ, the wider North Sea and the Baltic Sea (figure 5.51–5.54). CB28 was the most frequently detected and reached the highest atmospheric bulk concentrations of the targeted PCBs in the range of 1.2 pg/m³ to 15.5 pg/m³. Besides, CB52 was quantified in the majority of the air samples in bulk concentrations up to 10.3 pg/m³. In contrast CB138 and CB153, the congeners of comparable less volatility (saturation vapour pressures of 0.147 mPa and 0.139 mPa at 25 °C, respectively ^[139]), were observed in significantly lower abundances in the marine atmosphere. Their atmospheric concentrations ranged from <LOQ to 6.1 pg/m³ and 8.2 pg/m³, respectively.

The mean atmospheric PCB concentrations reported in this study (2009/2010) were slightly decreased in comparison to those reported in other studies of the North Atlantic atmosphere in the years 1990 to 2007. ^[67] However, they were still at the same order of magnitude. A significant long-term trend in atmospheric PCB concentrations was not detected considering seasonal and other temporal variation. The PCB concentrations above the Baltic Sea were at the same order of magnitude as their mean atmospheric concentrations reported in 1999. ^[140] They were significantly higher than those observed for the atmosphere of the North Sea and the German EEZ during this study (table 5.3).

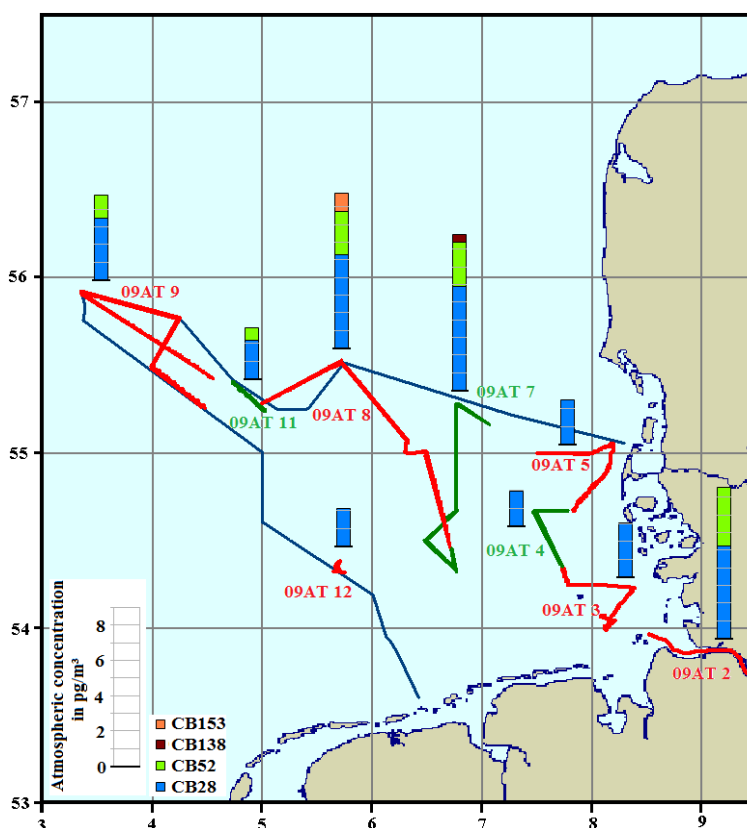


Figure 5.51: Atmospheric bulk concentrations of PCBs above the German EEZ in May/June 2009

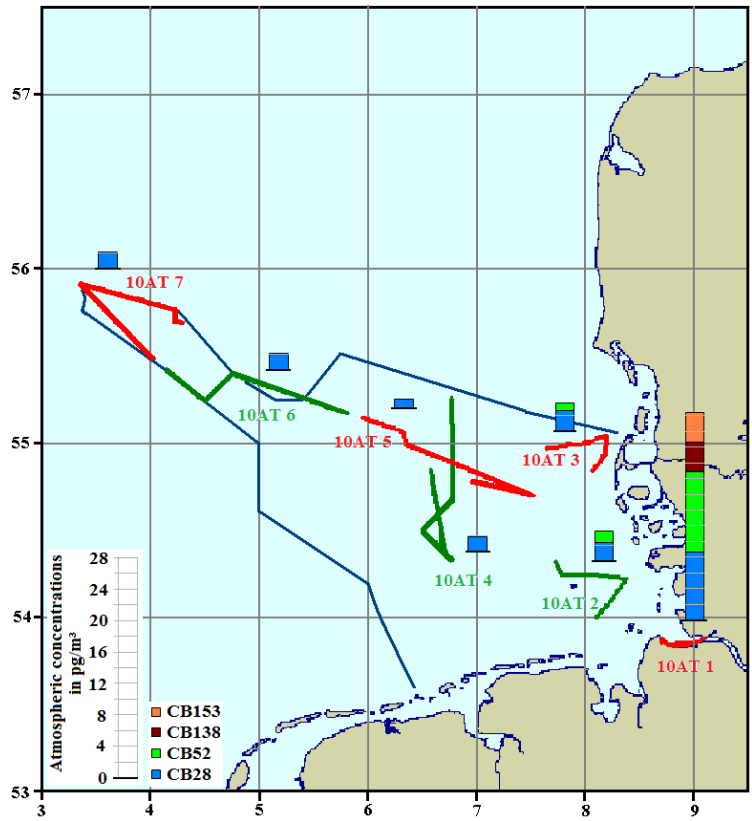


Figure 5.52: Atmospheric bulk concentrations of PCBs above the German EEZ in May 2010

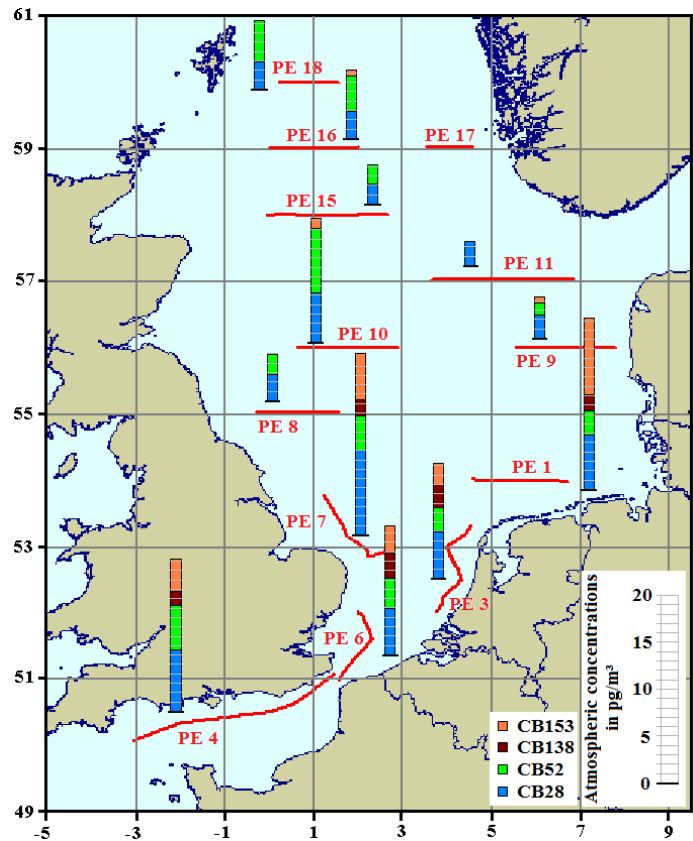


Figure 5.53: Atmospheric bulk concentrations of PCBs above the North Sea in Aug./Sep. 2009

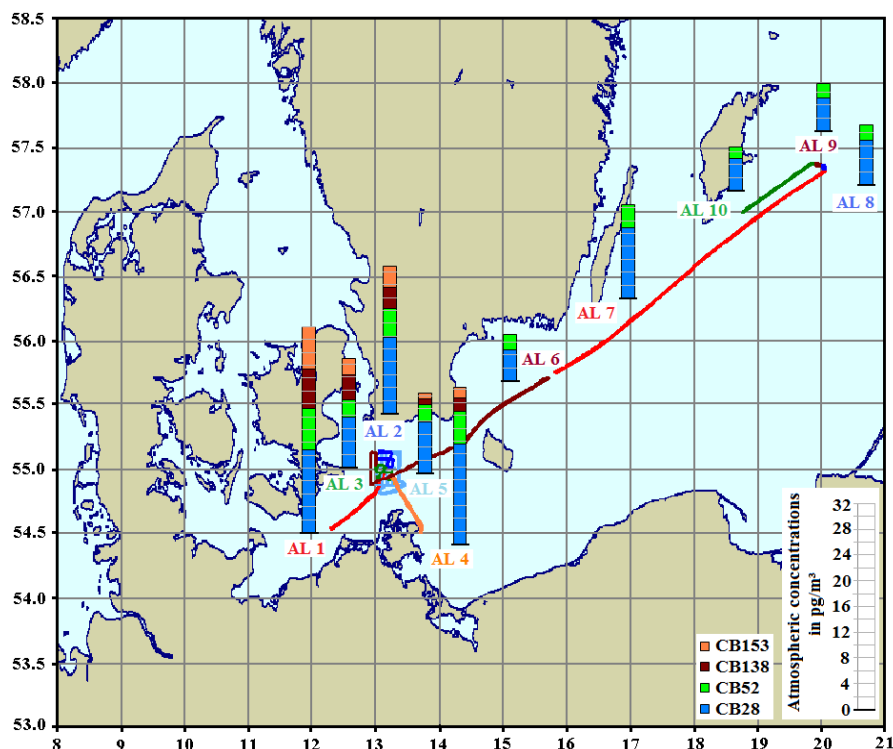


Figure 5.54: Concentrations of PCBs in the gaseous mass fraction of the atmosphere above the Baltic Sea in Apr. 2009

The atmospheric concentrations of PCBs were highly variable and strongly depended on the sampling site location and the air mass history, which pointed to strong continental sources. Lower concentrations were observed with increasing distance to continent. Only CB28 and low abundances of CB52 were observed in air masses, which had predominantly passed the sea (24 h air mass backward trajectories, refer to chapter 3.5 and annex 4). This could be due to their higher volatility (saturation vapour pressures of 21 mPa and 6.9 mPa at 25 °C, respectively ^[139]). These observations were consistent with similar investigations of the North Atlantic Ocean in 1990 reporting the advection of contaminated air masses as the dominant source of PCBs to the marine atmosphere. ^[141]

Comparison of atmospheric concentrations at sea and land based sampling sites

The seasonality of atmospheric PCB concentrations (figure 5.55) hindered a comparison of the results from sea and land based sampling sites, because the respective air sampling campaigns were performed in different seasons. The mean atmospheric concentrations (bulk concentrations) of the PCBs determined in Sülldorf/Hamburg in December 2010 were comparable to the mean atmospheric concentrations observed in the marine atmosphere in spring and summer (table 5.3). According to the seasonal passive sampler profile (figure 5.55(A)), the atmospheric PCB abundances in Sülldorf/Hamburg were approximately four times higher in summer (June/July 2010) than in winter (Nov./Dec. 2010). Considering these relations, the atmospheric concentrations

of PCBs above the continent during the research cruises from April to September were assumed to be up to four times higher than those observed in the marine atmosphere.

Table 5.3: Comparison of the atmospheric bulk concentrations of PCBs (in pg/m³) determined at sea and land based sampling sites, n = number of air samples, \bar{x}_{arithm} = arithmetic mean of the air concentrations in pg/m³, σ = standard deviation of the atmospheric concentrations in pg/m³

Sampling campaign	n	CB28		CB52		CB138		CB153	
		\bar{x}_{arithm}	$\pm \sigma$	\bar{x}_{arithm}	$\pm \sigma$	\bar{x}_{arithm}	$\pm \sigma$	\bar{x}_{arithm}	$\pm \sigma$
Baltic Sea (Apr. 2009)	10	8.9	3.7	3.4	1.5	1.6	2.2	1.5	2.2
German EEZ (May./Jun. 2009)	9	3.5	1.6	1.1	1.3	0.1	0.2	0.1	0.3
North Sea (Aug./Sep. 2009)	13	4.0	2.4	2.9	1.9	0.8	1.1	1.9	2.5
German EEZ (May 2010)	7	3.0	2.6	1.8	3.8	0.5	1.4	0.5	1.4
Sülldorf/Hamburg (Dec. 2010)	20	4.9	3.5	3.7	4.1	0.7	1.4	0.8	1.3

Seasonal variations in atmospheric PCB concentrations

A seasonal variation of atmospheric PCB abundances was observed at the sampling site Sülldorf/Hamburg (figure 5.55(A)). A correlation coefficient of 0.85 between the monthly mean air

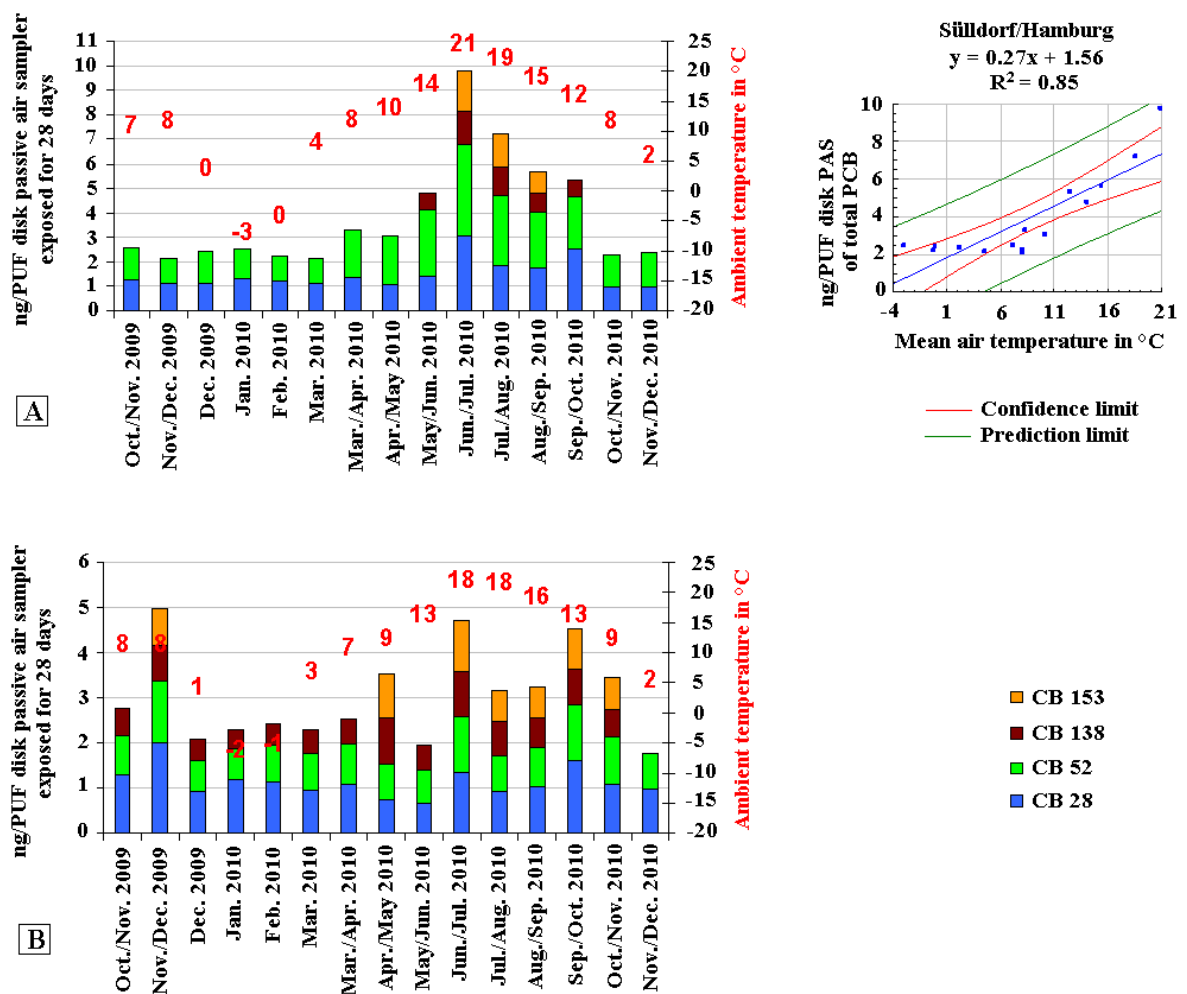


Figure 5.55: Seasonal variation in atmospheric abundances of PCBs at the PUF disk passive air sampler sampling sites Sülldorf/Hamburg (A) and Tinnum/Sylt (B)

temperatures and the atmospheric PCB levels was found. During the months of increased mean air temperatures (12 °C – 21 °C), even the less volatile congeners CB138 and CB153 were quantifiable in the urban ambient air. Beyond the months of highest PCB abundances, exclusively the more volatile congeners CB28 and CB52 could be quantified in constant atmospheric levels. These seasonal fluctuations could be explained by a stronger source in summer, namely revolatilisation from contaminated soil, influenced by ambient temperature.

In contrast, the passive sampler profile of the coastal sampling site Tinnum/Sylt (figure 5.55(B)) displayed no significant variations in atmospheric PCB abundances with season. CB138 and CB153 were more frequently quantified at Tinnum/Sylt than in Sülldorf/Hamburg. This was ascribed to the higher wind speeds at the coastal sampling site (refer to chapter 3.2.2), which enhanced the sampling rates and increased the particle intrusion to the PUF disk passive air sampler.

Besides, the PCB concentrations, in particular those of the higher molecular weight PCBs, were significantly increased in the North Sea atmosphere in Aug./Sep. than in the atmosphere of the German EEZ in spring (table 5.3). This could be caused by the enhanced volatilisation processes of PCBs from contaminated soil in the summer month, considering the predominant influence of the advection of continental air on the PCB concentrations in the marine atmosphere.

Gas-particle partitioning

Although observed in both mass fractions, the PCB concentrations plotted in figures 5.51-5.54 could be exclusively quantified in the gaseous mass fraction of the atmosphere (except CB153 in the air sample PE 7 of figure 5.53). A significant gas-particle partitioning of CB 138 and 153 could be documented by two air samples (R1S1, R1S2, refer to annex 1) collected in Sülldorf/Hamburg in December 2010. In contrast, the concentrations of CB28 and CB52 associated with particles could never be quantified. This was due to the higher molecular weight and thus lower volatility of CB138 and CB153 as well as the low ambient air temperatures, which favoured the adsorption to particulate matter. On average approximately 20 % of the bulk concentration of CB138 and CB53 was determined in the particle associated mass fraction of the two air samples, respectively.

Occurrence and distribution of PCBs in the surface seawater

PCBs were observed throughout all water sampling sites in the German EEZ (figures 5.56-5.57). In contrast to their occurrence in atmosphere, CB138 and CB153 were the main components in the surface water. They exhibited the strongest fluctuations in surface water concentrations. Maximum amplitudes of approximately 10 pg/L (EIDER to ENTE3/DTEND) were observed, with the highest abundances in the Elbe estuary (EIDER) and lowest at the western sampling sites (ENTE3/DTEND) in the open sea. In comparison, the decrease in surface water concentrations of

CB28 and CB52 was less pronounced. Maximum amplitudes of approximately 3.75 pg/L were observed within the German EEZ (EIDER/ENTE3), respectively (figure 5.56). The spatial distribution of the PCBs illustrated that the riverine inputs by Elbe, Ems and Weser were the major sources of PCBs to the surface water of the German EEZ.

The spatial distribution of PCBs in the surface water was influenced by the SPM level in the water column. All targeted PCBs adsorbed to the SPM. However, similar as observed for the gas-particle partitioning in the atmosphere, the affinity of the higher molecular weight PCBs CB138 and CB153 to SPM was stronger than that of CB28 and CB52 (annex 6).^[119] Thus, their concentrations at sampling sites with high SPM abundances, e.g., the Elbe and river estuaries, were significantly increased in comparison to the lower molecular weight PCBs CB28 and CB52, which in turn resulted in a higher concentration gradient towards the open sea.

The lower molecular weight PCBs were predominantly present in the aqueous mass fraction of the surface water.^[119] Nevertheless, their comparably small concentration gradients towards the open sea could not be fully addressed to their lower adsorption to SPM and a dilution effect with pristine water. Instead, a significant atmospheric deposition was considered, regarding the predominant occurrence of CB28 and CB52 in the marine atmosphere. Further indications for an atmospheric PCB input in the German EEZ were shown by the PCB patterns of the water samples. The PCB patterns displayed more variability towards the open sea than inside the river estuaries and the Elbe plume. Although the resuspension of PCB contaminated sediment may be an explanation for this observation, the most probable assumption was found to be the atmospheric deposition of PCBs to the surface water of the German EEZ.

Complementing observations could be documented for the surface water of the North Sea (figure 5.58). Highest PCB concentrations were determined inside the river estuaries of Thames (14) and Rhine (11, 12) and the exchange region with the Baltic Sea (41), displaying the dominant riverine input of PCBs to the surface seawaters. The PCB concentrations decreased towards the northern North Sea below the respective LOQs. Hence, there was no indication for a significant atmospheric deposition at the northern sampling sites. The PCB patterns were highly variable. Although CB138 and CB153 were the main components in the surface water of the river plumes, the lighter molecular weight PCBs CB28 and CB52 were more frequently observed towards the northern sampling sites. Atmospheric deposition as well as the resuspension of contaminated sediments was assumed to be the most probable contributors to the variability in PCB patterns.

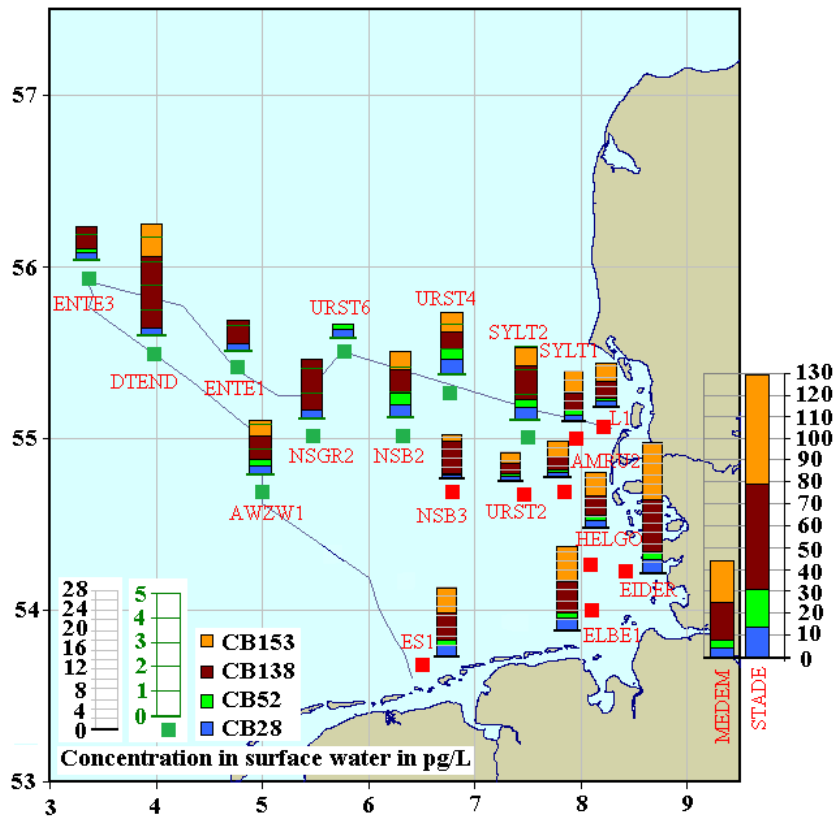


Figure 5.56: Occurrence and distribution of PCBs in the surface water (5m) of the German EEZ in May/June, 2009; Note the variable concentration scales displayed in the legend

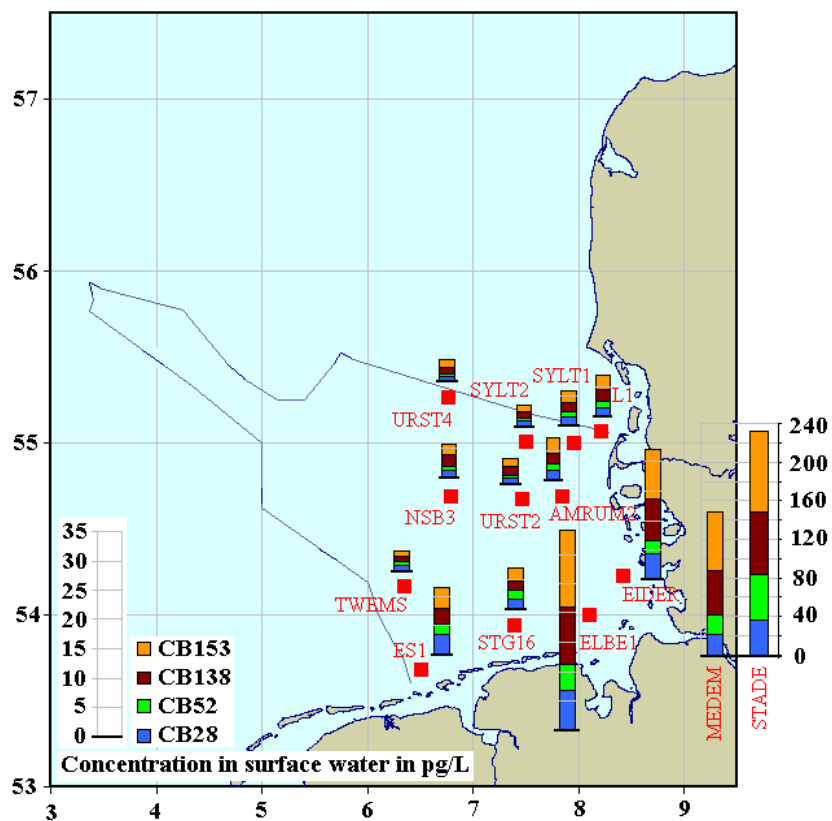


Figure 5.57: Occurrence and distribution of PCBs in the surface water (5m) of the German EEZ in May 2010

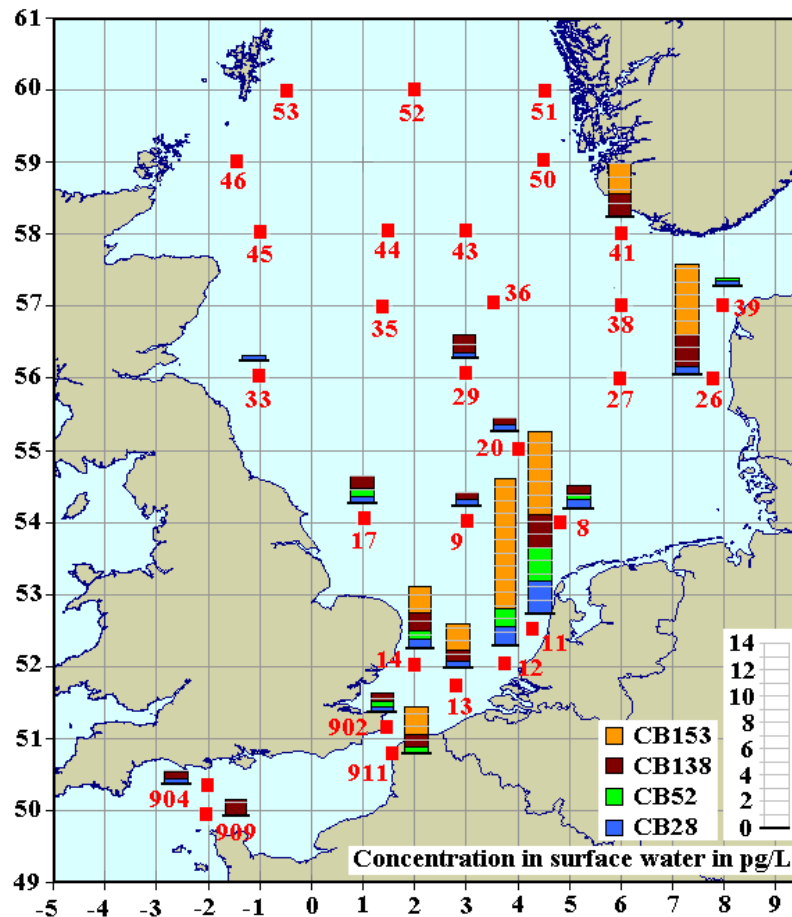


Figure 5.58: Occurrence and distribution of PCBs in the surface water (5m) of the North Sea in Aug./Sep. 2009

The occurrence and spatial distribution of PCBs in the surface water of the Baltic Sea (figure 5.59) differed from the observations in the German EEZ and the North Sea. Each targeted PCB was determined throughout all water sampling sites in the Baltic Sea, whereof CB28 and CB52 were the dominating congeners. The sum PCB concentrations varied between 8 pg/L and 17 pg/L and were comparable to those determined inside the river plume of the Rhine. The surface water concentrations slightly decreased towards the eastern sampling sites. A constant concentration of 8 pg/L for the sum of CB28 and CB52 was observed for all sampling sites east of 15°E. A shift in the PCB patterns towards the lower molecular weight PCBs CB28 and CB52 at the eastern sampling sites was observed. Considering the dominant occurrence of CB28 and CB52 in the Baltic Sea atmosphere (refer to figure 5.54), this shift might be partly caused by atmospheric deposition. A close to equilibrium distribution of the lower molecular weight congeners, could be supposed from the constant surface water concentrations at the eastern sampling sites as well as from the constant atmospheric concentrations of CB28 and CB52 in air masses, which had passed the Baltic Sea within the last 24 h.

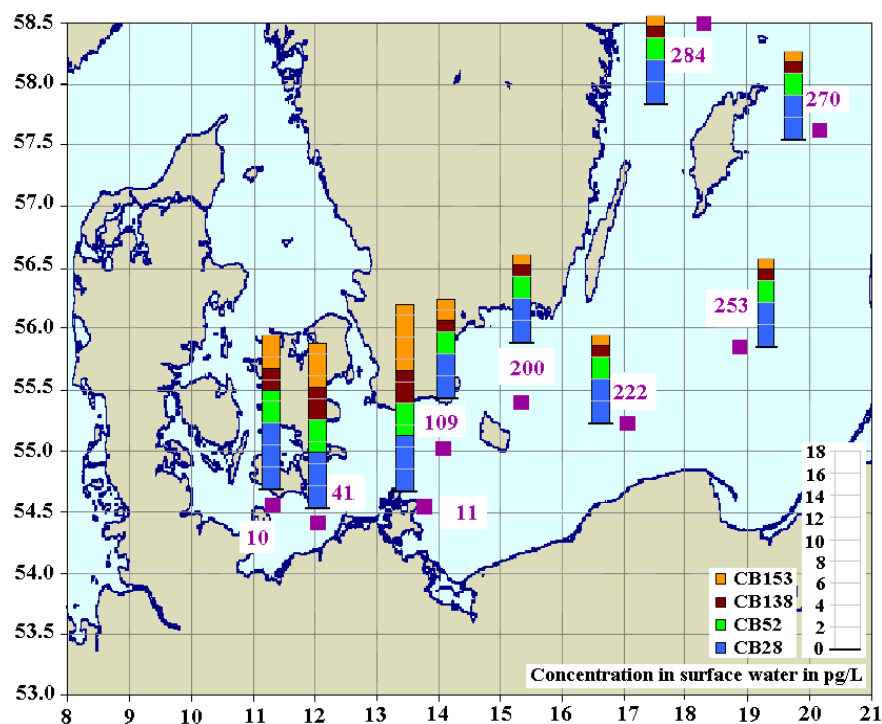


Figure 5.59: Occurrence and distribution of PCBs in the surface water (6 m) of the Baltic Sea in Feb. 2005

Net flux of diffusive gas exchange of PCBs between the marine atmosphere and the surface water

The surface water concentrations of the targeted PCBs discussed above were significantly biased by the particle associated mass fraction of the PCBs. Particle associated PCBs were not available for a free gaseous exchange with the atmosphere. Thus, the direction of the net flux of diffusive gas exchange of the targeted PCBs was not calculated in this study.

A recent study investigating the air-water exchange fluxes above the North Atlantic Ocean in 2005 reported a state close to phase equilibrium. However, atmospheric deposition was still dominating the PCB exchange, whereof tri -and tetrachlorinated congeners contributed to more than 70% of the total flux of the congeners studied. ^[67] In addition, several studies investigated PCB air-sea exchange in the Baltic Sea. The results were diverse. The Kattegat Sea region was found to be a potential source of PCBs to the atmosphere in 1999 ^[142], whereas another study reported a state close to phase equilibrium in the southern Baltic Sea between March and June 1999. ^[143] Another author derived net deposition of PCBs to the Baltic Sea as the annual mean. ^[144]

The predominant occurrence of CB28 and CB52 in the marine atmosphere of the North Sea and the Baltic Sea as well as the characteristic changes in PCB patterns towards the lower molecular weight congeners beyond river plumes were in agreement with the net depositional flux of PCBs reported in the previous studies. ^[67, 144, 145] In particular, the atmospheric deposition of the lower

molecular weight congeners CB28 and CB52 was indicated, which was consistent with the reported flux domination of tri- and tetrachlorinated PCBs. ^[67] The constant surface water concentrations at the eastern sampling sites of the Baltic Sea as well as the constant atmospheric concentrations of CB28 and CB52 in air masses, which had predominantly passed the Baltic Sea within 24 h, agreed with the state close to equilibrium reported in 1999. ^[143]

Conclusions

The rivers were the dominant input sources of PCBs to the surface waters. Nevertheless, the increased variability of PCB patterns as well as the characteristic shift towards the lower molecular weight congeners beyond river plumes and towards the eastern part of the Baltic Sea pointed to the occurrence of atmospheric deposition. CB28 and CB52 were the main components in atmosphere, whereas CB138 and CB53 were sporadically observed and exclusively in air masses originating from continent. Thus, the lower molecular weight congeners were expected to dominate the air-sea exchange fluxes. A state close to phase equilibrium, in particular of the lower molecular weight PCB congeners, was assumed for the study area in the Baltic Sea.

5.1.7 Triazine Herbicides

Triazine herbicides are intensively applied in industrial agriculture worldwide for the preemergence weed control in crops, vineyards and orchards. Besides, they are used as total herbicides on roads and railways. A variety of triazine herbicide compound classes (for example chlorotriazines, methoxytriazines and methylthiotriazines) were discovered and developed within the years 1950 to 1970. Simazine was the first registered triazine herbicide, followed by atrazine at the end of the 1950s in Europe and the United States. ^[146, 147] Today, the triazine herbicides raise concern as main contaminants of soil, surface waters and ground waters providing a toxicity potential for the environment, wildlife and humans. Thus, selected triazine herbicides such as simazine and atrazine were restricted in their usage in several countries, during the last decades. ^[148, 149] Nine triazine herbicides and a triazine metabolite are targeted in this study (table 3.10): Atrazine (ATRAZ) and its degradation product desethylatrazine (DEATRAZ), propazin (PROPAZ), simazine (SIMAZ) and terbuthylazine (TERBAZ) are chlorotriazines. Hexazinone (HEXAZIN) is a methoxytriazine. Ametryn (AMETRYN), irgarol (IRGAROL), prometryn (PROMETR) and terbutryn (TERBUTR) are methylthiotriazine herbicides.

Occurrence and distribution of triazine herbicides in the marine atmosphere

The triazine herbicides were scarcely detected in the atmosphere. An overview is given in table 5.4. Terbuthylazine was the most frequently observed triazine herbicide in the marine atmosphere of the German EEZ, the North Sea and the Baltic Sea. A maximum concentration of up to 156.05 pg/m³

was determined above the river Elbe in May/June 2009. The terbuthylazine concentrations in the marine atmosphere were highly variable (0.1 pg/m³ to 16.54 pg/m³) and were in relation to the air mass history (chapter 3.5). Highest concentrations were observed in air advected from the continent (air samples 09AT 7, 09AT 8 or AL1 – AL6), whereas either significantly decreased concentrations or concentrations below the LOQ were determined in the air masses (AL 7 - AL10), which had passed the sea within the last 24 hours (figure 5.60-5.61). This indicated strong primary sources of terbuthylazine at the continent polluting the marine atmosphere by advection of continental air. The highest terbuthylazine concentrations observed in the marine atmosphere (and in air advected from the continent, 09AT 7, 09AT 8) were approximately 10 times lower than the concentration measured in air sampled along the river Elbe (09AT 2).

Table 5.4: Occurrence and concentrations (pg/m³) of triazine herbicides in the atmosphere above the German EEZ, the wider North Sea, the Baltic Sea and Sülldorf/Hamburg; range = range of atmospheric concentrations above the LOQ in pg/m³; n/n = number of positive analysed air samples/number of total analysed air samples

Sampling site	German EEZ		German EEZ		North Sea	
Date	27.05 - 03.06.09		18.05 - 23.05.10		21.08 - 07.09.09	
	range	n/n	range	n/n	range	n/n
AMETRYN	<LOQ	0/9	<LOD	0/7	<LOD	0 / 13
ATRAZ	<LOQ	0/9	<LOD	0/7	0.94	1 / 13
DEATRAZ	<LOD	0/9	<LOD	0/7	<LOD	0 / 13
HEXAZIN	<LOD	0/9	<LOD	0/7	<LOD	0 / 13
IRGAROL	<LOD	0/9	<LOD	0/7	<LOD	0 / 13
PROMETR	<LOQ	0/9	<LOD	0/7	<LOD	0 / 13
PROPAZ	<LOD	0/9	<LOD	0/7	<LOD	0 / 13
SIMAZ	<LOD	0/9	<LOD	0/7	0.7	1 / 13
TERBAZ	0.73 - 156.05	8/9	0.47 - 4.73	3/7	0.21 - 0.72	2 / 13
TERBUTR	0.30	1/9	<LOQ	0/7	<LOD	0 / 13

Sampling site	Baltic Sea		Sülldorf/Hamburg	
Date	26.04. - 04.05.09		15.11 - 15.12.10	
	range	n/n	range	n/n
AMETRYN	<LOD	0/10	<LOD	0/20
ATRAZ	1.09 - 3.21	6/10	<LOD	0/20
DEATRAZ	0.13 - 1.08	5/10	<LOD	0/20
HEXAZIN	<LOD	0/10	<LOD	0/20
IRGAROL	<LOD	0/10	0.09 - 0.10	2/20
PROMETR	0.20 - 0.54	4/10	<LOD	0/20
PROPAZ	<LOD	0/10	<LOD	0/20
SIMAZ	0.21 - 0.85	2/10	<LOD	0/20
TERBAZ	0.10 - 9.17	10/10	0.08	1/20
TERBUTR	<LOD	0/10	0.10 - 21.32	17/20

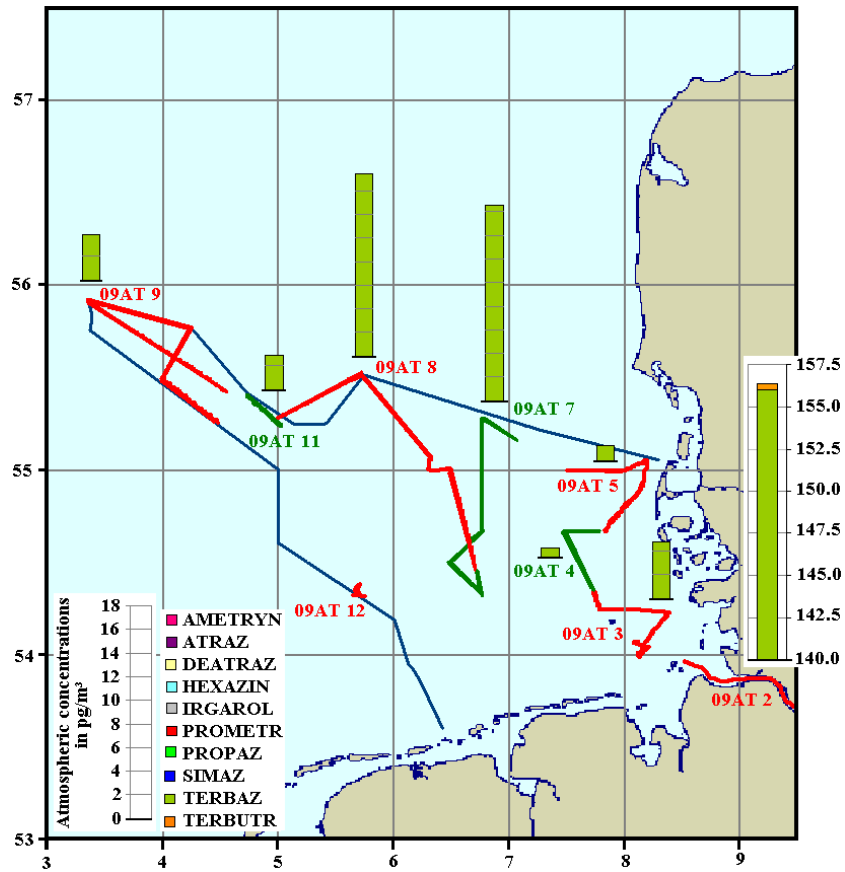


Figure 5.60: Atmospheric bulk concentrations of triazine herbicides above the German EEZ in May/June, 2009

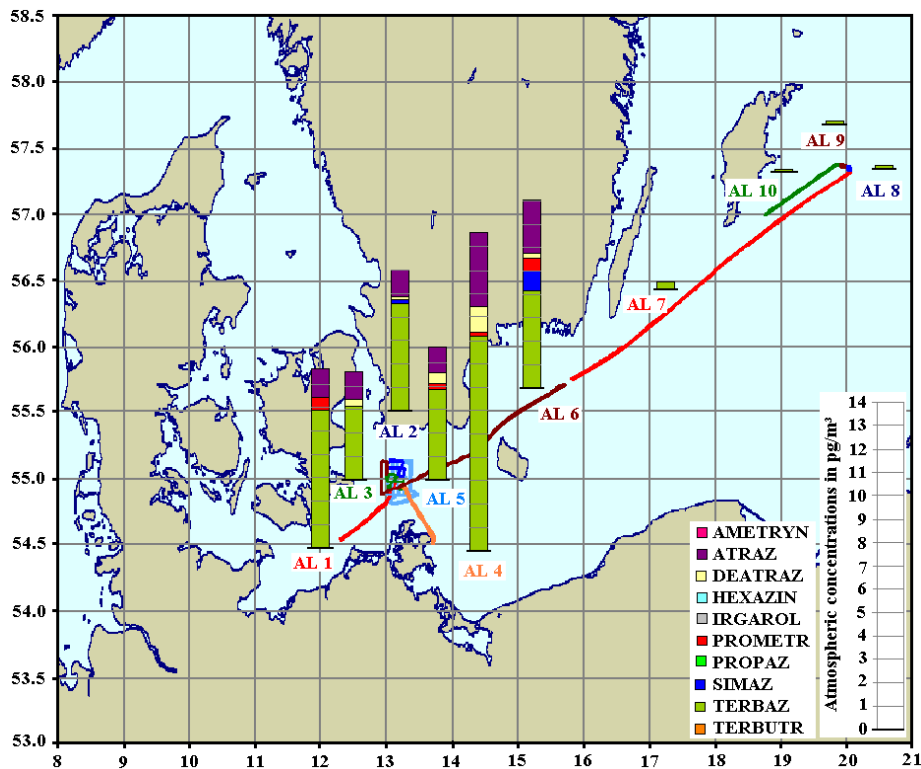


Figure 5.61: Concentrations of triazine herbicides in the gaseous mass fraction of the atmosphere above the Baltic Sea in Apr. 2009

In contrast to the atmosphere of the German EEZ and the wider North Sea, an extended spectrum of triazine herbicides was observed in the marine atmosphere of the Baltic Sea (figure 5.61). In addition to terbuthylazine, even simazine, prometryn, desethylatrazine and atrazine could be quantified in air advected from the continent at the sampling sites west of 16°E in maximum concentrations of 9.17 pg/m³, 0.85 pg/m³, 0.54 pg/m³, 1.08 pg/m³ and 3.21 pg/m³, respectively. The Baltic Sea is an inland water body with highly industrialised riparian countries, whereas the North Sea is only partly bordered and is open to the Atlantic Ocean (English Channel in the south and the Norwegian sea in the north) and to the Baltic Sea (Skagerrak). In addition, only a small part of the Baltic Sea atmosphere was investigated in this study exhibiting sampling sites predominantly close to the continent. Thus a higher pollution level of the marine atmosphere above the Baltic Sea, especially by currently used pesticides in industrial agriculture could be expected. Furthermore, the larger air sample volumes (factor 2 – 3) collected during the Baltic Sea campaign might contribute to the wider spectrum of triazine herbicides detected (chapter 3.2).

Hexazinone, propazine and ametryn could not be quantified neither during the sampling campaigns on sea nor during the sampling campaign in Sülldorf/Hamburg, but irgarol and terbutryn were episodically observed. In particular, terbutryn revealed elevated concentration levels of up to 21.32 pg/m³ in the atmosphere of Sülldorf/Hamburg in November/December 2010. These significantly increased concentrations during a season of limited weed growth indicated the influence of further significant primary sources of terbutryn beyond the industrial agriculture. This was supported by the comparison of the seasonal profiles of atmospheric concentrations of terbutryn and terbuthylazine as discussed below.

Seasonal variations in atmospheric concentrations

Terbuthylazine was the most frequently quantified triazine herbicide in the atmosphere of the German EEZ in May/June 2009. In contrast, it was scarcely found and in significant lower concentrations during the sampling campaign in the North Sea in August/September 2009 and in the German EEZ in May 2010 (table 5.4). These observations were in agreement with the seasonal fluctuations of atmospheric terbuthylazine levels monitored by the PUF disk passive air samplers in Sülldorf/Hamburg and Tinum/Sylt (figure 5.62). At both sampling sites, significantly increased atmospheric abundances of terbuthylazine were observed in the months from May to July, whereas the atmospheric concentrations were below or close to the LOQ beyond this period. This provided evidence that terbuthylazine was a currently used pesticide in industrial agriculture in Europe with a main application season from May to July. During the main application season it was intensively emitted into the atmosphere by spray drift or volatilisation (saturation vapour pressure of

0.149 mPa at 25 °C, ^[150]) and transported to the marine atmosphere by advection of contaminated air masses, as demonstrated in this study. Thus, secondary sources such as revolatilisation processes from contaminated soil, appeared to cause negligible input of triazine herbicides to the atmosphere. In consequence, a significant atmospheric deposition of terbuthylazine to the surface water of the German EEZ, the wider North Sea and the Baltic Sea was exclusively expected for the months of the main agricultural application season.

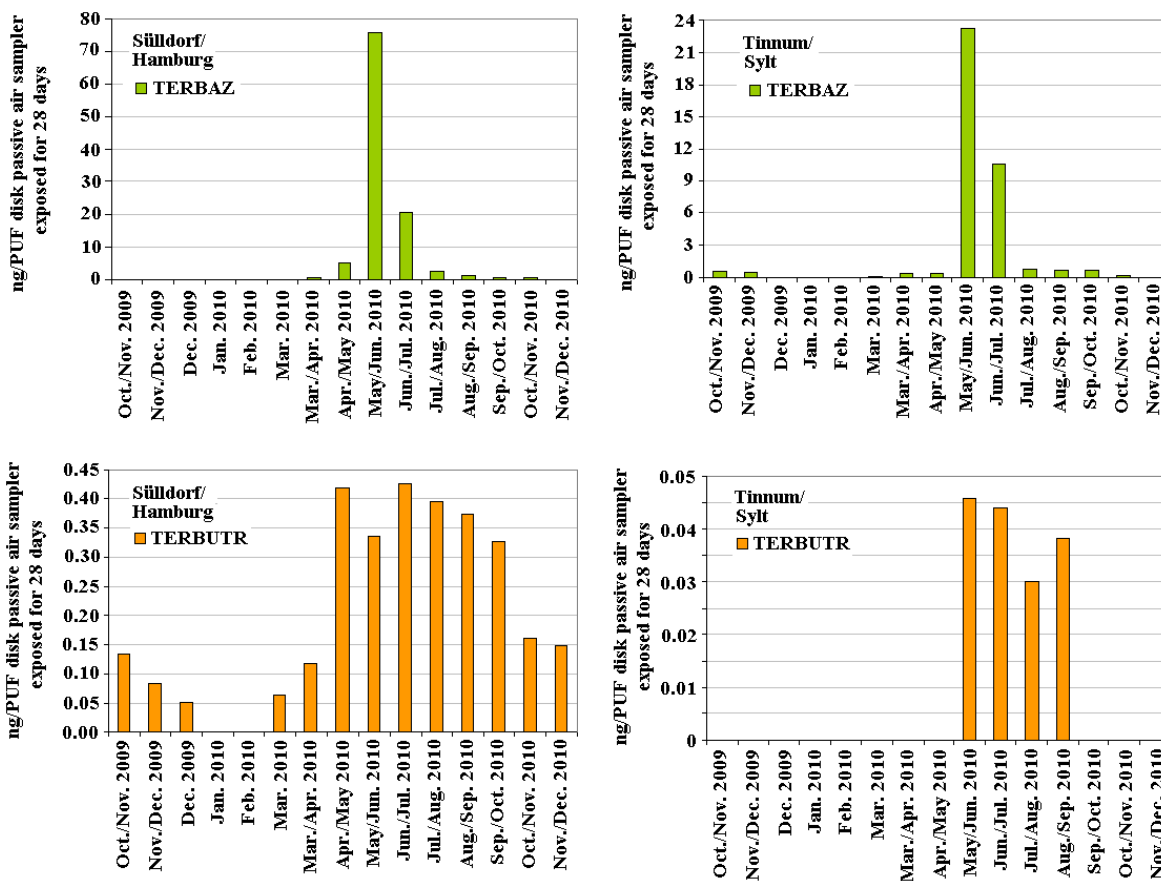


Figure 5.62: Seasonal variations in atmospheric levels of the triazine herbicides terbuthylazine and terbutryn observed at the sampling sites Sülldorf/Hamburg and Tinnum/Sylt

In addition, a seasonal profile of the atmospheric occurrence of terbutryn could be monitored by the PUF disk passive air samplers. It has been reported that terbutryn is a widely used biocide, e.g., in antifouling paints for facades and in roof paints. ^[151, 152] In consequence, a variety of potential emission sources to the atmosphere exist throughout the year. The seasonal profiles of terbutryn (figure 5.62) gave evidence to its predominant application as biocide: Although highest atmospheric abundances were observed within the months from May 2010 to October 2010, a pronounced main application season as determined for terbuthylazine, could not be documented. Terbutryn was quantified almost throughout the year in the urban atmosphere of Sülldorf/Hamburg,

except of the months January 2010 and February 2010. This pointed to several diffusive primary emission sources of terbutryn to the atmosphere, beyond an application as herbicide in agriculture. Moreover, terbutryn was found in significantly lower abundances in the atmosphere than terbuthylazine, regarding the total amount collected at the PUF disk passive air samplers. Maximum concentrations of 0.45 ng/PUF disk PAS and 75.88 ng/PUF disk PAS were determined, respectively.

Except of terbuthylazine and terbutryn, no further triazine herbicides could be quantified by the PUF disk passive air samplers exposed in Tinum/Sylt and Sülldorf/Hamburg.

Gas-particle partitioning

Terbuthylazine and terbutryn underwent gas-particle partitioning in the atmosphere, which was in relation to their semi-volatile properties (saturation vapour pressures of 0.149 mPa and 0.280 mPa at 25 °C, respectively ^[150]). On average approximately 70 % of the total terbuthylazine concentration was determined in the particle associated mass fraction at 12 °C, whereas terbutryn was almost exclusively quantified in the particulate matter fraction of the air samples.

In consequence of their strong adsorption to atmospheric particulate matter as well as their episodically occurrence in the marine atmosphere, a significant long range transport potential in atmosphere to higher altitudes could not be expected. But, indications for long range transport of atrazine and desethylatrazine were found in previous studies reporting their occurrence in the Arctic. ^[153, 154]

Occurrence and distribution of triazine herbicides in the surface seawater

The triazine herbicides are highly water soluble (e.g., water solubilities of terbuthylazine and terbutryn were 8.5 mg/L and 25 mg/L at 20°C, respectively) and adsorb negligibly to the SPM (e.g., the logK_{OW} of terbuthylazine and terbutryn are 3.21 and 3.74, respectively). ^[150] In consequence, their spatial distribution in surface water was unaffected by the SPM level in the water column and was predominantly influenced by punctual sources like riverine input or the Baltic Sea outflow as well as the prevailing sea currents. The targeted triazine herbicides displayed similar distribution patterns throughout the surface water of the German EEZ and the North Sea (figure 5.63 -5.65). Highest concentrations were quantified in the water samples of the river Elbe and inside the estuaries of Rhine (11, 12), Elbe (e.g., HELGO, AMRU2, SYLT1, 26), Ems (ES1, TWEMS, STG16) and Weser (ELBE1). Besides, remarkably increased surface water concentrations were determined at the sampling sites monitoring the Baltic Sea outflow (26, 39 40, 41, 50, 51). A significant decline in surface water concentrations towards the open sea was observed. In addition, seasonal fluctuations in surface water concentrations at the sampling sites in the estuary (MEDEM)

and the plume of the river Elbe (HELGO) were documented indicating the extent and continuous application of individual triazine herbicides, especially in the summer months (figure 5.66).

The spatial distributions of simazine, desethylatrazine, hexazinone, prometryn, propazin, ametryn, terbutryn and irgarol in the surface water of the German EEZ and the North Sea were comparable and predominantly differed in the extent of the concentration gradients from the coastal sampling sites to the open sea as summarized in table 5.5. For this reason and due to their negligible occurrence in the marine atmosphere their occurrence in surface water was not discussed in detail here.

Table 5.5: Concentration ranges of the triazine herbicides in the surface water of the German EEZ, the wider North Sea and the Baltic Sea; min. /max. = minimum/maximum concentrations in pg/L

Sampling site Sampling season pg/L	German EEZ May/Jun. 2009		German EEZ May 2010		North Sea Aug./Sep. 2009		Baltic Sea Jun./Jul. 2008	
	min.	max.	min.	max.	min.	max.	min.	max.
AMETRYN	9	522	22	532	11	37	<LOQ	42
ATRAZ	512	3961	561	3985	515	1267	957	2650
DEATRAZ	140	6250	142	2730	123	1134	424	1049
HEXAZIN	<LOQ	2523	10	2714	<LOQ	58	27	98
IRGAROL	<LOQ	3531	<LOQ	1896	<LOQ	507	178	4525
PROMETR	<LOQ	1576	5	1688	2	41	5	359
PROPAZ	8	392	<LOQ	388	<LOQ	31	39	202
SIMAZ	100	4566	114	3097	82	573	606	2953
TERBAZ	54	28730	32	7500	14	1386	177	731
TERBUTR	<LOQ	2952	9	3341	4	253	6	50

Terbutylazine revealed the strongest decline in surface water concentrations of the targeted triazine herbicides (table 5.5). A maximum concentration of 28.7 ng/L was observed in the river Elbe in May/June 2009. The surface water concentrations gradually decreased to a minimum of 54 pg/L towards the western sampling sites of the German EEZ (figure 5.63-5.64). Terbutylazine was quantified throughout all water sampling sites in the North Sea. The concentrations ranged from 14 pg/L in the north to 1.4 ng/L at the coastal sampling sites in the south (figure 5.65). Considering the seasonally increased concentrations in the marine atmosphere, it was assumed that the transport of terbutylazine to the remote sampling sites in the northern North Sea could be partly attributed to atmospheric deposition. The comparison of three monitoring cruises in the German EEZ in May/June 2009, September 2009 and November 2009 showed a strong seasonality of the surface water concentrations of terbutylazine. As illustrated in figure 5.66, the amplitude of the seasonal fluctuations decreased with increasing distance to the estuary and river plume of the Elbe. Moreover, a shift in the season of maximum surface water concentrations was observed, which added evidence to the perception of atmospheric deposition of terbutylazine during the

main application season. The maximum surface water concentrations at the western sampling sites of the German EEZ in May/June could be related to the seasonally increased atmospheric abundances of terbuthylazine monitored by the PUF disk passive air samplers in May/June 2010 (figure 5.62). In contrast, the surface water concentrations of terbuthylazine at the coastal sampling sites were higher in September. This was attributed to the dominant riverine input of terbuthylazine masking the minor atmospheric deposition. The time lag between the maximum of the atmospheric

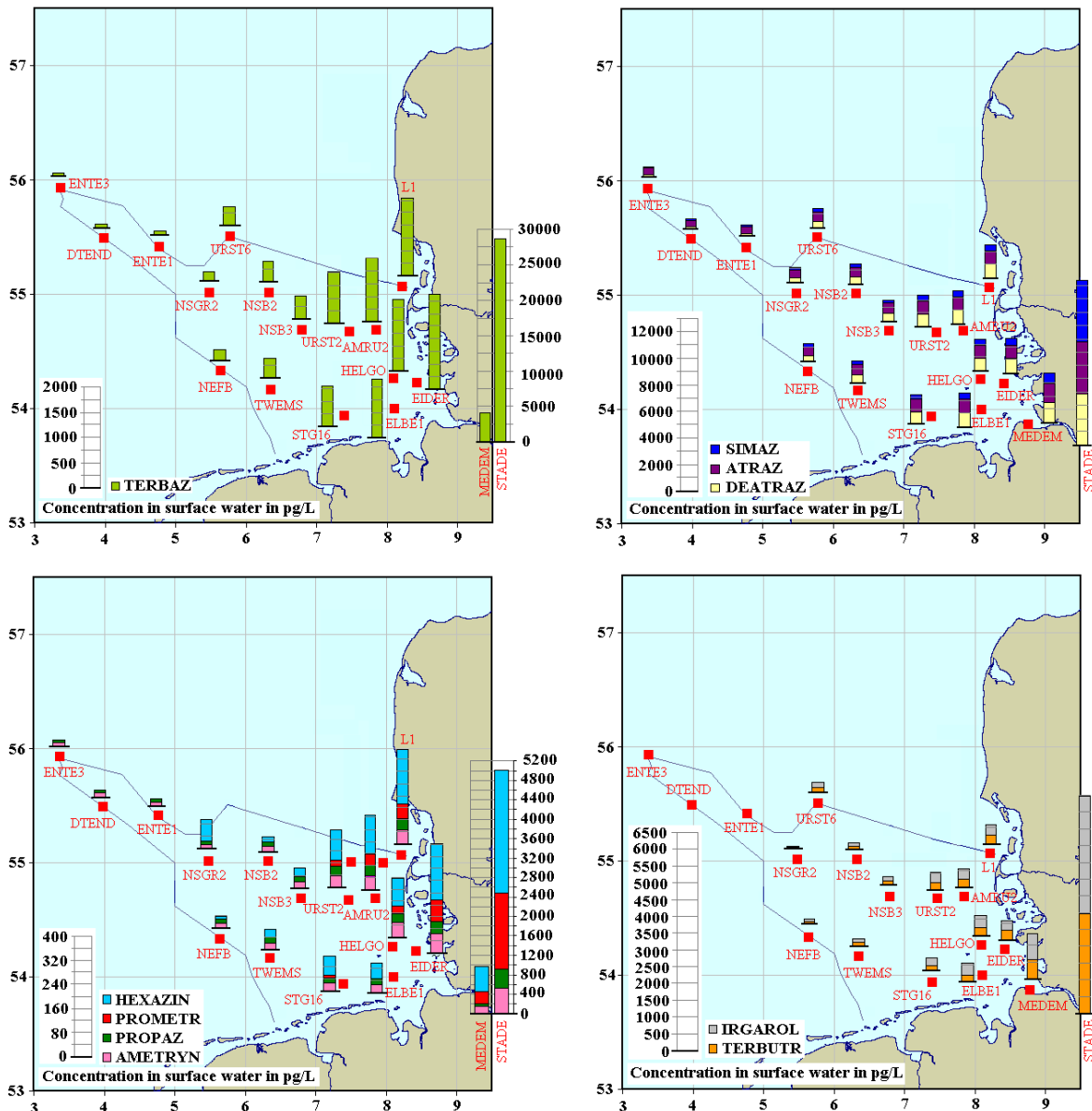


Figure 5.63: Occurrence and distribution of triazine herbicides in the aqueous phase of the surface water (5m) of the German EEZ in May/June, 2010; Note the increased concentration scale of terbuthylazine, hexazinone, prometryn, propazin and ametryn at the sampling sites STADE, MEDEM and SYLT1, respectively

terbuthylazine abundances and the maximum in the surface water concentrations of the Elbe estuary was uncertain due to discontinuous water sampling (no data in July, August and October).

However, such a time lag could be expected because riverine transport of organic pollutants was presumably delayed against atmospheric deposition due to sorption in soils and characteristic runoff, while regional transport in the atmosphere was fast. Similar conclusions, concerning the significance of the atmospheric deposition to the surface water of the German EEZ beyond river plumes had been already reported in former studies during the 1990s for atrazine, terbuthylazine and simazine. [155, 156] The seasonally increased abundances in the atmosphere and in the surface water as well as the strong decline in surface water concentrations from the estuaries towards the open sea gave evidence that terbuthylazine was currently the most extensively applied triazine herbicide in central and northwestern Europe.

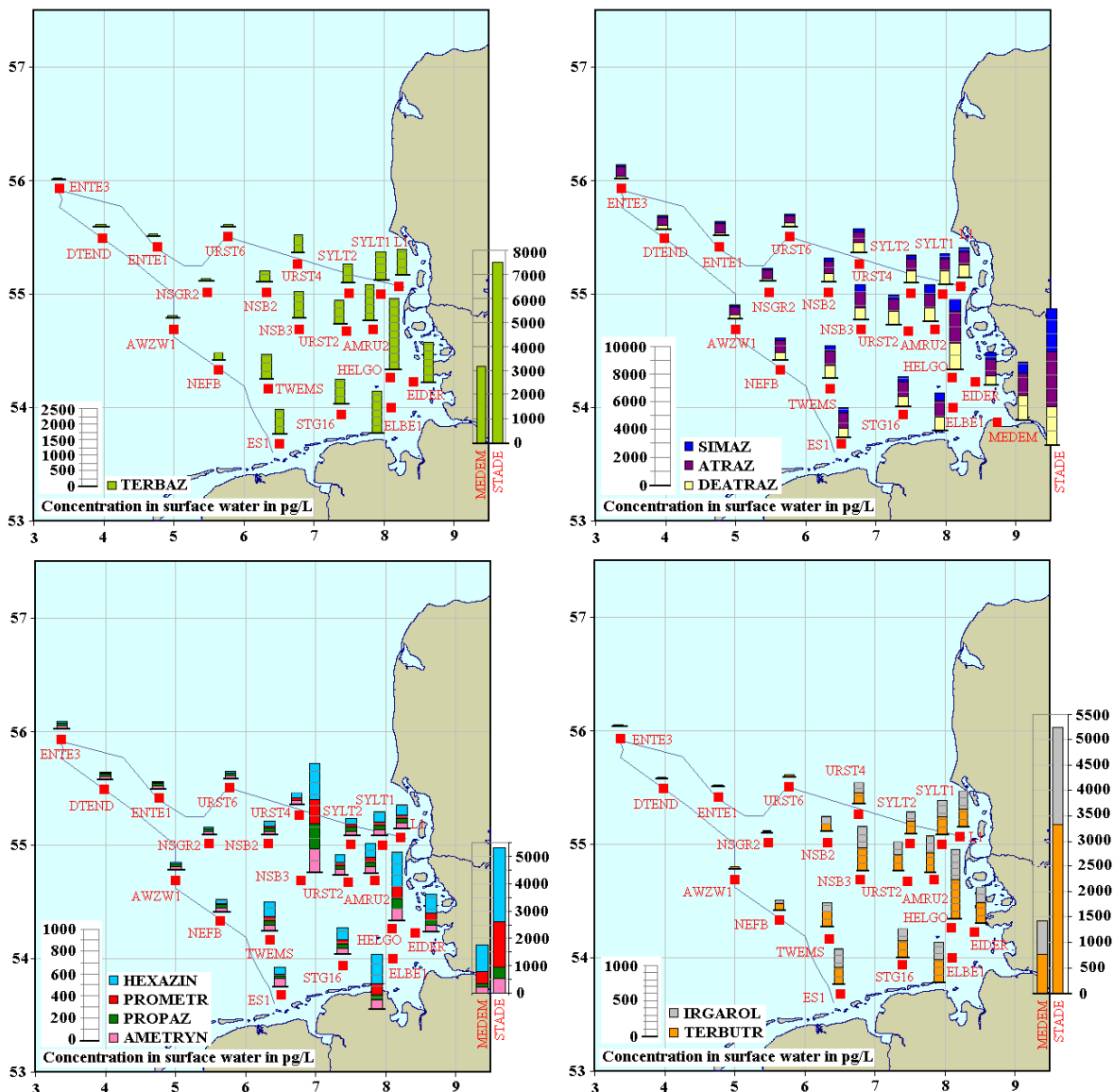


Figure 5.64: Occurrence and distribution of triazine herbicides in the aqueous phase of the surface water (5m) of the German EEZ in May 2010; Note the increased concentration scale of terbuthylazine, hexazinone, prometryn, propazin, ametryn, irgarol and terbuthryn at the sampling sites STADE and MEDEM, respectively

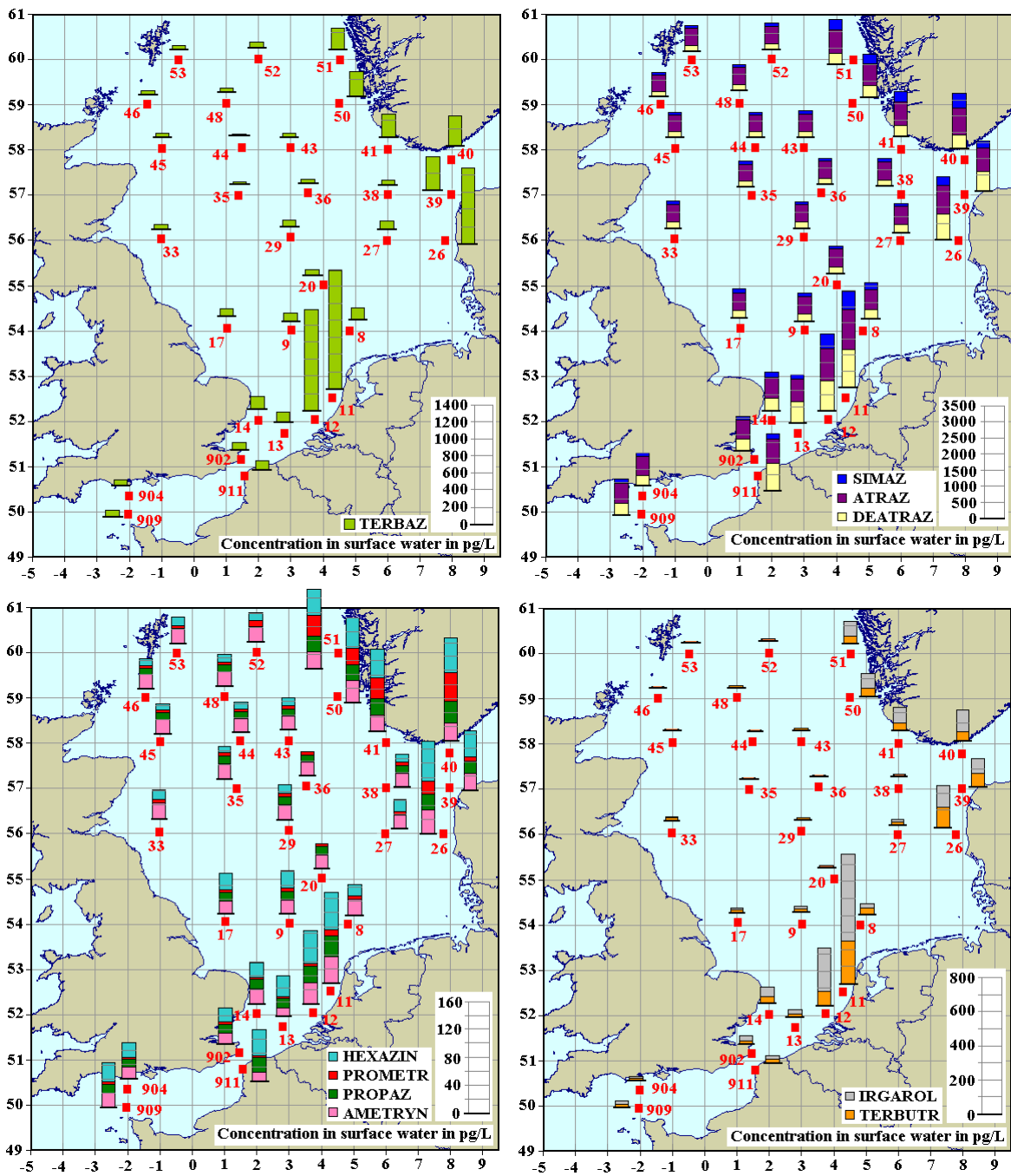


Figure 5.65: Occurrence and distribution of triazine herbicides in the aqueous phase of the surface water (5m) of the North Sea in Aug./Sep. 2009

Atrazine and its metabolite desethylatrazine were the dominant triazine herbicides in the surface water of the German EEZ and the wider North Sea. Maximum surface water concentrations of approximately 4 ng/L and 6 ng/L were quantified in the Elbe, respectively. Both compounds reached almost constant surface water concentrations of approximately 0.55 ng/L and 0.15 ng/L beyond the river plumes and estuaries, respectively. On average the surface water concentrations of

atrazine in the central and in the northern North Sea were approximately more than twice as high as the sum of the concentrations of the other targeted triazine herbicides. This could be partly attributed to higher atmospheric deposition fluxes in the past. ^[155, 156] Although the application was restricted nowadays, the spatial distribution of atrazine in the surface water was still dominated by the riverine inputs of Elbe and Rhine as well as by the input of the Baltic Sea outflow.

The spatial distribution of the triazine herbicides in the surface water of the Baltic Sea (figure 5.67) differed from their occurrence in the North Sea. This could be attributed to the limited water exchange rates of an inland sea and the highly industrialised riparian countries. On average the total surface water concentration of the targeted triazine herbicides in the Baltic Sea was seven times higher than in the North Sea and comparable to the mean sum concentration in the Elbe estuary. In comparison to the North Sea and the German EEZ, small concentration gradients were observed (table 5.5). The surface water concentrations of the triazine herbicides in the central Baltic Sea were less variable. A significant decrease was observed towards the northern sampling sites in the Bothnian Bay (35, 37, BB3) as well as towards the water exchange region with the North Sea (Skagerrak). The main components in the surface water of the Baltic Sea were simazine, atrazine, irgarol and the metabolite desethylatrazine with mean concentrations of 2.3 ng/L, 2.0 ng/L, 1 ng/L and 0.8 ng/L, respectively. The distribution patterns of the triazine herbicides in the surface water of the Baltic Sea gave no indications for the influence of atmospheric deposition.

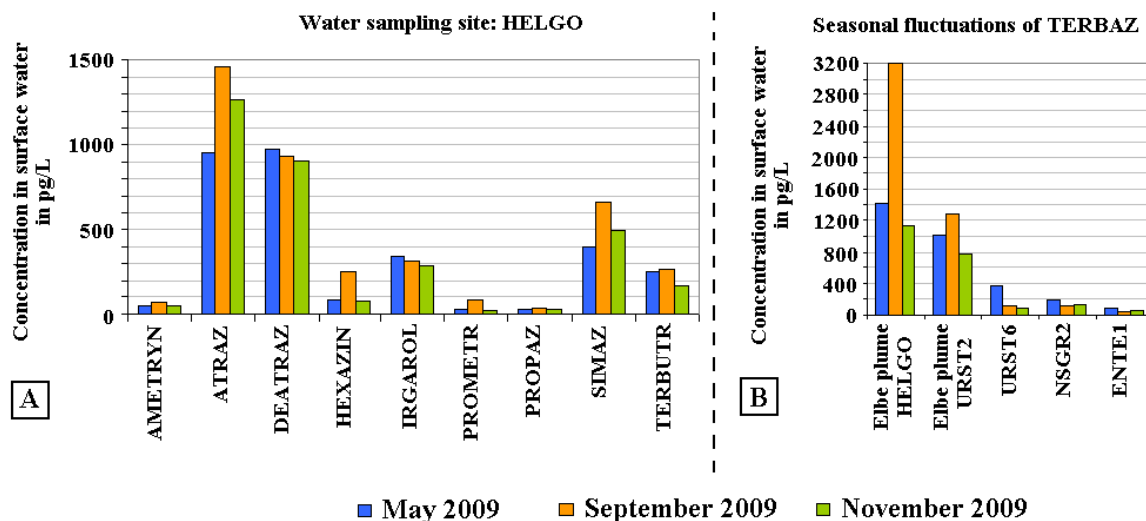


Figure 5.66: Seasonal variations in the surface water concentrations (5 m) of the triazine herbicides in the estuary of the river Elbe (A) and of terbuthylazine at selected sampling sites throughout the German EEZ (B)

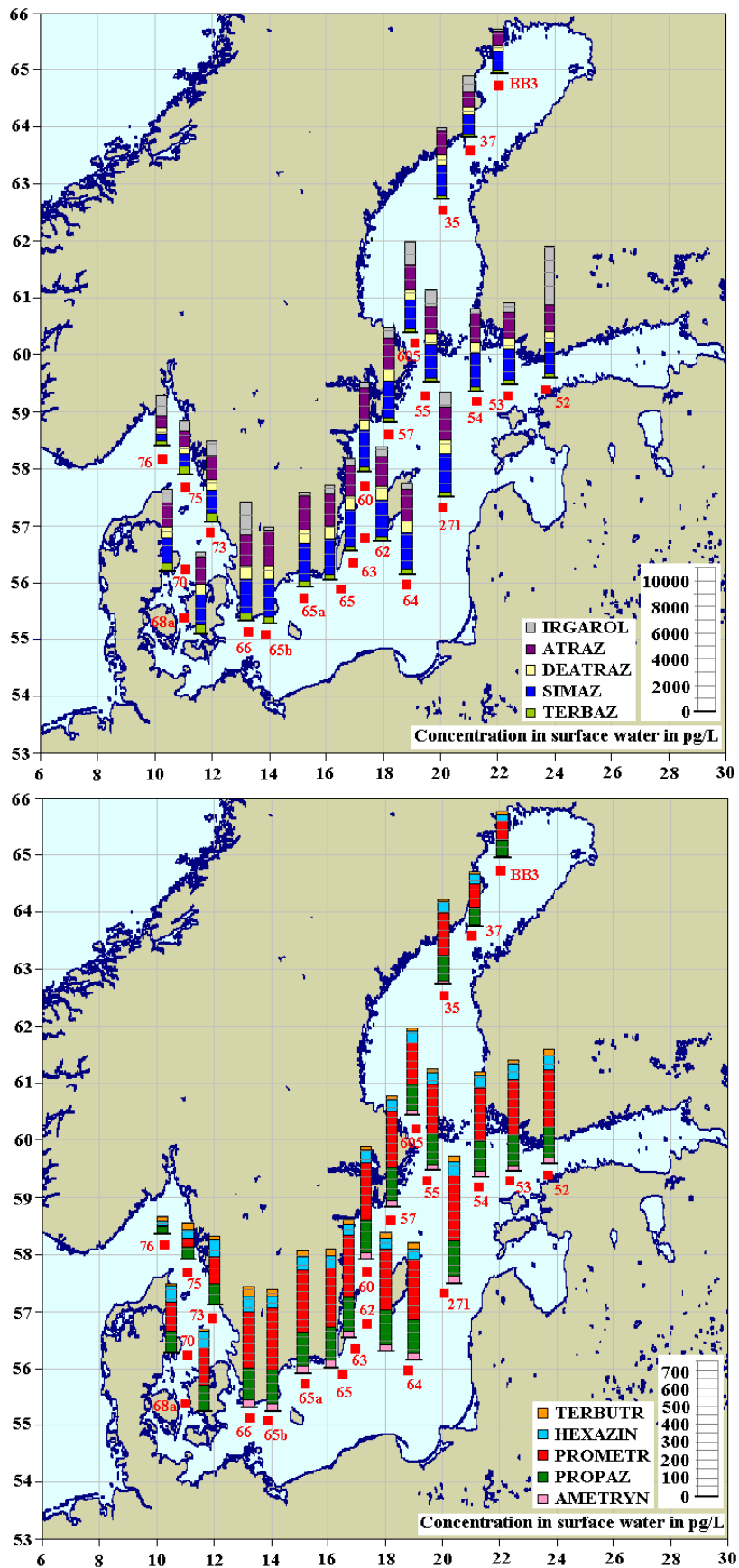


Figure 5.67: Occurrence and distribution of triazine herbicides in the aqueous phase of the surface water (6m) of the Baltic Sea in Jun./Jul. 2008

Net flux of diffusive gas exchange of triazine herbicides between the marine atmosphere and the surface water

The direction of the net flux of diffusive gas exchange between the marine atmosphere and the surface water was calculated for terbuthylazine within the German EEZ in May/June 2009 (figure 5.68 A) and for terbuthylazine and atrazine within the Baltic Sea (figure 5.68 B). Note that the surface water concentrations (June/July 2008) and the atmospheric concentrations (April 2009) of the Baltic Sea originated from different seasons. Considering the seasonal fluctuations in surface seawater concentrations monitored for the German EEZ the direction of the net flux might be severely biased.

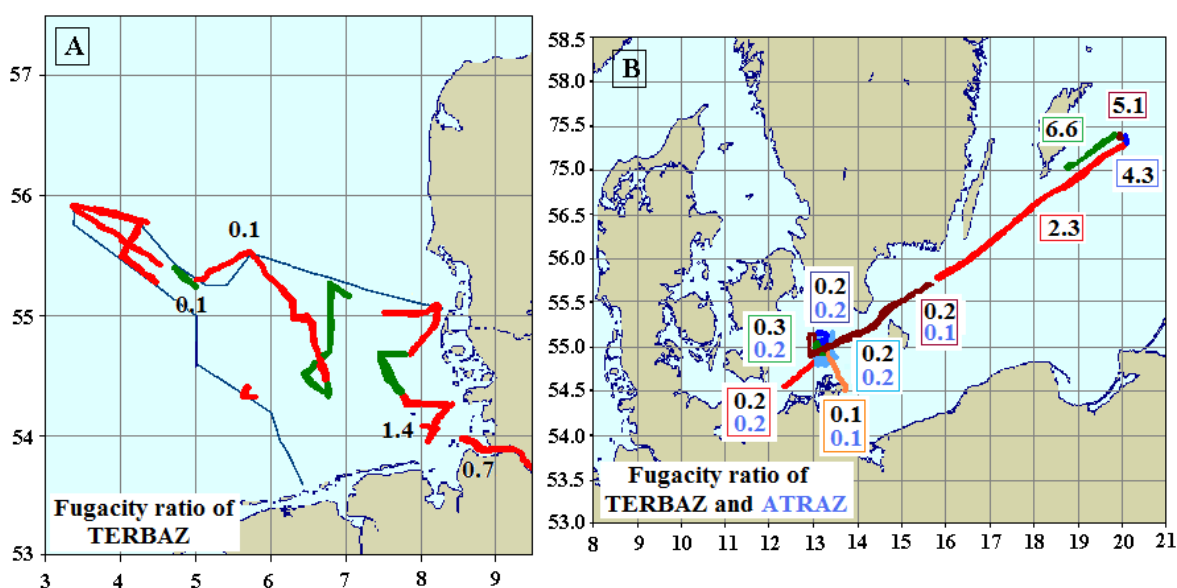


Figure 5.68: Net flux of diffusive gas exchange of terbuthylazine and atrazine; Fugacity ratio < 0.5: Atmosphere → Sea; Fugacity ratio > 2: Sea → Atmosphere; (A) German EEZ May/Jun. 2009; (B) Baltic Sea Apr. 2009

The fugacity ratios pointed to a predominant atmospheric deposition of terbuthylazine and atrazine to the surface seawaters. In regions of highest surface water concentrations and lowest atmospheric abundances, the flux might change to an outgassing, as calculated for the sampling sites in the Baltic Sea east of 16°E. A close to phase equilibrium was determined for two sampling sites in the river plume of the Elbe.

However, diffusive gas exchange was not expected to be a major atmospheric deposition process of triazine herbicides, because they occurred predominantly in the particle associated mass fraction of the atmosphere. Thus, they were more prone to dry particulate as well as wet deposition processes. Besides, triazine herbicides were scarcely quantified in the marine atmosphere displaying the negligible revolatilisation from contaminated surface waters.

Conclusions

Major input pathways of triazine herbicides to the surface seawaters were the rivers: Highest concentration gradients from the coastal sampling sites towards the open sea according to the sea currents as well as seasonal fluctuations in surface water concentrations demonstrated current usage. The strongest gradient was observed for terbuthylazine suggesting an intensified application.

Terbuthylazine was the only of the targeted triazine herbicides, which could be episodically quantified in the marine atmosphere. A seasonality of its atmospheric abundances was observed, which could be attributed to the main application period in agriculture in May/June. The air mass backward trajectory analysis demonstrated the transport of terbuthylazine into the marine atmosphere by advection of contaminated air masses from land. An atmospheric deposition of terbuthylazine was indicated by the seasonal fluctuations in the surface water at the sampling sites in the open sea as well as by the estimation of the direction of the net flux of diffusive gas exchange. Dry particulate as well as wet deposition were expected to be the major removal processes of terbuthylazine due to its predominant occurrence in the particle associated mass fraction of the atmosphere. Revolatilisation of terbuthylazine from the significantly contaminated surface waters was assumed to be negligible, because it was only scarcely detected in the marine atmosphere beyond the main application season.

This study gave evidence that atmospheric deposition could be an important input pathway of triazine herbicides to the surface seawaters. Regarding the main sea currents of the North Sea, the remarkably high triazine herbicide abundances (in particular atrazine) at the remote sampling sites in the northern North Sea had to be attributed to significantly pre-contaminated surface water presumably due to atmospheric deposition in the past.

5.1.8 Organophosphate Insecticides

Organophosphates are widely used in industrial agriculture as well as in home, garden and in veterinary practices for the control of insect pests. They are highly toxic substances even for humans, which act by an inhibition of the cholinesterase activity after inhalation, dermal absorption, ingestion and eye contact. ^[157 - 159] Organophosphates exhibit a short persistence in the environment. ^[160-162] Hydrolysis rates (half lives) ranging from a few hours to 130 days at a water temperature of 20 °C and pH 7.4 are reported in the literature. ^[161] Six organophosphate insecticides are targeted in this study (table 3.10): chlorfenvinphos (CHLORFENV), malathion (MALATH), azinphos-ethyl (AZINPH-E), azinphos-methyl (AZINPH-M), diazinone (DIAZINON) and dimethoate (DIMETH).

Occurrence and distribution of organophosphate insecticides in the atmosphere

Organophosphates were only sporadically detected in the marine as well as in the continental atmosphere. An overview is listed in table 5.6. Concentrations above the LOQs were solely observed for diazinone, dimethoate and malathion in 13, 2 and 2 out of 59 active air samples, respectively. Atmospheric concentrations of chlorfenvinphos were observed below the LOQ, whereas azinphos-ethyl and azinphos-methyl were never detected by active air sampling. Maximum concentrations of diazinone, dimethoate and malathion were close to the LOQ with 2.66 pg/m³, 0.32 pg/m³ and 0.25 pg/m³, respectively. Organophosphates were exclusively observed in air masses, which had passed the continent within the last 24 hours. It was concluded that their occurrence in the marine atmosphere was determined by the advection of contaminated air from the continent.

Table 5.6: Occurrence and bulk concentrations (pg/m³) of organophosphate insecticides in the atmosphere above the German EEZ, North Sea, Baltic Sea and Sülldorf/Hamburg; range = range of atmospheric concentrations above the LOQ in pg/m³; n/n = number of positive analysed air samples/number of total analysed air samples

Sampling site	German EEZ		German EEZ		North Sea	
Date	27.05. - 03.06.09		18.05. - 23.05.10		21.08. - 07.09.09	
	range	n/n	range	n/n	range	n/n
AZINPH-E	<LOD	0/9	<LOD	0/7	<LOD	0/13
AZINPH-M	<LOD	0/9	<LOD	0/7	<LOD	0/13
CHLORFENV	<LOD	0/9	<LOD	0/7	<LOQ	0/13
DIAZINON	<LOD	0/9	<LOD	0/7	0.37 - 2.66	4/13
DIMETH	<LOQ	0/9	<LOD	0/7	<LOQ	0/13
MALATH	0.21	1/9	<LOD	0/7	<LOD	0/13

Sampling site	Baltic Sea		Sülldorf/Hamburg	
Date	26.04. - 04.05.09		15.11. - 15.12.10	
	range	n/n	range	n/n
AZINPH-E	<LOD	0/10	<LOD	0/20
AZINPH-M	<LOD	0/10	<LOD	0/20
CHLORFENV	<LOD	0/10	<LOD	0/20
DIAZINON	0.12 - 1.27	3/10	0.92 - 1.63	6/20
DIMETH	0.15 - 0.32	2/10	<LOQ	0/20
MALATH	0.25	1/10	<LOD	0/20

The passive air sampler profiles (figure 5.69) displayed a sporadically presence of dimethoate and diazinone at very low abundances in the atmosphere at the urban (Sülldorf/Hamburg) and coastal (Tinum/Sylt) sampling site, respectively. This pointed to a variety of minor and diffusive primary sources to the atmosphere. In addition, the occurrence of azinphos-methyl in the atmosphere of Sülldorf/Hamburg in May/June 2010 could be documented. Azinphos-ethyl, chlorfenvinphos and malathion were not detected in any PUF disk passive air sample.

Diazinone was the most frequently detected organophosphate in the atmosphere throughout the year exhibiting less variability in the atmospheric concentration levels. In contrast, dimethoate revealed a less pronounced seasonal profile in the air of Sülldorf/Hamburg. Highest atmospheric concentration levels were determined in May/June, whereas it could not be quantified from December to April. This seasonal profile might be attributed to a main application season of dimethoate in agriculture.

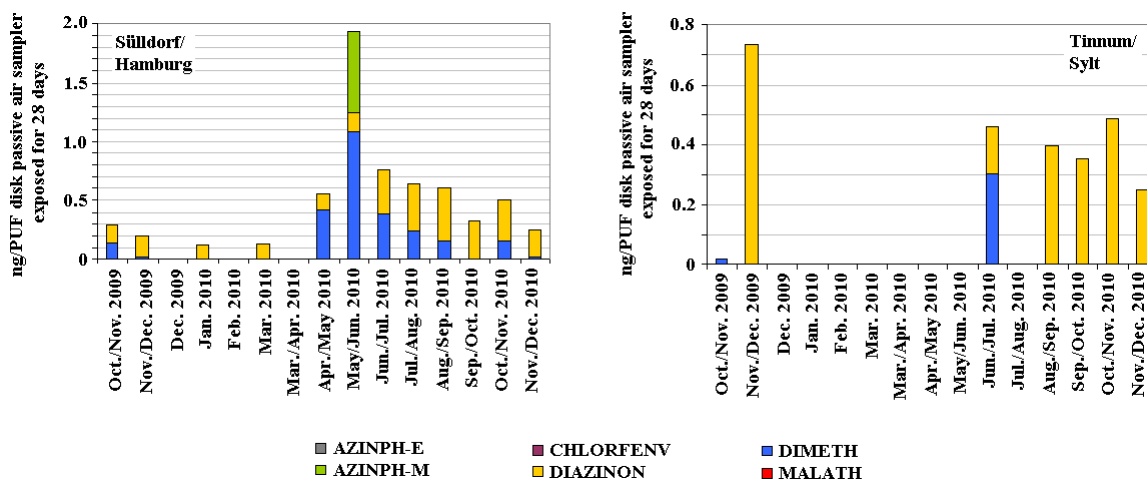


Figure 5.69: Seasonal variations in the atmospheric abundances of the organophosphate insecticides observed at the sampling sites Sülldorf/Hamburg and Tinnum/Sylt

Organophosphates are semi-volatile (e.g., saturation vapour pressures of dimethoate and diazinone at 25 °C are 1.1 mPa and 12 mPa, respectively ^[150]) and thus undergo gas-particle partitioning in the atmosphere. They were predominantly found in the gaseous mass fraction.

Occurrence and distribution of organophosphate insecticides in the surface seawater

Diazinone was the most frequently observed organophosphate insecticide in the surface water of the German EEZ and the wider North Sea (figures 5.70-5.72). Maximum surface water concentrations of approximately 400 pg/L and 23 pg/L were determined in the Elbe (STADE) and in the river plume of the Rhine (11), respectively. However, diazinone displayed no typical concentration gradient from the coastal sampling sites towards the open sea, which would be characteristic for a predominant riverine input. In contrast, it was quantified in concentrations > 5 pg/L throughout the entire German EEZ and even at the sampling sites in the central North Sea beyond river plumes and estuaries. In consequence, atmospheric deposition was assumed to be an important input pathway of diazinone to the surface seawaters. The sporadic occurrence of diazinone in air advected from the continent as well as the short persistence of organophosphates in the environment supported this perception.

Dimethoate was less frequently detected in surface water than diazinone corresponding to their abundances in the atmosphere. However, dimethoate displayed similar distribution patterns in the German EEZ and the wider North Sea. Although highest concentrations of up to 200 pg/L were observed in the Elbe and the Elbe plume, it exhibited not the characteristic concentration gradient typical for riverine input. Instead, dimethoate was episodically observed even at the northern sampling sites in the North Sea, which pointed to atmospheric deposition.

Azinphos-methyl and chlorfenvinphos were exclusively observed in the river plumes of Elbe (EIDER) and Rhine (11), whereas malathion occurred even in the central German EEZ (TWEMS, NSB3). This sporadic occurrence indicated an atmospheric deposition, because neither azinphos-methyl nor chlorfenvinphos and malathion could be determined in the surface water of the Elbe.

Organophosphate insecticides could not be detected in the surface water of the Baltic Sea in June/July 2008, although their presence in the Baltic Sea atmosphere may suggested an atmospheric deposition flux similar as for the North Sea region. Their absence could be related to the significantly decreased salt content of the Baltic Sea surface water, which tended to accelerate the degradation of organophosphates. For example, it was reported that the persistence of diazinone in seawater was significantly higher than in comparison to freshwater (San Diego creek watershed in southern California, USA) due to an inhibition of microbial degradation. [162]

Significant seasonal fluctuations of organophosphate concentrations in the surface waters could not be observed.

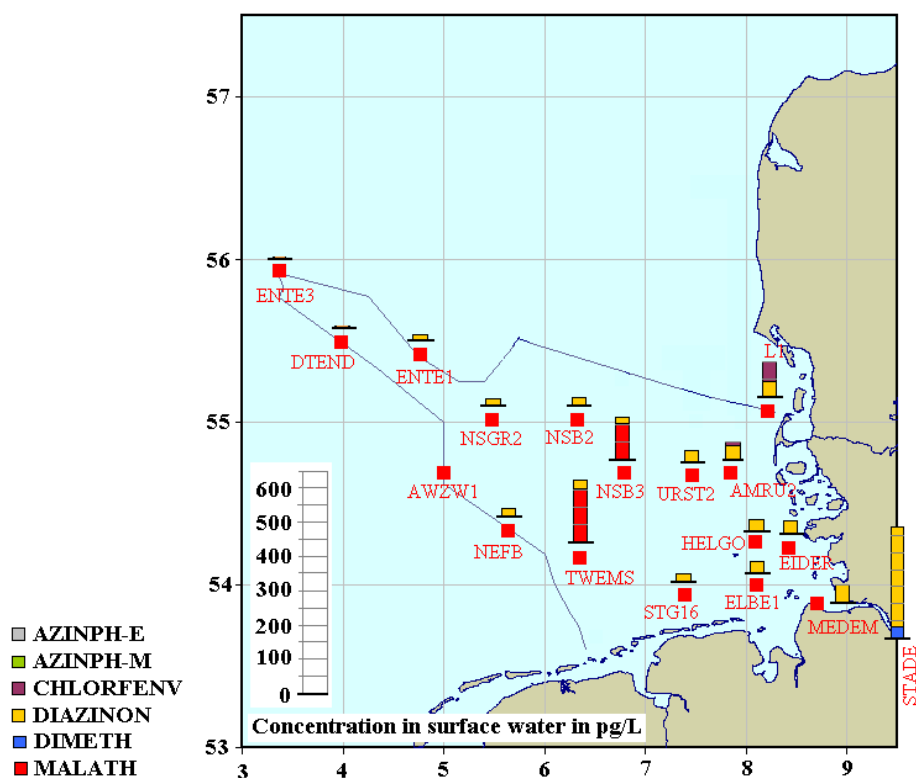


Figure 5.70: Occurrence and distribution of organophosphate insecticides in the aqueous phase of the surface water (5m) of the German EEZ in May/Jun. 2009

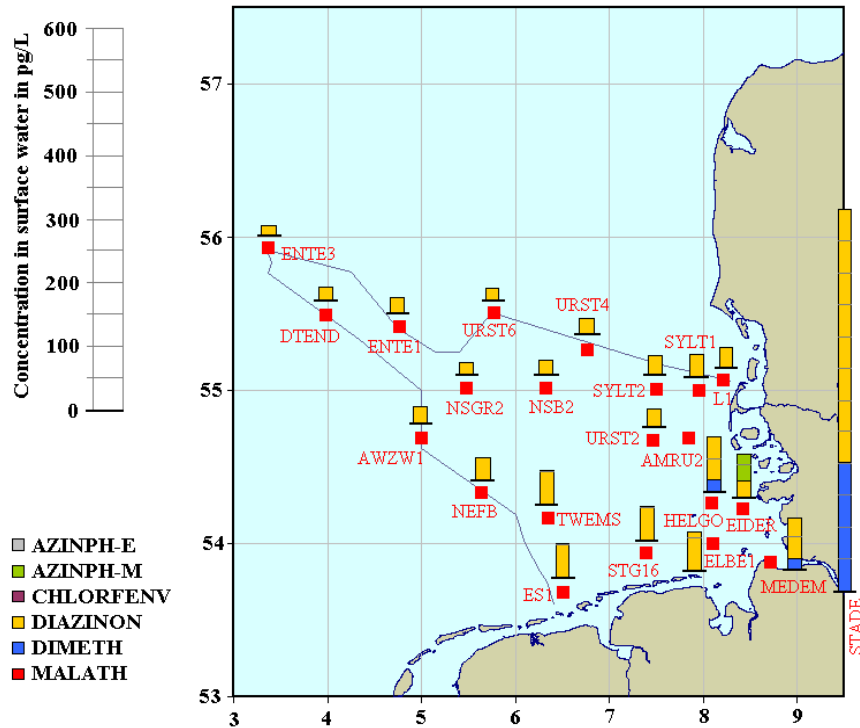


Figure 5.71: Occurrence and distribution of organophosphate insecticides in the aqueous phase of the surface water (5m) of the German EEZ in May 2010

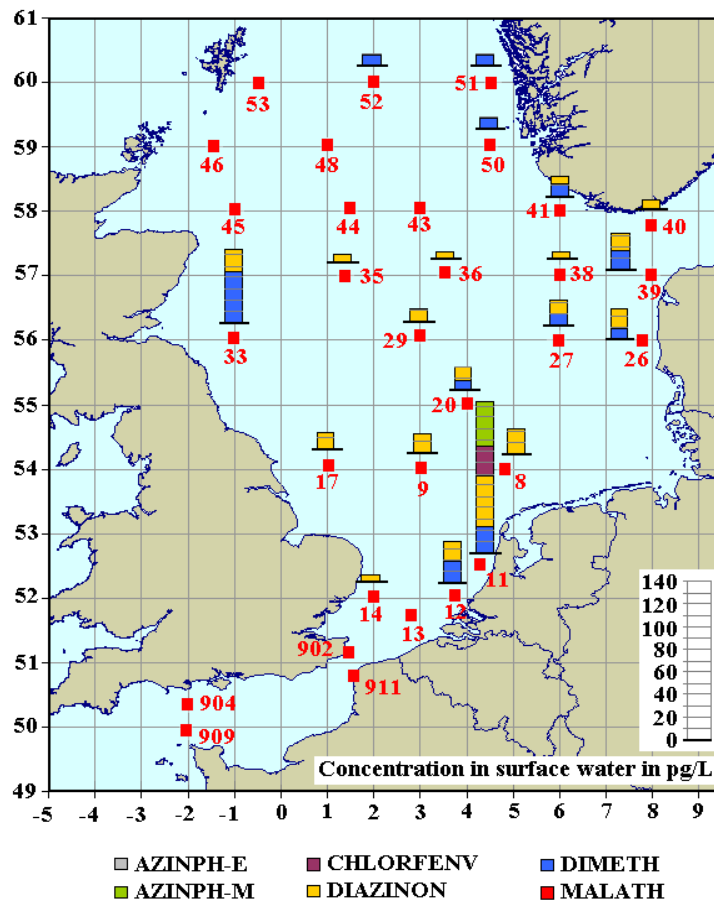


Figure 5.72: Occurrence and distribution of organophosphate insecticides in the aqueous phase of the surface water (5m) of the North Sea in Aug./Sep. 2009

Net flux of diffusive gas exchange of organophosphate insecticides between the marine atmosphere and the surface water

Due to the limited data, the direction of the net flux of diffusive gas exchange could be exclusively investigated for diazinone at three sampling sites in the North Sea (figure 5.73). Whenever occurring in the atmosphere, a dry gaseous deposition of diazinone was calculated supporting the conclusions derived from the spatial distribution of organophosphates in surface seawater and the marine atmosphere.

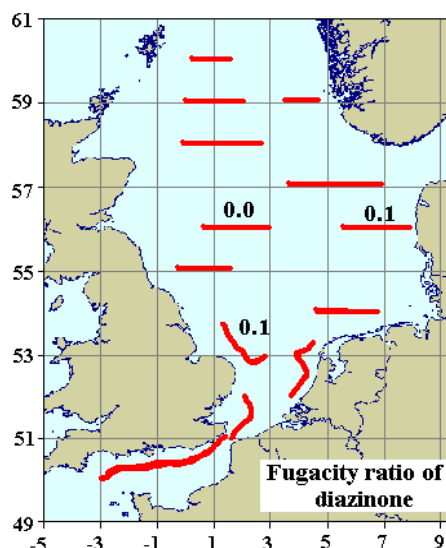


Figure 5.73: Net flux of diffusive gas exchange of diazinone between the surface water and the atmosphere of the North Sea in Aug./Sep. 2009; Fugacity ratio < 0.5: Atmosphere → Sea; Fugacity ratio > 2: Sea → Atmosphere

Conclusions

The targeted organophosphate insecticides were minor surface seawater contaminants. This could be attributed to their short persistence in the environment. ^[162] The absence of the typical concentration gradients from the coastal sampling sites towards the open sea, the presence of diazinone and dimethoate at sampling sites in the central and northern North Sea, the sporadic occurrence in the marine atmosphere originating from air advected from the continent as well as the calculation of the direction of the net flux of diffusive gas exchange provided evidence that atmospheric deposition was the major input pathway of organophosphates to the surface seawaters.

5.1.9 Phenylurea Herbicides

Phenylurea herbicides are intensively applied worldwide since their discovery after the Second World War. They are used for the pre or post emergence weed control in cereals cropping, orchards and cotton fields. Besides, the phenylurea herbicide diuron acts as an algicide in antifouling paints and as total herbicide on roads and railway tracks. Due to their high water solubilities and limited

biodegradation they have come into focus as toxic contaminants of groundwater and surface waters in recent years. ^[163, 164] Six phenylurea herbicides are targeted in this study (table 3.10): diuron (DIURON), fenuron (FENUR), isoproturon (ISOPRUR), chlorotoluron (CHLORTUR), linuron (LINUR) and methabenzthiazuron (METHABZT).

Occurrence and distribution of phenylurea herbicides in the marine atmosphere

Diuron was the most frequently observed phenylurea herbicide in the atmosphere of the German EEZ and the wider North Sea. The atmospheric abundances of diuron were highly variable. Atmospheric concentrations of diuron above the German EEZ in spring 2009 (figure 5.74) and 2010 (figure 5.75) were detected in the range of <LOQ to 20.5 pg/m³ with an arithmetic mean of 4.0 pg/m³ and in the range of 1.6 pg/m³ to 19.2 pg/m³ with an arithmetic mean of 6.6 pg/m³, respectively. In contrast, concentrations of diuron in the range of 0.1 pg/m³ to 38 pg/m³ with an arithmetic mean of 33 pg/m³ were determined in the atmosphere above the North Sea in August/September 2009 (figure 5.76). On average the concentrations of diuron in the marine atmosphere were observed at levels approximately six times higher in summer than in spring. In addition, significantly increased atmospheric diuron abundances could be sporadically determined, e.g., up to 148 pg/m³ in the atmosphere of the North Sea (PE 16) and up to 20 pg/m³ in the atmosphere of the German EEZ (09AT 9). Neither the spatial distribution in the atmosphere nor the sporadic and remarkably increased atmospheric abundances of diuron could be related to the air mass history. A similar distribution pattern in the atmosphere could be documented for fenuron. It was temporarily determined in the marine atmosphere, apparently not related to air mass history. Typical concentrations were found in the range of <LOQ to 5.0 pg/m³. Even sporadically high atmospheric abundances of fenuron were observed, similar to the occurrence of diuron. For example, up to 18 pg/m³ (PE1) and 105 pg/m³ (10AT 5) could be determined in the atmosphere above the German EEZ in May 2010 (figure 5.75) and above the North Sea in August/September 2009 (figure 5.76), respectively. Chlorotoluron, isoproturon and linuron were scarcely detected in the marine atmosphere of the German EEZ and the wider North Sea (figure 5.74-5.76). They occurred independently of each other predominantly in air masses, which had passed the continent within the last 24 hours (chapter 3.5). Atmospheric concentrations of <1 pg/m³, 0.2 pg/m³ to 2.6 pg/m³ and 1 pg/m³ to 3 pg/m³ could be determined, respectively. Methabenzthiazuron was never detected in any air sample.

Phenylurea herbicides were most frequently detected in the atmosphere of the Baltic Sea, in particular at the sampling sites west of 16°E (figure 5.77). This might be attributed to the proximity of those sampling sites to the continent as well as to the increased sample volumes of a factor 2 to 3 of the Baltic Sea campaign (chapter 3.2). All targeted phenylurea herbicides except methabenzthiazuron were detected. Isoproturon was most frequently observed and reached the

highest concentrations among the phenylurea herbicides in the marine atmosphere of the Baltic Sea, as high as 22 pg/m³. This finding was corresponding with the fact that isoproturon was currently the most intensively applied pesticide in European cereal production. ^[163] Fenuron, linuron, chlortoluron and diuron were quantified in maximum concentrations of 11.6 pg/m³, 5.4 pg/m³, 3.4 pg/m³ and 1.4 pg/m³, respectively. The highest atmospheric abundances and a diversified spectrum of phenylurea herbicides could be determined at the sampling sites west of 16°E (AL1 – AL6), which were affected by air masses travelling over land. In contrast, the sampling sites east of 16°E (AL7 – AL10) showed lowest atmospheric concentrations and a decreased spectrum of phenylurea herbicides. Exclusively fenuron, isoproturon and diuron could be quantified at these sampling sites. This was ascribed to the influence of air masses passing the sea within the last 24 hours (air mass backward trajectory analysis in chapter 3.5 and annex 4). However, different concentration gradients from the western to the eastern sampling sites were documented for the individual phenylurea herbicides. The atmospheric concentrations of chlortoluron, linuron and isoproturon displayed a significant decrease in relation to the air mass history, whereas on average diuron and fenuron were quantified in the same concentrations throughout all sampling sites. In addition, fenuron displayed a sporadically increased atmospheric concentration of 11.6 pg/m³ (AL6), whereas its average atmospheric concentration was approximately 2.5 pg/m³.

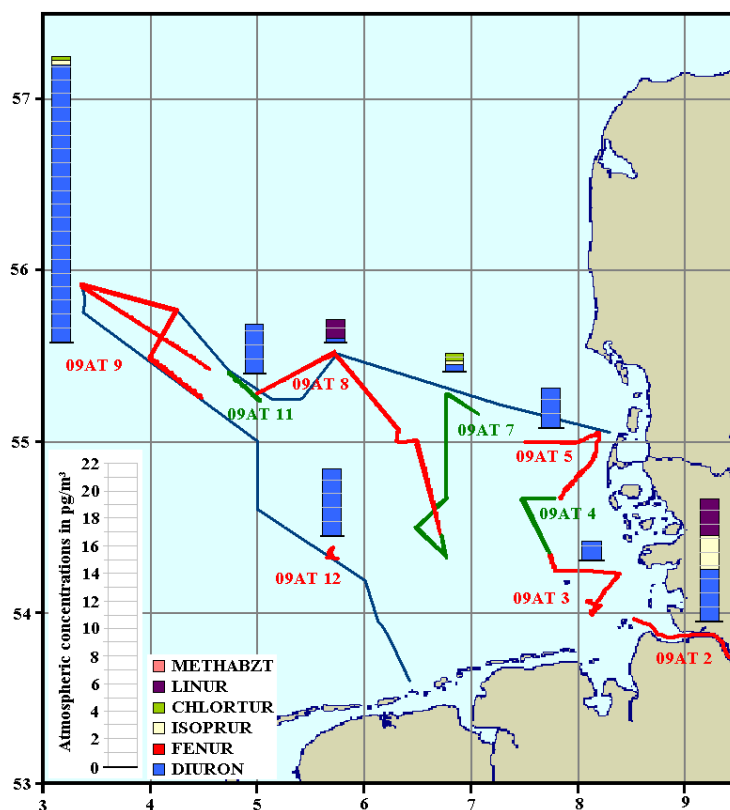


Figure 5.74: Atmospheric bulk concentrations of phenylurea herbicides above the German EEZ in May/June, 2009

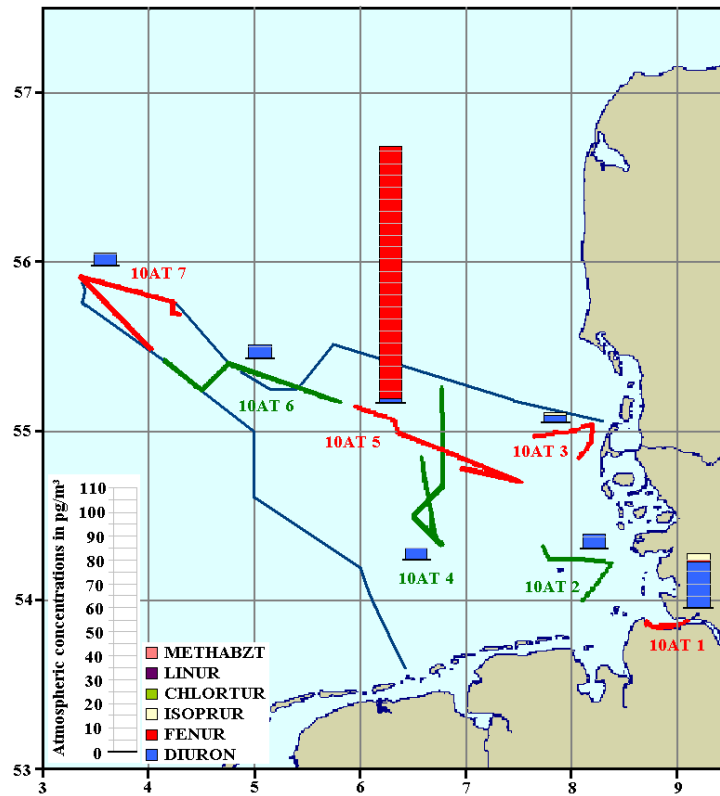


Figure 5.75: Atmospheric bulk concentrations of phenylurea herbicides above the German EEZ in May 2010

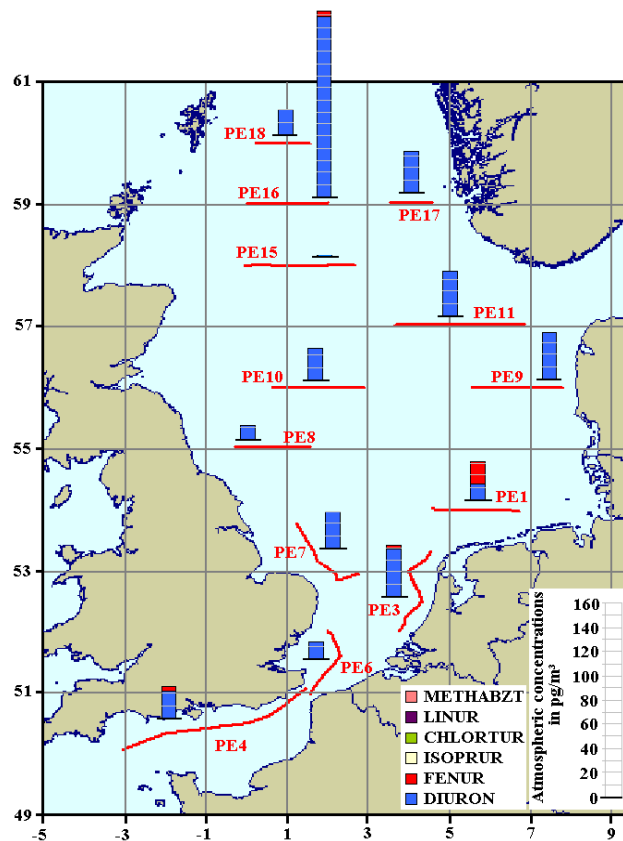


Figure 5.76: Atmospheric bulk concentrations of phenylurea herbicides above the North Sea in Aug./Sep. 2009

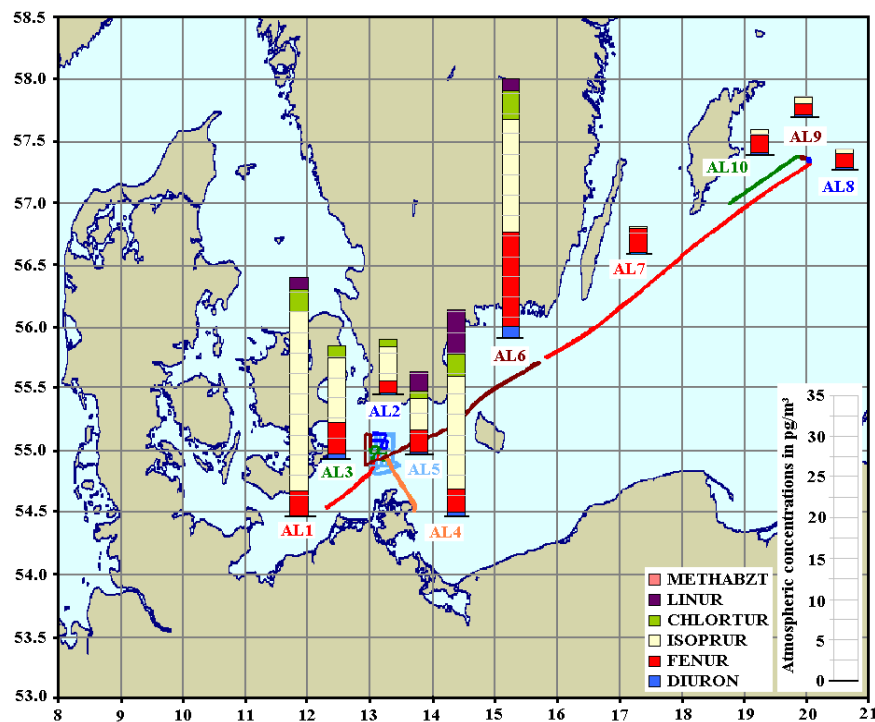


Figure 5.77: Concentrations of phenylurea herbicides in the gaseous mass fraction of the atmosphere above the Baltic Sea in Apr. 2009

To sum up, the occurrence of isoproturon, chlortoluron and linuron in the marine atmosphere of the German EEZ, the wider North Sea and the Baltic Sea was determined by the advection of air masses from continent. In contrast, the atmospheric abundances of diuron and fenuron did not follow the same pattern: The side-by-side air sampling experiments performed in Sülldorf/Hamburg in December 2010 (chapter 3.2/4.1.1 and annex 1) displayed temporarily increased atmospheric abundances of diuron and fenuron, which were significantly different to the concentration determined in the air sample collected side by side. In contrast, isoproturon displayed no significant aberrations in side-by-side air sampling experiments (table 5.7). For this reason, the remarkably increased concentrations of diuron in the air samples 09AT 9 and PE 16 as well as fenuron in the air samples 10AT 5 and AL 6 could be regarded as outliers. Furthermore, the method validation (chapter 4) gave no indication for a systematic error in air sample analysis or an interference in mass transitions of the mass spectrometer methods. Thus, the results of diuron and fenuron plotted in figures 5.74 – 77 may be accepted as true environmental concentrations. However, questions came up concerning the atypical occurrence of diuron and fenuron in air masses of different origin in the atmosphere. In consequence, further verifications of the performances of the air sample preparation methods and mass spectrometer analysis of diuron and fenuron would be necessary for a supplementary validation of these results. As listed in table 5.7 aberrations in the concentrations of air samples collected side-by-side predominantly originated from the analysis of the gaseous mass fraction of the atmosphere. Hence, an important complement

of the method validation might be an investigation of the matrix influence on the ionisation process in the ion source of the mass spectrometer, e.g. by post-column infusion experiments. ^[165] Excluding a systematic error in air sample analysis, it could be supposed that local sources at the sampling sites itself significantly contributed to the diuron and fenuron abundances. Possible local sources of diuron and fenuron could be the biocide containing antifouling paints, which were presumably ubiquitous at all ship based sampling sites and were even applied during sea cruises. However, fumigation from antifouling paints did not explain the outliers in side-by-side sampling experiments in Sülldorf/Hamburg.

Table 5.7: Atmospheric concentrations of diuron and fenuron in Sülldorf/Hamburg in December 2010 determined during the side-by-side air sampling experiments

Diuron [pg/m ³]	Active air sampler 1			Active air sampler 2		
	cp	cg	sum	cp	cg	sum
R1	0.64	0.00	0.64	0.59	0.36	0.95
R2	0.94	2.96	3.90	0.83	4.11	4.94
R3	0.52	0.00	0.52	0.53	0.00	0.53
R4	2.14	0.00	2.14	2.41	9.72	12.14
R5	0.33	0.00	0.33	0.00	9.15	9.15
R6	0.75	5.06	5.81	0.00	0.00	0.00
R7	0.00	0.00	0.00	0.00	0.00	0.00
R8	2.81	0.00	2.81	0.97	9.53	10.51
R9	0.00	6.88	6.88	0.00	6.66	6.66
R10	0.00	7.59	7.59	0.00	5.82	5.82

Fenuron [pg/m ³]	Active air sampler 1			Active air sampler 2		
	cp	cg	sum	cp	cg	sum
R1	1.50	0.89	2.39	0.68	0.66	1.35
R2	0.77	0.34	1.11	0.46	0.26	0.72
R3	1.98	0.68	2.66	1.34	48.21	49.55
R4	2.90	0.34	3.23	1.39	0.00	1.39
R5	0.68	0.31	0.99	0.48	0.00	0.48
R6	0.39	0.47	0.86	0.21	0.51	0.72
R7	0.34	1.95	2.29	0.32	1.71	2.04
R8	0.00	1.82	1.82	0.00	0.00	0.00
R9	0.62	0.00	0.62	0.43	0.00	0.43
R10	0.64	0.00	0.64	0.50	0.00	0.50

Isoproturon [pg/m ³]	Active air sampler 1			Active air sampler 2		
	cp	cg	sum	cp	cg	sum
R1	18.91	0.25	19.16	19.76	0.00	19.76
R2	0.49	0.00	0.49	0.54	0.00	0.54
R3	2.06	0.00	2.06	2.41	0.00	2.41
R4	2.00	0.00	2.00	1.93	0.00	1.93
R5	0.51	0.00	0.51	0.46	0.00	0.46
R6	0.29	0.00	0.29	0.27	0.00	0.27
R7	0.00	0.00	0.00	0.00	0.00	0.00
R8	0.30	0.04	0.34	0.26	0.00	0.26
R9	0.49	0.00	0.49	0.31	0.00	0.31
R10	0.32	0.00	0.32	0.41	0.00	0.41

Seasonal variations in atmospheric concentrations

The PUF disk passive air samplers exposed at Tinnum/Sylt and Sülldorf/Hamburg displayed seasonal profiles in the atmospheric abundances of diuron, chlortoluron and isoproturon. In contrast, the atmospheric occurrence of fenuron, linuron and methabenzthiazuron was not documented by the passive air samplers (figure 5.78).

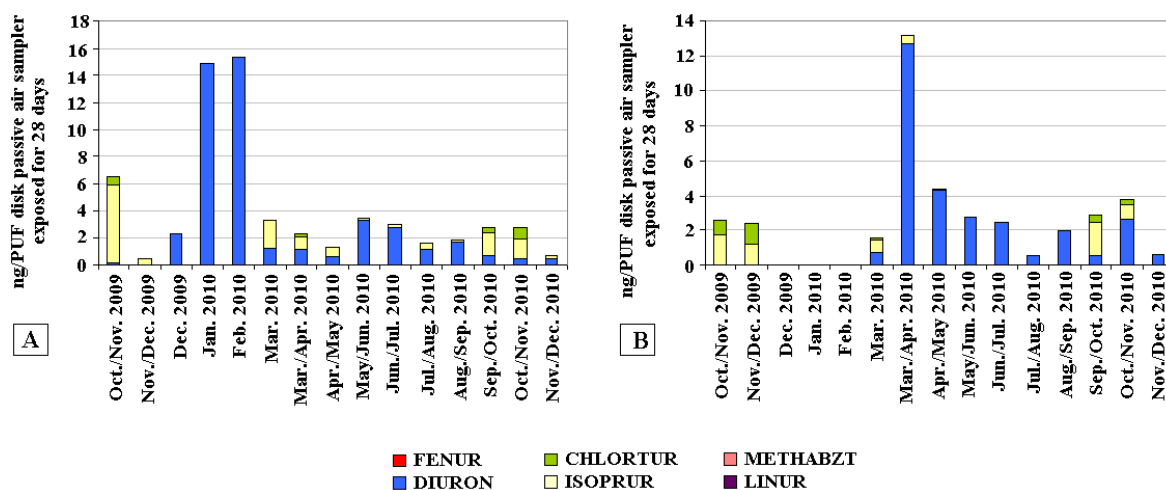


Figure 5.78: Seasonal variations in the atmospheric abundances of phenylurea herbicides observed at the sampling sites Sülldorf/Hamburg (A) and Tinnum/Sylt (B)

Isoproturon was detected almost throughout the entire year at the sampling site Sülldorf/Hamburg. Highest atmospheric abundances were monitored within September to November. A comparable seasonal profile, but decreased concentrations could be documented for the coastal sampling site Tinnum/Sylt. Chlortoluron displayed the same seasonality as isoproturon with lower atmospheric abundances. The increased atmospheric concentrations of isoproturon and chlortoluron in autumn might be related to agricultural usage, i.e. the pre-emergence weed control in winter crops.

Diuron was the most frequently observed phenylurea herbicide and was detected almost throughout the year. Highest atmospheric abundances were documented for January to February 2010 in Sülldorf/Hamburg, whereas the highest concentrations at Tinnum/Sylt were monitored in March/April. The disagreement of the periods of maximum concentrations of diuron as well as the comparability of atmospheric abundances at the individual sampling sites might be related to diffusive and predominantly local sources to the atmosphere. In addition, a rapid transformation of diuron during atmospheric transport was observed in a previous study supporting this perception.

[166] Similar observations were reported for the occurrence of diuron in rain water samples from urban and rural sampling sites in the Alsace region in eastern France: Diuron was detected throughout the year with episodic maxima in wet deposition samples. [57] This temporal pattern

corresponded to the atmospheric abundances of diuron monitored using the PUF disk passive air samplers. No pronounced seasonality of diuron was observed at any of the sampling sites.

Gas-particle partitioning

The phenylurea herbicides underwent gas-particle partitioning in the atmosphere. Chlortoluron, isoproturon and linuron were predominantly present in the particle associated mass fraction of the atmosphere (> 80 % of the bulk atmospheric concentration). In contrast diuron and fenuron were primarily quantified in the gaseous mass fraction (> 80 % of the bulk atmospheric concentration). The occurrence of the phenylurea herbicides in the particle associated mass fraction was only partly consistent with their vapour pressures. Only fenuron and linuron are semivolatile (5.0 mPa and 0.2 mPa at 25 °C, respectively ^[150]) indicating a significant occurrence in the gaseous mass fraction of the atmosphere. However, linuron was detected in the particle associated mass fraction, whereas diuron occurred predominantly in the gaseous mass fraction of the atmosphere. This might be attributed to blow-on and blow-off effects accompanied with active air sampling methods (chapter 3.1.1) and provided further indications of a systematic error in the analysis of phenylurea herbicides as discussed above.

Occurrence and distribution of phenylurea herbicides in the surface seawater

The targeted phenylurea herbicides displayed similar distribution patterns throughout the surface waters of the German EEZ (figure 5.79 – 5.80) and the wider North Sea. (figure 5.81), which were comparable to those of the triazine herbicides summarized in chapter 5.1.7. Important input sources of phenylurea herbicides to the surface seawaters were the rivers. This was displayed by the characteristic river plumes, especially of the Elbe and the Rhine as well as the strong decreasing concentrations beyond these regions in relation to the prevailing sea currents (chapter 3.6). Besides, the outflow of the Baltic Sea affected the occurrence of phenylurea herbicides in the northeast of the North Sea. Diuron was quantified in the highest concentrations of the targeted phenylurea herbicides. It was observed throughout all sampling sites of the German EEZ and the North Sea in concentrations ranging from 150 pg/L to 15000 pg/L and 130 pg/L to 2700 pg/L, respectively. Isoproturon, chlortoluron and fenuron displayed the same overall distribution, but were detected in significantly lower concentrations ranging from 11 pg/L to 980 pg/L, 6 pg/L to 830 pg/L and 7 pg/L to 87 pg/L in the North Sea in Aug./Sep. 2009, respectively. In contrast, methabenzthiazuron and linuron could be exclusively determined at sampling sites inside or adjacent to river plumes and the Baltic Sea outflow. Maximum concentrations in the ranges of 100 pg/L to 150 pg/L and 100 pg/L to 325 pg/L were quantified within the sampling campaigns in the river plumes, respectively. It might be assumed that the overall occurrence of diuron, isoproturon, chlortoluron and fenuron at northern sampling sites, which were influenced by the

inflow of the Atlantic Ocean originated from atmospheric deposition. In particular, the increased concentrations of diuron might be attributed to atmospheric transport and deposition processes, considering the predominant occurrence in the atmosphere described above. In addition, the application of diuron as biocide in antifouling paints for ship maintenance ^[163, 164] could be additionally contributed to the widespread distribution in surface seawater and the increased surface water concentrations.

In contrast, the concentration gradients documented for the Baltic Sea (figure 5.82) were lower and displayed less variation in the surface water concentrations of phenylurea herbicides in the central Baltic Sea. Lowest concentrations of the sum of these substances were detected in the Bothnian Bay (35, 37, BB3), which were comparable to those observed in the central and northern North Sea. Highest abundances of phenylurea herbicides were quantified adjacent to the Gulf of Finland (52, 53, 54) and in the western Baltic Sea, Kattegat and Skagerrak. All targeted phenylurea herbicides, except linuron were detected throughout all sampling sites. Linuron was exclusively observed in the southern Baltic Sea. The spatial distributions of phenylurea herbicides in the surface water of the Baltic Sea showed no indications of atmospheric deposition.

Seasonal fluctuations in the surface water concentrations of phenylurea herbicides could be observed in the German EEZ in 2009 (figure 5.83). The amplitude of the seasonal variations decreased with increasing distance to the river estuary of the Elbe. Highest surface water concentrations of isoproturon, chlortoluron, linuron and methabenzthiazuron were determined in May. In contrast, maximum abundances of fenuron were quantified in November. Diuron displayed no significant seasonal profile in surface seawater concentrations, which was consistent with its atmospheric abundances. The different seasons of maximum surface water concentrations of the individual phenylurea herbicides were consistent with their application in pre- as well as post-emergence wheat control, not necessarily in combination with each other and during the whole vegetation period. In consequence, the seasonal fluctuations of phenylurea herbicide abundances in the surface water might be only partly coincide with their seasonal variations in atmosphere, due to differences in atmospheric and hydrospheric transports. Although atmospheric concentrations of chlortoluron and isoproturon were quantified in autumn, an occurrence could even be observed in spring at both sampling sites, which partly confirmed the seasonal profile in surface seawater concentrations.

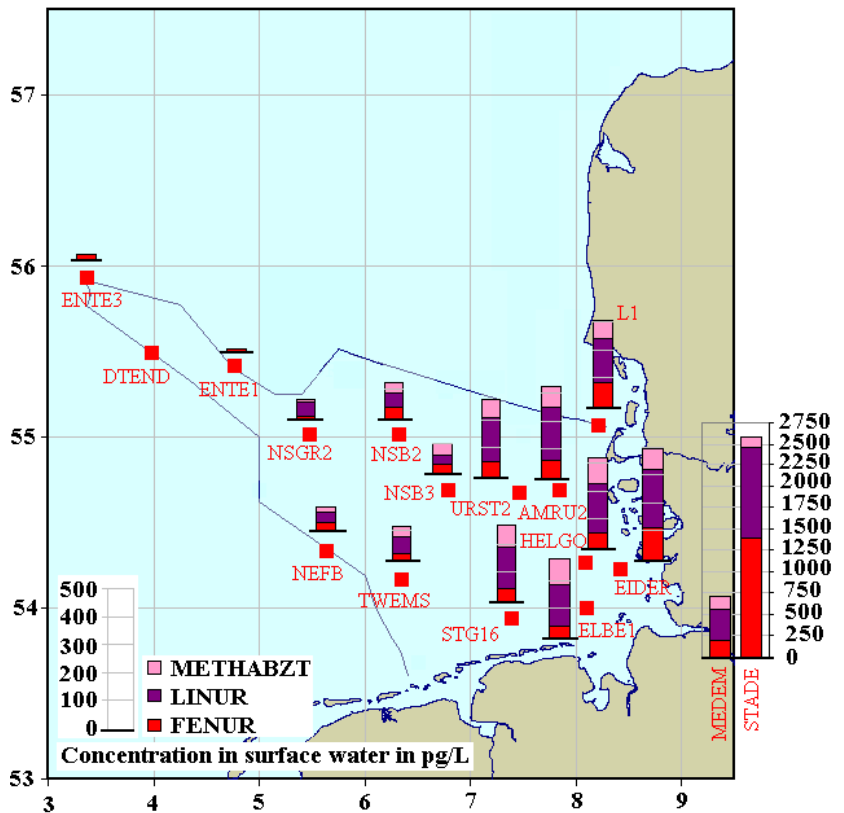
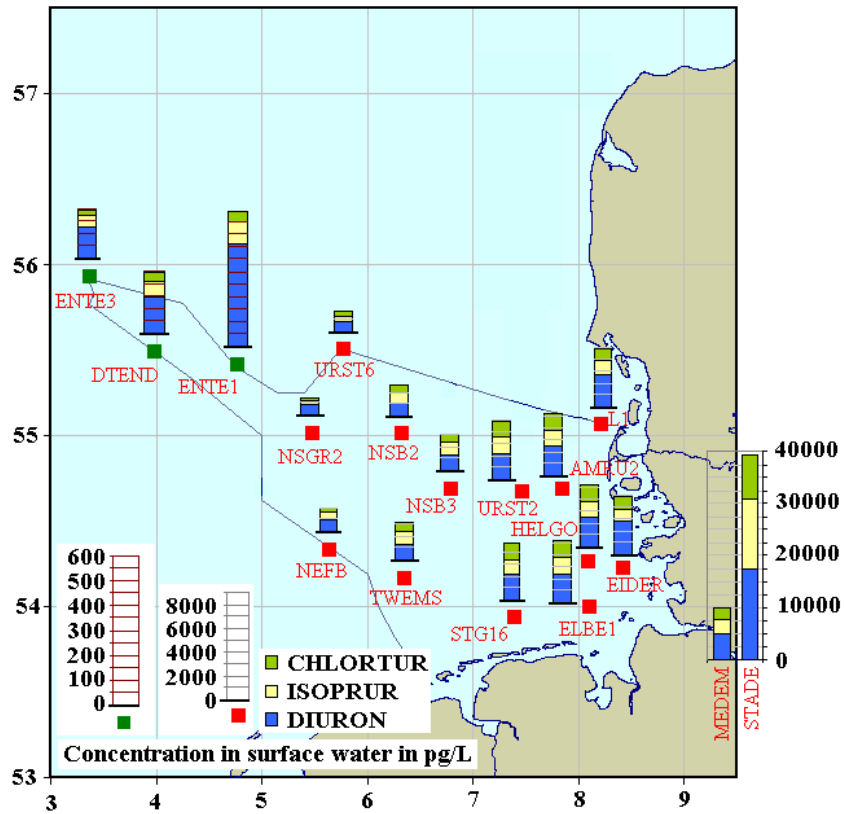


Figure 5.79: Occurrence and distribution of phenylurea herbicides in the aqueous phase of the surface water (5 m) of the German EEZ in May/Jun. 2009; Note the different concentration scales in both figures

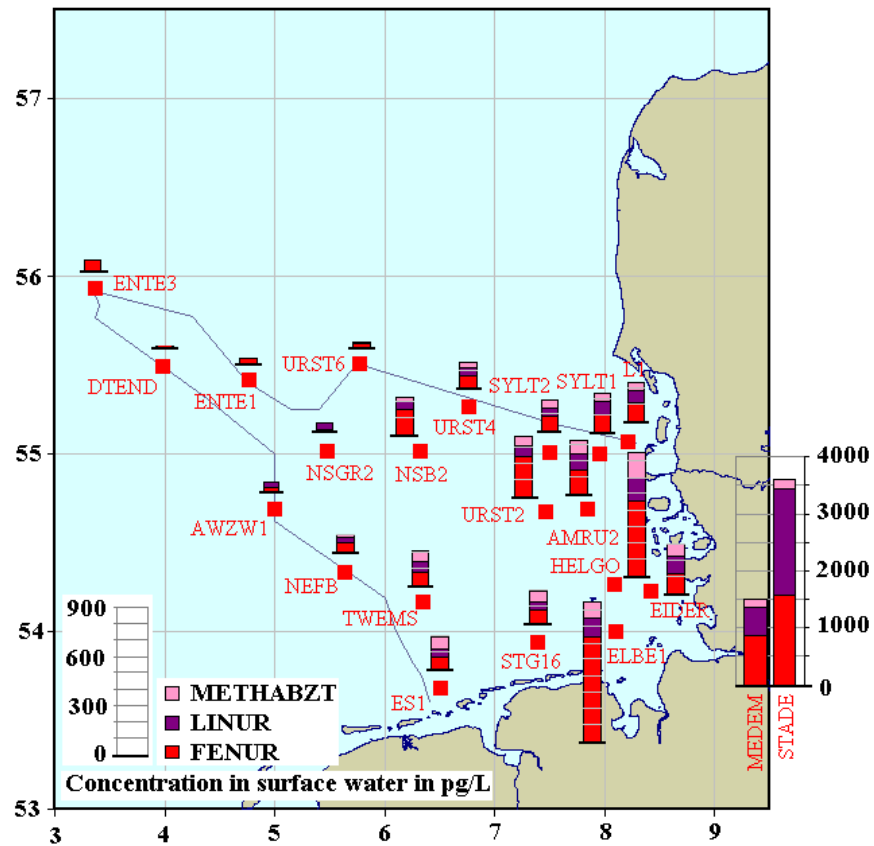
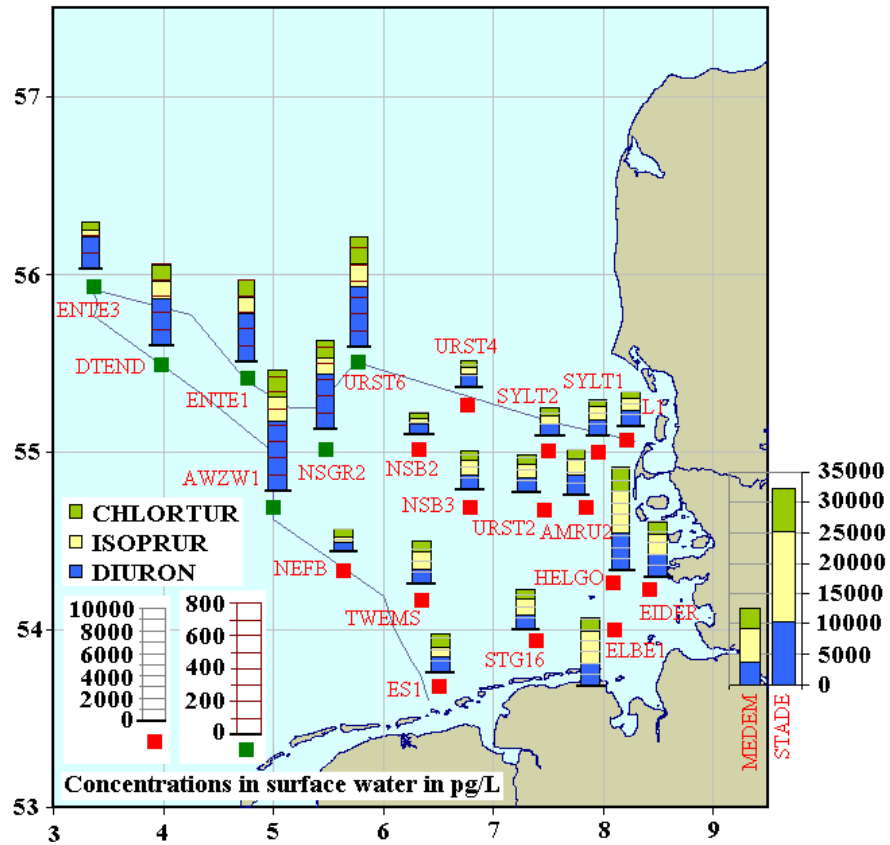


Figure 5.80: Occurrence and distribution of phenylurea herbicides in the aqueous phase of the surface water (5 m) of the German EEZ in May 2010; Note the different concentration scales in both figures

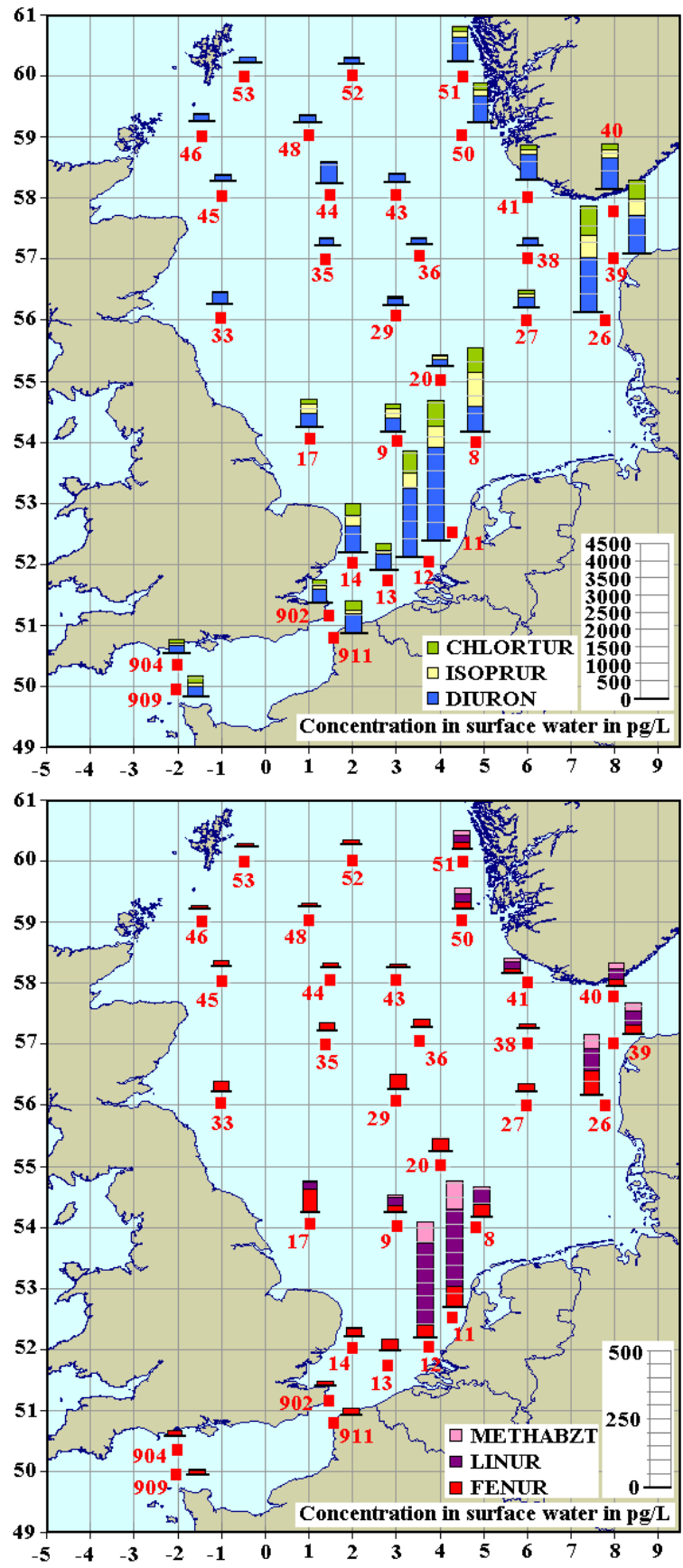


Figure 5.81: Occurrence and distribution of phenylurea herbicides in the aqueous phase of the surface water (5 m) of the North Sea in Aug./Sep. 2009

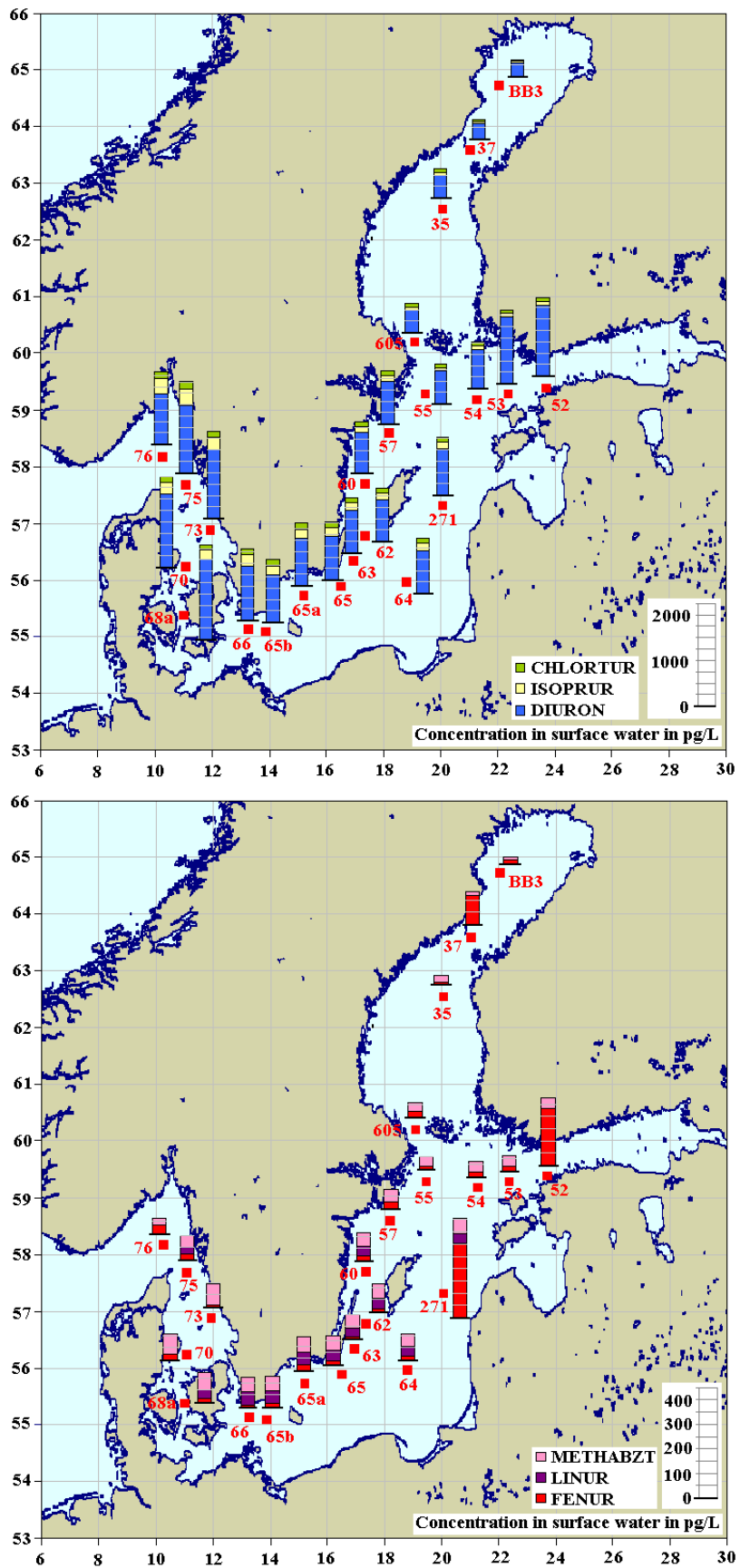


Figure 5.82: Occurrence and distribution of phenylurea herbicides in the aqueous phase of the surface water (6 m) of the Baltic Sea in Jun./Jul. 2008

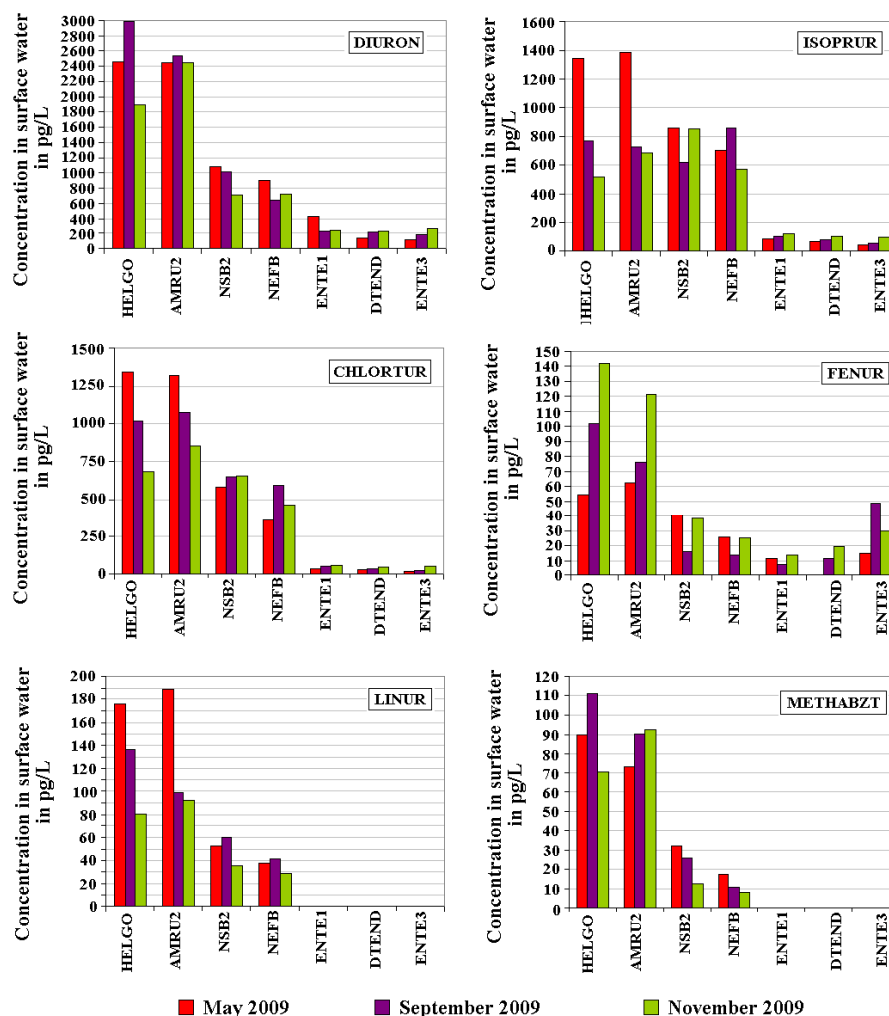


Figure 5.83: Seasonal variations in the surface water concentrations (5 m) of the phenylurea herbicides displayed for selected sampling sites in the German EEZ in 2009; The sampling sites are sorted from left to right by increasing meridional distance from the Elbe estuary

Net flux of diffusive gas exchange of phenylurea herbicides between the marine atmosphere and the surface water

The direction of the net flux of diffusive gas exchange of phenylurea herbicides between the marine atmosphere and the surface water was calculated for isoproturon, chlortoluron and linuron within the Baltic Sea. The results always indicated a net atmospheric deposition with fugacity ratios (f_w/f_a) of 0.0. The fugacity ratios could not be calculated for the German EEZ and the wider North Sea, because isoproturon, chlortoluron and linuron were exclusively quantified in the particle associated mass fraction of the marine atmosphere. Diuron and fenuron were predominantly observed in the gaseous mass fraction of the atmosphere and prone to dry gaseous deposition. However, the inconsistencies in atmospheric abundances and gas-particle partitioning discussed above would require additional investigations in order to reach consistent conclusions.

Methabenzthiazuron was never detected in any air sample and thus was not expected to undergo significant gaseous exchange processes.

The Henry's law constants for the individual phenylurea herbicides are $<0.7 \text{ mPa m}^3 \text{ mol}^{-1}$ [150]. In consequence, a dry gaseous atmospheric deposition of phenylurea herbicides would be supposed, whenever occurring in the gaseous mass fraction of the marine atmosphere. Besides, the low HLCs pointed to a negligible revolatilisation processes of phenylurea herbicides from surface seawater.

Conclusions

The spatial distribution of phenylurea herbicides in the surface water of the German EEZ and the wider North Sea indicated that the rivers and the Baltic Sea outflow were major input sources. Furthermore, the results of this study pointed to an atmospheric deposition of phenylurea herbicides, which might significantly contributed to the surface seawater contamination beyond coastal sampling sites.

All targeted phenylurea herbicides except of methabenzthiazuron were detected in the marine atmosphere. The occurrence of isoproturon, chlortoluron and linuron was found to be determined by the advection of continental contaminated air masses. They were predominantly present in the particle associated mass fraction limiting their lifetimes in atmosphere due to their vulnerability to dry as well as wet deposition processes. In addition, their Henry's Law Constants pointed to an atmospheric deposition of the gaseous mass fraction as well as to a negligible revolatilisation from the contaminated surface waters. Although, diuron and fenuron revealed similar vapour pressures, $\log K_{OWS}$ and HLCs as the other targeted phenylurea herbicides, they did not follow the same distribution patterns. [150] The overall occurrence of diuron as well as the sporadic occurrence of fenuron in the marine atmosphere was unaffected by the air mass history. Besides, both components were observed throughout all water sampling sites, whereas the surface water concentrations of chlortoluron, isoproturon, linuron and methabenzthiazurion decreased below LOQ at the remote sampling sites. In contrast, fenuron and diuron were even detected in remarkably amounts in the northern North Sea, where the sea currents were determined by the inflow of the Atlantic Ocean. The widespread distribution of diuron and fenuron in the surface seawater indicated atmospheric deposition. Moreover, the application of diuron as biocide in antifouling paints [163, 164] for ship maintenance might have contributed to its widespread distribution.

Pronounced seasonal concentration profiles of phenylurea herbicides were neither detected in air nor in surface seawaters. This could be attributed to their on-going usage for pre-and post-emergence weed control during the entire vegetation period as well as their application as biocides, e.g., on roads and railway tracks. [163, 164]

5.1.10 Phenoxyalkanoic acid and Thiadiazine Herbicides

Phenoxyalkanoic acid herbicides have been discovered and registered after the Second World War in the 1950s. Besides their extensive application for post-emergence weed control in industrial agriculture, they are also used as home and garden herbicides and even occur in industrial products, e.g. as root protection agents in flat roof sealings. Although phenoxyalkanoic acids undergo microbial as well as photochemical decomposition their high mobility in soil enables the penetration of the ground water, which has raised concern in recent years. ^[167-169] Four phenoxyalkanoic acids of which two are phenoxyacetic acids (24-D, MCPA) and further two are phenoxypropionic acids (DICHLPR, MECOPR) are targeted in this study. Bentazone (BENTAZ) is a thiadiazine herbicide. It is used as a post-emergence herbicide in early spring to summer for the weed control in industrial agriculture. Bentazone is rapidly degraded in the environment and reveals half lives in soil of 3-21 days. Nevertheless, it was regionally observed in the groundwater. ^[170]

Occurrence and distribution of phenoxyalkanoic acids and bentazone in the marine atmosphere

Data of the targeted phenoxyalkanoic acids was exclusively available for the particle associated mass fraction of the atmosphere above the German EEZ and the wider North Sea (figures 5.84-5.86), due to their instability during Soxhlet extraction. Atmospheric concentrations of phenoxyalkanoic acids above the Baltic Sea were not available, because only the adsorber cartridges were provided to this study, which were extracted in the Soxhlet apparatus.

All targeted phenoxyalkanoic acids occurred sporadically and independent of each other in the particle associated mass fraction of the marine atmosphere. MCPA was the most frequently observed phenoxyalkanoic acid. It could be quantified in concentrations ranging from 0.47 pg/m³ to 11.1 pg/m³. The phenoxypropionic acids mecoprop and dichlorprop could be determined in the atmosphere above the river Elbe in concentrations ranging between 1.4 pg/m³ to 3.1 pg/m³ and 2.1 pg/m³ to 7.3 pg/m³, respectively. Besides, mecoprop was even detected in a single air sample of the marine atmosphere (PE 7) in a concentration of 0.5 pg/m³. The phenoxyethanoic acids occurred more frequently and in higher concentrations in the marine atmosphere than the phenoxypropionic acids. This might be attributed to the higher volatility of the phenoxyethanoic acids ^[150] increasing the chances for input and longer residence times in the atmosphere and thus the transport and distribution by advection of contaminated air masses.

Phenoxyalkanoic acids were almost exclusively present in the air advected from the continent (24 hours backward trajectories, chapter 3.5 and annex 4) and at sampling sites close to the coast. A relation of the atmospheric abundances of phenoxyalkanoic acids to the air mass history could be

partly observed. For example, 24-D was exclusively observed in highest concentrations in the air masses originating from France (PE 6, PE 4) during the research cruise in the North Sea in Aug./Sep. 2009 (figure 5.86). Besides, MCPA occurred in highest abundances in the air masses passing land (09AT 2, 09AT 7, 09AT 8) during the sampling campaign in the German EEZ in May/Jun. 2009 (figure 5.84). However, the air mass history did not facilitate a sufficient interpretation of the spatial distribution of phenoxyalkanoic acids in the marine atmosphere. This had been already observed for further currently used pesticides targeted in this study, e.g., for the phenylurea herbicides fenuron and diuron (chapter 5.1.9) and might be attributed to the widespread usage of herbicides in antifouling agents and as biocides resulting in a variety of diffusive sources to the environment beyond agriculture. Moreover, blow off effects (chapter 3.1.1) from the GFFs during active air sampling could not be excluded to distort the particle collection and thus the results illustrated in figures 5.84-5.86.

The thiadiazine herbicide bentazone was stable during Soxhlet extraction. Hence, a complete data set for bentazone could be documented. Bentazone was exclusively detected in three air samples of the marine atmosphere obtained during the research cruise in the German EEZ in May/Jun. 2009 and a single air sample of the Baltic Sea (AL2). The concentrations were highly variable even in those air masses exhibiting identical 24 hours air mass backward trajectories (09AT 7, 09AT 8). The bulk concentrations of bentazone varied between 0.1 pg/m^3 and 12.0 pg/m^3 .

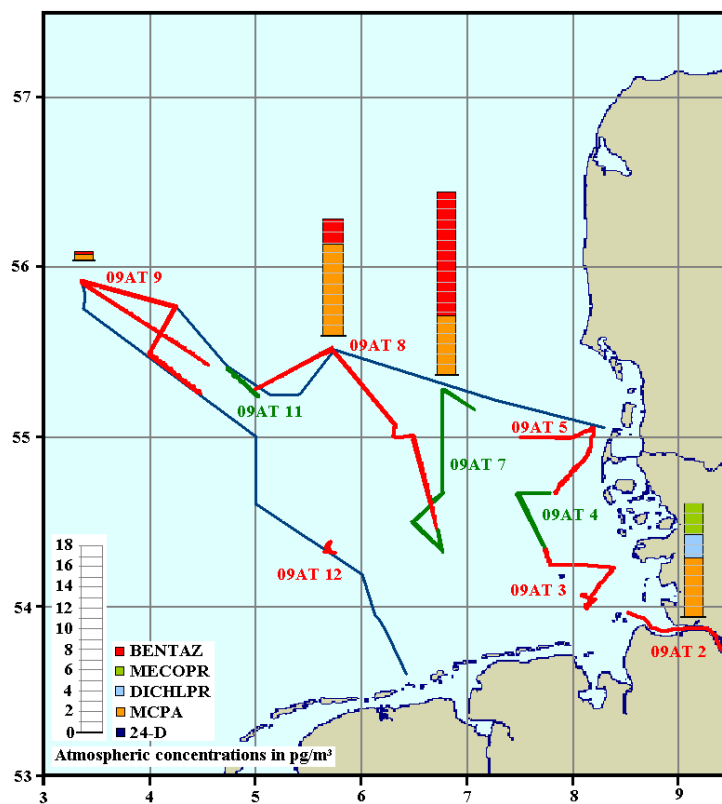


Figure 5.84: Atmospheric concentrations of phenoxyalkanoic acids (gaseous mass fraction) and bentazone (bulk concentrations) above the German EEZ in May/Jun. 2009

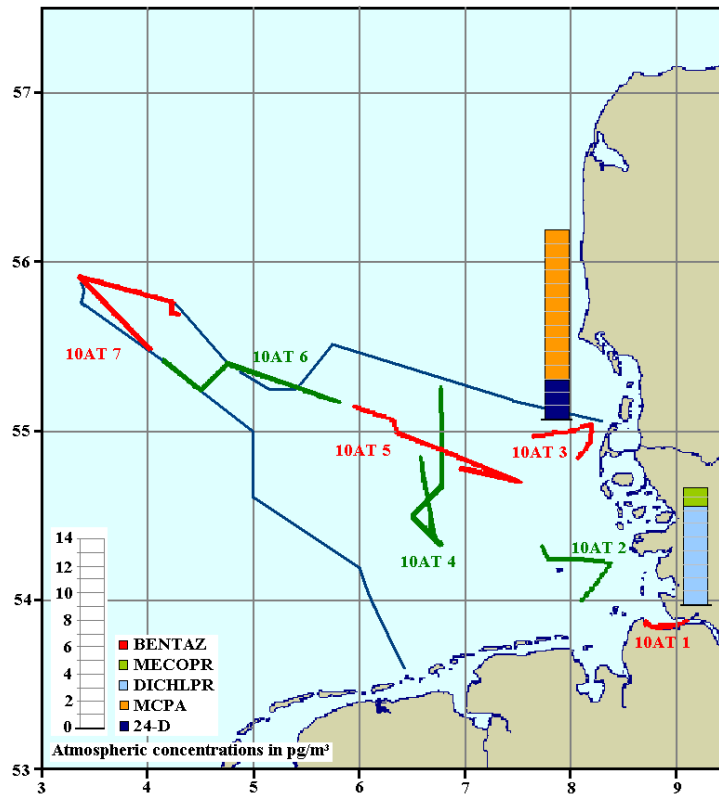


Figure 5.85: Atmospheric concentrations of phenoxyalkanoic acids (gaseous mass fraction) and bentazone (bulk concentrations) above the German EEZ in May 2010

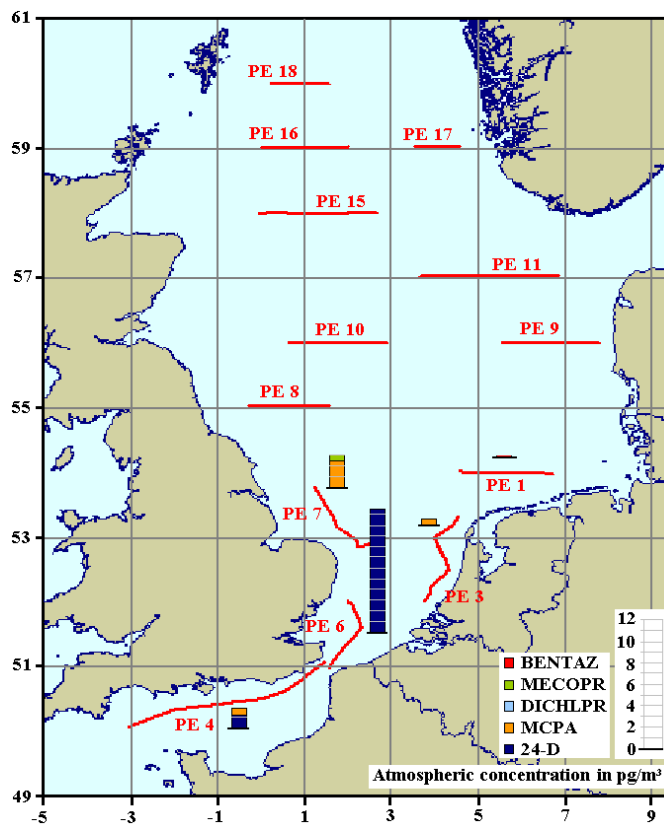


Figure 5.86: Atmospheric concentrations of phenoxyalkanoic acids (gaseous mass fraction) and bentazone (bulk concentrations) above the North Sea in Aug./Sep. 2009

Seasonal variations in atmospheric bentazone concentrations

A seasonal profile of bentazone could be monitored by the PUF disk passive air samplers in Sülldorf/Hamburg and Tinnum/Sylt (figure 5.87). Bentazone was exclusively quantified from early spring (March) to early summer (June), which was in agreement with the main application season in agriculture.^[170] The active air sampling campaigns in the German EEZ (figures 5.84-5.85) took place during this season. However, bentazone could be exclusively detected in the marine atmosphere during the sampling campaign in 2009 (figure 5.84). This might be related to the prevailing air masses from the open sea collected in 2010 (chapter 3.5).

Seasonal profiles of phenoxyalkanoic acid herbicides in the atmosphere could not be investigated, due to their transformation during the Soxhlet extraction of the PUF disk passive air samples.

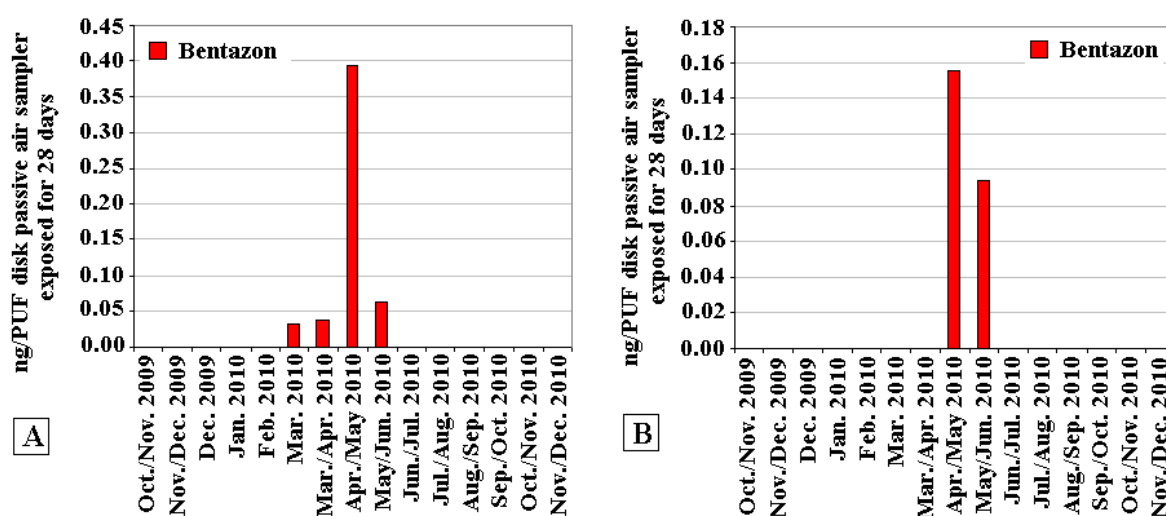


Figure 5.87: Seasonal variations in the atmospheric abundances of bentazone observed at the sampling sites Sülldorf/Hamburg (A) and Tinnum/Sylt (B)

Gas-particle partitioning

Phenoxyalkanoic acids underwent gas-particle partitioning in the atmosphere. Although, they were detected in both mass fractions of the atmosphere during this study, their partly transformation during Soxhlet extraction prevented the estimation of the major mass fraction.

However, the vapour pressures of phenoxyalkanoic acids could be used as an indicator for their partitioning behaviour in atmosphere. The vapour pressures of mecoprop and dichlorprop were found to be $< 10 \cdot 10^{-5}$ Pa (20 °C)^[150], pointing to a predominant occurrence in the particle associated mass fraction of the atmosphere, respectively. In comparison, 24-D and MCPA exhibited significantly increased vapour pressure of 11 mPa (20°C) and 0.8 mPa (25 °C), respectively.^[150] In consequence major atmospheric abundances were assumed in the gaseous mass fraction of the atmosphere. In the case of 24-D the vapour pressure was found to be as high as those of the organophosphate insecticides occurring in the gaseous mass fraction of the atmosphere.

The thiadiazine herbicide bentazone (vapour pressure of 0.45 mPa, ^[150]) was observed to undergo gas-particle partitioning. It was predominantly detected in the particle associated mass fraction of the atmosphere.

Occurrence and distribution of phenoxyalkanoic acids and bentazone in the surface seawater

Highest concentrations of phenoxyalkanoic acids and bentazone in the surface water of the German EEZ and the wider North Sea were determined inside of the river plumes and the Baltic Sea outflow (figures 5.88-5.90). A decrease in the concentrations in relation to the prevailing sea currents gave evidence that riverine input is a major source of phenoxyalkanoic acids and bentazone to the surface seawater. However, characteristics in their occurrences and spatial distributions, in particular at water sampling sites at the open sea indicated the contribution of atmospheric deposition to the surface seawater contamination. MCPA and mecoprop reached the highest surface water concentrations of the targeted phenoxyalkanoic acids and were quantified throughout all sampling sites in the German EEZ. They were even detected at the remote sampling sites in the northern North Sea, where the surface seawater composition was dominated by the inflow from the Atlantic Ocean (chapter 3.6). Considering, the photochemical as well as microbial degradation of phenoxyalkanoic acids in the environment ^[167], their occurrence at remote sampling sites was presumably related to atmospheric deposition. The phenoxyethanoic acids were predominantly detected and in highest abundances (ranging from 8 pg/L to 40 pg/L) at the sampling sites in the northern North Sea, whereas mecoprop was a major surface water contaminant at the coastal sampling sites. This observation might be related to the more frequent occurrence of phenoxyethanoic acids than phenoxypropionic acids in the marine atmosphere and thus to a higher atmospheric deposition of MCPA and 24-D. 24-D was temporarily detected at the western sampling sites of the German EEZ and in the northern North Sea. This sporadic and temporal occurrence could not be exclusively attributed to a dilution effect with the background water of the open sea and might be interpreted as further indicator of atmospheric deposition.

Bentazone could be exclusively detected at the coastal sampling sites of the North Sea, as well as inside the river plume of the Elbe and at the sampling sites in the central German EEZ in maximum concentrations of 200 pg/L, 1500 pg/L and 500 pg/L, respectively. Bentazone was rapidly degraded in the environments in half lives of 3 to 21 days. ^[170] In consequence, it was supposed that the occurrence of bentazone, e.g., in the central North Sea beyond river plumes and estuaries, rather originated from the more dynamic atmospheric transport and subsequent deposition than from the comparable slower riverine transport and dilution along the prevailing sea currents.

The occurrence and distribution of phenoxyalkanoic acids and bentazone in the surface water of the Baltic Sea (figure 5.91) displayed no characteristics pointing to the occurrence of atmospheric

deposition, as observed for the German EEZ and the wider North Sea. The surface water of the central Baltic Sea exhibited more or less homogenous concentrations and compositions. A decrease in the surface water concentrations could be observed at the sampling sites in the Bothnian Bay (35, 37, BB3) as well as in Skagerrak (70, 73, 75, 76). The average sum concentration of the targeted phenoxyalkanoic acids in the surface water at the sampling sites of the central Baltic Sea was approximately 2000 pg/L and was comparable to those observed in the Elbe plume. The bentazone concentrations were similar to those determined in the central German EEZ (approximately 30 pg/L). The phenoxyethanoic acids, in particular 24-D, reached the highest surface water concentrations in the Baltic Sea, whereas the surface water of the German EEZ and the North Sea exhibited higher abundances of mecoprop. On average the phenoxypropionic acids built up only a sixth of the sum concentration of the targeted phenoxyalkanoic acids in the surface seawater of the central Baltic Sea. Reasons for the differences in surface water composition and concentration between the Baltic Sea and the North Sea were multiple and could be only speculative at this point: The low water exchange rates as well as the increased chances of atmospheric deposition of an inland sea might have significantly contributed to the higher surface water contamination of the Baltic Sea. In addition, variable microbial activities in the surface seawater could influence the transformation of the pesticides causing aberrations of the contamination status of the surface seawaters.

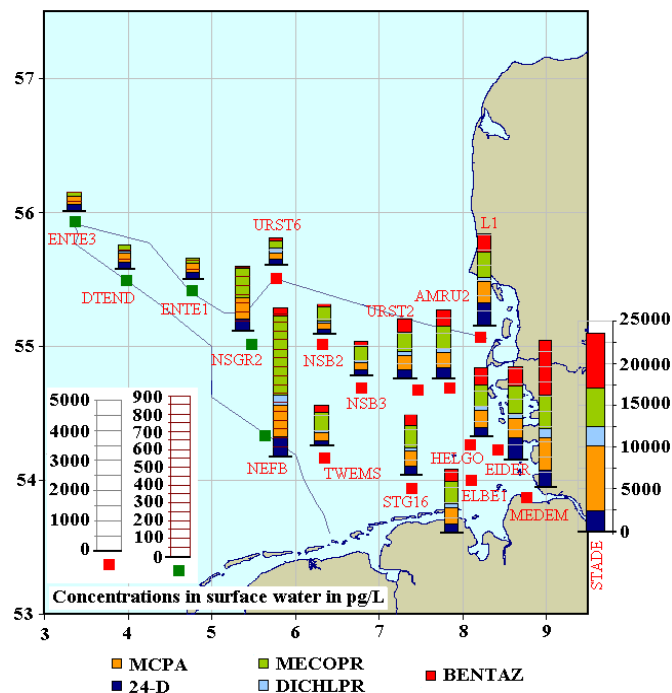


Figure 5.88: Occurrence and spatial distribution of phenoxyalkanoic acids and bentazone in the aqueous phase of the surface water (5 m) of the German EEZ in May/June, 2009; Note the variable concentration scales displayed in the legend

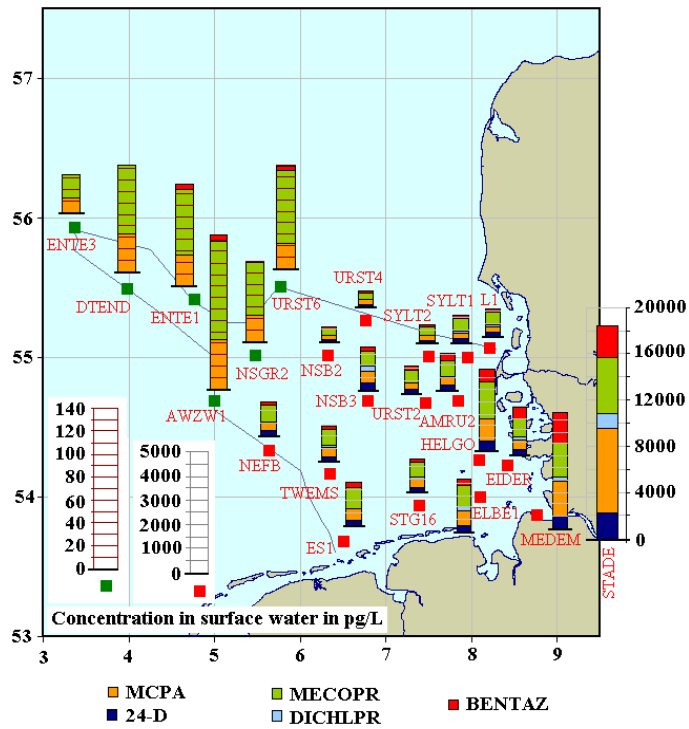


Figure 5.89: Occurrence and spatial distribution of phenoxyalkanoic acids and bentazone in the aqueous phase of the surface water (5 m) of the German EEZ in May 2010; Note the variable concentration scales displayed in the legend

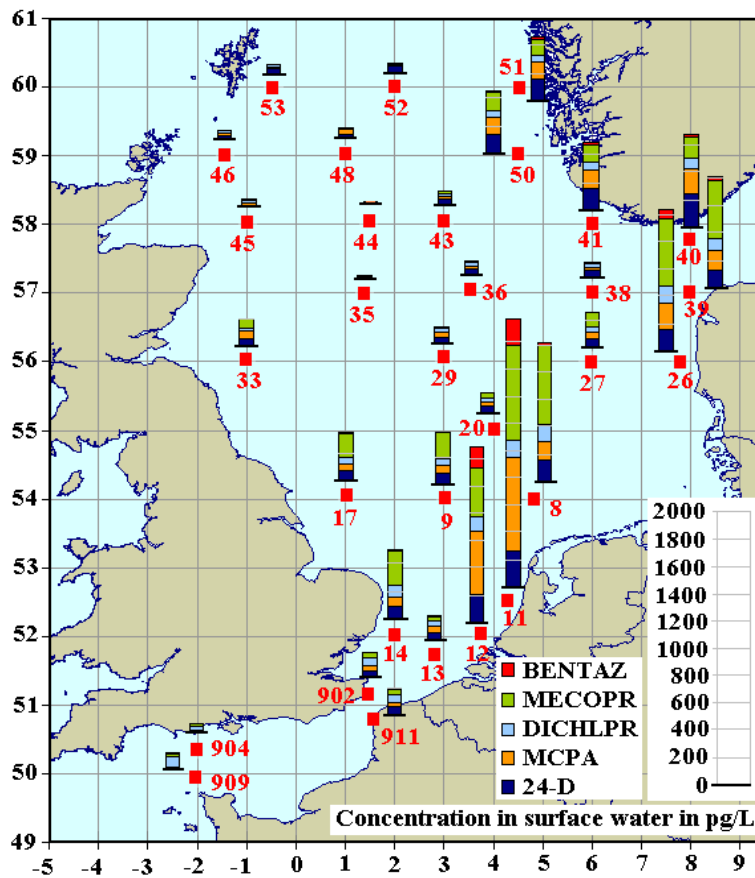


Figure 5.90: Occurrence and spatial distribution of phenoxyalkanoic acids and bentazone in the aqueous phase of the surface water (5 m) of the North Sea in Aug./Sep. 2009

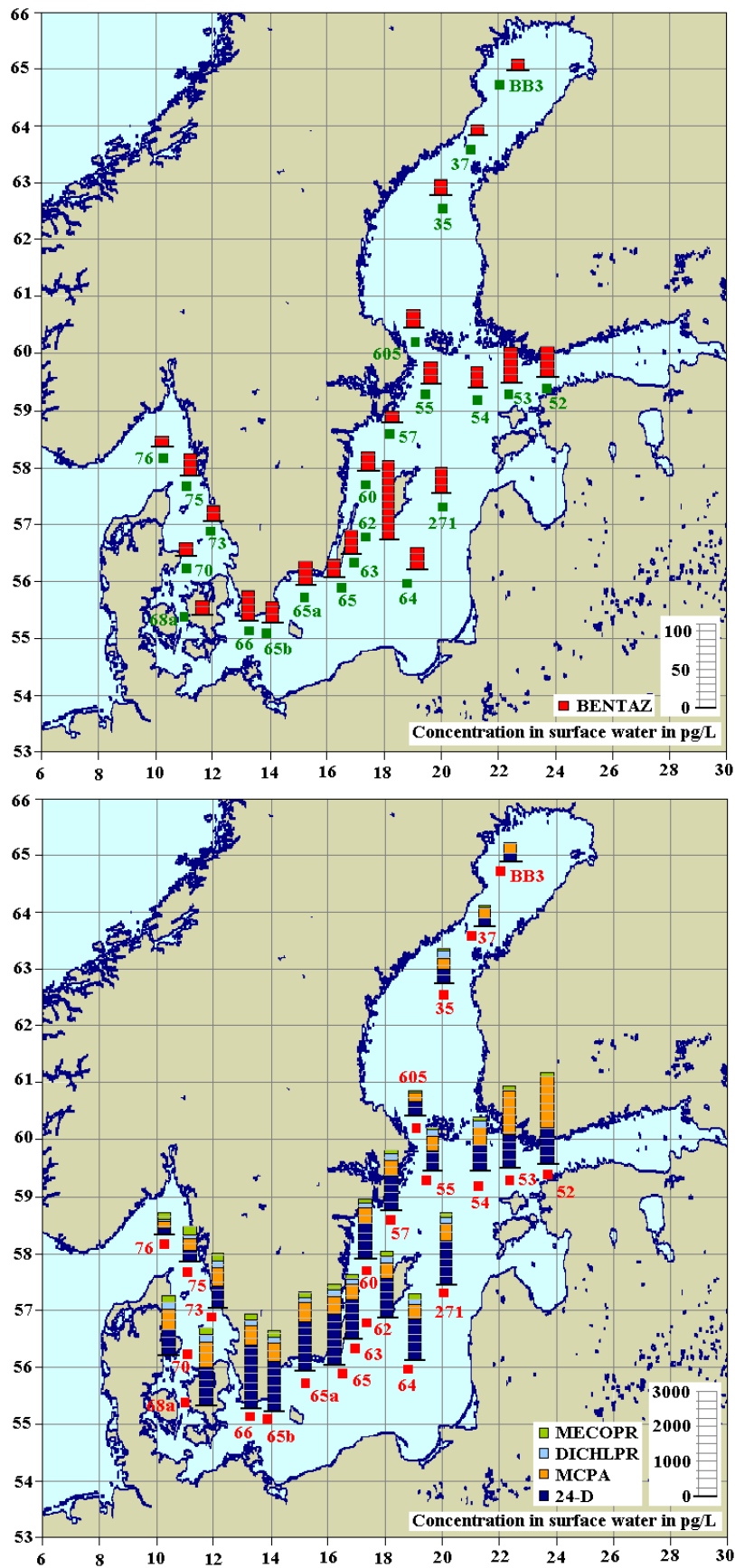


Figure 5.91: Occurrence and spatial distribution of phenoxyalkanoic acids and bentazone in the aqueous phase of the surface water (6 m) of the Baltic Sea in Jun./Jul. 2008

Seasonal fluctuations of phenoxyalkanoic acids and bentazone in the surface seawater

The phenoxyethanoic acids exhibited highest abundances in the surface seawater during spring. The seasonal fluctuations of 24-D could be observed at sampling sites in the river plume of the Elbe (HELGO, AMRU2), whereas in the case of MCPA it was even documented at the sampling sites in the open sea (ENTE1, DTEND, ENTE3). In particular the seasonal profiles of MCPA monitored at the western sampling of the German EEZ beyond river plumes and estuaries pointed to the occurrence of atmospheric deposition. This assumption was additionally confirmed by the observation of MCPA as the most frequently detected phenoxyalkanoic acid in the particle associated mass fraction of the marine atmosphere providing the chance of atmospheric deposition. In contrast, the phenoxypropionic acids, mecoprop and dichlorprop, displayed no pronounced seasonality in the surface seawater (figure 5.92).

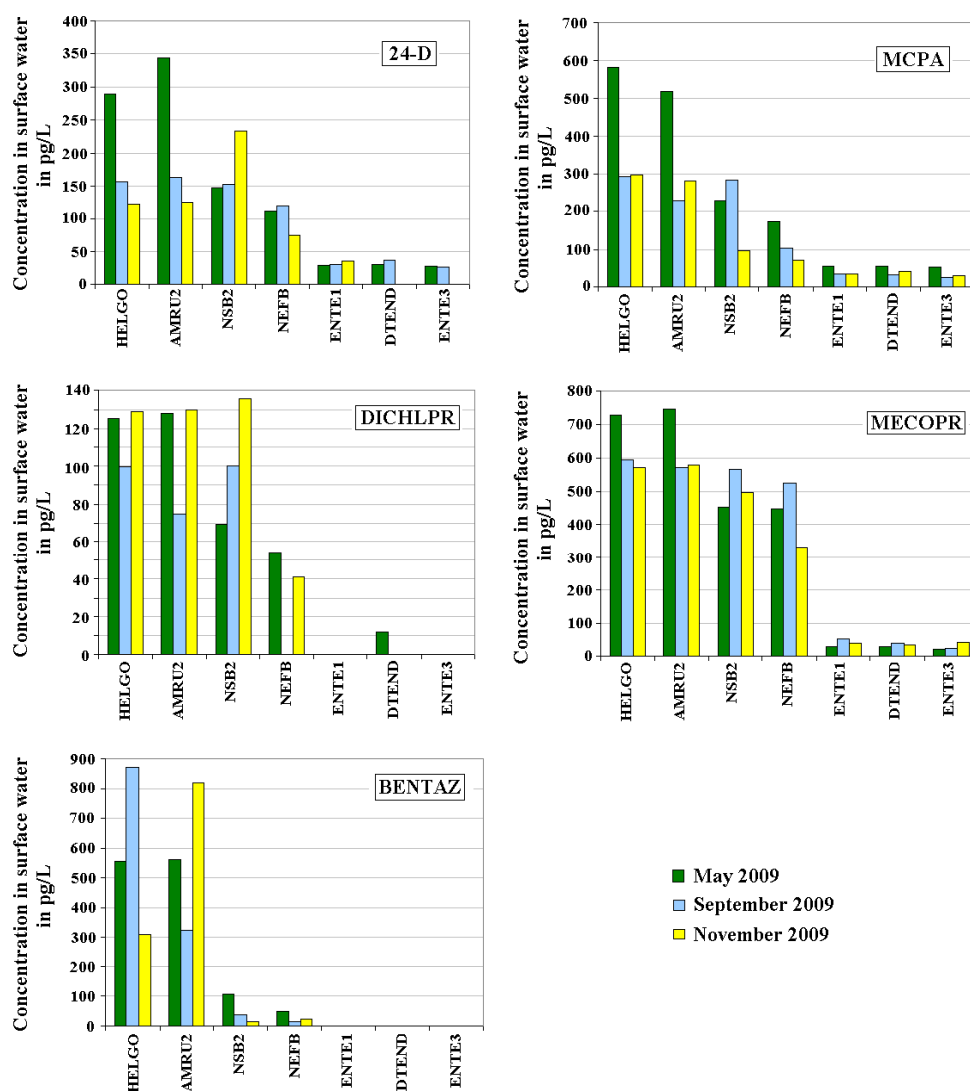


Figure 5.92: Seasonal variations in the surface water concentrations (5 m) of the phenoxyalkanoic acids and bentazone displayed for selected sampling sites in the German EEZ in 2009; The sampling sites are sorted from left to right by increasing meridional distance from the Elbe estuary

The seasonal profile of bentazone in the surface seawater was negligible inside the river plume of the Elbe. However, significantly increased abundances could be quantified in spring beyond the coastal sampling sites. This might point to an intensified atmospheric deposition during the main application season of bentazone ranging from early spring to early summer. Bentazone occurred sporadically in both mass fractions of the atmosphere and predominantly in air masses which had passed the continent within the last 24 hours. Thus, advection of continental contaminated air masses and atmospheric deposition was supposed to be an important input pathway of bentazone, in particular to the surface waters, which were found to be less influenced by riverine input and the Baltic Sea outflow (figure 5.92).

Net flux of diffusive gas exchange of phenoxyalkanoic acids and bentazone between the marine atmosphere and the surface seawater

The concentrations of the phenoxyalkanoic acids in the gaseous mass fraction of the atmosphere could not be quantified, due to their transformation during the Soxhlet extraction of the adsorber cartridges. Hence, the direction of the net flux of diffusive gas exchange between the marine atmosphere and the surface seawater was exclusively calculated for the thiadiazine herbicide bentazone. Bentazone was predominantly present in the particle associated mass fraction of the atmosphere. Thus, the atmospheric deposition of bentazone was assumed to be rather dominated by dry particle and wet deposition processes than by dry gaseous deposition. However, 3 atmospheric concentrations of bentazone could be quantified in the gaseous mass fraction during the research cruise in the German EEZ in May/Jun. 2009 as well as in a single air sample of the Baltic Sea campaign in Apr. 2009. The calculated fugacity ratios were 0.0 and indicated a net gaseous atmospheric deposition of bentazone to the surface seawaters. The Henry's Law Constants of the phenoxyalkanoic acids were found to be as low as that of bentazone.^[150] Hence, a dry gaseous deposition might be also assumed for the compound class of phenoxyalkanoic acid herbicides.

Conclusions

Riverine input was found to be an important source of the targeted phenoxyalkanoic acids and bentazone to the surface seawater. In addition, this study provided evidence that atmospheric deposition could be a significant contributor to the surface seawater contamination.

Exclusively the particle associated mass fraction of phenoxyalkanoic acids in the atmosphere was investigated in this study. However, relations in atmospheric abundances as well as characteristics in surface water distributions indicated atmospheric deposition. In particular, the occurrence of phenoxyethanoic acids (24-D and MCPA) in the surface water at the remote sampling sites in the northern North Sea, the seasonal fluctuations in surface water concentrations as well as the most frequent occurrence in the particle associated mass fraction pointed to a significant atmospheric

deposition to the surface water at the open sea. In comparison, the phenoxypropionic acids mecoprop and dichlorprop were less frequently detected in the atmosphere as well as in the surface water of the northern North Sea. Seasonal fluctuations in surface water concentrations within the German EEZ were not observed. It might be concluded that the atmospheric deposition of phenoxyethanoic acids exceeded the atmospheric deposition of phenoxypropionic acids.

The thiadiazine herbicide bentazone exhibited a seasonal profile in atmospheric concentrations, which correlated with the main agricultural application season from early spring (March) to early summer (June). The air mass history as well as the spatial distribution and seasonal fluctuations in surface water displayed the advection of air masses from continent and a subsequent atmospheric deposition to the surface seawaters, especially during the main application season. Bentazone was predominantly present in the particle associated mass fraction of the atmosphere. Hence, dry particle and wet deposition fluxes were supposed to overcome the dry gaseous deposition.

5.1.11 Dinitroaniline, Chloroacetanilide and Carbamate Pesticides

This chapter summarizes individual representatives of three further compound classes of currently used pesticides (CUPs) targeted in this study. They are in public focus due to their occurrence in surface and ground waters as well as due to the possible health hazards for humans and wildlife. The dinitroaniline pesticides pendimethalin (PENDIMETH) and trifluralin (TRIFLU) are applied as long residual and soil incorporated preemergence herbicides in agriculture, in particular for the protection of the winter grain. The usage of trifluralin is prohibited in the EU since 2008, whereas pendimethalin is still extensively applied. ^[171-173] Metolachlor (METOLA) and metazachlor (METAZCHL) belong to the pesticide group of chloroacetanilide herbicides, which are also extensively applied to the preemergence weed control in agriculture. ^[174] Pirmicarb (PIRIMIC) and carbendazim (CARBEND) contain the carbamate group as a common structure characteristic. Both pesticides are extensively applied in agriculture and fruit growing, whereof pirimicarb is used as a selective insecticide against aphids and carbendazim as a fungicide. ^[175, 176]

Occurrence and distribution of dinitroaniline, chloroacetanilide and carbamate pesticides in the marine atmosphere

All targeted representatives of chloroacetanilide, carbamate and dinitroaniline pesticides, except of pirimicarb could be quantified in the marine atmosphere of the German EEZ, the wider North Sea and the Baltic Sea (figures 5.93-5.96). Their concentrations and spatial distribution in the atmosphere were highly variable and strongly depended on the air mass history and the season.

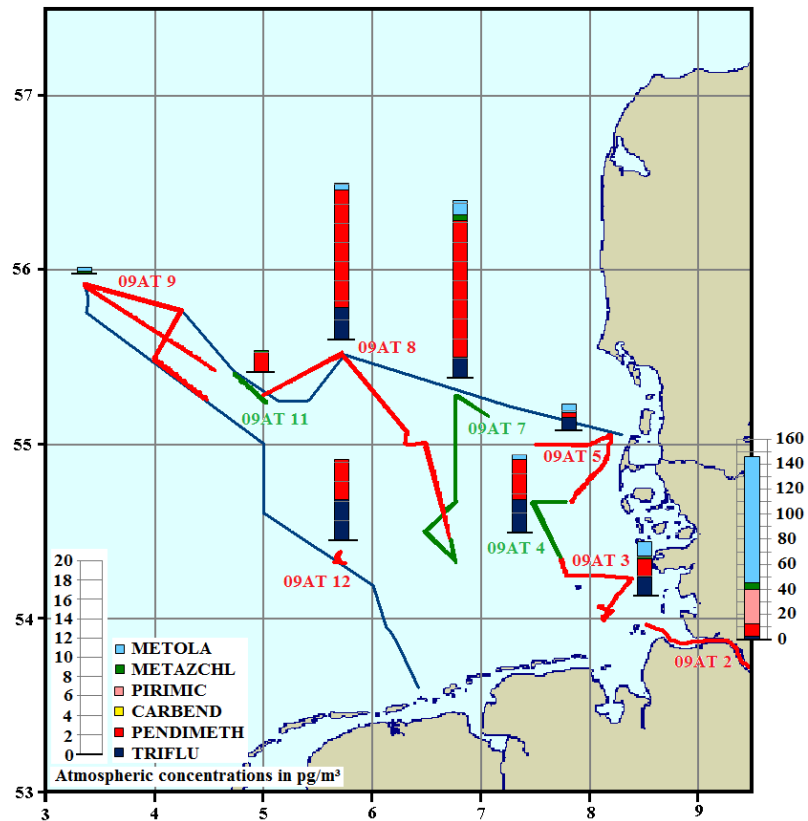


Figure 5.93: Atmospheric bulk concentrations of dinitroaniline, chloroacetanilide and carbamate pesticides above the German EEZ in May/June. 2009

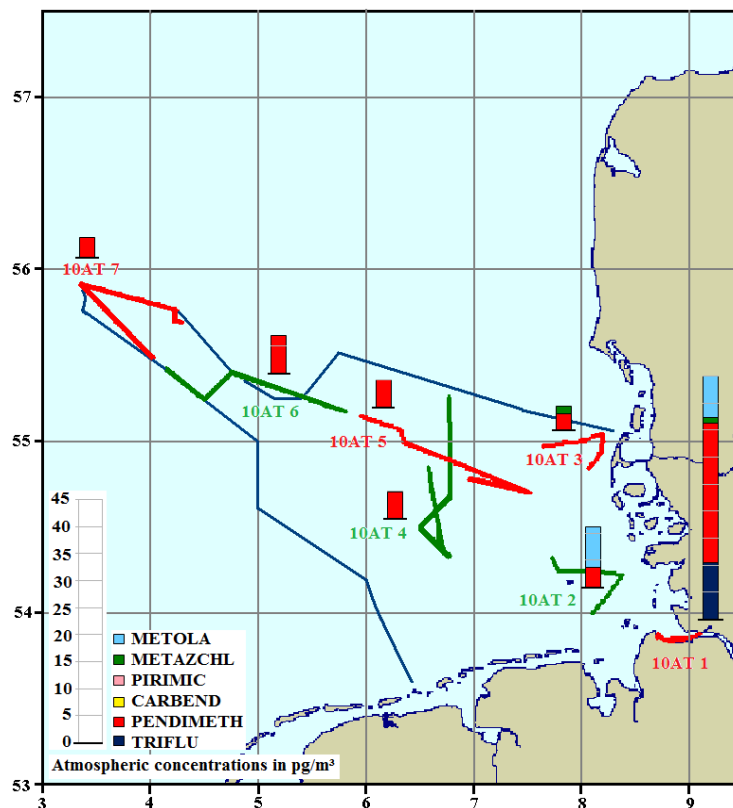


Figure 5.94: Atmospheric bulk concentrations of dinitroaniline, chloroacetanilide and carbamate pesticides above the German EEZ in May 2010

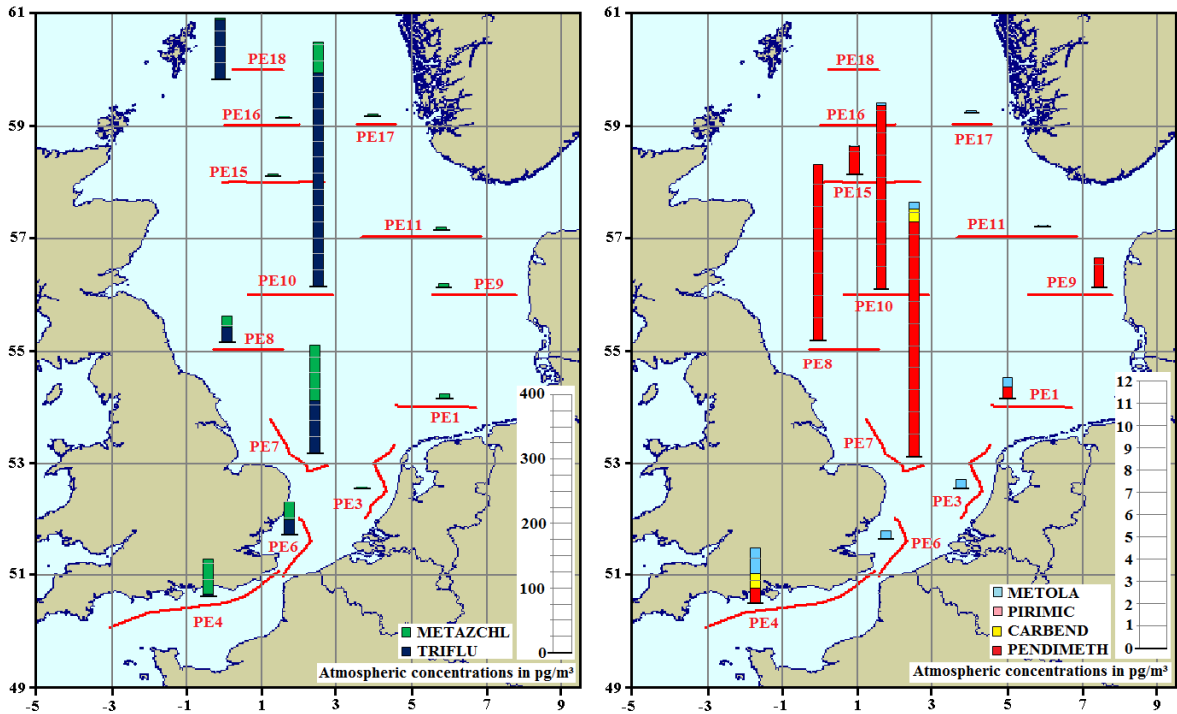


Figure 5.95: Atmospheric bulk concentrations of dinitroaniline, chloroacetanilide and carbamate pesticides above the North Sea in Aug./Sep. 2009

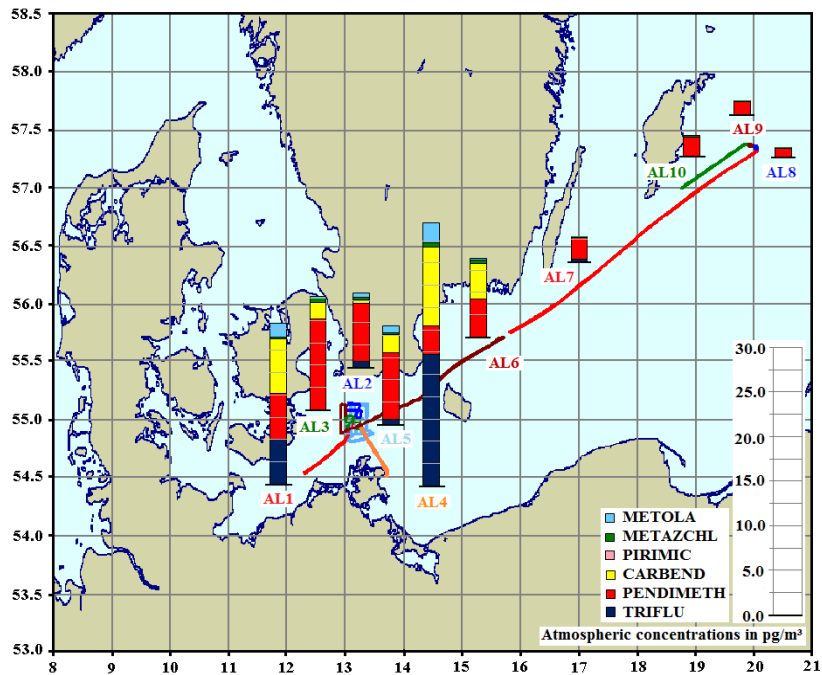


Figure 5.96: Concentrations of dinitroaniline, chloroacetanilide and carbamate pesticides in the gaseous mass fraction of the atmosphere above the Baltic Sea in Apr. 2009

The dinitroaniline pesticides trifluralin and pendimethalin were most frequently observed in the marine atmosphere and displayed the highest variability in their atmospheric concentrations. Trifluralin could be quantified in concentrations ranging from <LOQ to 331 pg/m^3 , whereas

pendimethalin reached maximum concentrations of up to 26 pg/m³ above the river Elbe. Highest abundances could be quantified in the air masses, which had passed the continent within the last 24 hours, like PE7/PE10/PE18 (figure 5.95), 10AT1 (figure 5.94), 09AT7/09AT8 (figure 5.93) and AL1-AL6 (figure 5.96). Hence, advection of contaminated air from the continent was supposed to be the major input source of trifluralin and pendimethalin to the marine atmosphere. Furthermore, the air mass history of the air samples PE 7, PE 8, PE 10 and PE18 gave evidence to current primary sources of pendimethalin and trifluralin in England during the research cruise in Aug./Sep. 2009 (figure 5.95). In addition, a widespread spatial distribution of the targeted dinitroaniline pesticides in the marine atmosphere was shown by their occurrence independent of the air mass history: For example, trifluralin and pendimethalin were detected in decreased abundances of approximately 4-5 pg/m³ in air masses of the open sea (24 h backward trajectories) at sampling sites in the central German EEZ in May/June 2009 (figure 5.93). Furthermore, pendimethalin could be quantified in the air samples of the German EEZ in May 2010 (figure 5.94), which predominantly originated from the open sea (24 h backward trajectories). Furthermore, pendimethalin was observed in concentrations of approximately 2.5 pg/m³ at the sampling sites east of 16°E (AL7-AL10) of the Baltic Sea in air masses which had passed the sea within the last 24 hours (figure 5.96).

Although less frequently observed, the chloroacetanilide herbicides metolachlor and metazachlor displayed a similar distribution pattern as described for trifluralin and pendimethalin. In general, significantly increased atmospheric concentrations were determined in air masses, which had passed the continent within the last 24 h giving evidence that advection of contaminated air from continent was the major input pathway of chloroacetanilides to the marine atmosphere. Besides, a widespread distribution was indicated by the presence of chloroacetanilides in the air masses originating from the open sea (24 h backward trajectories). However, this general distribution pattern significantly changed with season. Metazachlor exhibited an overall distribution throughout all sampling sites and highest atmospheric concentrations in the range of 1 pg/m³ to 88 pg/m³ in the atmosphere of the North Sea in Aug./Sep. 2009 (figure 5.95). Highest pollution levels were observed in the air masses originating from central England (PE7/PE10) and France (PE4/PE6) indicating current primary sources. During the research cruises in the German EEZ and the Baltic Sea in spring metazachlor revealed significantly decreased concentrations of less than 1.5 pg/m³, which could be attributed to a seasonally decrease in current primary sources. In contrast, metolachlor exhibited highest concentrations in the marine atmosphere during the research cruises in spring (figures 5.93, 5.94 and 5.96). Metolachlor was most frequently detected (7 of 9 air samples) in the marine atmosphere of the German EEZ in May/Jun. 2009 (figure 5.95) with a maximum concentration of 101 pg/m³ above the river Elbe and average concentrations of

approximately 1 pg/m³ in the marine atmosphere. The seasonalities in atmospheric concentrations of the chloroacetanilide herbicides in the marine atmosphere were also monitored by the PUF disk passive air sampling campaigns in Sülldorf/Hamburg and Tinum/Sylt and could be related to the main agricultural application seasons, as discussed below.

Pirimicarb, a carbamate insecticide, was never detected in the marine atmosphere of the German EEZ, the North Sea and the Baltic Sea. However, it could be quantified in a single air sample collected above the river Elbe in May/June 2009 (figure 5.93) in a concentration of 28 pg/m³. The fungicide carbendazim was never detected in the marine atmosphere above the German EEZ, but was sporadically observed in the marine atmosphere of the North Sea in air masses originating from central England (PE7) and France (PE4) in concentrations of 0.6 p/m³ and 0.7 pg/m³, respectively (figure 5.95). In addition, it was quantified in air advected from the continent (AL1-AL6) above the Baltic Sea in concentrations of up to 6.1 pg/m³ at the sampling sites west of 16°E (figure 5.96). Hence, advection of contaminated air from land was shown to be the major input pathway of the targeted carbamate pesticides to the marine atmosphere.

Seasonal fluctuations in atmospheric concentrations

All targeted representatives of chloroacetanilide, carbamate and dinitroaniline pesticides, except of carbendazim, displayed seasonal variations in their atmospheric abundances in the atmosphere of Sülldorf/Hamburg and Tinum/Sylt (figure 5.97).

The dinitroaniline pesticides trifluralin and pendimethalin could be quantified throughout the year, but reached significantly increased atmospheric concentration levels in the months from September to November. This seasonality was attributed to their main application in agriculture as preemergence herbicides for the protection of the winter grain.^[172] The above mentioned current primary source of trifluralin and pendimethalin in central England (Aug./Sep. 2009) could be related to this main agricultural application season monitored by the PUF disk passive air samplers. In addition, pendimethalin displayed a second small seasonal increase in atmospheric abundances in spring (May/June) at the sampling site Sülldorf/Hamburg, which might be in relation to an application as preemergence herbicide for the protection of the summer grain. Trifluralin was quantified in significantly lower amounts on the PUF disks than pendimethalin, which might display the prohibition of application in the EU states since 2008.^[173] The occurrence of pendimethalin and trifluralin in the atmosphere above the continent throughout the year provided an ongoing and widespread contamination of the marine atmosphere, which was shown by the presence of pendimethalin and trifluralin in the air masses originating from the open sea (24 h backward trajectories). A previous study classified trifluralin as a pesticide, which occurred episodically in the rain water of the Alsace region in eastern France in concentrations of a few to

10 ng/L depending on current local sources. [57] This classification was not supported by the results of this study, which rather pointed to the occurrence of trifluralin in rain water throughout the year and a seasonally extended wet deposition in the months from September to November at the sampling sites Sülldorf/Hamburg and Tinnum/Sylt.

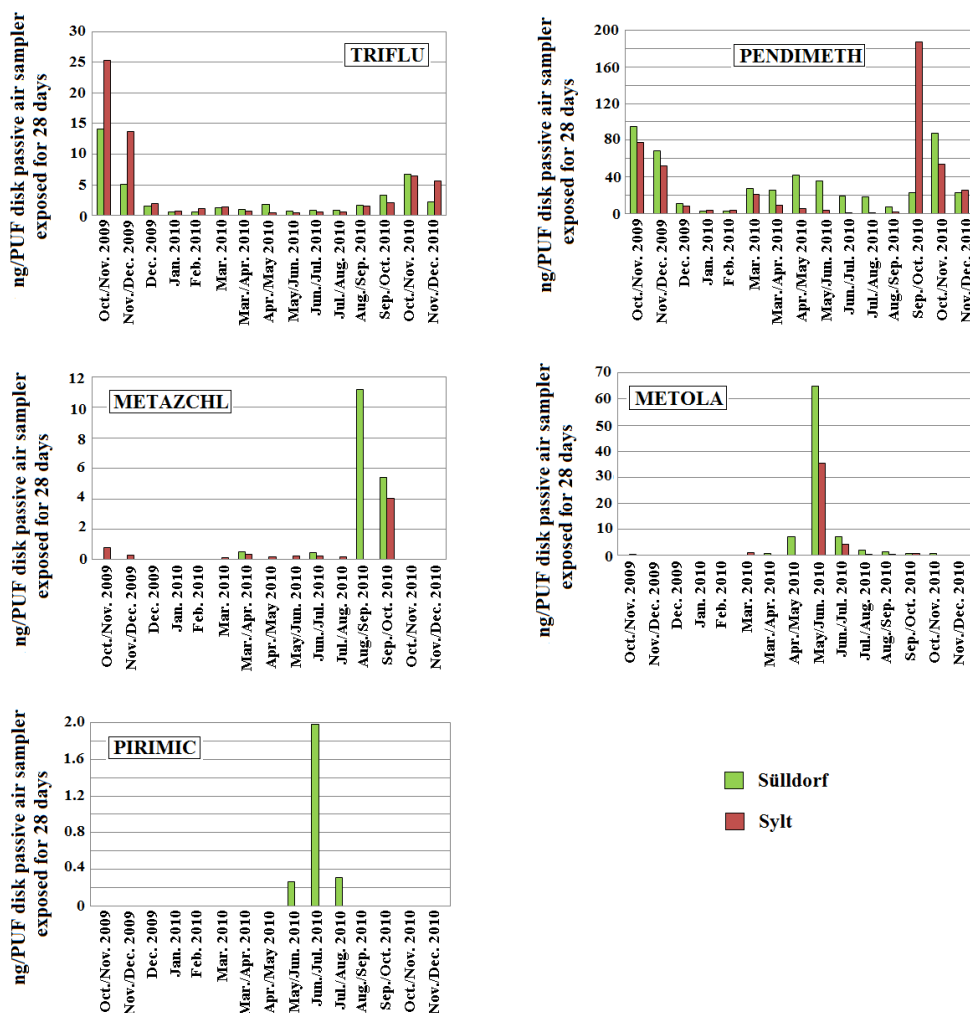


Figure 5.97: Seasonal variations in the atmospheric abundances of dinitroaniline, chloroacetanilide and carbamate pesticides at the sampling sites Sülldorf/Hamburg and Tinnum/Sylt

In contrast, atmospheric abundances of metolachlor and metazachlor could be exclusively documented in the months from March to November. The chloroacetanilide herbicides displayed different periods of maximum atmospheric concentrations, which were found to be related to the seasons of preemergence weed control in agriculture. Metolachlor exhibited highest atmospheric abundances in the months from May to June indicating a predominant application as preemergence herbicide for the protection of the summer grain. In contrast, metazachlor revealed increased atmospheric concentrations from August to October pointing to an extensive usage for the weed control of the winter grain. As described above, these seasonalities were even documented by the

active air sampling campaigns in the marine atmosphere and provided evidence to the widespread distribution of currently used pesticides during their main agricultural application seasons by advection of contaminated air from the continent. The seasonality of atmospheric metolachlor abundances was also documented by rain water samples of the Alsace region in eastern France, reporting strong seasonal effects associated with the period of application. ^[57]

The fungicide carbendazim could not be detected in any PUF disk passive air sample, whereas the insecticide pirimicarb displayed a less pronounced seasonal profile in its atmospheric concentrations. Atmospheric abundances of pirimicarb were exclusively quantified in the months from May to August and decreased below the LOQ beyond this period. Considering this seasonality, the single active air sample exhibiting a pirimicarb concentration of 28 $\mu\text{g}/\text{m}^3$ in May/Jun. 2009 might be related to a current application. The results of the passive air sampling studies pointed to marginal primary local sources of the targeted carbamate pesticides to the atmosphere of central and northwestern Europe.

Gas-particle partitioning

Trifluralin and pendimethalin underwent gas particle partitioning in the atmosphere. In correlation to their vapour pressures of 6.1 mPa (25°C) and 4.0 mPa (25°C), respectively, ^[150] they were predominantly present in the gaseous mass fraction of the atmosphere. The particle associated abundances of trifluralin were exclusively determined below the LOQ, whereas pendimethalin was quantified in both mass fraction of the atmosphere. On average approximately 80 % of total pendimethalin was present in the gaseous mass fraction of the atmosphere. The particle associated and the gaseous mass fractions of pendimethalin were plotted in % against the ambient air temperatures in figure 5.98, where 100 % referred to the sum concentration of all air samples exhibiting pendimethalin abundances in both mass fractions for the respective air temperatures.

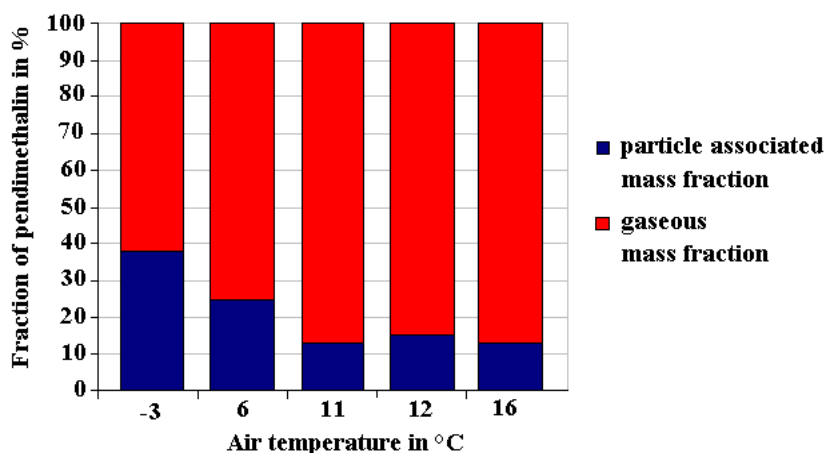


Figure 5.98: Gas-particle partitioning of pendimethalin in correlation with the ambient air temperatures

Similar to the gas-particle partitioning described for the PAHs in chapter 5.1.1, a correlation in the gas-particle partitioning behaviour of pendimethalin with the ambient air temperature was documented. Low air temperatures favoured the adsorption of pendimethalin to the particulate mass fraction of the atmosphere, which was displayed by the increase of the particle associated pendimethalin abundances to approximately 38 % in winter and its decrease to approximately 13 % during summer.

Metolachlor and metazachlor were also found to undergo gas-particle partitioning in the atmosphere (vapour pressures of 4.2 mPa (25 °C) and 93 µPa (20 °C), respectively. ^[150]). Both chloroacetanilides were predominantly present in the particle associated mass fraction of the atmosphere, although the vapour pressure of metolachlor rather pointed to higher abundances in the gaseous phase. On average, >85 % of metazachlor and >60 % of metolachlor was quantified in the particle associated mass fraction of the atmosphere (calculated from the air samples exhibiting quantifiable concentration in both mass fractions). A correlation in the gas-particle partitioning of the chloroacetanilides with the ambient air temperature could not be investigated due to the limited data.

The vapour pressures of pirimicarb and carbendazim ($9.7 \cdot 10^{-4}$ Pa (25 °C) and $9.9 \cdot 10^{-8}$ Pa (20 °C), respectively, ^[150]) pointed to a predominant occurrence in the particle associated mass fraction of the atmosphere. This presumption was confirmed for the insecticide pirimicarb. Pirimicarb was detected in a single active air sample in a concentration of 28 pg/m³, whereof 24 pg (86 %) were quantified in the particle associated mass fraction and 4 pg (14 %) in the gaseous mass fraction of the atmosphere (figure 5.95). The gas-particle partitioning of carbendazim could not be evaluated due to the limited atmospheric data. Carbendazim was exclusively detected in the particle associated mass fraction of the North Sea atmosphere (figure 5.93). However, evidence to a significant gas-particle partitioning was provided by its occurrence in the gaseous mass fraction of the Baltic Sea atmosphere (figure 5.94).

Occurrence and distribution of dinitroaniline, chloroacetanilide and carbamate pesticides in the surface seawater

Pendimethalin and trifluralin displayed an anomalous spatial distribution in the surface water of the German EEZ and the wider North Sea, which was never observed for any other currently used pesticide targeted in this study (figures 5.99 – 5.101). This provided evidence to a predominant atmospheric input of the dinitroanilines herbicides to the surface seawaters. For example, the surface water concentrations of pendimethalin at the western sampling sites of the German EEZ (ENTE1, DTEND, ENTE3) in 2010 (figure 5.100) were observed to be as high as in the river plume of the Elbe (EIDER, ELBE1, HELGO), but were still up to two times lower than those determined in the central German EEZ (NSB3, AWZW1). In 2009 (figure 5.99) the surface water

concentrations in the Elbe plume were higher than those at the western sampling sites, but were still significantly lower than the maximum concentrations of 206 pg/L quantified in the central German EEZ (URST6, NEFB). Similar results were obtained for the surface water of the wider North Sea (figure 5.101). The surface water concentrations at the sampling sites inside the river plumes (14, 11, 12) and the Baltic Sea outflow (39, 40, 41, 50, 51) were significantly increased indicating a riverine input and an outflow from the Baltic Sea. However, sampling sites in the central North Sea (9, 8, 17, 10, 27, 29, 33) displayed concentration levels of pendimethalin (up to 48 pg/L), which partly exceeded the abundances in the river source regions (20 pg/L to 30 pg/L). This might be presumably related to an extended atmospheric deposition to these sea regions.

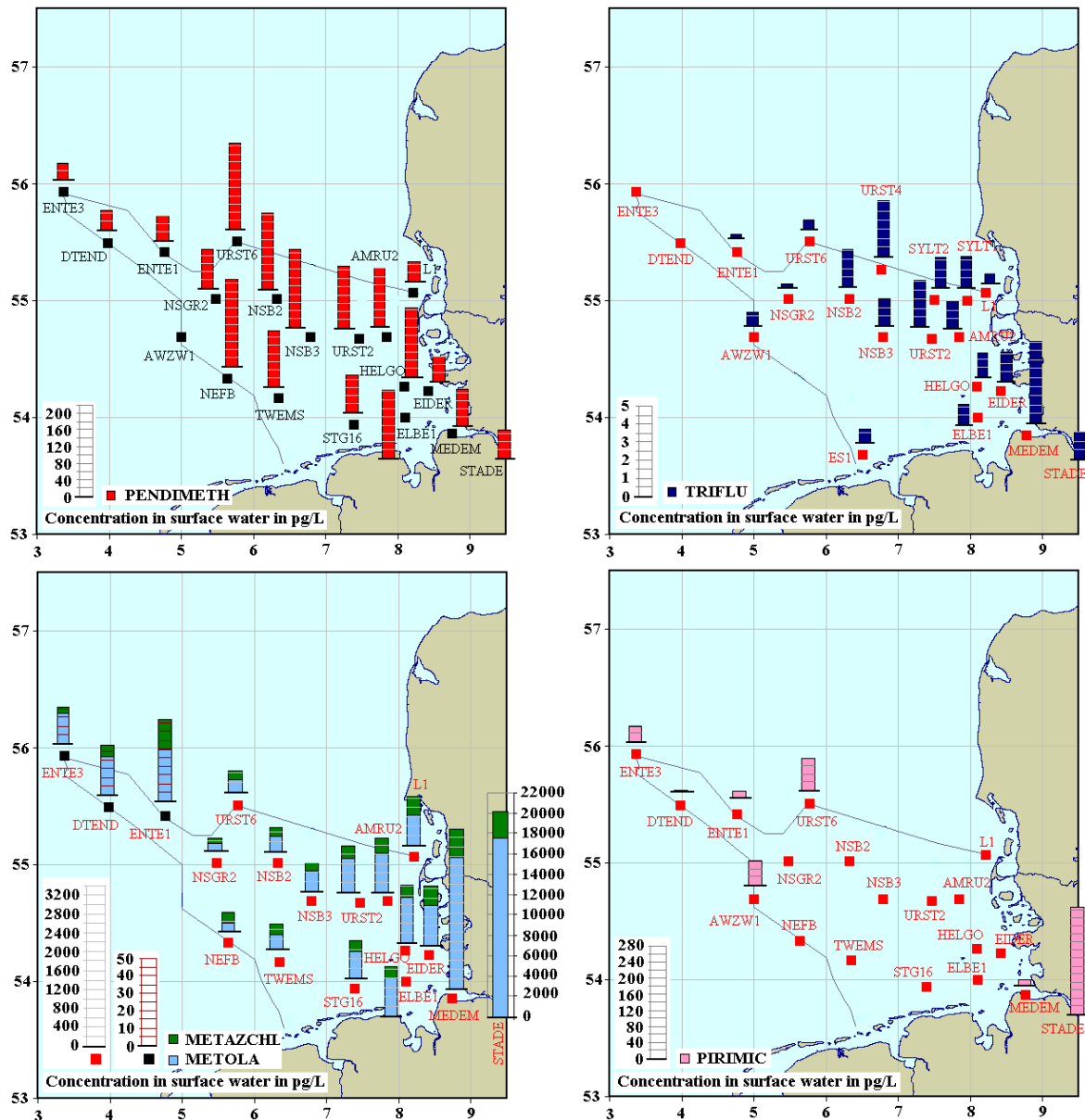


Figure 5.99: Occurrence and distribution of dinitroaniline, chloroacetanilide and carbamate pesticides in the aqueous phase of the surface water (5 m) of the German EEZ in May/Jun. 2009

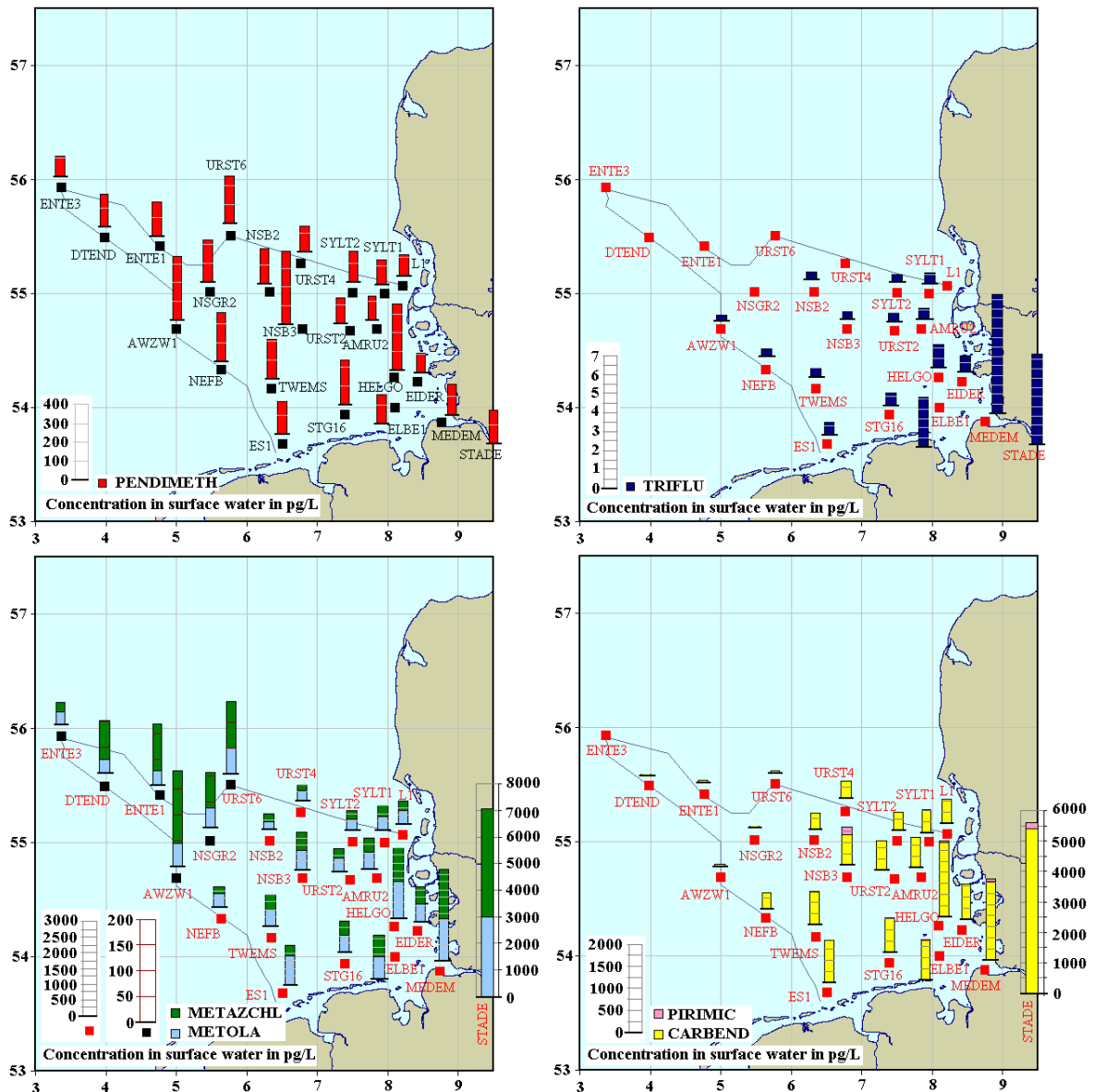


Figure 5.100: Occurrence and distribution of dinitroaniline, chloroacetanilide and carbamate pesticides in the aqueous phase of the surface water (5 m) of the German EEZ in May 2010

Lowest surface water concentrations of pendimethalin (<10 pg/L) were detected in the northern North Sea, where the surface water composition was dominated by the inflow of the Atlantic Ocean. The occurrence of pendimethalin at these remote sampling sites gave further evidence to a significant atmospheric deposition of pendimethalin to the surface water of the North Sea.

Trifluralin displayed similar distribution patterns, which pointed to predominant atmospheric input sources to the surface waters. However, the typical concentration profile, which emerged from a predominant input by the river Elbe and the prevailing sea currents could be observed within the German EEZ in the year 2010 (figure 5.100), whereas it was masked by an extended atmospheric deposition in 2009 (figure 5.99). The occurrence and distribution of trifluralin in the surface water of the North Sea pointed to a predominant atmospheric input (figure 5.101)

exceeding the riverine input: Highest surface water concentrations of up to 36 pg/L were determined in the central North Sea (17, 20, 29, 33, 35, 36), whereas trifluralin abundances in the Baltic Sea outflow and the river plumes were comparable to those determined in the northern North Sea. Trifluralin was less frequently detected than pendimethalin and reached significantly lower surface water concentrations. This might be attributed to the decreased atmospheric abundances of trifluralin in comparison to pendimethalin and thus a decreased atmospheric depositional flux to the surface seawaters. For this reason, the typical concentration profiles emerging from riverine input and sea currents could be partly observed during seasons of decreased atmospheric trifluralin abundances.

To sum up, the typical concentration profiles, which emerged from a predominant riverine input, the Baltic Sea outflow and the prevailing sea currents were found to be less pronounced for the dinitroaniline herbicides than those described, e.g., in chapter 5.17 and 5.19. Highest surface water concentrations were quantified at the sampling sites in the central German EEZ and the central North Sea instead inside the river plumes. This pointed to atmospheric deposition as a major source of the surface seawater contamination.

Surface water concentrations of trifluralin in the Baltic Sea were not available. However, the occurrence of pendimethalin was investigated in June/July 2008 for the entire sea region (figure 5.102). Pendimethalin was quantified throughout all sampling sites (except of 605) in concentration ranging from 14 pg/L to 133 pg/L. Highest surface water concentrations were determined in the southern central Baltic Sea (66, 65b, 65a, 65) and lowest in the Bothnian Bay (35, 37, BB3). The distribution pattern of pendimethalin in the surface water of the Baltic Sea agreed with those of other currently used pesticides and provided no evidence for an extended atmospheric deposition of the dinitroaniline herbicides.

In contrast, the chloroacetanilide herbicides displayed strong concentration gradients from the river plumes to the open sea according to the prevailing sea currents indicating a predominant riverine input of metolachlor and metazachlor to the surface water of the German EEZ and the North Sea (figures 5.99 – 5.101). However, characteristics in their distribution patterns, in particular at the water sampling sites in the open sea, pointed to a significant seasonal contribution of atmospheric deposition to the contamination of the surface seawater. For example, metolachlor significantly exceeded the surface water concentrations of metazachlor at the sampling sites inside the river plumes in the southern North Sea (14, 13, 12, 11, 26) and the English Channel (902, 904, 909, 911) (figure 5.101). In contrast, the sampling sites in the central North Sea (9, 8, 17, 20, 27, 29, 33, 35, 36, 43) exhibited higher levels of metazachlor than of metolachlor. Considering, the predominant occurrence of metazachlor in the atmosphere of the North Sea in Aug./Sep. 2009 and the current primary sources in central England and France (figure 5.93), this shift in the distribution

patterns might be influenced by a seasonally increased atmospheric deposition. In addition, the occurrence of metolachlor and metazachlor at the northern sampling sites of the North Sea, which were dominated by the inflow of the Atlantic Ocean and thus unaffected by riverine input, provided evidence to the significant contribution of atmospheric deposition to the surface water contamination beyond coastal sampling sites. Furthermore, seasonal variations in the distribution patterns of metolachlor and metazachlor were observed in the surface water of the German EEZ (figures 5.99 - 5.100). In May 2010, the surface water concentrations of metazachlor exceeded those of metolachlor, whereas metolachlor reached higher abundances than metazachlor in May/June 2009 throughout all sampling sites, respectively. Moreover, the surface water concentration of metolachlor at the sampling site STADE was approximately six times higher in 2009 than in 2010 indicating current primary sources of metolachlor and a high riverine input. However, the predominant occurrence of metolachlor throughout all sampling sites in the German EEZ in May/June 2009 might not be exclusively related to high riverine input. Considering the more frequent occurrence of metolachlor in the atmosphere above the German EEZ in May/June 2009 (figure 5.95) and the PUF disk passive air sampler profiles (figure 5.97) monitoring current primary sources from May to June, atmospheric deposition was presumably a significant input source of metolachlor to the surface seawater during this season.

The spatial distributions of the chloroacetanilide herbicides in the surface water of the Baltic Sea in June/July 2008 displayed no characteristics indicating the occurrence of atmospheric deposition (figure 5.102). Metolachlor and metazachlor were detected throughout all sampling sites in concentrations ranging from 8 pg/L to 137 pg/L and 14 pg/L to 151 pg/L, respectively. They displayed a similar distribution pattern, exhibiting highest surface water concentrations in the sea region Skagerrak/Kattegat (68a, 70, 73, 75, 76) and a gradual decrease towards the north western Baltic Sea.

The carbamate insecticide pirimicarb was never detected in the surface water of the North Sea and the Baltic Sea, but was sporadically quantified at individual sampling sites in the German EEZ (figures 5.99 and 5.100). Highest abundances of 265 pg/L in May/June 2009 and 215 pg/L in May 2010 were determined at the sampling site STADE, respectively. In addition, pirimicarb was detected at the sampling site MEDEM in the Elbe estuary, a few individual sampling sites in the central German EEZ and even at the sampling sites west of 5°E in the open North Sea (ENTE3, DTEND, ENTE1). Concentrations in the range of 3 pg/L to 198 pg/L were determined. The sporadic occurrence of pirimicarb, in particular at the sampling sites beyond river plumes and the high variability in surface water concentrations pointed to a predominant atmospheric input to the surface water of the German EEZ. Considering the seasonality in the atmospheric pirimicarb abundances, a significant atmospheric deposition was exclusively suggested for the months from

May to August. The spatial distribution of pirimicarb in the surface seawater was comparable to those of the organophosphate insecticides described in chapter 5.1.8. Analogous to the organophosphates, pirimicarb was found to have a short persistence in the environment due to a rapid transformation by photochemistry and microbial degradation. ^[177-179] Thus, atmospheric transport and subsequent deposition was assumed to be a major input pathway of pirimicarb to the surface seawater.

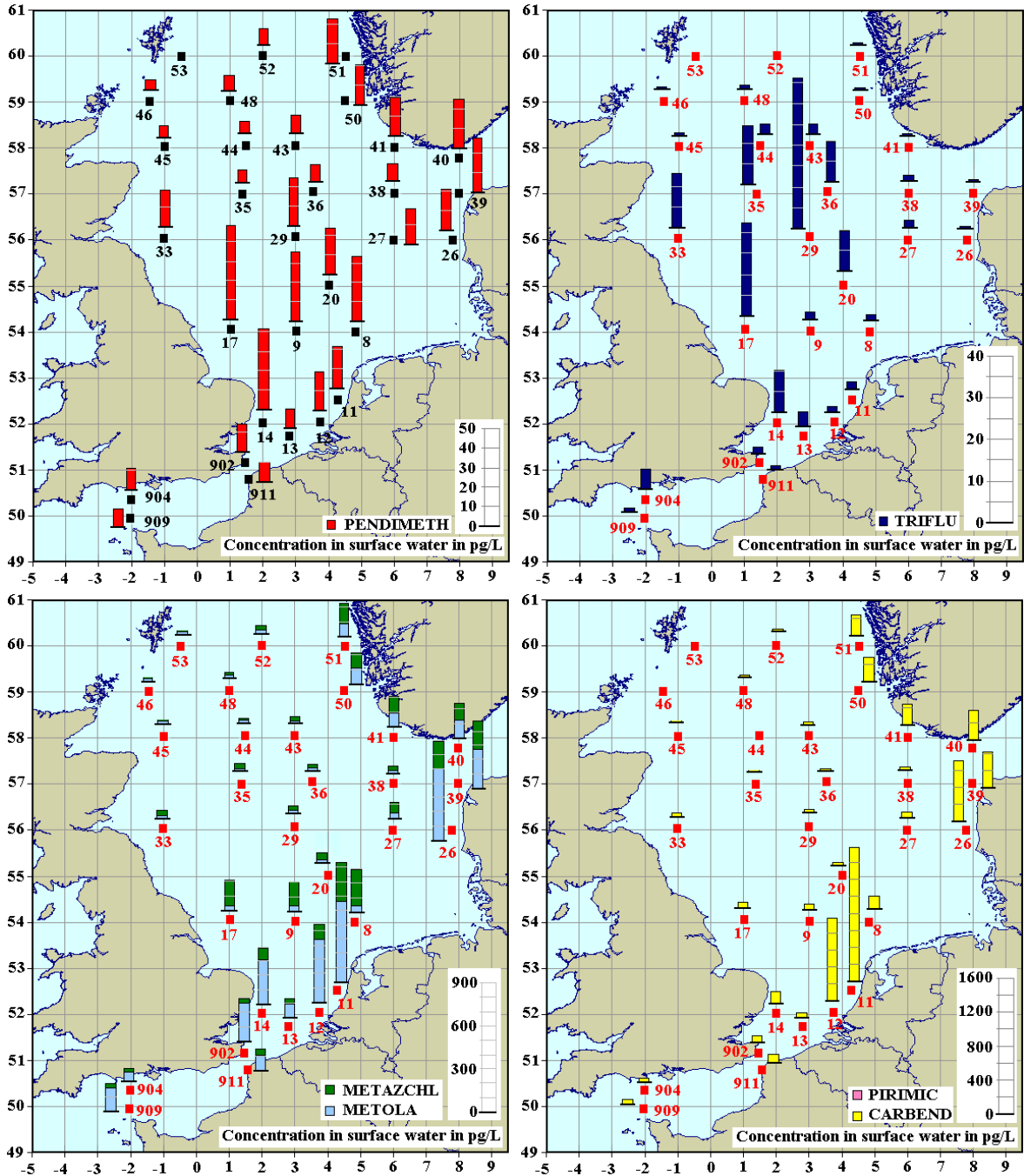


Figure 5.101: Occurrence and distribution of dinitroaniline, chloroacetanilide and carbamate pesticides in the aqueous phase of the surface water (5 m) of the North Sea in Aug./Sep. 2009

The carbamate fungicide carbendazim displayed the typical concentration profile in the surface water of the German EEZ and the North Sea emerging from a predominant riverine input, the outflow of the Baltic Sea and a subsequent dilution along the prevailing sea currents (figures 5.100 and 5.101). Surface water concentrations in the range of 3.0 pg/L to 5.3 ng/L and 5.3 pg/L to 1.6 ng/L were quantified in the German EEZ in May 2010 and in the North Sea in Aug./Sep. 2009, respectively. Carbendazim was even detected at the western sampling sites of the German EEZ and at the remote sampling sites in the northern North Sea, which were dominated by the inflow from the Atlantic Ocean and thus unaffected by riverine input. This could point to the occurrence of atmospheric deposition, although carbendazim was never detected in the atmosphere of the German EEZ and occurred only sporadically in the atmosphere of the North Sea. Surface water concentrations of carbendazim for the German EEZ in May/Jun. 2009 and for the Baltic Sea in Jun./Jul. 2008 were not available.

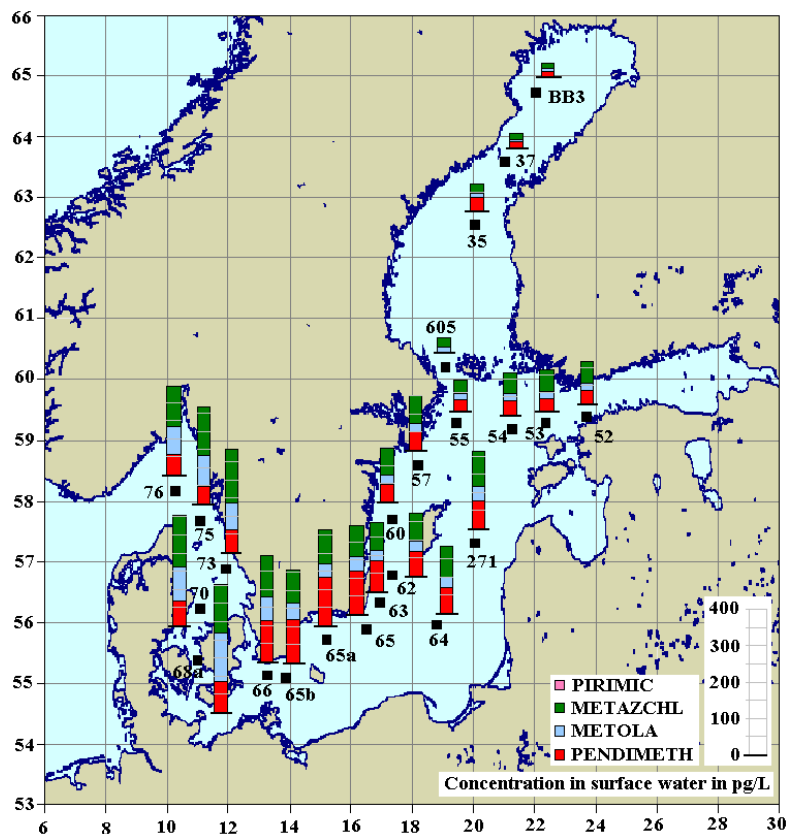


Figure 5.102: Occurrence and distribution of dinitroaniline, chloroacetanilide and carbamate pesticides in the aqueous phase of the surface water (6 m) of the Baltic Sea in Jun./Jul. 2008

Seasonal fluctuations in the surface seawater concentrations

The seasonal fluctuations in surface water concentrations observed in the German EEZ in 2009 (figure 5.103) correlated with the seasonal variations in atmospheric concentrations and thus with the individual application periods in agriculture as discussed above (figure 5.97).

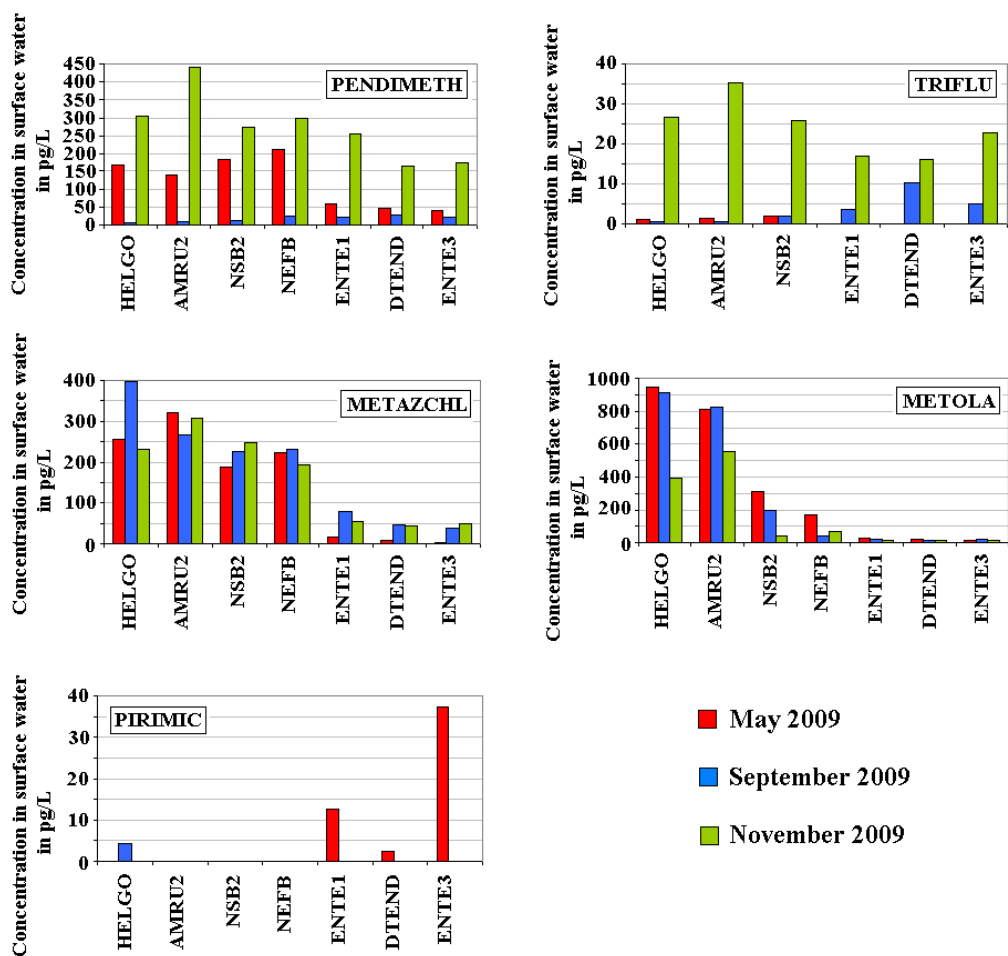


Figure 5.103: Seasonal variations in the surface water concentrations (5 m) of the dinitroaniline, chloroacetanilide and carbamate pesticides displayed for selected sampling sites in the German EEZ in 2009; The sampling sites are sorted by increasing meridional distance from the Elbe estuary from the left to the right

Pendimethalin and trifluralin exhibited a seasonal maximum in surface water concentrations in November 2009 throughout all sampling sites in the German EEZ, which was in relation to the maximum in the atmospheric abundances from September to November. Besides, pendimethalin displayed a second, but less pronounced seasonal increase in surface water concentrations in May 2009, which was even monitored in the air of Sülldorf/Hamburg. The strong correlation in seasonal variations of the surface seawater concentrations and the atmospheric abundances throughout all sampling sites provided further evidence to a strong atmospheric deposition of the dinitroanilines herbicides into the surface seawaters, in particular during their main agricultural application seasons.

Metolachlor displayed highest surface water concentrations in May 2009, which agreed with the maximum in atmospheric concentrations from May to June. The seasonal profiles in surface water concentrations were well pronounced at the sampling sites inside the river plume of the Elbe and in the central German EEZ, but were not observed at the western sampling sites in the open sea.

These observations confirmed the predominant riverine input of metolachlor to the surface seawater. In contrast, metazachlor revealed increased surface water concentrations in September and November 2009. This seasonal profile was also well pronounced at the western sampling sites of the German EEZ, which were less affected by variations in riverine input. Considering the season of maximum atmospheric abundances of metazachlor, atmospheric deposition was supposed to be a major contributor to the surface seawater contamination during the main agricultural application period.

A seasonal profile in the surface water concentrations of pirimicarb was not monitored, because it was only sporadically quantified in the surface water of the German EEZ presumably due to its short persistence in the environment. However, it was most frequently quantified in May 2009 at the western sampling sites of the German EEZ, which was within the season exhibiting atmospheric abundances of pirimicarb. These results supported the perception that atmospheric deposition was the major input pathway of pirimicarb to the surface water of the German EEZ. A seasonal profile in surface water concentrations of carbendazim could not be investigated, because the surface seawater concentrations for May 2009 were not available.

Net flux of diffusive gas exchange of dinitroaniline, chloroacetanilide and carbamate pesticides between the marine atmosphere and the surface seawater

The direction of the net flux of diffusive gas exchange was calculated for the dinitroaniline and the chloroacetanilide herbicides, whenever they were present in the gaseous mass fraction of the atmosphere. Surface water concentrations of trifluralin in the Baltic Sea were not available. Hence, the gaseous net flux of trifluralin within the Baltic Sea region could not be determined. Moreover, pirimicarb and carbendazim were excluded from these calculations either due to surface seawater concentrations below LOQ or due to their absence in the gaseous mass fraction of the marine atmosphere. It had to be considered that the surface water concentrations of the Baltic Sea originated from a research cruise performed nine months before the active air sampling campaign of the Baltic Sea. Thus, seasonalities in surface water concentrations presumably biased the calculated fugacity ratios of the Baltic Sea. The results were summarized in figure 5.104.

Pendimethalin and trifluralin occurred in highest abundances in the gaseous mass fraction of the atmosphere and were thus prone to dry gaseous deposition. Due to the spatial distribution of pendimethalin in the marine atmosphere and in the surface water, atmospheric deposition was concluded to be the major input pathway to the surface seawater. This conclusion was confirmed by the fugacity ratios for pendimethalin indicating net dry gaseous deposition throughout the German EEZ, the wider North Sea and the Baltic Sea. Besides, a close to phase equilibrium was indicated for pendimethalin at the coastal sampling sites of the German EEZ in 2010. Although

trifluralin displayed a similar spatial distribution in the marine atmosphere and a comparable anomalous distribution in the surface seawater as pendimethalin, a trend to net dry gaseous deposition was exclusively determined for the sampling sites exhibiting highest atmospheric concentrations. Instead, a close to phase equilibrium or even net volatilisation was determined for the majority of the sampling sites in the German EEZ and the North Sea. However, high atmospheric abundances of trifluralin presumably caused by current usage, were observed to significantly lower the fugacity ratios, which pointed to the occurrence of net dry gaseous deposition. Thus, the fugacity ratios supported the perception that atmospheric deposition was the major input source of trifluralin and pendimethalin to the surface sea water during their main application season in agriculture.

An overall dry gaseous deposition was calculated for metazachlor and metolachlor throughout the German EEZ, the wider North Sea and the Baltic Sea. However, dry particle and wet deposition were assumed to exceed the gaseous deposition, considering the predominant occurrence of the chloroacetanilide herbicides in the particle associated mass fraction of the atmosphere.

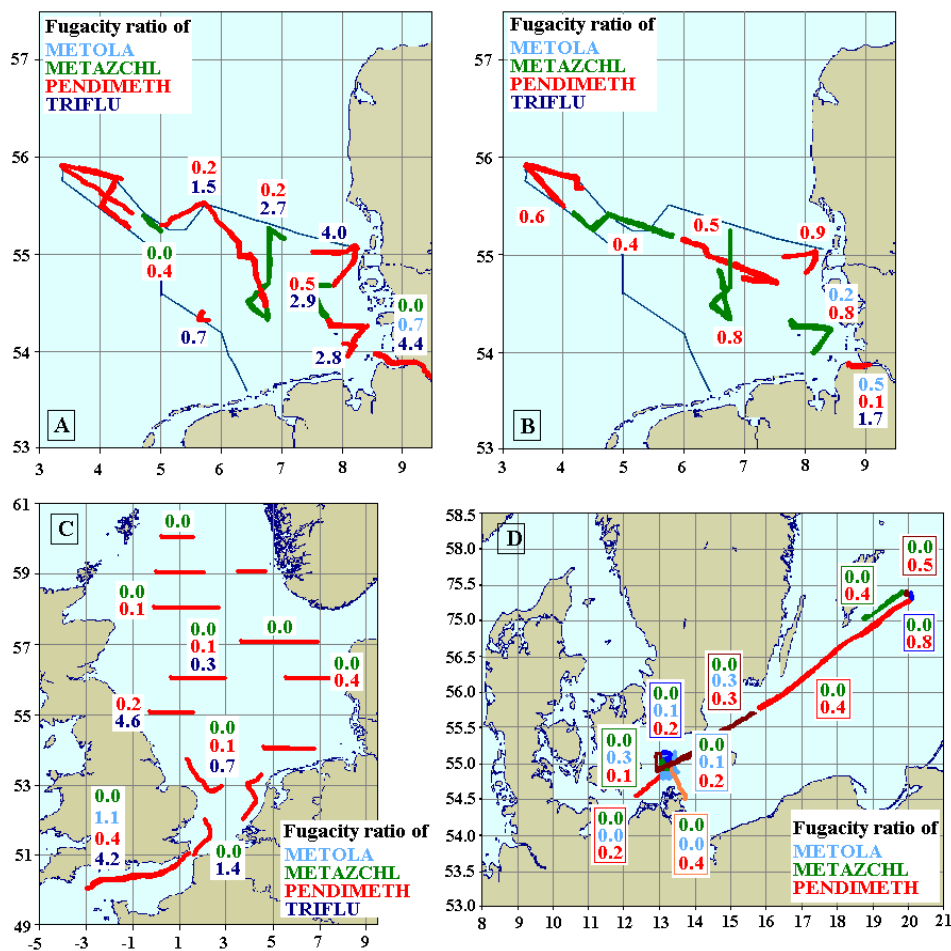


Figure 5.104: Net flux of diffusive gas exchange of the dinitroaniline and chloroacetanilide herbicides; Fugacity ratio < 0.5: Atmosphere → Sea; Fugacity ratio > 2: Sea → Atmosphere; (A) German EEZ May/June 2009; (B) German EEZ May 2010; (C) North Sea Aug./Sep. 2009; (D) Baltic Sea Apr. 2009

Conclusions

The dinitroaniline herbicides displayed a widespread distribution in the marine atmosphere, which was found to be determined by the advection of contaminated air from land. Both components were quantifiable throughout the entire year in the continental atmosphere, but exhibited seasons of significantly increased abundances. Those could be related to the periods of their application as preemergence herbicides, in particular for the protection of the winter grain in autumn. The same seasonality was observed in the surface water throughout all sampling sites of the German EEZ. The dinitroaniline herbicides revealed anomalous distribution patterns in the surface seawater of the German EEZ and the North Sea, which could be excluded to emerge from riverine input and the prevailing sea currents. Instead, the high surface water concentrations in the central North Sea and the German EEZ strongly pointed to atmospheric deposition as a major input pathway, especially during the main agricultural application seasons. Their dominant occurrence in the gaseous mass fraction of the atmosphere made them prone to long range transport and gaseous exchange processes with the surface seawater. The fugacity ratios confirmed an overall dry gaseous deposition of pendimethalin throughout the entire sea regions of the German EEZ, the wider North Sea and the Baltic Sea, whereas a close to phase equilibrium or even net volatilisation was indicated for trifluralin. However, high atmospheric abundances of trifluralin presumably caused by current usage, were observed to significantly lower the fugacity ratios, which pointed to the occurrence of net dry gaseous deposition.

The occurrence and concentrations of the chloroacetanilide herbicides in the atmosphere were strongly related to the periods of preemergence weed control in agriculture. The same seasonality was observed in the surface seawater of the German EEZ. Metolachlor was found to be predominantly applied for the protection of the summer grain, whereas metazachlor reached highest environmental abundances in autumn during the sowing of the winter grain. The advection of contaminated air from land provided a widespread distribution of the chloroacetanilides in the marine atmosphere during the periods of current agricultural usage. These seasonally increased atmospheric concentrations significantly contributed to the surface seawater contamination, in particular at the sampling sites of the open sea. The major mass fraction of the chloroacetanilides in the atmosphere was particle associated. Thus, dry particle and wet deposition fluxes were supposed to overcome the dry gaseous deposition to the surface seawater. However, rivers and the outflow of the Baltic Sea were found to be the dominant input sources of the chloroacetanilides to the surface seawater, as indicated by the typical concentration profiles emerging from a prevailing riverine transport and the sea currents.

The carbamate insecticide pirimicarb exhibited a short persistence in the environment.^[177-179] It was neither detected in the marine atmosphere nor in the surface water of the North Sea and the Baltic Sea. However, seasonally increased atmospheric abundances from May to June could be monitored in the continental atmosphere of Sülldorf/Hamburg. During this season, it was even sporadically detected in the surface water of the German EEZ. It was concluded that atmospheric deposition was a major input pathway of pirimicarb to the surface seawater. The occurrence and distribution of pirimicarb in the marine environment was similar to that described for the organophosphate insecticides in chapter 5.1.8.

In contrast, the fungicide carbendazim displayed the typical concentration profile in the surface seawaters indicating a predominant riverine input. In addition, carbendazim was never detected in the atmosphere of the German EEZ and occurred only sporadically in the air of the North Sea. However, the occurrence of carbendazim at sampling sites in the western German EEZ and in the northern North Sea, which were unaffected by riverine input pointed to the occurrence of atmospheric deposition.

5.1.12 Perfluorinated compounds

Perfluorinated compounds (PFCs), in particular those of the type perfluoroalkyl sulfonate (PFSA) and perfluoroalkyl carboxylate (PFCA), are used in a wide range of commercial products. During the last decades, they have been extensively applied as industrial surfactants, additives, refrigerants, oil, water and stain repellents for paper, leather and textile as well as in fire fighting foams. Besides, they are constituents of fluoropolymers like polytetrafluoroethylene (PTFE) and polyvinylidene fluoride (PVDF). Production, application and waste disposal are their most important emission sources to the environment. Perfluorinated surfactants exhibit an extreme persistence and are globally distributed throughout all environmental media. PFCs are assimilated by water organisms like water plants and fishes providing an accumulation along the food chain and thus an increased toxicity potential.^[180, 181] Nine linear perfluorinated compounds are targeted in this study (table 3.10), of which three are perfluoroalkyl sulfonates (PFBS, PFHXS, PFOS), five are perfluoroalkyl carboxylates (PFHXA, PFHPA, PFOA, PFNOA, PFDEA) and one is a volatile precursor compound (PFOSA) of the class perfluorinated sulfonamides.

Occurrence and distribution of PFCs in the marine atmosphere

The targeted perfluorinated compounds could be quantified in very low concentrations of less than 1.5 pg/m³ in the marine atmosphere, which were either close or below the LOQ. However, a limited data set was obtained (figures 5.105- 5.107). The occurrence and spatial distributions of the perfluorinated compounds in the marine atmosphere of the German EEZ (figures 5.105 and 5.106)

and the wider North Sea (figure 5.107) were found to be less affected by the air mass history (chapter 3.5). Instead, an increase in the atmospheric concentrations and thus a wider spectrum of the targeted PFCs was observed with decreasing distance to the continent. This might indicate complex and diffusive emission sources of the targeted PFCs to the marine atmosphere, which were not primarily dominated by the advection of air from land.

Fluorotelomer alcohols, perfluorinated sulfonamides and perfluorinated sulfonamido ethanols are volatile precursor compounds of the targeted PFCs. They occur in the gaseous mass fraction of the atmosphere and are thus prone to long range transport.^[54] A widespread distribution of precursor compounds, especially of the fluorotelomer alcohols, was reported for the atmosphere above the German EEZ in 2007.^[55] It was assumed that the formation of PFSA and PFCA from precursor compounds might be an important factor influencing their occurrence and spatial distribution in the marine atmosphere. Furthermore, wave breaking processes could provide a direct transport of PFCs from the water column to the marine atmosphere (chapter 2.3.2).

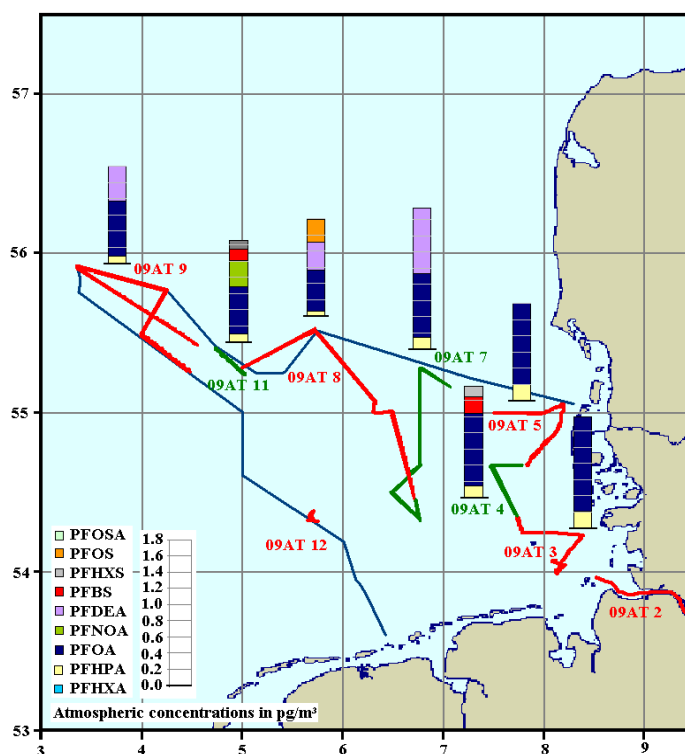


Figure 5.105: Atmospheric bulk concentrations of the PFCs above the German EEZ in May/June. 2009

PFOA was most frequently quantified in the marine atmosphere. It was detected throughout all sampling sites in the German EEZ and was overall present in the North Sea atmosphere. Exclusively the sampling sites in the northern North Sea (PE16, PE17, PE18) exhibited lowest atmospheric abundances of PFOA below LOQ. PFOA was quantified in almost constant atmospheric concentrations in the range of 0.5 pg/m^3 to 1.5 pg/m^3 . PFOS could be detected in

similar concentrations (0.1 pg/m³ to 1.5 pg/m³) at the majority of the sampling sites. However, its spatial distribution displayed a more sporadic character than observed for PFOA. This was displayed by a comparison of sea and land based sampling sites in figure 5.108: The significantly increased contamination level of the air of Sülldorf/Hamburg and at sea based sampling sites in proximity to the coast suggested that PFOS was primarily emitted from continental sources to the marine atmosphere. In contrast, PFOA exhibited similar mean atmospheric concentrations (0.7 pg/m³) throughout all sampling sites, which might point to further input pathways of PFOA to the marine atmosphere beyond air mass advection from land. It was assumed that PFOA underwent sea air exchange via wave breaking processes and sea spray causing an ongoing contamination of the marine atmosphere independent from current sources at the continent. Lab experiments supported this perception. It was observed that deprotonated PFOA was concentrated on the surface of fine aerosol bubbles, as they might be build by bubble bursting processes in the water column of the surface seawater. [182]

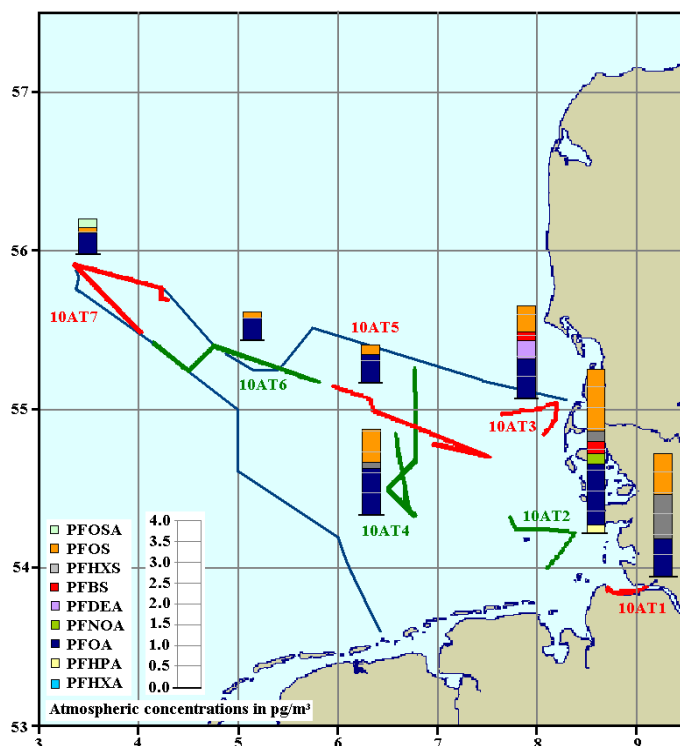


Figure 5.106: Atmospheric bulk concentrations of the PFCs above the German EEZ in May 2010

All other targeted PFCs were sporadically, but less frequently quantified in the marine atmosphere than PFOS and PFOA (figures 5.105- 5.107). A sequence emerging from their frequency of atmospheric concentrations above the LOQ might be as follows: PFHPA, PFNOA/PFHXS, PFBS, PFDEA, PFHXA/PFOA. The occurrence and spatial distribution of the PFCs in the marine atmosphere of the Baltic Sea could not be described, due to the missing

concentration data of the particulate mass fraction. Seasonal fluctuations in atmospheric concentrations of PFCs were neither observed in Tinnum/Sylt nor in Sülldorf/Hamburg.

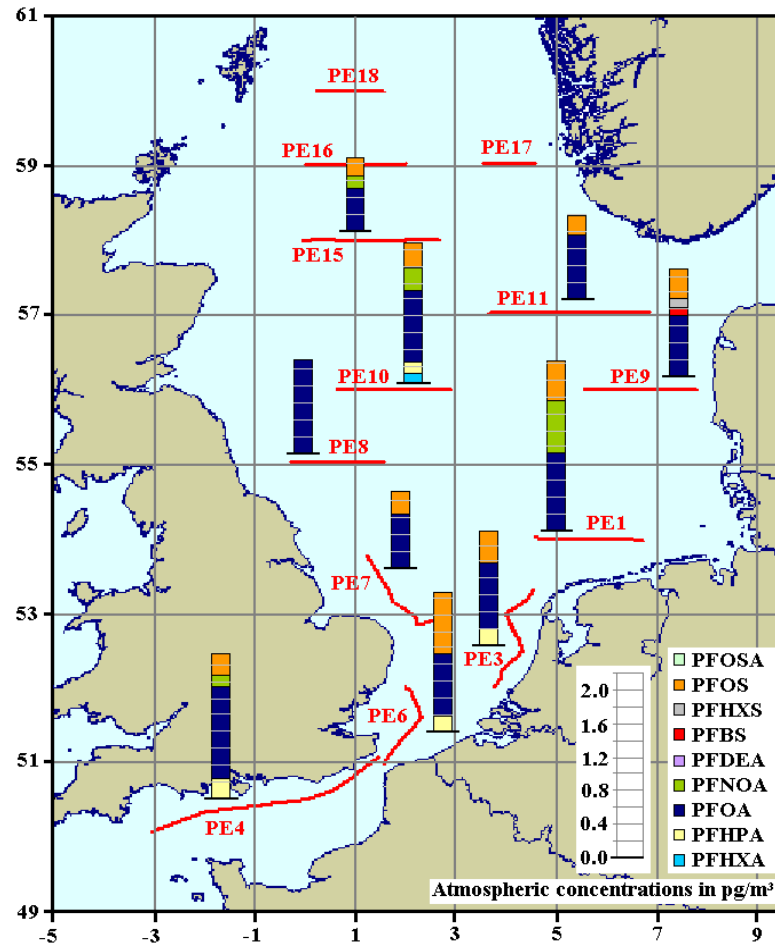


Figure 5.107: Atmospheric bulk concentrations of PFCs above the North Sea in Aug./Sep. 2009

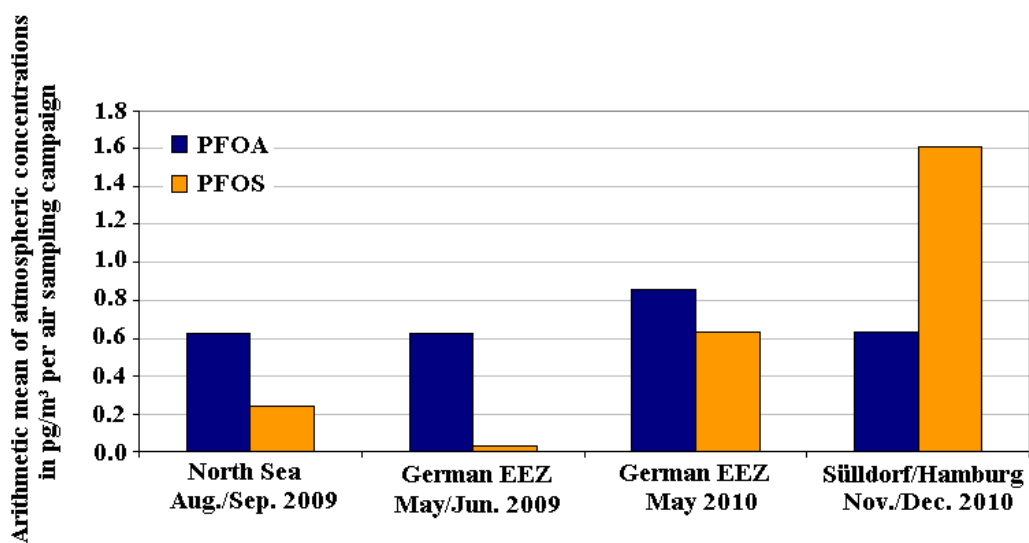


Figure 5.108: Arithmetic mean bulk concentrations of PFOS and PFOA in pg/m³ at sea and land based sampling sites

Gas-particle partitioning

It has been reported that the PFSA and PFCA occur in the particle associated mass fraction of the atmosphere, whereas the more volatile precursor compounds are present in the gaseous mass fraction. ^[55] In this study, the PFCs could be extracted from the GFFs as well as from the adsorber cartridges. However, the gas-particle partitioning of the targeted PFCs could not be evaluated, due to the very low concentration levels close to the LOQs. Moreover, the low concentrations might be additionally biased by the blow-on and blow-off effects related to active air sampling (chapter 3.1.1).

Occurrence and distribution of PFCs in the surface seawater

The targeted PFCs displayed the typical distribution patterns in the surface water of the German EEZ and the wider North Sea emerging from a predominant riverine input and a subsequent distribution along the prevailing sea currents (chapter 3.6). The main surface water contaminants of the targeted PFCs were PFOA and PFOS reaching mean concentrations of 1.2 ng/L to 1.5 ng/L and 0.8 ng/L to 1.2 ng/L inside the river plume of the Elbe (ELBE, EIDER, HELGO) within the German EEZ (figures 5.109 and 5.110), respectively. Their surface water concentrations decreased to <200 pg/L and <100 pg/L at the western sampling sites of the German EEZ beyond the river plumes, respectively. The surface water of the wider North Sea (figure 5.111) exhibited highest PFOA and PFOS concentrations inside the river plumes of the Rhine and the Thames (8, 11, 12, 13, 14), but also in the region of the Baltic Sea outflow (39, 40, 41, 50, 51). Concentrations of up to 3.0 ng/L and 2.8 ng/L were quantified, which decreased to less than 300 pg/L and 80 pg/L towards the sampling sites in the central and northern North Sea, respectively. PFOA reached higher surface seawater concentrations than all other targeted PFCs throughout all sampling sites. This might support the perception that PFOA was introduced to the marine atmosphere via wave breaking processes as discussed above.

The other targeted PFCs displayed similar distribution patterns as described for PFOS and PFOA. They differed in the extent of the concentration gradients between the coastal sampling sites inside the river plumes and of the open sea. All targeted PFCs could be detected throughout all sampling sites.

A shift in the surface seawater composition of PFCs from the coastal to the remote sampling sites was observed (figure 5.113). As an example PFOA, PFNOA and PFOSA exhibited a higher fraction on the total PFC composition at the remote sampling sites, whereas PFOS and PFBS revealed increased fractions at the coastal sampling sites. Other PFC components like PFHXA, PFHPA, PFDEA and PFHXS displayed almost constant fractions on the total PFC burden throughout all sampling sites. These observations suggested that the transport in the water phase

was not the only important input and distribution mechanism of PFCs, as this might result in a more homogenous surface seawater composition.

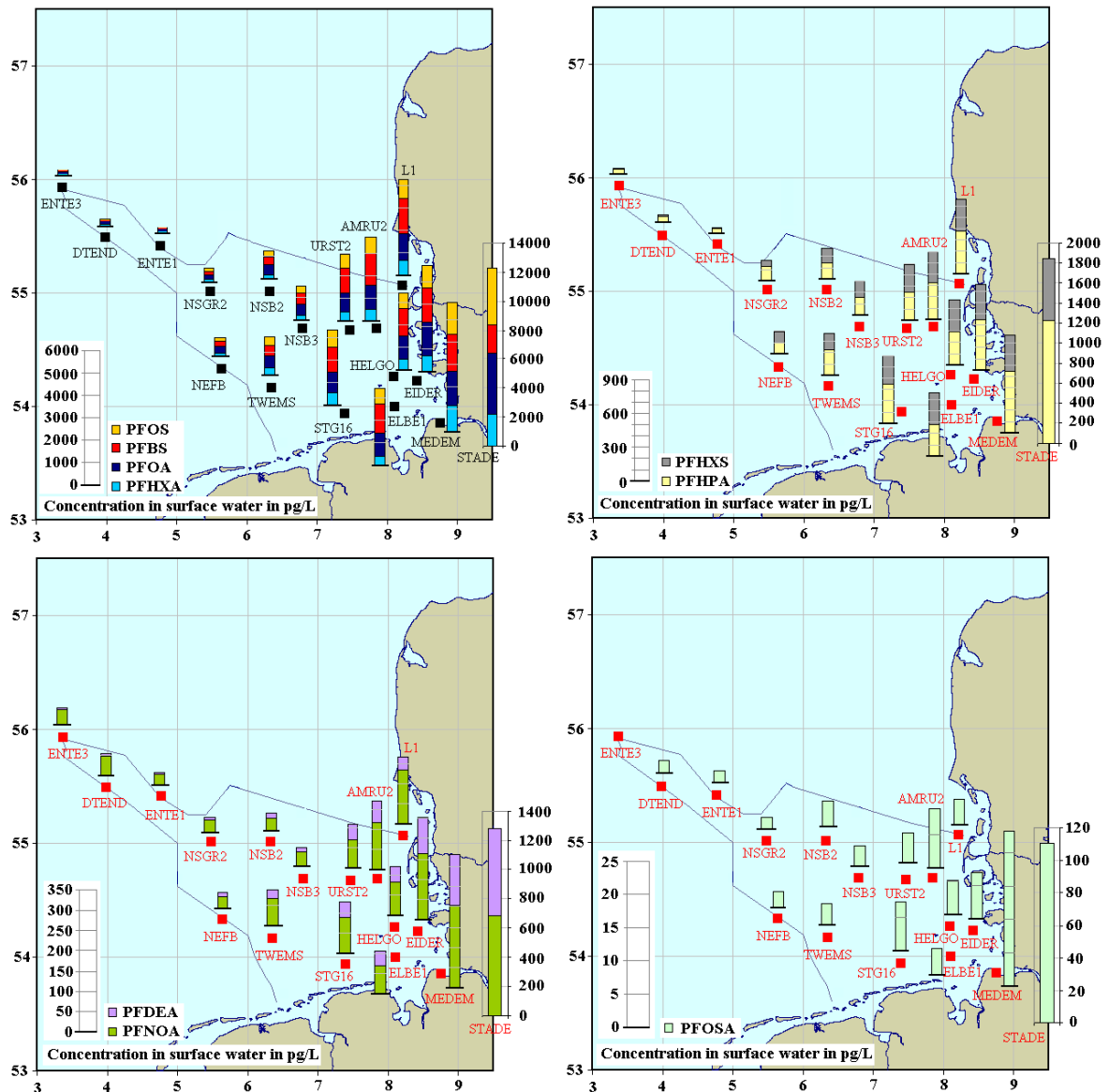


Figure 5.109: Occurrence and distribution of PFCs in the aqueous phase of the surface water (5 m) of the German EEZ in May/June, 2009

The surface water of the Baltic Sea displayed an almost homogenous PFC composition and only slow concentration gradients (figure 5.112). All targeted PFCs were detected throughout all sampling sites, except of PFOSA, which occurred only sporadically in three water samples collected in the central Baltic Sea (65, 65b, 62). The sum concentrations of the PFCs at individual sampling sites varied between 1.9 ng/L and 0.8 ng/L and were comparable with those quantified in the central German EEZ. The surface water composition was similar to that of the North Sea at the sampling sites beyond the river plumes (figure 5.113). Highest sum concentrations were determined in the central Baltic Sea (62), whereas lowest were observed in the Bothnian Bay (37).

Individual PFC compounds displayed a slightly different spatial distribution, e.g., PFBS and PFOA exhibited highest surface water concentrations in the region of Skagerrak and Kattegat (68a, 70, 73, 75). The homogeneous and widespread distribution of the PFCs in the surface water of the Baltic Sea might point to a second transport mechanism beyond the distribution by the prevailing sea currents, as it was also suggested by the PFC patterns in the surface waters of the German EEZ and the wider North Sea (figure 5.113). In recent years, it has been hypothesized that the formation of PFCAs and PFSA from their volatile precursor compounds, which undergo long-range transport in the atmosphere, efficiently contribute to the widespread distribution of the PFCs. In contrast, PFCAs and PFSA are not expected to travel long distances in the atmosphere, because of their low volatility and efficient elimination by wet and dry deposition. [54, 55]

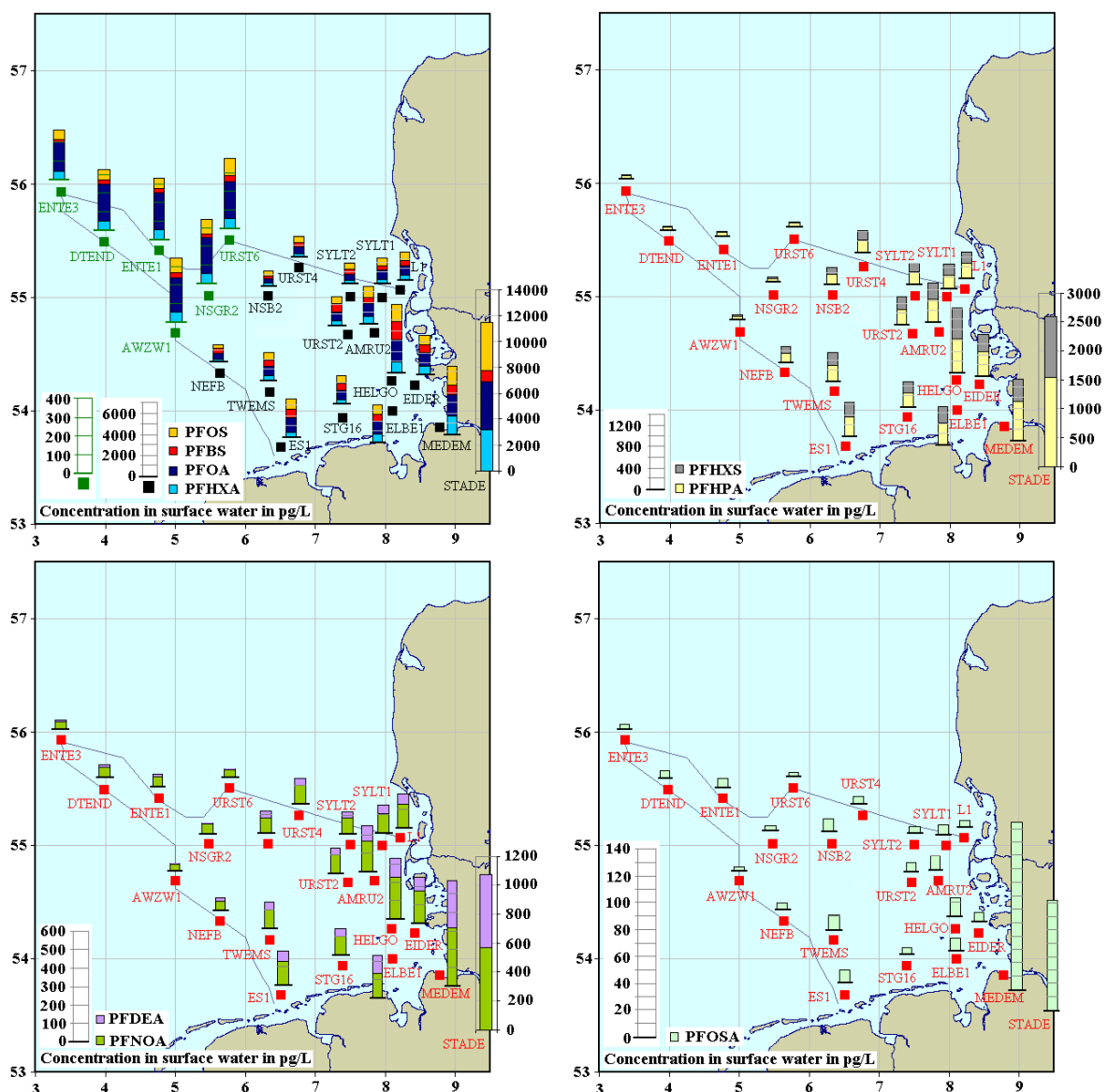


Figure 5.110: Occurrence and distribution of PFCs in the aqueous phase of the surface water (5 m) of the German EEZ in May 2010

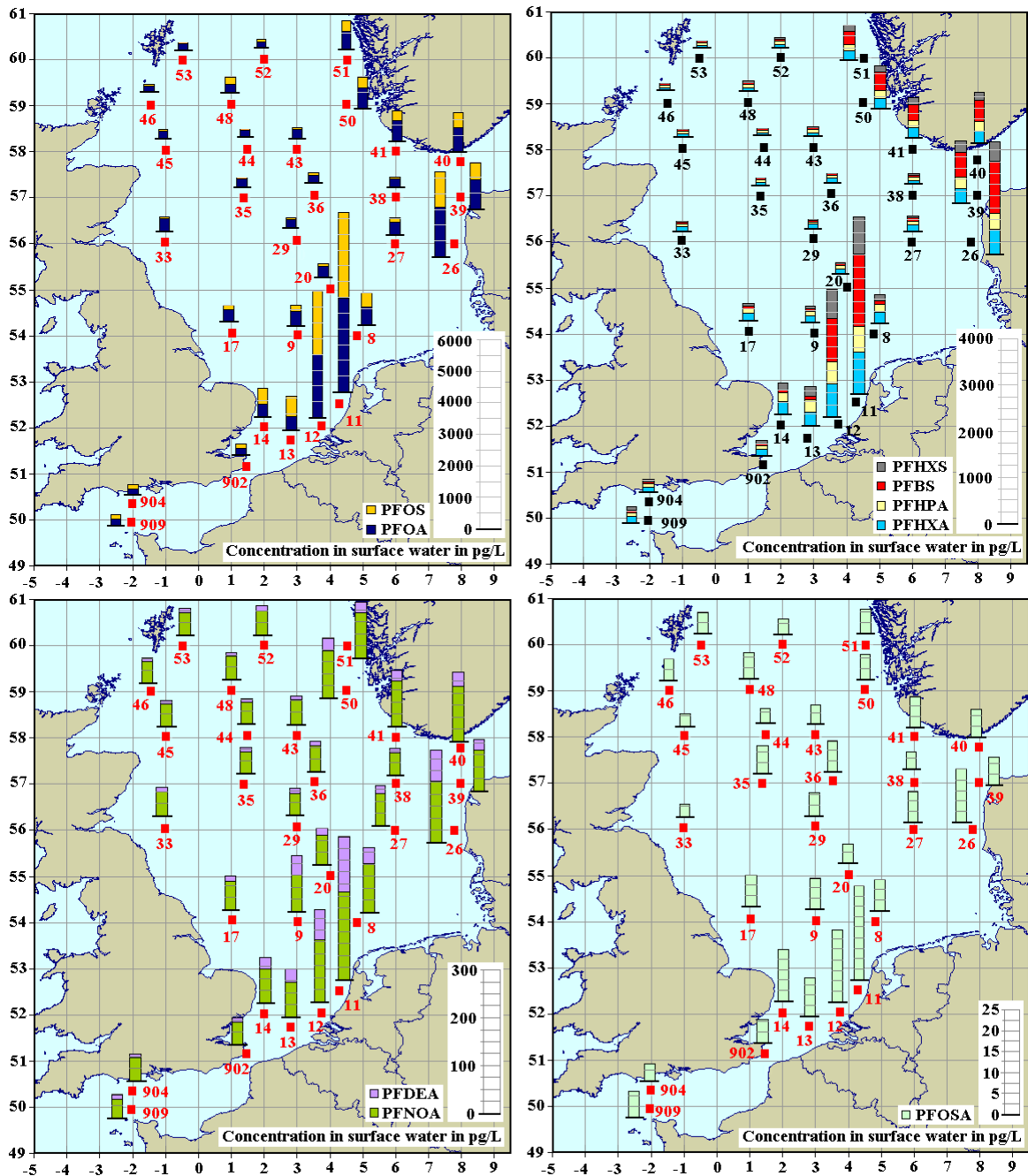


Figure 5.11: Occurrence and distribution of PFCs in the aqueous phase of the surface water (5 m) of the North Sea in Aug./Sep. 2009

The concentrations and spatial distribution of the PFCs in the surface water of the North Sea and the Baltic Sea had been already documented for the year 2005 and were in agreement with the results of the years 2008 to 2010 reported in this study. ^[183] A significant seasonality in the surface water concentrations of the targeted PFCs was not observed.

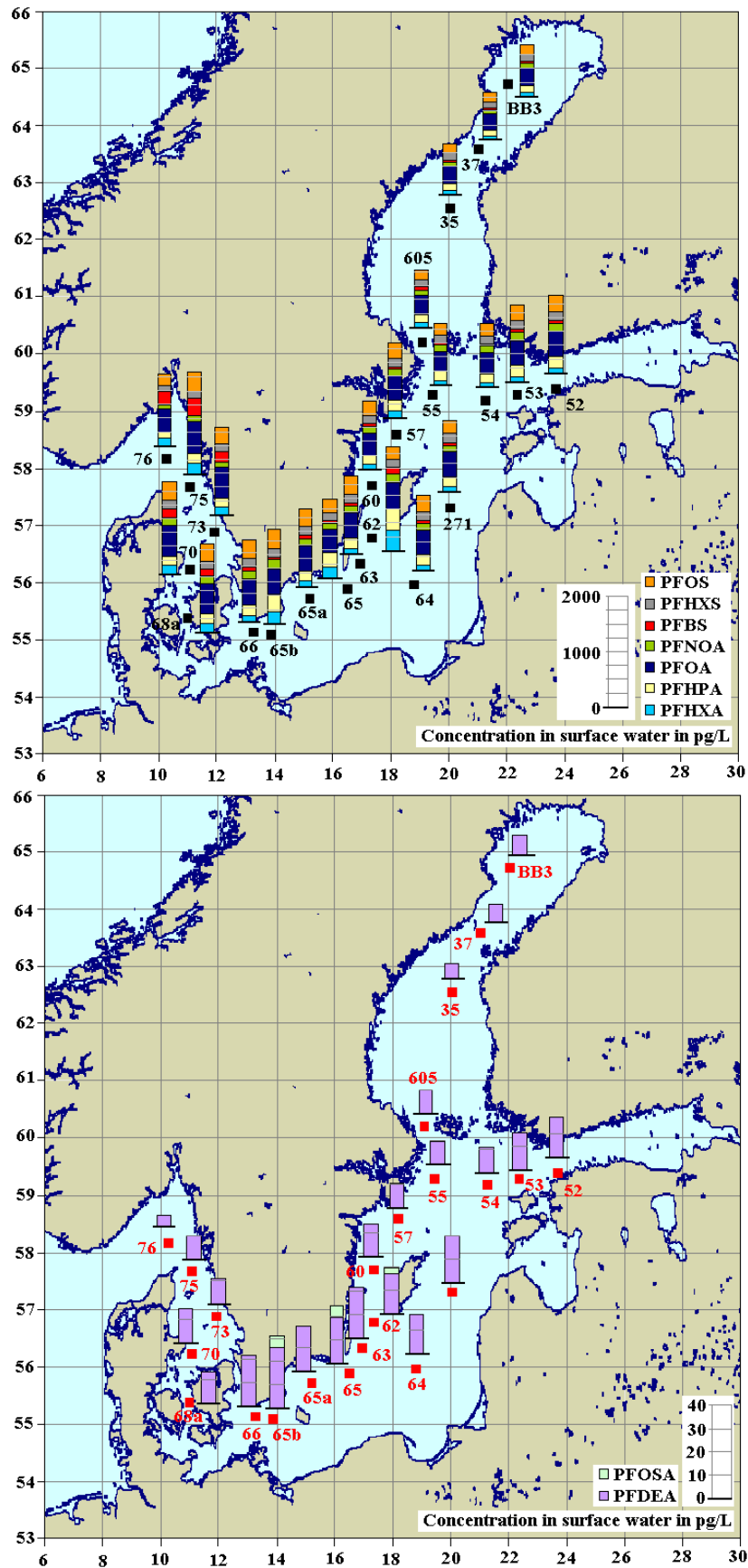


Figure 5.112: Occurrence and distribution of PFCs in the aqueous phase of the surface water (6 m) of the Baltic Sea in Jun./Jul. 2008

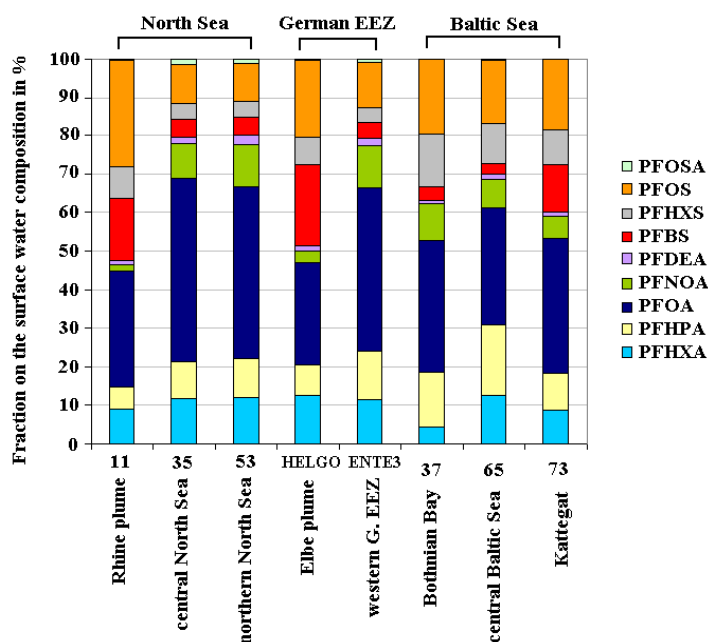


Figure 5.113: Composition of the targeted PFCs in the surface water (5-6 m) of the North Sea, the German EEZ and the Baltic Sea

Net flux of diffusive gas exchange of PFCs between the marine atmosphere and the surface water

The direction of the net flux of diffusive gas exchange of PFCs between the marine atmosphere and the surface seawater was not calculated, because the PFCs were predominantly associated with particulate mass fraction of the atmosphere and were thus not prone to dry gaseous deposition. The atmospheric abundances determined in the gaseous mass fraction were presumably affected by blow off effects from the GFF to the adsorber cartridge (chapter 3.1.1). Furthermore, the targeted perfluorinated compounds revealed surface active properties limiting the validity of the Henry's Law and the approach for the calculation of the direction of the net flux of diffusive gas exchange.

Conclusions

The targeted PFC compounds displayed the typical spatial distribution in the surface seawater emerging from riverine input and a distribution in relation to the sea currents. Thus, the transport in the water column was confirmed to be a main distribution pathway of PFCs in the environment. However, the widespread distribution of the targeted PFCs throughout all sampling sites in the German EEZ, the wider North Sea and the Baltic Sea as well as the shift in the surface water composition from the coastal to the remote sampling sites and the variability in the concentration gradients within the individual PFCs indicated a further input pathway to the surface seawater. The targeted PFCs occurred in very low concentrations near or below the respective LOQ in the marine atmosphere. Thus, atmospheric deposition might not be a major contamination source of the

surface seawater. Instead, the continuous and widespread occurrence of PFOA in the marine atmosphere apparently unaffected by the air mass history pointed to a sea-air exchange via wave breaking processes. In addition, the negligible vapour pressures of the targeted PFCs and thus the predominant occurrence in the particle associated mass fraction of the atmosphere indicated negligible long range transport potential. However, atmospheric transport and subsequent deposition might be the most probable explanation on the widespread distribution of the PFCs. In recent studies, it has been hypothesized that the distribution of PFCAs and PFSA in the environment is supported by their formation from the more volatile precursor compounds like fluorotelomer alcohols, perfluorinated sulfonamides and perfluorinated sulfonamido ethanols, which are able to travel great distances in the atmosphere. Those compounds have been found to be overall present in the marine atmosphere of the German EEZ. ^[55]

5.1.13 Organophosphorus and Brominated Flame Retardants

Organic flame retardants have been extensively applied during the last decades. Individual brominated flame retardants of the class of polybrominated diphenylethers are nowadays banned under the Stockholm Convention (chapter 1.2). Flame retardants reduce the inflammability of a variety of industrial and commercial products. In addition, non halogenated organophosphorus compounds are additionally used as plasticizers, antifoaming agents and as additives in hydraulic fluids. ^[184] Three non-halogenated organophosphorus compounds are targeted in this study (table 3.10): TBEP (Tris(2-butoxyethyl)phosphate), TBP (Tributyl phosphate) and TPP (Triphenyl phosphate). Besides, three isomers of the brominated flame retardant hexabromocyclododecane (α -HBCD, β -HBCD and γ -HBCD) are investigated, whereof β - and γ -HBCD are quantified as sum parameter.

Occurrence and distribution of organophosphorus and brominated flame retardants in the marine atmosphere

The organophosphorus flame retardants exhibited extraordinarily increased blank values (chapter 4.2), which were assumed to originate from multiple sources throughout the cleaning, sample preparation and analysis procedures. In consequence, the limits of quantification were remarkably increased (chapter 4.3) and the concentrations above the LOQs revealed a decreased reliability. Nevertheless, their occurrence in the marine atmosphere was confirmed by this study. The tree targeted non-chlorinated organophosphorus flame retardants were quantified in concentrations, which marked them as main organic contaminants of the marine atmosphere. They displayed a widespread spatial distribution throughout almost all sampling sites. In addition, their atmospheric abundances partly corresponded to the air mass history indicating a distribution based

on the advection of contaminated air from land. TBP and TPP were more frequently quantified and in a significantly higher concentration range than TBEP. TBEP was never detected in the marine atmosphere of the German EEZ, but occurred in the atmosphere of the wider North Sea and in a single air sample of the Baltic Sea. It was also scarcely detected in the urban atmosphere of Sülldorf/Hamburg. The concentration levels of the targeted organophosphorus flame retardants in the marine and continental atmosphere were comparable (table 5.8).

The occurrence of organophosphorus flame retardants and plasticizers in the atmosphere of the North Sea was still reported for the year 2010 during another study. The influence of industrialised regions on the atmospheric abundances was documented by an air mass backward trajectory analysis. The concentration ranges were in agreement with the results of this study with 4 – 290 pg/m³, n.d. – 150 pg/m³, n.d. – 80 pg/m³ for TPP, TBP and TBEP, respectively. The chlorinated organophosphorus compound TCPP (tris(2-chloroisopropyl)phosphate) was reported to be the predominant flame retardant in the atmosphere. ^[184]

Table 5.8: Occurrence and bulk concentrations (pg/m³) of organophosphorus and brominated flame retardants in the atmosphere above the German EEZ, the wider North Sea, the Baltic Sea and Sülldorf/Hamburg; range = range of atmospheric concentrations above the LOQ in pg/m³; n/n = number of positive analysed air samples/number of total analysed air samples

Sampling site	German EEZ		German EEZ		North Sea	
Date	27.05 - 03.06.09		18.05 - 23.05.10		21.08 - 07.09.09	
	range	n/n	range	n/n	range	n/n
TBEP	< LOD	0/9	< LOD	0/7	2.8 - 33.5	7/13
TBP	11.9 - 41.0	6/9	28.1 - 108.1	7/7	14.3 - 156.3	11/13
TPP	4.2 - 36.3	7/9	4.8 - 1922.2	7/7	7.0 - 1041.7	12/13
HBCD-A	< LOD	0/9	< LOD	0/7	< LOD	0/13
HBCD-BG	< LOD	0/9	< LOD	0/7	< LOD	0/13

Sampling site	Baltic Sea		Sülldorf/Hamburg	
Date	26.04. - 04.05.09		15.11 - 15.12.10	
	range	n/n	range	n/n
TBEP	32.9	1/10	4.1 - 12.5	5/20
TBP	27.2 - 92.6	9/10	21.3 - 305.9	20/20
TPP	5.8 - 238.8	10/10	9.3 - 128.6	12/20
HBCD-A	< LOQ	0/10	1.5 - 2.2	6/20
HBCD-BG	2.1 - 5.6	4/10	2.7 - 7.7	5/20

In contrast, the hexabromocyclododecane isomers were never detected in the marine atmosphere of the German EEZ and the Baltic Sea. Exclusively the sum concentration of β - and γ -HBCD could be sporadically quantified in air advected from the continent above the Baltic Sea. Besides, the three targeted isomers were sporadically observed in the urban atmosphere of Sülldorf/Hamburg. The atmospheric concentrations were < 2.2 pg/m³ for the α - isomer and < 7.7 pg/m³ for the sum parameter of β - and γ -HBCD (table 5.8). The concentrations correlated with the lower

concentration range in the air of urban and rural sampling sites in Sweden (2-610 pg/m³) reviewed in 2006. ^[185]

Gas-particle partitioning

The non-chlorinated organophosphorus flame retardants were detected in both mass fractions of the atmosphere, but were predominantly associated with the particulate matter. This was in agreement with a previous study documenting a mean particulate associated mass fraction of 86 ± 25 % for the sum of eight organophosphorus compounds on the bulk concentration. The occurrence of organophosphorus compounds in the gaseous mass fraction was reported to be affected by the fine aerosol particles in the marine atmosphere providing a passing through the filter and an accumulation on the adsorber cartridge. ^[184]

The HBCD isomers were exclusively detected in the particulate mass fraction of the atmosphere. This was consistent with the results of previous studies reporting a majority of the airborne HBCD abundances associated with the particulate matter and only a minor mass fraction in the gaseous phase. ^[185]

Occurrence and distribution of organophosphorus and brominated flame retardants in the surface seawater

Surface water concentrations of organophosphorus flame retardants were not available, due to the remarkably increased field and laboratory blanks preventing a reliable quantification. The brominated flame retardant HBCD could not be quantified in the surface water of the German EEZ, the wider North Sea and the Baltic Sea. Except a single concentration of 152 pg/L could be determined for the sum parameter of the β - and γ - isomer in a surface water sample of a coastal sampling site in proximity to the island Sylt (L1) in May/Jun. 2009. The absence of HBCD from the aqueous phase of the surface water might be attributed to the hydrophobic properties and the strong adsorption of HBCD to particulate matter, which indicated a predominant occurrence in soil and sediments. However, HBCD could not even be detected in the sediments of coastal waters investigated in previous studies. ^[185] Thus, significant abundances of HBCD in the surface seawater might be neither expected for the aqueous nor for the particulate phase.

Net flux of diffusive gas exchange of organophosphorus and brominated flame retardants between the marine atmosphere and the surface water

The direction of the net flux of diffusive gas exchange could not be calculated due to the missing surface water concentrations of the organophosphorus flame retardants and the low concentration levels of HBCD in the marine environment. Moreover, the flame retardants were predominantly

distributed in the particle associated mass fraction of the atmosphere, which made them rather prone to dry particle and wet deposition than to dry gaseous deposition.

Conclusions

The organophosphorus flame retardants were observed to be major contaminants of the marine atmosphere pointing to a significant contribution of atmospheric deposition to the pollution of the surface seawater. Their predominant occurrence in particulate mass fraction made them vulnerable to an efficient scavenging by wet and dry deposition processes. Further investigations with a wider spectrum of organophosphorus flame retardants will be necessary to assess the current environmental pollution of the marine environment. In addition, a blank optimization will be required for future examinations in order to increase the reliability of the results.

In contrast, the HBCD isomers were observed to be negligible contaminants of the atmosphere. In addition, they were not detected in the surface seawater. Thus, HBCD was found to be a minor contaminant of the marine environment of the German EEZ, the wider North Sea and the Baltic Sea.

5.1.14 Pharmaceuticals

Pharmaceuticals exhibiting a considerable persistence in the environment, display a widespread distribution in limnic waterbodies. Their occurrence in the ground and tap water has raised concern in recent years. The major input pathways of pharmaceuticals to the aquatic systems are the effluents of waste water treatment plants. Six organic compounds, which are extensively applied as active ingredients in pharmaceutical formulations for human medicine are targeted in this study. Primidone (PRIMID) and carbamazepine (CARBAMAZ) are antiepileptic drugs. Carbamazepine is persistent and is used as a marker of anthropogenic influences in the aquatic environment. Diclofenac (DICLOF) and naproxen (NAPROX) are nonsteroidal anti-inflammatory drugs, which additionally exhibit analgetic properties. Furthermore, clofibrac acid (CLOFIBRS), a blood lipid regulator and the sedative oxazepam (OXAZEP) are targeted. ^[186-191]

Occurrence and distribution of pharmaceuticals in the marine atmosphere

Pharmaceuticals were extremely rare in the atmosphere. Exclusively five positive findings could be documented for the marine atmosphere and sixteen for the continental atmosphere of Sülldorf/Hamburg. They were not detected in the PUF disk passive air samplers exposed in Sülldorf/Hamburg and Tinum/Sylt. However, all targeted pharmaceuticals, except of naproxen and oxazepam, could be at least observed in the atmosphere as summarized in table 5.9. The most frequently quantified pharmaceutical was carbamazepine. It was quantified in ten of twenty active air samples of Sülldorf/Hamburg in concentrations of up to 17 pg/m³.

Primidone was detected in a similar concentration range as carbamazepine, but occurred less frequently with a total of seven positive findings. Diclofenac was observed in a single air sample of the marine atmosphere in a concentration of 2.74 pg/m³. Clofibric acid occurred in two air samples collected in Sülldorf/Hamburg in concentrations of 2.54 pg/m³ to 2.76 pg/m³. Atmospheric data of clofibric acid, diclofenac and naproxen was only available for the particle associated mass fraction, due to their instability during soxhlet extraction preventing a reliable quantification.

The results indicated that direct primary sources of pharmaceuticals to the atmosphere did not exist. The scarcely positive findings in the atmosphere were assumed to originate from secondary emission sources of the widespread contaminated surface waters.

Table 5.9: Occurrence and bulk concentrations of carbamazepine, primidone and oxazepam and concentrations of clofibric acid, diclofenac and naproxen in the particle associated mass fraction of the atmosphere of the German EEZ, the wider North Sea, the Baltic Sea and of Sülldorf/Hamburg, respectively; range = range of atmospheric concentrations above the LOQ in pg/m³, n/n = number of positive analysed air samples/number of total analysed air samples

Sampling site	German EEZ		German EEZ		North Sea	
Date	27.05. - 03.06.09		18.05. - 23.05.10		21.08. - 07.09.09	
	range	n/n	range	n/n	range	n/n
CARBAMAZ	< LOD	0/10	< LOD	0/7	< LOD	0/13
PRIMID	5.09 - 46.01	3/9	< LOD	0/7	< LOD	0/13
DICLOF	2.74	1/9	< LOD	0/7	< LOD	0/13
NAPROX	< LOD	0/10	< LOD	0/7	< LOD	0/13
CLOFIBRS	< LOD	0/10	< LOD	0/7	< LOD	0/13
OXAZEP	< LOD	0/10	< LOD	0/7	< LOD	0/13

Sampling site	Baltic Sea		Sülldorf/Hamburg	
Date	26.04. - 04.05.09		15.11. - 15.12.10	
	range	n/n	range	n/n
CARBAMAZ	0.25	1/10	0.17 - 17.36	10/20
PRIMID	< LOD	0/10	1.65 - 11.49	4/20
DICLOF	< LOQ	0/10	< LOD	0/20
NAPROX	< LOD	0/10	< LOD	0/20
CLOFIBRS	< LOD	0/10	2.54 - 2.76	2/20
OXAZEP	< LOD	0/10	< LOD	0/20

Gas-particle partitioning

The extremely rare atmospheric concentrations of pharmaceuticals in the atmosphere were predominantly related to the particle associated mass fraction. Individual positive findings in the adsorber cartridge could be probably ascribed to blow off effects from the GFFs (chapter 3.1.1). These findings were in agreement with the low vapour pressures of $1.97 \cdot 10^{-5}$ Pa (25 °C),

$4.85 \cdot 10^{-7}$ Pa (25 °C), $8.19 \cdot 10^{-6}$ Pa (25 °C), $2.52 \cdot 10^{-4}$ Pa (25 °C) and $5 \cdot 10^{-10}$ Pa (25 °C) of carbamazepine, primidone, diclofenac, naproxen and oxazepam, respectively. The vapour pressure of clofibrac acid (15 mPa at 25 °C) indicated an occurrence in the gaseous mass fraction. ^[150] However, it was also exclusively quantified on the GFFs of two active air samples.

Occurrence and distribution of pharmaceuticals in the surface seawater

Carbamazepine displayed a widespread distribution throughout the surface waters of the German EEZ and the wider North Sea giving evidence to its increased persistence in the aquatic environment (figures 5.114- 5.116). The distribution patterns correlated with the prevailing sea currents (chapter 3.6) and confirmed a major riverine input pathway or in the case of the wider North Sea also the input by the outflow of the Baltic Sea. Highest surface water concentrations were quantified in the river Elbe and its estuary with up to 86 ng/L (STADE, figure 5.115). The carbamazepine abundances sharply decreased towards the open sea, but were still present at the remote sampling sites in the northern North Sea in concentrations ranging from 30 pg/L to 100 pg/L. The occurrence of carbamazepine at sampling sites in the northern North Sea suggested a significant precontamination of the Atlantic Ocean. However, atmospheric deposition was assumed to be not a significant contributor to the widespread distribution of carbamazepine due to its extremely rare occurrence in the marine atmosphere. Primidone exhibited a similar distribution pattern in the surface seawater as carbamazepine, but reached significantly lower surface water concentrations within the German EEZ and the wider North Sea (figures 5.114- 5.116). Highest abundances of up to 35 ng/L were quantified in the river Elbe, whereas lowest were observed at the northern sampling sites of the North Sea in a range of 25 pg/L to 70 pg/L. In contrast, oxazepam and clofibrac acid were almost exclusively quantified in coastal surface waters of the German EEZ and the wider North Sea inside of the river plumes and the region of the Baltic Sea outflow (figures 5.114- 5.116). The concentrations of oxazepam and clofibrac acid ranged from 0.6 ng/L to 9 ng/L and from 5 pg/L to 800 pg/L within the German EEZ and from 80 pg/L to 1.3 ng/L and 8 pg/L to 55 pg/L within the North Sea, respectively. Diclofenac could be never observed in the surface water of the wider North Sea. In addition, it was only sporadically quantified within the German EEZ exhibiting highest concentrations of up to 55 ng/L in the Elbe and within the Elbe estuary (figures 5.114 and 5.115). However, in May/Jun. 2009, it was even detected at the central and western sampling sites of the German EEZ in concentrations exceeding those inside the river plume of the Elbe. This pointed to a further input pathway beyond the riverine transport, whereof an atmospheric deposition of diclofenac or any other of the targeted pharmaceuticals might be excluded.

The Baltic Sea displayed an almost homogenous surface water composition of carbamazepine, primidone and clofibrac acid (figure 5.117). They were detected throughout all sampling sites.

Highest surface water concentrations could be quantified in the southern central Baltic Sea. Slightly decreasing concentrations were observed towards the Bothnian Bay (35, 37, BB3) and the region of Kattegat and Skagerrak (70, 73, 75, 76). The surface seawater concentrations of carbamazepine, primidone and clofibric acid ranged from 0.6 ng/L to 2.3 ng/L, from 0.6 ng/L to 2.4 ng/L and from 26 pg/L to 152 pg/L, respectively. The surface water concentration of primidone in the Baltic Sea was at the same order of magnitude as that of carbamazepine. Oxazepam was exclusively quantified in the region of Kattegat and Skagerrak (68a, 70, 73, 75, 76) as well as at individual sampling sites in the northern central Baltic Sea (52, 53, 605) in concentrations ranging from 195 pg/L to 526 pg/L. Diclofenac was sporadically observed throughout the entire sea region, except the Bothnian Bay. The surface water concentrations of diclofenac ranged from 30 pg/L to 98 pg/L. A single surface water concentration of 3 ng/L was quantified.

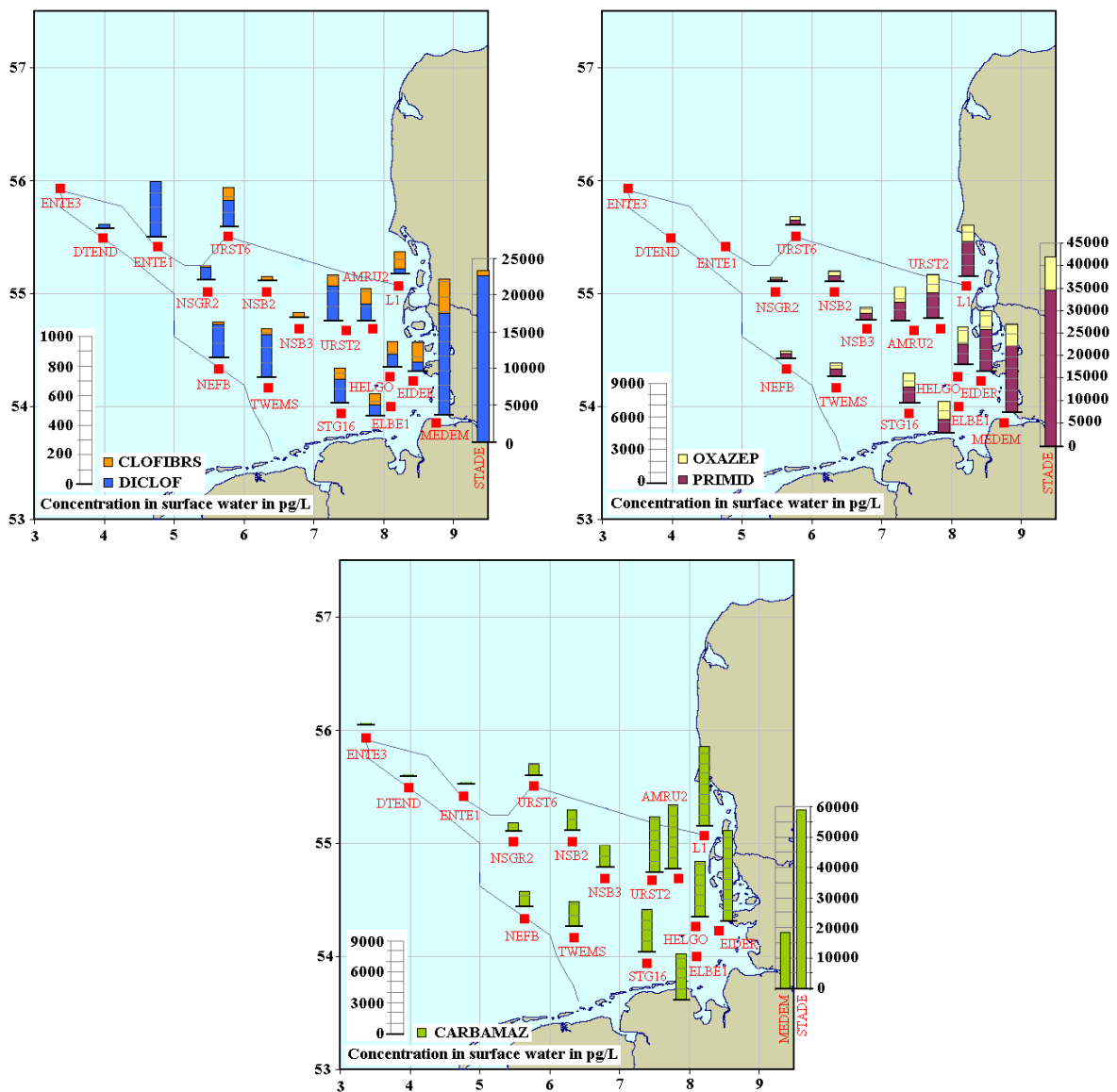


Figure 5.114: Occurrence and spatial distribution of pharmaceuticals in the aqueous phase of the surface water of the German EEZ in May/June, 2009

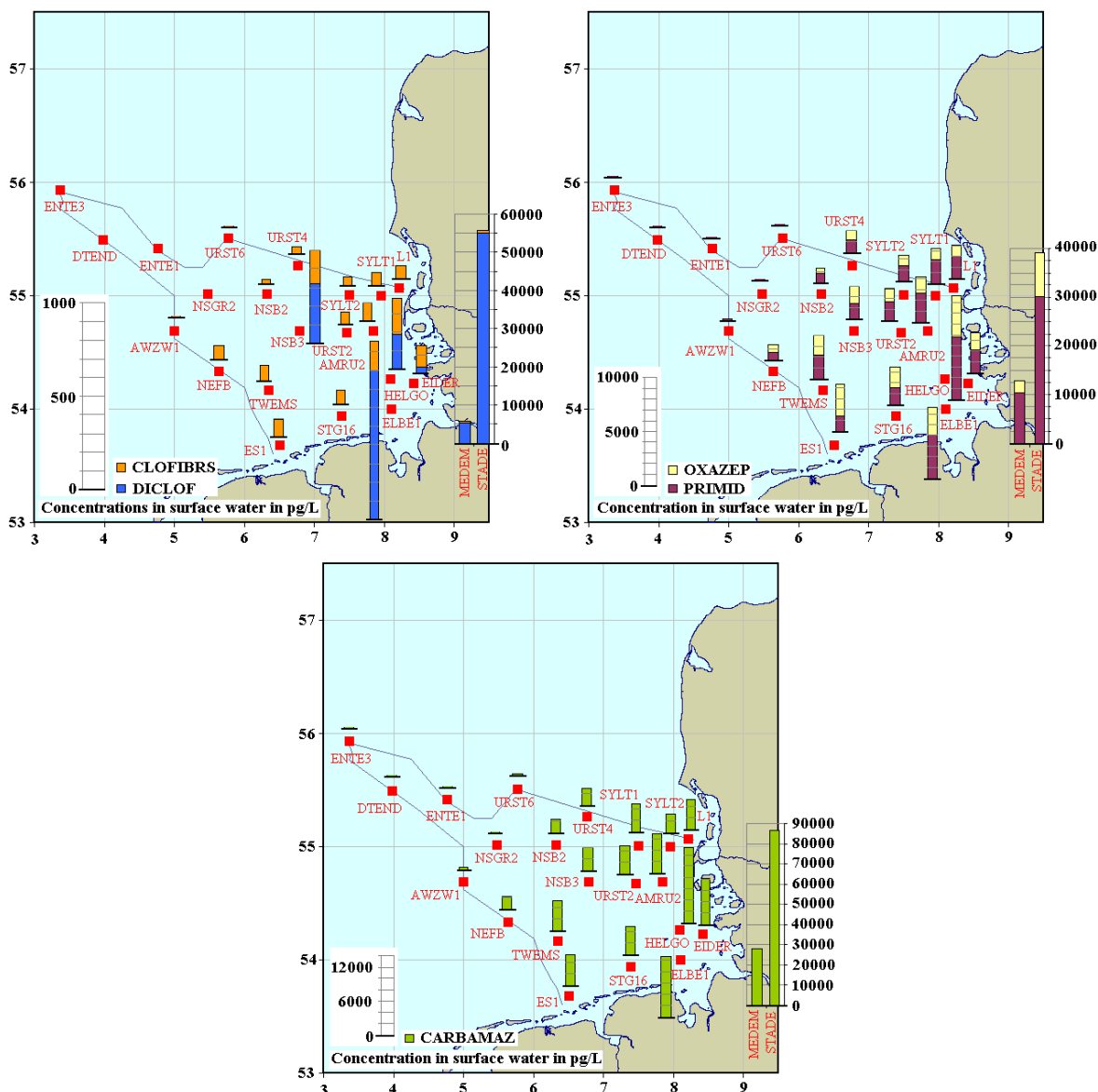


Figure 5.115: Occurrence and spatial distribution of pharmaceuticals in the aqueous phase of the surface water of the German EEZ in May 2010

Surface water concentrations of naproxen were neither available for the German EEZ nor for the North Sea or the Baltic Sea. Seasonal fluctuations in the surface water concentrations of pharmaceuticals in the German EEZ within the year 2009 could not be observed.

The high water solubilities and the low to moderate vapour pressures of the targeted pharmaceuticals were in agreement with their widespread distribution in the surface seawater and their negligible occurrence in the atmosphere. Besides, their low $\log K_{OWs}$ were found in the range of 0.91 to 3.18 indicating to a negligible adsorbance to suspended particulate matter in the water column. Exclusively diclofenac revealed an increased $\log K_{OW}$ of 4.51 indicating a marginal tendency to particle adsorption.^[150] In conclusion, the occurrence and spatial distribution of the

targeted pharmaceuticals in the surface seawater depended predominantly on the current river load and the prevailing sea currents, whereas the influence of atmospheric deposition and sedimentation processes in the water column was presumed to be negligible.

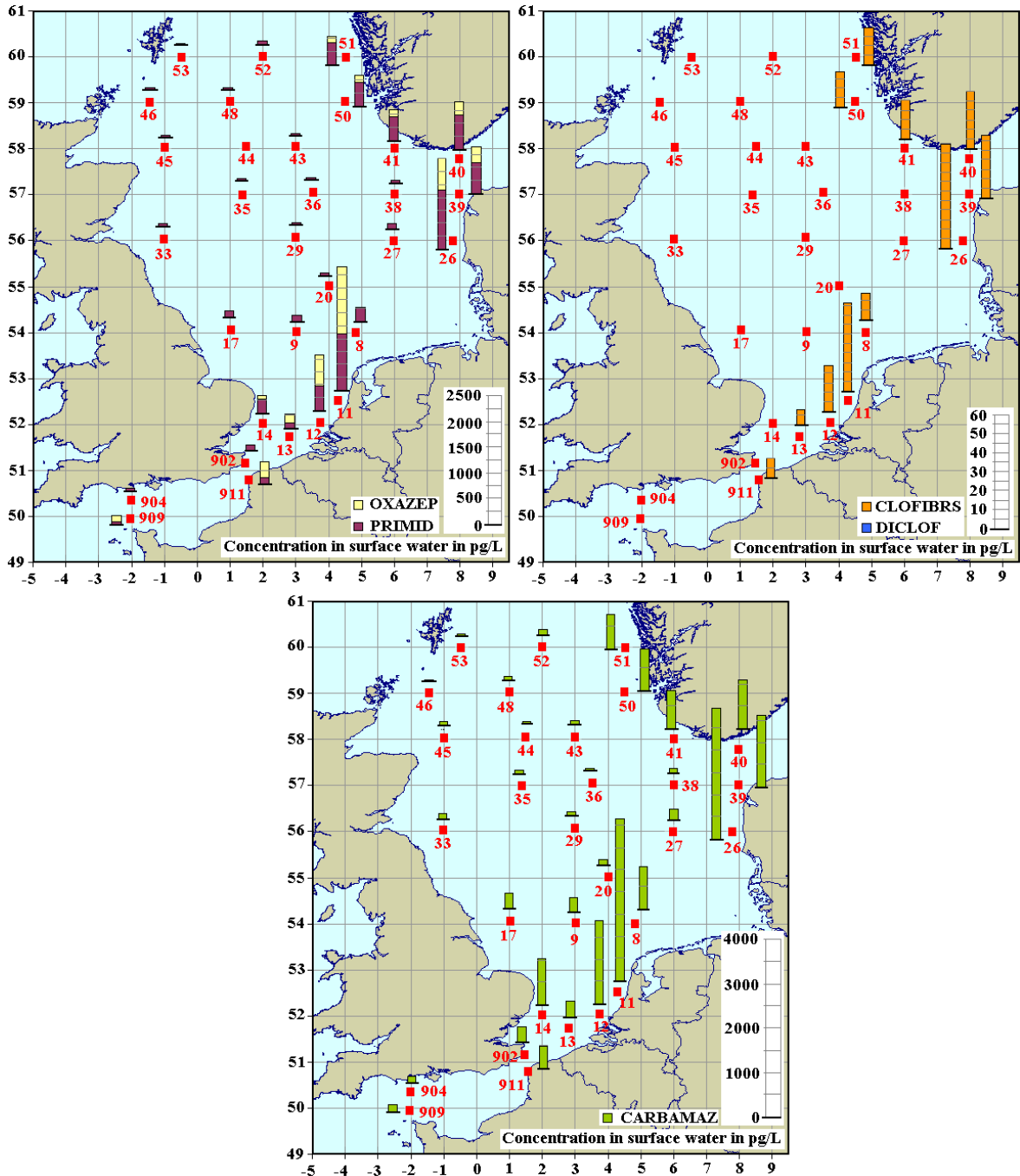


Figure 5.116: Occurrence and spatial distribution of pharmaceuticals in the aqueous phase of the surface water of the North Sea in Aug./Sep. 2009

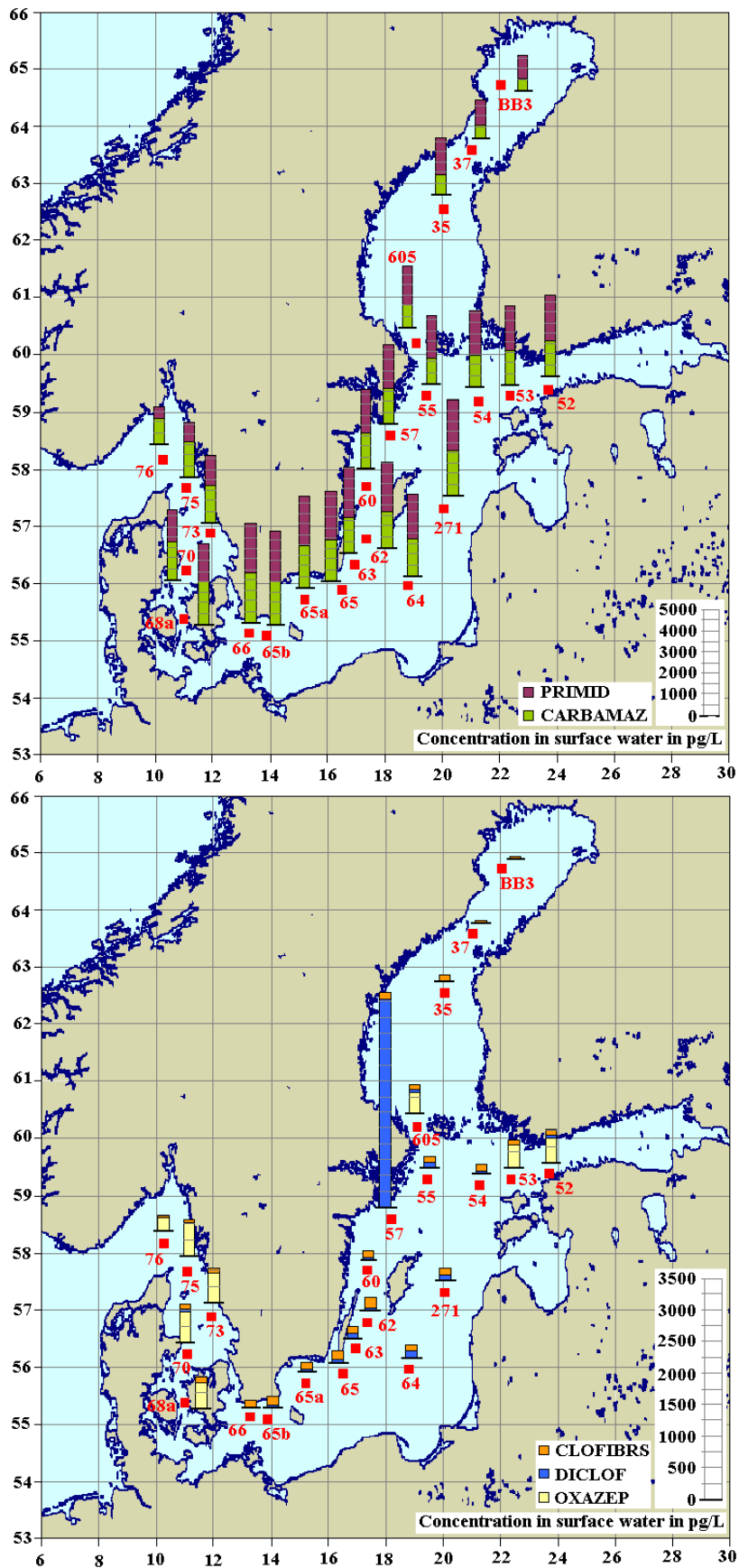


Figure 5.117: Occurrence and spatial distribution of pharmaceuticals in the aqueous phase of the surface water of the Baltic Sea in Jun./Jul. 2008

Net flux of diffusive gas exchange of pharmaceuticals between the marine atmosphere and the surface water

The targeted pharmaceuticals were extremely rare in the atmosphere. Thus, atmospheric deposition was excluded to be an important input pathway of pharmaceuticals to the surface seawaters. In addition, pharmaceuticals occurred in the particle associated mass fraction of the atmosphere making them rather prone to wet and dry particulate deposition processes than to dry gaseous deposition.

Conclusions

The targeted pharmaceuticals exhibited a widespread distribution in the surface seawaters of the German EEZ, the wider North Sea and the Baltic Sea. In particular the antiepileptic drugs carbamazepine and primidone were detected throughout all surface water sampling sites indicating their high persistence in the aquatic environment. Riverine input was found to be the major contamination source of the surface seawaters, which was displayed by the correlation of the spatial distribution of the pharmaceuticals with the prevailing sea currents. In contrast, the targeted pharmaceuticals were extremely rare in the atmosphere. Exclusively carbamazepine was episodically detected in the urban atmosphere of Sülldorf/Hamburg. Thus, atmospheric deposition could be excluded to be a significant contributor to the widespread surface seawater contamination.

5.2 Vertical distributions of organic contaminants in the North Sea atmosphere

Complementing investigations on the vertical distribution of organic pollutants in the marine atmosphere of the North Sea were performed in order to assess the representativeness of the active air sampling data on the contamination of the marine atmospheric boundary layer. Besides, further indications on sources and seasonalities of the target compounds in the marine atmosphere were expected from these investigations. To my knowledge this was the first study reporting vertical profiles of organic pollutants in the marine atmospheric boundary layer.

Three passive air sampling campaigns were performed on the research platforms FINO 1 and FINO 3 in the German EEZ in the period from August to September 2010. Three modified PUF disk passive air samplers (chapter 3.1.2) were installed in 40 m, 60 m and 80 m height of the 80 m to 90 m masts positioned on these stations (approximately 20 m above the sea level). The PUF disks were simultaneously exposed at the individual heights. The first two sampling campaigns were performed almost in parallel (time delay of 7 days) at FINO1 located at the Borkum Riffgrund (40 km distance to the coast) and at FINO 3 west of the island Sylt (70 km distance to the coast) for

a sampling duration of 50 days in August/September, respectively (figure 3.13). The third sampling campaign was performed at FINO1 for a shorter period of 34 days in September/October.

5.2.1 Influence of the vertical wind velocity profile on the sampling rates

As discussed in chapter 3.1.2, the seasonal and vertical profiles monitored by the passive air samplers were based on the total amounts of target analytes accumulated on the PUF disks. As reported previously and confirmed by the passive air sampling campaigns of this study the wind shielding effect of the “flying saucer” design was insufficient at wind velocities > 4 m/s. ^[109] Average wind velocities during the sampling campaigns on the FINO platforms ranged from 8 m/s to 9 m/s (meteorological data from the deep sea island Heligoland, chapter 3.2.2). Thus, a strong relation of the sampling rates to the wind velocity had to be expected. In consequence, the variability of the wind velocities with increasing height had to be investigated. Meteorological parameters, including the wind speed were monitored at the FINO stations at the respective heights. However, at the time of this study, these instruments were not fully operative. Nevertheless, a single vertical wind profile could be obtained from the FINO 3 platform from 10 August to the 1 September 2010 (figure 5.118). This profile displayed constant wind velocities at 40 m, 60 m and 80 m height above the FINO platform indicating similar sampling rates. Moreover, the profile displayed an average wind velocity (figure 5.118) comparable to that measured on the island Heligoland. Thus, the meteorological data of Heligoland (chapter 3.2.2) was considered to be representative for the sampling campaigns performed at the FINO platforms.

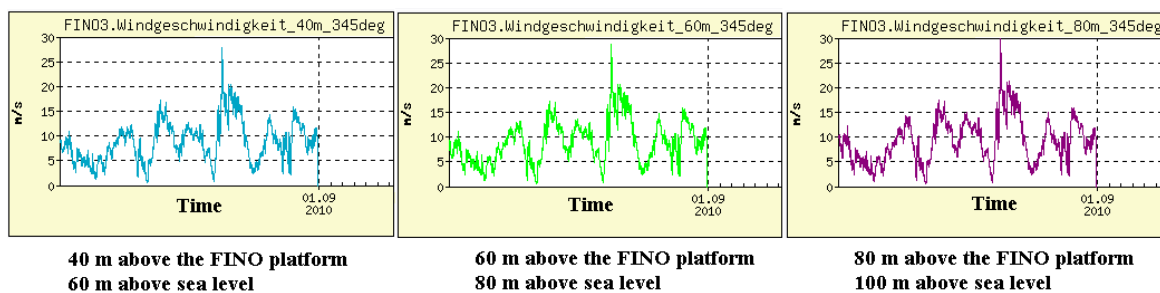


Figure 5.118: Vertical wind profile monitored at the FINO 3 platform in the period of the 10 August to the 1 September 2010

The PUF disks of the second FINO 1 and the FINO 3 campaign were spiked with PRCs prior to exposure. The recoveries of the PRCs in the air samples were useful indicators for the variation of the sampling rate with height. Comparable PRC recoveries indicated comparable sampling rates and thus, comparable air samples. In contrast, a decrease of PRC recoveries with increasing height would point to an increase in the wind velocity and thus an increase in the sampling rates with increasing height. In such a case, the vertical concentration gradients would be significantly biased and might display either a slighter decrease or even an increase in atmospheric concentrations with

increasing height. A previous study reported such a reflection of the wind profile with height by the deuration compounds as well as by the targeted PCBs and organochlorine pesticides at rather low average wind velocities of 0.3 m/s to 4.5 m/s. The study was performed with PUF disks and SPMD at a 100 m tower at a forest site, 30 km north of Uppsala, Sweden. ^[33] Despite of the same method and elevation heights these results were in disagreement to the results of this study. The PRC recoveries of this study (table 5.10) including four PCBs and isotopically labeled lindane displayed no significant aberrations with elevation, which was in agreement with the constant wind velocities monitored by the FINO 3 platform (figure 5.118).

Table 5.10: Recovery (%) of PRCs in the PUF disk passive air samples exposed at the FINO research platforms

Recovery in %	FINO3 A	FINO3 C	FINO 3 E	FINO1 G	FINO1 H	FINO1 I
Exposure height [m ASL]	60	80	100	60	80	100
Sampling duration [d]	50	50	50	34	34	34
SIMAZ-D ₁₀	72	75	69	70	74	67
PROMETR-D ₆	4	0	0	3	3	2
HCHG- ¹³ C ₆ D ₆	17	11	15	32	23	22
CB30	9	1	1	6	5	4
CB104	36	30	33	52	48	47
CB145	60	56	57	79	75	78
CB204	89	97	93	93	90	96
PHEN-D ₁₀	31	4	7	26	18	15
FLU-D ₁₀	89	88	80	108	98	91
BAA-D ₁₂	58	38	41	77	82	68

The discrepancies of the recoveries of the PRC compounds were < 10 % and thus, lower than the standard deviations calculated for the reproducibility of the PUF disk air sample preparation method (chapter 4.2.3). Only PHEN-D₁₀, FLU-D₁₀ and BAA-D₁₂ revealed amplitudes >10 %, which ranged from 11 % to 27 %, 9 % to 17 % and 9% to 20 %, respectively. The PRC recoveries decreased with height, eventually reflecting increasing wind velocities. However, the deuterium labeled PAH compounds FLU-D₁₀ and BAA-D₁₂ even exhibited increased standard deviations in the reproducibility of the air sample preparation method of 15 % and 11 %, respectively (chapter 4.2.3). Hence, the vertical fluctuations on PRC recoveries of FLU-D₁₀ and BAA-D₁₂ were found to be insignificant. In contrast, the maximum amplitude of PHEN-D₁₀ significantly exceeded the standard deviations in air sample preparation of 3 % (chapter 4.2.3). Hence, the sampling rates of the targeted low molecular weight PAHs (ACY, ACE, FL, PHEN) might be expected to increase with increasing height. Nevertheless, correction factors were not applied, due to the indication of constant sampling rates by nine out of ten PRCs and the vertical wind profile obtained from FINO3 illustrating wind velocity being independent of exposure height. It was supposed that the total amounts accumulated on the PUF disks at different heights were directly comparable.

5.2.2 Vertical profiles of PAH abundances in the marine atmosphere

Considering a maximum error of 10 % to 20 % of the PAH's concentrations, the vertical profiles displayed either an even distribution (FINO 1, Aug./Sep. 2010) or only slightly decreasing PAH concentrations with height (FINO 3; FINO 1 in Sep./Oct. 2010) in the marine atmosphere (figure 5.119). This vertical concentration gradient was less negative than reported for the urban atmospheric boundary layer in Toronto, Canada. There, the sharply decreasing PAH levels with height were attributed to the high emissions at ground level near the CN tower. ^[192] Although the shipping traffic in the German EEZ provided potential ground level emissions, they might have been negligible in comparison to those in Toronto.

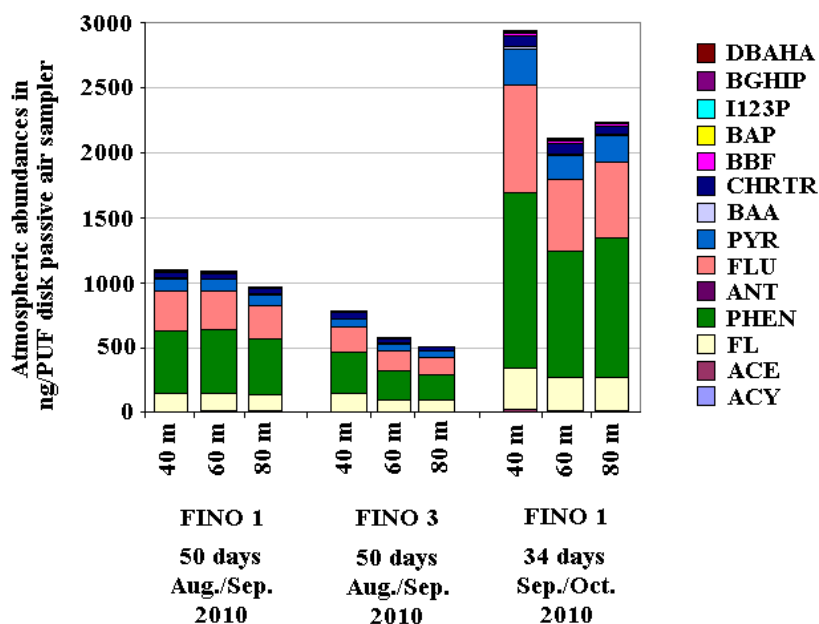


Figure 5.119: Vertical gradients of the atmospheric abundances of PAHs in the marine atmosphere of the German EEZ in the period of August to October 2010; The respective heights refer to the position on the 80 to 90 m masts installed 20 m above the sea level

However, more significant were the aberrations between the tree sampling campaigns, which pointed to the influence of continental emission sources on the PAH abundances in the marine atmosphere: The vertical profiles monitored at FINO 1 and FINO 3 in Aug./Sep. 2010 were similar in the PAH composition and in their total abundances accumulated on the PUF disks, whereas the vertical profile documented in Sep./Oct. revealed three times higher total abundances and an extended spectrum of the targeted PAHs independent of the shorter exposure time. On the one hand, with 9 m/s vs. 8 m/s the mean wind speed was slightly higher during the later campaign. Increased wind velocities did not only accelerated the accumulation of the target compounds on the PUF disk, but also supported the particle intrusion in the passive air sampler. In consequence also an extended spectrum of particle associated high molecular weight PAHs could be monitored by

the PUF disk passive air sampler in Sep./Oct. 2010. On the other hand, the higher PAH abundances of the sampling campaign in Sep./Oct. 2010 could be attributed to the beginning of the heating period. Increased PAH emissions to the atmospheric boundary layer, longer atmospheric lifetimes as well as higher abundances of particle associated high molecular weight PAHs in the atmosphere are related to this season. ^[69]

To sum up, the vertical distributions of the PAHs in the marine atmospheric boundary layer up to a height of 100 m above sea level pointed to a marginal pollution of the marine atmosphere by shipping traffic and a more dominant input from distant sources due to advection of contaminated air masses from land.

The PAH patterns of the vertical profiles were similar to the PUF disk passive air samples collected in Sülldorf/Hamburg and Tinnum /Sylt. The most abundant components were phenanthrene, fluoranthene, fluorene and pyrene. However, differing from the active air sampling data where fluorene was found to be the second most abundant PAH compound in the marine atmosphere (chapter 5.1.1), fluoranthene exhibited similar or even higher concentrations on the PUF disk passive air samplers. Apart from the differences in sources influencing the sites, this might be attributable to differences in wind speed (and, hence, sampling efficiency) and temperature (and, hence, gas-particle partitioning).

5.2.3 Vertical profiles of organochlorine pesticides and PCBs in the marine atmosphere

The vertical profiles of the organochlorine pesticides and PCBs were similar to that of the PAHs, discussed above. The atmospheric abundances of organochlorine pesticides and PCBs displayed an even distribution or only slightly decreasing concentrations with elevation, not significantly exceeding the standard error of approximately 10 % to 20 % of the total sum concentration (figure 5.120). These observations were in contrast to the investigations of other authors, who reported strong ground level emissions of PCBs and HCHs as well as variable vertical distributions of organochlorine pesticides during different sampling periods on the CN tower in Toronto, Canada. ^[192, 193] Ground level emissions of organochlorine pesticides and PCBs in the marine atmosphere might occur as outgassing from the surface seawater or an active air-sea exchange via wave breaking processes generating contaminated sea spray. Furthermore, PCB emissions from ships were expected, albeit considered to be low. ^[194] No data were available to assess this possible source. However, the almost even distribution up to a height of 100 m above sea level supported the perception that the marine atmospheric boundary layer was well mixed and that ground level emissions were too low to sustain a negative vertical gradient. Instead constant atmospheric abundances with height indicated advection as the predominant source of pollution.

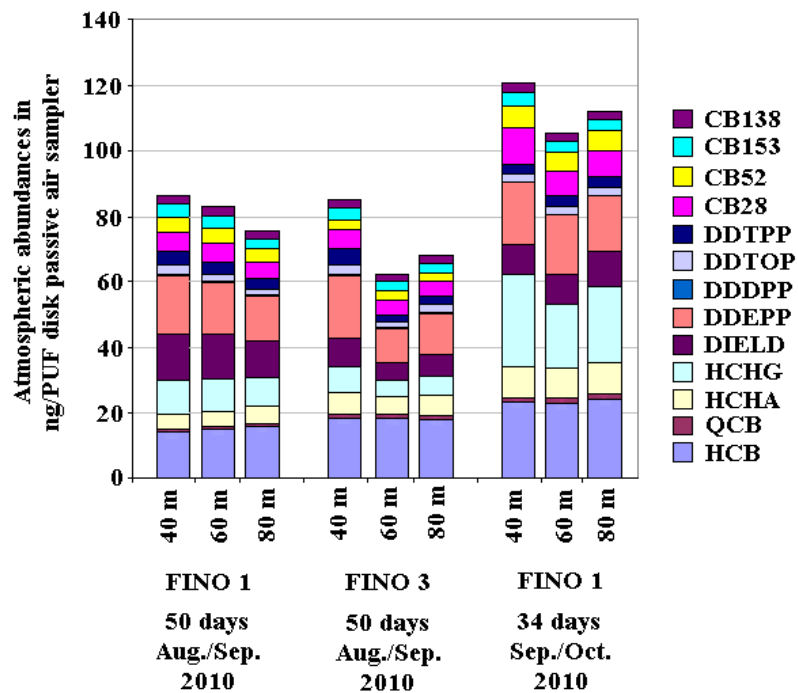


Figure 5.120: Vertical gradients of the atmospheric abundances of organochlorine pesticides and PCBs in the marine atmosphere of the German EEZ in the period of August to October 2010; The respective heights refer to the position on the 80 to 90 m masts installed 20 m above the sea level

Significant aberrations were only observed between the individual sampling campaigns. The vertical profiles monitored at FINO 1 and FINO 3 in Aug./Sep. 2010 were similar in the PCB and OCP abundances, whereas increased concentrations could be quantified on the PUF disks of the FINO 1 air sampling campaign in Sep./Oct. 2010. This might be attributed to the higher average wind speed of 9 m/s during this campaign (chapter 3.2.2) overcompensating for the influence of the shorter exposure time.

5.2.4 Vertical profiles of polar pesticides in the marine atmosphere

The currently most used triazine herbicide terbuthylazine, two organophosphate insecticides (dimethoate and diazinone), four phenylurea herbicides (chlortoluron, isoproturon, diuron and linuron) as well as the targeted chloroacetanilides (metolachlor, metazachlor) and dinitroaniline (trifluralin, pendimethalin) herbicides could be quantified. The vertical profiles of the polar pesticides (figure 5.121) displayed no distinct trends in their abundances with elevation giving evidence to a well mixed marine atmospheric boundary layer up to 100 m above sea level and thus a dominant input from distant sources by advection, presumably from land. Their vertical profiles monitored in a period from late summer to autumn confirmed the seasonalities in the atmospheric distributions of polar pesticides during this season as discussed in chapters 5.1.7 to 5.1.11.

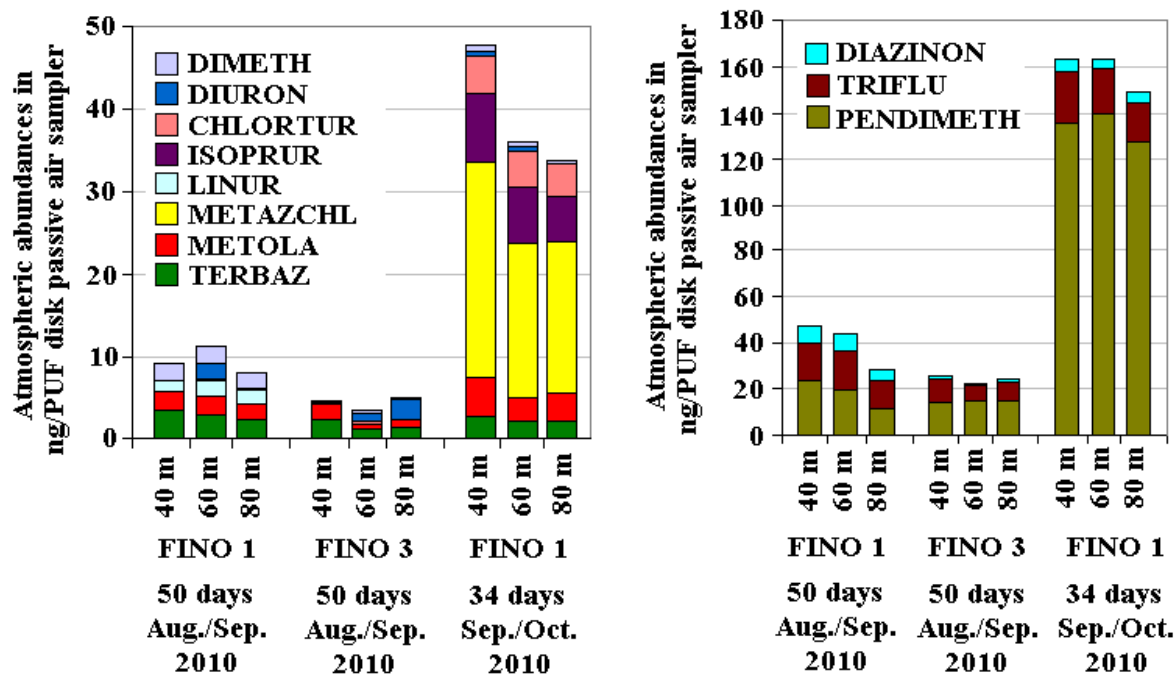


Figure 5.121: Vertical gradients of the atmospheric abundances of polar pesticides in the marine atmosphere of the German EEZ in the period of August to October 2010; The respective heights refer to the position on the 80 to 90 m masts installed 20 m above the sea level

Metazachlor, isoproturon and chlortoluron were monitored by the passive air samplers exposed at FINO 1 in Sep./Oct. 2009, but never in samples collected during the earlier profiling experiments. These findings were in correlation to their main agricultural application season documented by the passive air samplers at Tinnum/Sylt and Sülldorf/Hamburg. In addition, pendimethalin exhibited significantly increased abundances on the PUF disks in Sep./Oct. than in Aug./Sep. This observation agreed with the seasonal profiles monitored at land based sampling sites, which documented the atmospheric occurrence of pendimethalin throughout the year and highest atmospheric abundances in autumn due to its application as winter grain protective herbicide. Trifluralin was applied in a similar way as pendimethalin, but exhibited significantly lower atmospheric abundances due to restriction in application in recent years. In consequence, a characteristic increase in the atmospheric abundances in Sep./Oct. could not be observed. The organophosphate insecticides displayed no distinct seasonal profiles (chapter 5.1.8). Their occurrence in the vertical profiles of the marine atmospheric boundary layer supported the assumption of the dominant atmospheric input of the highly biodegradable insecticides to the sea surface. Terbutylazine and metolachlor were detected throughout all vertical profiles and elevations in almost constant abundances, whereas the occurrences of diuron and linuron were highly variable. Quantifiable concentrations of diuron were obtained for only 1-2 samples (heights) per vertical profile. Linuron was exclusively detected in the first vertical profile originating from FINO 1 in Aug./Sep. 2010, consistent with its sporadic occurrence in the marine atmosphere.

Contrary to the seasonal profiles of the PAHs, PCBs and OCPs, the abundances of the currently used pesticides accumulated on the PUF disks of the FINO 1 sampling campaign in Sep./Oct. 2010 were not significantly higher than those quantified in Aug./Sep. 2010. The reason was unclear, but might be presumably explained by the variability of primary sources.

To sum up, the vertical profiles of currently used pesticides in the marine atmospheric boundary layer gave further evidence on the extended transport of currently used pesticides to the marine atmosphere, especially in the period of their main agricultural application season and, thus, even further indications for a significant atmospheric deposition.

5.2.5 Vertical profiles of perfluorinated compounds in the marine atmosphere

The perfluorinated compounds were primarily associated with the particulate mass fraction of the atmosphere. They were quantified in very low concentrations in active air samples of the marine atmosphere, which were either close to or below the LOQ. Besides, they occurred only sporadically in the passive air samples collected in Sülldorf/Hamburg and Tinum/Sylt (chapter 5.1.12). Considering these observations, it was remarkable that the entire spectrum of the targeted PFCs was shown in all elevations of the vertical profiles (figure 5.122). This gave evidence to an extended particle intrusion to the passive air samplers at average wind speeds of 8 m/s to 9 m/s.

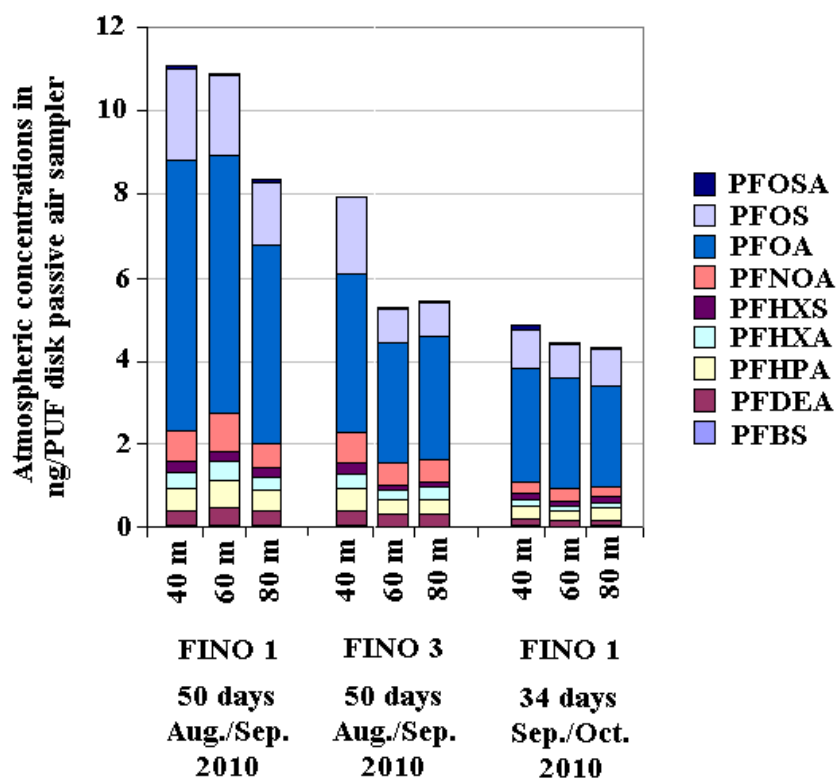


Figure 5.122: Vertical gradients of the atmospheric abundances of perfluorinated compounds in the marine atmosphere of the German EEZ in the period of August to October 2010; The respective heights refer to the position on the 80 to 90 m masts installed 20 m above the sea level

Similar to the other organic contaminants targeted in this study, the PFCs displayed an almost even vertical distribution (FINO 1, Sep./Oct. 2010) in the marine atmosphere and a trend of slightly decreasing abundances with elevation (FINO 1 in Aug./Sep. 2010, FINO3). Hence, it might be concluded that the pollution of the marine atmosphere was dominated by the advection of contaminated air masses from land. Nothing could be concluded regarding the possible influence of active sea-air exchange via wave breaking processes (chapter 5.1.12). Contrary to the vertical profiles discussed above, highest PFC abundances were collected during the FINO 1 campaign in Aug./Sep. 2010, whereas lowest were quantified during the campaign in Sep./Oct. 2010 exhibiting a shorter exposure time. Furthermore, the vertical profiles of FINO 1 and FINO 3 in Aug./Sep. 2010 revealed higher aberrations than observed for the other pollutant classes. On the one hand, this might be ascribed to the variability in continental primary sources. On the other hand, it had to be considered that particle collection by passive air samplers was not reproducible limiting the validity of the results. ^[31]

In summary, the vertical profiles gave evidence to a well mixed boundary layer up to a height of 100 m above sea level. Ground level emissions due to shipping traffic or sea-air exchange were concluded to be at a minimum. Instead, the even distributions with height pointed to a predominant pollution of the marine atmosphere by advection of contaminated air masses from land. Seasonalities in the atmospheric occurrence of currently used pesticides were confirmed by the vertical profiles suggesting an extended atmospheric input to the sea surface during agricultural application seasons. Moreover, the insufficient wind dampening effect of the “flying saucer” protection chamber at high sea sampling sites was reflected by the results.

5.3 Estimations of the dry particle and wet deposition fluxes to the surface seawaters

The occurrence and significant contribution of atmospheric deposition to the surface seawater contamination has been documented by this study for the majority of the targeted organic contaminants as discussed in detail in chapters 5.1 and 5.2. This chapter summarizes the estimations of the dry particle and wet deposition fluxes to the surface seawaters, as defined in chapters 2.4.3 and 2.4.4, respectively. A quantification of the dry gaseous deposition (chapter 2.4.2) was not possible on the basis of the current data, because this would require more detailed knowledge, e.g., about the meteorological conditions and mass transfer rate coefficients. However, the direction of the net flux of diffusive gas exchange has been calculated as already discussed in chapter 5.1.

5.3.1 Wet deposition

Rain water samples from the marine environment were not available for this study, due to the absence of significant amounts of precipitation during the research cruises. In addition, knowledge of scavenging ratios of organic pollutants was quite sparse (table 5.11) and mostly not applicable to the conditions of the marine atmosphere of the North Sea and the Baltic Sea.

Table 5.11: Scavenging ratios

Pollutant	Scav. ratio	F_{wet} (ng m ⁻² d ⁻¹)	Sampling site	Year	Ref.
ACY	600 ^[a]	0.314	suburban (Czech Rep.)	2006-2008	[104]
ACE	450 ^[a]	0.277	suburban (Czech Rep.)	2006-2008	[104]
PHEN	6100 ^[a]	5.792	suburban (Czech Rep.)	2006-2008	[104]
ANT	1800 ^[a]	1.152	suburban (Czech Rep.)	2006-2008	[104]
FLU	31000 ^[a]	8.817	suburban (Czech Rep.)	2006-2008	[104]
PYR	16000 ^[a]	6.308	suburban (Czech Rep.)	2006-2008	[104]
BAA	5100 ^[a]	1.411	suburban (Czech Rep.)	2006-2008	[104]
BBF	15000 ^[a]	3.749	suburban (Czech Rep.)	2006-2008	[104]
CB28	26000 ^[b]	n.a.	eastern Mediterranean Sea	2000-2001	[195]
CB52	15000 ^[b]	n.a.	eastern Mediterranean Sea	2000-2001	[195]
CB138	19000 ^[b]	n.a.	eastern Mediterranean Sea	2000-2001	[195]
	55000 ^[a]	0.01 - 18.1	Baltic Sea	1990-1992	[145]
CB153	43000 ^[b]	n.a.	eastern Mediterranean Sea	2000-2001	[195]
	45000 ^[a]	0.01 - 10.1	Baltic Sea	1990-1992	[145]
HCB	485 ^[c]	n.a.	Enewetak Atoll, Pacific	1981	[196]
HCHA	4179 ^[c]	n.a.	Enewetak Atoll, Pacific	1981	[196]
HCHG	3154 ^[c]	n.a.	Enewetak Atoll, Pacific	1981	[196]
DIELD	54000 ^[c]	n.a.	Enewetak Atoll, Pacific	1981	[196]
DDEPP	1100 ^[c]	n.a.	Enewetak Atoll, Pacific	1981	[196]

[a] total scav. ratio W_r , [b] scav. ratio of the gaseous mass fraction, [c] estimated values

An estimation of the wet deposition fluxes (of the compounds listed in table 5.11) based on the yearly mean precipitation amount (750 mm), the atmospheric bulk concentration and the scavenging ratio (chapter 2.4.4, equation 18) resulted in 1000 to 10000 times higher fluxes than quantified at coastal sampling sites of the North Sea and the Baltic Sea (table 5.12).

In consequence, estimated wet deposition fluxes were exclusively based on the monthly rain water samples collected and analysed by the UBA at a coastal sampling site of the North Sea (Tinnum/Sylt) and of the Baltic Sea (Zingst). Only a decreased selection of the targeted pollutants of this study was investigated by the UBA, including the PCBs, individual PAHs and chlorinated pesticides. The annual wet deposition fluxes at Tinnum and Zingst were calculated and applied to the sea area of the North Sea and the Baltic Sea, respectively. The results were summarized in table 5.12 for 2009 and 2010. In order to assess the contribution of the estimated wet deposition fluxes to the surface seawater contamination, water concentrations were calculated based on the annual deposition per square meter and a subsequent distribution in a water column of 25 m depth.

The depth of the imaginary water column was derived from the vertical profiles of salinity and temperature of the German EEZ. ^[197]

Table 5.12: Annual wet deposition fluxes of organic pollutants to the coastal sampling sites Tinnum and Zingst (calculated from the data of the UBA, annex 8) as well as estimated wet deposition fluxes to the surface seawater of the German EEZ, the wider North Sea and the Baltic Sea

F_{Wet}	Tinnum/Sylt [ng m ⁻² y ⁻¹]		Zingst [ng m ⁻² y ⁻¹]		G. EEZ [kg y ⁻¹]		North Sea [kg y ⁻¹]		Baltic Sea [kg y ⁻¹]	
	2009	2010	2009	2010	2009	2010	2009	2010	2009	2010
HCB	39	32	184	38	1.1	0.9	22	19	76	16
HCHA	126	122	100	146	3.6	3.5	72	70	41	60
HCHG	593	529	531	574	17	15	341	304	219	237
ALD	4.4	4.7	17	6	0.1	0.1	2.5	2.7	7.1	2.4
DIELD	68	65	26	34	1.9	1.9	39	38	11	14
END	15	16	20	16	0.4	0.5	8.7	9.3	8.2	6.6
DDTPP	36	22	139	144	1.0	0.6	21	13	57	60
DDTOP	8.2	8.7	28	27	0.2	0.2	4.7	5.0	11	11
DDEPP	26	15	43	53	0.7	0.4	15	8.7	18	22
DDPP	12	7.2	24	26	0.3	0.2	6.7	4.2	9.9	11
CB28	162	25	114	85	4.6	0.7	93	14	47	35
CB52	76	22	42	65	2.2	0.6	44	12	17	27
CB138	154	341	176	242	4.4	9.7	89	196	73	100
CB153	167	365	181	183	4.8	10.4	96	210	75	76
PHEN	12776	11577	11019	12276	365	331	7346	6657	4551	5070
ANT	482	411	498	721	14	12	277	236	206	298
FLU	12429	10025	13650	16247	355	287	7147	5764	5638	6710
PYR	8048	6030	10351	10502	230	172	4628	3467	4275	4337
BAA	2298	1926	3593	3806	66	55	1321	1108	1484	1572
CHRTR	6932	6080	8110	10603	198	174	3986	3496	3349	4379
BAP	2092	2007	2324	3949	60	57	1203	1154	960	1631
I123P	3085	2502	3165	5225	88	72	1774	1439	1307	2158
BGHIP	2900	2552	2896	5277	83	73	1667	1467	1196	2179
DBAHA	593	536	607	933	17	15	341	308	251	386

All in all the surface seawater concentrations derived from the annual wet deposition fluxes were in the same order of magnitude as the real surface seawater concentrations observed in the German EEZ, the wider North Sea and the Baltic Sea (table 5.13). A difference of at most a factor of 10 is observed. Considering the different pollution levels of the coastal/continental and marine atmosphere (chapter 5.1), the annual wet deposition fluxes to the sea surface were presumably overestimated, in particular beyond coastal waters. However, the comparison of estimated vs. real water concentrations confirmed that the calculated wet deposition fluxes in table 5.12 were in the true order of magnitude and that atmospheric deposition was an important contribution to the surface seawater contamination.

Table 5.13: Surface seawater concentrations calculated from the annual wet deposition fluxes and real water concentrations observed in 5-6 m of depth; n.a. = not available

C _{Water} [pg/L]	Estimated concentrations based on F_{wet}				Real concentrations in the open sea and at coastal sampling sites					
	North Sea		Baltic Sea		German EEZ 2009		North Sea 2009		Baltic Sea 2005/(2009)	
	2009	2010	2009	2010	ENTE1	HELGO	48	11	200/(28)	11/(35)
HCB	1.6	1.3	7.4	1.5	2.1	2.9	3.3	3.5	8	10
HCHA	5.0	4.9	4.0	5.8	44	46	38	20	(78)	(127)
HCHG	24	21	21	23	33	79	18	62	(88)	(138)
ALD	0.2	0.2	0.7	0.2	<LOD	<LOD	<LOD	<LOD	n.a.	n.a.
DIELD	2.7	2.6	1.0	1.4	8.6	9.1	4.8	16	n.a.	n.a.
END	0.6	0.6	0.8	0.6	<LOD	<LOD	<LOD	<LOD	n.a.	n.a.
DDTPP	1.5	0.9	5.6	5.8	0.28	0.88	<LOD	<LOD	3	5
DDTOP	0.3	0.3	1.1	1.1	n.a.	n.a.	n.a.	n.a.	n.a.	n.a.
DDEPP	1.0	0.6	1.7	2.1	0.22	2.8	<LOD	1.4	4	13
DDDPP	0.5	0.3	1.0	1.0	0.38	8.5	<LOD	1.8	5	11
CB28	6.5	1.0	4.6	3.4	0.24	1.3	<LOD	2.5	4	5
CB52	3.0	0.9	1.7	2.6	<LOD	0.87	<LOD	2.5	2	3
CB138	6.2	14	7.0	9.7	0.95	4.3	<LOD	2.6	1	3
CB153	6.7	15	7.2	7.3	<LOD	4.8	<LOD	6.2	1	6
PHEN	511	463	441	491	215	413	188	383	1290	1258
ANT	19	16	20	29	n.a.	n.a.	<LOD	<LOD	19	70
FLU	497	401	546	650	113	454	34	185	1204	1911
PYR	322	241	414	420	<LOD	242	<LOD	80	432	782
BAA	92	77	144	152	n.a.	n.a.	<LOD	18	69	199
CHRTR	277	243	324	424	19	169	15	62	185	325
BAP	84	80	93	158	<LOD	108	<LOD	<LOD	54	264
I123P	123	100	127	209	n.a.	126	<LOD	26	76	384
BGHIP	116	102	116	211	n.a.	n.a.	<LOD	31	78	410
DBAHA	24	21	24	37	n.a.	n.a.	<LOD	<LOD	13	<LOD

5.3.2 Dry particle deposition

Estimations on the dry particle deposition of organic contaminants to the surface seawater were based on a deposition velocity of 0.02 cm/s (17.28 m/d) derived from the characteristic MMD of a maritime aerosol size distribution and an empirical relation to the deposition velocity at a relative humidity of 99 % (chapter 2.4.3). The dry particle deposition was quantified for individual target compounds exhibiting overall atmospheric abundances in the particle associated mass fraction (chapter 5.1). An overview of the estimated dry particle deposition fluxes to the surface seawater of the German EEZ and the wider North Sea was given in table 5.14. Fluxes were calculated in units of $\text{pg m}^{-2} \text{d}^{-1}$ for the respective season of the air sampling campaigns. An extrapolation to an annual deposition in units of g/year was discarded for the CUPs and PAHs, due to the significant seasonalities in atmospheric concentrations (chapter 5.1). The annual dry particulate deposition fluxes of PFCs and organophosphorus flame retardants to the German EEZ and the North Sea was summarized in table 5.15. The dry particulate deposition to the Baltic Sea could not be quantified,

because pollutant concentrations of the particulate associated mass fraction of the Baltic Sea atmosphere were not available for this study.

Table 5.14: Estimations of the dry particulate deposition fluxes to the surface seawater of the German EEZ and the North Sea

Organic pollutant	F_{DD} (pg m ⁻² d ⁻¹)					
	German EEZ - May/Jun. 2009/2010			North Sea - Aug./Sep. 2009		
	Min.	Max.	Mean	Min.	Max.	Mean
BAA	<LOD	253	65	<LOD	443	34
CHRTR	<LOD	768	325	<LOD	<LOD	<LOD
BBF	<LOD	471	147	<LOD	1301	100
BAP	<LOD	326	95	<LOD	861	66
I123P	<LOD	328	138	<LOD	787	61
BGHIP	<LOD	329	136	<LOD	831	158
DBAHA	<LOD	305	66	<LOD	<LOD	<LOD
TERBAZ	<LOD	2179	175	<LOD	<LOD	<LOD
CHLORTUR	<LOD	9.8	1.0	<LOD	<LOD	<LOD
ISOPRUR	<LOD	43	6.8	<LOD	2.4	0.2
LINUR	<LOD	47	4.4	<LOD	<LOD	<LOD
24-D	<LOD	51	5.0	<LOD	199	17
MCPA	<LOD	191	34	<LOD	42	5.1
DICHLPR	<LOD	125	10	<LOD	<LOD	<LOD
MECOPR	<LOD	54	4.9	<LOD	9.2	0.7
BENTAZ	<LOD	196	15	<LOD	1.2	0.1
PENDIMETH	<LOD	180	21	<LOD	17	2.0
CARBEND	<LOD	<LOD	<LOD	<LOD	12	1.6
METAZCHL	<LOD	74	8.5	19	1468	314
METOLA	<LOD	1463	100	<LOD	13	3.1
PFHPA	<LOD	3.5	1.2	<LOD	2.2	0.2
PFHXA	<LOD	<LOD	<LOD	<LOD	2.1	0.2
PFHXS	<LOD	4.2	0.4	<LOD	<LOD	<LOD
PFNOA	<LOD	5.5	0.6	<LOD	4.7	0.9
PFOA	<LOD	25	13	<LOD	19	11
PFOS-1	<LOD	26	5.1	<LOD	13	4.3
PFOSA-1	<LOD	3.5	0.2	<LOD	<LOD	<LOD
TBP	<LOD	739	389	<LOD	1401	661
TPP	<LOD	627	171	<LOD	488	220

The biggest uncertainty propagating in these calculations originated from the choice of a fixed deposition velocity. In reality the particle deposition velocity was highly fluctuating corresponding to atmospheric turbulence and mass size distribution of the targeted substances. A correspondingly large range of deposition velocities were reported in literature (0.1 – 7.2 cm/s). These differed from compound to compound and from site to site. Some studies differentiated according to substance, whereas others applied a general deposition velocity. ^[58, 59, 99, 198-201] Moreover, the blow-on and blow-off effects associated with active air sampling methodologies (chapter 3.1.1) might bias the pollutant concentrations quantified in the particle associated mass fraction of the atmosphere to

some extent. Deposition velocities of relevant studies (target compounds with highest mass fraction in the particulate phase of the atmosphere) were summarized in table 5.16.

Table 5.15: Estimations of the annual dry particle deposition fluxes of PFCs and organophosphorus flame retardants to the surface seawater of the German EEZ and the North Sea

Organic pollutant	F_{DD} (g y ⁻¹)					
	German EEZ			North Sea		
	Min.	Max.	Mean	Min.	Max.	Mean
PFHPA	<LOD	37	12	<LOD	465	36
PFHXA	<LOD	<LOD	<LOD	<LOD	432	33
PFHXS	<LOD	44	4.1	<LOD	<LOD	<LOD
PFNOA	<LOD	58	6.6	<LOD	996	187
PFOA	<LOD	261	132	<LOD	4082	2279
PFOS-1	<LOD	269	53	<LOD	2675	897
PFOSA-1	<LOD	37	2.3	<LOD	<LOD	<LOD
TBP	<LOD	7711	4060	<LOD	294089	138695
TPP	<LOD	6545	1780	<LOD	102442	46138

Table 5.16: Dry particulate deposition fluxes (F_{DD}), deposition velocities (v_D) and concentrations in the particulate mass fraction in the atmosphere (c_p) reported in the literature

Pollutant	F_{DD} (ng m ⁻² d ⁻¹)	v_D (cm s ⁻¹)	c_p (pg m ⁻³)	Sampling site	Year	Ref.
CHRTR	38	0.5	88	coastal (Sandy Hook)	1997-2001	[102]
	15	0.5	35	coastal (Tuckerton)	1997-2001	[102]
	18	0.5	42	coastal (Delaware Bay)	1997-2001	[102]
	18	0.5	42	coastal (Alloway Creek)	1997-2001	[102]
BAP	18	0.5	42	coastal (Sandy Hook)	1997-2001	[102]
	4.8	0.5	11	coastal (Tuckerton)	1997-2001	[102]
	7.2	0.5	17	coastal (Delaware Bay)	1997-2001	[102]
	12	0.5	28	coastal (Alloway Creek)	1997-2001	[102]
I123P	50	0.5	116	coastal (Sandy Hook)	1997-2001	[102]
	13	0.5	30	coastal (Tuckerton)	1997-2001	[102]
	20	0.5	46	coastal (Delaware Bay)	1997-2001	[102]
	23	0.5	53	coastal (Alloway Creek)	1997-2001	[102]
BGHIP	38	0.5	88	coastal (Sandy Hook)	1997-2001	[102]
	13	0.5	30	coastal (Tuckerton)	1997-2001	[102]
	9.5	0.5	22	coastal (Delaware Bay)	1997-2001	[102]
	23	0.5	53	coastal (Alloway Creek)	1997-2001	[102]
CB 138	n/a	0.42	n/a	eastern Mediterranean Sea	2000-2001	[99]
CB 153	n/a	0.40	n/a	eastern Mediterranean Sea	2000-2001	[99]
TBP	0.17 - 25.9	0.2	1 - 150	German EEZ of the North Sea	2010	[184]
TPP	0.69 - 50.1	0.2	4 - 290	German EEZ of the North Sea	2010	[184]
MCPA	n.a.	0.53	n.a.	Canadian Prairies	May-July 2002	[58]
24-D	n.a.	0.36	n.a.	Canadian Prairies	May-July 2002	[58]
Pesticides	n.a.	0.2	n.a.	Canadian agricultural regions	2004-2005	[59]

6. Summary

The aim of this study was the assessment of the exchange processes of organic pollutants between the marine atmosphere and the surface seawater of the German EEZ, the wider North Sea and the Baltic Sea with emphasis upon the occurrence and contribution of atmospheric deposition to the seawater contamination. 87 organic pollutants, routinely monitored as surface seawater contaminants by the BSH, were targeted in this study. Concentrations of polycyclic aromatic hydrocarbons (PAHs), organochlorine pesticides (OCPs), polychlorinated biphenyls (PCBs), currently used pesticides (CUPs), perfluorinated compounds (PFCs), organophosphorus / brominated flame retardants and pharmaceuticals were simultaneously quantified in the surface seawater and the marine atmosphere during two research cruises in the German EEZ in May/Jun. 2009 and May 2010 as well as during a further research cruise in the North Sea in Aug./Sep. 2009. Air samples of the gaseous mass fraction of the Baltic Sea atmosphere of April 2009 were provided by the University of Hamburg. Air samples were collected using high-volume active air samplers operated on the top deck of the respective research vessels. Furthermore, PUF disk passive air samples were exposed at an urban land based sampling site (Sülldorf/Hamburg) and at a rural coastal sampling site (Tinum/Sylt) between October 2009 and December 2010, respectively. Moreover, PUF disks were installed at the FINO research platforms in the German EEZ in various heights above sea level. Seasonal and vertical fluctuations of atmospheric concentrations could be successfully monitored by passive air sampling providing further indications of sources, occurrences and distributions of the organic pollutants in the marine atmosphere. The application of standard active and passive air sampling methodologies at research ships required a continuing optimization and adaptation of the sampling equipment and sampler design to the extreme weather and working conditions at sea. Methods of sample preparation were developed and validated which allowed the reliable quantification of 87 organic pollutants from a single air sample (GFFs, PUF disks, PUF plugs, PUF/XAD-2/PUF adsorber cartridges). Estimations on wet deposition fluxes to the surface seawater were based on substance concentration levels in precipitation at Zingst (Baltic Sea) and Tinum/Sylt (German EEZ/North Sea) provided by the Federal Environmental Agency of Germany for 2009 and 2010. Dry particulate fluxes were derived from the concentrations of organic pollutants in the particle associated mass fraction of the marine aerosol and an estimated deposition velocity of 0.02 cm/s.

All processes contributing to air-sea exchange of organic pollutants, i.e. atmospheric deposition and volatilisation from the surface seawater could be documented in this study. The most frequently observed exchange mechanism of the target analytes was the atmospheric deposition. A significant contribution of atmospheric deposition to the surface water contamination of the open

sea could be demonstrated for phenanthrene, fluorene, lindane, dieldrin, *p,p'*-DDE and CUPs. While the spatial distribution of most target compounds in the surface seawater appeared to be dominated by riverine input and subsequent transport with sea currents, increased surface water concentrations beyond river plumes and/or characteristic changes in distribution patterns with season were found and might be ascribed to the influence of atmospheric deposition. The occurrence and widespread distribution of organic contaminants in the marine atmosphere as well as seasonally extended atmospheric concentrations were in agreement with these perceptions: For example, fluorene and phenanthrene, the main PAH components in the marine atmosphere, displayed almost constant or only slightly decreasing surface water concentrations throughout the German EEZ unaffected by the suspended particulate matter and riverine fresh water content. In contrast, other PAH components occurring in lower atmospheric abundances revealed strong concentration gradients from the coastal waters to the open sea. Similar observations are made for the DDT metabolites. Although *p,p'*-DDD was quantified in higher concentrations than *p,p'*-DDE in the coastal surface waters, exclusively *p,p'*-DDE could be quantified in the central North Sea. This shift in distribution patterns pointed to an atmospheric deposition of *p,p'*-DDE, which was found to be the main DDT metabolite in the marine atmosphere. A further example was dieldrin. Dieldrin exhibited increased surface water concentrations in the south-central part of the North Sea (Dogger Bank region), which could be excluded to originate from riverine input due to the prevailing sea currents. However, elevated atmospheric concentrations of dieldrin were observed in air masses originating from central England above or in proximity to this sea region. These might be possible sources of dieldrin to the Dogger Bank. In particular, the CUPs exhibited highest variability in atmospheric concentrations, which were consistent with the seasonal changes of their concentrations in surface seawater. Correlations in the seasons of highest atmospheric abundances and highest concentrations in the surface seawater, in particular in regions beyond riverine input, were assumed to originate rather from a fast atmospheric transport and subsequent deposition than from the comparable slower riverine transport and distribution along the sea currents. Such correlations were observed for a variety of the targeted CUPs: Terbutylazine was found to be the currently most extensively used triazine herbicide with a main application season in May/June. Metolachlor exhibited the same main application season. The phenoxethanoic acids (24-D, MCPA) exhibited highest air and water concentrations in spring, whereas pendimethalin, trifluralin and metazachlor had a main application season from September to October. Furthermore, anomalous distribution patterns in the surface seawater as observed for trifluralin and pendimethalin, which were incoherent with the prevailing sea currents and riverine sources, but consistent with their seasonally increased atmospheric abundances, gave evidence that atmospheric deposition was a major source of surface seawater pollution. Other CUPs exhibiting a short persistence in the environment like pirimicarb and the organophosphate herbicides were scarcely detected in the

marine atmosphere and the surface seawater. However, their sporadic occurrence in air and water even at remote sampling sites might indicate an atmospheric deposition to the surface seawater. Air mass history indicated that advection of contaminated air masses from the continent resulted in a widespread distribution of organic pollutants in the marine atmosphere and deposition to the surface seawater. This was additionally suggested by the vertical pollutant profiles obtained from the FINO stations, which displayed an almost even distribution with height. Air-sea exchange close to equilibrium was documented for some “classical” OCPs like hexachlorobenzene and α -HCH and was even assumed for the low molecular weight PCBs (CB28 and CB 52) in the Baltic Sea environment. Besides, hexachlorocyclohexane isomers (α -HCH, lindane) and fluorene, a low molecular weight PAH, displayed a significant trend of net volatilisation from highly contaminated coastal waters (river plume of the Elbe) in summer. The targeted pharmaceuticals and PFCs were scarcely detected in the marine atmosphere in concentrations close to or below the respective LOQs. In consequence, the contribution of atmospheric deposition to the surface seawater contamination by these pollutants was expected to be negligible. In contrast, the continuous and widespread occurrence of PFOA in the marine atmosphere independent of air mass history indicated a marine particle source, such as sea spray (occurring in wave breakings and during precipitation). Organophosphorus flame retardants were found to be major contaminants of the marine atmosphere. Although surface water data was not available, the increased concentrations and their predominant occurrence in the particle associated mass fraction was indicative of an extended atmospheric deposition to the surface seawater.

7. Zusammenfassung

Ziel dieser Studie war eine Untersuchung der Austauschprozesse von organischen Schadstoffen zwischen der marinen Atmosphäre und dem Oberflächenwasser der Deutschen Ausschließlichen Wirtschaftszone (AWZ), der Nordsee und der Ostsee unter besonderer Berücksichtigung des Beitrags von atmosphärischen Depositionsprozessen zur Meerwasserbelastung. Es wurden 87 organische Schadstoffe in dieser Studie untersucht, die auch als Zielsubstanzen im aktuellen Monitoringprogramm des BSH für die Meerwasseranalyse geführt werden. Polyzyklische aromatische Kohlenwasserstoffe (PAKs), „klassische“ chlorierte Pestizide (OCPs), polychlorierte Biphenyle (PCBs), aktuell verwendete Pestizide (CUPs), perfluorierte Verbindungen (PFCs), Phosphorflammschutzmittel, bromierte Flammschutzmittel und Pharmazeutika wurden jeweils simultan im Oberflächenwasser und der marinen Atmosphäre während zwei Forschungsfahrten in der deutschen AWZ im Mai/Juni 2009 und im Mai 2010 sowie während einer weiteren Fahrt in der Nordsee im August/September 2009 analysiert. Luftproben des gasförmigen Anteils organischer Schadstoffe in der Ostseeatmosphäre von April 2009 wurden von der Universität Hamburg zur Verfügung gestellt. Die Luftproben wurden mit Hilfe eines High-volume-Aktivsammlers auf dem Peildeck der jeweiligen Forschungsschiffe genommen. Zusätzlich wurden Passivsammlerproben an einem städtischen (Sülldorf/Hamburg) und an einem ländlichen küstennahen (Tinnum/Sylt) Beprobungsort in einem jeweiligen Zeitraum von Oktober 2009 bis Dezember 2010 gesammelt. Zudem wurden weitere Passivsammler in verschiedenen Höhen auf den FINO-Forschungsplattformen in der Deutschen AWZ installiert. Saisonale und vertikale Konzentrationsschwankungen konnten mit Hilfe der Passivsammler erfolgreich aufgezeichnet werden und ermöglichten einen tieferen Einblick in Eintragspfade, Vorkommen und Verteilung organischer Schadstoffe in der Atmosphäre. Die Anwendung der aktuellen aktiven und passiven Luftprobenahmeverfahren auf Forschungsschiffen erforderte eine fortwährende Optimierung und Anpassung von Geräten und Zubehör an die extremen Wetter- und Arbeitsbedingungen auf See. Es wurden Analysemethoden entwickelt und validiert, die eine zuverlässige Quantifizierung von allen 87 Schadstoffen in einer einzigen Luftprobe (GFFs, PUF Scheiben, PUF Zylinder, PUF/XAD-2/PUF Adsorberkartusche) ermöglichten. Die Eintragsberechnungen von organischen Schadstoffen durch Nassdeposition ins Oberflächenwasser der Meere basierten auf Depositionsdaten von Zingst (Ostsee) und Tinnum/Sylt (Deutsche AWZ, Nordsee), die vom Umweltbundesamt (Deutschland) für die Jahre 2009 und 2010 zur Verfügung gestellt wurden. Der Eintrag durch atmosphärische Partikel wurde anhand der Schadstoffkonzentration in atmosphärischen Schwebstoffen und unter Annahme einer allgemeinen Sedimentationsgeschwindigkeit von 0,02 cm/s geschätzt.

Alle Prozesse die zu dem Austausch von organischen Schadstoffen zwischen Ozean und Atmosphäre beitragen (atmosphärischer Eintrag, Verflüchtigung), konnten in dieser Studie beobachtet werden. Der am häufigste beobachtete Austauschprozess der Zielsubstanzen war die atmosphärische Deposition. Ein signifikanter Beitrag atmosphärischer Deposition zur Oberflächenwasserbelastung der Meere wurde für Phenanthren, Fluoren, Lindan, Dieldrin, *p,p'*-DDE und CUPs nachgewiesen. Obwohl die räumliche Verteilung im Oberflächenwasser der meisten Zielsubstanzen auf hohe Flusseinträge und die vorherrschenden Meeresströmungen zurückzuführen war, konnten erhöhte Wasserkonzentrationen außerhalb der Flussfahnen und/oder charakteristische jahreszeitliche Schwankungen im Verteilungsmuster des Oberflächenwassers als Hinweis auf atmosphärische Depositionsprozesse gedeutet werden. Das Vorkommen und die weiträumige Verteilung organischer Schadstoffe in der marinen Atmosphäre sowie saisonal erhöhte Luftkonzentrationen bestätigten diese Annahmen: Zum Beispiel zeigten Fluoren und Phenanthren, die Hauptkomponenten der untersuchten PAHs in der marinen Atmosphäre, nahezu gleichbleibende Wasserkonzentrationen in der Deutschen AWZ, die unbeeinflusst vom Schwebstoff- und Süßwassergehalt waren. Andere PAH Komponenten, die in wesentlich geringeren Luftkonzentrationen gefunden wurden, bildeten dagegen starke Konzentrationsgradienten im Oberflächenwasser aus. Hinweise auf atmosphärische Deposition wurden auch im Verteilungsmuster der DDT-Metabolite gefunden. Obwohl *p,p'*-DDD in höheren Konzentrationen im küstennahen Oberflächenwasser gefunden wurde, war ausschließlich noch das *p,p'*-DDE auf den weiter nördlich gelegenen Probenahmestationen der zentralen Nordsee messbar. Dies deutete auf eine atmosphärische Deposition von *p,p'*-DDE hin, da ausschließlich das *p,p'*-DDE und nicht das *p,p'*-DDD in der marinen Atmosphäre gefunden wurde. Ein weiteres Beispiel war Dieldrin. Dieldrin wies erhöhte Wasserkonzentrationen im südlichen Teil der zentralen Nordsee (Dogger-Bank) auf, die aufgrund der vorherrschenden Meeresströmungen nicht auf Flusseinträge zurückzuführen waren. In diesem Seegebiet wurden auch stark erhöhte Dieldrin Konzentrationen in den aus England stammenden Luftmassen (Rückwärtstrajektorien von 24 Stunden) quantifiziert, die über atmosphärische Depositionsprozesse zur Meerwasserbelastung in diesem Seegebiet beigetragen haben könnten. Insbesondere die CUPs zeigten erhebliche Schwankungen in den Luftkonzentrationen, die mit den saisonalen Schwankungen der jeweiligen Wasserkonzentrationen im küstennahen Oberflächenwasser sowie in der offenen See übereinstimmten. Es wurde angenommen, dass diese Übereinstimmungen der saisonalen Schwankungen im Oberflächenwasser der offenen See (unbeeinflusst von Flusseinträgen) und der Atmosphäre überwiegend durch atmosphärische Depositionsprozesse verursacht wurden und nur im geringeren Maße durch den vergleichsweise langsamen Transport in der Wasserphase mit den Meeresströmungen: So wurde zum Beispiel beobachtet, dass Terbutylazin das damals meist genutzte Triazin-Herbizid war und hauptsächlich von Mai bis Juni ausgebracht wurde. Für Metolachlor wurde die gleiche

Hauptanwendungszeit gefunden. Die Phenoxyessigsäuren (24-D und MCPA) wiesen die höchsten Wasser- und Luftkonzentrationen im Frühjahr auf, wohingegen Pendimethalin, Trifluralin und Metazachlor in höchsten Mengen im September und Oktober ausgebracht wurden. Zudem wurden atypische Verteilungsmuster im Oberflächenwasser für Trifluralin und Pendimethalin gefunden, die nicht auf die vorherrschenden Meeresströmungen und Flusseinträge zurückzuführen waren, aber in Verbindung mit dem Auftreten episodisch erhöhter Luftkonzentrationen standen. Dies erbrachte den Beweis, dass atmosphärische Depositionsprozesse wichtige Eintragspfade organischer Schadstoffen ins Oberflächenwasser sind. Andere CUPs wie Pirimicarb und die Phosphorsäureester, die eine geringe Persistenz in der Umwelt haben, wurden nur selten in der Atmosphäre und im Oberflächenwasser detektiert. Jedoch deuteten die sporadisch gemessenen Konzentrationen insbesondere außerhalb der Küstengebiete auf eine mögliche atmosphärische Deposition dieser Stoffe ins Oberflächenwasser hin. Eine Rückverfolgung der Luftströmungen (Herkunftsanalyse mittels Rückwärtstrajektorien) zeigte, dass die Advektion von belasteten kontinentalen Luftmassen, eine Ursache der weiträumigen Verteilung organischer Schadstoffe in der marinen Atmosphäre war und die atmosphärische Deposition der Schadstoffe ins Oberflächenwasser der Meere ermöglichte. Die Advektion als Haupteintragspfad organischer Schadstoffe in die marine Atmosphäre wurde durch die vertikalen Konzentrationsprofile (von den FINO-Forschungsplattformen) bestätigt, die nahezu gleichbleibende Schadstoffkonzentrationen mit der Höhe dokumentierten. Für einzelne „klassische“ chlorierte Pestizide wie Hexachlorbenzol und α -HCH näherten sich die Austauschprozesse zwischen Meer und Atmosphäre einer Gleichgewichtseinstellung an. Eine Gleichgewichtseinstellung der PCBs kleinster Molmasse (CB 28 und CB 52) im Ostseeraum wird vermutet. Zudem zeigten die HCH-Isomere (α -HCH, Lindan) und Fluoren in den Sommermonaten die Tendenz aus dem küstennahen hochbelasteten Oberflächenwasser (Elbfahne) auszugasen. Die Pharmazeutika und PFCs wurden nur selten in der Atmosphäre detektiert und in Konzentrationen die nahe bzw. unter der Bestimmungsgrenze lagen. Demzufolge war anzunehmen, dass die atmosphärische Deposition dieser Stoffe einen unerheblichen Beitrag zur Meerwasserbelastung leistete. Jedoch deuteten die kontinuierlichen und weiträumigen Vorkommen von PFOA in der marinen Atmosphäre auf einen aktiven Meer-Atmosphäre-Austausch durch Wellenbrechungsprozesse hin. Die Phosphorflammschutzmittel bildeten eine Hauptschadstoffklasse der marinen Atmosphäre. Obwohl entsprechende Oberflächenwasserkonzentrationen nicht zur Verfügung standen, deuteten die erhöhten Luftkonzentrationen und die starke Partikeladsorption auf starke atmosphärische Eintragspfade ins Oberflächenwasser der Meere hin.

8. Perspectives

Further long time studies are required to verify and complement the results of this study. But first of all additional adaptations of the passive air sampling methodology to the exposure conditions in the marine atmosphere should be aspired. Although the current modified “flying saucer” design resisted the increased wind speeds at the open sea, the sampling rates were still significantly influenced by wind velocities exceeding 4-5 m/s. ^[109] Average wind speeds in the marine atmosphere were observed in the range of 8 m/s to 9 m/s preventing a semi-quantitative analysis of the atmospheric abundances during this study. In consequence, a modification of the sampler design to a more efficient wind dampening effect is proposed. The first attempt may be the usage of “dome”-housings, because wind-tunnel experiments documented constant sampling rates up to a wind velocity of 20 m/s. ^[109] An efficient wind dampening would improve the validity of future trend investigations based on the total amount of target analytes accumulated on the PUF disks. Moreover, the determination of sampling rates for the major target compounds and pollutant classes would be facilitated. Calibration of sampling rates should be performed with the help of low volume active air samplers as mentioned in chapter 1.2. In order to evaluate the reliability of the calculated sampling rates, the calibration procedures should be performed at least at two sampling sites exhibiting significant differences in the average wind velocities. Sülldorf/Hamburg, Sylt and Heligoland may be proposed as adequate and accessible sampling sites. Thereafter, vertical pollutant profiles should be monthly monitored at the FINO research platforms, in order to improve the knowledge of the seasonality and distribution of organic pollutants in the marine atmosphere.

Another field of activity should be the collection of monthly wet and dry particle deposition samples at the sampling sites Sülldorf/Hamburg, Sylt, Heligoland and FINO in order to verify and complement the estimations on the deposition fluxes to the surface seawater. The calculation of scavenging ratios for the major target compounds may enable estimations of wet deposition fluxes to the surface seawater by knowledge of the current atmospheric concentrations.

Besides, the spectrum of targeted pollutants may be extended in future investigations. For example, fluorotelomer alcohols, perfluorinated sulfonamides, perfluorinated sulfonamido ethanols, short chained PFCs, polybrominated diphenyl ethers (PBDEs), organophosphorus flame retardants, phthalates and endosulfan may be expected in significant abundances in the marine atmosphere. In contrast, the pharmaceuticals and the organic compounds of short persistence like the organophosphate insecticides and pirimicarb could be excluded from future investigations, because they were found to be negligible contaminants of the marine atmosphere and the surface seawater. The data of this and future studies may be incorporated to current mass balance models in order to review the results of current investigations and to model future trends in the surface seawater pollution.

9. Experimental

9.1 List of materials

The tables below list the solvents, chemicals and further materials applied during this study.

Table 9.1: List of solvents

Solvent	CAS	Purity	Hazard Pictogram	Hazard Statements	Precautionary Statements
Acetone	67-64-1	SupraSolv®	GHS02; GHS07	H225; H319; H336; EUH066	P210; P233; P305+P351+P338
Dichloromethane	75-09-2	SupraSolv®	GHS08	H351	P281; P308+P313
<i>n</i> -Hexane	110-54-3	SupraSolv®	GHS02; GHS07; GHS08; GHS09	H225; H304; H361; H373; H315; H336; H411	P210; P240; P273; P301+P310; P331; P302+P352; P403+P235
Methanol	67-56-1	SupraSolv®	GHS02; GHS06; GHS08	H225; H301+ H311+H331; H370	P210; P280; P302+P352; P403+P235

Supplier: Merck, Darmstadt, Germany

Table 9.2: List of chemicals (common names); P = Purity in %, S = Supplier

Chemical	CAS	P	S	Hazard Pictogram	Hazard Statements	Precautionary Statements
2,4-D	94-75-7	99.3	1	GHS05; GHS07	H302; H335; H318; H317; H412	P273; P280; P305+P351+P338; P302+P352
Acenaphthene	83-32-9	99.9	2	GHS07; GHS09	H315; H319; H335; H410	P261; P273; P305+P351+P338; P501
Acenaphthene-D ₁₀	15067-26-2	99	3	GHS07; GHS09	H315; H319; H335; H410	P261; P273; P305+P351+P338; P501
Acenaphthylene	208-96-8	99.9	2	GHS06; GHS08	H301+ H311+H331; H370	P260; P280; P301+P310; P311
Acetic acid (glacial)	64-19-7	100	4	GHS02; GHS05	H226; H314	P280; P305+P351+P338; P370; P378; P310
Aldrin	309-00-2	99.3	8	GHS06; GHS08; GHS09	H301; H311; H351; H372; H410	P273; P280; P301+P310; P314; P501;
Ametryn	834-12-8	98.5	1	GHS07; GHS09	H302; H410	P273; P501
Ammonium acetate	631-61-8	>97	4	GHS07	H315; H319; H335	P261; P305+P351+P338
Anthracene	120-12-7	99.8	2	GHS09	H410	P273
Anthracene-D ₁₀	1719-06-8	98	3	GHS09	H410	P273
Atrazine	1912-24-9	99.5	1	GHS07; GHS08; GHS09	H317; H373; H410	P273; P280; P501
Atrazine-D ₅	163165-75-1	99	1	GHS07; GHS08; GHS09	H317; H373; H410	P273; P280; P501
Azinphos-ethyl	2642-71-9	98	1	GHS06; GHS09	H300; H311; H410	P264; P273; P280; P301+P310; P312; P501

Table 9.2 continued:

Chemical	CAS	P	S	Hazard Pictogram	Hazard Statements	Precautionary Statements
Azinphos-methyl	86-50-0	98.5	1	GHS06, GHS09	H300; H311;H317; H330; H410	P260; P264; P273; P280; P284; P301+P310
Azinphos-methyl-D ₆	N/A	99.5	1	GHS06, GHS09	H300; H311;H317; H330; H410	P260; P264; P273; P280; P284; P301+P310
Bentazon	25057-89-0	97	1	GHS07	H302; H317; H319; H412	P273; P280; P305+P351+P338
Benzo[<i>a</i>]anthracene	56-55-3	97.9	2	GHS08; GHS09	H350; H410	P201; P273; P308+P313; P501
Benzo[<i>a</i>]anthracene-D ₁₂	1718-53-2	98	3	GHS08; GHS09	H350; H410	P201; P273; P308+P313; P501
Benzo[<i>a</i>]pyrene	50-32-8	98	2	GHS07; GHS08; GHS09	H317; H340; H350;H360; H410	P201; P273; P280; P308+P313; P501
Benzo[<i>b</i>]fluoranthene	205-99-2	99.9	2	GHS08, GHS09	H350; H410	P201, P273; P308+P313; P501
Benzo[<i>e</i>]pyrene-D ₁₂	192-97-2	98	3	GHS08, GHS09	H350; H410	P201, P273; P308+P313; P501
Benzo[<i>g,h,i</i>]perylene	191-24-2	99.1	2	GHS09	H410	P273; P501
Benzo[<i>g,h,i</i>]perylene-D ₁₂	93951-66-7	98	3	GHS09	H410	P273; P501
Carbamazepine	298-46-4	99	1	GHS07; GHS08	H302; H317; H334	P261; P280; P342; P311
Carbendazim	10605-21-7	99	1	GHS08, GHS09	H340; H360; H410	P201; P273; P308+P313; P501
Chlorfenvinphos	470-90-6	97	1	GHS06; GHS09	H300; H311; H410	P264; P273; P280; P301+P310; P312; P501
Chlortoluron	15545-48-9	98	1	GHS08; GHS09	H351; H361; H410	P273; P281; P501
Chromabond® Sorbenz SiOH	7631-86-9	95-100	5	GHS05	H314	-
Chrysene	218-01-9	98.7	2	GHS08; GHS09	H341; H350; H410	P201; P273; P281; P308+P313; P501
Clofibric acid	882-09-7	99	6	GHS07	H302	-
Desethylatrazine	6190-65-4	98	1	GHS07	H302; H319; H332	P305+P351+P338
Desethylatrazine-D ₆	N/A	99	1	GHS07	H302; H319; H332	P305+P351+P338
Diazinone	333-41-5	99.5	1	GHS07; GHS09	H302; H410	P273; P501
Dibenzo[<i>a,h</i>]anthracene	53-70-3	99.6	2	GHS08; GHS09	H350; H410	P201; P202; P273; P281; P308+P313; P391; P405; P501
Dichlorprop	120-36-5	99	1	GHS05; GHS07	H302; H312; H315; H318	P280; P305+P351+P338
Diclofenac	15307-79-6	98.8	1	GHS06	H301	P301+P310
Dieldrin	60-57-1	99.2	7	GHS06; GHS08; GHS09	H301; H310; H351; H372; H410	P273; P280; P301+P310; P302; P350; P501
Dimethoate	60-51-5	98	1	GHS07	H302; H312	P280
Diuron	330-54-1	97.7	1	GHS07; GHS08; GHS09	H302; H351; H373; H410	P273; P281; P501
Diuron-D ₆	N/A	99.5	1	GHS07; GHS08; GHS09	H302; H351; H373; H410	P273; P281; P501
Endrin	72-20-8	98	8	GHS06; GHS09	H300; H311; H410	P264; P273; P280; P301+P310; P312; P501
Fenuron	101-42-8	99	1	GHS07	H319; H335	P261; P305+P351+P338

Table 9.2 continued:

Chemical	CAS	P	S	Hazard Pictogram	Hazard Statements	Precautionary Statements
Fluoranthene	206-44-0	98.2	2	GHS07	H302	-
Fluoranthene-D ₁₀	93951-69-0	98	3	GHS07	H302	-
Fluorene	86-73-7	98.6	2	GHS09	-	P273; P391
Hexachlorobenzene	118-74-1	>98.0	3	GHS08; GHS09	H350; H372; H410	P201; P273; P308+P313; P501
Hexachlorobenzene- ¹³ C ₆	93952-14-8	99.5	1	GHS08; GHS09	H350; H372; H410	P201; P273; P308+P313; P501
Hexazinone	51235-04-2	99	1	GHS07; GHS09	H319; H302; H410	P273; P305+P351+P338; P501
Indeno[1,2,3- <i>cd</i>]pyrene	193-39-5	99.9	2	GHS08	H351	P281
Irgarol	28159-98-0	98.5	1	GHS07; GHS09	H317; H400	P273; P280
Isodrin	465-73-6	98.1	1	GHS06; GHS09	H300; H310; H330; H410	P260; P264; P273; P280; P284; P301+P310
Isoproturon	34123-59-6	99	1	GHS08; GHS09	H351; H410	P273; P281; P501
Lindane	58-89-9	99.9	8	GHS06; GHS08; GHS09	H301; H312; H332; H362; H373; H410	P263; P273; P280; P301+P310; P501
Lindane- ¹³ C ₆ D ₆	58-89-9	98	3	GHS06; GHS08; GHS09	H301; H312; H332; H362; H373; H410	P263; P273; P280; P301+P310; P501
Linuron	330-55-2	99.5	1	GHS06; GHS07; GHS09	H302; H351; H360Df; H373; H410	P201; P273; P281; P308+P313; P501
Malathion	121-75-5	99.5	1	GHS07; GHS09	H302; H317; H410	P273; P280; P501
Malathion-D ₁₀	N/A	99.0	5	GHS07; GHS09	H302; H317; H410	P273; P280; P501
MCPA	94-74-6	97.5	1	GHS05; GHS07; GHS09	H302; H315; H318; H410	P273; P280; P305+P351+P338; P501
MCPA-D ₃	N/A	99.0	1	GHS05; GHS07; GHS09	H302; H315; H318; H410	P273; P280; P305+P351+P338; P501
Mecoprop	93-65-2	98.8	1	GHS05; GHS07; GHS09	H302; H315; H318; H410	P273; P280; P305+P351+P338; P501
Mecoprop-D ₃	N/A	99.5	1	GHS05; GHS07; GHS09	H302; H315; H318; H410	P273; P280; P305+P351+P338; P501
Metazachlor	67129-08-2	99.5	1	GHS07	H302	-
Methabenzthiazuron	18691-97-9	99.0	1	GHS09	H410	P273; P501
Metolachlor	51218-45-2	97.0	1	GHS07	H302	-
Naproxen	22204-53-1	99.0	1	GHS07	H302	-
<i>o,p'</i> -DDT	789-02-6	99.0	1	GHS06; GHS08; GHS09	H301; H351; H372; H410	P273; P281; P301+P310; P314; P501
Oxazepam	604-75-1	99.0	5	GHS08	H351	P281
<i>p,p'</i> -DDD	72-54-8	99.0	8	GHS06; GHS08; GHS09	H301; H312; H351; H410	P273; P280; P301+P310; P501
<i>p,p'</i> -DDE	72-55-9	99.0	8	GHS06; GHS08; GHS09	H302; H351; H410	P273; P281; P501
<i>p,p'</i> -DDT	50-29-3	99.0	8	GHS06; GHS08; GHS09	H301; H351; H372; H410	P273; P281; P301+P310; P314; P501

Table 9.2 continued:

Chemical	CAS	P	S	Hazard Pictogram	Hazard Statements	Precautionary Statements
<i>p,p'</i> -DDT-D ₈	93952-18-2	99	9	GHS06; GHS08; GHS09	H301; H351; H372; H410	P273; P281; P301+P310; P314; P501
PCB 28	7012-37-5	99.9	1	GHS08; GHS09	H373; H410	P273; P501
PCB 30	35693-92-6	96.5	1	GHS03; GHS07; GHS08; GHS09	H225; H304; H315; H336; H373; H410	P210; P261; P273; P301+P310; P331; P501
PCB 52	35693-99-3	99.0	1	GHS08; GHS09	H373; H410	P273; P501
PCB 52- ¹³ C ₁₂	N/A	>98	3	GHS08; GHS09	H373; H410	P273; P501
PCB 104	56558-16-8	99	1	GHS08; GHS09	H373; H410	P273; P501
PCB 138	35065-28-2	99.0	1	GHS08; GHS09	H373; H410	P273; P501
PCB 145	74472-40-5	99.5	1	GHS08; GHS09	H373; H410	P273; P501
PCB 153	35065-27-1	99.0	10	GHS08; GHS09	H373; H410	P273; P501
PCB 153- ¹³ C ₁₂	N/A	99.6	3	GHS08; GHS09	H373; H410	P273; P501
PCB 185	52712-05-7	99.9	1	GHS08; GHS09	H373; H410	P273; P501
PCB 204	74472-52-9	99.5	1	GHS08; GHS09	H373; H410	P273; P501
Pendimethalin	40487-42-1	98.0	1	GHS07, GHS09	H317; H410	P273; P280; P501
Pentachlorobenzene	608-93-5	99.9	3	GHS02; GHS07; GHS09	H228; H302; H410	P201; P273; P501
Perfluorobutanesulfonic acid	375-73-5	>98.0	11	GHS02; GHS06; GHS08	H225; H301+ H311+H331; H370	P210; P233; P240; P280; P302+P352; P304+P340 ; P309+P310, P410; P235
Perfluorodecanoic acid	335-76-2	>98.0	11	GHS02; GHS06; GHS08	H225; H301+ H311+H331; H370	P210; P233; P240; P280; P302+P352; P304+P340 ; P309+P310, P410; P235
Perfluoroheptanoic acid	375-85-9	>98.0	11	GHS02; GHS06; GHS08	H225; H301+ H311+H331; H370	P210; P233; P240; P280; P302+P352; P304+P340 ; P309+P310, P410; P235
Perfluorohexanesulfonic acid	3871-99-6	>98.0	11	GHS02; GHS06; GHS08	H225; H301+ H311+H331; H370	P210; P233; P240; P280; P302+P352; P304+P340 ; P309+P310, P410; P235
Perfluorohexanesulfonic acid- ¹⁸ O ₂	N/A	>98.0	11	GHS02; GHS06; GHS08	H225; H301+ H311+H331; H370	P210; P233; P240; P280; P302+P352; P304+P340 ; P309+P310, P410; P235
Perfluorohexanoic acid	307-24-2	>98.0	11	GHS02; GHS06; GHS08	H225; H301+ H311+H331; H370	P210; P233; P240; P280; P302+P352; P304+P340; P309+P310, P410; P235
Perfluorononanoic acid	375-95-1	>98.0	11	GHS02; GHS06; GHS08	H225; H301+ H311+H331; H370	P210; P233; P240; P280; P302+P352; P304+P340 ; P309+P310, P410; P235
Perfluorooctanesulfonamide	754-91-6	>98.0	11	GHS02; GHS06; GHS08	H225; H301+ H311+H331; H370	P210; P233; P240; P280; P302+P352; P304+P340 ; P309+P310, P410; P235
Perfluorooctanesulfonic acid	1763-23-1	>98.0	11	GHS02; GHS06; GHS08	H225; H301+ H311+H331; H370	P210; P233; P240; P280; P302+P352; P304+P340 ; P309+P310, P410; P235

Table 9.2 continued:

Chemical	CAS	P	S	Hazard Pictogram	Hazard Statements	Precautionary Statements
Perfluorooctanesulfonic acid- ¹³ C ₄	N/A	>98.0	11	GHS02; GHS06; GHS08	H225; H301+ H311+H331; H370	P210; P233; P240; P280; P302+P352; P304+P340 ; P309+P310, P410; P235
Perfluorooctanoic acid	335-67-1	>98.0	11	GHS02; GHS06; GHS08	H225; H301+ H311+H331; H370	P210; P233; P240; P280; P302+P352; P304+P340 ; P309+P310, P410; P235
Perfluorooctanoic acid- ¹³ C ₂	N/A	>98.0	11	GHS02; GHS06; GHS08	H225; H301+ H311+H331; H370	P210; P233; P240; P280; P302+P352; P304+P340 ; P309+P310, P410; P235
Perylene-D ₁₂	1520-96-3	98	3	GHS09	H410	P273; P501
Phenanthrene	85-01-8	99.9	2	GHS07; GHS09	H302; H315; H319; H335; H410	P261; P273; P305+P351+P338; P501
Phenanthrene-D ₁₀	1517-22-2	98	3	GHS07; GHS09	H302; H315; H319; H335; H410	P261; P273; P305+P351+P338; P501
Pirimicarb	23103-98-2	99.0	1	GHS02; GHS07	H225; H302; H312; H319; H332;	P210, P280; P305+P351+P338
Primidone	125-33-7	99.0	1	GHS07; GHS08	H302; H351	P281
Prometryn	7287-19-6	99.3	1	GHS07; GHS09	H332; H400	P273
Prometryn-D ₆ (isopropyl D ₆)	N/A	98.0	1	GHS07; GHS09	H332; H400	P273
Propazin	139-40-2	98.0	1	GHS08; GHS09	H351; H410	P273; P281; P501
Pyrene	129-00-0	96.6	2	GHS07; GHS09	H319; H410	P273; P305+P351+P338; P501
Simazine	122-34-9	99.5	1	GHS08; GHS09	H351; H410	P273; P281; P501
Simazine-D ₁₀	220621-39-6	98.5	1	GHS08; GHS09	H351; H410	P273; P281; P501
Terbutylazine	5915-41-3	99.0	1	GHS07	H302; H332	-
Terbutylazine-D ₅	N/A	98.0	1	GHS07	H302; H332	-
Terbutryn	886-50-0	97.5	1	GHS07; GHS09	H319; H400	P273; P305+P351+P338
Tetrabromobisphenol A- ¹³ C ₂	N/A	>98.0	11	GHS09	H410	P273; P501
Tributyl phosphate	126-73-8	99.5	1	GHS07; GHS09	H302; H315; H351	P281
Trifluralin	1582-09-8	97.5	1	GHS07; GHS08; GHS09	H317; H351; H410	P273; P280; P501
Trifluralin-D ₁₄	N/A	98	1	GHS07; GHS08; GHS09	H317; H351; H410	P273; P280; P501
Triphenyl phosphate	115-86-6	99.5	1	GHS09	H400	P273
Triphenylene	217-59-4	97.0	2	GHS05	H318	P305+P351+P338
Tris(2-butoxy-ethyl)phosphate	78-51-3	93.0	1	GHS07	H312; H315; H319; H332; H335	P261; P280; P305+P351+P338
α-Hexabromocyclododecane	3194-55-6	>98.0	11	GHS09	H410	P273; P501
α-Hexabromocyclododecane-D ₁₈	N/A	98.0	11	GHS09	H410	P273; P501
α-Hexachlorocyclohexane	319-84-6	99.3	8	GHS06; GHS08; GHS09	H301; H312; H332; H362; H373; H410	P263; P273; P280; P301+P310; P501

Table 9.2 continued:

Chemical	CAS	P	S	Hazard Pictogram	Hazard Statements	Precautionary Statements
β -Hexabromocyclododecane	3194-55-6	>98.0	11	GHS09	H410	P273; P501
β -Hexachlorocyclohexane	319-85-7	99.0	8	GHS06; GHS08; GHS09	H301; H312; H332; H362; H373; H410	P263; P273; P280; P301+P310; P501
γ -Hexabromocyclododecane	3194-55-6	>98.0	11	GHS09	H410	P273; P501
δ -Hexachlorocyclohexane	319-86-8	99.2	8	GHS06; GHS08; GHS09	H301; H312; H332; H362; H373; H410	P263; P273; P280; P301+P310; P501
ϵ -Hexachlorocyclohexane	6108-10-7	99.9	1	GHS06; GHS08; GHS09	H301; H312; H332; H362; H373; H410	P263; P273; P280; P301+P310; P501

S1 = Ehrenstorfer, Augsburg, Germany; **S2** = Supelco, Bellefonte, USA; **S3** = Cambridge Isotope Laboratories, Andover, UK; **S4** = Merck, Darmstadt, Germany; **S5** = Macherey-Nagel, Düren, Germany; **S6** = Campro Scientific, Berlin, Germany; **S7** = Institute of organic and industrial chemistry, Warsaw, Poland; **S8** = Riedel-de Haen, Seelze, Germany; **S9** = Chiron, Trondheim, Norway; **S10** = Promochem, Wesel, Germany; **S11** = Wellington, Southgate, Canada

Table 9.3: Further materials, S = Supplier

Material	S	Material	S
Aluminium foil	1	ORBO 2500 PUF/XAD-2/PUF cartridges (Supelco)	9
Baker-10 SPE system	2	Parafilm- stretch sealing film	1
Chromacol crimp caps with PP septum	3	Pasteur pipettes	1
Chromacol crimp caps with PTFE septum	3	Plastic bags with pressure lock, 20x30 cm	1
Chromacol PTFE sealing disks for screw caps, blue	3	PTFE sealing disks N11 for screw caps, white	5
Chromacol vials with crimp (2 mL, 0.5 mL)	3	PUF disks	10
Chromacol vials with screw cap (2 mL, 0.5 mL)	3	Rack for silica gel clean up	11
Condensor, NS 60/46	1	Round bottom flasks, 500 mL	1
Electromantle for 500 mL round bottom flasks	1	Screw cap, 8 mm, PP, with hole	1
Empty SPE tubes, PP, 6 mL	2	Screw cap, 8 mm, PP, without hole	1
G8-Viton sealing disks for screw caps	4	Snap-cap wide neck bottle, 10 mL	12
Glass columns 3 mL	5	Soxhlet-extractors, 300 mL	1
Glass fibre filters; MN 85 / 90 BF, 15 cm diameter	5	Steriplan petri dish, 17 cm diameter	12
Glass fibre frits for glass columns 3mL	5	Supelpak-2 (purified XAD-2)	9
Glasses for Büchi-parallel-evaporator racks 12 and 4	6	Syringe filters; Phenex Nylon 0.25 μ m; 2.5 mm diameter	2
Microliter syringes (25 μ L, 50 μ L, 100 μ L, 250 μ L, 500 μ L)	7	Vakuum exsiccators	1
Mucasol ®	8	Volumetric flasks (10 mL, 20 mL, 50 mL, 100 mL)	1
Narrow-neck bottles (2 L, 500 mL)	1	Volumetric pipettes (0.5 mL, 1 mL, 2 mL, 2.5 mL, 3 mL, 5 mL, 10 mL, 30 mL, 100 mL)	1

S1 = Omnilab, Bremen, Germany; **S2** = Phenomenex, Aschaffenburg, Germany; **S3** = Chromacol, Welwyn Garden City, UK; **S4** = Chromatographie Service GmbH, Langerwehe, Germany; **S5** = Macherey-Nagel, Düren, Germany; **S6** = Büchi Labortechnik, Essen, Germany; **S7** = Hamilton, Bonaduz, Switzerland; **S8** = Merz, Frankfurt, Germany; **S9** = Sigma-Aldrich, Taufkirchen, Germany; **S10** = RECETOX, Masaryk University in Brno, Czech Republic; **S11** = Mechanic workshop, BSH, (figure 8.1); **S12** = VWR, Darmstadt, Germany

9.2 List of instruments

GC-MS/MS:

GC	Varian CP-3800 (Varian Associates, Sunnyvale, USA)
MS	Varian 1200 Quadrupole MS/MS (Varian Associates, Sunnyvale, USA)
Carrier gas	Helium 5.0 (Linde, Hamburg, Germany)
Autosampler	CTC Combi PAL (CTC Analytics AG, Zwingen, Switzerland)
Column	Varian Factor Four Capillary Column VF-5ms, 30 m length, 0.25 µm film thickness (Varian Associates, Sunnyvale, USA)
Software	Varian Workstation Toolbar 6.9.2

HPLC-MS/MS:

HPLC	Agilent Series 1100 consisting of a binary pump, micro vacuum degaser, thermostatic column oven, autosampler and control (Agilent, Santa Clara, California)
MS	AB Sciex QTrap® 5500 with Turbo Ion Spray and APCI probe (AB Sciex, Darmstadt, Germany)
Column	two coupled columns Synergi Hydro RP, 8 nm pore size, 4 µm particle size, 75 mm x 2 mm Synergi Polar RP, 8 nm pore size, 4 µm particle size, 50 mm x 2 mm equipped with a security guard Aqua C18, 12.5 nm pore size, 4 mm x 2 mm (Phenomenex, Aschaffenburg, Germany)
Software	Analyst 1.5

Parallel-evaporator:

Vacuum controller V-850/855 (Büchi Labortechnik, Essen, Germany)
Vacuum pump V-700/710 (Büchi Labortechnik, Essen, Germany)
Distillation Chiller B-741 (Büchi Labortechnik, Essen, Germany)
Syncore® Accessories, including the racks R4 and R12 (Büchi Labortechnik, Essen, Germany)

High-volume active air sampler:

Digitel DHM-60 (Riemer-Messtechnik, Hausen/Rhön, Germany),
High-volume sampler borrowed from the Helmholtz-Zentrum Geesthacht-Centre for Materials and Coastal Research (HZG) was used for the active air sampling campaign in the German EEZ in May/June 2009, description in ^[55]
High-volume sampler tested by the University of Hamburg during the sea cruise in the Baltic Sea in April 2009, description in ^[91]

Passive air sampler:

PUF disk passive air sampler in “flying saucer” design (RECETOX, Masaryk University, Brno, Czech Republic)

Centrifuge:

Centrifuge Sigma 2-15, (Sigma, Osterode, Germany)

Analytical Balance:

Mettler AT200 (Sartorius, Göttingen, Germany)

Water deionisation and purification system:

Milli-Q-Academic-A10 (Millipore, Milford, USA)

9.3 Standard Solutions

At this point the compositions of applied standard solutions are summarized in order to avoid the extended listing of the spiked compounds and concentrations in running texts. The target analytes, performance reference compounds and internal standards are subdivided in LC and GC standards depending on their methods of quantification.

9.3.1 Performance reference compound (PRC) standard solutions**Table 9.4: PRC-LC (methanol solution)**

Compound	Concentration
SIMAZ-D ₁₀	10.0 ng/mL
PROMETR-D ₆	10.0 ng/mL

Table 9.5: PRC-GC (hexane solution)

Compound	Concentration
PHEN-D ₁₀	40.8 ng/mL
FLU-D ₁₀	39.0 ng/mL
BAA-D ₁₂	41.3 ng/mL
HCHG- ¹³ C ₆ D ₆	19.1 ng/mL

Compound	Concentration
CB 30	9.8 ng/mL
CB 104	7.5 ng/mL
CB 145	12.7 ng/mL
CB 204	10.3 ng/mL

9.3.2 Internal standard (IS) solutions**Table 9.6: IS-LC (methanol solution)**

Compound	Concentration
ATRAZ-D ₅	10.3 ng/mL
AZINPHOS-M-D ₆	10.0 ng/mL
DEATRAZ-D ₆	10.0 ng/mL
DIURON-D ₆	9.2 ng/mL
HBCDA-D ₁₈	10.0 ng/mL
MALATH-D ₁₀	10.2 ng/mL

Compound	Concentration
MCPA-D ₃	10.0 ng/mL
MECOPR-D ₃	10.3 ng/mL
PFHXS- ¹⁸ O ₂	10.0 ng/mL
PFOA- ¹³ C ₂	9.8 ng/mL
PFOS ³ C ₄	10.0 ng/mL
TERBAZ-D ₅	10.0 ng/mL

Table 9.7: IS-GC (hexane solution)

Compound	Concentration
ACE-D ₁₀	268.0 ng/mL
ANT-D ₁₀	256.0 ng/mL
BEP-D ₁₂	196.0 ng/mL
BGHIP-D ₁₂	184.0 ng/mL
PER-D ₁₂	192.0 ng/mL
HCB- ¹³ C ₆	32.0 ng/mL

Compound	Concentration
DDTPP-D ₈	32.3 ng/mL
TRIFLU-D ₁₄	29.1 ng/mL
HCHE	40.0 ng/mL
CB 52- ¹³ C ₁₂	25.6 ng/mL
CB 185	32.0 ng/mL
CB 153- ¹³ C ₁₂	25.6 ng/mL

9.3.3 Spike standard solutions of target compounds

Table 9.8: Spike-LC (methanol solution)

Compound	Concentration	Compound	Concentration	Compound	Concentration
24-D	19.3 ng/ml	HBCDA	20.0 ng/ml	PFHPA	22.0 ng/ml
AMETRYN	24.6 ng/ml	HBCDB	20.0 ng/ml	PFHXA	20.4 ng/ml
ATRAZ	21.2 ng/ml	HBCDG	20.0 ng/ml	PFHXS	20.0 ng/ml
AZINPHOS-E	20.2 ng/ml	HEXAZIN	25.5 ng/ml	PFNOA	20.0 ng/ml
AZINPHOS-M	21.4 ng/ml	IRGAROL	23.0 ng/ml	PFOA	22.0 ng/ml
BENTAZ	23.6 ng/ml	ISOPRUR	22.0 ng/ml	PFOS	19.4 ng/ml
CARBAMAZ	20.2 ng/ml	LINUR	22.9 ng/ml	PFOSA	15.0 ng/ml
CARBEND	20.0 ng/ml	MALATH	24.3 ng/ml	PIRIMIC	20.6 ng/ml
CHLORFENV	24.2 ng/ml	MCPA	19.9 ng/ml	PRIMID	20.2 ng/ml
CHLORTUR	20.8 ng/ml	MECOPR	19.5 ng/ml	PROMETR	23.0 ng/ml
CLOFIBRS	36.5 ng/ml	METAZCHL	20.4 ng/ml	PROPAZ	19.7 ng/ml
DEATRAZ	28.8 ng/ml	METHABZT	20.0 ng/ml	SIMAZ	19.7 ng/ml
DIAZINON	23.8 ng/ml	METOLA	20.0 ng/ml	TBEP	21.2 ng/ml
DICHLPR	21.0 ng/ml	NAPROX	20.0 ng/ml	TBP	20.0 ng/ml
DICLOF	20.6 ng/ml	OXAZEP	18.4 ng/ml	TERBAZ	26.0 ng/ml
DIMETH	25.6 ng/ml	PENDIMETH	21.8 ng/ml	TERBUTR	19.4 ng/ml
DIURON	22.0 ng/ml	PFBS	18.1 ng/ml	TPP	20.0 ng/ml
FENUR	22.2 ng/ml	PFDEA	19.9 ng/ml		

Table 9.9: Spike-GC (hexane solution)

Compound	Concentration	Compound	Concentration	Compound	Concentration
ACE	455.0 ng/mL	END	54.2 ng/mL	CB 153	65.5 ng/mL
ACY	542.0 ng/mL	FLU	622.0 ng/mL	CB 28	47.0 ng/mL
ALD	53.3 ng/mL	FL	458.0 ng/mL	CB 52	27.3 ng/mL
ANT	445.0 ng/mL	HCB	53.3 ng/mL	PHEN	451.0 ng/mL
BAA	576.0 ng/mL	I123P	436.0 ng/mL	PYR	462.0 ng/mL
BAP	427.0 ng/mL	ISOD	56.0 ng/mL	QCB	64.0 ng/mL
BBF	502.0 ng/mL	DDTOP	60.9 ng/mL	TRIFLU	56.8 ng/mL
BGHIP	448.0 ng/mL	DDDPP	65.0 ng/mL	HCHA	50.5 ng/mL
CHR	520.0 ng/mL	DDEPP	63.5 ng/mL	HCHB	59.0 ng/mL
DBAHA	473.0 ng/mL	DDTPP	50.3 ng/mL	HCHG	50.8 ng/mL
DIELD	55.8 ng/mL	CB 138	60.6 ng/mL	HCHD	50.3 ng/mL

9.4 Processing methods

9.4.1 Pre-cleaning of sampling material

PUF plugs, PUF disks and XAD-2 are rinsed with tap water and undergo Soxhlet-extraction with acetone, hexane and methanol for 12 h, respectively. The pre-cleaned adsorber materials are dried in a vacuum desiccator for periods ranging from 24 h to 48 h. Thereafter the PUF plugs and PUF disks are wrapped twofold in aluminium foil, sealed in zip-lock plastic backs and stored in a freezer (-20 °C) until usage. The XAD-2 resin is transferred to a pre-cleaned glass jar with screw cap and keep frozen (-20 °C) until exposure.

Adsorber cartridges are assembled under the clean-bench. PUF/XAD-2/PUF adsorber cartridges are equipped with pre-cleaned gauze insertions to prevent a loss of XAD-2 during sampling. A smaller PUF plug of dimensions of 250 mm x 550 mm is placed above the insertion to prevent from the clogging of the gauze pores by the XAD-2 resin. Thereafter, 10 g of XAD-2 resin and a second PUF plug of dimensions of 500 mm x 550 mm are placed inside the cartridge. PUF plug adsorber cartridges solely consist of a PUF plug with dimensions of 500 mm x 550 mm and are exposed without gauze insertion. The assembled adsorber cartridges are wrapped in aluminium foil, sealed in plastic bags and stored in the freezer (-20 °C) until usage.

Glass fibre filters are baked at 500 °C in a muffle furnace for 24 h. Subsequently GFFs are separately placed in pre-cleaned petri dishes. The petri dishes are sealed with parafilm, wrapped in aluminium foil and stored in a freezer at -20°C.

Laboratory glass jars, petri dishes and adsorber cartridge housings are cleaned in a 2 % mucasol® solution if required. Then they are rinsed with tap water and put in the dishwasher. Finally all laboratory equipment is twofold solvent rinsed with acetone, hexane and methanol, respectively. Last materials consisting of glass and metal are baked at 300 °C overnight.

9.4.2 Sample collection

GFFs, adsorber cartridges and PUF disks are defrosted. Thereafter, the adsorber cartridges and PUF disks are spiked with 1 mL PRC-LC (table 9.4) and PRC-GC (table 9.5) standard solution, respectively. GFF and adsorber cartridge are inserted in their respective solvent-rinsed sampler holders prior to their transportation to the high-volume active air sampler. The pre-installation in the laboratory of the research ship simplified the sample collection during bad weather periods and additionally prevents the contamination of sampling material, e.g., from sea spray and smoke during transportation to the sampling site. PUF disks are equipped with a stainless steel ring enabling the insertion inside the protection chamber. They are wrapped in aluminium foil during their transport to the sampling site.

After exposure, the PUF disks and adsorber cartridges are wrapped in aluminium foil, sealed in zip-lock plastic bags and stored in the freezer (-20 °C) until extraction. The GFF samples are placed in petri dishes, sealed with parafilm, wrapped in aluminium foil and placed in the freezer (-20 °C). Sampling parameters are listed in chapter 3.2. Figure 8.1 illustrates the insertion of the sampling materials in their respective sampler holders.

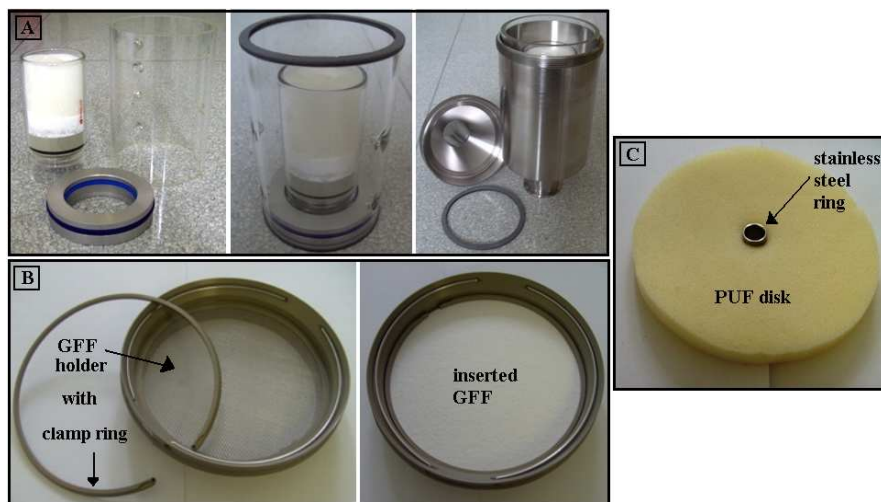


Figure 9.1. Insertion of the sampling material in respective sampler holders; (A) Adsorber cartridge; (B) Glass fibre filter; (C) PUF disk with stainless steel ring

Field blanks are defrosted and exposed to ambient air in laboratory during pre-installation of the sampling material in respective sampler holders. Thereafter, PUF disk and adsorber cartridge field blanks were spiked with 1 mL PRC-LC and PRC-GC standard solutions. Finally, they are packed as usual for storage in the freezer until extraction. At least three field blanks of each sampling material were obtained for each sampling campaign. Field blanks are listed in chapter 4. Field blank data is tabulated in the annex 2.

9.4.3 Sample preparation

Extraction

All air samples are defrosted prior to extraction and spiked with 0.5 mL of the internal standard solutions IS GC (table 9.7) and IS LC (table 9.6), respectively. Each air sample is twofold extracted by solvent mixtures of acetone, hexane and methanol. Both extracts are unified to a homogenous acetone/hexane/methanol solution.

PUF disks and adsorber cartridges are Soxhlet-extracted by the solvent mixtures acetone/hexane (60/40, 210 mL/140 mL) and acetone/methanol (90/10, 315 mL/35 mL) for a duration of 3 hours, respectively. The air samples are placed inside the Soxhlet extractor using a blunt-nosed thumb forcep. The stainless steel ring of the PUF disk is removed prior to extraction. XAD-2 is an

electrostatic material and a significant amount remains inside the adsorber cartridge housing. Therefore, the inside of the cartridge glass housing is rinsed with the first extraction solvent mixture. All Soxhlet extractors are equipped with a pasteur pipette for purposes of pressure compensation and wrapped with aluminium foil. The two successive extracts are unified in a narrow neck bottle, wrapped with aluminium foil and stored overnight in a refrigerator (7 °C).

GFFs are placed for two hours in the solvent mixtures acetone/hexane (60/40, 60 mL/40 mL) and acetone/methanol (90/10, 90 mL/10 mL), respectively. Most internal standards immediately evaporate from the GFF surfaces with insufficient atmospheric particle coating. For this reason, internal standards are spiked into the first extraction solvent. Finally, both extracts are unified in a narrow neck bottle, wrapped with aluminium foil and stored overnight in a refrigerator (7 °C). GFF extraction is performed in petri dishes. The extracts are transferred to the narrow neck bottle using a volumetric pipette.

Evaporation

The next day the acetone/hexane/methanol extracts are evaporated in a parallel evaporation system (Büchi). Parallel evaporation provides the simultaneous evaporation of 4 (rack 4) to 12 (rack 12) air samples depending on the solvent volume. In order to obtain a common and constant evaporation process of all air samples time-pressure gradients are programmed.

Target compounds are quantified by GC-MS/MS and LC-MS/MS systems requiring distinct solvents and clean-up procedures. Hence, each air sample extract is divided in two aliquot parts (GC-aliquot and LC-aliquot) prior to evaporation. The narrow neck bottles are twofold rinsed with ~ 3 mL acetone improving the quantitative transfer of the extracts to the Büchi glass jars. Thereafter, solvent volumes of ~ 350 mL (PUF disk, adsorber cartridge) and ~ 100 mL (GFF) are obtained. Hence, GFF extracts are evaporated at rack 12, whereas PUF disk and adsorber cartridge extracts have to be evaporated at rack 4.

The evaporation process finishes at a final volume of 1.0 – 1.5 mL. Acetone is the remaining solvent. Büchi parameters and time-pressure gradients are listed in tables 9.10 and 9.11.

Table 9.10: Büchi evaporation parameters and time-pressure gradient for the evaporation of 350 mL acetone/hexane/methanol (75/20/5, v/v/v) solvent mixture at rack 4

Heating plate:	40 °C	Time pressure gradient:			
Water recirculation cooler:	20 °C	Step	Pressure in mbar		Duration in minutes
Water condenser:	10 °C		Start	End	
Rotation speed:	160 rpm	1	1000	500	2
Total duration:	105 min	2	500	400	3
		3	400	270	35
		4	270	250	20
		5	250	250	45

Table 9.11: Büchi evaporation parameters and time-pressure gradient for the evaporation of 100 mL acetone/hexane/methanol (75/20/5, v/v/v) solvent mixture at rack 12

Heating plate: 45 °C
 Water recirculation cooler: 20 °C
 Water condenser: 10 °C
 Rotation speed: 250 rpm
 Total duration: 43 min

Time pressure gradient:

Step	Pressure in mbar		Duration in minutes
	Start	End	
1	1000	400	2
2	400	300	3
3	300	220	23
4	220	220	15

Solvent exchange

After the first evaporation step the GC-aliquot is replenished with 40 mL hexane and the LC-aliquot is filled up with 40 mL methanol. Both extracts undergo a second parallel evaporation step ending at a total volume of ~1.0 mL hexane and methanol extract, respectively. Büchi parameters and time-pressure gradients are listed in tables 9.12 to 9.15.

Table 9.12: Büchi evaporation parameters and time-pressure gradient for the evaporation of 40 mL hexane at rack 4

Heating plate: 40 °C
 Water recirculation cooler: 20 °C
 Water condenser: 10 °C
 Rotation speed: 160 rpm
 Total duration: 20 min

Time pressure gradient:

Step	Pressure in mbar		Duration in minutes
	Start	End	
1	1000	250	3
2	250	180	3
3	180	170	4
4	170	170	10

Table 9.13: Büchi evaporation parameters and time-pressure gradient for the evaporation of 40 mL methanol at rack 4

Heating plate: 40 °C
 Water recirculation cooler: 20 °C
 Water condenser: 10 °C
 Rotation speed: 160 rpm
 Total duration: 50 min

Time pressure gradient:

Step	Pressure in mbar		Duration in minutes
	Start	End	
1	1000	250	3
2	250	120	5
3	120	120	42

Table 9.14: Büchi evaporation parameters and time-pressure gradient for the evaporation of 40 mL hexane at rack 12

Heating plate: 45 °C
 Water recirculation cooler: 20 °C
 Water condenser: 10 °C
 Rotation speed: 250 rpm
 Total duration: 20 min

Time pressure gradient:

Step	Pressure in mbar		Duration in minutes
	Start	End	
1	1000	250	2
2	250	160	3
3	160	160	15

Table 9.15: Büchi evaporation parameters and time-pressure gradient for the evaporation of 40 mL methanol at rack 12

Heating plate: 45 °C
Water recirculation cooler: 20 °C
Water condenser: 10 °C
Rotation speed: 250 rpm
Total duration: 51 min

Time pressure gradient:

Step	Pressure in mbar		Duration in minutes
	Start	End	
1	1000	200	2
2	200	150	2
3	150	120	3
4	120	120	44

Centrifugation

The extracts are transferred to 2 mL glass vials and evaporated under a gentle stream of nitrogen to a total volume of approx. 1.5 mL. Additionally, the Büchi glass jars are solvent rinsed either with hexane or methanol (~ 2mL) depending on the solvent of the aliquot. Subsequently the vials are capped and centrifuged for 10 minutes at 3000 rpm. The pellet is discarded, whereas the supernatant is transferred to a 1.0 mL glass vial and evaporated under a gentle stream of nitrogen to an end-volume of 0.5 mL. The extracts are stored in a refrigerator (7 °C) until clean-up.

Clean-up

The storage in the refrigerator causes a further irreversible precipitation of PUF matrix in the methanol extract, which may not be removed by centrifugation. Therefore, all methanol aliquots, except those originating from GFFs, undergo a final syringe filtration. The methanol extracts are evaporated under a gentle stream of nitrogen to a volume of 250 µL. Nylon syringe filters with 0.25 µm pore size and equipped with an empty SPE cartridge are pre-cleaned by rinsing them with approx. 5.0 mL methanol. The remaining solvent is blown out via a stream of nitrogen. Thereafter, a 1.0 mL glass vial is placed under the syringe filter and the sample is transferred to the SPE cartridge using a pasteur pipette. The methanol extract is blown out via nitrogen. Syringe filter, glass vial and pasteur pipette are rinsed twofold with 0.250 mL methanol and the remaining solvent in the filter is again blown out with nitrogen. Finally, the filtered extracts are evaporated under a gentle stream of nitrogen to an end-volume of 0.5 mL and stored in the refrigerator (7 °C) until quantification at the LC-MS/MS system. It has been observed that the PUF precipitation in the methanol aliquot is partly reversible, if the solvent volume increases. For this reason, the rinsing of syringe filters after filtration is limited to max. 500 µL in order to avoid a further precipitation during the final evaporation step.

Silica gel is used as clean-up material for the hexane-aliquot analysed at the GC-MS/MS system. It is heated for 2 h at 150 °C, mixed with 6 % Milli-Q-Water and homogenized for 1 h on a horizontal flask shaker. Thereafter, 3 mL glass columns are equipped with a glass fibre frit, filled

with 0.5 g activated silica gel and topped with a second frit. Then the glass columns are rinsed with 10 mL dichloromethane and 10 mL hexane, respectively. The silica gel must remain in the solvent after rinsing. Once the meniscus of the solvent touches the upper glass fibre frit, the glass column is placed above a snap-cap wide neck bottle and the air-sample extract is transferred to the silica gel. The silica gel is eluted with 5 mL of a hexane/dichloromethane solution (70/30, v/v), as soon as the meniscus of the extract touches the upper glass fibre frit. Vial and pasteur pipette is rinsed with the elution solvent. After elution, the extracts are transferred to a 1.0 mL glass vial and evaporated under a gentle stream of nitrogen to an end-volume of 500 µL. These GC extracts are stored in the refrigerator (7 °C) until quantification.

9.4.4 Quality control samples

Table 9.16 lists the spiked amounts of target analytes, performance reference compounds and internal standards to laboratory blanks and spike control samples. Quality control samples are described in detail in chapter 4. Recovery results of target analytes and performance reference compounds are calculated against single-point calibration standards (“GC-Cal” and “LC-Cal”). They are analysed at least in triplicate per sample preparation sequence. Their composition is tabulated in tables 9.17 - 9.18.

Table 9.16: Amounts of target analytes, performance reference compounds and internal standard added to laboratory blanks and spike control samples; Absolute concentrations may be calculated from tables 9.4 – 9.9

Volume of added solutions in µL	PRC-LC (table 9.4)	PRC-GC (table 9.5)	IS-LC (table 9.6)	IS-GC (table 9.7)	Spike-LC (table 9.8)	Spike-GC (table 9.9)
Laboratory blanks:						
Soxhlet blank	1000	1000	500	500	-	-
Petri dish blank	1000	1000	500	500	-	-
2.0 L bottle blank	1000	1000	500	500	-	-
0.5 L bottle blank	1000	1000	500	500	-	-
Evaporation-350mL blank	500	500	250	250	-	-
Evaporation-100mL blank	500	500	250	250	-	-
Syringe filtration blank	500	-	250	-	-	-
Silica gel blank	-	500	-	250	-	-
Spike samples:						
PUF disk	1000	1000	500	500	250	200
GFF	1000	1000	500	500	250	200
PUF plug adsorber cartridge	1000	1000	500	500	250	200
PUF/XAD-2/PUF adsorber cartridge	1000	1000	500	500	250	200
Evaporation-350mL spike	500	500	250	250	125	100
Evaporation-100mL spike	500	500	250	250	125	100
Syringe filtration spike	500	-	250	-	125	-
Silica gel spike	-	500	-	250	-	100

Table 9.17: Composition of the single-point calibration standard LC-Cal (methanol solution)

Compound		Concentration		Compound		Concentration		Compound		Concentration	
24-D	A	4.8	ng/mL	HBCDA-D ₁₈	IS	5.0	ng/mL	PFHXS	A	5.0	ng/mL
AMETRYN	A	6.2	ng/mL	HBCDB	A	5.0	ng/mL	PFHXS- ¹⁸ O ₂	IS	5.0	ng/mL
ATRAZ	A	5.3	ng/mL	HBCDG	A	5.0	ng/mL	PFNOA	A	5.0	ng/mL
ATRAZ-D ₅	IS	5.1	ng/mL	HEXAZIN	A	6.4	ng/mL	PFOA	A	5.5	ng/mL
AZINPH-E	A	5.1	ng/mL	ISOPRU	A	5.5	ng/mL	PFOA- ¹³ C ₂	IS	4.9	ng/mL
AZINPH-M	A	5.4	ng/mL	IRGAROL	A	5.8	ng/mL	PFOS	A	4.9	ng/mL
AZINPH-M-D ₆	IS	5.0	ng/mL	LINUR	A	5.7	ng/mL	PFOS- ¹³ C ₄	IS	5.0	ng/mL
BENTAZ	A	5.9	ng/mL	MALATH	A	6.1	ng/mL	PFOSA	IS	3.8	ng/mL
CARBAMAZ	A	5.1	ng/mL	MALATH-D ₁₀	IS	5.1	ng/mL	PIRIMIC	A	5.2	ng/mL
CARBEND	A	5.0	ng/mL	MCPA	A	5.0	ng/mL	PRIMID	A	5.0	ng/mL
CHLORFENV	A	6.1	ng/mL	MCPA-D ₃	IS	5.0	ng/mL	PROMETR	A	5.8	ng/mL
CHLORTUR	A	5.2	ng/mL	MECOPR	A	4.9	ng/mL	PROMETR-D ₆	PRC	10.0	ng/mL
CLOFIBRS	A	9.1	ng/mL	MECOPR-D ₃	IS	5.2	ng/mL	PROPAZ	A	4.9	ng/mL
DEATRAZ	A	7.2	ng/mL	METAZCHL	A	5.1	ng/mL	SIMAZ	A	4.9	ng/mL
DEATRAZ-D ₆	IS	5.0	ng/mL	METHABZT	A	5.0	ng/mL	SIMAZ-D ₁₀	PRC	10.0	ng/mL
DIAZINON	A	6.0	ng/mL	METOLA	A	5.0	ng/mL	TBEP	A	5.3	ng/mL
DICHLPR	A	5.3	ng/mL	NAPROX	A	5.0	ng/mL	TBP	A	5.0	ng/mL
DICLOF	A	5.1	ng/mL	OXAZEP	A	4.6	ng/mL	TERBAZ	A	6.5	ng/mL
DIMETH	A	6.4	ng/mL	PENDIMETH	A	5.5	ng/mL	TERBAZ-D ₅	IS	5.0	ng/mL
DIURON	A	5.5	ng/mL	PFBS	A	4.5	ng/mL	TERBUTR	A	4.8	ng/mL
DIURON-D ₆	IS	4.6	ng/mL	PFDEA	A	5.0	ng/mL	TPP	A	5.0	ng/mL
FENUR	A	5.6	ng/mL	PFHPA	A	5.5	ng/mL				
HBCDA	A	5.0	ng/mL	PFHXA	A	5.1	ng/mL				

A = target analyte; IS = internal standard; PRC = performance reference compound

Table 9.18: Composition of the single-point calibration standard GC-Cal (hexane solution)

Compound		Conc.		Compound		Conc.		Compound		Conc.	
ACE	A	91.0	ng/mL	CB 185	IS	16.0	ng/mL	HCB	A	10.7	ng/mL
ACE-D ₁₀	IS	134.0	ng/mL	CB 204	PRC	10.3	ng/mL	HCB- ¹³ C ₆	IS	16.0	ng/mL
ACY	A	108.4	ng/mL	CB 28	A	9.4	ng/mL	HCHA	A	10.1	ng/mL
ALD	A	10.7	ng/mL	CB 30	PRC	9.8	ng/mL	HCHB	A	11.8	ng/mL
ANT	A	89.0	ng/mL	CB 52	A	5.5	ng/mL	HCHD	A	10.1	ng/mL
ANT-D ₁₀	IS	128.0	ng/mL	CB 52- ¹³ C ₁₂	IS	12.8	ng/mL	HCHE	IS	20.0	ng/mL
BAA	A	115.2	ng/mL	CHR	A	104.0	ng/mL	HCHG	A	10.2	ng/mL
BAA-D ₁₂	PRC	41.3	ng/mL	DBAHA	A	94.6	ng/mL	HCHG- ¹³ C ₆ D ₆	PRC	19.1	ng/mL
BAP	A	85.4	ng/mL	DDDPP	A	13.0	ng/mL	I123P	A	87.2	ng/mL
BBF	A	100.4	ng/mL	DDEPP	A	12.7	ng/mL	ISOD	A	11.2	ng/mL
BEP-D ₁₂	IS	98.0	ng/mL	DDT-D ₈	IS	16.2	ng/mL	PER-D ₁₂	IS	96.0	ng/mL
BGHIP	A	89.6	ng/mL	DDTOP	A	12.2	ng/mL	PHEN	A	90.2	ng/mL
BGHIP-D ₁₂	IS	92.0	ng/mL	DDTPP	A	10.1	ng/mL	PHEN-D ₁₀	PRC	40.8	ng/mL
CB 104	PRC	7.5	ng/mL	DIELD	A	11.2	ng/mL	PYR	A	92.4	ng/mL
CB 138	A	12.1	ng/mL	END	A	10.8	ng/mL	QCB	A	12.8	ng/mL
CB 145	PRC	12.7	ng/mL	FL	A	91.6	ng/mL	TRIFLU	A	11.4	ng/mL
CB 153	A	13.1	ng/mL	FLU	A	124.4	ng/mL	TRIFLU-D ₁₄	IS	14.6	ng/mL
CB 153- ¹³ C ₁₂	IS	12.8	ng/mL	FLU-D ₁₀	PRC	39.0	ng/mL				

A = target analyte; IS = internal standard; PRC = performance reference compound

9.5 Mass spectrometry - Acquisition methods

Target analytes are analysed with GC-MS, GC-MS/MS and HPLC-MS/MS methods described below. Certified calibration standards are adopted from the routine mass spectrometer analyses of the BSH monitoring programme. The calibration ranges of GC-MS, GC-MS/MS and HPLC-MS/MS target analytes go from 10 ng/mL to 500 ng/mL, from 0.5 ng/mL to 80 ng/mL and from 0 ng/mL to 10 ng/mL with average internal standard concentrations of 100 ng/mL, 15 ng/mL and 5 ng/mL, respectively).

9.5.1 GC-MS

Injector program:

Method type:	splitless	Carrier control mode:	Flow control
Equilibration time:	5 s	Transfer time:	3 min
End time:	75 min	Transfer column flow:	1 mL/min
Initial temperature:	60 °C	Start column flow:	1 mL/min
Ramp rate:	10 °C/s	End column flow:	1 mL/min
Final temperature:	280 °C	Split flow:	25 mL/min
Temperature control:	Keep current temperature	Injection volume:	2 µL

Table 9.19: GC gradient program (GC-MS method)

Temperature in °C	Ramp rate in °C/min	Hold in min	Total in min
60	0.0	0.2	0.2
100	5.0	0.1	8.3
320	3.5	4.0	75.2

Table 9.20: MS parameters (MS method type: segmented SIM); -Q = Qualifier; Ret. = retention time in minutes, S = segment, Q1 = Q1 mass (m/z)

Compound	Ret.	S	Q1	Compound	Ret.	S	Q1	Compound	Ret.	S	Q1
ACE	20.8	1	154	BAP	55.7	4	252	FLU	37.9	3	202
ACE-D ₁₀	20.6	1	164	BBF	54.0	4	252	FLU-D ₁₀	37.8	3	212
ACE-Q	20.8	1	152	BEP-D ₁₂	55.3	4	264	I123P	61.5	5	276
ACY	19.7	1	152	BGHIP	62.7	5	276	PER-D ₁₂	56.1	4	264
ANT	30.5	2	178	BGHIP-D ₁₂	62.6	5	288	PHEN	30.2	2	178
ANT-D ₁₀	30.4	2	188	CHRTR	47.6	3	228	PHEN-D ₁₀	30.0	2	188
BAA	47.4	3	228	DBAHA	61.8	5	278	PYR	39.3	3	202
BAA-D ₁₂	47.2	3	240	FL	24.1	2	166				

Scan time of segments: 0.4 s; CHRTR : chrysene and triphenylene are analysed as sum parameter

9.5.2 GC-MS/MS

Injector program:

Method type:	large volume	Carrier control mode:	Flow control
Equilibration time:	5 s	Transfer time:	2 min
End time:	40 min	Sample sweep column flow:	1 mL/min
Initial temperature:	60 °C	Transfer column flow:	1 mL/min
Ramp rate:	15 °C/s	Start column flow:	1 mL/min
Final temperature:	300 °C	End column flow:	1 mL/min
Temperature control:	Keep current temperature	Vent flow:	60 mL/min
Vent mode:	Fixed time	Split flow:	25 mL/min
Vent time:	8 s	Injection volume:	6 µL

Table 9.21: GC gradient program (GC-MS/MS method)

Temperature in °C	Ramp rate in °C/min	Hold in min	Total in min
60	0.0	0.2	0.2
100	10.0	0.1	4.3
320	7.0	3.5	39.2

Table 9.22: MS parameters (MS method type: segmented MRM); -Q = Qualifier; Ret. = retention time in minutes, S = segment, Q1 = Q1 mass (m/z), Q3 = Q3 mass (m/z), CE = collision energy in V

Compound	Ret.	S	mass transition		CE
			Q1	Q3	
ALD	20.7	7	262.8	192.8	30
CB28	19.4	6	258.0	185.9	15
CB30	17.5	4	257.9	185.9	20
CB52	20.3	7	292.0	221.8	15
CB52-Q	20.3	7	220.0	149.8	15
CB52- ¹³ C ₁₂	20.3	7	304.0	232.1	25
CB104	20.7	7	325.9	253.9	25
CB138	25.6	11	359.8	289.5	15
CB145	23.3	9	359.8	289.8	30
CB153	24.9	10	359.8	289.5	15
CB153- ¹³ C ₁₂	24.9	10	371.9	301.9	25
CB185	26.4	12	393.7	358.6	10
CB204	27.0	12	429.7	357.9	30
DDPP	24.6	10	235.1	165.0	20
DDPP-Q1	24.6	10	199.1	163.1	20
DDPP-Q2	24.6	10	235.0	199.6	10
DDEPP	23.4	9	317.8	246.0	22
DDTOP	24.6	10	235.1	165.0	20
DDTOP-Q1	24.6	10	199.1	163.1	20
DDTOP-Q2	24.6	10	235.0	199.6	10
DDTPP	25.6	11	235.1	165.0	20
DDTPP-Q1	25.6	11	235.0	199.6	10
DDTPP-D ₈	25.5	11	243.0	207.6	10
DIELD	23.6	9	277.0	241.4	10
DIELD-Q	23.6	9	262.8	192.8	30
END	24.1	9	262.8	192.8	30
HCB	16.7	3	283.7	248.7	25
HCB- ¹³ C ₆	16.7	3	289.8	254.8	15
HCHA	16.6	3	181.0	145.1	15
HCHA-Q	16.6	3	219.0	182.6	10
HCHB	17.4	4	219.0	182.6	10
HCHD	18.5	5	219.0	182.6	10
HCHE	18.8	5	219.0	182.6	10
HCHG	17.7	4	219.0	182.6	10
HCHG- ¹³ C ₆ D ₆	17.5	4	227.9	190.9	10
ISOD	21.6	8	193.1	157.6	20
ISOD-Q	21.6	8	262.8	192.8	22
QCB	13.7	1	249.8	214.7	15
TRIFLU	16.0	2	306.0	263.8	10
TRIFLU-D ₁₄	15.9	2	315.3	267.1	10

Scan time of segments: 0.25 s – 0.45 s

9.5.3 HPLC-MS/MS

Composition of eluents:

Eluent A: Milli-Q-water buffered with 5 mMol/L acetic acid and 5 mMol/L ammonium acetate

Eluent B: Methanol buffered with 5 mMol/L acetic acid and 5 mMol/L ammonium acetate

Injection volume: 4 μ L

Column temperature: 29 °C

Table 9.23: HPLC gradient program

Step	Total Time in minutes	Flow rate in μ L/min	Composition of mobile phase	
			Eluent A in %	Eluent B in %
0	7.00	300	85	15
1	0.10	300	85	15
2	0.30	300	60	40
3	22.00	300	5	95
4	28.00	300	5	95

Table 9.24: Common scheduled MRM parameters in positive (p) and negative (n) ESI mode

Parameter	ESI mode		Parameter	ESI mode	
	p	n		p	n
Curtain gas (CUR)	25 psi	25 psi	Temperature (TEM)	400 °C	400 °C
Collision gas (CAD)	Medium	Medium	Ion Spray Voltage (IS)	5500 V	-4500 V
Ion Source gas 1 (GS1)	50 psi	50 psi	Entrance potential (EP)	10 V	-10 V
Ion Source gas 2 (GS2)	35 psi	35 psi	Collision cell exit potential (CXP)	12 V	-12 V

Table 9.25: Scheduled MRM mass transition parameters in positive (p) and negative (n) ESI mode; -Q = Qualifier, Ret. = retention time in minutes; M = ESI mode, m. trans. = mass transition, Q1 = Q1 mass (m/z), Q3 = Q3 mass (m/z), DP = declustering potential in V, CE = collision energy in V

Compound	Ret.	M	mass transition		DP	CE	Compound	Ret.	M	mass transition		DP	CE
			Q1	Q3						Q1	Q3		
24-D	8.4	n	219.0	160.8	-35	-19	DICLOF	15.7	p	296.1	250.0	60	5
AMETRYN	15.2	p	228.1	186.1	60	26	DIMETH	7.7	p	230.1	199.0	40	13
ATRAZ	13.0	p	216.1	174.1	60	25	DIURON	13.7	p	233.1	72.1	60	23
ATRAZ-D ₅	12.9	p	221.2	179.2	60	25	DIURON-D ₆	13.6	p	239.1	78.0	40	23
AZINPH-E	18.8	p	346.2	132.2	60	23	FENUR	7.4	p	165.1	72.0	40	22
AZINPH-M	16.4	p	318.1	132.1	60	21	FENUR-Q	7.4	p	165.1	120.1	40	25
AZINPH-M-D ₆	16.4	p	324.0	132.0	60	21	HBCD-A	23.9	n	640.5	78.8	-50	-50
BENTAZ	5.7	n	239.1	131.9	-60	-35	HBCD-A-D ₁₈	23.7	n	657.6	78.8	-50	-50
CARBAMAZ	11.9	p	237.1	194.1	60	28	HBCD-A-Q	23.9	n	640.5	80.8	-50	-50
CARBEND	8.7	p	192.1	160.0	60	25	HBCD-BG	24.7	n	640.6	78.8	-50	-50
CHLORFENV	19.2	p	361.0	155.0	60	17	HBCD-BG-Q	24.7	n	640.6	80.8	-50	-50
CHLORTUR	12.6	p	213.1	72.1	40	24	HEXAZIN	11.7	p	253.2	170.9	60	23
CLOFIBRS	9.4	n	213.1	126.9	-35	-21	IRGAROL	17.8	p	254.2	198.1	60	26
DEATRAZ	8.0	p	188.1	146.0	40	24	ISOPRUR	13.2	p	207.2	72.1	40	23
DEATRAZ-D ₆	8.0	p	194.1	147.1	40	24	LINUR	15.2	p	249.1	160.2	60	26
DIAZINON	19.4	p	305.2	169.2	60	35	MALATH	16.9	p	331.2	127.0	60	16
DICHLPR	10.1	n	233.0	160.8	-35	-21	MALATH-D ₁₀	16.8	p	341.1	132.1	60	16

Table 9.25 continued:

Compound	Ret.	M	mass transition		DP	CE	Compound	Ret.	M	mass transition		DP	CE
			Q1	Q3						Q1	Q3		
MCPA	8.6	n	199.1	140.9	-35	-19	PFOA-Q	15.1	n	413.0	168.8	-30	-24
MCPA-D ₃	8.5	n	202.1	144.0	-35	-19	PFOS	16.7	n	499.0	79.9	-85	-101
MECOPR	10.2	n	213.1	140.9	-35	-21	PFOS- ¹³ C ₄	16.7	n	502.9	79.9	-30	-101
METAZCHL	13.8	p	278.2	134.0	40	32	PFOSA	19.6	n	498.1	77.9	-85	-83
METHABZT	13.7	p	222.1	165.1	60	24	PFOS-Q	16.7	n	499.0	98.9	-85	-66
METOLA	17.7	p	284.2	252.1	60	21	PIRIMIC	12.8	p	239.2	182.2	60	22
NAPROX	13.4	p	231.1	185.1	60	22	PRIMID	7.4	p	219.1	162.1	60	18
NAPROX-Q	13.4	p	231.1	170.1	60	37	PROMETR	17.0	p	242.2	158.1	60	33
OXAZEP	13.5	p	287.1	241.1	60	31	PROMETR-D ₆	16.9	p	248.1	206.1	60	27
PENDIMETH	22.7	p	282.2	212.1	40	14	PROMETR-D ₆ -Q	16.9	p	248.1	158.1	60	33
PENDIMETH-Q	22.7	p	282.2	194.2	40	23	PROPAZ	14.9	p	230.3	188.1	60	24
PFBS	8.6	n	299.0	79.9	-45	-65	SIMAZ	10.9	p	202.1	132.2	60	26
PFDEA	18.1	n	513.0	468.8	-30	-17	SIMAZ-D ₁₀	10.8	p	212.1	137.1	60	27
PFHPA	13.1	n	363.1	318.8	-30	-14	SIMAZ-D ₁₀ -Q	10.8	p	212.1	132.1	60	27
PFHXA	10.6	n	313.1	268.8	-30	-13	TBEP	21.1	p	399.3	299.2	60	18
PFHXS	13.3	n	399.0	79.9	-85	-85	TBP	20.2	p	267.2	99.1	60	26
PFHXS- ¹⁸ O ₂	13.3	n	402.9	84.0	-85	-85	TERBAZ	15.4	p	230.3	174.1	60	23
PFNOA	16.6	n	463.0	418.8	-30	-16	TERBAZ-D ₅	15.3	p	235.1	179.1	60	23
PFOA	15.1	n	413.0	368.8	-30	-14	TERBUTR	17.5	p	242.2	186.1	60	26
PFOA- ¹³ C ₂	15.1	n	415.0	369.8	-30	-14	TPP	19.6	p	327.2	152.1	60	51

MRM detection window in positive ESI mode: 80 s, MRM detection window in negative ESI mode: 100 s, HBCDBG: HBCDB and HBCDG are analysed as sum parameter

9.6 Mass spectrometry - Quantification methods

9.6.1 GC-MS

Common integration parameters:

Integration window:	± 0.250 min	Peak size reject:	500 counts
Peak width:	0.5 s at ½ Ht	Smoothing method:	5 point smooth, mean
Slope sensitivity:	20 SN	Spikes:	Remove spikes
Tangent:	10 %	Spike factor threshold:	5

Table 9.26: GC-MS analytes and their corresponding internal standards; -Q = Qualifier

Analyte	Internal standard	Analyte	Internal standard	Analyte	Internal standard
ACE	ACE-D ₁₀	BAP	BEP-D ₁₂	FLU	PER-D ₁₂
ACE-Q	ACE-D ₁₀	BBF	BEP-D ₁₂	FLU-D ₁₀	PER-D ₁₂
ACY	ANT-D ₁₀	BGHIP	BGHIP-D ₁₂	I123P	BGHIP-D ₁₂
ANT	ANT-D ₁₀	CHR/TR	PER-D ₁₂	PHEN	ANT-D ₁₀
BAA	PER-D ₁₂	DBAHA	BGHIP-D ₁₂	PHEN-D ₁₀	ANT-D ₁₀
BAA-D ₁₂	PER-D ₁₂	FL	ACE-D ₁₀	PYR	PER-D ₁₂

9.6.2 GC-MS/MS

Common integration parameters:

Integration window:	± 0.250 min	Peak size reject:	500 counts
Peak width:	4 s at ½ Ht	Smoothing method:	5 point smooth, mean
Slope sensitivity:	20 SN	Spikes:	Remove spikes
Tangent:	0 %	Spike factor threshold:	5

Table 9.27: GC-MS/MS analytes and their corresponding internal standards; -Q = Qualifier

Analyte	Internal standard	Analyte	Internal standard	Analyte	Internal standard
ALD	CB52- ¹³ C ₁₂	DDDPP-Q1	CB185	HCB	HCB- ¹³ C ₆
CB28	CB52- ¹³ C ₁₂	DDDPP-Q2	CB185	HCHA	CB52- ¹³ C ₁₂
CB30	CB52- ¹³ C ₁₂	DDEPP	CB185	HCHA-Q	CB52- ¹³ C ₁₂
CB52	CB52- ¹³ C ₁₂	DDTOP	DDTPP-D ₈	HCHB	HCHE
CB52-Q	CB52- ¹³ C ₁₂	DDTOP-Q1	DDTPP-D ₈	HCHD	HCHE
CB104	CB52- ¹³ C ₁₂	DDTOP-Q2	DDTPP-D ₈	HCHG	CB52- ¹³ C ₁₂
CB138	CB185	DDTPP	DDTPP-D ₈	HCHG- ¹³ C ₆ D ₆	CB52- ¹³ C ₁₂
CB145	CB153- ¹³ C ₁₂	DDTPP-Q	DDTPP-D ₈	ISOD	CB52- ¹³ C ₁₂
CB153	CB153- ¹³ C ₁₂	DIELD	CB153- ¹³ C ₁₂	ISOD-Q	CB52- ¹³ C ₁₂
CB204	CB185	DIELD-Q	CB153- ¹³ C ₁₂	QCB	HCB- ¹³ C ₆
DDDPP	CB185	END	CB185	TRIFLU	TRIFLU-D ₁₄

9.6.3 HPLC-MS/MS

Common integration parameters:

Retention window:	30 s	Base Sub Window:	0.6 min
Smoothing width:	3 points	Peak Splitting Factor:	2
Noise percent:	90 %		

A few target analytes, labeled n.q. in the table below, are transformed during Soxhlet-extraction. Thus the corresponding internal standard of some target analytes may differentiate depending on the extraction technique as summarized in table 9.28.

Table 9.28: HPLC-MS/MS analytes and their corresponding internal standards; n.q. = not quantified; -Q = Qualifier; Adsorber = PUF disks and adsorber cartridges

Analyte	Internal standard		Analyte	Internal standard	
	GFF	Adsorber		GFF	Adsorber
24-D	MCPA-D ₃	n.q.	CHLORTUR	DIURON-D ₆	ATRAZ-D ₅
AMETRYN	TERBAZ-D ₅	TERBAZ-D ₅	CLOFIBRS	MECOPR-D ₃	n.q.
ATRAZ	ATRAZ-D ₅	ATRAZ-D ₅	DEATRAZ	DEATRAZ-D ₆	DEATRAZ-D ₆
AZINPH-E	AZINPH-M-D ₆	AZINPH-M-D ₆	DIAZINON	TERBAZ-D ₅	TERBAZ-D ₅
AZINPH-M	AZINPH-M-D ₆	AZINPH-M-D ₆	DICHLPR	MECOPR-D ₃	n.q.
BENTAZ	MECOPR-D ₃	PFHXS- ¹⁸ O ₂	DICLOF	DIURON-D ₆	n.q.
CARBAMAZ	DIURON-D ₆	ATRAZ-D ₅	DIMETH	ATRAZ-D ₅	ATRAZ-D ₅
CARBEND	DEATRAZ-D ₆	DEATRAZ-D ₆	DIURON	DIURON-D ₆	DIURON-D ₆
CHLORFENV	TERBAZ-D ₅	TERBAZ-D ₅	FENUR	ATRAZ-D ₅	ATRAZ-D ₅

Table 9.28 continued:

Analyte	Internal standard		Analyte	Internal standard	
	GFF	Adsorber		GFF	Adsorber
FENUR-Q	ATRAZ-D ₅	ATRAZ-D ₅	PFHXA	PFOS- ¹³ C ₄	PFOA- ¹³ C ₂
HBCDA	HBCDA-D ₁₈	HBCDA-D ₁₈	PFHXS	PFHXS- ¹⁸ O ₂	PFHXS- ¹⁸ O ₂
HBCDA-Q	HBCDA-D ₁₈	HBCDA-D ₁₈	PFNOA	PFOS- ¹³ C ₄	PFOA- ¹³ C ₂
HBCDBG	HBCDA-D ₁₈	HBCDA-D ₁₈	PFOA	PFOA- ¹³ C ₂	PFOA- ¹³ C ₂
HBCDBG-Q	HBCDA-D ₁₈	HBCDA-D ₁₈	PFOA-Q	PFOA- ¹³ C ₂	PFOA- ¹³ C ₂
HEXAZIN	ATRAZ-D ₅	ATRAZ-D ₅	PFOS	PFOS- ¹³ C ₄	PFOS- ¹³ C ₄
IRGAROL	TERBAZ-D ₅	TERBAZ-D ₅	PFOSA	PFOS- ¹³ C ₄	PFOS- ¹³ C ₄
ISOPRUR	DIURON-D ₆	ATRAZ-D ₅	PFOS-Q	PFOS- ¹³ C ₄	PFOS- ¹³ C ₄
LINUR	DIURON-D ₆	DEATRAZ-D ₆	PIRIMIC	ATRAZ-D ₅	ATRAZ-D ₅
MALATH	MALATH-D ₁₀	MALATH-D ₁₀	PRIMID	DEATRAZ-D ₆	DEATRAZ-D ₆
MCPA	MCPA-D ₃	n.q.	PROMETR	TERBAZ-D ₅	TERBAZ-D ₅
MECOPR	MECOPR-D ₃	n.q.	PROMETR-D ₆	TERBAZ-D ₅	TERBAZ-D ₅
METAZCHL	ATRAZ-D ₅	ATRAZ-D ₅	PROMETR-D ₆ -Q	TERBAZ-D ₅	TERBAZ-D ₅
METHABZT	TERBAZ-D ₅	TERBAZ-D ₅	PROPAZ	TERBAZ-D ₅	TERBAZ-D ₅
METOLA	TERBAZ-D ₅	TERBAZ-D ₅	SIMAZ	ATRAZ-D ₅	ATRAZ-D ₅
NAPROX	DIURON-D ₆	n.q.	SIMAZ-D ₁₀	ATRAZ-D ₅	ATRAZ-D ₅
NAPROX-Q	DIURON-D ₆	n.q.	SIMAZ-D ₁₀ -Q	ATRAZ-D ₅	ATRAZ-D ₅
OXAZEP	DIURON-D ₆	TERBAZ-D ₅	TBEP	TERBAZ-D ₅	TERBAZ-D ₅
PENDIMETH	TERBAZ-D ₅	TERBAZ-D ₅	TBP	TERBAZ-D ₅	TERBAZ-D ₅
PENDIMETH-Q	TERBAZ-D ₅	TERBAZ-D ₅	TERBAZ	TERBAZ-D ₅	TERBAZ-D ₅
PFBS	PFHXS- ¹⁸ O ₂	PFHXS- ¹⁸ O ₂	TERBUTR	TERBAZ-D ₅	TERBAZ-D ₅
PFDEA	PFOS- ¹³ C ₄	PFOA- ¹³ C ₂	TPP	TERBAZ-D ₅	TERBAZ-D ₅
PFHPA	PFOS- ¹³ C ₄	PFOA- ¹³ C ₂			

9.7 Calculation of atmospheric concentrations

Peak integration results obtained from Varian Workstation Toolbar and Analyst display concentration data in units of ng/mL extract. Extract concentrations are corrected by the arithmetic mean of field blank data. Thereafter, concentrations are controlled for LOQ and LOD (refer to chapter 4). Finally, the related absolute mass numbers (ng) are divided by the volume of sampled air producing atmospheric concentrations of target analytes in units of ng/m³.

10. References

- [1] BSH, BLMP Meeresumwelt - Zustandsbericht 1997-1998 für Nordsee und Ostsee, 2002. Available (14.09.2011): <http://www.blmp-online.de/Seiten/Berichte.html>
- [2] OSPAR Commission, Quality status report 2010, 2010. Available (14.09.2011): <http://qsr2010.ospar.org/en/downloads.html>
- [3] HELCOM Commission, HELCOM Activities 2010 Overview, 2011. Available (14.09.2011): http://www.helcom.fi/publications/en_GB/publications/
- [4] UNECE, Handbook for the 1979 Convention on Long-range Transboundary Air Pollution and its protocols, 2004.
- [5] Ilyina, T., Lammel, G., Pohlmann, T., Mass budgets and contribution of individual sources and sinks to the abundance of γ -HCH, α -HCH and PCB 153 in the North Sea. *Chemosphere*, 2008. 72(8): p. 1132-1137.
- [6] EMEP, EMEP Status Report on Persistent Organic Pollutants in the Environment, 2010. Available (14.09.2011): http://emep.int/publ/common_publications.html
- [7] Breivik, K., Wania, F., Mass budgets, pathways, and equilibrium states of two hexachlorocyclohexanes in the Baltic Sea environment. *Environ. Sci. Technol.*, 2002. 36(5): p. 1024-1032.
- [8] Sehili, A.M., Lammel, G., Global fate and distribution of polycyclic aromatic hydrocarbons emitted from Europe and Russia. *Atmos. Environ.*, 2007. 41(37): p. 8301-8315.
- [9] AMAP, AMAP Assessment 2009: Persistent Organic Pollutants in the Arctic. *Sci. Total Environ.*, 2010. 408: p. 2851-3051.
- [10] Interim Secretariat for the Stockholm Convention on Persistent Organic Pollutants UNEP Chemicals, Stockholm Convention on Persistent Organic Pollutants (POPs)-Text and Annexes, 2001.
- [11] UNEP Chemicals, Website on the Stockholm Convention (14.09.2011): <http://chm.pops.int/Home/tabid/2121/mctl/ViewDetails/EventModID/871/EventID/142/xmid/6921/language/en-US/Default.aspx>
- [12] Gobas, F.A.P.C., de Wolf, W., Burkhard, L.P., Verbruggen, E., Plotzke, K., Revisiting bioaccumulation criteria for POPs and PBT assessments. *Integr. Environ. Assess. Manag.*, 2009. 5(4): p. 624-637
- [13] The Co-operative group, Persistent, bioaccumulative and toxic (PBT) chemicals- Sustainability Report, 2009.
- [14] EMEP Homepage, Sampling Sites of the EMEP measurement network, available (14.09.2011): <http://tarantula.nilu.no/projects/ccc/network/index.html>
- [15] Yusà, V., Coscollà, C., Mellouki, W., Pastor, A., de la Guardia, M., Sampling and analysis of pesticides in ambient air. *J. Chromatogr. A*, 2009. 1216(15): p. 2972-2983.
- [16] Galarneau, E., Bidleman, T., Blanchard, P., Seasonality and interspecies differences in particle/gas partitioning of PAHs observed by the Integrated Atmospheric Deposition Network (IADN). *Atmos. Environ.*, 2006. 40(1): p. 182-197.
- [17] Hung, H., Blanchard, P., Halsall, C., Bidleman, T., Stern, G., Fellin, P., Muir, D., Barrie, L., Jantunen, L., Helm, P., Temporal and spatial variabilities of atmospheric polychlorinated biphenyls (PCBs), organochlorine (OC) pesticides and polycyclic aromatic hydrocarbons (PAHs) in the Canadian Arctic: Results from a decade of monitoring. *Sci. Total Environ.*, 2005. 342(1-3): p. 119-144.

- [18] He, J., Balasubramanian, R., Semi-volatile organic compounds (SVOCs) in ambient air and rainwater in a tropical environment: Concentrations and temporal and seasonal trends. *Chemosphere*, 2010. 78(6): p. 742-751.
- [19] Eatough, D. J., Tang, H., Cui, W., Machir, J., Determination of the size distribution and chemical composition of fine particulate semivolatile organic material in urban environments using diffusion denuder technology. *Inhalation Toxicol.*, 1995. 7(5): p. 691-710.
- [20] Krieger, M.S., Hites, R. A., Diffusion denuder for the collection of semivolatile organic compounds. *Environ. Sci. Technol.*, 1992. 26(8): p. 1551-1555.
- [21] Peters, A. J., Lane, D. A., Gundel, L. A., Northcott, G. L., Jones, K. C., A comparison of high volume and diffusion denuder samplers for measuring semivolatile organic compounds in the atmosphere. *Environ. Sci. Technol.*, 2000. 34(23): p. 5001-5006.
- [22] Gouin, T., Harner, T., Blanchard, P., Mackay, D., Passive and active air samplers as complementary methods for investigating persistent organic pollutants in the Great Lakes Basin. *Environ. Sci. Technol.*, 2005. 39(23): p. 9115-9122.
- [23] Pozo, K., Harner, T., Wania, F., Muir, D. C. G., Jones, K. C., Barrie, L. A., Toward a global network for persistent organic pollutants in air: Results from the GAPS study. *Environ. Sci. Technol.*, 2006. 40(16): p. 4867-4873.
- [24] Hayward, S.J., Gouin, T., Wania, F., Comparison of four active and passive sampling techniques for pesticides in air. *Environ. Sci. Technol.*, 2010. 44(9):p. 3410-3416.
- [25] Wania, F., Shen, L., Lei, Y. D., Teixeira, C., Muir, D. C. G., Development and calibration of a resin-based passive sampling system for monitoring persistent organic pollutants in the atmosphere. *Environ. Sci. Technol.*, 2003. 37(7): p. 1352-1359.
- [26] Shoeib, M., Harner, T., Lee, S. C., Lane, D., Zhu, J., Sorbent-impregnated polyurethane foam disk for passive air sampling of volatile fluorinated chemicals. *Anal. Chem.*, 2008. 80(3): p. 675-682.
- [27] Söderström, H.S., Bergqvist, P. A., Passive air sampling using semipermeable membrane devices at different wind-speeds in situ calibrated by performance reference compounds. *Environ. Sci. Technol.*, 2004. 38(18): p. 4828-4834.
- [28] Harner, T., Farrar, N. J., Shoeib, M., Jones, K. C., Gobas, F. A. P. C., Characterization of polymer-coated glass as a passive air sampler for persistent organic pollutants. *Environ. Sci. Technol.*, 2003. 37(11): p. 2486-2493.
- [29] Tao, S., Cao, J., Wang, W., Zhao, J., Wang, Z., Cao, H., Xing, B., A Passive sampler with improved performance for collecting gaseous and particulate phase polycyclic aromatic hydrocarbons in air. *Environ. Sci. Technol.*, 2009. 43(11): p. 4124-4129.
- [30] Bartkow, M., Booij, K., Kennedy, K., Muller, J., Hawker, D., Passive air sampling theory for semivolatile organic compounds. *Chemosphere*, 2005. 60(2): p. 170-176.
- [31] Melymuk, L., Robson, M., Helm, P. A., Diamond, M. L., Evaluation of passive air sampler calibrations: Selection of sampling rates and implications for the measurement of persistent organic pollutants in air. *Atmos. Environ.*, 2011. 45: p. 1867-1875.
- [32] Pozo, K., Harner, T., Shoeib, M., Urrutia, R., Barra, R., Parra, O., Focardi, S., Passive-sampler derived air concentrations of persistent organic pollutants on a north-south transect in Chile. *Environ. Sci. Technol.*, 2004. 38(24): p. 6529-6537.
- [33] Moeckel, C., Harner, T., Nizzetto, L., Strandberg, B., Lindroth, A., Jones, K. C., Use of deuration compounds in passive air samplers: Results from active sampling-supported field deployment, potential uses, and recommendations. *Environ. Sci. Technol.*, 2009. 43(9): p. 3227-3232.

- [34] Klánová, J., Čupr, P., Kohoutek, J., Harner, T., Assessing the influence of meteorological parameters on the performance of polyurethane foam-based passive air samplers. *Environ. Sci. Technol.*, 2007. 42(2): p. 550-555.
- [35] Shoeib, M., Harner, T., Characterization and Comparison of Three Passive Air Samplers for Persistent Organic Pollutants. *Environ. Sci. Technol.*, 2002. 36(19): p. 4142-4151.
- [36] Hazrati, S., Harrad, S., Calibration of polyurethane foam (PUF) disk passive air samplers for quantitative measurement of polychlorinated biphenyls (PCBs) and polybrominated diphenyl ethers (PBDEs): Factors influencing sampling rates. *Chemosphere*, 2007. 67(3): p. 448-455.
- [37] Chaemfa, C., Wild, E., Davison, B., Barber, J. L., Jones, K. C., A study of aerosol entrapment and the influence of wind speed, chamber design and foam density on polyurethane foam passive air samplers used for persistent organic pollutants. *J. Environ. Monit.*, 2009. 11(6): p. 1135-1139.
- [38] Harner, T., Bidleman, T. F., Octanol-air partition coefficient for describing particle/gas partitioning of aromatic compounds in urban air. *Environ. Sci. Technol.*, 1998. 32(10):p. 1494-1502.
- [39] Bartkow, M. E., Jones, K. C., Kennedy, K. E., Holling, N., Hawker, D. W., Müller, J. F., Evaluation of performance reference compounds in polyethylene-based passive air samplers. *Environ. Pollut.*, 2006. 144(2): p. 365-370.
- [40] US EPA, Compendium of Methods for the Determination of Toxic Organic Compounds in Ambient Air-Compendium Method TO-10A, Second Edition, 1999. Available (14.09.2011): <http://www.epa.gov/ttnamti1/files/ambient/airtox/to-10ar.pdf>
- [41] EC and US EPA, Atmospheric Deposition of Toxic Substances to the Great Lakes : IADN Results trough 2005, 2005. Available (14.09.2011): <http://www.ec.gc.ca/rs-mn/default.asp?lang=En&n=0525D4AD-1>
- [42] Richter, B. E., Jones, B. A., Ezzell, J. L., Porter, N. L., Avdalovic, N., Pohl, C., Accelerated solvent extraction: a technique for sample preparation. *Anal. Chem.*, 1996. 68(6): p. 1033-1039.
- [43] Björklund, E., Nilsson, T., Bøwadt, S., Pressurised liquid extraction of persistent organic pollutants in environmental analysis. *TrAC*, 2000. 19(7): p. 434-445.
- [44] Babic, S., Petrovic, M., Kastelan-Macan, M., Ultrasonic solvent extraction of pesticides from soil. *J. Chromatogr., A*, 1998. 823(1-2): p. 3-9.
- [45] Camel, V., Microwave-assisted solvent extraction of environmental samples. *TrAC*, 2000. 19(4): p. 229-248.
- [46] Camel, V., Recent extraction techniques for solid matrices-supercritical fluid extraction, pressurized fluid extraction and microwave-assisted extraction: their potential and pitfalls. *Analyst*, 2001. 126(7): p. 1182-1193.
- [47] Skoog, D.A., Leary, J.J., *Instrumentelle Analytik: Grundlagen, Geräte, Anwendungen*. 1996: Springer Verlag.
- [48] Jaward, F. M., Farrar, N. J., Harner, T., Sweetman, A. J., Jones, K. C., Passive air sampling of PCBs, PBDEs, and organochlorine pesticides across Europe. *Environ. Sci. Technol.*, 2004. 38(1): p. 34-41.
- [49] Dreyer, A., Weinberg, I., Temme, C., Ebinghaus, R., Polyfluorinated compounds in the atmosphere of the Atlantic and Southern Oceans: evidence for a global distribution. *Environ. Sci. Technol.*, 2009. 43(17): p. 6507-6514.
- [50] Xie, Z., Ebinghaus, R., Analytical methods for the determination of emerging organic contaminants in the atmosphere. *Anal. Chim. Acta*, 2008. 610(2): p. 156-178.

- [51] de Kok, T. M. C. M., Driee, H. A. L., Hogervorst, J. G. F., Briedé, J. J., Toxicological assessment of ambient and traffic-related particulate matter: a review of recent studies. *Mutat. Res., Rev. Mutat. Res.*, 2006. 613(2-3): p. 103-122.
- [52] Gibson, T. L., Nitro derivatives of polynuclear aromatic hydrocarbons in airborne and source particulate matter. *Atmos. Environ.*, 1982. 16(8): p. 2037-2040.
- [53] Viras, L. G., Athanasiou, K., Siskos, P. A., Determination of mutagenic activity of airborne particulates and of the benzo[*a*]pyrene concentrations in Athens atmosphere. *Atmos. Environ.*, 1990. 24(2): p. 267-274.
- [54] Dreyer, A., Shoeib, M., Fiedler, S., Barber, J. L., Harner, T., Schramm, K. W., Jones, K. C., Ebinghaus, R., Field intercomparison on the determination of volatile and semivolatile polyfluorinated compounds in air. *Environ. Chem.*, 2010. 7(4): p. 350.
- [55] Dreyer, A., Ebinghaus, R., Polyfluorinated compounds in ambient air from ship-and land-based measurements in northern Germany. *Atmos. Environ.*, 2009. 43(8): p. 1527-1535.
- [56] Jahnke, A., Ahrens, L., Ebinghaus, R., Temme, C., Urban versus remote air concentrations of fluorotelomer alcohols and other polyfluorinated alkyl substances in Germany. *Environ. Sci. Technol.*, 2007. 41(3): p. 745-752.
- [57] Scheyer, A., Morville, S., Mirabel, P., Millet, M., Pesticides analysed in rainwater in Alsace region (eastern France): comparison between urban and rural sites. *Atmos. Environ.*, 2007. 41(34): p. 7241-7252.
- [58] Waite, D.T., Bailey, P., Sproull, J. F., Quiring, D. V., Chau, D. F., Bailey, J., Cessna, A. J., Atmospheric concentrations and dry and wet deposits of some herbicides currently used on the Canadian Prairies. *Chemosphere*, 2005. 58(6): p. 693-703.
- [59] Yao, Y., Harner, T., Blanchard, P., Tuduri, L., Waite, D., Poissant, L., Murphy, C., Belzer, W., Aulagnier, F., Sverko, E., Pesticides in the atmosphere across Canadian agricultural regions. *Environ. Sci. Technol.*, 2008. 42(16): p. 5931-5937.
- [60] Jaward, F. M., Barber, J. L., Booij, K., Jones, K. C., Spatial distribution of atmospheric PAHs and PCNs along a north-south Atlantic transect. *Environ. Pollut.*, 2004. 132(1): p. 173-181.
- [61] Bethan, B., Dannecker, W., Gerwig, H., Hühnerfuss, H., Schulz, M., Seasonal dependence of the chiral composition of α -HCH in coastal deposition at the North Sea. *Chemosphere*, 2001. 44(4): p. 591-597.
- [62] Ding, X., Wang, X., Xie, Z., Xiang, C., Mai, B., Sun, L., Zheng, M., Sheng, G., Fu, J., Pöschl, U., Atmospheric polycyclic aromatic hydrocarbons observed over the North Pacific Ocean and the Arctic area: Spatial distribution and source identification. *Atmos. Environ.*, 2007. 41(10): p. 2061-2072.
- [63] Crimmins, B.S., Particulate polycyclic aromatic hydrocarbons in the Atlantic and Indian Ocean atmospheres during the Indian Ocean Experiment and Aerosols99: Continental sources to the marine atmosphere. *J. Geophys. Res.*, 2004. 109, D05308, doi:10.1029/2003JD004192
- [64] Preston, M. R., Merrett, J., The distribution and origins of the hydrocarbon fraction of particulate material in the North Sea atmosphere. *Mar. Pollut Bull.*, 1991. 22(10): p. 516-522.
- [65] Tsapakis, M., Stephanou, E. G., Polycyclic aromatic hydrocarbons in the atmosphere of the Eastern Mediterranean. *Environ. Sci. Technol.*, 2005. 39(17): p. 6584-6590.

- [66] Lohmann, R., Gioia, R., Jones, K.C., Nizzetto, L., Temme, C., Xie, Z., Schulz-Bull, D., Hand, I., Morgan, E., Jantunen, L., Organochlorine pesticides and PAHs in the surface water and atmosphere of the North Atlantic and Arctic Ocean. *Environ. Sci. Technol.*, 2009. 43(15): p. 5633-5639.
- [67] Gioia, R., Nizzetto, L., Lohmann, R., Dachs, J., Temme, C., Jones, K.C., Polychlorinated biphenyls (PCBs) in air and seawater of the Atlantic Ocean: Sources, trends and processes. *Environ. Sci. Technol.*, 2008. 42(5): p. 1416-1422.
- [68] van den Berg, F., Kubiak, R., Benjey, W. G., Majewski, M. S., Yates, S. R., Reeves, G. L., Smelt, J. H., van der Linden, A. M. A., Emission of pesticides into the air. *Water Air Soil Pollut.*, 1999. 115(1): p. 195-218.
- [69] Lammel, G., Novák, J., Landlová, L., Dvorská, A., Klánová, J., Čupr, P., Kohoutek, J., Reimer, E., Škrdlíková, L., Sources and distributions of polycyclic aromatic hydrocarbons and toxicity of polluted atmosphere aerosols, in: *Urban Airborne Particulate Matter*, Zereini, F., Wiseman, C. L. S., Editors. 2011, Springer Berlin Heidelberg. p. 39-62.
- [70] Bidleman, T.F., Atmospheric processes. *Environ. Sci. Technol.*, 1988. 22(4): p.361-367.
- [71] van Pul, W. A. J., Bidleman, T. F., Brorström-Lundén, E., Builtjes, P. J. H., Dutchak, S., Duyzer, J. H., Gryning, S. E., Jones, K. C., van Dijk, H. F. G., van Jaarsveld, J. A., Atmospheric transport and deposition of pesticides: an assessment of current knowledge. *Water Air Soil Pollut.*, 1999. 115(1): p. 245-256.
- [72] Bidleman, T.F., Atmospheric transport and air-surface exchange of pesticides. *Water, Air, Soil Pollut.*, 1999. 115(1): p. 115-166.
- [73] Pankow, J.F., Fundamentals and mechanisms of gas/particle partitioning in the atmosphere, in: *Gas and particle phase measurements of atmospheric organic compounds*, Lane, D. A., Editor. 1999, Gordon and Breach Amsterdam p. 25–37.
- [74] Lei, Y., Is rain or snow a more efficient scavenger of organic chemicals? *Atmos. Environ.*, 2004. 38(22): p. 3557-3571.
- [75] Atkinson, R., Kwok, E., Arey, J., Photochemical processes affecting the fate of pesticides in the atmosphere, *BCPC, Pests and Disease*, 6A-2 (1992), pp. 469–476
- [76] Quante, M., The role of clouds in atmospheric transport and chemistry, in: *Persistent Pollution - Past, Present and Future*, Quante, M., Ebinghaus, R., Flöser, G., Editors. 2011, Springer Berlin Heidelberg. p. 299-316.
- [77] Gouin, T., Mackay, D., Jones, K. C., Harner, T., Meijer, S. N., Evidence for the “grasshopper” effect and fractionation during long-range atmospheric transport of organic contaminants. *Environ. Pollut.*, 2004. 128(1-2): p. 139-148.
- [78] Lammel, G., Semeena, V. S., Guglielmo, F., Ilyina, T., Leip, A., Bestimmung des Ferntransports von persistenten organischen Spurenstoffen und der Umweltexposition mittels Modelluntersuchungen. *Umweltwissenschaften und Schadstoff-Forschung*, 2006. 18(4): p. 254-261.
- [79] Wania, F., Westgate, J. N., On the mechanism of mountain cold-trapping of organic chemicals. *Environ. Sci. Technol.*, 2008. 42(24): p. 9092-9098.
- [80] Wania, F., Mackay, D., Global fractionation and cold condensation of low volatility organochlorine compounds in polar regions. *Ambio*, 1993. 22: p. 10-18.
- [81] Lammel, G., Zetzsch, C., POPs – schwer abbaubare Chemikalien. *CHIUZ*, 2007. 41(3): p. 276-284.
- [82] United Nations Environment Programme (UNEP): Regionally based assessment of persistent toxic substances-Global Report 2003, UNEP Chemicals, Châtelaine, Switzerland

- [83] Matthias, V., Aerosols as transport vehicles of persistent pollutants, in: Persistent Pollution - Past, Present and Future, Quante, M., Ebinghaus, R., Flöser, G., Editors. 2011, Springer Berlin Heidelberg. p. 267-286.
- [84] Schnelle-Kreis, J., Sklorz, M., Herrmann, H., Zimmermann, R., Atmosphärische Aerosole: Quellen, Vorkommen, Zusammensetzung. *CHIUZ*, 2007. 41(3): p. 220-230.
- [85] Deutscher Wetterdienst (DWD), Globales Master Portlet; available (15.09.11): http://www.google.de/imgres?imgurl=http://www.dwd.de/bvbw/generator/DWDWWW/Content/Forschung/FEHP/GAW/IMG/aerosole_pd_de.property%3Ddefault.jpg&imgrefurl=http://www.dwd.de/bvbw/appmanager/bvbw/dwdwwwDesktop%3Bjsessionid%3D1OKgNBjhZCffpys3z2Qx32XRB2nbCDhp
- [86] Allen, J. O., Dookeran, N. M., Smith, K. A., Sarofim, A. F., Taghizadeh, K., Lafleur, A. L., Measurement of polycyclic aromatic hydrocarbons associated with size-segregated atmospheric aerosols in Massachusetts. *Environ. Sci. Technol.*, 1996. 30(3): p. 1023-1031.
- [87] Bidleman, T. F., McConnell, L. L., A review of field experiments to determine air-water gas exchange of persistent organic pollutants. *Sci. Total Environ.*, 1995. 159(2-3): p. 101-117.
- [88] Jurado, E., Jaward, F. M., Lohmann, R., Jones, K. C., Simó, R., Dachs, J., Atmospheric dry deposition of persistent organic pollutants to the Atlantic and inferences for the global oceans. *Environ. Sci. Technol.*, 2004. 38(21): p. 5505-5513.
- [89] Williams, R. M., A model for the dry deposition of particles to natural water surfaces. *Atmos. Environ.*, 1982. 16(8): p. 1933-1938.
- [90] Dachs, J., Lohmann, R., Ockenden, W. A., Méjanelle, L., Eisenreich, S. J., Jones, K. C., Oceanic biogeochemical controls on global dynamics of persistent organic pollutants. *Environ. Sci. Technol.*, 2002. 36(20): p. 4229-4237.
- [91] Rueß, J., Ozean/Atmosphäre-Austauschprozesse von unpolaren und polaren organischen Xenobiotika. 2010, PhD thesis, Department of Chemistry, University Hamburg.
- [92] Jurado, E., Dachs, J., Seasonality in the “grasshopping” and atmospheric residence times of persistent organic pollutants over the oceans. *Geophys. Res. Lett.*, 2008. 35(17)
- [93] Berrojalbiz, N., Dachs, J., del Vento, S., Ojeda, M. J., Valle, M. C., Castro-Jiménez, J., Mariani, G., Wollgast, J., Hanke, G., Persistent organic pollutants in mediterranean seawater and processes affecting their accumulation in plankton. *Environ. Sci. Technol.*, 2011: p. 4315-4322.
- [94] O'Dowd, C. D., de Leeuw, G., Marine aerosol production: a review of the current knowledge. *Philos. Transact. A Math. Phys. Eng. Sci.*, 2007. 365: p. 1753.
- [95] Norris, S. J., Brooks, I.M., Smith, M.H., Hill, M.K., Brooks, B. J., de Leeuw, G., In-situ measurements of aerosol production from individual whitecaps during SEASAW. in 15th Conference on Air-Sea Interaction. 2007. Portland, Oregon. Available (02.04.2012): http://ams.confex.com/ams/15isa14m/techprogram/paper_124984.htm
- [96] Woolf, D. K., Bubbles, in *Encyclopedia of Ocean Sciences*. 2001, Academic Press. p. 352-357.
- [97] Paterson, S., Mackay, D., Gladman, A., A fugacity model of chemical uptake by plants from soil and air. *Chemosphere*, 1991. 23(4): p. 539-565.
- [98] Bidleman, T. F., McConnell, L. L., A review of field experiments to determine air-water gas exchange of persistent organic pollutants. *Sci. Total Environ.*, 1995. 159(2-3): p. 101-117.

- [99] Mandalakis, M., Apostolaki, M., Stephanou, E. G., Stavrakakis, S., Mass budget and dynamics of polychlorinated biphenyls in the eastern Mediterranean Sea. *Global Biogeochem. Cycles*, 2005. 19(3): p. 1-16 (GB3018).
- [100] Jaenicke, R., Aerosol physics and chemistry, in Landolt-Börnstein New Series, Fischer, G., Editor. 1988, Springer Berlin Heidelberg. p. 391-456.
- [101] Slinn, S., Slinn, W., Predictions for particle deposition on natural waters. *Atmos. Environ.* (1967), 1980. 14(9): p. 1013-1016.
- [102] Gigliotti, C. L., Totten, L. A., Offenberg, J. H., Dachs, J., Reinfelder, J. R., Nelson, E. D., Glenn, T. R., Eisenreich, S. J., Atmospheric concentrations and deposition of polycyclic aromatic hydrocarbons to the mid-atlantic east coast region. *Environ. Sci. Technol.*, 2005. 39(15): p. 5550-5559.
- [103] Bester, K., Hühnerfuss, H., Neudorf, B., Thiemann, W., Atmospheric deposition of triazine herbicides in Northern Germany and the German Bight (North Sea). *Chemosphere*, 1995. 30(9): p. 1639-1653.
- [104] Škrdlíková, L., Landlová, L., Klánová, J., Lammel, G., Wet deposition and scavenging efficiency of gaseous and particulate phase polycyclic aromatic compounds at a central European suburban site. *Atmos. Environ.*, 2011. 45(25): p. 4305-4312.
- [105] John, A. C., Probenahme und chemische Analytik von Korngrößenfraktionierten Immissions- und Emissionsaerosolen, Fakultät für Naturwissenschaften. 2002, Gerhard-Mercator-Universität Duisburg.
- [106] Bedienungsanleitung von 2005, High-Volume Sampler Digital DHM-60, Riemer Probenahmesysteme und Analysetechnik
- [107] Kavouras, I. G., Lawrence, J., Koutrakis, P., Stephanou, E. G., Oyola, P., Measurement of particulate aliphatic and polynuclear aromatic hydrocarbons in Santiago de Chile: source reconciliation and evaluation of sampling artifacts. *Atmos. Environ.*, 1999. 33(30): p. 4977-4986.
- [108] Mandalakis, M., Stephanou, E. G., Polychlorinated biphenyls associated with fine particles (PM_{2.5}) in the urban environment of Chile: concentration levels, and sampling volatilization losses. *Environ. Toxicol. Chem.*, 2002. 21(11): p. 2270-2275.
- [109] Tuduri, L., Harner, T., Hung, H., Polyurethane foam (PUF) disks passive air samplers: Wind effect on sampling rates. *Environ. Pollut.*, 2006. 144(2): p. 377-383.
- [110] Draxler R. R., Rolph, G. D., 2003. Hysplit Model access via NOAA ARL READY Website (<http://ready.arl.noaa.gov/HYSPLIT.php>). NOAA Air Resources Laboratory, Silver Spring, Maryland.
- [111] MUDAB-Marine Environmental Data Base of the German Oceanographic Data Centre (DOD), Hamburg, Germany. Data request (30.02.2011) provided at the DOD website: <http://www.bsh.de/de/Meeresdaten/Umweltschutz/DOD-Datenbank/index.jsp>
- [112] Motelay-Massei, A., Garban, B., Tiphagne-Larcher, K., Chevreuil, M., Ollivon, D., Mass balance for polycyclic aromatic hydrocarbons in the urban watershed of Le Havre (France): Transport and fate of PAHs from the atmosphere to the outlet. *Water Res.*, 2006. 40(10): p. 1995-2006.
- [113] Sehili, A.M., Lammel, G., Global fate and distribution of polycyclic aromatic hydrocarbons emitted from Europe and Russia. *Atmos. Environ.*, 2007. 41(37): p. 8301-8315.
- [114] Motelay-Massei, A., Ollivon, D., Garban, B., Tiphagne-Larcher, K., Zimmerlin, I., Chevreuil, M., PAHs in the bulk atmospheric deposition of the Seine river basin: Source identification and apportionment by ratios, multivariate statistical techniques and scanning electron microscopy. *Chemosphere*, 2007. 67(2): p. 312-321.

- [115] Ollivon, D., Blanchoud, H., Motelay-Massei, A., Garban, B. et al., Atmospheric deposition of PAHs to an urban site, Paris, France. *Atmos. Environ.*, 2002. 36(17): p. 2891-2900.
- [116] Tasdemir, Y., Esen, F., Dry deposition fluxes and deposition velocities of PAHs at an urban site in Turkey. *Atmos. Environ.*, 2007. 41(6): p. 1288-1301.
- [117] Lohmann, R., Lammel, G., Adsorptive and absorptive contributions to the gas-particle partitioning of polycyclic aromatic hydrocarbons: state of knowledge and recommended parametrization for modeling. *Environ. Sci. Technol.*, 2004. 38(14): p. 3793-3803.
- [118] Dachs, J., Eisenreich, S. J., Adsorption onto aerosol soot carbon dominates gas-particle partitioning of polycyclic aromatic hydrocarbons. *Environ. Sci. Technol.*, 2000. 34(17): p. 3690-3697.
- [119] Schulz-Bull, D., Hand, I., Lerz, A., Schneider, R., Trost, E., Wodarg, D., Regionale Verteilung chlorierter Kohlenwasserstoffe (CKW) und polycyclischer aromatischer Kohlenwasserstoffe (PAK) im Pelagial und Oberflächensediment in der deutschen ausschließlichen Wirtschaftszone (AWZ) im Jahr 2010, Bericht vom Leibnitz-Institut für Ostseeforschung der Universität Rostock im Auftrag des BSH, Hamburg, Rostock, Juni 2011.
- [120] Bailey, R.E., Global hexachlorobenzene emissions. *Chemosphere*, 2001. 43(2): p. 167-182.
- [121] Bailey, R.E., Pentachlorobenzene—Sources, environmental fate and risk characterization. 2007, Euro Chlor.
- [122] Bailey, R.E., Van Wijk, D., Thomas, P.C., Sources and prevalence of pentachlorobenzene in the environment. *Chemosphere*, 2009. 75(5): p. 555-564.
- [123] Courtney, K.D., Hexachlorobenzene (HCB): a review. *Environ. Res.*, 1979. 20(2): p. 225.
- [124] Lammel, G., Klánová, J., Kohoutek, J., Prokeš, R., Ries, L., Stohl, A., Observation and origin of organochlorine compounds and polycyclic aromatic hydrocarbons in the free troposphere over central Europe. *Environ. Pollut.*, 2009. 157(12): p. 3264-3271.
- [125] Shen, L., Wania, F., Compilation, evaluation, and selection of physical-chemical property data for organochlorine pesticides. *J. Chem. Eng. Data*, 2005. 50(3): p. 742-768.
- [126] Vijgen, J., Abhilash, P. C., Li, Y. F., Lal, R., Forter, M., Torres, J., Singh, N., Yunus, M., Tian, C., Schäffer, A., Weber, R., Hexachlorocyclohexane (HCH) as new Stockholm Convention POPs—a global perspective on the management of Lindane and its waste isomers. *Environ. Sci. Pollut. Res.*, 2010. 18(2): p. 152-162.
- [127] Bidleman, T. F., Jantunen, L. M., Falconer, R. L., Barrie, L. A., Fellin, P., Decline of hexachlorocyclohexane in the Arctic atmosphere and reversal of air sea gas exchange. *Geophys. Res. Lett.*, 1995. 22(3): p. 219-222.
- [128] Bottenheim J. W., Ashu D., Gong S.-L., Higachi K., Li Y.-F., Long range transport of air pollution to the Arctic, in: *Intercontinental Transport of Air Pollution*, Stohl A., Editors. 2004, Springer Berlin Heidelberg. p. 13-39.
- [129] Faller, J., Hühnerfuss, H., König, W. A., Ludwig, P., Gas chromatographic separation of the enantiomers of marine organic pollutants:: Distribution of α -HCH enantiomers in the North Sea. *Mar. Pollut. Bull.*, 1991. 22(2): p. 82-86.
- [130] Bethan, B., Dannecker, W., Gerwig, H., Hühnerfuss, H., Schulz, M., Seasonal dependence of the chiral composition of α -HCH in coastal deposition at the North Sea. *Chemosphere*, 2001. 44(4): p. 591-597.
- [131] Jorgenson, J.L., Aldrin and dieldrin: a review of research on their production, environmental deposition and fate, bioaccumulation, toxicology, and epidemiology in the United States. *Environ. Health Pers.*, 2001. 109(Suppl 1): p. 113-139.

- [132] Nielsen, T. G., Løkkegaard, B., Richardson, K., Pedersen, F. B., Hansen, L., Structure of plankton communities in the Dogger Bank area (North Sea) during a stratified situation. *Mar. Ecol. Prog. Ser.*, 1993. 95(1-2): p. 115-131.
- [133] Foght, J., April, T., Biggar, K., Aislabie, J., Bioremediation of DDT-contaminated soils: a review. *Biomed. J.*, 2001. 5(3): p. 225-246.
- [134] Snedeker, S.M., Pesticides and breast cancer risk: a review of DDT, DDE, and dieldrin. *Environ. Health Pers.*, 2001. 109(Suppl 1): p. 35.
- [135] Aislabie, J., Richards, N., H. Boul, H., Microbial degradation of DDT and its residues—a review. *N. Zeal. J. Agric. Res.*, 1997. 40(2): p. 269-282.
- [136] Iwata, H., Tanabe, S., Sakai, N., Tatsukawa, R., Distribution of persistent organochlorines in the oceanic air and surface seawater and the role of ocean on their global transport and fate. *Environ. Sci. Technol.*, 1993. 27(6): p. 1080-1098.
- [137] Safe, S., Bandiera, S., Sawyer, T., Robertson, L., Safe, L., Parkinson, A., Thomas, P.E., Ryan, D.E., Reik, L.M., Levin, W., Denomme, M.A., Fujita, T., PCBs: structure–function relationships and mechanism of action. *Environ. Health Pers.*, 1985. 60: p. 47-56.
- [138] Mills III, S.A., Thal, D. I., Barney, J., A summary of the 209 PCB congener nomenclature. *Chemosphere*, 2007. 68(9): p. 1603-1612.
- [139] Paasivirta, J., Sinkkonen, S., Mikkelsen, P., Rantio, T., Wania, F., Estimation of vapor pressures, solubilities and Henry's law constants of selected persistent organic pollutants as functions of temperature. *Chemosphere*, 1999. 39(5): p. 811-832.
- [140] Bruhn, R., Lakaschus, S., McLachlan, M.S., Air/sea gas exchange of PCBs in the southern Baltic Sea. *Atmos. Environ.*, 2003. 37(24): p. 3445-3454.
- [141] Schreitmüller, J., Vigneron, M., Bacher, R., Ballschmiter, K., Pattern analysis of polychlorinated biphenyls (PCB) in marine air of the Atlantic Ocean. *Intern. J. Environ. Chem.*, 1994. 57(1): p. 33-52.
- [142] Sundqvist, K.L., Wingfors, H., Brorstöm-Lundén, E., Wiberg, K., Air-sea gas exchange of HCHs and PCBs and enantiomers of α -HCH in the Kattegat Sea region. *Environ. Pollut.*, 2004. 128(1-2): p. 73-83.
- [143] Bruhn, R., Lakaschus, S., McLachlan, M.S., Air/sea gas exchange of PCBs in the southern Baltic Sea. *Atmos. Environ.*, 2003. 37(24): p. 3445-3454.
- [144] Axelman, J., Näf, C., Bandh, C., Ishaq, R., Pettersen, H., Zebühr, Y., Broman, D., Dynamics and distribution of hydrophobic organic compounds in the Baltic Sea, in: *A Systems Analysis of the Baltic Sea*, Wulff, F.V., Rahm, L.A., Larsson, P., Editors. 2001, Springer Berlin Heidelberg, p. 257-287.
- [145] Agrell, C., Larsson, P., Okla, L., Agrell, J., PCB congeners in precipitation, wash out ratios and depositional fluxes within the Baltic Sea region, Europe. *Atmos. Environ.*, 2002. 36(2): p. 371-383.
- [146] Heri, W., Pfister, F., Carroll, B., Parshley, T., Nabors, J.B., History of the discovery and development of triazine herbicides, in: *The Triazine Herbicides – 50 years Revolutionizing Agriculture*, LeBaron, H.M., McFarland, J. E., Burnside, O.C., Editors. 2008, Elsevier Professional, p. 29-46
- [147] Heri, W., Pfister, F., Carroll, B., Parshley, T., Nabors, J.B., Production, development, and registration of triazine herbicides, in: *The Triazine Herbicides – 50 years Revolutionizing Agriculture*, LeBaron, H.M., McFarland, J. E., Burnside, O.C., Editors. 2008, Elsevier Professional, p. 47-60

- [148] Skark, C., Zullei-Seibert, N., The occurrence of pesticides in groundwater - Results of case studies. *Int. J. Environ. Anal. Chem.*, 1995. 58(1-4): p. 387-396.
- [149] Ackerman, F., The economics of atrazine. *Int. J. Occup. Environ. Health*, 2007. 13(4): p. 437-445.
- [150] SRC PhysProp Database, output from the free online database at 24.01.12, available under: www.syrres.com
- [151] Jungnickel, C., Stock, F., Brandsch, T., Ranke, J., Risk assessment of biocides in roof paint. *Environ. Sci. Pollut. Res.*, 2008. 15(3): p. 258-265.
- [152] Burkhardt, M., Junghans, M., Zuleeg, S., Boller, M., Schoknecht, U., Lamani, X., Bester, K., Vonbank, R., Simmler, H., Boller, M., Biozide in Gebäudefassaden-ökotoxikologische Effekte, Auswaschung und Belastungsabschätzung für Gewässer. *Umweltwiss. Schadstoff. Forsch.*, 2009. 21(1): p. 36-47.
- [153] Macdonald, R. W., Barrie, L. A., Bidleman, T. F., Diamond, M. L., Gregor, D. J., Semkin, R. G., Strachan, W. M. J., Li, Y. F., Wania, F., Alaee, M., Alexeeva, L. B., Backus, S. M., Bailey, R., Bewers, J. M., Gobeil, C., Halsall, C. J., Harner, T., Hoff, J. T., Jantunen, L. M. M., Lockhart, W. L., Mackay, D., Muir, D. C. G., Pudykiewicz, J., Reimer, K. J., Smith, J. N., Stern, G. A., Schroeder, W. H., Wagemann, R., Yunker, M. B., Contaminants in the Canadian Arctic: 5 years of progress in understanding sources, occurrence and pathways. *Sci Total Environ.*, 2000. 254(2-3): p. 93-234.
- [154] Hermanson, M. H., Isaksson, E., Teixeira, C., Muir, D. C. G., Compher, K. M., Li, Y. F., Igarashi, M., Kamiyama, K., Current-use and legacy pesticide history in the Austfonna ice cap, Svalbard, Norway. *Environ. Sci. Technol.*, 2005. 39(21): p. 8163-8169.
- [155] Bester, K., Hühnerfuss, H., Neudorf, B., Thiemann, W., Atmospheric deposition of triazine herbicides in Northern Germany and the German Bight (North Sea). *Chemosphere*, 1995. 30(9): p. 1639-1653.
- [156] Hühnerfuss, H., Bester, K., Landgraff, O., Pohlmann, T., Selke, K., Annual balances of hexachlorocyclohexanes, polychlorinated biphenyls and triazines in the German Bight* 1. *Mar. Pollut. Bull.*, 1997. 34(6): p. 419-426.
- [157] Karr, C.J., Solomon, G.M., Brock-Utne, A.C., Health effects of common home, lawn, and garden pesticides. *Pediatr. Clin. N. Am.*, 2007. 54(1): p. 63-80.
- [158] Coronado, G.D., Thompson, B., Strong, L., Griffith, W.C., Islas, I., Agricultural task and exposure to organophosphate pesticides among farmworkers. *Environ. Health Persp.*, 2004. 112(2): p. 142.
- [159] Belden, J.B., Lydy, M.J., Impact of atrazine on organophosphate insecticide toxicity. *Environ. Toxicol. Chem.*, 2000. 19(9): p. 2266-2274.
- [160] Freed, V.H., Chiou, C.T., Schmedding, D.W., Degradation of selected organophosphate pesticides in water and soil. *J. Agric. Food Chem.*, 1979. 27(4): p. 706-708.
- [161] Freed, V.H., Schmedding, D.W., Kohnert, R., Haque, R., Physical chemical properties of several organophosphates: Some implication in environmental and biological behavior. *Pestic. Biochem. Physiol.*, 1979. 10(2): p. 203-211.
- [162] Bondarenko, S., Gan, J., Haver, D.L., Kabashima, J.N., Persistence of selected organophosphate and carbamate insecticides in waters from a coastal watershed. *Environ. Toxicol. Chem.*, 2004. 23(11): p. 2649-2654.
- [163] Sørensen, S.R., Bending, G.D., Jacobsen, C.S., Walker, A., Aamand, J., Microbial degradation of isoproturon and related phenylurea herbicides in and below agricultural fields. *FEMS Microbiol. Ecol.*, 2003. 45(1): p. 1-11.

- [164] Giacomazzi, S., Cochet, N., Environmental impact of diuron transformation: a review. *Chemosphere*, 2004. 56(11): p. 1021-1032.
- [165] Choi, B. K., Hercules, D. M., Gusev, A. I., LC-MS/MS signal suppression effects in the analysis of pesticides in complex environmental matrices. *Fresenius J. Anal. Chem.*, 2001. 369(3): p. 370-377.
- [166] Masclet, P., Contamination of lake water by pesticides via atmospheric transport, in *Geosciences and water resources: Environmental data modelling*, Bardinnet, C., Royer, J. J., Editors. 1997, Springer Berlin Heidelberg, p. 85-92.
- [167] Gintautas, P.A., Daniel, S. R., Macalady, D. L., Phenoxyalkanoic acid herbicides in municipal landfill leachates. *Environ. Sci. Technol.*, 1992. 26(3): p. 517-521.
- [168] Bucheli, T.D., Müller, S.R., Voegelin, A., Schwarzenbach, R.P., Bituminous roof sealing membranes as major sources of the herbicide (R, S)-mecoprop in roof runoff waters: potential contamination of groundwater and surface waters. *Environ. Sci. Technol.*, 1998. 32(22): p. 3465-3471.
- [169] Leistra, M., Boesten, J. J. T. I., Pesticide contamination of groundwater in Western Europe. *Agric., Ecosyst. Environ.*, 1989. 26(3-4): p. 369-389.
- [170] Huber, R., Otto, S., Environmental behavior of bentazon herbicide. *Rev. Environ. Contam. Toxicol.*, 1994. 137: p. 111-134.
- [171] Grover, R., Wolt, J. D., Cessna, A. J., Schiefer, H. B., Environmental fate of trifluralin, in *Reviews of environmental contamination and toxicology*, Ware, G. W., Editor. 1997, Springer Berlin Heidelberg, 153: p. 1-16.
- [172] Zimdahl, R. L., Catizone, P., Butcher, A. C., Degradation of pendimethalin in soil. *Weed Sci.*, 1984. 32: p. 408-412.
- [173] Pflanzenschutz-Warndienst für den Gemüsebau - Abteilung Pflanzenbau und Pflanzenschutz, Landwirtschaftskammer Schleswig-Holstein, January 2008.
- [174] Junghans, M., Backhaus, T., Faust, M., Scholze, M., Grimme, L. H., Predictability of combined effects of eight chloroacetanilide herbicides on algal reproduction. *Pest Manage. Sci.*, 2003. 59(10): p. 1101-1110.
- [175] Helgesen, R.G., Tauber, M. J., Pirimicarb, an aphicide nontoxic to three entomophagous arthropods. *Environ. Ent.*, 1974. 3(1): p. 99-101.
- [176] Saien, J., Khezrianjoo, S., Degradation of the fungicide carbendazim in aqueous solutions with UV/TiO₂ process: Optimization, kinetics and toxicity studies. *J. Hazard. Mater.*, 2008. 157(2-3): p. 269-276.
- [177] Chen, T., Fu, F., Chen, Z., Li, D., Zhang, L., Chen, G., Study on the photodegradation and microbiological degradation of pirimicarb insecticide by using liquid chromatography coupled with ion-trap mass spectrometry. *J. Chromatogr. A*, 2009. 1216(15): p. 3217-3222.
- [178] Szeto, S.Y., Vernon, R.S., Brown, M. J., Degradation of dimethoate and pirimicarb in asparagus. *J. Agric. Food Chem.*, 1985. 33(4): p. 763-767.
- [179] Romero, E., Schmitt, P., Mansour, M., Photolysis of pirimicarb in water under natural and simulated sunlight conditions. *Pestic. Sci.*, 1994. 41(1): p. 21-26.
- [180] Schultz, M. M., Barofsky, D. F., Field, J. A., Fluorinated alkyl surfactants. *Environ. Eng. Sci.*, 2003. 20(5): p. 487-501.
- [181] Giesy, J. P., Kannan, K., Global distribution of perfluorooctane sulfonate in wildlife. *Environ. Sci. Technol.*, 2001. 35(7): p. 1339-1342.

- [182] McMurdo, C. J., Ellis, D. A., Webster, E., Butler, J., Christensen, R. D., Reid, L. K., Aerosol enrichment of the surfactant PFO and mediation of the water– air transport of gaseous PFOA. *Environ. Sci. Technol.*, 2008. 42(11): p. 3969-3974.
- [183] Theobald, N., Caliebe, C., Gerwinski, W., Hühnerfuss, H., Lepom, P., Occurrence of perfluorinated organic acids in the North and Baltic seas. Part 1: Distribution in sea water. *Environ. Sci. Pollut. Res.*, 2011. 18(7): p. 1057-1069.
- [184] Möller, A., Xie, Z., Caba, A., Sturm, R., Ebinghaus, R., Organophosphorus flame retardants and plasticizers in the atmosphere of the North Sea. *Environ. Pollut.*, 2011. 159(12): p. 3660-3665.
- [185] Covaci, A., Gerecke, A. C., Law, R. J., Voorspoels, S., Kohler, M., Heeb, N. V., Leslie, H., Allchin, C. R., de Boer, J., Hexabromocyclododecanes (HBCDs) in the environment and humans: a review. *Environ. Sci. Technol.*, 2006. 40(12): p. 3679-3688.
- [186] Clara, M., Strenn, B., Kreuzinger, N., Carbamazepine as a possible anthropogenic marker in the aquatic environment: investigations on the behaviour of carbamazepine in wastewater treatment and during groundwater infiltration. *Water Res.*, 2004. 38(4): p. 947-954.
- [187] Christidis, D., Kalogerakis, D., Chan, T. Y., Mauri, D., Alexiou, G., Terzoudi, A., Is primidone the drug of choice for epileptic patients with QT-prolongation? A comprehensive analysis of literature. *Seizure*, 2006. 15(1): p. 64-66.
- [188] Todd, P. A., Clissold, S. P., Naproxen. A reappraisal of its pharmacology, and therapeutic use in rheumatic diseases and pain states. *Drugs*, 1990. 40(1): p. 91-137.
- [189] Davies, N. M., Anderson, K. E., Clinical pharmacokinetics of diclofenac. Therapeutic insights and pitfalls. *Clin. Pharmacokinet.*, 1997. 33(3): p. 184-213.
- [190] Stan, H. J., Heberer, T., Linkerhägner, M., Occurrence of clofibric acid in the aquatic system - Is the use in human medical care the source of the contamination of surface, ground and drinking water? *Vom Wasser*, 1994. 83: p. 57-68.
- [191] Greenblatt, D.J., Clinical pharmacokinetics of oxazepam and lorazepam. *Clin. Pharmacokinet.*, 1981. 6(2): p. 89-105.
- [192] Farrar, N.J., Harner, T., Shoeib, M., Sweetman, A., Jones, K. C., Field deployment of thin film passive air samplers for persistent organic pollutants: A study in the urban atmospheric boundary layer. *Environ. Sci. Technol.*, 2005. 39(1): p. 42-48.
- [193] Moreau-Guigon, E., Motelay-Massei, A., Harner, T., Pozo, K., Diamond, M., Chevreuril, M., Blanchoud, H., Vertical and temporal distribution of persistent organic pollutants in Toronto. 1. Organochlorine pesticides. *Environ. Sci. Technol.*, 2007. 41(7): p. 2172-2177.
- [194] Cooper, D., HCB, PCB, PCDD and PCDF emissions from ships. *Atmos. Environ.*, 2005. 39(27): p. 4901-4912.
- [195] Mandalakis, M., Stephanou, E. G., Wet deposition of polychlorinated biphenyls in the eastern Mediterranean. *Environ. Sci. Technol.*, 2004. 38(11): p. 3011-3018.
- [196] Tucker, W. A., Preston, A. L., Procedures for estimating atmospheric deposition properties of organic chemicals. *Water, Air, Soil Pollut.*, 1984. 21(1): p. 247-260.
- [197] Federal Maritime and Hydrographic Agency of Germany (BSH), Umweltbericht zum Raumordnungsplan für die deutsche ausschließliche Wirtschaftszone (AWZ) in der Nordsee. 21.08.2009
- [198] Vardar, N., Odabasi, M., Holsen, T. M., Particulate dry deposition and overall deposition velocities of polycyclic aromatic hydrocarbons. *J. Environ. Eng.*, 2002. 128(3): p. 269-274.

- [199] Tasdemir, Y., Esen, F., Dry deposition fluxes and deposition velocities of PAHs at an urban site in Turkey. *Atmos. Environ.*, 2007. 41(6): p. 1288-1301.
- [200] Odabasi, M., Sofuoglu, A., Vardar, N., Tasdemir, Y., Holsen, T. M., Measurement of dry deposition and air-water exchange of polycyclic aromatic hydrocarbons with the water surface sampler. *Environ. Sci. Technol.*, 1999. 33(3): p. 426-434.
- [201] Franz, T.P., Eisenreich, S. J., Holsen, T. M., Dry deposition of particulate polychlorinated biphenyls and polycyclic aromatic hydrocarbons to Lake Michigan. *Environ. Sci. Technol.*, 1998. 32(23): p. 3681-3688.
- [202] Bamford, H. A., Poster, D. I. L., Baker, J. E., Temperature dependence of Henry's law constants of thirteen polycyclic aromatic hydrocarbons between 4 °C and 31 °C. *Environ. Toxicol. Chem.*, 1999. 18(9): p. 1905-1912.
- [203] Sahsuvar, L., Helm, P. A., Jantunen, L. M., Bidleman, T. F., Henry's law constants for α -, β -, and γ -hexachlorocyclohexanes (HCHs) as a function of temperature and revised estimates of gas exchange in Arctic regions. *Atmos. Environ.*, 2003. 37(7): p. 983-992.
- [204] Abraham, M.H., Enomoto, K., Clarke, E. D., Rosés, M., Ràfols, C., Fuguet, E., Henry's law constants or air to water partition coefficients for 1, 3, 5-triazines by an LFER method. *J. Environ. Monit.*, 2007. 9(3): p. 234-239.
- [205] Rice, C. P., Chernyak, S. M., McConnell, L. L., Henry's law constants for pesticides measured as a function of temperature and salinity. *J. Agric. Food Chem.*, 1997. 45(6): p. 2291-2298.
- [206] Fendinger, N. J., Glotfelty, D. E., Henry's law constants for selected pesticides, PAHs and PCBs. *Environ. Toxicol. Chem.*, 1990. 9(6): p. 731-735.

11. Annexes

Annex 1(A1): Atmospheric concentrations of target analytes

A1 Table 1: Atmospheric concentrations of target compounds in pg/m³ determined by high-volume active air sampling; sample names correspond with the active air sampling campaigns tabulated in chapter 3; n.q. = not quantified; PXP = PUF/XAD-2/PUF adsorber cartridge; P pl = PUF plug adsorber cartridge; <LOQ and replaced by LOQ/2, = signal <LOD and replaced by LOD/2; = no signal detected; = signal < 0 after blank subtraction; = signal > upper calibration range

pg/m ³	AL 1	AL 2	AL 3	AL 4	AL 5	AL 6	AL 7	AL 8	AL 9	AL 10	09AT 2		09AT 3	
											GFF	PXP	GFF	PXP
24-D	n.q.	n.q.	n.q.	n.q.	n.q.	n.q.	n.q.	n.q.	n.q.	n.q.	1.74	n.q.	0.00	n.q.
ACE	24.45	19.86	24.08	80.92	26.85	15.96	26.22	10.81	11.91	10.76	0.00	303.1	2.42	60.82
ACY	0.00	0.00	0.00	11.59	10.07	0.00	0.00	11.14	0.00	9.17	0.00	34.28	0.00	29.83
ALD	0.00	0.00	0.00	0.00	0.00	0.00	0.00	0.00	0.00	0.00	0.00	0.00	0.00	0.00
AMETRYN	0.00	0.00	0.00	0.00	0.00	0.00	0.00	0.00	0.00	0.00	0.00	0.00	0.00	0.00
ANT	45.97	30.00	33.26	76.60	32.83	22.80	17.63	21.41	21.41	0.00	0.00	26.84	0.00	29.17
ATRAZ	1.23	1.09	1.19	3.21	1.12	2.29	0.05	0.07	0.00	0.00	0.00	0.00	0.00	0.00
AZINPH-E	0.00	0.00	0.00	0.00	0.00	0.00	0.00	0.00	0.00	0.00	0.00	0.00	0.00	0.00
AZINPH-M	0.00	0.00	0.00	0.00	0.00	0.00	0.00	0.00	0.00	0.00	0.00	0.00	0.00	0.00
BAA	5.93	0.00	2.38	8.65	0.00	0.00	0.00	0.00	0.00	0.00	14.65	14.63	11.05	11.11
BAP	10.52	0.00	7.83	12.50	0.00	0.00	0.00	0.00	0.00	0.00	18.87	16.23	0.00	12.08
BBF	15.17	5.51	12.46	17.68	8.15	0.00	0.00	4.74	0.00	5.34	27.25	0.00	0.00	3.68
BENTAZ	0.01	0.11	0.00	0.00	0.00	0.03	0.00	0.00	0.00	0.00	0.07	0.07	0.00	0.00
BGHIP	5.77	0.00	5.06	7.93	1.54	0.00	0.00	0.00	0.00	0.00	19.04	14.81	10.84	5.50
CARBAMAZ	0.00	0.00	0.00	0.00	0.00	0.25	0.00	0.00	0.00	0.00	0.00	0.00	0.00	0.00
CARBEND	6.11	0.36	1.86	8.80	2.03	4.03	0.00	0.00	0.00	0.00	0.00	0.00	0.00	0.00
CB138	6.11	3.25	3.90	2.06	0.88	0.63	0.38	0.46	0.21	0.48	0.00	0.77	0.00	0.00
CB153	6.62	3.28	2.59	1.67	0.89	0.63	0.38	0.46	0.21	0.48	1.04	1.04	0.82	0.27
CB28	12.91	11.80	7.80	15.54	7.89	4.85	10.87	6.95	5.16	4.92	0.00	5.26	0.00	3.04
CB52	6.39	4.56	2.63	5.15	2.75	2.32	3.72	2.33	2.23	1.74	0.00	3.30	0.00	0.55
CHLORFENV	0.00	0.00	0.00	0.00	0.00	0.00	0.00	0.00	0.00	0.00	0.00	0.00	0.00	0.00
CHLORTUR	2.68	0.89	1.37	2.84	0.97	3.40	0.05	0.07	0.03	0.07	0.00	0.00	0.00	0.00
CHRTR	0.00	0.00	0.00	0.00	0.00	0.00	0.00	0.00	0.00	0.00	44.45	44.82	34.09	33.55
CLOFIBRS	n.q.	n.q.	n.q.	n.q.	n.q.	n.q.	n.q.	n.q.	n.q.	n.q.	0.00	n.q.	0.00	n.q.
DBAHA	0.00	0.00	0.00	0.00	0.00	0.00	0.00	0.00	0.00	0.00	17.64	0.00	0.00	0.00
DDDPP	0.00	0.00	0.00	0.00	0.09	0.13	0.08	0.09	0.12	0.00	0.00	0.70	0.00	0.55
DDEPP	8.52	6.33	4.84	7.99	3.25	1.52	0.70	0.76	0.86	1.00	1.04	3.51	0.00	0.82
DDTOP	2.19	1.12	1.10	1.34	0.71	0.57	0.40	0.46	0.55	0.49	0.00	0.70	0.00	0.55
DDTPP	3.61	1.99	1.65	2.77	1.08	0.60	0.44	0.55	0.56	0.63	0.70	1.59	0.00	0.55
DEATRAZ	0.00	0.13	0.30	1.08	0.44	0.25	0.00	0.00	0.00	0.00	0.00	0.00	0.00	0.00
DIAZINON	1.27	0.12	0.00	0.86	0.06	0.00	0.00	0.00	0.00	0.00	0.00	0.00	0.00	0.00
DICHLPR	n.q.	n.q.	n.q.	n.q.	n.q.	n.q.	n.q.	n.q.	n.q.	n.q.	2.13	n.q.	0.00	n.q.
DICLOF	n.q.	n.q.	n.q.	n.q.	n.q.	n.q.	n.q.	n.q.	n.q.	n.q.	0.00	n.q.	0.00	n.q.
DIELD	0.00	0.00	0.00	0.00	0.00	0.00	0.00	0.00	0.00	0.00	0.00	1.39	0.00	1.81
DIMETH	0.32	0.06	0.03	0.09	0.15	0.03	0.00	0.00	0.00	0.00	0.14	0.35	0.00	0.11
DIURON	0.11	0.16	0.58	0.54	0.23	1.39	0.16	0.22	0.25	0.19	0.35	3.78	0.00	0.00
END	0.00	0.00	0.00	0.00	0.00	0.00	0.00	0.00	0.00	0.00	0.00	0.00	0.00	0.00

A1 Table 1 continued:

pg/m ³	AL 1	AL 2	AL 3	AL 4	AL 5	AL 6	AL 7	AL 8	AL 9	AL 10	09AT 2		09AT 3	
											GFF	PXP	GFF	PXP
FENUR	3.07	1.57	3.87	2.84	2.74	11.55	2.91	1.87	1.39	2.20	0.00	0.07	0.00	0.00
FL	789.2	377.0	629.9	795.3	359.9	416.5	244.4	267.1	303.9	286.8	13.51	769.3	10.67	334.2
FLU	277.8	133.5	113.3	259.7	123.9	72.93	64.52	76.34	67.98	89.62	7.66	49.17	6.05	12.32
HBCDA	0.00	0.00	0.48	0.14	0.31	0.45	0.00	0.00	0.00	0.11	0.56	0.00	0.00	0.00
HBCDBG	0.00	0.17	2.13	2.08	2.25	5.64	0.00	0.00	0.00	0.61	0.56	0.00	0.44	0.00
HCB	32.04	24.63	31.73	20.51	35.17	33.44	16.48	21.50	30.42	26.96	0.00	74.53	0.16	62.25
HCHA	6.66	5.97	6.08	9.12	6.38	3.67	4.00	4.25	3.82	4.00	0.00	10.79	0.00	4.28
HCHB	0.00	0.78	0.00	0.54	0.00	0.00	0.00	0.00	0.00	0.00	0.00	1.39	0.00	0.00
HCHD	0.34	0.00	0.29	0.00	0.00	0.00	0.16	0.00	0.00	0.00	0.00	1.39	0.00	0.00
HCHG	6.83	12.88	5.57	7.82	4.20	3.05	2.64	2.25	1.92	2.19	0.00	9.47	0.00	1.10
HEXAZIN	0.00	0.00	0.00	0.00	0.00	0.00	0.00	0.00	0.00	0.00	0.00	0.00	0.00	0.00
I123P	7.65	0.00	6.95	9.28	4.15	0.00	0.00	0.00	0.00	3.28	19.01	15.72	11.59	0.00
IRGAROL	0.00	0.00	0.00	0.00	0.00	0.00	0.00	0.00	0.00	0.00	0.07	0.00	0.00	0.00
ISOD	0.53	0.00	0.00	0.00	0.28	0.00	0.00	0.00	0.00	0.00	0.00	0.00	0.00	0.00
ISOPRUR	22.02	4.11	8.06	13.71	3.82	13.94	0.25	0.38	0.72	0.76	2.40	0.07	0.00	0.00
LINUR	1.43	0.29	0.48	5.39	2.44	1.47	0.09	0.00	0.00	0.34	2.72	0.00	0.00	0.00
MALATH	0.00	0.25	0.00	0.00	0.00	0.00	0.00	0.00	0.00	0.00	0.00	0.00	0.00	0.00
MCPA	n.q.	n.q.	n.q.	n.q.	n.q.	n.q.	n.q.	n.q.	n.q.	n.q.	5.75	n.q.	0.00	n.q.
MECOPR	n.q.	n.q.	n.q.	n.q.	n.q.	n.q.	n.q.	n.q.	n.q.	n.q.	3.12	n.q.	0.00	n.q.
METAZCHL	0.22	0.24	0.47	0.52	0.20	0.42	0.08	0.09	0.11	0.23	4.26	0.55	0.32	0.00
METHABZT	0.00	0.01	0.00	0.00	0.00	0.00	0.00	0.00	0.00	0.00	0.00	0.00	0.00	0.00
METOLA	1.53	0.53	0.21	2.24	0.76	0.19	0.02	0.01	0.00	0.00	84.68	16.75	1.48	0.00
NAPROX	n.q.	n.q.	n.q.	n.q.	n.q.	n.q.	n.q.	n.q.	n.q.	n.q.	0.00	n.q.	0.00	n.q.
OXAZEP	0.00	0.00	0.16	0.00	0.00	0.00	0.00	0.00	0.00	0.00	0.00	0.00	0.00	0.00
PENDIMETH	5.13	6.53	10.17	3.20	7.55	4.26	2.46	0.99	1.51	2.13	10.40	1.67	1.87	0.44
PFBS	0.03	0.00	0.00	0.00	0.00	0.09	0.00	0.00	0.00	0.00	0.00	0.14	0.00	0.11
PFDEA	0.04	0.02	0.00	0.00	0.00	0.19	0.00	0.00	0.00	0.00	0.00	0.00	0.00	0.00
PFHPA	0.00	0.01	0.02	0.02	0.01	0.34	0.00	0.00	0.00	0.01	0.14	0.00	0.20	0.00
PFHXA	0.00	0.02	0.04	0.03	0.02	0.11	0.00	0.00	0.04	0.03	0.07	0.00	0.11	0.00
PFHXS	0.00	0.00	0.00	0.00	0.00	0.07	0.00	0.00	0.00	0.00	0.07	0.14	0.11	0.11
PFNOA	0.00	0.00	0.00	0.00	0.00	0.38	0.00	0.00	0.00	0.00	0.07	0.00	0.05	0.00
PFOA	0.12	0.06	0.10	0.09	0.20	0.29	0.06	0.00	0.00	0.07	0.42	0.00	1.18	1.21
PFOS	0.00	0.00	0.00	0.00	0.00	0.46	0.00	0.00	0.00	0.04	0.14	0.63	0.38	0.49
PFOSA	0.00	0.03	0.00	0.04	0.03	0.00	0.00	0.00	0.04	0.03	0.00	0.00	0.00	0.00
PHEN	1222	769.1	530.1	1294	579.9	334.8	324.4	349.0	298.3	285.8	11.84	874.0	3.13	454.0
PIRIMIC	0.00	0.00	0.00	0.00	0.00	0.00	0.00	0.00	0.00	0.00	23.84	3.80	0.00	0.00
PRIMID	0.00	0.00	0.00	0.00	0.00	0.00	0.00	0.00	0.00	0.00	0.00	0.00	0.00	0.00
PROMETR	0.54	0.01	0.02	0.20	0.27	0.52	0.01	0.00	0.00	0.00	0.35	0.00	0.27	0.00
PROPAZ	0.00	0.00	0.00	0.00	0.00	0.00	0.00	0.00	0.00	0.00	0.00	0.00	0.00	0.00
PYR	123.6	63.88	55.45	132.5	61.34	41.27	31.04	30.91	26.88	35.84	4.18	20.89	3.30	16.50
QCB	3.75	1.65	2.60	2.17	1.51	1.94	1.21	1.43	2.04	1.82	0.00	14.68	0.00	15.26
SIMAZ	0.00	0.21	0.00	0.00	0.06	0.85	0.00	0.00	0.00	0.00	0.00	0.00	0.00	0.00
TBEP	0.00	0.00	0.81	0.73	0.00	32.90	0.00	1.68	0.00	0.58	0.00	0.00	0.00	0.00
TBP	92.60	42.46	53.90	52.95	35.41	81.34	9.85	30.38	33.18	27.18	18.81	0.00	7.04	30.90
TERBAZ	5.89	4.55	3.13	9.17	3.86	4.16	0.29	0.15	0.13	0.10	126.1	29.95	2.83	2.03
TERBUTR	0.00	0.00	0.00	0.00	0.00	0.00	0.00	0.00	0.00	0.00	0.30	0.00	0.00	0.00
TPP	41.09	25.06	24.88	33.39	25.40	238.8	5.75	18.04	12.10	9.89	10.88	9.82	10.35	0.00
TRIFLU	5.09	0.72	0.29	14.82	0.57	0.27	0.33	0.20	0.09	0.20	1.04	2.11	0.00	1.85

A1 Table 1 continued:

pg/m ³	09AT 4		09AT 5		09AT 7		09AT 8		09AT 9		09AT 11		09AT 12	
	GFF	PXP	GFF	PXP	GFF	PXP	GFF	PXP	GFF	PXP	GFF	PXP	GFF	PXP
24-D	0.00	n.q.	0.00	n.q.	0.00	n.q.	0.00	n.q.	0.00	n.q.	0.00	n.q.	0.00	n.q.
ACE	0.00	23.90	0.00	20.65	0.00	90.67	0.87	56.52	0.00	32.93	1.32	14.51	0.00	13.53
ACY	0.00	5.62	0.00	6.23	0.00	6.22	0.00	2.96	0.00	3.63	0.00	4.51	0.00	9.44
ALD	0.00	0.00	0.00	0.00	0.00	0.00	0.00	0.00	0.00	0.00	0.00	0.00	0.00	0.00
AMETRYN	0.04	0.00	0.00	0.00	0.00	0.08	0.00	0.00	0.00	0.05	0.00	0.00	0.06	0.00
ANT	0.00	0.00	0.00	6.23	0.00	6.22	0.00	0.00	0.00	0.00	0.00	4.51	0.00	0.00
ATRAZ	0.00	0.00	0.00	0.00	0.00	0.00	0.10	0.00	0.05	0.12	0.17	0.00	0.00	0.00
AZINPH-E	0.00	0.00	0.00	0.00	0.00	0.00	0.00	0.00	0.00	0.00	0.00	0.00	0.00	0.00
AZINPH-M	0.00	0.00	0.00	0.00	0.00	0.00	0.00	0.00	0.00	0.00	0.00	0.00	0.00	0.00
BAA	0.00	7.65	0.00	8.62	8.75	8.65	5.23	4.89	4.81	4.91	0.00	0.00	0.00	0.00
BAP	0.00	0.00	0.00	8.34	13.44	8.85	13.02	7.04	5.46	0.00	6.16	6.15	0.00	6.29
BBF	0.00	2.51	6.23	2.78	23.17	2.78	19.85	3.94	18.89	1.62	0.00	2.02	0.00	4.21
BENTAZ	0.00	0.00	0.00	0.00	11.33	0.65	1.99	0.40	0.16	0.14	0.00	0.06	0.00	0.00
BGHIP	0.00	0.00	0.00	0.00	16.35	8.97	14.75	7.03	7.22	2.42	6.18	3.01	0.00	0.00
CARBAMAZ	0.00	0.00	0.00	0.00	0.00	0.00	0.00	0.00	0.00	0.00	0.00	0.00	0.00	0.00
CARBEND	0.00	0.00	0.00	0.00	0.00	0.00	0.00	0.00	0.00	0.00	0.00	0.00	0.00	0.00
CB138	0.00	0.00	0.00	0.00	0.00	0.46	0.00	0.65	0.00	0.80	0.00	0.33	0.00	0.69
CB153	0.56	0.19	0.00	0.62	0.00	0.62	0.30	1.01	0.00	0.36	0.00	0.15	0.94	0.31
CB28	0.00	2.00	0.00	2.52	0.00	5.92	0.00	5.32	0.00	3.51	0.15	2.19	0.31	2.13
CB52	0.00	0.37	0.00	0.42	0.00	2.48	0.00	2.44	0.00	1.33	0.00	0.71	0.00	0.63
CHLORFENV	0.00	0.00	0.00	0.00	0.00	0.00	0.00	0.00	0.00	0.00	0.00	0.00	0.00	0.00
CHLORTUR	0.00	0.00	0.00	0.00	0.57	0.00	0.00	0.00	0.35	0.00	0.00	0.00	0.00	0.00
CHRTR	0.00	22.10	0.00	25.15	25.89	27.44	14.88	18.36	16.27	17.81	17.28	17.87	0.00	36.90
CLOFIBRS	0.00	n.q.	0.00	n.q.	0.00	n.q.	0.00	n.q.	0.00	n.q.	0.00	n.q.	0.00	n.q.
DBAHA	0.00	0.00	0.00	0.00	10.59	6.22	2.46	2.96	6.10	0.00	0.00	0.00	0.00	0.00
DDDPP	0.00	0.37	0.00	0.42	0.00	0.41	0.00	0.20	0.00	0.24	0.00	0.00	0.00	0.00
DDEPP	0.00	0.56	0.00	0.62	0.00	1.43	0.00	1.15	0.00	0.36	0.00	0.45	0.00	0.94
DDTOP	0.00	0.37	0.00	0.00	0.00	0.41	0.00	0.43	0.00	0.49	0.00	0.30	0.00	0.00
DDTPP	0.00	0.37	0.00	0.42	0.00	0.95	0.00	0.54	0.00	0.52	0.00	0.30	0.00	0.63
DEATRAZ	0.00	0.00	0.00	0.00	0.00	0.00	0.00	0.00	0.00	0.00	0.00	0.00	0.00	0.00
DIAZINON	0.00	0.00	0.00	0.00	0.00	0.00	0.00	0.00	0.00	0.00	0.00	0.00	0.00	0.00
DICHLPR	0.00	n.q.	0.00	n.q.	0.00	n.q.	0.00	n.q.	0.00	n.q.	0.00	n.q.	0.00	n.q.
DICLOF	0.00	n.q.	0.00	n.q.	0.00	n.q.	2.74	n.q.	0.00	n.q.	0.00	n.q.	0.00	n.q.
DIELD	0.00	2.00	0.00	2.18	0.00	2.28	0.00	2.79	0.00	1.93	0.00	2.29	0.00	1.26
DIMETH	0.00	0.07	0.00	0.00	0.00	0.08	0.00	0.04	0.00	0.05	0.00	0.00	0.00	0.13
DIURON	0.19	1.38	0.00	2.78	0.21	0.42	0.24	0.00	4.75	15.40	0.35	3.19	0.00	4.81
END	0.00	0.00	0.00	0.00	0.00	0.00	0.00	0.00	0.00	0.00	0.00	0.00	0.00	0.00
FENUR	0.00	0.00	0.00	0.04	0.04	0.12	0.06	0.06	0.00	0.07	0.00	0.03	0.00	0.06
FL	7.26	228.6	0.00	173.6	8.04	446.0	3.82	536.3	4.69	265.6	5.83	199.5	12.20	156.1
FLU	4.12	2.81	4.57	9.31	4.56	19.62	2.17	32.13	2.66	18.12	3.31	6.74	6.92	14.09
HBCDA	0.00	0.00	0.00	0.00	0.00	0.00	0.00	0.16	0.00	0.00	0.00	0.00	0.00	0.50
HBCDBG	0.30	0.00	0.33	0.00	0.00	0.00	0.00	0.00	0.00	0.00	0.00	0.00	0.50	0.50
HCB	0.00	56.35	0.00	51.40	0.00	72.80	0.06	50.66	0.07	44.02	0.09	48.71	0.00	64.02
HCHA	0.00	4.43	0.00	4.36	0.00	5.86	0.00	5.25	0.00	4.95	0.00	5.06	0.00	5.03
HCHB	0.00	0.00	0.00	0.00	0.00	0.00	0.00	0.00	0.00	0.00	0.00	0.00	0.00	0.00
HCHD	0.00	0.00	0.00	0.83	0.00	0.83	0.00	0.00	0.00	0.00	0.00	0.00	0.00	0.00
HCHG	0.00	0.75	0.00	2.22	0.00	6.82	0.00	6.48	0.00	3.43	0.00	4.07	0.00	0.44
HEXAZIN	0.00	0.00	0.00	0.00	0.00	0.00	0.00	0.00	0.00	0.00	0.00	0.00	0.00	0.00
I123P	0.00	0.00	0.00	0.00	16.52	9.72	15.22	7.27	7.34	5.27	6.64	0.00	0.00	0.00
IRGAROL	0.00	0.00	0.00	0.00	0.00	0.00	0.00	0.00	0.00	0.00	0.00	0.00	0.00	0.00

A1 Table 1 continued:

pg/m ³	09AT 4		09AT 5		09AT 7		09AT 8		09AT 9		09AT 11		09AT 12	
	GFF	PXP	GFF	PXP	GFF	PXP	GFF	PXP	GFF	PXP	GFF	PXP	GFF	PXP
ISOD	0.00	0.00	0.00	0.00	0.00	0.00	0.00	0.00	0.00	0.00	0.00	0.00	0.00	0.00
ISOPRUR	0.00	0.00	0.00	0.00	0.28	0.00	0.06	0.00	0.23	0.00	0.09	0.00	0.00	0.06
LINUR	0.00	0.00	0.00	0.00	0.00	0.00	1.35	0.49	0.00	0.00	0.00	0.00	0.00	0.00
MALATH	0.00	0.00	0.00	0.00	0.00	0.00	0.00	0.21	0.00	0.00	0.00	0.00	0.00	0.00
MCPA	0.00	n.q.	0.00	n.q.	5.68	n.q.	8.84	n.q.	0.56	n.q.	0.00	n.q.	0.00	n.q.
MECOPR	0.00	n.q.	0.00	n.q.	0.00	n.q.	0.00	n.q.	0.00	n.q.	0.00	n.q.	0.00	n.q.
METAZCHL	0.00	0.00	0.00	0.00	0.61	0.00	0.06	0.00	0.21	0.07	0.00	0.19	0.00	0.19
METHABZT	0.00	0.00	0.00	0.00	0.00	0.00	0.00	0.00	0.00	0.00	0.00	0.00	0.00	0.00
METOLA	0.51	0.00	0.86	0.91	1.46	0.00	0.72	0.00	0.34	0.00	0.12	0.00	0.00	1.38
NAPROX	0.00	n.q.	0.00	n.q.	0.00	n.q.	0.00	n.q.	0.00	n.q.	0.00	n.q.	0.00	n.q.
OXAZEP	0.00	0.00	0.00	0.00	0.00	0.00	0.00	0.00	0.00	0.00	0.00	0.00	0.00	0.00
PENDIMETH	0.19	4.13	0.45	0.33	1.90	12.27	0.00	12.20	0.00	0.58	0.15	1.94	0.89	3.27
PFBS	0.00	0.21	0.04	0.08	0.00	0.08	0.00	0.04	0.00	0.05	0.00	0.14	0.00	0.13
PFDEA	0.00	0.00	0.00	0.21	0.00	0.82	0.00	0.35	0.00	0.43	0.00	0.00	0.00	0.00
PFHPA	0.14	0.07	0.19	0.08	0.13	0.08	0.06	0.04	0.10	0.15	0.10	0.06	0.13	0.13
PFHXA	0.07	0.11	0.08	0.12	0.04	0.12	0.04	0.06	0.05	0.22	0.03	0.09	0.00	0.19
PFHXS	0.07	0.13	0.08	0.08	0.08	0.08	0.04	0.04	0.00	0.05	0.03	0.11	0.06	0.13
PFNOA	0.11	0.00	0.12	0.00	0.12	0.21	0.06	0.00	0.07	0.12	0.32	0.15	0.19	0.00
PFOA	0.91	0.82	1.01	0.91	0.79	0.00	0.50	0.00	0.67	0.53	0.59	0.66	0.38	1.38
PFOS	0.26	1.01	0.29	1.12	0.29	0.37	0.28	0.53	0.17	0.65	0.00	0.81	0.00	1.70
PFOSA	0.00	0.00	0.00	0.00	0.00	0.00	0.06	0.00	0.22	0.60	0.00	0.75	0.00	0.00
PHEN	2.13	92.54	2.37	139.0	2.36	300.1	3.35	360.0	4.11	211.6	15.18	94.92	3.59	94.64
PIRIMIC	0.00	0.00	0.00	0.00	0.00	0.00	0.00	0.00	0.00	0.00	0.00	0.00	0.00	0.00
PRIMID	0.00	0.00	0.00	0.00	46.01	0.00	5.09	0.00	9.76	0.00	0.00	0.00	0.00	0.00
PROMETR	0.19	0.00	0.21	0.00	0.21	0.00	0.10	0.00	0.12	0.00	0.15	0.00	0.31	0.00
PROPAZ	0.00	0.00	0.00	0.00	0.00	0.00	0.00	0.00	0.00	0.00	0.00	0.00	0.00	0.00
PYR	0.00	0.00	2.49	4.16	2.49	4.15	3.53	13.62	1.45	7.25	1.80	3.01	3.77	6.29
QCB	0.00	12.37	0.00	11.64	0.00	15.98	0.00	9.83	0.00	11.72	0.00	10.79	0.00	14.91
SIMAZ	0.00	0.00	0.00	0.00	0.00	0.00	0.76	0.00	0.00	0.00	0.00	0.00	0.00	0.00
TBEP	0.00	0.00	0.00	0.00	0.00	0.00	0.00	2.30	0.00	0.00	0.00	0.00	0.00	0.00
TBP	4.79	21.04	5.32	23.36	18.74	0.00	40.96	0.00	11.88	0.00	10.92	16.90	17.31	35.35
TERBAZ	0.73	0.37	1.32	1.25	16.54	1.24	9.37	6.06	3.86	0.73	0.91	2.01	0.00	1.89
TERBUTR	0.00	0.00	0.00	0.00	0.08	0.00	0.04	0.00	0.00	0.00	0.00	0.00	0.00	0.13
TPP	1.87	0.00	14.89	5.86	36.28	5.85	13.62	8.33	19.47	0.00	4.22	4.24	3.15	8.87
TRIFLU	0.00	3.37	0.00	1.32	0.00	2.05	0.00	3.22	0.00	0.36	0.00	0.45	0.00	4.13

pg/m ³	PE 1		PE 3		PE 4		PE 6		PE 7		PE 8		PE 9	
	GFF	PXP	GFF	PXP	GFF	PXP	GFF	PXP	GFF	PXP	GFF	PXP	GFF	PXP
24-D	0.36	n.q.	0.00	n.q.	1.17	n.q.	11.51	n.q.	0.00	n.q.	0.00	n.q.	0.00	n.q.
ACE	0.00	44.98	0.00	303.9	0.00	150.8	0.00	57.61	0.00	157.2	0.00	293.9	0.00	31.61
ACY	0.00	0.00	0.00	0.00	0.00	90.52	0.00	0.00	0.00	0.00	0.00	0.00	0.00	148.3
ALD	0.00	0.00	0.00	0.00	0.00	0.00	0.00	0.00	0.00	0.00	0.00	0.00	0.00	0.00
AMETRYN	0.00	0.00	0.00	0.00	0.00	0.00	0.00	0.00	0.00	0.00	0.00	0.00	0.00	0.00
ANT	0.00	0.00	0.00	0.00	0.00	97.81	0.00	0.00	0.00	0.00	0.00	0.00	0.00	73.98
ATRAZ	0.00	0.00	0.00	0.00	0.00	0.00	0.94	0.00	0.00	0.00	0.00	0.00	0.00	0.00
AZINPH-E	0.00	0.00	0.00	0.00	0.00	0.00	0.00	0.00	0.00	0.00	0.00	0.00	0.00	0.00
AZINPH-M	0.00	0.00	0.00	0.00	0.00	0.00	0.00	0.00	0.00	0.00	0.00	0.00	0.00	0.00
BAA	0.00	0.00	0.00	0.00	0.00	0.00	0.00	0.00	19.92	0.00	25.61	0.00	15.80	0.00
BAP	0.00	0.00	11.78	0.00	6.75	0.00	20.16	0.00	13.95	0.00	49.84	22.79	11.06	0.00
BBF	0.00	0.00	16.83	0.00	9.65	9.65	28.80	0.00	19.92	0.00	75.32	0.00	15.80	0.00

A1 Table 1 continued:

pg/m ³	PE 1		PE 3		PE 4		PE 6		PE 7		PE 8		PE 9	
	GFF	PXP	GFF	PXP	GFF	PXP	GFF	PXP	GFF	PXP	GFF	PXP	GFF	PXP
BENTAZ	0.07	0.00	0.00	0.00	0.00	0.01	0.00	0.00	0.00	0.00	0.00	0.00	0.00	0.02
BGHIP	0.00	29.66	17.62	22.20	11.91	0.00	14.40	0.00	19.92	0.00	48.10	0.00	7.90	0.00
CARBAMAZ	0.00	0.00	0.00	0.00	0.00	0.00	0.00	0.00	0.00	0.00	0.00	0.00	0.00	0.00
CARBEND	0.00	0.00	0.00	0.00	0.67	0.00	0.00	0.00	0.57	0.00	0.00	0.00	0.00	0.00
CB138	0.67	1.73	0.00	2.49	0.29	1.48	0.00	2.63	0.60	1.75	0.00	0.82	0.00	0.57
CB153	1.09	8.22	0.82	2.33	0.15	3.47	0.00	2.91	3.25	1.67	0.00	0.36	0.00	0.67
CB28	0.00	5.84	0.00	4.93	0.00	6.61	0.00	4.91	0.00	9.06	0.00	2.78	0.00	2.47
CB52	0.00	2.51	0.00	2.56	0.00	4.71	0.00	3.31	0.00	3.63	0.00	2.18	0.00	1.28
CHLORFENV	0.00	0.47	0.00	0.00	0.00	0.00	0.00	0.00	0.00	0.00	0.00	0.00	0.00	0.00
CHLORTUR	0.00	0.00	0.00	0.00	0.00	0.00	0.00	0.00	0.00	0.00	0.00	0.00	0.00	0.00
CHRTR	0.00	0.00	16.83	0.00	9.65	0.00	0.00	0.00	0.00	0.00	22.79	0.00	0.00	0.00
CLOFIBRS	0.00	n.q.	0.00	n.q.	0.00	n.q.	0.00	n.q.	0.00	n.q.	0.00	n.q.	0.00	n.q.
DBAHA	0.00	0.00	0.00	0.00	0.00	0.00	0.00	0.00	0.00	0.00	22.79	0.00	0.00	0.00
DDDPP	0.67	0.67	0.00	0.50	0.00	0.29	0.00	0.00	0.00	0.60	0.00	0.68	0.00	0.00
DDEPP	0.67	2.47	0.00	1.71	0.29	1.34	0.00	2.49	0.00	13.13	0.00	2.04	0.00	1.31
DDTOP	0.00	0.67	0.00	0.50	0.00	0.67	0.00	0.86	0.00	1.46	0.00	0.68	0.00	0.00
DDTPP	0.81	2.13	0.00	1.45	0.00	1.90	0.00	1.60	0.00	2.05	0.00	0.88	0.00	0.71
DEATRAZ	0.00	0.00	0.00	0.00	0.00	0.00	0.00	0.00	0.00	0.00	0.00	0.00	0.00	0.00
DIAZINON	0.00	0.00	0.00	0.00	0.00	0.00	0.00	0.00	0.00	0.79	0.00	0.00	0.00	0.37
DICHLPR	0.00	n.q.	0.00	n.q.	0.00	n.q.	0.00	n.q.	0.00	n.q.	0.00	n.q.	0.00	n.q.
DICLOF	0.00	n.q.	0.00	n.q.	0.00	n.q.	0.00	n.q.	0.00	n.q.	0.00	n.q.	0.00	n.q.
DIELD	0.00	1.76	0.50	2.46	0.00	3.52	0.00	2.29	0.00	11.36	0.68	3.11	0.00	1.90
DIMETH	0.00	0.00	0.34	0.00	0.00	0.00	0.12	0.00	0.00	0.00	0.00	0.00	0.00	0.00
DIURON	0.00	12.59	0.00	38.81	0.00	21.82	0.00	14.11	0.00	30.41	0.00	11.36	0.00	37.83
END	0.00	0.00	0.00	0.00	0.00	0.00	0.00	0.00	0.00	0.00	0.00	0.00	0.00	0.00
FENUR	0.78	17.23	0.37	2.93	0.42	3.66	0.14	2.07	0.10	0.48	0.05	0.55	0.03	0.38
FL	0.00	571.2	0.00	772.7	0.00	762.4	0.00	767.6	0.00	1054	0.00	1094	0.00	442.7
FLU	22.49	138.8	16.83	68.44	9.65	111.5	28.80	46.68	19.92	74.07	59.31	142.1	0.00	148.6
HBCDA	0.00	0.00	0.27	0.00	0.00	0.00	0.00	0.00	0.32	0.00	0.36	0.00	0.00	0.00
HBCDBG	0.36	0.00	0.27	0.00	0.15	0.15	0.46	0.46	0.00	0.00	0.00	0.00	0.25	0.00
HCB	0.47	64.13	0.10	57.29	0.06	57.16	0.00	67.66	0.00	55.96	0.14	54.38	0.00	58.95
HCHA	0.00	4.63	0.00	4.52	0.00	5.32	0.00	5.23	0.00	5.02	0.00	4.62	0.00	4.73
HCHB	0.00	0.00	0.00	0.00	0.00	0.59	0.00	0.86	0.00	0.60	0.00	0.68	0.00	0.00
HCHD	0.00	0.00	0.00	0.00	0.00	0.29	0.00	0.86	0.00	0.60	0.00	0.00	0.00	0.00
HCHG	0.00	5.66	0.00	3.71	0.00	15.16	0.86	9.00	0.00	15.74	0.00	3.24	0.00	2.05
HEXAZIN	0.00	0.00	0.00	0.00	0.00	0.00	0.00	0.00	0.00	0.00	0.00	0.00	0.00	0.00
I123P	0.00	0.00	13.46	0.00	7.72	0.00	0.00	0.00	15.94	0.00	45.55	0.00	0.00	0.00
IRGAROL	0.00	0.00	0.00	0.00	0.00	0.00	0.00	0.00	0.00	0.00	0.00	0.00	0.00	0.00
ISOD	1.01	0.00	0.76	0.00	0.00	0.00	1.30	0.00	2.24	0.00	0.00	0.00	0.00	0.00
ISOPRUR	0.00	0.00	0.00	0.00	0.14	0.00	0.06	0.00	0.00	0.00	0.00	0.00	0.00	0.00
LINUR	0.00	0.00	0.00	0.00	0.00	0.00	0.00	0.00	0.00	0.30	0.00	0.00	0.00	0.00
MALATH	0.00	0.00	0.00	0.00	0.00	0.00	0.00	0.00	0.00	0.00	0.00	0.00	0.00	0.00
MCPA	0.00	n.q.	0.47	n.q.	0.63	n.q.	0.29	n.q.	2.46	n.q.	0.00	n.q.	0.00	n.q.
MECOPR	0.00	n.q.	0.00	n.q.	0.00	n.q.	0.00	n.q.	0.53	n.q.	0.00	n.q.	0.00	n.q.
METAZCHL	6.70	0.00	1.22	0.03	50.37	4.31	27.50	0.36	84.94	3.32	16.50	0.11	5.35	0.29
METHABZT	0.00	0.00	0.00	0.00	0.00	0.00	0.00	0.00	0.00	0.00	0.00	0.00	0.00	0.00
METOLA	0.44	0.11	0.37	0.00	0.73	0.43	0.35	0.00	0.29	0.04	0.00	0.00	0.05	0.03
NAPROX	0.00	n.q.	0.00	n.q.	0.00	n.q.	0.00	n.q.	0.00	n.q.	0.00	n.q.	0.00	n.q.
OXAZEP	0.00	0.00	0.00	0.00	0.00	0.00	0.00	0.00	0.00	0.00	0.00	0.00	0.00	0.00
PENDIMETH	0.51	0.63	0.17	0.17	0.04	0.65	0.12	0.29	0.20	10.61	0.99	6.91	0.06	1.33
PFBS	0.00	0.07	0.00	0.03	0.00	0.00	0.00	0.06	0.00	0.06	0.00	0.07	0.00	0.11

A1 Table 1 continued:

pg/m ³	PE 1		PE 3		PE 4		PE 6		PE 7		PE 8		PE 9	
	GFF	PXP	GFF	PXP	GFF	PXP	GFF	PXP	GFF	PXP	GFF	PXP	GFF	PXP
PFDEA	0.00	0.00	0.17	0.00	0.10	0.00	0.00	0.00	0.00	0.00	0.00	0.00	0.00	0.00
PFHPA	0.07	0.00	0.05	0.20	0.03	0.24	0.00	0.19	0.06	0.00	0.05	0.00	0.05	0.00
PFHXA	0.07	0.13	0.05	0.00	0.03	0.16	0.09	0.00	0.06	0.12	0.07	0.00	0.05	0.00
PFHXS	0.07	0.00	0.05	0.03	0.02	0.00	0.06	0.06	0.04	0.04	0.07	0.05	0.05	0.11
PFNOA	0.23	0.38	0.08	0.00	0.05	0.13	0.06	0.00	0.04	0.00	0.05	0.00	0.08	0.00
PFOA	0.94	1.51	0.78	0.37	1.10	0.65	0.74	0.00	0.65	1.33	1.13	0.00	0.71	0.00
PFOS	0.48	0.36	0.39	0.27	0.27	0.15	0.74	0.00	0.27	0.32	0.15	0.36	0.34	0.73
PFOSA	0.20	1.98	0.15	0.00	0.02	0.85	0.06	0.00	0.04	1.75	0.05	0.00	0.03	0.00
PHEN	0.00	477.7	0.00	771.4	9.65	1372	0.00	910.2	19.92	1060	58.63	1050	0.00	748.8
PIRIMIC	0.00	0.00	0.00	0.00	0.00	0.00	0.00	0.00	0.00	0.00	0.00	0.00	0.00	0.00
PRIMID	0.00	0.00	0.00	0.00	0.00	0.00	0.00	0.00	0.00	0.00	0.00	0.00	0.00	0.00
PROMETR	0.04	0.00	0.03	0.00	0.00	0.00	0.06	0.00	0.00	0.00	0.00	0.00	0.03	0.00
PROPAZ	0.00	0.00	0.00	0.00	0.00	0.00	0.00	0.00	0.00	0.00	0.00	0.00	0.00	0.00
PYR	0.00	479.9	13.46	144.8	7.72	110.8	23.04	34.05	15.94	23.55	42.86	80.78	0.00	137.8
QCB	0.00	10.71	0.00	8.01	0.00	9.22	0.00	8.25	0.00	8.91	0.00	9.55	0.00	8.90
SIMAZ	0.70	0.00	0.00	0.00	0.00	0.00	0.00	0.00	0.00	0.00	0.00	0.00	0.00	0.00
TBEP	0.81	17.95	0.61	0.00	0.35	2.75	1.04	0.00	0.72	0.00	0.82	0.00	0.00	33.52
TBP	40.54	0.00	39.09	0.00	71.98	21.18	37.81	0.00	47.47	0.00	9.21	0.00	14.26	4.90
TERBAZ	0.00	0.20	0.00	0.03	0.00	0.21	0.00	0.06	0.00	0.18	0.00	0.05	0.00	0.14
TERBUTR	0.00	0.00	0.00	0.00	0.02	0.00	0.06	0.00	0.04	0.00	0.05	0.00	0.00	0.00
TPP	20.30	131.1	19.77	0.00	23.83	281.5	28.25	0.00	22.72	38.73	13.14	0.00	3.45	429.5
TRIFLU	0.00	1.44	0.00	1.08	0.00	2.63	2.72	19.89	0.60	80.65	0.00	23.07	0.00	1.01

pg/m ³	PE 10		PE 11		PE 15		PE 16		PE 17		PE 18		10AT 1	
	GFF	PXP	GFF	PXP	GFF	PXP	GFF	PXP	GFF	PXP	GFF	PXP	GFF	PXP
24-D	0.00	n.q.	0.00	n.q.	0.00	n.q.	0.00	n.q.	0.00	n.q.	0.00	n.q.	0.00	n.q.
ACE	0.00	92.30	0.00	0.00	0.00	0.00	0.00	0.00	0.00	0.00	0.00	70.43	2.64	273.0
ACY	0.00	0.00	0.00	0.00	0.00	0.00	0.00	0.00	0.00	0.00	0.00	0.00	9.42	16.58
ALD	0.00	0.00	0.00	0.00	0.00	0.00	0.00	0.00	0.00	0.00	0.00	0.00	0.00	0.00
AMETRYN	0.00	0.00	0.00	0.00	0.00	0.00	0.00	0.00	0.00	0.00	0.00	0.00	0.00	0.00
ANT	0.00	0.00	0.00	0.00	0.00	0.00	0.00	0.00	0.00	0.00	0.00	0.00	9.42	110.2
ATRAZ	0.00	0.00	0.00	0.00	0.00	0.00	0.00	0.00	0.00	0.00	0.00	0.00	0.00	0.00
AZINPH-E	0.00	0.00	0.00	0.00	0.00	0.00	0.00	0.00	0.00	0.00	0.00	0.00	0.00	0.00
AZINPH-M	0.00	0.00	0.00	0.00	0.00	0.00	0.00	0.00	0.00	0.00	0.00	0.00	0.00	0.00
BAA	0.00	0.00	0.00	0.00	0.00	0.00	0.00	0.00	0.00	0.00	0.00	0.00	9.52	22.04
BAP	12.33	0.00	11.25	0.00	0.00	0.00	0.00	0.00	0.00	0.00	24.65	0.00	12.78	7.60
BBF	17.62	0.00	16.07	0.00	0.00	0.00	0.00	0.00	0.00	0.00	0.00	0.00	0.00	0.00
BENTAZ	0.00	0.02	0.03	0.00	0.00	0.00	0.00	0.00	0.00	0.05	0.07	0.00	0.06	0.00
BGHIP	21.21	0.00	8.03	0.00	0.00	0.00	0.00	0.00	23.56	0.00	17.61	0.00	11.97	0.00
CARBAMAZ	0.00	0.00	0.00	0.00	0.00	0.00	0.00	0.00	0.00	0.00	0.00	0.00	0.00	0.00
CARBEND	0.00	0.00	0.00	0.00	0.00	0.00	0.00	0.00	0.00	0.00	0.00	0.00	0.00	0.00
CB138	0.00	0.63	0.00	0.58	0.00	0.19	0.00	0.78	0.00	0.57	0.00	0.42	0.00	3.71
CB153	0.00	1.08	0.00	0.26	0.26	0.26	0.35	0.74	0.00	0.28	0.00	0.56	0.00	3.81
CB28	0.00	5.25	0.00	2.60	0.00	2.16	0.00	2.94	0.00	1.04	0.00	2.86	0.63	8.70
CB52	0.00	6.93	0.00	0.58	0.00	1.99	0.00	3.69	0.00	1.70	0.00	4.48	0.00	10.26
CHLORFENV	0.00	0.00	0.00	0.00	0.00	0.00	0.00	0.00	0.00	0.00	0.00	0.00	0.00	0.00
CHLORTUR	0.00	0.00	0.00	0.00	0.00	0.00	0.00	0.00	0.00	0.00	0.00	0.00	0.00	0.00
CHRTR	0.00	0.00	0.00	0.00	0.00	0.00	0.00	0.00	0.00	0.00	0.00	0.00	28.84	34.16
CLOFIBRS	0.00	n.q.	0.00	n.q.	0.00	n.q.	0.00	n.q.	0.00	n.q.	0.00	n.q.	0.00	n.q.
DBAHA	0.00	0.00	0.00	0.00	0.00	0.00	0.00	0.00	0.00	0.00	0.00	0.00	16.51	9.42

A1 Table 1 continued:

pg/m ³	PE 10		PE 11		PE 15		PE 16		PE 17		PE 18		10AT 1	
	GFF	PXP	GFF	PXP	GFF	PXP	GFF	PXP	GFF	PXP	GFF	PXP	GFF	PXP
DDPP	0.00	0.53	0.00	0.16	0.00	0.00	0.00	0.00	0.00	0.00	0.00	0.35	0.00	0.63
DDEPP	0.00	12.54	0.00	1.39	0.00	1.39	0.00	1.45	0.00	1.41	0.00	2.34	0.00	3.79
DDTOP	0.00	1.65	0.00	0.48	0.00	0.00	0.00	0.00	0.00	0.00	0.00	1.06	0.00	1.29
DDTPP	0.00	1.85	0.00	0.64	0.00	0.72	0.00	0.77	0.00	1.25	0.00	1.11	0.00	1.45
DEATRAZ	0.00	0.00	0.00	0.00	0.00	0.00	0.00	0.00	0.00	0.00	0.00	0.00	0.00	0.00
DIAZINON	0.00	2.66	0.00	0.16	0.00	0.00	0.00	0.00	0.00	0.47	0.00	1.06	0.00	0.00
DICHLPR	0.00	n.q.	0.00	n.q.	0.00	n.q.	0.00	n.q.	0.00	n.q.	0.00	n.q.	7.26	n.q.
DICLOF	0.00	n.q.	0.00	n.q.	0.00	n.q.	0.00	n.q.	0.00	n.q.	0.00	n.q.	0.00	n.q.
DIELD	0.00	12.97	0.00	2.44	0.00	1.54	0.00	1.54	0.00	2.41	0.00	2.57	0.00	1.26
DIMETH	0.00	0.00	0.00	0.00	0.00	0.00	0.00	0.00	0.00	0.00	0.00	0.00	0.00	0.00
DIURON	0.00	26.23	0.00	36.35	0.00	0.97	0.00	148.7	0.00	33.64	0.00	20.26	0.00	19.22
END	0.00	0.00	0.00	0.00	0.00	0.00	0.00	0.00	0.00	0.00	0.00	0.00	0.00	0.00
FENUR	0.04	0.42	0.03	0.39	0.03	1.15	0.04	4.42	0.09	0.00	0.07	0.85	0.66	0.00
FL	0.00	654.4	0.00	179.1	0.00	187.4	0.00	185.6	0.00	207.1	0.00	560.7	7.35	519.8
FLU	17.62	84.38	16.07	5.05	0.00	57.15	0.00	126.6	0.00	14.80	35.22	84.93	4.02	291.4
HBCDA	0.00	0.00	0.00	0.00	0.00	0.00	0.00	0.00	0.00	0.00	0.00	0.00	0.00	0.00
HBCDBG	0.00	0.00	0.26	0.00	0.26	0.00	0.00	0.00	0.75	0.00	0.56	0.00	0.50	0.00
HCB	0.00	51.55	0.10	52.25	0.00	48.50	0.00	65.18	0.00	70.04	0.21	68.00	0.19	88.40
HCHA	0.00	3.23	0.00	5.60	0.00	4.90	0.00	4.64	0.00	5.80	0.00	4.46	0.94	8.82
HCHB	0.00	0.53	0.00	0.00	0.00	0.48	0.00	0.65	0.00	1.41	0.00	0.00	0.00	1.26
HCHD	0.00	0.00	0.00	0.00	0.00	0.00	0.00	0.00	0.00	0.00	0.00	0.00	0.00	1.26
HCHG	0.00	9.52	0.00	2.00	0.00	1.30	0.00	1.87	0.00	1.23	0.00	2.46	0.00	7.38
HEXAZIN	0.00	0.00	0.00	0.00	0.00	0.00	0.00	0.00	0.00	0.00	0.00	0.00	0.00	0.00
I123P	14.09	0.00	0.00	0.00	0.00	0.00	0.00	0.00	0.00	0.00	0.00	0.00	14.54	0.00
IRGAROL	0.00	0.00	0.00	0.00	0.00	0.00	0.00	0.00	0.00	0.00	0.00	0.00	0.00	0.00
ISOD	0.00	0.00	0.00	0.00	0.00	0.00	0.00	0.00	0.00	0.00	0.00	0.00	0.00	0.00
ISOPRUR	0.00	0.00	0.00	0.00	0.00	0.00	0.00	0.00	0.00	0.00	0.00	0.00	2.52	0.06
LINUR	0.28	0.00	0.00	0.00	0.00	0.00	0.00	0.00	0.00	0.00	0.00	0.00	0.00	0.00
MALATH	0.00	0.00	0.00	0.00	0.00	0.00	0.00	0.00	0.00	0.00	0.00	0.00	0.00	0.00
MCPA	0.00	n.q.	0.00	n.q.	0.00	n.q.	0.00	n.q.	0.00	n.q.	0.00	n.q.	0.00	n.q.
MECOPR	0.00	n.q.	0.00	n.q.	0.00	n.q.	0.00	n.q.	0.00	n.q.	0.00	n.q.	1.38	n.q.
METAZCHL	33.75	13.30	3.02	0.34	1.80	0.59	1.10	0.11	1.92	0.00	2.28	0.44	1.12	0.06
METHABZT	0.00	0.00	0.00	0.00	0.00	0.00	0.00	0.00	0.00	0.00	0.00	0.00	0.00	0.00
METOLA	0.15	0.09	0.00	0.03	0.00	0.03	0.00	0.04	0.00	0.09	0.00	0.00	1.89	5.73
NAPROX	0.00	n.q.	0.00	n.q.	0.00	n.q.	0.00	n.q.	0.00	n.q.	0.00	n.q.	0.00	n.q.
OXAZEP	0.00	0.00	0.00	0.00	0.00	0.00	0.00	0.00	0.00	0.00	0.00	0.00	0.00	0.00
PENDIMETH	0.07	8.23	0.00	0.45	0.00	1.26	0.22	0.00	0.47	1.32	0.35	0.35	2.82	22.95
PFBS	0.04	0.04	0.00	0.05	0.03	0.05	0.00	0.07	0.00	0.09	0.11	0.11	0.00	0.11
PFDEA	0.00	0.00	0.00	0.00	0.00	0.00	0.00	0.00	0.00	0.00	0.00	0.00	0.00	0.00
PFHPA	0.13	0.00	0.05	0.00	0.03	0.00	0.07	0.00	0.00	0.00	0.07	0.00	0.09	0.00
PFHXA	0.12	0.11	0.05	0.27	0.03	0.00	0.07	0.13	0.09	0.28	0.07	0.21	0.09	0.00
PFHXS	0.04	0.00	0.05	0.05	0.05	0.05	0.04	0.00	0.00	0.09	0.07	0.00	0.09	1.06
PFNOA	0.27	0.00	0.08	0.00	0.16	0.00	0.04	0.00	0.00	0.00	0.00	0.00	0.16	0.00
PFOA	0.85	1.18	0.77	1.08	0.50	0.35	0.22	0.48	0.19	3.16	0.35	0.00	0.89	0.00
PFOS	0.30	0.00	0.22	0.26	0.22	0.26	0.04	1.00	0.09	0.75	0.07	0.00	1.00	0.57
PFOSA	0.16	1.55	0.03	1.41	0.03	1.40	0.04	1.91	0.00	12.49	0.32	0.00	0.06	0.00
PHEN	0.00	643.0	0.00	193.5	0.00	280.5	0.00	508.7	0.00	92.94	0.00	512.4	3.83	1144
PIRIMIC	0.00	0.00	0.00	0.00	0.00	0.00	0.00	0.00	0.00	0.00	0.00	0.00	0.00	0.00
PRIMID	0.00	0.00	0.00	0.00	0.00	0.00	0.00	0.00	0.00	0.00	0.00	0.00	0.00	0.00
PROMETR	0.00	0.00	0.03	0.00	0.03	0.00	0.04	0.00	0.09	0.00	0.00	0.00	0.00	0.00

A1 Table 1 continued:

pg/m ³	PE 10		PE 11		PE 15		PE 16		PE 17		PE 18		10AT 1	
	GFF	PXP	GFF	PXP	GFF	PXP	GFF	PXP	GFF	PXP	GFF	PXP	GFF	PXP
PROPAZ	0.00	0.00	0.00	0.00	0.00	0.00	0.00	0.00	0.00	0.00	0.00	0.00	0.00	0.00
PYR	14.09	20.82	12.86	0.00	0.00	56.53	0.00	76.95	0.00	0.00	0.00	41.63	4.96	148.9
QCB	0.00	9.01	0.00	10.32	0.00	7.04	0.00	10.42	0.00	7.75	0.00	9.69	0.94	22.22
SIMAZ	0.00	0.00	0.00	0.00	0.00	0.00	0.00	0.00	0.00	0.00	0.00	0.00	0.00	0.00
TBEP	0.63	0.00	0.00	0.00	0.00	6.00	0.00	13.78	0.00	14.03	0.00	19.67	16.90	12.31
TBP	62.77	16.33	6.49	4.98	22.34	4.94	22.37	20.12	57.44	43.69	81.09	75.20	37.48	70.61
TERBAZ	0.00	0.72	0.00	0.03	0.00	0.00	0.00	0.04	0.00	0.00	0.00	0.07	0.28	2.48
TERBUTR	0.00	0.00	0.00	0.00	0.00	0.00	0.00	0.00	0.00	0.00	0.00	0.00	0.09	0.09
TPP	22.81	34.25	7.56	0.00	7.00	0.00	4.73	733.3	3.39	0.00	7.68	1042	5.30	1917
TRIFLU	0.00	331.2	0.00	1.03	0.00	1.02	0.00	1.39	0.00	3.02	0.00	91.84	0.94	10.36

pg/m ³	10AT 2		10AT 3		10AT 4		10AT 5		10AT 6		10AT 7		RIS1	
	GFF	PXP	GFF	PXP	GFF	PXP	GFF	PXP	GFF	PXP	GFF	PXP	GFF	P pl
24-D	0.00	n.q.	2.92	n.q.	0.00	n.q.	0.00	n.q.	0.00	n.q.	0.00	n.q.	0.00	n.q.
ACE	6.07	29.41	0.00	41.12	1.37	34.42	2.17	13.86	1.61	44.79	1.65	24.41	0.00	902.3
ACY	7.28	4.27	0.00	3.51	0.00	0.00	0.00	0.00	0.00	3.37	0.00	3.46	9.86	602.1
ALD	0.00	0.00	0.00	0.00	0.00	0.00	0.00	0.00	0.00	0.00	0.00	0.00	0.00	0.00
AMETRYN	0.00	0.00	0.00	0.00	0.00	0.00	0.00	0.00	0.00	0.00	0.00	0.00	0.00	0.00
ANT	0.00	7.28	0.00	5.99	0.00	4.90	0.00	7.76	0.00	0.00	0.00	5.89	17.36	368.5
ATRAZ	0.00	0.00	0.00	0.00	0.00	0.00	0.00	0.00	0.00	0.00	0.00	0.00	0.00	0.00
AZINPH-E	0.00	0.00	0.00	0.00	0.00	0.00	0.00	0.00	0.00	0.00	0.00	0.00	0.00	0.00
AZINPH-M	0.00	0.00	0.00	0.00	0.00	0.00	0.00	0.00	0.00	0.00	0.00	0.00	0.00	0.00
BAA	0.00	1.60	2.99	0.00	2.45	0.00	0.00	0.00	5.84	0.00	5.82	0.00	178.1	50.72
BAP	0.00	0.00	3.99	0.00	3.27	0.00	0.00	0.00	10.11	0.00	8.21	0.00	341.3	3.21
BBF	7.28	0.00	12.70	0.00	4.90	0.00	7.76	0.00	19.59	0.00	14.71	0.00	691.2	8.37
BENTAZ	0.00	0.00	0.04	0.00	0.00	0.00	0.00	0.00	0.00	0.00	0.00	0.00	0.00	0.00
BGHIP	0.00	0.00	6.98	0.00	6.33	0.00	8.19	0.00	9.68	0.00	7.97	0.00	415.2	2.57
CARBAMAZ	0.00	0.00	0.00	0.00	0.00	0.00	0.00	0.00	0.00	0.00	0.00	0.00	16.60	0.17
CARBEND	0.00	0.00	0.26	0.00	0.00	0.00	0.00	0.00	0.00	0.00	0.00	0.00	0.00	0.00
CB138	0.00	0.97	0.00	0.80	0.00	0.65	0.00	1.03	0.00	0.77	0.00	0.79	0.96	2.46
CB153	0.00	0.73	0.36	0.60	0.00	0.49	0.00	0.26	0.00	0.58	0.35	0.20	0.77	2.68
CB28	0.49	2.30	0.00	2.56	0.00	1.86	0.52	1.17	0.00	2.04	0.39	2.11	0.22	8.09
CB52	0.00	1.49	0.00	0.99	0.00	0.39	0.00	0.62	0.00	0.46	0.00	0.47	0.00	7.52
CHLORFENV	0.00	0.00	0.00	0.00	0.00	0.00	0.00	0.00	0.00	0.00	0.00	0.00	0.00	0.00
CHLORTUR	0.00	0.00	0.00	0.00	0.00	0.00	0.00	0.00	0.00	0.00	0.00	0.00	0.17	0.00
CHRTR	21.21	4.03	19.84	3.31	15.14	2.71	22.91	4.29	20.59	3.18	19.34	3.26	315.0	110.4
CLOFIBRS	0.00	n.q.	0.00	n.q.	0.00	n.q.	0.00	n.q.	0.00	n.q.	0.00	n.q.	0.00	n.q.
DBAHA	0.00	0.00	0.00	0.00	0.00	0.00	0.00	0.00	10.07	0.00	0.00	0.00	61.46	0.00
DDPP	0.00	0.49	0.00	0.40	0.00	0.33	0.00	0.00	0.00	0.38	0.00	0.39	0.00	0.00
DDEPP	0.00	1.95	0.00	0.60	0.00	0.49	0.00	0.78	0.00	0.58	0.00	0.59	0.65	4.14
DDTOP	0.00	0.49	0.00	0.40	0.00	0.33	0.00	0.52	0.00	0.38	0.00	0.39	0.00	0.88
DDTPP	0.00	0.49	0.00	0.40	0.00	0.33	0.00	0.52	0.00	0.38	0.00	0.39	0.70	0.88
DEATRAZ	0.00	0.00	0.00	0.00	0.00	0.00	0.00	0.00	0.00	0.00	0.00	0.00	0.00	0.00
DIAZINON	0.00	0.00	0.00	0.00	0.00	0.00	0.00	0.00	0.00	0.00	0.00	0.00	0.52	0.54
DICHLPR	0.00	n.q.	0.00	n.q.	0.00	n.q.	0.00	n.q.	0.00	n.q.	0.00	n.q.	0.00	n.q.
DICLOF	0.00	n.q.	0.00	n.q.	0.00	n.q.	0.00	n.q.	0.00	n.q.	0.00	n.q.	0.32	n.q.
DIELD	0.00	0.97	0.00	0.80	0.00	1.55	0.00	1.03	0.00	1.79	0.00	0.79	0.00	4.31
DIMETH	0.00	0.00	0.00	0.00	0.00	0.00	0.00	0.00	0.00	0.00	0.00	0.00	0.03	0.00
DIURON	0.00	6.11	0.00	3.04	0.00	4.83	0.00	1.60	0.00	5.75	0.00	5.51	0.64	0.00
END	0.00	0.00	0.00	0.00	0.00	0.00	0.00	0.00	0.00	0.00	0.00	0.00	0.00	0.00

A1 Table 1 continued:

pg/m ³	10AT 2		10AT 3		10AT 4		10AT 5		10AT 6		10AT 7		RIS1	
	GFF	PXP	GFF	PXP	GFF	PXP	GFF	PXP	GFF	PXP	GFF	PXP	GFF	P pl
FENUR	0.00	0.00	0.00	0.00	0.00	0.00	0.00	105.5	0.00	0.00	0.10	0.00	1.50	0.89
FL	5.68	228.2	0.00	329.5	3.82	437.0	0.00	236.2	4.49	652.3	4.60	367.8	11.48	2491
FLU	3.11	24.32	2.56	0.00	2.09	0.00	3.31	0.00	2.45	0.00	2.52	0.00	156.6	1417
HBCDA	0.00	0.00	0.00	0.00	0.00	0.00	0.00	0.41	0.00	0.31	0.00	0.31	1.78	0.00
HBCDBG	0.39	0.00	0.00	0.00	0.26	0.00	0.41	0.00	0.31	0.00	0.31	0.00	4.44	0.10
HCB	0.15	65.09	0.00	70.47	0.10	66.88	0.16	61.12	0.12	76.38	0.12	69.71	0.93	42.81
HCHA	0.73	3.32	0.00	3.19	0.49	2.99	0.00	2.74	0.00	3.29	0.00	3.10	0.00	14.15
HCHB	0.00	0.00	0.00	0.00	0.00	0.00	0.00	0.00	0.00	0.00	0.00	0.00	0.00	0.84
HCHD	0.00	0.00	0.00	0.80	0.00	0.65	0.00	0.00	0.00	0.00	0.00	0.00	0.00	0.92
HCHG	0.00	2.19	0.00	2.73	0.00	1.88	0.00	1.03	0.00	2.43	0.00	2.59	0.00	61.88
HEXAZIN	0.00	0.00	0.00	0.00	0.00	0.00	0.00	0.00	0.00	0.00	0.00	0.00	0.00	0.00
I123P	0.00	0.00	8.52	0.00	7.18	0.00	5.17	0.00	11.62	0.00	9.59	0.00	362.4	3.21
IRGAROL	0.00	0.00	0.00	0.00	0.00	0.00	0.00	0.00	0.00	0.00	0.00	0.00	0.10	0.00
ISOD	0.00	0.00	0.00	0.00	0.00	0.00	0.00	0.00	0.00	0.00	0.00	0.00	0.00	0.00
ISOPRUR	0.05	0.05	0.90	0.00	0.00	0.00	0.00	0.00	0.04	0.00	0.04	0.00	18.91	0.25
LINUR	0.00	0.00	0.00	0.00	0.00	0.00	0.00	0.00	0.00	0.00	0.00	0.00	0.00	0.00
MALATH	0.00	0.00	0.00	0.00	0.00	0.00	0.00	0.00	0.00	0.00	0.00	0.00	0.00	0.00
MCPA	0.00	n.q.	11.06	n.q.	0.00	n.q.	0.00	n.q.	0.00	n.q.	0.00	n.q.	1.80	n.q.
MECOPR	0.00	n.q.	0.00	n.q.	0.00	n.q.	0.00	n.q.	0.00	n.q.	0.00	n.q.	0.00	n.q.
METAZCHL	0.12	0.05	1.36	0.00	0.08	0.00	0.05	0.00	0.04	0.00	0.04	0.00	0.44	0.00
METHABZT	0.00	0.00	0.00	0.00	0.00	0.00	0.00	0.00	0.00	0.00	0.00	0.00	0.00	0.00
METOLA	0.55	7.00	0.10	0.56	0.08	0.00	0.05	0.00	0.00	0.54	0.04	0.00	0.67	0.06
NAPROX	0.00	n.q.	0.00	n.q.	0.00	n.q.	0.00	n.q.	0.00	n.q.	0.00	n.q.	0.00	n.q.
OXAZEP	0.00	0.00	0.00	0.00	0.00	0.00	0.00	0.00	0.00	0.00	0.00	0.00	0.00	0.00
PENDIMETH	0.30	3.56	0.77	2.12	0.07	4.91	0.10	5.00	0.08	6.89	0.24	3.67	9.86	80.60
PFBS	0.05	0.28	0.00	0.20	0.00	0.06	0.00	0.09	0.00	0.07	0.00	0.07	0.25	0.01
PFDEA	0.00	0.00	0.00	0.44	0.00	0.00	0.00	0.00	0.00	0.00	0.00	0.00	0.06	0.20
PFHPA	0.18	0.00	0.06	0.00	0.05	0.00	0.05	0.00	0.04	0.00	0.06	0.00	0.00	0.08
PFHXA	0.07	0.15	0.06	0.00	0.03	0.00	0.00	0.00	0.00	0.00	0.06	0.00	0.00	0.06
PFHXS	0.24	0.13	0.06	0.04	0.12	0.03	0.05	0.05	0.00	0.04	0.00	0.00	0.04	0.01
PFNOA	0.27	0.29	0.04	0.00	0.08	0.00	0.05	0.00	0.04	0.00	0.04	0.00	0.04	0.12
PFOA	1.45	0.34	0.93	0.82	1.11	0.67	0.65	0.36	0.51	0.00	0.49	0.00	0.04	0.35
PFOS	1.49	1.30	0.64	1.07	0.81	0.88	0.22	0.00	0.16	0.35	0.13	0.35	4.12	0.10
PFOSA	0.05	0.00	0.10	0.00	0.08	0.00	0.05	0.00	0.10	0.00	0.20	0.00	0.24	0.08
PHEN	2.96	69.70	2.44	211.0	1.99	188.0	3.15	74.25	7.01	220.7	2.40	174.5	110.5	5699
PIRIMIC	0.00	0.00	0.00	0.00	0.00	0.00	0.00	0.00	0.00	0.00	0.00	0.00	0.00	0.00
PRIMID	0.00	0.00	0.00	0.00	0.00	0.00	0.00	0.00	0.00	0.00	0.00	0.00	0.00	0.00
PROMETR	0.00	0.00	0.00	0.00	0.00	0.00	0.00	0.00	0.04	0.00	0.04	0.00	0.00	0.00
PROPAPZ	0.00	0.00	0.00	0.00	0.00	0.00	0.00	0.00	0.00	0.00	0.00	0.00	0.00	0.00
PYR	3.83	0.00	3.15	0.00	2.58	0.00	4.08	0.00	3.03	0.00	3.10	0.00	156.3	1014
QCB	0.73	18.88	0.00	20.83	0.00	15.05	0.00	13.52	0.00	18.19	0.00	14.67	0.00	3.50
SIMAZ	0.00	0.00	0.00	0.00	0.00	0.00	0.00	0.00	0.00	0.00	0.00	0.00	0.00	0.00
TBEP	13.06	0.00	0.00	0.00	0.00	0.00	13.91	0.00	10.32	0.00	10.57	0.00	4.12	0.00
TBP	42.75	6.27	31.53	18.97	32.69	20.32	40.00	41.63	28.94	4.95	28.08	0.00	83.75	6.75
TERBAZ	0.10	4.73	0.47	0.20	0.07	0.00	0.00	0.00	0.00	0.00	0.00	0.20	0.10	0.03
TERBUTR	0.00	0.05	0.00	0.00	0.00	0.00	0.00	0.00	0.00	0.00	0.00	0.00	8.32	0.07
TPP	6.67	0.00	11.36	0.00	6.25	0.00	4.78	0.00	4.88	0.00	8.93	0.00	19.86	0.95
TRIFLU	0.00	0.73	0.00	0.60	0.00	0.49	0.00	0.78	0.00	0.58	0.00	0.59	0.00	5.41

A1 Table 1 continued:

pg/m ³	R1S2		R2S1		R2S2		R3S1		R3S2		R4S1		R4S2	
	GFF	P pl	GFF	P pl	GFF	P pl	GFF	P pl	GFF	PXP	GFF	P pl	GFF	PXP
24-D	0.00	n.q	0.00	n.q	0.00	n.q	0.00	n.q	0.00	n.q	7.48	n.q	8.84	n.q
ACE	2.27	747.6	0.00	514.2	0.00	512.5	0.00	1691	0.00	3299	0.00	573.5	0.00	1450
ACY	14.69	506.9	4.12	234.8	9.52	208.6	22.19	2485	24.00	3670	6.80	480.3	7.27	849.7
ALD	0.00	0.00	0.00	0.00	0.00	0.00	0.00	0.00	0.00	0.00	0.00	0.00	0.00	0.00
AMETRYN	0.00	0.00	0.00	0.00	0.00	0.00	0.00	0.00	0.00	0.00	0.00	0.00	0.00	0.00
ANT	21.09	430.3	4.12	217.8	8.48	246.1	31.77	1008	35.48	1164	6.80	181.2	7.27	199.0
ATRAZ	0.00	0.00	0.00	0.00	0.00	0.00	0.00	0.00	0.00	0.00	0.00	0.00	0.00	0.00
AZINPH-E	0.00	0.00	0.00	0.00	0.00	0.00	0.00	0.00	0.00	0.00	0.00	0.00	0.00	0.00
AZINPH-M	0.00	0.00	0.00	0.00	0.00	0.00	0.00	0.00	0.00	0.00	0.00	0.00	0.00	0.00
BAA	180.2	58.56	70.85	12.71	81.89	13.24	432.4	73.60	487.6	84.72	141.0	8.50	153.7	9.09
BAP	342.9	0.00	94.41	0.00	108.8	0.00	703.0	0.00	809.2	0.00	203.1	0.00	230.6	0.00
BBF	716.8	2.84	243.6	0.00	276.9	0.00	1151	0.00	1330	0.00	591.4	0.00	660.6	0.00
BENTAZ	0.00	0.00	0.00	0.00	0.00	0.00	0.00	0.00	0.00	0.00	0.00	0.00	0.00	0.00
BGHIP	425.6	0.00	126.6	0.00	142.3	0.00	599.1	0.00	659.0	0.00	262.5	0.00	286.6	0.00
CARBAMAZ	17.36	0.00	1.52	0.00	0.25	0.00	0.00	0.00	0.00	0.00	0.00	0.00	0.00	0.00
CARBEND	0.00	0.00	0.00	0.00	0.00	0.00	0.00	0.00	0.00	0.00	0.00	0.00	0.00	0.00
CB138	0.84	3.40	0.00	1.76	0.63	2.14	1.23	3.31	1.30	1.00	0.00	1.02	0.00	0.84
CB153	0.75	3.50	0.00	1.01	0.48	2.08	0.94	2.01	1.00	2.35	0.78	1.67	1.69	0.65
CB28	0.58	8.49	0.00	6.50	0.00	6.82	0.00	12.24	0.00	11.99	0.00	5.36	0.00	3.84
CB52	0.00	8.38	0.00	7.28	0.00	8.14	0.00	12.34	0.00	11.56	0.00	3.73	0.00	1.31
CHLORFENV	0.00	0.00	0.00	0.00	0.00	0.00	0.00	0.00	0.00	0.00	0.00	0.00	0.00	0.00
CHLORTUR	0.98	0.00	0.10	0.00	0.04	0.00	0.08	0.00	0.22	0.00	0.55	0.00	1.21	0.00
CHRTR	321.2	129.7	140.7	33.36	160.9	35.75	652.1	119.2	721.9	124.2	309.6	26.25	335.7	9.60
CLOFIBRS	0.00	n.q	0.00	n.q	0.00	n.q	0.00	n.q	0.00	n.q	2.76	n.q	2.54	n.q
DBAHA	63.12	0.00	17.87	0.00	19.39	0.00	90.92	0.00	103.0	0.00	40.84	0.00	44.82	0.00
DDPP	0.00	0.00	0.00	0.00	0.00	0.00	0.00	0.00	0.00	0.00	0.00	0.00	0.00	0.00
DDEPP	0.62	5.23	0.51	9.26	0.53	10.86	2.33	17.38	2.63	22.28	0.85	6.76	0.91	8.65
DDTOP	0.00	1.26	0.00	1.41	0.00	1.67	0.82	2.70	0.87	3.12	0.00	1.14	0.00	1.41
DDTPP	0.76	1.45	0.70	1.65	0.78	2.03	2.00	2.90	2.40	3.35	0.51	1.31	0.55	1.62
DEATRAZ	0.00	0.00	0.00	0.00	0.00	0.00	0.00	0.00	0.00	0.00	0.00	0.00	0.00	0.00
DIAZINON	0.37	1.26	0.10	0.10	0.11	0.00	1.03	0.42	0.92	0.22	0.93	0.00	0.96	0.00
DICHLPR	0.00	n.q	0.00	n.q	0.00	n.q	0.00	n.q	0.00	n.q	0.00	n.q	0.00	n.q
DICLOF	0.28	n.q	0.16	n.q	0.17	n.q	0.33	n.q	0.35	n.q	0.00	n.q	0.29	n.q
DIELD	0.00	4.61	0.00	2.66	0.00	2.64	0.00	4.46	0.00	4.75	0.00	3.73	0.00	3.95
DIMETH	0.06	0.00	0.04	0.00	0.04	0.00	0.08	0.00	0.22	0.00	0.00	0.00	0.00	0.00
DIURON	0.59	0.36	0.94	2.96	0.83	4.11	0.52	0.00	0.53	0.00	2.14	0.24	2.41	9.72
END	0.00	0.00	0.00	0.00	0.00	0.00	0.00	0.00	0.00	0.00	0.00	0.00	0.00	0.00
FENUR	0.68	0.66	0.77	0.34	0.46	0.26	1.98	0.68	1.34	48.21	2.90	0.34	1.39	0.00
FL	13.43	2382	5.15	2378	10.68	2784	22.99	6856	25.43	8646	17.08	2717	18.27	3665
FLU	193.5	2150	84.74	1486	96.45	1995	371.2	2940	414.5	3644	277.6	942.9	289.7	1114
HBCDA	1.92	0.00	0.16	0.00	0.53	0.00	2.18	0.33	2.20	0.00	0.85	0.27	0.91	0.00
HBCDBG	4.23	0.00	0.16	0.00	0.53	0.17	2.73	0.33	1.09	0.00	0.85	0.27	0.91	0.00
HCB	0.82	38.91	0.00	63.61	0.00	69.19	0.00	68.81	0.00	96.00	0.00	67.82	0.00	95.34
HCHA	0.00	13.84	0.00	7.80	0.00	7.93	0.00	7.68	0.00	11.06	0.00	5.48	0.00	6.27
HCHB	0.00	0.74	0.00	0.62	0.00	0.63	0.00	0.00	0.00	0.00	0.00	0.00	0.00	0.00
HCHD	0.00	0.86	0.00	0.72	0.00	0.74	0.00	1.44	0.00	1.52	0.00	1.19	0.00	0.00
HCHG	0.76	60.60	0.00	25.99	0.00	26.04	0.00	35.86	0.00	45.79	0.00	16.63	0.00	16.32
HEXAZIN	0.00	0.00	0.00	0.00	0.00	0.00	0.00	0.00	0.00	0.00	0.00	0.00	0.00	0.00
I123P	370.2	0.00	122.5	0.00	136.5	0.00	601.3	0.00	669.7	0.00	286.6	0.00	316.4	0.00
IRGAROL	0.09	0.00	0.02	0.00	0.02	0.00	0.08	0.00	0.09	0.00	0.00	0.00	0.00	0.00

A1 Table 1 continued:

pg/m ³	R1S2		R2S1		R2S2		R3S1		R3S2		R4S1		R4S2	
	GFF	P pl	GFF	P pl	GFF	P pl	GFF	P pl	GFF	PXP	GFF	P pl	GFF	PXP
ISOD	0.00	0.00	0.00	0.00	0.00	0.00	0.00	0.00	0.00	0.00	0.00	0.00	0.00	0.00
ISOPRUR	19.76	0.03	0.49	0.02	0.54	0.00	2.06	0.04	2.41	0.04	2.00	0.03	1.93	0.04
LINUR	0.00	0.00	0.00	0.00	0.00	0.00	0.00	0.00	0.00	0.00	0.00	0.00	0.00	0.00
MALATH	0.00	0.00	0.00	0.00	0.00	0.00	0.00	0.00	0.00	0.00	0.00	0.00	0.00	0.00
MCPA	1.48	n.q	0.00	n.q	0.00	n.q	0.00	n.q	0.00	n.q	0.00	n.q	0.00	n.q
MECOPR	0.00	n.q	0.00	n.q	0.00	n.q	0.00	n.q	0.00	n.q	0.00	n.q	0.00	n.q
METAZCHL	0.29	0.00	0.13	0.00	0.16	0.00	0.22	0.00	0.34	0.00	0.00	0.00	0.00	0.00
METHABZT	0.00	0.00	0.00	0.00	0.00	0.00	0.00	0.00	0.00	0.00	0.00	0.00	0.00	0.00
METOLA	0.77	0.28	0.42	0.04	0.35	0.04	0.70	0.08	0.99	0.09	1.14	0.07	1.22	0.04
NAPROX	0.00	n.q	0.00	n.q	0.00	n.q	0.00	n.q	0.00	n.q	0.00	n.q	0.00	n.q
OXAZEP	0.00	0.00	0.00	0.00	0.00	0.00	0.00	0.00	0.00	0.00	0.00	0.00	0.00	0.00
PENDIMETH	9.21	98.99	11.60	66.64	11.78	75.41	59.79	150.6	71.86	179.4	41.74	56.52	40.67	78.61
PFBS	0.22	0.01	0.00	0.02	0.00	0.02	0.08	0.04	0.09	0.13	0.00	0.03	0.00	0.26
PFDEA	0.05	0.06	0.04	0.10	0.04	0.11	0.08	0.21	0.09	0.96	0.00	0.17	0.00	1.05
PFHPA	0.00	0.02	0.00	0.02	0.00	0.02	0.00	0.04	0.00	0.13	0.00	0.03	0.00	0.11
PFHXA	0.00	0.02	0.00	0.04	0.00	0.04	0.00	0.08	0.00	0.30	0.00	0.07	0.00	0.25
PFHXS	0.05	0.01	0.00	0.02	0.00	0.02	0.00	0.04	0.00	0.04	0.00	0.03	0.00	0.04
PFNOA	0.03	0.11	0.00	0.06	0.00	0.02	0.00	0.04	0.00	0.13	0.00	0.10	0.00	0.00
PFOA	0.03	0.11	0.02	0.21	0.06	0.21	0.22	0.12	0.13	1.52	0.24	0.34	0.35	1.27
PFOS	3.99	0.03	0.07	0.06	0.09	0.17	0.86	0.12	1.10	0.80	0.20	0.10	0.18	1.14
PFOSA	0.20	0.07	0.04	0.04	0.04	0.04	0.27	0.00	0.09	0.09	0.03	0.07	0.04	0.07
PHEN	135.4	6350	53.81	5026	62.03	5687	214.4	11725	239.5	13618	159.7	3641	177.8	4081
PIRIMIC	0.00	0.00	0.00	0.00	0.00	0.00	0.00	0.00	0.00	0.00	0.00	0.00	0.00	0.00
PRIMID	1.65	0.00	0.00	0.00	0.53	0.00	2.89	0.00	11.49	0.00	0.00	0.00	0.00	0.00
PROMETR	0.00	0.00	0.00	0.00	0.00	0.00	0.00	0.00	0.00	0.04	0.00	0.00	0.00	0.00
PROPAZ	0.00	0.00	0.00	0.00	0.00	0.00	0.00	0.00	0.00	0.00	0.00	0.00	0.00	0.00
PYR	190.4	1392	76.22	893.3	86.96	1188	348.7	1863	383.1	2120	250.0	569.2	263.1	613.5
QCB	0.00	2.24	0.00	4.00	0.00	3.81	0.00	5.72	0.00	12.53	0.00	6.30	0.00	12.95
SIMAZ	0.00	0.00	0.00	0.00	0.00	0.00	0.00	0.00	0.00	0.00	0.00	0.00	0.00	0.00
TBEP	4.72	0.00	1.54	0.00	1.58	0.00	11.17	0.00	12.47	0.00	2.55	0.00	2.73	0.00
TBP	0.00	43.27	50.01	3.60	56.12	3.68	133.2	7.18	199.3	12.64	34.25	0.00	52.26	0.00
TERBAZ	0.09	0.08	0.00	0.02	0.06	0.02	0.00	0.04	0.00	0.09	0.00	0.00	0.00	0.04
TERBUTR	7.70	0.02	1.23	0.02	1.31	0.02	6.95	0.08	7.86	0.04	18.46	0.03	21.32	0.04
TPP	20.10	6.59	12.03	4.57	11.40	11.70	36.96	0.00	42.92	0.00	119.9	7.55	128.6	0.00
TRIFLU	0.00	5.56	0.00	18.46	0.00	21.67	0.00	8.57	0.00	11.43	0.00	2.90	0.00	3.55

pg/m ³	R5S1		R5S2		R6S1		R6S2		R7S1		R7S2		R8S1	
	GFF	P pl	GFF	PXP	GFF	P pl	GFF	P pl	GFF	P pl	GFF	P pl	GFF	PXP
24-D	0.00	n.q	0.00	n.q	0.00	n.q	0.00	n.q	0.00	n.q	0.00	n.q	0.00	n.q
ACE	0.00	393.6	0.00	793.7	0.00	786.8	0.00	863.9	0.00	1761	0.00	1806	0.00	1296
ACY	0.00	706.1	0.00	1063	26.95	838.4	29.53	913.9	15.83	2270	20.63	2467	134.7	1354
ALD	0.00	0.00	0.00	0.00	0.00	0.00	0.00	0.00	0.00	0.00	0.00	0.00	0.00	0.00
AMETRYN	0.00	0.00	0.00	0.00	0.00	0.00	0.00	0.00	0.00	0.00	0.00	0.00	0.00	0.00
ANT	0.00	180.2	0.00	189.8	23.57	311.5	26.53	383.5	22.81	443.6	30.45	562.0	85.78	145.8
ATRAZ	0.00	0.00	0.00	0.00	0.00	0.00	0.00	0.00	0.00	0.00	0.00	0.00	0.00	0.00
AZINPH-E	0.00	0.00	0.00	0.00	0.00	0.00	0.00	0.00	0.00	0.00	0.00	0.00	0.00	0.00
AZINPH-M	0.00	0.00	0.00	0.00	0.00	0.00	0.00	0.00	0.00	0.00	0.00	0.00	0.00	0.00
BAA	40.34	27.01	47.16	25.55	188.0	6.48	219.3	6.61	338.7	0.00	414.7	8.85	426.0	10.84
BAP	69.70	0.00	82.15	0.00	234.7	0.00	272.0	0.00	331.3	0.00	405.3	0.00	465.0	0.00
BBF	209.3	0.00	238.6	0.00	598.9	0.00	701.5	0.00	658.5	0.00	785.0	0.00	1059	0.00

A1 Table 1 continued:

pg/m ³	R5S1		R5S2		R6S1		R6S2		R7S1		R7S2		R8S1	
	GFF	P pl	GFF	PXP	GFF	P pl	GFF	P pl	GFF	P pl	GFF	P pl	GFF	PXP
BENTAZ	0.00	0.00	0.00	0.00	0.00	0.00	0.00	0.00	0.00	0.00	0.00	0.00	0.00	0.00
BGHIP	120.9	0.00	135.1	0.00	272.3	0.00	316.5	0.00	306.3	0.00	370.2	0.00	469.6	0.00
CARBAMAZ	0.00	0.00	0.00	0.00	0.26	0.00	0.73	0.00	0.22	0.00	0.07	0.00	4.18	0.00
CARBEND	0.00	0.00	0.00	0.00	0.00	0.00	0.00	0.00	0.00	0.00	0.00	0.00	0.00	0.00
CB138	0.00	0.88	0.00	0.71	0.00	0.78	0.79	0.79	0.00	1.05	1.06	1.06	1.30	1.00
CB153	0.00	0.47	0.71	0.55	0.00	0.41	0.61	0.42	0.80	0.56	0.81	0.57	2.06	0.00
CB28	0.00	4.70	0.00	3.49	0.00	4.50	0.00	5.49	0.59	1.78	0.00	4.03	0.00	0.74
CB52	0.00	2.78	0.00	1.11	0.00	3.20	0.00	3.98	0.00	2.59	0.00	3.32	0.00	1.56
CHLORFENV	0.00	0.00	0.00	0.00	0.00	0.00	0.00	0.00	0.00	0.00	0.00	0.00	0.00	0.00
CHLORTUR	0.00	0.00	0.00	0.00	0.00	0.00	0.00	0.00	0.00	0.00	0.00	0.00	0.00	0.00
CHRTR	92.97	56.91	107.5	24.40	378.1	9.07	445.4	18.94	544.5	12.19	655.7	12.39	810.3	11.45
CLOFIBRS	0.00	n.q	0.00	n.q	0.00	n.q	0.00	n.q	0.00	n.q	0.00	n.q	0.00	n.q
DBAHA	16.68	0.00	19.21	0.00	40.38	0.00	45.65	0.00	40.99	0.00	49.70	0.00	68.58	0.00
DDDP	0.00	0.00	0.00	0.00	0.00	0.00	0.00	0.00	0.00	0.00	0.00	0.00	0.87	0.00
DDEPP	0.00	4.05	0.77	4.47	0.65	3.98	0.66	4.67	0.87	2.48	1.78	3.39	2.59	2.28
DDTOP	0.00	0.44	0.00	1.04	0.00	0.39	0.00	0.89	0.70	0.52	0.71	0.53	0.87	0.00
DDTPP	0.44	0.93	0.46	1.14	0.80	0.78	0.90	0.94	1.41	0.52	1.59	0.53	1.94	0.00
DEATRAZ	0.00	0.00	0.00	0.00	0.00	0.00	0.00	0.00	0.00	0.00	0.00	0.00	0.00	0.00
DIAZINON	0.15	0.15	0.00	0.00	0.13	0.00	0.00	0.00	0.00	0.00	0.00	0.00	0.00	0.00
DICHLPR	0.00	n.q	0.00	n.q	0.00	n.q	0.00	n.q	0.00	n.q	0.00	n.q	0.00	n.q
DICLOF	0.00	n.q	0.00	n.q	0.00	n.q	0.21	n.q	0.28	n.q	0.00	n.q	0.35	n.q
DIELD	0.00	2.89	0.00	3.43	0.00	2.56	0.00	2.63	0.00	0.00	0.00	0.00	0.00	0.00
DIMETH	0.00	0.00	0.00	0.00	0.00	0.00	0.00	0.00	0.00	0.00	0.00	0.00	0.00	0.00
DIURON	0.33	0.59	0.00	9.15	0.75	5.06	0.00	0.00	0.00	0.00	0.00	0.71	2.81	1.26
END	0.00	0.00	0.00	0.00	0.00	0.00	0.00	0.00	0.00	0.00	0.00	0.00	0.00	0.00
FENUR	0.68	0.31	0.48	0.00	0.39	0.47	0.21	0.51	0.34	1.95	0.32	1.71	0.13	1.82
FL	0.00	2196	0.00	2422	22.68	3543	23.94	4235	18.74	3142	20.75	3841	150.2	3272
FLU	31.02	935.6	32.82	1001	348.5	1635	419.1	1582	464.6	1505	543.4	1932	1456	334.0
HBCDA	0.23	0.00	0.25	0.25	0.21	0.00	0.66	0.21	0.28	0.00	0.28	0.00	0.35	0.00
HBCDBG	0.23	0.00	0.25	0.00	0.21	0.21	0.21	0.21	0.28	0.00	0.28	0.00	6.10	0.00
HCB	0.00	58.15	0.00	74.23	0.00	72.75	0.00	86.07	0.00	77.09	2.51	87.91	0.00	79.59
HCHA	0.00	3.37	0.00	4.03	0.00	4.86	0.00	6.17	0.00	4.31	0.00	5.95	0.00	4.95
HCHB	0.00	0.00	0.00	0.00	0.00	0.00	0.00	0.00	0.00	0.00	0.00	0.00	0.00	0.00
HCHD	0.00	0.00	0.00	0.00	0.00	0.00	0.00	0.93	0.00	0.00	0.00	0.00	0.00	0.00
HCHG	0.00	13.21	0.92	14.69	0.00	10.05	0.00	12.47	0.00	7.70	0.00	9.57	0.00	5.12
HEXAZIN	0.00	0.00	0.00	0.00	0.00	0.00	0.00	0.00	0.00	0.00	0.00	0.00	0.00	0.00
I123P	108.3	0.00	126.1	0.00	285.4	0.00	334.5	0.00	281.2	0.00	336.0	0.00	476.1	0.00
IRGAROL	0.00	0.00	0.00	0.00	0.00	0.00	0.00	0.00	0.00	0.00	0.00	0.00	0.00	0.00
ISOD	0.00	0.00	0.00	0.00	0.00	0.00	0.00	0.00	0.00	0.00	0.00	0.00	0.00	0.00
ISOPRUR	0.51	0.03	0.46	0.03	0.29	0.03	0.27	0.03	0.10	0.03	0.11	0.04	0.30	0.04
LINUR	0.00	0.00	0.00	0.00	0.00	0.00	0.00	0.00	0.00	0.00	0.00	0.00	0.00	0.00
MALATH	0.00	0.00	0.00	0.00	0.00	0.00	0.00	0.00	0.00	0.00	0.00	0.00	0.00	0.00
MCPA	0.00	n.q	0.00	n.q	0.00	n.q	0.00	n.q	0.00	n.q	0.00	n.q	0.00	n.q
MECOPR	0.00	n.q	0.00	n.q	0.00	n.q	0.00	n.q	0.00	n.q	0.00	n.q	0.00	n.q
METAZCHL	0.00	0.00	0.00	0.00	0.00	0.00	0.00	0.00	0.00	0.00	0.00	0.00	0.00	0.00
METHABZT	0.00	0.00	0.00	0.00	0.00	0.00	0.00	0.00	0.00	0.00	0.00	0.00	0.00	0.00
METOLA	0.51	0.15	0.79	0.03	0.00	0.05	0.00	0.00	0.00	0.00	0.00	0.07	0.00	0.00
NAPROX	0.00	n.q	0.00	n.q	0.00	n.q	0.00	n.q	0.00	n.q	0.00	n.q	0.00	n.q
OXAZEP	0.00	0.00	0.00	0.00	0.00	0.00	0.00	0.00	0.00	0.00	0.00	0.00	0.00	0.00
PENDIMETH	5.20	44.84	7.72	58.88	19.36	10.37	19.54	20.58	12.08	1.05	12.74	4.78	5.19	0.22

A1 Table 1 continued:

pg/m ³	R5S1		R5S2		R6S1		R6S2		R7S1		R7S2		R8S1	
	GFF	P pl	GFF	PXP	GFF	P pl	GFF	P pl	GFF	P pl	GFF	P pl	GFF	PXP
PFBS	0.03	0.03	0.03	0.33	0.00	0.03	0.05	0.03	0.03	0.03	0.00	0.00	0.00	0.89
PFDEA	0.00	0.06	0.00	0.64	0.00	0.05	0.00	0.05	0.00	0.17	0.00	0.07	0.00	0.22
PFHPA	0.00	0.03	0.00	0.09	0.00	0.03	0.00	0.03	0.00	0.03	0.00	0.04	0.00	0.13
PFHXA	0.00	0.03	0.00	0.22	0.00	0.03	0.00	0.05	0.00	0.07	0.00	0.07	0.00	0.30
PFHXS	0.00	0.03	0.00	0.09	0.03	0.03	0.03	0.03	0.00	0.03	0.00	0.04	0.00	0.38
PFNOA	0.00	0.03	0.00	0.09	0.00	0.03	0.00	0.08	0.00	0.10	0.00	0.04	0.00	0.00
PFOA	0.03	0.09	0.09	1.08	0.16	0.08	0.23	0.08	0.20	0.35	0.11	0.35	0.13	0.52
PFOS	0.03	0.09	0.03	1.83	0.39	0.08	0.44	0.08	1.92	0.28	2.64	0.11	0.35	3.28
PFOSA	0.06	0.00	0.06	0.06	0.03	0.00	0.00	0.00	0.00	0.00	0.00	0.00	0.00	0.00
PHEN	20.92	3587	21.61	3895	240.8	5544	282.9	6485	230.3	5747	281.7	6929	1362	4237
PIRIMIC	0.00	0.00	0.00	0.00	0.00	0.00	0.00	0.00	0.00	0.00	0.00	0.00	0.00	0.00
PRIMID	0.00	0.00	0.00	0.00	0.00	0.00	0.00	0.00	0.00	0.00	0.89	0.00	1.08	0.00
PROMETR	0.00	0.00	0.00	0.03	0.00	0.00	0.00	0.00	0.00	0.00	0.00	0.00	0.00	0.04
PROPAZ	0.00	0.00	0.00	0.00	0.00	0.00	0.00	0.00	0.00	0.00	0.00	0.00	0.00	0.00
PYR	31.62	678.5	34.80	645.1	313.4	1001	381.4	978.2	448.8	1009	536.3	1332	1190	133.0
QCB	0.00	5.22	0.00	10.46	0.00	6.29	0.00	5.96	0.00	10.28	0.00	8.17	0.00	14.40
SIMAZ	0.00	0.00	0.00	0.00	0.00	0.00	0.00	0.00	0.00	0.00	0.00	0.00	0.00	0.00
TBEP	2.20	0.00	6.36	0.00	0.65	0.00	0.66	0.00	0.87	0.00	0.89	0.00	3.25	0.00
TBP	21.27	5.12	80.01	0.00	71.95	4.53	77.94	4.63	37.20	6.10	40.28	6.20	35.02	0.00
TERBAZ	0.00	0.03	0.00	0.03	0.08	0.00	0.00	0.00	0.00	0.03	0.00	0.00	0.00	0.09
TERBUTR	0.06	0.03	0.10	0.00	0.39	0.00	0.46	0.03	0.33	0.00	0.37	0.00	0.33	0.00
TPP	4.13	6.50	4.34	0.00	3.65	1.92	9.91	0.00	10.72	0.00	4.99	7.86	2.04	0.00
TRIFLU	0.00	20.96	0.00	26.28	0.00	4.14	0.00	5.61	0.00	1.92	0.00	2.19	0.00	0.00

pg/m ³	R8S2		R9S1		R9S2		R10S1		R10S2	
	GFF	PXP	GFF	PXP	GFF	PXP	GFF	PXP	GFF	PXP
24-D	0.00	n.q	0.00	n.q	0.00	n.q	0.00	n.q	0.00	n.q
ACE	18.95	1513	0.00	1396	0.00	15792	0.00	2189	0.00	2346
ACY	191.6	1580	49.99	2024	50.70	2001	0.00	2094	6.21	1483
ALD	0.00	0.00	0.00	0.00	0.00	0.00	0.00	0.00	0.00	0.00
AMETRYN	0.00	0.00	0.00	0.00	0.00	0.00	0.00	0.00	0.00	0.00
ANT	108.5	194.7	44.26	338.6	49.58	391.3	6.07	216.5	6.21	243.7
ATRAZ	0.00	0.00	0.00	0.00	0.00	0.00	0.00	0.00	0.00	0.00
AZINPH-E	0.00	0.00	0.00	0.00	0.00	0.00	0.00	0.00	0.00	0.00
AZINPH-M	0.00	0.00	0.00	0.00	0.00	0.00	0.00	0.00	0.00	0.00
BAA	472.2	11.16	353.3	22.89	413.6	26.37	111.6	19.05	122.6	21.37
BAP	518.9	0.00	374.9	17.94	434.5	0.00	119.7	0.00	135.1	0.00
BBF	1160	0.00	998.2	21.99	1147	9.22	372.0	7.59	410.6	7.77
BENTAZ	0.00	0.00	0.00	0.00	0.00	0.00	0.00	0.00	0.00	0.00
BGHIP	513.9	7.54	407.8	6.03	466.7	0.00	189.1	0.00	209.3	15.72
CARBAMAZ	0.87	0.00	0.00	0.00	0.17	0.00	0.00	0.00	0.00	0.00
CARBEND	0.00	0.00	0.00	0.00	0.00	0.00	0.00	0.00	0.00	0.00
CB138	1.34	1.03	1.07	0.82	1.11	0.85	0.00	0.70	0.00	0.71
CB153	2.19	0.00	0.82	0.00	0.85	0.66	0.70	0.55	0.71	0.56
CB28	2.28	2.23	0.61	1.79	0.63	4.64	0.00	4.10	0.00	4.33
CB52	0.00	1.61	0.00	1.29	0.00	3.95	0.00	1.09	0.00	3.32
CHLORFENV	0.00	0.00	0.00	0.00	0.00	0.00	0.00	0.00	0.00	0.00
CHLORTUR	0.00	0.00	0.07	0.00	0.00	0.00	0.00	0.00	0.00	0.00
CHRTR	900.1	0.00	692.9	57.50	793.3	63.75	268.2	61.60	302.8	63.34
CLOFIBRS	0.00	n.q	0.00	n.q	0.00	n.q	0.00	n.q	0.00	n.q

A1 Table 1 continued:

pg/m ³	R8S2		R9S1		R9S2		R10S1		R10S2	
	GFF	PXP	GFF	PXP	GFF	PXP	GFF	PXP	GFF	PXP
DBAHA	81.93	0.00	62.28	0.00	70.76	0.00	30.65	0.00	36.86	0.00
DDPP	0.89	0.00	0.00	0.00	0.00	0.00	0.00	0.00	0.00	0.00
DDEPP	2.78	2.54	0.89	3.31	1.85	3.53	0.76	3.93	0.78	5.02
DDTOP	0.89	0.00	0.71	0.54	0.74	0.55	0.00	0.91	0.00	1.10
DDTPP	2.26	0.00	1.26	0.54	1.34	0.55	0.46	0.94	0.47	1.18
DEATRAZ	0.00	0.00	0.00	0.00	0.00	0.00	0.00	0.00	0.00	0.00
DIAZINON	0.00	0.00	0.18	0.00	0.00	0.00	0.15	0.15	0.00	0.16
DICHLPR	0.00	n.q	0.00	n.q	0.00	n.q	0.00	n.q	0.00	n.q
DICLOF	0.36	n.q	0.00	n.q	0.30	n.q	0.00	n.q	0.00	n.q
DIELD	0.00	0.00	0.00	0.00	0.00	3.70	0.00	3.43	0.00	3.70
DIMETH	0.00	0.00	0.00	0.00	0.00	0.00	0.00	0.00	0.00	0.00
DIURON	0.97	9.53	0.00	6.88	0.00	6.66	0.00	7.59	0.00	5.82
END	0.00	0.00	0.00	0.00	0.00	0.00	0.00	0.00	0.00	0.00
FENUR	0.13	1.87	0.62	4.46	0.43	4.61	0.64	1.28	0.50	1.30
FL	159.5	3876	41.07	3886	43.65	47624	7.59	3815	7.77	4152
FLU	1736	698.2	547.3	2010	634.7	2832	148.6	2147	174.0	2280
HBCDA	0.36	0.00	0.29	0.00	0.30	0.00	1.52	0.00	1.68	0.00
HBCDBG	7.71	0.00	0.29	0.00	0.30	0.00	0.76	0.00	0.78	0.00
HCB	0.00	88.98	0.00	89.67	0.00	97.66	0.00	86.81	0.00	95.03
HCHA	0.00	6.66	0.00	7.14	0.00	7.67	0.00	9.24	0.00	11.92
HCHB	0.00	0.00	0.00	0.00	0.00	0.00	0.00	0.00	0.00	0.00
HCHD	0.00	0.00	0.00	0.00	0.00	0.00	0.00	1.06	0.00	1.09
HCHG	0.00	6.28	0.00	14.03	0.00	16.63	0.00	39.63	0.00	45.15
HEXAZIN	0.00	0.00	0.00	0.00	0.00	0.00	0.00	0.00	0.00	0.00
I123P	527.9	0.00	413.6	8.93	476.2	0.00	185.7	0.00	207.1	0.00
IRGAROL	0.00	0.00	0.00	0.00	0.00	0.00	0.00	0.00	0.00	0.00
ISOD	0.00	0.00	0.00	0.00	0.00	0.00	0.00	0.00	0.00	0.00
ISOPRUR	0.26	0.00	0.49	0.04	0.31	0.04	0.32	0.03	0.41	0.00
LINUR	0.00	0.00	0.00	0.00	0.00	0.00	0.00	0.00	0.00	0.00
MALATH	0.00	0.00	0.00	0.00	0.00	0.00	0.00	0.00	0.00	0.00
MCPA	0.00	n.q	0.00	n.q	0.00	n.q	0.00	n.q	0.00	n.q
MECOPR	0.00	n.q	0.00	n.q	0.00	n.q	0.00	n.q	0.00	n.q
METAZCHL	0.00	0.00	0.11	0.00	0.11	0.00	0.00	0.00	0.00	0.00
METHABZT	0.00	0.00	0.00	0.00	0.00	0.00	0.00	0.00	0.00	0.00
METOLA	0.00	0.00	0.00	0.00	0.00	0.00	0.51	0.03	0.71	0.06
NAPROX	0.00	n.q	0.00	n.q	0.00	n.q	0.00	n.q	0.00	n.q
OXAZEP	0.00	0.00	0.00	0.00	0.00	0.00	0.00	0.00	0.00	0.00
PENDIMETH	5.78	0.67	5.91	3.19	6.15	3.56	5.09	32.51	6.50	47.16
PFBS	0.00	0.70	0.00	0.11	0.00	0.44	0.06	0.09	0.12	0.09
PFDEA	0.00	0.22	0.00	0.50	0.00	1.06	0.06	1.84	0.06	1.57
PFHPA	0.00	0.13	0.00	0.00	0.00	0.33	0.03	0.09	0.03	0.09
PFHXA	0.00	0.31	0.00	0.25	0.00	0.74	0.00	0.49	0.00	0.22
PFHXS	0.00	0.27	0.00	0.04	0.00	0.20	0.00	0.09	0.00	0.09
PFNOA	0.00	0.00	0.00	0.11	0.00	0.37	0.00	0.30	0.00	0.09
PFOA	0.16	0.54	0.23	1.25	0.11	3.20	2.07	2.87	2.36	1.09
PFOS	0.17	2.63	0.63	0.75	0.68	1.77	0.15	0.88	0.13	1.03
PFOSA	0.04	0.09	0.00	0.00	0.04	0.07	0.11	0.18	0.32	0.19
PHEN	1586	5077	373.8	7642	424.2	8752	69.48	7421	81.95	8229
PIRIMIC	0.00	0.00	0.00	0.00	0.00	0.00	0.09	0.00	0.09	0.00
PRIMID	4.04	0.00	0.89	0.00	0.00	0.00	0.00	0.00	0.00	0.00

A1 Table 1 continued:

pg/m ³	R8S2		R9S1		R9S2		R10S1		R10S2	
	GFF	PXP	GFF	PXP	GFF	PXP	GFF	PXP	GFF	PXP
PROMETR	0.00	0.00	0.00	0.04	0.00	0.04	0.00	0.00	0.00	0.00
PROPAZ	0.00	0.00	0.00	0.00	0.00	0.00	0.00	0.00	0.00	0.00
PYR	1407	493.1	497.6	1350	586.0	1770	135.5	1196	158.3	1391
QCB	0.00	16.84	0.00	12.10	0.00	13.80	0.00	11.01	0.00	11.92
SIMAZ	0.00	0.00	0.00	0.00	0.00	0.00	0.00	0.00	0.00	0.00
TBEP	3.35	0.00	0.00	0.00	0.00	7.41	2.28	0.00	2.33	0.00
TBP	34.25	0.00	27.41	0.00	25.73	10.73	87.99	0.00	305.9	9.04
TERBAZ	0.00	0.04	0.00	0.00	0.00	0.04	0.09	0.06	0.09	0.03
TERBUTR	0.30	0.00	0.18	0.04	0.18	0.00	0.06	0.03	0.06	0.00
TPP	2.10	0.00	1.68	0.00	1.73	526.6	9.29	0.00	15.06	0.00
TRIFLU	0.00	0.00	0.00	2.22	0.00	2.36	0.00	1.94	0.00	2.33

A1 Table 2: Atmospheric concentrations of target compounds in ng/PUF disk determined by passive air sampling; sample names correspond with the active air sampling campaigns tabulated in chapter 3; n.q. = not quantified; PXP = PUF/XAD-2/PUF adsorber cartridge; P pl = PUF plug adsorber cartridge; <LOQ and replaced by LOQ/2, = signal <LOD and replaced by LOD/2; 0 = no signal detected; 0 = signal < 0 after blank subtraction; signal > upper calibration range

ng/PUF disk	09AT A	09AT C	09AT E	09AT G	10AT A	10AT C	PE A	PE C	Sülld. G	Sülld. I	Sülld. K	Sülld. M	Sülld. O
24-D	n.q.	n.q.	n.q.	n.q.	n.q.	n.q.	n.q.	n.q.	n.q.	n.q.	n.q.	n.q.	n.q.
ACE	4.37	4.37	4.37	4.37	1.31	1.31	28.54	42.73	207.8	212.5	234.8	238.0	170.3
ACY	2.35	2.35	2.35	2.35	0.00	0.00	13.01	11.51	44.14	36.21	47.64	16.08	5.36
ALD	0.00	0.00	0.00	0.00	0.00	0.00	0.00	0.00	0.00	0.00	0.00	0.00	0.00
AMETRYN	0.00	0.00	0.00	0.00	0.00	0.00	0.00	0.00	0.00	0.00	0.00	0.00	0.00
ANT	0.00	0.00	0.00	0.00	0.00	0.00	62.58	106.4	42.27	30.72	60.00	68.33	31.49
ATRAZ	0.00	0.00	0.00	0.00	0.00	0.00	0.00	0.00	0.00	0.00	0.00	0.00	0.00
AZINPH-E	0.00	0.00	0.00	0.00	0.00	0.00	0.00	0.00	0.00	0.00	0.00	0.00	0.00
AZINPH-M	0.00	0.00	0.00	0.00	0.00	0.00	0.00	0.00	0.00	0.00	0.00	0.00	0.00
BAA	1.79	1.71	1.65	1.70	1.77	1.73	0.00	0.00	7.28	6.34	11.67	25.13	7.69
BAP	2.04	1.00	1.00	1.00	2.04	1.00	0.00	5.00	5.52	0.00	6.69	15.51	5.50
BBF	0.00	0.00	0.00	0.00	0.00	0.00	0.00	0.00	8.06	5.62	13.69	49.22	10.70
BENTAZ	0.32	0.15	0.28	0.10	0.10	0.01	0.00	0.00	0.00	0.00	0.00	0.00	0.00
BGHIP	1.79	1.77	1.67	1.65	1.67	1.67	0.00	0.00	4.72	0.00	6.33	16.99	5.08
CARBAMAZ	0.00	0.00	0.00	0.00	0.00	0.00	0.00	0.00	0.00	0.00	0.00	0.00	0.00
CARBEND	0.00	0.00	0.00	0.00	0.00	0.00	0.00	0.00	0.00	0.00	0.00	0.00	0.00
CB138	0.00	0.00	0.00	0.33	0.52	0.25	0.48	0.47	0.29	0.29	0.29	0.29	0.29
CB153	0.19	0.19	0.19	0.19	0.30	0.15	0.36	0.38	0.35	0.35	0.35	0.35	0.35
CB28	0.42	0.42	0.14	0.42	0.42	0.47	0.10	0.43	1.28	1.13	1.11	1.33	1.16
CB52	0.49	0.39	0.19	0.19	0.49	0.51	0.51	0.72	1.25	0.99	1.34	1.18	0.95
CHLORFENV	0.00	0.00	0.00	0.00	0.00	0.00	0.04	0.00	0.00	0.00	0.00	0.00	0.00
CHLORTUR	0.00	0.00	0.00	0.18	0.00	0.00	0.00	0.00	0.70	0.05	0.00	0.00	0.00
CHRTR	2.21	2.21	0.74	2.21	2.22	2.22	0.00	0.00	17.49	18.44	28.54	64.48	23.75
CLOFIBRS	n.q.	n.q.	n.q.	n.q.	n.q.	n.q.	n.q.	n.q.	n.q.	n.q.	n.q.	n.q.	n.q.
DBAHA	0.00	0.00	0.00	0.00	0.00	0.00	0.00	0.00	0.00	0.00	0.00	6.38	0.00
DDPP	0.10	0.10	0.10	0.10	0.10	0.10	0.15	0.00	0.13	0.13	0.13	0.13	0.13
DDEPP	0.49	0.41	0.15	0.36	0.15	0.15	0.69	0.81	1.65	0.99	0.86	0.78	0.64

A1 Table 2 continued:

ng/PUF disk	09AT A	09AT C	09AT E	09AT G	10AT A	10AT C	PE A	PE C	Süld. G	Süld. I	Süld. K	Süld. M	Süld. O
DDTOP	0.10	0.10	0.10	0.10	0.10	0.10	0.00	0.00	0.49	0.42	0.38	0.39	0.36
DDTPP	0.20	0.10	0.10	0.20	0.06	0.06	0.25	0.34	0.52	0.43	0.36	0.44	0.34
DEATRAZ	0.00	0.00	0.00	0.00	0.00	0.00	0.00	0.00	0.00	0.00	0.00	0.00	0.00
DIAZINON	0.22	0.00	0.00	0.00	0.00	0.00	1.14	0.96	0.15	0.18	0.00	0.12	0.00
DICHLPR	n.q.	n.q.	n.q.	n.q.	n.q.	n.q.	n.q.	n.q.	n.q.	n.q.	n.q.	n.q.	n.q.
DICLOF	n.q.	n.q.	n.q.	n.q.	n.q.	n.q.	n.q.	n.q.	n.q.	n.q.	n.q.	n.q.	n.q.
DIELD	1.25	1.09	0.89	0.95	0.86	0.89	0.81	0.91	0.47	0.76	0.20	0.20	0.20
DIMETH	0.05	0.12	0.05	0.05	0.00	0.00	0.11	0.10	0.14	0.02	0.00	0.00	0.00
DIURON	2.01	8.69	9.06	3.73	0.98	3.26	0.28	0.20	0.18	0.00	2.35	14.93	28.11
END	0.00	0.00	0.00	0.00	0.00	0.00	0.00	0.00	0.00	0.00	0.00	0.00	0.00
FENUR	0.00	0.00	0.00	0.03	0.00	0.06	0.08	0.04	0.03	0.08	0.03	0.00	0.03
FL	74.82	70.50	50.29	60.29	62.18	68.29	197.6	285.2	690.8	516.0	984.4	2477	858.5
FLU	8.60	8.60	2.87	8.60	3.17	3.17	122.2	179.3	206.2	241.7	442.6	856.5	388.4
HBCDA	0.00	0.00	0.00	0.00	0.00	0.00	0.08	0.00	0.00	0.08	0.00	0.00	0.00
HBCDBG	0.00	0.00	0.00	0.00	0.00	0.00	0.18	0.00	0.08	0.08	0.08	0.08	0.00
HCB	13.93	10.87	8.82	10.05	15.12	14.51	6.46	6.97	8.23	8.03	10.43	10.42	8.54
HCHA	1.71	1.26	1.08	1.24	1.30	1.48	0.94	0.92	1.15	1.17	0.94	1.02	0.96
HCHB	0.00	0.00	0.00	0.00	0.00	0.00	0.00	0.00	0.25	0.25	0.25	0.25	0.25
HCHD	0.00	0.00	0.00	0.00	0.00	0.00	0.00	0.00	0.20	0.20	0.20	0.20	0.20
HCHG	1.18	0.95	0.82	0.91	0.60	0.77	0.91	0.97	4.80	4.83	3.45	3.31	3.03
HEXAZIN	0.00	0.00	0.00	0.00	0.00	0.00	0.00	0.00	0.00	0.00	0.00	0.00	0.00
I123P	2.17	2.09	2.02	2.01	2.04	2.03	0.00	0.00	5.49	0.00	6.76	20.18	5.78
IRGAROL	0.00	0.00	0.00	0.00	0.00	0.00	0.00	0.00	0.00	0.00	0.00	0.00	0.00
ISOD	0.00	0.00	0.00	0.00	0.00	0.00	0.00	0.00	0.00	0.00	0.00	0.00	0.00
ISOPRUR	0.01	0.00	0.09	0.00	0.01	0.01	0.00	0.00	5.73	0.50	0.03	0.00	0.00
LINUR	0.00	0.00	0.00	0.00	0.00	0.00	0.00	0.00	0.00	0.00	0.00	0.00	0.00
MALATH	0.00	0.00	0.00	0.00	0.00	0.00	0.00	0.00	0.00	0.00	0.00	0.00	0.00
MCPA	n.q.	n.q.	n.q.	n.q.	n.q.	n.q.	n.q.	n.q.	n.q.	n.q.	n.q.	n.q.	n.q.
MECOPR	n.q.	n.q.	n.q.	n.q.	n.q.	n.q.	n.q.	n.q.	n.q.	n.q.	n.q.	n.q.	n.q.
METAZCHL	0.43	0.35	1.01	0.57	0.19	0.21	5.67	4.76	0.23	0.08	0.08	0.23	0.23
METHABZT	0.00	0.00	0.00	0.00	0.00	0.00	0.00	0.00	0.00	0.00	0.00	0.00	0.00
METOLA	13.06	12.86	8.67	10.56	0.00	0.00	0.03	0.08	0.22	0.22	0.00	0.00	0.00
NAPROX	n.q.	n.q.	n.q.	n.q.	n.q.	n.q.	n.q.	n.q.	n.q.	n.q.	n.q.	n.q.	n.q.
OXAZEP	0.00	0.00	0.00	0.00	0.00	0.00	0.00	0.00	0.00	0.00	0.00	0.00	0.00
PENDIMETH	5.56	4.41	3.46	2.57	4.25	3.39	0.91	0.93	94.90	68.48	11.36	2.42	2.72
PFBS	0.00	0.01	0.02	0.01	0.00	0.01	0.01	0.01	0.00	0.02	0.00	0.00	0.00
PFDEA	0.00	0.00	0.00	0.00	0.00	0.00	0.00	0.00	0.00	0.00	0.00	0.00	0.00
PFHPA	0.03	0.03	0.00	0.03	0.06	0.06	0.00	0.00	0.00	0.00	0.00	0.00	0.12
PFHXA	0.06	0.06	0.00	0.00	0.03	0.03	0.03	0.03	0.00	0.00	0.00	0.00	0.29
PFHXS	0.05	0.03	0.03	0.04	0.03	0.03	0.02	0.02	0.01	0.01	0.02	0.01	0.02
PFNOA	0.05	0.05	0.05	0.00	0.07	0.07	0.18	0.12	0.11	0.00	0.00	0.00	0.00
PFOA	0.24	0.24	0.24	0.24	0.19	0.19	0.41	0.47	0.00	0.00	0.00	0.00	0.91
PFOS	0.43	0.11	0.11	0.31	0.22	0.22	0.18	0.17	0.40	0.13	0.00	0.13	0.13
PFOSA	0.04	0.04	0.04	0.04	0.00	0.00	0.09	0.14	0.09	0.09	0.00	0.09	0.09
PHEN	81.25	34.71	34.71	77.41	51.81	57.13	917.2	1298	1032	970.7	1682	3636	1480
PIRIMIC	0.00	0.00	0.00	0.00	0.00	0.00	0.00	0.00	0.00	0.00	0.00	0.00	0.00
PRIMID	0.00	0.00	0.00	0.00	0.00	0.00	0.00	0.00	0.00	0.00	0.00	0.00	0.00
PROMETR	0.00	0.00	0.00	0.00	0.00	0.00	0.00	0.00	0.00	0.00	0.00	0.00	0.00
PROPAZ	0.00	0.00	0.00	0.00	0.00	0.00	0.00	0.00	0.00	0.00	0.00	0.00	0.00
PYR	0.00	0.00	0.00	5.80	4.93	4.93	133.7	169.6	111.3	136.3	243.3	357.7	175.9
QCB	1.57	1.48	1.45	1.52	1.78	1.80	0.66	0.66	1.37	1.36	1.72	2.04	1.99

A1 Table 2 continued:

ng/PUF disk	09AT A	09AT C	09AT E	09AT G	10AT A	10AT C	PE A	PE C	Sülld. G	Sülld. I	Sülld. K	Sülld. M	Sülld. O
SIMAZ	0.00	0.00	0.00	0.00	0.00	0.00	0.00	0.00	0.00	0.00	0.00	0.00	0.00
TBEP	0.00	0.00	0.00	0.00	0.00	0.00	0.17	0.36	0.18	0.18	0.18	0.18	0.54
TBP	0.00	0.00	0.00	0.00	0.00	0.00	0.00	0.00	8.29	8.29	8.29	8.29	8.29
TERBAZ	9.17	8.07	5.91	7.24	0.12	0.12	0.07	0.07	0.12	0.12	0.00	0.00	0.00
TERBUTR	0.00	0.00	0.00	0.00	0.00	0.00	0.00	0.00	0.13	0.08	0.05	0.00	0.00
TPP	1.88	1.88	1.88	1.88	0.74	2.22	2.12	0.82	0.00	0.00	2.09	0.00	6.28
TRIFLU	0.78	0.58	0.54	0.53	0.49	0.52	30.91	33.95	14.07	5.07	1.54	0.59	0.49

ng/PUF disk	Sülld. Q	Sülld. S	Sülld. U	Sülld. W	Sülld. Y	Sülld. Z	Sülld. AB	Sülld. AC	Sülld. AE	Sülld. AG	Sülld. AI	Sülld. AK	Sylt A
24-D	n.q	n.q	n.q	n.q	n.q	n.q	n.q	n.q	n.q	n.q	n.q	n.q	n.q
ACE	179.8	177.6	200.2	106.6	179.9	146.7	130.5	146.5	153.1	195.1	164.9	199.2	89.79
ACY	5.36	5.36	16.08	0.00	0.00	0.00	0.00	0.00	5.36	16.08	15.33	15.33	5.41
ALD	0.00	0.00	0.00	0.00	0.00	0.00	0.00	0.00	0.00	0.00	0.00	0.00	0.00
AMETRYN	0.00	0.00	0.00	0.00	0.00	0.00	0.00	0.00	0.00	0.00	0.00	0.00	0.00
ANT	32.20	16.07	19.91	8.92	11.60	10.65	12.97	14.96	15.51	26.98	16.89	65.93	14.51
ATRAZ	0.00	0.00	0.00	0.00	0.00	0.00	0.00	0.00	0.00	0.00	0.00	0.00	0.00
AZINPH-E	0.00	0.00	0.00	0.00	0.00	0.00	0.00	0.00	0.00	0.00	0.00	0.00	0.00
AZINPH-M	0.00	0.00	0.00	0.00	0.69	0.00	0.00	0.00	0.00	0.00	0.00	0.00	0.00
BAA	9.27	6.54	7.93	4.81	4.73	5.08	5.28	6.27	5.69	6.82	4.70	9.08	7.08
BAP	6.10	5.56	5.56	5.39	0.00	5.48	5.44	6.14	5.43	5.69	1.50	4.18	6.69
BBF	14.38	7.34	8.34	5.67	4.95	6.63	6.01	8.19	5.84	7.95	4.73	9.33	14.03
BENTAZ	0.00	0.03	0.04	0.39	0.06	0.02	0.02	0.00	0.00	0.00	0.00	0.00	0.00
BGHIP	6.07	4.85	4.99	0.00	0.00	4.69	4.88	5.37	4.65	4.99	2.00	4.01	6.64
CARBAMAZ	0.00	0.00	0.00	0.00	2.00	0.00	0.00	0.00	0.00	0.00	0.01	0.00	0.00
CARBEND	0.00	0.00	0.00	0.00	0.00	0.00	0.00	0.00	0.00	0.00	0.00	0.00	0.00
CB138	0.29	0.29	0.29	0.29	0.64	1.31	0.89	1.51	0.77	0.67	0.28	0.28	0.63
CB153	0.35	0.35	0.35	0.35	0.35	1.63	1.06	1.63	0.89	0.35	0.36	0.36	0.33
CB28	1.28	1.10	1.39	1.06	1.43	3.07	1.87	1.80	1.72	2.49	0.98	0.97	1.32
CB52	1.08	1.06	1.94	2.02	2.73	3.75	2.90	2.81	2.30	2.18	1.31	1.43	0.84
CHLORFENV	0.00	0.00	0.00	0.00	0.00	0.00	0.00	0.00	0.00	0.00	0.00	0.00	0.00
CHLORTUR	0.00	0.00	0.23	0.00	0.00	0.00	0.00	0.00	0.00	0.38	0.81	0.00	0.84
CHRTR	26.25	16.17	21.33	10.25	8.72	12.40	10.39	11.29	11.59	15.49	13.84	23.07	26.74
CLOFIBRS	n.q	n.q	n.q	n.q	n.q	n.q	n.q	n.q	n.q	n.q	n.q	n.q	n.q
DBAHA	0.00	0.00	0.00	0.00	0.00	0.00	0.00	0.00	0.00	0.00	0.00	0.00	0.00
DDPP	0.13	0.13	0.13	0.13	0.13	0.30	0.31	0.32	0.27	0.27	0.15	0.00	0.13
DDEPP	0.68	0.94	1.00	0.75	0.74	1.24	1.06	1.03	1.86	3.06	1.42	1.15	2.56
DDTOP	0.37	0.40	0.46	0.40	0.43	0.69	0.56	0.55	0.63	0.72	0.43	0.39	0.56
DDTPP	0.35	0.41	0.57	0.50	0.46	0.93	0.91	0.98	0.82	0.90	0.42	0.37	0.59
DEATRAZ	0.00	0.00	0.00	0.00	0.00	0.00	0.00	0.00	0.00	0.00	0.00	0.00	0.00
DIAZINON	0.00	0.12	0.00	0.13	0.17	0.37	0.42	0.37	0.45	0.32	0.34	0.23	0.00
DICHLPR	n.q	n.q	n.q	n.q	n.q	n.q	n.q	n.q	n.q	n.q	n.q	n.q	n.q
DICLOF	n.q	n.q	n.q	n.q	n.q	n.q	n.q	n.q	n.q	n.q	n.q	n.q	n.q
DIELD	0.20	0.55	0.46	0.54	0.63	0.83	0.67	0.62	0.88	0.75	1.90	1.75	0.83
DIMETH	0.00	0.00	0.00	0.42	1.08	0.38	0.18	0.32	0.15	0.05	0.16	0.02	0.02
DIURON	2.55	1.24	1.11	0.65	3.35	2.78	1.05	1.22	1.67	0.72	0.47	0.49	0.00
END	0.00	0.00	0.00	0.00	0.00	0.00	0.00	0.00	0.00	0.00	0.00	0.00	0.00
FENUR	0.03	0.00	0.03	0.08	0.08	0.03	0.08	0.08	0.03	0.03	0.03	0.03	0.00
FL	948.5	365.5	407.5	250.7	362.2	478.3	321.5	350.0	363.6	451.4	376.7	578.8	509.8
FLU	401.4	189.2	272.7	109.5	191.8	311.5	176.6	151.7	186.4	212.7	156.3	315.1	248.4
HBCDA	0.00	0.08	0.08	0.08	0.00	0.00	0.08	0.25	0.08	0.08	0.08	0.08	0.25

A1 Table 2 continued:

ng/PUF disk	Sülld. Q	Sülld. S	Sülld. U	Sülld. W	Sülld. Y	Sülld. Z	Sülld. AB	Sülld. AC	Sülld. AE	Sülld. AG	Sülld. AI	Sülld. AK	Sylt A
HBCDBG	0.08	0.08	0.08	0.25	0.08	0.00	0.08	1.86	0.25	0.08	0.08	0.08	0.66
HCB	8.58	8.95	9.30	8.91	8.27	7.46	8.80	8.77	10.02	12.48	9.87	10.07	10.46
HCHA	1.18	1.10	1.29	1.23	1.39	1.90	1.69	1.60	1.79	1.84	1.66	1.42	1.65
HCHB	0.25	0.25	0.25	0.25	0.25	0.25	0.25	0.25	0.25	0.25	0.00	0.00	0.25
HCHD	0.20	0.20	0.20	0.20	0.20	0.20	0.20	0.20	0.20	0.20	0.35	0.00	0.20
HCHG	3.68	4.34	6.60	7.33	8.46	15.15	10.16	9.92	7.91	7.18	5.13	4.34	3.10
HEXAZIN	0.00	0.00	0.00	0.00	0.00	0.00	0.00	0.00	0.00	0.00	0.00	0.00	0.00
I123P	6.75	5.48	5.54	5.44	0.00	5.46	5.46	5.71	5.44	5.61	1.50	3.58	7.22
IRGAROL	0.00	0.00	0.00	0.00	0.00	0.00	0.00	0.00	0.00	0.00	0.00	0.02	0.00
ISOD	0.00	0.00	0.00	0.00	0.00	0.00	0.00	0.00	0.00	0.00	0.00	0.00	0.00
ISOPRUR	0.03	2.08	1.04	0.66	0.11	0.21	0.55	0.50	0.18	1.70	1.51	0.21	1.77
LINUR	0.00	0.00	0.00	0.00	0.00	0.00	0.00	0.00	0.00	0.00	0.00	0.00	0.00
MALATH	0.00	0.00	0.00	0.00	0.00	0.00	0.00	0.00	0.00	0.00	0.00	0.00	0.00
MCPA	n.q	n.q	n.q	n.q	n.q	n.q	n.q	n.q	n.q	n.q	n.q	n.q	n.q
MECOPR	n.q	n.q	n.q	n.q	n.q	n.q	n.q	n.q	n.q	n.q	n.q	n.q	n.q
METAZCHL	0.00	0.23	0.51	0.23	0.23	0.45	0.23	0.23	11.17	5.44	0.21	0.00	0.78
METHABZT	0.00	0.00	0.00	0.00	0.00	0.00	0.00	0.00	0.00	0.00	0.00	0.00	0.00
METOLA	0.00	0.22	0.72	7.19	64.85	7.06	2.12	1.95	1.31	0.61	0.55	0.07	0.62
NAPROX	n.q	n.q	n.q	n.q	n.q	n.q	n.q	n.q	n.q	n.q	n.q	n.q	n.q
OXAZEP	0.00	0.00	0.00	0.00	0.00	0.00	0.00	0.00	0.00	0.00	0.00	0.00	0.00
PENDIMETH	3.62	26.98	25.12	42.16	35.39	19.23	19.99	16.06	7.34	22.61	88.01	22.60	77.57
PFBS	0.00	0.00	0.01	0.02	0.02	0.04	0.01	0.00	0.01	0.00	0.02	0.01	0.02
PFDEA	0.05	0.05	0.05	0.10	0.05	0.13	0.05	0.05	0.00	0.02	0.00	0.00	0.05
PFHPA	0.00	0.00	0.00	0.00	0.00	0.00	0.00	0.00	0.00	0.00	0.11	0.00	0.04
PFHXA	0.00	0.00	0.00	0.00	0.00	0.10	0.00	0.10	0.00	0.00	0.00	0.00	0.00
PFHXS	0.01	0.02	0.02	0.01	0.01	0.01	0.00	0.00	0.00	0.00	0.01	0.01	0.09
PFNOA	0.36	0.21	0.11	0.11	0.11	0.11	0.11	0.11	0.04	0.04	0.04	0.04	0.06
PFOA	0.00	0.00	0.00	0.00	0.00	0.00	0.00	0.00	0.00	0.00	0.00	0.00	0.21
PFOS	0.00	0.00	0.13	0.40	0.00	0.00	0.00	0.00	0.00	0.00	0.00	0.00	0.33
PFOSA	0.00	0.09	0.09	0.09	0.09	0.26	0.09	0.09	0.09	0.00	0.00	0.00	0.13
PHEN	1534	805.2	955.9	599.5	922.2	1371	864.4	859.6	906.1	937.9	762.8	1280	801.1
PIRIMIC	0.00	0.00	0.00	0.00	0.27	1.98	0.34	0.28	0.00	0.00	0.00	0.00	0.00
PRIMID	0.00	0.00	0.00	0.00	0.00	0.00	0.00	0.00	0.00	0.00	0.00	0.00	0.00
PROMETR	0.00	0.00	0.00	0.00	0.00	0.00	0.00	0.00	0.00	0.00	0.00	0.00	0.00
PROPAZ	0.00	0.00	0.00	0.00	0.00	0.00	0.00	0.00	0.00	0.00	0.00	0.00	0.00
PYR	182.9	92.85	147.8	52.74	67.46	105.7	76.33	62.14	81.55	111.0	85.27	195.0	99.10
QCB	1.87	1.51	1.58	1.17	1.01	0.57	0.69	0.69	0.98	1.29	1.25	1.57	1.73
SIMAZ	0.00	0.00	0.00	0.00	0.00	0.00	0.00	0.00	0.00	0.00	0.00	0.00	0.00
TBEP	0.18	0.18	0.54	0.54	0.54	0.00	0.00	0.18	0.18	0.18	0.53	0.53	0.52
TBP	8.29	0.00	0.00	0.00	8.29	8.29	8.29	8.29	8.29	8.29	7.98	7.98	3.21
TERBAZ	0.00	0.12	0.29	4.96	75.88	20.50	2.63	2.35	1.06	0.50	0.25	0.04	0.51
TERBUTR	0.00	0.06	0.12	0.42	0.34	0.42	0.39	0.40	0.37	0.33	0.16	0.15	0.00
TPP	0.00	0.00	0.00	6.28	6.28	6.28	2.09	2.09	2.09	2.09	2.01	2.01	5.54
TRIFLU	0.47	1.23	1.01	1.75	0.65	0.76	0.78	0.79	1.68	3.23	6.74	2.14	25.40

ng/PUF disk	Sylt C	Sylt E	Sylt G	Sylt H	Sylt I	Sylt K	Sylt M	Sylt O	Sylt Q	Sylt R	Sylt S	Sylt U	Sylt W
24-D	n.q	n.q	n.q	n.q	n.q	n.q	n.q	n.q	n.q	n.q	n.q	n.q	n.q
ACE	82.18	102.5	135.5	74.51	23.88	58.51	39.83	69.50	62.26	84.49	57.86	93.23	37.23
ACY	16.23	5.41	16.23	5.41	0.00	0.00	0.00	0.00	0.00	0.00	0.00	0.00	0.00
ALD	0.00	0.00	0.00	0.00	0.00	0.00	0.00	0.00	0.00	0.00	0.00	0.00	0.00

A1 Table 2 continued:

ng/PUF disk	Sylt C	Sylt E	Sylt G	Sylt H	Sylt I	Sylt K	Sylt M	Sylt O	Sylt Q	Sylt R	Sylt S	Sylt U	Sylt W
AMETRYN	0.00	0.00	0.00	0.00	0.00	0.00	0.00	0.00	0.00	0.00	0.00	0.00	0.00
ANT	13.29	31.48	29.03	20.04	8.32	6.22	6.93	7.16	7.65	8.69	41.36	11.94	8.31
ATRAZ	0.00	0.00	0.00	0.00	0.00	0.00	0.00	0.00	0.00	0.00	0.00	0.00	0.00
AZINPH-E	0.00	0.00	0.00	0.00	0.00	0.00	0.00	0.00	0.00	0.00	0.00	0.00	0.00
AZINPH-M	0.00	0.00	0.00	0.00	0.00	0.00	0.00	0.00	0.00	0.00	0.00	0.00	0.00
BAA	8.17	7.89	19.55	7.86	5.15	5.16	5.28	5.14	0.00	0.00	13.18	2.00	2.00
BAP	7.61	6.44	11.83	6.63	0.00	0.00	0.00	0.00	0.00	0.00	6.48	1.50	0.00
BBF	14.61	10.74	53.85	14.90	5.46	6.13	6.19	0.00	0.00	0.00	8.28	7.43	2.00
BENTAZ	0.00	0.00	0.00	0.00	0.00	0.01	0.16	0.09	0.01	0.00	0.00	0.00	0.00
BGHIP	7.23	5.86	17.76	6.84	0.00	0.00	0.00	0.00	0.00	0.00	5.70	2.00	0.00
CARBAMAZ	0.00	0.00	0.00	0.00	0.00	0.00	0.00	0.00	0.00	0.00	0.00	0.00	0.00
CARBEND	0.00	0.00	0.00	0.00	0.00	0.00	0.00	0.00	0.00	0.00	0.00	0.00	0.00
CB138	0.79	0.45	0.44	0.48	0.52	0.56	1.04	0.57	1.01	0.76	0.67	0.81	0.60
CB153	0.81	0.33	0.33	0.33	0.33	0.33	0.97	0.33	1.12	0.67	0.68	0.87	0.71
CB28	2.00	0.91	1.20	1.13	0.95	1.08	0.74	0.68	1.36	0.93	1.02	1.62	1.08
CB52	1.37	0.71	0.67	0.80	0.83	0.88	0.78	0.70	1.23	0.80	0.88	1.22	1.06
CHLORFENV	0.00	0.00	0.00	0.00	0.00	0.00	0.00	0.00	0.00	0.00	0.00	0.00	0.00
CHLORTUR	1.21	0.00	0.00	0.00	0.17	0.00	0.00	0.00	0.00	0.00	0.00	0.43	0.33
CHRTR	24.98	27.98	68.87	27.70	11.29	15.44	11.22	8.57	8.57	8.63	22.83	15.56	13.55
CLOFIBRS	n.q	n.q	n.q	n.q	n.q	n.q	n.q	n.q	n.q	n.q	n.q	n.q	n.q
DBAHA	0.00	0.00	7.15	0.00	0.00	0.00	0.00	0.00	0.00	0.00	0.00	0.00	0.00
DDPP	0.13	0.13	0.13	0.13	0.13	0.13	0.13	0.13	0.13	0.13	0.27	0.00	0.15
DDEPP	1.95	0.88	1.13	0.92	1.18	0.98	0.60	0.63	0.81	0.80	2.20	5.09	1.71
DDTOP	0.43	0.34	0.41	0.38	0.35	0.38	0.33	0.37	0.44	0.43	0.53	0.84	0.39
DDTPP	0.49	0.31	0.42	0.39	0.33	0.38	0.31	0.32	0.48	0.45	0.57	0.83	0.32
DEATRAZ	0.00	0.00	0.00	0.00	0.00	0.00	0.00	0.00	0.00	0.00	0.00	0.00	0.00
DIAZINON	0.73	0.00	0.00	0.00	0.00	0.00	0.00	0.00	0.15	0.00	0.40	0.35	0.49
DICHLPR	n.q	n.q	n.q	n.q	n.q	n.q	n.q	n.q	n.q	n.q	n.q	n.q	n.q
DICLOF	n.q	n.q	n.q	n.q	n.q	n.q	n.q	n.q	n.q	n.q	n.q	n.q	n.q
DIELD	1.93	0.54	0.20	0.51	0.83	0.94	0.84	0.73	1.28	1.37	1.58	2.39	2.40
DIMETH	0.00	0.00	0.00	0.00	0.00	0.00	0.00	0.05	0.30	0.03	0.05	0.00	0.00
DIURON	0.00	0.00	0.00	0.00	0.76	12.74	4.29	2.79	2.46	0.57	1.94	0.59	2.67
END	0.00	0.00	0.00	0.00	0.00	0.00	0.00	0.00	0.00	0.00	0.00	0.00	0.00
FENUR	0.00	0.00	0.00	0.00	0.00	0.00	0.00	0.00	0.00	0.07	0.00	0.00	0.00
FL	387.3	686.3	2287	747.3	173.0	188.1	106.1	150.3	161.6	145.5	152.6	239.9	167.9
FLU	217.1	438.3	909.6	386.6	115.4	157.2	106.8	122.7	136.4	92.58	212.4	182.2	175.6
HBCDA	0.25	0.66	0.08	0.08	0.00	0.00	0.08	0.08	0.08	0.25	0.00	0.00	0.00
HBCDBG	0.25	0.25	0.00	0.25	0.08	0.25	0.25	0.08	0.25	0.25	0.08	0.08	0.08
HCB	11.11	11.26	11.74	10.22	10.25	12.63	9.53	9.52	7.63	8.42	11.85	16.60	14.17
HCHA	1.58	0.97	1.31	0.99	0.84	1.20	1.09	1.20	1.48	1.68	2.21	2.79	2.14
HCHB	0.25	0.25	0.00	0.25	0.25	0.25	0.25	0.00	0.25	0.25	0.25	0.75	0.00
HCHD	0.20	0.00	0.00	0.20	0.00	0.20	0.00	0.00	0.20	0.20	0.20	0.35	0.00
HCHG	4.30	1.41	1.49	1.83	2.36	2.60	2.42	3.09	5.97	4.30	3.47	4.55	3.21
HEXAZIN	0.00	0.00	0.00	0.00	0.00	0.00	0.00	0.00	0.00	0.00	0.00	0.00	0.00
I123P	7.79	6.61	22.77	7.83	0.00	0.00	0.00	0.00	0.00	0.00	6.50	1.50	0.00
IRGAROL	0.00	0.00	0.00	0.00	0.00	0.00	0.00	0.00	0.00	0.00	0.00	0.00	0.00
ISOD	0.00	0.00	0.00	0.00	0.00	0.00	0.00	0.00	0.00	0.00	0.00	0.00	0.00
ISOPRUR	1.20	0.00	0.00	0.00	0.67	0.42	0.06	0.00	0.00	0.01	0.00	1.90	0.81
LINUR	0.00	0.00	0.00	0.00	0.00	0.00	0.00	0.00	0.00	0.00	0.00	0.00	0.00
MALATH	0.00	0.00	0.00	0.00	0.00	0.00	0.00	0.00	0.00	0.00	0.00	0.00	0.00
MCPA	n.q	n.q	n.q	n.q	n.q	n.q	n.q	n.q	n.q	n.q	n.q	n.q	n.q

A1 Table 2 continued:

ng/PUF disk	Sylt C	Sylt E	Sylt G	Sylt H	Sylt I	Sylt K	Sylt M	Sylt O	Sylt Q	Sylt R	Sylt S	Sylt U	Sylt W
MECOPR	n.q	n.q	n.q	n.q	n.q	n.q	n.q	n.q	n.q	n.q	n.q	n.q	n.q
METAZCHL	0.28	0.00	0.07	0.03	0.10	0.35	0.15	0.20	0.21	0.18	0.00	4.07	0.00
METHABZT	0.00	0.00	0.00	0.00	0.00	0.00	0.00	0.00	0.00	0.00	0.00	0.00	0.00
METOLA	0.27	0.03	0.00	0.19	1.31	0.32	0.23	35.69	4.39	0.45	0.54	0.85	0.26
NAPROX	n.q	n.q	n.q	n.q	n.q	n.q	n.q	n.q	n.q	n.q	n.q	n.q	n.q
OXAZEP	0.00	0.00	0.00	0.00	0.00	0.00	0.00	0.00	0.00	0.00	0.00	0.00	0.00
PENDIMETH	51.80	8.03	4.04	3.34	20.79	8.76	5.32	4.01	1.28	1.23	2.19	187.5	53.73
PFBS	0.28	0.00	0.00	0.02	0.01	0.01	0.05	0.02	0.02	0.02	0.03	0.01	0.03
PFDEA	0.16	0.00	0.00	0.00	0.05	0.05	0.11	0.05	0.14	0.14	0.22	0.05	0.05
PFHPA	0.26	0.00	0.00	0.04	0.00	0.04	0.12	0.00	0.04	0.00	0.04	0.04	0.12
PFHXA	0.04	0.00	0.00	0.04	0.00	0.04	0.13	0.04	0.04	0.00	0.04	0.00	0.00
PFHXS	0.74	0.02	0.03	0.08	0.02	0.04	0.34	0.02	0.02	0.03	0.02	0.06	0.18
PFNOA	0.17	0.00	0.06	0.00	0.00	0.06	0.17	0.06	0.17	0.17	0.17	0.16	0.16
PFOA	2.61	0.00	0.00	0.21	0.00	0.21	0.63	0.21	0.63	0.63	1.46	0.20	0.60
PFOS	3.39	0.04	0.04	0.27	0.04	0.13	0.35	0.13	0.13	0.35	2.20	0.61	0.93
PFOSA	0.04	0.00	0.00	0.00	0.00	0.00	0.00	0.04	0.04	0.00	0.00	0.00	0.00
PHEN	621.1	1210	3373	1167	262.6	318.1	249.4	321.7	342.7	266.5	355.7	449.0	337.3
PIRIMIC	0.00	0.00	0.00	0.00	0.00	0.00	0.00	0.00	0.00	0.00	0.00	0.00	0.00
PRIMID	0.00	0.00	0.00	0.00	0.00	0.00	0.00	0.00	0.00	0.00	0.00	0.00	0.00
PROMETR	0.00	0.00	0.00	0.00	0.00	0.00	0.00	0.00	0.00	0.00	0.00	0.00	0.00
PROPAZ	0.00	0.00	0.00	0.00	0.00	0.00	0.00	0.00	0.00	0.00	0.00	0.00	0.00
PYR	84.53	188.0	266.4	129.0	44.21	54.14	57.57	49.49	18.80	18.80	109.2	81.83	74.69
QCB	2.11	2.07	2.32	2.12	2.09	2.43	1.67	1.23	0.83	0.84	1.00	2.03	1.77
SIMAZ	0.00	0.00	0.00	0.00	0.00	0.00	0.00	0.00	0.00	0.00	0.00	0.00	0.00
TBEP	0.94	0.05	0.05	0.13	0.00	0.13	0.05	0.05	0.05	0.05	0.13	0.00	0.00
TBP	3.21	0.00	0.00	0.00	0.00	0.00	0.00	3.21	3.21	3.21	3.21	0.00	3.24
TERBAZ	0.39	0.01	0.03	0.00	0.11	0.36	0.33	23.25	10.63	0.70	0.61	0.62	0.23
TERBUTR	0.00	0.00	0.00	0.00	0.00	0.00	0.02	0.05	0.04	0.03	0.04	0.00	0.27
TPP	73.84	0.00	0.66	0.66	0.00	0.66	0.00	0.66	0.66	0.66	0.66	2.20	2.20
TRIFLU	13.74	1.98	0.69	1.10	1.36	0.67	0.47	0.45	0.50	0.50	1.45	2.09	6.46

ng/PUF disk	Sylt Y	FINO1 A	FINO1 B	FINO1 C	FINO1 G	FINO1 H	FINO1 I	FINO3 A	FINO3 C	FINO3 E
24-D	n.q	n.q	n.q	n.q	n.q	n.q	n.q	n.q	n.q	n.q
ACE	70.65	4.40	4.40	4.40	18.36	8.67	9.60	4.40	4.40	4.40
ACY	0.00	0.00	2.74	2.74	0.00	0.00	0.00	0.00	0.00	0.00
ALD	0.00	0.00	0.00	0.00	0.00	0.00	0.00	0.00	0.00	0.00
AMETRYN	0.00	0.00	0.00	0.00	0.00	0.00	0.00	0.00	0.00	0.00
ANT	30.52	0.00	0.00	0.00	0.00	0.00	0.00	0.00	0.00	0.00
ATRAZ	0.00	0.00	0.00	0.00	0.00	0.00	0.00	0.00	0.00	0.00
AZINPH-E	0.00	0.00	0.00	0.00	0.00	0.00	0.00	0.00	0.00	0.00
AZINPH-M	0.00	0.00	0.00	0.00	0.00	0.00	0.00	0.00	0.00	0.00
BAA	6.23	6.43	5.67	5.62	9.60	8.15	6.83	6.39	5.25	5.50
BAP	1.50	0.00	0.00	0.00	3.52	3.93	3.20	0.00	0.00	0.00
BBF	7.74	13.03	10.28	9.17	26.36	24.08	21.17	0.00	5.87	7.57
BENTAZ	0.00	0.03	0.01	0.01	0.00	0.00	0.00	0.01	0.00	0.01
BGHIP	2.00	5.73	5.69	0.00	5.31	5.56	4.15	5.83	0.00	0.00
CARBAMAZ	0.00	0.00	0.00	0.00	0.00	0.00	0.00	0.00	0.00	0.00
CARBEND	0.00	0.00	0.00	0.00	0.66	0.42	0.68	0.00	0.00	0.00
CB138	0.25	2.86	2.66	2.24	2.82	2.41	2.50	2.37	2.15	2.12
CB153	0.34	3.88	3.79	3.16	4.34	3.56	3.82	3.52	2.66	2.80

A1 Table 2 continued:

ng/PUF disk	Sylt Y	FINO1 A	FINO1 B	FINO1 C	FINO1 G	FINO1 H	FINO1 I	FINO3 A	FINO3 C	FINO3 E
CB28	0.97	5.98	5.92	5.10	10.64	7.59	7.92	5.72	4.35	4.17
CB52	0.81	4.58	4.44	3.73	6.84	5.41	5.93	3.42	2.85	2.94
CHLORFENV	0.00	0.00	0.00	0.00	0.00	0.00	0.00	0.00	0.00	0.00
CHLORTUR	0.00	0.00	0.11	0.19	4.59	4.23	3.86	0.00	0.48	0.00
CHRTR	24.82	49.21	44.78	38.48	91.11	71.77	65.62	37.08	24.73	27.78
CLOFIBRS	n.q.	n.q.	n.q.	n.q.	n.q.	n.q.	n.q.	n.q.	n.q.	n.q.
DBAHA	0.00	0.00	0.00	0.00	0.00	0.00	0.00	0.00	0.00	0.00
DDDP	0.00	0.48	0.43	0.41	0.00	0.00	0.00	0.42	0.31	0.42
DDEPP	1.07	18.31	15.91	13.51	18.95	18.49	17.54	18.92	9.99	12.53
DDTOP	0.33	2.77	2.42	2.09	2.46	2.46	2.42	3.37	1.87	2.16
DDTPP	0.25	4.00	3.57	3.06	3.29	3.25	3.09	4.54	2.37	2.94
DEATRAZ	0.00	0.00	0.00	0.00	0.00	0.00	0.00	0.00	0.00	0.00
DIAZINON	0.25	7.06	7.32	5.52	6.12	4.63	5.27	1.26	0.80	1.40
DICHLPR	n.q.	n.q.	n.q.	n.q.	n.q.	n.q.	n.q.	n.q.	n.q.	n.q.
DICLOF	n.q.	n.q.	n.q.	n.q.	n.q.	n.q.	n.q.	n.q.	n.q.	n.q.
DIELD	1.91	13.68	13.63	11.44	9.21	9.02	10.19	8.53	5.60	6.82
DIMETH	0.00	2.19	1.84	1.74	0.92	0.68	0.49	0.22	0.15	0.13
DIURON	0.66	0.00	2.12	0.00	0.48	0.56	0.00	0.00	1.05	2.45
END	0.00	0.00	0.00	0.00	0.00	0.00	0.00	0.00	0.00	0.00
FENUR	0.02	0.00	0.00	0.05	0.00	0.00	0.00	0.00	0.05	0.00
FL	374.6	143.0	143.3	136.0	327.7	263.4	259.8	147.5	91.15	91.96
FLU	362.9	302.4	283.6	250.2	835.0	554.7	589.5	193.9	147.6	128.7
HBCDA	0.25	0.00	0.00	0.00	0.00	0.00	0.00	0.00	0.00	0.00
HBCDBG	0.08	0.00	0.00	0.00	0.25	0.08	0.25	0.78	0.00	0.00
HCB	15.16	14.00	14.82	15.64	23.19	22.96	24.18	18.26	18.25	17.85
HCHA	1.98	4.75	4.87	5.48	9.70	8.94	10.07	6.70	5.58	6.10
HCHB	0.75	0.00	0.00	0.00	0.75	0.75	0.75	0.00	0.00	0.00
HCHD	0.00	0.20	0.20	0.20	0.37	0.37	0.37	0.00	0.00	0.20
HCHG	2.01	10.40	9.53	8.68	28.02	19.49	23.18	7.78	4.84	5.74
HEXAZIN	0.00	0.00	0.00	0.00	0.00	0.00	0.00	0.00	0.00	0.00
I123P	1.50	6.51	0.00	0.00	5.89	6.65	4.70	6.77	0.00	0.00
IRGAROL	0.00	0.00	0.00	0.00	0.00	0.00	0.00	0.00	0.00	0.00
ISOD	0.00	0.00	0.00	0.00	0.00	0.00	0.00	0.00	0.00	0.00
ISOPRUR	0.01	0.00	0.04	0.03	8.20	6.81	5.50	0.12	0.00	0.01
LINUR	0.00	1.16	1.85	1.82	0.00	0.00	0.00	0.00	0.00	0.00
MALATH	0.00	0.00	0.00	0.00	0.00	0.00	0.00	0.00	0.00	0.00
MCPA	n.q.	n.q.	n.q.	n.q.	n.q.	n.q.	n.q.	n.q.	n.q.	n.q.
MECOPR	n.q.	n.q.	n.q.	n.q.	n.q.	n.q.	n.q.	n.q.	n.q.	n.q.
METAZCHL	0.00	0.00	0.00	0.00	26.21	18.76	18.46	0.00	0.00	0.00
METHABZT	0.00	0.00	0.00	0.00	0.00	0.00	0.00	0.00	0.00	0.00
METOLA	0.03	2.58	2.23	1.79	4.60	2.77	3.28	1.90	0.59	0.88
NAPROX	n.q.	n.q.	n.q.	n.q.	n.q.	n.q.	n.q.	n.q.	n.q.	n.q.
OXAZEP	0.00	0.00	0.00	0.00	0.00	0.00	0.00	0.00	0.00	0.00
PENDIMETH	25.88	23.35	19.31	11.78	135.3	139.6	127.6	14.51	15.27	14.73
PFBS	0.01	0.05	0.05	0.05	0.04	0.01	0.04	0.05	0.02	0.02
PFDEA	0.00	0.37	0.45	0.35	0.15	0.14	0.11	0.35	0.33	0.29
PFHPA	0.04	0.51	0.64	0.49	0.34	0.24	0.32	0.54	0.30	0.36
PFHXA	0.00	0.39	0.45	0.32	0.12	0.12	0.12	0.31	0.27	0.30
PFHXS	0.06	0.27	0.24	0.19	0.14	0.11	0.12	0.28	0.11	0.12
PFNOA	0.05	0.73	0.90	0.57	0.31	0.34	0.27	0.73	0.52	0.54
PFOA	0.20	6.50	6.23	4.80	2.73	2.62	2.40	3.85	2.87	2.98

A1 Table 2 continued:

ng/PUF disk	Sylt Y	FINO1 A	FINO1 B	FINO1 C	FINO1 G	FINO1 H	FINO1 I	FINO3 A	FINO3 C	FINO3 E
PFOS	0.38	2.22	1.88	1.52	0.94	0.81	0.88	1.81	0.84	0.82
PFOSA	0.00	0.06	0.06	0.02	0.06	0.06	0.06	0.02	0.02	0.02
PHEN	997.6	485.5	493.6	425.7	1340	969.4	1075	311.3	231.3	199.9
PIRIMIC	0.00	0.00	0.00	0.00	0.00	0.00	0.00	0.00	0.00	0.00
PRIMID	0.00	0.00	0.00	0.00	0.00	0.00	0.00	0.00	0.00	0.00
PROMETR	0.00	0.00	0.00	0.00	0.00	0.00	0.00	0.00	0.00	0.00
PROPAZ	0.00	0.00	0.00	0.00	0.00	0.00	0.00	0.00	0.00	0.00
PYR	208.6	94.46	99.08	95.65	282.3	191.6	204.1	67.03	61.58	48.05
QCB	2.24	0.88	0.92	0.89	1.44	1.80	1.52	1.53	1.32	1.31
SIMAZ	0.00	0.00	0.00	0.00	0.00	0.00	0.00	0.00	0.00	0.00
TBEP	0.83	0.00	0.00	0.00	0.11	0.11	0.00	0.12	0.00	0.00
TBP	0.00	0.00	0.00	0.00	6.38	6.38	6.38	0.00	0.00	7.08
TERBAZ	0.02	3.31	2.92	2.40	2.86	2.27	2.24	2.37	1.15	1.44
TERBUTR	0.00	0.00	0.00	0.00	0.00	0.00	0.00	0.00	0.00	0.00
TPP	0.00	32.20	21.00	67.20	11.11	8.01	25.11	12.80	321.5	10.80
TRIFLU	5.67	16.78	16.97	11.70	22.37	19.37	16.41	10.22	6.36	8.12

Annex 2 (A2): Field blanks and control samples

Field blanks

A2 Table 1: Field blanks of Glass Fibre Filters (GFFs); Concentrations of target analytes in ng/mL blank extract

ng/mL	PE 2	PE 12	PE 13	09AT 1	09AT 6	09AT 10	09AT 13	10AT 8	10AT 9	10AT 10	10 Nov./ Dec. 1
24-D	0.0000	0.0000	0.0000	0.0000	0.0000	0.0000	0.0000	0.0000	0.0000	0.0000	0.0000
ACE	0.0000	0.0000	0.0000	2.4190	2.3070	2.2750	2.1160	2.0570	1.9100	1.9710	0.0000
ACY	0.0000	0.0000	0.0000	0.0000	0.0000	0.0000	0.0000	0.0000	0.0000	0.0000	0.0000
ALD	0.0000	0.0000	0.0000	0.0000	0.0000	0.0000	0.0000	0.0000	0.0000	0.0000	0.0000
AMETRYN	0.0000	0.0000	0.0000	0.0021	0.0000	0.0025	0.0017	0.0000	0.0000	0.0000	0.0034
ANT	0.0000	0.0000	0.0000	0.0000	0.0000	0.0000	0.0000	0.0000	0.0000	0.0000	0.0000
ATRAZ	0.0000	0.0000	0.0000	0.0000	0.0000	0.0000	0.0000	0.0000	0.0000	0.0000	0.0000
AZINPH-E	0.0000	0.0000	0.0000	0.0000	0.0000	0.0000	0.0000	0.0000	0.0000	0.0000	0.0000
AZINPH-M	0.0000	0.0000	0.0000	0.0000	0.0000	0.0000	0.0000	0.0000	0.0000	0.0000	0.0000
BAA	0.0000	0.0000	0.0000	0.0000	0.0000	0.0000	0.0000	0.0000	0.0000	0.0000	0.0000
BAP	0.0000	0.0000	0.0000	0.0000	0.0000	0.0000	0.0000	0.0000	0.0000	0.0000	0.0000
BBF	0.0000	0.0000	0.0000	0.0000	0.0000	0.0000	0.0000	0.0000	0.0000	0.0000	0.0000
BENTAZ	0.0000	0.0000	0.0000	0.0000	0.0000	0.0000	0.0000	0.0000	0.0000	0.0000	0.0000
BGHIP	0.0000	0.0000	0.0000	0.0000	0.0000	0.0000	0.0000	0.0000	0.0000	0.0000	0.0000
CARBAMAZ	0.0000	0.0000	0.0000	0.0000	0.0000	0.0000	0.0000	0.0000	0.0000	0.0000	0.0000
CARBEND	0.0000	0.0000	0.0000	0.0000	0.0000	0.0000	0.0000	0.0000	0.0000	0.0000	0.0000
CB138	0.0000	0.0000	0.0000	0.0000	0.0000	0.0000	0.0000	0.0000	0.0000	0.0000	0.0000
CB153	0.0000	0.2350	0.0000	0.0000	0.0000	0.0000	0.0000	0.0000	0.2650	0.0000	0.0000
CB28	0.0000	0.0000	0.0000	0.0000	0.1640	0.0000	0.0000	0.0000	0.0000	0.0000	0.0000
CB52	0.0000	0.0000	0.0000	0.0000	0.0000	0.0000	0.0000	0.0000	0.0000	0.0000	0.0000
CHLORFENV	0.0000	0.0000	0.0000	0.0000	0.0000	0.0000	0.0000	0.0000	0.0000	0.0000	0.0000

A2 Table 1 continued:

ng/mL	PE 2	PE 12	PE 13	09AT 1	09AT 6	09AT 10	09AT 13	10AT 8	10AT 9	10AT 10	10 Nov./ Dec. 1
CHLORTUR	0.0000	0.0000	0.0000	0.0000	0.0000	0.0000	0.0000	0.0000	0.0000	0.0000	0.0000
CHRTR	0.0000	0.0000	0.0000	0.0000	0.0000	0.0000	0.0000	0.0000	0.0000	0.0000	0.0000
CLOFIBRS	0.0000	0.0000	0.0000	0.0000	0.0000	0.0000	0.0000	0.0000	0.0000	0.0000	0.0000
DBAHA	0.0000	0.0000	0.0000	0.0000	0.0000	0.0000	0.0000	0.0000	0.0000	0.0000	0.0000
DDDP	0.0000	0.0000	0.0000	0.0000	0.0000	0.0000	0.0000	0.0000	0.0000	0.0000	0.0000
DDEPP	0.0000	0.0000	0.0000	0.0000	0.0000	0.0000	0.0000	0.0000	0.0000	0.0000	0.0000
DDTOP	0.0000	0.0000	0.0000	0.0000	0.0000	0.0000	0.0000	0.0000	0.0000	0.0000	0.0000
DDTPP	0.0000	0.0000	0.0000	0.0000	0.0000	0.0000	0.0000	0.0000	0.0000	0.0000	0.0000
DEATRAZ	0.0000	0.0000	0.0000	0.0000	0.0000	0.0000	0.0000	0.0000	0.0000	0.0000	0.0000
DIAZINON	0.0000	0.0000	0.0000	0.0000	0.0000	0.0000	0.0000	0.0000	0.0000	0.0000	0.0000
DICHLPR	0.0000	0.0000	0.0000	0.0000	0.0000	0.0000	0.0000	0.0000	0.0000	0.0000	0.0000
DICLOF	0.0000	0.0000	0.0000	0.0000	0.0000	0.0000	0.0000	0.0000	0.0000	0.0000	0.0000
DIELD	0.0000	0.0000	0.0000	0.0000	0.0000	0.0000	0.0000	0.0000	0.0000	0.0000	0.0000
DIMETH	0.0000	0.0000	0.0000	0.0000	0.0000	0.0000	0.0000	0.0000	0.0000	0.0000	0.0000
DIURON	0.0000	0.0000	0.0000	0.0000	0.0000	0.0000	0.0000	0.0000	0.0000	0.0000	0.0000
END	0.0000	0.0000	0.0000	0.0000	0.0000	0.0000	0.0000	0.0000	0.0000	0.0000	0.0000
FENUR	0.0050	0.0000	0.0000	0.0000	0.0000	0.0000	0.0000	0.0000	0.0000	0.0000	0.0000
FL	0.0000	0.0000	0.0000	0.0000	0.0000	5.2170	5.2030	4.9390	4.9090	4.9310	0.0000
FLU	0.0000	0.0000	0.0000	2.9460	0.0000	2.9430	2.9450	3.8110	3.7960	3.7960	0.0000
HBCDA	0.0000	0.0000	0.0000	0.0000	0.0000	0.0000	0.0000	0.0000	0.0000	0.0000	0.0025
HBCDBG	0.0000	0.0000	0.0000	0.0000	0.0000	0.0000	0.0014	0.0058	0.0020	0.0010	0.0022
HCB	0.1870	0.1820	0.1950	0.1450	0.1470	0.1540	0.1490	0.1430	0.1480	0.1500	0.0000
HCHA	0.0000	0.0000	0.0000	0.0000	0.0000	0.0000	0.0000	0.0000	0.0000	0.0000	0.0000
HCHB	0.0000	0.0000	0.0000	0.0000	0.0000	0.0000	0.0000	0.0000	0.0000	0.0000	0.0000
HCHD	0.0000	0.0000	0.0000	0.0000	0.0000	0.0000	0.0000	0.0000	0.0000	0.0000	0.0000
HCHG	0.0000	0.0000	0.0000	0.0000	0.0000	0.0000	0.0000	0.0000	0.0000	0.0000	0.0000
HEXAZIN	0.0000	0.0000	0.0000	0.0000	0.0000	0.0000	0.0000	0.0000	0.0000	0.0000	0.0000
I123P	0.0000	0.0000	0.0000	0.0000	0.0000	0.0000	0.0000	0.0000	0.0000	0.0000	0.0000
IRGAROL	0.0000	0.0000	0.0000	0.0000	0.0000	0.0000	0.0000	0.0000	0.0000	0.0000	0.0000
ISOD	0.0000	0.0000	0.0000	0.0000	0.0000	0.0000	0.0000	0.0000	0.0000	0.0000	0.0000
ISOPRUR	0.0000	0.0000	0.0000	0.0000	0.0000	0.0000	0.0000	0.0000	0.0000	0.0000	0.0000
LINUR	0.0000	0.0000	0.0000	0.0000	0.0000	0.0000	0.0000	0.0000	0.0000	0.0000	0.0000
MALATH	0.0000	0.0000	0.0000	0.0000	0.0000	0.0000	0.0000	0.0000	0.0000	0.0000	0.0000
MCPA	0.0000	0.0000	0.0000	0.0000	0.0000	0.0000	0.0000	0.0000	0.0000	0.0000	0.0000
MECOPR	0.0000	0.0000	0.0000	0.0000	0.0000	0.0000	0.0000	0.0000	0.0000	0.0000	0.0000
METAZCHL	0.0000	0.0000	0.0000	0.0000	0.0000	0.0000	0.0000	0.0000	0.0000	0.0000	0.0000
METHABZT	0.0000	0.0000	0.0000	0.0000	0.0000	0.0000	0.0000	0.0000	0.0000	0.0000	0.0000
METOLA	0.0000	0.0000	0.0000	0.0320	0.0530	0.0309	0.0199	0.0400	0.0439	0.0372	0.0000
NAPROX	0.0000	0.0000	0.0000	0.0000	0.0000	0.0000	0.0000	0.0000	0.0000	0.0000	0.0000
OXAZEP	0.0000	0.0000	0.0000	0.0000	0.0000	0.0000	0.0000	0.0000	0.0000	0.0000	0.0000
PENDIMETH	0.0054	0.0000	0.0000	0.0581	0.0757	0.0000	0.0526	0.0692	0.0721	0.0956	0.0720
PFBS	0.0009	0.0000	0.0000	0.0033	0.0034	0.0027	0.0028	0.0067	0.0052	0.0069	0.0025
PFDEA	0.0000	0.0000	0.0000	0.0000	0.0000	0.0000	0.0000	0.0000	0.0000	0.0000	0.0000
PFHPA	0.0306	0.0261	0.0179	0.0056	0.0141	0.0111	0.0055	0.0165	0.0101	0.0175	0.0079
PFHXA	0.0268	0.0179	0.0039	0.0000	0.0160	0.0035	0.0007	0.0212	0.0105	0.0152	0.0088
PFHXS	0.0004	0.0000	0.0001	0.0011	0.0025	0.0019	0.0002	0.0022	0.0024	0.0028	0.0014
PFNOA	0.0474	0.0356	0.0404	0.0115	0.0256	0.0282	0.0125	0.0367	0.0296	0.0419	0.0000
PFOA	0.0764	0.0554	0.0629	0.0165	0.0743	0.0465	0.0202	0.0488	0.0484	0.0519	0.0341
PFOS	0.0312	0.0111	0.0139	0.0315	0.0873	0.0390	0.0068	0.0105	0.0063	0.0062	0.0187
PFOSA	0.0460	0.0052	0.0093	0.0518	0.1118	0.0547	0.0200	0.0286	0.0184	0.0353	0.0197

A2 Table 1 continued:

ng/mL	PE 2	PE 12	PE 13	09AT 1	09AT 6	09AT 10	09AT 13	10AT 8	10AT 9	10AT 10	10 Nov./Dec. 1
PHEN	0.0000	0.0000	0.0000	3.1040	2.8530	2.9750	3.1320	3.4180	3.1770	3.2370	0.0000
PIRIMIC	0.0000	0.0000	0.0000	0.0000	0.0000	0.0000	0.0000	0.0000	0.0000	0.0000	0.0000
PRIMID	0.0000	0.0000	0.0000	0.0000	0.0000	0.0000	0.0000	0.0000	0.0000	0.0000	0.0000
PROMETR	0.0466	0.0498	0.0424	0.0813	0.0775	0.0819	0.0846	0.0775	0.0749	0.0766	0.0865
PROPAZ	0.0000	0.0000	0.0000	0.0000	0.0000	0.0000	0.0000	0.0000	0.0000	0.0000	0.0000
PYR	0.0000	0.0000	0.0000	3.5760	3.5720	3.5730	3.5750	4.7130	4.6740	4.6730	0.0000
QCB	0.0000	0.0000	0.0000	0.0000	0.0000	0.0000	0.0000	0.0000	0.0000	0.0000	0.0000
SIMAZ	0.0000	0.0000	0.0000	0.0000	0.0000	0.0000	0.0000	0.0000	0.0000	0.0000	0.0000
TBEP	0.5682	0.1558	0.5024	2.8514	4.0810	3.5298	9.5082	8.2680	0.8925	5.6074	0.7770
TBP	2.8200	1.5700	1.8700	2.1100	2.3400	2.3100	2.2800	1.8400	2.1800	1.9600	2.4600
TERBAZ	0.2080	0.1149	0.1469	0.1005	0.0311	0.0490	0.0790	0.0797	0.0836	0.0770	0.0668
TERBUTR	0.0000	0.0000	0.0000	0.0000	0.0000	0.0000	0.0000	0.0000	0.0000	0.0000	0.0000
TPP	1.6400	1.0900	1.3100	0.4720	0.7210	0.6510	0.4120	0.4840	0.5420	0.5830	0.5380
TRIFLU	0.0000	0.0000	0.0000	0.0000	0.0000	0.0000	0.0000	0.0000	0.0000	0.0000	0.0000

ng/mL	10 Nov./ Dec. 2	10 Nov./ Dec. 3
24-D	0.0000	0.0000
ACE	0.0000	0.0000
ACY	0.0000	0.0000
ALD	0.0000	0.0000
AMETRYN	0.0051	0.0049
ANT	0.0000	0.0000
ATRAZ	0.0000	0.0000
AZINPH-E	0.0000	0.0000
AZINPH-M	0.0000	0.0000
BAA	0.0000	0.0000
BAP	0.0000	0.0000
BBF	0.0000	0.0000
BENTAZ	0.0000	0.0000
BGHIP	0.0000	0.0000
CARBAMAZ	0.0000	0.0000
CARBEND	0.0000	0.0000
CB138	0.0000	0.0000
CB153	0.0000	0.0000
CB28	0.0000	0.4940
CB52	0.0000	0.0000
CHLORFENV	0.0000	0.0000
CHLORTUR	0.0000	0.0000
CHRTR	0.0000	0.0000
CLOFIBRS	0.0000	0.0000
DBAHA	0.0000	0.0000
DDDP	0.0000	0.0000
DDEPP	0.0000	0.0000
DDTOP	0.0000	0.0000
DDTPP	0.0000	0.0000
DEATRAZ	0.0000	0.0000
DIAZINON	0.0000	0.0000

ng/mL	10 Nov./ Dec. 2	10 Nov./ Dec. 3
DICHLPR	0.0000	0.0000
DICLOF	0.0000	0.0000
DIELD	0.0000	0.0000
DIMETH	0.0000	0.0000
DIURON	0.0000	0.0000
END	0.0000	0.0000
FENUR	0.0000	0.0000
FL	0.0000	0.0000
FLU	0.0000	0.0000
HBCDA	0.0016	0.0008
HBCDBG	0.0036	0.0024
HCB	0.0000	0.0000
HCHA	0.0000	0.0000
HCHB	0.0000	0.0000
HCHD	0.0000	0.0000
HCHG	0.0000	0.0000
HEXAZIN	0.0000	0.0000
I123P	0.0000	0.0000
IRGAROL	0.0000	0.0000
ISOD	0.0000	0.0000
ISOPRUR	0.0000	0.0000
LINUR	0.0000	0.0000
MALATH	0.0000	0.0000
MCPA	0.0000	0.0000
MECOPR	0.0000	0.0000
METAZCHL	0.0000	0.0000
METHABZT	0.0000	0.0000
METOLA	0.0000	0.0000
NAPROX	0.0000	0.0000
OXAZEP	0.0000	0.0000
PENDIMETH	0.0563	0.0484

ng/mL	10 Nov./ Dec. 2	10 Nov./ Dec. 3
PFBS	0.0028	0.0043
PFDEA	0.0000	0.0000
PFHPA	0.0070	0.0126
PFHXA	0.0065	0.0070
PFHXS	0.0007	0.0012
PFNOA	0.0000	0.0000
PFOA	0.0408	0.0434
PFOS	0.0233	0.0147
PFOSA	0.0119	0.0149
PHEN	0.0000	0.0000
PIRIMIC	0.0000	0.0000
PRIMID	0.0000	0.0000
PROMETR	0.0968	0.0835
PROPAZ	0.0000	0.0000
PYR	0.0000	0.0000
QCB	0.0000	0.0000
SIMAZ	0.0000	0.0000
TBEP	0.9328	0.4261
TBP	2.9400	2.1700
TERBAZ	0.1053	0.0424
TERBUTR	0.0000	0.0000
TPP	1.5800	0.3480
TRIFLU	0.0000	0.0000

A2 Table 2: Field blanks of PUF plug adsorber cartridges; Concentrations of target analytes in ng/mL blank extract; n.q. = not quantified

ng/mL	AL 11	AL 12	AL 13	10 Nov./Dec. 1	10 Nov./Dec. 2	10 Nov./Dec. 3
24-D	n.q.	n.q.	n.q.	n.q.	n.q.	n.q.
ACE	3.9140	0.0000	0.0000	4.3870	3.7820	3.7570
ACY	0.0000	0.0000	0.0000	16.3460	4.3410	4.6830
ALD	0.0000	0.0000	0.0000	0.0000	0.0000	0.0000
AMETRYN	0.0000	0.0000	0.0000	0.0000	0.0000	0.0000
ANT	0.0000	0.0000	0.0000	0.0000	0.0000	0.0000
ATRAZ	0.0000	0.0000	0.0000	0.0000	0.0000	0.0000
AZINPH-E	0.0000	0.0000	0.0000	0.0000	0.0000	0.0000
AZINPH-M	0.0000	0.0000	0.0000	0.0000	0.0000	0.0000
BAA	0.0000	0.0000	0.0000	0.0000	0.0000	0.0000
BAP	0.0000	0.0000	0.0000	0.0000	0.0000	0.0000
BBF	0.0000	0.0000	0.0000	0.0000	0.0000	0.0000
BENTAZ	0.0000	0.0000	0.0000	0.0000	0.0000	0.0000
BGHIP	0.0000	0.0000	0.0000	0.0000	0.0000	0.0000
CARBAMAZ	0.0000	0.0000	0.0000	0.0000	0.0000	0.0000
CARBEND	0.0000	0.0000	0.0000	0.0000	0.0000	0.0000
CB138	0.2520	0.4390	0.1820	0.0000	0.0000	0.0000
CB153	0.2940	0.4800	0.2670	0.0000	0.4130	0.4120
CB28	0.0000	0.0000	0.0000	0.4960	0.0000	0.0000
CB52	0.0000	0.0000	0.0000	0.0000	0.0000	0.0000
CHLORFENV	0.0000	0.0000	0.0000	0.0000	0.0000	0.0000
CHLORTUR	0.0000	0.0000	0.0000	0.0046	0.0145	0.0227
CHRTR	0.0000	0.0000	0.0000	0.0000	0.0000	0.0000
CLOFIBRS	n.q.	n.q.	n.q.	n.q.	n.q.	n.q.
DBAHA	0.0000	0.0000	0.0000	0.0000	0.0000	0.0000
DDPP	0.0000	0.0000	0.0690	0.0000	0.0000	0.0000
DDEPP	0.0000	0.0000	0.0000	0.0000	0.0000	0.0000
DDTOP	0.0000	0.0000	0.0000	0.0000	0.0000	0.0000
DDTPP	0.0000	0.0000	0.0000	0.0000	0.0000	0.0000
DEATRAZ	0.0000	0.0000	0.0000	0.0000	0.0000	0.0000
DIAZINON	0.0000	0.0000	0.0000	0.0000	0.0000	0.0000
DICHLPR	n.q.	n.q.	n.q.	n.q.	n.q.	n.q.
DICLOF	n.q.	n.q.	n.q.	n.q.	n.q.	n.q.
DIELD	0.0000	0.0000	0.0000	0.0000	0.0000	0.0000
DIMETH	0.0000	0.0000	0.0000	0.0000	0.0000	0.0000
DIURON	0.0000	0.0000	0.0000	0.1197	0.0709	0.2394
END	0.0000	0.0000	0.0000	0.0000	0.0000	0.0000
FENUR	0.1068	0.0165	0.0000	0.0048	0.0053	0.0158
FL	0.0000	9.8660	0.0000	6.4720	5.0770	4.8750
FLU	2.1760	0.0000	0.0000	4.6970	2.7740	2.7140
HBCDA	0.2212	0.1315	0.1714	0.0000	0.0000	0.0000
HBCDBG	0.5900	0.3240	0.2805	0.0000	0.0000	0.0074
HCB	0.2130	0.2040	0.2280	0.0000	0.0000	0.0000
HCHA	0.1240	0.0000	0.0000	0.0000	0.0000	0.0000
HCHB	0.0000	0.0000	0.0000	0.0000	0.0000	0.0000
HCHD	0.0000	0.0000	0.0000	0.0000	0.0000	0.0000
HCHG	0.2240	0.1550	0.2120	0.0000	0.0000	0.0000
HEXAZIN	0.0000	0.0000	0.0000	0.0000	0.0000	0.0000
I123P	0.0000	0.0000	0.0000	0.0000	0.0000	0.0000
IRGAROL	0.0000	0.0000	0.0000	0.0000	0.0000	0.0000

A2 Table 2 continued:

ng/mL	AL 11	AL 12	AL 13	10 Nov./Dec. 1	10 Nov./Dec. 2	10 Nov./Dec. 3
ISOD	0.0000	0.0000	0.2210	0.0000	0.0000	0.0000
ISOPRUR	0.0000	0.0000	0.0000	0.0040	0.0020	0.0000
LINUR	0.0000	0.0000	0.0000	0.0000	0.0000	0.0000
MALATH	0.0000	0.0000	0.0000	0.0000	0.0000	0.0000
MCPA	n.q.	n.q.	n.q.	n.q.	n.q.	n.q.
MECOPR	n.q.	n.q.	n.q.	n.q.	n.q.	n.q.
METAZCHL	0.0000	0.0000	0.0000	0.0000	0.0000	0.0000
METHABZT	0.0000	0.0000	0.0000	0.0000	0.0000	0.0000
METOLA	0.0000	0.0000	0.0000	0.0428	0.0405	0.0000
NAPROX	n.q.	n.q.	n.q.	n.q.	n.q.	n.q.
OXAZEP	0.0000	0.0000	0.0000	0.0000	0.0000	0.0000
PENDIMETH	0.3251	0.1533	0.1689	0.3342	0.1780	0.0561
PFBS	0.0013	0.0000	0.0000	0.0108	0.0099	0.0119
PFDEA	0.0421	0.0000	0.0000	0.0241	0.0197	0.0151
PFHPA	0.0302	0.0000	0.0000	0.0373	0.0290	0.0309
PFHXA	0.0886	0.0524	0.0638	0.0387	0.0358	0.0370
PFHXS	0.0183	0.0174	0.0178	0.0017	0.0025	0.0022
PFNOA	0.0000	0.0000	0.0000	0.0296	0.0220	0.0216
PFOA	0.1744	0.0200	0.0706	0.1774	0.1466	0.1565
PFOS	0.1128	0.0593	0.0693	0.0824	0.1205	0.0788
PFOSA	0.0296	0.0305	0.0891	0.0658	0.0848	0.0938
PHEN	10.9960	4.7420	3.8360	11.1040	9.0750	8.2260
PIRIMIC	0.0000	0.0000	0.0000	0.0000	0.0000	0.0000
PRIMID	0.0000	0.0000	0.0000	0.0000	0.0000	0.0000
PROMETR	0.0650	0.0537	0.0591	0.0807	0.0828	0.0767
PROPAZ	0.0000	0.0000	0.0000	0.0000	0.0000	0.0000
PYR	0.0000	0.0000	0.0000	10.9370	5.7590	6.6950
QCB	0.2410	0.2490	0.2370	0.4940	0.4920	0.0000
SIMAZ	0.0000	0.0000	0.0000	0.0000	0.0000	0.0000
TBEP	1.2921	0.1729	0.0493	0.6858	0.7759	0.7558
TBP	11.3300	6.9220	4.3930	8.8700	7.1800	7.7800
TERBAZ	0.0372	0.0474	0.0328	0.0304	0.0213	0.0274
TERBUTR	0.0000	0.0000	0.0000	0.0000	0.0000	0.0000
TPP	1.6690	1.1930	0.7855	2.5800	3.0700	1.7800
TRIFLU	0.2480	0.2070	0.2120	0.0000	0.0000	0.0000

A2 Table 3: Field blanks of PUF/XAD-2/PUF adsorber cartridges; Concentrations of target analytes in ng/mL blank extract; n.q. = not quantified

ng/mL	PE 2	PE 12	PE 13	09AT 1	09AT 6	09AT 10	09AT 13	10AT 8	10AT 9	10AT 10	10 Nov./Dec. 1
24-D	n.q.	n.q.	n.q.	n.q.	n.q.	n.q.	n.q.	n.q.	n.q.	n.q.	n.q.
ACE	0.0000	0.0000	0.0000	3.5610	2.8090	3.4080	2.8580	4.1260	4.4510	3.5890	4.1200
ACY	0.0000	7.9940	47.0300	0.0000	0.0000	0.0000	0.0000	4.3360	4.3680	3.6840	9.2740
ALD	0.0000	0.0000	0.0000	0.0000	0.0000	0.0000	0.0000	0.0000	0.0000	0.0000	0.0000
AMETRYN	0.0000	0.0000	0.0000	0.0000	0.0000	0.0000	0.0000	0.0000	0.0000	0.0000	0.0000
ANT	0.0000	0.0000	0.0000	0.0000	0.0000	0.0000	0.0000	0.0000	0.0000	0.0000	0.0000
ATRAZ	0.0000	0.0000	0.0000	0.0000	0.0000	0.0000	0.0000	0.0000	0.0000	0.0000	0.0000
AZINPH-E	0.0000	0.0000	0.0000	0.0000	0.0000	0.0000	0.0000	0.0000	0.0000	0.0000	0.0000
AZINPH-M	0.0000	0.0000	0.0000	0.0000	0.0000	0.0000	0.0000	0.0000	0.0000	0.0000	0.0000

A2 Table 3 continued:

ng/mL	PE 2	PE 12	PE 13	09AT 1	09AT 6	09AT 10	09AT 13	10AT 8	10AT 9	10AT 10	10 Nov./Dec. 1
BAA	0.0000	0.0000	0.0000	0.0000	0.0000	0.0000	0.0000	1.5760	1.6140	1.4800	0.0000
BAP	0.0000	0.0000	0.0000	0.0000	0.0000	0.0000	0.0000	3.9560	4.2340	1.8370	0.0000
BBF	0.0000	0.0000	0.0000	2.1430	2.7560	2.4020	3.2060	0.0000	0.0000	0.0000	0.0000
BENTAZ	0.0047	0.0035	0.0046	0.0000	0.0000	0.0000	0.0000	0.0000	0.0000	0.0000	0.0000
BGHIP	0.0000	0.0000	6.3880	0.0000	0.0000	0.0000	0.0000	9.2730	10.6340	1.8510	3.8570
CARBAMAZ	0.0000	0.0000	0.0000	0.0000	0.0000	0.0000	0.0000	0.0000	0.0000	0.0000	0.0000
CARBEND	0.0000	0.0000	0.0000	0.0000	0.0000	0.0000	0.0000	0.0000	0.0000	0.0000	0.0000
CB138	0.2870	0.2380	0.2160	0.2520	0.3820	0.4800	0.3700	0.0000	0.0000	0.0000	0.0000
CB153	0.1450	0.1360	0.1230	0.2280	0.2380	0.2330	0.2290	0.2190	0.2100	0.2070	0.4160
CB28	0.1960	0.2020	0.2120	0.1340	0.1020	0.1300	0.0940	0.1260	0.1140	0.0820	0.5060
CB52	0.1540	0.1460	0.0000	0.1800	0.1620	0.1580	0.1620	0.1940	0.1780	0.1520	0.0000
CHLORFENV	0.0000	0.1031	0.0000	0.0000	0.0000	0.0000	0.0000	0.7308	1.0835	0.5309	0.2824
CHLORTUR	0.0000	0.0000	0.0000	0.0000	0.0000	0.0000	0.0000	0.0000	0.0000	0.0000	0.0000
CHRTR	0.0000	0.0000	0.0000	0.0000	0.0000	0.0000	0.0000	4.5820	4.6560	4.3540	0.0000
CLOFIBRS	n.q.	n.q.	n.q.	n.q.	n.q.	n.q.	n.q.	n.q.	n.q.	n.q.	n.q.
DBAHA	0.0000	0.0000	5.7330	0.0000	0.0000	0.0000	0.0000	0.0000	0.0000	0.0000	0.0000
DDPP	0.0000	0.0000	0.0000	0.0000	0.0000	0.0000	0.0000	0.0000	0.0000	0.0000	0.0000
DDEPP	0.0000	0.0000	0.0000	0.0000	0.0000	0.0000	0.0000	0.0000	0.0000	0.0000	0.0000
DDTOP	0.0000	0.0000	0.0000	0.0000	0.0000	0.0000	0.0000	0.0000	0.0000	0.0000	0.0000
DDTPP	0.0000	0.0000	0.0000	0.0000	0.0000	0.0000	0.0000	0.0000	0.0000	0.0000	0.0000
DEATRAZ	0.0000	0.0000	0.0000	0.0000	0.0000	0.0000	0.0000	0.0000	0.0000	0.0000	0.0000
DIAZINON	0.0000	0.0000	0.0000	0.0000	0.0000	0.0000	0.0000	0.0000	0.0000	0.0000	0.0000
DICHLPR	n.q.	n.q.	n.q.	n.q.	n.q.	n.q.	n.q.	n.q.	n.q.	n.q.	n.q.
DICLOF	n.q.	n.q.	n.q.	n.q.	n.q.	n.q.	n.q.	n.q.	n.q.	n.q.	n.q.
DIELD	0.0000	0.0000	0.0000	0.0000	0.0000	0.0000	0.0000	0.0000	0.0000	0.0000	0.0000
DIMETH	0.0000	0.0000	0.0000	0.0000	0.0000	0.0051	0.0054	0.0000	0.0000	0.0000	0.0000
DIURON	0.0000	0.0000	0.0000	0.0000	0.0000	0.0000	0.0000	0.1131	0.0968	0.0654	0.2954
END	0.0000	0.0000	0.0000	0.0000	0.0000	0.0000	0.0000	0.0000	0.0000	0.0000	0.0000
FENUR	0.1223	0.3936	0.0652	0.0195	0.0247	0.0295	0.0299	2.7244	4.0477	10.0970	0.9708
FL	0.0000	0.0000	0.0000	9.5900	6.8800	7.6430	6.8470	7.6530	8.0150	6.2750	4.9700
FLU	7.9130	8.3720	7.3410	3.9880	3.7800	4.1350	3.7060	14.4890	16.4290	5.1830	13.9460
HBCDA	0.0570	0.0000	0.0000	0.0000	0.0000	0.0000	0.0000	0.0768	0.0667	0.0607	0.0000
HBCDBG	0.0170	0.0000	0.0000	0.0000	0.0000	0.0000	0.0000	0.0000	0.0000	0.0000	0.0000
HCB	0.2170	0.2400	0.2320	0.2040	0.1820	0.1930	0.1760	0.1850	0.1570	0.1550	0.7680
HCHA	0.1190	0.1180	0.1200	0.0000	0.0000	0.0000	0.0000	0.0000	0.0000	0.0000	0.0000
HCHB	0.0000	0.0000	0.0000	0.0000	0.0000	0.0000	0.0000	0.0000	0.0000	0.0000	0.0000
HCHD	0.0000	0.0000	0.0000	0.0000	0.0000	0.0000	0.0000	0.0000	0.0000	0.0000	0.0000
HCHG	0.2020	0.2240	0.2270	0.2530	0.2100	0.2170	0.2130	0.2100	0.2070	0.1930	0.0000
HEXAZIN	0.0000	0.0000	0.0000	0.0000	0.0000	0.0000	0.0000	0.0000	0.0000	0.0000	0.0000
I123P	0.0000	0.0000	6.4690	0.0000	0.0000	0.0000	0.0000	3.0180	3.3280	1.9760	0.0000
IRGAROL	0.0000	0.0000	0.0000	0.0000	0.0000	0.0000	0.0000	0.0000	0.0000	0.0000	0.0000
ISOD	0.0000	0.0000	0.0000	0.2150	0.0000	0.0000	0.0000	0.0000	0.0000	0.0000	0.0000
ISOPRUR	0.0000	0.0000	0.0000	0.0038	0.0000	0.0000	0.0068	0.0000	0.0000	0.0000	0.0000
LINUR	0.0000	0.0000	0.0000	0.0000	0.0000	0.0000	0.0000	0.0000	0.0000	0.0000	0.0000
MALATH	0.0000	0.0000	0.0000	0.0000	0.0000	0.0000	0.0000	0.0000	0.0000	0.0000	0.0000
MCPA	n.q.	n.q.	n.q.	n.q.	n.q.	n.q.	n.q.	n.q.	n.q.	n.q.	n.q.
MECOPR	n.q.	n.q.	n.q.	n.q.	n.q.	n.q.	n.q.	n.q.	n.q.	n.q.	n.q.
METAZCHL	0.0000	0.0000	0.0000	0.0000	0.0000	0.0000	0.0234	0.0000	0.0000	0.0000	0.0000
METHABZT	0.0000	0.0000	0.0000	0.0000	0.0000	0.0000	0.0000	0.0000	0.0000	0.0000	0.0000
METOLA	0.0000	0.0253	0.0000	0.9500	0.7230	0.4720	0.6370	0.2050	0.4570	0.5000	0.0360

A2 Table 3 continued:

ng/mL	PE 2	PE 12	PE 13	09AT 1	09AT 6	09AT 10	09AT 13	10AT 8	10AT 9	10AT 10	10 Nov./Dec. 1
NAPROX	n.q.	n.q.	n.q.	n.q.	n.q.	n.q.	n.q.	n.q.	n.q.	n.q.	n.q.
OXAZEP	0.0000	0.0000	0.0000	0.0000	0.0000	0.0000	0.0000	0.0000	0.0000	0.0000	0.0000
PENDIMETH	0.1747	0.1977	0.1267	0.3287	0.3374	0.2282	0.1998	0.1420	0.1780	0.1507	0.0818
PFBS	0.0143	0.0153	0.0118	0.0236	0.0334	0.0184	0.0273	0.0157	0.0155	0.0258	0.0098
PFDEA	0.0000	0.0000	0.0000	0.0000	0.0000	0.0000	0.0000	0.0000	0.0000	0.0000	0.0272
PFHPA	0.0000	0.0000	0.0000	0.0475	0.0858	0.0591	0.0780	0.0822	0.0570	0.0757	0.0494
PFHXA	0.1111	0.1304	0.0927	0.0899	0.1274	0.0580	0.0791	0.1294	0.0720	0.0867	0.0544
PFHXS	0.0066	0.0166	0.0078	0.0183	0.0152	0.0087	0.0158	0.0304	0.0165	0.0080	0.0265
PFNOA	0.0000	0.0000	0.0000	0.1041	0.1882	0.1101	0.1992	0.2292	0.1091	0.1411	0.0632
PFOA	0.3383	0.4805	0.2854	0.2942	0.6910	0.4706	0.8761	0.3284	0.2535	0.3053	0.2513
PFOS	0.0782	0.2722	0.1409	0.2722	0.2683	0.2595	0.4189	0.1118	0.1993	0.3266	0.1157
PFOSA	1.4175	1.5000	0.6098	1.0500	0.9300	0.5310	0.6818	0.1545	0.1695	0.3240	0.0960
PHEN	12.409	11.304	15.559	9.5460	6.5670	7.8410	6.5160	17.278	16.953	8.8210	16.043
PIRIMIC	0.0000	0.0000	0.0000	0.0000	0.0000	0.0000	0.0000	0.0000	0.0000	0.0000	0.0000
PRIMID	0.0000	0.0000	0.0000	0.0000	0.0000	0.0000	0.0000	0.0000	0.0000	0.0000	0.0000
PROMETR	0.0682	0.0549	0.0677	0.0683	0.0767	0.0810	0.0749	0.0781	0.0704	0.0738	0.0757
PROPAZ	0.0000	0.0000	0.0000	0.0000	0.0000	0.0000	0.0000	0.0000	0.0000	0.0000	0.0000
PYR	9.9720	21.991	8.8600	4.9250	4.7040	5.3910	4.5400	57.805	70.371	9.5560	58.416
QCB	0.1730	0.1820	0.1810	0.2170	0.2140	0.2140	0.1930	0.2270	0.2150	0.1950	0.4940
SIMAZ	0.0000	0.0000	0.0000	0.0000	0.0000	0.0000	0.0000	0.0000	0.0000	0.0000	0.0000
TBEP	0.7102	0.7982	0.3858	3.6146	3.8372	5.5544	3.5192	3.2860	6.8476	1.7914	1.1554
TBP	6.6700	4.6400	6.4600	19.300	23.700	22.400	27.700	0.6970	0.0000	1.2800	14.300
TERBAZ	0.0579	0.0590	0.0384	0.4108	0.2613	0.2132	0.3744	0.0896	0.1664	0.1846	0.0241
TERBUTR	0.0000	0.0000	0.0000	0.0000	0.0000	0.0000	0.0000	0.0000	0.0000	0.0000	0.0000
TPP	10.400	34.500	21.400	3.1500	5.6500	2.3000	4.6800	35.200	49.100	8.2200	11.800
TRIFLU	0.0000	0.0000	0.3120	0.0000	0.0000	0.0000	0.0000	0.0000	0.0000	0.0000	0.0000

ng/mL	10 Nov./ Dec. 2	10 Nov./ Dec. 3
24-D	n.q.	n.q.
ACE	3.7770	n.q.
ACY	6.2240	n.q.
ALD	0.0000	0.0000
AMETRYN	0.0000	0.0000
ANT	3.1200	n.q.
ATRAZ	0.0000	0.0000
AZINPH-E	0.0000	0.0000
AZINPH-M	0.0000	0.0000
BAA	0.0000	n.q.
BAP	0.0000	n.q.
BBF	0.0000	n.q.
BENTAZ	0.0000	0.0000
BGHIP	0.0000	n.q.
CARBAMAZ	0.0000	0.0000
CARBEND	0.0000	0.0000
CB138	0.4710	0.6400
CB153	0.4560	0.7470
CB28	0.5430	0.7550
CB52	0.4290	1.0830

ng/mL	10 Nov./ Dec. 2	10 Nov./ Dec. 3
CHLORFENV	0.0000	0.0539
CHLORTUR	0.0000	0.0000
CHRTR	6.0430	n.q.
CLOFIBRS	n.q.	n.q.
DBAHA	0.0000	n.q.
DDDPP	0.0000	0.0000
DDEPP	0.0000	0.0000
DDTOP	0.0000	0.0000
DDTPP	0.0000	0.0000
DEATRAZ	0.0000	0.0000
DIAZINON	0.0000	0.0000
DICHLPR	n.q.	n.q.
DICLOF	n.q.	n.q.
DIELD	0.0000	0.0000
DIMETH	0.0000	0.0000
DIURON	0.1142	0.0000
END	0.0000	0.0000
FENUR	0.3547	1.4122
FL	5.0520	n.q.
FLU	67.395	n.q.

ng/mL	10 Nov./ Dec. 2	10 Nov./ Dec. 3
HBCDA	0.0000	0.0000
HBCDBG	0.0000	0.0000
HCB	0.0000	0.7920
HCHA	0.0000	0.0000
HCHB	0.0000	0.0000
HCHD	0.0000	0.0000
HCHG	0.0000	0.0000
HEXAZIN	0.0000	0.0000
I123P	0.0000	n.q.
IRGAROL	0.0000	0.0000
ISOD	0.0000	0.0000
ISOPRUR	0.0028	0.0017
LINUR	0.0000	0.0000
MALATH	0.0000	0.0000
MCPA	n.q.	n.q.
MECOPR	n.q.	n.q.
METAZCHL	0.0000	0.0000
METHABZT	0.0000	0.0000
METOLA	0.0353	0.0377
NAPROX	n.q.	n.q.

A2 Table 3 continued:

ng/mL	10 Nov./Dec. 2	10 Nov./Dec. 3	ng/mL	10 Nov./Dec. 2	10 Nov./Dec. 3	ng/mL	10 Nov./Dec. 2	10 Nov./Dec. 3
OXAZEP	0.0000	0.0000	PFOS	0.0972	0.0881	SIMAZ	0.0000	0.0000
PENDIMETH	0.0486	0.1802	PFOSA	0.1125	0.1005	TBEP	2.2684	2.4274
PFBS	0.0111	0.0391	PHEN	32.775	n.q.	TBP	15.700	15.500
PFDEA	0.0180	0.0336	PIRIMIC	0.0000	0.0000	TERBAZ	0.0196	0.0230
PFHPA	0.0561	0.1142	PRIMID	0.0000	0.0000	TERBUTR	0.0000	0.0005
PFHXA	0.0461	0.0978	PROMETR	0.0759	0.0776	TPP	100.00	143.00
PFHXS	0.0042	0.0041	PROPAZ	0.0000	0.0000	TRIFLU	0.0000	0.0000
PFNOA	0.0502	0.1301	PYR	59.541	n.q.			
PFOA	0.2678	0.4772	QCB	0.4900	0.5160			

A2 Table 4: Field blanks of PUF disk passive air samplers; Concentrations of target analytes in ng/mL blank extract; n.q. = not quantified

ng/mL	PE B	PE D	09AT B	09AT D	09AT F	09AT H	10AT B	10AT D	Sülld. D	Sülld. F	Sülld. H
24-D	n.q.	n.q.	n.q.	n.q.	n.q.	n.q.	n.q.	n.q.	n.q.	n.q.	n.q.
ACE	0.0000	0.0000	5.3030	5.6250	3.4110	2.4770	2.5170	4.5640	0.0000	5.1910	4.2300
ACY	0.0000	0.0000	2.1150	2.1170	2.0270	0.0000	2.5660	6.7800	0.0000	30.629	22.405
ALD	0.0000	0.0000	0.0000	0.0000	0.0000	0.0000	0.0000	0.0000	0.0000	0.0000	0.0000
AMETRYN	0.0000	0.0000	0.0000	0.0000	0.0000	0.0000	0.0228	0.0000	0.0000	0.0000	0.0000
ANT	0.0000	0.0000	0.0000	0.0000	0.0000	0.0000	0.0000	0.0000	0.0000	0.0000	0.0000
ATRAZ	0.0000	0.0000	0.0000	0.0000	0.0000	0.0000	0.0000	0.0000	0.0000	0.0000	0.0000
AZINPH-E	0.0000	0.0000	0.0000	0.0000	0.0000	0.0000	0.0000	0.0000	0.0000	0.0000	0.0000
AZINPH-M	0.0000	0.0000	0.0000	0.0000	0.0000	0.0000	0.0000	0.0000	0.0000	0.0000	0.0000
BAA	0.0000	0.0000	0.0000	0.0000	0.0000	0.0000	0.0000	0.0000	0.0000	0.0000	0.0000
BAP	0.0000	0.0000	0.0000	0.0000	0.0000	0.0000	0.0000	0.0000	0.0000	0.0000	0.0000
BBF	0.0000	0.0000	0.0000	0.0000	0.0000	0.0000	0.0000	0.0000	0.0000	0.0000	0.0000
BENTAZ	0.0000	0.0000	0.0046	0.0071	0.0059	0.0047	0.0309	0.0069	0.0000	0.0000	0.0000
BGHIP	0.0000	0.0000	0.0000	0.0000	0.0000	0.0000	0.0000	0.0000	0.0000	0.0000	0.0000
CARBAMAZ	0.0000	0.0000	0.0000	0.0000	0.0000	0.0000	0.0000	0.0000	0.0943	0.0000	0.0000
CARBEND	0.0000	0.0000	0.0000	0.0000	0.0000	0.0000	0.0000	0.0000	0.0000	0.0000	0.0000
CB138	0.0000	0.0000	0.3110	0.8110	1.2470	0.4320	0.0000	0.0000	0.4080	0.3430	0.3430
CB153	0.1410	0.1370	0.2400	0.2910	0.3230	0.2610	0.2440	0.2410	0.4090	0.3280	0.3220
CB28	0.1380	0.1520	0.0000	1.0020	0.4000	0.2240	0.2340	0.2020	0.3120	0.3000	0.2920
CB52	0.1480	0.1620	0.0000	0.4140	0.2820	0.2000	0.0000	0.0000	0.3360	0.0000	0.0000
CHLORFENV	0.0000	0.0000	0.0000	0.0000	0.0000	0.0000	0.0000	0.0000	0.0000	0.0000	0.0000
CHLORTUR	0.0000	0.0000	0.0000	0.0000	0.0000	0.0000	0.0000	0.0000	0.0000	0.0887	0.0000
CHRTR	0.0000	0.0000	4.3140	4.3750	4.3430	4.3170	4.3220	4.3660	0.0000	0.0000	0.0000
CLOFIBRS	n.q.	n.q.	n.q.	n.q.	n.q.	n.q.	n.q.	n.q.	n.q.	n.q.	n.q.
DBAHA	0.0000	0.0000	0.0000	0.0000	0.0000	0.0000	0.0000	0.0000	0.0000	0.0000	0.0000
DDPP	0.0000	0.0000	0.0000	0.0000	0.0000	0.0000	0.0000	0.0000	0.0000	0.0000	0.0000
DDEPP	0.2350	0.2390	0.1900	0.1980	0.1970	0.1920	0.2060	0.1900	0.0000	0.0000	0.0000
DDTOP	0.0000	0.0000	0.0000	0.0000	0.0000	0.0000	0.0000	0.0000	0.0000	0.0000	0.0000
DDTPP	0.0000	0.0000	0.0000	0.0000	0.0000	0.0000	0.1380	0.0000	0.0000	0.0000	0.0000
DEATRAZ	0.0000	0.0000	0.0000	0.0000	0.0000	0.0000	0.0000	0.0000	0.0000	0.0000	0.0000
DIAZINON	0.0000	0.0000	0.0000	0.0000	0.0000	0.0000	0.0000	0.0000	0.0000	0.0000	0.0000
DICHLPR	n.q.	n.q.	n.q.	n.q.	n.q.	n.q.	n.q.	n.q.	n.q.	n.q.	n.q.
DICLOF	n.q.	n.q.	n.q.	n.q.	n.q.	n.q.	n.q.	n.q.	n.q.	n.q.	n.q.
DIELD	0.0000	0.0000	0.0000	0.0000	0.0000	0.0000	0.0000	0.0000	0.0000	0.0000	0.0000
DIMETH	0.0000	0.0000	0.0000	0.0000	0.0000	0.0000	0.0236	0.0000	0.0000	0.0000	0.0000

A2 Table 4 continued:

ng/mL	PE B	PE D	09AT B	09AT D	09AT F	09AT H	10AT B	10AT D	Sülld. D	Sülld. F	Sülld. H
DIURON	0.0000	0.0000	0.0000	0.0000	0.0000	0.0000	0.0000	0.0000	0.0000	0.0000	0.0000
END	0.0000	0.0000	0.0000	0.0000	0.0000	0.0000	0.0000	0.0000	0.0000	0.0000	0.0000
FENUR	0.0328	0.0122	0.0000	0.1035	0.0845	0.0224	0.0000	0.0428	0.0000	0.0444	0.0190
FL	0.0000	0.0000	11.374	18.381	8.8090	6.0770	6.1090	8.5710	6.8850	8.4360	7.8580
FLU	6.4490	6.5080	4.1440	11.297	8.4350	4.7520	4.1730	4.9960	4.1420	7.6600	6.7980
HBCDA	0.0000	0.0000	0.0000	0.0000	0.0000	0.0000	0.0000	0.0000	0.0000	0.0000	0.0000
HBCDBG	0.0051	0.0021	0.0000	0.0000	0.0000	0.0000	0.0000	0.0000	0.0000	0.0000	0.0000
HCB	0.2090	0.2140	0.1830	0.4300	0.2640	0.1730	0.1660	0.1670	0.2480	0.2620	0.2640
HCHA	0.1190	0.1210	0.0000	0.0000	0.0000	0.0000	0.0000	0.0000	0.0000	0.0000	0.0000
HCHB	0.0000	0.0000	0.0000	0.0000	0.0000	0.0000	0.0000	0.0000	0.0000	0.0000	0.0000
HCHD	0.0000	0.0000	0.0000	0.0000	0.0000	0.0000	0.0000	0.0000	0.0000	0.0000	0.0000
HCHG	0.2070	0.2810	0.2200	0.5240	0.3090	0.2150	0.2270	0.2180	0.2770	0.0000	0.0000
HEXAZIN	0.0000	0.0000	0.0000	0.1835	0.1618	0.0000	0.0000	0.0000	0.0000	0.0000	0.0000
I123P	0.0000	0.0000	0.0000	0.0000	0.0000	0.0000	0.0000	0.0000	0.0000	0.0000	0.0000
IRGAROL	0.0000	0.0000	0.0000	0.0000	0.0000	0.0000	0.0000	0.0000	0.0000	0.0000	0.0000
ISOD	0.0000	0.0000	0.0000	0.0000	0.0000	0.0000	0.0000	0.0000	0.0000	0.0000	0.0000
ISOPRUR	0.0000	0.0000	0.0000	0.0000	0.0000	0.0000	0.0037	0.0000	0.0753	0.0000	0.0136
LINUR	0.0000	0.0000	0.0000	0.0000	0.0000	0.0000	0.0000	0.0000	0.0000	0.0000	0.0000
MALATH	0.0000	0.0000	0.0000	0.0000	0.0000	0.0000	0.0000	0.0000	0.0000	0.0000	0.0000
MCPA	n.q.	n.q.	n.q.	n.q.	n.q.	n.q.	n.q.	n.q.	n.q.	n.q.	n.q.
MECOPR	n.q.	n.q.	n.q.	n.q.	n.q.	n.q.	n.q.	n.q.	n.q.	n.q.	n.q.
METAZCHL	0.0000	0.0000	0.0000	0.0000	0.0000	0.0000	0.0171	0.0000	0.5273	0.0000	0.0198
METHABZT	0.0000	0.0000	0.0000	0.0000	0.0000	0.0000	0.0000	0.0000	0.0000	0.0000	0.0000
METOLA	0.0000	0.0000	0.1410	0.3360	0.2060	0.2920	0.1940	0.2130	0.5000	0.0000	0.0289
NAPROX	n.q.	n.q.	n.q.	n.q.	n.q.	n.q.	n.q.	n.q.	n.q.	n.q.	n.q.
OXAZEP	0.0000	0.0000	0.0000	0.0000	0.0000	0.0000	0.0000	0.0000	0.0000	0.0000	0.0000
PENDIMETH	0.0811	0.1168	0.1043	0.3582	0.2260	0.1583	0.1572	0.1835	0.9118	0.1299	0.3538
PFBS	0.0072	0.0065	0.0118	0.0127	0.0172	0.0112	0.0417	0.0182	0.0000	0.0231	0.0128
PFDEA	0.0000	0.0000	0.0000	0.0000	0.0000	0.0000	0.0000	0.0000	0.0000	0.0000	0.0000
PFHPA	0.0000	0.0000	0.1153	0.1252	0.1427	0.0738	0.0761	0.0457	0.3536	0.3173	0.0592
PFHXA	0.0560	0.0507	0.0759	0.1233	0.2425	0.0354	0.1019	0.0595	0.3750	0.2986	0.0904
PFHXS	0.0031	0.0018	0.0037	0.0024	0.0053	0.0028	0.0217	0.0047	0.0160	0.0128	0.0072
PFNOA	0.0000	0.0000	0.2292	0.1962	0.1972	0.1341	0.2733	0.1972	0.0000	0.0000	0.0813
PFOA	0.1090	0.1034	0.9080	0.8618	1.0965	0.6513	0.8948	0.7339	6.2594	1.2012	0.3163
PFOS	0.0516	0.0174	0.1584	0.1244	0.1818	0.1536	0.3451	0.2819	0.4325	0.7562	0.3042
PFOSA	0.0280	0.0211	0.1440	0.1343	0.1943	0.1673	0.2790	0.2280	0.1748	0.5340	0.1973
PHEN	9.3060	9.8240	9.2730	43.650	13.253	7.4570	7.3100	12.006	5.5100	25.269	20.660
PIRIMIC	0.0000	0.0000	0.0000	0.0000	0.0000	0.0000	0.0000	0.0000	0.0000	0.0000	0.0000
PRIMID	0.0000	0.0000	0.0000	0.0000	0.0000	0.0000	0.0000	0.0000	0.0000	0.0000	0.0000
PROMETR	0.0490	0.0431	0.0667	0.0661	0.0646	0.0664	0.0971	0.0745	0.0605	0.0764	0.0781
PROPAZ	0.0000	0.0000	0.0000	0.0000	0.0000	0.0000	0.0000	0.0000	0.0000	0.0000	0.0000
PYR	0.0000	6.9930	4.9020	20.721	15.634	5.9470	5.0880	6.9120	4.6480	15.022	13.960
QCB	0.1540	0.1650	0.1820	0.1630	0.1570	0.1510	0.1560	0.1530	0.2220	0.2510	0.2480
SIMAZ	0.0000	0.0000	0.0000	0.0000	0.0000	0.0000	0.0000	0.0000	0.0000	0.0000	0.0000
TBEP	0.2449	0.2756	3.9538	4.0598	3.2224	3.8902	5.6392	0.0000	0.8353	0.4357	0.0914
TBP	5.9300	12.200	34.100	65.000	54.900	38.100	45.900	47.100	39.400	38.200	17.300
TERBAZ	0.0560	0.0871	0.1742	0.2249	0.1547	0.2405	0.1846	0.2028	0.2626	0.0341	0.0360
TERBUTR	0.0000	0.0000	0.3330	0.1742	0.1239	0.0000	0.0000	0.0000	0.0000	0.0000	0.0000
TPP	1.1400	1.3300	1.4400	2.7900	2.0700	2.1200	2.2200	3.0700	9.1000	6.1100	1.8900
TRIFLU	0.3100	0.2960	0.0000	0.0000	0.0000	0.0000	0.0000	0.0000	0.0000	0.0000	0.0000

A2 Table 4 continued:

ng/mL	Sülld. J	Sülld. L	Sülld. N	Sülld. P	Sülld. R	Sülld. T	Sülld. V	Sülld. X	Sülld. AA	Sülld. AD	Sülld. AF
24-D	n.q.	n.q.	n.q.	n.q.	n.q.	n.q.	n.q.	n.q.	n.q.	n.q.	n.q.
ACE	0.0000	0.0000	0.0000	0.0000	0.0000	0.0000	0.0000	0.0000	0.0000	0.0000	0.0000
ACY	6.7640	6.5130	11.601	8.3620	6.8140	5.2840	7.6660	6.7210	7.3410	4.9850	9.5780
ALD	0.0000	0.0000	0.0000	0.0000	0.0000	0.0000	0.0000	0.0000	0.0000	0.0000	0.0000
AMETRYN	0.0000	0.0000	0.0000	0.0241	0.0200	0.0198	0.0161	0.0196	0.0000	0.0000	0.0000
ANT	0.0000	0.0000	0.0000	0.0000	0.0000	0.0000	0.0000	0.0000	0.0000	0.0000	0.0000
ATRAZ	0.0000	0.0000	0.0000	0.0000	0.0000	0.0000	0.0000	0.0000	0.0000	0.0000	0.0000
AZINPH-E	0.0000	0.0000	0.0000	0.0000	0.0000	0.0000	0.0000	0.0000	0.0000	0.0000	0.0000
AZINPH-M	0.0000	0.0000	0.0000	0.0000	0.0000	0.0000	0.0000	0.0000	0.0000	0.0000	0.0000
BAA	0.0000	0.0000	0.0000	0.0000	0.0000	0.0000	0.0000	0.0000	0.0000	0.0000	0.0000
BAP	0.0000	0.0000	0.0000	0.0000	0.0000	0.0000	0.0000	0.0000	0.0000	0.0000	0.0000
BBF	0.0000	0.0000	0.0000	0.0000	0.0000	0.0000	0.0000	0.0000	0.0000	0.0000	0.0000
BENTAZ	0.0000	0.0000	0.0000	0.0000	0.0000	0.0000	0.0000	0.0000	0.0000	0.0000	0.0000
BGHIP	0.0000	0.0000	0.0000	0.0000	0.0000	0.0000	0.0000	0.0000	0.0000	0.0000	0.0000
CARBAMAZ	0.0000	0.0000	0.0000	0.0000	0.0000	0.0000	0.0000	0.0000	0.0000	0.0000	0.0000
CARBEND	0.0000	0.0000	0.0000	0.0000	0.0000	0.0000	0.0000	0.0000	0.0000	0.0000	0.0000
CB138	0.0000	0.0000	0.3740	0.0000	0.0000	0.0000	0.0000	0.0000	0.0000	0.0000	0.0000
CB153	0.0000	0.0000	0.3540	0.3200	0.3240	0.0000	0.0000	0.3260	0.0000	0.3180	0.0000
CB28	0.2880	0.2880	0.3000	0.2920	0.2920	0.2900	0.2980	0.2920	0.2900	0.2880	0.2900
CB52	0.0000	0.0000	0.0000	0.0000	0.0000	0.0000	0.0000	0.0000	0.0000	0.0000	0.0000
CHLORFENV	0.0000	0.0000	0.0000	0.0000	0.0000	0.0000	0.0000	0.0000	0.0000	0.0000	0.0000
CHLORTUR	0.0000	0.0000	0.0000	0.0000	0.0000	0.0000	0.0000	0.0000	0.0000	0.0000	0.0000
CHRTR	0.0000	0.0000	0.0000	0.0000	0.0000	0.0000	0.0000	0.0000	0.0000	0.0000	0.0000
CLOFIBRS	n.q.	n.q.	n.q.	n.q.	n.q.	n.q.	n.q.	n.q.	n.q.	n.q.	n.q.
DBAHA	0.0000	0.0000	0.0000	0.0000	0.0000	0.0000	0.0000	0.0000	0.0000	0.0000	0.0000
DDPP	0.0000	0.0000	0.0000	0.0000	0.0000	0.0000	0.0000	0.0000	0.0000	0.0000	0.0000
DDEPP	0.0000	0.0000	0.0000	0.3120	0.0000	0.0000	0.0000	0.3110	0.0000	0.3110	0.3080
DDTOP	0.0000	0.0000	0.0000	0.0000	0.0000	0.0000	0.0000	0.0000	0.0000	0.0000	0.0000
DDTPP	0.0000	0.0000	0.0000	0.0000	0.0000	0.0000	0.0000	0.0000	0.0000	0.0000	0.0000
DEATRAZ	0.0000	0.0000	0.0000	0.0000	0.0000	0.0000	0.0000	0.0000	0.0000	0.0000	0.0000
DIAZINON	0.0000	0.0000	0.0000	0.0000	0.0000	0.0000	0.0000	0.0000	0.0000	0.0000	0.0000
DICHLPR	n.q.	n.q.	n.q.	n.q.	n.q.	n.q.	n.q.	n.q.	n.q.	n.q.	n.q.
DICLOF	n.q.	n.q.	n.q.	n.q.	n.q.	n.q.	n.q.	n.q.	n.q.	n.q.	n.q.
DIELD	0.0000	0.0000	0.0000	0.0000	0.0000	0.0000	0.0000	0.0000	0.0000	0.0000	0.0000
DIMETH	0.0000	0.0000	0.0000	0.0000	0.0000	0.0000	0.0000	0.0000	0.0000	0.0000	0.0000
DIURON	0.0000	0.0000	0.0000	0.0000	0.0000	0.0000	0.0000	0.0000	0.0000	0.0000	0.0000
END	0.0000	0.0000	0.0000	0.0000	0.0000	0.0000	0.0000	0.0000	0.0000	0.0000	0.0000
FENUR	0.0056	0.0000	0.0000	0.0000	0.0000	0.0000	0.0331	0.1779	0.0575	0.0161	0.0102
FL	0.0000	0.0000	7.1820	6.8550	6.8720	0.0000	0.0000	6.8510	0.0000	0.0000	6.8670
FLU	4.1380	4.1610	10.261	4.9480	4.7020	4.1390	4.2790	9.0430	5.0490	4.2250	4.7150
HBCDA	0.0000	0.0000	0.0000	0.0357	0.0000	0.0000	0.0235	0.0131	0.0000	0.0000	0.0000
HBCDBG	0.0000	0.0000	0.0000	0.1640	0.0000	0.0000	0.0661	0.0270	0.0000	0.0000	0.0000
HCB	0.2390	0.2460	0.2480	0.2420	0.2490	0.2400	0.2460	0.2450	0.2490	0.2430	0.2450
HCHA	0.0000	0.0000	0.0000	0.0000	0.0000	0.0000	0.0000	0.0000	0.0000	0.0000	0.0000
HCHB	0.0000	0.0000	0.0000	0.0000	0.0000	0.0000	0.0000	0.0000	0.0000	0.0000	0.0000
HCHD	0.0000	0.0000	0.0000	0.0000	0.0000	0.0000	0.0000	0.0000	0.0000	0.0000	0.0000
HCHG	0.0000	0.0000	0.0000	0.0000	0.0000	0.0000	0.0000	0.0000	0.0000	0.0000	0.0000
HEXAZIN	0.0000	0.0000	0.0000	0.0000	0.0000	0.0000	0.0000	0.0000	0.0000	0.0000	0.0000
I123P	0.0000	0.0000	0.0000	0.0000	0.0000	0.0000	0.0000	0.0000	0.0000	0.0000	0.0000
IRGAROL	0.0000	0.0000	0.0000	0.0000	0.0000	0.0000	0.0000	0.0000	0.0000	0.0000	0.0000
ISOD	0.0000	0.0000	0.0000	0.0000	0.0000	0.0000	0.0000	0.0000	0.0000	0.0000	0.0000

A2 Table 4 continued:

ng/mL	Sülld. J	Sülld. L	Sülld. N	Sülld. P	Sülld. R	Sülld. T	Sülld. V	Sülld. X	Sülld. AA	Sülld. AD	Sülld. AF
ISOPRUR	0.0000	0.0000	0.0000	0.0000	0.0000	0.0000	0.0000	0.0000	0.0000	0.0000	0.0000
LINUR	0.0000	0.0000	0.0000	0.0000	0.0000	0.0000	0.0000	0.0000	0.0000	0.0000	0.0000
MALATH	0.0000	0.0000	0.0000	0.0000	0.0000	0.0000	0.0000	0.0000	0.0000	0.0000	0.0000
MCPA	n.q.	n.q.	n.q.	n.q.	n.q.	n.q.	n.q.	n.q.	n.q.	n.q.	n.q.
MECOPR	n.q.	n.q.	n.q.	n.q.	n.q.	n.q.	n.q.	n.q.	n.q.	n.q.	n.q.
METAZCHL	0.0082	0.0000	0.0000	0.0000	0.0388	0.0349	0.0272	0.0513	0.0141	0.0118	0.0147
METHABZT	0.0000	0.0000	0.0000	0.0000	0.0000	0.0000	0.0000	0.0000	0.0000	0.0000	0.0000
METOLA	0.0000	0.0000	0.0000	0.0000	0.0000	0.0000	0.0000	0.0388	0.0148	0.0810	0.0561
NAPROX	n.q.	n.q.	n.q.	n.q.	n.q.	n.q.	n.q.	n.q.	n.q.	n.q.	n.q.
OXAZEP	0.0000	0.0000	0.0000	0.0000	0.0000	0.0000	0.0000	0.0000	0.0000	0.0000	0.0000
PENDIMETH	0.1562	0.1179	0.1398	0.1714	0.1057	0.1136	0.0689	0.2118	0.2806	0.1179	0.1900
PFBS	0.0118	0.0140	0.0099	0.0144	0.0091	0.0116	0.0105	0.0381	0.0124	0.0193	0.0109
PFDEA	0.0000	0.0000	0.0000	0.0000	0.0000	0.0000	0.0000	0.0000	0.0000	0.0000	0.0000
PFHPA	0.1069	0.2569	0.6797	0.2976	0.3085	0.1241	0.0917	0.0683	0.0839	0.0896	0.0834
PFHXA	0.1549	0.2425	0.5146	0.3302	0.2975	0.1712	0.1885	0.1804	0.1671	0.1233	0.1325
PFHXS	0.0045	0.0152	0.0051	0.0077	0.0043	0.0047	0.0078	0.0099	0.0066	0.0060	0.0056
PFNOA	0.0000	0.1271	0.0000	0.0000	0.0000	0.1732	0.1221	0.0000	0.0000	0.0000	0.0000
PFOA	0.3119	0.7394	1.1681	0.6513	0.6590	0.4055	0.4188	0.8320	0.5168	0.3736	0.2975
PFOS	0.1254	0.4345	0.1128	0.1808	0.1740	0.1429	0.1302	0.2955	0.1264	0.1293	0.0820
PFOSA	0.0632	0.3000	0.1193	0.1620	0.1178	0.1545	0.2513	0.1763	0.1155	0.1290	0.0848
PHEN	5.6420	5.5190	24.550	9.8010	8.6310	5.0900	6.9730	11.520	8.7150	5.5310	11.892
PIRIMIC	0.0000	0.0000	0.0000	0.0000	0.0000	0.0000	0.0000	0.0000	0.0000	0.0000	0.0000
PRIMID	0.0000	0.0000	0.0000	0.0000	0.0000	0.0000	0.0000	0.0000	0.0000	0.0000	0.0000
PROMETR	0.0902	0.0843	0.0787	0.3393	0.3358	0.3082	0.3163	0.3071	0.0771	0.0813	0.0888
PROPAZ	0.0000	0.0000	0.0000	0.0000	0.0000	0.0000	0.0000	0.0000	0.0000	0.0000	0.0000
PYR	4.8670	5.1970	22.528	8.4200	6.8130	4.6770	4.9730	22.136	8.6260	5.3290	7.1830
QCB	0.2190	0.2210	0.2260	0.2230	0.2180	0.2170	0.2230	0.2180	0.2170	0.2150	0.2240
SIMAZ	0.0000	0.0000	0.0000	0.0000	0.0000	0.0000	0.0000	0.0000	0.0000	0.0000	0.0000
TBEP	0.1526	0.6466	0.6063	0.3562	0.2417	0.2703	0.2290	0.4017	0.3138	0.1304	0.7759
TBP	8.2500	27.600	30.200	23.900	21.600	10.600	10.600	19.500	15.100	13.800	11.700
TERBAZ	0.0463	0.0221	0.0000	0.0000	0.0225	0.0230	0.0000	0.0285	0.0322	0.0803	0.0462
TERBUTR	0.0000	0.0000	0.0000	0.0000	0.0000	0.0000	0.0000	0.0000	0.0000	0.0000	0.0061
TPP	2.1700	4.5100	8.5900	7.5000	5.1800	2.7500	2.6700	8.5500	4.0300	2.8000	2.8800
TRIFLU	0.0000	0.0000	0.0000	0.0000	0.0000	0.0000	0.0000	0.0000	0.0000	0.0000	0.0000

ng/mL	Sülld. AH	Sülld. AJ	Sülld. AL	Sylt B	Sylt D	Sylt F	Sylt J	Sylt L	Sylt N	Sylt P	Sylt T
24-D	n.q.	n.q.	n.q.	n.q.	n.q.	n.q.	n.q.	n.q.	n.q.	n.q.	n.q.
ACE	0.0000	2.7090	2.7240	4.2670	4.2320	4.2180	0.0000	4.1050	4.0980	4.1090	0.0000
ACY	10.424	5.2050	5.1770	20.438	19.455	21.774	7.4400	11.128	11.307	8.0510	5.6240
ALD	0.0000	0.0000	0.0000	0.0000	0.0000	0.0000	0.0000	0.0000	0.0000	0.0000	0.0000
AMETRYN	0.0000	0.0085	0.0063	0.0000	0.0000	0.0000	0.0000	0.0000	0.0000	0.0000	0.0000
ANT	0.0000	0.0000	0.0000	0.0000	0.0000	0.0000	0.0000	0.0000	0.0000	0.0000	0.0000
ATRAZ	0.0000	0.0000	0.0000	0.0000	0.0000	0.0000	0.0000	0.0000	0.0000	0.0000	0.0000
AZINPH-E	0.0000	0.0000	0.0000	0.0000	0.0000	0.0000	0.0000	0.0000	0.0000	0.0000	0.0000
AZINPH-M	0.0000	0.0000	0.0000	0.0000	0.0000	0.0000	0.0000	0.0000	0.0000	0.0000	0.0000
BAA	0.0000	0.0000	0.0000	0.0000	0.0000	0.0000	0.0000	0.0000	0.0000	0.0000	0.0000
BAP	0.0000	0.0000	0.0000	0.0000	0.0000	0.0000	0.0000	0.0000	0.0000	0.0000	0.0000
BBF	0.0000	0.0000	0.0000	0.0000	0.0000	0.0000	0.0000	0.0000	0.0000	0.0000	0.0000
BENTAZ	0.0000	0.0000	0.0000	0.0000	0.0000	0.0000	0.0000	0.0000	0.0000	0.0000	0.0000
BGHIP	0.0000	0.0000	0.0000	0.0000	0.0000	0.0000	0.0000	0.0000	0.0000	0.0000	0.0000

A2 Table 4 continued:

ng/mL	Sülld. AH	Sülld. AJ	Sülld. AL	Sylt B	Sylt D	Sylt F	Sylt J	Sylt L	Sylt N	Sylt P	Sylt T
CARBAMAZ	0.0000	0.0000	0.0000	0.0000	0.0000	0.0000	0.0000	0.0000	0.0000	0.0000	0.0000
CARBEND	0.0000	0.0000	0.0000	0.0000	0.0000	0.0000	0.0000	0.0000	0.0000	0.0000	0.0000
CB138	0.0000	0.0000	0.0000	0.0000	0.0000	0.0000	0.0000	0.0000	0.0000	0.0000	0.0000
CB153	0.3170	0.3680	0.0000	0.3230	0.3210	0.3210	0.3260	0.0000	0.3260	0.0000	0.3200
CB28	0.2900	0.3510	0.3500	0.2920	0.2940	0.2920	0.2940	0.2940	0.2940	0.2960	0.2980
CB52	0.0000	0.0000	0.0000	0.0000	0.0000	0.0000	0.0000	0.0000	0.3240	0.0000	0.0000
CHLORFENV	0.0000	0.0000	0.0000	0.0000	0.0000	0.0000	0.0000	0.0000	0.0000	0.0000	0.0000
CHLORTUR	0.0000	0.0000	0.0000	0.0000	0.0000	0.0000	0.0000	0.0000	0.0000	0.0000	0.0000
CHRTR	0.0000	0.0000	0.0000	0.0000	0.0000	0.0000	0.0000	0.0000	0.0000	0.0000	0.0000
CLOFIBRS	n.q.	n.q.	n.q.	n.q.	n.q.	n.q.	n.q.	n.q.	n.q.	n.q.	n.q.
DBAHA	0.0000	0.0000	0.0000	0.0000	0.0000	0.0000	0.0000	0.0000	0.0000	0.0000	0.0000
DDPP	0.0000	0.0000	0.0000	0.0000	0.0000	0.0000	0.0000	0.0000	0.0000	0.0000	0.0000
DDEPP	0.0000	0.0000	0.0000	0.0000	0.0000	0.3110	0.0000	0.0000	0.0000	0.0000	0.0000
DDTOP	0.0000	0.0000	0.0000	0.0000	0.0000	0.0000	0.0000	0.0000	0.0000	0.0000	0.0000
DDTPP	0.0000	0.0000	0.0000	0.0000	0.0000	0.0000	0.0000	0.0000	0.0000	0.0000	0.0000
DEATRAZ	0.0000	0.0000	0.0000	0.0000	0.0000	0.0000	0.0000	0.0000	0.0000	0.0000	0.0000
DIAZINON	0.0000	0.0000	0.0000	0.0000	0.0000	0.0000	0.0000	0.0000	0.0000	0.0000	0.0000
DICHLPR	n.q.	n.q.	n.q.	n.q.	n.q.	n.q.	n.q.	n.q.	n.q.	n.q.	n.q.
DICLOF	n.q.	n.q.	n.q.	n.q.	n.q.	n.q.	n.q.	n.q.	n.q.	n.q.	n.q.
DIELD	0.0000	0.0000	0.0000	0.0000	0.0000	0.0000	0.0000	0.0000	0.0000	0.0000	0.0000
DIMETH	0.0000	0.0000	0.0059	0.0000	0.0000	0.0000	0.0000	0.0000	0.0000	0.0000	0.0000
DIURON	0.0000	0.0000	0.0000	0.0000	0.0000	0.0000	0.0000	0.0000	0.0000	0.0000	0.0000
END	0.0000	0.0000	0.0000	0.0000	0.0000	0.0000	0.0000	0.0000	0.0000	0.0000	0.0000
FENUR	0.0101	0.0312	0.0180	0.0269	0.0404	0.0000	0.0000	0.0206	0.0238	0.1179	0.0000
FL	6.8730	5.7410	5.9140	7.3400	7.3680	7.3500	7.9730	7.1220	7.1430	6.9730	6.9560
FLU	4.8260	11.138	9.4980	8.4260	8.5370	4.1000	1.8160	5.7980	3.4520	2.6610	1.6820
HBCDA	0.0000	0.0338	0.0265	0.0000	0.0000	0.0000	0.0000	0.0000	0.0000	0.0000	0.0000
HBCDBG	0.0000	0.0158	0.0000	0.0000	0.0000	0.0000	0.0000	0.0000	0.0000	0.0000	0.0000
HCB	0.2430	0.6000	0.6010	0.2510	0.2540	0.2540	0.2530	0.2500	0.2640	0.2520	0.2480
HCHA	0.0000	0.0000	0.0000	0.0000	0.0000	0.0000	0.0000	0.0000	0.0000	0.0000	0.0000
HCHB	0.0000	0.0000	0.0000	0.0000	0.0000	0.0000	0.0000	0.0000	0.0000	0.0000	0.0000
HCHD	0.0000	0.0000	0.0000	0.0000	0.0000	0.0000	0.0000	0.0000	0.0000	0.0000	0.0000
HCHG	0.0000	0.0000	0.0000	0.0000	0.0000	0.0000	0.0000	0.0000	0.0000	0.0000	0.2620
HEXAZIN	0.0000	0.0000	0.0000	0.0000	0.0000	0.0000	0.0000	0.0000	0.0000	0.0000	0.0000
I123P	0.0000	0.0000	0.0000	0.0000	0.0000	0.0000	0.0000	0.0000	0.0000	0.0000	0.0000
IRGAROL	0.0000	0.0000	0.0000	0.0000	0.0000	0.0000	0.0000	0.0000	0.0000	0.0000	0.0000
ISOD	0.0000	0.0000	0.0000	0.0000	0.0000	0.0000	0.0000	0.0000	0.0000	0.0000	0.0000
ISOPRUR	0.0000	0.0040	0.0082	0.0000	0.0000	0.0000	0.0000	0.0000	0.0000	0.0000	0.0000
LINUR	0.0000	0.0000	0.0000	0.0000	0.0000	0.0000	0.0000	0.0000	0.0000	0.0000	0.0000
MALATH	0.0000	0.0000	0.0000	0.0000	0.0000	0.0000	0.0000	0.0000	0.0000	0.0000	0.0000
MCPA	n.q.	n.q.	n.q.	n.q.	n.q.	n.q.	n.q.	n.q.	n.q.	n.q.	n.q.
MECOPR	n.q.	n.q.	n.q.	n.q.	n.q.	n.q.	n.q.	n.q.	n.q.	n.q.	n.q.
METAZCHL	0.0000	0.0000	0.0000	0.0234	0.0319	0.0220	0.0162	0.0000	0.0000	0.0050	0.0000
METHABZT	0.0000	0.0000	0.0000	0.0000	0.0000	0.0000	0.0000	0.0000	0.0000	0.0000	0.0000
METOLA	0.0411	0.0574	0.0569	0.0197	0.0000	0.0374	0.0000	0.0000	0.0358	0.0000	0.0000
NAPROX	n.q.	n.q.	n.q.	n.q.	n.q.	n.q.	n.q.	n.q.	n.q.	n.q.	n.q.
OXAZEP	0.0000	0.0000	0.0000	0.0000	0.0000	0.0000	0.0000	0.0000	0.0000	0.0000	0.0000
PENDIMETH	0.0902	0.3320	0.2992	0.1900	0.2064	0.1736	0.2097	0.1627	0.1671	0.2075	0.1179
PFBS	0.0099	0.0185	0.0112	0.0127	0.0000	0.0099	0.0166	0.0082	0.0123	0.0200	0.0138
PFDEA	0.0000	0.0202	0.0213	0.0000	0.0000	0.0000	0.0000	0.0000	0.0000	0.0000	0.0000
PFHPA	0.1581	0.0660	0.0647	0.0727	0.1768	0.1098	0.1307	0.0479	0.0400	0.0000	0.0573

A2 Table 4 continued:

ng/mL	Sülld. AH	Sülld. AJ	Sülld. AL	Sylt B	Sylt D	Sylt F	Sylt J	Sylt L	Sylt N	Sylt P	Sylt T
PFHXA	0.1987	0.0413	0.0422	0.1060	0.1875	0.1386	0.1783	0.1223	0.0972	0.0795	0.1967
PFHXS	0.0027	0.0048	0.0086	0.0086	0.0056	0.0064	0.0040	0.0074	0.0023	0.0052	0.0021
PFNOA	0.0000	0.1161	0.0808	0.0000	0.2172	0.0000	0.1051	0.0000	0.1211	0.1912	0.0000
PFOA	0.4188	0.1962	0.1940	0.3372	0.4739	0.3604	0.3758	0.2876	0.4970	0.7064	1.0811
PFOS	0.0854	0.0651	0.0693	0.2002	0.1536	0.1458	0.0867	0.0964	0.1584	0.1905	0.1691
PFOSA	0.0990	0.0292	0.0441	0.2138	0.1350	0.1088	0.0451	0.0679	0.1245	0.0840	0.0652
PHEN	10.440	13.394	11.302	18.740	25.787	20.982	7.8530	17.430	12.868	8.3440	6.6070
PIRIMIC	0.0000	0.0000	0.0000	0.0000	0.0000	0.0000	0.0000	0.0000	0.0000	0.0000	0.0000
PRIMID	0.0000	0.0000	0.0000	0.0000	0.0000	0.0000	0.0000	0.0000	0.0000	0.0000	0.0000
PROMETR	0.0865	0.0697	0.0748	0.0775	0.0750	0.0783	0.0741	0.0767	0.0743	0.0711	0.0840
PROPAZ	0.0000	0.0000	0.0000	0.0000	0.0000	0.0000	0.0000	0.0000	0.0000	0.0000	0.0000
PYR	7.7330	16.852	11.511	24.933	24.303	11.508	4.4140	15.534	8.2580	7.7220	3.6460
QCB	0.2220	0.0000	0.0000	0.2350	0.2350	0.2440	0.2270	0.2270	0.2290	0.2210	0.2230
SIMAZ	0.0000	0.0000	0.0000	0.0000	0.0000	0.0000	0.0000	0.0000	0.0000	0.0000	0.0000
TBEP	0.2311	0.4717	0.4844	0.0754	0.1022	0.1021	0.1134	0.1002	0.0671	0.1442	0.2364
TBP	17.200	12.800	14.300	11.300	11.400	10.300	11.600	10.600	13.400	13.200	17.800
TERBAZ	0.0302	0.0385	0.0233	0.0322	0.0159	0.0371	0.0221	0.0218	0.0235	0.0000	0.0000
TERBUTR	0.0000	0.0136	0.0000	0.0000	0.0000	0.0021	0.0000	0.0027	0.0025	0.0000	0.0000
TPP	2.1900	2.6200	2.9800	1.5900	2.7700	2.1100	2.1100	2.0400	2.0000	3.2200	3.0500
TRIFLU	0.0000	0.0000	0.0000	0.0000	0.0000	0.0000	0.0000	0.0000	0.0000	0.0000	0.0000

ng/mL	Sylt V	Sylt X	Sylt Z	FINO 1 D	FINO 1 E	FINO 1 F	FINO 3 B	FINO 3 D	FINO 3 F	FINO 1 J	FINO 1 K	FINO 1 L
24-D	n.q.	n.q.	n.q.	n.q.	n.q.	n.q.	n.q.	n.q.	n.q.	n.q.	n.q.	n.q.
ACE	3.0620	2.8230	2.7170	4.0990	0.0000	0.0000	0.0000	4.1090	4.1010	2.7230	2.7120	2.7140
ACY	10.999	8.7470	4.6410	7.6560	5.5870	5.5130	6.3860	12.383	10.361	5.5550	5.2460	5.6590
ALD	0.0000	0.0000	0.0000	0.0000	0.0000	0.0000	0.0000	0.0000	0.0000	0.0000	0.0000	0.0000
AMETRYN	0.0264	0.0498	0.0082	0.0000	0.0514	0.0000	0.0139	0.0000	0.0000	0.0000	0.0000	0.0000
ANT	0.0000	0.0000	0.0000	0.0000	0.0000	0.0000	0.0000	0.0000	0.0000	0.0000	0.0000	0.0000
ATRAZ	0.0000	0.0000	0.0000	0.0000	0.0000	0.0000	0.0000	0.0000	0.0000	0.0000	0.0000	0.0000
AZINPH-E	0.0000	0.0000	0.0000	0.0000	0.0000	0.0000	0.0000	0.0000	0.0000	0.0000	0.0000	0.0000
AZINPH-M	0.0000	0.0000	0.0000	0.0000	0.0000	0.0000	0.0000	0.0000	0.0000	0.0000	0.0000	0.0000
BAA	0.0000	0.0000	0.0000	0.0000	0.0000	0.0000	0.0000	0.0000	0.0000	0.0000	0.0000	0.0000
BAP	0.0000	0.0000	0.0000	0.0000	0.0000	0.0000	0.0000	0.0000	0.0000	0.0000	0.0000	0.0000
BBF	0.0000	0.0000	0.0000	0.0000	0.0000	0.0000	0.0000	0.0000	0.0000	0.0000	0.0000	0.0000
BENTAZ	0.0000	0.0218	0.0000	0.0000	0.0472	0.0066	0.0143	0.0043	0.0181	0.0000	0.0000	0.0000
BGHIP	0.0000	0.0000	0.0000	0.0000	0.0000	0.0000	0.0000	0.0000	0.0000	0.0000	0.0000	0.0000
CARBAMAZ	0.0167	0.0280	0.0000	0.0000	0.0000	0.0000	0.0000	0.0000	0.0000	0.0000	0.0000	0.0000
CARBEND	0.0000	0.0000	0.0000	0.0000	0.0000	0.0000	0.0000	0.0000	0.0000	0.0000	0.0000	0.0000
CB138	0.0000	0.0000	0.0000	0.0000	0.0000	0.0000	0.0000	0.0000	0.0000	0.0000	0.0000	0.0000
CB153	0.0000	0.0000	0.0000	0.0000	0.0000	0.0000	0.0000	0.0000	0.0000	0.3720	0.0000	0.0000
CB28	0.3520	0.3500	0.0000	0.1960	0.1920	0.1900	0.1920	0.1900	0.1900	0.3520	0.3500	0.3500
CB52	0.0000	0.0000	0.0000	0.0000	0.0000	0.0000	0.0000	0.0000	0.0000	0.0000	0.0000	0.0000
CHLORFENV	0.0000	0.0000	0.0000	0.0000	0.0000	0.0000	0.0000	0.0000	0.0000	0.0000	0.0000	0.0000
CHLORTUR	0.0153	0.0285	0.0084	0.0000	0.0000	0.0000	0.0000	0.0000	0.0000	0.0000	0.0000	0.0051
CHRTR	0.0000	0.0000	0.0000	0.0000	0.0000	0.0000	0.0000	0.0000	0.0000	0.0000	0.0000	0.0000
CLOFIBRS	n.q.	n.q.	n.q.	n.q.	n.q.	n.q.	n.q.	n.q.	n.q.	n.q.	n.q.	n.q.
DBAHA	0.0000	0.0000	0.0000	0.0000	0.0000	0.0000	0.0000	0.0000	0.0000	0.0000	0.0000	0.0000
DDP	0.0000	0.0000	0.0000	0.0000	0.0000	0.0000	0.0000	0.0000	0.0000	0.0000	0.0000	0.0000
DDEPP	0.0000	0.0000	0.0000	0.0000	0.0000	0.0000	0.0000	0.0000	0.0000	0.0000	0.0000	0.0000
DDTOP	0.0000	0.0000	0.0000	0.0000	0.0000	0.0000	0.0000	0.0000	0.0000	0.0000	0.0000	0.0000

A2 Table 4 continued:

ng/mL	Sylt V	Sylt X	Sylt Z	FINO 1 D	FINO 1 E	FINO 1 F	FINO 3 B	FINO 3 D	FINO 3 F	FINO 1 J	FINO 1 K	FINO 1 L
DDTPP	0.0000	0.0000	0.0000	0.0000	0.0000	0.0000	0.0000	0.0000	0.0000	0.0000	0.0000	0.0000
DEATRAZ	0.0000	0.0000	0.0000	0.0000	0.0000	0.0000	0.0000	0.0000	0.0000	0.0000	0.0000	0.0000
DIAZINON	0.0000	0.0757	0.0000	0.0000	0.0000	0.0000	0.0000	0.0000	0.0000	0.0000	0.0000	0.0000
DICHLPR	n.q.	n.q.	n.q.	n.q.	n.q.	n.q.	n.q.	n.q.	n.q.	n.q.	n.q.	n.q.
DICLOF	n.q.	n.q.	n.q.	n.q.	n.q.	n.q.	n.q.	n.q.	n.q.	n.q.	n.q.	n.q.
DIELD	0.0000	0.0000	0.0000	0.0000	0.0000	0.0000	0.0000	0.0000	0.0000	0.0000	0.0000	0.0000
DIMETH	0.0221	0.0284	0.0000	0.0000	0.0436	0.0022	0.0085	0.0000	0.0000	0.0000	0.0000	0.0000
DIURON	0.0515	0.0200	0.0000	0.0000	0.0000	0.0000	0.0000	0.0000	0.0000	0.0000	0.0000	0.0183
END	0.0000	0.0000	0.0000	0.0000	0.0000	0.0000	0.0000	0.0000	0.0000	0.0000	0.0000	0.0000
FENUR	0.0409	0.0698	0.0217	0.0192	0.0416	0.0185	0.1027	0.1957	0.0792	0.0129	0.0120	0.0099
FL	6.6610	5.8600	5.7980	0.0000	0.0000	0.0000	0.0000	7.0260	6.9860	5.9170	5.7180	5.7750
FLU	9.8000	11.925	11.350	5.5090	2.2490	2.3390	2.4530	5.9100	6.5880	8.2360	7.9180	7.8820
HBCDA	0.0000	0.0327	0.0000	0.0000	0.0000	0.0000	0.0000	0.0000	0.0000	0.0000	0.0098	0.0079
HBCDBG	0.0151	0.0047	0.0183	0.0000	0.0000	0.0000	0.0000	0.0000	0.0000	0.0000	0.0000	0.0000
HCB	0.0000	0.0000	0.0000	0.0000	0.2290	0.0000	0.2360	0.2370	0.2390	0.0000	0.6010	0.5990
HCHA	0.0000	0.0000	0.0000	0.0000	0.0000	0.0000	0.0000	0.0000	0.0000	0.0000	0.0000	0.0000
HCHB	0.0000	0.0000	0.0000	0.0000	0.0000	0.0000	0.0000	0.0000	0.0000	0.0000	0.0000	0.0000
HCHD	0.0000	0.0000	0.0000	0.0000	0.0000	0.0000	0.0000	0.1580	0.0000	0.0000	0.6520	0.0000
HCHG	0.0000	0.0000	0.0000	0.0000	0.0000	0.0000	0.0000	0.0000	0.0000	0.0000	0.0000	0.0000
HEXAZIN	0.0000	0.0000	0.0000	0.0000	0.0000	0.0000	0.0000	0.0000	0.0000	0.0000	0.0000	0.0000
I123P	0.0000	0.0000	0.0000	0.0000	0.0000	0.0000	0.0000	0.0000	0.0000	0.0000	0.0000	0.0000
IRGAROL	0.0000	0.0000	0.0000	0.0000	0.0000	0.0000	0.0000	0.0000	0.0000	0.0000	0.0000	0.0000
ISOD	0.0000	0.0000	0.0000	0.0000	0.0000	0.0000	0.0000	0.0000	0.0000	0.0000	0.0000	0.0000
ISOPRUR	0.0232	0.0408	0.0217	0.0000	0.0400	0.0086	0.0123	0.0000	0.0000	0.0100	0.0082	0.0160
LINUR	0.0000	0.0000	0.0000	0.0000	0.0000	0.0000	0.0000	0.0000	0.0000	0.0000	0.0000	0.0000
MALATH	0.0000	0.0000	0.0000	0.0000	0.0000	0.0000	0.0000	0.0000	0.0000	0.0000	0.0000	0.0000
MCPA	n.q.	n.q.	n.q.	n.q.	n.q.	n.q.	n.q.	n.q.	n.q.	n.q.	n.q.	n.q.
MECOPR	n.q.	n.q.	n.q.	n.q.	n.q.	n.q.	n.q.	n.q.	n.q.	n.q.	n.q.	n.q.
METAZCHL	0.2142	0.0600	0.0000	0.0000	0.0000	0.0000	0.0000	0.0000	0.0000	0.0165	0.0098	0.0252
METHABZT	0.0000	0.0164	0.0000	0.0000	0.0000	0.0000	0.0000	0.0000	0.0000	0.0000	0.0000	0.0000
METOLA	0.1240	0.0880	0.0503	0.0752	0.1300	0.0889	0.0795	0.0595	0.0682	0.0487	0.0491	0.0511
NAPROX	n.q.	n.q.	n.q.	n.q.	n.q.	n.q.	n.q.	n.q.	n.q.	n.q.	n.q.	n.q.
OXAZEP	0.0000	0.0000	0.0000	0.0000	0.0000	0.0000	0.0000	0.0000	0.0000	0.0000	0.0000	0.0000
PENDIMETH	0.6224	0.8791	0.6192	0.0999	0.3374	0.1034	0.1125	0.0000	0.0917	0.2413	0.1572	0.2413
PFBS	0.0300	0.0520	0.0184	0.0130	0.0678	0.0405	0.0416	0.0168	0.0222	0.0107	0.0103	0.0103
PFDEA	0.0367	0.0408	0.0000	0.0000	0.0000	0.0000	0.0000	0.0000	0.0000	0.0184	0.0197	0.0271
PFHPA	0.0944	0.1230	0.0732	0.0681	0.1340	0.0660	0.0746	0.0725	0.1164	0.0798	0.1057	0.1208
PFHXA	0.0438	0.0865	0.0394	0.0694	0.1814	0.1182	0.1345	0.1121	0.1569	0.0490	0.0572	0.0577
PFHXS	0.0279	0.0312	0.0082	0.0041	0.0347	0.0080	0.0100	0.0064	0.0090	0.0063	0.0047	0.0067
PFNOA	0.1081	0.1211	0.0435	0.0000	0.0762	0.0992	0.0733	0.0591	0.0574	0.0716	0.0745	0.0465
PFOA	0.3042	0.4871	0.2480	0.5642	0.5664	0.4507	0.5257	0.5675	0.7229	0.2336	0.2645	0.2656
PFOS	0.1069	0.0911	0.0528	0.1720	0.1225	0.1059	0.1089	0.1128	0.1332	0.0893	0.0654	0.1040
PFOSA	0.0491	0.0609	0.0443	0.0960	0.0722	0.0497	0.0733	0.0615	0.0672	0.0833	0.0609	0.0953
PHEN	12.660	11.300	12.578	12.777	7.3980	8.1830	8.7810	16.533	15.166	8.3980	6.5050	7.6300
PIRIMIC	0.0138	0.0390	0.0000	0.0000	0.0000	0.0000	0.0000	0.0000	0.0000	0.0000	0.0000	0.0000
PRIMID	0.0000	0.0000	0.0000	0.0000	0.0000	0.0000	0.0000	0.0000	0.0000	0.0000	0.0000	0.0000
PROMETR	0.0999	0.1173	0.0821	0.0688	0.1277	0.0817	0.0975	0.0722	0.0714	0.0705	0.0743	0.0793
PROPAZ	0.0000	0.0000	0.0000	0.0000	0.0000	0.0000	0.0000	0.0000	0.0000	0.0000	0.0000	0.0000
PYR	10.465	15.594	16.575	15.040	5.7540	6.8330	6.5240	17.034	18.754	7.3660	6.5450	6.5130
QCB	0.0000	0.0000	0.0000	0.1790	0.1710	0.1720	0.1740	0.1810	0.1770	0.0000	0.0000	0.0000
SIMAZ	0.0000	0.0000	0.0000	0.0000	0.0000	0.0000	0.0000	0.0000	0.0000	0.0000	0.0000	0.0000

A2 Table 4 continued:

ng/mL	Sylt V	Sylt X	Sylt Z	FINO 1 D	FINO 1 E	FINO 1 F	FINO 3 B	FINO 3 D	FINO 3 F	FINO 1 J	FINO 1 K	FINO 1 L
TBEP	0.5194	0.5925	1.5582	0.3678	0.4632	0.4028	0.4537	0.5957	0.3424	0.3752	0.3275	0.3572
TBP	12.300	14.700	9.4700	14.400	14.200	14.500	16.400	27.300	31.300	12.000	12.100	14.200
TERBAZ	0.0668	0.0754	0.0454	0.0633	0.1095	0.0657	0.0410	0.0654	0.0506	0.0283	0.0242	0.0278
TERBUTR	0.5005	0.0907	0.0301	0.0000	0.0000	0.0000	0.0000	0.0000	0.0000	0.7918	0.0286	0.0099
TPP	11.400	8.2100	4.1900	2.9800	4.1300	3.3300	5.1200	2.7700	2.6500	2.3900	3.3500	3.8300
TRIFLU	0.0000	0.0000	0.0000	0.0000	0.0000	0.0000	0.0000	0.0000	0.0000	0.0000	0.0000	0.0000

Laboratory blanks

A2 Table 5: Laboratory blanks – Extraction blanks; Concentrations of target analytes in ng/mL blank extract; n.q. = not quantified

ng/mL	Soxhlet 1	Soxhlet 2	Soxhlet 3	Soxhlet 4	Soxhlet 5	Petri dish 1	Petri dish 2	Petri dish 3
24-D	n.q.	n.q.	n.q.	n.q.	n.q.	0.0000	0.0000	0.0000
ACE	0.0000	0.0000	1.3218	0.0000	0.0000	0.0000	0.0398	0.0000
ACY	0.0000	0.0000	0.0000	5.8062	0.0000	0.0000	0.0000	0.0000
ALD	0.0000	2.9232	0.0000	0.0000	0.0000	0.0000	0.0000	0.0000
AMETRYN	0.0000	0.0000	0.0000	0.0000	0.0051	0.0000	0.0000	0.0072
ANT	0.0000	0.0000	0.0000	0.0000	0.0000	0.0000	0.0000	0.0000
ATRAZ	0.0000	0.0000	0.0000	0.0000	0.0000	0.0000	0.0000	0.0000
AZINPH-E	0.0000	0.0000	0.0000	0.0000	0.0000	0.0000	0.0000	0.0000
AZINPH-M	0.0000	0.0000	0.0000	0.0000	0.0000	0.0000	0.0000	0.0000
BAA	0.0000	0.0000	0.0000	0.0000	0.0000	0.0000	0.0000	0.0000
BAP	0.0000	0.0000	0.0000	0.0000	0.0000	0.0000	0.0000	0.0000
BBF	0.0000	0.0000	0.0000	0.0000	0.0000	0.0000	0.0000	0.0000
BENTAZ	0.0000	0.0000	0.0000	0.0000	0.0000	0.0000	0.0000	0.0000
BGHIP	0.0000	0.0000	0.0000	0.0000	0.0000	0.0000	0.0000	0.0000
CARBAMAZ	0.0000	0.0000	0.0000	0.0000	0.0000	0.0000	0.0000	0.0000
CARBEND	0.0000	0.0000	0.0000	0.0000	0.0000	0.0000	0.0000	0.0000
CB138	0.0000	0.0000	0.0000	0.0000	0.0000	0.0000	0.0000	0.0000
CB153	0.0000	0.1940	0.0124	0.0000	0.0000	0.0000	0.0000	0.0000
CB28	0.0720	0.0335	0.0207	0.0000	0.0014	0.0000	0.0157	0.0000
CB52	0.0590	0.0000	0.0000	0.0000	0.0000	0.0000	0.0000	0.0000
CHLORFENV	0.0000	0.0000	0.0000	0.0000	0.0000	0.0000	0.0000	0.0000
CHLORTUR	0.0000	0.0000	0.0000	0.0000	0.0000	0.0000	0.0000	0.0000
CHRTR	0.0000	0.0000	0.0819	0.0000	0.0000	0.0000	0.0000	0.0000
CLOFIBRS	0.0000	0.0000	n.q.	n.q.	n.q.	0.0000	0.0000	0.0000
DBAHA	0.0000	0.0000	0.0000	0.0000	0.0000	0.0000	0.0000	0.0000
DDDP	0.0000	0.0000	0.0000	0.0000	0.0000	0.0000	0.0000	0.0000
DDEPP	0.0000	0.0000	0.0089	0.0000	0.0000	0.0000	0.0000	0.0000
DDTOP	0.0000	0.0000	0.0000	0.0000	0.0000	0.0000	0.0000	0.0000
DDTPP	0.0000	0.0000	0.0000	0.0000	0.0000	0.0000	0.0000	0.0000
DEATRAZ	0.0000	0.0000	0.0000	0.0000	0.0347	0.0000	0.0000	0.0000
DIAZINON	0.0000	0.0000	0.0000	0.0000	0.0000	0.0000	0.0000	0.0000
DICHLPR	n.q.	n.q.	n.q.	n.q.	n.q.	0.0000	0.0000	0.0000
DICLOF	n.q.	n.q.	n.q.	n.q.	n.q.	0.0000	0.0000	0.0000
DIELD	0.2990	0.0000	0.0000	0.0000	0.0000	0.0000	0.0000	0.0000
DIMETH	0.0000	0.0000	0.0000	0.0000	0.0000	0.0000	0.0000	0.0000
DIURON	0.0000	0.0000	0.0000	0.0000	0.0000	0.0000	0.0000	0.0000

A2 Table 5 continued:

ng/mL	Soxhlet 1	Soxhlet 2	Soxhlet 3	Soxhlet 4	Soxhlet 5	Petri dish 1	Petri dish 2	Petri dish 3
END	0.0000	0.0000	0.0000	0.0000	0.0000	0.0000	0.0000	0.0000
FENUR	0.0000	0.0053	0.0000	0.0000	0.0000	0.0000	0.0000	0.0000
FL	0.0000	0.0000	1.4782	0.0000	0.1019	0.0000	0.0515	0.0000
FLU	0.0000	0.0000	1.8909	0.0000	0.2146	0.0000	0.0047	0.0000
HBCDA	0.0296	0.0000	0.0000	0.0000	0.0056	0.0000	0.0000	0.0031
HBCDBG	0.0000	0.0000	0.0000	0.0000	0.0035	0.0000	0.0100	0.0060
HCB	0.1430	0.0289	0.0310	0.0228	0.0000	0.0117	0.0248	0.0000
HCHA	0.0000	0.0000	0.0000	0.0000	0.0000	0.0000	0.0000	0.0000
HCHB	0.1270	0.0143	0.0000	0.0000	0.0000	0.0000	0.0000	0.0000
HCHD	0.1720	0.0754	0.0000	0.0000	0.0000	0.0000	0.0000	0.0000
HCHG	1.0210	1.0412	0.5674	0.0000	0.0000	0.0000	0.6496	0.0000
HEXAZIN	0.0000	0.0000	0.0000	0.0000	0.0000	0.0000	0.0000	0.0000
I123P	0.0000	0.0000	0.0000	0.0000	0.0000	0.0000	0.0000	0.0000
IRGAROL	0.0000	0.0000	0.0000	0.0000	0.0000	0.0000	0.0000	0.0000
ISOD	0.2610	0.0000	0.0000	0.0000	0.0000	0.0000	0.0000	0.0000
ISOPRUR	0.0000	0.0102	0.0000	0.0000	0.0000	0.0000	0.0000	0.0000
LINUR	0.0000	0.0000	0.0000	0.0000	0.0000	0.0000	0.0000	0.0000
MALATH	0.0000	0.0000	0.0000	0.0000	0.0000	0.0000	0.0000	0.0000
MCPA	n.q.	n.q.	n.q.	n.q.	n.q.	0.0000	0.0000	0.0000
MECOPR	n.q.	n.q.	n.q.	n.q.	n.q.	0.0000	0.0000	0.0000
METAZCHL	0.0000	0.0000	0.0000	0.0000	0.0000	0.0000	0.0000	0.0000
METHABZT	0.0000	0.0000	0.0000	0.0000	0.0000	0.0000	0.0000	0.0000
METOLA	0.0000	0.0000	0.2390	0.0000	0.0371	0.0000	0.0000	0.0187
NAPROX	n.q.	n.q.	n.q.	n.q.	n.q.	0.0000	0.0000	0.0000
OXAZEP	0.0000	0.0000	0.0000	0.0000	0.0000	0.0000	0.0000	0.0000
PENDIMETH	0.1180	0.2184	0.0000	0.0000	0.0000	0.0000	0.0000	0.0249
PFBS	0.0000	0.0243	0.0128	0.0104	0.0060	0.0000	0.0083	0.0081
PFDEA	0.0000		0.0000	0.0000	0.0150	0.0622	0.0000	0.0000
PFHPA	0.0000	0.0121	0.0279	0.0603	0.0309	0.0000	0.0035	0.0170
PFHXA	0.0633	0.0254	0.0162	0.0604	0.0304	0.0000	0.0000	0.0000
PFHXS	0.0155	0.0025	0.0028	0.0022	0.0008	0.0000	0.0000	0.0007
PFNOA	0.0000	0.0000	0.0707	0.0000	0.0297	0.0170	0.0109	0.0466
PFOA	0.0074	0.0474	0.5598	0.4706	0.0959	0.0489	0.0429	0.0592
PFOS	0.0297	0.0223	0.1827	0.1371	0.0915	0.0000	0.0444	0.0000
PFOSA	0.0393	0.0224	0.2033	0.0522	0.0248	0.0167	0.0525	0.0175
PHEN	0.0000	0.0000	5.1662	0.6697	4.5562	0.0000	0.3732	0.0000
PIRIMIC	0.0000	0.0000	0.0000	0.0000	0.0000	0.0000	0.0000	0.0000
PRIMID	0.0000	0.0000	0.0000	0.0000	0.0000	0.0000	0.0000	0.0000
PROMETR	0.0671	0.0595	0.0616	0.0906	0.0975	0.0000	0.0726	0.0817
PROPAZ	0.0000	0.0000	0.0000	0.0000	0.0000	0.0000	0.0000	0.0000
PYR	0.0000	0.0000	0.9875	0.0000	0.0739	0.0000	0.0000	0.0000
QCB	0.1990	0.0304	0.0851	0.1069	0.0000	0.0029	0.0082	0.0000
SIMAZ	0.0000	0.0000	0.0000	0.0000	0.0000	0.0000	0.0000	0.0000
TBEP	0.1535	0.3413	6.0844	0.1972	0.6678	0.4070	3.9538	0.2692
TBP	3.3250	8.1000	39.5000	12.1000	13.1000	2.0600	1.6800	2.1800
TERBAZ	0.0313	0.0000	0.2496	0.0680	0.0447	0.0471	0.0378	0.0243
TERBUTR	0.0000	0.0000	0.0000	0.0000	0.0000	0.0000	0.0000	0.0000
TPP	0.6766	2.4600	1.6200	1.0600	0.3240	1.2100	0.3730	0.0000
TRIFLU	0.2260	2.2374	0.0000	0.0000	0.0000	0.0000	0.0000	0.0000

A2 Table 6: Laboratory blanks – Bottle blanks; Concentrations of target analytes in ng/mL blank extract; n.q. = not quantified

ng/mL	2.0 L bottle 1	2.0 L bottle 2	2.0 L bottle 3	2.0 L bottle 4	2.0 L bottle 5	0.5 L bottle 1	0.5 L bottle 2	0.5 L bottle 3
24-D	n.q.	n.q.	n.q.	n.q.	n.q.	0.0000	0.0000	0.0000
ACE	0.0000	0.0000	1.5914	0.0000	0.0000	0.0000	0.0000	0.0000
ACY	0.0000	0.0000	0.0000	1.0515	0.0000	0.0000	0.0000	0.0000
ALD	0.0000	0.0328	0.0000	0.0000	0.0000	0.0000	0.0000	0.0000
AMETRYN	0.0000	0.0000	0.0000	0.0000	0.0057	0.0000	0.0000	0.0053
ANT	0.0000	0.0000	0.0000	0.0000	0.0000	0.0000	0.0000	0.0000
ATRAZ	0.0000	0.0000	0.0000	0.0000	0.0000	0.0000	0.0000	0.0000
AZINPH-E	0.0000	0.0000	0.0000	0.0000	0.0000	0.0000	0.0000	0.0000
AZINPH-M	0.0000	0.0000	0.0000	0.0000	0.0000	0.0000	0.0000	0.0000
BAA	0.0000	0.0000	0.0000	0.0000	0.0000	0.0000	0.0000	0.0000
BAP	0.0000	0.0000	0.0000	0.0000	0.0000	0.0000	0.0000	0.0000
BBF	0.0000	0.0000	0.0000	0.0000	0.0000	0.0000	0.0000	0.0000
BENTAZ	0.0000	0.0000	0.0000	0.0000	0.0000	0.0000	0.0000	0.0000
BGHIP	0.0000	0.0000	0.0000	0.0000	0.0000	0.0000	0.0000	0.0000
CARBAMAZ	0.0000	0.0000	0.0000	0.0000	0.0000	0.0000	0.0000	0.0000
CARBEND	0.0000	0.0000	0.0000	0.0000	0.0000	0.0000	0.0000	0.0000
CB138	0.0000	0.0000	0.0000	0.0000	0.0000	0.0000	0.0000	0.0000
CB153	0.0000	0.0057	0.0000	0.0000	0.0000	0.0000	0.0000	0.0000
CB28	0.0000	0.0000	0.0083	0.0000	0.0000	0.0000	0.0012	0.0000
CB52	0.0000	0.0000	0.0000	0.0000	0.0000	0.0000	0.0000	0.0000
CHLORFENV	0.0000	0.0000	0.0000	0.0000	0.0000	0.0000	0.0000	0.0000
CHLORTUR	0.0000	0.0000	0.0000	0.0000	0.0000	0.0000	0.0000	0.0000
CHRTR	0.0000	0.0000	0.0000	0.0000	0.0000	0.0000	0.0000	0.0000
CLOFIBRS	n.q.	n.q.	n.q.	n.q.	n.q.	0.0000	0.0000	0.0000
DBAHA	0.0000	0.0000	0.0000	0.0000	0.0000	0.0000	0.0000	0.0000
DDPP	0.1010	0.0000	0.0000	0.0000	0.0000	0.0000	0.0000	0.0000
DDEPP	0.2330	0.0000	0.0000	0.0000	0.0000	0.0000	0.0000	0.0000
DDTOP	0.2370	0.0000	0.0000	0.0000	0.0000	0.0000	0.0000	0.0000
DDTPP	0.1210	0.0000	0.0000	0.0000	0.0000	0.0000	0.0000	0.0000
DEATRAZ	0.0000	0.0000	0.0000	0.0000	0.0291	0.0000	0.0000	0.0000
DIAZINON	0.0000	0.0000	0.0000	0.0000	0.0000	0.0000	0.0000	0.0000
DICHLPR	n.q.	n.q.	n.q.	n.q.	n.q.	0.0000	0.0000	0.0000
DICLOF	n.q.	n.q.	n.q.	n.q.	n.q.	0.0000	0.0000	0.0000
DIELD	0.2340	0.0000	0.0000	0.0000	0.0000	0.0000	0.0000	0.0000
DIMETH	0.0000	0.0000	0.0000	0.0000	0.0000	0.0000	0.0000	0.0000
DIURON	0.0000	0.0000	0.0000	0.0000	0.0000	0.0000	0.0000	0.0000
END	n.q.	0.0000	0.0000	0.0000	0.0000	0.0000	0.0000	0.0000
FENUR	0.0000	0.0000	0.0000	0.0000	0.0000	0.0000	0.0000	0.0038
FL	0.0000	0.0000	1.2469	0.0000	0.0000	0.0000	0.0309	0.0000
FLU	0.0000	0.0000	0.0420	0.0000	0.0000	0.0000	0.0031	0.0000
HBCDA	0.0197	0.0000	0.0000	0.0045	0.0035	0.0000	0.0000	0.0040
HBCDBG	0.0000	0.0000	0.0436	0.0000	0.0055	0.0000	0.0061	0.0029
HCB	0.0000	0.0139	0.0562	0.0000	0.0000	0.0124	0.0088	0.0000
HCHA	0.0940	0.0000	0.0000	0.0000	0.0000	0.0000	0.0000	0.0000
HCHB	0.1240	0.0074	0.0000	0.0000	0.0000	0.0000	0.0000	0.0000
HCHD	0.1580	0.0338	0.0000	0.0000	0.0000	0.0000	0.0000	0.0000
HCHG	1.4390	1.0171	0.5991	0.0000	0.0000	0.0000	0.6302	0.0000
HEXAZIN	0.0000	0.0000	0.0000	0.0000	0.0000	0.0000	0.0000	0.0000
I123P	0.0000	0.0000	0.0000	0.0000	0.0000	0.0000	0.0000	0.0000
IRGAROL	0.0000	0.0000	0.0000	0.0000	0.0000	0.0000	0.0000	0.0000

A2 Table 6 continued:

ng/mL	2.0 L bottle 1	2.0 L bottle 2	2.0 L bottle 3	2.0 L bottle 4	2.0 L bottle 5	0.5 L bottle 1	0.5 L bottle 2	0.5 L bottle 3
ISOD	0.0000	0.0000	0.0000	0.0000	0.0000	0.0000	0.0000	0.0000
ISOPRUR	0.0000	0.0000	0.0000	0.0000	0.0000	0.0000	0.0000	0.0000
LINUR	0.0000	0.0000	0.0000	0.0000	0.0000	0.0000	0.0000	0.0000
MALATH	0.0000	0.0000	0.0000	0.0000	0.0000	0.0000	0.0000	0.0000
MCPA	n.q.	n.q.	n.q.	n.q.	n.q.	0.0000	0.0000	0.0000
MECOPR	n.q.	n.q.	n.q.	n.q.	n.q.	0.0000	0.0000	0.0000
METAZCHL	0.0000	0.0000	0.0000	0.0000	0.0000	0.0000	0.0000	0.0000
METHABZT	0.0000	0.0000	0.0000	0.0000	0.0000	0.0000	0.0000	0.0000
METOLA	0.0000	0.0000	0.0000	0.0000	0.0458	0.0000	0.0000	0.0280
NAPROX	n.q.	n.q.	n.q.	n.q.	n.q.	0.0000	0.0000	0.0000
OXAZEP	0.0000	0.0000	0.0000	0.0000	0.0000	0.0000	0.0000	0.0000
PENDIMETH	0.0398	0.0000	0.0000	0.0779	0.0000	0.0000	0.0000	0.0258
PFBS	0.0000	0.0264	0.0074	0.0038	0.0026	0.0000	0.0052	0.0000
PFDEA	0.0000	0.0000	0.0000	0.0000	0.0000	0.0555	0.0000	0.0000
PFHPA	0.0000	0.0010	0.0000	0.0401	0.0148	0.0000	0.0090	0.0135
PFHXA	0.0721	0.0036	0.0000	0.0360	0.0079	0.0000	0.0000	0.0000
PFHXS	0.0130	0.0022	0.0000	0.0012	0.0000	0.0000	0.0000	0.0000
PFNOA	0.0000	0.0000	0.0560	0.0322	0.0056	0.0081	0.0172	0.0496
PFOA	0.0431	0.0121	0.0253	0.3857	0.0631	0.0228	0.0385	0.0421
PFOS	0.0000	0.0106	0.0026	0.0698	0.0072	0.0000	0.0560	0.0000
PFOSA	0.0508	0.0144	0.0352	0.0177	0.0115	0.0030	0.0893	0.0217
PHEN	0.0000	0.0000	1.1737	0.0000	0.0767	0.0000	0.1984	0.0000
PIRIMIC	0.0000	0.0000	0.0000	0.0000	0.0000	0.0000	0.0000	0.0000
PRIMID	0.0000	0.0000	0.0000	0.0000	0.0000	0.0000	0.0000	0.0000
PROMETR	0.0704	0.0850	0.0793	0.0944	0.1035	0.0000	0.0679	0.0879
PROPAZ	0.0000	0.0000	0.0000	0.0000	0.0000	0.0000	0.0000	0.0000
PYR	0.0000	0.0000	0.0277	0.0000	0.0000	0.0000	0.0000	0.0000
QCB	0.0000	0.0080	0.1166	0.0000	0.0000	0.0021	0.0000	0.0000
SIMAZ	0.0000	0.0000	0.0000	0.0000	0.0000	0.0000	0.0000	0.0000
TBEP	0.2179	0.3731	6.9642	0.1505	0.6890	0.2883	3.7736	0.3328
TBP	3.4470	5.0100	6.4300	11.4000	11.5000	1.5000	1.6300	2.0300
TERBAZ	0.1251	0.1755	0.0775	0.1047	0.1102	0.0199	0.0080	0.0394
TERBUTR	0.0000	0.0000	0.0000	0.0000	0.0000	0.0000	0.0000	0.0000
TPP	0.6003	1.8300	0.7760	0.9010	0.2840	0.9450	0.3720	0.0000
TRIFLU	0.0000	3.8313	0.0000	0.0000	0.0000	0.0000	0.0000	0.0000

A2 Table 7: Laboratory blanks – Evaporation blanks; Concentration of target analytes in ng/mL blank extract; n.q. = not quantified

ng/mL	Evapo- ration- 350 mL 1	Evapo- ration- 350 mL 2	Evapo- ration- 350 mL 3	Evapo- ration- 350 mL 4	Evapo- ration- 350 mL 5	Evapo- ration- 350 mL 6	Evapo- ration- 350 mL 7	Evapo- ration- 350 mL 8	Evapo- ration- 350 mL 9	Evapo- ration- 100 mL 1	Evapo- ration- 100 mL 2
24-D	0.0000	0.0000	0.0000	n.q.	n.q.	n.q.	n.q.	n.q.	n.q.	0.0000	0.0000
ACE	0.0000	0.0000	0.0000	0.0000	0.0000	0.0000	0.1149	0.0000	0.0774	0.0000	0.0000
ACY	0.0000	0.0000	0.0000	10.355	0.0000	5.3840	0.2710	1.5894	0.3455	4.6042	0.0000
ALD	0.0000	0.0000	0.0000	0.0308	0.0040	0.0076	0.0000	0.0000	0.0000	0.0000	0.0000
AMETRYN	0.0000	0.0000	0.0000	0.0000	0.0000	0.0000	0.0000	0.0068	0.0043	0.0000	0.0000
ANT	0.0000	0.0000	0.0000	0.0000	0.0000	0.0000	0.0000	0.0000	0.0000	0.0000	0.0000
ATRAZ	0.0000	0.0000	0.0000	0.0000	0.0000	0.0000	0.0000	0.0000	0.0000	0.0000	0.0000
AZINPH-E	0.0000	0.0000	0.0000	0.0000	0.0000	0.0000	0.0000	0.0000	0.0000	0.0000	0.0000

A2 Table 7 continued:

ng/mL	Evapo- ration- 350 mL 1	Evapo- ration- 350 mL 2	Evapo- ration- 350 mL 3	Evapo- ration- 350 mL 4	Evapo- ration- 350 mL 5	Evapo- ration- 350 mL 6	Evapo- ration- 350 mL 7	Evapo- ration- 350 mL 8	Evapo- ration- 350 mL 9	Evapo- ration- 100 mL 1	Evapo- ration- 100 mL 2
AZINPH-M	0.0000	0.0000	0.0000	0.0000	0.0000	0.0000	0.0000	0.0000	0.0000	0.0000	0.0000
BAA	0.0000	0.0000	0.0000	0.0000	0.0000	0.0000	0.0000	0.0000	0.0000	0.0000	0.0000
BAP	0.0000	0.0000	0.0000	0.0000	0.0000	0.0000	0.0000	0.0000	0.0000	0.0000	0.0000
BBF	0.0000	0.0000	0.0000	0.0000	0.0000	0.0000	0.0000	0.0000	0.0000	0.0000	0.0000
BENTAZ	0.0000	0.0000	0.0000	0.0000	0.0000	0.0000	0.0000	0.0000	0.0000	0.0000	0.0000
BGHIP	0.0000	0.0000	0.0000	0.0000	0.0000	0.0000	0.0000	0.0000	0.0000	0.0000	0.0000
CARBAMAZ	0.0000	0.0000	0.0000	0.0000	0.0000	0.0000	0.0000	0.0000	0.0000	0.0000	0.0000
CARBEND	0.0000	0.0000	0.0000	0.0000	0.0000	0.0000	0.0000	0.0000	0.0000	0.0000	0.0000
CB138	0.0000	0.0000	0.2390	0.0000	0.0000	0.0000	0.0000	0.0000	0.0000	0.0000	0.0000
CB153	0.0000	0.0000	0.0000	0.0000	0.0064	0.0082	0.0000	0.0000	0.0000	0.0000	0.0000
CB28	0.0730	0.0670	0.0700	0.0000	0.0000	0.0000	0.0095	0.0000	0.0000	0.0000	0.0000
CB52	0.0780	0.0610	0.0700	0.0000	0.0000	0.0000	0.0000	0.0000	0.0000	0.0000	0.0000
CHLORFENV	0.0000	0.0000	0.0000	0.0000	0.0000	0.0000	0.0000	0.0000	0.0000	0.0000	0.0000
CHLORTUR	0.0000	0.0000	0.0000	0.0000	0.0000	0.0000	0.0000	0.0000	0.0000	0.0000	0.0000
CHRTR	0.0000	0.0000	0.0000	0.0000	0.0000	0.0000	0.0208	0.0000	0.0000	0.0000	0.0000
CLOFIBRS	0.0000	0.0000	0.0000	n.q.	n.q.	n.q.	n.q.	n.q.	n.q.	0.0000	0.0000
DBAHA	0.0000	0.0000	0.0000	0.0000	0.0000	0.0000	0.0000	0.0000	0.0000	0.0000	0.0000
DDDPP	0.1010	0.0980	0.1020	0.0000	0.0000	0.0000	0.0000	0.0000	0.0000	0.0000	0.0000
DDEPP	0.0000	0.0000	0.0000	0.0000	0.0000	0.0000	0.0000	0.0000	0.0000	0.0000	0.0000
DDTOP	0.2350	0.2360	0.2370	0.0000	0.0000	0.0000	0.0000	0.0000	0.0000	0.0000	0.0000
DDTPP	0.1210	0.1220	0.1230	0.0000	0.0000	0.0000	0.0000	0.0000	0.0000	0.0000	0.0000
DEATRAZ	0.0000	0.0000	0.0000	0.0000	0.0000	0.0000	0.0000	0.0000	0.0000	0.0000	0.0000
DIAZINON	0.0000	0.0000	0.0000	0.0000	0.0000	0.0000	0.0000	0.0000	0.0000	0.0000	0.0000
DICHLPR	0.0000	0.0000	0.0000	n.q.	n.q.	n.q.	n.q.	n.q.	n.q.	0.0000	0.0000
DICLOF	0.0000	0.0374	0.0000	n.q.	n.q.	n.q.	n.q.	n.q.	n.q.	0.0000	0.0000
DIELD	0.2610	0.2220	0.2460	0.0000	0.0000	0.0000	0.0000	0.0000	0.0000	0.0000	0.0000
DIMETH	0.0000	0.0000	0.0000	0.0000	0.0000	0.0000	0.0000	0.0000	0.0000	0.0000	0.0000
DIURON	0.0000	0.0000	0.0000	0.0000	0.0000	0.0000	0.0000	0.0000	0.0000	0.0000	0.0000
END	n.q.	n.q.	n.q.	0.0000	0.0000	0.0000	0.0000	0.0000	0.0000	0.0000	0.0000
FENUR	0.0000	0.0000	0.0000	0.0000	0.0000	0.0024	0.0000	0.0000	0.0000	0.0000	0.0000
FL	0.0000	0.0000	0.0000	0.0000	0.0000	0.0000	0.0687	0.0000	0.0000	0.0000	0.0000
FLU	0.0000	0.0000	0.0000	0.0000	0.0000	0.0000	0.0295	0.0000	0.0000	0.0000	0.0000
HBCDA	0.0352	0.0238	0.0395	0.0000	0.0000	0.0000	0.0448	0.0000	0.0007	0.0000	0.0000
HBCDBG	0.0030	0.0000	0.0000	0.0000	0.0000	0.0000	0.1220	0.0000	0.0023	0.0000	0.0000
HCB	0.1280	0.0000	0.1310	0.0594	0.0181	0.0529	0.0185	0.0000	0.0282	0.0217	0.0216
HCHA	0.1010	0.0000	0.0000	0.0246	0.0000	0.0000	0.0000	0.0000	0.0000	0.0000	0.0000
HCHB	0.1270	0.2230	0.2570	0.0108	0.0037	0.0060	0.0000	0.0000	0.0000	0.0000	0.0000
HCHD	0.1490	0.1570	0.1540	0.0098	0.0000	0.0186	0.0000	0.0000	0.0000	0.0000	0.0099
HCHG	0.1670	0.3220	0.1770	0.0055	0.0058	0.0112	0.0000	0.0000	0.0000	0.0070	0.0000
HEXAZIN	0.0000	0.0000	0.0000	0.0000	0.0000	0.0000	0.0000	0.0000	0.0000	0.0000	0.0000
I123P	0.0000	0.0000	0.0000	0.0000	0.0000	0.0000	0.0000	0.0000	0.0000	0.0000	0.0000
IRGAROL	0.0000	0.0000	0.0000	0.0000	0.0000	0.0000	0.0000	0.0000	0.0000	0.0000	0.0000
ISOD	0.0000	0.0000	0.2700	0.0000	0.0000	0.0000	0.0000	0.0000	0.0000	0.0000	0.0000
ISOPRUR	0.0000	0.0000	0.0000	0.0000	0.0000	0.0000	0.0000	0.0000	0.0000	0.0000	0.0000
LINUR	0.0000	0.0000	0.0000	0.0000	0.0000	0.0000	0.0000	0.0000	0.0000	0.0000	0.0000
MALATH	0.0000	0.0000	0.0000	0.0000	0.0000	0.0000	0.0000	0.0000	0.0000	0.0000	0.0000
MCPA	0.0000	0.0000	0.0000	n.q.	n.q.	n.q.	n.q.	n.q.	n.q.	0.0000	0.0000
MECOPR	0.0000	0.0000	0.0000	n.q.	n.q.	n.q.	n.q.	n.q.	n.q.	0.0000	0.0000
METAZCHL	0.0000	0.0000	0.0000	0.0000	0.0000	0.0000	0.0000	0.0000	0.0000	0.0000	0.0000
METHABZT	0.0000	0.0000	0.0000	0.0000	0.0000	0.0000	0.0000	0.0000	0.0000	0.0000	0.0000

A2 Table 7 continued:

ng/mL	Evapo- ration- 350 mL 1	Evapo- ration- 350 mL 2	Evapo- ration- 350 mL 3	Evapo- ration- 350 mL 4	Evapo- ration- 350 mL 5	Evapo- ration- 350 mL 6	Evapo- ration- 350 mL 7	Evapo- ration- 350 mL 8	Evapo- ration- 350 mL 9	Evapo- ration- 100 mL 1	Evapo- ration- 100 mL 2
METOLA	0.0000	0.0000	0.0000	0.0000	0.0000	0.0000	0.0000	0.0000	0.0000	0.0000	0.0000
NAPROX	0.0000	0.0000	0.0000	n.q.	n.q.	n.q.	n.q.	n.q.	n.q.	0.0000	0.0000
OXAZEP	0.0000	0.0000	0.0000	0.0000	0.0000	0.0000	0.0000	0.0000	0.0000	0.0000	0.0000
PENDIMETH	0.0976	0.0867	0.1038	0.0000	0.0000	0.0000	0.0000	0.1010	0.0000	0.0000	0.0000
PFBS	0.0000	0.0000	0.0000	0.0240	0.0240	0.0232	0.0071	0.0042	0.0000	0.0000	0.0000
PFDEA	0.0000	0.0000	0.0000	0.0000	0.0000	0.0000	0.0000	0.0000	0.0000	0.0513	0.0556
PFHPA	0.0000	0.0000	0.0000	0.0278	0.0112	0.0102	0.0201	0.0305	0.0214	0.0000	0.0000
PFHXA	0.0714	0.0592	0.0654	0.0159	0.0090	0.0135	0.0000	0.0299	0.0170	0.0000	0.0000
PFHXS	0.0152	0.0128	0.0133	0.0034	0.0035	0.0011	0.0000	0.0035	0.0000	0.0000	0.0000
PFNOA	0.0000	0.0000	0.0000	0.0000	0.0000	0.0000	0.1111	0.0389	0.0165	0.0243	0.0199
PFOA	0.0404	0.0022	0.0383	0.0618	0.0387	0.0364	0.5025	0.4342	0.1011	0.0217	0.0194
PFOS1	0.0000	0.0000	0.0151	0.0146	0.0061	0.0100	0.0806	0.0743	0.0152	0.0000	0.0000
PFOSA1	0.0275	0.0220	0.0425	0.0554	0.0155	0.0291	0.0885	0.0218	0.0825	0.0066	0.0065
PHEN	0.0000	0.0000	0.0000	0.0000	0.0000	0.0000	0.4127	0.0000	0.0338	0.0000	0.0000
PIRIMIC	0.0000	0.0000	0.0000	0.0000	0.0000	0.0000	0.0000	0.0000	0.0000	0.0000	0.0000
PRIMID	0.0000	0.0000	0.0000	0.0000	0.0000	0.0000	0.0000	0.0000	0.0000	0.0000	0.0000
PROMETR	0.0750	0.0806	0.0749	0.0699	0.0737	0.0767	0.0685	0.0998	0.0875	0.0000	0.0000
PROPAZ	0.0000	0.0000	0.0000	0.0000	0.0000	0.0000	0.0000	0.0000	0.0000	0.0000	0.0000
PYR	0.0000	0.0000	0.0000	0.0000	0.0000	0.0000	0.1987	0.0000	0.0000	0.0000	0.0000
QCB	0.1920	0.1890	0.2390	0.0808	0.0038	0.0154	0.0258	0.0242	0.0000	0.0099	0.0093
SIMAZ	0.0000	0.0000	0.0000	0.0000	0.0000	0.0000	0.0000	0.0000	0.0000	0.0000	0.0000
TBEP	0.1943	0.1297	0.0848	0.3403	0.2947	0.3901	3.8372	0.1897	0.3466	0.1558	0.2003
TBP	2.5630	2.5060	3.0260	5.4500	4.0100	4.0000	9.6600	12.200	4.4700	1.1600	1.1400
TERBAZ	0.0995	0.1353	0.1017	0.0000	0.0000	0.0144	0.0116	0.1456	0.0415	0.0265	0.0395
TERBUTR	0.0000	0.0000	0.0000	0.0000	0.0000	0.0000	0.0000	0.0000	0.0000	0.0000	0.0000
TPP	0.6523	0.3970	0.7407	1.4400	1.2600	1.1000	0.7040	0.8850	0.0000	0.5660	0.5160
TRIFLU	0.0000	0.0000	0.2690	0.0050	2.5730	0.6717	0.0000	0.0000	0.0000	0.0000	0.0000

ng/mL	Evapo- ration- 100 mL 3	Evapo- ration- 100 mL 4	Evapo- ration- 100 mL 5
24-D	0.0000	0.0000	0.0000
ACE	0.0000	0.3208	0.0000
ACY	0.0000	0.3767	0.0000
ALD	0.0000	0.0000	0.0000
AMETRYN	0.0000	0.0000	0.0060
ANT	0.0000	0.0000	0.0000
ATRAZ	0.0000	0.0000	0.0000
AZINPH-E	0.0000	0.0000	0.0000
AZINPH-M	0.0000	0.0000	0.0000
BAA	0.0000	0.0000	0.0000
BAP	0.0000	0.0000	0.0000
BBF	0.0000	0.0000	0.0000
BENTAZ	0.0000	0.0000	0.0000
BGHIP	0.0000	0.0000	0.0000
CARBAMAZ	0.0000	0.0000	0.0000
CARBEND	0.0000	0.0000	0.0000
CB138	0.0000	0.0000	0.0000
CB153	0.0000	0.0000	0.0000

ng/mL	Evapo- ration- 100 mL 3	Evapo- ration- 100 mL 4	Evapo- ration- 100 mL 5
CB28	0.0095	0.0134	0.0000
CB52	0.0000	0.0000	0.0000
CHLORFENV	0.0000	0.0000	0.0000
CHLORTUR	0.0000	0.0000	0.0000
CHRTR	0.0000	0.0000	0.0000
CLOFIBRS	0.0000	0.0000	0.0000
DBAHA	0.0000	0.0000	0.0000
DDPP	0.0000	0.0000	0.0049
DDEPP	0.0000	0.0000	0.0000
DDTOP	0.0000	0.0000	0.0000
DDTPP	0.0000	0.0000	0.0000
DEATRAZ	0.0000	0.0000	0.0000
DIAZINON	0.0000	0.0000	0.0000
DICHLPR	0.0000	0.0000	0.0000
DICLOF	0.0000	0.0000	0.0000
DIELD	0.0000	0.0000	0.0000
DIMETH	0.0000	0.0000	0.0000
DIURON	0.0000	0.0000	0.0000

A2 Table 7 continued:

ng/mL	Evapo- ration- 100 mL 3	Evapo- ration- 100 mL 4	Evapo- ration- 100 mL 5
END	0.0000	0.0000	0.0000
FENUR	0.0000	0.0000	0.0000
FL	0.0000	0.2943	0.0000
FLU	0.0000	0.0156	0.0000
HBCDA	0.0000	0.0000	0.0038
HBCDBG	0.0000	0.0063	0.0006
HCB	0.0232	0.0386	0.0000
HCHA	0.0000	0.0000	0.0000
HCHB	0.0000	0.0000	0.0000
HCHD	0.0098	0.0000	0.0000
HCHG	0.0113	0.0000	0.0000
HEXAZIN	0.0000	0.0000	0.0000
I123P	0.0000	0.0000	0.0000
IRGAROL	0.0000	0.0000	0.0000
ISOD	0.0000	0.0000	0.0000
ISOPRUR	0.0000	0.0000	0.0000
LINUR	0.0000	0.0000	0.0000
MALATH	0.0000	0.0000	0.0000
MCPA	0.0000	0.0000	0.0000
MECOPR	0.0000	0.0000	0.0000
METAZCHL	0.0000	0.0000	0.0000
METHABZT	0.0000	0.0000	0.0000
METOLA	0.0000	0.0000	0.0247
NAPROX	0.0000	0.0000	0.0000
OXAZEP	0.0000	0.0000	0.0000

ng/mL	Evapo- ration- 100 mL 3	Evapo- ration- 100 mL 4	Evapo- ration- 100 mL 5
PENDIMETH	0.0000	0.0000	0.0210
PFBS	0.0000	0.0000	0.0000
PFDEA	0.0000	0.0000	0.0000
PFHPA	0.0000	0.0000	0.0138
PFHXA	0.0000	0.0000	0.0000
PFHXS	0.0000	0.0000	0.0012
PFNOA	0.0000	0.0096	0.0391
PFOA	0.0000	0.0176	0.0346
PFOS1	0.0000	0.0000	0.0000
PFOSA1	0.0000	0.0236	0.0241
PHEN	0.0000	0.3371	0.0000
PIRIMIC	0.0000	0.0000	0.0000
PRIMID	0.0000	0.0000	0.0000
PROMETR	0.0000	0.0669	0.0769
PROPAZ	0.0000	0.0000	0.0000
PYR	0.0000	0.0150	0.0000
QCB	0.0230	0.0392	0.0000
SIMAZ	0.0000	0.0000	0.0000
TBEP	0.0000	2.1730	0.2714
TBP	0.0000	2.2500	2.1000
TERBAZ	0.0000	0.0172	0.0302
TERBUTR	0.0000	0.0000	0.0000
TPP	0.0000	0.2560	0.0000
TRIFLU	0.0000	0.0000	0.0000

A2 Table 8: Laboratory blanks – Clean-up blanks; Concentration of target analytes in ng/mL blank extract; n.q. = not quantified; S.f. = syringe filtration

ng/mL	Silica- gel 1	Silica- gel 2	Silica- gel 3	Silica- gel 4	Silica- gel 5	Silica- gel 6	Silica- gel 7	Silica- gel 8	Silica- gel 9	S.f. 1	S.f. 2	S.f. 3
24-D	n.q.	n.q.	n.q.	n.q.	n.q.	n.q.	n.q.	n.q.	n.q.	0.0000	0.0000	0.0000
ACE	0.0000	0.0000	0.0000	0.0000	0.0000	0.0000	0.0387	0.0000	0.0000	n.q.	n.q.	n.q.
ACY	0.0000	0.0000	0.0000	0.0000	0.0000	0.0000	0.0000	0.0000	0.0000	n.q.	n.q.	n.q.
ALD	0.0570	0.1900	n.q.	0.0000	0.0000	0.0000	0.0000	0.0000	0.0000	n.q.	n.q.	n.q.
AMETRYN	n.q.	n.q.	n.q.	n.q.	n.q.	n.q.	n.q.	n.q.	n.q.	0.0000	0.0049	0.0055
ANT	0.0000	0.0000	0.0000	0.0000	0.0000	0.0000	0.0000	0.0000	0.0000	n.q.	n.q.	n.q.
ATRAZ	n.q.	n.q.	n.q.	n.q.	n.q.	n.q.	n.q.	n.q.	n.q.	0.0000	0.0000	0.0000
AZINPH-E	n.q.	n.q.	n.q.	n.q.	n.q.	n.q.	n.q.	n.q.	n.q.	0.0000	0.0000	0.0000
AZINPH-M	n.q.	n.q.	n.q.	n.q.	n.q.	n.q.	n.q.	n.q.	n.q.	0.0000	0.0000	0.0000
BAA	0.0000	0.0000	0.0000	0.0000	0.0000	0.0000	0.0000	0.0000	0.0000	n.q.	n.q.	n.q.
BAP	0.0000	0.0000	0.0000	0.0000	0.0000	0.0000	0.0000	0.0000	0.0000	n.q.	n.q.	n.q.
BBF	0.0000	0.0000	0.0000	0.0000	0.0000	0.0000	0.0000	0.0000	0.0000	n.q.	n.q.	n.q.
BETAZ	n.q.	n.q.	n.q.	n.q.	n.q.	n.q.	n.q.	n.q.	n.q.	0.0000	0.0000	0.0000
BGHIP	0.0000	0.0000	0.0000	0.0000	0.0000	0.0000	0.0000	0.0000	0.0000	n.q.	n.q.	n.q.
CARBAMAZ	n.q.	n.q.	n.q.	n.q.	n.q.	n.q.	n.q.	n.q.	n.q.	0.0000	0.0000	0.0000
CARBEND	n.q.	n.q.	n.q.	n.q.	n.q.	n.q.	n.q.	n.q.	n.q.	0.0000	0.0000	0.0000
CB138	0.0000	0.0000	0.0000	0.0000	0.0000	0.0000	0.0000	0.0000	0.0000	n.q.	n.q.	n.q.
CB153	0.0000	0.0000	0.0000	0.0000	0.0000	0.0000	0.0000	0.0000	0.0000	n.q.	n.q.	n.q.
CB28	0.0610	0.0610	0.0600	0.0000	0.0016	0.0006	0.0035	0.0000	0.0000	n.q.	n.q.	n.q.

A2 Table 8 continued:

ng/mL	Silica-gel 1	Silica-gel 2	Silica-gel 3	Silica-gel 4	Silica-gel 5	Silica-gel 6	Silica-gel 7	Silica-gel 8	Silica-gel 9	S.f. 1	S.f. 2	S.f. 3
CB52	0.0000	0.0000	0.0000	0.0000	0.0000	0.0000	0.0000	0.0000	0.0000	n.q.	n.q.	n.q.
CHLORFENV	n.q.	n.q.	n.q.	n.q.	n.q.	n.q.	n.q.	n.q.	n.q.	0.0000	0.0000	0.0000
CHLORTUR	n.q.	n.q.	n.q.	n.q.	n.q.	n.q.	n.q.	n.q.	n.q.	0.0000	0.0000	0.0000
CHRTR	0.0000	0.0000	0.0000	0.0000	0.0000	0.0000	0.0000	0.0000	0.0000	n.q.	n.q.	n.q.
CLOFIBRS	n.q.	n.q.	n.q.	n.q.	n.q.	n.q.	n.q.	n.q.	n.q.	0.0000	0.0000	0.0000
DBAHA	0.0000	0.0000	0.0000	0.0000	0.0000	0.0000	0.0000	0.0000	0.0000	n.q.	n.q.	n.q.
DDPP	0.1000	0.1000	0.0000	0.0000	0.0000	0.0000	0.0000	0.0000	0.0000	n.q.	n.q.	n.q.
DDEPP	0.2320	0.0000	0.0000	0.0000	0.0000	0.0000	0.0000	0.0000	0.0000	n.q.	n.q.	n.q.
DDTOP	0.2430	0.2450	0.2480	0.0000	0.0000	0.0000	0.0000	0.0000	0.0000	n.q.	n.q.	n.q.
DDTPP	0.1290	0.1420	0.1430	0.0000	0.0000	0.0000	0.0000	0.0000	0.0000	n.q.	n.q.	n.q.
DEATRAZ	n.q.	n.q.	n.q.	n.q.	n.q.	n.q.	n.q.	n.q.	n.q.	0.0000	0.0000	0.0000
DIAZINON	n.q.	n.q.	n.q.	n.q.	n.q.	n.q.	n.q.	n.q.	n.q.	0.0000	0.0000	0.0000
DICHLPR	n.q.	n.q.	n.q.	n.q.	n.q.	n.q.	n.q.	n.q.	n.q.	0.0000	0.0000	0.0000
DICLOF	n.q.	n.q.	n.q.	n.q.	n.q.	n.q.	n.q.	n.q.	n.q.	0.0000	0.0000	0.0000
DIELD	0.2480	0.0000	0.0000	0.0000	0.0000	0.0000	0.0000	0.0000	0.0000	n.q.	n.q.	n.q.
DIMETH	n.q.	n.q.	n.q.	n.q.	n.q.	n.q.	n.q.	n.q.	n.q.	0.0000	0.0000	0.0000
DIURON	n.q.	n.q.	n.q.	n.q.	n.q.	n.q.	n.q.	n.q.	n.q.	0.0000	0.0000	0.0000
END	0.0000	0.0000	n.q.	0.0000	0.0000	0.0000	0.0000	0.0000	0.0000	n.q.	n.q.	n.q.
FENUR	n.q.	n.q.	n.q.	n.q.	n.q.	n.q.	n.q.	n.q.	n.q.	0.0000	0.0000	0.0000
FL	0.0000	0.0000	0.0000	0.0000	0.0000	0.0000	0.0034	0.0000	0.0000	n.q.	n.q.	n.q.
FLU	0.0000	0.0000	0.0000	0.0000	0.0000	0.0000	0.0000	0.0000	0.0000	n.q.	n.q.	n.q.
HBCDA	n.q.	n.q.	n.q.	n.q.	n.q.	n.q.	n.q.	n.q.	n.q.	0.0000	0.0000	0.0024
HBCDBG	n.q.	n.q.	n.q.	n.q.	n.q.	n.q.	n.q.	n.q.	n.q.	0.0000	0.0000	0.0004
HCB	0.1190	0.1160	0.1170	0.0278	0.0091	0.0180	0.0092	0.0000	0.0000	n.q.	n.q.	n.q.
HCHA	0.0000	0.0000	0.0000	0.0000	0.0000	0.0000	0.0000	0.0000	0.0000	n.q.	n.q.	n.q.
HCHB	0.0000	0.1310	0.1250	0.0000	0.0000	0.0000	0.0000	0.0000	0.0000	n.q.	n.q.	n.q.
HCHD	0.1480	0.1570	0.1510	0.0000	0.0000	0.0000	0.0000	0.0000	0.0000	n.q.	n.q.	n.q.
HCHG	0.1830	0.1500	0.1570	0.0000	0.0000	0.0000	0.0000	0.0000	0.0000	n.q.	n.q.	n.q.
HEXAZIN	n.q.	n.q.	n.q.	n.q.	n.q.	n.q.	n.q.	n.q.	n.q.	0.0000	0.0000	0.0000
I123P	0.0000	0.0000	0.0000	0.0000	0.0000	0.0000	0.0000	0.0000	0.0000	n.q.	n.q.	n.q.
IRGAROL	n.q.	n.q.	n.q.	n.q.	n.q.	n.q.	n.q.	n.q.	n.q.	0.0000	0.0000	0.0000
ISOD	0.0000	0.0000	0.0000	0.0000	0.0000	0.0000	0.0000	0.0000	0.0000	n.q.	n.q.	n.q.
ISOPRUR	n.q.	n.q.	n.q.	n.q.	n.q.	n.q.	n.q.	n.q.	n.q.	0.0000	0.0000	0.0026
LINUR	n.q.	n.q.	n.q.	n.q.	n.q.	n.q.	n.q.	n.q.	n.q.	0.0000	0.0000	0.0000
MALATH	n.q.	n.q.	n.q.	n.q.	n.q.	n.q.	n.q.	n.q.	n.q.	0.0000	0.0000	0.0000
MCPA	n.q.	n.q.	n.q.	n.q.	n.q.	n.q.	n.q.	n.q.	n.q.	0.0000	0.0000	0.0000
MECOPR	n.q.	n.q.	n.q.	n.q.	n.q.	n.q.	n.q.	n.q.	n.q.	0.0000	0.0000	0.0000
METAZCHL	n.q.	n.q.	n.q.	n.q.	n.q.	n.q.	n.q.	n.q.	n.q.	0.0000	0.0000	0.0000
METHABZT	n.q.	n.q.	n.q.	n.q.	n.q.	n.q.	n.q.	n.q.	n.q.	0.0000	0.0000	0.0000
METOLA	n.q.	n.q.	n.q.	n.q.	n.q.	n.q.	n.q.	n.q.	n.q.	0.0000	0.0000	0.0267
NAPROX	n.q.	n.q.	n.q.	n.q.	n.q.	n.q.	n.q.	n.q.	n.q.	0.0000	0.0000	0.0000
OXAZEP	n.q.	n.q.	n.q.	n.q.	n.q.	n.q.	n.q.	n.q.	n.q.	0.0000	0.0000	0.0000
PENDIMETH	n.q.	n.q.	n.q.	n.q.	n.q.	n.q.	n.q.	n.q.	n.q.	0.0000	0.0000	0.0271
PFBS	n.q.	n.q.	n.q.	n.q.	n.q.	n.q.	n.q.	n.q.	n.q.	0.0000	0.0000	0.0000
PFDEA	n.q.	n.q.	n.q.	n.q.	n.q.	n.q.	n.q.	n.q.	n.q.	0.0000	0.0000	0.0000
PFHPA	n.q.	n.q.	n.q.	n.q.	n.q.	n.q.	n.q.	n.q.	n.q.	0.0030	0.0233	0.0104
PFHXA	n.q.	n.q.	n.q.	n.q.	n.q.	n.q.	n.q.	n.q.	n.q.	0.0000	0.0244	0.0000
PFHXS	n.q.	n.q.	n.q.	n.q.	n.q.	n.q.	n.q.	n.q.	n.q.	0.0000	0.0000	0.0000
PFNOA	n.q.	n.q.	n.q.	n.q.	n.q.	n.q.	n.q.	n.q.	n.q.	0.0594	0.0000	0.0000
PFOA	n.q.	n.q.	n.q.	n.q.	n.q.	n.q.	n.q.	n.q.	n.q.	0.0320	0.0383	0.0388
PFOS	n.q.	n.q.	n.q.	n.q.	n.q.	n.q.	n.q.	n.q.	n.q.	0.1448	0.0000	0.0000

A2 Table 8 continued:

ng/mL	Silica-gel 1	Silica-gel 2	Silica-gel 3	Silica-gel 4	Silica-gel 5	Silica-gel 6	Silica-gel 7	Silica-gel 8	Silica-gel 9	S.f. 1	S.f. 2	S.f. 3
PFOSA	n.q.	n.q.	n.q.	n.q.	n.q.	n.q.	n.q.	n.q.	n.q.	0.0196	0.0167	0.0064
PHEN	0.0000	0.0000	0.0000	0.0000	0.0000	0.0000	0.2063	0.0000	0.0000	n.q.	n.q.	n.q.
PIRIMIC	n.q.	n.q.	n.q.	n.q.	n.q.	n.q.	n.q.	n.q.	n.q.	0.0000	0.0000	0.0000
PRIMID	n.q.	n.q.	n.q.	n.q.	n.q.	n.q.	n.q.	n.q.	n.q.	0.0000	0.0000	0.0000
PROMETR	n.q.	n.q.	n.q.	n.q.	n.q.	n.q.	n.q.	n.q.	n.q.	0.0570	0.0699	0.0700
PROPAZ	n.q.	n.q.	n.q.	n.q.	n.q.	n.q.	n.q.	n.q.	n.q.	0.0000	0.0000	0.0000
PYR	0.0000	0.0000	0.0000	0.0000	0.0000	0.0000	0.0046	0.0000	0.0000	n.q.	n.q.	n.q.
QCB	0.0000	0.0000	0.1860	0.0000	0.0000	0.0000	0.0026	0.0000	0.0000	n.q.	n.q.	n.q.
SIMAZ	n.q.	n.q.	n.q.	n.q.	n.q.	n.q.	n.q.	n.q.	n.q.	0.0000	0.0000	0.0000
TBEP	n.q.	n.q.	n.q.	n.q.	n.q.	n.q.	n.q.	n.q.	n.q.	1.1130	0.0835	0.1134
TBP	n.q.	n.q.	n.q.	n.q.	n.q.	n.q.	n.q.	n.q.	n.q.	0.5750	0.0418	0.0000
TERBAZ	n.q.	n.q.	n.q.	n.q.	n.q.	n.q.	n.q.	n.q.	n.q.	0.0000	0.0139	0.0139
TERBUTR	n.q.	n.q.	n.q.	n.q.	n.q.	n.q.	n.q.	n.q.	n.q.	0.0000	0.0000	0.0000
TPP	n.q.	n.q.	n.q.	n.q.	n.q.	n.q.	n.q.	n.q.	n.q.	0.3260	0.0000	0.0000
TRIFLU	0.2130	0.0000	0.0000	0.0000	0.0000	0.0000	0.0000	0.0000	0.0000	n.q.	n.q.	n.q.

Spike controls

A2 Table 9: Recovery of target compounds in spike control samples; n.q. = not quantified; PXP = PUF/XAD-2/PUF adsorber cartridge; E. = evaporation, S.f. = syringe filtration

%	GFF 1	GFF 2	GFF 3	GFF 4	GFF 5	GFF 6	GFF 7	GFF 8	GFF 9	PUF disk 1	PUF disk 2	PUF disk 3	PUF disk 4	PUF disk 5	PUF disk 6
24-D	93	88	92	102	105	107	105	104	103	n.q.	n.q.	n.q.	n.q.	n.q.	n.q.
ACE	97	100	98	137	103	102	103	103	103	71	133	99	98	100	102
ACY	81	88	89	123	97	92	100	101	101	78	83	49	42	45	70
ALD	80	91	78	108	68	70	72	74	73	87	85	89	92	95	97
AMETRYN	114	114	114	156	146	129	132	142	134	93	88	114	110	113	99
ANT	95	97	97	138	104	103	104	106	104	128	71	97	95	96	100
ATRAZ	103	101	100	100	102	99	101	101	102	96	95	96	96	97	94
AZINPH-E	104	104	109	131	121	114	116	120	126	104	106	120	160	121	188
AZINPH-M	102	97	104	105	101	105	105	102	105	102	102	98	93	92	101
BAA	90	89	88	132	98	90	91	94	102	104	115	96	98	96	113
BAP	98	101	97	147	104	102	101	98	96	109	83	88	84	94	85
BBF	108	111	106	151	108	105	104	104	104	97	105	107	109	110	110
BENTAZ	110	106	109	105	106	104	107	105	106	71	68	100	108	111	81
BGHIP	98	100	98	141	106	104	104	105	104	89	84	98	97	98	99
CARBAMAZ	98	98	97	108	110	107	108	105	109	99	97	101	100	103	81
CARBEND	60	49	60	110	130	81	87	90	94	86	91	91	76	86	29
CB138	85	95	89	139	106	103	103	101	100	107	107	97	94	98	99
CB153	92	96	94	137	102	102	110	102	102	109	105	96	98	101	99
CB28	84	96	88	128	98	93	101	103	95	104	93	92	96	97	100
CB52	93	101	90	134	101	96	106	99	100	103	100	92	93	97	100
CHLORFENV	107	102	102	117	104	102	108	107	115	152	143	105	104	93	91
CHLORTUR	97	98	97	102	99	100	103	99	103	87	82	85	80	89	49
CHRTR	91	88	87	132	97	90	92	97	103	119	122	96	101	97	120
CLOFIBRS	98	96	99	102	104	102	103	101	106	n.q.	n.q.	n.q.	n.q.	n.q.	n.q.
DBAHA	98	100	98	151	107	106	106	103	103	102	111	108	106	103	105
DDPP	77	84	77	134	107	100	102	112	110	102	93	87	89	90	98

A2 Table 9 continued:

%	GFF 1	GFF 2	GFF 3	GFF 4	GFF 5	GFF 6	GFF 7	GFF 8	GFF 9	PUF disk 1	PUF disk 2	PUF disk 3	PUF disk 4	PUF disk 5	PUF disk 6
DDEPP	90	105	88	166	127	132	112	125	118	105	100	101	100	102	111
DDTOP	101	126	108	235	200	253	147	171	140	85	92	80	83	80	99
DDTPP	102	101	98	153	127	125	109	115	107	93	96	90	92	91	95
DEATRAZ	99	97	103	107	102	100	104	103	104	97	101	99	97	99	107
DIAZINON	83	82	85	97	68	83	78	80	72	94	98	110	113	76	125
DICHLPR	101	97	101	100	102	102	100	102	104	n.q.	n.q.	n.q.	n.q.	n.q.	n.q.
DICLOF	90	89	87	121	111	107	109	106	110	n.q.	n.q.	n.q.	n.q.	n.q.	n.q.
DIELD	61	76	36	94	72	55	55	75	77	99	96	89	89	89	94
DIMETH	103	97	97	89	92	90	96	92	104	164	156	109	109	98	83
DIURON	99	98	99	106	106	106	104	103	108	101	104	121	116	117	114
END	61	73	36	134	97	70	80	83	104	129	106	96	89	92	154
FENUR	113	109	108	132	142	116	116	127	119	102	101	115	104	119	58
FL	105	106	103	146	105	106	105	109	106	126	190	141	135	138	123
FLU	59	53	52	97	71	60	65	64	82	98	112	89	83	80	108
HBCDA	92	87	91	87	87	92	94	87	100	89	88	81	76	85	46
HBCDBG	64	53	61	39	43	54	51	46	64	82	67	80	49	80	23
HCB	100	100	101	137	91	90	92	101	106	97	104	102	102	102	99
HCHA	28	12	17	4	4	2	5	13	23	71	73	86	85	88	89
HCHB	152	243	187	540	422	511	295	260	200	97	101	92	94	95	112
HCHD	0	0	0	0	0	0	0	0	0	64	34	82	75	64	55
HCHG	42	17	24	10	4	3	11	8	27	77	72	87	86	88	100
HEXAZIN	110	107	107	132	122	109	119	124	119	84	79	110	110	110	92
I123P	101	103	101	147	107	106	106	106	106	89	98	107	103	105	99
IRGAROL	123	119	124	157	164	136	142	154	138	79	75	94	93	91	88
ISOD	100	97	92	132	92	85	86	97	88	84	91	95	97	100	104
ISOPRUR	99	98	94	102	98	101	102	98	103	85	83	108	102	111	84
LINUR	92	93	91	97	91	97	94	89	99	94	92	107	107	116	99
MALATH	91	99	92	98	0	92	116	135	103	99	98	99	96	94	100
MCPA	98	95	98	107	107	108	107	107	109	n.q.	n.q.	n.q.	n.q.	n.q.	n.q.
MECOPR	101	96	100	100	104	101	102	102	105	n.q.	n.q.	n.q.	n.q.	n.q.	n.q.
METAZCHL	120	115	120	164	167	130	136	145	138	85	82	88	91	95	75
METHABZT	123	119	125	162	166	134	141	153	144	86	80	80	80	81	76
METOLA	108	105	108	138	128	119	119	125	122	97	95	130	132	130	120
NAPROX	84	86	83	109	100	98	97	96	100	n.q.	n.q.	n.q.	n.q.	n.q.	n.q.
OXAZEP	91	89	88	114	101	100	98	99	100	97	89	103	87	110	56
PENDIMETH	94	99	72	124	112	107	114	116	111	88	64	95	70	93	31
PFBS	97	98	100	242	262	281	245	281	316	114	117	123	123	120	107
PFDEA	99	100	102	101	103	103	101	105	103	88	112	125	113	117	111
PFHPA	104	104	108	102	103	104	107	105	105	64	80	88	78	77	75
PFHXA	103	104	106	102	103	104	105	106	105	68	90	102	93	86	85
PFHXS	100	99	103	103	104	102	103	105	104	98	97	103	101	100	97
PFNOA	100	100	102	102	103	102	103	105	104	80	103	121	108	110	90
PFOA	99	98	101	104	105	104	103	106	105	78	101	138	114	134	102
PFOS	100	100	103	104	104	104	105	105	105	99	99	108	104	109	97
PFOSA	98	97	102	101	102	102	102	105	104	89	86	107	99	107	56
PHEN	99	99	100	138	104	105	105	107	107	155	135	133	124	118	124
PIRIMIC	98	95	99	117	114	108	104	112	109	93	93	117	119	121	84
PRIMID	107	97	103	192	172	136	134	143	138	85	92	126	132	135	143
PROMETR	117	110	115	154	145	129	131	141	133	90	85	116	114	113	109
PROPAZ	102	100	103	109	103	107	107	108	109	102	99	91	92	92	108

A2 Table 9 continued:

%	GFF 1	GFF 2	GFF 3	GFF 4	GFF 5	GFF 6	GFF 7	GFF 8	GFF 9	PUF disk 1	PUF disk 2	PUF disk 3	PUF disk 4	PUF disk 5	PUF disk 6
PYR	61	57	56	101	75	64	67	66	84	126	128	101	89	86	118
QCB	99	99	99	139	104	99	143	102	109	74	78	66	69	68	91
SIMAZ	103	100	104	110	109	104	105	106	106	80	74	77	76	79	89
TBEP	121	130	131	134	134	137	126	132	124	91	86	85	79	87	99
TBP	124	123	120	239	169	137	141	172	155	136	138	822	810	794	320
TERBAZ	104	102	105	109	103	105	107	109	109	101	99	101	98	100	105
TERBUTR	114	113	114	150	144	129	130	140	131	88	85	114	112	110	105
TPP	104	103	100	885	111	94	105	98	114	81	79	106	121	112	135
TRIFLU	96	95	87	125	83	87	93	90	90	94	89	98	83	78	64

%	PUF disk 7	PUF disk 8	PUF disk 9	PUF disk 10	PUF disk 11	PUF plug 1	PUF plug 2	PUF plug 3	PUF plug 4	PUF plug 5	PUF plug 6	PXP 1	PXP 2	PXP 3	PXP 4
24-D	n.q.	n.q.	n.q.	n.q.	n.q.	n.q.	n.q.	n.q.	n.q.	n.q.	n.q.	n.q.	n.q.	n.q.	n.q.
ACE	98	97	103	104	104	89	97	86	104	104	104	148	168	138	99
ACY	64	66	68	70	62	176	175	168	54	59	68	87	136	112	49
ALD	99	102	89	80	89	79	72	74	79	92	89	81	85	85	95
AMETRYN	101	99	125	114	114	100	106	102	124	111	114	96	99	96	112
ANT	98	99	102	103	103	85	84	78	103	102	100	109	89	75	108
ATRAZ	95	95	104	103	103	101	99	100	104	104	104	97	99	99	104
AZINPH-E	204	163	190	220	271	102	97	100	134	164	192	104	112	111	203
AZINPH-M	102	95	117	120	113	103	101	102	107	110	106	95	101	101	108
BAA	113	103	104	129	112	97	92	88	119	175	123	97	82	117	140
BAP	77	91	96	77	96	100	97	93	84	58	92	98	92	94	122
BBF	110	111	108	107	109	102	101	96	110	103	111	101	104	109	143
BENTAZ	74	81	75	77	78	102	102	101	87	75	83	77	59	65	74
BGHIP	98	99	103	105	104	96	99	97	105	104	104	91	77	92	107
CARBAMAZ	81	79	93	76	77	101	101	101	107	91	93	100	102	103	103
CARBEND	58	77	70	50	60	102	107	103	98	59	49	89	88	89	47
CB138	99	99	104	108	107	100	101	103	109	106	106	109	103	109	97
CB153	99	99	102	107	109	99	102	101	110	103	107	106	106	108	100
CB28	99	99	96	105	101	94	87	91	102	98	99	96	106	105	104
CB52	101	101	100	113	108	100	94	96	108	104	107	105	104	106	115
CHLORFENV	91	90	111	89	92	99	95	98	97	97	96	185	167	165	100
CHLORTUR	55	54	81	60	62	103	94	99	105	81	81	90	95	97	92
CHRTR	125	110	107	142	114	99	90	88	122	188	134	138	129	139	143
CLOFIBRS	n.q.	n.q.	n.q.	n.q.	n.q.	n.q.	n.q.	n.q.	n.q.	n.q.	n.q.	n.q.	n.q.	n.q.	n.q.
DBAHA	105	101	112	111	118	102	95	91	118	118	112	110	94	107	103
DDPP	98	93	99	107	105	97	94	99	113	106	116	100	113	106	83
DDEPP	122	131	105	106	107	98	98	98	109	124	119	104	101	109	101
DDTOP	117	146	103	105	105	96	107	105	106	115	110	87	82	88	114
DDTPP	97	98	105	109	107	98	100	103	110	104	111	97	92	96	95
DEATRAZ	107	111	113	108	116	99	101	100	103	106	102	99	100	101	99
DIAZINON	117	113	111	119	117	103	99	101	91	105	106	87	94	86	133
DICHLPR	n.q.	n.q.	n.q.	n.q.	n.q.	n.q.	n.q.	n.q.	n.q.	n.q.	n.q.	n.q.	n.q.	n.q.	n.q.
DICLOF	n.q.	n.q.	n.q.	n.q.	n.q.	n.q.	n.q.	n.q.	n.q.	n.q.	n.q.	n.q.	n.q.	n.q.	n.q.
DIELD	90	95	74	61	69	73	77	71	81	79	74	90	105	97	81
DIMETH	81	85	97	99	98	102	99	100	92	86	86	177	151	159	98
DIURON	114	115	114	135	126	104	102	102	115	115	112	98	97	98	105
END	109	120	169	150	155	44	38	51	154	184	150	140	147	132	83

A2 Table 9 continued:

%	PUF disk 7	PUF disk 8	PUF disk 9	PUF disk 10	PUF disk 11	PUF plug 1	PUF plug 2	PUF plug 3	PUF plug 4	PUF plug 5	PUF plug 6	PXP 1	PXP 2	PXP 3	PXP 4
FENUR	64	72	95	92	90	101	100	100	113	102	94	98	98	97	410
FL	116	117	123	124	139	121	98	97	134	137	126	0	127	214	137
FLU	109	93	98	139	111	122	105	105	117	186	136	112	128	131	215
HBCDA	53	55	77	63	65	98	95	97	92	63	72	103	97	88	73
HBCDBG	27	30	60	47	37	102	99	100	92	24	31	93	83	68	43
HCB	97	98	105	98	85	90	99	87	91	104	104	99	95	100	96
HCHA	42	16	89	74	67	150	126	135	81	66	97	65	68	71	83
HCHB	144	208	106	119	110	94	97	96	122	141	186	102	98	100	124
HCHD	0	0	90	34	46	80	58	70	30	1	1	71	58	66	15
HCHG	50	22	86	77	62	81	81	83	72	59	57	67	82	73	88
HEXAZIN	93	91	96	81	79	105	105	103	103	98	96	93	90	97	100
I123P	98	103	108	100	111	102	95	92	109	92	105	77	86	83	124
IRGAROL	93	89	113	88	91	102	99	100	120	106	109	92	96	94	89
ISOD	102	102	93	91	88	86	80	87	88	103	88	83	79	84	106
ISOPRUR	88	94	100	88	91	101	93	98	116	94	98	91	98	93	98
LINUR	107	106	116	105	111	104	98	101	112	104	98	96	99	98	112
MALATH	97	99	97	97	91	101	101	101	99	92	86	96	95	96	113
MCPA	n.q.	n.q.	n.q.	n.q.	n.q.	n.q.	n.q.	n.q.	n.q.	n.q.	n.q.	n.q.	n.q.	n.q.	n.q.
MECOPR	n.q.	n.q.	n.q.	n.q.	n.q.	n.q.	n.q.	n.q.	n.q.	n.q.	n.q.	n.q.	n.q.	n.q.	n.q.
METAZCHL	79	79	98	79	81	100	107	102	118	107	103	93	98	97	112
METHABZT	82	84	99	81	84	100	103	101	118	97	95	95	98	99	109
METOLA	123	124	131	122	125	102	100	100	126	123	126	102	102	102	113
NAPROX	n.q.	n.q.	n.q.	n.q.	n.q.	n.q.	n.q.	n.q.	n.q.	n.q.	n.q.	n.q.	n.q.	n.q.	n.q.
OXAZEP	62	85	84	63	65	99	99	99	124	63	64	98	94	103	51
PENDIMETH	1	74	9	1	2	102	100	101	3	5	1	96	74	77	110
PFBS	102	104	511	462	507	100	100	100	355	379	827	105	98	104	123
PFDEA	94	101	100	121	121	100	101	100	110	129	112	100	106	112	99
PFHPA	64	70	98	102	107	98	97	98	95	104	96	90	89	93	73
PFHXA	63	73	89	86	90	96	98	98	83	89	85	91	87	90	75
PFHXS	95	96	105	106	105	102	101	101	105	104	106	100	98	103	109
PFNOA	78	85	118	114	118	99	100	100	104	122	110	97	99	103	100
PFOA	86	96	116	109	111	100	101	100	105	120	109	102	102	108	108
PFOS	97	98	110	106	110	100	100	100	107	108	109	102	102	103	110
PFOSA	65	69	99	83	99	100	99	100	105	85	93	88	100	91	99
PHEN	128	117	119	132	121	278	234	229	144	120	121	259	278	323	262
PIRIMIC	86	85	115	120	121	101	100	100	118	115	116	94	97	95	111
PRIMID	141	146	132	150	150	102	101	101	129	121	119	95	83	80	101
PROMETR	111	109	127	113	113	99	101	100	132	122	127	95	96	95	94
PROPAZ	105	106	104	98	94	100	99	100	109	110	111	102	101	102	113
PYR	114	98	101	142	120	211	143	156	124	199	134	207	160	240	248
QCB	100	93	102	99	91	60	85	78	92	96	73	69	76	70	69
SIMAZ	89	94	92	82	81	102	101	101	99	99	93	89	93	91	93
TBEP	105	101	187	139	115	99	97	99	113	122	89	109	106	101	212
TBP	327	270	533	387	385	101	99	100	385	422	415	116	120	108	244
TERBAZ	102	102	121	114	113	98	98	99	112	112	114	103	103	102	96
TERBUTR	112	107	126	107	110	103	101	101	127	115	117	95	100	97	94
TPP	116	111	281	73	77	99	95	98	102	192	191	152	103	102	4668
TRIFLU	0	0	86	0	91	51	82	425	n.q.	n.q.	n.q.	80	79	88	97

A2 Table 9 continued:

%	PXP 5	PXP 6	PXP 7	PXP 8	PXP 9	E.- 350 mL 1	E.- 350 mL 2	E.- 350 mL 3	E.- 350 mL 4	E.- 350 mL 5	E.- 350 mL 6	E.- 350 mL 7	E.- 350 mL 8	E.- 350 mL 9	E.- 100 mL 1
24-D	n.q.	n.q.	n.q.	n.q.	n.q.	n.q.	n.q.	n.q.	n.q.	n.q.	n.q.	n.q.	n.q.	n.q.	92
ACE	100	98	104	103	103	89	89	87	127	116	129	99	97	99	118
ACY	52	59	72	70	62	109	118	110	108	148	102	82	83	103	117
ALD	94	87	92	97	83	76	72	70	83	74	79	87	81	73	78
AMETRYN	116	120	114	120	121	98	99	98	107	105	112	109	119	125	105
ANT	102	99	103	104	101	83	85	83	94	89	75	96	97	103	115
ATRAZ	95	101	101	103	103	103	100	100	95	96	94	95	92	97	93
AZINPH-E	117	155	174	127	154	122	113	117	93	98	99	101	102	115	97
AZINPH-M	100	109	107	106	105	104	106	101	94	95	96	96	95	103	96
BAA	101	111	131	110	117	95	94	91	112	100	104	77	91	104	87
BAP	100	81	80	94	84	94	99	97	95	109	92	101	98	95	110
BBF	105	102	105	109	106	102	102	97	96	97	96	108	114	106	114
BENTAZ	71	65	65	83	69	2085	1342	2328	87	88	87	94	94	100	94
BGHP	95	98	102	104	102	97	99	97	86	98	91	95	98	103	98
CARBAMAZ	93	112	91	100	102	107	110	107	123	120	132	139	164	147	95
CARBEND	64	58	57	78	59	97	99	94	61	52	65	111	154	105	104
CB138	95	95	101	105	104	99	96	98	101	104	98	98	96	99	91
CB153	98	99	99	104	99	103	98	101	105	109	109	102	99	97	97
CB28	106	101	92	99	95	94	86	83	105	98	106	91	90	103	87
CB52	103	98	102	104	102	95	92	87	105	102	104	95	99	97	90
CHLORFENV	116	81	91	89	114	180	197	193	86	93	88	115	101	97	99
CHLORTUR	95	105	74	100	93	117	115	113	117	114	126	134	152	144	95
CHRTR	97	113	127	110	129	97	97	90	124	91	98	76	90	100	106
CLOFIBRS	n.q.	n.q.	n.q.	n.q.	n.q.	n.q.	n.q.	n.q.	n.q.	n.q.	n.q.	n.q.	n.q.	n.q.	96
DBAHA	109	101	99	108	114	98	103	98	101	105	103	98	97	86	116
DDPP	112	97	103	106	107	113	115	113	133	138	133	110	108	76	96
DDEPP	94	110	123	111	109	82	87	87	101	101	98	97	103	93	80
DDTOP	82	112	108	107	102	85	85	96	76	76	73	85	103	152	79
DDTPP	91	91	104	107	107	97	94	103	93	93	89	96	102	120	94
DEATRAZ	98	96	98	101	92	96	98	99	96	96	96	96	95	99	95
DIAZINON	117	103	100	94	86	84	91	89	77	82	75	72	88	89	82
DICHLPR	n.q.	n.q.	n.q.	n.q.	n.q.	n.q.	n.q.	n.q.	n.q.	n.q.	n.q.	n.q.	n.q.	n.q.	93
DICLOF	n.q.	n.q.	n.q.	n.q.	n.q.	n.q.	n.q.	n.q.	n.q.	n.q.	n.q.	n.q.	n.q.	n.q.	96
DIELD	86	86	81	78	79	85	89	90	109	118	113	83	94	39	80
DIMETH	104	71	88	82	110	151	184	183	89	97	84	112	95	95	97
DIURON	105	107	116	113	115	112	108	109	97	94	92	95	95	102	93
END	95	96	202	163	146	99	100	41	256	271	254	100	151	65	153
FENUR	143	141	104	104	105	106	98	102	101	102	107	98	117	121	102
FL	137	126	125	122	125	100	103	99	243	244	249	108	108	92	161
FLU	117	92	135	107	111	74	72	69	89	71	75	39	65	79	65
HBCDA	102	46	45	86	80	83	98	92	88	95	82	94	84	84	88
HBCDBG	112	17	25	78	35	78	81	91	75	82	71	82	57	66	88
HCB	99	100	101	98	99	99	97	101	100	100	97	101	100	93	99
HCHA	87	18	83	81	80	129	130	143	69	69	72	51	37	16	87
HCHB	96	179	116	118	111	100	104	100	96	100	97	121	139	103	106
HCHD	85	0	46	1	97	101	106	98	104	111	106	0	0	0	109
HCHG	96	24	75	78	83	103	96	88	84	84	84	61	46	20	92
HEXAZIN	104	85	93	94	110	94	107	100	94	110	97	139	105	104	99

A2 Table 9 continued:

%	PXP 5	PXP 6	PXP 7	PXP 8	PXP 9	E.-350 mL 1	E.-350 mL 2	E.-350 mL 3	E.-350 mL 4	E.-350 mL 5	E.-350 mL 6	E.-350 mL 7	E.-350 mL 8	E.-350 mL 9	E.-100 mL 1
I123P	110	96	99	108	101	94	99	98	96	93	78	100	98	99	109
IRGAROL	106	113	101	117	115	89	99	96	115	110	124	121	134	131	110
ISOD	98	92	103	99	95	88	88	88	80	78	81	93	97	92	90
ISOPRUR	99	108	98	111	109	126	117	117	115	112	123	130	149	147	94
LINUR	109	123	100	112	100	130	123	124	106	98	110	98	131	136	95
MALATH	106	91	96	97	97	96	99	99	92	91	92	96	93	100	96
MCPA	n.q.	n.q.	n.q.	n.q.	n.q.	n.q.	n.q.	n.q.	n.q.	n.q.	n.q.	n.q.	n.q.	n.q.	91
MECOPR	n.q.	n.q.	n.q.	n.q.	n.q.	n.q.	n.q.	n.q.	n.q.	n.q.	n.q.	n.q.	n.q.	n.q.	95
METAZCHL	101	117	95	110	110	100	103	102	105	105	117	115	127	133	106
METHABZT	110	123	89	114	108	96	101	97	112	108	121	115	128	132	107
METOLA	128	125	115	122	120	101	106	103	97	93	97	95	109	113	100
NAPROX	n.q.	n.q.	n.q.	n.q.	n.q.	n.q.	n.q.	n.q.	n.q.	n.q.	n.q.	n.q.	n.q.	n.q.	97
OXAZEP	135	79	62	120	70	108	113	110	118	111	126	128	135	133	94
PENDIMETH	120	37	32	5	19	86	94	73	54	82	74	78	70	33	86
PFBS	107	100	580	634	389	112	108	109	98	95	98	95	94	134	96
PFDEA	114	109	115	116	106	91	91	93	96	96	95	92	94	100	98
PFHPA	90	88	89	104	93	82	85	85	98	98	99	95	94	102	99
PFHXA	92	84	76	94	87	83	88	85	97	96	99	94	95	104	99
PFHXS	109	99	100	111	102	101	101	102	99	98	98	95	96	99	98
PFNOA	99	98	112	117	107	83	86	87	95	95	95	94	97	101	96
PFOA	103	96	104	114	105	101	101	101	101	99	99	102	96	100	98
PFOS	105	101	107	113	105	101	101	100	99	98	99	99	94	99	100
PFOSA	107	109	123	148	156	96	99	99	92	95	92	96	93	98	99
PHEN	162	115	124	119	118	95	96	97	95	72	101	100	98	111	83
PIRIMIC	108	115	113	113	111	95	96	94	89	90	87	85	97	107	93
PRIMID	127	112	118	125	118	93	110	101	100	95	88	116	157	153	108
PROMETR	116	123	119	128	125	96	101	100	99	98	104	105	118	128	107
PROPAZ	113	110	101	110	104	100	100	100	95	95	96	96	96	106	93
PYR	134	138	146	112	110	72	67	68	68	96	75	43	68	85	71
QCB	73	80	98	96	92	99	101	112	89	92	94	98	103	91	97
SIMAZ	81	89	87	99	93	93	98	97	95	99	98	96	96	105	95
TBEP	248	175	112	0	115	108	117	113	125	123	139	143	149	105	114
TBP	244	99	317	295	276	105	118	117	107	117	106	237	289	246	99
TERBAZ	104	106	110	113	111	100	100	98	96	96	98	97	96	104	94
TERBUTR	112	125	111	121	118	95	99	99	107	106	111	107	119	123	103
TPP	8797	296	301	64	125	91	129	116	85	94	91	133	118	616	100
TRIFLU	98	111	74	109	86	83	95	94	81	87	116	79	83	75	98

%	E.-100 mL 2	E.-100 mL 3	E.-100 mL 4	E.-100 mL 5	S.f. 1	S.f. 2	S.f. 3	S.f. 4	S.f. 5	S.f. 6	Silica-gel 1	Silica-gel 2	Silica-gel 3	Silica-gel 4	Silica-gel 5
24-D	94	93	90	98	n.q.	n.q.	n.q.	89	93	88	n.q.	n.q.	n.q.	n.q.	n.q.
ACE	107	116	99	100	n.q.	n.q.	n.q.	n.q.	n.q.	n.q.	90	90	91	108	110
ACY	90	104	95	92	n.q.	n.q.	n.q.	n.q.	n.q.	n.q.	95	96	97	120	99
ALD	83	84	88	89	n.q.	n.q.	n.q.	n.q.	n.q.	n.q.	94	91	104	102	107
AMETRYN	102	101	107	113	95	96	108	95	98	99	n.q.	n.q.	n.q.	n.q.	n.q.
ANT	112	101	97	102	n.q.	n.q.	n.q.	n.q.	n.q.	n.q.	92	89	91	116	85
ATRAZ	92	92	95	100	96	96	101	94	93	93	n.q.	n.q.	n.q.	n.q.	n.q.

A2 Table 9 continued:

%	E.- 100 mL 2	E.- 100 mL 3	E.- 100 mL 4	E.- 100 mL 5	S.f. 1	S.f. 2	S.f. 3	S.f. 4	S.f. 5	S.f. 6	Silica- gel 1	Silica- gel 2	Silica- gel 3	Silica- gel 4	Silica- gel 5
AZINPH-E	100	96	97	104	93	96	105	98	102	97	n.q.	n.q.	n.q.	n.q.	n.q.
AZINPH-M	97	95	97	101	93	99	103	95	99	97	n.q.	n.q.	n.q.	n.q.	n.q.
BAA	88	86	82	93	n.q.	n.q.	n.q.	n.q.	n.q.	n.q.	90	90	94	111	94
BAP	121	99	96	100	n.q.	n.q.	n.q.	n.q.	n.q.	n.q.	88	87	91	107	92
BBF	112	96	102	101	n.q.	n.q.	n.q.	n.q.	n.q.	n.q.	89	87	91	99	82
BENTAZ	95	95	95	98	87	71	79	79	75	82	n.q.	n.q.	n.q.	n.q.	n.q.
BGHIP	100	103	98	101	n.q.	n.q.	n.q.	n.q.	n.q.	n.q.	92	94	95	95	86
CARBAMAZ	94	93	94	106	103	93	103	98	100	99	n.q.	n.q.	n.q.	n.q.	n.q.
CARBEND	105	107	109	103	92	94	92	81	37	85	n.q.	n.q.	n.q.	n.q.	n.q.
CB138	100	103	95	99	n.q.	n.q.	n.q.	n.q.	n.q.	n.q.	88	86	91	109	111
CB153	99	103	95	101	n.q.	n.q.	n.q.	n.q.	n.q.	n.q.	95	92	94	109	109
CB28	88	99	89	95	n.q.	n.q.	n.q.	n.q.	n.q.	n.q.	85	81	82	111	109
CB52	101	104	92	103	n.q.	n.q.	n.q.	n.q.	n.q.	n.q.	90	89	93	107	108
CHLORFENV	98	98	99	107	101	100	107	99	101	103	n.q.	n.q.	n.q.	n.q.	n.q.
CHLORTUR	95	92	94	103	101	97	104	97	97	98	n.q.	n.q.	n.q.	n.q.	n.q.
CHRTR	96	92	82	94	n.q.	n.q.	n.q.	n.q.	n.q.	n.q.	90	88	94	117	93
CLOFIBRS	95	96	96	100	n.q.	n.q.	n.q.	97	96	96	n.q.	n.q.	n.q.	n.q.	n.q.
DBAHA	114	115	99	105	n.q.	n.q.	n.q.	n.q.	n.q.	n.q.	91	88	92	106	86
DDDPP	106	120	96	105	n.q.	n.q.	n.q.	n.q.	n.q.	n.q.	82	76	77	124	117
DDEPP	92	92	85	93	n.q.	n.q.	n.q.	n.q.	n.q.	n.q.	88	95	99	114	112
DDTOP	84	82	87	99	n.q.	n.q.	n.q.	n.q.	n.q.	n.q.	137	151	170	96	98
DDTPP	93	96	98	105	n.q.	n.q.	n.q.	n.q.	n.q.	n.q.	94	87	97	94	99
DEATRAZ	96	96	95	102	98	96	100	98	97	97	n.q.	n.q.	n.q.	n.q.	n.q.
DIAZINON	84	85	82	83	92	94	109	72	25	92	n.q.	n.q.	n.q.	n.q.	n.q.
DICHLPR	95	96	97	100	n.q.	n.q.	n.q.	99	94	96	n.q.	n.q.	n.q.	n.q.	n.q.
DICLOF	94	93	93	107	n.q.	n.q.	n.q.	86	94	99	n.q.	n.q.	n.q.	n.q.	n.q.
DIELD	96	96	90	81	n.q.	n.q.	n.q.	n.q.	n.q.	n.q.	96	98	89	127	109
DIMETH	94	94	96	109	102	99	101	93	90	98	n.q.	n.q.	n.q.	n.q.	n.q.
DIURON	93	94	96	108	94	98	102	96	97	95	n.q.	n.q.	n.q.	n.q.	n.q.
END	189	192	106	155	n.q.	n.q.	n.q.	n.q.	n.q.	n.q.	52	38	39	116	87
FENUR	101	98	103	114	101	99	104	96	96	99	n.q.	n.q.	n.q.	n.q.	n.q.
FL	154	175	106	104	n.q.	n.q.	n.q.	n.q.	n.q.	n.q.	92	88	92	116	120
FLU	65	62	59	70	n.q.	n.q.	n.q.	n.q.	n.q.	n.q.	95	93	100	102	100
HBCDA	17722	88	89	94	94	99	100	106	105	103	n.q.	n.q.	n.q.	n.q.	n.q.
HBCDBG	16916	86	84	86	96	94	103	101	100	100	n.q.	n.q.	n.q.	n.q.	n.q.
HCB	97	99	98	96	n.q.	n.q.	n.q.	n.q.	n.q.	n.q.	91	95	92	98	100
HCHA	74	88	95	69	n.q.	n.q.	n.q.	n.q.	n.q.	n.q.	90	94	94	96	99
HCHB	98	103	100	119	n.q.	n.q.	n.q.	n.q.	n.q.	n.q.	91	82	93	100	100
HCHD	106	108	105	1	n.q.	n.q.	n.q.	n.q.	n.q.	n.q.	82	79	81	100	101
HCHG	77	89	98	75	n.q.	n.q.	n.q.	n.q.	n.q.	n.q.	94	93	96	92	94
HEXAZIN	97	97	102	114	104	99	104	99	103	100	n.q.	n.q.	n.q.	n.q.	n.q.
I123P	114	108	99	103	n.q.	n.q.	n.q.	n.q.	n.q.	n.q.	89	86	91	94	79
IRGAROL	109	107	113	120	98	97	104	95	100	99	n.q.	n.q.	n.q.	n.q.	n.q.
ISOD	91	89	92	93	n.q.	n.q.	n.q.	n.q.	n.q.	n.q.	94	95	111	93	95
ISOPRUR	93	89	92	102	104	101	109	92	96	95	n.q.	n.q.	n.q.	n.q.	n.q.
LINUR	91	88	87	95	100	104	119	96	94	97	n.q.	n.q.	n.q.	n.q.	n.q.
MALATH	94	96	97	110	92	96	98	94	93	97	n.q.	n.q.	n.q.	n.q.	n.q.
MCPA	93	92	94	101	n.q.	n.q.	n.q.	100	97	97	n.q.	n.q.	n.q.	n.q.	n.q.
MECOPR	96	94	95	99	n.q.	n.q.	n.q.	99	97	98	n.q.	n.q.	n.q.	n.q.	n.q.

A2 Table 9 continued:

%	E.- 100 mL 2	E.- 100 mL 3	E.- 100 mL 4	E.- 100 mL 5	S.f. 1	S.f. 2	S.f. 3	S.f. 4	S.f. 5	S.f. 6	Silica- gel 1	Silica- gel 2	Silica- gel 3	Silica- gel 4	Silica- gel 5
METAZCHL	107	105	109	120	106	100	107	97	101	101	n.q.	n.q.	n.q.	n.q.	n.q.
METHABZT	105	105	112	118	95	94	104	94	94	98	n.q.	n.q.	n.q.	n.q.	n.q.
METOLA	100	98	96	102	98	96	111	96	96	97	n.q.	n.q.	n.q.	n.q.	n.q.
NAPROX	93	96	94	108	n.q.	n.q.	n.q.	86	87	93	n.q.	n.q.	n.q.	n.q.	n.q.
OXAZEP	92	91	92	96	103	98	114	96	87	97	n.q.	n.q.	n.q.	n.q.	n.q.
PENDIMETH	91	91	81	70	97	97	109	98	91	94	n.q.	n.q.	n.q.	n.q.	n.q.
PFBS	98	97	95	127	91	84	88	93	93	95	n.q.	n.q.	n.q.	n.q.	n.q.
PFDEA	98	96	94	98	97	98	102	102	99	100	n.q.	n.q.	n.q.	n.q.	n.q.
PFHPA	100	99	98	99	94	93	101	96	97	96	n.q.	n.q.	n.q.	n.q.	n.q.
PFHXA	100	98	98	101	84	93	99	84	87	88	n.q.	n.q.	n.q.	n.q.	n.q.
PFHXS	99	100	95	100	96	95	100	99	98	97	n.q.	n.q.	n.q.	n.q.	n.q.
PFNOA	98	97	92	98	96	99	100	97	96	91	n.q.	n.q.	n.q.	n.q.	n.q.
PFOA	98	98	95	101	94	97	101	99	100	99	n.q.	n.q.	n.q.	n.q.	n.q.
PFOS	99	99	95	100	95	94	102	103	101	100	n.q.	n.q.	n.q.	n.q.	n.q.
PFOSA	99	100	93	99	98	99	108	106	102	100	n.q.	n.q.	n.q.	n.q.	n.q.
PHEN	99	93	99	101	n.q.	n.q.	n.q.	n.q.	n.q.	n.q.	93	91	93	90	107
PIRIMIC	96	94	93	102	100	97	109	96	94	95	n.q.	n.q.	n.q.	n.q.	n.q.
PRIMID	107	108	106	119	101	103	119	96	94	96	n.q.	n.q.	n.q.	n.q.	n.q.
PROMETR	105	107	105	114	99	97	112	98	100	102	n.q.	n.q.	n.q.	n.q.	n.q.
PROPAZ	94	94	96	104	94	95	107	97	95	96	n.q.	n.q.	n.q.	n.q.	n.q.
PYR	77	73	62	71	n.q.	n.q.	n.q.	n.q.	n.q.	n.q.	93	88	96	116	87
QCB	92	97	96	101	n.q.	n.q.	n.q.	n.q.	n.q.	n.q.	91	100	103	103	103
SIMAZ	95	94	97	104	101	93	102	99	96	96	n.q.	n.q.	n.q.	n.q.	n.q.
TBEP	112	113	110	106	85	102	99	109	104	107	n.q.	n.q.	n.q.	n.q.	n.q.
TBP	97	95	122	119	96	97	118	93	86	86	n.q.	n.q.	n.q.	n.q.	n.q.
TERBAZ	94	93	97	103	95	96	106	96	96	97	n.q.	n.q.	n.q.	n.q.	n.q.
TERBUTR	103	101	105	114	95	96	108	96	98	100	n.q.	n.q.	n.q.	n.q.	n.q.
TPP	98	97	99	73	103	102	388	140	98	101	n.q.	n.q.	n.q.	n.q.	n.q.
TRIFLU	99	100	99	99	n.q.	n.q.	n.q.	n.q.	n.q.	n.q.	91	87	96	99	99

%	Silica- gel 6	Silica- gel 7	Silica- gel 8	Silica- gel 9
24-D	n.q.	n.q.	n.q.	n.q.
ACE	106	99	99	102
ACY	102	98	102	97
ALD	106	98	94	104
AMETRYN	n.q.	n.q.	n.q.	n.q.
ANT	110	98	100	104
ATRAZ	n.q.	n.q.	n.q.	n.q.
AZINPH-E	n.q.	n.q.	n.q.	n.q.
AZINPH-M	n.q.	n.q.	n.q.	n.q.
BAA	99	111	104	104
BAP	98	97	98	99
BBF	86	100	101	101
BENAZ	n.q.	n.q.	n.q.	n.q.
BGHIP	114	99	100	102
CARBAMAZ	n.q.	n.q.	n.q.	n.q.
CARBEND	n.q.	n.q.	n.q.	n.q.
CB138	115	95	99	105

%	Silica- gel 6	Silica- gel 7	Silica- gel 8	Silica- gel 9
CB153	104	102	98	104
CB28	110	100	94	101
CB52	104	98	99	106
CHLORFENV	n.q.	n.q.	n.q.	n.q.
CHLORTUR	n.q.	n.q.	n.q.	n.q.
CHRTR	118	111	105	106
CLOFIBRS	n.q.	n.q.	n.q.	n.q.
DBAHA	98	100	100	104
DDDPP	117	99	97	116
DDEPP	115	101	100	102
DDTOP	101	99	97	100
DDTPP	101	98	99	103
DEATRAZ	n.q.	n.q.	n.q.	n.q.
DIAZINON	n.q.	n.q.	n.q.	n.q.
DICHLPR	n.q.	n.q.	n.q.	n.q.
DICLOF	n.q.	n.q.	n.q.	n.q.
DIELD	113	104	99	89

A2 Table 9 continued:

%	Silica-gel 6	Silica-gel 7	Silica-gel 8	Silica-gel 9	%	Silica-gel 6	Silica-gel 7	Silica-gel 8	Silica-gel 9
DIMETH	n.q.	n.q.	n.q.	n.q.	OXAZEP	n.q.	n.q.	n.q.	n.q.
DIURON	n.q.	n.q.	n.q.	n.q.	PENDIMETH	n.q.	n.q.	n.q.	n.q.
END	93	92	69	113	PFBS	n.q.	n.q.	n.q.	n.q.
FENUR	n.q.	n.q.	n.q.	n.q.	PFDEA	n.q.	n.q.	n.q.	n.q.
FL	119	98	97	105	PFHPA	n.q.	n.q.	n.q.	n.q.
FLU	90	105	100	96	PFHXA	n.q.	n.q.	n.q.	n.q.
HBCDA	n.q.	n.q.	n.q.	n.q.	PFHXS	n.q.	n.q.	n.q.	n.q.
HBCDBG	n.q.	n.q.	n.q.	n.q.	PFNOA	n.q.	n.q.	n.q.	n.q.
HCB	98	101	98	103	PFOA	n.q.	n.q.	n.q.	n.q.
HCHA	102	101	96	101	PFOS	n.q.	n.q.	n.q.	n.q.
HCHB	99	99	100	103	PFOSA	n.q.	n.q.	n.q.	n.q.
HCHD	100	98	101	104	PHEN	102	99	101	103
HCHG	96	99	95	107	PIRIMIC	n.q.	n.q.	n.q.	n.q.
HEXAZIN	n.q.	n.q.	n.q.	n.q.	PRIMID	n.q.	n.q.	n.q.	n.q.
I123P	84	101	99	103	PROMETR	n.q.	n.q.	n.q.	n.q.
IRGAROL	n.q.	n.q.	n.q.	n.q.	PROPАЗ	n.q.	n.q.	n.q.	n.q.
ISOD	98	98	95	96	PYR	117	105	100	95
ISOPRUR	n.q.	n.q.	n.q.	n.q.	QCB	101	102	102	106
LINUR	n.q.	n.q.	n.q.	n.q.	SIMAZ	n.q.	n.q.	n.q.	n.q.
MALATH	n.q.	n.q.	n.q.	n.q.	TBEP	n.q.	n.q.	n.q.	n.q.
MCPA	n.q.	n.q.	n.q.	n.q.	TBP	n.q.	n.q.	n.q.	n.q.
MECOPR	n.q.	n.q.	n.q.	n.q.	TERBAZ	n.q.	n.q.	n.q.	n.q.
METAZCHL	n.q.	n.q.	n.q.	n.q.	TERBUTR	n.q.	n.q.	n.q.	n.q.
METHABZT	n.q.	n.q.	n.q.	n.q.	TPP	n.q.	n.q.	n.q.	n.q.
METOLA	n.q.	n.q.	n.q.	n.q.	TRIFLU	99	101	99	103
NAPROX	n.q.	n.q.	n.q.	n.q.					

A2 Table 10: Soxhlet extraction efficiency – Peak areas of labeled analytes (IS and PRCs) in the extract of the first sample preparation and in the extract of the second sample preparation

Peak area	1		2		3	
	Sample Preparation 1	Sample Preparation 2	Sample Preparation 1	Sample Preparation 2	Sample Preparation 1	Sample Preparation 2
ACE-D ₁₀	4.27E+06	2.19E+04	9.25E+05	5.49E+02	3.93E+05	0.00E+00
ANT-D ₁₀	9.40E+06	7.49E+03	1.86E+09	0.00E+00	1.08E+09	0.00E+00
ATRAZ-D ₅	4.94E+05	1.07E+04	4.89E+05	0.00E+00	5.03E+05	0.00E+00
AZINPH-M-D ₆	9.55E+04	1.58E+03	1.03E+05	0.00E+00	1.06E+05	1.06E+01
BAA-D ₁₂	1.51E+06	2.09E+03	1.81E+05	0.00E+00	1.42E+05	0.00E+00
BEP-D ₁₂	1.32E+07	1.80E+05	1.91E+09	0.00E+00	1.76E+09	0.00E+00
BGHIP-D ₁₂	1.01E+07	1.85E+05	1.31E+09	0.00E+00	1.18E+09	2.62E+03
CB104	2.66E+05	3.71E+03	9.34E+09	7.57E+02	6.87E+09	3.19E+03
CB145	8.66E+05	1.20E+04	1.94E+10	1.18E+03	1.65E+10	9.40E+03
CB153- ¹³ C ₁₂	7.77E+05	1.82E+03	1.70E+10	0.00E+00	1.36E+10	2.85E+03
CB185	2.06E+05	4.40E+03	5.57E+09	0.00E+00	4.07E+09	1.87E+03
CB204	4.46E+05	5.74E+03	8.88E+09	8.67E+02	7.55E+09	4.86E+03
CB30	4.91E+05	6.98E+03	1.18E+10	2.17E+04	7.18E+09	6.32E+03
CB52- ¹³ C ₁₂	4.73E+05	1.50E+04	1.37E+10	8.70E+03	9.55E+09	5.34E+03
DDTPP-D ₈	2.80E+05	3.70E+03	7.51E+09	2.40E+03	3.70E+09	8.66E+02
DEATRAZ-D ₆	1.78E+05	3.34E+03	1.84E+05	0.00E+00	1.87E+05	0.00E+00

A2 Table 10 continued:

Peak area	1		2		3	
	Sample Preparation 1	Sample Preparation 2	Sample Preparation 1	Sample Preparation 2	Sample Preparation 1	Sample Preparation 2
DIURON-D ₆	2.25E+05	4.45E+03	1.91E+05	0.00E+00	1.92E+05	0.00E+00
FLU-D ₁₀	1.81E+06	0.00E+00	2.29E+05	0.00E+00	1.67E+05	0.00E+00
HBCDA-D ₁₈	1.79E+05	3.77E+03	7.53E+04	0.00E+00	9.33E+04	0.00E+00
HC ¹³ B	2.59E+05	0.00E+00	9.49E+09	1.70E+04	4.89E+09	7.94E+03
HCH	1.65E+05	2.61E+03	6.61E+09	0.00E+00	4.56E+09	5.31E+03
HCHG- ¹³ C ₆ D ₆	1.21E+05	6.09E+02	5.21E+09	8.71E+02	2.53E+09	0.00E+00
MALATH-D ₁₀	9.79E+04	1.62E+03	1.64E+05	0.00E+00	1.09E+05	0.00E+00
MCPA-D ₃	2.47E+04	2.17E+04	1.81E+05	5.56E+03	2.86E+04	8.26E+03
MECOPROP-D ₃	4.48E+04	4.38E+04	3.31E+05	1.98E+03	4.99E+04	1.77E+04
PER-D ₁₂	9.81E+06	1.54E+05	1.29E+09	0.00E+00	1.23E+09	0.00E+00
PFHXS- ¹⁸ O ₂	1.76E+06	7.73E+05	1.45E+06	2.12E+04	1.18E+06	1.16E+05
PFOA- ¹³ C ₂	2.38E+06	1.31E+06	1.96E+06	3.82E+05	1.73E+06	4.31E+05
PFOS- ¹³ C ₄	2.22E+06	8.94E+05	1.51E+06	1.61E+04	1.22E+06	1.02E+05
PHEN-D ₁₀	1.09E+06	2.11E+03	2.48E+05	0.00E+00	1.04E+05	0.00E+00
PROMETR-D ₆	6.66E+05	1.60E+05	4.88E+04	0.00E+00	6.60E+05	0.00E+00
SIMAZ-D ₁₀	1.33E+04	8.14E+03	1.71E+04	0.00E+00	1.68E+05	7.63E+03
TERBAZ-D ₅	7.54E+05	0.00E+00	7.93E+05	0.00E+00	7.76E+05	0.00E+00
TRIFLU-D ₁₄	1.73E+05	0.00E+00	7.24E+09	7.89E+02	5.80E+05	0.00E+00

Peak area	4		5		6	
	Sample Preparation 1	Sample Preparation 2	Sample Preparation 1	Sample Preparation 2	Sample Preparation 1	Sample Preparation 2
ACE-D ₁₀	4.51E+05	9.73E+02	3.88E+05	0.00E+00	5.43E+05	1.28E+03
ANT-D ₁₀	1.15E+09	0.00E+00	1.01E+09	0.00E+00	1.36E+09	0.00E+00
ATRAZ-D ₅	4.53E+05	0.00E+00	5.79E+05	0.00E+00	5.60E+05	0.00E+00
AZINPH-M-D ₆	7.56E+04	0.00E+00	1.02E+05	0.00E+00	9.64E+04	8.59E+00
BAA-D ₁₂	1.29E+05	0.00E+00	1.19E+05	0.00E+00	1.47E+05	0.00E+00
BEP-D ₁₂	1.77E+09	0.00E+00	1.49E+09	0.00E+00	1.77E+09	0.00E+00
BGHP-D ₁₂	1.22E+09	9.51E+02	9.38E+05	6.40E+02	1.11E+09	1.06E+03
CB104	7.90E+09	6.27E+02	7.09E+09	9.34E+02	8.31E+09	1.93E+03
CB145	1.70E+10	3.04E+03	1.59E+10	0.00E+00	1.82E+10	1.99E+03
CB153- ¹³ C ₁₂	1.43E+10	3.84E+03	1.26E+10	1.16E+03	1.41E+10	0.00E+00
CB185	4.53E+09	0.00E+00	3.76E+09	0.00E+00	4.33E+09	0.00E+00
CB204	7.99E+09	0.00E+00	7.01E+09	0.00E+00	7.74E+09	0.00E+00
CB30	1.00E+10	6.14E+03	8.72E+09	1.57E+03	1.06E+10	7.98E+02
CB52- ¹³ C ₁₂	1.14E+10	3.96E+03	1.01E+10	0.00E+00	1.19E+10	3.45E+03
DDTPP-D ₈	4.34E+09	2.18E+03	3.36E+09	0.00E+00	3.82E+09	2.08E+03
DEATRAZ-D ₆	1.68E+05	0.00E+00	2.18E+05	0.00E+00	2.16E+05	0.00E+00
DIURON-D ₆	1.79E+05	0.00E+00	2.31E+05	0.00E+00	1.85E+05	0.00E+00
FLU-D ₁₀	1.72E+05	0.00E+00	1.53E+05	0.00E+00	1.73E+05	0.00E+00
HBCDA-D ₁₈	7.89E+04	0.00E+00	9.49E+04	0.00E+00	6.22E+04	0.00E+00
HC ¹³ B	6.74E+09	5.51E+03	5.86E+09	2.12E+03	7.66E+09	1.27E+04
HCH	5.85E+09	1.77E+03	4.97E+09	1.53E+03	5.60E+09	3.96E+03
HCHG- ¹³ C ₆ D ₆	3.75E+09	0.00E+00	3.13E+09	1.00E+03	3.56E+09	0.00E+00
MALATH-D ₁₀	9.19E+04	0.00E+00	9.05E+04	0.00E+00	8.32E+04	0.00E+00
MCPA-D ₃	1.04E+03	1.28E+03	2.01E+03	1.06E+03	6.59E+03	7.05E+03
MECOPROP-D ₃	3.33E+03	6.77E+03	3.62E+03	4.98E+03	2.51E+04	2.84E+04
PER-D ₁₂	1.31E+09	0.00E+00	1.04E+09	0.00E+00	1.28E+09	0.00E+00
PFHXS- ¹⁸ O ₂	9.99E+05	9.84E+04	1.27E+06	1.56E+05	1.22E+06	9.24E+03

A2 Table 10 continued:

Peak area	4		5		6	
	Sample Preparation 1	Sample Preparation 2	Sample Preparation 1	Sample Preparation 2	Sample Preparation 1	Sample Preparation 2
PFOA- ¹³ C ₂	1.27E+06	3.51E+05	1.64E+06	5.75E+05	1.58E+06	4.07E+05
PFOS- ¹³ C ₄	1.02E+06	8.40E+04	1.35E+06	1.41E+05	1.35E+06	5.46E+03
PHEN-D ₁₀	1.07E+05	0.00E+00	8.58E+04	8.52E+02	1.35E+05	0.00E+00
PROMETR-D ₆	6.34E+05	0.00E+00	7.72E+05	0.00E+00	6.98E+05	0.00E+00
SIMAZ-D ₁₀	1.49E+05	0.00E+00	1.92E+05	0.00E+00	1.85E+05	7.55E+03
TERBAZ-D ₅	7.14E+05	0.00E+00	9.00E+05	0.00E+00	8.69E+05	0.00E+00
TRIFLU-D ₁₄	5.05E+05	0.00E+00	3.03E+04	0.00E+00	2.19E+09	1.31E+03

Peak area	7		Peak area	7	
	Sample Preparation 1	Sample Preparation 2		Sample Preparation 1	Sample Preparation 2
ACE-D ₁₀	5.55E+05	0.00E+00	FLU-D ₁₀	1.48E+05	0.00E+00
ANT-D ₁₀	1.23E+09	0.00E+00	HBCDA-D ₁₈	5.59E+04	0.00E+00
ATRAZ-D ₅	4.86E+05	0.00E+00	HCB- ¹³ C ₆	6.07E+09	4.65E+03
AZINPH-M-D ₆	7.97E+04	8.59E+00	HCHE	4.33E+09	4.87E+03
BAA-D ₁₂	1.15E+05	0.00E+00	HCHG- ¹³ C ₆ D ₆	2.74E+09	7.99E+02
BEP-D ₁₂	1.66E+09	9.34E+02	MALATH-D ₁₀	7.14E+04	0.00E+00
BGHIP-D ₁₂	1.03E+09	6.64E+02	MCPA-D ₃	1.88E+03	1.11E+03
CB104	6.80E+09	9.33E+02	MECOPROP-D ₃	5.46E+03	1.04E+04
CB145	1.63E+10	0.00E+00	PER-D ₁₂	1.21E+09	5.08E+02
CB153- ¹³ C ₁₂	1.26E+10	0.00E+00	PFHXS- ¹⁸ O ₂	1.11E+06	1.56E+04
CB185	3.75E+09	0.00E+00	PFOA- ¹³ C ₂	1.20E+06	6.00E+05
CB204	6.62E+09	0.00E+00	PFOS- ¹³ C ₄	1.29E+06	1.09E+04
CB30	8.08E+09	7.35E+03	PHEN-D ₁₀	1.22E+05	0.00E+00
CB52- ¹³ C ₁₂	9.80E+09	5.66E+03	PROMETR-D ₆	5.99E+05	0.00E+00
DDTPP-D ₈	2.89E+09	9.27E+02	SIMAZ-D ₁₀	1.58E+05	7.14E+03
DEATRAZ-D ₆	1.85E+05	0.00E+00	TERBAZ-D ₅	7.84E+05	0.00E+00
DIURON-D ₆	1.55E+05	0.00E+00	TRIFLU-D ₁₄	1.95E+04	5.89E+02

A2 Table 11: Efficiency of the GFF extraction – Peak areas of labeled analytes (IS and PRCs) in the extract of the first sample preparation and in the extract of the second sample preparation

Peak area	1		2		3	
	Sample Preparation 1	Sample Preparation 2	Sample Preparation 1	Sample Preparation 2	Sample Preparation 1	Sample Preparation 2
ACE-D ₁₀	1.23E+04	0.00E+00	3.13E+03	6.45E+02	0.00E+00	6.84E+02
ANT-D ₁₀	5.58E+05	7.63E+02	5.20E+05	5.02E+02	1.91E+05	5.84E+02
ATRAZ-D ₅	4.10E+05	7.38E+03	4.23E+05	6.00E+03	4.04E+05	6.63E+03
AZINPH-M-D ₆	7.12E+04	1.74E+03	7.96E+04	1.21E+03	9.61E+04	1.79E+03
BAA-D ₁₂	2.41E+05	0.00E+00	2.17E+05	0.00E+00	2.03E+05	6.10E+02
BEP-D ₁₂	3.02E+09	2.47E+04	3.15E+09	1.47E+04	2.66E+09	1.39E+04
BGHIP-D ₁₂	2.26E+09	9.30E+03	2.32E+09	5.13E+03	1.96E+09	1.03E+04
CB104	3.84E+09	3.25E+04	4.15E+09	3.30E+04	4.02E+09	4.49E+04
CB145	1.08E+10	9.97E+04	1.26E+10	1.00E+05	1.21E+10	1.45E+05
CB153- ¹³ C ₁₂	8.35E+09	1.57E+05	1.02E+10	2.38E+05	9.94E+09	1.69E+05
CB185	2.70E+09	3.84E+04	3.23E+09	5.41E+04	3.17E+09	4.77E+04
CB204	5.41E+09	5.40E+04	6.40E+09	5.61E+04	6.33E+09	3.93E+04

A2 Table 11 continued:

Peak area	1		2		3	
	Sample Preparation 1	Sample Preparation 2	Sample Preparation 1	Sample Preparation 2	Sample Preparation 1	Sample Preparation 2
CB30	2.93E+09	1.28E+04	2.37E+09	1.84E+04	2.96E+09	4.21E+04
CB52- ¹³ C ₁₂	3.22E+09	3.59E+04	3.93E+09	5.30E+04	3.52E+09	6.76E+04
DDTPP-D ₈	7.00E+05	1.74E+04	1.30E+09	8.15E+03	6.57E+05	6.69E+03
DEATRAZ-D ₆	1.59E+05	3.84E+03	1.70E+05	2.74E+03	1.69E+05	3.91E+03
DIURON-D ₆	2.91E+05	4.47E+03	3.02E+05	3.16E+03	2.85E+05	4.65E+03
FLU-D ₁₀	1.83E+05	0.00E+00	1.67E+05	0.00E+00	1.70E+05	1.22E+03
HBCDA-D ₁₈	9.96E+04	5.38E+03	9.91E+04	3.71E+03	1.02E+05	4.57E+03
HCB- ¹³ C ₆	3.81E+05	0.00E+00	2.33E+05	1.06E+04	1.10E+05	5.68E+02
HCHE	4.56E+05	2.30E+04	9.14E+05	1.58E+04	4.09E+05	2.03E+04
HCHG- ¹³ C ₆ D ₆	8.68E+05	1.39E+04	1.15E+09	5.68E+03	8.65E+05	1.85E+04
MALATH-D ₁₀	7.38E+03	3.44E+02	5.11E+03	7.10E+02	1.58E+04	9.02E+02
MCPA-D ₃	2.06E+05	2.44E+04	2.05E+05	1.73E+04	1.86E+05	2.36E+04
MECOPROP-D ₃	3.59E+05	3.83E+04	3.53E+05	2.67E+04	3.39E+05	3.68E+04
PER-D ₁₂	2.23E+09	0.00E+00	2.20E+09	0.00E+00	1.73E+09	0.00E+00
PFHXS- ¹⁸ O ₂	1.41E+06	1.92E+04	1.39E+06	1.28E+04	1.33E+06	2.06E+04
PFOA- ¹³ C ₂	2.36E+06	3.86E+04	2.34E+06	2.93E+04	2.19E+06	4.56E+04
PFOS- ¹³ C ₄	1.47E+06	1.95E+04	1.46E+06	1.27E+04	1.39E+06	2.23E+04
PHEN-D ₁₀	6.61E+04	5.97E+02	5.01E+04	1.03E+03	5.90E+04	0.00E+00
PROMETR-D ₆	6.74E+05	1.42E+04	6.98E+05	1.11E+04	6.62E+05	1.18E+04
SIMAZ-D ₁₀	1.42E+05	9.66E+03	1.43E+05	6.66E+03	1.42E+05	8.58E+03
TERBAZ-D ₅	6.37E+05	1.36E+04	6.67E+05	9.22E+03	6.45E+05	1.57E+04
TRIFLU-D ₁₄	2.26E+05	1.88E+04	2.87E+09	2.17E+04	2.34E+09	3.13E+04

Peak area	4		5		6	
	Sample Preparation 1	Sample Preparation 2	Sample Preparation 1	Sample Preparation 2	Sample Preparation 1	Sample Preparation 2
ACE-D ₁₀	1.00E+09	6.20E+03	3.11E+06	0.00E+00	2.51E+06	0.00E+00
ANT-D ₁₀	2.21E+09	1.01E+03	8.07E+06	0.00E+00	7.02E+06	0.00E+00
ATRAZ-D ₅	5.48E+05	8.96E+03	4.28E+05	8.90E+03	8.05E+05	7.73E+03
AZINPH-M-D ₆	1.30E+05	1.88E+03	5.39E+04	1.44E+03	1.24E+05	1.64E+03
BAA-D ₁₂	3.09E+05	8.10E+02	1.72E+06	0.00E+00	1.58E+06	0.00E+00
BEP-D ₁₂	3.99E+09	1.48E+04	5.72E+06	0.00E+00	5.07E+06	0.00E+00
BGHIP-D ₁₂	2.82E+09	1.72E+04	4.51E+06	0.00E+00	4.10E+06	0.00E+00
CB104	1.26E+10	1.33E+05	5.06E+06	3.72E+03	3.54E+06	5.11E+03
CB145	3.16E+10	3.45E+05	1.26E+07	3.02E+04	1.04E+07	3.80E+04
CB153- ¹³ C ₁₂	2.92E+10	2.95E+05	1.19E+07	4.17E+04	1.02E+07	4.66E+04
CB185	9.79E+09	6.98E+04	4.66E+06	9.81E+03	4.02E+06	8.13E+03
CB204	1.60E+10	1.37E+05	7.19E+06	1.61E+04	6.37E+06	2.25E+04
CB30	1.37E+10	1.50E+05	7.98E+06	9.19E+03	4.46E+06	1.20E+04
CB52- ¹³ C ₁₂	1.83E+10	2.07E+05	7.61E+06	1.43E+04	5.39E+06	1.20E+04
DDTPP-D ₈	8.33E+09	2.59E+04	6.13E+06	1.02E+04	4.97E+06	1.28E+04
DEATRAZ-D ₆	1.99E+05	2.84E+03	1.31E+05	3.90E+03	3.03E+05	4.72E+03
DIURON-D ₆	2.50E+05	3.86E+03	1.62E+05	4.60E+03	3.52E+05	6.08E+03
FLU-D ₁₀	3.76E+05	0.00E+00	2.15E+06	0.00E+00	1.87E+06	0.00E+00
HBCDA-D ₁₈	9.44E+04	1.79E+03	4.27E+04	1.88E+03	1.10E+05	2.32E+03
HCB- ¹³ C ₆	1.11E+10	1.23E+05	5.78E+06	3.82E+03	3.31E+06	8.92E+03
HCHE	9.76E+09	8.75E+04	3.41E+06	4.02E+03	2.28E+06	2.95E+03
HCHG- ¹³ C ₆ D ₆	5.87E+09	6.50E+04	5.80E+06	4.08E+03	3.51E+06	4.27E+03
MALATH-D ₁₀	2.04E+05	3.04E+03	9.12E+04	1.83E+03	1.83E+05	1.09E+03

A2 Table 11 continued:

Peak area	4		5		6	
	Sample Preparation 1	Sample Preparation 2	Sample Preparation 1	Sample Preparation 2	Sample Preparation 1	Sample Preparation 2
MCPA-D ₃	1.75E+05	2.58E+03	1.56E+05	4.02E+03	2.79E+05	4.34E+03
MECOPROP-D ₃	3.05E+05	4.49E+03	2.60E+05	5.91E+03	4.21E+05	6.93E+03
PER-D ₁₂	2.51E+09	0.00E+00	4.57E+06	0.00E+00	4.06E+06	0.00E+00
PFHXS- ¹⁸ O ₂	1.25E+06	1.86E+04	1.27E+06	3.65E+04	2.36E+06	3.47E+04
PFOA- ¹³ C ₂	1.13E+06	3.08E+04	1.41E+06	2.81E+04	1.92E+06	5.21E+04
PFOS- ¹³ C ₄	1.31E+06	2.13E+04	1.32E+06	3.56E+04	2.39E+06	3.37E+04
PHEN-D ₁₀	2.51E+05	0.00E+00	2.76E+06	0.00E+00	2.26E+06	0.00E+00
PROMETR-D ₆	8.02E+05	1.29E+04	8.19E+05	2.10E+04	1.69E+06	2.01E+04
SIMAZ-D ₁₀	1.86E+05	8.71E+03	2.52E+05	1.73E+04	5.43E+05	1.83E+04
TERBAZ-D ₅	8.78E+05	1.30E+04	1.21E+06	3.53E+04	2.24E+06	3.70E+04
TRIFLU-D ₁₄	9.63E+09	1.13E+05	5.92E+06	4.90E+03	3.05E+06	4.79E+03

Peak area	7		8		9	
	Sample Preparation 1	Sample Preparation 2	Sample Preparation 1	Sample Preparation 2	Sample Preparation 1	Sample Preparation 2
ACE-D ₁₀	6.80E+06	0.00E+00	4.61E+06	0.00E+00	5.78E+06	0.00E+00
ANT-D ₁₀	8.48E+06	1.13E+03	6.14E+06	0.00E+00	7.14E+06	0.00E+00
ATRAZ-D ₅	5.85E+05	1.21E+04	7.70E+05	1.45E+04	7.30E+05	1.12E+04
AZINPH-M-D ₆	5.58E+04	1.01E+03	7.34E+04	9.88E+02	9.07E+04	1.36E+03
BAA-D ₁₂	1.38E+06	0.00E+00	1.12E+06	0.00E+00	1.13E+06	0.00E+00
BEP-D ₁₂	5.14E+06	0.00E+00	4.65E+06	0.00E+00	4.49E+06	0.00E+00
BGHIP-D ₁₂	3.19E+06	0.00E+00	2.94E+06	0.00E+00	2.86E+06	0.00E+00
CB104	7.25E+05	9.13E+02	6.12E+05	2.57E+03	7.19E+05	2.33E+03
CB145	2.53E+06	6.99E+03	2.22E+06	9.41E+03	2.52E+06	1.42E+04
CB153- ¹³ C ₁₂	2.66E+06	8.49E+03	2.30E+06	7.50E+03	2.81E+06	1.33E+04
CB185	1.00E+06	1.30E+03	8.85E+05	1.58E+03	1.15E+06	2.98E+03
CB204	1.77E+06	3.17E+03	1.57E+06	3.08E+03	1.88E+06	4.54E+03
CB30	1.00E+06	1.35E+03	8.54E+05	1.21E+03	1.03E+06	4.35E+03
CB52- ¹³ C ₁₂	1.12E+06	2.26E+03	1.04E+06	8.73E+02	1.10E+06	3.52E+03
DDTPP-D ₈	3.31E+05	0.00E+00	2.06E+05	0.00E+00	5.78E+05	8.69E+02
DEATRAZ-D ₆	2.79E+05	6.35E+03	3.56E+05	5.93E+03	3.49E+05	4.95E+03
DIURON-D ₆	4.59E+05	8.02E+03	4.46E+05	5.80E+03	4.38E+05	7.21E+03
FLU-D ₁₀	1.66E+06	0.00E+00	1.24E+06	0.00E+00	1.35E+06	0.00E+00
HBCDA-D ₁₈	1.11E+05	2.16E+03	1.24E+05	1.97E+03	1.27E+05	1.85E+03
HCB- ¹³ C ₆	7.78E+05	6.33E+02	6.83E+05	5.76E+02	8.31E+05	0.00E+00
HCHE	1.09E+05	0.00E+00	7.91E+04	0.00E+00	1.43E+05	6.17E+02
HCHG- ¹³ C ₆ D ₆	2.88E+05	5.44E+02	2.67E+05	1.43E+03	3.90E+05	2.15E+03
MALATH-D ₁₀	0.00E+00	0.00E+00	7.17E+03	0.00E+00	3.87E+03	0.00E+00
MCPA-D ₃	2.65E+05	2.19E+04	2.40E+05	2.15E+04	2.56E+05	2.40E+04
MECOPROP-D ₃	4.60E+05	2.77E+04	4.30E+05	2.75E+04	4.50E+05	2.85E+04
PER-D ₁₂	3.53E+06	0.00E+00	3.17E+06	0.00E+00	3.10E+06	0.00E+00
PFHXS- ¹⁸ O ₂	2.18E+06	3.36E+04	2.08E+06	2.86E+04	2.12E+06	3.31E+04
PFOA- ¹³ C ₂	3.02E+06	4.73E+04	2.90E+06	3.97E+04	2.94E+06	4.78E+04
PFOS- ¹³ C ₄	2.21E+06	3.39E+04	2.08E+06	2.83E+04	2.13E+06	3.21E+04
PHEN-D ₁₀	2.91E+06	0.00E+00	2.09E+06	0.00E+00	2.43E+06	0.00E+00
PROMETR-D ₆	1.49E+06	2.61E+04	1.64E+06	2.47E+04	1.58E+06	2.60E+04
SIMAZ-D ₁₀	4.08E+05	2.10E+04	5.18E+05	2.08E+04	5.01E+05	1.88E+04
TERBAZ-D ₅	8.29E+05	0.00E+00	1.04E+06	0.00E+00	9.72E+05	3.60E+02
TRIFLU-D ₁₄	2.81E+05	0.00E+00	2.92E+05	1.72E+03	5.26E+05	1.40E+03

Annex 3 (A3): Recoveries of performance reference compounds (PRCs)

Reproducibility of the sample preparation methods

A3 Table 1: Reproducibility of the sample preparation for GFFs; Recoveries (%) of Performance Reference Compounds spiked prior extraction to the environmental samples

%	SIMAZ-D ₁₀	PROMETR-D ₆	HCHG- ¹³ C ₆ D ₆	CB30	CB104	CB145	CB204	PHEN-D ₁₀	FLU-D ₁₀	BAA-D ₁₂
R1S1	87	52	122	98	100	98	96	102	80	101
R1S2	86	52	123	105	101	105	99	110	78	104
R2S1	97	80	89	66	100	93	95	97	76	98
R2S2	99	76	86	71	99	94	95	96	73	96
R3S1	97	71	100	83	98	97	97	98	74	100
R3S2	100	76	106	81	100	96	98	96	72	98
R4S1	100	76	106	81	100	96	98	96	72	98
R4S2	98	94	85	65	99	93	97	96	71	100
R5S1	98	101	71	61	102	95	98	102	71	95
R5S2	99	100	96	76	99	92	94	96	68	96
R6S1	96	66	102	77	99	93	96	97	75	102
R6S2	96	67	93	70	98	95	100	96	74	101
R7S1	99	58	104	77	98	95	99	96	78	104
R7S2	100	52	89	72	100	93	98	96	75	104
R8S1	98	55	104	78	99	95	101	95	79	105
R8S2	98	51	102	79	99	100	101	105	84	106
R9S1	98	43	99	75	101	97	102	99	74	103
R9S2	92	38	95	72	96	91	96	94	72	100
R10S1	98	90	89	68	98	94	95	99	75	103
R10S2	97	83	94	72	99	93	98	104	78	107

A3 Table 2: Reproducibility of the sample preparation for PUF plug adsorber cartridges; Recoveries (%) of Performance Reference Compounds spiked prior extraction to the environmental samples

%	SIMAZ-D ₁₀	PROMETR-D ₆	HCHG- ¹³ C ₆ D ₆	CB30	CB104	CB145	CB204	PHEN-D ₁₀	FLU-D ₁₀	BAA-D ₁₂
AL 1	104	77	92	88	85	76	92	127	118	121
AL 2	102	73	76	81	85	78	92	129	115	119
AL 3	102	81	86	76	82	76	94	131	117	116
AL 4	97	72	94	83	83	74	92	127	112	119
AL 5	103	72	90	83	85	74	92	125	114	114
AL 6	102	65	93	88	91	79	96	131	113	101
AL 7	105	74	91	87	85	80	93	122	100	109
AL 8	102	72	91	85	87	78	94	129	115	110
AL 9	103	78	90	85	85	79	91	125	113	101
AL 10	97	75	82	84	84	76	90	125	111	119

A3 Table 3: Reproducibility of the sample preparation for PUF/XAD-2/PUF adsorber cartridges; Recoveries (%) of Performance Reference Compounds spiked prior extraction to the environmental samples

%	SIMAZ-D ₁₀	PROMETR-D ₆	HCHG- ¹³ C ₆ D ₆	CB30	CB104	CB145	CB204	PHEN-D ₁₀	FLU-D ₁₀	BAA-D ₁₂
R3S2	93	108	117	84	102	98	96	100	99	117
R4S2	94	108	100	71	99	96	95	101	104	119
R5S2	93	106	100	71	103	95	99	98	104	118
R8S1	96	110	91	65	102	95	97	100	108	123
R8S2	94	107	109	91	98	96	98	103	98	114
R9S1	98	105	98	73	100	91	100	103	107	119
R9S2	88	111	102	74	97	89	94	100	106	121
R10S1	96	107	98	75	98	95	96	102	108	120
R10S2	95	105	104	84	86	95	98	103	100	115

A3 Table 4: Reproducibility of the sample preparation for PUF disks; Recoveries (%) of Performance Reference Compounds spiked prior extraction to the environmental samples

WF in %	SIMAZ-D ₁₀	PROMETR-D ₆	HCHG- ¹³ C ₆ D ₆	CB30	CB104	CB145	CB204	PHEN-D ₁₀	FLU-D ₁₀	BAA-D ₁₂
Sülld. G	86	80	93	74	93	82	101	98	95	105
Sylt A	86	74	94	74	94	81	91	104	113	123
Sylt C	87	64	89	76	92	80	91	103	114	117
Sylt E	79	56	90	76	93	80	93	99	134	126
Sylt G	65	67	100	80	93	79	108	99	112	118
Sylt H	80	54	91	74	92	80	106	99	119	121
Sylt I	83	55	93	82	93	80	103	98	130	129
Sylt K	85	63	93	79	93	80	89	100	127	131
Sylt M	88	45	93	85	91	81	92	97	119	124
FINO1 A	92	48	78	88	96	79	103	99	145	144
FINO1 B	87	50	74	84	94	79	98	99	142	144
FINO1 C	84	45	77	86	91	82	95	99	145	142

Data of desorption experiments

A3 Table 5: Desorption from PUF plug adsorber cartridges; Recoveries (%) of Performance Reference Compounds spiked prior to air sampling, V = Volume of sampled air in m³

WF in %	V	PROMETR-D ₆	SIMAZ-D ₁₀	HCHG- ¹³ C ₆ D ₆	CB30	CB104	CB145	CB204	PHEN-D ₁₀	FLU-D ₁₀	BAA-D ₁₂
10 Nov./Dec. 1	0	113	95	94	68	102	96	101	104	102	107
10 Nov./Dec. 2	0	114	93	91	74	105	93	100	103	104	119
10 Nov./Dec. 3	0	109	94	92	69	101	94	95	96	92	103
R1S1	779	87	94	116	79	104	101	95	97	104	119
R1S2	879	82	95	107	53	98	99	93	92	104	111
R2S1	485	88	89	106	80	103	96	98	105	112	118
R2S2	475	93	90	104	80	99	98	97	101	117	121
R3S1	244	101	95	104	75	100	95	98	99	92	108
R4S1	294	97	93	95	70	98	96	96	98	89	109
R5S1	342	98	94	100	69	101	97	99	102	102	115
R6S1	386	97	91	98	63	98	97	100	97	117	123
R6S2	378	95	93	102	74	101	95	97	97	93	106
R7S1	287	96	89	98	67	99	105	96	100	100	107
R7S2	282	103	91	94	68	100	94	101	96	101	109

A3 Table 6: Desorption from PUF/XAD-2/PUF adsorber cartridges; Recoveries (%) of Performance Reference Compounds spiked prior to air sampling; V = Volume of sampled air in m³; 09AT 14 = Break off air sample from the research cruise in the German EEZ in May/Jun. 2009, excluded from further data interpretation

%	V	PROMETR-D ₆	SIMAZ-D ₁₀	HCHG- ¹³ C ₆ D ₆	CB30	CB104	CB145	CB204	PHEN-D ₁₀	FLU-D ₁₀	BAA-D ₁₂
09AT 1	0	102	98	87	64	91	83	88	104	97	99
09AT 2	144	82	93	97	68	90	82	91	104	106	119
09AT 3	182	79	94	93	65	92	80	92	113	137	148
09AT 4	267	79	93	90	62	94	81	93	103	84	106
09AT 5	241	82	90	88	55	91	80	92	127	157	152
09AT 6	0	107	98	79	60	92	83	95	114	93	107
09AT 7	241	72	98	109	70	94	80	97	102	100	116
09AT 8	508	72	97	100	53	93	78	96	102	108	122
09AT 9	414	66	95	92	58	96	77	119	120	136	147
09AT 10	0	113	100	92	65	93	81	95	110	89	101
09AT 11	332	79	96	100	49	92	80	97	109	107	121
09AT 12	159	84	100	93	64	91	79	94	115	107	117
09AT 13	0	106	100	91	70	94	82	92	109	84	99
09AT 14	17	102	99	91	65	91	80	95	110	80	103
10AT 1	159	87	91	92	74	91	78	84	98	85	104
10AT 2	206	88	92	96	74	90	79	88	105	118	127
10AT 3	250	91	98	93	72	89	81	93	104	122	134
10AT 4	306	79	96	93	72	91	80	90	102	88	111
10AT 5	193	87	92	103	77	92	81	87	103	83	103
10AT 6	261	85	96	101	73	92	81	88	100	86	104
10AT 7	254	89	97	91	73	92	81	91	102	92	110
10AT 8	0	102	86	91	75	91	79	87	101	75	100
10AT 9	0	105	91	88	72	91	81	100	105	76	98
10AT 10	0	105	87	84	58	89	82	90	107	73	94
PE 1	222	76	98	91	75	86	79	83	118	117	131
PE 2	0	98	100	59	55	83	81	92	107	108	99
PE 3	297	69	99	71	52	85	74	88	126	126	110
PE 4	518	65	98	85	69	84	74	87	132	135	149
PE 6	174	81	97	66	65	83	77	89	113	137	119
PE 7	251	83	98	71	59	85	76	87	130	130	138
PE 8	219	81	95	69	69	81	75	88	122	130	115
PE 9	316	77	101	71	59	86	74	89	114	144	151
PE 10	284	84	102	78	65	84	77	93	118	153	127
PE 11	311	75	93	74	65	86	75	91	107	117	114
PE 12	0	96	97	62	67	82	76	92	92	126	122
PE 13	0	97	99	75	78	84	77	96	111	103	112
PE 14	194	84	90	65	72	86	73	84	163	161	152
PE 15	314	79	99	80	67	83	75	93	109	124	119
PE 17	106	89	99	63	65	83	78	92	100	121	115
PE 18	142	88	98	74	71	83	74	93	107	115	122
10 Nov./Dec. 1	0	99	89	93	77	99	95	98	109	112	129
10 Nov./Dec. 2	0	109	95	90	81	103	94	95	109	152	157
10 Nov./Dec. 3	0	103	94	104	84	79	91	93	106	99	118

Stability tests of exposed air sampling materials

A3 Table 7: Stability of frozen PUF/XAD-2/PUF adsorber cartridges; Recoveries (%) of Performance Reference Compounds in field blanks spiked prior to storage, D = Duration in weeks; PXP = PUF/XAD-2/PUF

%	D	PROMETR-D ₆	SIMAZ-D ₁₀	HCHG- ¹³ C ₆ D ₆	CB30	CB104	CB145	CB204	PHEN-D ₁₀	FLU-D ₁₀	BAA-D ₁₂
09AT 1	55.9	102	98	87	64	91	83	88	104	97	99
09AT 6	55.6	107	98	79	60	92	83	95	114	93	107
09AT 10	55.7	113	100	92	65	93	81	95	110	89	101
09AT 13	55.7	106	100	91	70	94	82	92	109	84	99
10AT 8	5.4	102	86	91	75	91	79	87	101	75	100
10AT 9	5.6	105	91	88	72	91	81	100	105	76	98
10AT 10	5.6	105	87	84	58	89	82	90	107	73	94
PE 2	28.9	98	100	59	55	83	81	92	107	108	99
PE 12	27.9	96	97	62	67	82	76	92	92	126	122
PE 13	28.0	97	99	75	78	84	77	96	111	103	112
PXP 1	0.0	83	82	76	72	92	80	91	103	80	103
PXP 2	0.0	112	89	82	74	94	82	94	100	70	91
PXP 3	0.0	116	90	62	77	92	81	97	106	80	100
PXP 4	0.0	93	99	69	67	94	83	97	96	99	109
PXP 5	0.0	97	97	86	78	90	81	92	93	96	93
PXP 6	0.0	94	98	81	77	92	86	98	84	107	109

A3 Table 8: Stability of frozen PUF disks; Recoveries (%) of Performance Reference Compounds in field blanks spiked prior to storage, D = Duration in weeks

%	D	PROMETR-D ₆	SIMAZ-D ₁₀	HCHG- ¹³ C ₆ D ₆	CB30	CB104	CB145	CB204	PHEN-D ₁₀	FLU-D ₁₀	BAA-D ₁₂
10AT B	7.7	98	100	77	84	91	82	92	111	85	99
10AT D	7.7	102	100	87	81	94	81	94	115	89	104
FINO1 D	0.0	93	96	88	74	94	83	93	107	133	134
FINO1 E	0.0	102	89	97	81	93	83	90	115	133	128
FINO1 F	0.0	103	87	93	77	94	83	89	124	135	129
FINO1 J	5.0	96	93	90	76	100	92	93	116	121	122
FINO1 K	5.0	101	94	103	93	103	101	98	119	104	106
FINO1 L	5.0	101	89	93	80	101	95	91	117	104	100
FINO3 B	12.1	110	81	96	76	93	79	95	126	120	127
FINO3 D	12.3	98	80	88	73	91	82	98	120	139	143
FINO3 F	12.3	99	80	86	70	89	79	97	119	123	123
PUF disk 1	0.0	109	106	72	70	89	84	96	119	81	86
PUF disk 2	0.0	108	104	76	71	90	84	97	120	78	86
PUF disk 3	0.0	105	107	75	72	90	85	100	112	75	85
Sülld. D	0.0	95	95	102	84	93	82	93	98	98	115
Sülld. F	0.0	102	101	98	82	92	80	94	101	98	112
Sülld. H	0.0	104	98	78	73	94	80	93	101	123	130
Sülld. AA	15.1	98	99	98	79	92	80	90	108	107	118
Sülld. AD	11.1	105	93	99	75	91	77	89	103	123	124
Sülld. AF	7.3	118	96	105	77	93	84	93	119	110	113
Sülld. AH	4.0	114	84	86	74	90	77	85	101	100	109
Sülld. AJ	4.7	103	93	52	77	96	95	94	100	103	108
Sülld. AL	4.7	98	91	82	74	100	95	95	113	117	116
Sylt B	0.0	100	97	87	70	90	80	92	103	128	134
Sylt D	0.0	96	94	92	72	92	79	91	106	131	136
Sylt F	0.0	101	98	88	71	90	80	91	104	115	117
Sylt J	0.0	98	94	94	81	94	81	108	104	123	124

A3 Table 8 continued:

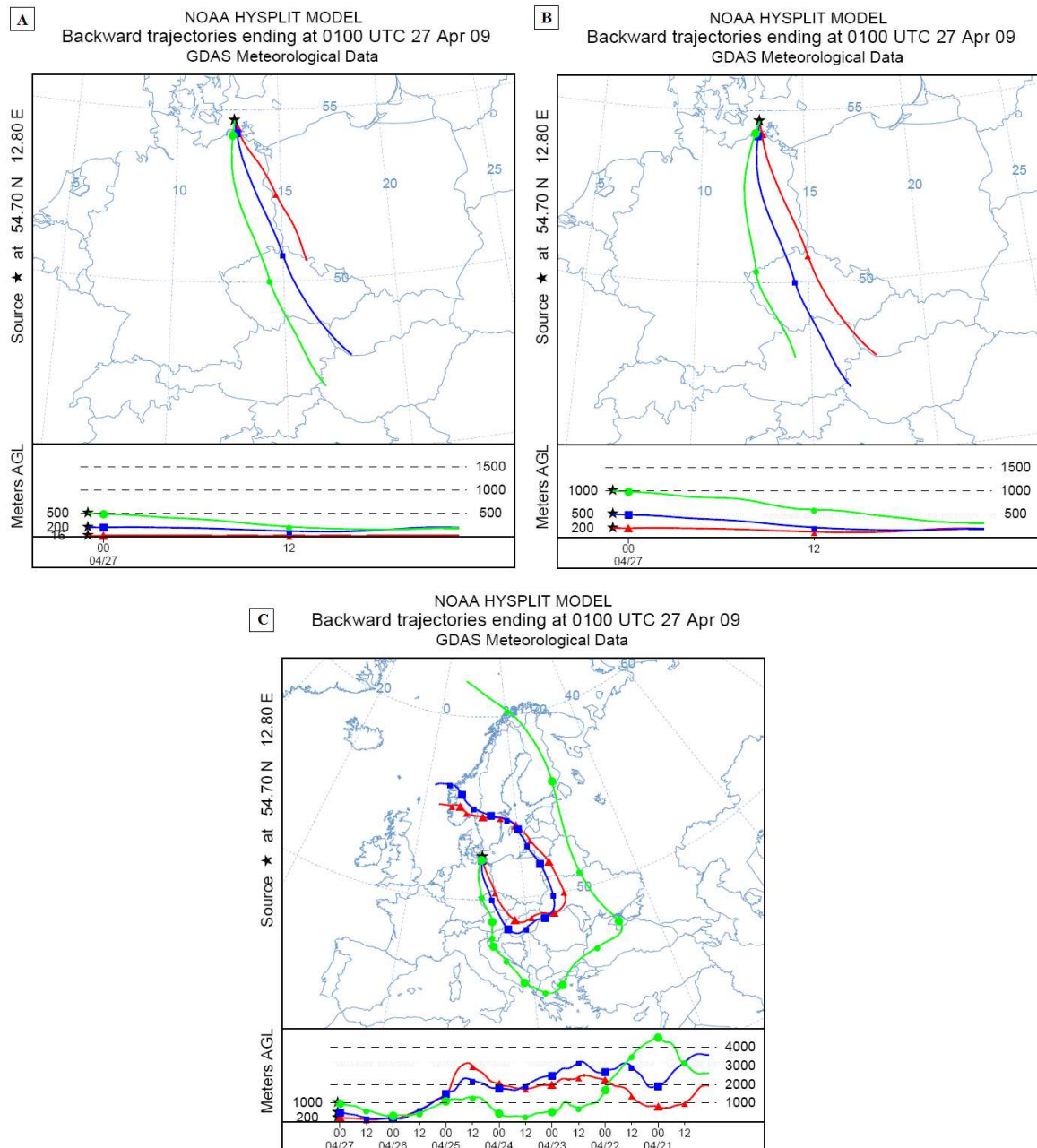
%	D	PROMETR-D ₆	SIMAZ-D ₁₀	HCHG- ¹³ C ₆ D ₆	CB30	CB104	CB145	CB204	PHEN-D ₁₀	FLU-D ₁₀	BAA-D ₁₂
Sylt L	0.0	96	92	93	72	89	81	91	104	135	138
Sylt N	0.0	91	93	95	77	95	80	91	106	120	123
Sylt P	24.1	87	90	94	78	91	82	92	100	109	120
Sylt T	24.4	97	86	104	82	95	80	88	112	105	116
Sylt V	4.6	108	88	96	82	102	95	96	135	111	121
Sylt X	4.6	101	83	88	77	98	91	91	101	105	113
Sylt Z	4.7	101	82	72	70	98	91	92	103	115	118

A3 Table 9: PRC recoveries (%) in the PUF disk passive air samples spiked prior to exposure at Tinnum/Sylt (28 days), Sülldorf/Hamburg (28 days) and at the FINO platforms

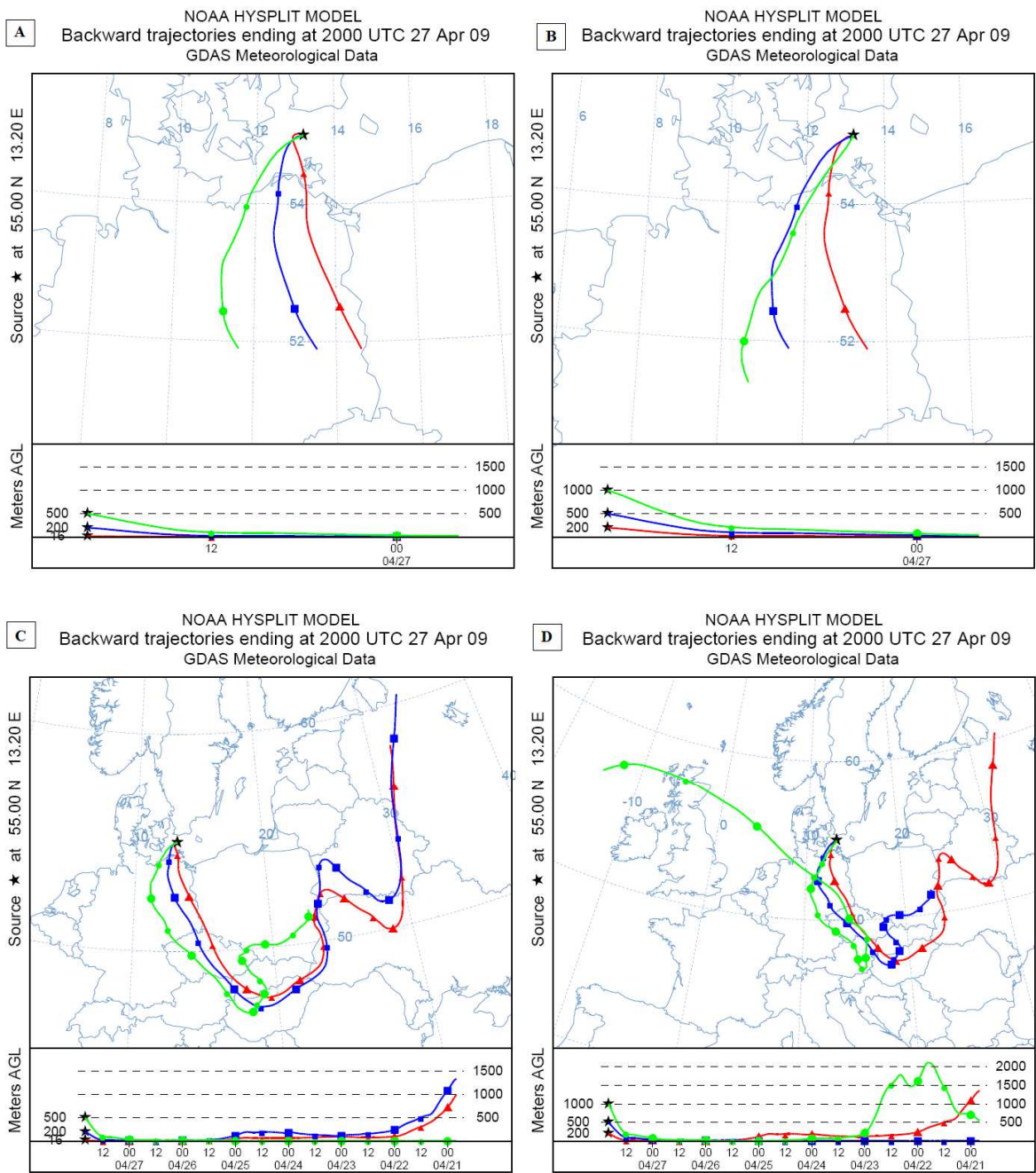
%	SIMAZ-D ₁₀	PROMETR-D ₆	HCHG- ¹³ C ₆ D ₆	CB30	CB104	CB145	CB204	PHEN-D ₁₀	FLU-D ₁₀	BAA-D ₁₂
Sülld. I	84	57	90	61	89	83	98	97	120	121
Sülld. K	85	41	99	64	88	80	93	91	118	116
Sülld. M	87	44	92	63	90	83	93	98	128	116
Sülld. O	83	39	92	67	92	83	96	108	153	149
Sülld. Q	70	28	100	69	93	82	95	106	145	146
Sülld. S	83	17	97	68	91	84	96	102	138	130
Sülld. U	73	25	90	60	88	83	101	102	148	124
Sülld. W	81	10	82	57	86	82	104	102	116	127
Sülld. Y	79	15	91	66	89	78	93	88	101	92
Sülld. Z	67	5	69	44	76	75	96	69	96	75
Sülld. AB	73	9	82	45	81	79	89	67	97	78
Sülld. AC	78	11	78	51	82	77	91	75	89	82
Sülld. AE	82	12	80	51	80	75	89	78	107	95
Sülld. AG	79	25	83	54	83	75	90	83	100	99
Sülld. AI	86	31	96	59	95	93	96	86	106	101
Sülld. AK	81	50	97	65	98	94	97	91	113	108
Sylt O	77	13	80	66	85	79	94	91	118	104
Sylt Q	85	12	73	63	81	76	98	87	110	98
Sylt R	84	15	80	63	81	79	96	88	105	100
Sylt S	90	16	89	72	88	79	90	95	107	100
Sylt U	79	11	80	63	91	94	98	87	109	95
Sylt W	87	10	72	47	88	91	94	74	135	100
Sylt Y	82	20	100	76	98	93	94	95	123	103
FINO3 A	72	4	17	9	36	60	89	31	89	58
FINO3 C	75	0	11	1	30	56	97	4	88	38
FINO3 E	69	0	15	1	33	57	93	7	80	41
FINO1 G	70	3	32	6	52	79	93	26	108	77
FINO1 H	74	3	23	5	48	75	90	18	98	82
FINO1 I	67	2	22	4	47	78	96	15	91	68

Annex 4 (A4) : Air mass backward trajectories – Original Hysplit 4.9 plottings

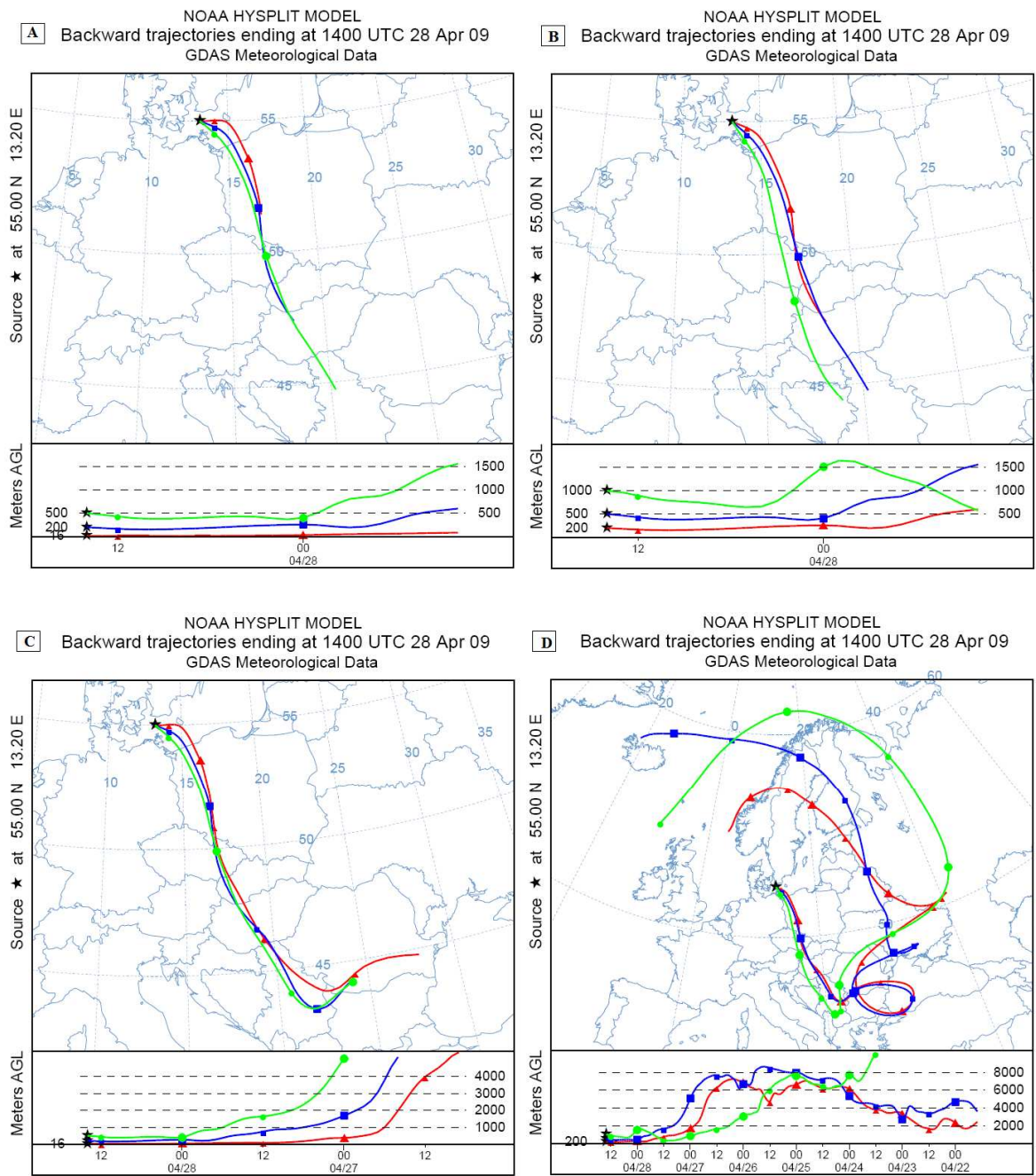
Air mass backward trajectories of air samples collected during the research cruise in the Baltic Sea in Apr. 2009



A4 Figure 1: Air mass backward trajectories of the air sample AL 1; (A) 24 h, 16 m, 200 m, 500 m arrival height; (B) 24 h; 200 m, 500 m, 1000 m arrival height; (C) 168 h; 500 m, 200 m, 1000 m arrival height

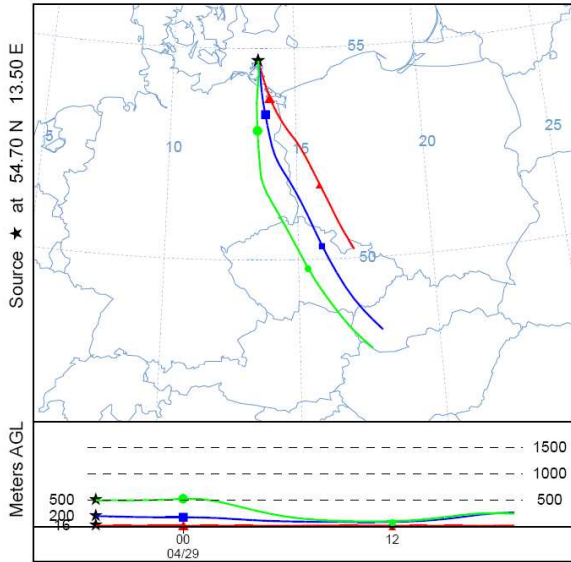


A4 Figure 2: Air mass backward trajectories of the air sample AL 2; (A) 24 h, 16 m, 200 m, 500 m arrival height; (B) 24 h; 200 m, 500 m, 1000 m arrival height; (C) 168 h; 16 m; 200 m; 500 m; (D) 168 h; 500 m, 200 m, 1000 m arrival height

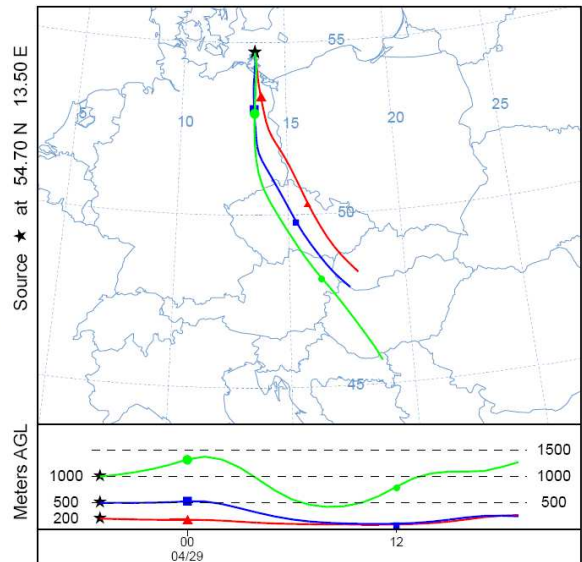


A4 Figure 3: Air mass backward trajectories of the air sample AL 3; (A) 24 h, 16 m, 200 m, 500 m arrival height; (B) 24 h; 200 m, 500 m, 1000 m arrival height; (C) 60 h; 16 m; 200 m; 500 m; (D) 168 h; 500 m, 200 m, 1000 m arrival height

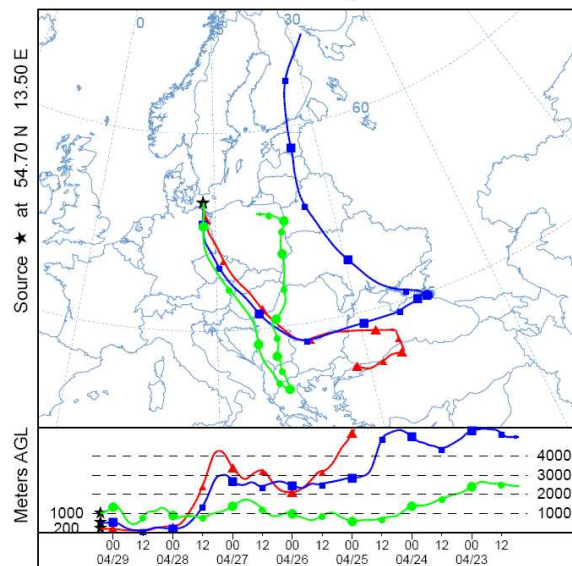
A NOAA HYSPLIT MODEL
Backward trajectories ending at 0500 UTC 29 Apr 09
GDAS Meteorological Data



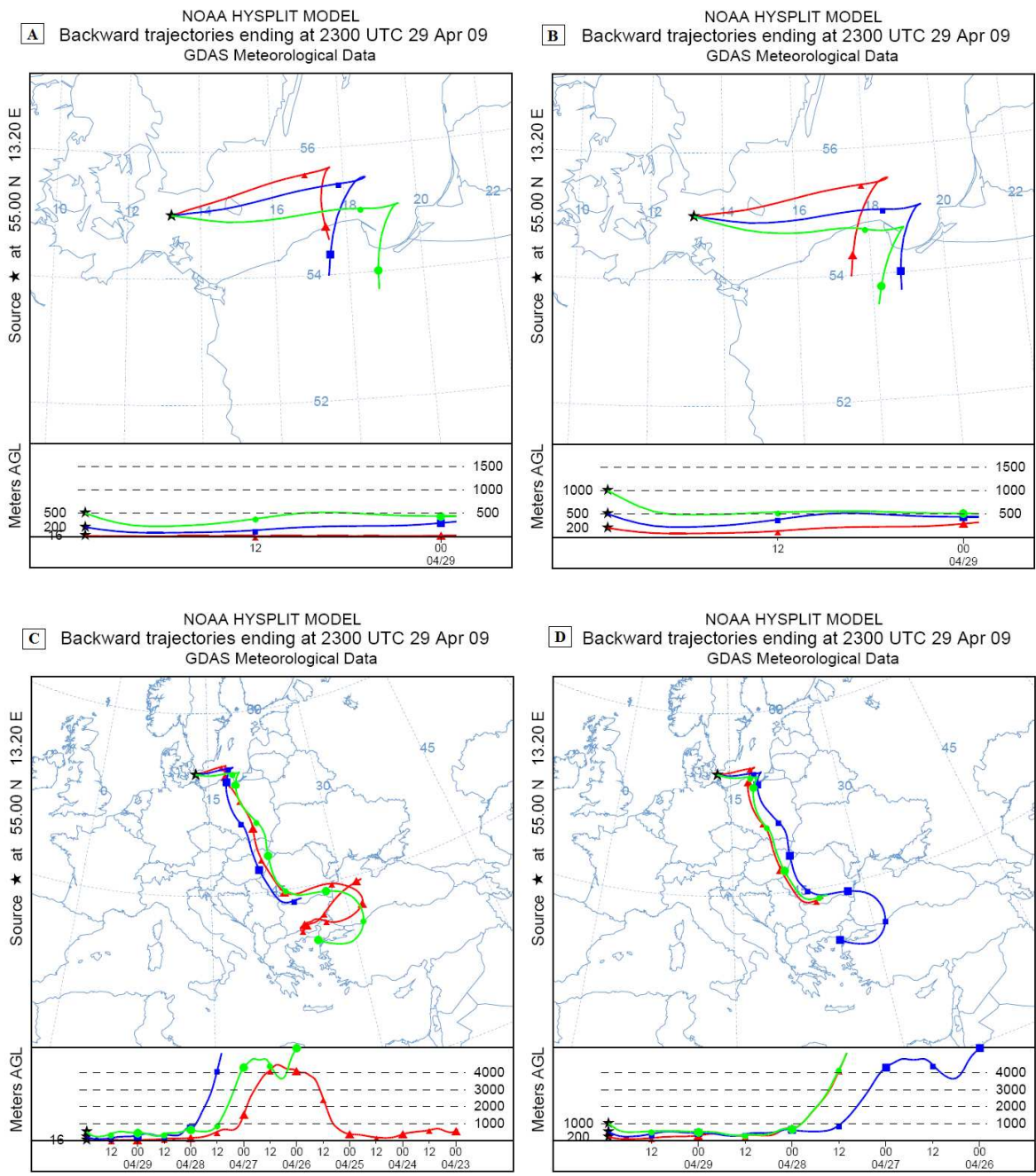
B NOAA HYSPLIT MODEL
Backward trajectories ending at 0500 UTC 29 Apr 09
GDAS Meteorological Data



C NOAA HYSPLIT MODEL
Backward trajectories ending at 0500 UTC 29 Apr 09
GDAS Meteorological Data

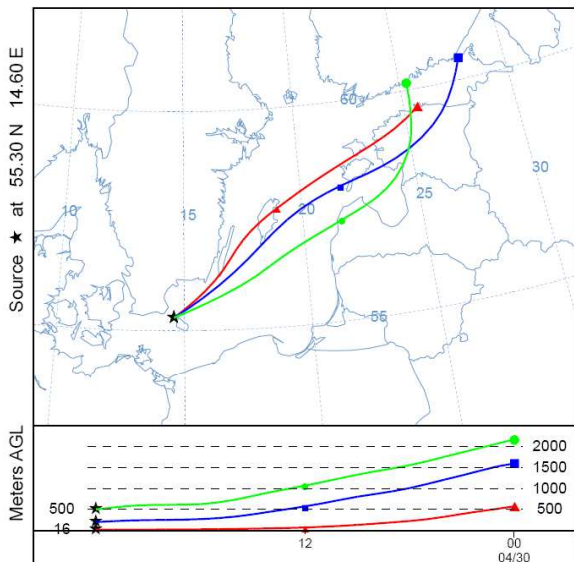


A4 Figure 4: Air mass backward trajectories of the air sample AL 4; (A) 24 h, 16 m, 200 m, 500 m arrival height; (B) 24 h; 200 m, 500 m, 1000 m arrival height; (C) 168 h; 200 m, 500 m, 1000 m arrival height

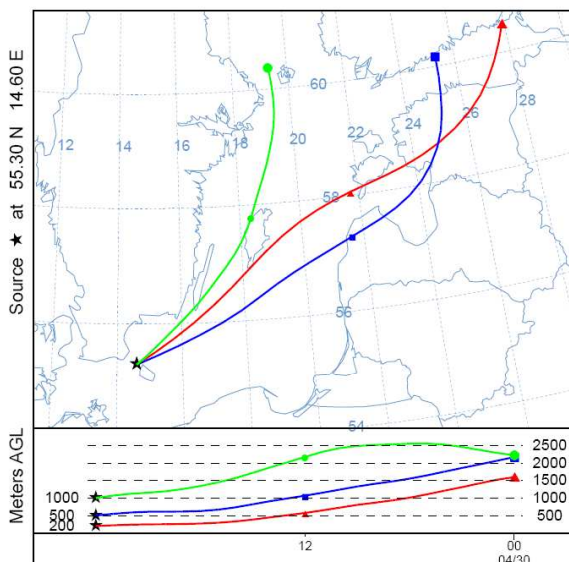


A4 Figure 5: Air mass backward trajectories of the air sample AL 5; (A) 24 h, 16 m, 200 m, 500 m arrival height; (B) 24 h; 200 m, 500 m, 1000 m arrival height; (C) 168 h; 16 m, 200 m, 500 m arrival height; (D) 96 h; 200 m, 500 m, 1000 m arrival height

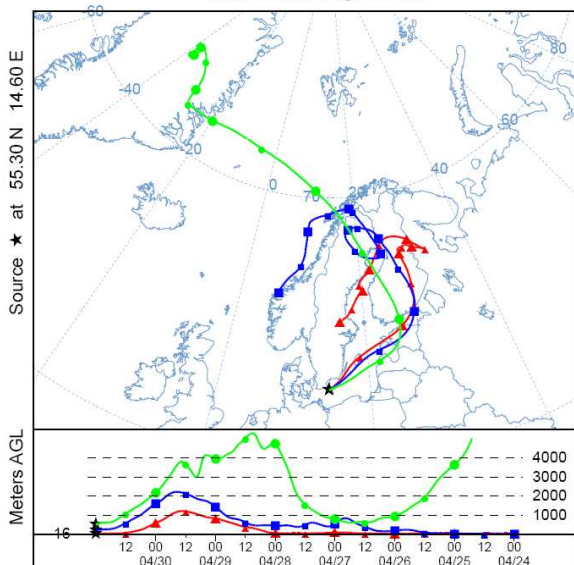
A NOAA HYSPLIT MODEL
Backward trajectories ending at 0000 UTC 01 May 09
GDAS Meteorological Data



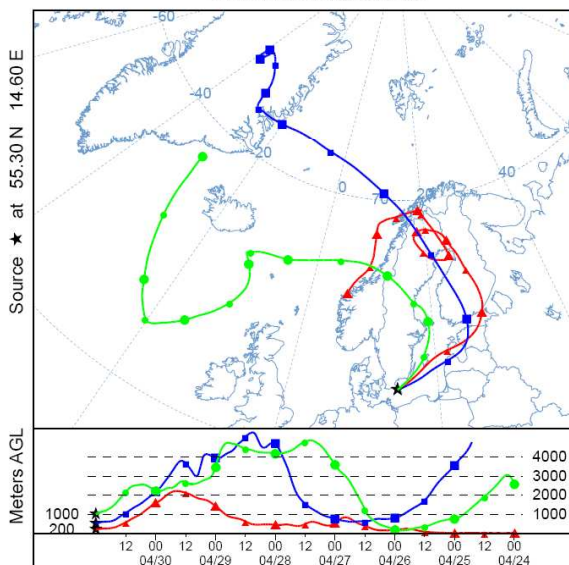
B NOAA HYSPLIT MODEL
Backward trajectories ending at 0000 UTC 01 May 09
GDAS Meteorological Data



C NOAA HYSPLIT MODEL
Backward trajectories ending at 0000 UTC 01 May 09
GDAS Meteorological Data

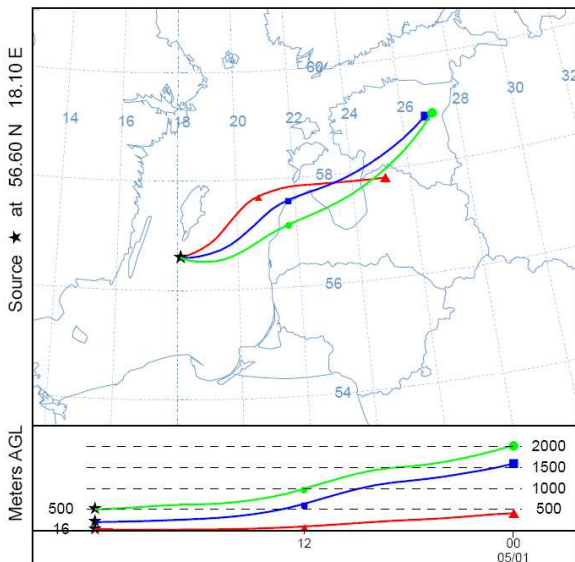


D NOAA HYSPLIT MODEL
Backward trajectories ending at 0000 UTC 01 May 09
GDAS Meteorological Data

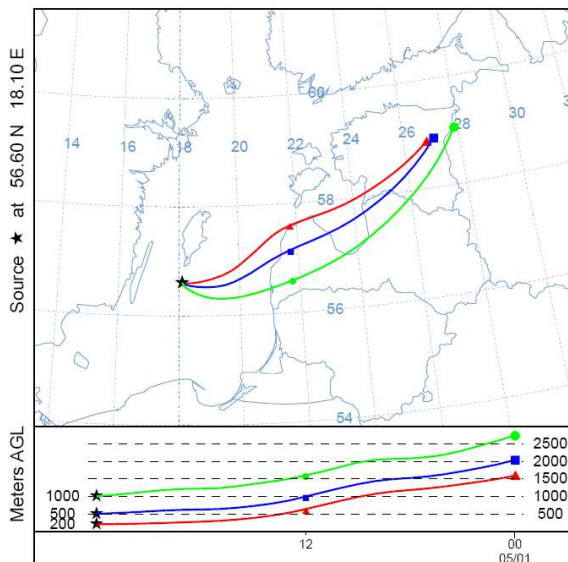


A4 Figure 6: Air mass backward trajectories of the air sample AL 6; (A) 24 h, 16 m, 200 m, 500 m arrival height; (B) 24 h; 200 m, 500 m, 1000 m arrival height; (C) 168 h; 16 m, 200 m, 500 m arrival height; (D) 168 h; 200 m, 500 m, 1000 m arrival height

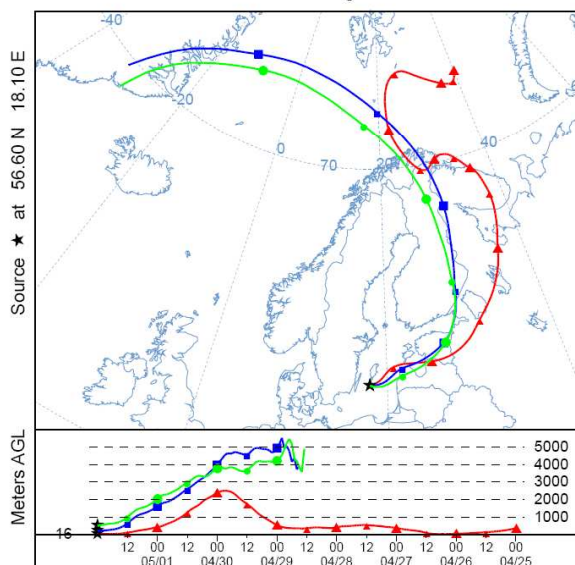
A NOAA HYSPLIT MODEL
Backward trajectories ending at 0000 UTC 02 May 09
GDAS Meteorological Data



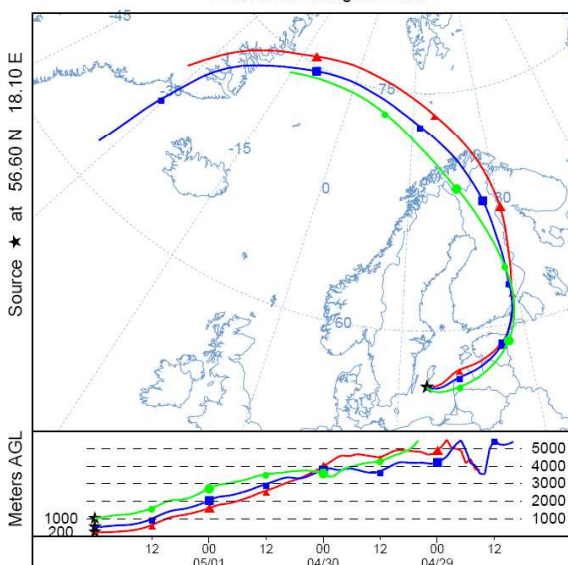
B NOAA HYSPLIT MODEL
Backward trajectories ending at 0000 UTC 02 May 09
GDAS Meteorological Data



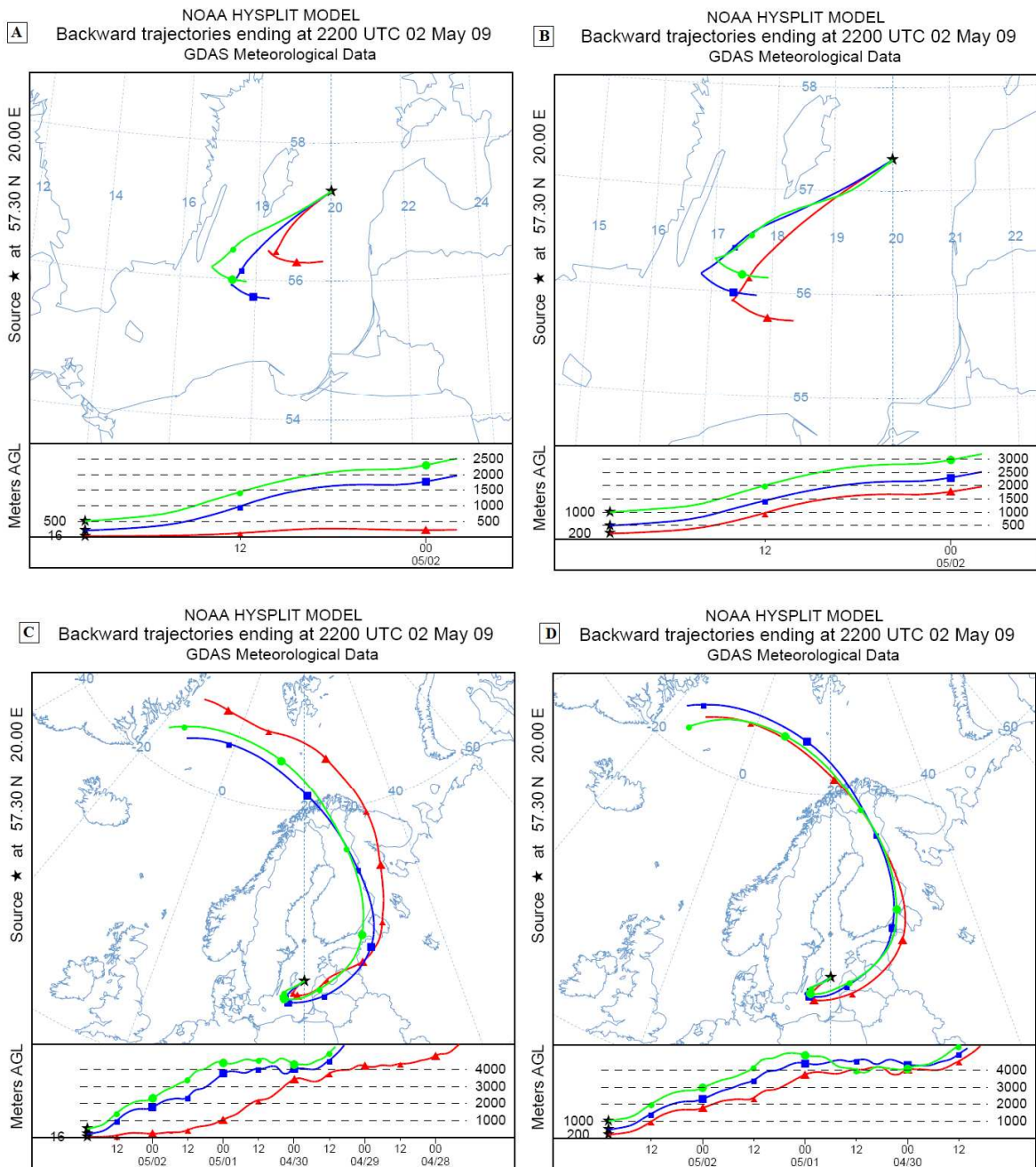
C NOAA HYSPLIT MODEL
Backward trajectories ending at 0000 UTC 02 May 09
GDAS Meteorological Data



D NOAA HYSPLIT MODEL
Backward trajectories ending at 0000 UTC 02 May 09
GDAS Meteorological Data

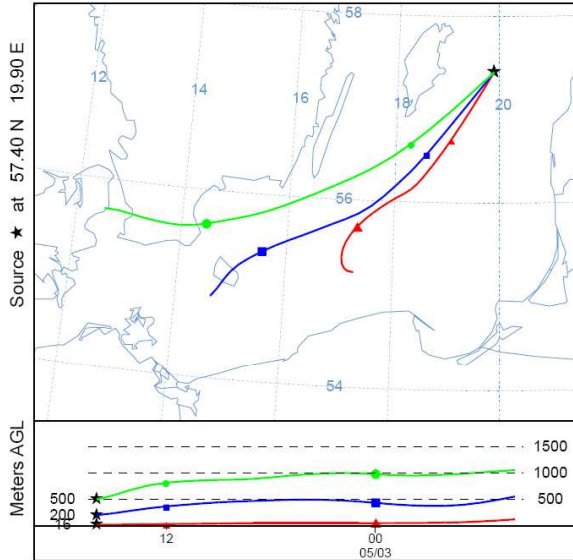


A4 Figure 7: Air mass backward trajectories of the air sample AL 7; (A) 24 h, 16 m, 200 m, 500 m arrival height; (B) 24 h; 200 m, 500 m, 1000 m arrival height; (C) 168 h; 16 m, 200 m, 500 m arrival height; (D) 84 h; 200 m, 500 m, 1000 m arrival height

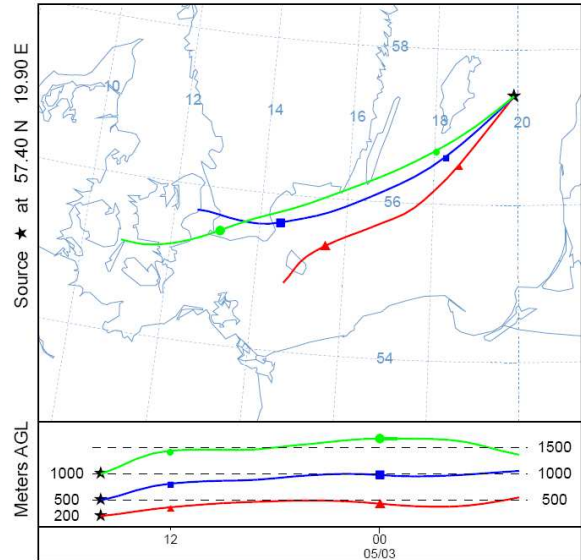


A4 Figure 8: Air mass backward trajectories of the air sample AL 8; (A) 24 h; 16 m, 200 m, 500 m arrival height; (B) 24 h; 200 m, 500 m, 1000 m arrival height; (C) 120 h; 16 m, 200 m, 500 m arrival height; (D) 84 h; 200 m, 500 m, 1000 m arrival height

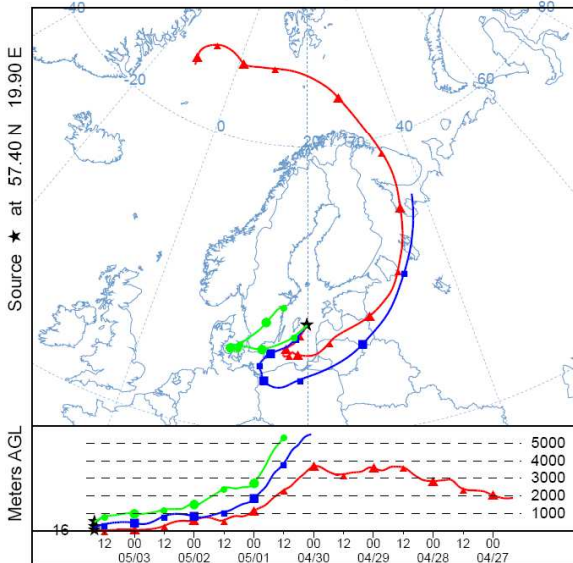
A NOAA HYSPLIT MODEL
Backward trajectories ending at 1600 UTC 03 May 09
GDAS Meteorological Data



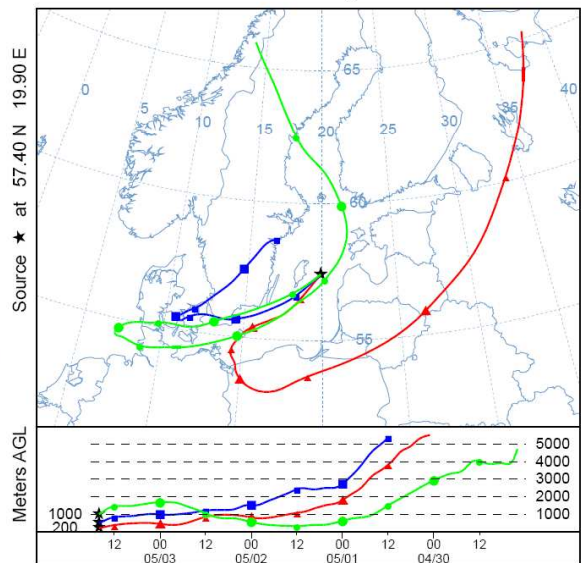
B NOAA HYSPLIT MODEL
Backward trajectories ending at 1600 UTC 03 May 09
GDAS Meteorological Data



C NOAA HYSPLIT MODEL
Backward trajectories ending at 1600 UTC 03 May 09
GDAS Meteorological Data

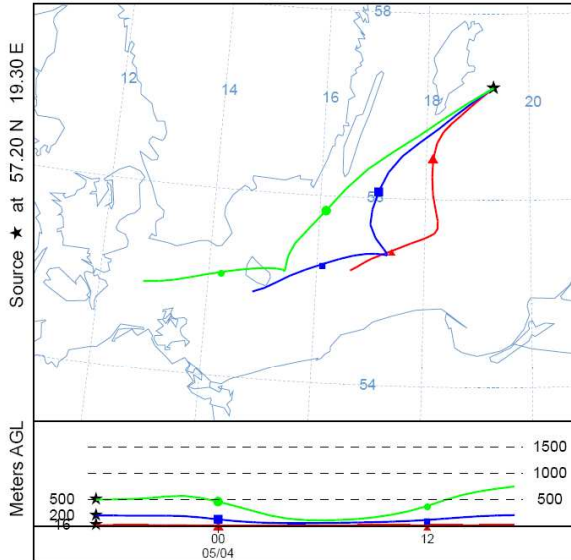


D NOAA HYSPLIT MODEL
Backward trajectories ending at 1600 UTC 03 May 09
GDAS Meteorological Data

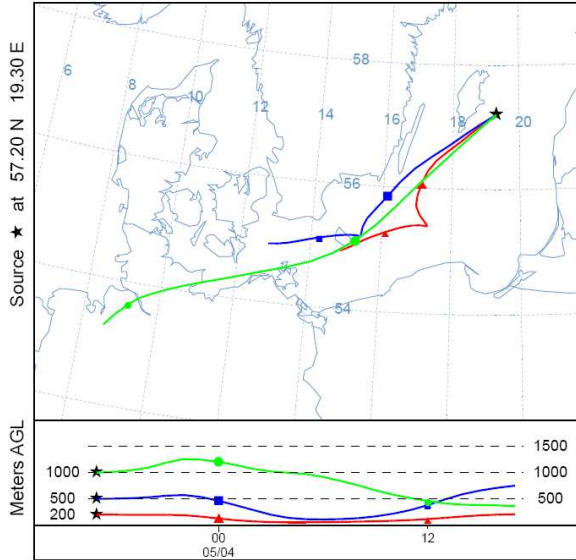


A4 Figure 9: Air mass backward trajectories of the air sample AL 9; (A) 24 h, 16 m, 200 m, 500 m arrival height; (B) 24 h; 200 m, 500 m, 1000 m arrival height; (C) 168 h; 16 m, 200 m, 500 m arrival height; (D) 108 h; 200 m, 500 m, 1000 m arrival height

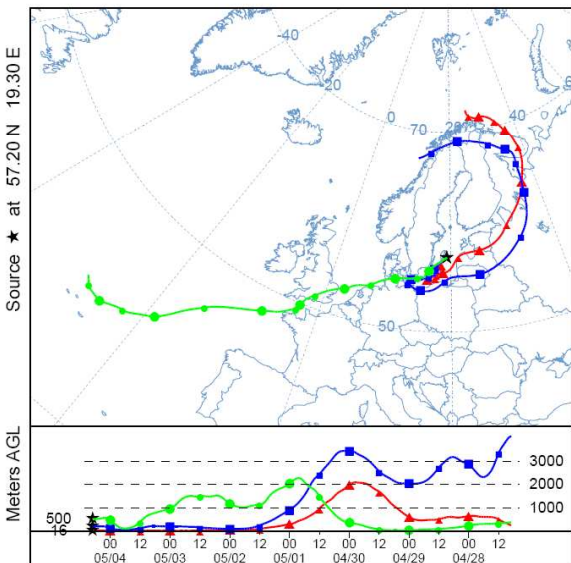
A NOAA HYSPLIT MODEL
Backward trajectories ending at 0700 UTC 04 May 09
GDAS Meteorological Data



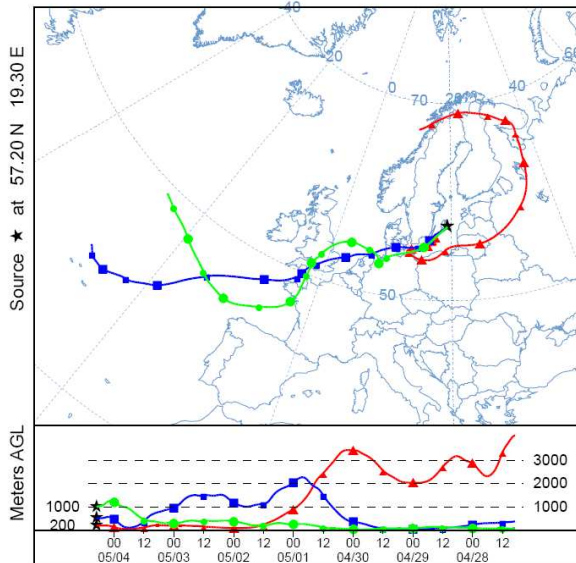
B NOAA HYSPLIT MODEL
Backward trajectories ending at 0700 UTC 04 May 09
GDAS Meteorological Data



C NOAA HYSPLIT MODEL
Backward trajectories ending at 0700 UTC 04 May 09
GDAS Meteorological Data

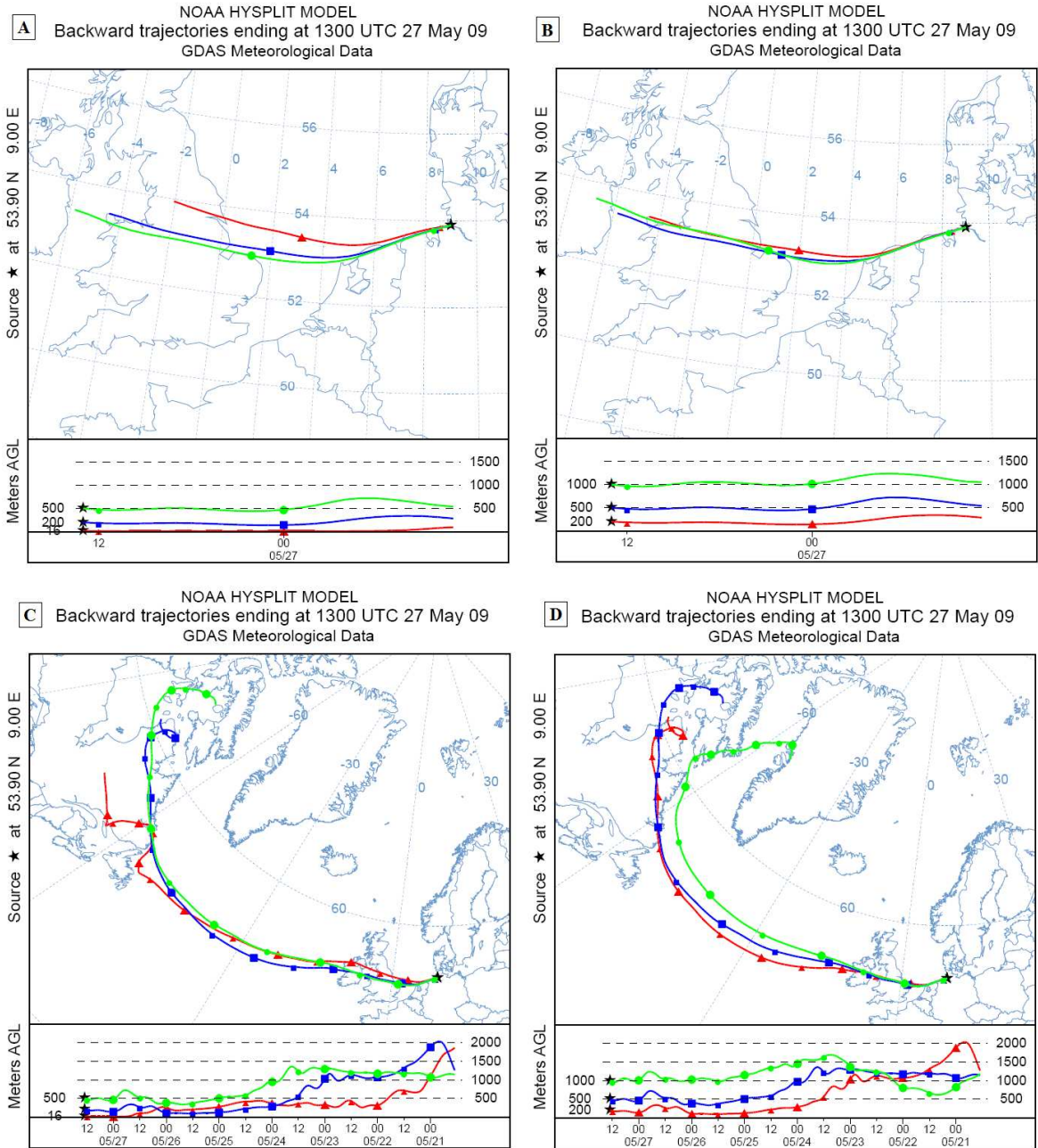


D NOAA HYSPLIT MODEL
Backward trajectories ending at 0700 UTC 04 May 09
GDAS Meteorological Data

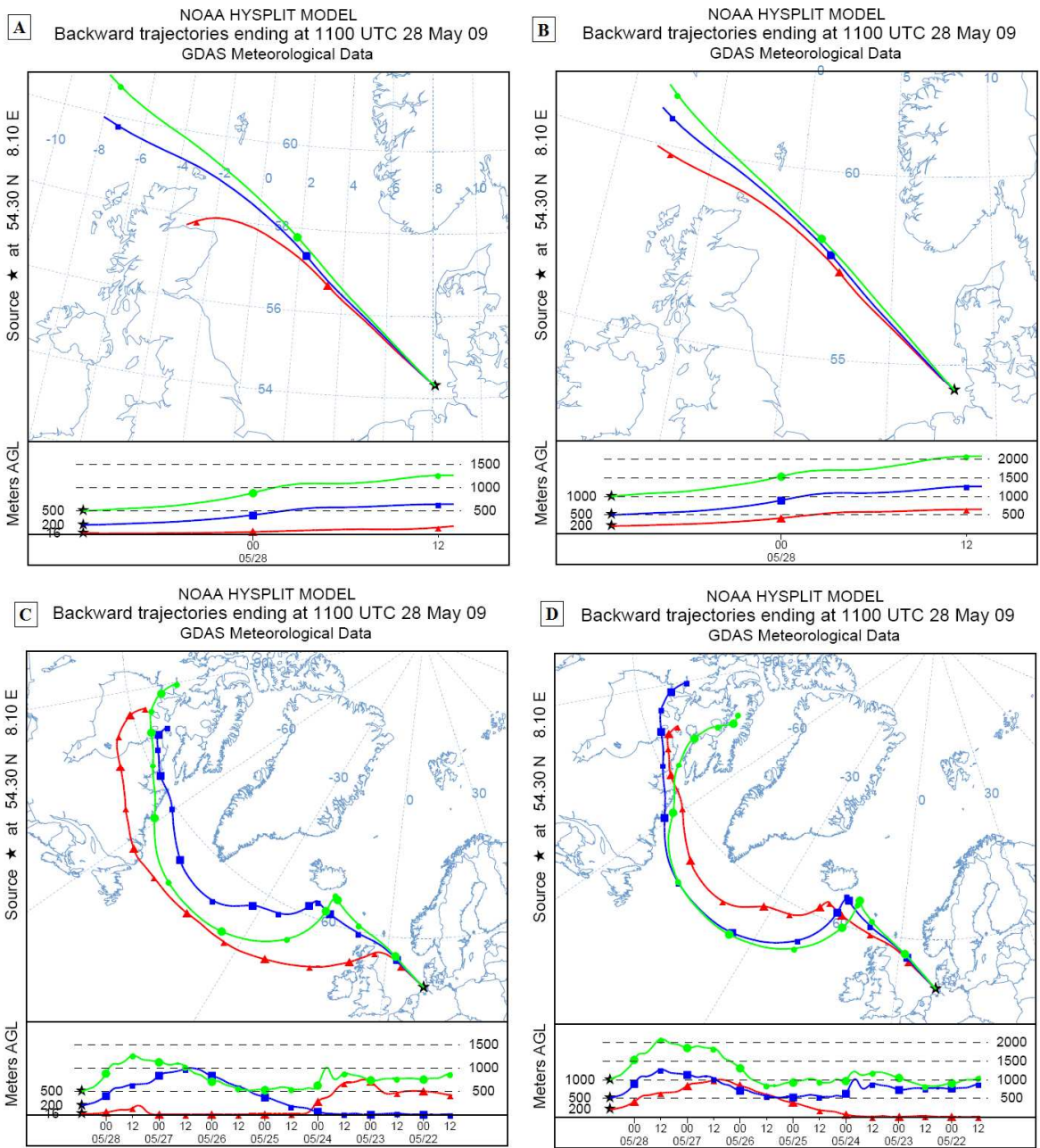


A4 Figure 10: Air mass backward trajectories of the air sample AL 10; (A) 24 h, 16 m, 200 m, 500 m arrival height; (B) 24 h; 200 m, 500 m, 1000 m arrival height; (C) 168 h; 16 m, 200 m, 500 m arrival height; (D) 168 h; 200 m, 500 m, 1000 m arrival height

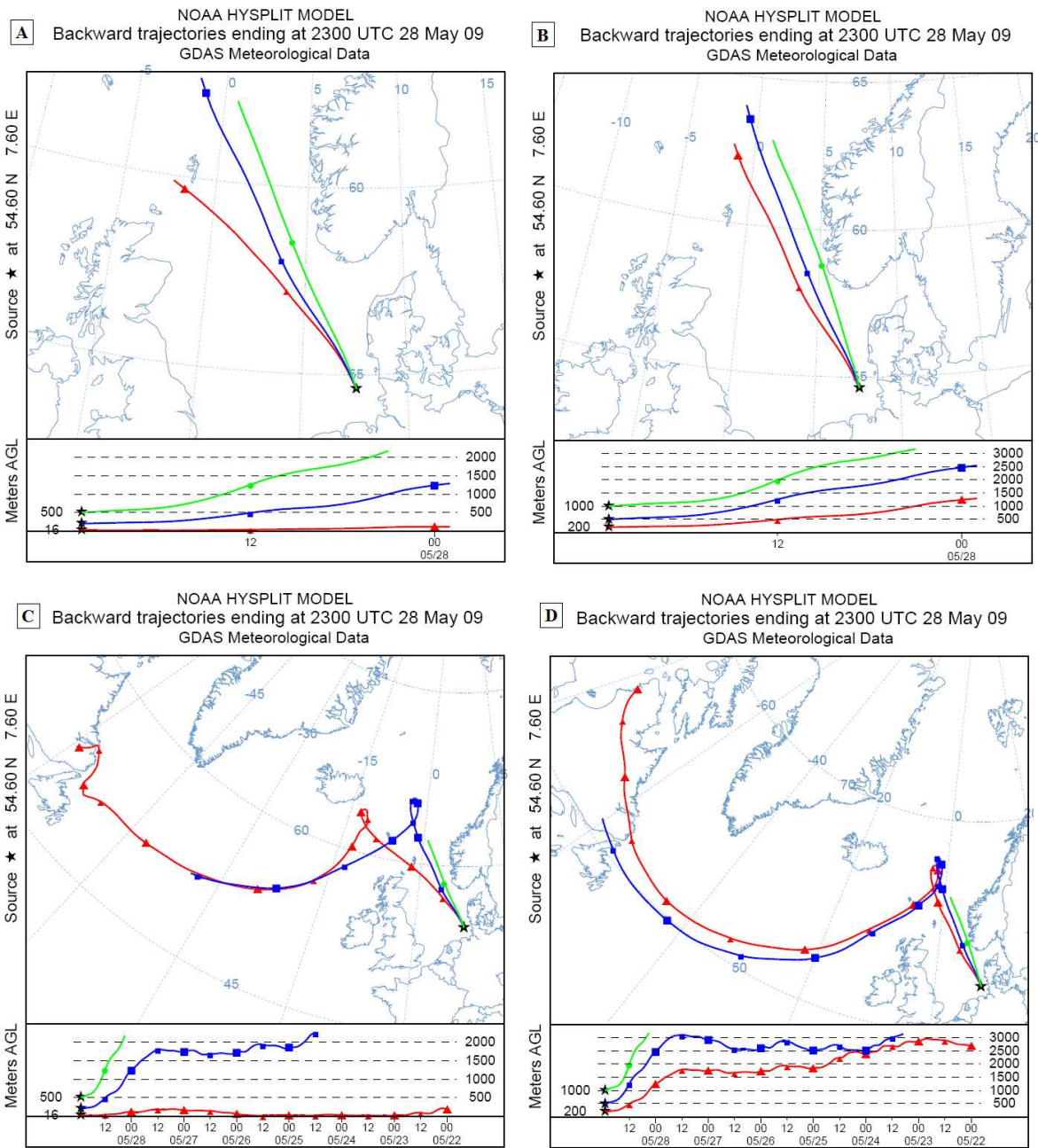
Air mass backward trajectories of air samples collected during the research cruise in the German EEZ in May/June. 2009



A4 Figure 11: Air mass backward trajectories of the air sample 09AT 2; (A) 24 h, 16 m, 200 m, 500 m arrival height; (B) 24 h; 200 m, 500 m, 1000 m arrival height; (C) 168 h; 16 m, 200 m, 500 m arrival height; (D) 168 h; 200 m, 500 m, 1000 m arrival height

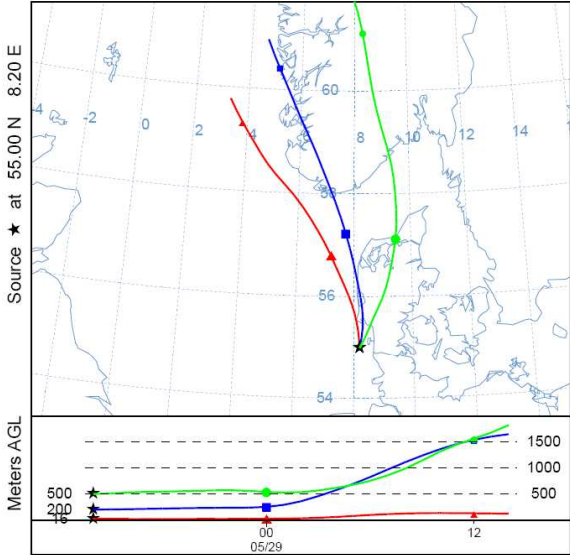


A4 Figure 12: Air mass backward trajectories of the air sample 09AT 3; (A) 24 h, 16 m, 200 m, 500 m arrival height; (B) 24 h; 200 m, 500 m, 1000 m arrival height; (C) 168 h; 16 m, 200 m, 500 m arrival height; (D) 168 h; 200 m, 500 m, 1000 m arrival height

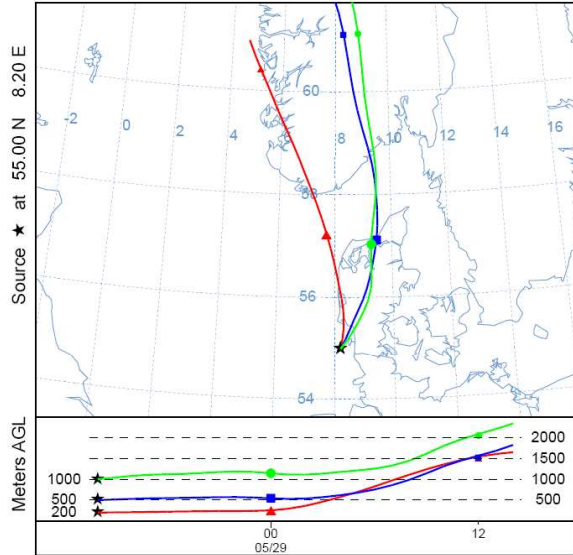


A4 Figure 13: Air mass backward trajectories of the air sample 09AT 4; (A) 24 h, 16 m, 200 m, 500 m arrival height; (B) 24 h; 200 m, 500 m, 1000 m arrival height; (C) 168 h; 16 m, 200 m, 500 m arrival height; (D) 168 h; 200 m, 500 m, 1000 m arrival height

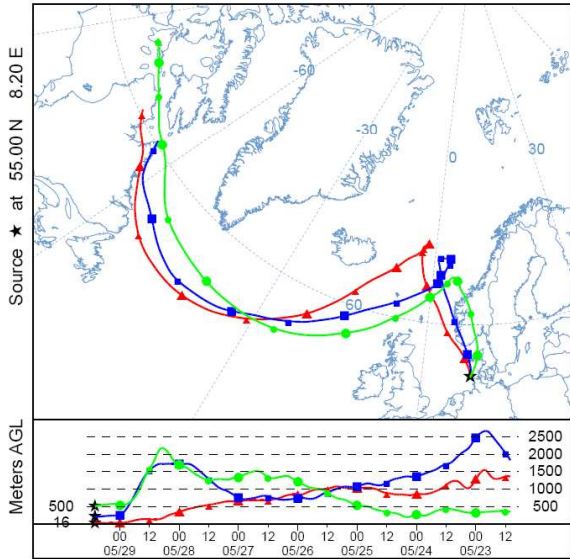
A NOAA HYSPLIT MODEL
Backward trajectories ending at 1000 UTC 29 May 09
GDAS Meteorological Data



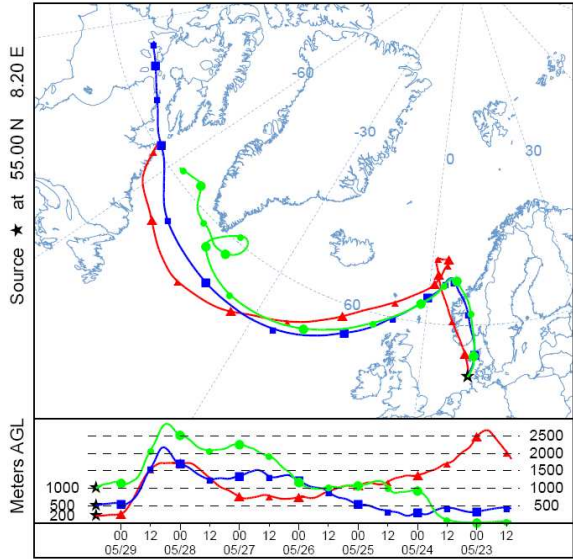
B NOAA HYSPLIT MODEL
Backward trajectories ending at 1000 UTC 29 May 09
GDAS Meteorological Data



C NOAA HYSPLIT MODEL
Backward trajectories ending at 1000 UTC 29 May 09
GDAS Meteorological Data

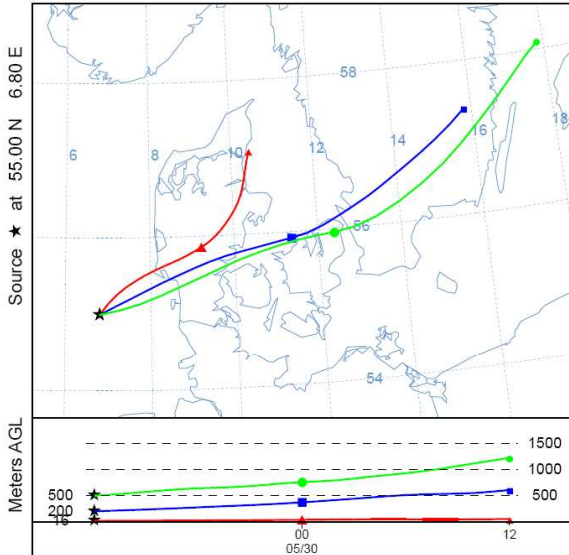


D NOAA HYSPLIT MODEL
Backward trajectories ending at 1000 UTC 29 May 09
GDAS Meteorological Data

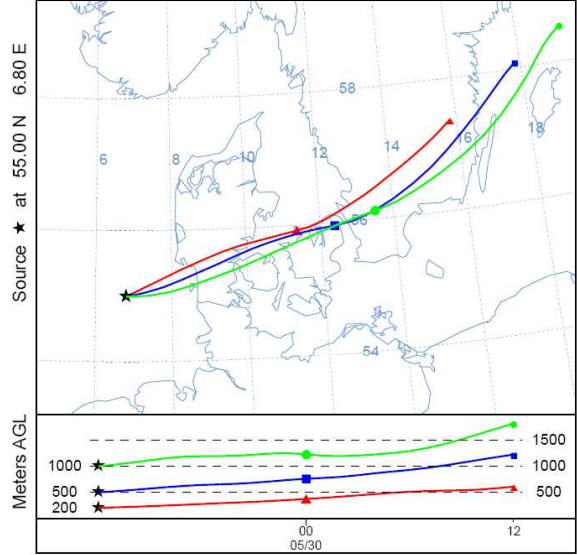


A4 Figure 14: Air mass backward trajectories of the air sample 09AT 5; (A) 24 h, 16 m, 200 m, 500 m arrival height; (B) 24 h; 200 m, 500 m, 1000 m arrival height; (C) 168 h; 16 m, 200 m, 500 m arrival height; (D) 168 h; 200 m, 500 m, 1000 m arrival height

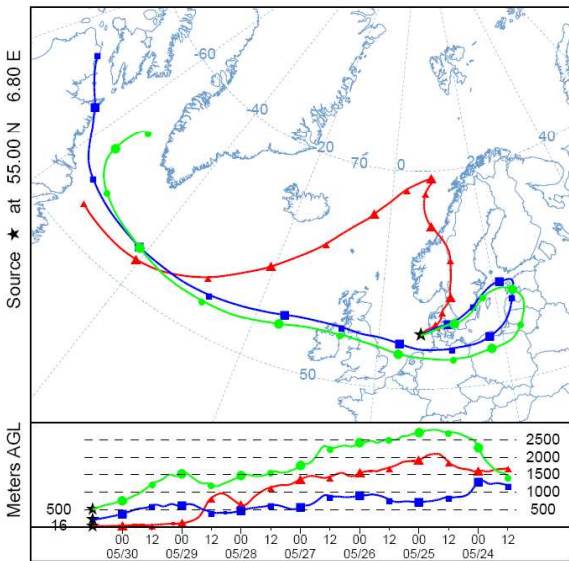
A NOAA HYSPLIT MODEL
Backward trajectories ending at 1200 UTC 30 May 09
GDAS Meteorological Data



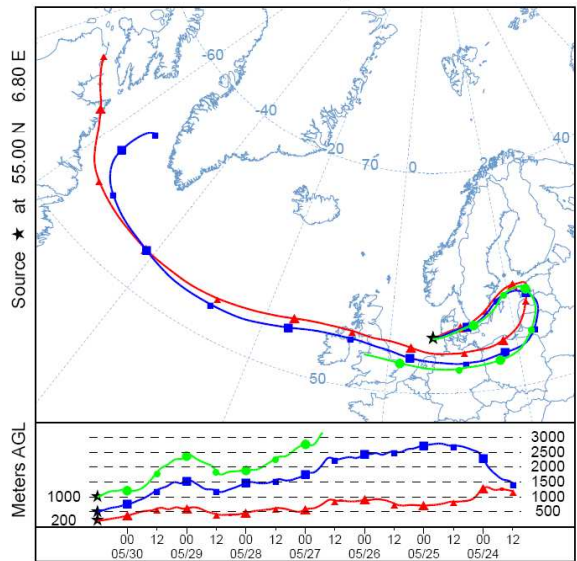
B NOAA HYSPLIT MODEL
Backward trajectories ending at 1200 UTC 30 May 09
GDAS Meteorological Data



C NOAA HYSPLIT MODEL
Backward trajectories ending at 1200 UTC 30 May 09
GDAS Meteorological Data

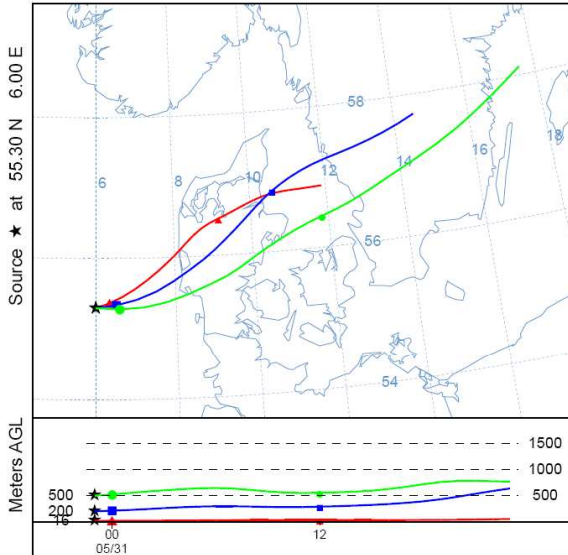


D NOAA HYSPLIT MODEL
Backward trajectories ending at 1200 UTC 30 May 09
GDAS Meteorological Data

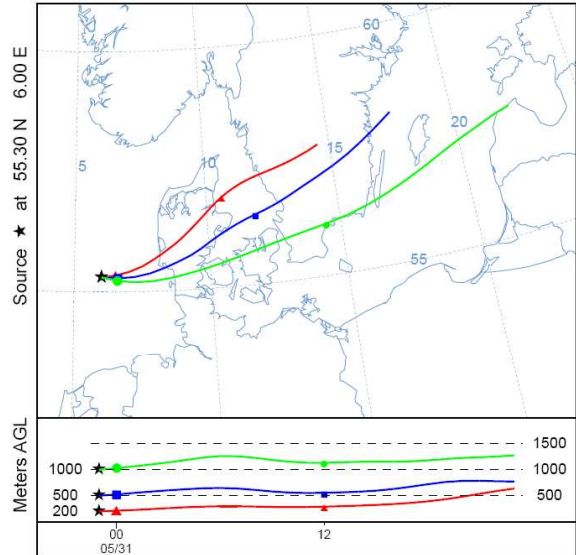


A4 Figure 15: Air mass backward trajectories of the air sample 09AT 7; (A) 24 h, 16 m, 200 m, 500 m arrival height; (B) 24 h; 200 m, 500 m, 1000 m arrival height; (C) 168 h; 16 m, 200 m, 500 m arrival height; (D) 168 h; 200 m, 500 m, 1000 m arrival height

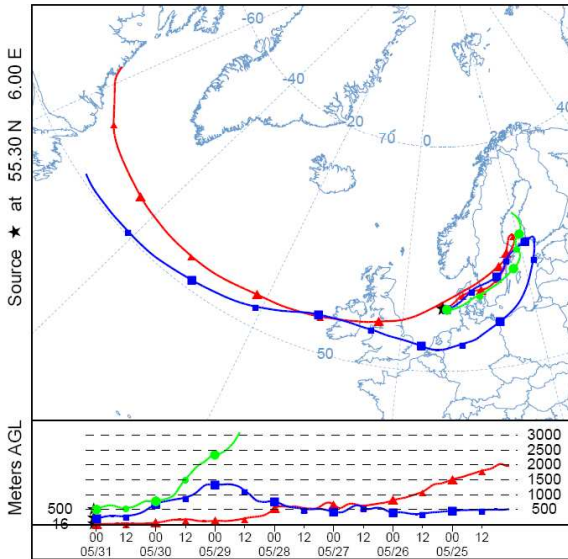
A NOAA HYSPLIT MODEL
Backward trajectories ending at 0100 UTC 31 May 09
GDAS Meteorological Data



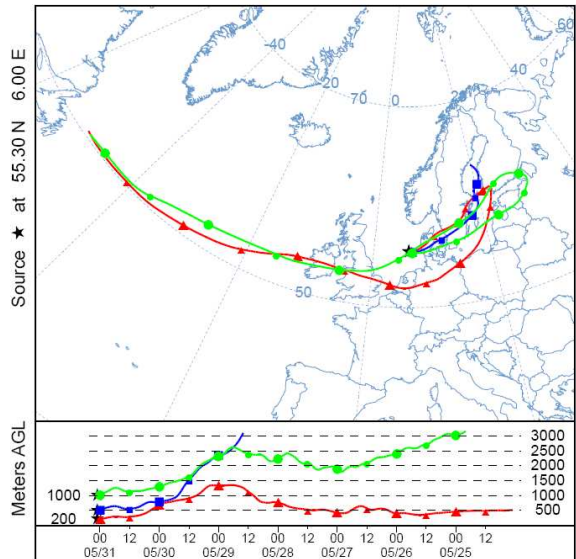
B NOAA HYSPLIT MODEL
Backward trajectories ending at 0100 UTC 31 May 09
GDAS Meteorological Data



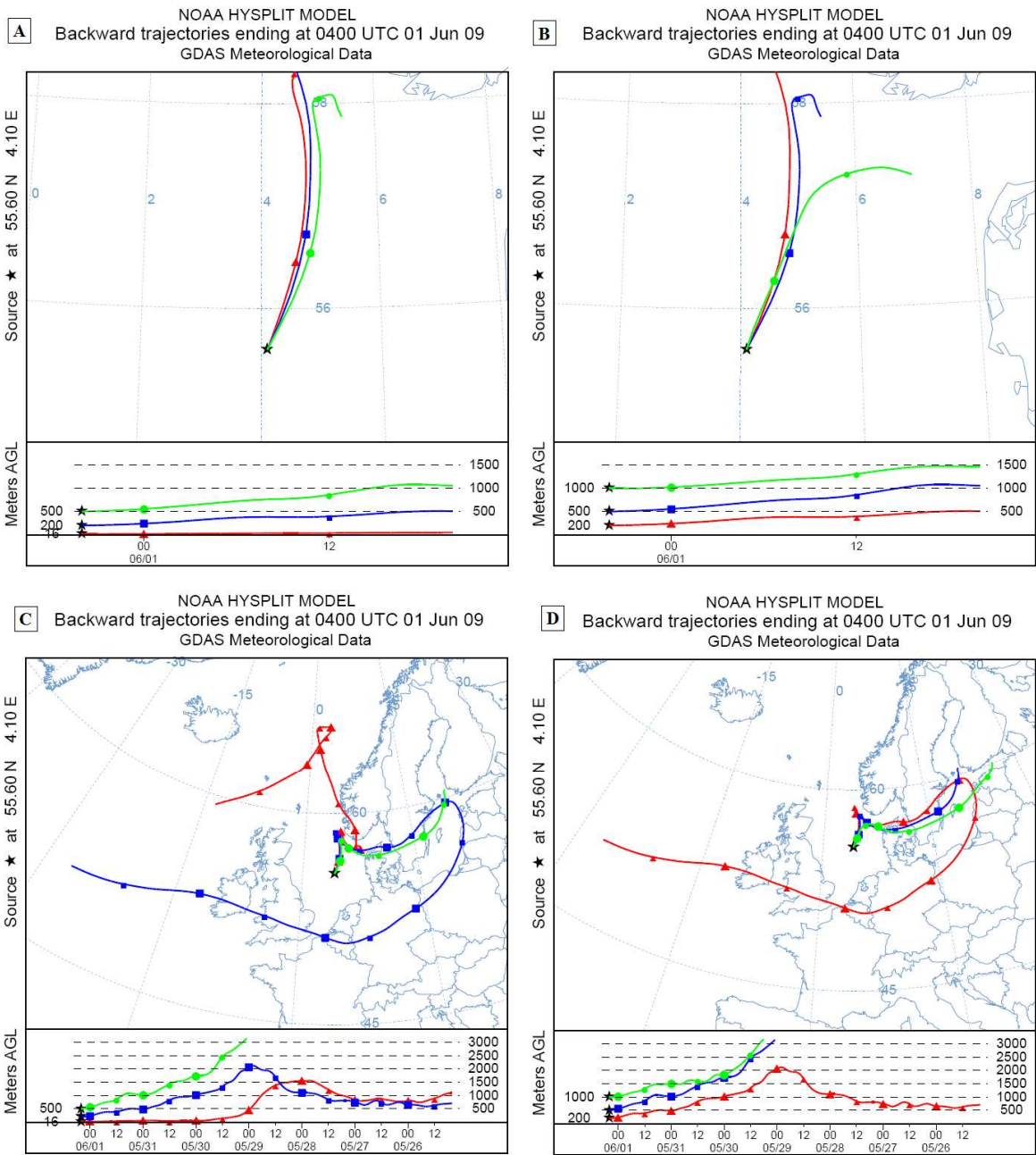
C NOAA HYSPLIT MODEL
Backward trajectories ending at 0100 UTC 31 May 09
GDAS Meteorological Data



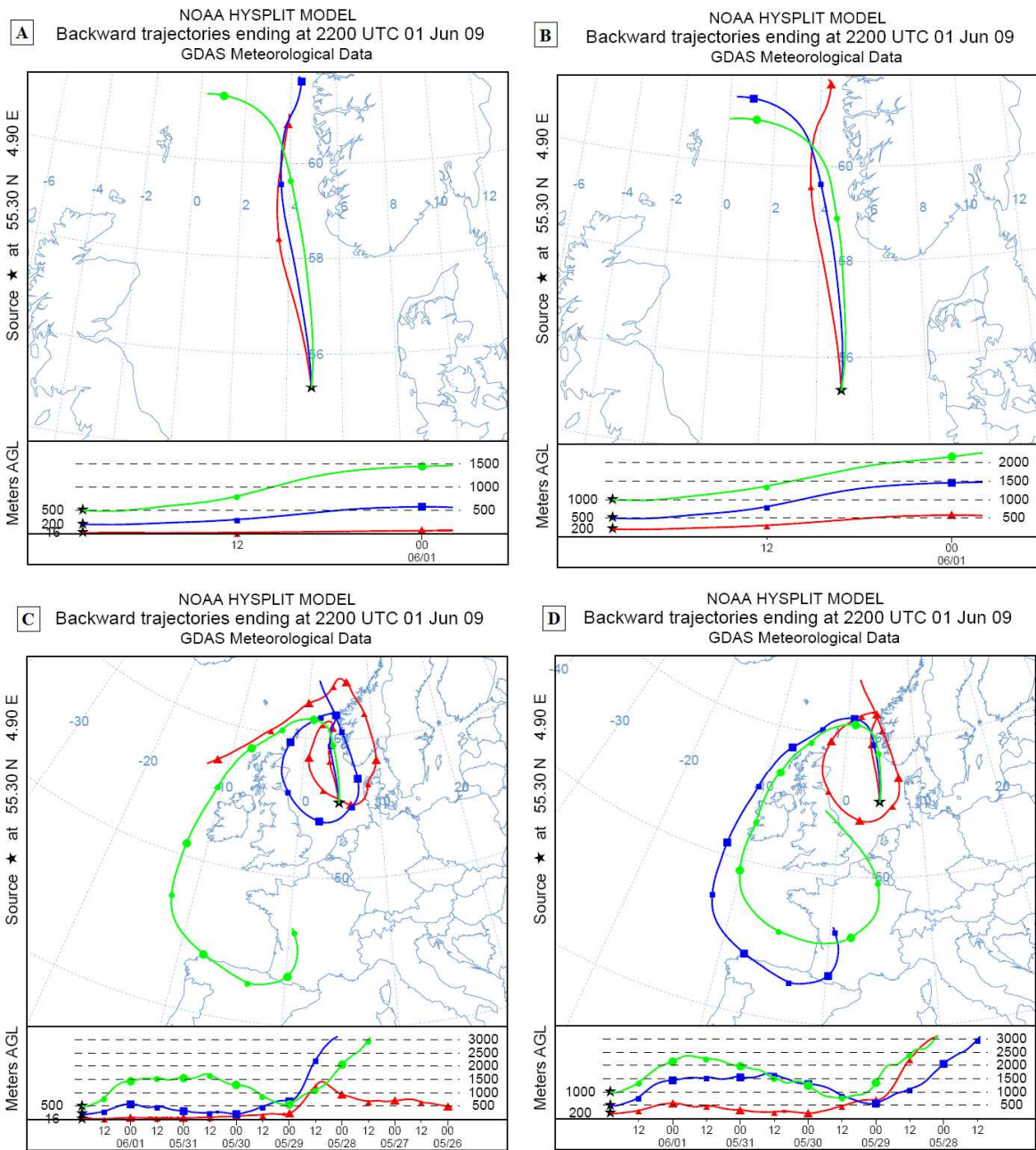
D NOAA HYSPLIT MODEL
Backward trajectories ending at 0100 UTC 31 May 09
GDAS Meteorological Data



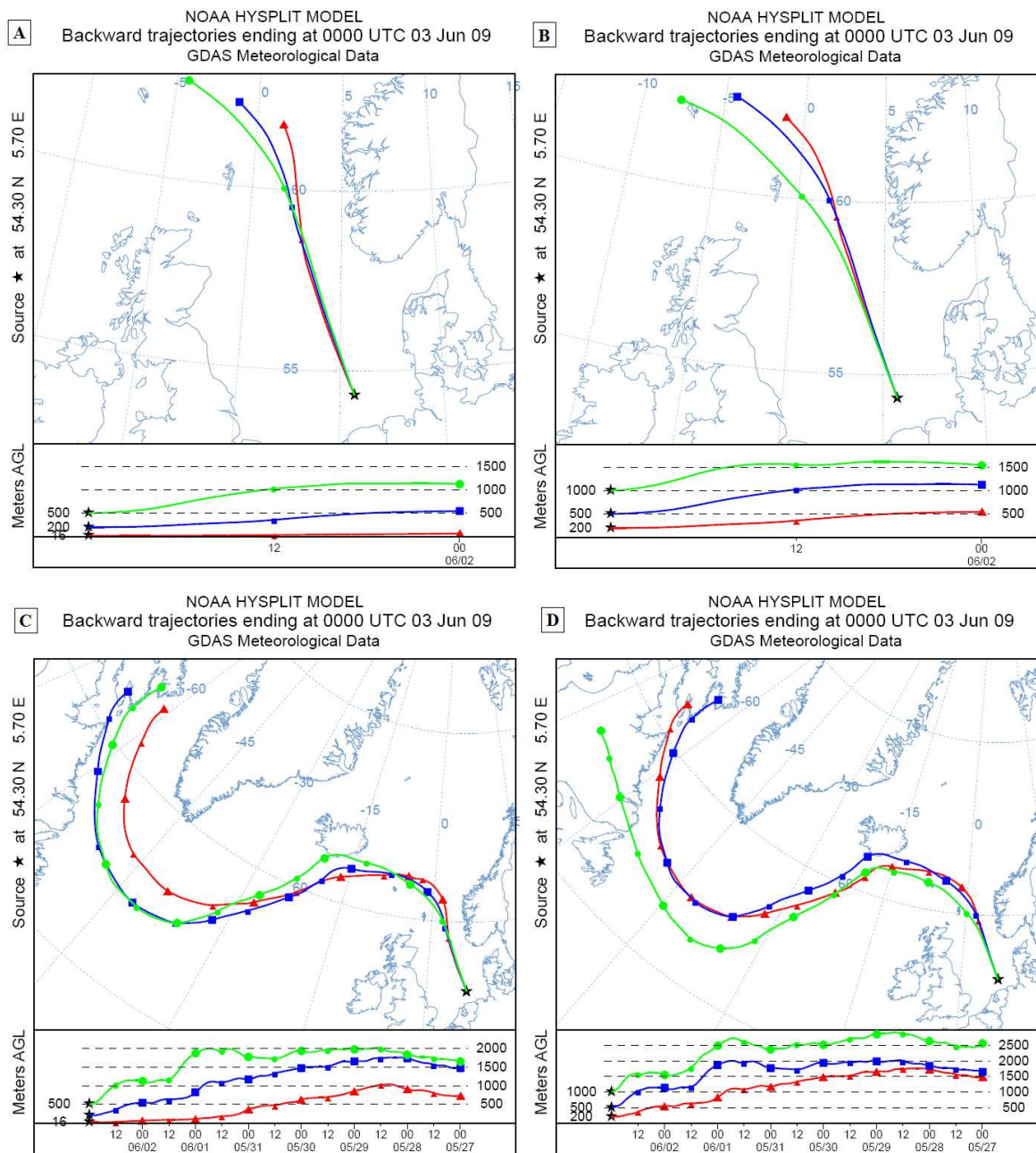
A4 Figure 16: Air mass backward trajectories of the air sample 09AT 8; (A) 24 h, 16 m, 200 m, 500 m arrival height; (B) 24 h; 200 m, 500 m, 1000 m arrival height; (C) 168 h; 16 m, 200 m, 500 m arrival height; (D) 168 h; 200 m, 500 m, 1000 m arrival height



A4 Figure 17: Air mass backward trajectories of the air sample 09AT 9; (A) 24 h, 16 m, 200 m, 500 m arrival height; (B) 24 h; 200 m, 500 m, 1000 m arrival height; (C) 168 h; 16 m, 200 m, 500 m arrival height; (D) 168 h; 200 m, 500 m, 1000 m arrival height

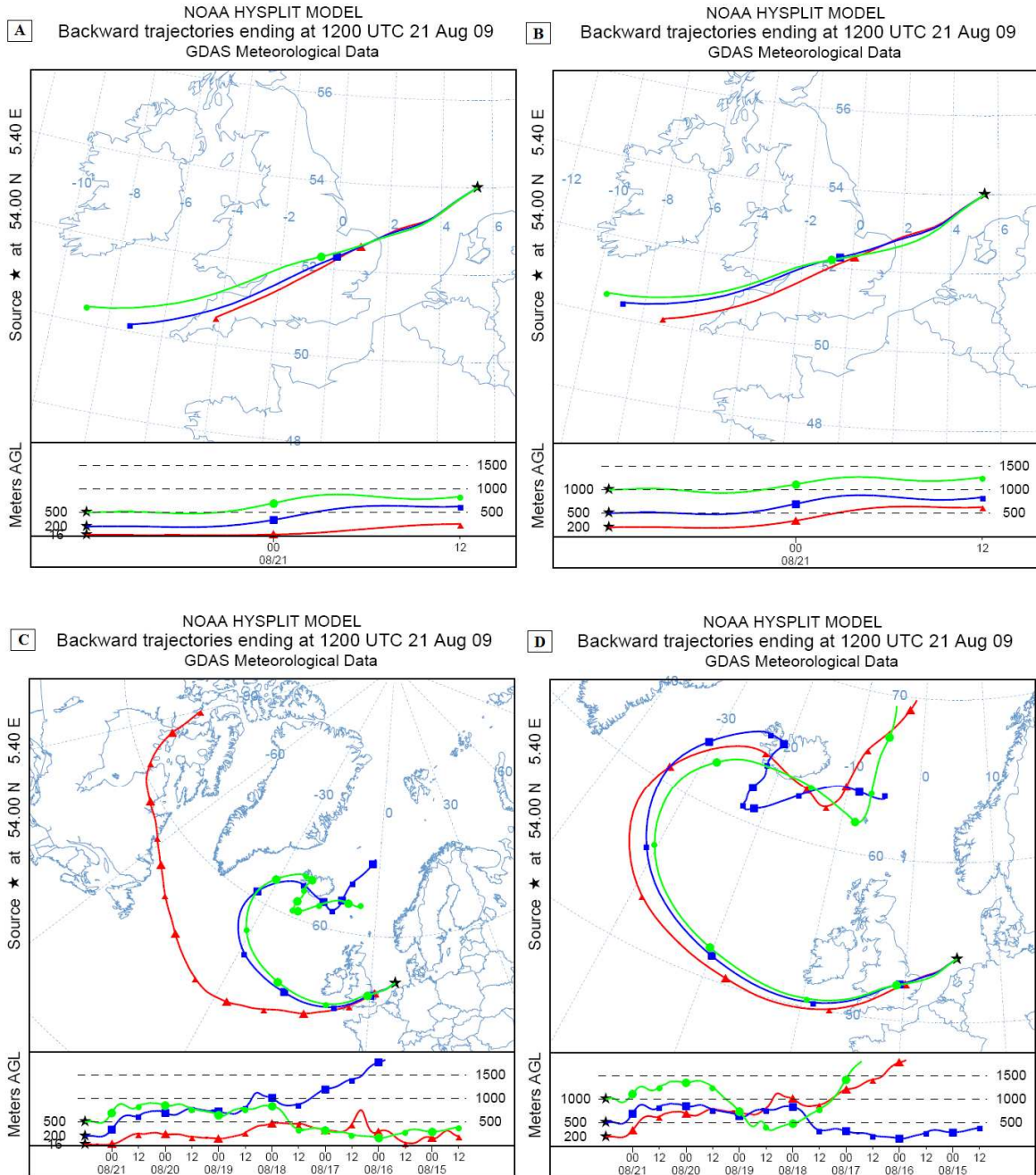


A4 Figure 18: Air mass backward trajectories of the air sample 09AT 11; (A) 24 h, 16 m, 200 m, 500 m arrival height; (B) 24 h; 200 m, 500 m, 1000 m arrival height; (C) 168 h; 16 m, 200 m, 500 m arrival height; (D) 72 h; 200 m, 500 m, 1000 m arrival height



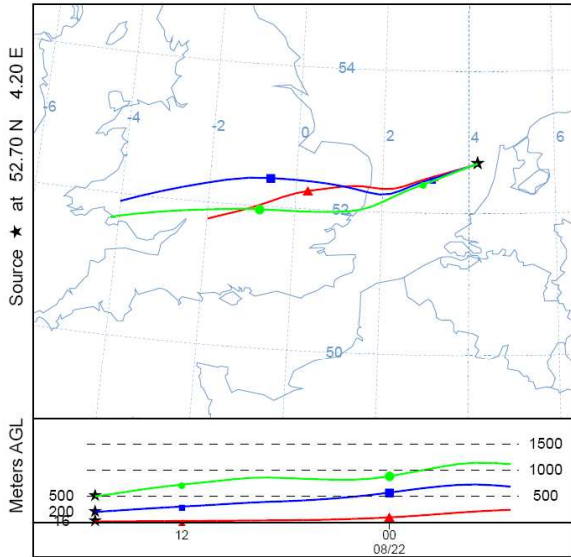
A4 Figure 19: Air mass backward trajectories of the air sample 09AT 12; (A) 24 h, 16 m, 200 m, 500 m arrival height; (B) 24 h; 200 m, 500 m, 1000 m arrival height; (C) 168 h; 16 m, 200 m, 500 m arrival height; (D) 168 h; 200 m, 500 m, 1000 m arrival height

Air mass backward trajectories of air samples collected during the research cruise in the North Sea in Aug./Sep. 2009

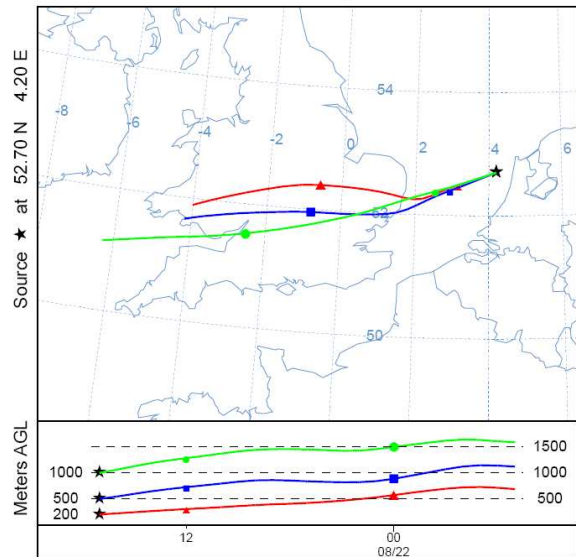


A4 Figure 20: Air mass backward trajectories of the air sample PE 1; (A) 24 h, 16 m, 200 m, 500 m arrival height; (B) 24 h; 200 m, 500 m, 1000 m arrival height; (C) 168 h; 16 m, 200 m, 500 m arrival height; (D) 168 h; 200 m, 500 m, 1000 m arrival height

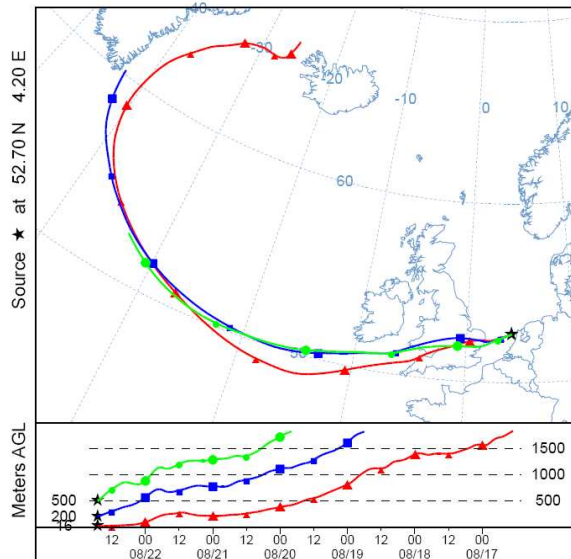
A NOAA HYSPLIT MODEL
Backward trajectories ending at 1700 UTC 22 Aug 09
GDAS Meteorological Data



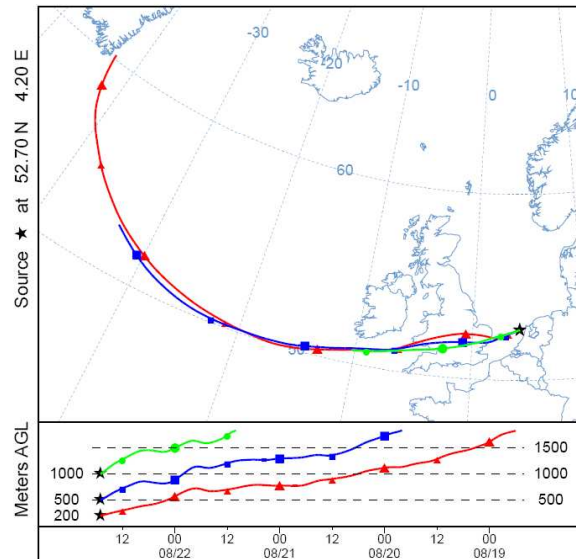
B NOAA HYSPLIT MODEL
Backward trajectories ending at 1700 UTC 22 Aug 09
GDAS Meteorological Data



C NOAA HYSPLIT MODEL
Backward trajectories ending at 1700 UTC 22 Aug 09
GDAS Meteorological Data

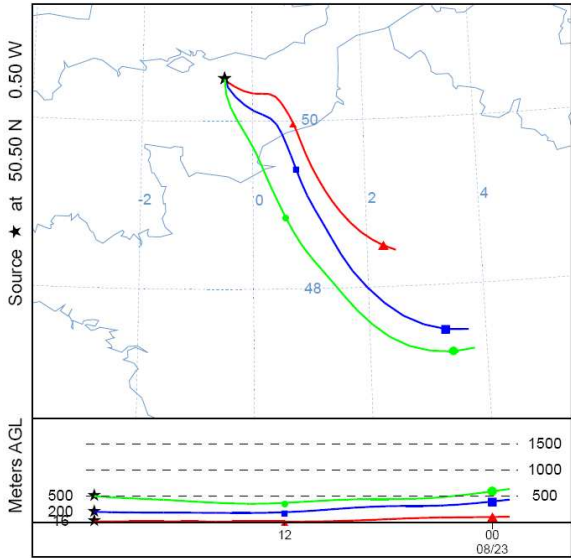


D NOAA HYSPLIT MODEL
Backward trajectories ending at 1700 UTC 22 Aug 09
GDAS Meteorological Data

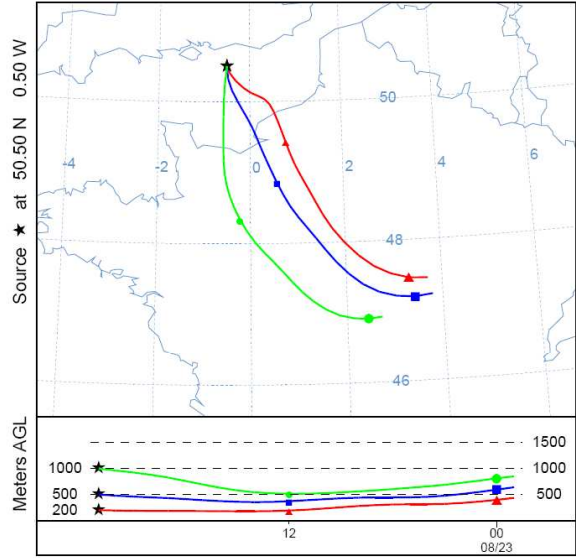


A4 Figure 21: Air mass backward trajectories of the air sample PE 3; (A) 24 h; 16 m, 200 m, 500 m arrival height; (B) 24 h; 200 m, 500 m, 1000 m arrival height; (C) 144 h; 16 m, 200 m, 500 m arrival height; (D) 96 h; 200 m, 500 m, 1000 m arrival height

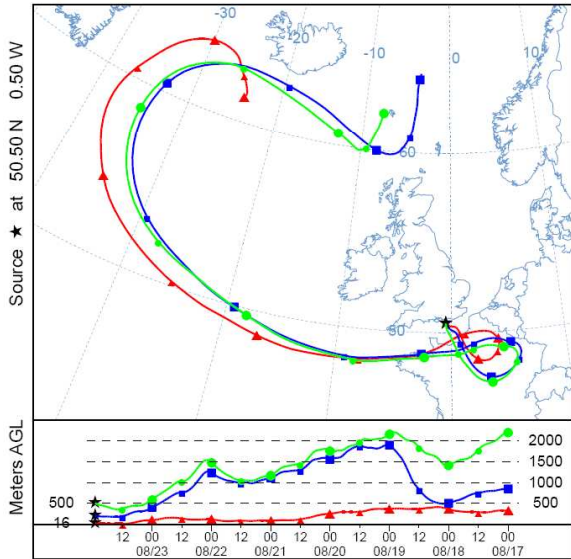
A NOAA HYSPLIT MODEL
Backward trajectories ending at 2300 UTC 23 Aug 09
GDAS Meteorological Data



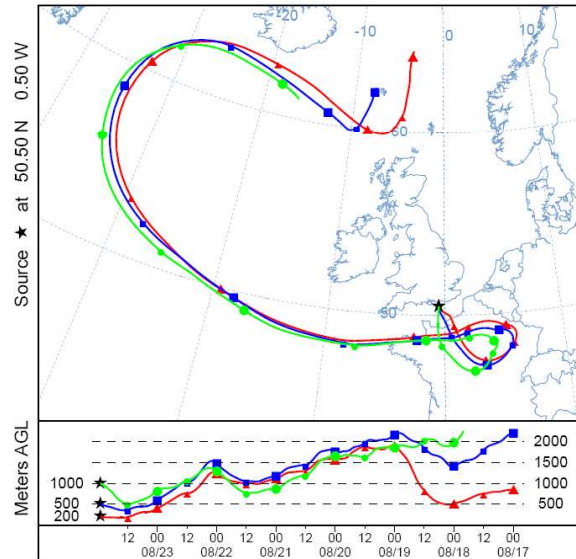
B NOAA HYSPLIT MODEL
Backward trajectories ending at 2300 UTC 23 Aug 09
GDAS Meteorological Data



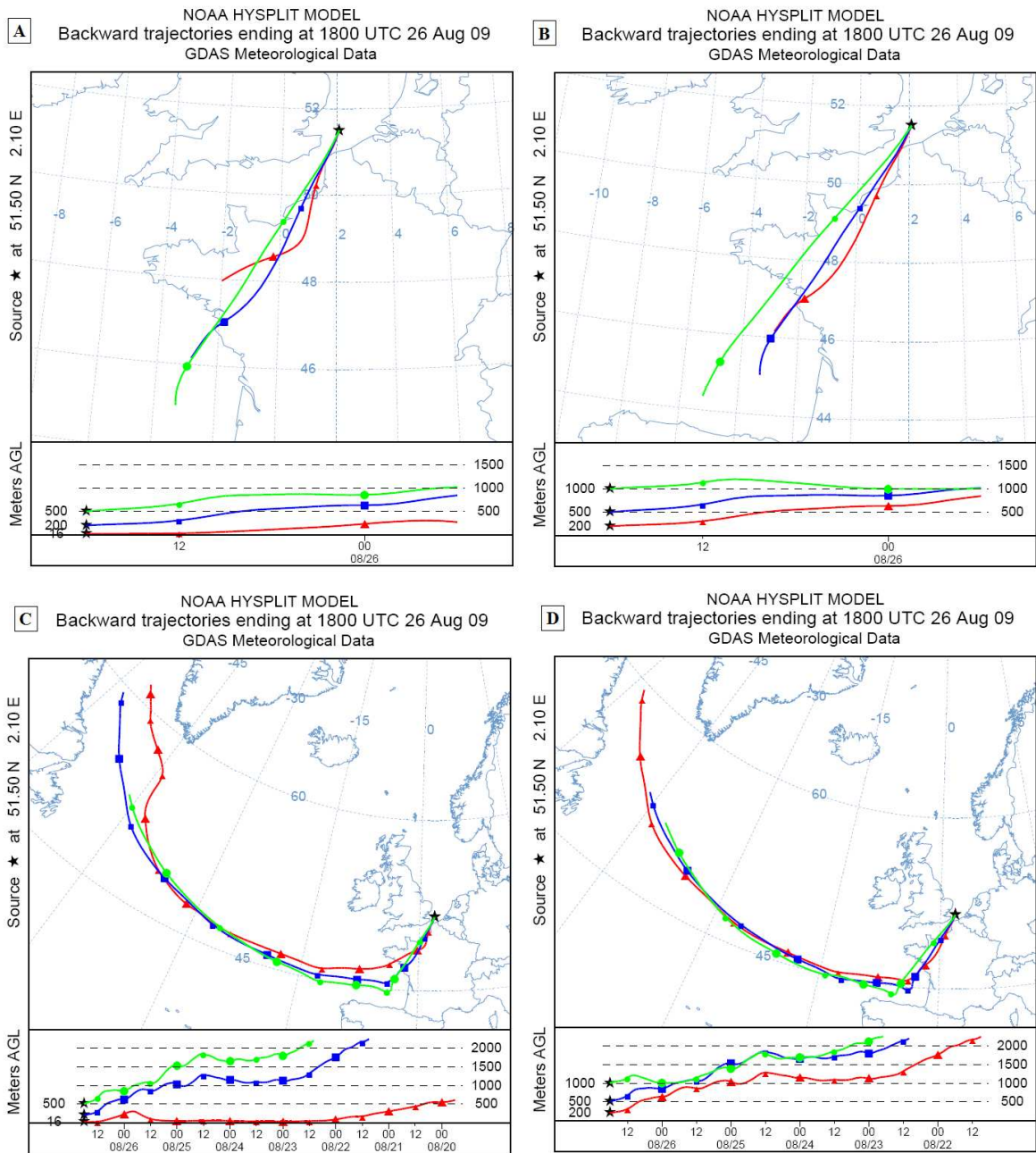
C NOAA HYSPLIT MODEL
Backward trajectories ending at 2300 UTC 23 Aug 09
GDAS Meteorological Data



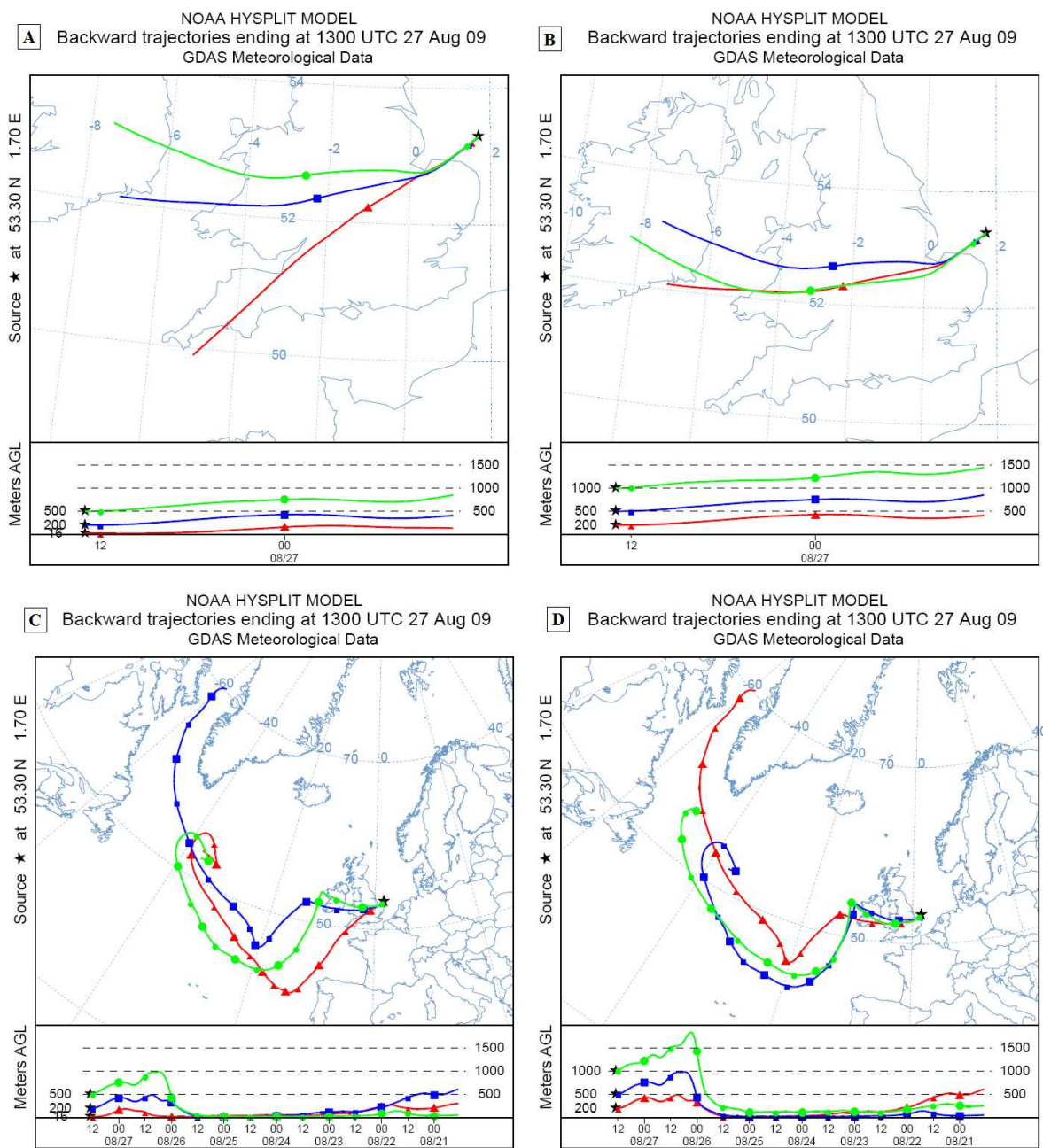
D NOAA HYSPLIT MODEL
Backward trajectories ending at 2300 UTC 23 Aug 09
GDAS Meteorological Data



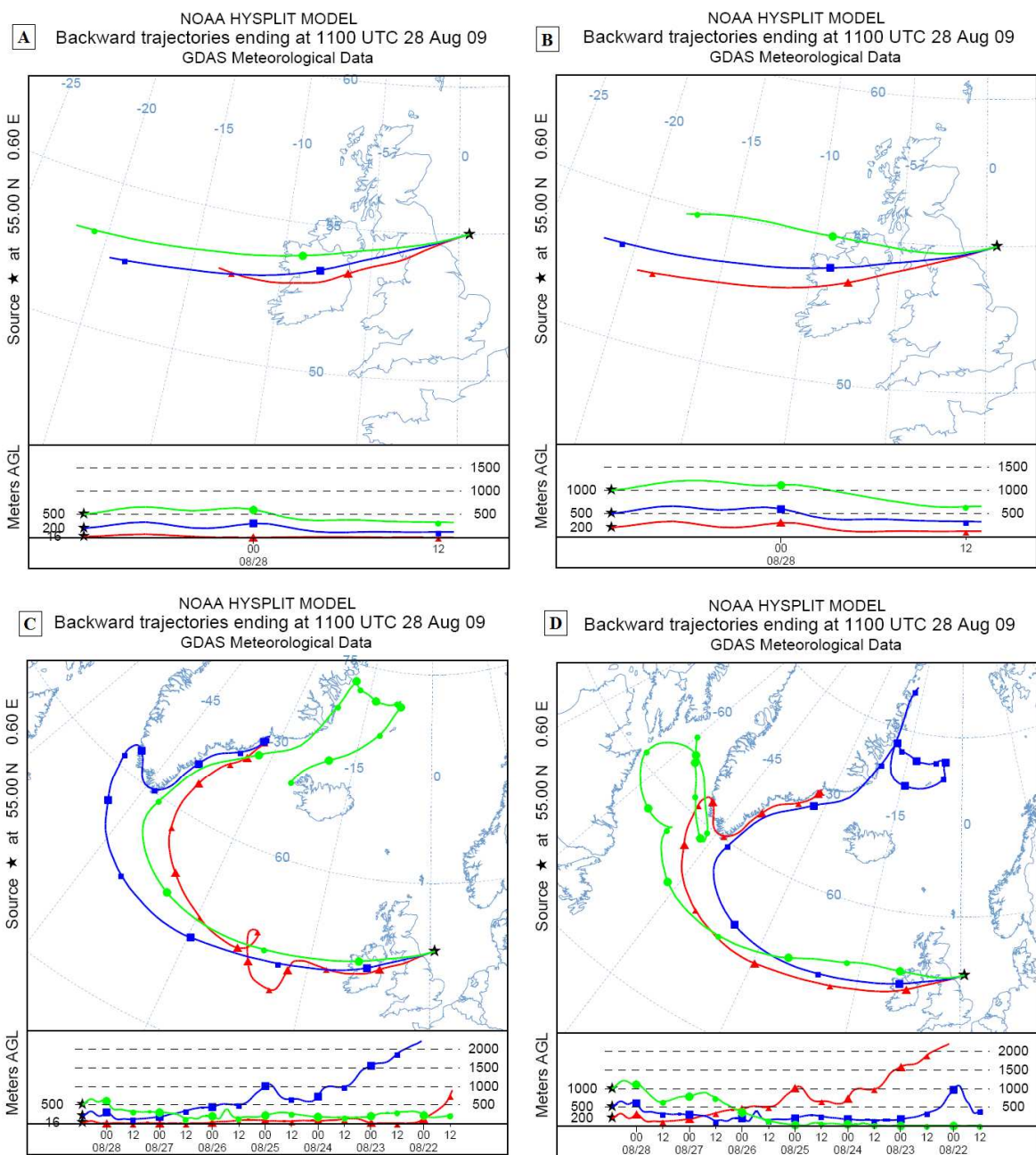
A4 Figure 22: Air mass backward trajectories of the air sample PE 4; (A) 24 h, 16 m, 200 m, 500 m arrival height; (B) 24 h; 200 m, 500 m, 1000 m arrival height; (C) 168 h; 16 m, 200 m, 500 m arrival height; (D) 168 h; 200 m, 500 m, 1000 m arrival height



A4 Figure 23: Air mass backward trajectories of the air sample PE 6; (A) 24 h, 16 m, 200 m, 500 m arrival height; (B) 24 h; 200 m, 500 m, 1000 m arrival height; (C) 168 h; 16 m, 200 m, 500 m arrival height; (D) 132 h; 200 m, 500 m, 1000 m arrival height

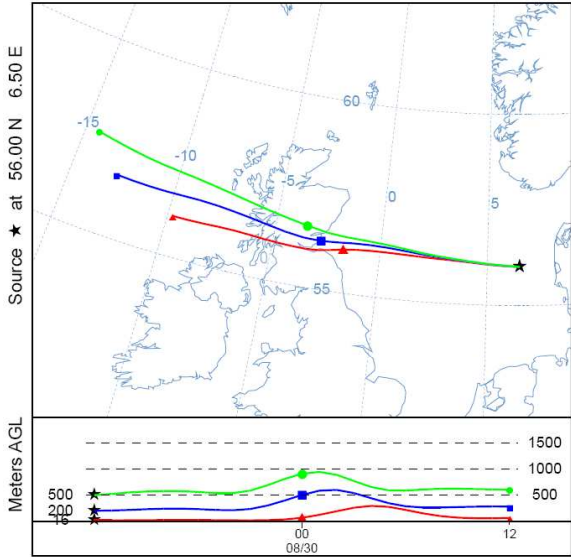


A4 Figure 24: Air mass backward trajectories of the air sample PE 7; (A) 24 h, 16 m, 200 m, 500 m arrival height; (B) 24 h; 200 m, 500 m, 1000 m arrival height; (C) 168 h; 16 m, 200 m, 500 m arrival height; (D) 168 h; 200 m, 500 m, 1000 m arrival height

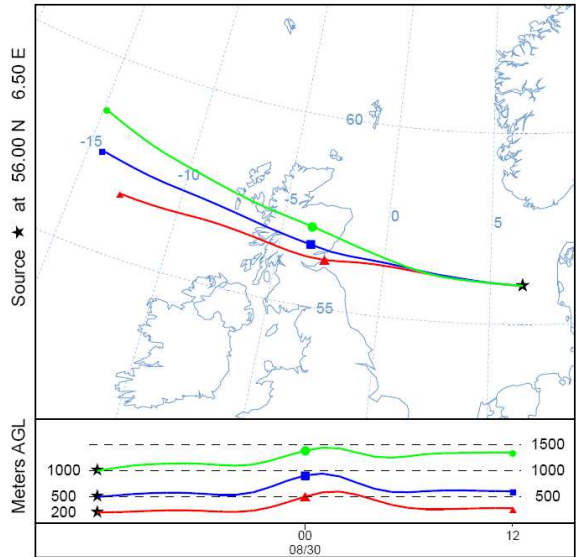


A4 Figure 25: Air mass backward trajectories of the air sample PE 8; (A) 24 h, 16 m, 200 m, 500 m arrival height; (B) 24 h; 200 m, 500 m, 1000 m arrival height; (C) 168 h; 16 m, 200 m, 500 m arrival height; (D) 168 h; 200 m, 500 m, 1000 m arrival height

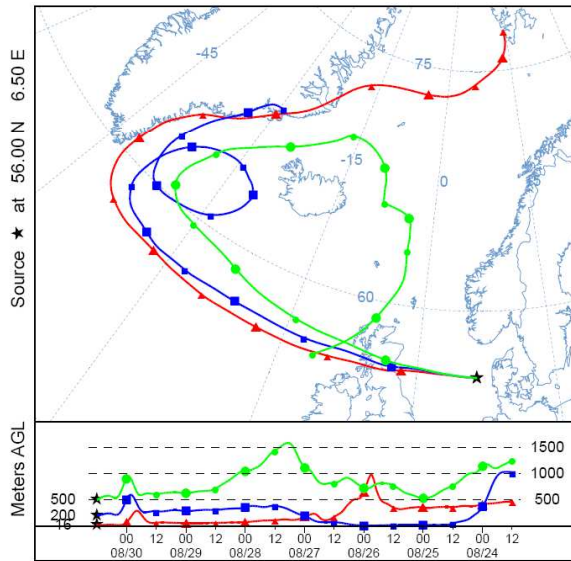
A NOAA HYSPLIT MODEL
Backward trajectories ending at 1200 UTC 30 Aug 09
GDAS Meteorological Data



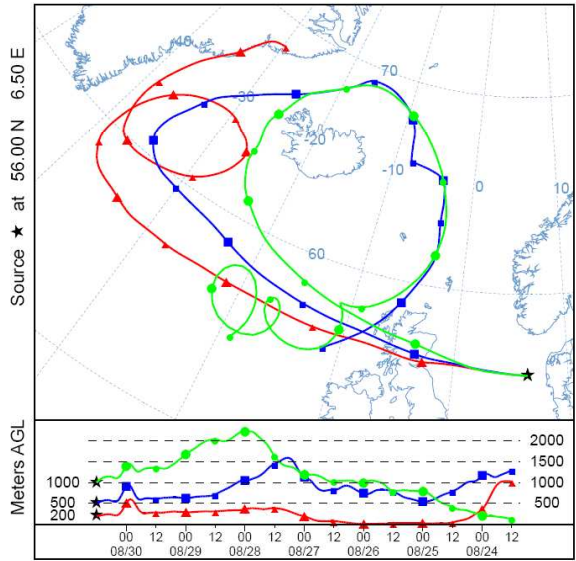
B NOAA HYSPLIT MODEL
Backward trajectories ending at 1200 UTC 30 Aug 09
GDAS Meteorological Data



C NOAA HYSPLIT MODEL
Backward trajectories ending at 1200 UTC 30 Aug 09
GDAS Meteorological Data

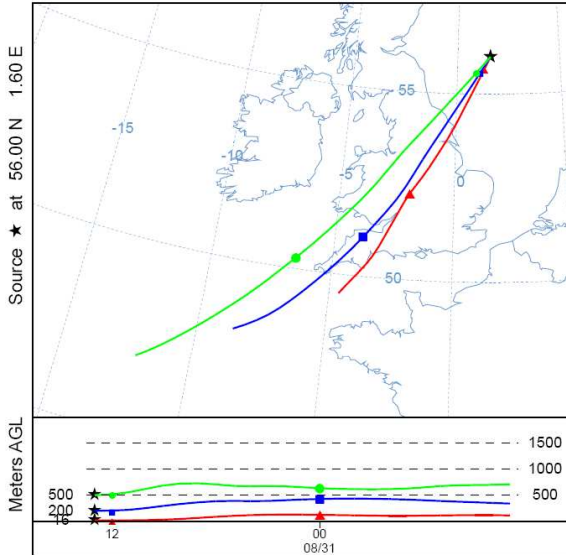


D NOAA HYSPLIT MODEL
Backward trajectories ending at 1200 UTC 30 Aug 09
GDAS Meteorological Data

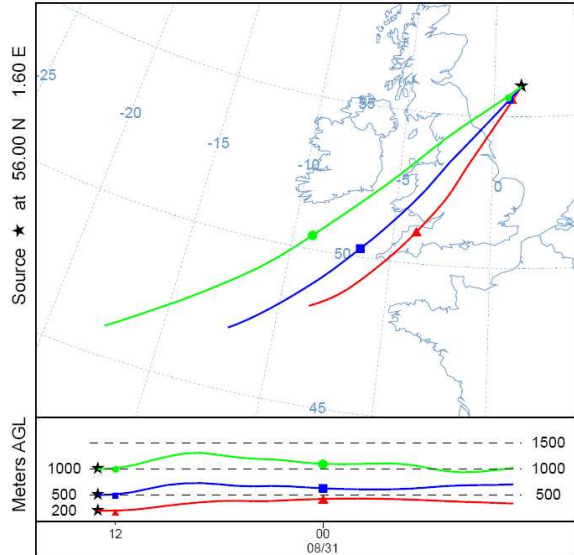


A4 Figure 26: Air mass backward trajectories of the air sample PE 9; (A) 24 h, 16 m, 200 m, 500 m arrival height; (B) 24 h; 200 m, 500 m, 1000 m arrival height; (C) 168 h; 16 m, 200 m, 500 m arrival height; (D) 168 h; 200 m, 500 m, 1000 m arrival height

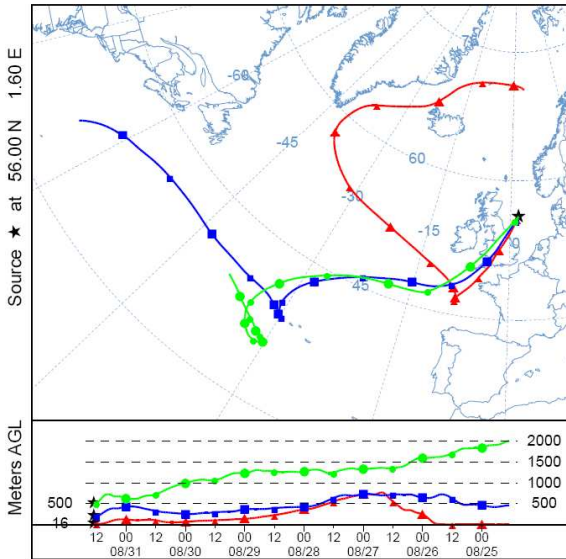
A NOAA HYSPLIT MODEL
Backward trajectories ending at 1300 UTC 31 Aug 09
GDAS Meteorological Data



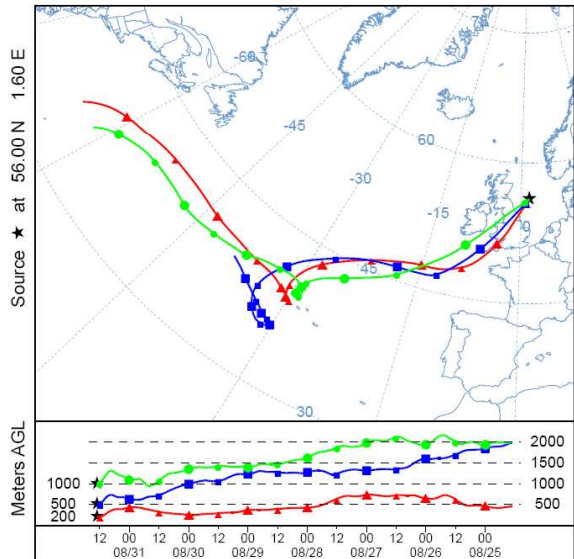
B NOAA HYSPLIT MODEL
Backward trajectories ending at 1300 UTC 31 Aug 09
GDAS Meteorological Data



C NOAA HYSPLIT MODEL
Backward trajectories ending at 1300 UTC 31 Aug 09
GDAS Meteorological Data

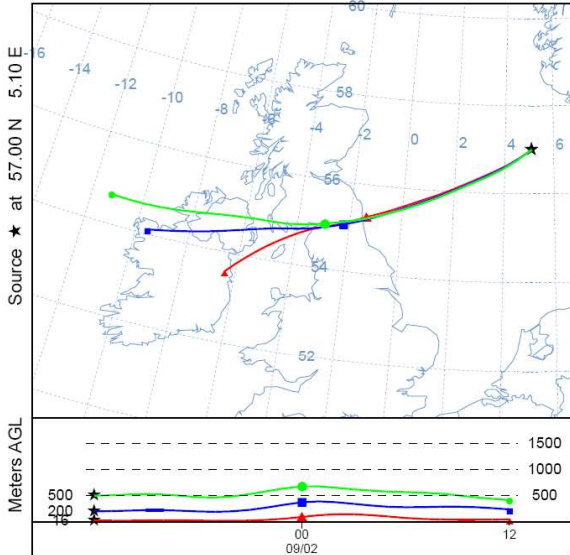


D NOAA HYSPLIT MODEL
Backward trajectories ending at 1300 UTC 31 Aug 09
GDAS Meteorological Data

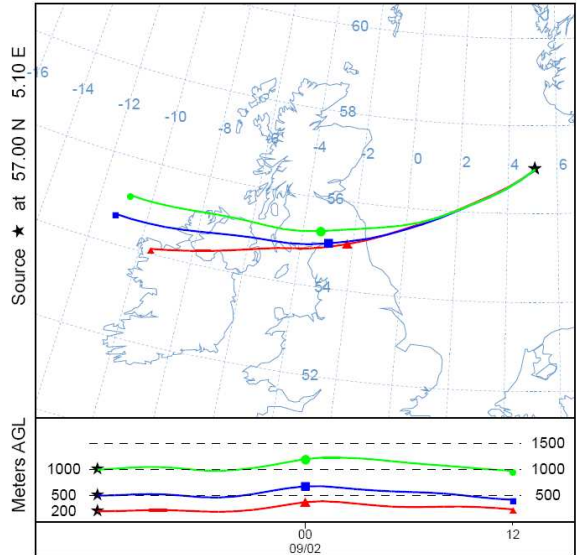


A4 Figure 27: Air mass backward trajectories of the air sample PE 10; (A) 24 h, 16 m, 200 m, 500 m arrival height; (B) 24 h; 200 m, 500 m, 1000 m arrival height; (C) 168 h; 16 m, 200 m, 500 m arrival height; (D) 168 h; 200 m, 500 m, 1000 m arrival height

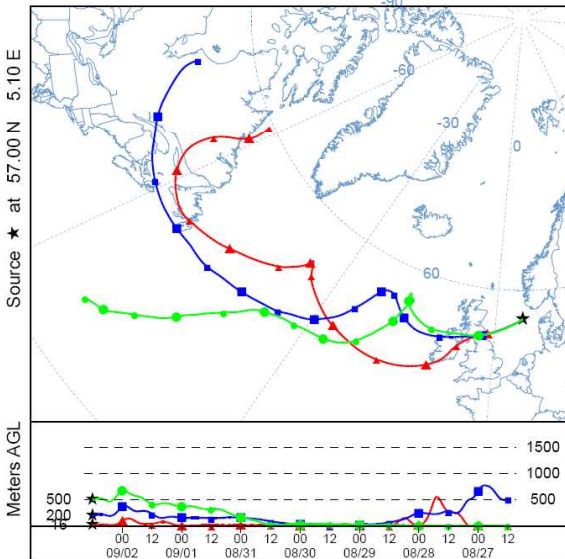
A NOAA HYSPLIT MODEL
Backward trajectories ending at 1200 UTC 02 Sep 09
GDAS Meteorological Data



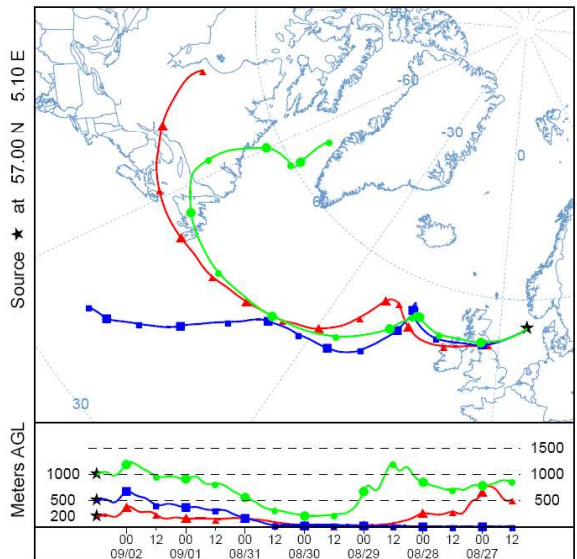
B NOAA HYSPLIT MODEL
Backward trajectories ending at 1200 UTC 02 Sep 09
GDAS Meteorological Data



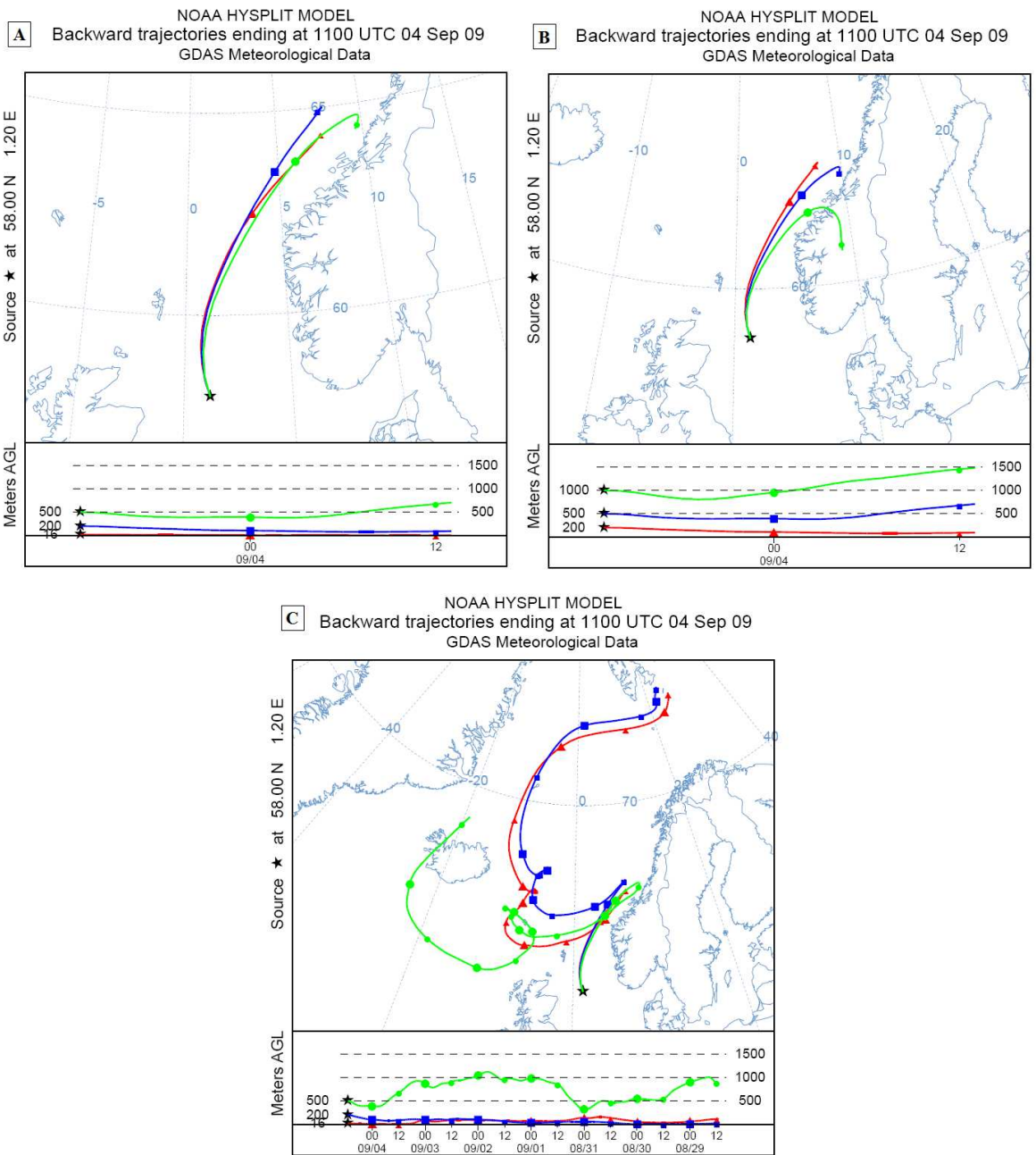
C NOAA HYSPLIT MODEL
Backward trajectories ending at 1200 UTC 02 Sep 09
GDAS Meteorological Data



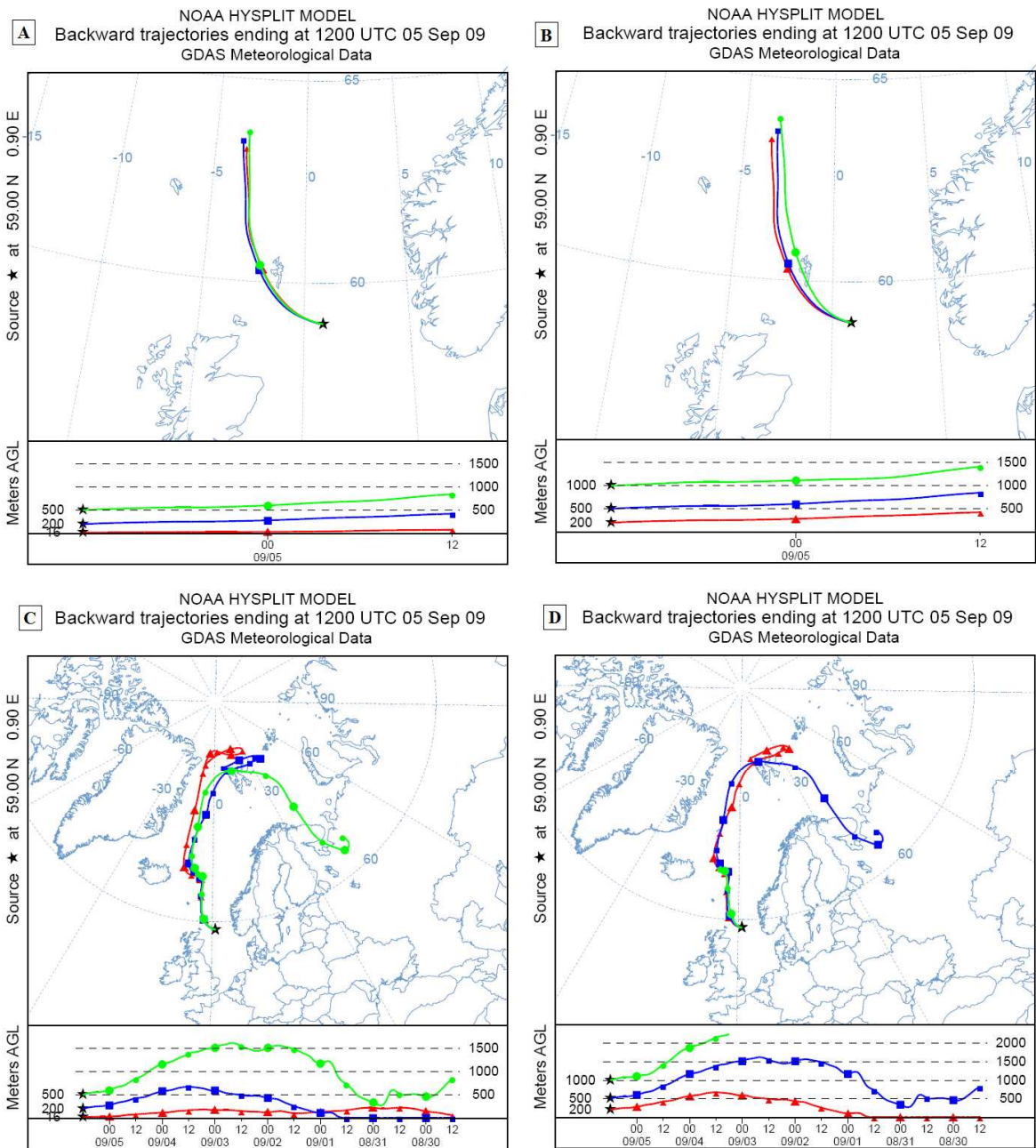
D NOAA HYSPLIT MODEL
Backward trajectories ending at 1200 UTC 02 Sep 09
GDAS Meteorological Data



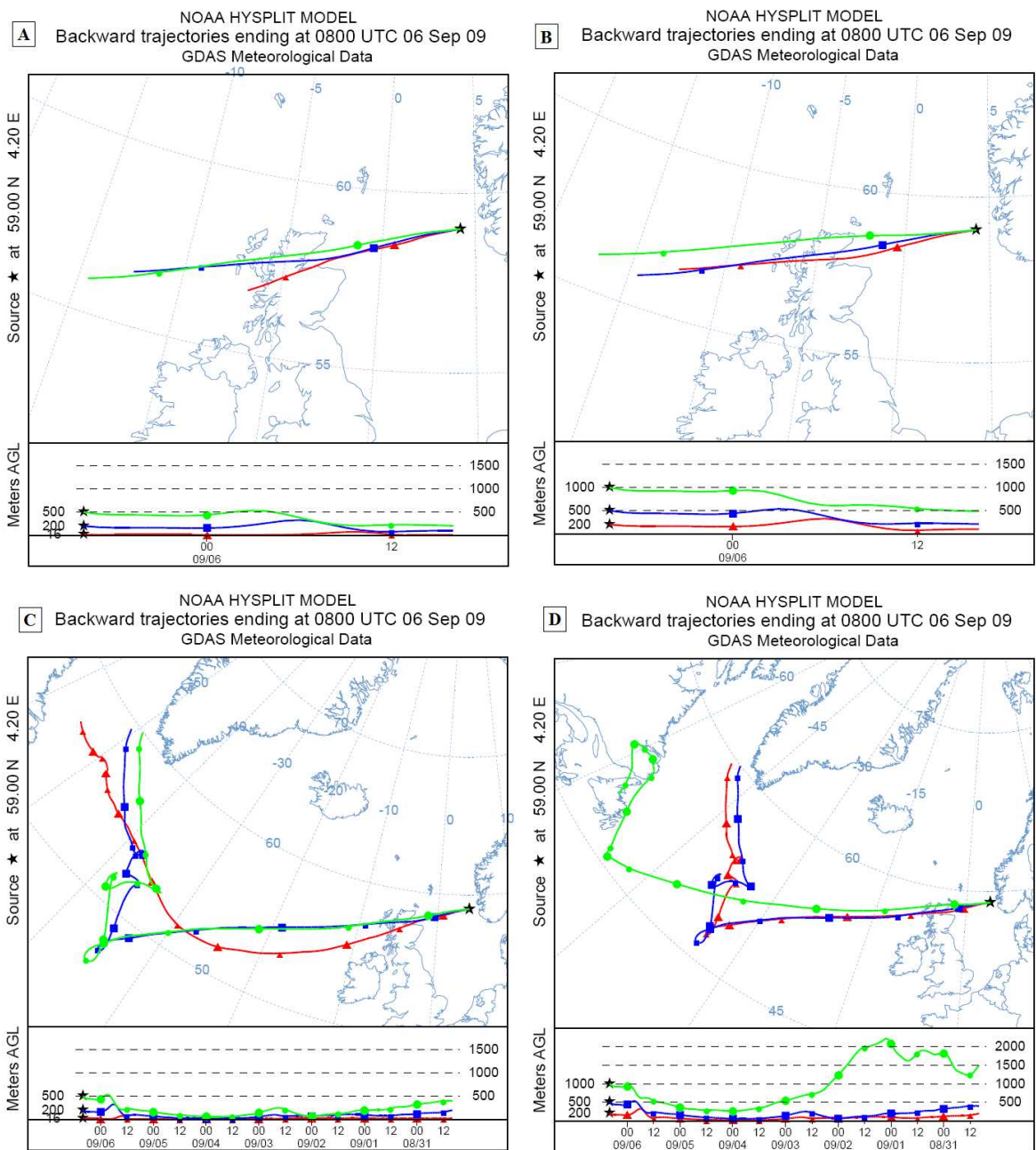
A4 Figure 28: Air mass backward trajectories of the air sample PE 11; (A) 24 h, 16 m, 200 m, 500 m arrival height; (B) 24 h; 200 m, 500 m, 1000 m arrival height; (C) 168 h; 16 m, 200 m, 500 m arrival height; (D) 168 h; 200 m, 500 m, 1000 m arrival height



A4 Figure 29: Air mass backward trajectories of the air sample PE 15; (A) 24 h, 16 m, 200 m, 500 m arrival height; (B) 24 h; 200 m, 500 m, 1000 m arrival height; (C) 168 h; 16 m, 200 m, 500 m arrival height

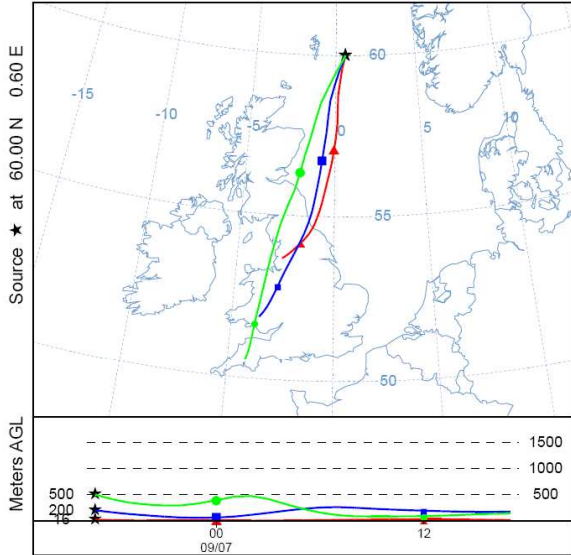


A4 Figure 30: Air mass backward trajectories of the air sample PE 16; (A) 24 h, 16 m, 200 m, 500 m arrival height; (B) 24 h; 200 m, 500 m, 1000 m arrival height; (C) 168 h; 16 m, 200 m, 500 m arrival height; (D) 168 h; 200 m, 500 m, 1000 m arrival height

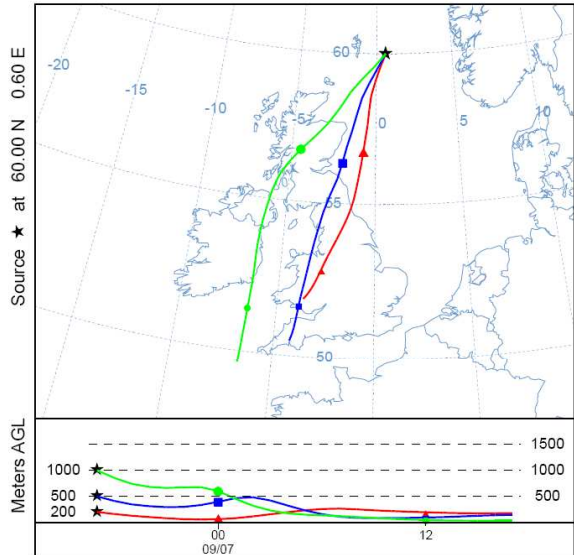


A4 Figure 31: Air mass backward trajectories of the air sample PE 17; (A) 24 h, 16 m, 200 m, 500 m arrival height; (B) 24 h; 200 m, 500 m, 1000 m arrival height; (C) 168 h; 16 m, 200 m, 500 m arrival height; (D) 168 h; 200 m, 500 m, 1000 m arrival height

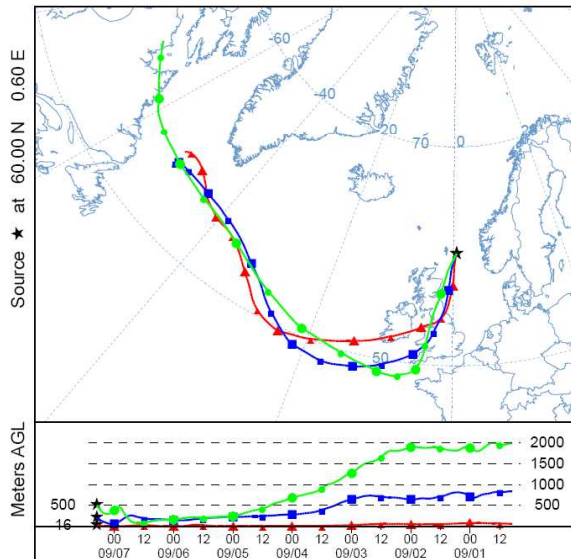
A NOAA HYSPLIT MODEL
Backward trajectories ending at 0700 UTC 07 Sep 09
GDAS Meteorological Data



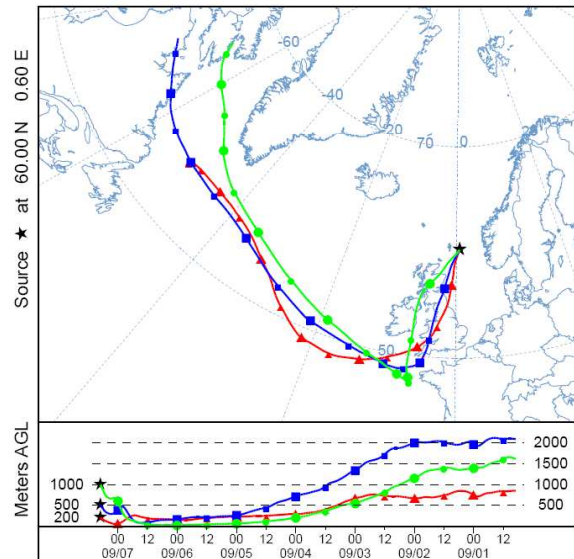
B NOAA HYSPLIT MODEL
Backward trajectories ending at 0700 UTC 07 Sep 09
GDAS Meteorological Data



C NOAA HYSPLIT MODEL
Backward trajectories ending at 0700 UTC 07 Sep 09
GDAS Meteorological Data

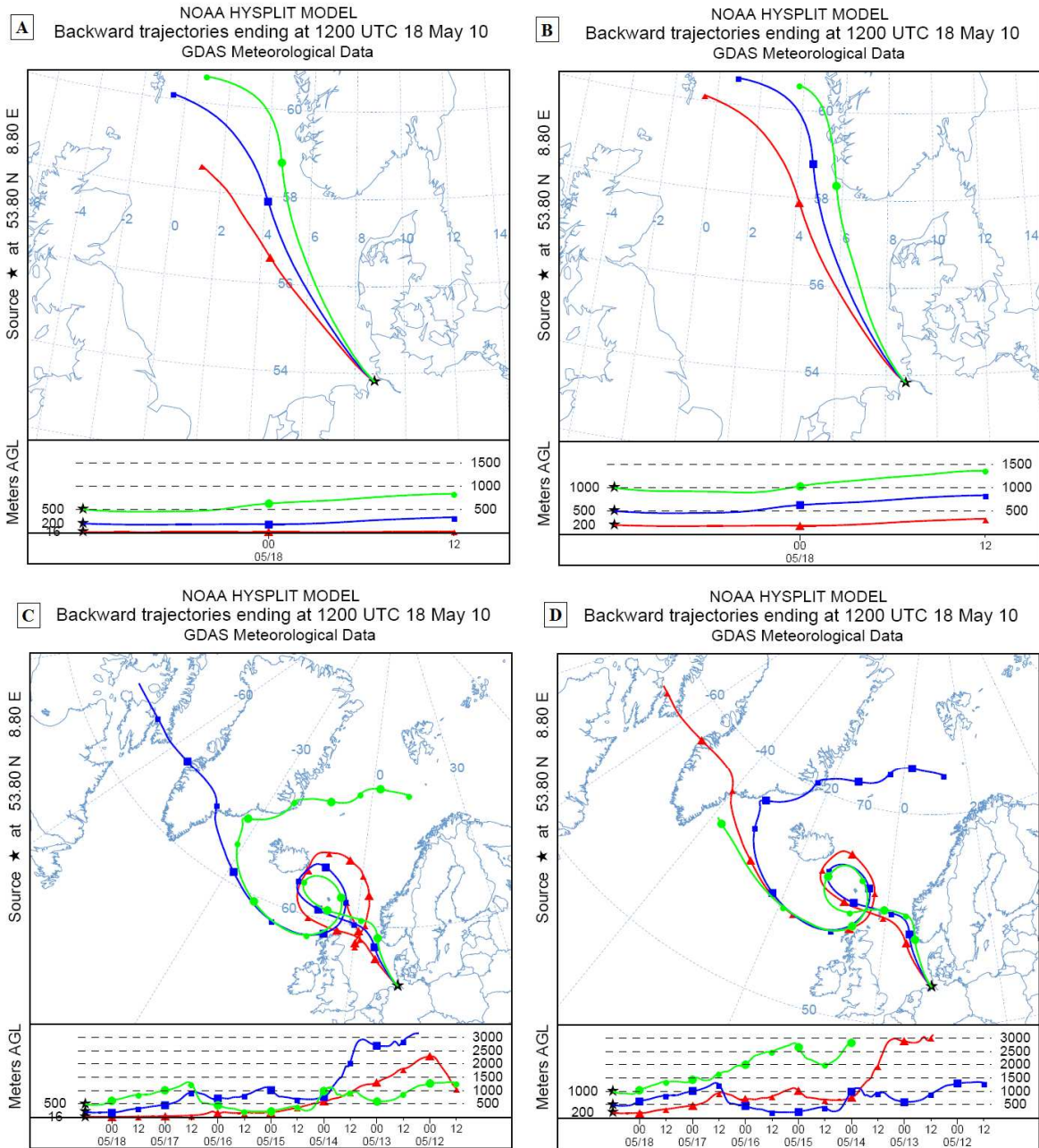


D NOAA HYSPLIT MODEL
Backward trajectories ending at 0700 UTC 07 Sep 09
GDAS Meteorological Data



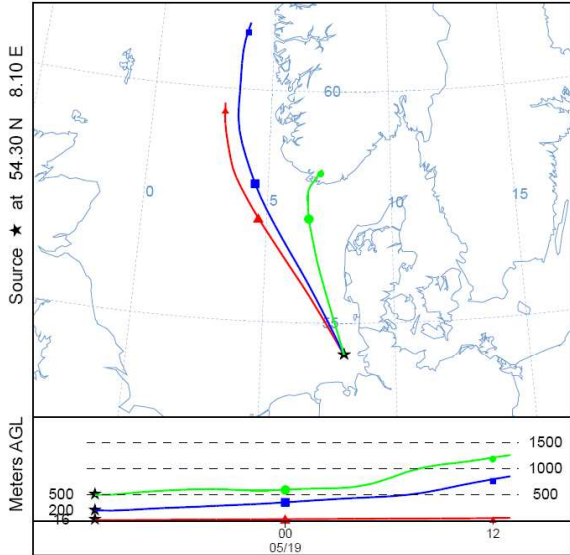
A4 Figure 32: Air mass backward trajectories of the air sample PE 18; (A) 24 h, 16 m, 200 m, 500 m arrival height; (B) 24 h; 200 m, 500 m, 1000 m arrival height; (C) 168 h; 16 m, 200 m, 500 m arrival height; (D) 168 h; 200 m, 500 m, 1000 m arrival height

Air mass backward trajectories of air samples collected during the research cruise in the German EEZ in May 2010

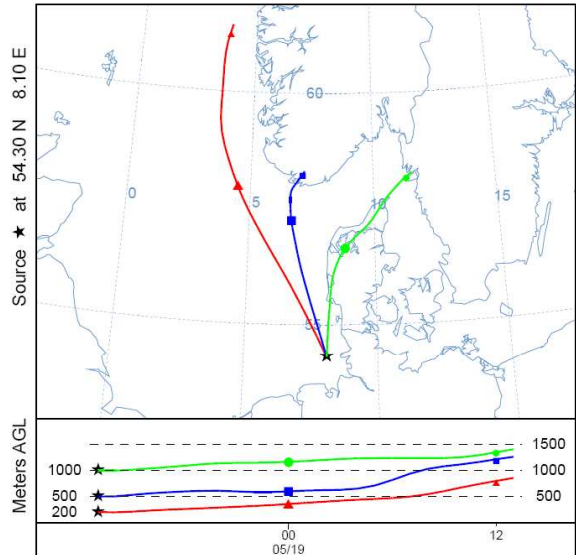


A4 Figure 33: Air mass backward trajectories of the air sample 10AT 1; (A) 24 h, 16 m, 200 m, 500 m arrival height; (B) 24 h; 200 m, 500 m, 1000 m arrival height; (C) 168 h; 16 m, 200 m, 500 m arrival height; (D) 168 h; 200 m, 500 m, 1000 m arrival height

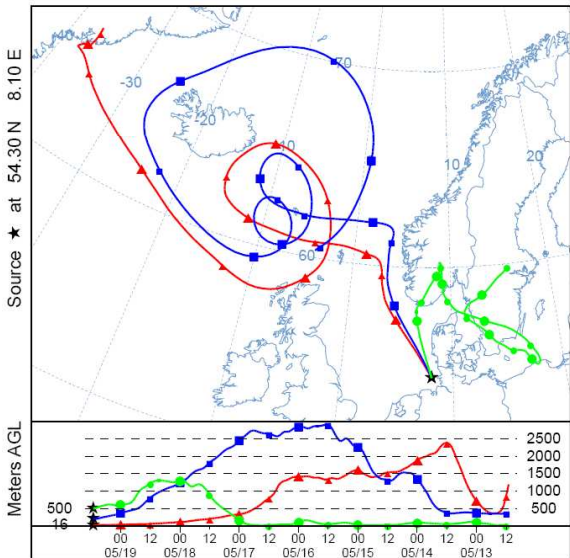
A NOAA HYSPLIT MODEL
Backward trajectories ending at 1100 UTC 19 May 10
GDAS Meteorological Data



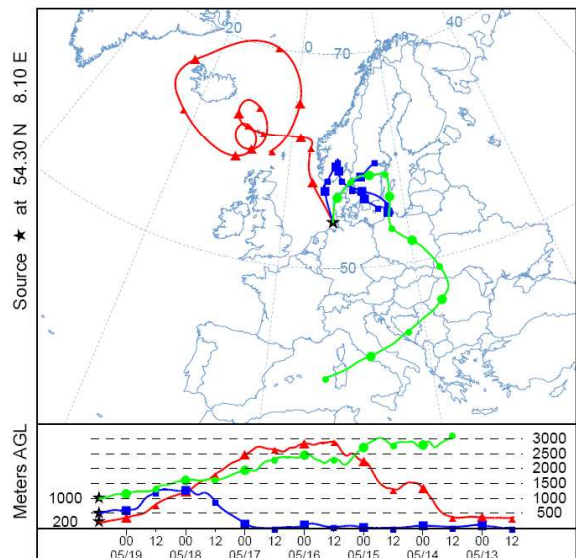
B NOAA HYSPLIT MODEL
Backward trajectories ending at 1100 UTC 19 May 10
GDAS Meteorological Data



C NOAA HYSPLIT MODEL
Backward trajectories ending at 1100 UTC 19 May 10
GDAS Meteorological Data

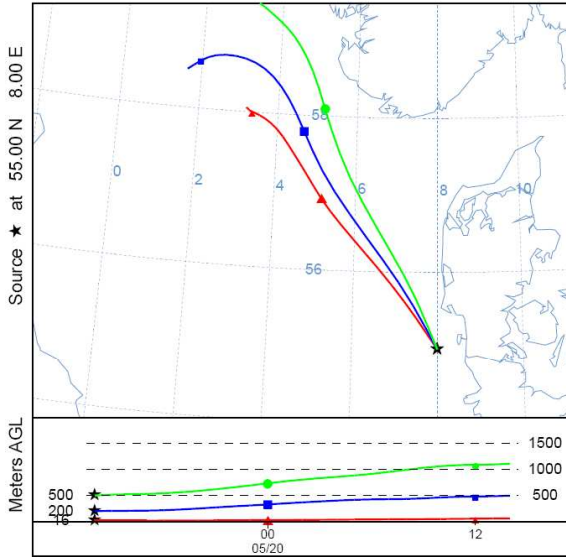


D NOAA HYSPLIT MODEL
Backward trajectories ending at 1100 UTC 19 May 10
GDAS Meteorological Data

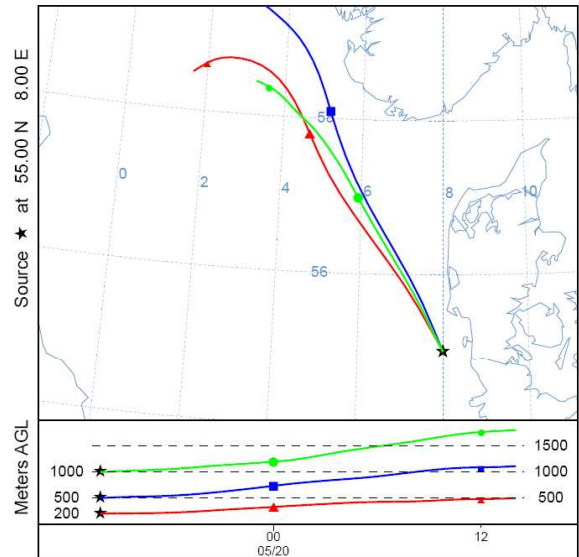


A4 Figure 34: Air mass backward trajectories of the air sample 10AT 2; (A) 24 h, 16 m, 200 m, 500 m arrival height; (B) 24 h; 200 m, 500 m, 1000 m arrival height; (C) 168 h; 16 m, 200 m, 500 m arrival height; (D) 168 h; 200 m, 500 m, 1000 m arrival height

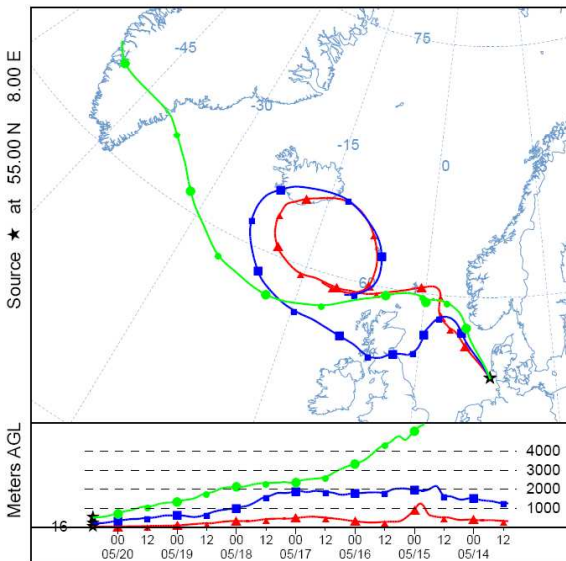
A NOAA HYSPLIT MODEL
Backward trajectories ending at 1000 UTC 20 May 10
GDAS Meteorological Data



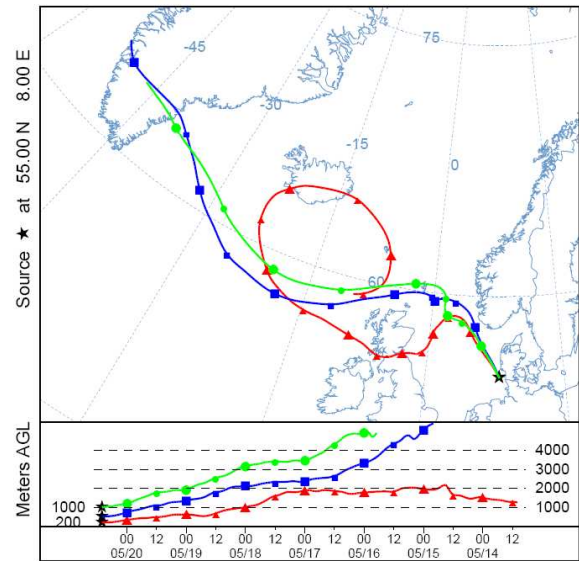
B NOAA HYSPLIT MODEL
Backward trajectories ending at 1000 UTC 20 May 10
GDAS Meteorological Data



C NOAA HYSPLIT MODEL
Backward trajectories ending at 1000 UTC 20 May 10
GDAS Meteorological Data

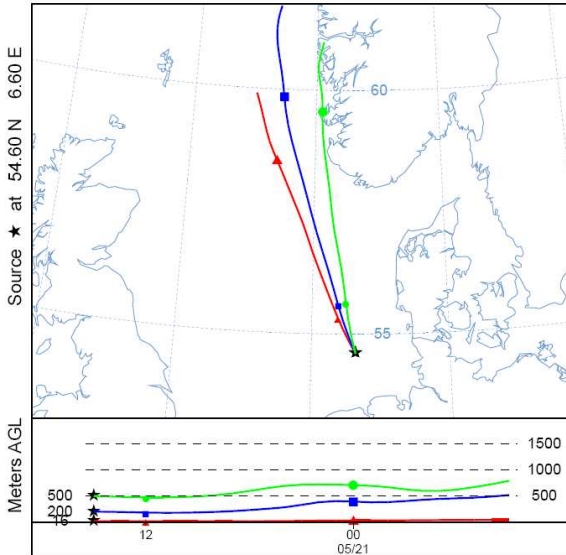


D NOAA HYSPLIT MODEL
Backward trajectories ending at 1000 UTC 20 May 10
GDAS Meteorological Data

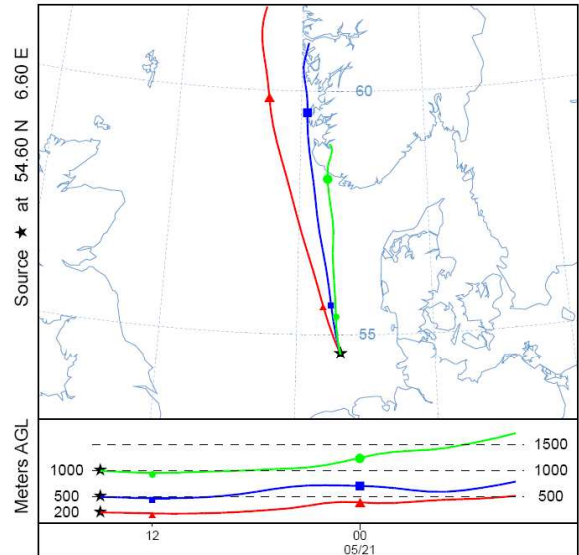


A4 Figure 35: Air mass backward trajectories of the air sample 10AT 3; (A) 24 h, 16 m, 200 m, 500 m arrival height; (B) 24 h; 200 m, 500 m, 1000 m arrival height; (C) 168 h; 16 m, 200 m, 500 m arrival height; (D) 168 h; 200 m, 500 m, 1000 m arrival height

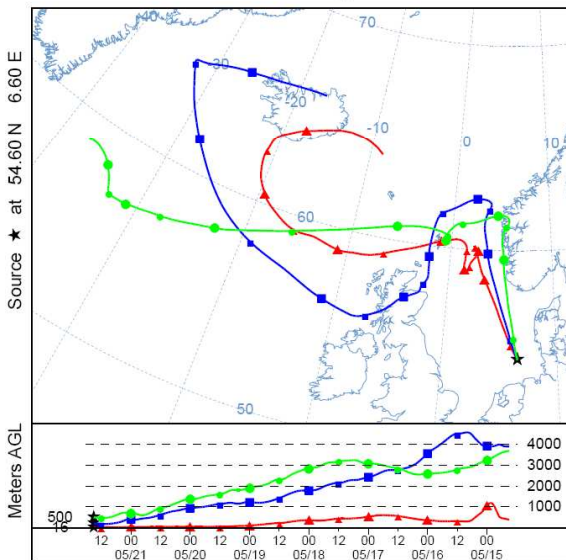
A NOAA HYSPLIT MODEL
Backward trajectories ending at 1500 UTC 21 May 10
GDAS Meteorological Data



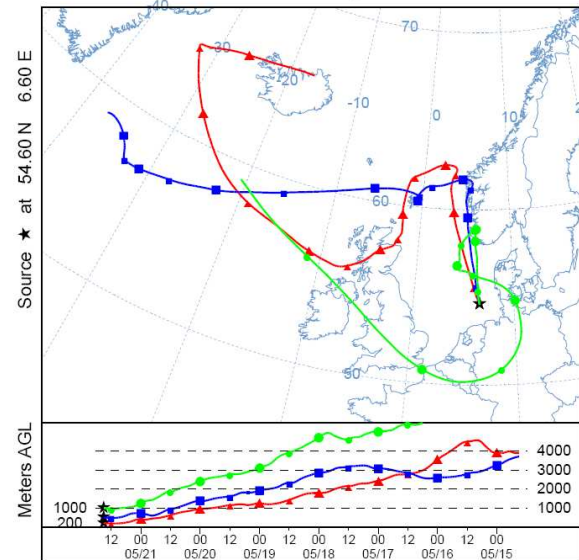
B NOAA HYSPLIT MODEL
Backward trajectories ending at 1500 UTC 21 May 10
GDAS Meteorological Data



C NOAA HYSPLIT MODEL
Backward trajectories ending at 1500 UTC 21 May 10
GDAS Meteorological Data

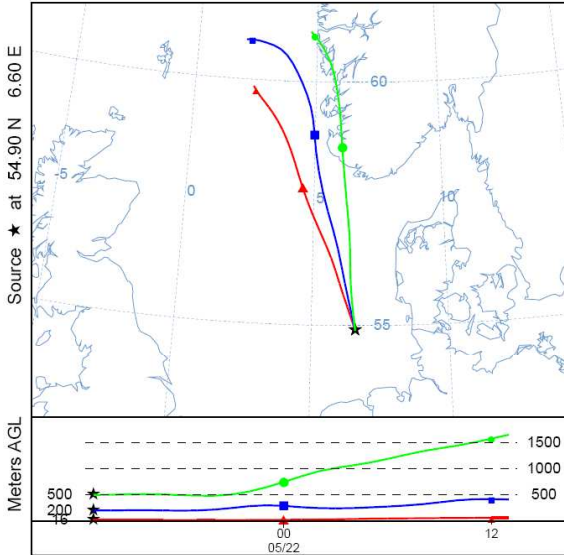


D NOAA HYSPLIT MODEL
Backward trajectories ending at 1500 UTC 21 May 10
GDAS Meteorological Data

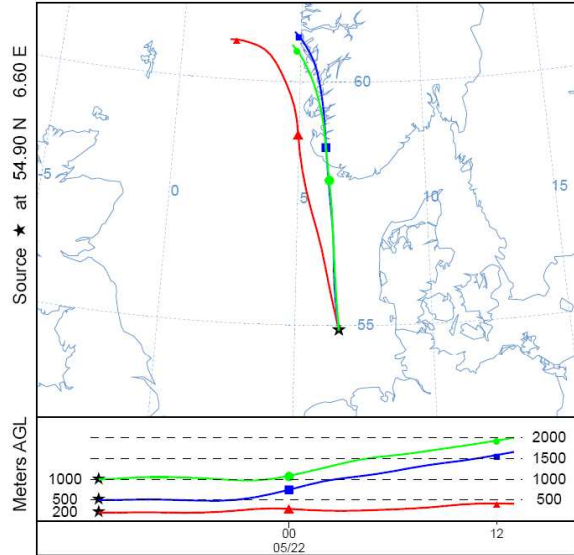


A4 Figure 36: Air mass backward trajectories of the air sample 10AT 4; (A) 24 h, 16 m, 200 m, 500 m arrival height; (B) 24 h; 200 m, 500 m, 1000 m arrival height; (C) 168 h; 16 m, 200 m, 500 m arrival height; (D) 168 h; 200 m, 500 m, 1000 m arrival height

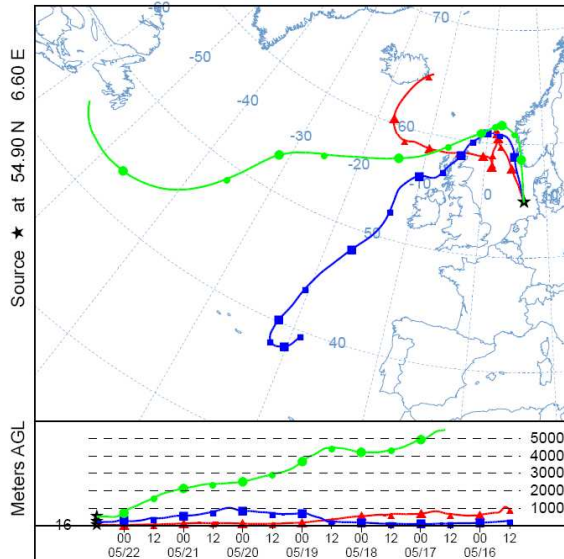
A NOAA HYSPLIT MODEL
Backward trajectories ending at 1100 UTC 22 May 10
GDAS Meteorological Data



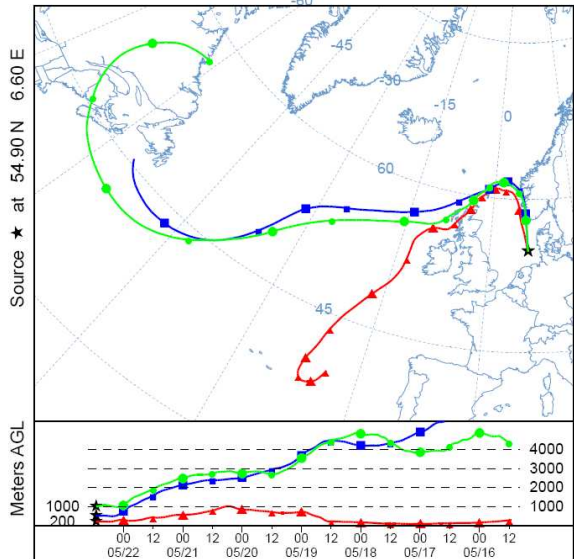
B NOAA HYSPLIT MODEL
Backward trajectories ending at 1100 UTC 22 May 10
GDAS Meteorological Data



C NOAA HYSPLIT MODEL
Backward trajectories ending at 1100 UTC 22 May 10
GDAS Meteorological Data

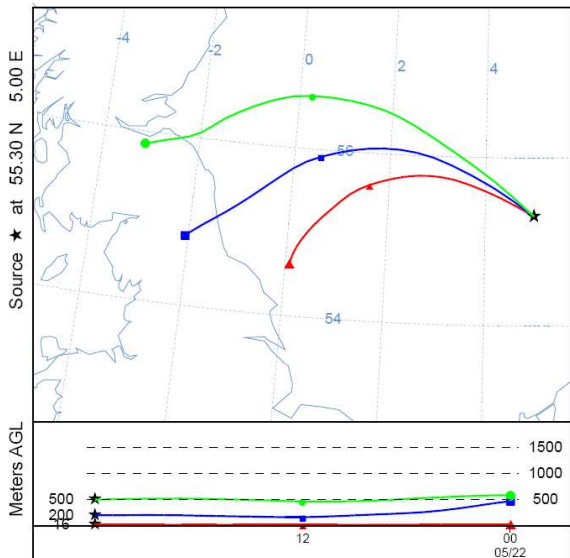


D NOAA HYSPLIT MODEL
Backward trajectories ending at 1100 UTC 22 May 10
GDAS Meteorological Data

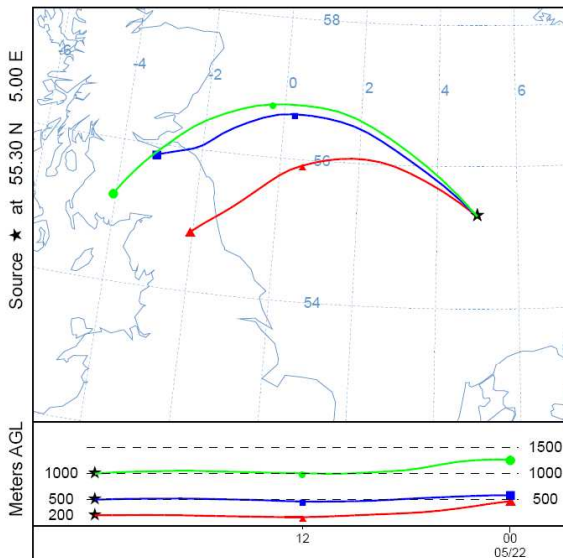


A4 Figure 37: Air mass backward trajectories of the air sample 10AT 5; (A) 24 h, 16 m, 200 m, 500 m arrival height; (B) 24 h; 200 m, 500 m, 1000 m arrival height; (C) 168 h; 16 m, 200 m, 500 m arrival height; (D) 168 h; 200 m, 500 m, 1000 m arrival height

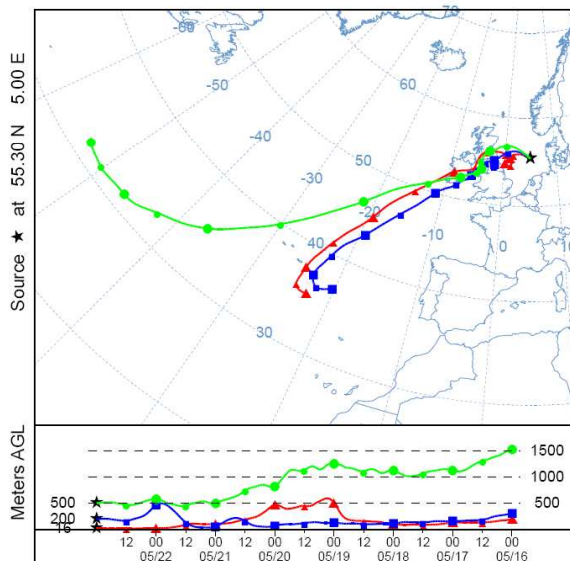
A NOAA HYSPLIT MODEL
Backward trajectories ending at 0000 UTC 23 May 10
GDAS Meteorological Data



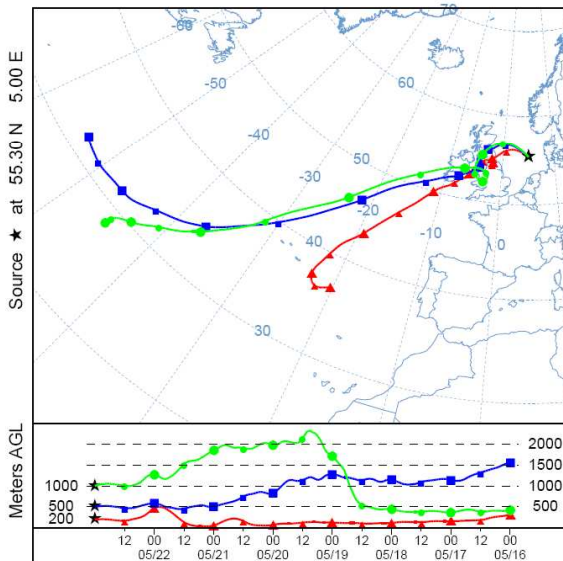
B NOAA HYSPLIT MODEL
Backward trajectories ending at 0000 UTC 23 May 10
GDAS Meteorological Data



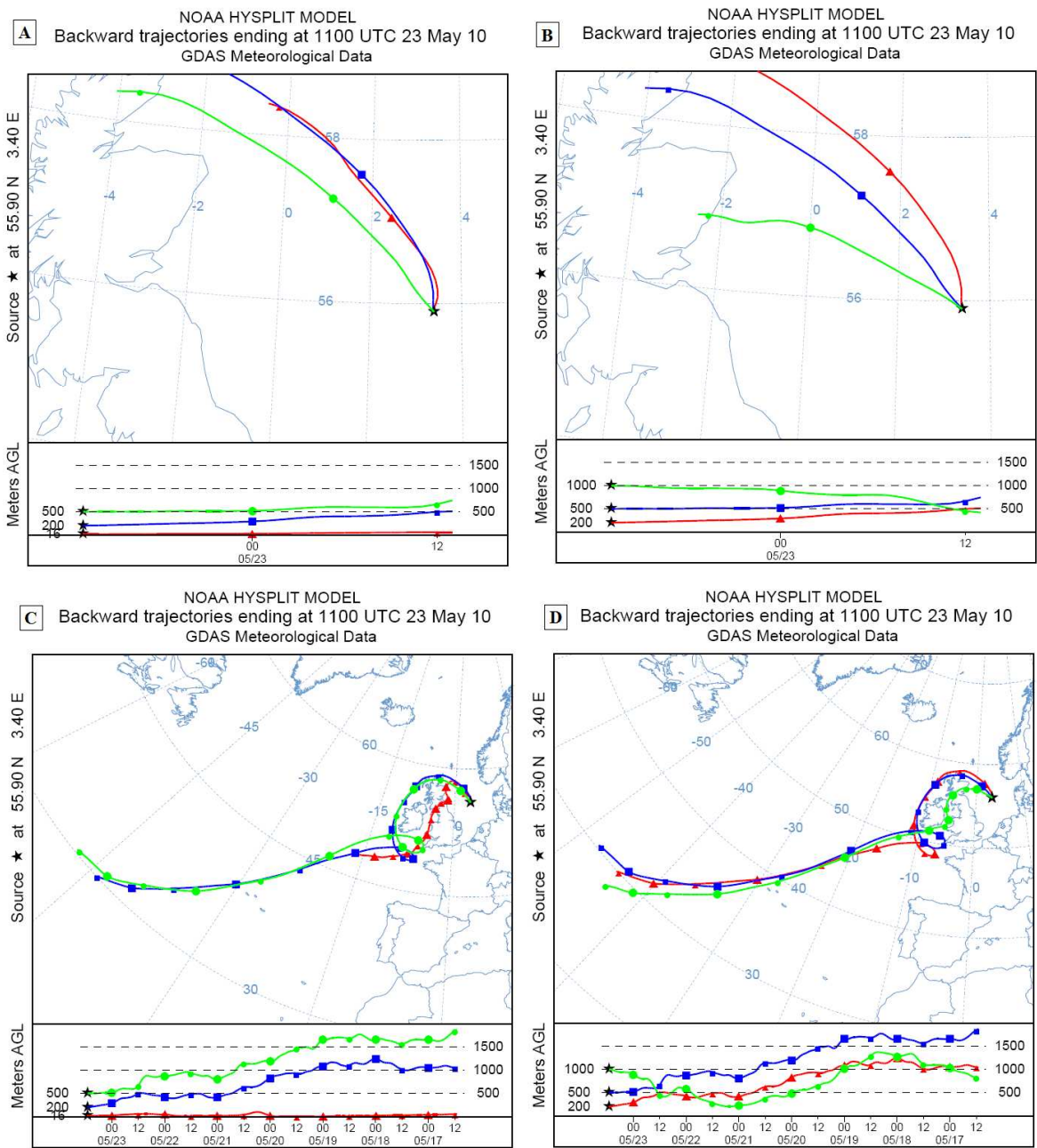
C NOAA HYSPLIT MODEL
Backward trajectories ending at 0000 UTC 23 May 10
GDAS Meteorological Data



D NOAA HYSPLIT MODEL
Backward trajectories ending at 0000 UTC 23 May 10
GDAS Meteorological Data



A4 Figure 38: Air mass backward trajectories of the air sample 10AT 6; (A) 24 h, 16 m, 200 m, 500 m arrival height; (B) 24 h; 200 m, 500 m, 1000 m arrival height; (C) 168 h; 16 m, 200 m, 500 m arrival height; (D) 168 h; 200 m, 500 m, 1000 m arrival height

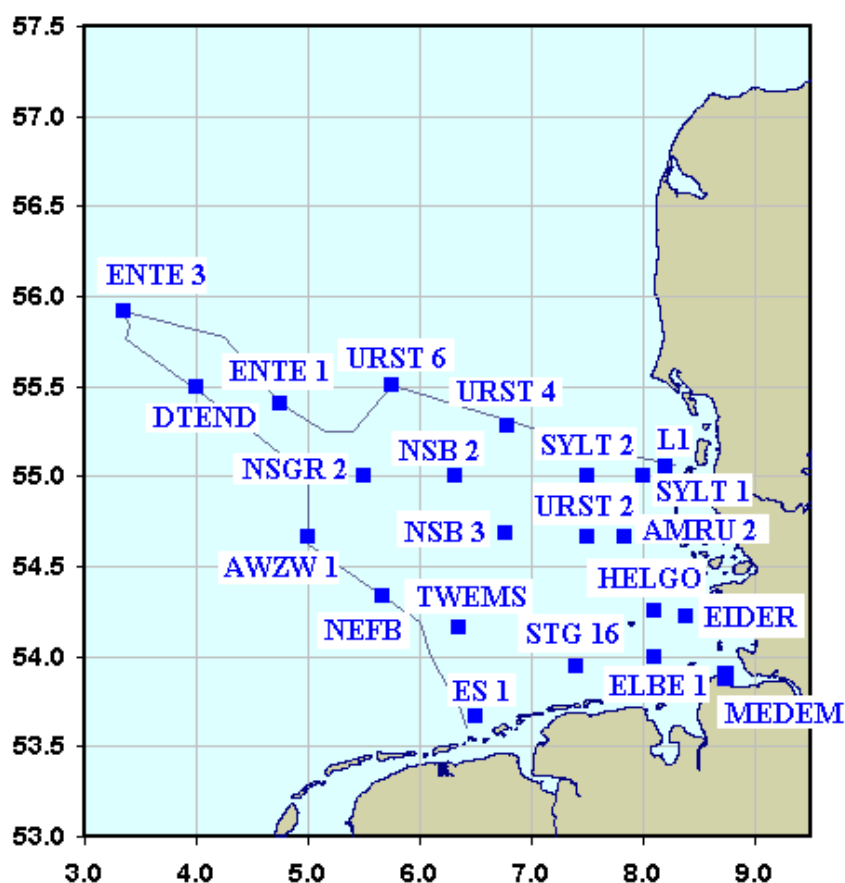


A4 Figure 39: Air mass backward trajectories of the air sample 10AT 7; (A) 24 h, 16 m, 200 m, 500 m arrival height; (B) 24 h; 200 m, 500 m, 1000 m arrival height; (C) 168 h; 16 m, 200 m, 500 m arrival height; (D) 168 h; 200 m, 500 m, 1000 m arrival height

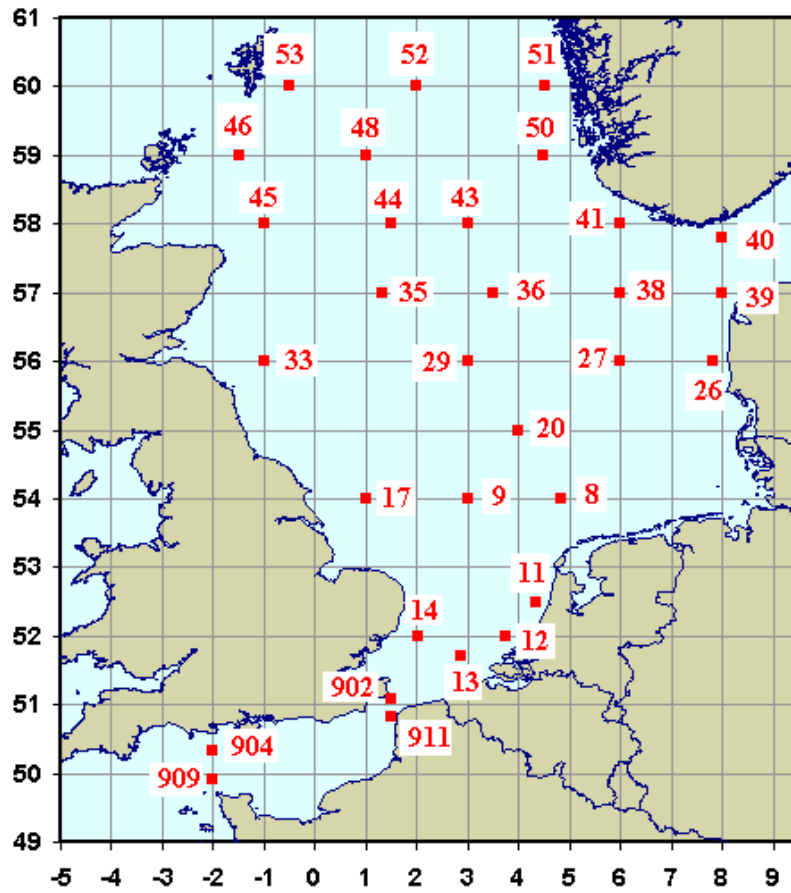
Annex 5 (A5): Surface water concentrations of target analytes

The data tabulated below is provided for this study from the Federal Maritime and Hydrographic Agency of Germany in Hamburg. Baltic Sea surface water concentrations from 2005 (A5 Table 4) and 2009 (A5 Table 6) are determined by the Institute for Baltic Sea Research (IOW) in Warnemünde and are extracted from the MUDAB database. ^[111]

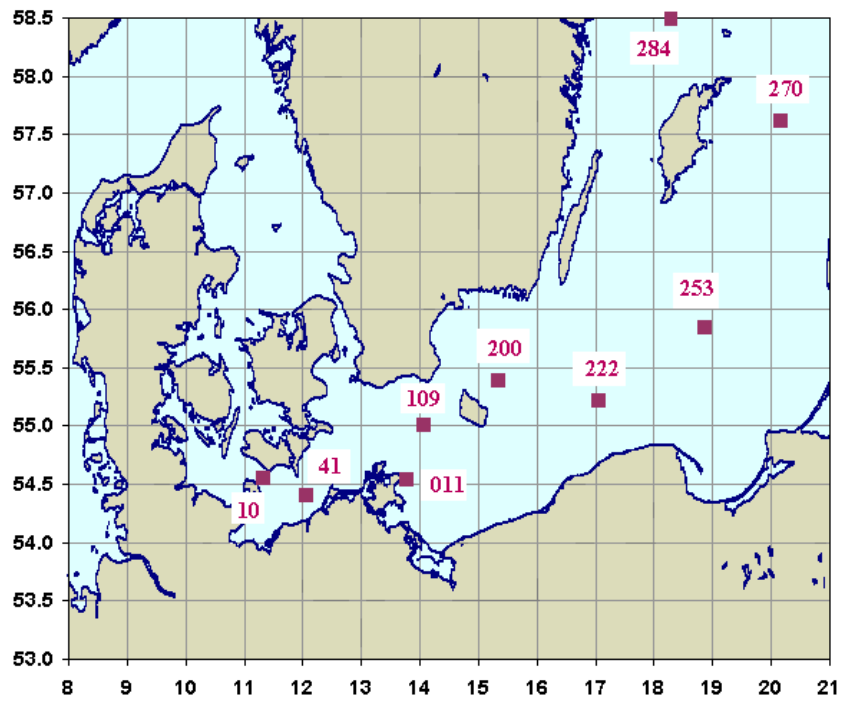
A5 figures 1 and 2 illustrate the water sampling sites for the determination of organic pollutants in the surface water of the German EEZ and North Sea, respectively. A further sampling site is placed on the river Elbe (STADE: 53.6 °N; 9.5 °W). Baltic Sea surface water sampling sites are illustrated in A5 figures 3 to 5 for the monitoring cruises in 2005 (PAHs, OCPs, PCBs and Trifluralin), 2008 (Polar Pesticides, PFCs, PBFRs and pharmaceuticals) and 2009 (HCHs), respectively. Surface water concentrations of target compounds are listed in A5 tables 1-8.



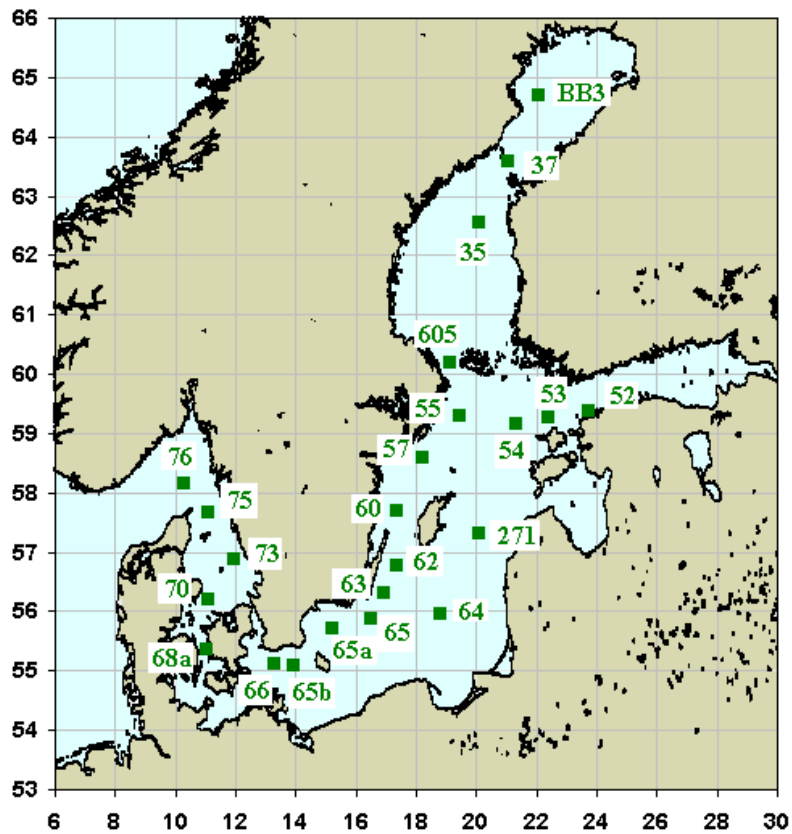
A5 Figure 1: Observational network of BSH water sampling sites in the German EEZ



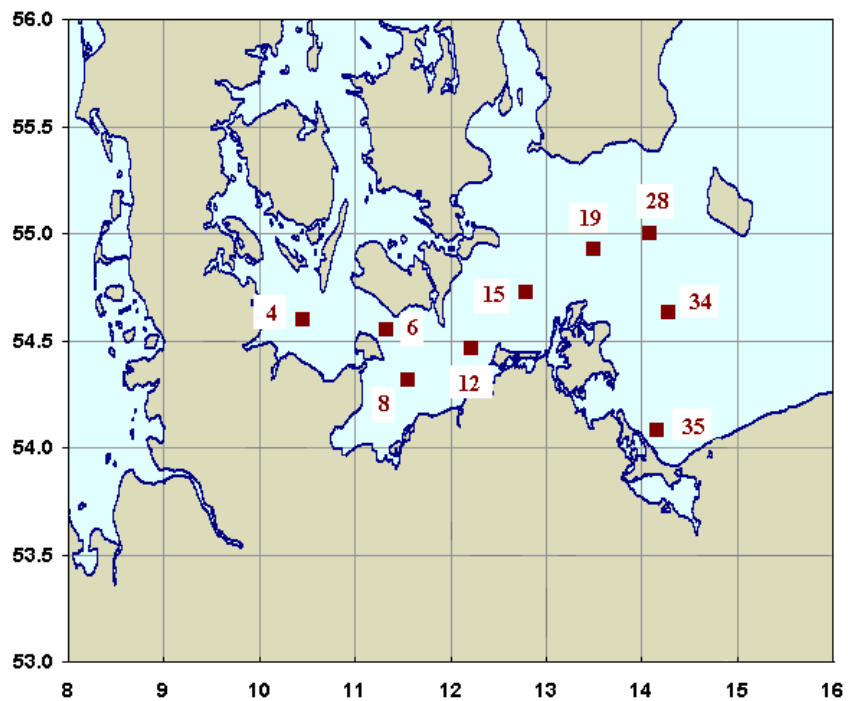
A5 Figure 2: Observational network of BSH water sampling sites in the North Sea



A5 Figure 3: Observational network of water sampling sites in the Baltic Sea for the research cruise in Feb. 2005



A5 Figure 4: Observational network of water sampling sites in the Baltic Sea for the research cruise in Jun./Jul. 2008



A5 Figure 5: Observational network of water sampling sites in the Baltic Sea for the research cruise in Jul. 2009

A5 Table 1: Surface water concentrations (5 m, A5 figure 1) in ng/L determined during the research cruise in the German EEZ in May/Jun. 2009; with respective LOQs, PSU= Practical Salinity units; SPM = Suspended particulate matter in mg/L; n.a.=data not available;

ng/L	AMRU2	AWZW1	DTEND	EIDER	ELBE1	ENTE1	ENTE3	ES1	HELGO	L1
24-D	0.3445	n.a.	0.0305	0.7218	0.2818	0.0293	0.0279	n.a.	0.2895	0.7344
ACE	n.a.	n.a.	n.a.	n.a.	n.a.	n.a.	n.a.	n.a.	n.a.	n.a.
ACY	n.a.	n.a.	n.a.	n.a.	n.a.	n.a.	n.a.	n.a.	n.a.	n.a.
ALD	0.0000	0.0000	0.0000	0.0000	0.0000	0.0000	0.0000	0.0000	0.0000	0.0000
AMETRYN	0.0464	n.a.	0.0110	0.0623	0.0250	0.0092	0.0094	n.a.	0.0487	0.0473
ANT	n.a.	n.a.	n.a.	n.a.	n.a.	n.a.	n.a.	n.a.	n.a.	n.a.
ATRAZ	1.0333	n.a.	0.5119	1.0832	1.1045	0.5469	0.5299	n.a.	0.9590	1.0450
AZINPH-E	0.0000	0.0000	0.0000	0.0000	0.0000	0.0000	0.0000	n.a.	0.0000	0.0000
AZINPH-M	0.0000	0.0000	0.0000	0.0000	0.0000	0.0000	0.0000	n.a.	0.0078	0.0000
BAA	n.a.	n.a.	n.a.	n.a.	n.a.	n.a.	n.a.	n.a.	n.a.	n.a.
BAP	0.0561	0.0000	0.0000	0.4624	0.1634	0.0000	0.0000	0.1463	0.1082	0.0478
BBF	n.a.	n.a.	n.a.	n.a.	n.a.	n.a.	n.a.	n.a.	n.a.	n.a.
BENTAZ	0.5619	n.a.	0.0000	0.6467	0.3982	0.0000	0.0000	n.a.	0.5572	0.6220
BGHIP	n.a.	n.a.	n.a.	n.a.	n.a.	n.a.	n.a.	n.a.	n.a.	n.a.
CARBAMAZ	6.1974	n.a.	0.0578	8.7249	4.4282	0.0760	0.0450	n.a.	5.3078	7.6331
CARBEND	n.a.	n.a.	n.a.	n.a.	n.a.	n.a.	n.a.	n.a.	n.a.	n.a.
CB138	0.0026	0.0010	0.0029	0.0108	0.0063	0.0009	0.0009	0.0055	0.0043	0.0033
CB153	0.0031	0.0006	0.0014	0.0115	0.0072	0.0005	0.0002	0.0050	0.0048	0.0036
CB28	0.0009	0.0003	0.0002	0.0026	0.0022	0.0002	0.0002	0.0019	0.0013	0.0011
CB52	0.0006	0.0003	0.0002	0.0015	0.0013	0.0001	0.0002	0.0012	0.0009	0.0006
CHLORFENV	0.0103	0.0000	0.0000	0.0000	0.0000	0.0000	0.0000	n.a.	0.0000	0.0564
CHLORTUR	1.3208	n.a.	0.0324	0.9890	1.4456	0.0364	0.0193	n.a.	1.3416	0.8954
CHRTR	0.1020	0.0218	0.0238	0.6225	0.2714	0.0189	0.0252	0.2135	0.1690	0.1497
CLOFIBRS	0.1086	n.a.	0.0000	0.1323	0.0697	0.0000	0.0000	n.a.	0.0862	0.1159
DBAHA	n.a.	n.a.	n.a.	n.a.	n.a.	n.a.	n.a.	n.a.	n.a.	n.a.
DDPP	0.0076	0.0008	0.0004	0.0206	0.0055	0.0004	0.0003	0.0028	0.0085	0.0079
DDEPP	0.0024	0.0003	0.0003	0.0069	0.0031	0.0002	0.0001	0.0021	0.0028	0.0027
DDTOP	n.a.	n.a.	n.a.	n.a.	n.a.	n.a.	n.a.	n.a.	n.a.	n.a.
DDTPP	0.0010	0.0003	0.0002	0.0014	0.0007	0.0003	0.0001	0.0007	0.0009	0.0007
DEATRAZ	1.0368	n.a.	0.1401	1.0757	1.0397	0.1483	0.1421	n.a.	0.9749	1.0310
DIAZINON	0.0383	0.0000	0.0052	0.0362	0.0322	0.0103	0.0053	n.a.	0.0322	0.0426
DICHLPR	0.1281	n.a.	0.0120	0.1743	0.1155	0.0000	0.0000	n.a.	0.1250	0.1512
DICLOF	0.1091	n.a.	0.0273	0.0639	0.0749	0.3756	0.0150	n.a.	0.0871	0.0324
DIELD	0.0119	0.0116	0.0073	0.0137	0.0167	0.0086	0.0062	0.0196	0.0091	0.0128
DIMETH	0.0000	0.0000	0.0000	0.0000	0.0000	0.0000	0.0000	n.a.	0.0015	0.0000
DIURON	2.4485	n.a.	0.1438	2.8109	2.3607	0.4139	0.1252	n.a.	2.4595	2.6462
END	0.0000	0.0000	0.0052	0.0000	0.0000	0.0000	0.0000	0.0000	0.0000	0.0000
FENUR	0.0628	n.a.	0.0011	0.1106	0.0404	0.0107	0.0145	n.a.	0.0538	0.0868
FL	0.3729	0.4668	0.3618	0.4645	0.6670	0.3940	0.3415	0.4225	0.4193	0.4074
FLU	0.3100	0.1022	0.1042	1.3047	0.7348	0.1134	0.1374	0.5341	0.4541	0.4368
HBCDA	0.0000	0.0000	0.0000	0.0000	0.0000	0.0000	0.0000	n.a.	0.0000	0.0000
HBCDBG	0.0000	0.0000	0.0000	0.0000	0.0000	0.0000	0.0000	n.a.	0.0000	0.1520
HCB	0.0029	0.0025	0.0018	0.0057	0.0049	0.0021	0.0020	0.0041	0.0029	0.0045
HCHA	0.0610	0.0352	0.0389	0.0871	0.0450	0.0437	0.0458	0.0416	0.0455	0.0812
HCHB	0.0734	0.0080	0.0084	0.0965	0.0234	0.0083	0.0082	0.0232	0.0488	0.0673
HCHD	0.0133	0.0014	0.0006	0.0174	0.0074	0.0007	0.0005	0.0065	0.0089	0.0141
HCHG	0.0854	0.0538	0.0276	0.1129	0.0959	0.0333	0.0248	0.0969	0.0793	0.0993
HEXAZIN	0.1299	n.a.	0.0018	0.1873	0.0511	0.0000	0.0008	n.a.	0.0919	0.1835
I123P	0.0635	0.0019	0.0022	0.5179	0.2161	0.0016	0.0015	0.1523	0.1265	0.0577

A5 Table 1 continued:

ng/L	AMRU2	AWZW1	DTEND	EIDER	ELBE1	ENTE1	ENTE3	ES1	HELGO	L1
IRGAROL	0.2933	n.a.	0.0000	0.2657	0.3393	0.0000	0.0000	n.a.	0.3473	0.2956
ISOD	0.0000	0.0000	0.0000	0.0000	0.0000	0.0000	0.0000	0.0000	0.0000	0.0000
ISOPRUR	1.3860	n.a.	0.0671	1.0208	1.4410	0.0875	0.0459	n.a.	1.3420	1.2870
LINUR	0.1891	n.a.	0.0187	0.2097	0.1444	0.0171	0.0140	n.a.	0.1765	0.1570
MALATH	0.0000	0.0000	0.0000	0.0000	0.0000	0.0000	0.0000	n.a.	0.0000	0.0000
MCPA	0.5191	n.a.	0.0550	0.6273	0.5568	0.0560	0.0532	n.a.	0.5806	0.7176
MECOPR	0.7449	n.a.	0.0293	0.9048	0.7703	0.0290	0.0229	n.a.	0.7293	0.8151
METAZCHL	0.3213	n.a.	0.0073	0.4090	0.2417	0.0174	0.0034	n.a.	0.2550	0.3998
METHABZT	0.0730	n.a.	0.0000	0.0752	0.0910	0.0000	0.0000	n.a.	0.0898	0.0633
METOLA	0.8130	0.0000	0.0218	0.8420	0.8050	0.0297	0.0172	n.a.	0.9530	0.6420
NAPROX	n.a.	n.a.	n.a.	n.a.	n.a.	n.a.	n.a.	n.a.	n.a.	n.a.
OXAZEP	1.5916	n.a.	0.0000	1.7296	1.4812	0.0000	0.0000	n.a.	1.5180	1.4720
PENDIMETH	0.1398	0.0000	0.0462	0.0592	0.1627	0.0591	0.0378	n.a.	0.1660	0.0463
PFBS	1.4102	n.a.	0.0314	1.5278	1.3108	0.0234	0.0229	n.a.	1.2475	1.5458
PFDEA	0.0528	n.a.	0.0061	0.0893	0.0353	0.0040	0.0044	n.a.	0.0387	0.0326
PFHPA	0.3217	n.a.	0.0518	0.4436	0.2734	0.0367	0.0376	n.a.	0.2954	0.3832
PFHXA	0.5207	n.a.	0.0672	0.6950	0.4066	0.0464	0.0513	n.a.	0.4759	0.6359
PFHXS	0.2780	n.a.	0.0134	0.3160	0.2860	0.0145	0.0124	n.a.	0.2810	0.2820
PFNOA	0.1161	n.a.	0.0476	0.1632	0.0705	0.0279	0.0352	n.a.	0.0813	0.1321
PFOA	1.0623	n.a.	0.1576	1.4987	1.0171	0.1422	0.1190	n.a.	1.0072	1.2342
PFOS	0.7348	n.a.	0.0644	1.0303	0.6785	0.0389	0.0446	n.a.	0.6648	0.8340
PFOSA	0.0089	n.a.	0.0020	0.0071	0.0040	0.0018	0.0014	n.a.	0.0050	0.0038
PHEN	0.3443	0.2433	0.1836	0.7522	0.7243	0.2149	0.2154	0.4561	0.4134	0.3770
PIRIMIC	0.0000	0.0588	0.0026	0.0000	0.0000	0.0129	0.0373	n.a.	0.0000	0.0000
PRIMID	2.3106	n.a.	0.0328	3.7636	1.2613	0.0363	0.0252	n.a.	1.8162	3.1481
PROMETR	0.0385	n.a.	0.0000	0.0731	0.0000	0.0000	0.0000	n.a.	0.0278	0.0483
PROPAZ	0.0325	n.a.	0.0090	0.0400	0.0216	0.0111	0.0082	n.a.	0.0272	0.0354
PYR	0.1086	0.0045	0.0042	0.8670	0.4082	0.0025	0.0050	0.2958	0.2417	0.1722
QCB	0.0008	0.0009	0.0006	0.0024	0.0024	0.0008	0.0009	0.0015	0.0009	0.0024
SIMAZ	0.4172	n.a.	0.1004	0.4664	0.4300	0.1181	0.1053	n.a.	0.3966	0.4320
TBEP	n.a.	n.a.	n.a.	n.a.	n.a.	n.a.	n.a.	n.a.	n.a.	n.a.
TBP	n.a.	n.a.	n.a.	n.a.	n.a.	n.a.	n.a.	n.a.	n.a.	n.a.
TERBAZ	1.2467	n.a.	0.0673	1.8720	1.1661	0.0798	0.0538	n.a.	1.4170	1.5470
TERBUTR	0.2536	n.a.	0.0000	0.2943	0.2004	0.0000	0.0000	n.a.	0.2468	0.2710
TPP	n.a.	n.a.	n.a.	n.a.	n.a.	n.a.	n.a.	n.a.	n.a.	n.a.
TRIFLU	0.0015	0.0007	0.0000	0.0016	0.0011	0.0001	0.0001	0.0007	0.0013	0.0005
SPM [mg/L]	2.63	0.56	0.65	28.88	11.75	0.09	n.a.	n.a.	n.a.	3.60
PSU	31.00	34.49	35.00	29.38	32.56	34.78	35.07	31.84	n.a.	29.87

ng/L	MEDEM	NEFB	NSB2	NSB3	NSGR2	STADE	STG16	SYLT1	SYLT2	TWEMS
24-D	0.5288	0.1110	0.1467	0.1631	0.0607	2.4222	0.2856	n.a.	n.a.	0.1563
ACE	n.a.	n.a.	n.a.	n.a.	n.a.	n.a.	n.a.	n.a.	n.a.	n.a.
ACY	n.a.	n.a.	n.a.	n.a.	n.a.	n.a.	n.a.	n.a.	n.a.	n.a.
ALD	0.0000	n.a.	0.0000	0.0000	0.0000	0.0000	n.a.	0.0000	0.0000	n.a.
AMETRYN	0.1589	0.0112	0.0165	0.0182	0.0105	0.5224	0.0241	n.a.	n.a.	0.0174
ANT	n.a.	n.a.	n.a.	n.a.	n.a.	n.a.	n.a.	n.a.	n.a.	n.a.
ATRAZ	1.4549	0.6616	0.7370	0.7572	0.6117	3.9613	0.9335	n.a.	n.a.	0.7498
AZINPH-E	0.0000	0.0000	0.0000	0.0000	0.0000	0.0000	0.0000	n.a.	n.a.	0.0000
AZINPH-M	0.0000	0.0000	0.0000	0.0000	0.0000	0.0000	0.0000	n.a.	n.a.	0.0000
BAA	n.a.	n.a.	n.a.	n.a.	n.a.	n.a.	n.a.	n.a.	n.a.	n.a.
BAP	0.7308	n.a.	0.0000	0.0056	0.0000	1.2916	n.a.	0.0239	0.0018	n.a.

A5 Table 1 continued:

ng/L	MEDEM	NEFB	NSB2	NSB3	NSGR2	STADE	STG16	SYLT1	SYLT2	TWEMS
BBF	n.a.	n.a.	n.a.	n.a.	n.a.	n.a.	n.a.	n.a.	n.a.	n.a.
BENTAZ	1.8259	0.0491	0.1087	0.1637	0.0120	6.5732	0.3558	n.a.	n.a.	0.2097
BGHP	n.a.	n.a.	n.a.	n.a.	n.a.	n.a.	n.a.	n.a.	n.a.	n.a.
CARBAMAZ	18.6024	1.4356	1.8400	2.0321	0.7026	58.7391	4.0844	n.a.	n.a.	2.3354
CARBEND	n.a.	n.a.	n.a.	n.a.	n.a.	n.a.	n.a.	n.a.	n.a.	n.a.
CB138	0.0169	n.a.	0.0010	0.0063	0.0021	0.0481	n.a.	0.0037	0.0013	n.a.
CB153	0.0195	n.a.	0.0007	0.0014	0.0003	0.0507	n.a.	0.0045	0.0008	n.a.
CB28	0.0039	n.a.	0.0005	0.0005	0.0003	0.0130	n.a.	0.0012	0.0005	n.a.
CB52	0.0036	n.a.	0.0005	0.0004	0.0002	0.0177	n.a.	0.0007	0.0003	n.a.
CHLORFENV	0.0000	0.0000	0.0000	0.0000	0.0000	0.0000	0.0000	n.a.	n.a.	0.0000
CHLORTUR	2.3920	0.3630	0.5834	0.7561	0.2444	8.4448	1.3832	n.a.	n.a.	0.8060
CHRTR	0.8493	n.a.	0.0222	0.0293	0.0210	1.5413	n.a.	0.1106	0.0323	n.a.
CLOFIBRS	0.2290	0.0222	0.0250	0.0323	0.0115	0.7756	0.0739	n.a.	n.a.	0.0373
DBAHA	n.a.	n.a.	n.a.	n.a.	n.a.	n.a.	n.a.	n.a.	n.a.	n.a.
DDPP	0.0875	n.a.	0.0000	0.0000	0.0006	0.3937	n.a.	0.0079	0.0018	n.a.
DDEPP	0.0169	n.a.	0.0005	0.0006	0.0002	0.0880	n.a.	0.0025	0.0006	n.a.
DDTOP	n.a.	n.a.	n.a.	n.a.	n.a.	n.a.	n.a.	n.a.	n.a.	n.a.
DDTPP	0.0088	n.a.	0.0000	0.0003	0.0002	0.0418	n.a.	0.0008	0.0003	n.a.
DEATRAZ	1.4976	0.4003	0.5256	0.6019	0.3197	3.8448	0.8899	n.a.	n.a.	0.6221
DIAZINON	0.0508	0.0199	0.0183	0.0194	0.0143	0.2939	0.0202	n.a.	n.a.	0.0253
DICHLPR	0.2783	0.0543	0.0691	0.0661	0.0000	2.2050	0.1134	n.a.	n.a.	0.0859
DICLOF	0.6894	0.2192	0.0212	0.0215	0.0882	22.6380	0.1595	n.a.	n.a.	0.2871
DIELD	0.0158	n.a.	0.0091	0.0070	0.0117	0.0115	n.a.	0.0143	0.0117	n.a.
DIMETH	0.0000	0.0000	0.0000	0.0000	0.0000	0.0309	0.0000	n.a.	n.a.	0.0000
DIURON	4.9410	0.8949	1.0793	1.2407	0.7664	17.2386	2.1521	n.a.	n.a.	1.2407
END	0.0000	n.a.	0.0000	0.0000	0.0000	0.0000	n.a.	0.0013	0.0000	n.a.
FENUR	0.1879	0.0254	0.0406	0.0291	0.0115	1.4011	0.0446	n.a.	n.a.	0.0212
FL	0.6193	n.a.	0.2956	0.2994	0.5350	0.6447	n.a.	0.4731	0.5072	n.a.
FLU	2.0743	n.a.	0.1065	0.1212	0.1317	3.0415	n.a.	0.4026	0.2379	n.a.
HBCDA	0.0000	0.0000	0.0000	0.0041	0.0000	0.0000	0.0019	n.a.	n.a.	0.0000
HBCDBG	0.0000	0.0000	0.0000	0.0018	0.0000	0.0000	0.0000	n.a.	n.a.	0.0000
HCB	0.0132	n.a.	0.0022	0.0020	0.0024	0.1877	n.a.	0.0046	0.0029	n.a.
HCHA	0.2042	n.a.	0.0284	0.0258	0.0372	1.2945	n.a.	0.0790	0.0372	n.a.
HCHB	0.2992	n.a.	0.0097	0.0100	0.0087	1.3319	n.a.	0.0697	0.0285	n.a.
HCHD	0.0601	n.a.	0.0028	0.0038	0.0015	0.3580	n.a.	0.0151	0.0078	n.a.
HCHG	0.1618	n.a.	0.0569	0.0508	0.0510	0.5103	n.a.	0.0954	0.0604	n.a.
HEXAZIN	0.5007	0.0090	0.0172	0.0266	0.0720	2.5225	0.0627	n.a.	n.a.	0.0236
I123P	0.5558	n.a.	0.0051	0.0104	0.0015	0.9850	n.a.	0.0295	0.0044	n.a.
IRGAROL	0.7532	0.0600	0.1001	0.1311	0.0308	3.5305	0.2289	n.a.	n.a.	0.1150
ISOD	0.0000	n.a.	0.0000	0.0000	0.0000	0.0044	n.a.	0.0008	0.0000	n.a.
ISOPRUR	2.6510	0.7040	0.8580	1.0120	0.3487	13.6400	1.2430	n.a.	n.a.	1.0461
LINUR	0.3828	0.0376	0.0526	0.0338	0.0471	1.0635	0.1433	n.a.	n.a.	0.0596
MALATH	0.0000	0.0000	0.0000	0.1023	0.0000	0.0000	0.0000	n.a.	n.a.	0.1532
MCPA	1.1116	0.1737	0.2283	0.2710	0.1211	7.7514	0.5022	n.a.	n.a.	0.2680
MECOPR	1.1115	0.4466	0.4524	0.4817	0.1599	4.6898	0.7508	n.a.	n.a.	0.6006
METAZCHL	0.6069	0.2244	0.1867	0.1805	0.1132	2.5500	0.2244	n.a.	n.a.	0.2213
METHABZT	0.1320	0.0175	0.0321	0.0407	0.0078	0.1050	0.0814	n.a.	n.a.	0.0354
METOLA	2.7800	0.1690	0.3140	0.4180	0.1370	17.6000	0.5600	n.a.	n.a.	0.3010
NAPROX	n.a.	n.a.	n.a.	n.a.	n.a.	n.a.	n.a.	n.a.	n.a.	n.a.
OXAZEP	1.9596	0.2447	0.4379	0.5686	0.1040	7.4244	1.2788	n.a.	n.a.	0.5226
PENDIMETH	0.0867	0.2097	0.1845	0.1878	0.0937	0.0678	0.0877	n.a.	n.a.	0.1332
PFBS	1.6453	0.1898	0.3869	0.5062	0.1709	1.9617	1.1029	n.a.	n.a.	0.4303

A5 Table 1 continued:

ng/L	MEDEM	NEFB	NSB2	NSB3	NSGR2	STADE	STG16	SYLT1	SYLT2	TWEMS
PFDEA	0.1271	0.0082	0.0124	0.0113	0.0043	0.5988	0.0381	n.a.	n.a.	0.0205
PFHPA	0.5424	0.1010	0.1394	0.1570	0.1186	1.2298	0.3525	n.a.	n.a.	0.2295
PFHXA	1.1617	0.1325	0.1824	0.2109	0.1202	2.2112	0.5533	n.a.	n.a.	0.3210
PFHXS	0.3260	0.0896	0.1250	0.1470	0.0581	0.6190	0.2450	n.a.	n.a.	0.1420
PFNOA	0.2022	0.0294	0.0306	0.0344	0.0318	0.6817	0.0891	n.a.	n.a.	0.0671
PFOA	1.5318	0.3075	0.4210	0.4904	0.2116	4.1876	0.9235	n.a.	n.a.	0.5301
PFOS	1.4094	0.1662	0.2498	0.2867	0.1128	3.9658	0.7844	n.a.	n.a.	0.4218
PFOSA	0.0233	0.0023	0.0039	0.0030	0.0018	0.1103	0.0073	n.a.	n.a.	0.0031
PHEN	1.1354	n.a.	0.2307	0.2152	0.2895	1.6979	n.a.	0.4341	0.4085	n.a.
PIRIMIC	0.0114	0.0000	0.0000	0.0000	0.0000	0.2650	0.0000	n.a.	n.a.	0.0000
PRIMID	5.9834	0.3713	0.4944	0.5953	0.1988	34.5078	1.3823	n.a.	n.a.	0.6750
PROMETR	0.2427	0.0000	0.0000	0.0000	0.0000	1.5755	0.0086	n.a.	n.a.	0.0000
PROPAZ	0.0570	0.0167	0.0144	0.0190	0.0109	0.3924	0.0184	n.a.	n.a.	0.0223
PYR	1.7033	n.a.	0.0142	0.0225	0.0027	3.4069	n.a.	0.1206	0.0214	n.a.
QCB	0.0037	n.a.	0.0008	0.0008	0.0008	0.0302	n.a.	0.0030	0.0010	n.a.
SIMAZ	0.7331	0.2135	0.2421	0.2371	0.1663	4.5658	0.3582	n.a.	n.a.	0.2539
TBEP	n.a.	n.a.	n.a.	n.a.	n.a.	n.a.	n.a.	n.a.	n.a.	n.a.
TBP	n.a.	n.a.	n.a.	n.a.	n.a.	n.a.	n.a.	n.a.	n.a.	n.a.
TERBAZ	4.1860	0.2236	0.4082	0.4602	0.1859	28.7300	0.7995	n.a.	n.a.	0.3770
TERBUTR	0.5818	0.0629	0.0818	0.1007	0.0335	2.9524	0.1375	n.a.	n.a.	0.0997
TPP	n.a.	n.a.	n.a.	n.a.	n.a.	n.a.	n.a.	n.a.	n.a.	n.a.
TRIFLU	0.0045	n.a.	0.0020	0.0014	0.0002	0.0015	n.a.	0.0017	0.0017	n.a.
SPM [mg/L]	20.67	n.a.	1.13	1.53	0.20	16.55	n.a.	3.80	1.53	n.a.
PSU	n.a.	34.38	34.07	33.94	34.37	n.a.	32.49	30.72	32.48	33.81

ng/L	URST2	URST4	URST6	LOQ
24-D	0.2847	n.a.	0.1641	0.0250
ACE	n.a.	n.a.	n.a.	n.a.
ACY	n.a.	n.a.	n.a.	n.a.
ALD	0.0000	0.0000	0.0000	0.0040
AMETRYN	0.0377	n.a.	0.1133	0.0015
ANT	n.a.	n.a.	n.a.	n.a.
ATRAZ	0.9940	n.a.	0.7041	0.0050
AZINPH-E	0.0000	n.a.	n.a.	0.0050
AZINPH-M	0.0000	n.a.	n.a.	0.0250
BAA	n.a.	n.a.	n.a.	n.a.
BAP	0.0244	0.0019	0.0000	0.0040
BBF	n.a.	n.a.	n.a.	n.a.
BENTAZ	0.4441	n.a.	0.0893	0.0015
BGHIP	n.a.	n.a.	n.a.	n.a.
CARBAMAZ	5.2774	n.a.	1.0514	0.0015
CARBEND	n.a.	n.a.	n.a.	n.a.
CB138	0.0020	0.0007	0.0002	0.0004
CB153	0.0022	0.0008	0.0003	0.0005
CB28	0.0009	0.0006	0.0003	0.0001
CB52	0.0006	0.0004	0.0002	0.0002
CHLORFENV	0.0000	n.a.	n.a.	0.0050
CHLORTUR	1.2584	n.a.	0.3661	0.0050
CHRTR	0.0683	0.0379	0.0435	0.0010
CLOFIBRS	0.0843	n.a.	0.0850	0.0050
DBAHA	n.a.	n.a.	n.a.	n.a.

ng/L	URST2	URST4	URST6	LOQ
DDPP	0.0051	0.0011	0.0005	0.0001
DDEPP	0.0017	0.0007	0.0002	0.0001
DDTOP	n.a.	n.a.	n.a.	n.a.
DDTPP	0.0007	0.0003	0.0002	0.0001
DEATRAZ	0.9590	n.a.	0.4709	0.0050
DIAZINON	0.0295	n.a.	n.a.	0.0050
DICHLPR	0.1187	n.a.	0.1334	0.0050
DICLOF	0.2305	n.a.	0.1760	0.0250
DIELD	0.0123	0.0129	0.0094	0.0010
DIMETH	0.0000	n.a.	n.a.	0.0050
DIURON	2.2399	n.a.	0.8433	0.0050
END	0.0000	0.0000	0.0000	0.0020
FENUR	0.0543	n.a.	n.a.	0.0025
FL	0.5940	0.6010	1.0311	0.0200
FLU	0.3263	0.2759	0.2844	0.0130
HBCDA	0.0000	n.a.	n.a.	0.0250
HBCDBG	0.0000	n.a.	n.a.	0.0300
HCB	0.0035	0.0033	0.0025	0.0001
HCHA	0.0556	0.0357	0.0369	0.0001
HCHB	0.0515	0.0147	0.0081	0.0001
HCHD	0.0115	0.0064	0.0012	0.0001
HCHG	0.0847	0.0616	0.0433	0.0003
HEXAZIN	0.0995	n.a.	0.0000	0.0015
I123P	0.0303	0.0065	0.0042	0.0020
IRGAROL	0.2749	n.a.	0.1576	0.0015

A5 Table 1 continued:

ng/L	URST2	URST4	URST6	LOQ	ng/L	URST2	URST4	URST6	LOQ
ISOD	0.0000	0.0000	0.0000	0.0050	PFOS	0.5803	n.a.	n.a.	0.0015
ISOPRUR	1.3750	n.a.	0.4686	0.0025	PFOSA	0.0046	n.a.	n.a.	0.0015
LINUR	0.1524	n.a.	n.a.	0.0250	PHEN	0.5022	0.4475	0.6993	0.0370
MALATH	0.0000	n.a.	n.a.	0.0050	PIRIMIC	0.0000	n.a.	0.0787	0.0025
MCPA	0.4804	n.a.	0.2342	0.0050	PRIMID	1.6749	n.a.	0.4359	0.0250
MECOPR	0.6533	n.a.	0.2701	0.0050	PROMETR	0.0217	n.a.	0.1068	0.0015
METAZCHL	0.2693	n.a.	0.1846	0.0025	PROPAZ	0.0294	n.a.	0.1203	0.0050
METHABZT	0.0648	n.a.	n.a.	0.0025	PYR	0.0759	0.1311	0.0232	0.0070
METOLA	0.7120	n.a.	0.2550	0.0015	QCB	0.0012	0.0012	0.0008	0.0001
NAPROX	n.a.	n.a.	n.a.	n.a.	SIMAZ	0.3847	n.a.	0.2598	0.0050
OXAZEP	1.3340	n.a.	0.3358	0.0250	TBEP	n.a.	n.a.	n.a.	n.a.
PENDIMETH	0.1496	n.a.	0.2064	0.0050	TBP	n.a.	n.a.	n.a.	n.a.
PFBS	1.1029	n.a.	n.a.	0.0015	TERBAZ	1.0127	n.a.	0.3692	0.0015
PFDEA	0.0389	n.a.	n.a.	0.0025	TERBUTR	0.2284	n.a.	0.1316	0.0015
PFHPA	0.2503	n.a.	n.a.	0.0015	TTP	n.a.	n.a.	n.a.	n.a.
PFHXA	0.3862	n.a.	n.a.	0.0015	TRIFLU	0.0025	0.0031	0.0005	0.0001
PFHXS	0.2420	n.a.	n.a.	0.0015	SPM [mg/L]	1.77	0.92	0.4	
PFNOA	0.0706	n.a.	n.a.	0.0025	PSU	n.a.	33.85	34.37	
PFOA	0.8717	n.a.	n.a.	0.0015					

A5 Table 2: Surface water concentrations (5 m, A5 figure 1) in ng/L determined during the research cruise in the German EEZ in May 2010; with respective LOQs, PSU = Practical Salinity units; SPM = Suspended particulate matter in mg/L; n.a. = data not available

ng/L	AMRU2	AWZW1	DTEND	EIDER	ELBE1	ENTE1	ENTE3	ES1	HELGO	L1
24-D	0.1931	0.0179	0.0243	0.1878	0.2329	0.0182	0.0113	0.2008	0.3663	0.1248
ACE	n.a.	n.a.	n.a.	n.a.	n.a.	n.a.	n.a.	n.a.	n.a.	n.a.
ACY	n.a.	n.a.	n.a.	n.a.	n.a.	n.a.	n.a.	n.a.	n.a.	n.a.
ALD	0.0000	0.0000	0.0000	0.0000	0.0000	0.0007	0.0005	0.0000	0.0000	0.0000
AMETRYN	0.0465	0.0228	0.0233	0.0532	0.0702	0.0242	0.0222	0.0632	0.1024	0.0442
ANT	n.a.	n.a.	n.a.	n.a.	n.a.	n.a.	n.a.	n.a.	n.a.	n.a.
ATRAZ	1.0014	0.6410	0.6402	1.1778	1.1459	0.6145	0.6392	1.1300	2.3024	0.8944
AZINPH-E	0.0000	0.0000	0.0000	0.0000	0.0000	0.0000	0.0000	0.0000	0.0000	0.0000
AZINPH-M	0.0000	0.0000	0.0000	0.0435	0.0000	0.0000	0.0000	0.0000	0.0000	0.0000
BAA	n.a.	n.a.	n.a.	n.a.	n.a.	n.a.	n.a.	n.a.	n.a.	n.a.
BAP	0.0630	0.0000	0.0000	0.3990	0.4450	0.0000	0.0000	0.0670	0.1800	0.0500
BBF	n.a.	n.a.	n.a.	n.a.	n.a.	n.a.	n.a.	n.a.	n.a.	n.a.
BENTAZ	0.3132	0.0049	0.0012	0.4258	0.2522	0.0030	0.0006	0.1746	0.5209	0.1562
BGHIP	n.a.	n.a.	n.a.	n.a.	n.a.	n.a.	n.a.	n.a.	n.a.	n.a.
CARBAMAZ	6.7868	0.4515	0.1356	8.1426	10.6762	0.1797	0.0803	5.4331	13.2138	5.2724
CARBEND	0.6704	0.0503	0.0193	0.7837	0.8972	0.0328	0.0029	0.9653	1.6920	0.5313
CB138	0.0020	n.a.	n.a.	0.0071	0.0100	0.0003	0.0002	0.0027	n.a.	0.0021
CB153	0.0025	0.0003	0.0006	0.0086	0.0133	0.0004	0.0002	0.0036	0.0091	0.0024
CB28	0.0017	0.0004	0.0004	0.0043	0.0067	0.0006	0.0003	0.0033	0.0031	0.0015
CB52	0.0008	n.a.	n.a.	0.0022	0.0043	n.a.	n.a.	0.0018	0.0020	0.0008
CHLORFENV	0.0000	0.0000	0.0000	0.0000	0.0000	0.0000	0.0000	0.0000	0.0000	0.0000
CHLORTUR	0.8974	0.1656	0.1002	1.0462	1.3853	0.1066	0.0404	1.2293	2.2131	0.7064
CHRTR	0.1160	0.0070	0.0050	0.5570	0.6240	0.0050	0.0050	0.1160	0.2600	0.0960
CLOFIBRS	0.0957	0.0069	0.0000	0.1126	0.1550	0.0000	0.0000	0.0947	0.1988	0.0678
DBAHA	n.a.	n.a.	n.a.	n.a.	n.a.	n.a.	n.a.	n.a.	n.a.	n.a.
DDPP	0.0030	0.0003	0.0000	0.0111	0.0297	0.0000	0.0000	0.0016	0.0104	0.0024

A5 Table 2 continued:

ng/L	AMRU2	AWZW1	DTEND	EIDER	ELBE1	ENTE1	ENTE3	ES1	HELGO	L1
DDEPP	0.0019	0.0001	0.0002	0.0054	0.0105	0.0003	0.0001	0.0020	0.0055	0.0015
DDTOP	n.a.	n.a.	n.a.	n.a.	n.a.	n.a.	n.a.	n.a.	n.a.	n.a.
DDTPP	0.0016	0.0000	0.0000	0.0034	0.0096	0.0000	0.0000	0.0012	0.0036	0.0000
DEATRAZ	0.9196	0.1650	0.1760	0.5852	0.9426	0.1548	0.1419	0.6016	1.8259	0.8592
DIAZINON	0.0400	0.0243	0.0185	0.0246	0.0602	0.0225	0.0131	0.0530	0.0686	0.0302
DICHLPR	0.0000	0.0000	0.0000	0.1030	0.1342	0.0000	0.0000	0.0000	0.0000	0.0738
DICLOF	0.0123	0.0000	0.0000	0.0347	0.8020	0.0000	0.0000	0.0166	0.1833	0.0025
DIELD	0.0075	0.0076	0.0065	0.0078	0.0130	0.0110	0.0043	0.0126	0.0093	0.0059
DIMETH	0.0008	0.0000	0.0000	0.0007	0.0049	0.0000	0.0000	0.0032	0.0165	0.0000
DIURON	1.7491	0.4141	0.2775	1.9830	2.0280	0.2831	0.1901	1.3626	3.3171	1.4285
END	0.0000	0.0000	0.0000	0.0000	0.0000	0.0000	0.0002	0.0000	0.0071	0.0000
FENUR	0.1502	0.0173	0.0077	0.1244	0.6335	0.0244	0.0593	0.0675	0.4561	0.1112
FL	0.2900	0.3610	0.6120	0.2790	0.4290	0.8420	0.5250	0.3140	0.3450	0.2600
FLU	0.3390	0.1360	0.1250	1.0150	1.3900	0.1620	0.1220	0.3140	0.6100	0.2820
HBCDA	0.0000	0.0000	0.0032	0.0000	0.0000	0.0078	0.0000	0.0000	0.0000	0.0000
HBCDBG	0.0000	0.0000	0.0000	0.0000	0.0017	0.0060	0.0000	0.0000	0.0000	0.0000
HCB	0.0059	0.0039	0.0039	0.0087	0.0127	0.0065	0.0040	0.0068	0.0074	0.0053
HCHA	0.0601	0.0271	0.0341	0.0655	0.0996	0.0414	0.0321	0.0351	0.0598	0.0479
HCHB	0.0355	0.0068	0.0070	0.0521	0.0900	0.0089	0.0082	0.0255	0.0488	0.0276
HCHD	0.0190	0.0007	0.0000	0.0200	0.0435	0.0000	0.0000	0.0082	0.0166	0.0130
HCHG	0.0807	0.0306	0.0326	0.0867	0.1147	0.0395	0.0190	0.0772	0.0803	0.0684
HEXAZIN	0.1246	0.0156	0.0095	0.1614	0.2619	0.0105	0.0133	0.0628	0.3000	0.0903
I123P	0.0840	0.0000	0.0000	0.4970	0.5140	0.0000	0.0000	0.0810	0.1920	0.0590
IRGAROL	0.2404	0.0082	0.0008	0.2269	0.2458	0.0010	0.0000	0.2562	0.4291	0.2567
ISOD	0.0000	0.0000	0.0000	0.0000	0.0000	0.0000	0.0000	0.0000	0.0000	0.0000
ISOPRUR	1.4146	0.1497	0.1126	1.7831	2.7247	0.1040	0.0467	0.8369	3.6311	0.9632
LINUR	0.0955	0.0303	0.0235	0.0990	0.1153	0.0244	0.0132	0.0527	0.1434	0.0712
MALATH	0.0000	0.0000	0.0000	0.0000	0.0000	0.0000	0.0000	0.0000	0.0000	0.0000
MCPA	0.3572	0.0433	0.0337	0.4283	0.6322	0.0267	0.0132	0.4836	0.9187	0.2633
MECOPR	0.6477	0.0864	0.0597	0.7812	0.9184	0.0580	0.0204	0.9036	1.5191	0.4965
METAZCHL	0.4313	0.1418	0.0765	0.5735	0.6579	0.0919	0.0205	0.3499	1.0904	0.3395
METHABZT	0.0715	0.0034	0.0011	0.0772	0.1026	0.0004	0.0001	0.0726	0.1529	0.0540
METOLA	0.5231	0.0444	0.0252	0.5476	0.7014	0.0266	0.0231	0.9029	1.1660	0.3970
NAPROX	n.a.	n.a.	n.a.	n.a.	n.a.	n.a.	n.a.	n.a.	n.a.	n.a.
OXAZEP	1.4711	0.0000	0.0000	1.6624	2.5134	0.0000	0.0000	2.9808	3.8208	1.1132
PENDIMETH	0.1255	0.3375	0.1717	0.1033	0.1495	0.1808	0.1051	0.1713	0.3494	0.1105
PFBS	0.6414	0.0281	0.0213	0.6937	0.6313	0.0200	0.0150	0.8331	1.6887	0.5116
PFDEA	0.0809	0.0061	0.0081	0.0751	0.0963	0.0101	0.0080	0.0555	0.0973	0.0539
PFHPA	0.4303	0.0586	0.0510	0.4570	0.4090	0.0601	0.0474	0.3631	0.6305	0.2656
PFHXA	0.7107	0.0558	0.0478	0.7950	0.7453	0.0556	0.0431	0.4378	1.0137	0.4092
PFHXS	0.2965	0.0300	0.0164	0.3250	0.3035	0.0196	0.0140	0.2751	0.5821	0.2380
PFNOA	0.1653	0.0327	0.0549	0.1739	0.1362	0.0534	0.0417	0.1278	0.2300	0.1273
PFOA	1.1549	0.1806	0.1985	1.2816	1.2155	0.1955	0.1588	1.3433	2.1324	0.9152
PFOS	1.0478	0.0789	0.0525	0.9587	0.9382	0.0573	0.0441	1.0575	1.6077	0.7309
PFOSA	0.0099	0.0030	0.0057	0.0063	0.0087	0.0059	0.0037	0.0087	0.0133	0.0045
PHEN	0.3188	0.2058	0.3338	0.5708	0.7758	0.3988	0.2188	0.3958	0.4638	0.3098
PIRIMIC	0.0015	0.0000	0.0000	0.0020	0.0152	0.0000	0.0000	0.0000	0.0121	0.0000
PRIMID	2.7253	0.1352	0.0717	2.0715	4.0128	0.0778	0.0425	1.4187	5.7644	1.9807
PROMETR	0.0473	0.0056	0.0053	0.0620	0.0998	0.0052	0.0051	0.0164	0.1147	0.0350
PROPAZ	0.0429	0.0153	0.0165	0.0488	0.0512	0.0162	0.0150	0.0308	0.0877	0.0354
PYR	0.1390	0.0060	0.0320	0.7050	1.1260	0.0070	n.a.	0.1460	0.3690	0.1430
QCB	0.0018	0.0011	0.0011	0.0030	0.0049	0.0024	0.0012	0.0030	0.0027	0.0015

A5 Table 2 continued:

ng/L	AMRU2	AWZW1	DTEND	EIDER	ELBE1	ENTE1	ENTE3	ES1	HELGO	L1
SIMAZ	0.6618	0.1462	0.1293	0.5105	0.5133	0.1432	0.1239	0.3520	0.8624	0.3386
TBEP	n.a.	n.a.	n.a.	n.a.	n.a.	n.a.	n.a.	n.a.	n.a.	n.a.
TBP	n.a.	n.a.	n.a.	n.a.	n.a.	n.a.	n.a.	n.a.	n.a.	n.a.
TERBAZ	1.1365	0.0607	0.0487	1.2934	1.3585	0.0489	0.0322	0.8042	2.2958	0.8334
TERBUTR	0.2701	0.0225	0.0142	0.2795	0.3142	0.0152	0.0087	0.2371	0.5489	0.2416
TPP	n.a.	n.a.	n.a.	n.a.	n.a.	n.a.	n.a.	n.a.	n.a.	n.a.
TRIFLU	0.0006	0.0003	0.0000	0.0008	0.0026	0.0000	0.0000	0.0007	0.0012	0.0000
SPM [mg/L]	1.26	0.61	0.30	6.22	3.95	0.06	0.58	6.68	8.15	0.59
PSU	31.37	34.49	34.61	30.41	28.11	34.59	34.96	31.27	30.88	32.38

ng/L	MEDEM	NEFB	NSB2	NSB3	NSGR2	STADE	STG16	SYLT1	SYLT2	TWEMS
24-D	0.5031	0.1782	0.0730	0.2785	0.0183	2.2118	0.1498	0.1355	0.0888	0.1533
ACE	n.a.	n.a.	n.a.	n.a.	n.a.	n.a.	n.a.	n.a.	n.a.	n.a.
ACY	n.a.	n.a.	n.a.	n.a.	n.a.	n.a.	n.a.	n.a.	n.a.	n.a.
ALD	0.0000	0.0000	0.0000	0.0000	0.0005	0.0000	0.0000	0.0000	0.0000	0.0000
AMETRYN	0.2232	0.0320	0.0264	0.2045	0.0223	0.5322	0.0436	0.0437	0.0325	0.0434
ANT	n.a.	n.a.	n.a.	n.a.	n.a.	n.a.	n.a.	n.a.	n.a.	n.a.
ATRAZ	1.6397	0.8493	0.8352	1.1671	0.5719	3.9846	1.0340	0.8993	0.8458	1.0673
AZINPH-E	0.0000	0.0000	0.0000	n.a.	0.0000	0.0000	0.0000	0.0000	0.0000	0.0000
AZINPH-M	0.0000	0.0000	0.0000	n.a.	0.0000	0.0000	0.0000	0.0000	0.0000	0.0000
BAA	n.a.	n.a.	n.a.	n.a.	n.a.	n.a.	n.a.	n.a.	n.a.	n.a.
BAP	2.1220	0.0000	0.0000	0.0000	0.0000	1.9870	0.0240	0.0300	0.0000	0.0000
BBF	n.a.	n.a.	n.a.	n.a.	n.a.	n.a.	n.a.	n.a.	n.a.	n.a.
BENTAZ	1.2923	0.1303	0.1048	0.1278	0.0006	2.7789	0.1351	0.1422	0.1017	0.1706
BGHIP	n.a.	n.a.	n.a.	n.a.	n.a.	n.a.	n.a.	n.a.	n.a.	n.a.
CARBAMAZ	27.9137	2.1777	2.3496	4.0339	0.2054	86.7539	4.9155	4.9590	3.4172	5.2956
CARBEND	1.7710	0.3523	0.3515	0.6598	0.0293	5.3950	0.7623	0.5278	0.3929	0.7368
CB138	0.0458	0.0011	0.0006	0.0018	0.0006	0.0657	0.0017	0.0018	0.0009	0.0007
CB153	0.0615	0.0012	0.0006	0.0019	0.0006	0.0822	0.0022	0.0020	0.0012	0.0009
CB28	0.0208	0.0007	0.0007	0.0012	0.0007	0.0362	0.0017	0.0014	0.0009	0.0009
CB52	0.0204	n.a.	n.a.	0.0007	n.a.	0.0473	0.0013	0.0007	0.0006	0.0007
CHLORFENV	0.0000	0.0000	0.0000	n.a.	0.0000	0.0000	0.0000	0.0000	0.0000	0.0000
CHLORTUR	3.2895	0.7260	0.4934	0.8959	0.1085	7.5036	0.9337	0.7141	0.6093	0.9596
CHRTR	2.5920	0.1240	0.0090	0.0070	0.0110	2.4640	0.0660	0.0690	0.0070	0.0310
CLOFIBRS	0.3419	0.0747	0.0257	0.1790	0.0043	0.8082	0.0738	0.0689	0.0468	0.0844
DBAHA	n.a.	n.a.	n.a.	n.a.	n.a.	n.a.	n.a.	n.a.	n.a.	n.a.
DDPP	0.1540	0.0014	0.0005	0.0009	0.0004	0.6090	0.0032	0.0023	0.0007	0.0037
DDEPP	0.0566	0.0011	0.0004	0.0009	0.0002	0.1631	0.0017	0.0014	0.0007	0.0016
DDTOP	n.a.	n.a.	n.a.	n.a.	n.a.	n.a.	n.a.	n.a.	n.a.	n.a.
DDTPP	0.0591	0.0009	0.0005	0.0007	0.0000	0.1941	0.0008	0.0011	0.0006	0.0010
DEATRAZ	1.7050	0.4527	0.5374	0.7796	0.1464	2.7302	0.6813	0.8891	0.7812	0.8515
DIAZINON	0.0634	0.0340	0.0214	n.a.	0.0173	0.3972	0.0520	0.0350	0.0295	0.0529
DICHLPR	0.2024	0.0000	0.0000	0.2002	0.0000	1.2747	0.0580	0.0604	0.0000	0.0686
DICLOF	5.3251	0.0017	0.0000	0.3163	0.0000	54.9692	0.0179	0.0094	0.0037	0.0114
DIELD	0.0144	0.0126	0.0079	0.0063	0.0118	0.0132	0.0085	0.0070	0.0061	0.0085
DIMETH	0.0152	0.0000	0.0000	n.a.	0.0000	0.2032	0.0033	0.0000	0.0000	0.0043
DIURON	3.8529	0.7027	0.8323	1.2934	0.3296	10.4398	1.2869	1.4340	1.0178	1.3110
END	0.0000	0.0000	0.0000	0.0000	0.0014	0.0000	0.0000	0.0000	0.0000	0.0000
FENUR	0.8710	0.0527	0.1589	n.a.	0.0074	1.5646	0.0755	0.1026	0.0837	0.0774
FL	0.7090	0.4900	0.4610	0.3760	0.8800	0.6750	0.5300	0.3520	0.4450	0.5030
FLU	5.4930	0.1800	0.1350	0.1380	0.2680	4.8770	0.3030	0.2710	0.1130	0.2530

A5 Table 2 continued:

ng/L	MEDEM	NEFB	NSB2	NSB3	NSGR2	STADE	STG16	SYLT1	SYLT2	TWEMS
HBCDA	0.0000	0.0000	0.0000	n.a.	0.0000	0.0000	0.0000	0.0000	0.0000	0.0000
HBCDBG	0.0000	0.0000	0.0000	n.a.	0.0000	0.0269	0.0000	0.0000	0.0000	0.0000
HCB	0.0550	0.0044	0.0058	0.0043	0.0063	0.2933	0.0060	0.0056	0.0049	0.0059
HCHA	0.2900	0.0256	0.0365	0.0361	0.0362	1.1742	0.0477	0.0540	0.0362	0.0520
HCHB	0.2708	0.0114	0.0126	0.0199	0.0084	0.9568	0.0322	0.0282	0.0174	0.0326
HCHD	0.1504	0.0062	0.0058	0.0103	0.0000	0.3890	0.0154	0.0138	0.0090	0.0212
HCHG	0.2424	0.0472	0.0544	0.0565	0.0348	0.5080	0.0727	0.0752	0.0553	0.0773
HEXAZIN	0.9694	0.0405	0.0485	0.3296	0.0107	2.7136	0.1097	0.0925	0.0611	0.1313
I123P	2.0180	0.0060	0.0000	0.0000	0.0000	1.5940	0.0350	0.0370	0.0000	0.0060
IRGAROL	0.6644	0.0538	0.0823	0.2938	0.0045	1.8964	0.1687	0.2338	0.1427	0.1294
ISOD	0.0000	0.0000	0.0000	0.0000	0.0000	0.0000	0.0000	0.0000	0.0000	0.0000
ISOPRUR	5.1964	0.5476	0.5902	1.1825	0.1002	14.5860	1.3563	1.0632	0.7763	1.4872
LINUR	0.4683	0.0328	0.0368	n.a.	0.0382	1.8875	0.0553	0.0764	0.0549	0.0683
MALATH	0.0000	0.0000	0.0000	n.a.	0.0000	0.0000	0.0000	0.0000	0.0000	0.0000
MCPA	1.4371	0.3753	0.1393	0.5012	0.0222	7.3663	0.3800	0.2548	0.1851	0.4207
MECOPR	1.3601	0.7172	0.2740	0.6380	0.0473	4.8185	0.5978	0.5149	0.3655	0.6415
METAZCHL	1.5820	0.2445	0.2222	0.5825	0.0690	4.0759	0.4311	0.3449	0.2880	0.4927
METHABZT	0.1580	0.0203	0.0260	n.a.	0.0013	0.1449	0.0621	0.0580	0.0392	0.0618
METOLA	1.3020	0.4052	0.2358	0.5983	0.0378	3.0070	0.5212	0.4146	0.3321	0.4967
NAPROX	n.a.	n.a.	n.a.	n.a.	n.a.	n.a.	n.a.	n.a.	n.a.	n.a.
OXAZEP	2.6634	0.7873	0.5549	1.5999	0.0000	9.0445	1.8584	1.1344	0.9283	1.7903
PENDIMETH	0.1631	0.2603	0.1833	0.3918	0.2262	0.1752	0.2325	0.1301	0.1625	0.2122
PFBS	0.8210	0.4182	0.3127	n.a.	0.0205	0.8087	0.6222	0.4807	0.3928	0.5758
PFDEA	0.2604	0.0148	0.0412	n.a.	0.0059	0.5109	0.0431	0.0444	0.0368	0.0424
PFHPA	0.7301	0.1698	0.1816	n.a.	0.0591	1.5328	0.2561	0.2425	0.2148	0.2899
PFHXA	1.7160	0.2033	0.2207	n.a.	0.0549	3.1966	0.3607	0.3364	0.2819	0.4217
PFHXS	0.4104	0.1257	0.1338	n.a.	0.0227	1.0570	0.2276	0.2264	0.1798	0.2362
PFNOA	0.3151	0.0510	0.0797	n.a.	0.0522	0.5665	0.0991	0.1061	0.0847	0.0991
PFOA	2.1147	0.5492	0.4598	n.a.	0.1903	3.7226	0.8867	0.8341	0.6211	0.9024
PFOS	1.8468	0.3590	0.4089	n.a.	0.0739	3.7266	0.6856	0.7326	0.5836	0.6820
PFOSA	0.1242	0.0050	0.0089	n.a.	0.0035	0.0818	0.0049	0.0065	0.0046	0.0108
PHEN	2.2778	0.2658	0.3628	0.3118	0.4358	2.2688	0.4608	0.3638	0.3278	0.4218
PIRIMIC	0.0718	0.0000	0.0000	0.1980	0.0000	0.2154	0.0024	0.0000	0.0000	0.0021
PRIMID	10.2615	0.6514	0.8189	1.4187	0.0745	30.0783	1.5619	2.1804	1.4267	2.2107
PROMETR	0.4429	0.0124	0.0141	0.2118	0.0055	1.6882	0.0379	0.0353	0.0221	0.0442
PROPAZ	0.1256	0.0242	0.0255	0.2299	0.0166	0.3881	0.0379	0.0356	0.0316	0.0365
PYR	4.3890	0.0510	0.0170	0.0190	0.0060	4.5880	0.0750	0.0970	0.0170	0.0250
QCB	0.0179	0.0016	0.0018	0.0013	0.0018	0.0302	0.0027	0.0013	0.0017	0.0014
SIMAZ	0.7993	0.2295	0.2673	0.5128	0.1159	3.0966	0.3608	0.3531	0.3060	0.3818
TBEP	n.a.	n.a.	n.a.	n.a.	n.a.	n.a.	n.a.	n.a.	n.a.	n.a.
TBP	n.a.	n.a.	n.a.	n.a.	n.a.	n.a.	n.a.	n.a.	n.a.	n.a.
TERBAZ	3.1837	0.2408	0.3637	0.8622	0.0498	7.4997	0.7934	0.8736	0.5851	0.8059
TERBUTR	0.7628	0.0918	0.1056	0.3213	0.0155	3.3406	0.2274	0.2454	0.1632	0.2012
TPP	n.a.	n.a.	n.a.	n.a.	n.a.	n.a.	n.a.	n.a.	n.a.	n.a.
TRIFLU	0.0063	0.0004	0.0004	0.0004	0.0000	0.0048	0.0007	0.0006	0.0004	0.0005
SPM [mg/L]	25.53	0.70	0.90	1.14	0.12	3.17	1.28	0.87	0.36	0.83
PSU	n.a.	33.65	33.83	32.71	34.59	n.a.	31.89	32.46	33.28	31.47

ng/L	URST2	URST4	URST6	LOQ
24-D	0.1301	0.0911	0.0184	0.0250
ACE	n.a.	n.a.	n.a.	n.a.

ng/L	URST2	URST4	URST6	LOQ
ACY	n.a.	n.a.	n.a.	n.a.
ALD	0.0000	0.0000	0.0000	0.0040

A5 Table 2 continued:

ng/L	URST2	URST4	URST6	LOQ	ng/L	URST2	URST4	URST6	LOQ
AMETRYN	0.0394	0.0301	0.0215	0.0015	HCHG	0.0571	0.0471	0.0330	0.0003
ANT	n.a.	n.a.	n.a.	n.a.	HEXAZIN	0.0753	0.0509	0.0116	0.0015
ATRAZ	0.8768	0.7246	0.5615	0.0050	I123P	0.0130	0.0000	0.0000	0.0020
AZINPH-E	0.0000	0.0000	0.0000	0.0050	IRGAROL	0.1825	0.1463	0.0104	0.0015
AZINPH-M	0.0000	0.0000	0.0000	0.0250	ISOD	0.0000	0.0000	0.0000	0.0050
BAA	n.a.	n.a.	n.a.	n.a.	ISOPRUR	1.1869	0.6959	0.1407	0.0025
BAP	0.0090	0.0000	0.0000	0.0040	LINUR	0.0696	0.0569	0.0180	0.0250
BBF	n.a.	n.a.	n.a.	n.a.	MALATH	0.0000	0.0000	0.0000	0.0050
BENTAZ	0.1800	0.0892	0.0024	0.0015	MCPA	0.2938	0.1676	0.0215	0.0050
BGHP	n.a.	n.a.	n.a.	n.a.	MECOPR	0.5197	0.3121	0.0649	0.0050
CARBAMAZ	5.0105	3.0916	0.3315	0.0015	METAZCHL	0.3247	0.1983	0.0910	0.0025
CARBEND	0.6361	0.3798	0.0417	0.0015	METHABZT	0.0511	0.0363	0.0028	0.0025
CB138	0.0014	0.0009	0.0002	0.0004	METOLA	0.4118	0.2888	0.0503	0.0015
CB153	0.0014	0.0013	0.0002	0.0005	NAPROX	n.a.	n.a.	n.a.	n.a.
CB28	0.0009	0.0008	0.0005	0.0002	OXAZEP	1.1730	0.7749	0.0000	0.0250
CB52	0.0005	0.0005	n.a.	0.0004	PENDIMETH	0.1353	0.1353	0.2508	0.0050
CHLORFENV	0.0000	0.0000	0.0000	0.0050	PFBS	0.7942	0.3470	0.0362	0.0015
CHLORTUR	0.8316	0.4934	0.1594	0.0050	PFDEA	0.0424	0.0378	0.0072	0.0025
CHRTR	0.0220	n.a.	0.0070	0.0010	PFHPA	0.2777	0.2262	0.0614	0.0015
CLOFIBRS	0.0658	0.0412	0.0051	0.0050	PFHXA	0.4592	0.2972	0.0550	0.0015
DBAHA	n.a.	n.a.	n.a.	n.a.	PFHXS	0.2291	0.1797	0.0315	0.0015
DDDPP	0.0013	0.0000	0.0003	0.0001	PFNOA	0.0983	0.1009	0.0386	0.0025
DDEPP	0.0013	0.0005	0.0002	0.0001	PFOA	0.7870	0.6610	0.1922	0.0015
DDTOP	n.a.	n.a.	n.a.	n.a.	PFOS	0.6123	0.6146	0.0922	0.0015
DDTTP	0.0007	0.0005	0.0000	0.0001	PFOSA	0.0063	0.0057	0.0027	0.0015
DEATRAZ	0.9063	0.6794	0.1776	0.0050	PHEN	0.3008	0.2878	0.2938	0.0370
DIAZINON	0.0275	0.0234	0.0172	0.0050	PIRIMIC	0.0010	0.0000	0.0000	0.0025
DICHLPR	0.0000	0.0000	0.0000	0.0050	PRIMID	1.7647	1.2058	0.1055	0.0250
DICLOF	0.0083	0.0025	0.0000	0.0250	PROMETR	0.0318	0.0210	0.0056	0.0015
DIELD	0.0067	0.0059	0.0071	0.0010	PROPAZ	0.0367	0.0000	0.0168	0.0050
DIMETH	0.0000	0.0000	0.0000	0.0050	PYR	0.0460	0.0120	0.0070	0.0070
DIURON	1.2638	1.1167	0.3655	0.0050	QCB	0.0022	0.0009	0.0009	0.0001
END	0.0000	0.0000	0.0000	0.0020	SIMAZ	0.3055	0.2635	0.1140	0.0050
FENUR	0.2453	0.0655	0.0193	0.0025	TBEP	n.a.	n.a.	n.a.	n.a.
FL	0.4030	n.a.	n.a.	0.0040	TBP	n.a.	n.a.	n.a.	n.a.
FLU	0.1700	0.0900	0.1850	0.0130	TERBAZ	0.7584	0.5565	0.0618	0.0015
HBCDA	0.0000	0.0000	0.0000	0.0250	TERBUTR	0.2169	0.1538	0.0215	0.0015
HBCDBG	0.0000	0.0000	0.0000	0.0300	TPP	n.a.	n.a.	n.a.	n.a.
HCB	0.0046	0.0047	0.0052	0.0001	TRIFLU	0.0005	0.0000	0.0000	0.0001
HCHA	0.0382	0.0326	0.0290	0.0001	SPM [mg/L]	0.71	0.59	0.31	
HCHB	0.0261	0.0182	0.0064	0.0001	PSU	32.41	33.47	34.59	
HCHD	0.0108	0.0071	0.0006	0.0001					

A5 Table 3: Surface water concentrations (5 m, A5 figure 2) in ng/L determined during the research cruise in the North Sea in Aug./Sep. 2009; with respective LOQs, PSU = Practical Salinity units; SPM = Suspended particulate matter in mg/L; n.a. = data not available

ng/L	GN008	GN009	GN011	GN012	GN013	GN014	GN017	GN020	GN026	GN027	GN029
24-D	0.1496	0.0723	0.2577	0.2036	0.0454	0.0803	0.0633	0.0398	0.1534	0.0527	0.0355
ACE	0.0290	0.0220	0.0710	0.0470	0.0230	0.0610	0.0430	0.0140	0.0110	0.0000	0.0190
ACY	0.0190	0.0000	0.0000	0.0530	0.0090	0.0320	0.0140	0.0000	0.0000	0.0000	0.0000

A5 Table 3 continued:

ng/L	GN008	GN009	GN011	GN012	GN013	GN014	GN017	GN020	GN026	GN027	GN029
ALD	0.0000	0.0000	0.0000	0.0000	0.0000	0.0000	0.0000	0.0000	0.0000	0.0000	0.0000
AMETRYN	0.0221	0.0186	0.0366	0.0293	0.0107	0.0213	0.0176	0.0182	0.0332	0.0191	0.0205
ANT	0.0000	0.0000	0.0000	0.0000	0.0000	0.0270	0.0000	0.0000	0.0000	0.0000	0.0000
ATRAZ	0.6231	0.5564	1.2670	1.0174	0.7184	0.6562	0.5598	0.5628	0.8915	0.5739	0.5640
AZINPH-E	0.0000	0.0038	0.0000	0.0000	0.0000	0.0000	0.0000	0.0000	0.0000	0.0000	0.0000
AZINPH-M	0.0000	0.0000	0.0391	0.0000	0.0000	0.0000	0.0000	0.0000	0.0000	0.0000	0.0000
BAA	0.0530	0.0000	0.0180	0.0190	0.0070	0.1340	0.0090	0.0000	0.0200	0.0160	0.0050
BAP	0.0700	0.0000	0.0000	0.0000	0.0000	0.2050	0.0120	0.0070	0.0000	0.0070	0.0060
BBF	0.1470	0.0000	0.1580	0.3030	0.0220	0.3170	0.0400	0.0000	0.0000	0.0000	0.0000
BENTAZ	0.0218	0.0045	0.1908	0.1508	0.0096	0.0106	0.0059	0.0005	0.0741	0.0052	0.0003
BGHIP	0.0710	0.0000	0.0310	0.0840	0.0110	0.1810	0.0110	0.0000	0.1070	0.0000	0.0000
CARBAMAZ	0.9514	0.3084	3.6497	1.8805	0.3680	1.0413	0.3276	0.0954	2.9521	0.2356	0.0645
CARBEND	0.1380	0.0700	1.5800	0.9690	0.0603	0.1290	0.0703	0.0338	0.7060	0.0691	0.0277
CB138	0.0007	0.0006	0.0026	0.0000	0.0009	0.0014	0.0009	0.0006	0.0024	0.0000	0.0015
CB153	0.0013	0.0010	0.0062	0.0099	0.0020	0.0020	0.0007	0.0007	0.0053	0.0004	0.0007
CB28	0.0007	0.0004	0.0025	0.0015	0.0004	0.0007	0.0005	0.0004	0.0006	0.0000	0.0003
CB52	0.0004	0.0000	0.0025	0.0013	0.0000	0.0006	0.0006	0.0002	0.0000	0.0000	0.0000
CHLORFENV	0.0000	0.0000	0.0247	0.0000	0.0000	0.0000	0.0000	0.0000	0.0000	0.0000	0.0000
CHLORTUR	0.6861	0.1680	0.7580	0.6382	0.2257	0.3524	0.1444	0.0480	0.8341	0.0874	0.0232
CHRTR	0.1350	0.0270	0.0620	0.0650	0.0240	0.2350	0.0390	0.0120	0.0440	0.0190	0.0090
CLOFIBRS	0.0138	0.0000	0.0461	0.0241	0.0077	0.0000	0.0000	0.0000	0.0548	0.0000	0.0000
DBAHA	0.0070	0.0000	0.0000	0.0000	0.0000	0.0180	0.0000	0.0000	0.0000	0.0000	0.0000
DDPP	0.0022	0.0009	0.0018	0.0013	0.0000	0.0021	0.0000	0.0000	0.0012	0.0007	0.0000
DDEPP	0.0012	0.0006	0.0014	0.0012	0.0006	0.0023	0.0008	0.0005	0.0010	0.0004	0.0003
DDTOP	n.a.	n.a.	n.a.	n.a.	n.a.	n.a.	n.a.	n.a.	n.a.	n.a.	n.a.
DDTPP	0.0000	0.0000	0.0000	0.0000	0.0000	0.0000	0.0000	0.0000	0.0000	0.0000	0.0000
DEATRAZ	0.2680	0.1956	1.1337	0.9134	0.6323	0.3786	0.1898	0.1732	0.7655	0.2160	0.1603
DIAZINON	0.0219	0.0159	0.0455	0.0182	0.0000	0.0063	0.0140	0.0113	0.0180	0.0113	0.0113
DICHLPR	0.1187	0.0527	0.1302	0.1082	0.0429	0.0824	0.0478	0.0288	0.1187	0.0355	0.0295
DICLOF	0.0077	0.0086	0.0223	0.0090	0.0000	0.0100	0.0070	0.0068	0.0103	0.0063	0.0138
DIELD	0.0155	0.0109	0.0161	0.0120	0.0043	0.0115	0.0092	0.0098	0.0114	0.0094	0.0058
DIMETH	0.0000	0.0000	0.0233	0.0179	0.0000	0.0000	0.0040	0.0079	0.0091	0.0102	0.0023
DIURON	0.7254	0.4000	2.7121	1.9962	0.4346	0.7426	0.4038	0.1908	1.5921	0.2770	0.1807
END	0.0000	0.0000	0.0000	0.0000	0.0000	0.0000	0.0000	0.0030	0.0000	0.0000	0.0000
FENUR	0.0467	0.0229	0.0710	0.0459	0.0404	0.0260	0.0825	0.0467	0.0875	0.0261	0.0544
FL	0.2900	0.2860	0.3240	0.2940	0.1570	0.3130	0.3160	0.2890	0.1540	0.3060	0.2160
FLU	0.4158	0.1268	0.1848	0.2138	0.0718	0.5448	0.1538	0.0678	0.1638	0.0698	0.0578
HBCDA	0.0000	0.0086	0.0000	0.0000	0.0052	0.0000	0.0000	0.0000	0.0109	0.0049	0.0036
HBCDBG	0.0000	0.0064	0.0049	0.0024	0.0020	0.0000	0.0000	0.0000	0.0078	0.0025	0.0000
HCB	0.0028	0.0034	0.0035	0.0029	0.0021	0.0029	0.0026	0.0048	0.0037	0.0034	0.0023
HCHA	0.0277	0.0272	0.0204	0.0168	0.0083	0.0174	0.0267	0.0361	0.0343	0.0374	0.0402
HCHB	0.0113	0.0086	0.0309	0.0098	0.0063	0.0090	0.0092	0.0094	0.0283	0.0082	0.0077
HCHD	0.0018	0.0000	0.0081	0.0068	0.0000	0.0019	0.0000	0.0000	0.0063	0.0000	0.0000
HCHG	0.0499	0.0394	0.0622	0.0476	0.0205	0.0431	0.0330	0.0359	0.0648	0.0390	0.0311
HEXAZIN	0.0168	0.0252	0.0533	0.0465	0.0302	0.0208	0.0239	0.0000	0.0581	0.0169	0.0124
I123P	0.0710	0.0000	0.0260	0.0280	0.0130	0.1890	0.0150	0.0000	0.0000	0.0000	0.0000
IRGAROL	0.0276	0.0115	0.5067	0.2582	0.0288	0.0545	0.0100	0.0040	0.1264	0.0182	0.0020
ISOD	0.0070	0.0000	0.0000	0.0000	0.0000	0.0000	0.0000	0.0000	0.0000	0.0000	0.0000
ISOPRUR	0.9837	0.2388	0.5944	0.4280	0.1056	0.3020	0.2481	0.0807	0.6333	0.1147	0.0507
LINUR	0.0516	0.0306	0.2894	0.3013	0.0147	0.0000	0.0271	0.0196	0.0792	0.0220	0.0099
MALATH	0.0000	0.0000	0.0000	0.0000	0.0000	0.0000	0.0000	0.0000	0.0000	0.0000	0.0000
MCPA	0.1370	0.0626	0.6888	0.4615	0.0449	0.0693	0.0533	0.0323	0.1975	0.0543	0.0327

A5 Table 3 continued:

ng/L	GN008	GN009	GN011	GN012	GN013	GN014	GN017	GN020	GN026	GN027	GN029
MECOPR	0.5918	0.1872	0.7010	0.3539	0.0340	0.2564	0.1775	0.0381	0.4895	0.1014	0.0179
METAZCHL	0.2580	0.1613	0.2743	0.1073	0.0390	0.0846	0.1735	0.0529	0.1892	0.0693	0.0352
METHABZT	0.0093	0.0039	0.0972	0.0740	0.0013	0.0048	0.0034	0.0000	0.0523	0.0031	0.0000
METOLA	0.0440	0.0416	0.5619	0.4355	0.0944	0.3046	0.0324	0.0176	0.5031	0.0409	0.0188
NAPROX	n.a.	n.a.	n.a.	n.a.	n.a.	n.a.	n.a.	n.a.	n.a.	n.a.	n.a.
OXAZEP	0.0000	0.0000	1.3064	0.6017	0.1711	0.0798	0.0000	0.0000	0.6118	0.0000	0.0000
PENDIMETH	0.0329	0.0355	0.0217	0.0199	0.0095	0.0411	0.0481	0.0234	0.0213	0.0182	0.0243
PFBS	0.0709	0.0501	1.5820	0.9519	0.0795	0.0636	0.0538	0.0326	1.1490	0.0676	0.0269
PFDEA	0.0333	0.0417	0.1164	0.0625	0.0268	0.0227	0.0115	0.0136	0.0651	0.0154	0.0103
PFHPA	0.1744	0.1031	0.5654	0.4725	0.2586	0.1845	0.1081	0.0691	0.3433	0.0932	0.0578
PFHXA	0.2249	0.1219	0.8864	0.7111	0.2835	0.2596	0.1329	0.0836	0.5215	0.1176	0.0713
PFHXS	0.1476	0.0664	0.8016	0.6256	0.2035	0.1600	0.0614	0.0345	0.4188	0.0555	0.0250
PFNOA	0.1026	0.0742	0.1814	0.1290	0.0732	0.0707	0.0587	0.0600	0.1268	0.0673	0.0439
PFOA	0.5730	0.4336	2.9589	1.9935	0.4234	0.3779	0.3694	0.3255	1.5825	0.3795	0.2525
PFOS	0.4417	0.1772	2.7517	2.0208	0.6347	0.5106	0.1413	0.1001	1.0818	0.1459	0.0592
PFOSA	0.0074	0.0073	0.0226	0.0171	0.0090	0.0124	0.0074	0.0045	0.0126	0.0073	0.0053
PHEN	0.3214	0.2434	0.3834	0.4054	0.2114	0.5304	0.2254	0.1714	0.1684	0.1984	0.1704
PIRIMIC	0.0000	0.0000	0.0022	0.0000	0.0000	0.0000	0.0000	0.0000	0.0000	0.0000	0.0000
PRIMID	0.2633	0.1110	1.0796	0.4631	0.0962	0.2724	0.1150	0.0499	1.1402	0.0926	0.0419
PROMETR	0.0041	0.0053	0.0084	0.0049	0.0016	0.0030	0.0037	0.0039	0.0186	0.0044	0.0052
PROPAZ	0.0000	0.0116	0.0308	0.0232	0.0145	0.0130	0.0116	0.0118	0.0226	0.0000	0.0113
PYR	0.2585	0.1355	0.0795	0.1225	0.0305	0.3235	0.0455	0.0195	0.0815	0.0335	0.0085
QCB	0.0016	0.0012	0.0036	0.0020	0.0011	0.0006	0.0009	0.0012	0.0008	0.0007	0.0007
SIMAZ	0.2004	0.1224	0.5732	0.4517	0.1396	0.1505	0.1284	0.1063	0.2858	0.1056	0.0879
TBEP	n.a.	n.a.	n.a.	n.a.	n.a.	n.a.	n.a.	n.a.	n.a.	n.a.	n.a.
TBP	n.a.	n.a.	n.a.	n.a.	n.a.	n.a.	n.a.	n.a.	n.a.	n.a.	n.a.
TERBAZ	0.1289	0.0842	1.3858	1.1866	0.1108	0.1413	0.0792	0.0567	0.8867	0.0833	0.0613
TERBUTR	0.0380	0.0183	0.2526	0.0801	0.0157	0.0392	0.0187	0.0074	0.1194	0.0136	0.0087
TPP	n.a.	n.a.	n.a.	n.a.	n.a.	n.a.	n.a.	n.a.	n.a.	n.a.	n.a.
TRIFLU	0.0014	0.0018	0.0019	0.0014	0.0033	0.0102	0.0223	0.0096	0.0005	0.0019	0.0361
SPM [mg/L]	1.02	0.18	0.98	1.41	0.26	5.16	0.24	0.08	0.76	0.19	0.06
PSU	34.47	34.55	32.74	34.16	34.81	34.98	34.50	34.89	33.02	34.90	34.98

ng/L	GN033	GN035	GN036	GN038	GN039	GN040	GN041	GN043	GN044	GN045	GN046
24-D	0.0373	0.0239	0.0327	0.0394	0.1235	0.2326	0.1525	0.0303	0.0195	0.0144	0.0254
ACE	0.0500	0.0140	0.0000	0.0000	0.0090	0.0000	0.0110	0.0000	0.0000	0.0090	0.0060
ACY	0.0000	0.0000	0.0000	0.0000	0.0000	0.0000	0.0000	0.0000	0.0000	0.0000	0.0000
ALD	0.0000	0.0000	0.0000	0.0000	0.0000	n.a.	0.0000	0.0000	0.0000	0.0000	0.0000
AMETRYN	0.0219	0.0209	0.0182	0.0183	0.0232	0.0246	0.0225	0.0185	0.0192	0.0199	0.0195
ANT	0.0000	0.0000	0.0000	0.0000	0.0000	0.0000	0.0000	0.0000	0.0000	0.0000	0.0000
ATRAZ	0.5645	0.5289	0.5393	0.5734	0.7394	0.8239	0.7322	0.5564	0.5262	0.5211	0.5146
AZINPH-E	0.0000	0.0000	0.0000	0.0000	0.0000	0.0000	0.0000	0.0000	0.0000	0.0000	0.0000
AZINPH-M	0.0000	0.0000	0.0000	0.0000	0.0000	0.0000	0.0000	0.0000	0.0000	0.0000	0.0000
BAA	0.0040	0.0070	0.0000	0.0000	0.0140	0.0000	0.0000	0.0000	0.0000	0.0000	0.0000
BAP	0.0090	0.0080	0.0000	0.0000	0.0190	0.0000	0.0000	0.0000	0.0000	0.0000	0.0000
BBF	0.0000	0.0400	0.0000	0.0000	0.0510	0.0000	0.0000	0.0000	0.0000	0.0000	0.0000
BENTAZ	0.0016	0.0000	0.0000	0.0002	0.0323	0.0190	0.0134	0.0000	0.0000	0.0000	0.0000
BGHIP	0.0000	0.0000	0.0000	0.0000	0.0180	0.0000	0.0000	0.0000	0.0000	0.0000	0.0000
CARBAMAZ	0.1112	0.0531	0.0451	0.0752	1.6075	1.1020	0.8321	0.0701	0.0324	0.0542	0.0304
CARBEND	0.0428	0.0104	0.0182	0.0320	0.4190	0.3450	0.2430	0.0278	0.0000	0.0060	0.0000
CB138	0.0000	0.0000	0.0000	0.0000	0.0004	n.a.	0.0018	0.0000	0.0000	0.0000	0.0000

A5 Table 3 continued:

ng/L	GN033	GN035	GN036	GN038	GN039	GN040	GN041	GN043	GN044	GN045	GN046
CB153	0.0003	0.0001	-0.0002	-0.0002	0.0001	n.a.	0.0022	-0.0005	-0.0005	0.0002	0.0003
CB28	0.0003	0.0000	0.0000	0.0000	0.0003	n.a.	0.0000	0.0000	0.0000	0.0000	0.0000
CB52	0.0000	0.0000	0.0000	0.0000	0.0003	n.a.	0.0000	0.0000	0.0000	0.0000	0.0000
CHLORFENV	0.0000	0.0000	0.0000	0.0000	0.0000	0.0000	0.0000	0.0000	0.0000	0.0000	0.0000
CHLORTUR	0.0194	0.0095	0.0138	0.0192	0.5232	0.1872	0.1360	0.0128	0.0059	0.0087	0.0055
CHRTR	0.0160	0.0130	0.0000	0.0000	0.0440	0.0258	0.0000	0.0000	0.0000	0.0000	0.0000
CLOFIBRS	0.0000	0.0000	0.0000	0.0000	0.0330	0.0299	0.0201	0.0000	0.0000	0.0000	0.0000
DBAHA	0.0000	0.0000	0.0000	0.0000	0.0000	0.0000	0.0000	0.0000	0.0000	0.0000	0.0000
DDPP	0.0000	0.0000	0.0000	0.0000	0.0007	n.a.	0.0000	0.0000	0.0000	0.0000	0.0000
DDEPP	0.0003	0.0003	0.0003	0.0002	0.0007	n.a.	0.0000	0.0000	0.0000	0.0002	0.0002
DDTOP	n.a.	n.a.	n.a.	n.a.	n.a.	n.a.	n.a.	n.a.	n.a.	n.a.	n.a.
DDTPP	0.0000	0.0000	0.0000	0.0000	0.0000	n.a.	0.0000	0.0000	0.0000	0.0000	0.0000
DEATRAZ	0.1627	0.1367	0.1518	0.1539	0.5846	0.4108	0.3293	0.1457	0.1332	0.1360	0.1230
DIAZINON	0.0194	0.0066	0.0052	0.0056	0.0162	0.0078	0.0061	0.0039	0.0032	0.0000	0.0000
DICHLPR	0.0236	0.0000	0.0297	0.0270	0.0940	0.0803	0.0643	0.0174	0.0000	0.0145	0.0121
DICLOF	0.0138	0.0052	0.0053	0.0069	0.0000	0.0105	0.0066	0.0067	0.0058	0.0074	0.0055
DIELD	0.0045	0.0059	0.0063	0.0059	0.0110	n.a.	0.0053	0.0034	0.0052	0.0039	0.0046
DIMETH	0.0453	0.0021	0.0025	0.0040	0.0166	0.0000	0.0114	0.0039	0.0023	0.0026	0.0019
DIURON	0.3204	0.1693	0.1337	0.1719	1.0731	0.9149	0.7184	0.2143	0.5781	0.1515	0.1967
END	0.0000	0.0000	0.0000	0.0000	0.0000	n.a.	0.0000	0.0000	0.0000	0.0000	0.0000
FENUR	0.0343	0.0281	0.0285	0.0153	0.0320	0.0220	0.0149	0.0092	0.0134	0.0184	0.0071
FL	0.2240	0.2350	0.1590	0.1290	0.1230	0.0751	0.0890	0.1430	0.2490	0.0850	0.0750
FLU	0.0698	0.0358	0.0308	0.0278	0.1148	0.0333	0.0588	0.0238	0.0278	0.0208	0.0218
HBCDA	0.0048	0.0000	0.0000	0.0000	0.0000	0.0000	0.0000	0.0000	0.0000	0.0000	0.0000
HBCDBG	0.0000	0.0000	0.0000	0.0000	0.0000	0.0000	0.0000	0.0000	0.0000	0.0000	0.0000
HCB	0.0028	0.0037	0.0031	0.0033	0.0033	n.a.	0.0026	0.0020	0.0031	0.0030	0.0042
HCHA	0.0339	0.0418	0.0436	0.0451	0.0290	n.a.	0.0424	0.0325	0.0481	0.0338	0.0422
HCHB	0.0073	0.0083	0.0082	0.0085	0.0147	n.a.	0.0249	0.0080	0.0083	0.0088	0.0093
HCHD	0.0000	0.0000	0.0000	0.0000	0.0039	n.a.	0.0000	0.0000	0.0000	0.0000	0.0000
HCHG	0.0232	0.0191	0.0270	0.0277	0.0553	n.a.	0.0397	0.0181	0.0176	0.0126	0.0143
HEXAZIN	0.0138	0.0105	0.0000	0.0121	0.0360	0.0505	0.0426	0.0127	0.0106	0.0096	0.0096
I123P	0.0000	0.0000	0.0000	0.0000	0.0190	0.0000	0.0000	0.0000	0.0000	0.0000	0.0000
IRGAROL	0.0030	0.0010	0.0008	0.0029	0.0854	0.1232	0.0897	0.0011	0.0000	0.0005	0.0000
ISOD	0.0000	0.0000	0.0000	0.0000	0.0000	n.a.	0.0000	0.0000	0.0000	0.0000	0.0000
ISOPRUR	0.0350	0.0196	0.0271	0.0349	0.5166	0.2024	0.1602	0.0242	0.0129	0.0173	0.0110
LINUR	0.0198	0.0000	0.0085	0.0087	0.0500	0.0364	0.0266	0.0000	0.0000	0.0000	0.0000
MALATH	0.0000	0.0000	0.0000	0.0000	0.0000	0.0000	0.0000	0.0000	0.0000	0.0000	0.0000
MCPA	0.0640	0.0152	0.0229	0.0241	0.1439	0.1846	0.1310	0.0249	0.0079	0.0182	0.0098
MECOPR	0.0683	0.0087	0.0090	0.0140	0.4134	0.1638	0.1277	0.0153	0.0000	0.0094	0.0000
METAZCHL	0.0383	0.0335	0.0300	0.0296	0.1962	0.1135	0.1221	0.0313	0.0167	0.0108	0.0076
METHABZT	0.0000	0.0000	0.0000	0.0004	0.0307	0.0213	0.0141	0.0000	0.0000	0.0000	0.0000
METOLA	0.0183	0.0158	0.0188	0.0200	0.2764	0.1246	0.0886	0.0159	0.0172	0.0176	0.0166
NAPROX	n.a.	n.a.	n.a.	n.a.	n.a.	n.a.	n.a.	n.a.	n.a.	n.a.	n.a.
OXAZEP	0.0000	0.0000	0.0000	0.0000	0.3146	0.2493	0.1463	0.0000	0.0000	0.0000	0.0000
PENDIMETH	0.0187	0.0064	0.0086	0.0086	0.0279	0.0251	0.0200	0.0090	0.0058	0.0057	0.0054
PFBS	0.0370	0.0217	0.0258	0.0392	0.5466	0.4544	0.3398	0.0230	0.0214	0.0205	0.0187
PFDEA	0.0098	0.0085	0.0104	0.0086	0.0235	0.0293	0.0228	0.0097	0.0075	0.0082	0.0081
PFHPA	0.0648	0.0459	0.0605	0.0587	0.2319	0.2032	0.1671	0.0579	0.0400	0.0454	0.0370
PFHXA	0.0777	0.0574	0.0718	0.0688	0.3091	0.2499	0.2032	0.0692	0.0506	0.0579	0.0500
PFHXS	0.0298	0.0199	0.0255	0.0291	0.2543	0.1815	0.1408	0.0244	0.0171	0.0192	0.0168
PFNOA	0.0498	0.0435	0.0528	0.0459	0.0849	0.1140	0.0938	0.0500	0.0434	0.0450	0.0434
PFOA	0.3755	0.2306	0.2183	0.2380	0.9231	0.7560	0.6200	0.2643	0.1735	0.2207	0.1625

A5 Table 3 continued:

ng/L	GN033	GN035	GN036	GN038	GN039	GN040	GN041	GN043	GN044	GN045	GN046
PFOS	0.0779	0.0498	0.0683	0.0680	0.5388	0.4530	0.3441	0.0533	0.0366	0.0428	0.0395
PFOSA	0.0029	0.0064	0.0072	0.0041	0.0064	0.0066	0.0073	0.0046	0.0034	0.0029	0.0049
PHEN	0.2624	0.1814	0.0864	0.0674	0.1044	0.0000	0.1324	0.1614	0.2654	0.0714	0.0734
PIRIMIC	0.0000	0.0000	0.0000	0.0000	0.0000	0.0000	0.0000	0.0000	0.0000	0.0000	0.0000
PRIMID	0.0633	0.0353	0.0364	0.0521	0.5963	0.6740	0.4551	0.0447	0.0238	0.0366	0.0276
PROMETR	0.0051	0.0046	0.0044	0.0051	0.0070	0.0414	0.0291	0.0041	0.0039	0.0045	0.0043
PROPAZ	0.0000	0.0108	0.0097	0.0109	0.0179	0.0308	0.0238	0.0099	0.0089	0.0089	0.0082
PYR	0.0195	0.0095	0.0085	0.0065	0.0895	0.0000	0.0215	0.0065	0.0085	0.0075	0.0075
QCB	0.0009	0.0008	0.0007	0.0007	0.0006	n.a.	0.0005	0.0005	0.0009	0.0006	0.0008
SIMAZ	0.0981	0.1004	0.0819	0.1065	0.2319	0.4526	0.3073	0.1002	0.0873	0.0877	0.0868
TBEP	n.a.	n.a.	n.a.	n.a.	n.a.	n.a.	n.a.	n.a.	n.a.	n.a.	n.a.
TBP	n.a.	n.a.	n.a.	n.a.	n.a.	n.a.	n.a.	n.a.	n.a.	n.a.	n.a.
TERBAZ	0.0477	0.0213	0.0341	0.0478	0.3860	0.3522	0.2625	0.0337	0.0140	0.0283	0.0346
TERBUTR	0.0160	0.0075	0.0055	0.0072	0.0766	0.0526	0.0422	0.0092	0.0041	0.0076	0.0046
TPP	n.a.	n.a.	n.a.	n.a.	n.a.	n.a.	n.a.	n.a.	n.a.	n.a.	n.a.
TRIFLU	0.0130	0.0142	0.0097	0.0014	0.0005	n.a.	0.0004	0.0025	0.0024	0.0007	0.0004
SPM [mg/L]	0.27	0.17	0.14	0.13	0.89	0.34	0.08	0.08	0.05	0.15	0.05
PSU	34.45	35.06	35.04	34.94	33.98	30.90	32.08	34.88	35.16	35.09	35.20

ng/L	GN048	GN050	GN051	GN052	GN053	GN902	GN904	GN909	GN911	LOQ
24-D	0.0256	0.1380	0.1534	0.0409	0.0268	0.0353	0.0157	0.0206	0.0499	0.0250
ACE	0.0000	0.0280	0.0130	0.0000	0.0000	0.0290	0.0200	0.0130	0.0240	0.0010
ACY	0.0000	0.0140	0.0000	0.0000	0.0000	0.0000	0.0000	0.0000	0.0000	0.0010
ALD	0.0000	0.0000	0.0000	0.0000	0.0000	0.0000	0.0000	0.0000	0.0000	0.0040
AMETRYN	0.0195	0.0309	0.0243	0.0211	0.0210	0.0147	0.0158	0.0197	0.0120	0.0015
ANT	0.0000	0.0000	0.0000	0.0000	0.0000	0.0000	0.0000	0.0000	0.0000	0.0030
ATRAZ	0.5426	0.6998	0.7373	0.5349	0.5406	0.6020	0.5896	0.6440	0.7420	0.0050
AZINPH-E	0.0000	0.0000	0.0000	0.0000	0.0000	0.0000	0.0000	0.0000	0.0000	0.0050
AZINPH-M	0.0000	0.0000	0.0000	0.0000	0.0000	0.0000	0.0000	0.0000	0.0000	0.0250
BAA	0.0000	0.0000	0.0000	0.0000	0.0000	0.0190	0.0070	0.0030	0.0160	0.0010
BAP	0.0000	0.0000	0.0000	0.0000	0.0000	0.0260	0.0100	0.0000	0.0200	0.0040
BBF	0.0000	0.0000	0.0000	0.0000	0.0000	0.0460	0.0200	0.0000	0.0370	0.0020
BENTAZ	0.0000	0.0131	0.0111	0.0000	0.0000	0.0023	0.0022	0.0068	0.0146	0.0015
BGHIP	0.0000	0.0000	0.0000	0.0000	0.0000	0.0250	0.0090	0.0050	0.0160	0.0020
CARBAMAZ	0.0572	0.9362	0.7855	0.1092	0.0379	0.3286	0.1203	0.1537	0.4802	0.0015
CARBEND	0.0168	0.2900	0.2470	0.0249	0.0053	0.0781	0.0481	0.0580	0.0950	0.0015
CB138	0.0000	0.0000	0.0000	0.0000	0.0000	0.0006	0.0006	0.0012	0.0011	0.0004
CB153	0.0002	0.0003	0.0003	0.0003	0.0004	0.0008	0.0004	0.0008	0.0020	0.0019
CB28	0.0000	0.0000	0.0000	0.0000	0.0000	0.0003	0.0003	0.0000	0.0000	0.0001
CB52	0.0302	0.0000	0.0000	0.0000	0.0000	0.0005	0.0000	0.0000	0.0004	0.0002
CHLORFENV	0.0000	0.0000	0.0000	0.0000	0.0000	0.0000	0.0000	0.0000	0.0000	0.0050
CHLORTUR	0.0108	0.1769	0.1321	0.0177	0.0073	0.1767	0.0971	0.1567	0.2716	0.0050
CHRTR	0.0150	0.0220	0.0140	0.0060	0.0000	0.0410	0.0180	0.0000	0.0300	0.0010
CLOFIBRS	0.0000	0.0183	0.0191	0.0000	0.0000	0.0000	0.0000	0.0000	0.0099	0.0050
DBAHA	0.0000	0.0000	0.0000	0.0000	0.0000	0.0000	0.0000	0.0000	0.0000	0.0040
DDPP	0.0000	0.0005	0.0000	0.0000	0.0000	0.0000	0.0000	0.0000	0.0000	0.0001
DDEPP	0.0002	0.0004	0.0003	0.0002	0.0002	0.0005	0.0003	0.0003	0.0005	0.0002
DDTOP	n.a.	n.a.	n.a.	n.a.	n.a.	n.a.	n.a.	n.a.	n.a.	n.a.
DDTPP	0.0000	0.0000	0.0000	0.0000	0.0000	0.0000	0.0000	0.0006	0.0000	0.0001
DEATRAZ	0.1488	0.3449	0.3296	0.1482	0.1338	0.3501	0.2899	0.3321	0.8447	0.0050
DIAZINON	0.0000	0.0000	0.0000	0.0000	0.0000	0.0000	0.0000	0.0000	0.0000	0.0050

A5 Table 3 continued:

ng/L	GN048	GN050	GN051	GN052	GN053	GN902	GN904	GN909	GN911	LOQ
DICHLPR	0.0000	0.0500	0.0517	0.0000	0.0198	0.0638	0.0234	0.0758	0.0570	0.0050
DICLOF	0.0064	0.0188	0.0070	0.0000	0.0059	0.0000	0.0000	0.0060	0.0203	0.0250
DIELD	0.0048	0.0067	0.0054	0.0036	0.0035	0.0049	0.0052	0.0031	0.0039	0.0010
DIMETH	0.0046	0.0095	0.0096	0.0088	0.0028	0.0022	0.0024	0.0045	0.0000	0.0050
DIURON	0.1863	0.7561	0.6978	0.1322	0.1286	0.3958	0.2331	0.2974	0.5257	0.0050
END	0.0000	0.0000	0.0000	0.0000	0.0000	0.0000	0.0000	0.0000	0.0000	0.0020
FENUR	0.0112	0.0216	0.0226	0.0147	0.0104	0.0133	0.0185	0.0139	0.0223	0.0025
FL	0.1750	0.1250	0.0880	0.0590	0.0370	0.1370	0.0870	0.0410	0.1200	0.0040
FLU	0.0338	0.0718	0.0568	0.0168	0.0108	0.1088	0.0598	0.0288	0.0888	0.0130
HBCDA	0.0000	0.0000	0.0000	0.0000	0.0000	0.0000	0.0000	0.0000	0.0000	0.0250
HBCDBG	0.0000	0.0000	0.0000	0.0000	0.0000	0.0020	0.0000	0.0000	0.0000	0.0250
HCB	0.0033	0.0032	0.0025	0.0025	0.0027	0.0023	0.0031	0.0018	0.0021	0.0001
HCHA	0.0381	0.0394	0.0354	0.0420	0.0321	0.0101	0.0098	0.0081	0.0077	0.0001
HCHB	0.0094	0.0248	0.0259	0.0118	0.0084	0.0065	0.0052	0.0052	0.0059	0.0001
HCHD	0.0000	0.0000	0.0000	0.0000	0.0000	0.0000	0.0000	0.0000	0.0000	0.0001
HCHG	0.0182	0.0411	0.0352	0.0188	0.0123	0.0222	0.0169	0.0138	0.0199	0.0046
HEXAZIN	0.0120	0.0431	0.0392	0.0119	0.0111	0.0198	0.0210	0.0272	0.0376	0.0015
I123P	0.0000	0.0000	0.0000	0.0000	0.0000	0.0270	0.0090	0.0050	0.0190	0.0020
IRGAROL	0.0012	0.0853	0.0870	0.0065	0.0005	0.0346	0.0134	0.0207	0.0205	0.0015
ISOD	0.0000	0.0000	0.0000	0.0000	0.0000	0.0000	0.0000	0.0002	0.0000	0.0050
ISOPRUR	0.0216	0.1926	0.1628	0.0253	0.0122	0.0890	0.0555	0.1091	0.1279	0.0025
LINUR	0.0000	0.0330	0.0261	0.0000	0.0000	0.0064	0.0056	0.0079	0.0000	0.0250
MALATH	0.0000	0.0000	0.0000	0.0000	0.0000	0.0000	0.0000	0.0000	0.0000	0.0050
MCPA	0.0217	0.1171	0.1201	0.0118	0.0124	0.0318	0.0110	0.0091	0.0334	0.0050
MECOPR	0.0150	0.1326	0.1209	0.0108	0.0071	0.0431	0.0162	0.0182	0.0432	0.0050
METAZCHL	0.0195	0.1059	0.1390	0.0361	0.0057	0.0328	0.0158	0.0229	0.0441	0.0025
METHABZT	0.0000	0.0161	0.0145	0.0000	0.0000	0.0023	0.0018	0.0047	0.0022	0.0025
METOLA	0.0166	0.1091	0.0876	0.0242	0.0195	0.2663	0.0659	0.1663	0.1030	0.0015
NAPROX	n.a.	n.a.	n.a.	n.a.	n.a.	n.a.	n.a.	n.a.	n.a.	n.a.
OXAZEP	0.0000	0.1472	0.1187	0.0000	0.0000	0.0000	0.0000	0.0984	0.2962	0.0250
PENDIMETH	0.0079	0.0207	0.0224	0.0081	0.0041	0.0139	0.0111	0.0093	0.0103	0.0050
PFBS	0.0313	0.3884	0.2914	0.0530	0.0193	0.0502	0.0418	0.0504	n.a.	0.0015
PFDEA	0.0081	0.0255	0.0222	0.0102	0.0094	0.0096	0.0078	0.0084	n.a.	0.0025
PFHPA	0.0495	0.1674	0.1469	0.0472	0.0405	0.0848	0.0658	0.0898	n.a.	0.0015
PFHXA	0.0647	0.2129	0.1788	0.0649	0.0500	0.1155	0.0905	0.1217	n.a.	0.0015
PFHXS	0.0582	0.1422	0.1292	0.0307	0.0176	0.0841	0.0642	0.0822	n.a.	0.0015
PFNOA	0.0470	0.0979	0.0937	0.0499	0.0450	0.0455	0.0464	0.0387	n.a.	0.0025
PFOA	0.2391	0.6203	0.5626	0.1562	0.1825	0.1692	0.1541	0.1725	n.a.	0.0015
PFOS	0.2241	0.3695	0.3176	0.0689	0.0397	0.1662	0.1325	0.1669	n.a.	0.0015
PFOSA	0.0060	0.0060	0.0056	0.0035	0.0046	0.0054	0.0041	0.0062	n.a.	0.0015
PHEN	0.1884	0.1614	0.1174	0.0614	0.0404	0.1834	0.1474	0.0734	0.1454	0.0370
PIRIMIC	0.0000	0.0000	0.0000	0.0000	0.0000	0.0000	0.0000	0.0000	0.0000	0.0025
PRIMID	0.0393	0.4520	0.4208	0.0681	0.0266	0.0950	0.0508	0.0556	0.1170	0.0250
PROMETR	0.0047	0.0249	0.0284	0.0078	0.0048	0.0035	0.0032	0.0043	0.0022	0.0015
PROPAZ	0.0094	0.0214	0.0225	0.0000	0.0000	0.0120	0.0106	0.0117	0.0214	0.0050
PYR	0.0065	0.0185	0.0115	0.0045	0.0045	0.0475	0.0215	0.0095	0.0425	0.0070
QCB	0.0006	0.0005	0.0003	0.0005	0.0004	0.0007	0.0010	0.0007	0.0006	0.0012
SIMAZ	0.0935	0.2833	0.3161	0.1220	0.1018	0.1214	0.1116	0.1118	0.1512	0.0050
TBEP	n.a.	n.a.	n.a.	n.a.	n.a.	n.a.	n.a.	n.a.	n.a.	n.a.
TBP	n.a.	n.a.	n.a.	n.a.	n.a.	n.a.	n.a.	n.a.	n.a.	n.a.
TERBAZ	0.0327	0.2802	0.2439	0.0530	0.0320	0.0785	0.0574	0.0620	0.0937	0.0015
TERBUTR	0.0085	0.0479	0.0411	0.0055	0.0061	0.0141	0.0088	0.0172	0.0233	0.0015

A5 Table 3 continued:

ng/L	GN048	GN050	GN051	GN052	GN053	GN902	GN904	GN909	GN911	LOQ
TPP	n.a.	n.a.	n.a.	n.a.	n.a.	n.a.	n.a.	n.a.	n.a.	n.a.
TRIFLU	0.0008	0.0004	0.0005	0.0000	0.0000	0.0015	0.0048	0.0008	0.0010	0.0001
SPM [mg/L]	0.07	0.26	0.23	0.05	0.06	1.46	1.15	0.73	1.21	
PSU	34.98	32.59	32.33	34.76	35.23	35.04	35.16	35.10	34.62	

A5 Table 4: Surface water concentrations (5 m, A5 figure 3) in ng/L of the Baltic Sea in Feb. 2005; data >LOQs, PSU = Practical Salinity units; SPM = Suspended particulate matter in mg/L; n.a. = data not available

ng/L	T10	T109	T200	T222	T253	T270	T284	T41	TO11	LOQ
ANT	0.0330	0.0180	0.0190	0.0240	0.0240	0.0310	0.0220	0.0230	0.0700	n.a.
BAA	0.0600	0.0640	0.0690	0.0820	0.0980	0.1230	0.1040	0.0750	0.1990	n.a.
BAP	0.0650	0.0540	0.0540	0.0490	0.0640	0.0790	0.0700	n.a.	0.2640	n.a.
BBF	0.2410	0.2160	0.1850	0.1880	0.2150	0.2790	0.2620	0.2820	0.6100	n.a.
BGHIP	0.1410	0.1040	0.0780	0.0720	0.0920	0.1120	0.1040	0.1880	0.4100	n.a.
CB 138	0.0020	0.0010	0.0010	0.0010	0.0010	0.0010	0.0010	0.0030	0.0030	n.a.
CB 153	0.0030	0.0020	0.0010	0.0010	0.0010	0.0010	0.0010	0.0040	0.0060	n.a.
CB 28	0.0060	0.0040	0.0040	0.0040	0.0040	0.0040	0.0040	0.0050	0.0050	n.a.
CB 52	0.0030	0.0020	0.0020	0.0020	0.0020	0.0020	0.0020	0.0030	0.0030	n.a.
CHRTR	0.1420	0.1610	0.1850	0.2050	0.2290	0.2950	0.2790	0.1570	0.3250	n.a.
DBAHA	0.0240	0.0180	0.0130	0.0120	0.0150	0.0190	0.0170	0.0320	n.a.	n.a.
DDDPP	0.0090	0.0070	0.0050	0.0070	0.0060	0.0080	0.0060	0.0070	0.0110	n.a.
DDEPP	0.0070	0.0060	0.0040	0.0050	0.0040	0.0030	0.0030	0.0060	0.0130	n.a.
DDTPP	0.0050	0.0040	0.0030	0.0030	0.0020	0.0030	0.0020	0.0050	0.0050	n.a.
FLU	1.1620	1.1920	1.2040	1.8040	1.3050	1.5170	1.3170	1.1800	1.9110	n.a.
HCB	0.0100	0.0080	0.0080	0.0070	0.0090	0.0080	0.0090	0.0090	0.0100	n.a.
I123P	0.1440	0.1070	0.0760	0.0730	0.0990	0.1190	0.1110	0.1990	0.3840	n.a.
PHEN	1.5150	0.9340	1.2900	1.7890	1.2340	1.6090	1.5730	1.2720	1.2580	n.a.
PYR	0.4340	0.4440	0.4320	0.6220	0.5220	0.6190	0.5510	0.4470	0.7820	n.a.
SPM [mg/L]	n.a.	n.a.	n.a.	n.a.	n.a.	n.a.	n.a.	n.a.	n.a.	
PSU	n.a.	n.a.	n.a.	n.a.	n.a.	n.a.	n.a.	n.a.	n.a.	

A5 Table 5: Surface water concentrations (6 m, A5 figure 4) in ng/L of the Baltic Sea in Jun./Jul. 2008; with respective LOQs, PSU = Practical Salinity units; SPM = Suspended particulate matter in mg/L; n.a. = data not available

ng/L	35	37	52	53	54	55	57	60	62	63	64	65
24-D	0.3890	0.2409	1.0277	0.9458	0.7395	0.5537	0.9644	1.0113	1.1194	1.1213	1.1648	1.4465
AMETRYN	0.0164	0.0066	0.0285	0.0283	0.0273	0.0266	0.0345	0.0347	0.0371	0.0362	0.0365	0.0400
ATRAZ	1.8341	1.1480	2.0125	2.0114	2.1792	2.0327	2.4500	2.4649	2.4182	2.4861	2.4596	2.4904
AZINPH-E	0.0000	0.0000	0.0000	0.0000	0.0000	0.0000	0.0000	0.0000	0.0000	0.0000	0.0000	0.0000
AZINPH-M	0.0000	0.0000	0.0000	0.0000	0.0000	0.0000	0.0000	0.0000	0.0000	0.0000	0.0000	0.0000
BENTAZ	0.0189	0.0122	0.0389	0.0456	0.0272	0.0281	0.0129	0.0245	0.1034	0.0295	0.0281	0.0233
CARBAMAZ	0.9116	0.5983	1.6510	1.5933	1.4417	1.1778	1.6621	1.6479	1.6995	1.6732	1.7602	1.8693
CARBEND	n.a.	n.a.	n.a.	n.a.	n.a.	n.a.	n.a.	n.a.	n.a.	n.a.	n.a.	n.a.
CHLORFENV	0.0000	0.0000	0.0000	0.0000	0.0000	0.0000	0.0000	0.0000	0.0000	0.0000	0.0000	0.0000
CHLORTUR	0.0655	0.0413	0.0844	0.0861	0.0860	0.0761	0.1099	0.1052	0.1133	0.1214	0.1194	0.1232
CLOFIBRS	0.0742	0.0309	0.0878	0.0883	0.0936	0.0939	0.1142	0.0985	0.1525	0.1079	0.1048	0.1222
DEATRAZ	0.7806	0.5532	0.8813	0.8637	0.8909	0.8853	0.8456	0.8443	0.9880	1.0034	0.8716	0.9891
DIAZINON	0.0000	0.0000	0.0000	0.0000	0.0000	0.0000	0.0000	0.0000	0.0000	0.0000	0.0000	0.0000
DICHLPR	0.2024	0.0000	0.0000	0.0000	0.1819	0.1790	0.2122	0.1242	0.1810	0.1302	0.1343	0.2057

A5 Table 5 continued:

ng/L	35	37	52	53	54	55	57	60	62	63	64	65
DICLOF	0.0204	0.0177	0.0502	0.0210	0.0363	0.0654	3.2938	0.0343	0.0391	0.0706	0.0984	0.0559
DIMETH	0.0000	0.0000	0.0000	0.0000	0.0000	0.0000	0.0000	0.0000	0.0000	0.0000	0.0000	0.0000
DIURON	0.5033	0.3362	1.5548	1.4559	0.8471	0.7172	0.9421	0.8962	0.9155	0.9528	0.9556	0.9745
FENUR	0.0072	0.1182	0.2331	0.0208	0.0190	0.0120	0.0278	0.0204	0.0124	0.0089	0.0147	0.0178
HBCDA	0.0000	0.0000	0.0000	0.0000	0.0000	0.0000	0.0000	0.0017	0.0000	0.0000	0.0000	0.0000
HBCDBG	0.0000	0.0000	0.0000	0.0000	0.0000	0.0000	0.0000	0.0017	0.0000	0.0000	0.0000	0.0000
HEXAZIN	0.0635	0.0518	0.0797	0.0808	0.0687	0.0699	0.0628	0.0679	0.0633	0.0640	0.0601	0.0744
IRGAROL	0.1992	1.2397	4.5253	0.7949	0.4080	1.3260	0.7677	0.3763	0.7160	0.4380	0.4441	0.6683
ISOPRUR	0.0686	0.0398	0.0908	0.0861	0.0895	0.0765	0.1219	0.1135	0.1318	0.1448	0.1375	0.1763
LINUR	0.0000	0.0000	0.0000	0.0000	0.0000	0.0000	0.0000	0.0397	0.0420	0.0338	0.0379	0.0421
MALATH	0.0000	0.0000	0.0000	0.0000	0.0000	0.0000	0.0000	0.0000	0.0000	0.0000	0.0000	0.0000
MCPA	0.3231	0.2939	1.4610	1.2575	0.5032	0.4297	0.4433	0.4391	0.4527	0.4447	0.4366	0.5022
MECOPR	0.0701	0.0425	0.1197	0.1219	0.1015	0.0818	0.1220	0.1243	0.1349	0.1397	0.1398	0.1435
METAZCHL	0.0254	0.0146	0.0617	0.0616	0.0566	0.0371	0.0739	0.0722	0.0779	0.0749	0.0829	0.0853
METHABZT	0.0305	0.0157	0.0412	0.0414	0.0439	0.0373	0.0522	0.0517	0.0563	0.0574	0.0561	0.0575
METOLA	0.0127	0.0082	0.0208	0.0201	0.0199	0.0172	0.0243	0.0251	0.0291	0.0276	0.0280	0.0376
NAPROX	n.a.	n.a.	n.a.	n.a.	n.a.	n.a.	n.a.	n.a.	n.a.	n.a.	n.a.	n.a.
OXAZEP	0.0000	0.0000	0.3784	0.3406	0.0000	0.0000	0.0000	0.0000	0.0000	0.0000	0.0000	0.0000
PENDIMETH	0.0361	0.0172	0.0359	0.0339	0.0394	0.0299	0.0515	0.0493	0.0684	0.0855	0.0714	0.1208
PFBS	0.0397	0.0287	0.0547	0.0621	0.0526	0.0476	0.0526	0.0487	0.1196	0.0561	0.0585	0.0417
PFDEA	0.0064	0.0073	0.0170	0.0159	0.0105	0.0094	0.0104	0.0138	0.0169	0.0217	0.0163	0.0194
PFHPA	0.1366	0.1230	0.2364	0.2209	0.1674	0.1706	0.1938	0.1723	0.3920	0.1967	0.1930	0.2614
PFHXA	0.0475	0.0359	0.0706	0.0721	0.0515	0.0642	0.1154	0.0697	0.3627	0.0823	0.0803	0.1828
PFHXS	0.1291	0.1155	0.1530	0.1469	0.1462	0.1376	0.1482	0.1483	0.1430	0.1483	0.1456	0.1480
PFNOA	0.0718	0.0813	0.1571	0.1658	0.1077	0.1058	0.1284	0.1165	0.1579	0.1445	0.1323	0.1078
PFOA	0.3293	0.2902	0.4344	0.4312	0.3957	0.3671	0.4343	0.4117	0.4736	0.4448	0.4374	0.4380
PFOS	0.1591	0.1665	0.2899	0.2897	0.2270	0.2149	0.2715	0.2625	0.2380	0.3288	0.2956	0.2366
PFOSA	0.0000	0.0000	0.0000	0.0000	0.0000	0.0000	0.0000	0.0000	0.0027	0.0000	0.0000	0.0052
PIRIMIC	0.0000	0.0000	0.0000	0.0000	0.0000	0.0000	0.0000	0.0000	0.0000	0.0000	0.0000	0.0000
PRIMID	1.7506	1.2199	2.1492	2.0775	2.1361	2.0372	2.0321	2.0513	2.3358	2.3762	2.0674	2.3701
PROMETR	0.2386	0.1304	0.3211	0.3103	0.2966	0.2744	0.3141	0.3212	0.3358	0.3396	0.3345	0.3257
PROPAZ	0.1392	0.0990	0.1740	0.1738	0.1691	0.1726	0.1824	0.1819	0.1920	0.1898	0.1861	0.1842
SIMAZ	2.3921	1.5557	2.3734	2.3537	2.6115	2.5535	2.8054	2.8083	2.7906	2.7828	2.8123	2.7227
TBEP	n.a.	n.a.	n.a.	n.a.	n.a.	n.a.	n.a.	n.a.	n.a.	n.a.	n.a.	n.a.
TBP	n.a.	n.a.	n.a.	n.a.	n.a.	n.a.	n.a.	n.a.	n.a.	n.a.	n.a.	n.a.
TERBAZ	0.2266	0.1902	0.2857	0.2898	0.2886	0.2592	0.3224	0.3095	0.3528	0.3413	0.3416	0.3895
TERBUTR	0.0128	0.0129	0.0296	0.0231	0.0213	0.0184	0.0269	0.0264	0.0298	0.0280	0.0283	0.0324
TPP	n.a.	n.a.	n.a.	n.a.	n.a.	n.a.	n.a.	n.a.	n.a.	n.a.	n.a.	n.a.
SPM [mg/L]	n.a.	n.a.	n.a.	n.a.	n.a.	n.a.	n.a.	n.a.	n.a.	n.a.	n.a.	n.a.
PSU	n.a.	n.a.	n.a.	n.a.	n.a.	n.a.	n.a.	n.a.	n.a.	n.a.	n.a.	n.a.

ng/L	65a	65b	66	68a	70	73	75	76	605	271	BB3	LOQ
24-D	1.3935	1.4147	1.7910	1.0808	0.7221	0.6216	0.2992	0.1784	0.3710	1.2564	0.2409	0.0250
AMETRYN	0.0396	0.0405	0.0421	0.0000	0.0000	0.0000	0.0000	0.0000	0.0205	0.0403	0.0048	0.0015
ATRAZ	2.5796	2.6497	2.4309	2.0677	1.8373	1.8691	1.1809	0.9565	1.8617	2.5318	1.1193	0.0050
AZINPH-E	0.0000	0.0000	0.0000	0.0000	0.0000	0.0000	0.0000	0.0000	0.0000	0.0000	0.0000	0.0050
AZINPH-M	0.0000	0.0000	0.0000	0.0000	0.0000	0.0000	0.0000	0.0000	0.0000	0.0000	0.0000	0.0250
BENTAZ	0.0297	0.0273	0.0382	0.0174	0.0163	0.0194	0.0290	0.0116	0.0236	0.0327	0.0136	0.0015
CARBAMAZ	1.9280	2.0008	2.3283	1.9876	1.7773	1.7318	1.6530	1.1768	0.9995	2.0938	0.5544	0.0015
CARBEND	n.a.	n.a.	n.a.	n.a.	n.a.	n.a.	n.a.	n.a.	n.a.	n.a.	n.a.	n.a.
CHLORFENV	0.0000	0.0000	0.0000	0.0000	0.0000	0.0000	0.0000	0.0000	0.0000	0.0000	0.0000	0.0050

A5 Table 5 continued:

ng/L	65a	65b	66	68a	70	73	75	76	605	271	BB3	LOQ
CHLORTUR	0.1328	0.1345	0.1426	0.1152	0.1272	0.1349	0.1812	0.1559	0.0653	0.1230	0.0294	0.0050
CLOFIBRS	0.1051	0.1318	0.1037	0.0938	0.0808	0.0767	0.0498	0.0304	0.0846	0.1158	0.0260	0.0050
DEATRAZ	1.0413	1.0489	1.0413	0.8927	0.8001	0.7723	0.5753	0.4241	0.7953	0.9924	0.5008	0.0050
DIAZINON	0.0000	0.0000	0.0000	0.0000	0.0000	0.0000	0.0029	0.0012	0.0000	0.0000	0.0000	0.0050
DICHLPR	0.1491	0.1849	0.1717	0.2338	0.2066	0.1906	0.1206	0.0830	0.0000	0.1399	0.0000	0.0050
DICLOF	0.0301	0.0315	0.0243	0.0197	0.0459	0.0160	0.0162	0.0162	0.0299	0.0614	0.0185	0.0250
DIMETH	0.0000	0.0000	0.0002	0.0000	0.0000	0.0000	0.0000	0.0000	0.0000	0.0000	0.0000	0.0050
DIURON	1.0384	1.0460	1.1924	1.7502	1.6174	1.5130	1.4823	1.1068	0.4992	1.0097	0.2964	0.0050
FENUR	0.0248	0.0161	0.0102	0.0152	0.0238	0.0089	0.0247	0.0376	0.0260	0.3048	0.0171	0.0025
HBCDA	0.0000	0.0000	0.0000	0.0000	0.0000	0.0000	0.0000	0.0000	0.0000	0.0070	0.0000	0.0250
HBCDBG	0.0000	0.0000	0.0000	0.0000	0.0000	0.0000	0.0000	0.0000	0.0000	0.0070	0.0000	0.0250
HEXAZIN	0.0754	0.0721	0.0836	0.0980	0.0946	0.0957	0.0478	0.0274	0.0626	0.0756	0.0420	0.0015
IRGAROL	0.2998	0.3098	2.4691	0.3882	1.0196	1.0566	0.7274	1.5629	1.7331	1.1719	0.1777	0.0015
ISOPRUR	0.1964	0.1975	0.2453	0.2221	0.2494	0.2696	0.3680	0.3333	0.0718	0.1536	0.0360	0.0025
LINUR	0.0507	0.0523	0.0509	0.0328	0.0247	0.0209	0.0271	0.0177	0.0000	0.0381	0.0000	0.0250
MALATH	0.0000	0.0000	0.0000	0.0000	0.0000	0.0000	0.0000	0.0000	0.0000	0.0000	0.0000	0.0050
MCPA	0.5542	0.5304	0.5674	0.7008	0.5648	0.5206	0.3441	0.1601	0.2641	0.5042	0.2528	0.0050
MECOPR	0.1543	0.1526	0.1757	0.2179	0.2138	0.2195	0.2324	0.1815	0.0596	0.1504	0.0270	0.0050
METAZCHL	0.0928	0.0903	0.1104	0.1337	0.1403	0.1507	0.1338	0.1112	0.0242	0.0969	0.0136	0.0025
METHABZT	0.0605	0.0578	0.0593	0.0735	0.0847	0.0870	0.0488	0.0244	0.0305	0.0628	0.0128	0.0025
METOLA	0.0388	0.0451	0.0672	0.1365	0.0918	0.0712	0.0843	0.0769	0.0148	0.0372	0.0083	0.0015
NAPROX	n.a.	n.a.	n.a.	n.a.	n.a.	n.a.	n.a.	n.a.	n.a.	n.a.	n.a.	n.a.
OXAZEP	0.0000	0.0000	0.0000	0.3908	0.4730	0.4623	0.5256	0.1949	0.3307	0.0000	0.0000	0.0250
PENDIMETH	0.1329	0.1204	0.1133	0.0830	0.0705	0.0627	0.0488	0.0562	0.0000	0.0789	0.0142	0.0050
PFBS	0.0630	0.0366	0.0725	0.1309	0.1764	0.2001	0.3260	0.2668	0.0563	0.0573	0.0424	0.0015
PFDEA	0.0193	0.0257	0.0217	0.0132	0.0146	0.0108	0.0099	0.0043	0.0096	0.0198	0.0084	0.0025
PFHPA	0.1880	0.3112	0.1999	0.1849	0.1652	0.1556	0.1592	0.1106	0.1588	0.1863	0.1420	0.0015
PFHXA	0.0851	0.2031	0.1002	0.1437	0.1433	0.1383	0.1959	0.1397	0.0666	0.0709	0.0523	0.0015
PFHXS	0.1552	0.1501	0.1516	0.1507	0.1449	0.1442	0.1277	0.0917	0.1322	0.1532	0.1131	0.0015
PFNOA	0.1352	0.1685	0.1511	0.1308	0.1184	0.0962	0.0912	0.0547	0.0921	0.1205	0.0887	0.0025
PFOA	0.4606	0.4816	0.4691	0.5471	0.5770	0.5583	0.5954	0.4205	0.3534	0.4519	0.3143	0.0015
PFOS	0.3125	0.3444	0.3268	0.3204	0.3348	0.2945	0.3477	0.2185	0.1730	0.2426	0.1756	0.0015
PFOSA	0.0000	0.0052	0.0000	0.0010	0.0000	0.0000	0.0006	0.0009	0.0000	0.0000	0.0000	0.0015
PIRIMIC	0.0000	0.0000	0.0000	0.0000	0.0000	0.0000	0.0000	0.0000	0.0000	0.0000	0.0000	0.0025
PRIMID	2.3984	2.4105	2.3560	1.7970	1.5448	1.4318	0.9209	0.5696	1.8445	2.3954	1.0917	0.0250
PROMETR	0.3414	0.3407	0.3145	0.2055	0.1578	0.1486	0.0499	0.0053	0.2329	0.3590	0.1078	0.0015
PROPAZ	0.1911	0.1905	0.1780	0.1427	0.1208	0.1147	0.0647	0.0389	0.1472	0.2016	0.0853	0.0050
SIMAZ	2.8743	2.8841	2.6302	2.2278	1.9414	1.8293	0.9692	0.6056	2.2789	2.9530	1.4366	0.0050
TBEP	n.a.	n.a.	n.a.	n.a.	n.a.	n.a.	n.a.	n.a.	n.a.	n.a.	n.a.	n.a.
TBP	n.a.	n.a.	n.a.	n.a.	n.a.	n.a.	n.a.	n.a.	n.a.	n.a.	n.a.	n.a.
TERBAZ	0.4298	0.4560	0.5227	0.7310	0.6530	0.6443	0.5940	0.2865	0.2181	0.3524	0.1773	0.0015
TERBUTR	0.0341	0.0323	0.0500	0.0061	0.0132	0.0201	0.0299	0.0173	0.0158	0.0327	0.0130	0.0015
TPP	n.a.	n.a.	n.a.	n.a.	n.a.	n.a.	n.a.	n.a.	n.a.	n.a.	n.a.	n.a.
SPM [mg/L]	n.a.	n.a.	n.a.	n.a.	n.a.	n.a.	n.a.	n.a.	n.a.	n.a.	n.a.	
PSU	n.a.	n.a.	n.a.	n.a.	n.a.	n.a.	n.a.	n.a.	n.a.	n.a.	n.a.	

A5 Table 6: Surface water concentrations (5 m, A5 figure 5) in ng/L of the Baltic Sea in Jul. 2009; data >LOQs, PSU = Practical Salinity units; SPM = Suspended particulate matter in mg/L; n.a. = data not available

ng/L	HCHA	HCHB	HCHG	LOQ
4	0.128	0.18	0.16	n.a.
6	0.105	0.205	0.127	n.a.
8	0.145	0.249	0.154	n.a.
12	0.128	0.25	0.145	n.a.
15	0.178	0.285	0.16	n.a.
19	0.141	0.296	0.158	n.a.
28	0.078	0.157	0.088	n.a.
34	0.153	0.303	0.157	n.a.
35	0.127	0.272	0.138	n.a.
SPM [mg/L]	n.a.	n.a.	n.a.	
PSU	n.a.	n.a.	n.a.	

A5 Table 7: Surface water concentrations (5 m, A5 figure 5) in ng/L of the German EEZ in September 2009; PSU = Practical Salinity units; SPM = Suspended particulate matter in mg/L; n.a. = data not available

ng/L	AMRU2	AWZW1	DTEND	EIDER	ELBE1	ENTE1	ENTE3	ES1	HELGO	L1
24-D	0.1621	0.1033	0.0375	0.1776	0.2104	0.0302	0.0267	0.2326	0.1563	0.1911
AMETRYN	0.0800	0.0188	0.0138	0.0816	0.1032	0.0168	0.0197	0.0363	0.0724	0.0750
ATRAZ	1.2532	0.5788	0.5820	1.4231	1.5611	0.6818	0.5905	1.5293	1.4656	1.2744
AZINPH-E	0.0000	0.0000	0.0000	0.0000	0.0000	0.0000	0.0000	0.0000	0.0000	0.0000
AZINPH-M	0.0000	0.0000	0.0000	0.0000	0.0000	0.0000	0.0000	0.0000	0.0000	0.0000
BENTAZ	0.3240	0.0000	0.0000	0.7516	0.9601	0.0000	0.0000	0.1967	0.8717	0.2262
CARBAMAZ	7.0062	0.5298	0.0879	8.8665	10.2111	0.1466	0.0771	4.2260	8.2902	7.2792
CARBEND	1.4500	0.1220	0.0376	1.6800	1.8600	0.0564	0.0395	1.7000	1.5200	1.4500
CHLORFENV	0.0000	0.0000	0.0000	0.0000	0.0000	0.0000	0.0000	0.0000	0.0000	0.0000
CHLORTUR	1.0712	0.3078	0.0332	1.1336	1.1128	0.0512	0.0217	0.6791	1.0223	1.0712
CLOFIBRS	0.0757	0.0073	0.0000	0.0835	0.0807	0.0000	0.0000	0.0573	0.0689	0.0798
DEATRAZ	0.8784	0.2146	0.1670	1.0613	1.1333	0.1915	0.1670	1.1203	0.9360	0.9504
DIAZINON	0.0186	0.0157	0.0138	0.0236	0.0261	0.0117	0.0125	0.0227	0.0145	0.0182
DICHLPR	0.0748	0.0000	0.0000	0.1176	0.0838	0.0000	0.0000	0.0706	0.0995	0.0876
DICLOF	0.1050	0.3252	0.0221	0.0416	0.0659	0.0664	0.0063	0.0212	0.0225	0.0104
DIMETH	0.0000	0.0000	0.0000	0.0000	0.0008	0.0000	0.0000	0.0289	0.0022	0.0000
DIURON	2.5364	0.4656	0.2097	3.1842	3.6234	0.2229	0.1900	2.2399	2.9866	2.7011
FENUR	0.0756	0.0066	0.0109	0.1268	0.1201	0.0073	0.0484	0.0701	0.1022	0.0874
HBCDA	0.0000	0.0000	0.0000	0.0000	0.0000	0.0000	0.0000	0.0000	0.0000	0.0000
HBCDBG	0.0038	0.0000	0.0000	0.0000	0.0070	0.0000	0.0000	0.0000	0.0000	0.0000
HEXAZIN	0.1440	0.0144	0.0082	0.2370	0.3058	0.0118	0.0068	0.0645	0.2472	0.1542
IRGAROL	0.2576	0.0151	0.0005	0.2657	0.3600	0.0034	0.0014	0.5532	0.3151	0.2519
ISOPRUR	0.7271	0.4444	0.0813	0.8195	0.8690	0.1085	0.0561	0.4774	0.7700	0.7491
LINUR	0.0987	0.0372	0.0150	0.1249	0.1891	0.0000	0.0144	0.1536	0.1364	0.1012
MALATH	0.0000	0.0000	0.0000	0.0000	0.0000	0.0000	0.0000	0.0000	0.0000	0.0000
MCPA	0.2283	0.0747	0.0324	0.2481	0.3305	0.0343	0.0276	0.6213	0.2918	0.2491
MECOPR	0.5704	0.2984	0.0388	0.5831	0.6279	0.0521	0.0243	0.6913	0.5938	0.5704
METAZCHL	0.2662	0.2254	0.0461	0.3478	0.4896	0.0818	0.0375	0.3284	0.3968	0.2723
METHABZT	0.0903	0.0058	0.0000	0.1110	0.1210	0.0000	0.0000	0.0813	0.1110	0.0861
METOLA	0.8280	0.0473	0.0133	1.0200	1.0900	0.0182	0.0181	0.4770	0.9170	0.8580
NAPROX	n.a.	n.a.	n.a.	n.a.	n.a.	n.a.	n.a.	n.a.	n.a.	n.a.

A5 Table 7 continued:

ng/L	AMRU2	AWZW1	DTEND	EIDER	ELBE1	ENTE1	ENTE3	ES1	HELGO	L1
OXAZEP	1.1592	0.0000	0.0000	1.2144	1.3984	0.0000	0.0000	1.1592	1.2788	1.1868
PENDIMETH	0.0107	0.0228	0.0293	0.0069	0.0073	0.0229	0.0246	0.0119	0.0059	0.0118
PFBS	0.8109	0.0288	0.0160	0.8109	0.8425	0.0167	0.0144	0.6816	0.7422	0.8678
PFDEA	0.0452	0.0057	0.0038	0.0534	0.0566	0.0034	0.0032	0.0765	0.0479	0.0437
PFHPA	0.2745	0.0733	0.0347	0.3140	0.3371	0.0374	0.0315	0.3832	0.3316	0.2855
PFHXA	0.4239	0.0774	0.0337	0.5136	0.5635	0.0396	0.0308	0.5768	0.5462	0.4310
PFHXS	0.2960	0.0420	0.0152	0.3330	0.3550	0.0177	0.0132	0.3490	0.3090	0.3090
PFNOA	0.1081	0.0432	0.0266	0.1371	0.1311	0.0293	0.0214	0.1261	0.1241	0.1121
PFOA	1.1902	0.2347	0.1411	1.4877	1.5208	0.1510	0.1355	1.2563	1.2563	1.2783
PFOS	0.9720	0.1341	0.0399	1.1858	1.2539	0.0480	0.0305	1.4774	1.1275	0.9817
PFOSA	0.0058	0.0008	0.0011	0.0079	0.0096	0.0010	0.0005	0.0129	0.0080	0.0059
PIRIMIC	0.0000	0.0000	0.0000	0.0000	0.0077	0.0000	0.0000	0.0000	0.0043	0.0000
PRIMID	2.3913	0.1524	0.0558	3.2187	3.8947	0.0574	0.0433	1.1200	2.9766	2.7142
PROMETR	0.0695	0.0042	0.0029	0.1055	0.1242	0.0039	0.0045	0.0117	0.0889	0.0685
PROPAZ	0.0375	0.0145	0.0145	0.0474	0.0476	0.0141	0.0149	0.0311	0.0388	0.0364
SIMAZ	0.5255	0.1594	0.1200	0.6986	0.7410	0.1427	0.1220	0.6042	0.6603	0.5796
TBEP	n.a.	n.a.	n.a.	n.a.	n.a.	n.a.	n.a.	n.a.	n.a.	n.a.
TBP	n.a.	n.a.	n.a.	n.a.	n.a.	n.a.	n.a.	n.a.	n.a.	n.a.
TERBAZ	2.3010	0.1010	0.0471	3.4060	4.4070	0.0387	0.0391	1.2064	3.1980	2.3790
TERBUTR	0.2381	0.0231	0.0061	0.2730	0.3078	0.0090	0.0083	0.2372	0.2614	0.2217
TPP	n.a.	n.a.	n.a.	n.a.	n.a.	n.a.	n.a.	n.a.	n.a.	n.a.
TRIFLU	0.0007	0.0045	0.0103	0.0007	0.0012	0.0035	0.0049	0.0020	0.0006	0.0007
SPM [mg/L]	n.a.	n.a.	n.a.	n.a.	n.a.	n.a.	n.a.	n.a.	n.a.	n.a.
PSU	n.a.	n.a.	n.a.	n.a.	n.a.	n.a.	n.a.	n.a.	n.a.	n.a.

ng/L	MEDEM	NEFB	NSB2	NSB3	NSGR2	STADE	STG16	SYLT1	SYLT2	TWEMS
24-D	0.6051	0.1187	0.1525	0.1563	0.0861	n.a.	0.1496	0.1920	0.1457	0.1255
AMETRYN	0.3573	0.0233	0.0208	0.0249	0.0171	n.a.	0.0478	0.0729	0.0487	0.0225
ATRAZ	3.8657	0.5671	0.7115	1.2107	0.5915	n.a.	1.3169	0.9282	0.9080	1.0301
AZINPH-E	0.0000	0.0000	0.0000	0.0000	0.0000	n.a.	0.0000	0.0000	0.0000	0.0000
AZINPH-M	0.0000	0.0000	0.0000	0.0000	0.0000	n.a.	0.0000	0.0000	0.0000	0.0000
BENTAZ	6.7146	0.0157	0.0379	0.0759	0.0000	n.a.	0.1567	0.2356	0.1779	0.0594
CARBAMAZ	40.1367	0.9625	1.7389	2.8409	0.5045	n.a.	4.0036	6.6018	4.7012	1.9917
CARBEND	5.6600	0.1970	0.5020	0.8960	0.1390	n.a.	1.2100	1.4100	1.1200	0.7090
CHLORFENV	0.0000	0.0000	0.0000	0.0000	0.0000	n.a.	0.0000	0.0000	0.0000	0.0000
CHLORTUR	2.7768	0.5918	0.6469	0.6084	0.2153	n.a.	0.7114	1.0608	0.9287	0.5096
CLOFIBRS	0.1779	0.0000	0.0174	0.0337	0.0046	n.a.	0.0546	0.0746	0.0596	0.0232
DEATRAZ	2.5632	0.2722	0.5414	0.8107	0.2434	n.a.	0.9144	0.9662	0.8381	0.7488
DIAZINON	0.1107	0.0203	0.0162	0.0219	0.0123	n.a.	0.0138	0.0162	0.0126	0.0143
DICHLPR	0.0916	0.0000	0.1001	0.1124	0.0000	n.a.	0.0696	0.0794	0.0711	0.0596
DICLOF	2.0580	0.0262	0.0368	0.0047	0.0075	n.a.	0.0276	0.0161	0.0087	0.0246
DIMETH	0.0000	0.0000	0.0000	0.0018	0.0000	n.a.	0.0008	0.0000	0.0000	0.0000
DIURON	11.6388	0.6324	1.0157	1.5043	0.4864	n.a.	1.9325	2.4925	1.9105	1.3066
FENUR	0.5860	0.0136	0.0160	0.0334	0.0087	n.a.	0.0496	0.0593	0.0410	0.0266
HBCDA	0.0000	0.0000	0.0000	0.0000	0.0000	n.a.	0.0000	0.0000	0.0032	0.0000
HBCDBG	0.0000	0.0000	0.0000	0.0000	0.0000	n.a.	0.0000	0.0000	0.0117	0.0000
HEXAZIN	1.9492	0.0097	0.0208	0.0386	0.0276	n.a.	0.0538	0.1068	0.0601	0.0387
IRGAROL	1.4720	0.0269	0.1507	0.2944	0.0181	n.a.	0.3473	0.2392	0.1921	0.2461
ISOPRUR	3.5640	0.8613	0.6171	0.4609	0.3069	n.a.	0.4587	0.7304	0.6952	0.3828
LINUR	1.2606	0.0411	0.0601	0.0996	0.0332	n.a.	0.0959	0.0882	0.0936	0.0795
MALATH	0.0000	0.0000	0.0000	0.0000	0.0000	n.a.	0.0000	0.0000	0.0000	0.0000

A5 Table 7 continued:

ng/L	MEDEM	NEFB	NSB2	NSB3	NSGR2	STADE	STG16	SYLT1	SYLT2	TWEMS
MCPA	0.9597	0.1032	0.2829	0.4208	0.0709	n.a.	0.3593	0.2710	0.2233	0.2848
MECOPR	0.9155	0.5226	0.5655	0.5879	0.2291	n.a.	0.6065	0.5538	0.5304	0.3832
METAZCHL	1.8768	0.2336	0.2275	0.2499	0.1958	n.a.	0.2346	0.2091	0.1754	0.1816
METHABZT	0.2130	0.0104	0.0258	0.0473	0.0054	n.a.	0.0752	0.0836	0.0673	0.0383
METOLA	4.3000	0.0423	0.2010	0.4440	0.0584	n.a.	0.4580	0.7730	0.5400	0.2990
NAPROX	n.a.	n.a.	n.a.	n.a.	n.a.	n.a.	n.a.	n.a.	n.a.	n.a.
OXAZEP	4.3332	0.0000	0.2861	0.6845	0.0000	n.a.	0.9476	1.1132	0.8326	0.5078
PENDIMETH	0.0093	0.0259	0.0141	0.0118	0.0205	n.a.	0.0106	0.0145	0.0141	0.0150
PFBS	0.9311	0.0380	0.1754	0.3544	0.0485	n.a.	0.5180	0.8434	0.6192	0.2911
PFDEA	0.2532	0.0112	0.0141	0.0217	0.0057	n.a.	0.0442	0.0382	0.0403	0.0190
PFHPA	0.8455	0.1008	0.1318	0.1845	0.0593	n.a.	0.2273	0.2734	0.2383	0.1603
PFHXA	1.6202	0.1192	0.1600	0.2374	0.0664	n.a.	0.3128	0.4239	0.3454	0.2048
PFHXS	0.6160	0.0689	0.1330	0.2080	0.0424	n.a.	0.2480	0.2880	0.2330	0.1840
PFNOA	0.4304	0.0556	0.0527	0.0648	0.0341	n.a.	0.0918	0.1011	0.0912	0.0511
PFOA	3.0966	0.2821	0.5135	0.8695	0.2094	n.a.	1.0667	1.2012	0.9742	0.6491
PFOS	2.8285	0.2469	0.4150	0.6668	0.1108	n.a.	0.8301	0.9040	0.8291	0.5492
PFOSA	0.0533	0.0011	0.0016	0.0019	0.0009	n.a.	0.0075	0.0051	0.0063	0.0038
PIRIMIC	0.1268	0.0000	0.0000	0.0000	0.0000	n.a.	0.0000	0.0000	0.0000	0.0000
PRIMID	16.9512	0.2442	0.4591	0.7527	0.1514	n.a.	1.2007	2.5326	1.6144	0.5660
PROMETR	0.8096	0.0042	0.0055	0.0088	0.0044	n.a.	0.0139	0.0612	0.0347	0.0066
PROPAZ	0.2120	0.0158	0.0211	0.0272	0.0130	n.a.	0.0273	0.0393	0.0273	0.0244
SIMAZ	2.6174	0.1840	0.2440	0.4103	0.1555	n.a.	0.4487	0.4182	0.3385	0.3523
TBEP	n.a.	n.a.	n.a.	n.a.	n.a.	n.a.	n.a.	n.a.	n.a.	n.a.
TBP	n.a.	n.a.	n.a.	n.a.	n.a.	n.a.	n.a.	n.a.	n.a.	n.a.
TERBAZ	26.5200	0.1178	0.4225	0.7943	0.1109	n.a.	0.9100	2.0930	1.3390	0.6461
TERBUTR	1.2584	0.0397	0.0893	0.1558	0.0242	n.a.	0.1742	0.2120	0.1578	0.1220
TPP	n.a.	n.a.	n.a.	n.a.	n.a.	n.a.	n.a.	n.a.	n.a.	n.a.
TRIFLU	0.0149	0.0061	0.0020	0.0011	0.0028	0.0030	0.0006	0.0007	0.0006	0.0015
SPM [mg/L]	n.a.	n.a.	n.a.	n.a.	n.a.	n.a.	n.a.	n.a.	n.a.	n.a.
PSU	n.a.	n.a.	n.a.	n.a.	n.a.	n.a.	n.a.	n.a.	n.a.	n.a.

ng/L	URST2	URST4	URST6	LOQ
24-D	0.1457	0.1583	0.0863	0.0250
AMETRYN	0.0493	0.0260	0.0148	0.0015
ATRAZ	0.9165	1.0939	0.5852	0.0050
AZINPH-E	0.0000	0.0000	0.0000	0.0050
AZINPH-M	0.0000	0.0000	0.0000	0.0250
BENTAZ	0.2026	0.0820	0.0000	0.0015
CARBAMAZ	4.8023	2.3860	0.5095	0.0015
CARBEND	1.1000	0.7020	0.1390	0.0015
CHLORFENV	0.0000	0.0000	0.0000	0.0050
CHLORTUR	0.9048	0.6188	0.2163	0.0050
CLOFIBRS	0.0584	0.0269	0.0059	0.0050
DEATRAZ	0.8568	0.7315	0.2750	0.0050
DIAZINON	0.0176	0.0000	0.0129	0.0050
DICHLPR	0.0612	0.0718	0.0000	0.0050
DICLOF	0.0158	0.0102	0.0146	0.0250
DIMETH	0.0000	0.0000	0.0000	0.0050
DIURON	1.8776	1.2517	0.4853	0.0050
FENUR	0.0350	0.0297	0.0142	0.0025
HBCDA	0.0000	0.0000	0.0000	0.0250

ng/L	URST2	URST4	URST6	LOQ
HBCDBG	0.0000	0.0000	0.0000	0.0300
HEXAZIN	0.0629	0.0397	0.0248	0.0015
IRGAROL	0.2001	0.2542	0.0185	0.0015
ISOPRUR	0.6578	0.4818	0.2893	0.0025
LINUR	0.0811	0.0793	0.0296	0.0250
MALATH	0.0000	0.0000	0.0000	0.0050
MCPA	0.2203	0.3285	0.0755	0.0050
MECOPR	0.5460	0.5294	0.2272	0.0050
METAZCHL	0.1785	0.2519	0.1918	0.0025
METHABZT	0.0627	0.0400	0.0052	0.0025
METOLA	0.5200	0.3660	0.0610	0.0015
NAPROX	n.a.	n.a.	n.a.	n.a.
OXAZEP	0.8814	0.4572	0.0000	0.0250
PENDIMETH	0.0106	0.0124	0.0222	0.0050
PFBS	0.6247	0.2703	0.0578	0.0015
PFDEA	0.0429	0.0157	0.0046	0.0025
PFHPA	0.2536	0.1592	0.0544	0.0015
PFHXA	0.3730	0.1936	0.0589	0.0015
PFHXS	0.2370	0.1670	0.0458	0.0015

A5 Table 7 continued:

ng/L	URST2	URST4	URST6	LOQ	ng/L	URST2	URST4	URST6	LOQ
PFNOA	0.0960	0.0573	0.0283	0.0025	TBEP	n.a.	n.a.	n.a.	n.a.
PFOA	0.9874	0.6854	0.2061	0.0015	TBP	n.a.	n.a.	n.a.	n.a.
PFOS	0.9166	0.4928	0.1001	0.0015	TERBAZ	1.2857	0.5720	0.1140	0.0015
PFOSA	0.0060	0.0025	0.0009	0.0015	TERBUTR	0.1588	0.1287	0.0246	0.0015
PIRIMIC	0.0000	0.0000	0.0000	0.0025	TPP	n.a.	n.a.	n.a.	n.a.
PRIMID	1.6548	0.6135	0.1786	0.0250	TRIFLU	0.0007	0.0009	0.0024	0.0001
PROMETR	0.0313	0.0079	0.0037	0.0015	SPM [mg/L]	n.a.	n.a.	n.a.	
PROPAZ	0.0281	0.0231	0.0134	0.0050	PSU	n.a.	n.a.	n.a.	
SIMAZ	0.3444	0.3414	0.1437	0.0050					

A5 Table 8: Surface water concentrations (5 m, A5 figure 5) in ng/L of the German EEZ in November 2009; PSU = Practical Salinity units; SPM = Suspended particulate matter in mg/L; n.a. = data not available

ng/L	AMRU2	AWZW1	DTEND	EIDER	ELBE1	ENTE1	ENTE3	ES1	HELGO	L1
24-D	0.1247	0.0000	0.0232	0.1694	0.1366	0.0354	0.0213	0.1387	0.1221	0.1312
AMETRYN	0.1049	4.9403	0.0208	0.1380	0.0000	0.0200	0.0224	0.0567	0.0531	0.0754
ATRAZ	1.3031	6.7872	0.5991	1.4730	0.0000	0.5994	0.5994	1.2797	1.2680	1.2882
AZINPH-E	0.0000	0.0000	0.0000	0.0000	0.0000	0.0000	0.0000	0.0000	0.0000	0.0000
AZINPH-M	0.0000	0.0000	0.0000	0.0000	0.0000	0.0000	0.0000	0.0000	0.0000	0.0000
BENTAZ	0.8202	0.6602	0.0000	1.2534	0.5639	0.0000	0.0000	0.1860	0.3057	0.7611
CARBAMAZ	7.6543	0.4257	0.0942	13.2744	6.7272	0.1034	0.1132	4.4595	4.8316	8.4954
CARBEND	1.5930	0.0938	0.0389	2.0470	1.4630	0.0407	0.0414	1.5850	1.3690	1.6100
CHLORFENV	0.0000	0.0000	0.0000	0.0000	0.0000	0.0000	0.0000	0.0000	0.0000	0.0000
CHLORTUR	0.8537	78.0312	0.0488	0.9316	0.0000	0.0577	0.0532	0.5301	0.6849	0.9964
CLOFIBRS	0.0570	0.0000	0.0000	0.0750	0.0456	0.0000	0.0000	0.0326	0.0412	0.0627
DEATRAZ	0.9444	2.8094	0.1534	1.1385	0.0000	0.1584	0.1649	0.8608	0.9050	0.9867
DIAZINON	0.0215	3.4641	0.0143	0.0293	0.0000	0.0132	0.0197	0.0329	0.0179	0.0142
DICHLPR	0.1301	0.0000	0.0000	0.1436	0.1012	0.0000	0.0000	0.0523	0.1290	0.0931
DICLOF	0.0548	0.0130	0.0062	0.5104	0.0235	0.0105	0.0082	0.0166	0.0110	0.0163
DIMETH	0.0000	0.0000	0.0000	0.0033	0.0000	0.0000	0.0000	0.0054	0.0022	0.0000
DIURON	2.4452	128.3562	0.2256	3.3511	0.0000	0.2364	0.2655	1.9193	1.8941	2.5122
FENUR	0.1217	0.2860	0.0192	0.2098	0.0000	0.0133	0.0296	0.0661	0.1421	0.1741
HBCDA	0.0057	0.0000	0.0000	0.0000	0.0000	0.0000	0.0000	0.0037	0.0000	0.0000
HBCDBG	0.0000	0.0000	0.0000	0.0000	0.0000	0.0000	0.0000	0.0000	0.0000	0.0000
HEXAZIN	0.1567	0.1645	0.0084	0.2719	0.0000	0.0112	0.0099	0.0545	0.0792	0.1908
IRGAROL	0.3550	4.3367	0.0042	0.5061	0.0000	0.0057	0.0047	0.5165	0.2890	0.2608
ISOPRUR	0.6828	114.2900	0.1061	0.9423	0.0000	0.1211	0.1018	0.4873	0.5188	0.7277
LINUR	0.0925	9.8166	0.0122	0.1176	0.0000	0.0134	0.0138	0.0759	0.0806	0.0751
MALATH	0.0000	0.0000	0.0000	0.0000	0.0000	0.0000	0.0000	0.0000	0.0000	0.0000
MCPA	0.2802	0.0000	0.0403	0.3270	0.2876	0.0328	0.0301	0.3751	0.2971	0.2091
MECOPR	0.5780	9.5297	0.0317	0.6669	0.5984	0.0392	0.0402	0.5558	0.5685	0.5252
METAZCHL	0.3083	1.8472	0.0439	0.5899	0.0000	0.0545	0.0503	0.2902	0.2326	0.3231
METHABZT	0.0927	0.0053	0.0000	0.1194	0.0890	0.0000	0.0000	0.0650	0.0705	0.0890
METOLA	0.5546	5.7910	0.0164	0.7071	0.0000	0.0148	0.0143	0.2905	0.3914	0.6441
NAPROX	n.a.	n.a.	n.a.	n.a.	n.a.	n.a.	n.a.	n.a.	n.a.	n.a.
OXAZEP	1.0571	0.0000	0.0000	1.7121	1.0019	0.0000	0.0000	1.1675	0.7961	0.9816
PENDIMETH	0.4407	40.8299	0.1648	0.5429	0.0000	0.2569	0.1755	0.9865	0.3039	0.5651
PFBS	0.7583	8.2020	0.0144	0.7804	0.5918	0.0199	0.0173	0.6288	0.5892	0.8824
PFDEA	0.0293	1.2998	0.0031	0.0355	0.0391	0.0044	0.0028	0.0269	0.0283	0.0251
PFHPA	0.2908	16.2724	0.0304	0.3559	0.2553	0.0422	0.0313	0.2292	0.2236	0.3350

A5 Table 8 continued:

ng/L	AMRU2	AWZW1	DTEND	EIDER	ELBE1	ENTE1	ENTE3	ES1	HELGO	L1
PFHXA	0.4568	18.4745	0.0380	0.5932	0.3642	0.0524	0.0333	0.3680	0.3202	0.5160
PFHXS	0.2889	12.8500	0.0147	0.3254	0.2524	0.0161	0.0157	0.2790	0.2463	0.3061
PFNOA	0.0884	11.4414	0.0291	0.1112	0.0938	0.0400	0.0267	0.0679	0.0720	0.0999
PFOA	1.1494	61.1830	0.1352	1.3433	1.0384	0.1455	0.1632	0.8987	0.9575	1.1538
PFOS	0.7919	31.5220	0.0342	0.9114	0.7781	0.0496	0.0326	0.6583	0.7001	0.8135
PFOSA	0.0048	0.3676	0.0016	0.0068	0.0051	0.0019	0.0013	0.0076	0.0045	0.0045
PIRIMIC	0.0000	0.0000	0.0000	0.0073	0.0005	0.0000	0.0000	0.0000	0.0000	0.0000
PRIMID	2.1966	0.1172	0.0454	4.0743	1.7890	0.0531	0.0501	1.0494	1.2633	2.5931
PROMETR	0.0656	1.2144	0.0033	0.1214	0.0000	0.0035	0.0034	0.0084	0.0221	0.0798
PROPAZ	0.0306	2.8269	0.0126	0.0477	0.0000	0.0139	0.0144	0.0238	0.0258	0.0369
SIMAZ	0.5903	1.8578	0.1418	0.7192	0.0000	0.1403	0.1432	0.5072	0.4915	0.5982
TBEP	n.a.	n.a.	n.a.	n.a.	n.a.	n.a.	n.a.	n.a.	n.a.	n.a.
TBP	n.a.	n.a.	n.a.	n.a.	n.a.	n.a.	n.a.	n.a.	n.a.	n.a.
TERBAZ	2.1398	20.9560	0.0436	3.3722	0.0000	0.0434	0.0371	0.8819	1.1261	2.3101
TERBUTR	0.2500	4.8787	0.0118	0.3995	0.0000	0.0121	0.0141	0.1868	0.1656	0.2420
TPP	n.a.	n.a.	n.a.	n.a.	n.a.	n.a.	n.a.	n.a.	n.a.	n.a.
TRIFLU	0.0353	0.0301	0.0162	0.0435	0.0266	0.0172	0.0228	0.0273	0.0267	0.0407
SPM [mg/L]	n.a.	n.a.	n.a.	n.a.	n.a.	n.a.	n.a.	n.a.	n.a.	n.a.
PSU	n.a.	n.a.	n.a.	n.a.	n.a.	n.a.	n.a.	n.a.	n.a.	n.a.

ng/L	MEDEM	NEFB	NSB2	NSB3	NSGR2	STADE	STG16	SYLT1	SYLT2	TWEMS
24-D	0.2600	0.0753	0.2320	0.0365	0.0677	2.9423	0.1274	0.1322	0.1163	0.0632
AMETRYN	0.2155	0.0216	0.0222	0.0203	0.0240	0.5045	0.0827	0.0675	0.0471	0.0206
ATRAZ	1.9615	0.6145	0.7346	0.7404	0.6789	4.9468	1.4422	1.3275	0.8962	0.5596
AZINPH-E	0.0000	0.0000	0.0000	0.0000	0.0000	0.0000	0.0000	0.0000	0.0000	0.0000
AZINPH-M	0.0000	0.0000	0.0000	0.0000	0.0000	0.0000	0.0000	0.0000	0.0000	0.0000
BENTAZ	2.3642	0.0231	0.0150	0.0189	0.0083	34.7628	0.4968	0.8470	0.2423	0.0120
CARBAMAZ	27.5093	1.0363	1.1940	0.5618	0.7608	58.6784	6.8414	8.1962	2.9915	0.6316
CARBEND	3.1660	0.1859	0.2034	0.1713	0.1241	12.7500	1.7990	1.6260	0.8010	0.1129
CHLORFENV	0.0000	0.0000	0.0000	0.0000	0.0000	0.0000	0.0000	0.0000	0.0000	0.0000
CHLORTUR	1.2636	0.4648	0.6553	0.4188	0.3930	3.4944	0.7327	0.8915	0.7561	0.2886
CLOFIBRS	0.1283	0.0000	0.0000	0.0000	0.0000	0.9152	0.0519	0.0540	0.0341	0.0079
DEATRAZ	1.5134	0.3080	0.3083	0.4847	0.2075	3.4632	1.0028	0.9765	0.7282	0.2004
DIAZINON	0.0577	0.0166	0.0131	0.0145	0.0162	0.4247	0.0213	0.0153	0.0148	0.0173
DICHLPR	0.1091	0.0411	0.1357	0.0205	0.0504	0.9277	0.1462	0.1025	0.0931	0.0000
DICLOF	2.5529	0.0047	0.0070	0.0031	0.0142	61.4519	0.0246	0.0342	0.0094	0.0096
DIMETH	0.0077	0.0000	0.0000	0.0000	0.0000	0.2660	0.0063	0.0000	0.0005	0.0000
DIURON	5.7206	0.7172	0.7080	0.8343	0.4946	13.7799	2.3739	2.4980	1.4065	0.4950
FENUR	0.4169	0.0251	0.0382	0.0377	0.0328	2.2629	0.0830	0.1263	0.0492	0.0196
HBCDA	0.0000	0.0000	0.0000	0.0030	0.0000	0.0000	0.0000	0.0000	0.0000	0.0055
HBCDBG	0.0000	0.0000	0.0000	0.0000	0.0000	0.0000	0.0000	0.0000	0.0000	0.0000
HEXAZIN	0.6782	0.0120	0.0000	0.0215	0.0106	2.2002	0.1266	0.1770	0.0451	0.0078
IRGAROL	0.8871	0.0424	0.0352	0.1326	0.0257	1.7906	0.3879	0.3260	0.2280	0.0339
ISOPRUR	1.6390	0.5672	0.8509	0.3958	0.5822	10.7932	0.5645	0.6982	0.6421	0.4047
LINUR	0.2248	0.0282	0.0354	0.0427	0.0415	0.6993	0.0826	0.0894	0.0663	0.0283
MALATH	0.0000	0.0000	0.0000	0.0000	0.0000	0.0000	0.0000	0.0000	0.0000	0.0000
MCPA	0.4751	0.0696	0.0968	0.0611	0.0507	3.7159	0.3141	0.2316	0.2336	0.0501
MECOPR	0.8037	0.3275	0.4961	0.1356	0.3197	4.8058	0.6150	0.5578	0.5401	0.2134
METAZCHL	1.3168	0.1928	0.2467	0.1348	0.2034	9.6002	0.2966	0.3122	0.1818	0.1480
METHABZT	0.1375	0.0078	0.0124	0.0085	0.0087	0.1028	0.0949	0.0943	0.0546	0.0069
METOLA	1.2080	0.0682	0.0422	0.1285	0.0360	2.1270	0.5146	0.5745	0.3098	0.0258

A5 Table 8 continued:

ng/L	MEDEM	NEFB	NSB2	NSB3	NSGR2	STADE	STG16	SYLT1	SYLT2	TWEMS
NAPROX	n.a.	n.a.	n.a.	n.a.	n.a.	n.a.	n.a.	n.a.	n.a.	n.a.
OXAZEP	2.9017	0.0000	0.0000	0.1106	0.0000	11.8680	1.1224	0.9982	0.5450	0.0000
PENDIMETH	0.6152	0.2981	0.2735	0.3130	0.1994	0.7418	0.4894	0.4931	0.3922	0.3666
PFBS	0.9212	0.0396	0.0386	0.1664	0.0229	0.9727	0.7651	0.7597	0.5778	0.0255
PFDEA	0.0718	0.0058	0.0082	0.0151	0.0062	0.5803	0.0262	0.0257	0.0287	0.0061
PFHPA	0.5485	0.0944	0.0964	0.1217	0.0699	1.5910	0.3081	0.2980	0.2677	0.0683
PFHXA	0.9370	0.1244	0.1130	0.1587	0.0780	2.0625	0.4814	0.4523	0.3728	0.0834
PFHXS	0.4291	0.0846	0.0790	0.1191	0.0517	1.3630	0.2929	0.2963	0.1947	0.0523
PFNOA	0.2026	0.0479	0.0522	0.0512	0.0485	0.8101	0.0921	0.0883	0.0948	0.0372
PFOA	1.8227	0.2413	0.2893	0.3647	0.2676	6.1624	1.0865	1.1659	0.7884	0.2304
PFOS	1.4045	0.2150	0.1969	0.3216	0.1498	5.9302	0.8283	0.8018	0.6913	0.1786
PFOSA	0.0158	0.0032	0.0018	0.0030	0.0005	0.0991	0.0054	0.0044	0.0033	0.0014
PIRIMIC	0.0270	0.0000	0.0000	0.0000	0.0000	0.2944	0.0000	0.0000	0.0000	0.0000
PRIMID	9.1991	0.2883	0.2691	0.1514	0.1682	48.5531	1.7678	2.3833	0.8314	0.1780
PROMETR	0.3374	0.0024	0.0034	0.0010	0.0035	1.2455	0.0408	0.0731	0.0131	0.0026
PROPAZ	0.0852	0.0138	0.0134	0.0163	0.0147	0.4283	0.0329	0.0317	0.0233	0.0152
SIMAZ	1.1749	0.2011	0.2717	0.2409	0.2041	3.9458	0.6095	0.5879	0.3292	0.1639
TBEP	n.a.	n.a.	n.a.	n.a.	n.a.	n.a.	n.a.	n.a.	n.a.	n.a.
TBP	n.a.	n.a.	n.a.	n.a.	n.a.	n.a.	n.a.	n.a.	n.a.	n.a.
TERBAZ	8.7620	0.1760	0.1495	0.3484	0.1310	22.7630	1.6926	2.2464	0.7433	0.1158
TERBUTR	0.7357	0.0391	0.0404	0.0671	0.0297	4.4209	0.2313	0.2482	0.1440	0.0296
TPP	n.a.	n.a.	n.a.	n.a.	n.a.	n.a.	n.a.	n.a.	n.a.	n.a.
TRIFLU	0.0663	0.0395	0.0260	0.0200	0.0261	0.0629	0.0461	0.0366	0.0160	0.0365
SPM [mg/L]	n.a.	n.a.	n.a.	n.a.	n.a.	n.a.	n.a.	n.a.	n.a.	n.a.
PSU	n.a.	n.a.	n.a.	n.a.	n.a.	n.a.	n.a.	n.a.	n.a.	n.a.

ng/L	URST2	URST4	URST6	LOQ
24-D	0.1190	0.1188	0.0331	0.0250
AMETRYN	0.0405	0.0212	0.0193	0.0015
ATRAZ	0.9090	0.7233	0.5837	0.0050
AZINPH-E	0.0000	0.0000	0.0000	0.0050
AZINPH-M	0.0000	0.0000	0.0000	0.0250
BENTAZ	0.2619	0.0539	0.0000	0.0015
CARBAMAZ	2.9804	1.2536	0.3002	0.0015
CARBEND	0.7908	0.4201	0.0570	0.0015
CHLORFENV	0.0000	0.0000	0.0000	0.0050
CHLORTUR	0.7197	0.4977	0.1582	0.0050
CLOFIBRS	0.0361	0.0120	0.0000	0.0050
DEATRAZ	0.7497	0.5407	0.1980	0.0050
DIAZINON	0.0129	0.0104	0.0121	0.0050
DICHLPR	0.0994	0.0585	0.0000	0.0050
DICLOF	0.0081	0.0055	0.0107	0.0250
DIMETH	0.0000	0.0000	0.0000	0.0050
DIURON	1.4944	0.9219	0.3390	0.0050
FENUR	0.0771	0.0268	0.0221	0.0025
HBCDA	0.0000	0.0000	0.0051	0.0250
HBCDBG	0.0000	0.0000	0.0000	0.0300
HEXAZIN	0.0470	0.0280	0.0122	0.0015
IRGAROL	0.2145	0.1324	0.0121	0.0015
ISOPRUR	0.5999	0.4446	0.2483	0.0025
LINUR	0.0709	0.0454	0.0212	0.0250

ng/L	URST2	URST4	URST6	LOQ
MALATH	0.0000	0.0000	0.0000	0.0050
MCPA	0.2216	0.1554	0.0249	0.0050
MECOPR	0.5388	0.3344	0.1116	0.0050
METAZCHL	0.1756	0.1317	0.1435	0.0025
METHABZT	0.0517	0.0240	0.0036	0.0025
METOLA	0.2948	0.1339	0.0313	0.0015
NAPROX	n.a.	n.a.	n.a.	n.a.
OXAZEP	0.5291	0.2529	0.0000	0.0250
PENDIMETH	0.3784	0.2741	0.1833	0.0050
PFBS	0.4837	0.1898	0.0268	0.0015
PFDEA	0.0235	0.0097	0.0050	0.0025
PFHPA	0.2005	0.1458	0.0506	0.0015
PFHXA	0.2737	0.1883	0.0554	0.0015
PFHXS	0.2028	0.1329	0.0306	0.0015
PFNOA	0.0668	0.0531	0.0414	0.0025
PFOA	0.8256	0.4183	0.1949	0.0015
PFOS	0.5908	0.3208	0.0798	0.0015
PFOSA	0.0019	0.0024	0.0005	0.0015
PIRIMIC	0.0000	0.0000	0.0000	0.0025
PRIMID	0.8936	0.3280	0.1028	0.0250
PROMETR	0.0126	0.0040	0.0032	0.0015
PROPAZ	0.0246	0.0175	0.0143	0.0050
SIMAZ	0.3297	0.2368	0.1434	0.0050
TBEP	n.a.	n.a.	n.a.	n.a.

A5 Table 8 continued:

ng/L	URST2	URST4	URST6	LOQ
TBP	n.a.	n.a.	n.a.	n.a.
TERBAZ	0.7696	0.3600	0.0784	0.0015
TERBUTR	0.1332	0.0732	0.0179	0.0015
TPP	n.a.	n.a.	n.a.	n.a.

ng/L	URST2	URST4	URST6	LOQ
TRIFLU	0.0198	0.0250	0.0190	0.0001
SPM [mg/L]	n.a.	n.a.	n.a.	
PSU	n.a.	n.a.	n.a.	

Annex 6 (A6): Concentrations of target analytes in suspended particulate matter

A6 Table 1: Concentrations (ng/g) of target analytes in suspended particulate matter collected at four water sampling sites (refer to A4 figure 1) by centrifugation of surface water; TOC = Concentration (mg/g) of total organic carbon in the suspended particulate matter, n.a. = not available

ng/g	EIDER	DTEND	L1	URST6	LOQ
CB138	0.79	0.20	0.82	0.19	0.13
CB153	1.05	0.23	0.96	0.25	0.07
CB28	0.50	0.00	0.34	0.10	n.a.
CB52	0.23	0.11	0.24	0.17	0.11
DDDPP	1.05	0.18	0.45	0.39	n.a.
DDEPP	0.57	0.26	0.35	0.21	n.a.
DDTPP	0.00	0.00	0.00	2.39	n.a.
HCB	0.61	0.30	0.47	0.34	0.22
HCHA	0.00	0.00	0.00	0.00	0.07
HCHG	0.48	0.21	0.00	0.00	0.29
ACE	24.17	0.00	0.00	0.00	12.68
ACY	17.53	0.00	0.00	0.00	n.a.
ANT	27.72	0.00	13.90	0.00	8.07
BAA	48.90	10.23	25.13	9.73	n.a.
BAP	50.52	0.00	28.35	7.84	n.a.
BBF	115.77	23.77	83.95	19.69	n.a.
BGHIP	83.60	11.10	65.52	6.25	n.a.
CHRTR	67.39	21.24	45.62	15.63	n.a.
DBAHA	26.56	7.64	13.69	0.00	n.a.
FL	18.33	1.87	7.21	0.90	8.27
FLU	112.34	33.46	70.97	25.04	8.57
I123P	105.11	52.42	73.14	11.30	n.a.
PHEN	105.59	25.74	58.74	29.72	37.02
PYR	91.42	22.53	59.28	21.06	22.22
TOC [mg/g]	50	185	88	215	n.a.

Annex 7 (A7): Henry's law constants of target analytes

A7 Table 1: Henry's law constants applied for the calculation of the net flux of diffusive gas exchange of target analytes between the surface water and the atmosphere; Surface water temperature (5 m) of the German EEZ in May/Jun. = 10°C; Surface water temperature (5m) of the North Sea in Aug./Sep. = 17 °C; Surface water temperature (5m) of the Baltic Sea in Apr. = 7 °C

Organic Compound	H [Pa m ³ mol ⁻¹]			Reference
	7 °C	10 °C	17 °C	
FL	2.69	3.33	5.61	interpolated for respective water temperatures from [202]
PHEN	1.22	1.51	2.50	interpolated for respective water temperatures from [202]
HCB	11.20	16.00	26.40	interpolated/extrapolated for respective water temperatures from [125]
QCB	17.27	24.67	41.80	interpolated/extrapolated for respective water temperatures from [125]
HCHA	0.12	0.15	0.32	interpolated for respective water temperatures from [203]
HCHG	0.05	0.06	0.12	interpolated for respective water temperatures from [203]
DIELD	0.28	0.4	0.68	extrapolated for respective water temperatures from [125]
TERBAZ	$4.44 \cdot 10^{-3}$	$4.49 \cdot 10^{-3}$	$4.60 \cdot 10^{-3}$	calculated for respective water temperatures from Kw by $H = (RT)/Kw$ after [204]
ATRAZ	$2.33 \cdot 10^{-4}$	$2.35 \cdot 10^{-4}$	$2.41 \cdot 10^{-4}$	calculated for respective water temperatures from Kw by $H = (RT)/Kw$ after [204]
DIAZINON	-	-	$8.46 \cdot 10^{-3}$	extrapolated for respective water temperatures from [150]
ISOPRUR	$3.18 \cdot 10^{-6}$	-	-	extrapolated for respective water temperatures from [150]
CHLORTUR	$5.11 \cdot 10^{-6}$	-	-	extrapolated for respective water temperatures from [150]
LINUR	$1.77 \cdot 10^{-4}$	-	-	extrapolated for respective water temperatures from [150]
BENTAZ	$7.73 \cdot 10^{-5}$	$1.10 \cdot 10^{-4}$	-	extrapolated for respective water temperatures from [150]
TRIFLU	7.53	9.22	11.35	extrapolated for respective water temperatures from [205]
PENDIMETH	$2.43 \cdot 10^{-2}$	$3.47 \cdot 10^{-2}$	$5.90 \cdot 10^{-2}$	extrapolated for respective water temperatures from [206]
METOLA	$2.74 \cdot 10^{-3}$	$3.91 \cdot 10^{-3}$	$6.65 \cdot 10^{-3}$	extrapolated for respective water temperatures from [205]
METAZCHL	$2.01 \cdot 10^{-5}$	$2.88 \cdot 10^{-5}$	$4.89 \cdot 10^{-5}$	extrapolated for respective water temperatures from [150]

Annex 8 (A8): Concentrations of organic compounds in rain water samples

The following data is provided to this study by the Federal Environmental Agency (UBA), Luftmessnetz, Paul-Ehrlich-Str. 29, 63225 Langen, 2011".

A8 Table 1: Concentrations (ng/L) of organic compounds in monthly rain water samples collected in Zingst in 2009 and 2010, respectively

ng/L	January		February		March		April	
	2009	2010	2009	2010	2009	2010	2009	2010
HCB	0.1562	0.0567	0.0493	0.0701	0.0285	0.0454	0.3934	0.1634
HCHA	0.2507	0.1369	0.1396	0.1931	0.1598	0.1672	0.2577	0.2636
HCHG	1.6026	1.1804	0.7057	1.4038	0.6633	1.6134	4.2646	1.2106
ALD	0.0626	0.0066	0.0211	0.0280	0.0132	0.0329	0.0607	0.0122
DIELD	0.1289	0.0804	0.0407	0.0753	0.0729	0.1161	0.0911	0.0798
END	0.1606	0.0535	0.0540	0.0596	0.0339	0.1269	0.1135	0.0328
DDTPP	0.3329	0.2429	0.4418	0.3818	0.2211	0.2353	0.6860	0.3052
DDTOP	0.0876	0.0518	0.0884	0.0797	0.0478	0.0582	0.1158	0.0735
DDEPP	0.0775	0.0809	0.0938	0.0996	0.0532	0.0559	0.4924	0.0902
DDDPP	0.0508	0.0714	0.0662	0.1149	0.0477	0.0383	0.4055	0.0464
CB28	0.6976	0.2601	0.2200	1.1067	0.1271	0.1797	1.8455	0.1718
CB52	0.2660	0.1857	0.0839	0.7954	0.0485	0.0724	0.6933	0.0540
CB138	1.3302	0.1127	0.4195	0.1257	0.2424	0.2675	5.3935	0.4444
CB153	1.2404	0.1438	0.3912	0.1603	0.2260	0.3411	5.9953	0.5654
PHEN	15.9157	70.6696	26.4893	46.6263	9.9825	15.8356	11.9028	23.9771
ANT	1.9819	6.4307	1.2602	2.3911	0.4244	0.4717	0.8059	0.5410
FLU	33.6571	120.8189	48.0849	56.3933	11.4421	14.7531	5.3016	29.1070
PYR	28.1527	70.7273	31.4970	33.1138	7.9501	6.7598	4.0145	14.4857
BAA	10.8705	24.8079	8.0312	8.8801	1.6078	2.5078	2.4904	5.8371
CHRTR	35.7064	58.8699	40.8086	26.4050	5.4130	5.0631	1.7420	16.4068
BAP	10.2776	26.3507	9.7333	8.9764	1.7139	2.3902	2.3358	5.9046
I123P	16.5603	42.8679	18.9634	14.7583	2.6119	2.9726	2.7081	5.7318
BGHIP	14.3612	40.8705	15.8322	13.9050	2.4834	3.1058	2.5425	7.9200
DBAHA	2.5625	7.6287	2.7753	2.5349	0.4267	0.7231	0.8412	1.4240
Deposition [L/m ²]	9.1	37.4	28.9	33.6	50.0	15.8	4.4	19.5

ng/L	May		June		July		August	
	2009	2010	2009	2010	2009	2010	2009	2010
HCB	0.0291	0.0320	0.0258	0.0329	0.0624	0.0424	2.1152	0.0407
HCHA	0.2341	0.2116	0.1772	0.1839	0.1312	0.1664	0.1707	0.1520
HCHG	1.8977	0.7944	1.0898	1.4391	1.3285	1.0085	1.2594	0.6022
ALD	0.0067	0.0025	0.0032	0.0074	0.0119	0.0098	0.1392	0.0031
DIELD	0.0566	0.0369	0.0341	0.0461	0.0382	0.0292	0.0260	0.0338
END	0.0173	0.0067	0.0082	0.0184	0.0776	0.0199	0.0582	0.0058
DDTPP	0.2573	0.2409	0.0800	0.1484	0.2004	0.1970	0.1563	0.1626
DDTOP	0.0490	0.0242	0.0163	0.0409	0.0395	0.0296	0.0368	0.0317
DDEPP	0.1231	0.0410	0.0323	0.0506	0.0243	0.0546	0.0258	0.0938
DDDPP	0.0346	0.0246	0.0206	0.0110	0.0738	0.0164	0.0466	0.0255
CB28	0.1367	0.0785	0.1210	0.1046	0.4549	0.0665	0.3609	0.0193
CB52	0.0514	0.0110	0.0455	0.0303	0.1412	0.0735	0.1466	0.0213
CB138	0.3995	0.0905	0.3537	0.2492	0.3582	0.1519	0.5191	0.2912

A8 Table 1 continued:

ng/L	May		June		July		August	
	2009	2010	2009	2010	2009	2010	2009	2010
CB153	0.4441	0.1151	0.3931	0.3171	0.3841	0.1429	0.5466	0.2207
PHEN	7.8298	9.0704	4.8508	6.9728	7.4591	2.5404	16.7495	4.4292
ANT	0.4252	0.3540	0.1466	0.2500	0.2515	0.2508	0.3701	0.1598
FLU	9.6393	13.0528	4.3165	5.6697	4.8963	5.2651	5.3352	4.0557
PYR	8.4986	8.8593	4.2774	1.5300	4.5089	4.0000	5.5099	1.9462
BAA	1.4412	3.0709	0.8650	1.2357	0.8462	0.9340	0.8419	0.6966
CHRTR	3.7417	9.6302	2.4233	3.0730	3.0073	2.0352	2.2911	2.0222
BAP	1.3603	4.3517	1.1199	1.6759	1.1230	1.5909	1.0064	0.9128
I123P	1.2562	4.5571	1.2599	1.4545	0.8875	1.7858	0.8861	1.2212
BGHIP	1.3097	5.6881	1.3256	2.0628	0.8755	1.7887	0.8155	1.1365
DBAHA	0.2641	1.1830	0.2278	0.4453	0.1105	0.2763	0.1045	0.2209
Deposition [L/m ²]	60.0	95.6	67.8	34.7	43.8	49.5	41.1	170.7

ng/L	September		October		November		December	
	2009	2010	2009	2010	2009	2010	2009	2010
HCB	2.0077	0.0678	0.0311	0.0570	0.0366	0.0332	0.0622	0.0534
HCHA	0.1263	0.2324	0.2089	0.2418	0.2041	0.1738	0.1796	0.1251
HCHG	0.6271	0.5400	0.5643	0.4001	0.6120	0.3570	0.6406	0.6963
ALD	0.1713	0.0057	0.0065	0.0109	0.0076	0.0044	0.0130	0.0140
DIELD	0.0437	0.0169	0.0590	0.0232	0.0464	0.0592	0.0272	0.0309
END	0.0830	0.0115	0.0153	0.0280	0.0180	0.0114	0.0307	0.0360
DDTPP	0.2233	0.1101	0.5380	0.1610	0.1683	0.0962	0.1309	0.2889
DDTOP	0.0330	0.0171	0.1132	0.0154	0.0325	0.0221	0.0163	0.0832
DDEPP	0.0278	0.0547	0.1715	0.0641	0.0670	0.0401	0.0600	0.0989
DDDPP	0.0513	0.0095	0.0515	0.0354	0.0265	0.0204	0.0116	0.0792
CB28	0.2806	0.0384	0.1625	0.0592	0.0797	0.0263	0.1169	0.0788
CB52	0.0908	0.0425	0.0787	0.1451	0.0179	0.0260	0.0460	0.0779
CB138	0.4052	0.0878	0.1410	1.9138	0.0189	0.0616	0.0322	0.1845
CB153	0.3895	0.0826	0.1140	1.0883	0.0182	0.0469	0.0310	0.1405
PHEN	9.5501	6.5537	41.3564	10.4508	16.7249	9.9536	59.0740	57.2892
ANT	0.2105	0.1765	2.4299	0.3518	0.3634	0.3162	2.5774	4.5851
FLU	4.1680	5.9163	55.5334	10.7283	19.4799	9.7796	84.1113	85.4890
PYR	4.4222	4.4052	43.7291	8.5758	12.1343	8.0456	62.0984	60.2352
BAA	0.6456	1.1216	21.6529	3.0905	2.9397	2.4619	19.2790	27.0059
CHRTR	2.2694	3.4412	33.8057	8.4360	9.2125	6.1042	46.5335	83.0390
BAP	0.8745	1.7581	8.8242	2.8906	2.4351	2.0998	14.4785	24.5858
I123P	0.8052	2.4143	9.6554	3.8692	3.8173	2.4797	21.6649	29.0444
BGHIP	0.7542	2.1656	8.2275	4.0907	3.9165	2.5028	20.7921	29.0501
DBAHA	0.1216	0.3499	2.4611	0.5848	0.6022	0.3624	4.0559	4.7450
Deposition [L/m ²]	38.2	85.7	86.7	63.2	73.8	142.2	43.3	47.5

A8 Table 2: Concentrations (ng/L) of organic compounds in monthly rain water samples collected in Tinnum/Sylt in 2009 and 2010, respectively

ng/L	January		February		March		April	
	2009	2010	2009	2010	2009	2010	2009	2010
HCB	0.0507	0.0225	0.0544	0.0476	0.0777	0.0905	0.1380	0.0423
HCHA	0.2135	0.0934	0.1870	0.2026	0.1497	0.2530	0.2949	0.2252
HCHG	0.7764	0.3123	0.8703	1.0113	0.7396	2.5803	1.7309	1.0030

A8 Table 2 continued:

ng/L	January		February		March		April	
	2009	2010	2009	2010	2009	2010	2009	2010
ALD	0.0105	0.0078	0.0080	0.0071	0.0089	0.0164	0.0204	0.0088
DIELD	0.0827	0.1044	0.0577	0.0920	0.1152	0.1642	0.1277	0.1608
END	0.0269	0.0631	0.0205	0.0575	0.0402	0.1225	0.0522	0.0237
DDTPP	0.0463	0.0565	0.0371	0.0597	0.0968	0.0461	0.3433	0.1260
DDTOP	0.0088	0.0093	0.0081	0.0085	0.0461	0.0182	0.0819	0.0400
DDEPP	0.0099	0.0278	0.0102	0.0253	0.0456	0.0539	0.4546	0.0652
DDDPP	0.0078	0.0190	0.0067	0.0174	0.0628	0.0370	0.1006	0.0314
CB28	0.0287	0.0314	0.3944	0.0286	0.0285	0.0610	0.6475	0.0545
CB52	0.0111	0.0360	0.1303	0.0328	0.0243	0.0699	0.2433	0.0390
CB138	0.0407	0.1329	0.0419	0.1212	0.0405	0.2581	1.8925	0.3211
CB153	0.0358	0.1695	0.0369	0.1546	0.0356	0.3292	2.1036	0.4085
PHEN	13.8130	33.3259	18.2465	36.9569	7.1279	23.4737	62.2292	23.3598
ANT	0.5011	2.0142	0.9103	1.3014	0.4477	1.3686	4.2775	0.9083
FLU	8.9831	38.0320	16.0516	42.3960	9.5776	22.9865	52.7939	38.1306
PYR	6.6260	21.6801	12.7845	20.9712	7.5641	14.6883	42.7140	23.3429
BAA	2.2305	6.6162	4.2503	4.3168	2.3557	4.3444	11.5334	7.0496
CHRTR	6.3730	22.9296	9.1460	25.4552	5.6763	7.5753	22.7802	32.9688
BAP	3.3436	5.4144	5.4514	3.8405	3.1891	4.6354	12.4538	7.7614
I123P	5.6830	9.2836	7.4229	11.0905	4.1384	4.4366	10.5747	9.1255
BGHIP	5.7572	8.6200	7.4689	9.6520	4.3059	4.8641	10.8041	12.4740
DBAHA	0.9501	2.0148	1.2251	2.0551	0.8430	1.2919	2.5765	2.4179
Deposition [L/m ²]	38.0	31.7	36.9	34.8	38.2	16.3	12.7	26.9

ng/L	May		June		July		August	
	2009	2010	2009	2010	2009	2010	2009	2010
HCB	0.0242	0.0239	0.0437	0.0471	0.0411	0.0670	0.1325	0.0340
HCHA	0.0910	0.1986	0.1216	0.2293	0.1448	0.1634	0.1632	0.1391
HCHG	1.1382	1.1882	0.6130	0.9250	0.9924	1.2322	1.1896	0.5498
ALD	0.0035	0.0050	0.0068	0.0150	0.0039	0.0043	0.0029	0.0037
DIELD	0.0555	0.0961	0.0442	0.0970	0.0596	0.0419	0.0756	0.0465
END	0.0090	0.0134	0.0173	0.0824	0.0254	0.0086	0.0193	0.0075
DDTPP	0.0300	0.0441	0.0153	0.0328	0.0153	0.0206	0.0338	0.0179
DDTOP	0.0072	0.0088	0.0112	0.0173	0.0042	0.0128	0.0105	0.0111
DDEPP	0.0303	0.0368	0.0547	0.0725	0.0070	0.0072	0.0269	0.0063
DDDPP	0.0037	0.0080	0.0067	0.0158	0.0058	0.0071	0.0261	0.0062
CB28	0.1136	0.0307	0.2051	0.0606	0.0930	0.0288	0.8720	0.0250
CB52	0.0427	0.0220	0.0770	0.0434	0.0397	0.0318	0.4719	0.0276
CB138	0.3319	0.1812	0.5993	0.3572	0.3353	0.0658	0.2117	0.0570
CB153	0.3689	0.2306	0.6661	0.4544	0.3639	0.0618	0.2297	0.0536
PHEN	9.8469	14.7771	5.8473	11.4442	6.8767	24.2514	16.4357	4.8157
ANT	0.5092	0.6355	0.3282	0.7412	0.1566	0.4804	0.3067	0.1457
FLU	7.7132	15.3892	5.2145	6.7383	4.8519	9.3471	4.6880	4.9049
PYR	7.0087	10.5144	1.2103	2.2235	3.5393	5.3786	3.9007	3.1120
BAA	2.0104	4.1742	3.5130	7.3796	0.8221	1.4646	0.3615	0.9799
CHRTR	4.2912	8.1326	4.3674	16.0141	2.7593	4.3950	1.3731	2.4030
BAP	2.4502	4.3533	1.4690	3.5836	1.0999	2.1427	0.3295	1.2815
I123P	1.8793	3.1866	1.2944	5.6785	0.9929	2.3922	0.1947	1.2286
BGHIP	1.8729	4.7701	0.4011	1.1224	0.9561	2.4607	0.2350	1.1462
DBAHA	0.4018	1.1037	0.4011	1.1224	0.1157	0.4810	0.0373	0.2503
Deposition [L/m ²]	72.2	47.7	40.0	24.2	66.2	114.4	104.9	131.9

A8 Table 2 continued:

ng/L	September		October		November		December	
	2009	2010	2009	2010	2009	2010	2009	2010
HCB	0.0313	0.0473	0.0233	0.0429	0.0211	0.0279	0.0398	0.0510
HCHA	0.1469	0.2014	0.1679	0.1520	0.1910	0.1428	0.1497	0.1116
HCHG	0.3231	0.3905	0.5443	0.4360	0.5541	0.3980	0.4371	0.2583
ALD	0.0051	0.0058	0.0049	0.0046	0.0044	0.0064	0.0083	0.0163
DIELD	0.0987	0.0914	0.0899	0.1095	0.1062	0.1385	0.1310	0.0878
END	0.0336	0.0102	0.0115	0.0119	0.0104	0.0164	0.0196	0.0419
DDTPP	0.0976	0.0243	0.0296	0.0213	0.0349	0.0175	0.0575	0.0172
DDTOP	0.0044	0.0151	0.0061	0.0053	0.0055	0.0059	0.0104	0.0144
DDEPP	0.0074	0.0239	0.0195	0.0169	0.0383	0.0063	0.0332	0.0325
DDDPP	0.0162	0.0084	0.0099	0.0044	0.0088	0.0049	0.0074	0.0158
CB28	0.0980	0.0339	0.0504	0.0260	0.0828	0.0291	0.0133	0.0707
CB52	0.0418	0.0375	0.0149	0.0147	0.0272	0.0164	0.0086	0.0399
CB138	0.3530	0.0775	0.0379	0.1358	0.0421	2.9913	0.0206	0.3696
CB153	0.3832	0.0728	0.0451	0.1736	0.0359	3.0856	0.0198	0.4724
PHEN	5.9953	11.8591	15.9690	15.8116	15.0975	8.7959	47.7223	12.2962
ANT	0.6342	0.3082	0.5979	0.5654	0.5579	0.3079	1.2554	0.6458
FLU	8.5320	12.2454	13.9342	10.8567	14.6275	8.9678	71.7117	9.8923
PYR	5.6483	8.7706	9.8706	6.4955	8.2359	5.7293	40.4799	5.9307
BAA	2.6526	2.6936	2.3348	2.1177	2.3744	1.5306	10.3468	1.0962
CHRTR	8.9743	6.5603	7.4305	7.1059	6.9825	5.2154	40.0933	3.0141
BAP	2.2553	3.9119	2.3328	2.0596	2.1089	1.2794	6.7812	0.6924
I123P	2.2064	3.9810	3.0004	2.2319	2.9196	1.8296	17.2488	0.6845
BGHIP	2.1374	3.7778	2.9824	2.6544	2.8420	2.1879	15.0638	1.0031
DBAHA	0.3485	0.7452	0.5377	0.4491	0.5528	0.3012	3.4741	0.1644
Deposition [L/m²]	62.9	97.2	116.0	94.9	127.8	84.9	67.8	34.9

Declarations

I hereby state that the thesis entitled: „Atmospheric deposition of organic contaminants to the North Sea and the western Baltic Sea” is my work and that I have not used any other materials besides those cited. I clearly indicated those parts been taken from other works. This thesis has not been submitted for degree in any other university.

(Date)

(Signature)

I herewith declare that I did not undertake any previous attempt to receive a PhD.

(Date)

(Signature)